

## ABSTRACT

Title of Dissertation:           BRIDGE PIER SCOUR IN TIDAL ENVIRONMENTS

Donald R. Demetrius, Doctor of Philosophy, 2006

Dissertation directed by:   Professor Richard H. McCuen  
Department of Civil and Environmental Engineering

Scour depths in estuaries are often estimated using imprecise models that were developed for riverine systems and do not consider the various processes responsible for the removal of sediment in a tidal system. In a tidal or estuarine environment, the flow changes directions with the tide resulting in scour patterns that are quite different from those in upland rivers. At the other end of the spectrum of models used to determine pier scour are the multi-dimensional hydrodynamic models that include the tidal processes; however, these models are unattractive because they require extensive and costly data inputs and are characteristically computationally intensive and very complex. Also, not much accuracy is added to the process by the use of hydrodynamic models as the results they produce are used as inputs to less accurate empirical local scour equations.

In order to efficiently enhance the safety of bridges spanning tidal waterways, a multi-component continuous model (WAVES) was developed to predict bridge pier scour in tidal estuaries and facilitate a risk-based design approach for bridges. The WAVES program is the result of the application of accepted theories regarding the mechanism of bridge pier scour in general, along with the combination of tidal and riverine hydraulics. The basis of the model is the novel approach used in the quantification of the effects of the downflow and horseshoe vortex that most experts in the field identify as the agents responsible for scour around bridge piers.

Through the performance of this study, several conclusions were drawn. First, a number of scour models and equations currently in use may be inappropriate for bridge pier design and analysis in tidal environments. Second, a temporal model for tidal environments that provides a time history of scour significantly improves the usefulness of scour predictions over single-event models. The methodology employed by the WAVES program provides these improvements at reasonable costs. Third, the WAVES program facilitates a risk-based design approach by yielding estimates of the probability of scour depths over time and will help policy makers and designers to make important decisions regarding the design of safer new bridges and the safe use of existing bridges.

# **BRIDGE PIER SCOUR IN TIDAL ENVIRONMENTS**

**by**

**Donald R. Demetrius**

Dissertation submitted to the Faculty of the Graduate School of the  
University of Maryland, College Park in partial fulfillment  
of the requirements of the degree of  
Doctor of Philosophy  
2006

Advisory Committee:

Dr. Richard H. McCuen, Chair  
Dr. Kaye L. Brubaker  
Dr. Mohammad Modarres  
Dr. Glenn E. Moglen  
Dr. Yaron M. Sternberg

## **ACKNOWLEDGEMENTS**

The completion of this dissertation is an achievement that could not be possible without the help and support of a number of people. I am deeply indebted to Dr. Richard H. McCuen, not only for his technical expertise, but also for the patience and commitment to this project that he has shown over the years and Dr. Kaye Brubaker who, for a long time, served as a source of motivation. In addition, I would like to thank Dr. Dr. Mohammad Modarres, Glenn Moglen, and Dr. Yaron Sternberg for their input and expertise.

No undertaking of this magnitude can be accomplished without the help and support of friends and relatives. Very special thanks to Balthazar Barrie, Catherine Barrie, and in particular, Rose Barrie for the invaluable assistance they gave. Thanks to Simon Francis for the help he provided in reviewing this manuscript. Also, thanks to Vickie Demetrius and Nicole Groves who also provided me help and support in this endeavor.



# TABLE OF CONTENTS

LIST OF TABLES .....	xii
LIST OF FIGURES .....	xvi
NOTATIONS .....	xx
CHAPTER 1 - INTRODUCTION .....	1
1.1 INTRODUCTION .....	1
1.2 TYPES OF SCOUR .....	2
1.3 SCOUR IN TIDAL WATERWAYS .....	3
1.4 GOAL AND OBJECTIVES .....	4
1.5 IMPLICATIONS .....	5
CHAPTER 2 - LITERATURE REVIEW .....	7
2.1 INTRODUCTION .....	7
2.2 PIER SCOUR AND ITS MECHANISMS .....	9
2.2.1 Definition of Scour .....	9
2.2.2 General Scour .....	10
2.2.3 Contraction Scour .....	11
2.2.4 Local Scour .....	11
2.2.5 Total Pier Scour .....	11
2.3 BRIDGE PIER SCOUR IN AN ESTUARINE ENVIRONMENT .....	12
2.3.1 Estuary Classification .....	12
2.3.2 The Hydrologic and Hydraulic Process .....	14
2.3.3 Tidal, Storm Surge, and Riverine Hydrology .....	14
2.3.4 Estuarine Hydraulics .....	15
2.3.5 The Importance of Hydraulics to the Bridge Pier Scour Process .....	17
2.3.6 The Scour and Sedimentation Processes in Estuaries .....	17
2.4 THE DOWNFLOW DEVELOPMENT .....	19
2.4.1 Introduction .....	19
2.4.2 Theoretical Development of the Downflow .....	19
2.4.3 Research Supporting the Existence of the Downflow .....	21
2.4.4 Role of the Downflow in the Local Scour Process .....	24
2.5 THE VORTEX DEVELOPMENT .....	28
2.5.1 Introduction .....	28
2.5.2 Theoretical Background .....	28
2.5.3 Free Vortex .....	30
2.5.4 Forced Vortex .....	31
2.5.5 Real Vortex .....	32
2.5.6 Flow About a Circular Pier .....	34
2.5.7 The Vortex System During Development of the Scour Hole .....	35
2.6 CURRENT PIER SCOUR MODELS .....	46

2.6.1	Introduction.....	46
2.6.2	Comparative Scour Research.....	46
2.7	MODEL COMPONENTS FOR ESTUARINE BRIDGE SCOUR ANALYSIS .....	48
2.7.1	Introduction.....	48
2.7.2	The Riverine Hydrologic Component.....	48
2.7.3	The Tidal Hydrologic Component.....	49
2.7.4	The Hydraulic Component.....	52
2.7.5	Sediment Transport and Scour Models.....	54
2.8	HURRICANES AND ASSOCIATED MODELS .....	60
2.9	DEVELOPMENT OF A CONCEPTUAL MULTI-SCALE FRAMEWORK.....	63
2.9.1	Introduction.....	63
2.9.2	Available Methods of Scale Determination.....	63
2.9.3	The Melville-Coleman Approach .....	66
2.9.4	The Catchment Scale .....	66
2.9.5	The Stream Section Scale .....	68
2.9.6	The Bridge Far-Field Scale.....	69
2.9.7	The Bridge Near-Field Scale .....	69
2.9.8	The Local Scale.....	69
2.10	MODEL EVALUATION AND ANALYSIS.....	70
2.10.1	Introduction.....	70
2.10.2	Sensitivity Analysis .....	71
2.10.3	Sensitive Variables.....	72
2.10.4	Uncertainty Analysis.....	73
	CHAPTER 3 - MODEL DEVELOPMENT .....	75
3.1	INTRODUCTION .....	75
3.2	DEVELOPMENT OF THE SCALE APPROACH FOR ESTUARIES.....	75
3.2.1	Introduction.....	75
3.2.2	Open-Ocean Scale.....	78
3.2.3	Catchment Scale.....	79
3.2.4	Tidal Estuary Scale .....	79
3.2.5	Bridge Near-Field Scale.....	81
3.2.6	Local Scour Scale .....	82
3.3	MODEL FORMULATION .....	82
3.3.1	Introduction.....	82
3.3.2	Overview of the Model Structure .....	83
3.4	FORMULATION OF THE TIDAL COMPONENT.....	84
3.4.1	Introduction.....	84
3.4.2	Development of the Base Station Tidal Model.....	84
3.4.3	Determination of the Tidal Component at the Bridge Station .....	85
3.4.4	Determination of the Tidal Discharges at the Bridge Location .....	90
3.5	FORMULATION OF THE CATCHMENT COMPONENT.....	91
3.5.1	Introduction.....	91

3.5.2	Estimation of the Number and Duration of the Annual Storms.....	91
3.5.3	Estimation of Rainfall Depths.....	92
3.5.4	Determination of the Catchment Hydrograph.....	93
3.6	FORMULATION OF THE HYDRAULIC COMPONENT .....	94
3.6.1	Introduction.....	94
3.6.2	Estimation of the Resultant Flow Depth.....	94
3.6.3	Estimation of the Resultant Discharge.....	97
3.6.4	Estimation of the Resultant Velocity .....	97
3.7	DETERMINATION OF THE DOWNFLOW .....	98
3.7.1	Downflow Model Prior to the Beginning of Scour.....	98
3.7.1.1	The Turbulent Flow Profile .....	98
3.7.1.2	Impuse-Momentum Application.....	99
3.7.1.3	Width of the Stagnation Plane of a Circular Pier.....	101
3.7.1.4	Jet Equations .....	102
3.7.1.5	Treatment of the Boundary Layers .....	105
3.7.1.6	Development of a General Downflow Equation.....	106
3.7.2	Downflow Model After Scouring Begins.....	107
3.7.3	Calibration of the maximum downflow for $0 < d_s/d < 2.3$ .....	109
3.7.4	Estimation of the maximum downflow for $d_s/d > 2.3$ .....	110
3.7.5	Composite Maximum Downflow Equation.....	111
3.8	FORMULATION OF THE VORTEX MODEL .....	112
3.8.1	Introduction.....	112
3.8.2	Shear Stress and Tangential Velocity Equations for Vortex $S_0$ .....	113
3.8.3	Shear Stress and Tangential Velocity Equation for Vortex 1 .....	116
3.8.4	Shear Stress and Tangential Velocity for the Horseshoe Vortex System.....	117
3.8.5	Spatial Variation of $v_{th}$ and $\tau_{th}$ Across the Face of the Bridge Pier .....	118
3.8.6	Calibration of the Horseshoe Vortex Model Prior to the Full Development of the Scour Hole .....	119
3.8.6.1	Relationship between $d_s/D$ and $\theta$ .....	121
3.8.6.2	Relationship between $a/D$ and $\theta$ and $b/D$ and $\theta$ .....	121
3.8.6.3	Relationship between $a_m/a$ and $\theta$ .....	123
3.8.6.4	Determination of the Coordinates of the Center of the Vortex.....	124
3.8.6.5	Development of the Tangential Velocity of the Vortex.....	128
3.8.7	The Vortex Model after the Full Development of the Scour Hole .....	128
3.9	THE SCOUR COMPONENT.....	129
3.9.1	Introduction.....	129
3.9.2	General Scour Model .....	130
3.9.3	Contraction Scour Model .....	131
3.9.4	Time Varying Local Scour model.....	132
3.9.5	Determination of the Incipient Velocity $V_i$ .....	134
3.9.6	Development of the Ultimate Scour Model .....	137
3.9.7	Determination of the Time to Ultimate Scour $t_e$ .....	137
3.10	PROGRAM FUNCTIONS .....	138
3.10.1	Introduction.....	138
3.10.2	Determination of the Mean Ultimate Scour Depth.....	139
3.10.2.1	Design of New Bridges.....	139

3.10.2.2	The Analysis of Existing Bridges .....	140
3.10.3	Effect of Pier Diameter .....	140
3.10.4	Determination of the Probability and Risk of Failure.....	141
3.10.4.1	Design of New Bridges.....	141
3.10.4.2	The Analysis of Existing Bridges .....	143
3.10.5	Effect of Hurricanes.....	143
3.10.5.1	Design of New Bridges.....	143
3.10.5.2	The Analysis of Existing Bridges .....	144
3.10.6	Analysis of the Features to Prevent Failure by Scour.....	144
3.11	MODELING PROCESS AND ALGORITHM DEVELOPMENT.....	145
3.11.1	Assumptions and Conditions .....	145
3.11.2	Modeling Process.....	146
3.11.3	Determine Storm Event Variates .....	151
3.11.4	Determine Catchment Hydrograph for Each Storm.....	152
3.11.5	Determine Base Station Tidal Variates and Synthesize Tidal Model.....	153
3.11.6	Determine Tidal Elevations at Bridge Location .....	156
3.11.7	Determine Tidal Discharges at the Bridge Location.....	159
3.11.8	Determine the Combined Depth and Velocity at the Bridge Location.....	160
3.11.9	Determine Downflow and Vortex Velocity Vectors .....	161
3.11.10	Compute Scour (Sum of Local and Contraction Scour) .....	163
3.11.11	Program Execution Options.....	167
	CHAPTER 4 - SENSITIVITY AND ERROR ANALYSIS.....	170
4.1	INTRODUCION.....	170
4.1.1	Reasons and Challenges of a Sensitivity Analysis for Estuary Scour .....	170
4.1.2	Challenges with Sensitivity Analyses of Continuous Scour Simulations in a Tidal Environment .....	171
4.2	DEVELOPMENT OF BASELINE STUDY CONDITIONS.....	172
4.2.1	Identification of Input Variables and Parameters .....	172
4.2.2	Development of Baseline Conditions .....	174
4.2.2.1	Selection of the Data to be Analyzed.....	174
4.2.2.2	Selection of Simulation Length .....	174
4.2.2.3	Selection of Baseline Conditions.....	175
4.2.2.4	Data Range Constraints.....	177
4.3	VARIABLE AND PARAMETER SENSITIVITY ANALYSIS .....	180
4.3.1	Method of Sensitivity Analysis.....	180
4.3.2	Relative Sensitivity Results .....	181
4.3.3	Highly Sensitive Variables and Parameters.....	185
4.3.3.1	Introduction.....	185
4.3.3.2	Results for the Upstream Pier Face.....	186
4.3.3.3	Results for the Downstream Pier Face.....	192
4.3.3.4	Least Sensitive Variables and Surprising Results.....	197
4.4	PARAMETER SENSITIVITY OF MODEL COMPONENTS .....	197
4.5	COMPONENT UNCERTAINTY .....	200
4.6	VARIABLE ERROR AND UNCERTAINTY ANALYSES .....	203

CHAPTER 5 - MODEL APPLICATION.....	205
5.1 INTRODUCTION .....	205
5.1.1 Variations in Estuary and Watershed Conditions .....	205
5.1.2 Determination of Tidal or Catchment Dominated Estuaries Using the Simmons Ratio .....	206
5.1.3 Determination of Tidal or Catchment Dominated Estuaries Using the CE Ratio .....	209
5.1.4 General Discussion of the Bridge Location Conditions .....	209
5.1.5 Case Study Site Selection Rationale .....	210
5.2 DATA COMPILATION METHODS OF THE CASE STUDY SITES .....	211
5.2.1 Catchment Data.....	211
5.2.2 Tidal Data.....	212
5.2.2.1 Base Station Tidal Data .....	212
5.2.2.2 Bridge Station Tidal Data .....	213
5.2.3 Bridge Cross Section Data .....	213
5.2.4 Bridge Data .....	214
5.2.5 Bridge Estuary Data.....	215
5.2.6 Soil Data.....	216
5.2.7 Hurricane Data .....	217
5.3 THE MONIE BAY SITE .....	218
5.3.1 Estuary Conditions.....	218
5.3.2 Watershed Conditions.....	219
5.3.3 Simmons Ratio and Bridge Location Conditions .....	219
5.4 THE BLACK RIVER SITE.....	221
5.4.1 Estuary Conditions.....	221
5.4.2 Watershed Conditions.....	222
5.4.3 Simmons Ratio and Bridge Location Conditions .....	222
5.5 THE PATUXENT RIVER SITE .....	224
5.5.1 Estuary Conditions.....	224
5.5.2 Watershed Conditions.....	225
5.5.3 Simmons Ratio and Bridge Location Conditions .....	226
5.6 THE WICOMICO RIVER SITE .....	227
5.6.1 Estuary Conditions.....	227
5.6.2 Watershed Conditions.....	228
5.6.3 Simmons Ratio and Bridge Location Conditions .....	228
5.7 THE PATAPSCO RIVER SITE.....	230
5.7.1 Estuary Conditions.....	230
5.7.2 Watershed Conditions.....	231
5.7.3 Simmons Ratio and Bridge Location Conditions .....	231
CHAPTER 6 - CASE STUDIES: CONTINUOUS MODEL APPLICATION.....	234
6.1 INTRODUCTION .....	234
6.2 SIMULATION CONDITIONS AND ASSUMPTIONS .....	235

6.2.1	Continuous Simulations .....	235
6.2.2	Hurricane Event Simulations .....	238
6.3	THE MONIE BAY SITE .....	239
6.3.1	Specific Modeling Assumptions and Conditions .....	239
6.3.1.1	Hurricane Simulations .....	240
6.3.2	Continuous Simulation Results .....	241
6.3.2.1	Upstream Pier Face .....	243
6.3.2.2	Downstream Pier Face .....	244
6.3.3	Results of the Hurricane Event Simulations .....	246
6.4	THE BLACK RIVER AT BALTIMORE SITE .....	248
6.4.1	Specific Modeling Assumptions and Conditions .....	248
6.4.1.1	Hurricane Simulations .....	249
6.4.2	Continuous Simulation Results .....	250
6.4.2.1	Upstream Pier Face .....	251
6.4.2.2	Downstream Pier Face .....	252
6.4.3	Hurricane Event Simulation Results .....	253
6.5	THE PATUXENT RIVER AT BENEDICT SITE .....	255
6.5.1	Specific Modeling Assumptions and Conditions .....	255
6.5.2	Continuous Simulation Results .....	257
6.5.2.1	Upstream Pier Face .....	258
6.5.2.2	Downstream Pier Face .....	259
6.5.3	Hurricane Event Simulation Results .....	261
6.6	THE WICOMICO RIVER SITE .....	263
6.6.1	Specific Modeling Assumptions and Conditions .....	263
6.6.1.1	Hurricane Simulations .....	263
6.6.2	Continuous Simulation Results .....	264
6.6.2.1	Upstream Pier Face .....	265
6.6.2.2	Downstream Pier Face .....	267
6.6.3	Hurricane Event Simulation Results .....	268
6.7	BALTIMORE ON THE PATAPSCO RIVER SITE .....	270
6.7.1	Specific Modeling Assumptions and Conditions .....	270
6.7.1.1	Hurricane Simulations .....	271
6.7.2	Continuous Simulation Results .....	272
6.7.2.1	Upstream Pier Face .....	272
6.7.2.2	Downstream Pier Face .....	274
6.7.3	Hurricane Event Simulation Results .....	275
6.8	ANALYSIS OF RESULTS .....	276
6.8.1	Continuous Simulation Results .....	276
6.8.1.1	Risk of Pier Failure at the Tide Controlled Sites .....	279
6.8.1.2	Risk of Pier Failure Mixed-Controlled Sites .....	285
6.8.1.3	Risk of Pier Failure at a Catchment-Controlled Site .....	292
6.8.2	Hurricane Event Results .....	296
CHAPTER 7 - COMPARISON OF EXISTING MODELS WITH THE WAVES PROGRAM .....		300

7.1	INTRODUCTION .....	300
7.1.1	Benefits and Weaknesses of a Single-Event Model .....	300
7.1.2	Benefits and Weaknesses of Continuous Models .....	301
7.1.3	Rationale for Model Comparison Exercises .....	302
7.2	SUMMARY DESCRIPTION OF FORTY SINGLE-EVENT MODELS.....	302
7.2.1	Model Description .....	302
7.2.2	Summary of Required Inputs.....	307
7.3	COMPARISON OF WAVES WITH FORTY SINGLE-EVENT MODELS .....	309
7.3.1	Procedure .....	309
7.3.2	Results of the Comparative Exercises.....	311
7.3.2.1	Introduction.....	311
7.3.2.2	Summary of Results.....	312
7.3.3	Tide-Controlled Sites: Monie Bay and Black River .....	316
7.3.3.1	Upstream Pier Face .....	316
7.3.3.2	Downstream Pier Face .....	318
7.3.3.3	Maximum Predicted Pier Scour Results .....	319
7.3.4	Mixed-Control Sites: Patuxent and Wicomico Rivers.....	325
7.3.4.1	Upstream Pier Face .....	325
7.3.4.2	Downstream Pier Face .....	326
7.3.4.3	Maximum Predicted Pier Scour Results .....	327
7.3.5	Catchment-Controlled Site: Baltimore Patapsco .....	332
7.3.5.1	Upstream Pier Face .....	332
7.3.5.2	Downstream Pier Face .....	333
7.3.5.3	Maximum Predicted Scour Results.....	334
7.4	COMPARISON OF THE CONTINUOUS RESULTS FROM THE FIVE BENCHMARK MODELS AND WAVES.....	338
7.4.1	Discussion of the Single-Event Models Used.....	338
7.4.1.1	Rationale of Model Selection.....	338
7.4.1.2	Data Range Constraints of the Selected Models.....	339
7.4.2	Method of Developing Continuous Simulations from Single-Event Models .....	341
7.4.3	Summary of Results.....	342
7.4.3.1	Tide-Controlled Estuaries Monie Bay and Black River .....	342
7.4.3.2	Mixed Control Estuaries Patuxent at Benedict and Wicomico.....	346
7.4.3.3	Catchment-Controlled Estuary Baltimore at the Patapsco.....	350
7.4.4	Discussion of Results .....	352
7.4.4.1	Tide Controlled Estuaries Monie Bay and Black River.....	352
7.4.4.2	Mixed-Control Estuaries Patuxent at Benedict and Wicomico .....	354
7.4.4.3	Catchment-Controlled Estuary the Patapsco at Baltimore .....	356
7.5	CONCLUSIONS.....	358
7.5.1	Forty-Model Comparison.....	358
7.5.2	Continuous Simulations Comparison .....	359
	CHAPTER 8 - CONCLUSIONS .....	362
8.1	INTRODUCTION .....	362

8.2	THE THEORETICAL BASIS OF THE WAVES PROGRAM .....	363
8.3	DATA INPUT NEEDED FOR THE MULTI-SCALE FRAMEWORK .....	364
8.4	ESTUARY PIER SCOUR DATA FOR MODEL VALIDATION .....	366
8.5	THE BENEFITS OF A TIME DEPENDENT SCOUR MODEL .....	367
8.6	BENEFITS OF A RISK BASED-DESIGN APPROACH .....	368
8.7	THE USE OF CURRENT SCOUR EQUATIONS FOR ESTUARIES .....	370
8.8	HURRICANE SCOUR.....	372
8.9	IMPORTANT FEATURES OF PIER SCOUR IN ESTUARIES .....	373

CHAPTER 9 - RECOMMENDATIONS .....	375
-----------------------------------	-----

9.1	INTRODUCTION .....	375
9.2	THE NEED FOR A RISK-BASED DESIGN METHODOLOGY .....	375
9.3	IMPROVING THE SCIENCE OF PIER SCOUR PREDICTIONS .....	376
9.3.1	Further Research into the Scour Process .....	376
9.3.2	The Importance of Reliable Pier Scour Field Data .....	378
9.4	IMPROVING THE WAVES PROGRAM .....	379
9.4.1	Pier Geometry .....	379
9.4.2	Pier Type .....	380
9.4.3	Modeling Pressure Flow .....	381
9.4.4	Improving the Hydraulic Component .....	381
9.4.5	Model Calibration and Verification .....	382

## LIST OF APPENDICES

### APPENDIX A

Appendix A-1.....	WAVES Program Variable List
Appendix A-2.....	WAVES Program Fortran Codes

### APPENDIX B

Appendix B-1.....	Baseline Conditions and Results for the Sensitivity Analyses
Appendix B-2.....	Detailed Sensitivity Results

### APPENDIX C

Appendix C-1.....	HEC-6 Soil Particle Sizes
Appendix C-2.....	Location Maps of the Case Study Sites
Appendix C-3.....	USGS Simulations of the Case Study Catchments

### APPENDIX D

Appendix D-1.....	Determination of the Number of Simulations Required for Stabilization
Appendix D-2.....	Continuous and Hurricane Simulation Input Files for the Case Study Sites
Appendix D-3.....	Monie Bay Continuous Simulation Results
Appendix D-4.....	Monie Bay Hurricane Simulation Results



Appendix D-5.....	Black River Continuous Simulation Results
Appendix D-6.....	Black River Hurricane Simulation Results
Appendix D-7.....	Patuxent River Continuous Simulation Results
Appendix D-8.....	Patuxent River Hurricane Simulation Results
Appendix D-9.....	Wicomico River Continuous Simulation Results
Appendix D-10.....	Wicomico River Hurricane Simulation Results
Appendix D-11.....	Patapsco River Continuous Simulation Results
Appendix D-12.....	Patapsco River Hurricane Simulation Results
APPENDIX E	
Appendix E-1 .....	40-Model Comparison Codes
Appendix E-2 .....	40-Model Comparison Input Files
Appendix E-3 .....	40-Model Comparison Output Files (Scour Results)
Appendix E-4 .....	Benchmark Models Annual Series Codes
Appendix E-5 .....	Benchmark Models Annual Series Input Data
Appendix E-6 .....	Benchmark Models Annual Series Output Data (Scour Results)
APPENDIX F .....	The Physics of the Horseshoe Vortex and Downflow Formation
REFERENCES	

## LIST OF TABLES

Table 2.4-1	Specific conditions of experiment C2M, D2M, and C2R.....	27
Table 2.5-1	Mean position of oscillating vortices .....	40
Table 2.5-2	Location of the center of the mean vortices positions for $R=2,610$ .....	40
Table 2.5-3	Velocity on a vertical plane through the center of some vortices.....	41
Table 2.5-4	Velocity distribution along a horizontal plane through the center of vortex 1 .....	42
Table 2.5-5	Pressure distribution along the vertical stagnation line .....	43
Table 2.5-6	Bed shear stress.....	43
Table 2.5-7	Raw vortex data obtained from Melville et al .....	44
Table 2.5-8	Normalized vortex data.....	44
Table 2.7-1	Empirical local scour models .....	56
Table 2.9-1	Table of the Various Scales of an Estuary System .....	64
Table 2.9-2	Melville's Scale Approach to Riverine Bridge Scour Analysis .....	67
Table 3.2-1	Applicable Scales for Various Estuarine Regimes .....	76
Table 3.2-2	Estuarine Scale Approach for Bridge Scour Analysis .....	77
Table 3.5-1	Gamma variate constants for Baltimore .....	93
Table 3.7-1	Values of $V_d/U$ obtained from Ettema (1980) .....	111
Table 3.8-1	Normalized coordinates of the center of each vortex .....	124
Table 4.2-1	Input Data for Scour Model with the Acronym Shown.....	173
Table 4.2-2	Data ranges of the catchment variables observed in the review of the Chesapeake Bay estuaries.....	175
Table 4.2-3	Data ranges of the estuary variables observed in the review of the Chesapeake Bay estuaries.....	176
Table 4.2-4	Data ranges of the hydraulic (cross section) variables observed in the review of the Chesapeake Bay estuaries.....	176
Table 4.2-5	Data ranges of the scour variables observed in the review of the Chesapeake Bay estuaries .....	176
Table 4.2-6	Data ranges of the hurricane variables observed in the review of the Chesapeake Bay estuaries .....	177
Table 4.2-7	National Weather Service Classification of Hurricanes .....	179
Table 4.3-1	Summary of the relative sensitivity results for the single-event hurricane .....	182
Table 4.3-2	Summary of relative sensitivity results of 25-year simulation for the sensitive variables and parameters .....	182
Table 4.3-3	Annual Relative Sensitivity of the Upstream Pier Face Scour to Tide Peakedness.....	183
Table 4.3-4	Sensitivity of downstream face scour results to pier diameter .....	184
Table 4.3-5	The most sensitive variables for scour on the upstream pier face ranked in order of importance.....	187
Table 4.3-6	Relative Sensitivities (RS) for Hurricane Scour on the Upstream Pier Face .....	191
Table 4.3-7	Relative Sensitivities of Model Variables (RS) on the Downstream Pier Face Ranked .....	193

Table 4.3-8	Relative Sensitivity Results (RS) for Hurricane Scour on the Downstream Pier Face .....	196
Table 4.4-1	Mean Annual Sensitivity Results u/s Pier Face .....	198
Table 4.4-2	Final Scour Sensitivity Results for the u/s Pier Face .....	198
Table 4.4-3	Mean Annual Sensitivity results d/s Pier Face .....	200
Table 4.4-4	Final Scour Sensitivity Results d/s Pier Face .....	200
Table 4.6-1	Error Analysis for the Final Scour Results .....	204
Table 5.1-1	Case study site properties used to determine adjusted Simmons Ratios and the CE Ratio .....	208
Table 6.3-1	Summary of Monie Bay Continuous Simulation Variables and Pier Scour Results at the Upstream (U/S) and Downstream (D/S) Pier Faces .....	243
Table 6.3-2	Monie Bay Hurricane Scour Results for the Upstream (U/S) and Downstream (D/S) Pier Faces with 5 in. of Rainfall .....	247
Table 6.3-3	Monie Bay Hurricane Scour Results for the Upstream (U/S) and Downstream (D/S) Pier Faces with 5, 8, 12, and 16 in. of Rainfall .....	248
Table 6.4-1	Summary of the Black River Continuous Simulation Variables and Pier Scour Results at the Upstream (U/S) and Downstream (D/S) Pier Faces .....	250
Table 6.4-2	Black River Hurricane Scour Results for 7 in. of Rainfall at the Upstream (U/S) and Downstream (D/S) Pier Faces .....	254
Table 6.4-3	Scour in ft Predicted for a Category III Hurricane with Variable Rainfall Amounts of 5, 8, 12, and 16 in. on the Downstream (D/S) and Upstream (U/S) Pier Faces of the Black River Case Study Sites .....	254
Table 6.5-1	Summary of Patuxent at Benedict Continuous Simulation Variables at the Upstream (U/S) and Downstream (U/S) Pier Faces .....	257
Table 6.5-2	Patuxent at Benedict Hurricane Scour Results for Eight Inches of Rainfall .....	261
Table 6.5-3	Scour in ft Predicted for a Category III Hurricane with Variable Rainfall Amounts of 5, 8, 12, and 16 in. on the Downstream (D/S) and Upstream (U/S) Pier Faces of the Patuxent River Case Study Sites .....	262
Table 6.6-1	Summary of the Wicomico River Continuous Simulation Variables at the Upstream (U/S) and Downstream (D/S) Pier Faces .....	265
Table 6.6-2	The Wicomico River Hurricane Scour Results for 5 Inches of Rainfall. U/S Indicates Upstream and D/S Downstream .....	269
Table 6.6-3	Scour in Feet Predicted for a Category III Hurricane with Variable Rainfall Amounts of 5, 8, 12, and 16 in. on the Downstream (D/S) and Upstream (U/S) Pier Face at the Wicomico Case Study Site .....	270
Table 6.7-1	Summary of the Patapsco River Site Simulation Variables at the Upstream \ (U/S) and Downstream (D/S) Pier Faces .....	273

Table 6.7-2	The Patapsco River Site Hurricane Scour Results for the Upstream (U/S) and Downstream (D/S) Pier Faces with Eight Inches of Rainfall .....	275
Table 6.7-3	Scour in ft Predicted for a Category III Hurricane with Variable Rainfall Amounts of 5, 8, 12, and 16 in. on the Upstream (U/S) and Downstream (D/S) Pier Faces at the Patapsco River Case Study Sites.....	276
Table 6.8-1	Hypothetical Consequence Analysis for the Failure of the Bridge at Each Site.....	279
Table 6.8-2	Showing the computations of the risks associated with the failure of the bridge at Monie Bay when natural armoring was not considered.....	284
Table 6.8-3	Showing the computations of the risk associated with the failure of the bridge at Black River when natural armoring was not considered.....	284
Table 6.8-4	Showing the Computations for the Risk Analysis Associated With the Failure of the Bridge at the Patuxent River with Armoring.....	288
Table 6.8-5	Showing the Computations for the Risk Analysis Associated With the Failure of the Bridge at the Patuxent River without Armoring.....	288
Table 6.8-6	Showing the computations for the risk associated with the failure of the bridge at the Wicomico River site with and without natural armoring.....	291
Table 6.8-7	Showing the computations for the risk associated with the failure of the bridge at the Patapsco River site with natural armoring.....	294
Table 6.8-8	Showing the computations for the risk associated with the failure of the bridge at the Patapsco River site without natural armoring.....	294
Table 6.8-9	Summary of the hurricane scour results at the upstream (U/S) and downstream (D/S) pier face .....	299
Table 7.2-1	Univariate and bivariate models selected for the comparison exercise .....	304
Table 7.2-2	Models with three or more predictor variables selected for the comparison exercise.....	305
Table 7.2-3	Data Used in the Development of Some Models.....	306
Table 7.3-1	Data Obtained From the WAVES Upstream Pier Face Simulations for the Case Study Sites Used as Input Variables for the Models in the Comparative Scour Exercises .....	311
Table 7.3-2	Data Obtained From the WAVES Downstream Pier Face Simulations for the Case Study Sites Used as Input Variables for the Models in the Comparative Scour Exercises.....	311
Table 7.3-3	Results of the forty Model comparative study for the upstream pier face .....	314

Table 7.3-4	Results of the 40 Model comparative study for the downstream pier face .....	315
Table 7.3-5	Final predicted maximum scour results determined by the 40 models tested.....	317
Table 7.3-6	Mean and standard deviation for the pier scour results provided by the five benchmark models at Black River (BLK) and Monie Bay (MONIE) .....	320
Table 7.3-7	Mean and standard deviation for the pier scour results provided by the 40 models used in the comparative exercise at Black River and Monie Bay.....	321
Table 7.3-8	Mean and standard deviation for the pier scour results of the five benchmark models at the Patuxent (PAT) and Wicomico (WICO) Rivers .....	328
Table 7.3-9	Mean and standard deviation for the pier scour results of the 40 models used in the comparison exercise at the Patuxent (PAT) and Wicomico (WICO) Rivers .....	329
Table 7.3-10	Mean and standard deviation for the pier scour results of the five benchmark models at the Baltimore (BAL) Patapsco River site.....	334
Table 7.3-11	Mean and standard deviation for the pier scour results of the 40 models used in the comparison exercise at the Baltimore (BAL) Patapsco River site .....	336
Table 7.4-1	Data ranges and constraints of models used in the continuous comparison study.....	340
Table 8.3-1	WAVES Model Variable Input as a Function of Scales.....	365

## LIST OF FIGURES

Figure 2.4-1	The development of the downflow around bridge piers .....	21
Figure 2.4-2	Downflow in front of a pier according to Ettema (1980) .....	25
Figure 2.4-3	$y/d$ vs $V_d/U$ for three experiments by Ahmed and Rajaratnam (1998) .....	27
Figure 2.5-1	Circulation of a circular streamline .....	30
Figure 2.5-2	Diagram of a free vortex system with floating particles.....	31
Figure 2.5-3	Diagram of a forced vortex system with floating particles.....	32
Figure 2.5-4	The theoretical velocity profile of a real vortex.....	33
Figure 2.5-5	Plan view of the horizontal flow around cylindrical object.....	36
Figure 2.5-6	Streamline patterns and vortex systems (Baker 1979).....	38
Figure 2.5-7	$x/D$ - $y/D$ plane used by Baker (1979) to plot the mean position of each vortex .....	39
Figure 2.5-8	Spatial variation in shear stress around a cylindrical pier prior to development of the scour hole. This information was obtained from Briaud et al (1999) .....	45
Figure 3.2-1	The Open-Ocean Scale .....	79
Figure 3.2-2	The Catchment Scale .....	80
Figure 3.2-3	The Tidal Estuary Scale .....	81
Figure 3.3-1	Model Schematic .....	83
Figure 3.4-1	Explanation of the variables used in the determination of wave peakedness .....	87
Figure 3.4-2	Expected attenuation between Sewell point and Baltimore.....	88
Figure 3.4-3	Distorted tidal profile at bridge station b .....	89
Figure 3.7-1	Conceptual model of flow as a series of parallel jets.....	100
Figure 3.7-2	A circular pier in plan view showing streamlines impinging the pier .....	102
Figure 3.7-3	Conceptual jet orifices based on Daily and Harleman (1966) .....	103
Figure 3.7-4	Velocity components used to determine downflow velocity.....	104
Figure 3.7-5	Variation of magnitude and location of downflow with scour depth .....	107
Figure 3.7-6	Variation of $V_{dmax}/U$ with $d_s/d$ given by Equation 3.7-29 .....	112
Figure 3.8-1	Variation of tangential velocity or shear stress of the horseshoe vortex with location across the upstream face of the pier in terms of $\theta$ .....	119
Figure 3.8-2	Showing pier with diameter $D$ and scour hole with angle $\theta$ .....	120
Figure 3.8-3	Representation of a Power Model Relating $d_s/D$ to Scour Angle $\theta$ .....	121
Figure 3.8-4	Representation of a Sine Model Relating $a/D$ to $\theta$ .....	122
Figure 3.8-5	Representation of a Sine Model Relating $b/D$ to $\theta$ .....	122
Figure 3.8-6	Relationship Between $a_m/a$ and Scour Angle $\theta$ (degrees).....	123
Figure 3.8-7	Graphical determination of $x_c/D$ as a function of $d_s/D$ .....	125
Figure 3.8-8	Graphical determination of $y_c/D$ as a function of $d_s/D$ .....	125
Figure 3.8-9	Showing the Vortex and Scour Hole Geometry .....	127
Figure 3.11-1	Model Procedure Flowchart.....	147
Figure 3.11-2	The time base ( $T_b$ ) of each hydrograph in the Sequence of Simulated Storms .....	153

Figure 4.3-1	Sensitivity of the upstream pier face scour to wave peakedness .....	181
Figure 4.3-2	Sensitivity of the downstream pier face scour to the pier diameter .....	185
Figure 4.5-1	Scour at the upstream face of the pier predicted by the WAVES program with the local scour model computed with Eq. 4.5-1 compared with the scour predicted using the original WAVES algorithm .....	202
Figure 4.5-2	Scour at the downstream face of the pier predicted by the WAVES program with the local scour model computed with Eq. 4.5-1 compared with the scour predicted using the original WAVES algorithm .....	202
Figure 5.3-1	Monie Bay Cross Section Profile at the Proposed Bridge Location .....	220
Figure 5.4-1	Black River Site Cross Section Profile at the Proposed Bridge Location .....	224
Figure 5.5-1	Patuxent River Cross Section Profile at the Proposed Bridge Location .....	226
Figure 5.6-1	Wicomico River Cross Section Profile at the Proposed Bridge Location .....	229
Figure 5.7-1	Patapsco River Cross Section Profile at the Proposed Bridge Location .....	232
Figure 6.3-1	Temporal variation of pier scour for the downstream face obtained from the results of the Monie Bay simulations .....	245
Figure 6.4-1	Temporal variation of pier scour for the upstream face obtained from the results of the Black River simulations .....	251
Figure 6.4-2	Temporal variation of pier scour for the downstream face obtained from the results of the Black River simulations .....	253
Figure 6.5-1	Temporal variation of pier scour for the upstream face obtained from the results of the Patuxent at Benedict Simulations .....	259
Figure 6.5-2	Temporal variation of pier scour for the downstream face obtained from the results of the Patuxent at Benedict simulations .....	260
Figure 6.6-1	Temporal variation of pier scour for the upstream face obtained from the results of the Wicomico River Simulations .....	267
Figure 6.6-2	Temporal variation of pier scour for the downstream face obtained from the results of the Wicomico River Simulations .....	268
Figure 6.7-1	Temporal variation of pier scour for the upstream face obtained from the results of the Patapsco River Simulations .....	274
Figure 6.8-1	Final predicted ultimate scour for Monie Bay .....	280
Figure 6.8-2	Final predicted ultimate scour for Black River .....	281
Figure 6.8-3	Temporal Variations in the Probability of Failure of the Bridge at Monie Bay .....	283
Figure 6.8-4	Temporal Variations in the Risks of Failure for the Bridge at Monie Bay .....	283

Figure 6.8-5	Temporal Variations in the Probability of Failure of the Bridge at Black River.....	285
Figure 6.8-6	Temporal Variations in the Risks of Failure for the Bridge at Black River .....	285
Figure 6.8-7	Final predicted ultimate scour for the Patuxent River site.....	286
Figure 6.8-8	Final Predicted Ultimate Scour for the Wicomico River site .....	287
Figure 6.8-9	Temporal variations in the probability of failure of the bridge at the Patuxent River with armoring considered.....	289
Figure 6.8-10	Temporal variations in the probability of failure of the bridge at the Patuxent River without armoring considered .....	289
Figure 6.8-11	Temporal variations in the risks of failure for the bridge at the Patuxent River with armoring considered.....	290
Figure 6.8-12	Temporal variations in the risks of failure for the bridge at the Patuxent River without armoring considered.....	290
Figure 6.8-13	Temporal variations in the probability of failure of the bridge at the Wicomico River site with and without armoring considered.....	292
Figure 6.8-14	Temporal Variations in the Risks of Failure for the bridge at the Wicomico River site with and without natural armoring considered.....	292
Figure 6.8-15	Final predicted ultimate scour for the Patapsco River site .....	293
Figure 6.8-16	Temporal variations in the probability of failure of the bridge at the Patapsco River site with natural armoring considered .....	295
Figure 6.8-17	Temporal variations in the probability of failure of the bridge at the Patapsco River site without natural armoring considered .....	295
Figure 6.8-18	Temporal Variations in the Risks of Failure for the bridge at the Patapsco River site with natural armoring considered.....	296
Figure 6.8-19	Temporal Variations in the Risks of Failure for the bridge at the Patapsco River site without natural armoring considered .....	296
Figure 6.8-20	Typical Hurricane Discharge Variation with Time Produced by the WAVES Program.....	298
Figure 7.3-1	Probability histogram representing the 40-Model scour results for the tide-controlled Monie Bay site.....	322
Figure 7.3-2	Probability histogram representing the 40-Model scour results for the tide-controlled Black River site .....	323
Figure 7.3-3	Results of the 40-model study at Monie Bay in comparison to the Predicted Maximum Scour results obtained from the WAVES Program.....	324
Figure 7.3-4	Results of the 40-model study at Black River in comparison to the Predicted Maximum Scour results obtained from the WAVES Program.....	325
Figure 7.3-5	Probability histogram representing the 40-Model scour results for the mixed-control Patuxent River site .....	330



Figure 7.3-6	Probability histogram representing the 40-Model scour results for the mixed-control Wicomico River site.....	330
Figure 7.3-7	Results of the 40-model study at Patuxent at Benedict in comparison to the Predicted Maximum Scour results obtained from the WAVES Program .....	331
Figure 7.3-8	Results of the 40-model study at Wicomico River in comparison to the Predicted Maximum Scour results obtained from the WAVES Program .....	332
Figure 7.3-9	Probability histogram representing the 40-model scour results for the catchment-controlled Baltimore Patapsco River site .....	337
Figure 7.3-10	Results of the 40-model study at the Baltimore Patapsco site in comparison to the Predicted Maximum Scour results obtained from the WAVES Program .....	338
Figure 7.4-1	Monie Bay Upstream Pier Face .....	343
Figure 7.4-2	Monie Bay Downstream Pier Face .....	343
Figure 7.4-3	Black River Upstream Pier Face.....	345
Figure 7.4-4	Black River Downstream Pier Face.....	345
Figure 7.4-5	Patuxent River Upstream Pier Face .....	347
Figure 7.4-6	Patuxent River Downstream Pier Face .....	348
Figure 7.4-7	Wicomico River Upstream Pier Face .....	349
Figure 7.4-8	Wicomico River Downstream Pier Face.....	350
Figure 7.4-9	Baltimore Patapsco River Location Upstream Pier Face.....	352
Figure 7.4-10	Baltimore Patapsco River Location Downstream Pier Face.....	352

## NOTATIONS AND VARIABLES

$a$	= Length of the minor axis of the elliptical vortex (ft)
$a_c$	= Length of the minor axis of the circular vortex at the location of the maximum tangential velocity (ft)
$a_m$	= Length of the minor axis of the elliptical vortex at the location of the maximum tangential velocity (ft/s)
$A$	= Catchment basin area (mi <sup>2</sup> )
$\bar{A}$	= Tide attenuation factor
$A_b$	= Cross sectional area of the estuary at bridge location (ft <sup>2</sup> )
$A_c$	= Cross sectional area of the estuary mouth (ft <sup>2</sup> )
$A_m$	= Mean diurnal tidal amplitude (ft)
$b_{in}$	= The invert elevation at the bridge location (ft)
$A_s$	= Surface area of the estuary upstream of the bridge location (mi <sup>2</sup> )
$A_s$	= Standard deviation in the diurnal amplitude (ft)
$b$	= (Variance in the daily rainfall/ mean daily rainfall) , gamma function constant
$b$	= Pier diameter (ft)
$b$	= Estuary width (mi)
$b_{max}$	= Maximum estuary width (mi)
$b_{min}$	= Minimum estuary width (mi)
$B$	= Pier diameter (ft)
$B$	= Length of the major axis of the elliptical vortex (ft)
$b_o$	= Half the length of a rectangular orifice
$B_{in}$	= Channel invert at base station (ft)

$c$  = (Mean daily rainfall/ standard deviation in daily rainfall)<sup>2</sup>, gamma function constant

$C$  = Convex routing factor

$C_1$  = Orifice coefficient

$C_e$  = Wave celerity (ft/s)

$C_w$  = Weir coefficient

$CN$  = Curve number

$D$  = Rainfall duration (hr) or bridge pier diameter (ft)

$d$  = Particle diameter (mm) or bridge pier diameter (ft)

$D_p$  = Bridge pier diameter (ft)

$D_H$  = Hurricane distance of closest approach (to the bridge) (mi)

$(dd_s/dt)$  = Rate of scour (ft/s)

$d_{50}$  = Mean grain size, 50% smaller than (mm)

$d_{16}$  = Grain size, 16% smaller than (mm)

$d_{84}$  = Grain size, 84% smaller than (mm)

$d_{max}$  = Maximum grain size (mm)

$D_u$  = Unit hydrograph duration (hr)

$D_{uH}$  = Hurricane duration (hr)

$d_s$  = Local scour depth (ft)

$d_{se}$  = Equilibrium or ultimate scour depth (ft)

$F$  = Froude number of stream flow

$f,$  = Froude number of stream flow based on pier diameter

$F_b$	= Froude number of stream flow based on pier diameter
$F_{rc}$	= Froude number of stream flow for which bedload motion starts
$g$	= Acceleration due to gravity ( $\text{ft/s}^2$ )
$G_f$	= Volume of fresh water entering the estuary over one hydrograph step ( $\text{ft}^3$ )
$G_o$	= Volume of freshwater leaving the estuary over one hydrograph step ( $\text{ft}^3$ )
$H$	= Mean tidal range (ft)
$j$	= Horizontal jet layer in question in the development of the downflow model
$K$	= Mean tidal lag time in moving from base station B to bridge station b (hr)
$k$	= Contraction scour factor
$L$	= Length of catchment flow path (mi)
$L_e$	= Length of estuary above the bridge section (mi)
$L$	= Distance between the base station and the bridge station (mi)
$L_m$	= Mean lunar tidal amplitude (ft)
$L_s$	= Standard deviation in the lunar amplitude (ft)
$M_B$	= Mean tidal depth at base station (ft)
$M_e$	= Mean tidal elevation (ft)

$n$	= Manning's coefficient
$N_{bp}$	= Number of bridge piers
$N_d$	= Number of diurnal variates
$N_p$	= Number of rainfall ordinates
$N_R$	= Number of runoff ordinates
$N_u$	= Number of unit hydrograph ordinates
$P_{gy}$	= Stagnation pressure (lb/ft <sup>2</sup> )
$P_{sy}$	= Static pressure (lb/ft <sup>2</sup> )
$p$	= Peakedness of the wave at the base station
$p_m$	= Mean peakedness
$q$	= Discharge per unit width (cfs/ft)
$Q$	= Discharge (cfs)
$Q_{base}$	= Catchment base flow
$Q_f$	= Freshwater hydrograph discharge value (cfs)
$Q_F$	= Tidal discharge produced by the falling limb (cfs)
$Q_o$	= Discharge from the freshwater prism (cfs)
$Q_N$	= Tidal discharge predicted by Neill's equation (cfs)
$Q_R$	= Tidal discharge produced by the rising limb (cfs)
$Q_T$	= Total resultant discharge at bridge station (cfs)
$q_s$	= Sediment discharge rate (ft <sup>2</sup> /s)
$Q_{rising}$	= Horizontal discharge of an estuary directed upstream (ft/s)

$Q_{\text{falling}}$	= Horizontal discharge of an estuary directed downstream (ft/s)
$Q_s$	= Sediment flow rate (cfs)
$R$	= Channel hydraulic radius (ft)
$Re$	= Reynolds number
$R_H$	= Hurricane radius (mi)
$r$	= Variable distance from the center of a circular vortex (ft)
$r_c$	= Distance from the center of a circular vortex to the point where the maximum tangential velocity is reached (ft)
$S$	= Soil infiltration potential
$S_{fl}$	= Friction slope
$S_f$	= Fresh water storage (ft <sup>3</sup> )
$s$	= Specific gravity
$S_H$	= Hurricane surge (ft)
$S_s$	= Sediment particle specific weight (lb/ft <sup>3</sup> )
$S_t$	= Tidal storage (ft <sup>3</sup> )
$S_T$	= Total volumetric storage (ft <sup>3</sup> )
$t_b$	= Hydrograph time base (hr)
$T$	= Oscillation period (hr)
$T$	= Wave period (hr)
$t$	= Time (hr)
$\tau$	= Travel time of a wavelet from base station to the bridge station (hr)

$t_e$	= Time to reach equilibrium scour depth (ft)
$t_c$	= Time of concentration (hr)
$t_p$	= Time to peak (hr)
$T_b$	= Time at which each point on the attenuated wave arrives at the bridge station (hr)
$T_D$	= Diurnal period (hr)
$T_L$	= Lunar period (hr)
$T_s$	= Total scour depth (ft)
$U$	= Mean free stream horizontal velocity (ft/s)
$u$	= Horizontal component of the estuary velocity that varies vertically according to the turbulent flow profile (ft/s)
$U_c$	= Critical mean stream velocity that causes bedload movement (ft/s)
$U_i$	= Velocity causing incipient motion of a given bed particle size (ft/s)
$V$	= Velocity (ft/s)
$V_a$	= Stream velocity above which armoring is not possible (ft/s)
$V_{dmax}$	= Maximum downflow (ft/s)
$V_H$	= Hurricane tracking speed (mph)
$V_n$	= Net velocity (ft/s)
$V_{thm}$	= Maximum vortex tangential velocity (ft/s)
$V_d$	= Downflow velocity (ft/s)
$v_d$	= Velocity of downward jet (ft/s)
$v_n$	= Net velocity of vertical jet between adjoining layers (ft/s)

$v_u$  = Velocity of upward jet (ft/s)

$V_c$  = Maximum tangential velocity (ft/s)

$V_c$  = Horizontal velocity across the mouth of an estuary (ft/s)

$V_t$  = Vortex tangential velocity at any given distance from the center (ft/s)

$V_{\text{rising}}$  = Horizontal velocity of an estuary directed upstream (ft/s)

$V_{\text{falling}}$  = Horizontal velocity of an estuary directed downstream (ft/s)

$W_{\text{max}}$  = Maximum width of the estuary upstream of location b (ft)

$W_{b1u}$  = Upstream bottom width of the estuary at the near field distance (mi)

$W_{b1d}$  = Bottom width of the estuary at the near field distance on the downstream side of the bridge (ft)

$W_{b2}$  = Effective bottom width of the channel at the bridge location (ft)

$W_o$  = Width of the estuary at the bridge location b (ft)

$\chi$  = Length of estuary segment (ft)

$x$  = Distance along the horizontal axis measured from the center of the pier (ft)

$x_c/D$  = Normalized x coordinate of the center of the vortex ellipse when plot in the  $x/D, y/D$  plane

$Y$  = Flow depth (ft)

$y$  = Vertical displacement from estuary bed (ft)

$Y_m$  = Flow depth (ft)

$y_c/D$  = Normalized y coordinate of the center of the vortex ellipse when plot in the  $x/D, y/D$  plane

$Y_B$  = Tidal depth at base station (ft)



$y_b$	= Estuary depth at bridge station (ft)
$y_m$	= Average depth between the base station and the bridge station (ft)
$Y_s$	= Scour depth due to contraction scour (ft)
$Y_t$	= Attenuated time varying tidal depth at b (ft)
$Y_T$	= Total water depth at the bridge location (ft)
$z_i$	= Normal distribution of the diurnal amplitude
$z_j$	= Normal distribution of the lunar amplitude
$Z_s$	= Mean overbank slope
$\alpha$	= Gradation constant for sand and gravel
$\beta$	= Ratio of grain volume to total volume in the bed (porosity)
$\gamma$	= Specific weight of water (lb/ft <sup>3</sup> )
$\gamma_s$	= Specific weight of soil (lb/ft <sup>3</sup> )
$\gamma_w$	= Specific weight of water (lb/ft <sup>3</sup> )
$\xi$	= Vorticity (s <sup>-1</sup> )
$\eta$	= Tidal elevation (ft)
$\eta_B$	= Tidal elevations at base station (ft)
$\eta_b$	= Tidal elevations at bridge station (ft)
$\eta_r$	= Routed water surface elevation values at the bridge station (ft)
$\theta$	= Side angle of scour hole (degrees)
$\nu$	= Viscosity (lb.s/ft <sup>2</sup> )
$\nu$	= Kinematic viscosity (ft <sup>2</sup> /s)

$\rho$	= Density of water (slugs/ft <sup>3</sup> )
$\phi$	= Angle of internal friction of the estuary bed material (degrees)
$\phi_i$	= Phase angle of the diurnal wave (radians)
$\phi_J$	= Phase angle of the diurnal wave (radians)
$\sigma_d$	= Standard deviation grain size estimated as $d_{84}/d_{16}$
$\tau$	= Shear stress at a specific location (lbs/ft <sup>2</sup> )
$\tau_c$	= Critical shear stress which causes the insipient motion of a sediment particle of a given diameter (lbs/ft <sup>2</sup> )
$\tau_o$	= bed shear stress (lbs/ft <sup>2</sup> )
$\tau_{hm}$	= Maximum tangential shear stress (lbs/ft <sup>2</sup> )
$\tau_m$	= Free stream shear stress (lbs/ft <sup>2</sup> )
$\pi$	= 3.142
$\kappa$	= Von Karman constant
$\omega$	= Angular velocity (radians/sec)
$\Gamma$	= Circulation (ft <sup>2</sup> /sec)

# **CHAPTER 1**

## **INTRODUCTION**

### **1.1 INTRODUCTION**

At a time when the Nation is faced with the problem of maintaining or replacing its aging infrastructure, along with the increased cost of analysis, design, and construction, engineers are now challenged to develop technologies that are cost effective and accurate to ensure that our infrastructure will operate properly during its design life. One area of concern is in the design of bridges, particularly the design and construction of bridge piers located in areas susceptible to scour. Bridges that span tidal waterways must be designed to withstand scour from regular diurnal and semi-diurnal tidal flows, large storm-surge tidal flows, and the combination of these tidal flows with riverine flows. These bridges are extremely sensitive to the issues of cost and safety.

An example of cost related problems in tidal bridge design might be seen in the ever-increasing projected cost associated with the replacement of the Wilson Bridge over the tidal Potomac River. Also, a number of bridge failures caused by pier scour resulted in the loss of lives and costly property damage. The failure of the New York Thruway Bridge that crossed the Schoharie Creek, which resulted in the loss of 10 lives, is one obvious example.

Critical to the design of bridges across tidal waterways are models, which are able to accurately predict the degree of pier scour expected throughout the design life of the structure. Though accurate models currently exist, the cost of data collection and the complexity of these models make their use unpopular. Conversely, the less complex and

less expensive models are typically unable to provide accurate estimates of the expected scour. Also, because of their simplicity they may not incorporate all of the important variables that influence scour. Therefore, there exists a need for models that can accurately and economically predict the depth of scour during the design life of bridges over tidal waterways.

## **1.2 TYPES OF SCOUR**

Major damage to bridges at river crossings often occurs during discrete flooding events, however, the process of scour that eventually leads to the damage or failure of a bridge typically occurs over a long period of time. Scour induced pier failure may generally be attributed to a number of factors: first, the long-term flow duration characteristics of the runoff that occurred prior to the time of failure; second, the geomorphic and fluvial processes that affect the sediment transport potential of the riverine or estuarine system; and third, the geometry and configuration of the bridge piers.

The processes mentioned above give rise to three distinct types of scour: general scour, contraction scour, and local scour. Depending on the location and scale of the system, one or more of the scour types may be involved and will be spatially and temporally distributed within the flow field. Most current and popular scour models do not account for the temporal and spatial variation of scour; rather, they typically provide a single-valued estimate of the scour depth for a specific design discharge. Applications of such models are limited typically to narrow rivers and streams, and this makes their

use unsuitable for work involving estuaries of significant widths. On the other hand, current spatially and temporally distributed models are complex and costly to run.

### **1.3 SCOUR IN TIDAL WATERWAYS**

Scour depths in estuaries are often estimated using models developed for riverine systems. These models do not consider the various processes responsible for the removal of sediment in a tidal system. In a tidal or estuarine environment, the flow changes directions with the tide resulting in scour patterns that are quite different from those in a riverine environment. Scour in an estuarine environment can develop alternately from both in-coming and out-going tides. The mechanism of scour in tidal waterways also creates the possibility that less general scour could develop in estuaries because some of the material eroded in one phase of the tidal cycle could be deposited in the scour hole in the next phase. Also, material deposited during periods of low velocity flow may not have the same resistance to scour as would virgin soils, and therefore, re-suspension of the material may occur at much lower velocities than that required to scour virgin soil.

Waves and tidal motion play a significant role in the scour process in tidal waterways and researchers have developed various theories to explain the importance of each to the process of estuarine hydraulics. Other factors that affect scour at tidal sites include storm surges, the effects of estuary geometry on the reflection of waves, the potential for the formation of standing waves, the significant unsteadiness of tidal flows, the specific hydraulic and hydrologic regime of the estuarine environment, and the type of sediments that comprise the bed of the estuary.

## **1.4 GOAL AND OBJECTIVES**

Melville and Coleman (2000) have developed a conceptual framework for scour analyses in riverine environments based on the spatial and temporal scales appropriate to the different scour types. Under their scenario, the following five scales of scour processes are suggested: (1) the catchment scale; (2) the stream section scale; (3) the bridge far-field scale; (4) the bridge near-field scale; and, (5) the local scour scale. The conceptual model of Melville and Coleman is a useful representation in riverine environments; however, it is not adequate for the analyses of pier scour of bridges that are located in estuarine-tidal-riverine environments. For such designs a broader conceptual model is needed.

The goal of this study is to formulate, and test a multi-component model to predict bridge pier scour in tidal estuaries and to develop a methodology for bridge pier design in estuary-riverine environments. This goal will be achieved by meeting the following objectives:

1. Develop a conceptual multi-scale framework for modeling scour in tidal environments.
2. Based on the conceptual multi-scale framework, formulate a temporally varied multi-component model, which determines the water surface elevations, flow rates, velocities, and scour depth at the bridge location in the tidal environment system.
3. Perform sensitivity analyses of the model and its components to determine the importance of the coefficients and variables, particularly estuary geometry, so

that design engineers can properly use the model to obtain reasonably accurate scour results.

4. Compare the performance of the model with existing models and by such comparison evaluate the need for continuous time-dependent scour models as opposed to single-event, design-discharge models.
5. Show how the model may be used to facilitate a risk-based method for bridge pier designs.

## **1.5 IMPLICATIONS**

The development of a model to predict scour in tidal rivers and estuaries, along with the development of a procedure that provides a time varying estimate of total scour has very important implications for the design of bridge piers in estuarine environments. As a result of this research, the state of the science will be advanced in a number of ways.

First, the development of a conceptual temporal, multi-scale framework for modeling scour in tidal estuaries will enable all scales to be considered in a design but ultimately only data for the scales to which the particular design is sensitive would be required. Such a method would greatly reduce the overall complexity and cost of bridge pier designs. This would be achieved by requiring complex analyses only in situations where they are needed.

Second, the inclusion of a temporal hydraulic model component for tidal and estuarine environments should significantly improve the accuracy of scour predictions. Such a hydraulic model could also be used to perform continuous hydrologic and hydraulic simulations to provide a time history of scour. This could be achieved without

incurring unacceptable costs and hence lead to safer bridge pier designs and fewer bridge failures.

Third, sensitivity analyses of the developed model will clearly define the important parameters for different scenarios and conditions. Knowledge of the model sensitivities is necessary for the model user to properly apply the model and select the level of data required for a particular design scenario, which will make for easier application. Also, knowledge of the insensitive variables and parameters will allow for the elimination of such variables from the program thus simplifying the model

Fourth, an assessment of the model's performance, particularly in comparison with the Neill's equation, would be of interest to the Maryland State Highway Administration (SHA). The Neill's model is a simple representation of the continuity equation and is used to compute flow velocities (currents) resulting from tidal motion. It is applicable only to estuaries that exhibit prismatic behavior. The SHA is currently studying methods of improving the applicability of the Neill's equation and has a vested interest in the development of models that have the potential of providing a greater range of applicability and improved accuracy over the Neill's model.

Fifth, the prevailing assumption that bridge pier failure is primarily the result of single valued design storm events was earlier questioned. Clear knowledge regarding the significance of a continuous time dependent mechanism in the development of scour in tidal waterways is necessary. This would allow the user of time-variant models to more precisely assess the inaccuracies of their designs because of failure to account for dynamic conditions existing at the bridge pier.



## **CHAPTER 2**

### **LITERATURE REVIEW**

#### **2.1 INTRODUCTION**

This study was conducted for the purpose of improving tidal bridge pier scour modeling. The need for such a study grew out of concerns expressed by the civil engineering community, in particular the Maryland State Highway Administration (SHA), with regards to the inability of current tidal bridge pier scour models to provide accurate and reliable results at low cost. This position was also supported by Richardson et al. (1991) who acknowledged that, “the problems associated with estimating scour and providing cost effective and safe designs need to be addressed further in research and development programs”. Richardson et al. (1991) also cited the areas of the most pressing research needs among which was the need for computer software (models) for the analysis of all aspects of bridge scour.

The literature review is devoted to concepts concerning the modeling of bridge pier scour in the highly complex estuarine system environment. In particular, the literature survey focuses on: the assessment of the state of knowledge about the processes involved in tidal bridge pier scour; the assessment of the possibility of addressing model diversity through the use of a conceptual multi-scale approach to modeling; the assessment of the extent of deficiencies in current tidal bridge pier scour models; the examination of the methods of analyzing scour models; and the assessment of the performance of current bridge pier scour models through a comparative study of these models.

Assessment of the state of knowledge about the mechanisms of the various processes involved in bridge pier scour in a tidal environment provides a first step in determining the ability of existing and proposed theoretical deterministic models to correctly simulate the total tidal scour process. A deterministic model based on faulty theories will most likely produce faulty results. Accordingly, it is important to ensure that deterministic models are based on sound theories about the physical systems and also that they includes all significant processes.

Owing to the number of different flow regimes that exist in a tidal or estuarine system, along with the different types of processes associated with bridge scour, it is understandable that such wide variations in conditions would lead to great diversity in the types and scope of bridge scour models used within the tidal and estuarine environments. It is believed that one of the most cost effective ways of addressing this diversity is through a conceptual multi-scale approach to modeling. This method could be used to develop a system wherein model components could be tailored to address specific conditions and flow regimes. As a result, there is interest in determining the degree of success involved with the use of the scale approach as reported by other researchers.

The primary purpose of this study is the development of a model that addresses the areas of deficiency or greatest need in the existing tidal bridge pier scour modeling spectrum. It is, therefore, necessary to first assess the extent of deficiency in the current tidal bridge pier scour modeling system through a review of the work of other researchers. Examination of the types of analysis and methods generally used in this area of research is essential for the purpose of assessing the performance of existing or proposed models. In particular, the assessment of the methods used to determine model

reliability, the sensitivity to model parameters and variables, and the uncertainties associated with the use of such models are of great importance to this study. Parameter and variable sensitivity are also important in assessing the data needs, which bear a direct relationship to the cost of using the model. As an example, consider the bathymetry or cross-section geometry of an estuary reach. Such data can be acquired through direct measurement or from topographic maps and charts. If the results from an estuary model were shown to be very sensitive to bathymetry, then measured data would be required; otherwise topographic maps may prove adequate.

There is great diversity in the number and types of pier scour models currently in use. Most of these models were developed from laboratory studies, and field data from upland rivers. As a result, very few models being used today were designed specifically for estuaries or tidal rivers. Comparing the performance of existing models will help to determine which existing models are appropriate for use in estuaries and the conditions governing the use of these models. Comparing the performance of existing models will also assist in establishing the performance criteria for the proposed model, which will further serve as the basis of determining to what degree the goal of the study has been accomplished.

## **2.2 PIER SCOUR AND ITS MECHANISMS**

### **2.2.1 Definition of Scour**

Researchers (Melville and Coleman, 2000 and Richardson and Davis, 1995) have shown that bridge pier scour is comprised of the following processes: the hydrologic and hydraulic processes that establish the scour variables of discharge, velocity, and flow

depth; and the erosion and sediment transport processes, which establish the sediment flow rate variable that causes scour hole formation due to erosion and transport of sediment from the hole. Melville and Coleman (2000) also define scour as the lowering of the level of a river [estuary] bed such that a tendency to expose the foundations of a bridge exists. The amount of this reduction below an assumed natural level is termed the scour depth. The scour depth is a function of the depth of flow, the flow or circulation velocity, the density of the water, and the type and nature of the sediments on the estuary bed (or banks). Melville and Coleman (2000) further characterize scour in terms of general scour, contraction scour, and local scour.

### **2.2.2 General Scour**

According to Melville and Coleman (2000) general scour occurs irrespective of the existence of the bridge and can occur as either long-term or short-term scour; the two types being distinguished by the time taken for scour development. Short-term general scour is usually developed from a single or several closely placed floods. Long-term general scour has a considerably longer time scale, normally on the order of several years and includes progressive degradation and lateral bank erosion. Melville and Coleman (2000) further define progressive degradation as the quasi-permanent general lowering of the riverbed due to hydrometeorologic and geomorphologic changes in the catchment watershed.

### **2.2.3 Contraction Scour**

According to Melville and Coleman (2000), contraction scour is caused by the convergence of the flow as it approaches the bridge. At bridge crossings where the flow is relatively wide and shallow, the flow is predominantly two-dimensional (2-D) in the x-y horizontal plane and contracts further within the bridge opening, accelerating to the narrowest section called the vena contracta. Contraction scour is caused by the accelerated 2-D flow across the contracted section.

### **2.2.4 Local Scour**

Melville and Coleman (2000) defined local scour as the scour caused by the bridge pier or abutment. In addition, they defined two types of local scour; clear water and live bed scour. Clear water scour occurs when the bed material upstream of the scour area is at rest. In this case the maximum local scour depth is reached when the flow can no longer remove bed material from the scour area. Live bed scour occurs when there is general sediment transport by the river [estuary] with the equilibrium scour depth being reached when the rate of transport of material into the scour hole is equal to the rate of transport of material out of it.

### **2.2.5 Total Pier Scour**

Richardson et al. (1991) determined that the total scour at a highway crossing was comprised of three components: aggradation and degradation; contraction scour; and local scour. They further defined aggradation to be the long-term deposition of materials eroded from one section of a stream reach into another while degradation was the long-term lowering or scouring of the streambed. Their definitions of local scour and

contraction scour were consistent with the definitions of these terms presented by Melville and Coleman (2000).

## **2.3 BRIDGE PIER SCOUR IN AN ESTUARINE ENVIRONMENT**

### **2.3.1 Estuary Classification**

To fully understand the characteristics of estuaries, classification systems are established. One of the many methods of classification that is also important to the hydraulic character of an estuary is classification by salinity structure. The U.S. Army Corps of Engineers (1991) suggests that most estuary systems are coastal plain estuaries with individually unique salinity and flow characteristics that affect circulation. To understand estuary circulation Pritchard and Cameron (1963) classified estuaries as highly stratified, partially mixed, or well mixed.

Under the Pritchard and Cameron (1963) scheme, a highly stratified estuary is one in which the outgoing lighter fresh water overrides a denser incoming saltwater flow. The dense salt wedge will advance along the bottom until the freshwater flow forces can no longer be overcome. At this point, the tip of the salt wedge will be blunt at the rising tide and tapered during the falling tide. Mixing occurs only at the salt/freshwater interface by entrainment. As small amounts of salt water are mixed into the upper layers, more fluid enters the estuary at the bottom while more fluid leaves the system from the top layers giving rise to weak circulation currents.

A partially mixed estuary is one in which the tidal energy is dissipated by bottom friction produced turbulence. These turbulent eddies mix salt water upward and fresh water downward with a net upward flow of saline water. As the salinity of the surface

water is increased the outgoing surface flow is correspondingly increased. This causes an inward surface flow along the bottom. This well-defined two-layer flow is typical of partially mixed estuaries like the Chesapeake Bay estuaries. In partially mixed estuaries, the surface salinity increases steadily down the estuary with fresh water occurring only at the head of the estuary. Also, in partially mixed estuaries, river flow is low compared with the tidal prism, where the tidal prism is defined as the volume of water between the high and low tide elevations.

In estuaries where the tidal prism is much larger than river flow and the bottom friction is large enough to mix the entire water column, a well-mixed estuary results. If the estuary is wide, a coriolis force may form a horizontal flow separation, and in the northern hemisphere the seaward flow will occur on the right side (looking downstream) while the compensating landward flow will be on the left, which give rise to a net counter clockwise circulation. This results in the water surface being higher on the left during flood tide and higher on the right during ebb tide. An example of a well mixed estuary is found in the lower reaches of the Delaware River.

Simmons (1955) developed a ratio to define the estuary type in terms of mixing. The Simmons ratio is the ratio of the volume of river flow per tidal cycle to the volume of the tidal prism. When the ratio is 1.0 or greater, the estuary is highly stratified. When the ratio is between 0.2 and 0.5, the estuary is partially mixed. When it is less than 0.1, a well-mixed condition exists.

### **2.3.2 The Hydrologic and Hydraulic Process**

A hydrologic and hydraulic analysis of an estuarine system requires an understanding of those factors that influence estuary circulation, which in turn affects the velocity distribution in the estuarine flow field. Wang (1980) showed that circulation in estuaries is quite complex and depends on the relative magnitude of tidal variations, fresh water inflow, wind driven flow, waves created by tidal motion, and salinity gradients. The degree of complexity exhibited in the hydraulics of the estuarine system generates the need for a spatial classification of the estuary system. An estuarine system can be divided into three basic zones: tidal river, estuary, and open ocean. The tidal river zone is influenced predominantly by the advective fresh water flows generated by surface run-off from the catchment area. Tidal river flows are also affected by the changes in water surface elevations caused by the tides at the downstream boundary. Winds, tides, ocean currents, and the absence of fresh-water mixing characterize the ocean zone. The most complex of the three zones is the estuary zone whose properties depend on the degree of mixing of river (fresh) water and sea (saline) water giving rise to circulation currents.

### **2.3.3 Tidal, Storm Surge, and Riverine Hydrology**

Richardson and Edge (1997) discussed the need to develop accurate tidal, storm surge, and river flow information when modeling estuary hydraulics, as these three variables were the dominant features driving estuary hydrodynamics. In numerical models, the riverine flow represents the upstream boundary conditions while the water surface elevations caused by the tides and storm surges are used for the downstream boundary conditions.



Richardson and Edge (1997) define the tide range as the elevation change from low water to high water on a given cycle. For many locations two high tides and two low tides occur daily (semi-diurnal). The mean tide range is defined as the average difference between high and low tides for the year. Spring tide occurs when the sun and the moon combine to generate greater than normal tidal elevations, two spring tides occur each month with the new and full moons. Twice monthly the sun and the moon form a right angle with the earth, which gives rise to lower than normal tides called neap tides.

The U.S. Army Corps of Engineers (1991) defines a storm surge as a substantial rise in the sea level caused by reduced air pressure. Storm surges are generally associated with hurricanes, cyclones, and other severe weather conditions. While there is general belief in the scientific community that storm surges play a significant role in the development of scour in estuaries, not much research has been performed to determine the impacts of storm surges on scour mechanisms.

Fresh water flow enters an estuary from the drainage basins of rivers, ground water, and rain falling on the estuary water surface. In highly stratified estuaries and tidal rivers where freshwater flow dominates, estuary elevations are not independent of the catchment discharge, and this must be considered when developing estuary models. In contrast, the water levels in well mixed estuaries dominated by tidal fluctuations may be insensitive to riverine inputs.

#### **2.3.4 Estuarine Hydraulics**

Estuarine hydraulics provides the mechanism for the production and transport of sediment that causes bridge pier scour. Thurman (1993) described the mechanism of

tidal and ocean waves as not involving the mass transport of the fluid medium in the direction of the wave, but involved the medium moving in an orbital path (orbital waves), in the vertical plane. This results in a small net transport of water in the direction that the waveform is moving. This mechanism is particularly applicable to the ocean zone and suggests that purely ocean environments may experience much less general scour than riverine environments. Many researchers, including Pillsbury (1956) and the U. S. Army Corps of Engineers (1991), have determined that the primary cause of estuarine flows is attributed to the inward (flood) and outward (ebb) advection of water driven by changes in hydraulic energy head caused by tides or surges at the ocean interface, and the magnitude of these tide produced currents are a function of surface slope. Tidal waves (similar in structure to the shallow ocean waves) and wind driven surface waves also produce currents that contribute significantly to the movement of water in the estuarine environment. The effects of tidal waves can be amplified or damped by the geometry of the estuary and surface resistance. Finally, the presence of salinity and density gradients in estuaries also produces density driven currents.

The overall estuarine transport process is further complicated by the fact that different layers within an estuary undergo different modes of motion in various directions. Wang (1980) developed a study on circulation in the Chesapeake Bay in which he determined that the Chesapeake Bay was a partially mixed estuary and the circulation was driven by the tides, river runoff, salinity (density) gradients, and wind. Using gauges located at strategic points along the Bay, he further deduced that, although the Bay was dominated by tide driven waves, mass transport (including the transport of sediments) was mainly due to the wind and density induced circulation.

### **2.3.5 The Importance of Hydraulics to the Bridge Pier Scour Process**

The rate of bridge pier scour is directly related to two hydraulic variables: flow depth and flow velocity. Chiew (1984) and Johnson and McCuen (1991) showed that the rate and extent of the development of scour holes during local pier scour was dependent on the magnitude of the down flow which was in turn directly related to the velocity of the approaching flow. The jet of water in the downflow is related to the strength of the vortex created when the flow impinges on the pier and while the vortex itself contributes significantly to erosion, the vortex pattern is highly correlated to downflow. The importance of velocity and depth to the sediment transport and scour process is further supported by the structure of most empirical models developed to predict scour. Johnson (1995) compared seven widely used empirical scour models, all of which incorporated factors based on velocity and flow depth.

### **2.3.6 The Scour and Sedimentation Processes in Estuaries**

Melville and Coleman (2000) suggest that the flow at bridges over tidal waterways changes directions with the tide causing local scour to be developed alternately from two directions. They believe that under this scenario bridge pier scour can be assessed using the same principles as for rivers of unidirectional flow although typically less scour develops as some of the material eroded during one tide phase is deposited in the scour hole during the next phase. Melville and Coleman (2000) in discussing the mechanism of scour in tidal waterways indicated that general scour over an extended period may not be a critical cause of pier failure in estuarine conditions.

In a pier scour study on bridge structures over the Pamlico Sound in North Carolina, Shelden and Martin (1998) concluded that general scour and contraction scour were negligible, with only local scour being significant. This finding could be attributed to the bridge being located close to the mouth of an estuary with no constriction. Similar results were obtained by Hu et al. (1995) from a study on tidal marsh accretion (aggradation) using the SEDH sediment transport computer model.

Neill (1973) discussed the mechanism of sediment transport in estuaries. He concluded that under certain conditions stratified fresh water and salt water can flow simultaneously in opposite directions. Through the shoaling process, suspended sediments and dissolved solids carried by the river entering the estuary tend to flocculate on contact with the salt water whereby causing deposition or aggradation. The U.S. Army Corps of Engineers (1991) also identified salt-water intrusion as an important factor in estuary sedimentation because saline water enhances flocculation of suspended sediments while density currents will be responsible for moving sediments upstream along the bottom. As a result, suspended sediments may become trapped instead at the lower locations in an estuary causing aggradation rather than general scouring.

In summary, the literature reviewed strongly indicated that the portion of an estuary not subject to large advective flow velocities did not experience significant general scour. Further, the dominant scour mechanisms in estuaries were found to be local scour and contraction scour. Hence the importance of general scour depends on the magnitude of the daily flow velocities and location within the estuarine system.

## **2.4 THE DOWNFLOW DEVELOPMENT**

### **2.4.1 Introduction**

The body of existing research strongly indicates that the downflow phenomenon, caused by the presence of a pier obstruction placed in the stream flow, plays an extremely important role in the development of local scour around bridge piers. The downflow may be defined as the flow or discharge directed vertically downwards towards the streambed along the upstream face of a bridge pier or any other obstruction that is placed in the horizontal flow path. Available research suggests that the magnitude of the downflow is due to an adverse pressure gradient induced by the bridge pier, with the adverse pressure gradient in turn being a consequence of the vertical profile of the horizontal velocity of the stream.

### **2.4.2 Theoretical Development of the Downflow**

Researchers such as Grover and Harrington (1966) have studied the horizontal velocity profile of natural channels. By measuring the horizontal velocities in streams at various distances from the invert, they determined that the horizontal velocity profile of a stream was in close agreement with the logarithmic wake law expressed for turbulent flow, which could be described by:

$$u = U(y/Y_m)^n \quad (2.4-1)$$

where  $u$  is the velocity of a horizontal jet or streamline,  $U$  is the mean stream velocity,  $y$  is the displacement of the jet from the streambed,  $n$  is an empirical constant, and  $Y_m$  is the flow depth. A value for  $n$  of 0.18 shows good agreement with the data provided by Grover and Harrington (1966).

Figure 2.4-1 depicts the formation of the adverse pressure gradient from which the downflow originates. The coordinates  $x$  and  $y$  are two locations in the flow field that are in contact with the upstream face of the bridge pier. The static pressure prisms that are shown for both locations indicate that the static pressure varies directly with the distance from the surface. If  $P_s(y)$  is the static pressure at location  $y$  and  $P_s(x)$  the static pressure at location  $x$ , then as shown in Fig. 2.4-1,  $P_s(y)$  is greater than  $P_s(x)$ . If the turbulent stream velocity profile developed by Grover and Harrington (1966) is assumed, then  $u_x$  will be greater than  $u_y$ , where  $u_x$  and  $u_y$  are the horizontal velocities at levels  $x$  and  $y$ , respectively. The velocities at  $x$  and  $y$  are associated with stagnation pressures when the flows at these location impact the bridge pier.

Hung (1968) and Baker (1980) define the total stagnation pressure at each location after impact as the sum of the static pressure and the product of the velocity head at a given location and the fluid specific weight. Accordingly, the stagnation pressure at location  $y$  is:

$$P_g(y) = 0.5\rho u_y^2 + P_s(y) \quad (2.4-2)$$

The magnitude of the pressure developed from the impact of the normal horizontal flow at each location along the vertical face of a pier may be determined in terms of a pressure coefficient,  $C_p$ , given by Hung (1968) as:

$$C_p(y) = 2 [P_g(y) - P_s(y)] / \rho U^2 \quad (2.4-3)$$

where  $P_g(y)$  is the stagnation pressure at  $y$ , and  $U$  is the horizontal free stream velocity.

Figure 2.4-1 shows that, due to the increase in the slope of the velocity profile curve near the bottom of the channel, the difference in velocity heads between two levels in close proximity in this region will be significant while the static pressures will be

approximately the same. As a result, the stagnation pressure and pressure coefficient at the higher level will be greater than those at the lower level, thus inducing a downward flow velocity denoted as  $v_d$ .

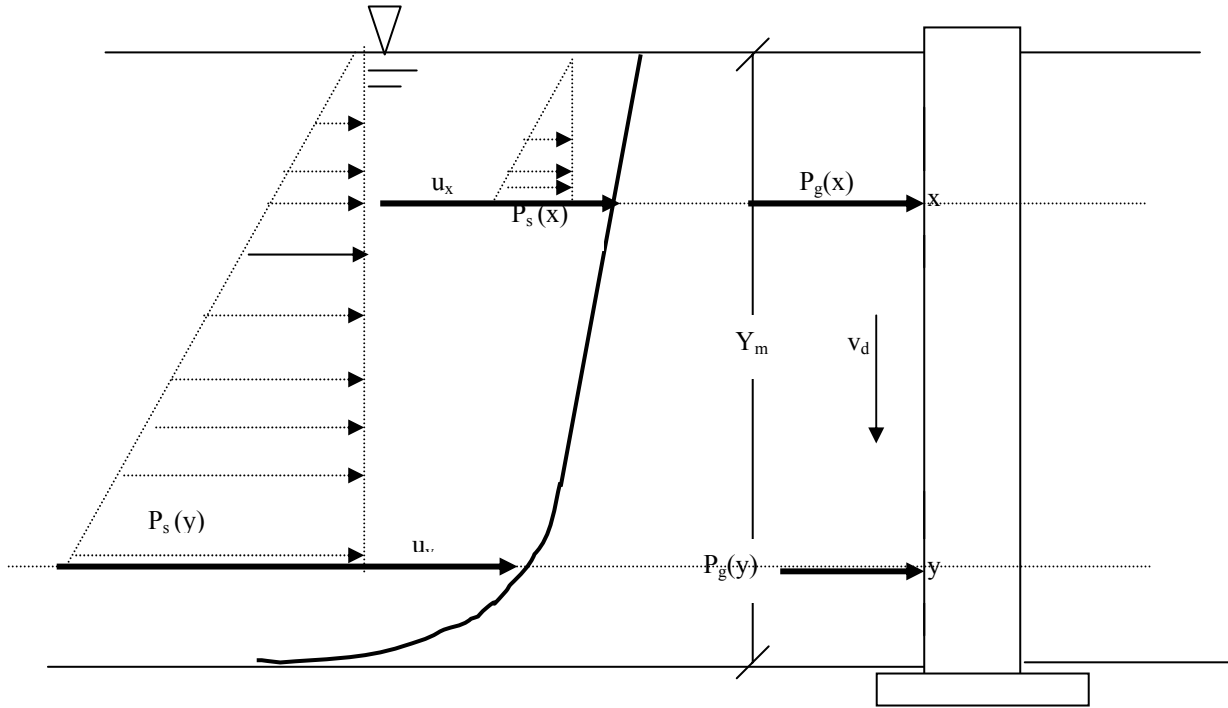


**Figure 2.4-1. The development of the downflow around bridge piers.  $x$  and  $y$  are two locations in contact with the upstream face of the bridge pier. The static pressure prisms  $P_s(y)$  and  $P_s(x)$  are shown for both locations. The curve represents the turbulent stream velocity profile developed by Grover and Harrington (1966) that induces a vertical adverse pressure gradient.**

### 2.4.3 Research Supporting the Existence of the Downflow

Shen et al. (1966) recorded the presence of the downflow in experiments they performed on the impacts caused by the presence of a pier in a flow field. Hung (1968) studied the velocity and pressure distributions near a circular cylinder in an open channel. He found that the secondary flows (downflows) along the front and rear of the cylinder were due to the resulting pressure gradient of the horizontal streamflow. Melville (1975)

measured the velocities of the flow at different stages in the development of the scour hole. He also found that a strong vertically downward flow also developed as the scour hole enlarged. Baker (1979, 1980) studied the formation of a turbulent horseshoe vortex around the base of a cylinder placed in a wind tunnel and determined that the pressure coefficient at the base of the cylinder was  $(u/U)^2$  where  $u$  was the velocity of the streamline that passed down the face of the cylinder and  $U$  was the free stream velocity. Baker's finding was an indication that  $u$  was equivalent to the downflow velocity at the base of the cylinder. Using the notation for the pressure coefficient in Eq. 2.4-3, then according to Baker:

$$C_{p0} = (V_d/U)^2 \quad (2.4-4)$$

Rearranging gives:

$$V_d = UC_{p0}^{0.5} \quad (2.4-5)$$

where  $V_d$  is the downflow, and  $C_{p0}$  represents the coefficient of pressure at the base of the cylinder on the stagnation plane.

Using wind tunnel experiments, Ettema (1980) measured the downflow induced by a cylindrical obstruction placed in the flow in the vertical plane of symmetry. He found that the downflow velocity varied with the vertical displacement from the channel bottom. He also found that at any given elevation the value of the downflow varied horizontally, with the downflow velocity being zero in contact with the pier and again some distance upstream of it. The velocity profiles shown in Fig. 2.4-2 are based on experimental data by Ettema (1980) and represent the maximum downflow distribution at any elevation, where  $d$  is the pier diameter and  $y$  is the distance from the channel invert.



Vennard and Street (1982) described secondary flow as the consequence of wall friction. They determined that the secondary flow was related to the horizontal velocity profile in a flow field. They reasoned that the stagnation pressure at the obstruction was greater at higher vertical levels in the flow field than at lower levels (as may be deduced from the velocity profile shown in Fig. 2.4-1). According to Vennard and Street (1982), this pressure difference maintained a downward secondary flow, thus inducing a vortex type motion with the core of the vortex being swept downstream around both sides of the projection.

Raudjkivi (1986) also conducted laboratory research into the flowfield developed around circular piers. He also believed that the downflow around bridge piers was primarily due to an adverse pressure gradient set up by the stagnation pressure produced by the pier obstruction. He reasoned that because the horizontal velocity in turbulent flow decreased with depth, then the stagnation pressure, which according to him is given by  $\rho u^2/2$ , also decreases with depth, thus setting up the adverse pressure gradient.

Dargahi (1989) conducted laboratory studies to determine the turbulent flow field around a circular cylinder. These studies revealed that the main flow characteristics around a cylinder were a relatively large secondary flow and a change in the vertical velocity profile when compared to the free stream condition. Though not mentioned by name, the large secondary flow identified by Dargahi is synonymous to the downflow found by the other researchers.

Melville and Coleman (2000) attributed the downflow velocity to an adverse pressure gradient induced by the bridge pier. According to Melville and Coleman the stagnation pressures on the face of a pier were highest near the surface, where the

deceleration is greatest, and decreases with depth. The resulting downward pressure gradient at the pier face generated the downflow.

#### **2.4.4 Role of the Downflow in the Local Scour Process**

Though the exact scour mechanism, and the role that the downflow plays in this process, have not yet been determined conclusively, many researchers have established relationships between the development of the downflow and the depth of the scour hole. There is also a distinct group of researchers that believe that the downflow is the actual agent of scour. Other researchers however, argue that the downflow is responsible for the formation of the horseshoe vortex, and it is this vortex that plays the direct role in the scour process.

Chiew (1984) determined that the rate of erosion of the scour hole formed around bridge piers was directly related to the magnitude of the downflow that was in turn due to the adverse pressure gradient induced by the bridge pier. Under Chiew's conceptual view of the scour process, the horseshoe vortex was directly responsible for the development of the scour hole. Chiew indicated that the jet of water in the downflow played an important role in the formation and strength of the vortex. However, it was the vortex that caused the erosion of the bed material around the pier, thus forming the scour hole.

Studies conducted by Ettema (1980) deduced that the magnitude of the downflow varied with the horizontal distance from the pier and the vertical distance from the bed. Ettema also found that the vertical location of the maximum downflow was dependent on scour depth ( $d_s$ ), while the horizontal location of the maximum downflow was 0.05 to 0.02 pier diameters upstream of the pier, being closer to the pier at lower elevations.

Figure 2.4-2 shows that the maximum value of  $V_{\text{dmax}}/U$  increases from 0.4 (at  $d_s/d = 0$ ) to 0.8 (at  $d_s/d = 2.3$ ), where  $V_{\text{dmax}}$  is the maximum downflow at a given elevation in the flow field and  $d$  is the diameter of the obstruction.

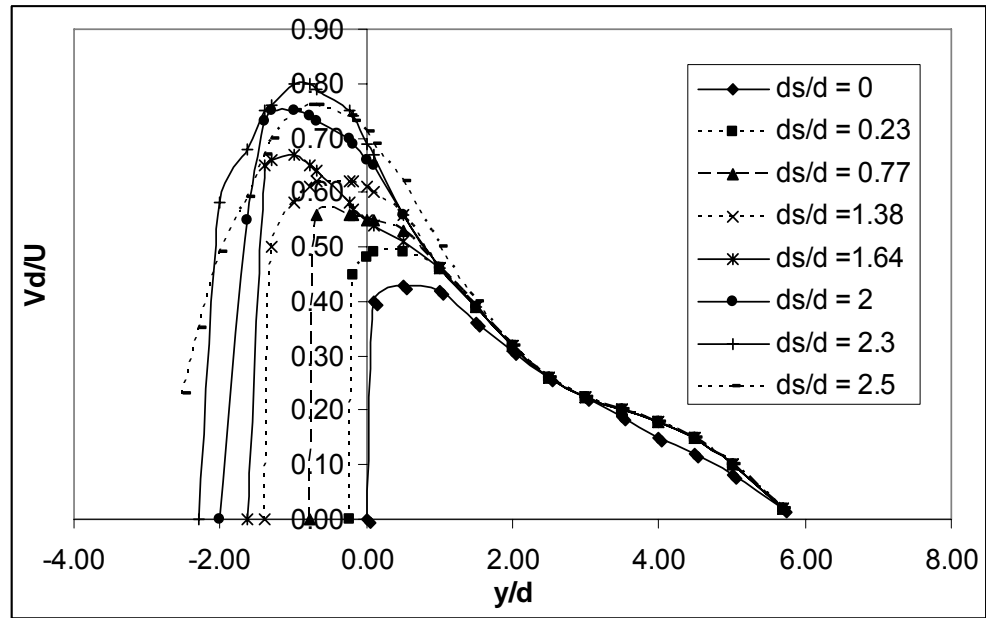


**Figure 2.4-2 Downflow in front of a pier according to Ettema (1980) for values of  $d_s/d = 0, 0.23, 0.77, 1.38, 1.64, 2.0, 2.3, 2.5$  where  $d_s$  represents scour depth,  $d$  the pier diameter, and  $y$  the vertical distance from the channel invert.**

Raudjkivi (1986) was also able to develop relationships between the magnitude of the downflow and the scour depth. He found that the downflow close to the base of a pier was approximately 40% of the mean free stream velocity when the scour depth was zero. He also determined that the downflow increased to a maximum value of 80% of the mean free stream velocity when the scour depth was 2.3 times the pier diameter.

Dargahi (1989) believed that the secondary flow or downflow did not play a direct role in the scour process but was responsible for the flow separation that occurred

just upstream of the pier obstruction, which eventually led to the development of a vortex system. He further observed that the downflow in the stagnation plane of the cylinder separated from the pier surface and rotated, thus forming a small anti-clockwise vortex at the base of the pier. From these laboratory studies, Dargahi determined that the pressure coefficient close to the base of the pier,  $C_{p0}$ , was 0.65. When this value of  $C_{p0}$  is substituted into Eq. 2.4-5, a simple expression for the magnitude of the maximum downflow velocity is derived:

$$V_d = 0.81U \quad (2.4-6)$$

Ahmed and Rajaratnam (1998) conducted laboratory flume experiments on the flow past cylindrical piers. The experiments were conducted using a flume 20 m long and 1.22 m wide. The flume was fitted with a sediment recess 0.2 m deep, 0.78 m wide and 0.78 m long. Cylindrical plexiglass piers of varying radii were used. In four of the experiments, the bed was allowed to scour in the sediment recess, while in another four experiments, the sand that formed the bed of the flume was glued to the bottom. They observed frontal downflow velocities as large as 95% of the approach velocity during the development of the scour hole. Results of three of their experiments are shown in Fig. 2.4-3. Table 2.4-1 also shows the specific conditions of each of the above experiments.

**Table 2.4-1. Specific conditions of experiment C2M, D2M, and C2R.**  
**d** is the pier diameter, **U** is the free stream velocity, **Y<sub>m</sub>** is the flow depth, **d<sub>s</sub>** is the scour depth, and **d<sub>r</sub>** is the scour radius

Expt.	d (m)	U (m/s)	Y <sub>m</sub> (m)	d <sub>s</sub> (m)	d <sub>r</sub> (m)
C2M	0.089	0.293	0.182	0.055	0.116
D2M	0.089	0.384	0.14	0.151	0.276
C2R	0.089	0.293	0.182	0	0

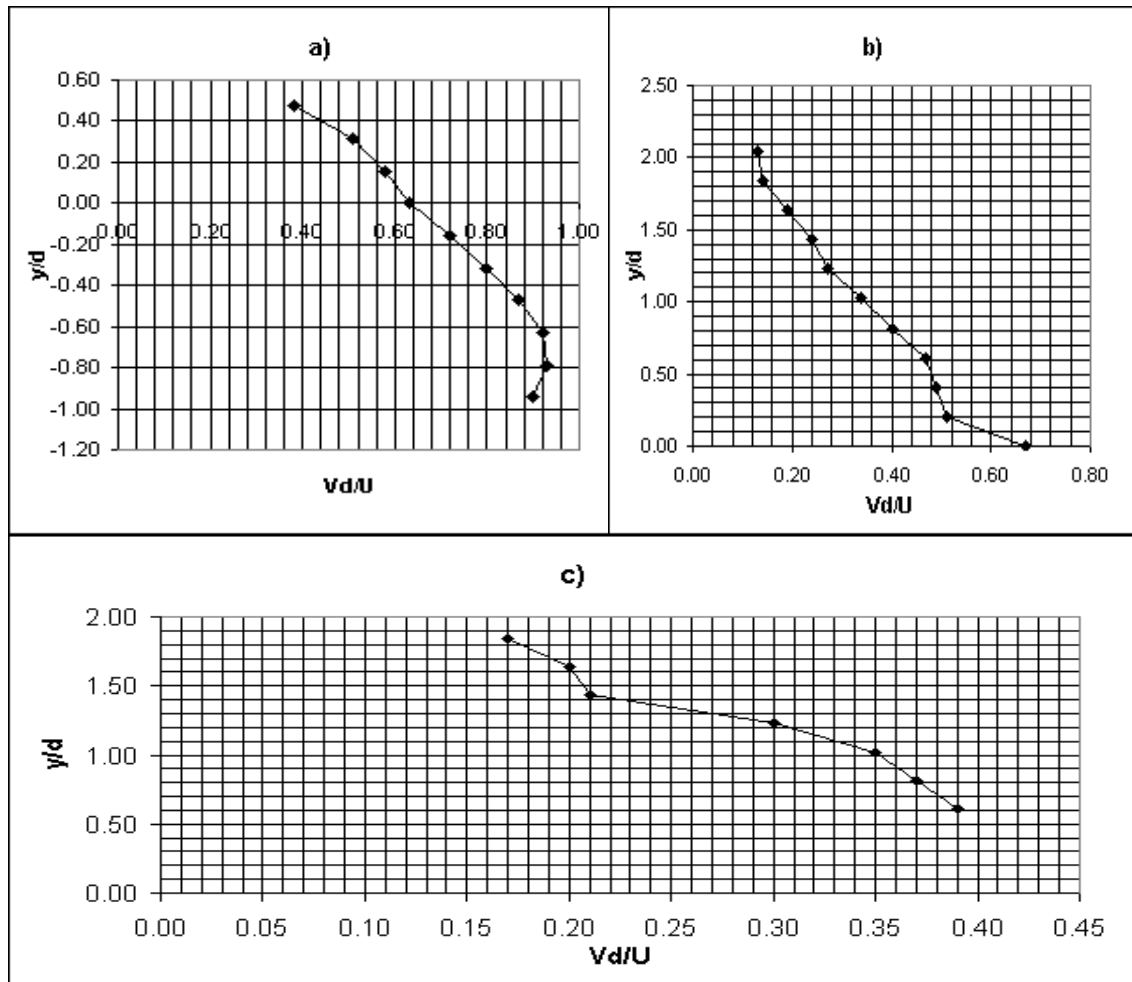


**Figure 2.4-3.  $y/d$  vs  $Vd/U$  for three experiments by Ahmed and Rajaratnam (1998).**  
**a) Results of experiment D2M with a mobile sand bed. b) Results from experiment C2M with a mobile sand bed. c) Results from experiment C2R with rigid sand bed.**

## **2.5 THE VORTEX DEVELOPMENT**

### **2.5.1 Introduction**

Many researchers see the horseshoe vortices, formed when an obstruction is placed in a flow field, as being directly responsible for the formation of the local scour hole. As a result, it was necessary to review the theoretical basis for the formation of the horseshoe vortex system as the first step in the development of a model to represent the behavior of the horseshoe vortex. Important fluid mechanics theories and relevant research findings can be used in the development of models to predict the properties of the horseshoe vortices. Details of the derivation of such theories may be found in fluid mechanic references such as Vennard and Street (1982) and Ahmed (1987).

### **2.5.2 Theoretical Background**

Vennard and Street (1982) indicated that the horseshoe vortex produced by projections from a boundary surface, for example a bridge pier, is caused by the vertical variation of the stagnation pressure that is induced by the obstruction in the flow field. They deduced that this pressure difference maintains a downward secondary flow, or downflow, that induces a vortex type motion. The core of the vortex is swept downstream around the sides of the projection by the streamwise longitudinal flow. Vennard and Street (1982) believed that the vortex strength was related to the downflow at the upstream face of the pier.

Theoretically, the strength of an induced vortex may be expressed in terms of its vorticity  $\xi$ , where  $\xi$  ( $S^{-1}$ ) is defined as the differential circulation per unit area enclosed and is given by:

$$\xi = (\partial v / \partial x - \partial u / \partial y) = \partial \Gamma / \partial x \partial y \quad (2.5-1)$$

where  $x$  is the distance moved in the horizontal direction,  $y$  is the vertical distance moved,  $v$  is the vertical velocity, and  $u$  the horizontal velocity.  $\Gamma$  ( $\text{ft}^2/\text{s}$ ) is a measure of the “swirl” in a fluid and is defined as the line integral of the tangential components of velocity around a closed curve fixed in the flow. In a two-dimensional flow field,  $\Gamma$  is given by:

$$\Gamma = (\partial v / \partial x - \partial u / \partial y) \, dx \, dy \quad (2.5-2)$$

For a flow field comprised of streamlines of concentric circles, the circulation in polar coordinates is given by:

$$\Gamma = v_t 2\pi r \quad (2.5-3)$$

where  $r$  is the radius of the particular circular path and  $v_t$  is the tangential velocity as shown in Fig. 2.5-1. The vorticity in polar coordinates is given by:

$$\xi = \partial v_t / \partial r + v_t / r - \partial v_r / r \partial \theta \quad (2.5-4)$$

where  $v_r$  is the radial component of the velocity, and  $\theta$  is the angle through which the streamline moves in a given time  $t$ . The dimensions suggest that  $\xi$  is related to the rate of change of the tangential velocity with distance from the center of the vortex. It may be shown that the vorticity of a vortex is also directly related to the angular velocity  $\omega$ , where  $\omega$  is defined as the rate of change of  $\theta$  with time. Vennard and Street (1982) define the angular velocity  $\omega$  in a vortex as the average rotation of the fluid element given by:

$$\omega = \frac{1}{2}\xi = \frac{1}{2}(\partial v / \partial x - \partial u / \partial y) \quad (2.5-5)$$

Equation 2.5-5 may also be expressed as:

$$\xi = 2\omega \quad (2.5-6)$$

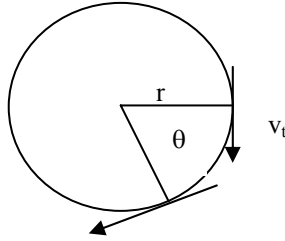


**Figure 2.5-1. Circulation of a circular streamline**

### **2.5.3 Free Vortex**

Ahmed (1987) defines a free vortex as a flow field with a concentric circle of streamlines with a velocity distribution such that the flow field is irrotational. In a free vortex, the radial component of velocity everywhere is zero, and the velocity distribution is characterized by the equation:

$$v_t r = C \quad (2.5-7)$$

where  $C$  is a constant. Thus, a free vortex may be defined as one in which two conditions are valid: (1) the product of the tangential velocity at a point and the radial distance of that point from the vortex center is constant and (2) the tangential velocity increases towards the vortex center.

Figure 2.5-2 shows the important features of a free vortex. The boxes with vertical lines in Fig. 2.5-2 represent solid particles floating in the free vortex. As shown in the figure, the orientation of the particles remains the same at all locations within the vortex field. This reflects the fact that, even though the flow path is circular, the flow remains irrotational. The velocity distribution, as indicated by the arrows in Fig. 2.5-2, shows that the velocity is greatest near the center of the vortex.



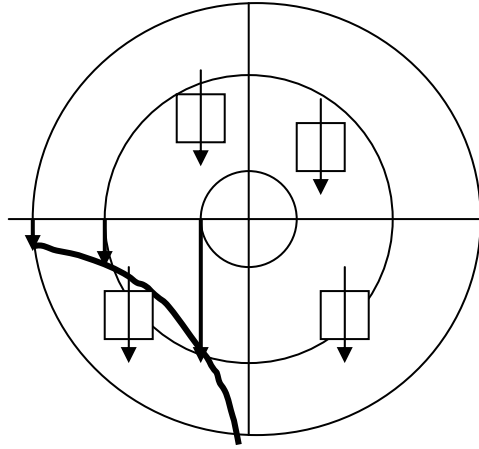


**Figure 2.5-2. Diagram of a free vortex system with floating particles represented by boxes. The concentric circles represent locations with a specific distance from the vortex center. The vertical arrow through each box represents the orientation of the particle. The tangential velocity distribution, as indicated by the heavier arrows, shows an increase in magnitude as the center of the vortex is approached. The heavy curved line, which represents the variation of the tangential velocity with distance from the center of the vortex, satisfies Eq. 2.5-7.**

#### 2.5.4 Forced Vortex

Vennard and Street (1982) defined a forced vortex as one in which the tangential velocity ( $v_t$ ) increases linearly with displacement from the vortex center and may be represented by:

$$v_t = r\omega \quad (2.5-8)$$

where  $r$  is the distance from the center of the vortex and  $\omega$  is its angular velocity. Note that in a forced vortex the orientation of the suspended particle changes with location in the flow field. Thus, the flow in a forced vortex is described as rotational and is depicted as shown in Fig. 2.5-3.

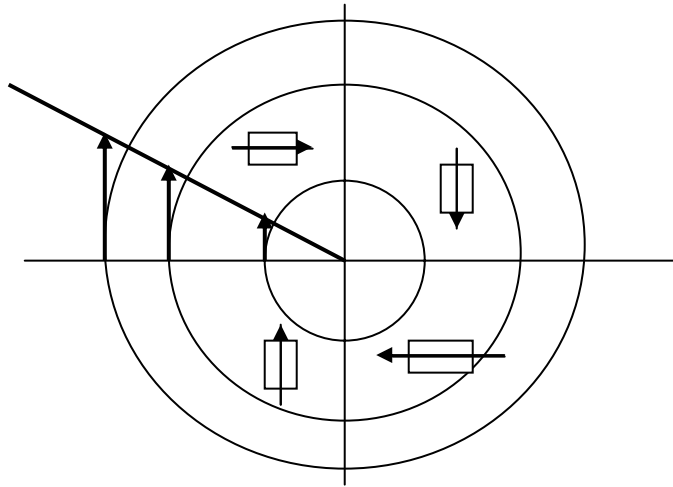


**Figure 2.5-3. Diagram of a forced vortex system with floating particles represented by boxes. The concentric circles represent locations with a specific distance from the vortex center. The vertical arrow through each box represents the orientation of the particles. The orientation of the particles within the vortex field changes with location. The tangential velocity distribution, as indicated by the heavier arrows, shows a linear increase in magnitude as the distance from the center vortex is increased.**

### **2.5.5 Real Vortex**

Current theory suggests that in a free vortex the tangential velocity at the center of the vortex approaches infinity. Since such a condition is impossible, totally free vortices are inadequate to represent a real flow field. Rankine was the first to suggest that vortices in real flow fields can be modeled as a combination of both free and forced conditions, with the forced vortex flow occurring at or near the vortex center and the free vortex flow occurring outside of this region, as depicted by Fig. 2.5-4.

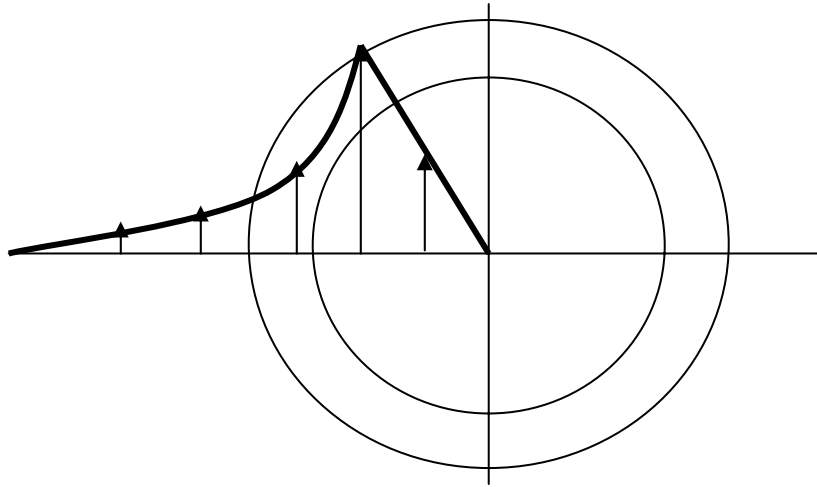


**Figure 2.5-4. The theoretical velocity profile of a real vortex indicated by the heavier curved and straight lines. The figure shows the tangential velocity increasing linearly with distance for regions close to the vortex center followed by a decrease in tangential velocity for distances further away from the center.**

Fluid Mechanics texts, such as Vennard and Street (1982), suggest that real or Rankine vortex can be represented by the following equation:

For the forced vortex region,  $r \leq r_m$ :

$$V_t = \omega_1 r \quad (2.5-9)$$

where  $\omega_1 = V_m / r_m \quad (2.5-10)$

Therefore:

$$V_t = V_m r / r_m \quad (2.5-11)$$

For the free vortex region  $r > r_m$ :

$$V_t = \omega_2 / r \quad (2.5-12)$$

where  $\omega_2 = V_m r_m \quad (2.5-13)$

Therefore:

$$V_t = V_m r_m / r \quad (2.5-14)$$

where  $V_t$  is the tangential velocity at radius  $r$ ,  $V_m$  is the maximum tangential velocity, and  $r_m$  is the radius of the maximum tangential velocity. Equations 2.5-13 and 2.5-14 can be combined as follows:

$$V_t = \begin{cases} V_m (r / r_m) & \text{for } r \leq r_m \\ V_m r_m / r & \text{for } r > r_m \end{cases} \quad (2.5-15)$$

Odgaard (1986) also developed the following model to represent a real vortex:

$$u/u_c = 1.4(r_c/r)[1 - \exp(-1.25(r^2/r_c^2))] \quad (2.5-16)$$

where  $u$  is the velocity of the vortex a distance  $r$  from the center,  $u_c$  is the maximum tangential velocity, and  $r_c$  is the distance from the center of the vortex to the point of maximum velocity.

### 2.5.6 Flow About a Circular Pier

The flow field in the  $x$ - $z$  plane set up by a cylindrical pier, where the  $x$  axis is taken along the horizontal direction and the  $z$  axis is directed into the paper, may be modeled using the hydromechanics flow theories of potential flow and stream functions. Although these theories specifically relate to non-viscous fluids, the models they produce provide reasonable estimates of the behavior of real fluids outside of the regions of the boundary layer set up by the cylinder. Using these theories, Ahmed (1987) determined that the tangential velocity ( $v_t$ ) and radial velocity ( $v_r$ ) about a cylinder at a given depth could be represented as:

$$v_t = -u(1 + a^2/r^2)\sin\theta \quad (2.5-17)$$

$$v_r = u(1 - a^2/r^2)\sin\theta \quad (2.5-18)$$

where the negative sign in Eq. 2.5-17 represents the direction of the tangential velocity with respect to  $u$ , which in turn is the flow velocity at a given depth taken without the cylinder in place,  $r$  and  $\theta$  are the polar coordinates of the point at which the velocities are to be determined, and  $a$  is the radius of the cylinder as shown in Fig. 2.5-5. At the surface,  $u$  is approximately equal to the free stream velocity  $U$ . Since the vertical velocity profile may be determined by Eq. 2.4-1, then Eqs. 2.5-17 and 2.5-18 may thus be used in conjunction with Eq. 2.4-1 to estimate the velocity at any point in the flow field affected by a cylinder.

Ahmed (1987) used the stagnation pressure to determine an expression for the pressure at any point in the flow field around the cylinder as represented by:

$$P_{(r,\theta,y)} = P_{oy} + 0.5\rho(u_y^2 - v_t^2_{(r,\theta,y)}) \quad (2.5-19)$$

where  $P_{oy}$  is the free stream static pressure and  $u_y$  is the velocity  $y$  feet from the channel invert. It should be noted that Eqs. 2.5-17, 2.5-18, and 2.5-19 provide estimates of the pressure and velocity at points in the flow field about the cylinder based on an inviscid fluid and, therefore, cannot predict the vortex properties (i.e., vorticity, angular velocity, tangential velocity) of real fluids. However, these models may be used to estimate the flow conditions from which the vortices are formed, and further to test the accuracy or validity of the downflow and vortex models that are developed.

### **2.5.7 The Vortex System During Development of the Scour Hole**

A considerable amount has been written about the various aspects of the horseshoe vortex system associated with flows around an object placed normal to the direction of flow. In particular, Baker (1979) and Dargahi (1989) have provided

significant contributions towards the understanding of the mechanism through which such vortex systems are developed.

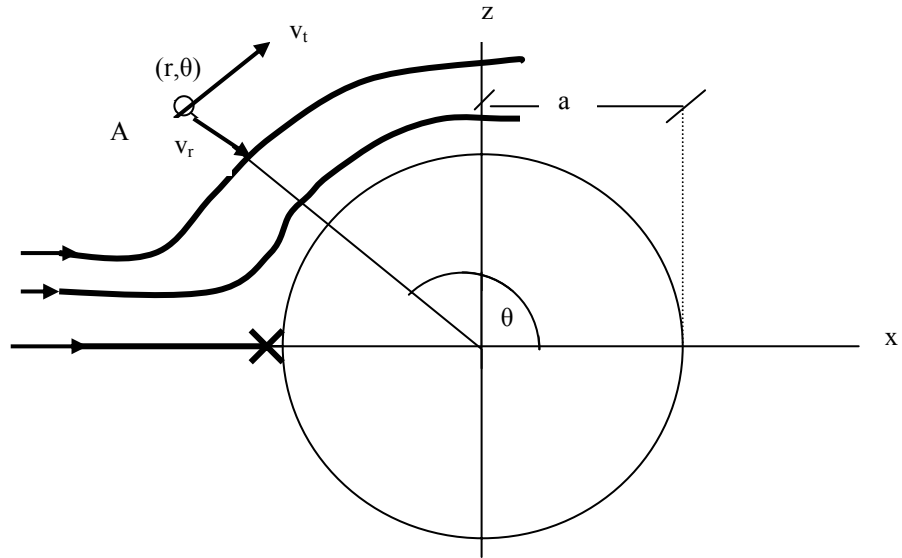


**Figure 2.5-5. Plan view of the horizontal flow around cylindrical object. “A” represents a location in the flow field with polar coordinates  $r$  and  $\theta$  relative to the center of the cylinder with radius  $a$ .  $v_r$  and  $v_t$  represent the radial and tangential velocities of location A. Three streamlines are shown depicted by arrows with heavy lines. The “X” on the streamline that approaches the cylinder normally indicates that the streamline is deflected vertically downwards by the cylinder.**

Baker (1979) conducted experiments using flow visualization in a smoke tunnel that had a cross section of 30.5 by 15.3 cm. A 7.6-cm diameter cylinder, 3.8 cm in height was mounted on a flat plate on the centerline of the tunnel working section. The flow pattern in the plane of symmetry upstream of the cylinder was determined using flow visualization techniques. In addition, measurements of the pressure and velocity distribution upstream of the cylinder were made.

Figure 2.5-6 shows the flow pattern seen in the smoke tunnel. At lower flow speeds, three vortices (1, 2, and 3) rotated in a clockwise direction and three smaller vortices (1a, 2a, and S<sub>0</sub>) rotated in a counter-clockwise direction. The exact number of vortices depended on the diameter of the obstruction and flow speed, with more vortices appearing as either the flow speed or diameter of the obstruction increased. Baker (1979) showed that the number of vortices was a function of the Reynolds number  $UD/\nu$  and a dimensionless parameter  $D/\delta$ , where  $\delta$  is the boundary layer thickness,  $D$  is the pier diameter, and  $\nu$  the kinematic viscosity. The quantity  $UD/\nu$  is defined as the pier Reynolds number, as it uses the pier diameter as the length dimension in the Reynolds equation in lieu of the flow depth or hydraulic radius. Above a certain flow speed ( $0.65 \text{ ms}^{-1}$ ), Baker found that the entire vortex system oscillated with Strouhal number ( $fU/D$ ) of the range from 0.26 to 0.6 with  $f$  from 0.8 to 1.4 hertz, where  $f$  is the oscillation frequency (hertz).

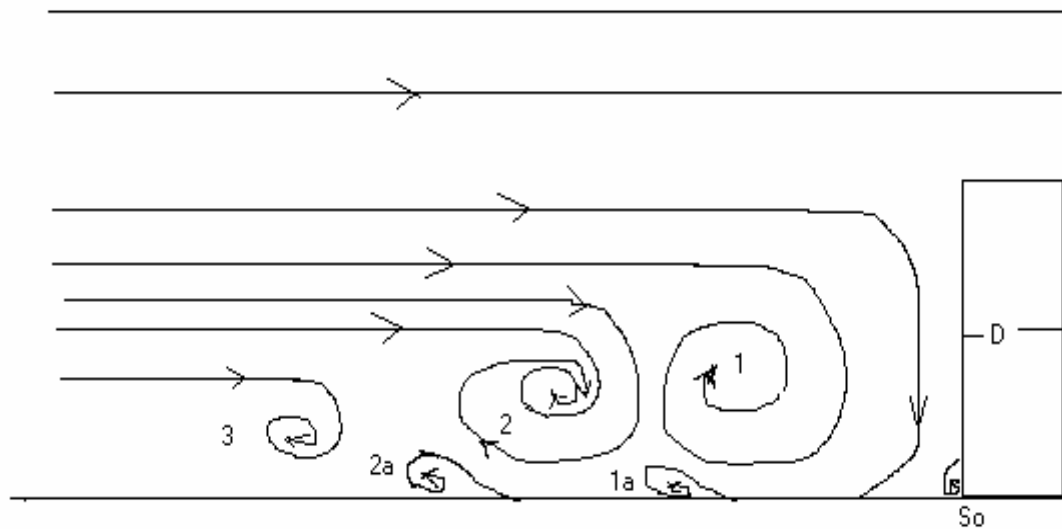
Baker (1979) plotted the mean position of each vortex in the  $x/D$ - $y/D$  plane using the convention shown in Fig. 2.5-7. The origin is taken as the vertical plane of symmetry through the center of the cylinder. Thus, values of  $x/D$  upstream of this plane were taken as negative, while values of  $x/D$  downstream of the plane were positive.

Table 2.5-1 shows the mean location of each of the vortices in the system for a pier Reynolds number of 16,000. Baker (1979) also showed that the mean position of vortex 1 was dependent on both the pier Reynolds number  $UD/\nu$  and  $D/\delta$ . Baker (1979) measured the pressure distribution in the plane of symmetry upstream of the cylinder for flows with pier Reynolds numbers in the range from 16,000 to 40,000. The coefficient of pressure,  $C_p$ , was computed for  $x/D$  values in the range from  $-2.0$  to  $-0.5$  (at the face of

the cylinder). It was found that  $C_p$  had a maximum value of 1.0 at  $x/D = 0.5$  and was gradually decreased to 0.2 at  $x/D = -2.0$ . The measurements also indicated a sharp drop in pressure at  $x/D = -0.72$ , where  $C_p$  was measured in the range from 0.30 to 0.35. Note that vortex 1 was centered at  $x/D = -0.72$  and  $C_p$  in this case is defined by the equation:

$$C_p = [P - P_o] / 0.5 \rho U^2 \quad (2.5-20)$$

where  $P_o$  is the free stream static pressure measured with no cylinder in place,  $P$  is the pressure measured at  $(x/D)$ , and  $P$  and  $C_p$  vary with  $x/D$ .



**Figure 2.5-6 Streamline patterns and vortex systems (Baker 1979) showing a weak counter clockwise vortex  $S_o$  at the base of the cylinder along with small counter clockwise vortices 1a, and 2a at the invert of the flume.**

Baker (1979) also determined the location of each vortex in the system at flow conditions that cause a pier Reynolds number of 2,610. The vortices were centered as shown in Table 2.5-2. The horizontal and vertical velocity components were also measured by Baker (1979) on lines drawn vertically through the centers of vortices 1, 2, 3, and 1a for flow conditions with a pier Reynolds number of 2,610. These results are presented in Table 2.5-3. In addition, Baker (1979) took velocity measurements along a



horizontal line through the center of vortex 1. The results are shown in Table 2.5-4.  $U$ ,  $u$ , and  $v$  in Tables 2.5-3 and 2.5-4 represent the mean free stream velocity, the horizontal component of the velocity at the point, and the vertical component of the velocity at the point in question. “ $u$ ” is negative when directed upstream while “ $v$ ” is negative when directed vertically downwards.

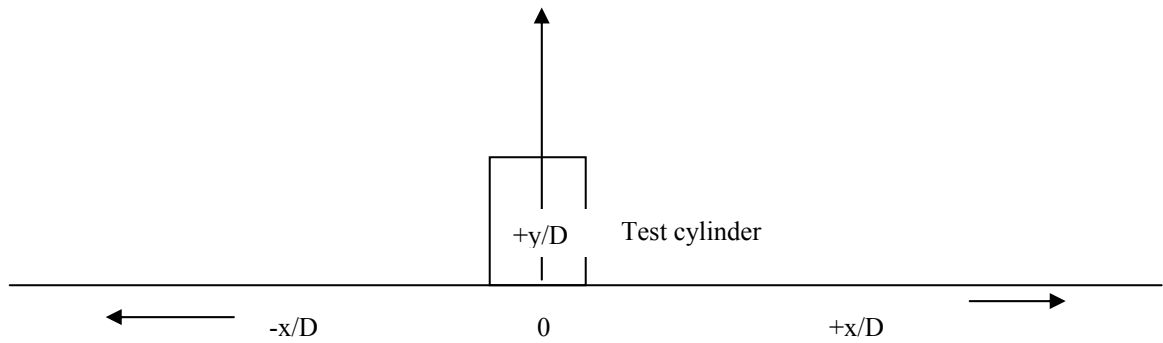


**Figure 2.5-7  $x/D$ - $y/D$  plane used by Baker (1979) to plot the mean position of each vortex. The figure shows the origin at the central axis of the cylinder. Values of  $x/D$  upstream of this plane were taken as negative while values of  $x/D$  downstream of the plane were positive.**

Using hydrogen bubble flow visualization, Dargahi (1989) also experimentally investigated the flow field around a circular cylinder mounted vertically. Pier Reynolds numbers ranging from 6,600 to 65,000 were used. Dargahi (1989) determined that the main characteristic of the flow upstream of the cylinder was a system of horseshoe vortices, similar to those identified by Baker (1978), which were shed quasi periodically with a frequency of 0.1 to 2 hertz. Dargahi (1989) also identified a relatively large secondary flow region that had a skewed horizontal velocity distribution in the vertical

direction. The implication being that the vortices produced affected the vertical velocity distribution in the flume used for the experiments.

**Table 2.5-1. Mean position of oscillating vortices where  $x/D$  is the normalized horizontal distance from the center of the cylinder and  $y/D$  is the normalized vertical distance from the invert of the test channel.**

Vortex Number from Fig. 2-8	Coordinates of the center of the mean vortex position	
	$x/D$	$y/D$
1	-0.72	0.045
2	-0.85	0.035
3	-0.95	0.023
$S_o$	-0.55	0.010
1a	-0.75	0.010
2a	-0.88	0.010

**Table 2.5-2. Location of the center of the mean vortices positions for  $R=2,610$**

Vortex Number	Coordinates of the center of the mean vortex position for $R=2610$	
	$x/D$	$y/D$
1	-0.66	0.045
2	-0.83	0.035
3	-0.88	0.025
1a	-0.73	0.025
2a	-0.85	0.010

Dargahi (1989) conducted experiments in a 22-m long, 1.5-m wide, and 0.65-m deep hydraulic flume, with a cylinder 0.15-m wide and 0.5-m high mounted vertically on the flume bed 18 m from the inlet. A uniformly graded sand was glued to the bed to provide surface roughness. Detailed measurements of pressure, velocity, and shear stress were made. He determined that for pier Reynolds number from 20,000 to 39,000 the vortex system was similar to that obtained by Baker with vortices 1, 2,  $S_o$ , 1a, and 2a being clearly identified. The flow visualization showed that vortex 1 was centered at  $x/D$

between -0.72 and -0.83, and the number of vortices increased to 9 when the pier Reynolds number was increased to 65,000.

**Table 2.5-3. Velocity on a vertical plane through the center of some vortices.  $D$  represents the pier diameter,  $y$  the vertical distance from the channel invert,  $u$  the horizontal velocity component,  $v$  the vertical velocity component, and  $U$  the free stream velocity.**

Vortex	1		2		3		1a	
y/D	u/U	v/U	u/U	v/U	u/U	v/U	u/U	v/U
0.00								
0.01		0.00		0	-0.09	0	0.1	0
0.02	-0.8	0.00	-0.25	0	-0.12	0	0.15	0
0.03	-0.6	0.02	-0.20	.03	0.00	0	0	0
0.04	-0.5	0.03	0	0		0	-0.11	0
0.05	-0.4	0.02	0.1	-0.02	0.40	0	-0.12	0
0.06	-0.3	0.01	0.2	-0.01	0.45	0	-0.13	0
0.07	0.0	0.0	0.25	0	0.50	0	-0.13	0
0.08	0.3	-0.04	0.3				0	0
0.09	0.4	-0.03	0.4			0.02		0
0.10	0.5	-.02	0.6	0.02	0.75	0.03	0.5	0

Pressure measurements taken by Dargahi (1989) showed a constant coefficient of pressure,  $C_p$ , of 0.5 in the range  $-0.80 < x/D < -0.70$ . This result was attributed to the presence of vortex 1.  $C_p$  fell gradually from 1.0 at  $x/D = -0.5$ , to 0.1 at  $x/D = -2.0$ . The pressure distribution was also measured along the vertical stagnation line at the upstream face of the cylinder. The results, shown in Table 2.5-5, indicate a pressure gradient caused by the non-uniform, or skewed, velocity distribution of the approach flow. He attributed the formation of vortex  $S_0$  to this pressure gradient.

Dargahi (1989) measured the streamwise longitudinal velocity distribution along the plane of symmetry upstream of the cylinder. Measurements were taken at 14 stations

in the region  $-2.5 < x/D < -0.63$ . The distribution agreed with the logarithmic and wake laws, described by Eq. 2.4-1, in the region  $-2.5 < x/D < -1.2$ , whereas in the region  $-1.1 < x/D < -0.63$ , the distribution was influenced by the adverse pressure gradient caused by the cylinder. The velocity profile in this range roughly exhibited the logarithmic form; however, the profile oscillated about a mean peak value of 19 cms with a minimum peak of 12 cms and a maximum peak of 24 cms. Note that the free stream velocity was 30 cms.

**Table 2.5-4. Velocity distribution along a horizontal plane through the center of vortex 1. D represents the pier diameter, x the horizontal distance from the center of the pier, u the horizontal velocity component, v the vertical velocity component, and U the free stream velocity.**

$x/D$	$u/U$	$v/U$
-0.50	0	
-0.52	0	-0.1
-0.54	0	-0.2
-0.56	0	-0.4
-0.58	-0.03	-0.45
-0.60	-0.05	-0.35
-0.62	-0.05	-0.40
-0.64	-0.03	-0.30
-0.66	0	0
-0.68	0.4	0.4
-0.70	0.70	0.45

Dargahi (1989) also determined the bed shear stress by measuring the horizontal velocity gradient at depth  $y/Y_m = 0.0025$ . The results were normalized by  $\tau_m$ , the free stream shear stress and shown in Table 2.5-6. He noted that significant increases of shear stress occurred close to the cylinder at lines drawn at 45 and 90 degrees to the forward stagnation plane. At these locations,  $\tau / \tau_m$  was 4.5 and 3.5, respectively. He also noted that  $\tau / \tau_m$  was equal to 1.5 in the plane of symmetry of the cylinder at the locations of

vortices 1a and 2 and that the horseshoe vortices located 45 degrees from the stagnation plane reached the maximum shear stress value of  $2.5\tau_m$ .

**Table 2.5-5. Pressure distribution along the vertical stagnation line where  $C_p$  represents the pressure coefficient,  $y$  the vertical distance from the channel invert, and  $Y_m$  the flow depth.**

$y/Y_m$	$C_p$
0.01	0.7
0.1	0.65
0.2	0.70
0.3	0.85
0.4	0.87
0.5	0.95
0.6	0.97
0.7	0.98
0.8	0.98
0.9	0.99
1.0	0.99

**Table 2.5-6. Bed shear stress at  $y/Y_m = 0.0025$ .  $\tau$  represents the bed shear stress, values of which are normalized by the free stream shear stress  $\tau_m$ .**

$x/D$	$\tau / \tau_m$
-0.5	-0.6
-0.6	-1.1
-0.7	-1.5
-0.8	-0.5
-0.9	0.02
-1.0	0.5
-1.1	0.55
-1.2	0.6
-1.3	0.7
-1.4	0.8
-1.5	0.9

A number of researchers, Richardson and Panchang (1998), Dey et al. (1995), Baker (1979), and Melville (1975), have studied the properties of the vortex after the development of the scour hole. Data obtained from these sources show that the vortex in the developed scour hole is elliptical in shape with the major axis of the ellipse being

perpendicular to the sloped side of the scour hole. Table 2.5-7 shows vortex parameters determined from the sources listed above.

**Table 2.5-7. Raw vortex data obtained from Melville (1975), Baker (1979), Dey et al. (1995), and Richardson and Panchang (1998)**

$\theta$	D	L	$d_s$	A	b	$a_m$	$x_c$	$y_m$	$V_m/U$	Ref
0.0									0.45	Baker(1979)
27.5	5.00	5.00	5.00	0.90	2.20	0.85	-5.00	-2.80	0.55	Richardson & Panchang(1998)
35.0	5.00	10.50	5.50	1.10	2.75	1.1	-6.00	-2.50	0.6	Richardson & Panchang(1998)
38.0	5.70	12.50	6.00	1.30	3.50	1.25	-6.35	-3.50	0.5	Melville(1975)
40.0	5.70	11.00	6.50	1.30	3.75	1.2	-6.85	-3.60	0.6	Dey(1995)

In Table 2.5-7 above,  $\theta$  is the slope angle of the side of the scour hole, D is the pier diameter, L is length of the sloped side of the scour hole,  $d_s$  is the scour depth, a is the minor axis of the vortex ellipse, b is its major axis,  $a_m$  is the distance along the minor axis to the point of maximum tangential velocity,  $x_c$  is the x-coordinate for the center of the vortex,  $V_m$  is the maximum tangential velocity, and U is the free stream velocity. The data shown in Table 2.5-7 were obtained from pier scour experiments conducted by the researchers using laboratory apparatus of various dimensions. In order to ensure comparison of pertinent results between experiments, all dimensions were normalized by the diameter of the pier used in each experiment and shown in Table 2.5-8. Also included is the normalized y-coordinate of the center of the vortex  $y_c/D$ .

**Table 2.5-8. Normalized vortex data obtained from Table 2.5-7**

$\theta$	$d_s/D$	$L/D$	$a/D$	$b/D$	$x_c/D$	$y_c/D$	$a_m/D$	$V_m/U$
0.0	0.00	0	0.10	0.10	-0.68	0.1	0.08	0.42
27.5	1.00	1.00	0.18	0.44	-1.00	-0.56	0.17	0.55
35.0	1.10	2.10	0.22	0.55	-1.20	-0.50	0.22	0.6
38.0	1.05	2.19	0.23	0.61	-1.11	-0.61	0.22	0.5
40.0	1.14	1.93	0.23	0.66	-1.20	-0.63	0.21	0.6

Briaud et al. (1999) evaluated the shear stresses that occurred around a cylindrical pier using numerical simulations. They used the CHIMERA-RANS method, which entailed dividing the region around the pier into three-dimensional blocks. The Reynolds-Averaged Navier Stokes (RANS) equation was then used to analyze the mesh system thus formed. One of the outputs of the CHIMERA-RANS computer simulations was the shear stress variation on the riverbed around the pier prior to the development of a scour hole (Fig. 2.5-8). Briaud et al. (1999) also found that minimum shear stresses were located at  $0^\circ$  and  $180^\circ$  as shown in Fig. 2.5-8 and in the stagnation plane, while the maximum shear stresses were found at  $45^\circ$ , and  $135^\circ$  to the horizontal.

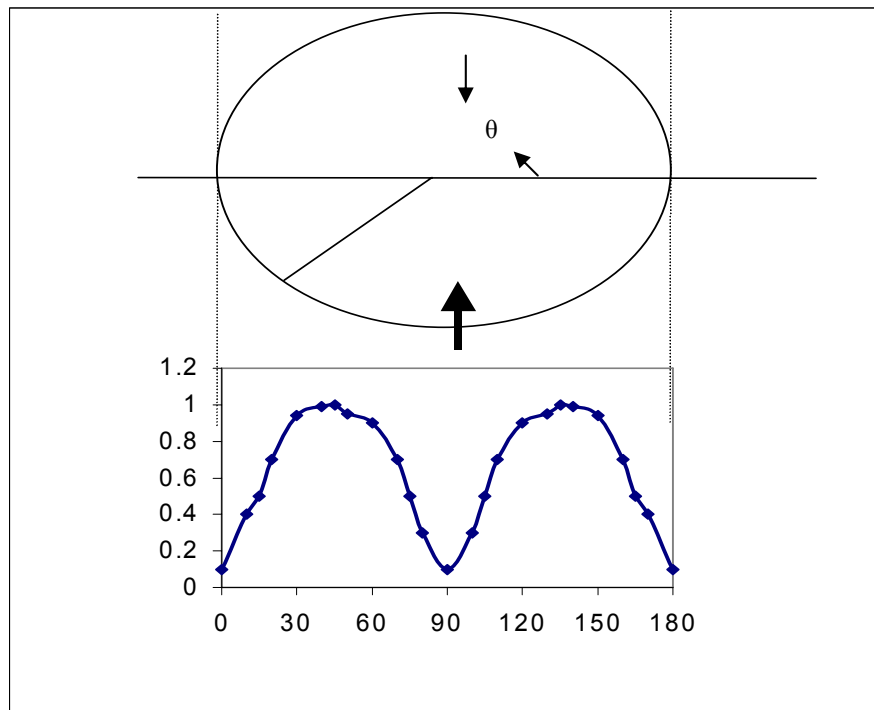


**Figure 2.5-8. Spatial variation in shear stress around a cylindrical pier prior to development of the scour hole. This information was obtained from Briaud et al. (1999). The arrow represents the direction of the oncoming flow. The y-axis shows the shear stress normalized by the maximum scour (located at  $45^\circ$ , and  $135^\circ$ ). The x-axis represents the location on the face of the pier from left to right in degrees.**

## **2.6 CURRENT PIER SCOUR MODELS**

### **2.6.1 Introduction**

Melville and Coleman (2000), along with many other researchers, have developed and discussed a myriad of models and processes applicable to the prediction of scour in riverine and tidal waterways. The acceptance of innovations to the tidal-estuarine modeling process will depend on the ability of the new models or processes to perform in a manner that shows a clear improvement in some respect over the current models and procedures. One method of assessing the performance of a given model is through comparison with current accepted models.

### **2.6.2 Comparative Scour Research**

Jain and Mordi (1986) conducted a comparative study of pier scour equations used in alluvial channels. Model results were compared to field data, collected by Inglis (1949) and Ahmed (1960), from railroad bridges in India. The models used in the study included Larras (1963), Laursen and Tosh (1956), Shen et al. (1969), Breusers et al. (1977), and Lacey (1930). The study results showed that model predictions of scour varied from observed values in the range of -48% to +51%. From these results Jain and Mordi concluded that the equation of Laursen and Tosh (1956) was probably the most accurate as it produced the lowest range of variation from the observed data (-12% to +30%) of all the models studied.

Johnson (1995) compared the following seven bridge-pier-scour equations using field data for both live-bed and clear-water scour: CSU HEC 18 (Richardson and Davis 1991); Melville and Sutherland (1988); Hancu (1971); Breusers et al. (1977); Shen et al.



(1969); Laursen and Tosh (1956) and Jain and Fischer (1979). Johnson also indicated that the data reflecting clear-water scour was of particular significance to bridges located in coastal areas. The study involved the examination of the limitations of each equation for the purpose of providing guidance to practicing bridge hydraulic engineers. The method used included a detailed review and identification of the sources of field data sets published in recent years. Through this method 515 data sets were identified. This process was followed by the computation of scour depths using seven bridge-pier-scour equations and all 515 cases. For each method the computed scour depth was compared to the observed scour depth by a factor ( $\beta$ ) representing the bias between the predicted and observed values:

$$\beta = d_{sc}/d_{so} \quad (2.6-1)$$

where  $d_s$  represents scour depth, and subscripts c and o represent computed and observed values respectively. The bias factor computed for each of the seven methods was then compared for various conditions including flow depth-to-pier width ratio, Froude Number, and velocity-to-critical scour velocity ratio. The coefficient of variance for each method was also computed and assisted in assessing the limitations of each equation.

The results of this study indicated that all the models tested, except Hancu (1971), showed positive biases for high stream velocities ( $V/V_c > 3$ ). The results also showed that at high velocity ranges Melville and Sutherland (1988) had the highest positive bias (300%) while the biases of the other models, excluding Hancu (1971), ranged from 21% found with the HEC 18 model to 41% found with the Laursen and Tosh equation. At very low velocities ( $V/V_c < 0.5$ ), all the models except Breusers et al., Hancu, and Shen et al., showed positive biases in the range of 270% to 400%. The equations of Breusers et

al., (1977) and Hancu (1971) had a bias of zero at very low velocities, while Shen et al., (1969) under-predicted by 50%.

## **2.7 MODEL COMPONENTS FOR ESTUARINE BRIDGE SCOUR ANALYSIS**

### **2.7.1 Introduction**

The assessment of scour in estuaries and tidal rivers presents a diverse and varied process and gives rise to a whole spectrum of models used in scour simulations and designs. The hydrodynamic multi-dimensional deterministic numerical models are at the complex end of the spectrum while at the other end, are the much simpler empirical models. Tidal bridge scour models typically consist of the following components: the tidal and riverine hydrologic components where both components are used to determine resultant estuary discharges, the hydraulic component where the associated velocities and water surface elevations are computed, and the sediment production and transport component where the computed velocities and flow depths are used to predict the amount of sediments that will be removed from the system that causes the resulting scour hole. In order to develop a model for the prediction of estuary scour, it was necessary to review the literature for research information related to all the components that would be included in such a model.

### **2.7.2 The Riverine Hydrologic Component**

Hydrologic methods used to determine the response of a catchment basin to rainfall inputs is an area that is well studied and beyond the scope of this dissertation. A large number of hydrologic methods are available for use in the development of the

catchment or riverine component of the model and relevant information on these may be found in most hydrologic texts. The SCS TR-55, and TR-20 models are of particular interest as these models are widely accepted by the engineering community and they require only a modest amount of field data to produce results. Details on the use and development of the TR-55 and TR-20 models can be found in the SCS technical releases TR-55 (1986) and TR-20 (1984).

### 2.7.3 The Tidal Hydrologic Component

Neill (1973) proposed the following equation for the estimation of the maximum natural tidal discharge:

$$Q_{\max} = (\Omega * \pi) / T \quad (2.7-1)$$

where  $\Omega$  = the tidal prism or the volume of water in the estuary between low and high tide levels and  $T$  = the tidal period or the time interval between successive high or low tide. The corresponding maximum velocity ( $V_{\max}$ ) through the inlet cross-section is given by:

$$V_{\max} = (\Omega * \pi) / (A * T) \quad (2.7-2)$$

where  $A$  is the cross-sectional area of the waterway opening at the mean water level.

Assuming a sinusoidal variation the discharge equation becomes:

$$Q = Q_{\max} \sin (2\pi t / T) \quad (2.7-3)$$

Neill states that the assumption of sinusoidal variation is correct only in estuaries with vertical shorelines, but it is acceptable if the relative difference between the estuary surface areas at low and high tides is small.

Chang (1998) modified the format of the Neill's equation and placed it in a form consistent with the continuity equation for steady flow. Chang's modification of Neill's equation can be represented as follows:

$$A_c * V_c = A_s * V_s \quad (2.7-4)$$

where:  $A_c$  is the cross-section area at the mouth of the estuary,  $V_c$  is the horizontal velocity across the mouth of the estuary,  $A_s$  is the total surface area of the estuary, and  $V_s$  is the velocity of rise or fall of the water surface at the estuary mouth. The horizontal tidal movement can be modeled as a sine wave where:

$$h(t) = H/2[1 - \cos(2\pi t/T)] \quad (2.7-5)$$

$V_s(t)$  is obtained by differentiating equation 2.7-5:

$$V_s(t) = (H\pi/T) \sin(2\pi t/T) \quad (2.7-6)$$

where  $H$  is the distance between high and low tides (the tidal range).

$V_c$  becomes:

$$V_c(t) = (A_s/A_c) (H\pi/T) \sin(2\pi t/T) \quad (2.7-7)$$

Maryland State Highway Administration (SHA) uses Chang's version of the Neill's equation in their bridge design work.

Neill's equation is commonly used for the estimation of tidal flows in estuaries. As a first-order approximation, Neill assumes that the water surface in an estuary rises or falls in response to flows through the cross-section at its mouth. In short estuaries, this assumption is appropriate as the water surface essentially remains horizontal and its rise and fall over the total surface area of the estuary exhibits a prismatic behavior. However, in longer estuaries, the water surface will not remain horizontal and the rate of change of tidal elevation will vary along the length of the estuary. In addition, the more realistically

modeled peak tidal flow will be lagged in time with respect to the peak tidal surge at the estuary mouth. Neill's equation provides a fast and inexpensive method for the determination of tidal flows; however, the use of this model is limited to specific conditions and assumptions not usually encountered in real situations.

Demetrius et al. (2002) developed the following regression equations to represent the tidal components in real estuaries, by the analysis of estuarine tidal mechanisms and model simulations:

$$V_{\text{falling}} = V_c(t) * (b_{\text{max}}/b)^{0.329} (H/y)^{-0.186} (L/cT) \text{ for } b_{\text{max}}/b > 1$$

$$V_c(t) \text{ otherwise} \quad (2.7-8)$$

where  $V_{\text{falling}}$  is the tidal velocity due to the falling tide directed downstream at the location of concern,  $V_c(t)$  is the velocity predicted by the Chang's modification of Neill's equation,  $b_{\text{max}}$  is the maximum estuary width upstream of the location of concern,  $b$  is the width of the estuary at the location of concern,  $H$  is the difference in height between high and low tide,  $y$  is the riverine or non-tidal component of the flow depth,  $L$  is the estuary length to location of interest,  $c$  is the wave celerity ( $gy$ )<sup>0.5</sup>, and  $T$  is the tidal period.

Similarly

$$V_{\text{rising}} = -V_c(t) * (b_{\text{max}}/b)^{0.053} (H/y)^{-0.138} (L/cT) \text{ for } b_{\text{max}}/b > 1$$

$$-V_c(t) \text{ otherwise} \quad (2.7-9)$$

where  $V_{\text{rising}}$  is the tidal velocity due to the rising tide directed upstream at the location of concern, hence the negative sign. The discharges predicted by Demetrius et al. (2000) are as follows:

$$Q_{\text{rising}} = Q_N \{1 + \sin[((L/cT) - 0.01)^{1.04} * (b_{\text{max}}/b)^{0.58} (H/y_m)^{-1.13}]\} \text{ for } (L/cT) > 0.01$$

$$Q_N \text{ otherwise} \quad (2.7-10)$$

While for the falling limb:

$$Q = Q_N(L/cT)^{0.09} (H/y_m)^{0.256} \quad (2.7-11)$$

#### **2.7.4 The Hydraulic Component**

Much research has been done in the development of hydrodynamic numerical models, which have the potential of providing accurate predictions of flow discharge, velocity, and flow depth, but which also require many more resources in terms of computational time, data, and money. The U.S. Army Corps of Engineers (1991) identifies two types of hydrodynamic models: coupled, and linked. Hydrodynamic models are said to be coupled if they model the processes of hydrodynamics and sediment transport simultaneously and interactively using the same spatial and temporal grid. In linked models, the output of the hydrodynamic process is used as the input for the sediment transport model. The U.S. Army Corps of Engineers also refers to the hydrodynamic models as numerical models, as they solve the hydrodynamic equations of mass and momentum numerically using either finite difference or finite element methods. The solutions of hydrodynamic equations using numerical methods have been investigated by many researchers including Muir (1978), Stelling (1980), and Prandle (1982). Shelden and Martin (1998) used the Army Corps of Engineers' two-dimensional RMA-2 finite element hydrodynamic computer model along with the FHWA HEC-18 scour model to determine scour depths in a North Carolina estuary. Although Shelden and Martin reported acceptable results, there appears to be a potential for the loss of accuracy when a hydrodynamic model is linked to an empirical scour model such as the HEC-18, owing to the uncertainty of the local scour component. Hu et al., (1995) also

used the RMA-2 linked to the SEDH finite element sediment transport model to determine the accretion (aggradation) process in a tidal marsh over a 5-year simulation period.

Hydrodynamic models along with numerical models for sediment transport have the potential of providing the most accurate predictions of estuary processes; however, these models have certain disadvantages. Hydrodynamic models require large investments of resources (time, money, trained personnel) and are subject to issues such as the stability of results and numerical dispersion. It is generally recommended in the literature that hydrodynamic models be considered only if there are adequate resources to support them or if the problem is sufficiently complex to warrant their use.

The next level of hydrologic-hydraulic modeling, in terms of accuracy, is one-dimensional unsteady flow models such as UNET (Barkau, 1996). The UNET algorithm is based on the solution of the finite difference approximation of the St. Venant equations in one dimension. UNET performs hydraulic computations for channels, overbanks, bridges, and culverts and includes potentially filled or inundated bay, estuary, and floodplain areas. UNET also has the ability to model the flows associated with a wide range of hydraulic structures including bridge piers. Disadvantages of UNET include the inability to model flows that are significantly two-dimensional. Also, like most finite difference models UNET is subject to issues of stability and truncation errors.

Next on the scale of potential accuracy are the conceptual models based on simple theory and the empirical models. The orifice approach presented by Richardson and Davis (1995) represents a simple conceptual model for constricted waterways such as inlets to enclosed tidal bays. Where energy loss is confined to the inlet channel and the

adjoining bay is only filled during a tidal cycle, the maximum flow velocity through the inlet may be computed as:

$$V_{\max} = C_d(2g\Delta H)^{1/2} \quad (2.7-12)$$

where  $C_d$  is the discharge coefficient and  $\Delta H$  is the maximum head differential. The discharge coefficient includes entrance and exit losses and friction loss through the channel. This approach has been applied to daily tides where the head differences can be measured. For storm-surge computations the head difference must be estimated, which in practical applications can be difficult.

### **2.7.5 Sediment Transport and Scour Models**

Numerical models of analytical descriptions have been developed by researchers to simulate general, contraction, and local scour. Most of these models use the outputs from hydraulic models for their scour simulations. The number of models and variations of them are significant, so only a few of these models are reviewed below.

CH3D of the U. S. Army Corps of Engineers (Engel et al., 1995) is a three-dimensional flow model that has been recently upgraded to simulate sediment transport and erodible boundary development. SEDH is a multi-dimensional finite element sediment transport and deposition model based on a sediment transport equation developed by Krone (1962). This model is used in circumstances where the most accurate results are required owing to its complexity, data requirements, and costs related to data gathering and simulations.

The U. S. Army Corps of Engineers HEC6 (1977) is a one-dimensional movable boundary open channel numerical model designed to predict changes in river profiles due



to scour or deposition. The model uses a continuous flow record to compute water surface profiles of the channel thereby providing energy slopes, velocity, and depth at each cross-section. Potential sediment transport rates are then computed at each section. These rates, combined with the duration of flow, permit a volumetric accounting of sediment within the reach. Numerical scour models present a significant limitation in their inability to predict local scour. Also, in order to confidently use numerical models to analyze and forecast scour, the process of acquiring the measured data required for the calibration and validation of these models may significantly impact available resources.

Melville and Coleman (2000) have outlined a wide range of empirical models that may be used to address all scour types. Included is an empirical model that predicts local scour due to wave action. Accordingly, the model was included in the comparative study of this dissertation to determine if it was applicable to tidal environments:

$$d_s/b = 2.0[1 - \exp(0.03 \{KC - 6\})] \quad (2.7-13)$$

$$KC = V_m T/b \quad (2.7-14)$$

where  $V_m$  is the maximum value of the oscillatory flow velocity due to the waves,  $T$  is the wave period,  $b$  is the pier width, and  $d_s$  is the scour depth.

Breusers (1965) also developed a simple empirical equation from the results of a study done on bridge pier local scour in tidal waterways. Breusers found that  $d_s$  was equal to 1.4 times the width of the bridge pier. Most of the above empirical equations are simple and easy to use; however, they are typically developed from laboratory data causing them to reflect idealistic conditions only and the range of the data used in their development. Table 2.7-1 shows a number of empirical local scour models currently in use.

**Table 2.7-1. Empirical local scour models**

<b>Eq #</b>	<b>Author/ Ref.</b>	<b>Scour Type</b>	<b>Equation</b>
1	Johnson (1991)	Both	$\Delta d_s / \Delta t = C(V_d - V_t)$ $V_t = C_1(2\rho_s + gdG \sin \phi / 3 [2(1 - \sin \phi)]^{0.5} - C_2 G \exp(-cV_o)$
2	Liu et al	Clear water	$d_s = d_{se} (1 - \exp[-ct/t_o/(1-t/t_m)])$
3	Shen et al	Clear water	$d_s = 2.23 \times 10^{-4} (Ub/v)^{0.619}$
4	Baker	Clear water	$d_s/b = (a_1 N - a_2) \tanh(a_3 y/b)$ ; $N = U/(\Delta \gamma_s d / \rho f)$
5	Breussers	Clear water	$d_s/b = f_1(U/U_c) [2 \tanh(y/b)] f_2(\text{shape}) f_3(\alpha, l/b)$
6	Ettema	Clear water	$d_s/b = K_1 \ln[dtv/b^3] + \ln K_2$
7	Jain 1981	Clear water	$d_s/b = 1.84 [y/b^{0.3}] [F_{rc}]^{0.25}$
8	Englis	Live bed	$d_{se}/b = 2.32 (q^{0.67}/b)^{0.78}$ lab data
9	Englis	Live bed	$d_{se} = 0.47 K (Q/f_1)^{0.33}$ field data
10	Laursen & Tosh	Live bed	$d_{se}/b = 1.5 (y/b)^{0.30}$
11	Hancu	Live bed	$d_{se}/b = 3.3 (d/b)^{0.20} (y/b)^{0.13}$
12	Coleman	Live bed	$d_{se}/b = 1.49 (U^2/gy)^{0.10}$
13	Breussers	Live bed	$d_{se} = 1.4(b)$
14	Basak et al	Live bed	$d_{se} = 0.558 b^{0.586}$
15	Neill	Live bed	$d_{se} = 1.34 K (q^2/f_1)^{0.5}$ field data
17	Railways Ministry, India	Live bed	$d_{se} = 0.47 K (Q f_1)^{0.33}$ River field data
18	Izzard & Bradley	Live bed	$d_{se} = 2.15 [Q/(B-b)]^{0.67}$ lab and field data
19	Jain & Fischer	Live bed	$d_{se}/b = 2.0 (y/b)^{0.5} [F_r - F_{rc}]^{0.25}$
20	HEC18		$d_s = 2y K_1 K_2 K_3 K_4 [b/y]^{0.65} F_r^{0.34}$
21	Laursen 1958	Live bed	$d_{se}/y = 0.182 (b/y) \{ [(d_{se}/11.5y) + 1]^{1.7} - 1 \}^{-1}$

**Table 2.7-1 (cont'd) Empirical local scour models**

<b>Eq #</b>	<b>Author/ Ref.</b>	<b>Scour Type</b>	<b>Equation</b>
22	Laursen 1958	Live bed	$d_{se}/b=1.11(y/b)^{0.5}$
23	Larras 1963		$d_s/b=1.05b^{0.75}$ for circular piers
24	Blench 1969		$d_s/b=1.8(y_r/b)^{0.75}-y/b$ ; $y_r = 1.48(q^2/1.9d^{0.5})^{0.33}$
25	Coleman 1971		$d_s/b=0.54(y/b)^{0.41}(U^2/gy)^{0.6}y^{0.41}$
26	Hancu 1971	Both	$d_s/b=2.42[(2V/V_c)-1](y/b)^{0.33}(V_c^2/gb)^{0.33}$ ( $2V/V_c$ )-1=1 for live bed
27	Chitale 1988		$d_s=2.5b$
28	Melville 1997	Both	$d_s=K_{yb} K_d [(V-(V_a-V_c)/V_c)]$ ; $K_{yb} = 2.4b$ for $b/y < 0.7$ , $2(by)^{0.5}$ for $0.7 < b/y < 5$ , $4.5y$ for $b/y > 5$ $K_d = 0.057 \log[2.44b/d_{50}]$ for $B/d_{50} \leq 25$ , 1 for $B/d_{50} > 25$
29	Ansri & Qadar 1994		$d_s=0.86b^3$ for $b < 2.2m$ ; $3.60b^{0.4}$ for $b > 2.2m$
30	Gao et al 1993	Both	$d_s=0.46K_\zeta b^{0.6} y^{0.15} d^{-0.07} [(V-V'_c)/(V_c-V'_c)]^\eta$ ; $\eta \leq 1$
31	Richardson & Davis 1995		$d_s/b=2K_3 K_4 [y/b]^{0.35} F_r^{0.43}$
32	Lacey		$ds=K(0.473)(Q d_{50}-0.57)^{0.33}$
33	Maza & Sanchez	Live bed	$dse/b=2Kf K5 (V^2/gb)- 30(d/b)$
34	Garde		$ds/y=4n_1 n_2 n_3 (1/\alpha) Fr^n$

Johnson and McCuen (1991) developed a local scour model to account for temporal and spatial variations of scour at a bridge pier. The model is represented as:

$$\Delta D/\Delta t = C(V_d - V_t) \quad (2.7-15)$$

where  $\Delta D/\Delta t$  is the rate of change of depth of the scour hole with time,  $V_d$  is the downward velocity responsible for local scour, and  $V_t$  is the termination velocity, which

is the magnitude of the downward velocity when it has decreased to a value that is no longer capable of causing erosion. Though not developed for estuarine conditions, it would be of interest to determine if the model could be applied to estuaries to account for the long-term flow duration of storms occurring prior to failure.

Most scour equations require the critical velocity of the channel bed material. However, the incipient velocity provides more realistic scour estimates because it accounts of scour that occurs prior to the velocity of the stream reaching its critical value. The incipient velocity may be determined by estimating the critical erosion velocity and adjusting this velocity with a reduction factor. Neill (1968) suggests the following equation to determine the critical velocity  $U_c$ :

$$U_c = 4.81[(S_s - 1)gd_{50}]^{0.5}[y/d_{50}]^{0.17} \quad (2.7-16)$$

where  $U_c$  is the critical velocity above which bed materials of size  $d_{50}$  or smaller will be transported and is measured in ft/sec.  $S_s$  is the specific gravity of the bed materials and  $y$  is the flow depth in meters. The median particle size,  $d_{50}$ , is measured in meters.  $U_c$  is also accepted by researchers as the velocity at which scour conditions change from clear water to live bed.

Melville and Sutherland (1988) used the following equation to determine the critical velocity associated with movement of the bed material:

$$U_c/v_{*c} = 5.75[\log(5.53Y/d_{50})] \quad (2.7-17)$$

in which  $Y$  is the flow depth in feet and  $d_{50}$  is the mean particle diameter in feet.  $v_{*c}$  is the shear velocity given by:

$$v_{*c} = 1.66 d_{50}^{0.5} \quad (2.7-18)$$

where  $d_{50}$  is in ft and  $v_{*c}$  is in ft/sec.

Using data from the Academy of Railway Sciences in China, Dongguang et al., (1993) determined that the incipient velocity of the bed materials in most rivers and waterways was lower than the critical velocity of the bed material. They developed the equations shown below to represent the incipient velocity  $V_i$  in ft/sec.:

$$V_i = 0.645 (d_{50}/B)U_c \quad (2.7-19)$$

If all the variables except  $d_{50}$  are expressed in English units the above equation becomes:

$$V_i = 0.476 (d_{50}/B)U_c \quad (2.7-20)$$

where  $d_{50}$  is in millimeters, and  $B$  represents the pier diameter in feet.

Melville and Coleman (2000) discuss natural armoring as the process by which finer materials of the channel bed are more frequently suspended by the flow thus causing a layer of larger sizes material at the surface of the bed. Richardson and Davis (2001) recommend against using this consideration in the design and analysis of bridge piers because it reduced the overall safety of pier designs. Melville and Coleman (2000) suggest the following process to determine the incipient velocity of a naturally armored stream. First the method is used only if the standard deviation of the channel bed soils is greater than 1.3. The standard deviation may be determined from:

$$\sigma = (d_{84}/d_{16})^{0.5} \quad (2.7-21)$$

where  $\sigma$  is the standard deviation of the particle sizes in the bed material. If the standard deviation in the soil particle sizes is greater than 1.3, then the mean armoring particle diameter is computed as:

$$d_{50a} = d_{max}/1.8 \quad (2.7-22)$$

where  $d_{50a}$  (mm) is the mean armoring particle diameter and  $d_{max}$  (mm) is the maximum soil particle size. Next critical armoring velocity  $U_{ca}$  is determined from:

$$U_{ca} = 4.81[(S_s - 1)gd_{50a}]^{0.5}[y/d_{50a}]^{0.17} \quad (2.7-23)$$

Finally, the incipient armoring velocity is given by:

$$U_a = 0.8U_{ca} \quad (2.7-24)$$

Combining equations 2.7-23 and 2.7-24 and substituting for the specific gravity of water and  $d_{50a}$  gives:

$$U_a = 1.328(d_{max}/1.8)^{0.33}y^{0.17} \quad (2.7-25)$$

where  $U_a$  and  $U_{ca}$  are in ft/s,  $y$  is in feet and  $d_{max}$  is in millimeters.

## 2.8 HURRICANES AND ASSOCIATED MODELS

Many dangerous and destructive tropical storms and hurricanes have occurred along the Atlantic and Gulf coast areas of the United States. Notable among these is the great storm of September 1900 that took the lives of over 6000 people in Galveston, Texas. In addition to the loss of lives, tropical storms have also caused the loss of billions of dollars in property damage. Among the hurricanes that affected the Chesapeake Bay area are Hazel (1954), Connie (1955), Dianne (1955), Donna (1960), Camile (1969), Agnes (1972), Eloise (1975), David (1979), Hugo (1989), Floyd (1999), Isabel (2003), and Charley (2004).

The National Weather Service has recorded the track of significant tropical storms that have occurred since 1900. From this data, the most likely track of storms with the greatest impact to the Chesapeake Bay area was determined. The storms are usually formed in the Tropical Atlantic and generally move towards the northwest. Landfall is typically made along the United States east coast at the Carolinas. The storms then track inland towards the north along a path that takes them parallel to the Chesapeake Bay.

According to the National Weather Service, the degree of impact on locations in the Chesapeake Bay area depends greatly on the path of the storm in relation to the location. Because of the anti-clockwise circulation of the winds in hurricanes, locations to the east side of the storm will be subjected to stronger wind forces than locations to the west of the hurricane. This is due to the fact that locations to the east of hurricanes will be exposed to the resultant wind velocities comprised of the hurricanes' northern translational velocity and the wind circulation velocity. These velocities oppose each other at locations to the west, side of the hurricane.

Much of the destructive impacts caused by hurricanes are due to the wind velocities and storm surge that accompany the hurricanes. The hurricane wind velocity is the resultant of the hurricane circulation and translational velocities. The hurricane storm surge is the rise in coastal, estuarine, or riverine water surface elevations caused by a combination of the hurricane winds and the reduced air pressure due to the hurricane. National Weather Service researchers are also convinced that the storm surge from a hurricane has the greatest destructive impact on the bridge pier (NOAA, 1977). There is conclusive evidence (NOAA, 1977) that the momentum and force of the surge wave have the greatest impact on the bridge pier and deck, and are the leading causes for failure of these structures in a hurricane event. However, little is known about the impact that a surge wave may have on the development of scour around a bridge pier.

The Saffir-Simpson hurricane scale is a 1-5 rating based on the hurricane's strength used by the National Weather Service to estimate the potential property damage and flooding expected from a hurricane. Hurricane wind speed is the determining factor in the scale as surge heights are dependent on the slope of the continental shelf and the

shape of the coastline at the location of the hurricane landfall. Category one hurricanes have a wind speed of 74-95 mph and a surge height of 4-5 ft. Category two hurricanes have a wind speed of 96-110 mph and a surge height of 6-8 ft. Category three hurricanes have a wind speed of 111-130 mph and a surge height of 9-12 ft. Category four hurricanes have a wind speed of 131-155 mph and a surge height of 13-18 ft. Finally, category five hurricanes have a wind speed greater than 155 mph and a surge height greater than 18 ft.

Most of the models developed to represent the hydraulic properties of hurricanes and their effects employ the use of sophisticated and costly three-dimensional hydrodynamic models. However, a few simple one-dimensional models are in existence. The U.S. Army Corps of Engineers (1986) developed the following simple temporal hurricane surge model for semi-diurnal tidal regimes:

$$Z(t) = S * \exp [ - ( t - t_m )^2 / 2t^2 ] \quad (2.8-1)$$

where  $Z$  is the surge height at a given time  $t$ ,  $S$  is the maximum surge value, and  $t_m$  is the time at which the maximum surge occurs. The U.S Army Corps of Engineers (1986) recommends regarding each parameter as stochastic being the realization of a random storm. The values may therefore be generated from random numbers if the distributions are determined.

Richardson and Edge (1997) used historical events to develop the following synthetic storm surge hydrograph:

$$S_t(t) = S_p * [1 - \exp (-D/t)] \quad (2.8-2)$$

In equation 2.8-2,  $D$  is  $R$  divided by  $f$ ,  $R$  is the hurricane radius in miles,  $f$  is the translational speed in miles per hour,  $S_p$  is the maximum surge in feet, and  $S_t$  is the surge



at a given time  $t$ . Richardson and Edge (1997) recommend that the values of  $R$  and  $f$  be determined from the National Weather Service hurricane classification data.

## **2.9 DEVELOPMENT OF A CONCEPTUAL MULTI-SCALE FRAMEWORK**

### **2.9.1 Introduction.**

Scour in estuaries and rivers is dependent on the hydrologic-hydraulic and the sedimentation-and-transport processes. Advective turbulence and dispersion in the form of eddy currents further impact sedimentation. Researchers have shown great interest in understanding the situations where advective turbulence dominates over eddy dispersion, and visa versa. The scale concept is one method used to determine the relative importance of these processes.

### **2.9.2 Available Methods of Scale Determination**

For the purpose of water quality modeling in surface waters, Chapra (1997) used parameters and variables from the advection-diffusion model to determine the scale of importance for dispersion or eddy dispersion. The one-dimensional advection-diffusion equation can be written as:

$$\partial C / \partial t = -U \partial C / \partial x + E \partial^2 C / \partial x^2 \quad (2.9-1)$$

where  $C$  is the concentration of the pollutant,  $U$  is advection (ft/sec),  $L$  is the length of the system (ft), and  $E$  is the diffusion coefficient (ft<sup>2</sup>/sec). The Peclet number,  $P_e$ , is a dimensionless quantity and was developed through a dimensionless analysis of Equation 2.9-1:

$$P_e = LU/E \quad (2.9-2)$$

According to Chapra (1997) if  $P_e$  is greater than 10, then advective or riverine flow dominates. If  $P_e$  is less than 0.1, then dispersion or the ocean process dominates. For  $P_e$  between 0.1 and 10, both dispersion and advection are important, and the environment is essentially estuarine. Chapra further defines an estuary as the region where a free flowing river meets the ocean. He treats the estuary system as a number of zones based on the interaction of advection and dispersion. Table 2.9-1 depicts these zones along with the relative importance of the two processes mentioned. The importance of the Peclet number in the analysis of bridge pier scour is that it may be used in determining the expected scour mechanisms. For example, it was discussed earlier that general scour, and to some extent contraction scour, do not contribute significantly to total scour in fully mixed or partially mixed estuaries that have low fresh water advection. By knowledge of the Peclet number, one could determine the degree of mixing expected in a particular estuary and hence deduce the expected scour mechanisms.

**Table 2.9-1. Table Of The Various Scales Of An Estuary System**

<b>Zone or Scale</b>	<b>Advection</b>	<b>Dispersion</b>	<b><math>P_e</math></b>
<b>River</b>	Yes	No	>10
<b>Tidal River</b>	Yes	Minimal	>10
<b>Estuary</b>	Yes	Yes	Between 0.1,10
<b>Bay</b>	Minimal	Yes	<0.1
<b>Ocean</b>	No	Yes	<0.1

Hydrodynamic models used in the designs for protection against bridge scour in estuarine environments utilize the ocean as a downstream boundary condition. A

problem arises in defining the correct method for determining the ocean boundary. Edge et al., (1998) have investigated a number of methods of defining the so-called ocean scale. The most promising method was the single design hydrograph (SDH) that produces a downstream boundary hydrograph based on data developed from storm surge elevations provided by FEMA and NOAA. The duration of the downstream hydrograph is equal to the average value of the historical data at the site considered and is combined with a mid-rising tide. This method has a significant disadvantage in that it does not provide any spatial references for the ocean boundary.

Metha and Prakash (1988) approached the hydrodynamic modeling of an enclosed bay in terms of two separate regimes of scale. One pertained to the channel through the land barrier. The other termed the near-field region as the region characterized by the ebb and flood circulation beyond the channel.

Another type of scaling estimation in estuarine environments affects the degree of wave damping or amplification. Savenije (1998) showed, through an analytical solution of the St. Venant equations in a La Grange reference frame, that the damping of the wave, and hence the water surface elevation, depends on the friction number  $g/C^2$ , where  $C$  is equal to  $(gy)^{1/2}$ . Wave amplification was dependent on the estuary shape number  $h/b$  and the wave range-to-depth ratio  $H/h$ . Here  $h$  is the depth of the estuary,  $H$  is the range of the wave, and  $b$  is the convergence length defined by:

$$b = -X / (\ln(B/B_0)) \quad (2.9-3)$$

where  $X$  is the distance from the mouth of the estuary,  $B$  is the average width, and  $B_0$  is the width at the mouth. The typical representation of the St. Venant equations assumes the Eulerian reference frame that conceptually depicts an observer viewing the flowing

system from a stationary position along its banks. In contrast, the La Grange reference frame depicts the observer moving along with the flow (say drifting in a boat). The choice of reference frames affects the treatment of the convective acceleration term in the St. Venant equation.

### **2.9.3 The Melville-Coleman Approach**

Melville and Coleman (2000) comprehensively studied the scour around bridge piers in riverine environments. They suggested that the scour of riverbeds at bridges is a complex problem that can be evaluated at many different levels of detail and that the total scour depth at a bridge foundation depends on aspects that range from very localized factors, such as the geometry of the foundations, to the geomorphic factors that must be considered at the wider catchment scale. Table 2.9-2 provides a comprehensive view of the bridge scour process with respect to the scales suggested by Melville and Coleman (2000).

Elements of the bridge pier scour process occur at different scales that require varying details to be adequately considered. To address the possible scales involved, the authors proposed a conceptual scale approach for a scour analysis framework. The Melville-Coleman approach consists of the following spatial scales earlier developed by Parola et al. (1996).

### **2.9.4 The Catchment Scale**

The catchment scale, which defines the limits of the catchment that contributes flow through the bridge, is used for the derivation of flood (Q) discharge hydrographs

and an estimation of the sediment flow ( $Q_s$ ) from the catchment area.  $Q_s$  is important as it helps in determining to what degree scour will be clear water scour or live bed scour.

Geomorphic characteristics and geomorphic evolution are also considered at this scale.

**Table 2.9-2. Melville and Coleman's (2000) Scale Approach to Riverine Bridge Scour Analysis**

	<i>Catchment</i>	<i>Stream</i>	<i>Far Field</i>	<i>Near Field</i>	<i>Local</i>
<b>Important Temporal Variables</b>	Time scale Time of concentration, Intensity Hydrograph time base	Peak or time varying discharge	Peak or time varying discharge, sediment yield	Peak or time varying discharge, sediment yield	Peak or time varying discharge, sediment yield
<b>Important Spatial Variables</b>	Area Precipitation Imperviousness Slope	Channel geometry Hydraulic parameters	Channel geometry Hydraulic parameters	Channel geometry Hydraulic parameters, pier geometry	Hydraulic parameters, pier geometry
<b>Process</b>	Hydrologic Geomorphic Sediment production	Fluvial, meander headcut	Fluvial, bed-form migration	Interaction of bridge structure	Local erosion at bridge foundation
<b>Outputs</b>	Q(discharge) Qs( sediment yield) Geomorphic Details	Long term general scour Depth	Short term general scour Depth	Localized scour depth	Local scour depth
<b>Type of Analysis</b>	Field inspection Hydrologic	Hydraulic, sediment transport	Hydraulic, sediment transport	Hydraulic, sediment transport, scour depth	Hydraulic, Scour depth
<b>Data req. and source</b>	Catchment characteristics from maps, field observations	Channel cross sections, Properties of bed and bank	Channel cross sections, Properties of bed and bank	Channel cross sections, Properties of bed and bank, Pier geometry	Pier geometry, Properties of bed and bank
<b>Type of Model</b>	1-D for transport empirical geomorphic relationships	1-D for transport empirical geomorphic relationships	1-D or 2-D	2-D for transport empirical scour relationships	empirical scour relationships 3-D hydro-mechanic
<b>Type of Scour</b>	Long term general Degradation Aggradation	Long term General	short term general	Contraction Scour	Local scour

The geomorphic characteristics and the geomorphic evolution of a catchment are based on the premise that river form and fluvial processes evolve simultaneously through mutual adjustment towards self stabilization. Leopold and Maddock (1953) were among

the first to establish the connection between stream geometry and stream hydrology.

Their work on the hydraulic geometry of streams led to the development of the following power equations:

$$W = aQ^b \quad (2.9-4)$$

$$H = cQ^d \quad (2.9-5)$$

$$U = eQ^f \quad (2.9-6)$$

where  $W$  is the stream width,  $H$  is the stream depth,  $U$  is the mean velocity,  $Q$  is the discharge (volumetric flow rate), and  $a$ ,  $b$ ,  $c$ ,  $d$ ,  $e$ , and  $f$  are constants determined from stage-discharge rating curves. Rosgen (1996) extended this relationship to include sediment discharge:

$$Q_s d_{50} = kQS \quad (2.9-7)$$

where  $Q_s$  is the sediment discharge,  $Q$  is the volumetric discharge,  $d_{50}$  is the mean particle size of the sediment material within the channel,  $S$  is the channel slope, and  $k$  is a constant. By assessing the geomorphic characteristics of the watershed streams, estimates of  $Q$  and  $Q_s$  can be made based on the empirical geomorphic relationships. Knowledge of the geomorphic evolution of the catchment is useful in assessing the nature of the sediment deposits and the expected rates of sedimentation.

### **2.9.5 The Stream Section Scale**

The stream section scale, which extends about 20 valley widths upstream and downstream of the bridge site, is used primarily to assess geomorphic changes that may lead to long-term general scour at the bridge site. These geomorphic changes include stream meander, the relative stability of the stream over the expected life of the bridge,

sediment migration, and the degradation/aggradation behavior of the stream channel that impact long-term general scour at the bridge site. The output from the stream section scale includes long-term general scour and sediment flow.

### **2.9.6 The Bridge Far-Field Scale**

The bridge far-field scale is used to determine water surface elevations for use in subsequent scour analyses. This scale is also used for the determination of short-term general scour. The spatial limits of the scale extend upstream and downstream from the bridge crossing at a sufficient distance for this purpose. However, relevant flow information is needed for at least three channel widths upstream and downstream of the bridge. Melville and Coleman (2000) indicated that at the bridge far-field scale the time scale is the duration of the flood hydrograph or a succession of hydrographs. The bridge far-field scale is different from the stream section scale in that long term general scour and stream stability are not assessed.

### **2.9.7 The Bridge Near-Field Scale**

This scale extends upstream and downstream from the bridge crossing to the cross sections where the flow velocities are unaffected by the presence of the bridge. The primary purpose of the bridge near-field scale is to determine contraction scour depths and the flow parameters for local scour depth estimation. Such flow parameters include details of the flow and velocity distribution in the main channel and adjoining floodplain, flow depth, and the rates of sediment transport. The time scale of the bridge near-field scale is also the duration of the flood hydrograph or a succession of hydrographs.

### **2.9.8 The Local Scale**

According to Melville and Coleman (2000), the purpose of analysis at the local scour scale is to estimate the local scour depths. The individual scour control volume encompasses the local scour hole formed around the piers and extends upstream and downstream to the extent of the influence of the pier foundation structure, while the time scale is the duration of a single flood. The flow at this scale is highly three-dimensional and, according to Melville and Coleman (2000), and it is not yet possible to model such flows numerically or analytically. Important factors at this scale include the three dimensional horseshoe vortex system, turbulence, boundary roughness, sediment transport characteristics, bed material characteristics, and phenomena such as armoring. The significant time scale is the duration of a single flood or succession of floods.

## **2.10 MODEL EVALUATION AND ANALYSIS**

### **2.10.1 Introduction**

An evaluation and analysis of the developed model is necessary to assess its performance with regards to the required goal and objectives. Included in the method of assessment is a detailed uncertainty and sensitivity analysis of the model. Johnson (1996) determined that hydraulic methods and designs are best analyzed using probabilistic and reliability methods, and that the estimation of reliability requires knowledge of the total uncertainty associated with the method. McCuen (2003) expresses the need for sensitivity analyses in modeling studies by stating “an understanding of the foundations of sensitivity analysis should ensure that the results are presented in ways that will ensure that the modeling efforts lead to the best possible decision”.



### 2.10.2 Sensitivity Analysis

McCuen (1973) defines sensitivity as the rate of change of one factor with respect to change in another factor. McCuen further defines two types of sensitivities, parametric sensitivity and component sensitivity. Parametric sensitivity is the rate of change of the model output with respect to the rate of change of the parameter of interest. Parametric sensitivity is mathematically defined as:

$$S_{p_i} = \partial\phi/\partial p_i \quad (2.10-1)$$

where  $S_{p_i}$  is the parametric sensitivity,  $\phi$  is the output function, and  $p_i$  is the parameter under consideration. According to McCuen, component sensitivity measures the effect of variation in the input function  $I$  on the output function  $\phi$ . The component sensitivity may therefore be defined as:

$$S_c = \partial\phi/\partial I \quad (2.10-2)$$

where  $S_c$  is the component sensitivity

Sensitivity can also be expressed in three forms: absolute, relative, and deviation.

If  $Y$  represents the criterion variable of a model and  $X$  the predictor variable then the absolute sensitivity  $S_a Y$  is defined as:

$$S_a Y = \partial Y/\partial X \quad (2.10-3)$$

The relative sensitivity  $S_r$  can be expressed as:

$$S_r Y = (\partial Y/\partial X)(X_i/Y_i) \quad (2.10-4)$$

$$\text{or} \quad S_r Y = (\Delta Y/Y_i)(X_i/\Delta X) \quad (2.10-5)$$

The deviation sensitivity  $S_D Y$  is defined as

$$S_D Y = (\partial Y/\partial X) * \Delta X \quad (2.10-6)$$

where  $(\partial Y/\partial X)$  represents the rate of change of the criterion variable (Y) with a predictor variable or component (X) and  $\Delta X$  is a measure of the error in the predictor variable.

Sensitivity analysis forms a very important aspect of all phases of model development. At the formulation phase, a sensitivity analysis identifies important parameters, variables, and model components, and compares the response of the formulated model with the response of the real system. In the calibration phase, a sensitivity analysis provides an indication of those parameters that may be fully and easily estimated using optimization. Sensitivity analyses are also important in the verification phase and provide a tool for the analysis of the uncertainty in the results. Chapra (1997) also provides procedures for using first-order sensitivity analysis along with perturbations to determine the sensitivities of model components, variables, and parameters.

### **2.10.3 Sensitive Variables**

The diversity of flow regimes and scales experienced in the estuarine system makes the identification of sensitive components, parameters, and variables a critical aspect of model development for estuaries and tidal waterways. Research to determine the sensitivity of the hydraulic outputs (discharge, velocity, and depth) to the geometry of estuaries and tidal waterways clearly indicate correlation between these variables. Savenije (1998) performed research that indicated that the amplification of estuary waves was dependent on the shape factor  $h/b$  and on the range-to-depth ratio  $H/h$  defined in Section 2.3.1. This result provides an indication of the degree to which hydraulic outputs may be expected to be sensitive to estuary geometry. Metha and Prakash (1998) also

showed that the discharge velocity and flow depth in the mouth of an enclosed bay was a function of the degree of constriction. Melville and Coleman (2000) also demonstrated that contraction scour would be sensitive to the degree of constriction in the mouths and outlets of constricted bays. Neill (1973) showed that the ability to model the estuary ebb and flood circulation by a simple continuity expression was sensitive to the length/depth ratio of the estuary, and further that this method could be used only when the estuary exhibited prismatic behavior.

#### **2.10.4 Uncertainty Analysis**

Generally, four types of uncertainties are associated with hydraulic methods: model uncertainty, physical parameter uncertainty, regression parameter uncertainty, and data uncertainty, all contributing to the total uncertainty of the method. According to Yeh and Tung (1993), model uncertainty arises from the inability of the model to perfectly reflect the system's true behavior. Model uncertainty can be represented by the coefficient of variation of the bias within the model (ratio of the predicted to observed value). Physical parameter uncertainty arises from the inability to accurately quantify parameters. Uncertainties are inherent in the assessment of hydraulic parameters such as Manning's roughness coefficient and estuary slopes, and the improper quantification of these uncertainties will lead to modeling errors. Physical parameter uncertainty can be expressed in terms of its coefficient of variation. Regression parameter uncertainty is a measure of the sensitivity of the model's structure to that of the physical system being modeled. One method of assessing regression parameter sensitivity is through a deviation sensitivity analysis discussed in Section 2.10.4.

Yeh and Tung (1993) described data uncertainty as including measurement errors, data inconsistencies, and data handling and transcription errors. To meaningfully apply the information obtained from measured data it is necessary to know the degree of uncertainty involved. Apmann (1970) classified errors in the measurement of physical quantities as systematic, random, or procedural. Random errors are deviations from the true quantities caused by chance fluctuations. Systematic errors, which are referred to as biases, are caused by the characteristics of the particular measuring device. Procedural errors occur when a continuous variable is estimated using a number of discrete measurements.

The uncertainty, and consequently the reliability, of the results provided by a model can be accurately assessed through a deviation sensitivity analysis. Equation 2.10-6 defines deviation sensitivity. However, for the purposes of an uncertainty analysis,  $\Delta Y$  represents the uncertainty in the results caused by a predictor variable (X),  $(\partial Y / \partial X)$  is the rate of change of the criterion variable or model result (Y) with the predictor variable, and  $\Delta X$  is the error in the predictor variable.

## **CHAPTER 3**

### **MODEL DEVELOPMENT**

#### **3.1 INTRODUCTION**

The basis for the research is the development of an estuary scour model and the application of the adapted Melville and Coleman (2000) multi-scale framework. The theoretical basis of each component of the model is presented. The functions of the model and the specific cases to which the model may be applied are introduced. The model was developed for application in tidal rivers and estuaries. The specific bridge pier configurations to which the model may be applied are for caisson, slab footing, and piled foundation piers where the channel invert is at or above the caisson, slab, or pile cap.

#### **3.2 DEVELOPMENT OF THE SCALE APPROACH FOR ESTUARIES**

##### **3.2.1 Introduction**

The development of a methodology for bridge pier design in estuary-riverine environments requires the adaptation of Melville and Coleman's (2000) multi-scale concept. Melville and Coleman's multi-scale concept was developed to facilitate bridge pier scour analysis in a riverine environment. While a system of scales based on the degree of spatial resolution may be appropriate for non-tidal rivers and floodplains, the same may not work for tidal waterways because of fundamental differences between these environments. In a riverine system, the hydrologic processes that consist of direct runoff and groundwater discharge are generated from the catchment above the bridge

being modeled. In the case of a tidal waterway, in addition to discharges generated by the catchment above the structure, the effects of tidal variations that originate downstream of the bridge must also be considered. This difference is further complicated by the fact that depending on the location within the estuary, or the type of estuary being considered, the freshwater input from the catchment area may not have a significant impact on the hydraulic behavior at the structure location. Another significant difference relates to the complex variations in the hydraulic regimes experienced in an estuarine system. The differences in the hydraulic regimes of the estuarine system were addressed in Section 2.9.2 using Chapra's (1997) method, which related these differences to the location within the estuary system. Table 3.2-1 depicts the applicability of Melville's spatial resolution scaled to the various estuary regimes presented by Chapra. Table 3.2-2 was prepared based on the considerations shown in Table 3.2-1 and depicts an adapted scale approach that could be used for estuary systems. Table 3.2-1 shows that some scales are not applicable to some regimes of the estuary system. Therefore, in developing a conceptual scale for tidal waterways the region of influence of that scale must also be determined.

**Table 3.2-1 Applicable Scales for Various Estuarine Regimes**

<b>ESTUARY HYDRAULIC REGIME</b>				
<b>Scale</b>	<b>Tidal River</b>	<b>Estuary</b>	<b>Bay</b>	<b>Ocean</b>
<b>Catchment</b>	Yes	Yes	No	No
<b>Stream Section</b>	Yes	No	No	No
<b>Bridge Far-Field</b>	Yes	Yes	No	No
<b>Bridge Near-Field</b>	Yes	Yes	Yes	Yes
<b>Bridge Local</b>	Yes	Yes	Yes	Yes

**Table 3.2-2 Estuarine Scale Approach for Bridge Scour Analysis**

	<b>Open Ocean</b>	<b>Catchment</b>	<b>Stream Section</b>	<b>Tidal</b>	<b>Bridge Far-field</b>	<b>Bridge Near-field</b>	<b>Bridge Local</b>
<b>Important Temporal Variables</b>	Tidal periods	Time of concentration  Time to peak Rainfall duration  Hydrograph duration	Tidal WSE	Tidal WSE	Peak or time varying discharge  Sediment yield  Depth	Peak or time varying discharge  Sediment yield  Depth	Peak or time varying discharge  Sediment yield  Depth
<b>Important Spatial Variables</b>	Tidal WSE  Tidal wavelength	Catchment area  Curve number	Tidal WSE  Geomorphic data  Soil type  Meander	Tidal WSE	Estuary geometry  Velocity  Depth	Estuary geometry  Velocity  Depth	Hydraulic parameters  Pier geometry
<b>Process</b>	Wave mechanics  Tidal hydraulics	SCS hydrology	Hydraulic  Continuity equation  Runoff hydrograph	Wave Mechanics  Tidal hydraulics  Runoff hydrograph	Bed-form migration	Interaction of bridge structure	Local erosion at bridge foundation
<b>Outputs</b>	Water surface elevation	Q(discharge)	Q(discharge)  Water surface elevation  Tidal currents	Q(discharge)  Water surface elevation  Tidal currents	Short term general scour  Depth	Contraction scour depth	Local scour depth
<b>Type of Analysis</b>	Hydraulic	Hydrologic	Hydraulic	Hydraulic	Hydraulic  Sediment transport	Hydraulic  Sediment transport  Scour depth	Hydraulic  Scour depth
<b>Data Required and Source</b>	Tidal records	Rainfall  Catchment area  Landuse and other hydrologic parameters	Tidal  Stream geometry  Geomorphic data	Tidal  Estuary geometry  Hydraulic parameters	Estuary cross-sections  Properties of bed and bank	Estuary geometry  Cross-sections  Properties of bed and bank  Pier geometry	Pier geometry  Properties of bed and bank
<b>Type of Model</b>	1-D  Empirical  Regression	SCS hydrologic model	Empirical	2-D or 3-D	1-D or 2-D	2-D for transport  Empirical scour equations	Empirical scour equations  3-D hydro-mechanics

Since the Melville–Coleman description of scales is not adequate for tidal analyses, an expanded description of scales was developed. This description has seven rather than five scales. These scales represent an expanded system derived from the Melville-Coleman model and Chapra’s description of estuary regimes. The first four scales are based on the flow regimes found in the estuarine system and are used to establish the hydraulic properties that will be used in the sediment transport and scour components of the model. The last three scales were adapted from Melville and Coleman’s approach because they were found to be applicable to the estuary flow regimes. They were determined based on the proximity to the bridge structure and are the scales that are used in the actual scour computations. In any design, the different scales will be of varying importance. The importance of any scale will influence the importance of the variables associated with that scale. On further analysis of the 7-scale approach, it was determined that only the following scales were needed to develop a model to predict estuarine or tidal river scour: the open-ocean, catchment, tidal estuary, Bridge Near-field, and Local Bridge scales.

### **3.2.2 Open-Ocean Scale**

The open-ocean scale is characterized by the absence of advective flows or frictional land effects. The tidal currents are driven only by ocean waves. The Peclet Number,  $P_e$ , and the Simmon’s Ratio are very low as dispersion is the only transport process present. This scale is important in that it provides for the development of a model for tidal variations that is not significantly influenced by riverine or catchment inputs. Figure 3.2-1 shows the open-ocean scale.



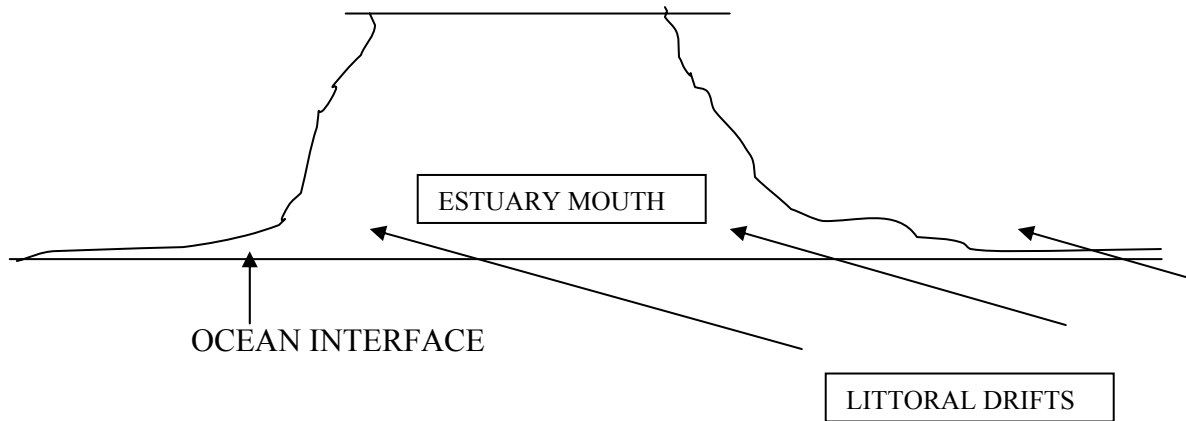


**Figure 3.2-1. The Open-Ocean Scale – Processes consist of tidal variations and sediment or sand aggradation due to accretion or littoral drifts. The region of influence for the aggradation process is limited to the lower estuary.**

### **3.2.3 Catchment Scale**

The catchment scale is important to rivers or creeks whose depth and flow properties are affected by tidal changes and estuaries. The discharge generated from surface runoff from the catchment area is significant to the modeling process. As in the case of purely riverine system, the catchment scale extends to the limits of the watershed producing freshwater flow through the bridge and is used for the estimation of discharge hydrographs from the catchment area. Figure 3.2-2 depicts the catchment scale.

### **3.2.4 Tidal Estuary Scale**

The tidal estuary scale encompasses a diverse regime. This scale includes stratified, partially mixed, and fully mixed estuaries. Stratified estuaries are characterized by high Peclet numbers and Simmons ratios and discharges from the catchment area that dominate the hydraulic properties at the bridge location; partially mixed estuaries have medium values of Peclet numbers and Simmons ratios and both the catchment discharge

and the tidal processes are significant; fully mixed estuaries have low Peclet numbers and Simmons ratios and are dominated by the tidal processes. Estuaries can further be classified according to length, depth, surface area, and entrance geometry, and these represent some of the variables that will be required as inputs to the scour model.

Figure 3.2-3 depicts the tidal estuary scale.

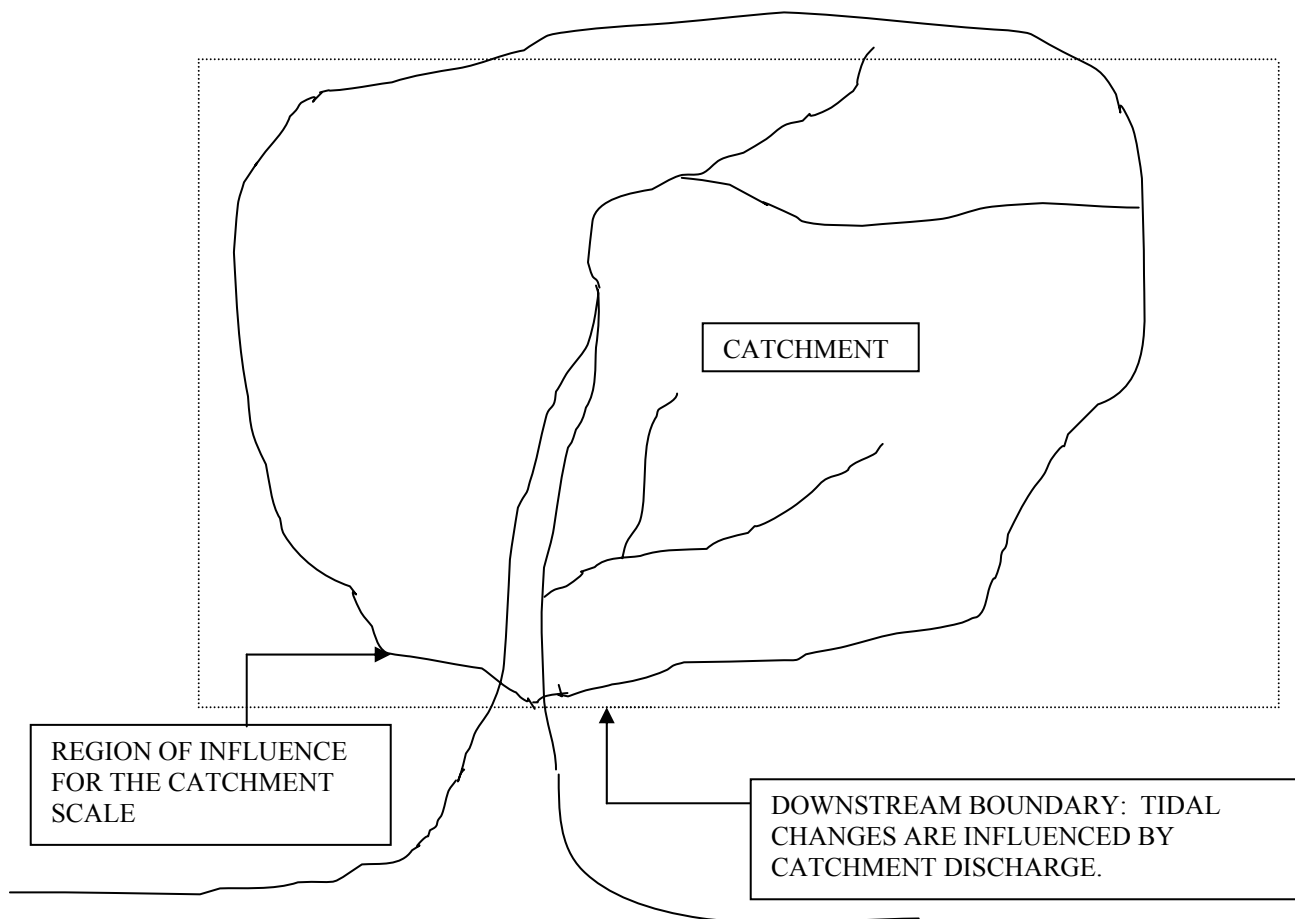


**Figure 3.2-2. The Catchment Scale – Processes consist of rainfall runoff hydrology and sediment flow. The region of influence of the catchment scale extends down the estuary to the point where the catchment discharge has no effect on the estuary water surface elevations.**

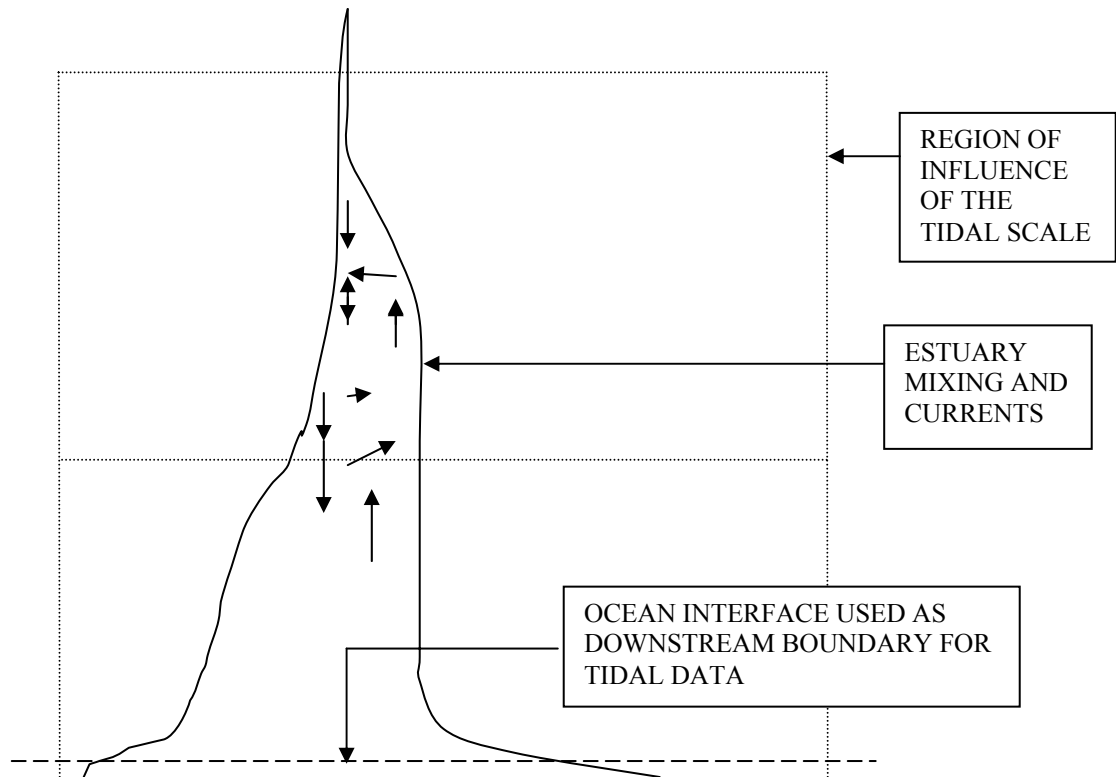


**Figure 3.2-3. The Tidal Estuary Scale – Processes include tidal variations, estuarine hydraulics, general scour, bank friction, density current formation, and mixing.**

### **3.2.5 Bridge Near-Field Scale**

The tidal bridge near-field scale is used to determine contraction scour depths and the flow parameters for local scour depth estimation. The tidal bridge near-field scale is very important to the modeling of constricted estuary entrances. Estuary geometry is an important variable of this scale. The spatial range of tidal bridge near-field scale extends 500 to 1000 times the pier diameter, while the temporal scale is measured in hours.

### **3.2.6 Local Scour Scale**

The individual scour control volumes encompass the local scour hole formed around the piers. At this scale the local scour depths at piers and abutments are estimated. The spatial range of this scale is the diameter of the scour hole when fully developed, while the temporal scale is in hours.

## **3.3 MODEL FORMULATION**

### **3.3.1 Introduction**

The tidal or estuarine system is comprised of different flow regimes that respond differently to individual model types and structures. To ensure accuracy, model components were developed to incorporate the needs of each regime and scale. Prior to starting the model formulation process a preliminary survey was conducted that targeted the Maryland State Highway Agency (SHA) and other transportation agencies. The purpose of this survey was to establish specific areas of need for which the model would be developed. Information regarding current design procedures, tolerable errors, accepted levels of risk, and resource-constraints were compiled. A survey of the number of bridges existing in the various estuarine hydraulic regimes was also completed. This information was used to develop model performance criteria and to determine the variables to be included in each model component, the appropriate temporal and spatial scales of the model, the model structure, and the specific range of estuarine hydraulic regimes that should be addressed.

### 3.3.2 Overview of the Model Structure

The model structure (see Figure 3.3-1) was based on the need to predict pier scour on an hourly basis over the life of the bridge structure and during extreme weather events. The model was intended to be used to estimate scour rates and ultimate scour over the life of the bridge and during hurricane events. The model was also designed to evaluate the effects of variables, conditions, and scour parameters.

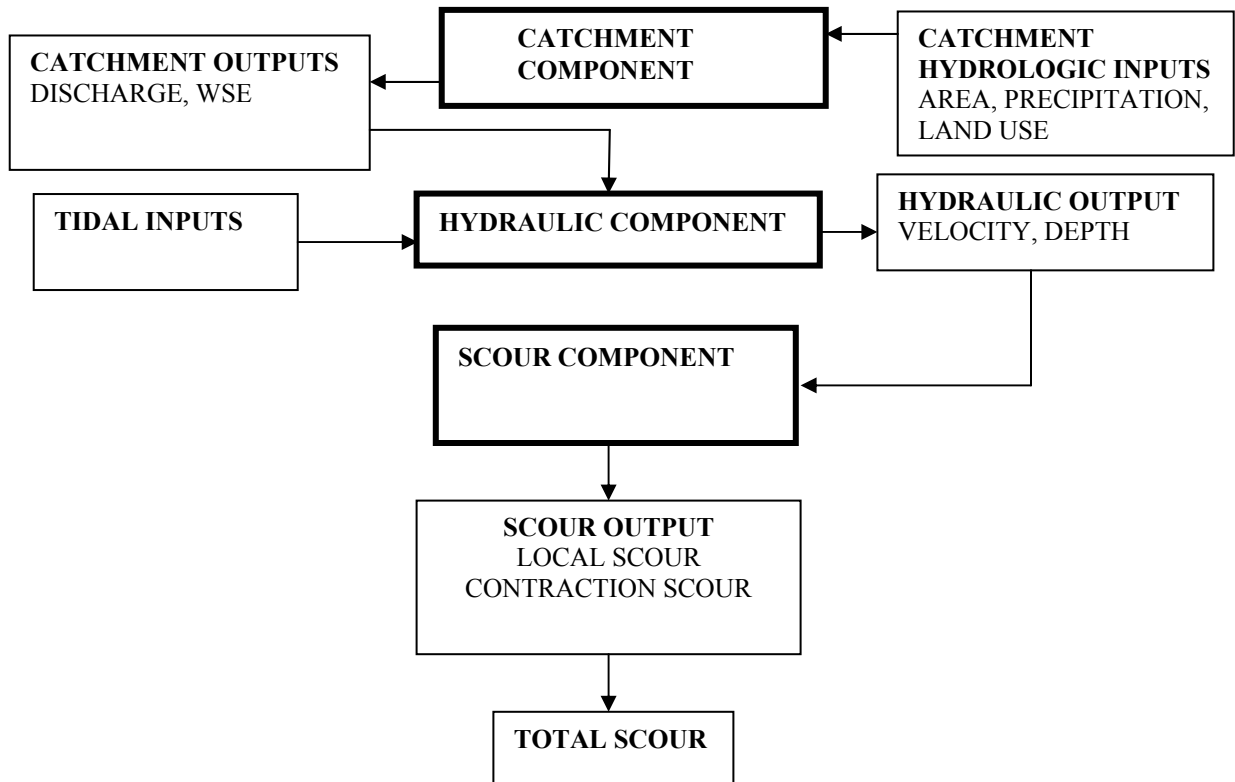


**Figure 3.3-1. Model Schematic**

Hydrologic variables include precipitation, catchment area and land use, catchment physiographic features and slopes, tidal data, and storm surge data. Hydraulic variables include estuary and stream geometry, cross-section, flow velocity, and flow

depth. Scour variables include sediment soil type and particle size, bridge pier size and geometry, and sediment flow. Melville and Coleman (2000) defined the range of measured scour depth to be between 1 ft and 30 ft. As a result the model was formulated to address a 10 percent higher scour range. As suggested by theory and observations made during the literature review, the model is comprised of four components: catchment, tidal, hydraulic and scour. A schematic of the model is presented in Fig. 3.3-1 and a discussion of the formulation of each component follows.

### **3.4 FORMULATION OF THE TIDAL COMPONENT**

#### **3.4.1 Introduction**

The development of the tidal component of the model relied heavily on the historical tidal data from the Chesapeake Bay provided by the National Oceanic and Atmospheric Administration (NOAA). Hourly tidal series data spanning a period of 50 years were used. The model was developed to produce hourly tidal values that covered the life of the bridge structure. This was accomplished by randomly generating a tidal profile to be associated with each hydrologic storm simulated. The duration of each tidal profile in hours was computed as the total number of hours in a year divided by the number of storms expected annually.

#### **3.4.2 Development of the Base Station Tidal Model**

The base station tidal model development was done at the ocean scale. Tidal data from NOAA stations located close enough to the mouth of the Chesapeake Bay estuary to be unaffected by riverine flows were used to develop a base station tidal model. The data

reflected the amplitudes and periods of the diurnal and lunar cycles and were used to develop a base station tidal model of the form:

$$\eta = M + z_i(f(t_m))(\bar{A}_1, S_{x/2})\sin(2\pi t/t_m + \phi_i) + z_j(\bar{A}_2, S_2)\sin(2\pi t/t_M + \phi_J) \quad (3.4-1)$$

where  $\eta$  is tide elevation in feet recorded with MSL as datum,  $M$  is the mean elevation in feet,  $X_m$  is the mean tidal range in feet,  $\bar{A}_1$  is the mean tidal amplitude ( $1/2$  the mean tidal range  $X_m$ ),  $\bar{A}_2$  is the mean lunar amplitude,  $\phi_i$  is the phase angle of the diurnal amplitude,  $\phi_J$  is the phase angle of the lunar amplitude,  $t_m$  is the mean diurnal period in hours,  $t_M$  is the mean bi-weekly lunar period in hours,  $S_{x/2}$  is the standard deviation in the diurnal amplitude, and  $S_2$  is the standard deviation in the lunar amplitude.

Tidal data from Sewell Point, located in the Norfolk, Virginia area were used to represent the base station producing the model below:

$$\eta = 5.80 + z_i(f(t_d))(1.21, 0.285)\sin(2\pi[t/12.32] + \phi_i) + z_j(f(t_L))(0.62, 0.28)*\sin(2\pi[t/356] + \phi_J) \quad (3.4-2)$$

in which  $z_i(f(t_d))$  describes the fact that normal variates were used to simulate the values of the diurnal amplitude. In this case a normal variate for the diurnal amplitude was generated after each diurnal period and remains constant for that period. Similarly,  $z_j(f(t_L))$  indicates a normal variate that represents the lunar amplitude. This was generated for each lunar period and remained constant for that period.

### 3.4.3 Determination of the Tidal Component at the Bridge Station

As discussed in Chapter 2, studies show that tidal waves are distorted and transformed as they propagate through an estuary. To obtain the wave properties at the bridge station the wave was routed using the convex routing procedure described below.

The base station tidal elevation ( $WSE_B$ ) may be represented as a function of time ( $t$ ) as follows:

$$WSE_B = f_1(t) \quad (3.4-3)$$

The water surface elevation at the bridge station ( $WSE_b$ ) was also determined as a function of  $t$ . The latter was done by making hourly measurements of the wave heights of the profile for a particular bridge station provided by NOAA over extended periods of time when the bridge station was least influenced by runoff from catchment storms:

$$WSE_b = f_2(t) \quad (3.4-4)$$

An attenuation factor,  $A$ , was next determined as the relationship between mean amplitude at bridge station  $b$  and the mean amplitude at base station  $B$  where:

$$WSE_{B(t=1)} = A * WSE_{b(t=1)} \quad (3.4-5)$$

For example, using Sewell Point as the base station and Baltimore on the Patapsco River as the bridge station, it was found that  $A$  was 0.6. The convex routing constant  $C$  is given by the equation:

$$C = \Delta t / K \quad (3.4-6)$$

where  $K$  is the mean lag time and  $\Delta t$  is one hour. Using Sewell Point as the base station and Baltimore on the Patapsco River as the bridge station,  $K/\Delta t$  was given by:

$$K/\Delta t = 3.694 + 19.164 * P - 21.247 * A \quad (3.4-7)$$

For a  $\Delta t$  of 1 hour  $K$  was determined as:

$$K = 3.694 + (19.164 * P) - (21.247 * A) \quad (3.4-8)$$

Equation 3.4-8 is defined for  $2/3 < P < 1$ ;  $0.4 < A < 1$ ; and  $2 < (K/\Delta t) < 10$ .  $P$  is defined as the mean peakedness of the wave at the base station where peakedness is given by:

$$P = [WSE_{B(t=tp-\Delta t)} / WSE_{B(t=tp)}] \quad (3.4-9)$$



where  $t_p$  is the time of one of the wave peaks in hours. Figure 3.4-1 explains the manner in which the variables were used to determine the wave peakedness. The water surface elevation at the bridge station at time  $t$  was determined by convex routing as:

$$WSE_{b(t=1)} = A * WSE_{B(t=1)} \quad (3.4-10)$$

$$(WSE_b)_{t+1} = C(WSE_B)_t + (1-C)(WSE_b)_t \quad (3.4-11)$$

The subscript  $t = 1$  indicates the initial elevation. Figure 3.4-2 shows the level of tidal attenuation expected between Sewell Point and Baltimore.

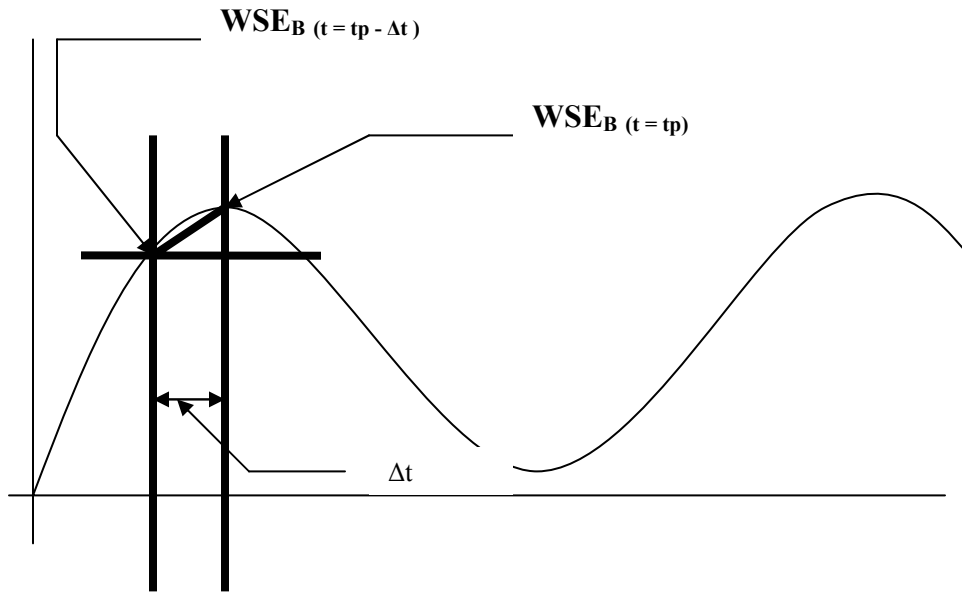


**Figure 3.4-1. Explanation of the variables used in the determination of wave peakedness**

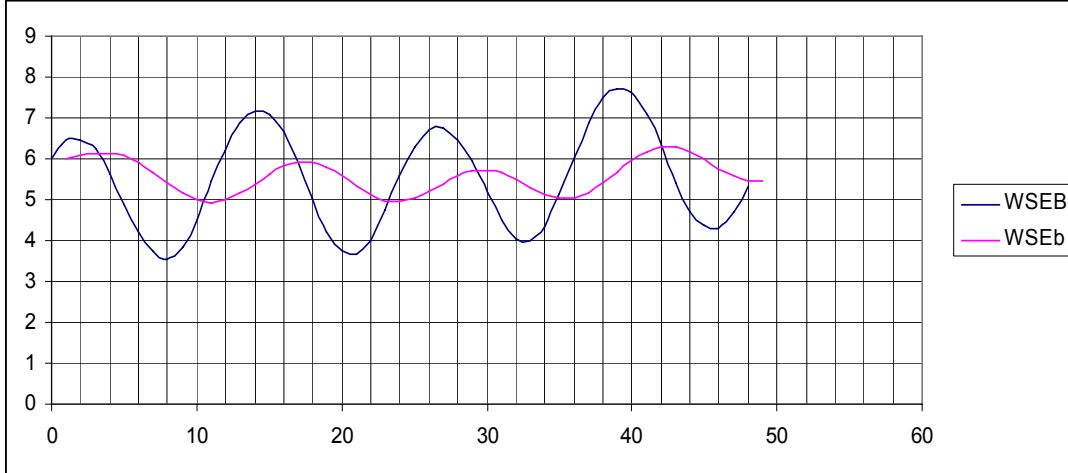


**Figure 3.4-2. Expected attenuation between Sewell point and Baltimore. The x-axis represents time in hrs while the y-axis represents tidal heights in feet.  $WSE_B$  represents the Sewell Point station, while  $WSE_b$  depicts the Baltimore station.**

In addition to being attenuated, the wave at the bridge station will also be distorted. Assuming that the attenuated wave profile is now located at base station B, this distortion may be computed using the assumption that every point on the attenuated wave becomes a wavelet and travels at its own velocity given by  $c = \sqrt{gy}$  where  $y$  is the average depth between the base station and the bridge station at any given time. First, the depths of the estuary at the base station and at the bridge location where the wave profile is required were determined and labeled  $Y_{(t)}$  and  $y_{(t)}$ , respectively. The wavelet travel speed at a given time  $t$  was, therefore, given by:

$$V_{(t)} = (g * (Y_{(t)} + y_{(t)})/2)^{0.5} \quad (3.4-12)$$

$$V_{(t)} = [g * [(WSE_{B(t)} - INV_B) + (WSE_{b(t)} - INV_b)]/2]^{0.5} \quad (3.4-13)$$

where  $WSE_{b(t)}$  represents the elevation of the attenuated wave as a function of  $t$ . The profile is distorted owing to the fact that the wave peak will arrive at the bridge location earlier than other points on the wave. The travel time  $t$  of each point on the wave was computed as:

$$t = L/[3600g * [(WSE_{B(t)} - INV_B) + (WSE_{b(t)} - INV_b)]/2]^{0.5} \quad (3.4-14)$$

The new time  $T$  at which each point on the attenuated wave arrives at the bridge station was given by:

$$T = t + L/[3600g * [(WSE_{B(t)} - INV_B) + (WSE_{b(t)} - INV_b)/2]]^{0.5} \quad (3.4-15)$$

where  $L$  is the distance between the bridge station and the base station and  $g$  is the acceleration due to gravity. Finally, the new hourly wave heights at the bridge station were determined by interpolation. When the times were adjusted the distorted tidal profile shown in Figure 3.4-3 was obtained.

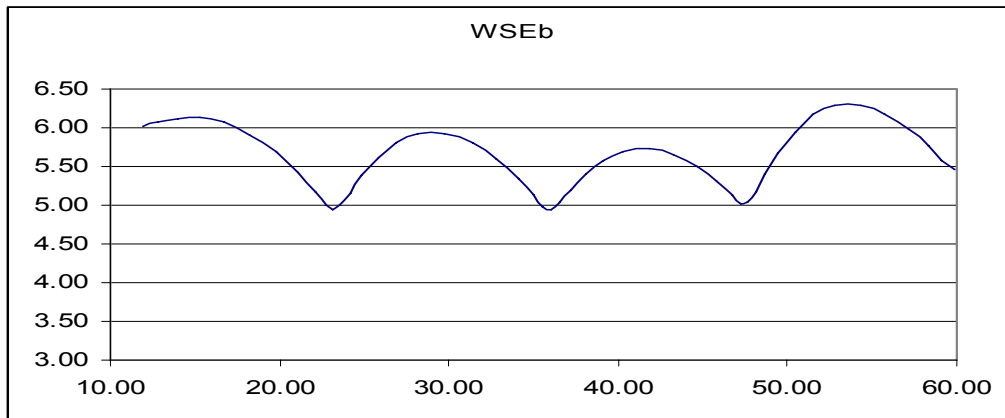


**Figure 3.4-3. Distorted tidal profile at bridge station b. The x-axis is in hours and the y-axis is in feet.**

When hurricane surges were considered, the Richardson and Edge (1997) equation was used to generate the surge values as a function of time:

$$S_t(t) = S_p * [1 - \exp(-D/t)] \quad (3.4-16)$$

in which  $D$  is  $R$  divided by  $f$ ,  $R$  is the hurricane radius in miles,  $f$  is the translational speed in miles per hour,  $S_p$  is the maximum surge in feet, and  $S_t$  is the surge at any given time  $t$ . The surge profile was then algebraically added to the distorted tidal profile and the resultant used to determine the tidal discharge.

### 3.4.4 Determination of the Tidal Discharges at the Bridge Location

The discharge generated by the tidal changes at the bridge location was determined using the modified Neill's (1968) equation. Neill predicted the discharge generated by tidal changes as:

$$Q_N = A_s * [\Delta \eta_b / \Delta t] \quad (3.4-17)$$

where  $Q_N$  is the Neill's predicted tidal discharge,  $A_s$  is the plan area of the estuary and  $[\Delta \eta_b]$  represents hourly change in tidal elevation. The term  $[\Delta \eta_b]$ , which is negative on the rising limb and positive on the falling limb of the tide is defined by:

$$[\Delta \eta_b(t)] = \eta_b(t) - \eta_b(t+1) \quad (3.4-18)$$

A study done by Demetrius et al. (2001) showed that tide generated discharges were dependent on the wave travel time, estuary shape, and the ratio of the mean tidal range to the mean depth. The equation is represented as:

$$Q_R = \begin{cases} Q_N \{1 + \sin[(L_w/C_e T_D) - 0.01]^{1.04} (W_m/W_o)^{0.58} (H/y_m)^{-1.13}\} & \text{for } (L_w/C_e T_D) > 0.01 \\ Q_N & \text{otherwise} \end{cases} \quad (3.4-19)$$

In Equation 3.4-19,  $Q_R$  is the actual tide generated discharge of the rising limb,  $W_m$  is the maximum width of the estuary upstream of location b,  $W_o$  is the width of the estuary at the bridge location b,  $C_e$  is the mean wave celerity given by  $(g * y_m)^{0.5}$ ,  $H$  is the mean tidal range for that tidal series,  $L_w$  is the length of the estuary above the bridge location,  $y_m$  is the mean depth at location b, and  $T_D$  is the tidal period. For the falling limb, the tide generated discharge  $Q_F$  is given by:

$$Q_F = Q_N (L / C_e T_D)^{0.09} (H / y_m)^{0.256} \quad (3.4-20)$$

### **3.5 FORMULATION OF THE CATCHMENT COMPONENT**

#### **3.5.1 Introduction**

Hydrologic input from the upstream catchment area was shown to be significant in the cases of the tidal river scale and the estuary scale. As a result, a hydrologic model was necessary to predict riverine flows to the study point in the estuary. For this study a hydrologic model based on the Soils Conservation Service's (SCS) model was used in conjunction with regional rainfall intensity-duration-frequency curves.

#### **3.5.2 Estimation of the Number and Duration of the Annual Storms**

One of the most important objectives of the model was to simulate the pier scour as a continuous process for the life of the bridge. The number of storms per year at the bridge location must be determined in order to simulate rainfall events over the life of the bridge. The number of storms per year was treated as a random variable with a mean of 80 storms determined from the rainfall data from the City of Baltimore. Kreeb and McCuen (2003) determined that approximately 77.2% of all storms in Maryland have durations less than 12 hours, while 22.8% of all storms have durations greater than 12 hours. In addition they proposed the following breakdown in storm duration (D); the proportion of storms for  $D < 12$  hr was 77.2%, the proportion of storms for  $12 < D < 24$  hr was 16.2 %, and the proportion of storms for  $D > 24$  hr was 6.6%.

This breakdown indicated that at Baltimore, with 80 storms annually, the number of storms with duration less than 12 hr was 62, the number of storms with duration between 12 and 24 hr was 13, and the number of storms with duration greater than 24 hr was 5. For durations greater than 24 hr, a duration of 36 hr was assumed. Also, of the 13

storms with duration between 12 hr and 24 hr, it was assumed that there were seven storms with durations of 18 hr and six storms with durations of 24 hr. All storms with a duration less than 12 hours were assumed to have a duration of 6 hr.

### 3.5.3 Estimation of Rainfall Depths

As the total rainfall depth for any storm is considered to be a random variate, the depth can be generated from the region's IDF curves (Nation Weather Service TP 40, 1961) using a Gamma PDF:

$$f(P) = x^{c-1} e^{-x/b} / b^c \Gamma(c) \quad (3.5-1)$$

where  $c$  is the mean daily rainfall divided by the square of the standard deviation in the daily rainfall amounts,  $b$  is the variance in the daily rainfall divided by the mean daily rainfall amount, and  $f(P)$  is the probability of occurrence of the rainfall event  $x$ . The standard deviation and mean rainfall can be determined from the IDF curves for that particular region. For a given value of duration  $D$ , the value of  $D$  was entered on an IDF curve for the region and the 2-yr and 100-yr intensities obtained. These intensities were converted to depths by multiplying the intensity values by the storm duration (in hrs). The standard deviation ( $S$ ) in daily rainfall was then given by:

$$S = \log(i_{100}/i_2) / z_{100} \quad (3.5-2)$$

where  $i_{100}$  is the intensity of the hundred-year storm,  $i_2$  is the intensity of the two-year storm and  $z_{100}$  is the normal variate associated with the hundred-year event. The mean daily rainfall was given by:

$$\text{Mean } x = \log x_2 \quad (3.5-3)$$

where  $x$  is the daily rainfall value and  $x_2$  is the rainfall associated with the 2-year storm.

The storm depth gamma variates were generated using:

$$\Gamma = -\text{bln}\left(\prod_{i=1}^c U_i\right) = -\text{bln}[u_1 * u_2 * \dots * u_{c-1} * u_c] \quad (3.5-4)$$

in which U represents a vector of uniformly distributed random numbers (0, 1),  $\Gamma$  is the rainfall depth in inches, and b and c were determined using the method above. Table 3.5-1 lists the Gamma variates of the rainfall data from the City of Baltimore.

**Table 3.5-1. Gamma variate constants for Baltimore**

D storm duration in hr	b	c
6	0.1	3
18	0.4	2
24	0.83	2
36	1.35	1

### 3.5.4 Determination of the Catchment Hydrograph

The rainfall response of the catchment area was modeled by the SCS dimensionless hydrograph method. The 24-hour type II storm distribution was used as the basis of the model with the 6-, 18-, and 36-hour distribution being developed from the appropriate adjustment of the 24-hour distribution. After determination of the SCS unit hydrograph by standard SCS procedures, the direct runoff hydrograph for each storm was obtained through the process of convolution. The base flow for the catchment area was determined using the expression:

$$\text{Baseflow (cfs)} = 1.02A^{0.9129} \quad (3.5-5)$$

Equation 3.5-5 was developed from a study titled: Estimation of Discharge, Runoff, and Baseflow in Ungaged Maryland Streams. The study was conducted by Stephen D. Preston and supervised by Dr. R. H. McCuen of the Civil and Environmental Engineering

Department, University of Maryland. The final hydrograph for each storm was obtained by adding the baseflow to the direct runoff hydrograph. The duration of each rainfall hydrograph was determined as the total hours in a year divided by the number of storms in a year as was the case with the tidal profiles.

### **3.6 FORMULATION OF THE HYDRAULIC COMPONENT**

#### **3.6.1 Introduction**

The hydraulic component of the model provides the important link between the tidal and catchment processes. The hydraulic component uses the tidal and catchment components as hydrologic inputs and converts these to time varying stream velocities that are the resultant of the catchment and tidal inputs. Prior to determining the resultant stream velocities the resultant discharges and flow depths must be computed.

The estimation of the resultant discharge obtained from the combination of the catchment and tidal discharges is a very important step in the model formulation process. Of equal importance is the estimation of the resultant flow depth derived from the tides and riverine effects. The determination of the resultant discharge and flow depths as a function of time allows the estimation of the estuary flow velocities, also as a function of time.

The next step in the process is the conversion of the time varying stream velocity to the downflow. The downflow is then used to develop the properties of the horseshoe vortex and to determine the vortex tangential velocity as a function of time. The variation of flow depth and the vortex tangential velocity with time are important inputs that are used by the scour component to estimate time varying scour depths.



### 3.6.2 Estimation of the Resultant Flow Depth

In order to determine the resultant flow depth at the bridge cross-section, it was necessary first to ensure that the estuary above the bridge cross-section was short enough to use the assumption that the tidal changes occurred at all points within the estuary at the same time. This assumption facilitated the use of the Neill's estuary discharge equation. This condition is met when  $L_w$ , the length of the estuary above the bridge, is defined by the following inequality:

$$L_w < T_D(g y_m)^{0.5} \quad (3.6-1)$$

in which  $T_D$  is the diurnal period in seconds,  $g$  is the acceleration due to gravity, and  $y_m$  is the mean tidal depth. It was also necessary to define a control volume that surrounded all surfaces of the estuary upstream of the bridge. Let the catchment inflow to the control volume be  $Q_f$ , the tidal inflow  $Q_R$ , the tidal outflow from the control volume  $Q_F$ , and the mean low tide depth at  $b$  represented as  $Y_x$ . Then the total tidal volume flowing into or out of the bridge control volume in one time increment will be  $Q_R$  or  $Q_F$ . For a time increment of one hour the tidal volume in or out of the control volume will be:

$$S_T = 3600 * \begin{cases} |Q_R| & \text{for the rising limb} \\ - Q_F & \text{for the falling limb} \end{cases} \quad (3.6-2)$$

The total volume of fresh water  $S_Q$ , flowing into the control volume over one time increment may be given by:

$$S_Q = Q_f * \Delta t \quad (3.6-3)$$

where  $S_Q$  is the volume of fresh water entering the estuary over one hydrograph step in cubic feet, and  $Q_f$  is the hydrograph discharge value at time  $t$ . If  $\Delta t$  is one hour then:

$$S_Q = 3600 Q_f \quad (3.6-4)$$

The total storage at time t may be computed using the continuity of mass as:

$$S_{(t)} = S_{(t-1)} + S_{Q(t)} + S_{T(t)} \quad (3.6-5)$$

or:

$$S_{(t)} = S_{(t-1)} + \begin{cases} 3600*[Q_f + |Q_R|]_{(t)} & \text{for the rising limb} \\ 3600*[Q_f - Q_F]_{(t)} & \text{for the falling limb} \end{cases} \quad (3.6-6)$$

where  $S_{(t)}$  is the total storage in the control volume at time step t, and  $S_{(t-1)}$  is the total storage at time t-1.  $S_{(t)}$  may also be estimated as the area of the estuary times its mean depth:

$$S_{(t)} = A_s * Y_{T(t)} \quad (3.6-7)$$

where  $A_s$  is the planar area of the estuary above the bridge section and  $Y_{T(t)}$  is the combined tidal and fresh water depth at any time t. At the initial condition,  $t = 1$ , it was assumed that the estuary would be at its mean tidal depth. Therefore, the combined depth  $Y_{T(1)}$  was given by:

$$Y_{T(1)} = A_m + Y_{bm} \quad (3.6-8)$$

where  $A_m$  is mean tidal amplitude at the bridge cross-section and  $Y_{bm}$  is the mean low tide depth. Similarly, the total storage at the first time step  $S_{(1)}$  was assigned the following value:

$$S_{(1)} = A_s * A_m \quad (3.6-9)$$

The resultant water depth ( $Y_T$ ) may be given by:

$$Y_{T(t)} = S_{(t)} / A_s \quad (3.6-10)$$

or:

$$Y_{T(t)} = \begin{cases} [S_{(t-1)} + 3600*[Q_f + |Q_R|]_{(t)}] / A_s & \text{for the rising limb} \\ [S_{(t-1)} + 3600*[Q_f - Q_F]_{(t)}] / A_s & \text{for the falling limb} \end{cases} \quad (3.6-11)$$

### 3.6.3 Estimation of the Resultant Discharge

The inputs required for this step are the time-varying tidal discharges at location b, the corresponding time-varying routed fresh water outflows, the total time-varying flow depth, and the cross-section geometry of the estuary at location b. The time-varying resultant or net discharge  $Q_{T(t)}$ , computed as the vector sum of the tidal discharges, and the routed fresh water discharges is determined by:

$$Q_{T(t)} = \begin{cases} Q_{f(t)} - |Q_{R(t)}| \\ Q_{f(t)} + Q_{F(t)} \end{cases} \quad (3.6-12)$$

The term  $|Q_{R(t)}|$  represents the absolute value of the time-varying tidal discharge of the rising limb of the tide,  $Q_{F(t)}$  is the tidal discharge of the falling limb,  $Q_{f(t)}$  is the time-varying catchment or freshwater discharge. Assuming freshwater discharges are always positive, then for the incoming tide (rising limb)  $Q_{R(t)} < 0$ , and for the outgoing tide  $Q_{F(t)} > 0$ . Therefore, the net discharge is computed as the vector sum of the tidal and fresh water discharges.

### 3.6.4 Estimation of the Resultant Velocity

The net velocity can then be computed from the net discharge and the area of the estuary cross section at the bridge location. The cross sectional area  $A_{x(t)}$  of the estuary at station b at any time t is determined by:

$$A_{x(t)} = W_o * Y_{T(t)} \quad (3.6-13)$$

where  $A_{x(t)}$  represents the cross sectional area of the estuary at bridge station b, and  $W_o$  is the estuary width at b. The net velocity  $v_{n(t)}$  is computed as:

$$v_{n(t)} = Q_{T(t)} / [W_o * Y_{T(t)}] \quad (3.6-14)$$

The magnitude and direction of  $v_{n(t)}$  determined by the sign of  $Q_{T(t)}$  can be used to determine the downflow. When  $v_{n(t)}$  is positive the downflow will be along the upstream face of the pier, and when  $v_{n(t)}$  is negative, the downflow will be along the downstream face of the pier.

### **3.7 DETERMINATION OF THE DOWNFLOW**

#### **3.7.1 Downflow Model Prior to the Beginning of Scour**

A downflow model that considers the flow in a river or estuary as a series of horizontal jets was developed using the following assumptions: (1) at any point in time the estuary or river was flowing with depth  $Y_m$  and with a turbulent velocity profile such that each horizontal jet has a velocity that varies with depth by the power law; (2) the free stream velocity  $U$  is approximately equal to the maximum horizontal velocity and can be determined with Manning's equation; (3) the horizontal flow profile is modeled as a series of horizontal jets each with area  $\Delta y$  (for a unit width into the paper); and (4) each horizontal jet within the stagnation plane impinges the bridge pier normally and is deflected vertically upwards and downwards, with one-half of the jet deflected in each direction, but at the same velocity as the impact jet.

##### **3.7.1.1 The Turbulent Flow Profile**

The vertical profile of the horizontal velocity of an estuary is an important element in the development of the downflow caused by the pier obstruction. The vertical profile of the horizontal velocity of a typical natural channel was obtained by fitting

stream velocity measurements taken by Grover and Harrington (1966) and is described by Equation 2.4-1 in Chapter 2 with the value of the exponent  $n$  being 0.18. Impulse-momentum principles were applied to the turbulent flow profile in order to derive an expression representing the downflow.

### 3.7.1.2 Impulse-Momentum Application

The total area of flow in the channel per unit width is  $Y_m$  and may be approximated by:

$$Y_m = \Sigma \Delta y \quad (3.7-1)$$

where  $\Delta y$  is the incremental height of each horizontal jet layer. The total estuary discharge per unit width  $q$  is approximated by an expression of the continuity equation:

$$q = \Sigma u \Delta y \quad (3.7-2)$$

Figure 3.7-1 depicts jets of the fluid at three levels (i, j, and k) separated by a vertical distance of  $\Delta y$  within a flowing waterway. The fluid at each level flows horizontally impinging on a cylindrical pier that deflects the flow vertically upwards and downwards. Each horizontal layer may thus be considered as a jet that impinges the pier normally. In the following discussion  $u$  is used to denote the horizontal velocity component, while  $v$  represents the vertical velocity component. If level  $j$  is used as an example, then the jet at this level impinges the pier with horizontal velocity component  $u_j$  and, based on the momentum theory, is deflected vertically upwards with velocity component  $v_{uj}$  and downwards with velocity component  $v_{dj}$ , so that:

$$v_{dj} = v_{uj} = u_j \quad (3.7-3)$$

Equation 3.7-4 is derived from the jet momentum theory of vanes. The momentum theory is based on the principle that the total momentum before a collision is equal to the total momentum after the collision:

$$\rho Q u \text{ (before)} = \rho Q u \text{ (after)} \quad (3.7-4)$$

It may be shown with the momentum theory that the discharge  $Q$ , in each vertical direction (up and down) is half the impinging discharge while the vertical velocities (again up and down) are equal to the impinging velocity. As a result the area of each vertical jet per unit width is  $0.5\Delta y$ .

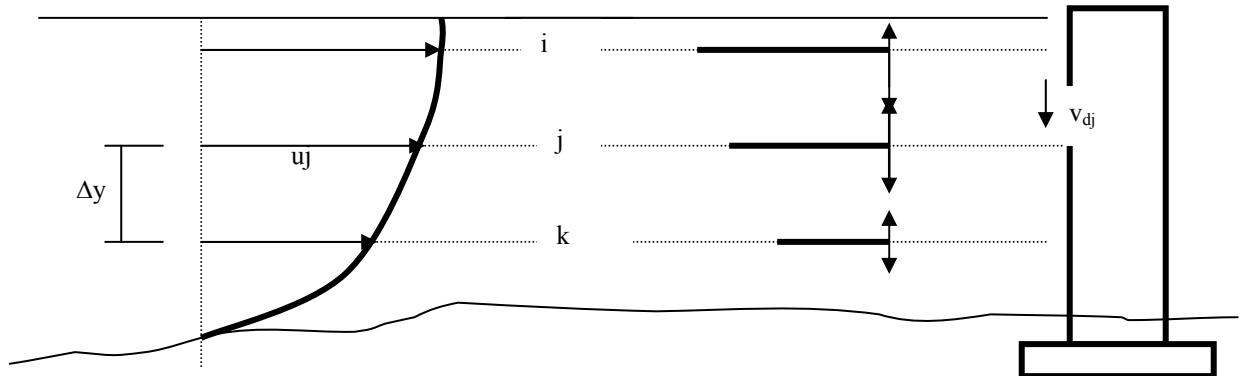


**Figure 3.7-1. Conceptual model of flow as a series of parallel jets. The horizontal jets at three levels are shown separated by a distance of  $\Delta y$ . Note that the velocity of each jet decreases with depth. Each jet is deflected vertically up and down on normal impact with the pier.**

### 3.7.1.3 Width of the Stagnation Plane of a Circular Pier

Dargahi (1989), Raudjkivi (1986), and others have identified the presence of a counter-clockwise vortex in the upstream stagnation plane of circular piers placed in a flow field. In order to develop a downflow model, it is necessary to estimate the width of the stagnation plane, which may then be assumed to be the width of the downflow jet. The width of the stagnation plane may be expressed in terms of the pier diameter using geometric considerations as shown in Figure 3.7-2.

The stagnation plane is the region in which streamlines that impinge on the pier are deflected vertically downwards. Theoretically, this plane should be no thicker than the normal axis shown. However, to conceptually model the downflow, a reasonable estimate of the thickness of the stagnation plane may be made and will include all streamlines on both sides of the normal axis, where the angle  $\theta$  (in radians) subtended by the normal axis and any radii is approximately zero. A relatively simple way of estimating the thickness of this plane is to examine the tangent of the angle  $\theta$  (see Figure 3.7-2). A safe approximation would be to include the region subtended by an angle of 0.10 radians. Using the tangent of the 0.10 radians, the length of the arc subtended by an angle of 0.10 radians is  $0.10d/2$  or  $0.05d$  where  $d$  is the diameter of the pier. Since the angle subtended by the approximate stagnation plane is  $2\theta$ , it may, therefore, be assumed that the thickness or width of each vertical jet is  $0.10d$ .

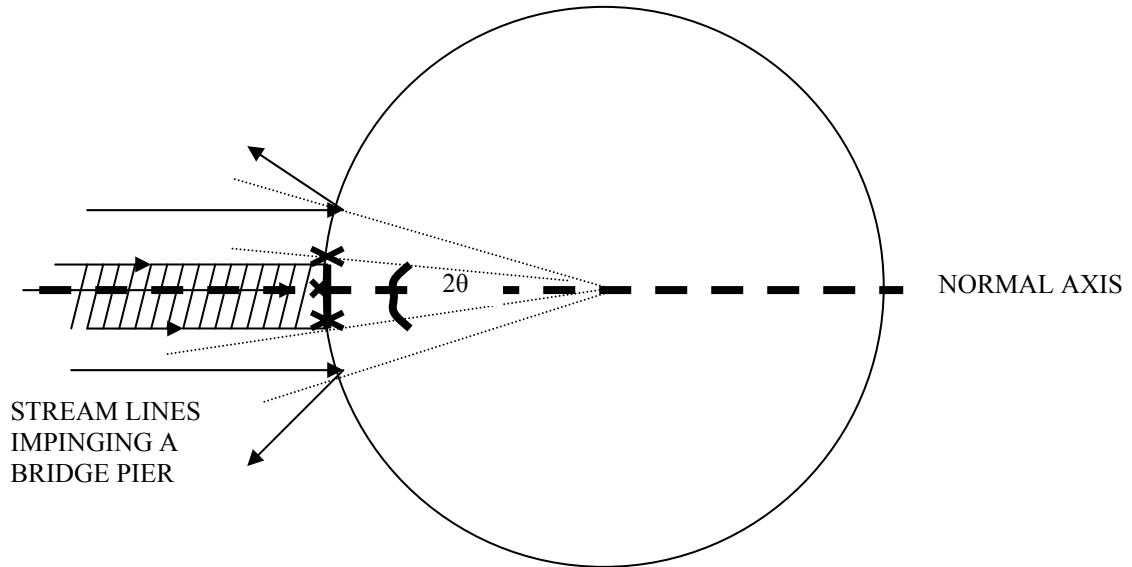


**Figure 3.7-2. A circular pier in plan view showing streamlines impinging the pier. The hatch-marked area represents the thickness of the stagnation plane that extends into the paper. Streamlines striking the pier within this region are deflected vertically downwards as indicated by the crosses.**

#### 3.7.1.4 Jet Equations

Daily and Harleman (1966) developed the following equation to represent the jet from a rectangular orifice:

$$v_y = v(2b_o/(yC_1))^{0.5} \quad (3.7-5)$$

where  $v_y$  is the velocity of the jet after traveling a distance  $y$  from the orifice,  $v$  is the velocity of the jet leaving the orifice,  $b_o$  is the half width of the orifice, and  $C_1$  is an empirical constant. According to Daily and Harleman (1966), the jet development length  $L_o$  is given by:

$$L_o = 2b_o/C_1 \quad (3.7-6)$$

where  $L_o$  varies with both the flow velocity and orifice width. The proposed conceptual jet model assumes that each location along the bridge pier that is impacted by the



horizontal jet acts as a rectangular orifice that generates an upward flow and downward flow as shown in Figure 3.7-3. As discussed earlier, the width of this orifice is assumed to be width of the stagnation plane for a circular pier,  $0.10d$ , and the height  $0.5\Delta y$ . The total downward flow velocity ( $V_{dj}$ ) due to the pier at level  $j$  is the vector sum of the downward velocity of the jet at that level ( $v_{dj}$ ), the upward velocity of the jet from level  $k$  when it arrives at level  $j$  ( $v_{uka}$ ), and ( $v_{ni}$ ), the net vertical velocity of the jet from level  $i$  when it arrives at level  $j$ . Subscript 'a' indicates that the velocity of the vertical jet from level  $k$  is reduced or adjusted on arriving at level  $j$ .  $v_{ni}$  is obtained by the vector sum of the downward velocity of the jet from level  $i$ , as it arrives at level  $j$ , and the upward velocity of the jet from level  $j$  as depicted in Figures 3.7-3 and 3.7-4.

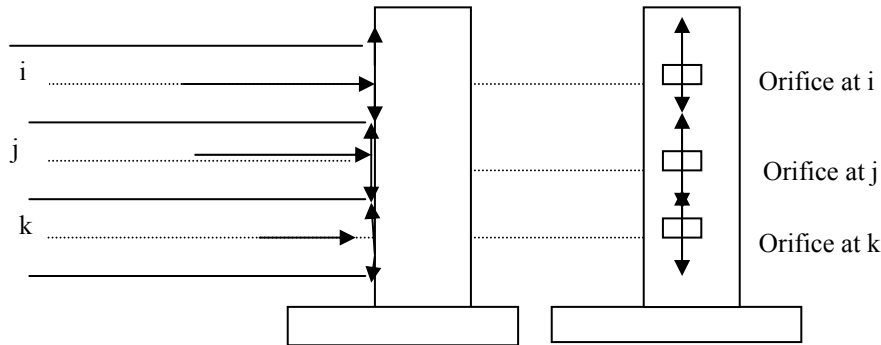


**Figure 3.7-3. Conceptual jet orifices based on Daily and Harleman (1966)**

Equation 3.7-5 is used to determine the velocity of the downward jet from the orifice at level  $i$  when it arrives at level  $j$ . Assuming that the height of each horizontal jet is  $\Delta y$ , then the downward jet from the orifice at level  $i$  travels a distance of  $\Delta y$  before arriving at the orifice at level  $j$ . The velocity of the downward jet from level  $i$  at level  $j$  is denoted as  $v_{dia}$  and is given by:

$$v_{dia} = v_{di}(0.10d/(\Delta y C_1))^{0.5} \quad (3.7-7)$$

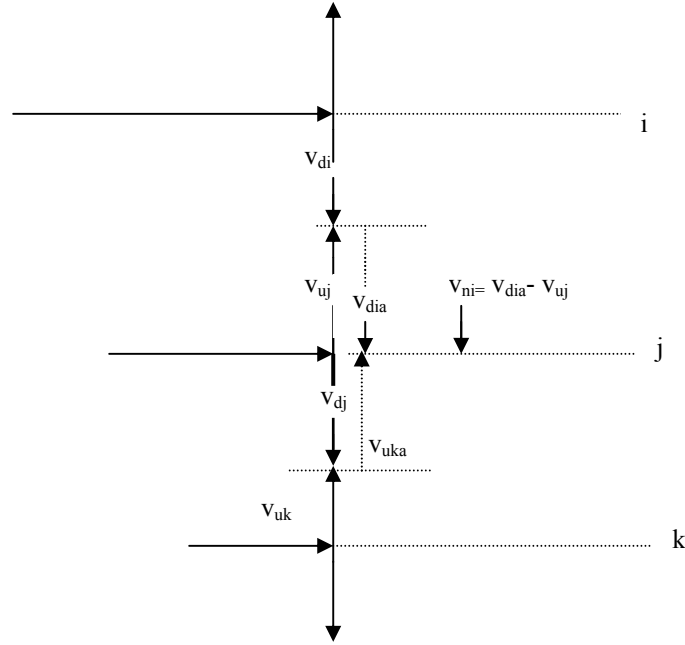


**Figure 3.7-4. Velocity components used to determine the downflow velocity**

The net velocity  $v_{ni}$ , defined as the vector sum of the velocities of the downward jet from level i when it arrives at level j and the upward jet from level j, is given by:

$$v_{ni} = v_{dia} - v_{uj} \quad (3.7-8)$$

Substituting for  $v_{dia}$  from Equation 3.7-7 gives:

$$v_{ni} = v_{di}(0.10d/(\Delta y C_1))^{0.5} - v_{uj} \quad (3.7-9)$$

Equation 3.7-9 determines the magnitude of the net velocity,  $v_{ni}$ , at level j. Similarly, the magnitude of the velocity of the upward jet from the orifice at level k, as it arrives at level j, denoted as  $v_{uka}$ , is given by:

$$v_{uka} = v_{uk}(0.10d/(\Delta y C_1))^{0.5} \quad (3.7-10)$$

The total downflow at level j (denoted by  $V_{dj}$ ) is the vector sum of  $v_{ni}$ ,  $v_{uka}$ , and  $v_{dj}$  and is given by:

$$V_{dj} = v_{dj} + v_{ni} - v_{uka} \quad (3.7-11)$$

where  $v_{dj}$  is the downward velocity from the orifice at level  $j$ . Substituting the expressions for  $v_{ni}$  and  $v_{uka}$  from Equations 3.7-9 and 3.7-10 into Equation 3.7-11 gives:

$$V_{dj} = v_{dj} + v_{di}(0.10d/(\Delta y C_1))^{0.5} - v_{uj} - v_{uk}(0.10d/(\Delta y C_1))^{0.5} \quad (3.7-12)$$

Rearranging gives:

$$V_{dj} = v_{dj} - v_{uj} + (v_{di} - v_{uk})(0.10d/(\Delta y C_1))^{0.5} \quad (3.7-13)$$

From the impulse-momentum principle,  $v_{dj}$  is equal to  $v_{uj}$ , hence Equation 3.7-13 may be further reduced to:

$$V_{dj} = (v_{di} - v_{uk})(0.10d/(\Delta y C_1))^{0.5} \quad (3.7-14)$$

In Equation 3.7-14,  $v_{di}$  is greater than  $v_{uk}$  because of the vertical profile of the horizontal velocity. As a result,  $V_{dj}$  increases as the vertical displacement from the channel invert decreases.  $V_{dj}$  also increases with  $d$  and decreases with  $\Delta y$ . The rationality and accuracy of the equation depend on the spacing ( $\Delta y$ ) considered between horizontal layers.

### 3.7.1.5 Treatment of the Boundary Layers

At the surface level (level 1), it is assumed the net input from the level above is zero and the downflow at the surface denoted by  $V_{d1}$  is given by:

$$V_{d1} = (v_{d1} - v_{u2})(0.10d/(\Delta y C_1))^{0.5} \quad (3.7-15)$$

where  $v_{u2}$  is the upward velocity from the jet at level 2 located just below level 1 the surface level. As indicated by the results of the study conducted by Ettema (1980), the downflow at the level in contact with the invert of the channel is zero prior to the onset of scour. According to the Clifford and Grover (1966) turbulent velocity profile and Ettema (1980), the horizontal velocity along the channel bottom is zero, so the downflow at the invert of the channel is 0.

### 3.7.1.6 Development of a General Downflow Equation

The terms in the first bracket of Equations 3.7-14 and 3.17-15 will approach  $\partial v$  as  $\Delta y$  approaches zero. Also, from the impulse-momentum principle,  $v_{d1} = u_1$ ,  $v_{u2} = u_2$ ,  $v_{di} = u_i$ , and  $v_{uk} = u_k$ ; therefore,  $\partial v = \partial u$  and the general expression for the downflow at a given location may be written as:

$$V_d = \partial u (0.10d/(\Delta y C_1))^{0.5} \quad (3.7-16)$$

Differentiating Equation 2.4-1 of Chapter 2, with respect to  $y$  for  $n$  equal 0.18, gives:

$$(\partial u / \partial y) = 0.18U / [Y_m^{0.18} y^{0.82}] \quad (3.7-17)$$

Expressing Equation 3.7-17 in terms of  $\partial u$  yields:

$$\partial u = 0.18U \partial y / [Y_m^{0.18} y^{0.82}] \quad (3.7-18)$$

Equation 3.7-14 determines the downflow in terms of levels  $i$  and  $k$  that are separated by a distance of  $2\Delta y$ . Therefore, substituting Equation 3.7-18 for  $\partial u$  and  $2\Delta y$  for  $\partial y$  in Equation 3.7-16 yields:

$$V_d = 0.114U(\Delta y d)^{0.5} / [Y_m^{0.18} y^{0.82} C_1^{0.5}] \quad (3.7-19)$$

Equation 3.7-19 is defined for all values of  $y$  except zero in which case the downflow will be zero according to Ettema (1980). The accuracy of  $V_d$  depends on the choice of  $\Delta y$ . Also, Equation 3.7-19 predicts the downflow velocity for values in the range for which  $y$  is greater than  $\Delta y$ . For  $y$  less than  $\Delta y$ , it is assumed that the downflow will decrease until it is zero at  $y$  equal zero. By determining the location ( $y$ ) at which the maximum downflow occurs, Equation 3.7-19 may be expressed in terms of the maximum downflow value:

$$V_{dmax} = 0.114U(\Delta y d)^{0.5} / [Y_m^{0.18} y_d^{0.82} C_1^{0.5}] \quad (3.7-20)$$

where  $V_{dmax}$  is the maximum downflow velocity and  $y_d$  is the distance of the location of the maximum downflow from the channel invert.

### 3.7.2 Downflow Model After Scouring Begins

Ettema (1980) showed that for each scour depth a maximum downflow value exists, and that this maximum downflow increases for the range of scour depths from zero to approximately 2.3 times the pier diameter, where the downflow is at its highest. The maximum downflow then decreases with any further increase in scour depth (see Fig. 2.4-2). Figure 3.7-5 represents the relationship between the maximum downflow and scour depth in the range of scour depth from zero to 2.3 times the pier diameter and derived from the maximum downflow values presented in Fig 2.4-2. The straight line is a regression model that fits the increase in maximum downflow with scour depth. The line is represented by the equation:

$$V_{dmax}/U = C_2(d_s/d) + C_3 \quad (3.7-21)$$

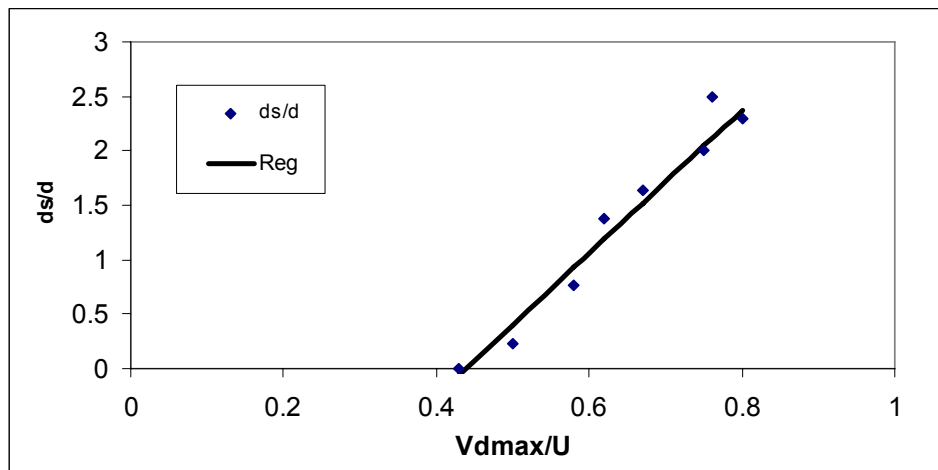


**Figure 3.7-5. Variation of the magnitude and location of the downflow with scour depth where  $d_s$  is the scour depth,  $d$  the pier diameter, and  $y$  the vertical distance from the invert of the channel. Reg in the key indicates a regression line.**

Based on these results, the variation in maximum downflow in the phase of increasing downflow during the development of the scour hole may be modeled by Equation 3.7-21 with the  $C_3$  constant term replaced by Equation 3.7-20 yielding:

$$V_{dmax}/U = C_2(d_s/d) + 0.114U(\Delta y d)^{0.5}/[Y_m^{0.18} y_d^{0.82} C_1^{0.5}] \quad (3.7-22)$$

The variation in maximum downflow was modeled as a logistic function in the range where the scour depth was greater than 2.3 times the pier diameter during the phase of decreasing downflow. The full composite model may be represented by:

$$V_{dmax}/U = \begin{cases} C_2(d_s/d) + 0.114U(\Delta y d)^{0.5}/[Y_m^{0.18} y_d^{0.82} C_1^{0.5}] & \text{for } d_s/d \leq 2.3 \\ [C_4(V_{dmax}/U)_{max}/(1+e^{C_5\{(d_s/d)-C_6\}})] + C_7(V_{dmax}/U)_{max} & \text{for } d_s/d > 2.3 \end{cases} \quad (3.7-23)$$

where  $d_s$  represents the scour depth,  $d$  the pier diameter, and  $(V_{dmax}/U)_{max}$  is the maximum value of  $V_{dmax}/U$ , which may be obtained from Fig. 3.7-5.

The constant  $C_1$  and the parameter  $\Delta y$  in Equation 3.7-22 were determined by performing simulations using a range of values for the variables  $U$ ,  $d$ , and  $Y_m$  to determine the value of  $V_d$  at each location  $y$ .  $C_1$  was estimated using methods developed by Daily and Harleman (1966). The results of these simulations showed that  $C_1$  should be in the range from 0.20 to 0.50 and that  $\Delta y$  should equal  $0.1d$  to provide results that agreed with Ettema's data, which yields:

$$V_d = 0.04Ud^{0.5}/[Y_m^{0.18} y^{0.82} C_1^{0.5}] \quad \text{for } y \geq 0.1d \quad (3.7-24)$$

For values of  $y < 0.1d$ , it is assumed that  $V_d$  decreases linearly and becomes zero at  $y$  equal zero.

As indicated above, if  $\Delta y$  was equal to  $0.1d$ , then the computed value of the maximum downflow ( $V_{dmax}$ ) would be in agreement with the maximum downflow predicted by Fig. 2.4-2 for  $d_s/d$  equal to zero. This was found to be located at a distance

of  $0.1d$  from the invert. Therefore, substituting  $0.1d$  for  $\Delta y$ , and  $y_d$  in Equation 3.7-22 yields:

$$V_{dmax} = 0.114U(0.1d*d)^{0.5}/[Y_m^{0.18}(0.1d)^{0.82}C_1^{0.5}] \quad (3.7-25)$$

which simplifies to:

$$V_{dmax} = 0.24Ud^{0.18}/[Y_m^{0.18}C_1^{0.5}] \quad (3.7-26)$$

where  $V_{dmax}$  is the maximum downflow and is generally located at a vertical distance  $0.1$  times the pier diameter from the invert. Equation 3.7-26 was calibrated against the values expressed in Table 3.7-1 by carrying out simulations where  $U$ ,  $d$ , and  $Y$  were varied. For  $C_1$  equal to  $0.24$ ,  $V_{dmax}/U$  was typically in the range from  $0.40$  to  $0.43$ , which provides reasonable agreement with Ettema's findings. Initially, it may appear that the equation predicts a decrease in downflow with flow depth, but under closer examination it may be observed that the velocity  $U$  is a function of  $Y_m$  as  $U$  increases with the hydraulic radius of the channel, which in turn increases with depth  $Y_m$ . The overall effect of the variation of the velocity  $U$  with  $Y_m$  is that  $V_{dmax}$  increases as  $Y_m$  increases.

### 3.7.3 Calibration of the maximum downflow for $0 < d_s/d < 2.3$

Equation 3.7-26 was calibrated against Table 3.7-1 for values of  $d_s/d$  in the range from  $0$  to  $2.3$ , and the data points shown on Fig. 3.7-5. It was found that, if  $C_2$  was equal to  $0.15$  and Equation 3.7-26 was substituted for  $C_3$ , then the straight line shown in Fig. 3.7-5 provided the best fit for the data points. The square of the correlation coefficient for this model is  $0.98$ . Based on these results, the variation in maximum downflow in the phase of increasing downflow during the development of the scour hole may be modeled by:

$$V_{dmax}/U = 0.15(d_s/d) + 0.24d^{0.18}/[Y_m^{0.18}C_1^{0.5}] \quad (3.7-27)$$

### 3.7.4 Estimation of the maximum downflow for $d_s/d > 2.3$

Table 3.7-1 shows a general decrease in the maximum downflow values when the scour depth  $d_s$  was greater than  $2.3d$ . Due to the lack of data provided by Ettema (1980) for downflow values corresponding to  $d_s/d > 2.3$ , the variation in maximum downflow in this region was modeled as a decreasing logistic function. It was found that if  $C_4$  was 0.50,  $C_5$  was 3.0,  $C_6$  was 6.0, and  $C_7$  was 0.50, then a smooth decreasing logistic curve was obtained. The model may be represented by:

$$V_{dmax}/U = [0.50(V_{dmax}/U)_{max}/(1+e^{3\{(d_s/d)-4\}})] + 0.50(V_{dmax}/U)_{max} \quad (3.7-28)$$

where  $d_s$  represents the scour depth,  $d$  the pier diameter, and  $(V_{dmax}/U)_{max}$  is the maximum value of  $V_{dmax}/U$ . Figure 4.2-2 shows that  $(V_{dmax}/U)_{max}$  is 0.785 and occurs at  $d_s/d = 2.3$ . By substituting 0.785 for  $(V_{dmax}/U)_{max}$  Equation 3.7-28 thus becomes:

$$V_{dmax}/U = [0.40/(1+e^{3\{(d_s/d)-4\}})] + 0.40 \quad (3.7-29)$$



**Table 3.7-1. Values of  $V_d/U$  obtained from Fig. 2.4-2 Ettema (1980).  $V_d$  is the downflow velocity,  $U$  is the mean free stream velocity,  $d_s$  is the scour depth,  $d$  is the pier diameter, and  $y$  is the displacement from the channel invert.**

$d_s/d$	0	0.23	0.77	1.38	1.64	2	2.3	2.5
$y/d$	$V_d/U$							
-2.50								0.23
-2.30							0.00	0.35
-2.00						0.00	0.58	0.49
-1.64					0.00	0.55	0.68	0.59
-1.38				0.00	0.65	0.73	0.75	0.67
-1.30				0.50	0.66	0.75	0.76	0.70
-1.00				0.58	0.67	0.75	0.80	0.75
-0.77			0.00	0.61	0.65	0.74	0.80	0.76
-0.67			0.56	0.62	0.64	0.73	0.79	0.76
-0.23		0.00	0.56	0.62	0.58	0.70	0.75	0.74
-0.18		0.45	0.56	0.62	0.57	0.69	0.74	0.73
0.00	0.00	0.48	0.55	0.61	0.55	0.66	0.69	0.71
0.10	0.40	0.49	0.55	0.60	0.54	0.65	0.67	0.69
0.50	0.43	0.49	0.53	0.56	0.51	0.56	0.56	0.62
1.00	0.42	0.46	0.46	0.46	0.46	0.46	0.46	0.50
1.50	0.36	0.39	0.39	0.39	0.39	0.39	0.39	0.40
2.00	0.31	0.32	0.32	0.32	0.32	0.32	0.32	0.32
2.50	0.26	0.26	0.26	0.26	0.26	0.26	0.26	0.26
3.00	0.23	0.23	0.23	0.23	0.23	0.23	0.23	0.23
3.50	0.19	0.20	0.20	0.20	0.20	0.20	0.20	0.20
4.00	0.15	0.18	0.18	0.18	0.18	0.18	0.18	0.18
4.50	0.12	0.15	0.15	0.15	0.15	0.15	0.15	0.15
5.00	0.08	0.10	0.10	0.10	0.10	0.10	0.10	0.10
5.69	0.02	0.02	0.02	0.02	0.02	0.02	0.02	0.02

### 3.7.5 Composite Maximum Downflow Equation

Summarizing, Ettema (1980) showed that the maximum downflow increased from approximately  $0.4U$  at  $d_s/d$  equal zero to a maximum value of approximately  $0.8U$  at  $d_s/d$  equal to approximately 2.3 and then decreased with further increases in  $d_s/d$ . The following composite model represents this relationship:

$$V_{dmax}/U = \left\{ \frac{0.15(d_s/d) + 0.24d^{0.18}/[Y_m^{0.18}C_1^{0.5}]}{[0.40/(1+e^{3\{(d_s/d)-4\}})] + 0.40} \right\} \quad (3.7-30)$$

The variation of  $V_{dmax}/U$  with  $d_s/d$  given by the composite model is shown in Fig. 3.7-6.



**Figure 3.7-6. The variation of  $V_{dmax}/U$  with  $d_s/d$  given by Equation 3.7-29**

### **3.8 FORMULATION OF THE VORTEX MODEL**

#### **3.8.1 Introduction**

The vortex component of the model will be used to compute scour around the sides of the pier and will provide estimates of the tangential velocity ( $v_t$ ) and shear stress ( $\tau$ ) associated with the flow in the vortex system. The strength of the vortex depends on the downflow velocity, as the downflow initiates the vortex development.  $v_t$  and  $\tau$  may then be expressed in terms of the downflow and used as inputs to an erosion model component that determines the rate of scour hole development. Studies have shown that depending on the Reynolds number, multiple vortices with varying strengths may be developed within the stagnation plane of a pier by a given flow condition. As these vortices are swept downstream by the streamwise flow, a dynamic horseshoe vortex system is formed. Researchers, such as Dargahi (1989) and Raudjkivi (1986), have shown that the horseshoe vortex system has the most significant impact on scour rates when compared to the stagnation plane vortices. In order to obtain a comprehensive vortex model, the approach used was first to determine the maximum downflow close to

the base of the pier in the vicinity of the vortex  $S_o$ . Next, using experimental data from the literature, the shear stress and tangential velocity of the stagnation plane vortex  $S_o$  were expressed in terms of the maximum downflow. The relationships between the shear stress and tangential velocity of vortex 1 and the vortex  $S_o$  were established. Similar relationships were then established between the horseshoe vortex system and vortex  $S_o$ . Using the latter relationships, models that relate the tangential velocity and shear stress of vortex 1 with the maximum downflow were formulated. Similarly, models were developed expressing the tangential velocity and shear stress of the horseshoe vortex in terms of the maximum downflow. For the purpose of the development of the vortex model, the vortex flow induced by the presence of the bridge pier was assumed to be a real vortex, where the region close to the center behaves as a forced vortex while the region further away from the center behaves as a free vortex.

### **3.8.2 Shear Stress and Tangential Velocity Equations for Vortex $S_o$**

The location and spin direction of vortex  $S_o$  supports the argument that the strength of this vortex ( $\xi$ ) is related to the downflow along the bridge pier. Table 2-6 shows a relatively low value of 0.6 for  $\tau_{S_o}/\tau_m$  at this location, where  $\tau_{S_o}$  represents the shear stress of vortex  $S_o$ . This indicates that  $S_o$  is a weak vortex that may not significantly affect the scour development process. However,  $S_o$  may be useful for simulating the strengths of the other vortices in the system. This forms the conceptual basis for a model to be developed. The direction of spin of vortex  $S_o$  indicates that this vortex was set up by a downflow velocity profile in the boundary layer along the vertical stagnation line of the cylinder.

Vennard and Street (1982) present the following method for determining the free stream shear stress,  $\tau_m$ , (lb/ft<sup>2</sup>) in a channel:

$$\tau_m = \gamma RS \quad (3.8-1)$$

where R is the hydraulic radius of the channel, and S is the friction slope which may be obtained by solving Manning's equation giving:

$$S = U^2 n^2 / [(1.49)^2 R^{1.333}] \quad (3.8-2)$$

where n is the Manning's roughness coefficient of the channel. Substituting Eq. 3.8-2 into Equation 3.8-1 yields:

$$\tau_m = \gamma R U^2 n^2 / [(1.49)^2 R^{1.333}] = 0.45 \gamma (nU)^2 / R^{0.33} \quad (3.8-3)$$

Dargahi (1989) shows that for vortex  $S_o$ :

$$\tau_{S_o} = 0.6 \tau_m \quad (3.8-4)$$

Equation 3.7-26 was developed to determine the maximum downflow prior to the commencement of scour. Rearranging Equation 3.7-26 in terms of the free stream velocity, U, yields:

$$U = 4.17 V_{dmax} Y_m^{0.18} C_1^{0.5} / d^{0.18} \quad (3.8-5)$$

Combining Equations 3.8-3, 3.8-4, and 3.8-5 gives:

$$\tau_{S_o} = 1.13 \gamma (n V_{dmax} Y_m^{0.18} C_1^{0.5} / d^{0.18})^2 / R^{0.33} \quad (3.8-6)$$

Equation 3.8-6 thus describes  $\tau_{S_o}$ , for vortex  $S_o$ , as a function of the maximum downflow  $V_{dmax}$ , the pier diameter d,  $Y_m$  the flow depth, R the free stream hydraulic radius.

Recall that the turbulent flow profile in a channel may be described by:

$$u = U(y/Y_m)^{0.18} \quad (3.8-7)$$

Assuming that the vorticity,  $\xi$ , is due primarily to the horizontal velocity gradient,  $\partial u / \partial y$ , and that  $\partial v / \partial x$  is negligible then:

$$\xi = - \partial u / \partial y \quad (3.8-8)$$

where the negative sign indicates that the direction of the vortex spin is opposite to the horizontal velocity gradient. By differentiating Equation 3.8-7 with respect to  $y$  it can be shown that:

$$\xi = 0.18U / (Y_m^{0.18} y^{0.82}) \quad (3.8-9)$$

Note that since we are interested only in the magnitude of  $\xi$ , the negative sign was dropped. Also, since  $\xi$  is twice  $\omega$  then:

$$\omega = 0.09U / (Y_m^{0.18} y^{0.82}) \quad (3.8-10)$$

Using the forced vortex assumption for the region close to the center of the vortex, the tangential velocity responsible for scour development would be given by:

$$v_t = r \omega = 0.09Ur / (Y_m^{0.18} y^{0.82}) \quad (3.8-11)$$

where  $r$  is the radius of the vortex, and  $U$  is given by Equation 3.8-5. Substituting Equation 3.8-5 for  $U$  and  $y$  as  $0.1d$  in Equation 3.8-11 gives:

$$v_t = 0.09 r (4.17V_{dmax} Y_m^{0.18} C_1^{0.5}) / [Y_m^{0.18} (y)^{0.82} d^{0.18}] \quad (3.8-12)$$

Simplifying Equation 3.8-12 yields:

$$v_t = 0.38C_1^{0.5} r V_{dmax} / (y^{0.82} d^{0.18}) \quad (3.8-13)$$

If the vortex system described by Table 2.5-1 was used as an example, then it could be deduced that  $y$ , the location of the center of vortex  $S_o$ , is the distance between the vortex center and the channel invert given as  $0.01d$  in Table 2.5-1. Similarly, the radius ( $r$ ) of vortex  $S_o$  was estimated by Dargahi (1989) to be  $0.05d$ . The tangential velocity of the vortex  $S_o$  at the channel invert, defined as  $v_{tSo}$ , can be obtained by substituting for the radius in Equation 3.8-13 yielding:

$$v_{tSo} = 0.83C_1^{0.5} V_{dmax} \quad (3.8-14)$$

### 3.8.3 Shear Stress and Tangential Velocity Equation for Vortex 1

Dargahi (1989) indicated that the shear stress associated with vortex  $S_o$ ,  $\tau_{S_o}$  was  $0.6\tau_m$  and that the shear stress associated with vortex 1,  $\tau_1$ , was  $1.5\tau_m$ . From these results it can be deduced that:

$$\tau_{S_o}/\tau_1 = 0.6 \tau_m / 1.5\tau_m = 0.4 \quad (3.8-15)$$

where  $\tau_1$  is the shear stress of vortex 1. Rearranging Equation 3.8-15 gives:

$$\tau_1 = 2.5\tau_{S_o} \quad (3.8-16)$$

An expression for  $\tau_1$  could thus be developed by multiplying Equation 3.8-6 by 2.5 giving:

$$\tau_1 = 2.83\gamma(nV_{dmax} Y_m^{0.18} C_1^{0.5}/d^{0.18})^2/R^{0.33} \quad (3.8-17)$$

The tangential velocity of vortex 1 ( $v_{t1}$ ) may be derived from Equation 3.8-13 if the radius of that vortex can be determined. From Table 2.5-4, the radius of vortex 1 is  $0.14d$  while  $y$  is  $0.045d$ . Substituting for  $r$  and  $y$  in Equation 3.8-13 gives:

$$v_{t1} = 1.2C_1^{0.5}V_{dmax} \quad (3.8-18)$$

Equation 3.8-18 expresses the tangential velocity of vortex 1 in the form of a simple and direct relationship with the maximum downflow. It can also be seen that the accuracy and rationality of Equation 3.8-18 will depend on the value of the Harlemann's (1966) jet constant.

### 3.8.4 Shear Stress and Tangential Velocity for the Horseshoe Vortex System

Dargahi (1989) noted that the ratio of the maximum shear stress of the horseshoe vortex to the channel free stream shear stress ( $\tau_{hm}/\tau_m$ ) was 4.5 at a line drawn at 45 degrees to the forward stagnation plane, and that  $\tau_{so}$  was equal to  $0.6\tau_m$ , where  $\tau_{hm}$  is the maximum shear stress of the horseshoe vortex, and  $\tau_{so}$  is the shear stress of the vortex  $S_o$  at the base of the pier in the stagnation plane. This indicates that the maximum value of the shear stress associated with the horseshoe vortex  $\tau_{hm}$  in this location was  $7.5\tau_{so}$  or  $(4.5*\tau_{so}/0.6)$ . This could be attributed to the intensification of the vortices as they are swept downstream by the horizontal flow in the channel. This observation is also supported by the stream function and potential flow Equations 2.5-17 and 2.5-18 that predict maximum horizontal velocities of 1.8 times the value of  $U$  at that section of the pier where the horseshoe vortex was located. Substituting for  $\tau_{so}$  from Equation 3.8-6 yields:

$$\tau_{hm} = 8.48\gamma(nV_{dmax} Y_m^{0.18} C_1^{0.5}/d^{0.18})^2/R^{0.33} \quad (3.8-19)$$

A model to predict the maximum tangential velocity of the horseshoe vortex,  $v_{thm}$ , was developed from Equation 3.8-18. Using the fact that the horizontal velocities in the plane oriented at 45 degrees to the stagnation plane of the pier was 1.8 times the value of  $U$ , the maximum tangential velocity of the horseshoe vortex may be estimated as:

$$v_{thm} = 1.8 * v_{tl} \quad (3.8-20)$$

Substituting for  $v_{tl}$  from Eq. 3.8-18 gives:

$$v_{thm} = 2.2C_1^{0.5}V_{dmax} \quad (3.8-21)$$

Because research has shown that the horseshoe vortex has the greatest impacts on scour rates, Equations 3.8-19 and 3.8-21 were the only equations considered for use in the scour component.

### 3.8.5 Spatial Variation of $v_{th}$ and $\tau_h$ Across the Face of the Bridge Pier

Using the data developed by Briaud et al. (1999), the following model was formulated and calibrated to determine the variation of the shear stress of the horseshoe vortex across the upstream face of the bridge pier:

$$\tau_{h\theta} / \tau_{hm} = 0.55 + 0.45(\sin 4\theta - 1.5) \quad (3.8-22)$$

where  $\theta$  is measured in radians. The assumption was made that the same relationship would explain the spatial variation in the tangential velocity of the horseshoe across the face of the pier:

$$V_{th\theta} / V_{thm} = 0.55 + 0.45(\sin 4\theta - 1.5) \quad (3.8-23)$$

In Equations 3.8-22 and 3.8-23  $\tau_{h\theta}$  is the shear stress of the horseshoe vortex at any location  $\theta$  along the upstream face of the pier,  $\tau_{hm}$  is the maximum shear stress of the horseshoe vortex,  $V_{th\theta}$  is the tangential velocity of the horseshoe vortex at any location  $\theta$  along the upstream face of the pier,  $V_{thm}$  is the maximum tangential velocity of the horseshoe vortex, and  $\theta$  is the angle, in radians, between a line drawn through the center of the pier perpendicular to the flow and a line drawn from the center of the pier to the point in question on its upstream face. Figure 3.8-1 shows the difference between the model results and those of Briaud et al. (1999). The solid line represents the model predictions while the points show the results of Briaud et al. Although the model appears



to under predict, the maximum values and the locations at which these occur are in very close agreement with the results of Briaud et al. (1999).

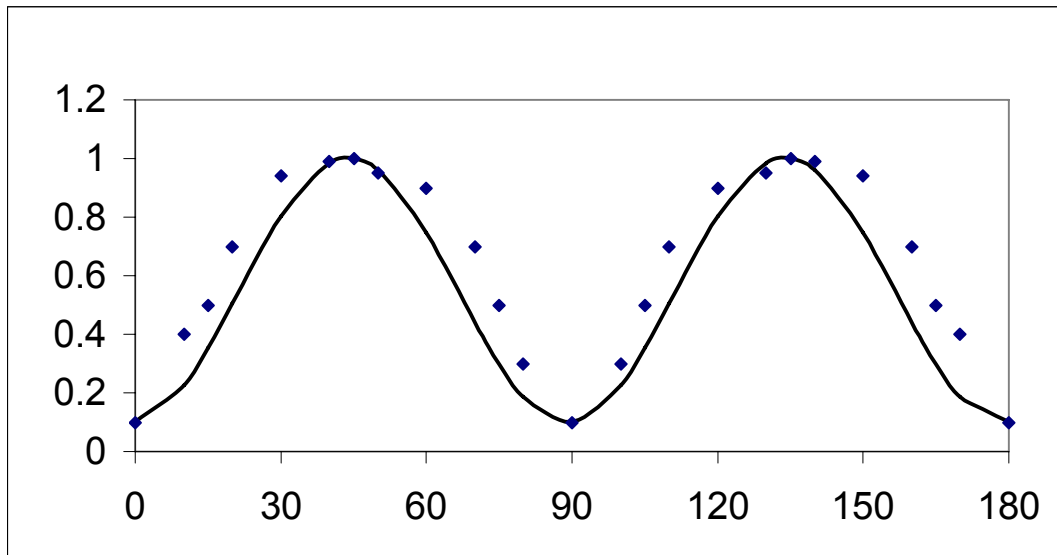


**Fig. 3.8-1. The variation of the tangential velocity or shear stress of the horseshoe vortex with location across the upstream face of the pier in terms of  $\theta$ . The y-axis represents the shear stress or tangential velocity at a given location normalized by the maximum shear stress or tangential velocity of the horseshoe vortex. The x-axis represents the location at the face of the pier in terms of  $\theta$  (degrees).**

### **3.8.6 Calibration of The Horseshoe Vortex Model Prior to the Full Development of the Scour Hole**

The body of research shows that the formation of the horseshoe vortex system occurs in two phases. The first phase starts at the onset of scour and ends at the development of the scour hole when the side slope of the hole becomes constant. During this phase the horseshoe vortex system is initially circular, and while growing transforms to an elliptical shape when the scour hole becomes fully developed. A number of assumptions were made in modeling the vortex in the first phase.

First, it was assumed that the vortex was a Rankine vortex with the inner core modeled as a forced vortex and the outer section modeled as a free vortex. Initially the

vortex system is circular and the tangential velocity is described by Equation 3.8-21. Second, to account for the change in shape that occurs later, the vortex was modeled as an ellipse with  $a$  as its minor axis perpendicular to the side of the scour hole and  $b$  its major axis parallel to the side of the scour hole. When the scour depth is zero,  $a$ , the minor axis of the ellipse is equal in length to,  $b$ , the major axis and the system conforms to its circular shape. As the scour hole develops,  $b$  increases and  $a$  decreases giving rise to an elliptical geometry. Third, the location of the center of the ellipse changed systematically with the development of the scour hole.

The data in Table 2.5-8 were used to determine  $a$ ,  $b$ , and  $V_{thm}$  as functions of scour depth and angle of the side of the scour hole  $\theta$ . Column 9 of Table 2.5-8 shows the variation between the ratio of the maximum tangential velocity to the mean stream velocity,  $V_m/U$ , and scour angle  $\theta$  in the stagnation plane of the bridge pier after the scour hole has been developed. By establishing numerical relationships between the variables listed, this information was used to develop a model representing the maximum tangential velocity of the horseshoe vortex after the full development of the scour hole.

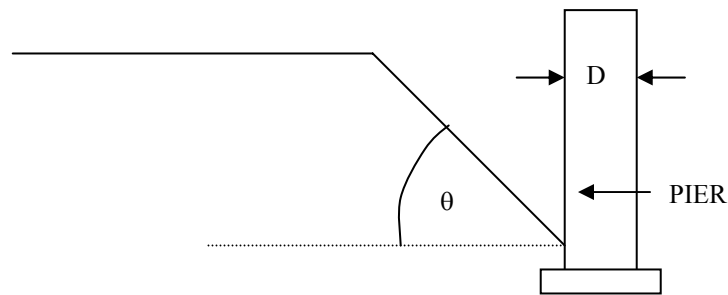


**Figure 3.8-2. Showing pier with diameter  $D$  and scour hole with angle  $\theta$**

### 3.8.6.1 Relationship between $d_s/D$ and $\theta$

Figure 3.8-3 shows a graphical depiction of the power model fitted to the normalized data provided in Table 2.5-8. The curve is a regression equation representing the relationship between  $d_s/D$  and  $\theta$ . From Figure 3.8-3 it may, therefore, be shown that:

$$\theta = 31(d_s/D)^2 \text{ for } \theta < \phi \quad (3.8-24)$$

where  $\phi$  is the angle of internal friction of the bed material. Since  $\theta$  cannot increase beyond the angle of internal friction,  $\phi$  will be its upper limit.

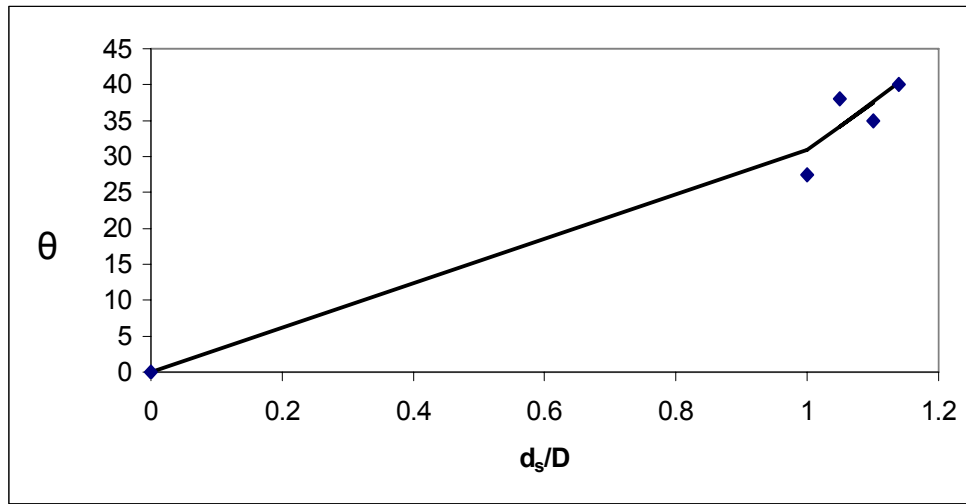


**Figure 3.8-3. Representation of a Power Model Relating  $d_s/D$  to Scour Angle  $\theta$**

### 3.8.6.2 Relationship between $a/D$ and $\theta$ and $b/D$ and $\theta$

The normalized data for  $a/D$  in Table 2.5-8 was plotted against  $\theta$ . Figure 3.8-4 shows the curve representing this relationship. Equation 3.8-25 is the model derived from Fig. 3.8-4 and used to express the relationship between  $a/D$  and  $\theta$ :

$$a/D = 0.08 + 0.23 \sin(\theta * 3.142/180) \quad (3.8-25)$$

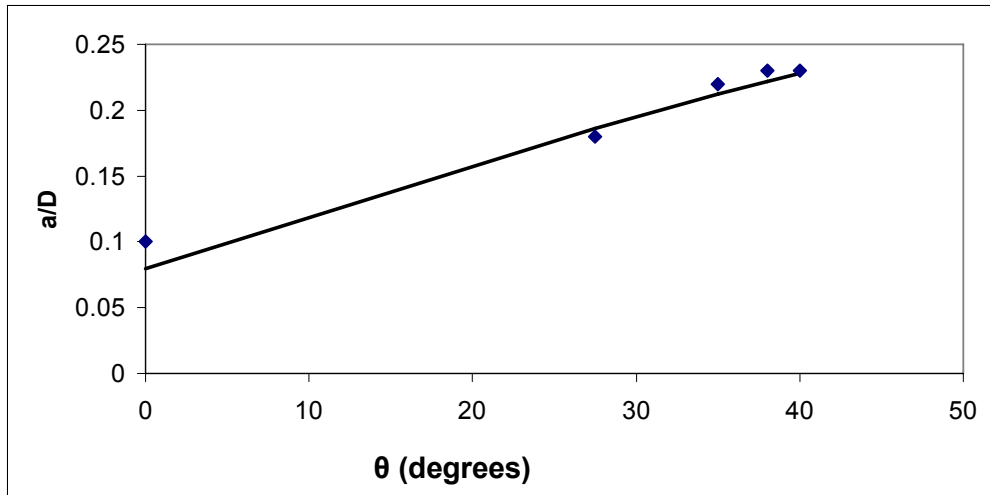


**Figure 3.8-4. Representation of a Sine Model Relating  $a/D$  to  $\theta$**

The normalized data in Table 2.5-8 was also used to develop a relationship between  $b/D$  and scour angle  $\theta$ . Figure 3.8-5 shows the plot of  $b/D$  against  $\theta$ . Equation 3.8-26 is an expression of the sine model used to describe this relationship:

$$b/D = 0.08 + 0.85\sin(\theta \cdot 3.142/180) \quad (3.8-26)$$

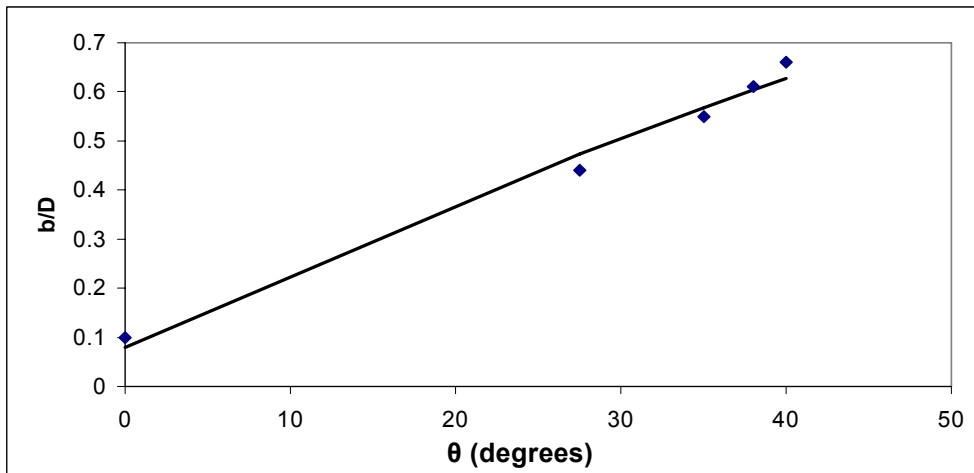


**Figure 3.8-5. Representation of a Sine Model Relating  $b/D$  to  $\theta$**

### 3.8.6.3 Relationship between $a_m/a$ and $\theta$

Let  $a_m$  be the distance along the minor axis of the ellipse from the center of the vortex to the point where the maximum velocity is reached. Table 2.5-8 provides data relating both  $(a_m/D)$  and  $(a/D)$  to scour angle  $\theta$ . It may then be shown that:

$$a_m/a = (a_m/D)/(a/D) \quad (3.8-27)$$

Figure 3.8-6 was developed by plotting the values determined for  $(a_m/a)$  against  $\theta$ . The regression model fitting this data may be expressed as:

$$a_m/a = -0.0002\theta^2 + 0.012\theta + 0.80 \quad (3.8-28)$$

Combining Equations 3.8-25 and 3.8-28 into Equation 3.8-27 gives:

$$a_m = D[-0.0002\theta^2 + 0.012\theta + 0.80][0.08 + 0.23\sin(\theta \cdot 3.142/180)] \quad (3.8-29)$$

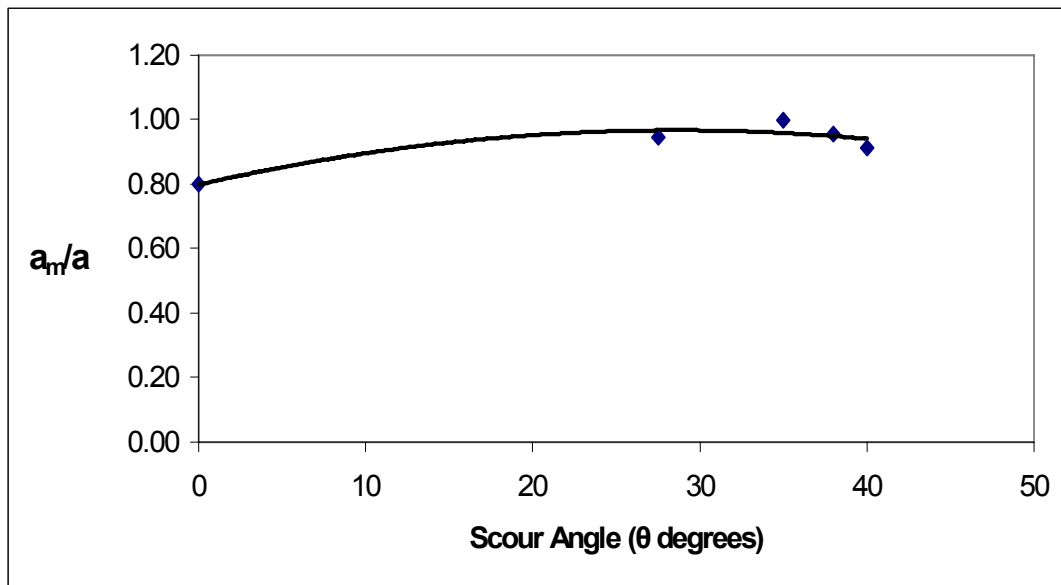


Figure 3.8-6. Relationship Between  $a_m/a$  and Scour Angle  $\theta$  (degrees)

### 3.8.6.4 Determination of the Coordinates of the Center of the Vortex

Let  $x_c/D$  and  $y_c/D$  be the normalized coordinates of the center of the vortex ellipse when plotted in the  $x/D$ ,  $y/D$  plane. The coordinates of the center of the horseshoe vortex along with the associated values of  $\theta$  and  $d_s/D$ , derived from the lab study data presented in Table 2.5-8, were tabulated in Table 3.8-1. The coordinates of the center of the elliptical vortex as a function of the scour angle can thus be represented by the following general equations:

$$x_c/D = f(d_s) \quad (3.8-30)$$

$$y_c/D = f(d_s) \quad (3.8-31)$$

The first step in the process of determining the center of the vortex in terms of the scour angle is to determine relationships between  $x_c/D$  and  $y_c/D$  in terms of the scour depth.

The following models were developed from the data in Table 3.8-1:

$$x_c/D = -0.68 - 0.4(d_s/D)^2 \quad (3.8-32)$$

$$y_c/D = 0.05 - 0.5(d_s/D)^3 \quad (3.8-33)$$

where  $x_c/D$  and  $y_c/D$  represent the normalized  $x$ ,  $y$  coordinates of the center of the vortex.

These models are represented graphically in Figures 3.8-7 and 3.8-8.

**Table 3.8-1: Normalized coordinates of the center of each vortex**

Theta	$d_s$	$d_s/D$	$x_c/D$	$y_c/D$
0.00	0.00	0.00	-0.68	0.05
27.50	5.00	1.00	-1.00	-0.56
35.00	5.50	1.10	-1.20	-0.50
38.00	6.00	1.05	-1.11	-0.61
40.00	6.50	1.14	-1.20	-0.63

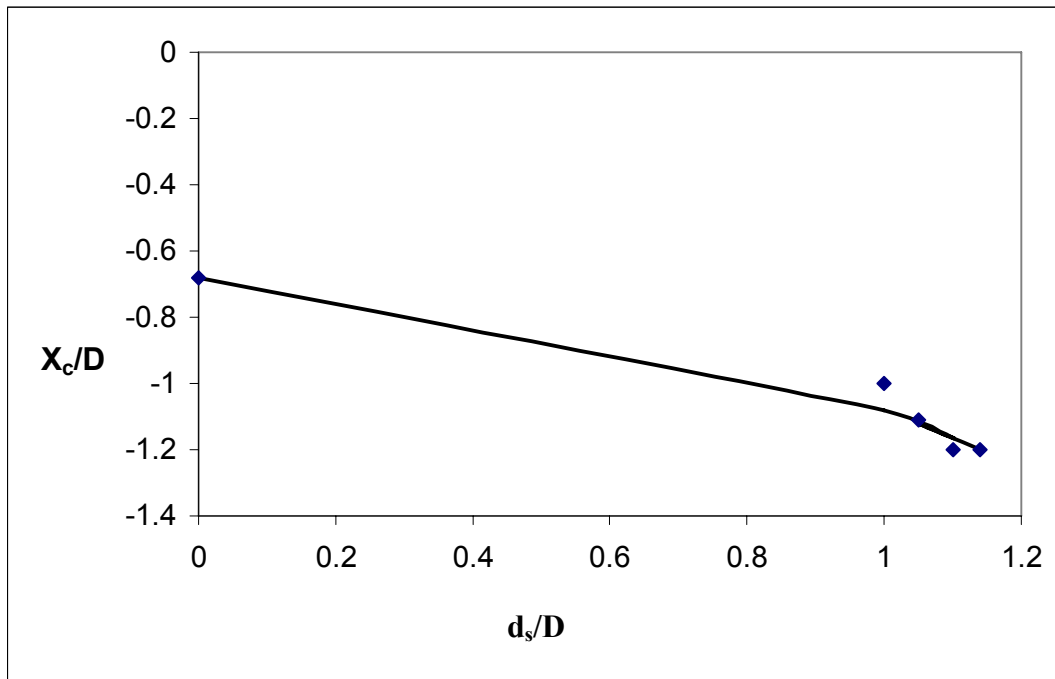


**Figure 3.8-7. Graphical determination of  $x_c/D$  as a function of  $d_s/D$**

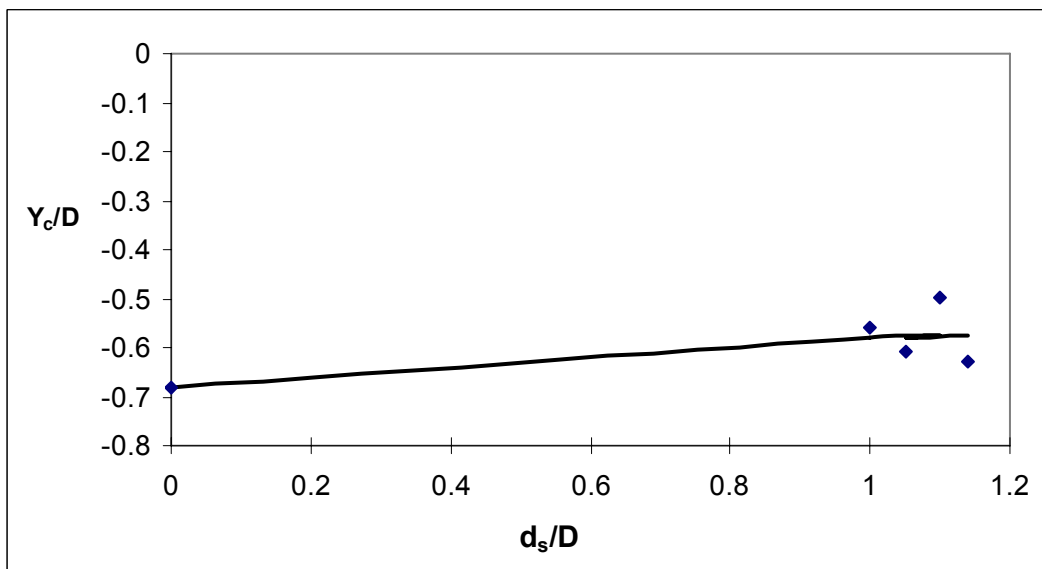


**Figure 3.8-8. Graphical determination of  $y_c/D$  as a function of  $d_s/D$**

It was then necessary to determine the coordinates of the point where the vortex is in contact with the side slope of the scour hole. Figure 3.8-9 shows a hypothetical elliptical vortex within the scour hole. The center of the vortex is at point A with coordinates  $(-x_c/D, -y_c/D)$ . The point on the side slope of the scour hole along axis  $a$  is point C with coordinates  $(-x_s/D, -y_s/D)$ . It can be seen from Figure 3.8-9, that the line from C to the  $x/D$  axis is the length of line CD +  $y_c/D$ . Therefore the ordinate  $y_s/D$  can be represented as:

$$-y_s/D = -(CD + y_c/D) \quad (3.8-34)$$

It can also be shown that angle CAB is equal to  $\theta$ ; therefore, the line CD is equal to  $AC \cdot \cos\theta$ , or  $a \cos\theta$ , where  $a$  is the length of the minor axis of the vortex.

Equation 3.8-34 can, therefore, be represented as:

$$-y_s/D = -(a \cos\theta + y_c/D) \quad (3.8-35)$$

Similarly it can be shown that the ordinate  $-x_s/D$  can be written as:

$$-x_s/D = -(CB + x_c/D) \quad (3.8-36)$$

or

$$-x_s/D = -(a \sin \theta + x_c/D) \quad (3.8-37)$$

The negative signs in Equations 3.8-36, and 3.8-37 indicate that the point C is in a negative quadrant of the  $x/D, y/D$  plane. The distances of point C from the streambed and the face of the pier are given by combining Equations 3.8-33 and 3.8-34 with Equations 3.8-36 and 3.8-37, respectively:

$$y_s/D = a \cos\theta + 0.05 - 0.5(d_s/D)^3 \quad (3.8-38)$$

$$x_s/D = a \sin \theta - 0.68 - 0.4(d_s/D)^2 \quad (3.8-39)$$



Equations 3.8-38 and 3.8-39 thus represent the coordinates of the point where the vortex is in contact with the side of the scour hole in terms of the scour angle and scour depth.

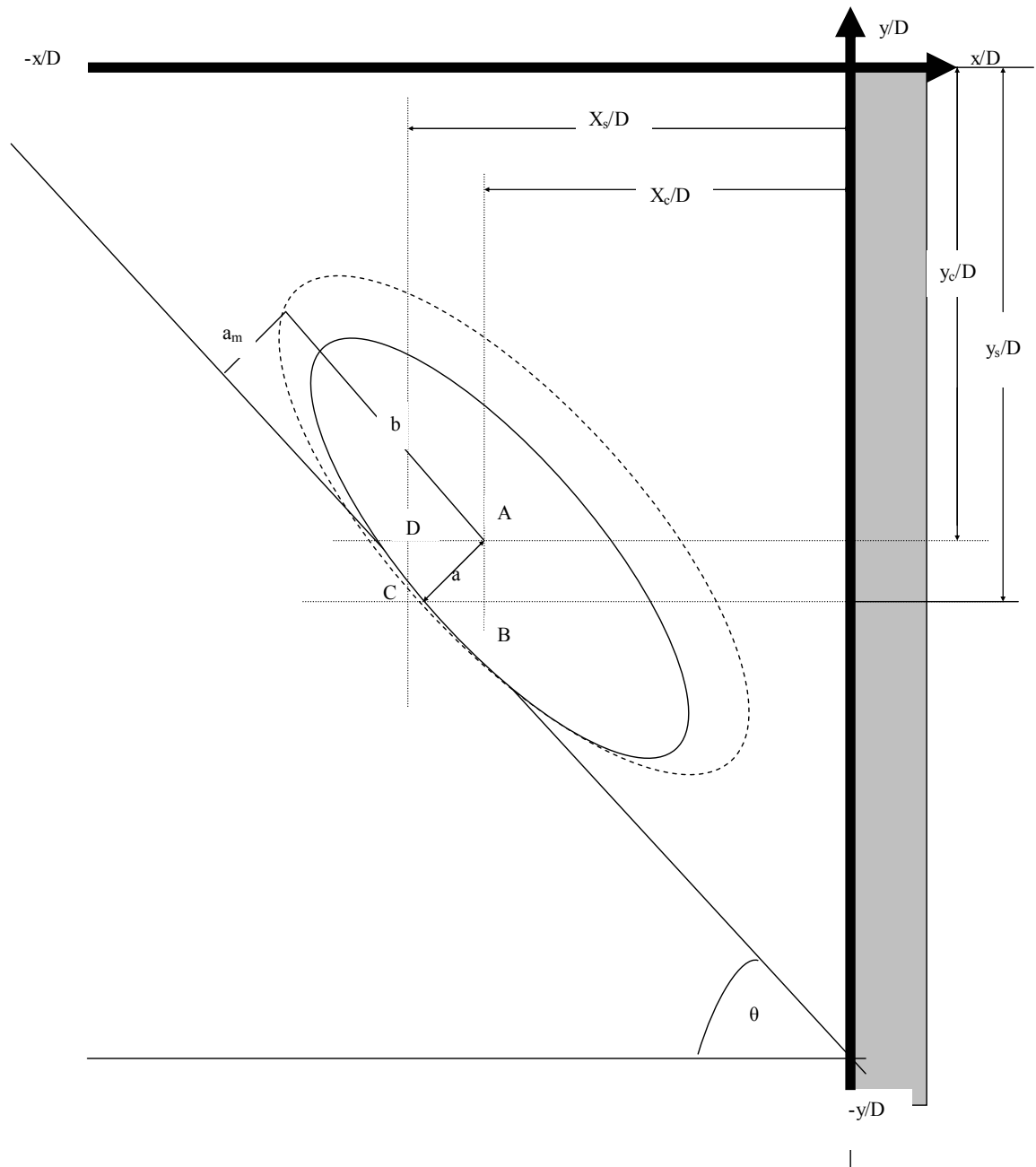


**Figure 3.8-9 Showing the Vortex and Scour Hole Geometry**

### 3.8.6.5 Development of the Tangential Velocity of the Vortex

Using Eq. 2.5-15 or Eq 2.5-16, with the assumption that the normal distance from the center of the vortex to the side of the scour hole is “ $a$ ” (where  $a$  is a function of  $\theta$ ), the following equations were developed to predict the tangential velocity of the vortex at point C. Changing the radius  $r$ , to minor axis  $a$ , in Equation 2.5-15 and Equation 2.5-16 gives:

$$V_t = \begin{cases} V_{thm} (a / a_m) & a \leq a_m \\ V_{thm} a_m / a & a > a_m \end{cases} \quad (3.8-40)$$

or

$$V_t = 1.4(a_m/a) V_{thm} [1 - \exp(-1.25(a^2/a_m^2))] \quad (3.8-41)$$

Recall the maximum tangential velocity  $V_{thm}$ , is determined from Equation 3.8-42 below developed in the prior sections:

$$V_{thm} = 2.24C_1^{0.5}V_{dmax} \quad (3.8-42)$$

### 3.8.7 The Vortex Model After the Full Development of the Scour Hole

The development of the scour hole is complete when the scour angle does not increase with the depth of scour. When this occurs, the side of the scour hole is assumed to be scoured evenly without further change in scour angle. This condition is reached when the scour angle is equal to the natural angle of repose (friction angle) of the bed material. The models developed to determine the tangential velocity, shape, and size of the horseshoe vortices during the development process are also used in this phase.

However in this phase the maximum tangential velocity is described by Equation 3.8-43 below which was developed from the data in Table 2.5-8.

$$V_{thm} = 2.7 V_{dmax} \quad (3.8-43)$$

### **3.9 THE SCOUR COMPONENT**

#### **3.9.1 Introduction**

Parola et al. (1995) concluded that the short-term prognosis is poor for the development of a numerical model of local scour that is of direct use to practicing engineers. In response to this message, a local scour model that was simple, practical, and easy to apply was considered. Accordingly, the local scour component of the model was developed as an empirical model based on the analysis of scour data. The literature also indicated that local scour was the most significant scour process in estuaries. As a result not much value would be added to the model by developing a contraction scour component that would be more complex and sophisticated than the local scour component; therefore, the decision was made to also use a contraction scour model that was simple and based on empirical relationships.

A model that accurately simulates the scour processes in estuarine environments must be able to reflect the wide range of conditions, scales, and processes that will be encountered. With the understanding that the estuarine scour process is extremely complex, it was necessary to eliminate insensitive or insignificant contributions through the use of appropriate simplifying assumptions. As a prelude to the development of the scour component, all important processes and the scales at which they occur were identified.

The modeling strategy considered can be summarized as follows. General scour  $d_{sg}$ , contraction scour  $d_{sc}$ , and local scour  $d_{sl}$ , were determined separately at each time increment with the total scour  $d_s$ , being the sum of the three scour components as represented by:

$$\Delta d_{s(t)} = \Delta d_{sg(t)} + \Delta d_{sc(t)} + \Delta d_{sl(t)} \quad (3.9-1)$$

Secondly, the total scour at any given time is given by:

$$d_{s(t)} = d_{s(t-1)} + \Delta d_{s(t)} \quad (3.9-2)$$

where  $d_{s(t)}$  is the total scour at time  $t$ ,  $d_{s(t-1)}$  is the total scour at one time increment earlier, and  $\Delta d_{s(t)}$  is the total scour that occurs during the time increment between  $t$  and  $t-1$ . The sensitivity of each scour component displayed in Equation 3.9-1, in estuarine environments, was determined from the literature. Scour components determined to be insensitive to the overall results were deleted where appropriate.

### 3.9.2 General Scour Model

The literature review showed that in estuarine conditions, general scour does not play as important a role as it does in the scour of upland rivers. The reason commonly cited is that the general scour that is generated on one tidal cycle is negated on the next cycle when the flow is reversed. However, most researchers recommend a careful analysis of the historical scour data to determine whether a general lowering or raising of the bed of the channel occurs. Due to the complexity of determining general scour, along with the relatively unimportant role it is expected to play in estuarine environments, the current model was not developed with an option to determine general

scour. However, general scour at the bridge location should be analyzed separately and the results obtained used to adjust the model results.

### 3.9.3 Contraction Scour Model

Contraction scour will occur if there is significant narrowing of the estuary at the bridge location and may be determined at the bridge near field scale. In the development of the contraction scour component the following contraction scour models were considered. The first considered was the Einstein–Brown bed load formula as modified by Straub (1985):

$$q_s = [g(S_s - 1)d_{50}^3]^{1/2}[\tau_o/(\tau_c - 1)]^3 \quad (3.9-3)$$

where  $q_s$  is the sediment flow rate per unit channel width,  $S_s$  is the specific weight of the mean particle size,  $d_{50}$  is the diameter of the mean particle size,  $\tau_o$  is the shear stress resulting from the flow, and  $\tau_c$  is the incipient shear stress for the mean particle size.

Henderson (1965) indicated that the Einstein–Brown model provided a better estimate of contraction scour than the Shields model with the source of inputs being obtained either by hydraulic calculations or soil sample measurements.

Contraction scour may also be determined by the method developed by Richardson and Davis (2001) with adjustments made for tidal situations. For the incoming or rising tide, contraction scour was given by:

$$Y_s = Y_T [(W_R/W_{be})K - 1] \quad (3.9-4)$$

where  $Y_s$  is the contraction due to flow depth  $Y_T$ ,  $W_R$  is the bottom width of the estuary at the near field distance on the downstream side of the bridge,  $W_{be}$  is the effective bottom width of the channel at the bridge location. The effective width excludes the piers

and abutment dimensions, and K is a factor that varies from 0.59 to 0.69 and depends on the type of bed material found in the estuary. For most estuaries the value of K is 0.65.

For the outgoing tide or falling limb, contraction scour was given by:

$$Y_s = Y_T [(W_F/W_{be})K - 1] \quad (3.9-5)$$

where  $W_F$  is the bottom width of the estuary at the upstream side of the bridge.

The third model considered was the Komura model (Richardson and Davis, 2001) expressed below as:

$$Y_s = Y_T(t) * (1.45 * (V(t) / (32.2 * Y_T(t)^{0.5})^{0.2} * K * ((1/\sigma_c)^{0.2}) - 1) \quad (3.9-6)$$

In Equation 3.9-6, K is a constant defined by the degree of constriction in the estuary at the bridge section and  $\sigma_c$  is the standard deviation in the soil particle size distribution.

The Komura equation (Richardson and Davis, 2001) is believed to provide the most meaningful estimates of contraction scour in estuarine conditions. This is due to the fact that the model is a function of stream velocity, which is not the case with the HEC18 equation (Richardson and Davis, 2001). Contraction scour was computed only when the terms  $[(W_R/W_{be})K - 1]$  and  $[(W_F/W_{be})K - 1]$  were greater than zero. The value of the contraction scour was based on the highest value of  $Y_T$  in the simulation to that time.  $Y_s$  was then incorporated into the computation of the local scour  $d_s$  at the end of the simulation at the end of each storm sequence.

### **3.9.4 Time Varying Local Scour Model**

The literature indicates that the local scour component is the most important of the scour components in both upland rivers and estuarine environments. Local scour is determined at the Local Scale with a temporal scale that may be expressed in hours over

the bridge life. Figure II-17 of Melville and Coleman (2000) provides data showing the variation of local scour with time. From this data, Melville and Coleman developed the following equation to represent the time to reach equilibrium scour under clear water conditions:

$$d_s/d_{se} = \exp \{-0.03[ABS[(V_c/V) \ln(t/t_e)]]^{1.6} \} \quad (3.9-7)$$

The author, after examining Melville and Coleman's (2000) data, determined that modifying the constants in the above equation provided a better fit. Hence, with modifications Melville and Coleman's equation may be written as:

$$d_s/d_{se} = \exp \{-0.08[ABS[(V_c/V) \ln(t/t_e)]]^{1.2} \} \quad (3.9-8)$$

In Equations 3.9-7 and 3.9-8,  $d_s$  is the scour at time  $t$ ,  $d_{se}$  is the equilibrium or ultimate scour depth,  $V_c$  is the critical erosion velocity of the bed material, and  $t_e$  is the time to ultimate scour. Differentiating Melville and Coleman's equation with respect to time gives the instantaneous scour rate as:

$$dd_s/dt = K1 * K2 * K3 \quad (3.9-9)$$

where:

$$K1 = \exp \{-0.08[ABS[(V_c/V) \ln(t/t_e)]]^{1.2} \} \quad (3.9-10)$$

$$K2 = \{ABS[\ln(t/t_e)]\}^{0.2} \quad (3.9-11)$$

$$K3 = 0.1 * (d_{se}/t) * (V_c/V)^{1.2} \quad (3.9-12)$$

Melville and Coleman's scour rate equation was adapted to the tangential velocity and the incipient velocity of the bed material and became:

$$K1 = \exp \{-0.08[ABS[(V_i/V_t) \ln(t/t_e)]]^{1.2} \} \quad (3.9-13)$$

$$K2 = \{ABS[\ln(t/t_e)]\}^{0.2} \quad (3.9-14)$$

$$K3 = 0.1 * (d_{se}/t) * (V_i/V_t)^{1.2} \quad (3.9-15)$$

where  $V_i$  is the incipient scour velocity of the bed material and  $V_t$  is the vortex tangential velocity.

### 3.9.5 Determination of the Incipient Velocity $V_i$

The time dependent local scour models presented in the previous section indicated the need to determine both the incipient velocity and the ultimate scour of the channel bed material. The incipient velocity may be determined by estimating the critical erosion velocity and adjusting this velocity with a reduction factor. Neill (1968) suggests the following equation to determine the critical velocity  $U_c$ :

$$U_c = 4.81[(S_s - 1)gd_{50}]^{0.5}[y/d_{50}]^{0.17} \quad (3.9-16)$$

where  $U_c$  is the velocity in ft/sec above which bed material of size  $d_{50}$  or smaller will be transported.  $S_s$  is the specific gravity of the bed materials and  $y$  is the flow depth in meters. The mean particle size,  $d_{50}$ , is measured in meters.  $U_c$  is also accepted by researchers as the velocity at which scour conditions change from clear water to live bed. Melville and Sutherland (1989) used the following equation to determine the critical velocity associated with movement of the bed material:

$$U_c/v_{*c} = 5.75[\log(5.53Y/d_{50})] \quad (3.9-17)$$

in which  $Y$  is the flow depth (ft),  $d_{50}$  is the mean particle diameter (ft), and  $v_{*c}$  is the shear velocity (ft/sec) given by:

$$v_{*c} = 1.66 d_{50}^{0.5} \quad (3.9-18)$$

Using data from the Academy of Railway Sciences in China, Dongguang et al. (1993) determined that the incipient velocity of the bed material in most rivers and



waterways was lower than the critical velocity of the bed material. They developed the following equations to represent the incipient velocity  $V_i$ :

$$V_i = 0.645 (d_{50} / B) U_c \quad (3.9-19)$$

In English units Eq. 3.9-19 becomes:

$$V_i = 0.476 (d_{50} / B) U_c \quad (3.9-20)$$

where  $d_{50}$  is expressed in millimeters, and  $B$  represents the pier diameter in ft.

Briaud et al (1999) identified  $\tau_c$  as the shear stress necessary for water to remove material from the channel bed. This model is particularly applicable to sand and gravel or cohesionless soil particles. The model is as follows:

$$\tau_c = 2(\rho_s - \rho_w)gd \tan \phi / 3\alpha \quad (3.9-21)$$

For consistent English units  $\rho_w$  must be in slugs ( $\rho_w = 1$ ), and  $\rho_s = 2.65$ ,  $d_{50}$ , the mean particle diameter must be in ft.  $\alpha$  is 5.7 for sand and 7.3 for gravel. The above equation was then combined to determine the incipient velocity of the bed particles by setting  $\tau_c$  equal to the hydraulic shear stress induced by the flow. The hydraulic shear stress related to flow in the channel is given by:

$$\tau = \gamma_w S^{1/4} (n V_i / 1.49)^{3/2} \quad \text{for uniform flow} \quad (3.9-22)$$

$$\tau = \gamma_w n^2 V_i^2 / [2.22 R_H^{1/3}] \quad \text{for non-uniform flow} \quad (3.9-23)$$

Setting  $\tau = \tau_c$  and solving for  $V_i$  gives:

$$V_i = \{2(\rho_s - 1)gd \tan \phi / [3\alpha \gamma_w S^{1/4}]\}^{0.67} (1.49/n) \quad \text{for uniform flow} \quad (3.9-24)$$

$$V_i = [2(\rho_s - 1)gd \tan \phi [2.22 R_H^{1/3}] / (3\alpha \gamma_w n^2)]^{0.5} \quad \text{for non-uniform flow} \quad (3.9-25)$$

where  $S$  is the friction slope of the channel,  $n$  is the Manning's coefficient,  $\gamma_w$  is the specific weight of water, and  $R_H$  is the hydraulic radius of the channel.

Zai-Jin-You (1998) developed the following equation to determine the incipient velocity of materials in an oscillation flow:

$$V_i = (v/2Kd) \{1 + [1 - (8\pi KBd^2/vT)]^{0.5}\} \quad (3.9-26)$$

where:

$$K = 0.053 \{d[(s-1)gd]^{0.5}/4v\}^{-0.87} \quad (3.9-27)$$

$$B = 280 \{d[(s-1)gd]^{0.5}/4v\}^{-0.67} \quad (3.9-28)$$

$v$  is the kinematic viscosity ( $\text{ft}^2/\text{s}$ ),  $d$  is the bed material grain size (mm),  $s$  is the specific gravity  $\rho_s/\rho_w$  (dimensionless), and  $T$  is the period of the oscillation (s). Equation 3.9-26 is valid for:

$$T \geq (T_{\min} = 8\pi KBd^2/v) \quad (3.9-29)$$

Natural channel armoring is a process that frequently occurs in some waterways, and thus should be considered in order to improve the accuracy of the model. Though most researchers in the field recommend that the estimation of pier scour should be done without considering natural armoring, the option to estimate the effects of natural armoring was included with the program. Natural armoring in non-uniformed sediments is significant only when the following relationship holds:

$$\sigma > 1.3 \quad (3.9-30)$$

where  $\sigma$  is the standard deviation of the particle sizes in the bed material given by:

$$\sigma = (d_{84}/d_{16})^{0.5} \quad (3.9-31)$$

If the standard deviation in the soil particle sizes is greater than 1.3, then:

$$U_a = 0.8U_{ca} \quad (3.9-32)$$

where  $U_{ca}$  is given by:

$$U_{ca} = 4.81[(S_s - 1)gd_{50a}]^{0.5}[y/d_{50a}]^{0.17} \quad (3.9-33)$$

and

$$d_{50a} = d_{\max}/1.8 \quad (3.9-34)$$

in which  $d_{50a}$  is the maximum soil particle size (mm).

### 3.9.6 Development of the Ultimate Scour Model

An empirical ultimate scour model was developed by comparing the importance of the variables in the models listed in Tables 2.7-1 and 2.7-2. The significance of each variable was determined by the magnitude of its power coefficient. Based on this analysis, it was found that the most important variables were the pier diameter ( $b$ ), the stream velocity ( $U$ ), the critical velocity of the bed material ( $U_c$ ), and the flow depth ( $y$ ). Ettema (1983) investigated the mechanism of local scour and suggested that the rate of scour could be more accurately described by the function  $\tanh(y/b)$ . Using this consideration the following general model was proposed for computing ultimate scour:

$$d_{se}/b = \tanh(y/b)(V_t - V_i)^{k_1} [u/(gb)^{0.5}]^{k_2} \quad (3.9-35)$$

The magnitude of coefficients  $k_1$  and  $k_2$  were determined by analysis of the power coefficients of the models presented in Tables 2.7-1 and 2.7-2. From this analysis it was determined that  $k_1$  should be 1.0 while  $k_2$  was assigned a value of 0.0. Equation 3.9-35 represents the ultimate scour depth that could be obtained with a particular vortex tangential velocity and bed material of a given incipient velocity.

### 3.9.7 Determination of the Time to Ultimate Scour $t_e$

The time to the ultimate scour depth ( $t_e$ ) may be determined from models developed by a number of researchers. The model developed by Hancu (1971) is broadly

accepted and is expressed as shown below. The equations were modified for use with the vortex tangential velocity and  $t_e$  was expressed in hours as:

$$t_e = 48.26 (b/V_t)[(V_t/V_i) - 0.4] \text{ for } y/b > 6 \quad (3.9-36)$$

and

$$t_e = 30.89 (b/V_t)[(V_t/V_i) - 0.4](y/b)^{0.25} \text{ for } y/b \leq 6 \quad (3.9-37)$$

### **3.10 PROGRAM FUNCTIONS**

#### **3.10.1 Introduction**

A clear understanding of the functions and capabilities of the proposed model is necessary prior to the development of the program algorithm. The model was developed to meet the needs of bridge engineers in designing safer bridges. As a result, it was anticipated that the model would be used for the design of new bridge piers, the analysis of existing piers, and the design and analysis of scour mitigating options for existing piers.

The design and construction of safer bridges is important to transportation departments and bridge operators. Accordingly, the program was developed to provide methods of analyzing the impacts of scour on various sizes of bridge piers. The program was also developed to provide information that could be used to assess the safety of the bridge from scour during various points of its design life, and also the time at which failure would occur after continuous scour.

Transportation departments responsible for the operation and maintenance of bridges over estuaries need to be able to forecast the risk of failure from continued use or from extreme weather events. As a part of their inspections and maintenance operations,

transportation departments must have the ability to assess the performance of various methods used to prevent or reduce pier scour around existing bridge piers. As a result, the program was also designed to analyze existing bridges.

### **3.10.2 Determination of the Mean Ultimate Scour Depth**

#### **3.10.2.1 Design of New Bridges**

The program was developed to determine the design dimensions, pier depth, and diameter of circular bridge piers in a given estuarine environment. The objective was to determine, through simulations, the expected scour depth that would be reached during the life of the bridge. Thus, by performing simulations for piers of a given diameter, a designer may ensure that the pier footing will be placed some distance below this expected scour depth, depending on the level of risk accepted.

The output provided by simulations involving various pier sizes and number of piers over the duration of the design life of the structure should include the ultimate scour depth and the time taken to reach the ultimate scour depth. The ultimate scour was defined as the maximum depth of scour that could be reached for that particular combination of pier size and soil properties. Other necessary outputs included the annual mean and standard deviation of the ultimate scour depth.

The mean ultimate scour depth may be determined from the time varying scour table, as the scour beyond which further increase over the succeeding years does not occur. Knowledge of the ultimate scour depth and the time to reach the ultimate scour depth will give designers the ability to predict the stability of the pier at the limit of the design life of the structure. This information could thus be used by bridge engineers to

design bridge piers so that the pier foundations will be located below the expected ultimate scour elevation.

#### **3.10.2.2 The Analysis of Existing Bridges**

The determination of the mean ultimate scour depth and time to scour is also relevant to the operation and maintenance of existing bridges. In the case of an existing facility, the pier diameter is fixed; however, other changes may take place in the environment that warrant periodic analyses. Among such changes are the hydrologic effects due to changes in land use practices in the watershed above the bridge. In this case it may be necessary to re-evaluate the ultimate scour and time to ultimate scour to assess these impacts on the life of the bridge.

#### **3.10.3 Effect of Pier Diameter**

An important function of the program should be providing bridge design engineers with the ability to optimize the size and number of piers that are necessary to provide the greatest safety at the lowest cost. This can be achieved by performing multiple simulations in which the number of piers and the pier diameters are varied. The results from the analyses of various pier sizes will be presented in the form discussed in Section 3.10.2.1. The determination of the impact of the pier size on scour depth will assist designers in optimizing bridge construction costs.

### 3.10.4 Determination of the Probability and Risk of Failure

#### 3.10.4.1 Design of New Bridges

Estimation of the risk of failure is one of the most important aspects of the design of bridges. Further, pier scour is but one of the mechanisms of failure that must be addressed in a comprehensive risk analysis of the structure. In general, the determination of failure risks must involve the estimation of the probability of failure along with the consequences of failure (in death toll or cost in dollars). The program must be designed to assist engineers and policy makers in performing this very important task.

In order to facilitate the performance of a risk analysis due to pier failure, it is necessary to estimate the pier depth at which failure is expected to occur, the probability of failure as a function of time, and the consequences of failure. The scour depth that causes failure along with the consequences of failure are determined in separate analyses that are beyond the scope of this dissertation. The probability of failure as a function of time may be determined by computing the probability of scour exceeding this failure depth each year. The annual probability of failure may be determined by the following equation:

$$P_r(F)_A = 1 - P_r(d_s < d_{sf})_A \quad (3.10-1)$$

where  $P_r(F)_A$  is the annual probability of failure,  $d_s$  is the annual scour depth,  $d_{sf}$  is the scour depth at which failure occurs, and  $P_r(d_s < d_{sf})_A$  is the annual probability that the scour depth will be less than the depth of scour that makes failure imminent. Finally, the failure risk as a function of time is determined by the product of the probability of failure each year and the consequences of failure.

Because the major portion of a risk analysis is performed outside of the proposed model, very little value would be added by designing the program to also determine the probability of failure for each year in the simulation. As a result, the time varying probability of failure and the time varying risk of failure are determined externally using the probability of scour results determined by the program. The program output needed for failure probability and risk analyses are histograms of the distribution of scour depths at specific years within the duration of the simulation. For example, histograms of the scour results can be provided at years 15, 25, 50, 75, and 100 of the simulation. The output may be presented in the form of a time varying table with associated mean scour depth and the standard deviation in the scour depth. Since other programs are available with more versatile graphics packages than possessed by Fortran, the histogram data are best presented in tabular form. For the years identified the table would show the number of scour simulation results in each range, the probability of scour in each range, and the cumulative probability of scour in each range.

Knowledge of the probability and risk of failure of a given design will assist designers and policy makers in designing safer bridges. The risk data will also allow design engineers to optimize bridge construction cost. It should also be noted that depending on the proposed use of the structure, funding availability, and the failure consequences, different structures would justify different probabilities and risks of failure.



#### **3.10.4.2 The Analysis of Existing Bridges**

The need to analyze existing structures for the probability and risk of failure is an important feature in the operation and maintenance of existing bridges. As stated in Section 3.10.2.2, environmental and other changes may warrant these analyses. As indicated with the design of new bridges, the program was developed to allow the estimation of the probability of failure of an existing structure whose current life and scour depth are known. The program was also developed to facilitate forecasting of the probability of failure during any of the future years of the life of the bridge. In conjunction with a consequence analysis, these results may also be used to determine the risk of failure of an existing bridge structure.

#### **3.10.5 Effect of Hurricanes**

##### **3.10.5.1 Design of New Bridges**

The objective of determining the pier scour impacts of hurricanes is to ensure that bridges are designed to withstand these catastrophic weather events. The program can then be used to perform simulations as a single-event model with a given hurricane tidal surge and rainfall amount. This single-event simulation determines any additional scour produced by the hurricane.

The output from a hurricane simulation is the expected mean scour depth caused by the event along with the standard deviation in the scour depth. It must be possible to vary both the hurricane surge and rainfall record in order to determine the scour depth associated with changes in each of these variables. This would enable the development of curves that could be used for scour forecasting. The results are presented as a table

with the pier diameter, pier depth, hurricane scour, and probability of scour. The results of a hurricane simulation can be used to predict the effects of various types and categories of hurricanes on the stability of the bridge structure.

#### **3.10.5.2 The Analysis of Existing Bridges**

The knowledge of the impact of hurricanes on an existing bridge with a known life and existing scour depth can help transportation and highway agencies to determine the safety of the structure during that event. With this information, these agencies are able to develop strategies regarding the use of such bridges during and immediately following a hurricane event. Such strategies may include closing the structure or limiting its access to certain users. The analysis of hurricane impacts on existing facilities generally entails the estimation of the increase in pier scour that would be caused by the hurricane over existing conditions. As a result, the required program output should be the mean scour depth and the standard deviation of the scour depth expected from the event. The expected scour depths could also be computed for different types of hurricanes and tabulated. From these results the probability of failure after or during the event could be determined while a risk analysis could be performed to determine if the facility should be closed or its access limited.

#### **3.10.6 Analysis of the Features to Prevent Failure by Scour**

The analysis of features incorporated around piers to prevent failure by scour is important in both the design of new bridges and the maintenance of existing bridges. The objective of these analyses is to determine the effects of using scour control or protection

measures. Such measures include, but are not limited to, rip rap channel armoring, pier collars, rock gabions, sacrificial piles, deflector vanes, pavement, sacked concrete, extended footing, underpinning, and spurs (groynes). The program does not need to possess the ability to analyze all of the options; however, measures that effectively raise the incipient velocity of the bed material (such as riprap and rock gabion) can be treated. The program must, therefore, be designed to recognize changes in the type of bed materials with depth.

The analysis of scour control measures would require performing simulations while varying the input to accommodate the control being considered. As a result, the ultimate scour depth obtained by the use of the scour reducing method is a required output. Also, for given scour reducing options, the time at which scouring will undermine the existing pier, as well as the probability and risk of failure with time, will be needed.

### **3.11 MODELING PROCESS AND ALGORITHM DEVELOPMENT**

#### **3.11.1 Assumptions and Conditions**

Having identified the various theoretical and empirical equations that may be used to determine scour in tidal waterways, it became necessary to develop the specific computer algorithms to best represent the model components. In order to develop a program with the capability of simulating scour over the life of a bridge, a number of assumptions were made.

First, the average bridge design life was assumed to be 50 years. A simulation time of 100 years was selected to ensure that the simulation extended significantly

beyond the design life of the bridge. Though the rainfall and tidal development were treated independently, it was assumed that weather conditions that caused high tide and surges would also contribute to significant rainfall. This effect may be observed when a hurricane progresses up an estuary. Initially the winds and low pressure cause significant tidal surges that travel up the estuary. As the hurricane system moves overland, high intensity rainstorms are produced, that later result in increased riverine discharges to the estuary.

Second, it was assumed that storms of durations 6, 18, 24, and 36 hrs could represent the annual distribution of storms events. The number of storms per year was based on the statistical data derived from regional curves. As an example, using the Baltimore curve, on average 80 events occur per year. The duration of each event was calculated to ensure that the simulation covered every hour of the bridge life.

Other assumptions included the fact that in a tidal environment scour occurs on both sides of the pier. As a result, scour was simulated at both the upstream and downstream pier faces. It was also assumed, based on the literature review, that for each vortex tangential velocity a unique ultimate or equilibrium scour depth was related to the magnitude of the tangential velocity. Finally, only singular circular bridge piers were modeled with only contraction and local scour being considered.

### **3.11.2 Modeling Process**

A clear presentation of the overall modeling process is necessary to efficiently create algorithms to describe the process. The important elements of the modeling

process are outlined below. Figure 3.11-1 also provides a graphical representation of the process.

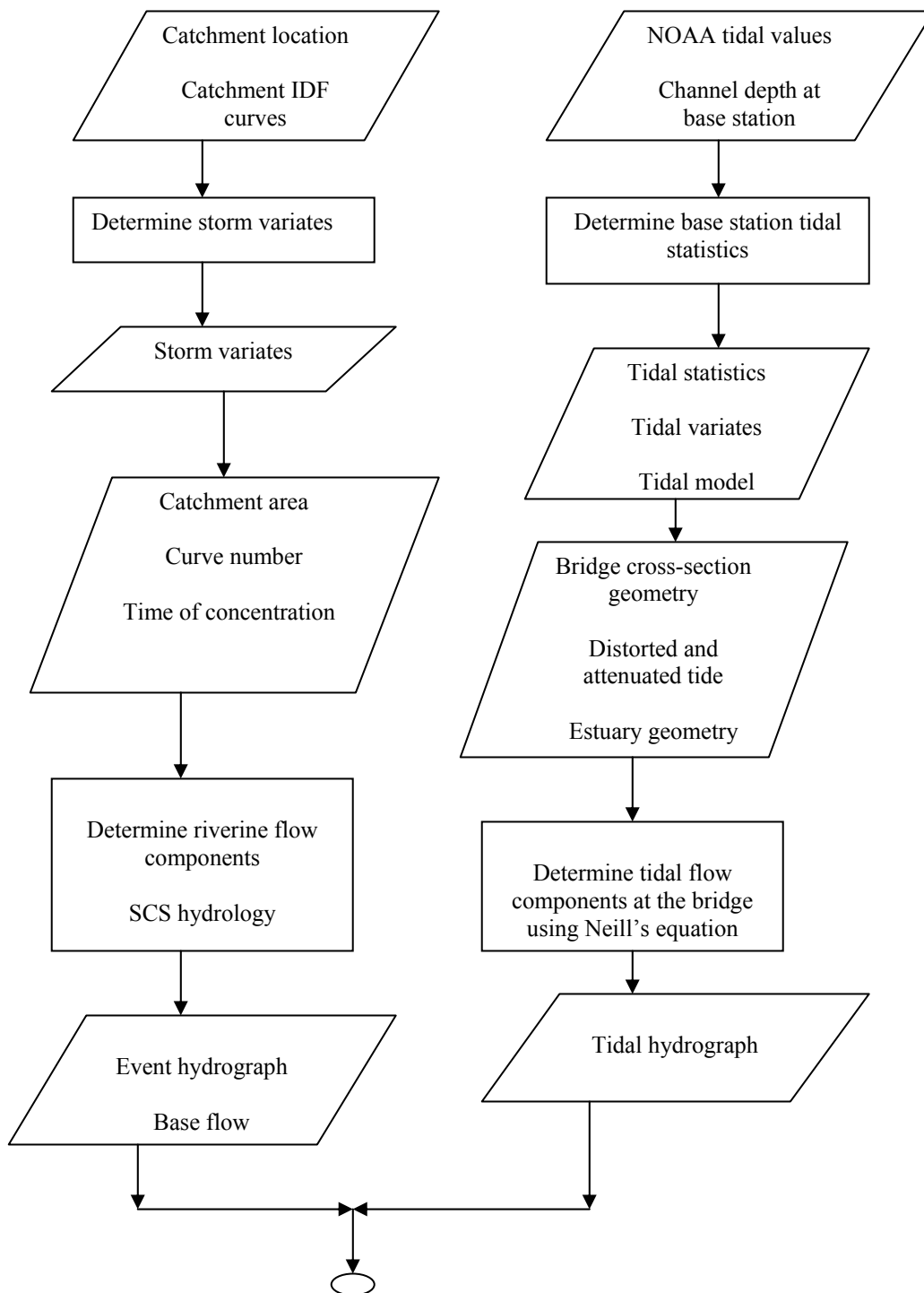


**Figure 3.11-1. Model Procedure Flowchart**

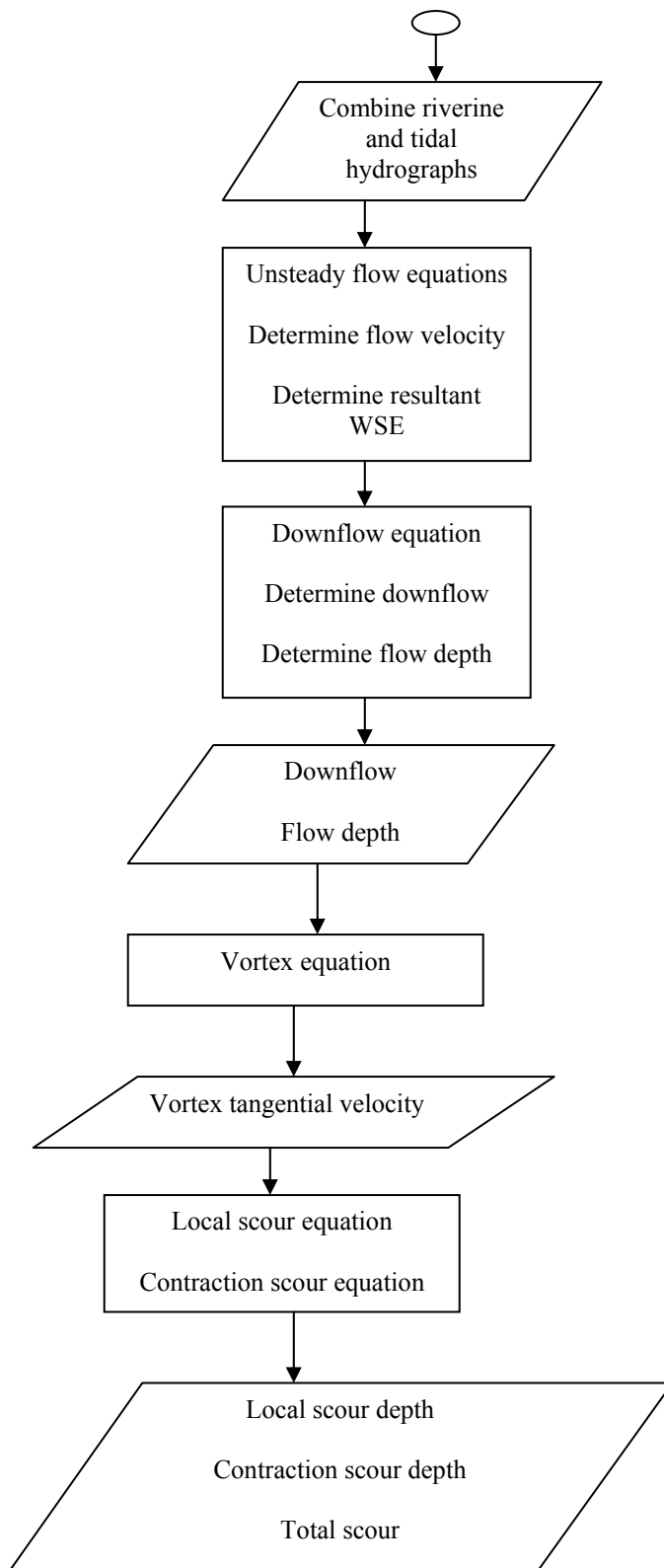


**Figure 3.11-1. Continued**

Regional rainfall data and IDF curves were used to estimate the number of scour producing storms along with the duration and magnitude of each storm for the simulation period. Scour was determined sequentially storm-to-storm and within each storm period. For each storm, the duration of the runoff hydrograph and the time that runoff starts in the tidal cycle were simulated randomly. The product of this process was a hydrograph representing the rainfall-runoff response of the catchment area above the bridge.

Tides from a gauged location within the estuary close enough to the ocean to be insignificantly impacted by riverine inputs were used. Such a station was referred to as the tidal base station. Tides from the tidal base station were synthesized, routed to the bridge location, transformed, and attenuated from a regular sinusoidal pattern to reflect the effect of frictional forces experienced as the tide moves into the estuary. The transformed tide was synthesized for a period that corresponds to the duration of the freshwater runoff hydrograph of the bridge catchment area. The changes in the tidal elevations with time were then transformed into tidal discharges using the modified Neill's Equation.

The next step in the process was the modeling of the combination of the riverine and tidal inputs at the bridge location. The riverine and tidal flow components were combined with the aggregation accounting for the direction of the two discharge vectors, upstream and downstream. The net velocity of the system was determined as a vector through the use of the steady flow continuity equation at each time step.

Using the combined velocity and water surface elevation, the downflow and vortex velocities at the bridge were computed. These served as inputs to a local scour model that produced a local scour depth. The channel contraction scour produced at the

bridge was also computed at each time increment based on the highest value of the flow velocity in each rainfall simulation period. The total scour at the upstream and downstream face of the pier was determined over the full simulation period by incorporating the depth of contraction and local scour. In addition, the channel bed elevation was lowered whenever the contraction scour values were greater than zero.

The program steps were written and compiled in Fortran 77. The program was identified by the acronym WAVES which means Watershed Vested Estuary Scour. Presented below is a summary of the steps required to simulate the scour process, which are later addressed in detail. The Fortran 77 codes used to represent the model may be found in Appendix A-2.

First, the number and duration of scour producing storms were determined and variates selected to represent the intensity and depth of each storm. Second, the riverine flow hydrograph at the bridge location was constructed. Third, the base station tidal statistics were determined and used to synthesize the base station tides. Fourth, tidal elevations at the bridge location were determined. Fifth, the tidal discharges at the bridge location were computed. Sixth, the routed riverine outflow from the bridge location and the combined tide–freshwater depths and water surface elevations (WSE) were determined. Seventh, the combined flow velocities at the bridge location in the upstream and downstream directions were determined. Eighth, the downflow and vortex velocity vectors were computed. Ninth, the local and contraction scour and the total scour as the sum of the local scour and contraction scour components were computed.



### 3.11.3 Determine Storm Event Variates

The inputs required for this step include the catchment regional location, the rainfall records of the catchment area, and the intensity–duration–frequency (IDF) and depth–duration–frequency (DDF) curves for that region. The case study sites investigated were all located in the Maryland tidal area, and it was assumed that the rainfall patterns of these sites could be represented by the Baltimore rainfall IDF and DDF curves. To ensure a level of variation in the annual number of storms, this variable was modeled as a normal variate, and a random number generator was used to determine the depth at the beginning of each simulation year.

The duration of each storm (6, 18, 24, or 36 hrs) and annual proportions of each duration were determined by methods described in Section 2.3.3. Variates representing the depth of each event were generated for these durations using the gamma function described below:

$$\Gamma = -b \ln(\prod_{i=1}^c U_i) = -b \ln[u_1 * u_2 * \dots * u_{c-1} * u_c] \quad (3.11-1)$$

in which  $U_i$  is a set of uniformly distributed random numbers (0,1),  $\Gamma$  represents the storm depth derived from the uniformed variates, while  $b$  and  $c$  are determined using regional rainfall data where:

$$c = (\text{mean daily rainfall} / \text{standard deviation in daily rainfall})^2 \quad (3.11-2)$$

$$b = (\text{variance in the daily rainfall} / \text{mean daily rainfall}) \quad (3.11-3)$$

The variates were generated by the program using a random number generator.

#### 3.11.4 Determine Catchment Hydrograph for Each Storm

The inputs required for the determination of the riverine hydrograph associated with each storm include the catchment area, the SCS curve number, the catchment time of concentration, the SCS design storm for that region, the SCS dimensionless unit hydrograph, the storm duration, and the rainfall depth. A catchment hydrograph was determined for each storm using the method described in Section 3.2.4. The time base of each hydrograph was extended to ensure full coverage of the simulation period.

The mean time base  $t_b$  (or duration) of the runoff hydrograph in hours was estimated by:

$$t_b = 8766/NO \quad (3.11-4)$$

where NO is the number of storms each year and 8766 represent the number of hours in a year. The mean time base was computed to set the upper limit of the duration of the hydrograph from each storm. The number of runoff ordinates for each storm  $N_R$ , is given by:

$$N_R = N_p + N_u - 1 \quad (3.11-5)$$

where  $N_p$  is the number of rainfall ordinates and  $N_u$  is the number of unit hydrograph ordinates. Since the computations were done hourly, it may be shown that:

$$N_p = D \quad (3.11-6)$$

in which D is the rainfall duration. Also, the number of unit hydrograph ordinates ( $N_u$ ) may be given by:

$$N_u = 5 t_p \quad (3.11-7)$$

or

$$N_u = 3.3 t_c \quad (3.11-8)$$

where  $t_c$  is the time of concentration of the catchment watershed and  $t_p$  is the hydrograph time to peak. Therefore, the number of rainfall ordinates would be:

$$[(D + 3.3 t_c)/\Delta t] - 1 \quad (3.11-9)$$

where  $D$  is the duration of the storm in question and  $\Delta t$  is the simulation time increment of 1.0 hr. The catchment base flow was computed using:

$$Q_{\text{base}} = 1.02A^{0.91} \quad (3.11-10)$$

where  $A$  represents the catchment area in square miles and  $Q_{\text{base}}$  is the base flow in cfs.

Development of the storm hydrograph used SCS procedures and the assumptions discussed earlier. Figure 3.11-2 depicts the sequencing of the storms to provide continuous simulations.

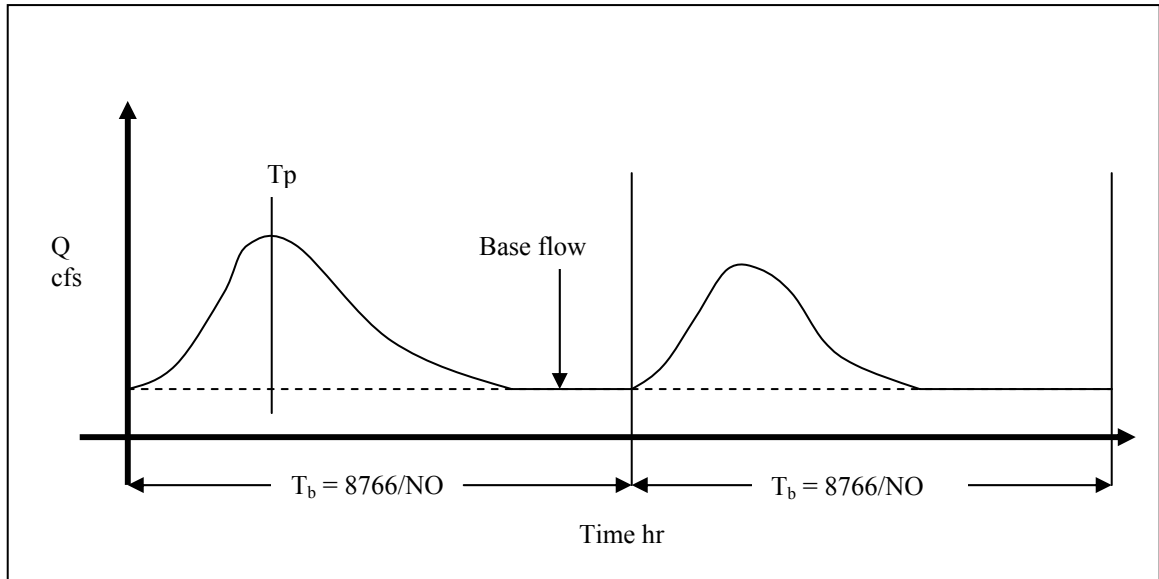


**Fig. 3.11-2. The time base ( $T_b$ ) of each hydrograph in the Sequence of Simulated Storms.  $T_b$  was computed to provide continuous simulations.**

### 3.11.5 Determine Base Station Tidal Variates and Synthesize Tidal Model

In order to synthesize the tidal model, tidal data from the tidal base station were gathered. The base station was selected far enough downstream of the bridge location so

that the tidal profile was not noticeably influenced by riverine flows. NOAA provides a source of historical tidal data through the network of stations they maintain. In order to determine the tidal variates, a statistical analysis of the historical tidal data was performed at the base station selected.

Tidal data from Sewell Point near Norfolk, Virginia, were analyzed to produce the statistics of the tides at the base station. The mean depth and the tidal statistics produced were used to synthesize the base station tidal model. The analysis of the tidal data involved fitting parameters of a tidal model by determining the mean and standard deviation of the tidal amplitudes related to both the diurnal and lunar periods. Also, the mean diurnal and lunar periods were determined. Random number simulations were used to generate variates to represent the diurnal and lunar amplitudes. New random variates were generated on each change of the diurnal or lunar cycle and kept constant throughout that cycle. The general tidal elevation model with the mean sea level (MSL) used as the datum may be represented as:

$$\eta = z_i(f(T_D))(A_m, A_{st})\sin[(2\pi(t/T_D)+\phi_i)] + z_j(L_m, L_s)*\sin[2\pi(t/T_L)+\phi_j] \quad (3.11-11)$$

where  $\eta$  is the tidal elevation (ft),  $A_m$  is the mean diurnal amplitude (ft),  $A_{st}$  is the standard deviation in the diurnal amplitude (ft),  $T_D$  is the mean diurnal period (hr),  $L_m$  is the mean lunar amplitude (hr),  $L_s$  is the standard deviation in the Lunar amplitude (hr),  $T_L$  is the mean lunar period (hr),  $t$  is the time variable in hours,  $\phi_i$  is the phase angle of the diurnal period,  $\phi_j$  is the phase angle of the lunar period,  $z_i(f(T_D))$  signifies the fact that normal variates for the diurnal amplitude will be changed on each new cycle.  $z_j(L_m, L_s)$  represents the normal variates to be generated for the lunar cycle. Note that only one

variate was used per storm simulation as the lunar cycle is much longer than the expected storm time base.

The general tidal depth variation model for the base station is given by:

$$Y_B = M + z_i(f(T_D))(A_m, A_{st})\sin[(2\pi(t/T_D) + \phi_i) + z_j(L_m, L_s)*\sin[(2\pi(t/T_L) + \phi_J)] \quad (3.11-12)$$

where  $Y_B$  is the time-varying tidal depth (ft) and  $M$  is the mean tidal depth at the base station (ft).  $M$  is given by:

$$M = M_w - B_{in} \quad (3.11-13)$$

where  $M_w$  is the mean tidal elevation and  $B_{in}$  is the invert of the base station. If MSL is taken as the datum then  $M$  is given by:

$$M = -B_{in} \quad (3.11-14)$$

The following sinusoidal tidal model was calibrated for the use of Sewell Point as a base station:

$$Y_B = 5.80 + z_i(f(T_D))(1.21, 0.285)\sin(2\pi[t/12.32] + \phi_i) + z_j(0.62, 0.28)*\sin(2\pi[t/356] + \phi_J) \quad (3.11-15)$$

where  $Y_B$  is the total tidal depth in feet at the base station at any time  $t$ ;  $z_i(f(T_D))$  denotes that the variates representing the diurnal amplitude will be generated from the normal distribution  $z_i(1.21, 0.285)$  and will change only with a change in the diurnal cycle ( $T_D = 12.32$  hrs). Similarly, the variates representing the lunar amplitude were generated from the normal distribution  $z_j(0.62, 0.28)$ . Only one lunar variate per storm event simulation is required as the lunar cycle ( $T_L = 356$  hrs) is much longer than the storm event base.

The duration of the tide associated with each storm event was set equal to the freshwater storm hydrograph duration. Therefore, the total number of variates per event simulation needed to represent the diurnal amplitude was given by:

$$N_d = t_b / T_D \quad (3.11-16)$$

### 3.11.6 Determine Tidal Elevations at Bridge Location

The inputs required for this step were the distance from tidal base station to bridge location, the estuary invert at the bridge location, the mean estuary depth at the bridge location, and the planar area of the estuary upstream of the bridge location. First, the average tidal amplitude ( $A_B$ ) at the base station was determined. The mean diurnal tidal amplitude ( $A_b$ ) at the bridge station was also estimated. This was done by estimating the water surface depths obtained from NOAA historical records from gauges closest to the bridge station. The tidal records used were those taken over extended periods when the station was not influenced by runoff from freshwater inflows. These periods were identified by the regularity of the tidal variations. Next, the tide attenuation factor,  $\bar{A}$ , determined as the relationship between mean amplitude at bridge station b and the mean amplitude at base station B was given by:

$$\bar{A} = A_b / A_B \quad (3.11-17)$$

For example, using Sewell Point as the base station B and Baltimore as the bridge station b, it was found that  $\bar{A}$  was 0.6.

The Sewell Point and Baltimore tidal measurements were used to develop a regression equation that related the mean lag time and the attenuation factor of the wave.  $K$  is the mean tidal lag time in moving from base station B, to bridge station b, and  $K$  was given by the regression equation:

$$K/\Delta t = 3.694 + 19.164 * p_m - 21.247 * \bar{A} \quad (3.11-18)$$

Equation 3.11-18 resulted in a standard error ratio ( $S_e/S_y$ ) of 0.338, which indicates good accuracy. In Equation 3.11-18,  $\bar{A}$  is the wave attenuation factor and  $p_m$  is the mean peakedness of the wave at the base station defined as the mean value of  $p$ , which was computed by:

$$p = [\eta_B \text{ at } (t = t_p - \Delta t)] / [\eta_B \text{ at } (t = t_p)] \quad (3.11-19)$$

where  $\eta_B$  at  $(t = t_p - \Delta t)$  represents the base station tidal elevation at the time increment before the peak tide and  $\eta_B$  at  $(t = t_p)$  represents the tidal elevation at the peak tide.

For  $\Delta t = 1$  hour the lag time is given by:

$$K = 3.694 + 19.164 * p_m - 21.247 * \bar{A} \quad (3.11-20)$$

The above equation is defined only for  $2/3 < p_m < 1$ ,  $0.4 < \bar{A} < 1$ , and  $2 < (K/\Delta t) < 10$

In order to obtain the wave properties at the bridge station, the wave was routed using the convex routing procedure described below. The convex routing factor,  $C$ , is given by:

$$C = \Delta t / K \quad (3.11-21)$$

while the routed water surface elevation values at the bridge station at any time  $t$  is given by :

$$\eta_b \text{ at time } (t+1) = \bar{A} * \eta_B \text{ at time } (t+1) \quad (3.11-22)$$

$$\eta_b \text{ time } (t+1) = C * \eta \text{ at time } t + (1-C) * \eta_b \text{ at time } t \quad (3.11-23)$$

In addition to being attenuated, the shape of the wave at the bridge station will also change due to frictional forces. The change in shape may be determined by computing the new time  $t_b$  at which each point on the attenuated wave arrives at the bridge station:

$$t_b = t_t + L_w / \{1800g * [(\eta_B - B_{in}) + (\eta_b - b_{in})]\}^{0.5} \quad (3.11-24)$$

The time, in hrs, described by  $t_b$ , was not be restricted to whole number values, accordingly interpolations was required to reflect the value of the transformed tidal elevation on an hourly basis.

Hurricane surges were incorporated into the tidal profile at the bridge by using a modified form of the Richardson and Edge (1997) equation. In the scheme used, the duration of the hurricane  $D$  (hrs) is given by:

$$D = R/f \quad (3.11-25)$$

where  $R$  is the hurricane radius in miles and  $f$  is the hurricane translational speed in miles per hour. Next, the position of the hurricane relative to the bridge was defined by the term  $H_{prm}$  such that:

$$H_{prm} = \begin{cases} R - H_{dis} & \text{for } H_{dis} < R \\ 0 & \text{for } H_{dis} > R \end{cases} \quad (3.11-26)$$

where  $H_{dis}$  is the expected closest distance that the hurricane will approach the bridge.

The terms derived above were then incorporated in the following model to estimate a value of the surge with respect to time:

$$S_t(t) = S_p * (H_{prm}/R) [1 - \exp(-((S_p * (H_{prm}/R))/R) * (t/(D-t)))] \quad (3.11-27)$$

In Equation 3.11-27,  $S_p$  is the maximum surge in feet, and  $S_t$  is the surge at any given time  $t$ . The surge profile was then algebraically added to the distorted tide profile and the resultant used to determine the tidal discharge.



### 3.11.7 Determine Tidal Discharges at the Bridge Location

The discharge generated by the tidal changes at location b is determined using the modified Neill's equation. Neill (1973) predicted the discharge generated by tidal changes as:

$$Q_N = A_s * [\Delta \eta_b / \Delta t] \quad (3.11-28)$$

By selecting a computational time step  $\Delta t$  of one hour Equation 3.11-30 becomes:

$$Q_N = A_s * [\Delta \eta_b] \quad (3.11-29)$$

where  $Q_N$  is the Neill's predicted tidal discharge,  $A_s$  is the plan area of the estuary, and  $[\Delta \eta_b]$  represents hourly change in tidal elevation. The term  $[\Delta \eta_b]$ , which is negative on the rising limb and positive on the falling limb of the tide, is defined by:

$$[\Delta \eta_{b(t)}] = \eta_{bf(t)} - \eta_{bf(t+1)} \quad (3.11-30)$$

Tidal discharges were found to depend on the wave travel time, estuary shape, and the ratio of the mean tidal range to the mean depth as described by the following equation:

$$Q_R = \begin{cases} Q_N \{1 + \sin[(L_w/C_e T_D) - 0.01] 1.04 (W_m/W_o)^{0.58} (H/y_m) - 1.13\} & \text{for } (L_w/C_e T_D) > 0.01 \\ Q_N & \text{otherwise} \end{cases} \quad (3.11-31)$$

where  $W_m$  is the maximum width of the estuary upstream of location b,  $W_o$  is the width of the estuary at the bridge location b,  $C_e$  is the mean wave celerity given by  $(g y_m)^{0.5}$ ,  $H$  is the mean tidal range for that tidal series,  $L_w$  is the distance from station B to station b, and  $y_m$  is the mean depth at location b. For the falling limb of the tide:

$$Q_F = Q_{Nt} (L / C_e T_D)^{0.09} (H / y_m)^{0.256} \quad (3.11-32)$$

### 3.11.8 Determine the Combined Depth and Velocity at the Bridge Location

The next step in the modeling process was the determination of the combined tide-fresh water flow depth and flow velocity. First it was necessary to determine the combined flow depth as a function of time from the following equation:

$$Y_{T(0)} = A_m + Y_{bm} \quad (3.11-33)$$

where  $A_m$  is mean tidal amplitude at the bridge cross section,  $Y_{T(0)}$  is the assumed estuary depth at the beginning of each simulation, and  $Y_{bm}$  is the mean low tide depth.

For time  $t$  greater than zero the following equation holds:

$$Y_{T(t)} = \begin{cases} [S_{(t-1)} + 3600*[Q_f + |Q_R|]_{(t)})/A_s & \text{for the rising limb} \\ [S_{(t-1)} + 3600*[Q_f - Q_F]_{(t)})/A_s & \text{for the falling limb} \end{cases} \quad (3.11-34)$$

In Equation 3.11-34,  $Y_{T(t)}$  represents the resultant water depth at any given time  $t$ ,  $A_s$  is the planar area of the estuary above the bridge section, and  $Q_f$  is the catchment discharge at time step  $t$ ,  $Q_R$  is the tidal discharge flowing into the estuary on the rising limb of the tide,  $Q_F$  is the tidal discharge flowing out of the estuary at the falling limb of the tide, and  $S_{(t-1)}$  is the estuary storage brought forward from the prior time increment. The estuary storage at the beginning of the simulation was assumed to be:

$$S_{(t-1)} = A_s * A_m \quad (3.11-35)$$

The process used by the algorithm in the hourly determination of the combined water depth was as follows. First, the total storage at time  $t=1$  hr was computed from the following equation:

$$Y_{T(1)} = S_{(1)}/A_s \quad (3.11-36)$$

where  $S_{(1)}$  is given by:

$$S_{(1)} = \begin{cases} [A_s * (A_m + Y_{bm}) + 3600 * [Q_f + |Q_R|]_{(1)}] & \text{for the rising limb} \\ [A_s * (A_m + Y_{bm}) + 3600 * [Q_f - Q_F]_{(1)}] & \text{for the falling limb} \end{cases} \quad (3.11-37)$$

Next the combined depth at time  $t=2$  hrs is computed as follows:

$$Y_{T(2)} = S_{(2)} / A_s \quad (3.11-38)$$

where  $S_{(2)}$  is given by:

$$S_{(2)} = \begin{cases} [S_{(1)} + 3600 * [Q_f + |Q_R|]_{(2)}] & \text{for the rising limb} \\ [S_{(1)} + 3600 * [Q_f - Q_F]_{(2)}] & \text{for the falling limb} \end{cases} \quad (3.11-39)$$

This process was repeated for all of the time increments in the tidal and catchment series.

The net stream velocity was then computed as:

$$v_{n(t)} = Q_{T(t)} / [W_o * Y_{T(t)}] \quad (3.11-40)$$

where  $W_o$  is the width of the estuary at the bridge station,  $Q_{T(t)}$  is the time-varying total discharge, and  $Y_{T(t)}$  is the time varying flow depth.

### 3.11.9 Determine Downflow and Vortex Velocity Vectors

The following steps, from the determination of the downflow to the computation of scour, were done sequentially for each velocity ordinate related to the storm-tidal series combination. The downflow was determined from the first velocity ordinate, next the vortex velocity at the same time step was computed, and followed by the local and contraction scour. The process was repeated with the next velocity ordinate and so on to the end of the storm-tidal series. The required input were the net estuary velocity, as a function of time, computed in Section 3.11.8, the total flow depth as a function of time computed in Section 3.11.7, and the bridge pier diameter. Other inputs included the existing scour depth at the beginning of the process, and the mean particle diameter and

the angle of internal friction of the bed material. The computed downflow velocity and the time varying total estuary discharge were also required.

The downflow was computed using the following equation:

$$V_{d(t)} / v_{n(t)} = \begin{cases} 0.15(d_s/d)_{(t)} + 0.24d^{0.18} / [Y_{T(t)}^{0.18} C_1^{0.5}] & \text{for } d_s/d \leq 2.3 \\ [0.40 / (1 + e^{3\{(d_s/d)(t) - 4\}})] + 0.40 & \text{for } d_s/d > 2.3 \end{cases} \quad (3.11-40)$$

where  $V_d$  (ft/s) is the downflow at that time (hrs),  $v_n$  is the net stream velocity (ft/s),  $d$  is the pier diameter (ft),  $d_s$  is the existing scour depth (ft),  $Y_T$  is the total depth of flow (ft), and  $C_1$  is the orifice coefficient. When the net velocity was negative, the downflow was evaluated at the downstream face of the pier. When the net velocity was positive the downflow was evaluated at the upstream face of the pier.

The following system of equations was used to determine the time varying vortex properties along the upstream and downstream faces of the bridge pier:

$$V_{t(t)} = \begin{cases} V_m(a/a_m)_{(t)} & a \leq a_m \\ V_m(a_m/a)_{(t)} & a > a_m \end{cases} \quad (3.11-43)$$

where  $V_t$  is the magnitude of the tangential velocity of the horseshoe vortex in contact with the side of the scour hole (ft/s),  $V_m$  is the maximum value of the tangential velocity (ft/s),  $a$  is the distance from the center of the vortex to the side of the scour hole along the minor axis of the vortex (ft), and  $a_m$  is the distance from the center of the vortex along the minor axis to the location of the maximum tangential velocity (ft). The variables listed are given by the following equations:

$$V_m(t) = \begin{cases} 2.24C_1^{0.5}V_{d(t)} & \text{for } \theta < \phi \\ 2.7 V_{d(t)} & \text{for } \theta = \phi \end{cases} \quad (3.11-44)$$

where  $\theta$  is the angle (in degrees) of the side slope of the scour hole and  $\phi$  is the angle of internal friction of the channel material in degrees. The distance from the center of the vortex along the minor axis to the location of the maximum tangential velocity ( $a_m$ ) is given by:

$$a_m/a = -0.0002\theta^2 + 0.012\theta + 0.80 \quad (3.11-45)$$

$$a_m = a[-0.0002\theta^2 + 0.012\theta + 0.80][0.08 + 0.23\sin(\theta * 3.142/180)] \quad (3.11-46)$$

$$\theta_{(t)} = \begin{cases} 31(d_s/d)^2 & \text{for } 31(d_s/d)^2 < \phi \\ \phi & \text{otherwise} \end{cases} \quad (3.11-47)$$

where  $a$  is the length of the minor axis of the vortex (ft),  $\theta$  is the angle of the scour hole (degrees),  $\phi$  is the angle of internal friction of the bed material,  $d_s$  is the depth of scour, and  $d$  is the pier diameter.

First, the angle of the side slope was computed based on the existing scour depth prior to the storm event using Eq. 3.11-47. Then the maximum tangential velocity was computed from Eq. 3.11-44. Following this, the distance  $a_m$ , from the center of the vortex to the side of the scour hole along the minor axis of the vortex, and  $a$ , the distance from the center of the vortex along the minor axis to the location of the maximum tangential velocity were computed using Equations 3.11-45 and 3.11-46, respectively. Finally the vortex tangential velocity at the side of the scour hole was computed from Eq. 3.11-43.

### 3.11.10 Compute Scour (Sum of Local and Contraction Scour)

The required inputs for this step are the tangential velocity of the horseshoe vortex determined in Section 3.11.9, the pier diameter, the total water depth in the estuary

at the bridge station, bed and bank soils properties and particle diameter, and the net velocity computed from Section 3.11.5. The process involves the computation of the total local scour depth over each storm event and summing it over one year of simulation then repeating this process for 100 years. The contraction scour was then computed based on the highest flow depth in each storm in the 100-yr simulation and added to the total local scour hourly. The flow velocity was then adjusted to account for the general lowering of the bed in the near-field contraction section.

The local scour was computed for the variable set of net velocity, downflow, and tangential velocity computed for a given time step. The process was then repeated for all the net velocities in the event series while summing the local scour values. Local scour was determined by the following set of equations. The total local scour at the end of the first time step was given by:

$$d_{si+1} = d_{si} + (dd_s/dt)_i (\Delta t) \quad (3.11-48)$$

For a computational time step of one hour Equation 3.11-48 becomes:

$$d_{si+1} = d_{si} + (dd_s/dt)_i \quad (3.11-49)$$

where  $d_{si+1}$  is the local scour at the end of the first time step,  $d_{si}$  is the local scour at the beginning of the first time step and  $(dd_s/dt)_i$  is the rate of scour over the first time step.

The process is repeated for the second and subsequent time steps. The scour rate produced during a given time step is given by:

$$dd_s/dt = K1 * K2 * K3 \quad (3.11-50)$$

where:

$$K1 = \exp\{-0.08[ABS[(V_i/V_t) \ln(t/t_e)]]^{1.2}\} \quad (3.11-51)$$

$$K2 = \{ABS[\ln(t/t_e)]\}^{0.2} \quad (3.11-52)$$

$$K3 = 0.1*(d_{se}/t)*(V_i/V_t)^{1.2} \quad (3.11-53)$$

The time variable of the simulation is denoted as  $t$ . The variable  $V_i$  is the velocity of incipient motion for the channel soil material, which was determined by the following models:

$$V_c = [2(\rho_s - 1)gd_{50}\text{Tan}\phi[2.22 Y_T^{1/3}]/(3\alpha\gamma_w n^2)]^{0.5} \quad (3.11-54)$$

or

$$V_c = 4.81[(S_s - 1)gd_{50}]^{0.5}[Y_T/d_{50}]^{0.17} \quad (3.11-55)$$

and

$$V_i = 0.476 (d_{50} / B)V_c \quad (3.11-56)$$

where  $B$  is the pier diameter (ft),  $V_i$  is the incipient velocity of the bed material (ft/s),  $V_c$  is the critical erosion velocity of the bed material (ft),  $d_{50}$  is the mean grain size (mm),  $S_s$  represents the specific gravity given by  $\rho_s/\rho_w$ ,  $\rho_s$  is the density of sand or clay material,  $\rho_w$  is the density of water,  $\phi$  is the angle of internal friction of the bed material,  $\alpha$  is a constant ranging from 5.3 for clays to 7.5 for sand,  $n$  is Manning's coefficient,  $\gamma_w$  is the specific weight of water (lb/ft<sup>3</sup>), and  $Y_T$  is the estuary depth (ft).

When natural armoring is considered the following process is used. First, the standard deviation of the soil material particle size is determined as:

$$\sigma > 1.3 \quad (3.11-57)$$

where  $\sigma$  is the standard deviation of the particle sizes in the bed material given by:

$$\sigma = (d_{84}/d_{16})^{0.5} \quad (3.11-58)$$

If the standard deviation in the soil particle sizes is greater than 1.3, then the mean armoring particle diameter is computed as:

$$d_{50a} = d_{\max}/1.8 \quad (3.11-59)$$

where  $d_{50a}$  is the maximum soil particle size. Next, critical armoring velocity  $U_{ca}$  is determined from:

$$U_{ca} = 4.81[(S_s - 1)gd_{50a}]^{0.5}[y/d_{50a}]^{0.17} \quad (3.11-60)$$

Finally, the incipient armoring velocity is given by:

$$U_a = 0.8U_{ca} \quad (3.11-61)$$

Combining Equations 3.11-60 and 3.11-61 and substituting for the specific gravity of water and  $d_{50a}$  gives:

$$U_a = 1.328(d_{\max}/1.8)^{0.33}y^{0.17} \quad (3.11-62)$$

The equilibrium or ultimate scour depth  $d_{se}$  associated with a given tangential velocity is given by :

$$d_{se}/d = \begin{cases} [\tanh(Y_T/d)][(V_t/V_i)] & \text{for } (V_t/V_i) > 0 \\ 0 & \text{otherwise} \end{cases} \quad (3.11-63)$$

where  $d_{se}$  (ft) is the ultimate scour depth for a given tangential velocity  $V_t$  (ft/s),  $V_i$  (ft/s) is the net estuary velocity,  $Y_T$  (ft) is the total estuary depth, and  $d$  (ft) is the pier diameter. The time to equilibrium scour,  $t_e$  (in hrs.), for a particular tangential velocity is given by:

$$t_e = \begin{cases} 48.26 (d/V_t)[(V_t/V_i)-0.4] & \text{for } (Y_T/d) > 6 \\ 30.89 (d/V_t)[(V_t/V_i)-0.4](Y_T/d)^{0.25} & \text{for } (Y_T/d) \leq 6 \end{cases} \quad (3.11-64)$$

Finally, the 100-yr simulations were repeated 1,000 times and the results discussed in Sections 3.10.1 through 3.10.4 were recorded.



### **3.11.11 Program Execution Options**

The WAVES program depends greatly on the equations that predict the various aspects of the pier scour process. In addition, researchers have not reached a clear consensus on the applicability of many of these equations. The assumed scour conditions are also variable and as such will have an effect on scour predictions. As a result, the WAVES program was developed with a number of capabilities and options to facilitate the complete analysis of the pier scour results predicted with the use of these equations. The options provided are: executing the program in the pier design or existing pier analysis mode, choice of the equation used to determine the critical erosion velocity of the bed material, choice of the equation used to determine contraction scour, executing the program with either considering or neglecting armoring, consideration of the Brubaker-Demetrius modifications to the Neill's tidal discharge equation, consideration of tide distortion, and the use of the Saffir-Simpson hurricane classification or specific hurricane properties.

The WAVES program was developed to facilitate the design of new bridge piers and the analysis of scour at existing facilities. The pier design option allows for the sizing of new piers (diameter and depth) by starting the scour simulations with zero scour. In contrast, the existing pier analysis option assumes the existence of some degree of scour at the start of the simulation.

The determination on the critical erosion velocity of the channel bed material plays an important role in the pier scour process. The literature review conducted revealed a number of equations that were developed for this purpose. The literature review did not reveal a clear consensus among researches regarding the comparative

accuracy of these models. Accordingly, three of the most widely used critical erosion velocity models were included in the WAVES program as options. These models include the HEC18 model, the Neill's critical velocity model, and the SRICOS critical velocity model. These models are all described in Chapter 2.

The WAVES program was also developed with the ability to predict contraction scour where the estuary cross section geometry warrants this consideration. Three popular contraction scour models identified in the literature and discussed in Chapter 2 were included as options in the WAVES program. The contraction scour models provided as options, were the Straub's, Neill's, and Komura's contraction scour equations.

Though not recommended for consideration by most researchers, natural channel armoring was included as an option for the WAVES program simulations. The natural armoring method used was based on the method developed for the HEC18 model. Natural armoring was included in the WAVES program so that its effects could be analyzed by prospective model users through the direct comparison of the scour results produced with and without consideration of this option.

The tidal process also plays an important role in the development of pier scour. The tidal process includes many complicated tidal effects with two of the most important effects included as options in the WAVES program. These options are the Brubaker-Demetrius modification to the Neill's estuary discharge equation and the consideration of tidal distortion in the computation of the tidal discharges. Both these effects are discussed in detail in Chapter 2.

The single-event hurricane simulation was included in the WAVES program to determine the impacts of a single hurricane event in the scouring of bridge piers. The hurricane option provides for the modeling of hurricanes of specific strength categories based on the Saffir-Simpson hurricane classification. In addition, the hurricane option allows for the modeling of hurricanes where specific characteristics such as expected surge, wind speed, and the hurricane size are used as inputs.

## **CHAPTER 4**

### **SENSITIVITY AND ERROR ANALYSIS**

#### **4.1 INTRODUCTION**

##### **4.1.1 Reasons and Challenges of a Sensitivity Analysis for Estuary Scour**

One of the objectives of this study was to perform sensitivity analyses of the model and its components to determine the importance of the coefficients, parameters, and variables, design engineers can then properly use the model to obtain the best possible accuracy in bridge designs. By providing information on the most sensitive variables to design engineers who use the model, the sensitivity analysis will assist in improving the accuracy of the design by establishing the performance criteria for the input variables. Variable and parameter sensitivity analyses are also useful during the model formulation phase because they help to determine the variables that should be included in the model and those that may be omitted, thus ensuring that the model will not be unnecessarily complex. The variable sensitivities may also serve as a method of examining the rationality of the model output. The response of a rational model to the model input variables and parameters must be consistent with the theoretical and empirical performance of these variables (parameters). An error analysis may be used to determine the propagation of errors on the overall reliability and accuracy of the model, while an uncertainty analysis is an important aspect of model verification and helps to establish the reliability of the model.

As discussed in Chapter 3, the scour model includes tidal, catchment, hydraulic, and scour components. A number of variables and parameters, upon which the final

scour results depend, exist within each of these components. A component sensitivity analysis allows the ranking of these components with regard to the overall model response to the component changes. This analysis will further assist in determining the importance of each component and hence will also be helpful in the formulation phase by facilitating revisions to the model to ensure that the level of complexity of each component is appropriate. Owing to the degree of complexity involved in the interactions of these components to produce estimates of scour, a traditional component sensitivity analysis that involves the analyses of the inputs and outputs of each component was difficult to perform. Instead, a comparison of the number of sensitive variables and the degree of sensitivity of such variables within each component was made.

#### **4.1.2 Challenges with the Sensitivity Analyses of Continuous Simulations in a Tidal Environment**

A unique feature of estuarine and tidal scour is that scour can be initiated by either upstream or downstream flows on the downstream or upstream pier face. Accordingly, it is likely that scour initiated from the upstream and downstream faces will respond differently to each component and variable. This is due to the fact that in a tidal or estuarine environment the catchment components produce discharges and velocities that are directed downstream thus impacting the upstream pier face. Conversely, the tidal flows are periodically directed upstream and will more likely impact the downstream face of the pier. As a result, it would be expected that scour on the upstream pier face will be more sensitive to the variables of the catchment component, while the downstream pier face should be more susceptible to the variables of the tidal process. In order to verify

this postulation, separate sensitivity analyses were performed for scour on the upstream and downstream pier faces.

Another objective of this study was to compare the scour that resulted from continuous simulations with those obtained from current models that are based on single events or design storms. In order to achieve this objective in a concise way, the model was designed to provide annual cumulative scour over the life of the bridge structure for both the upstream and downstream pier faces. Depending on the estuary conditions, it was expected that the variation of scour with time would be different for the upstream and downstream pier faces. Further, for the upstream or downstream pier faces, the rate of scour and the sensitivities of the variables were also expected to vary with time. As a result, making annual comparisons between variables would be difficult. In order to facilitate the process of comparing the sensitivities of the variables, it was necessary to determine the mean sensitivity of each variable, which is the sum of the annual sensitivity divided by the simulation period.

## **4.2 DEVELOPMENT OF BASELINE STUDY CONDITION**

### **4.2.1 Identification of Input Variables and Parameters**

In order to develop the baseline study conditions, it was necessary to review the list of input data used by the program and select those variables and coefficients that would be used in the analysis. The sensitivity analyses were used to identify the most important variables. A list of all the input variables used by the program is shown in Table 4.2-1.

**Table 4.2-1. Input Data for Scour Model with the Acronym Shown**

Acronym	Variable
ALPHA	A constant defined by soil type and particle size
AS	Estuary plan area (mi <sup>2</sup> )
B6, B18, B24, B36	Gamma distribution variable b
C1	Orifice factor for downflow computation
C6,C18, C24, C36	Gamma distribution variable c
CBA	Catchment basin area (mi <sup>2</sup> )
CN	Curve number
D16	Soils gradation data d16, 16% finer than (mm)
D50	Soils gradation data d50, 50% finer than (mm)
D84	Soils gradation data d84, 84% finer than (mm)
DMAX	Soils gradation data maximum particle size (mm)
DT	Base station diurnal period (hr)
HDIST	Closest distance of approach to the bridge (mi)
HRAD	Hurricane radius (mi)
HSPEED	Hurricane translation speed (mph)
HURAIN	Hurricane rainfall (in.)
IBS	Base station invert (ft)
IRS	Bridge station invert (ft)
LE	Estuary length above bridge station (mi)
LT	Base station lunar period (hr)
LW	Distance between bridge and base station (mi)
MDA	Base station diurnal amplitude (ft)
MDR	Bridge station mean depth (ft)
MLA	Base station lunar amplitude (ft)
MLT	Bridge station mean low tide depth (ft)
MLTE	Bridge station mean low tide elevation (ft)
MTR	Bridge station diurnal amplitude (ft)
MXSURG	Hurricane surge (ft)
NBP	Number of bridge piers
PD	Pier diameter (ft)
PHI	Soil angle of repose (phi angle) (degrees)
PKM	Base station wave peakedness amplitude (ft)
SDA	Standard deviation in base station diurnal amplitude (ft)
SLA	Standard deviation in base station lunar amplitude (ft)
TMCON	Time of Concentration (hr)
UESTZ	Estuary over bank side slope UESTZ:1
WB	Estuary width at bridge station (mi)
WD	Estuary width at near field distance below bridge station (mi)
WM	Maximum estuary width above bridge station (mi)
WTBMLT	Estuary width at bridge station (ft)
WU	Estuary width at near field distance above bridge station (mi)
XABMLE	Estuary in bank area at bridge cross section (ft <sup>2</sup> )

## **4.2.2 Development of Baseline Conditions**

### **4.2.2.1 Selection of the Data to be Analyzed**

Preliminary sensitivity simulations were performed for all of the input variables to identify parameters and variables that would be selected for more comprehensive sensitivity analyses. The data to be analyzed were selected based on three criteria. First, the data consisted of variables whose values would be subject to the judgment of the bridge design engineer or the program user. For example, the pier diameter variable (PD) was selected as the pier size would need to be determined by the bridge design engineer; however, the invert (IRS) of the bridge station would not be selected by the user, as once the design engineer selects a bridge location, the invert is fixed as a variable. Second, the data consisted of parameters and variables that indicated significant sensitivities during the preliminary simulation exercise. The bridge location tidal amplitude (MTR) was selected because it was found that both the upstream and downstream pier face scour was significantly affected by the magnitude of this variable. Third, the data variables and parameters were selected to ensure that all of the components of the model were represented in the analysis.

### **4.2.2.2 Selection of Simulation Length**

Many simulations were required to conduct the sensitivity analyses using continuous simulations. This in turn required a large amount of computer time, as the duration of each simulation was 100 years. As a result, it was necessary to use a shorter simulation for the sensitivity studies. With a large number of variables to be analyzed, the exercise would be made more efficient if a simulation duration that was just long



enough to produce significant changes in the scour results was used. A simulation length of 25 years was selected for the sensitivity analyses because the maximum scour was achieved within this period in most of the test runs done as part of the preliminary sensitivity study.

#### 4.2.2.3 Selection of Baseline Conditions

The scenario selected for the sensitivity analysis of the baseline conditions was based on observations made on the tidal rivers and estuaries of the Chesapeake Bay system. A review of the Chesapeake Bay estuaries revealed that most of these systems could be defined as well mixed with data ranges that conformed to those displayed in Tables 4.2-2 through 4.2-6. In addition, the bridge cross section was selected to be narrow and shallow enough to ensure that significant velocities would be developed within the cross section, which would give rise to significant scour. The relative size of the estuary and catchment areas were selected such that scour on the upstream and downstream faces of the piers was expected to be similar in magnitude. A rule of thumb was established from the preliminary simulations when it was found that a 4-mi<sup>2</sup>-estuary caused scour that was roughly equivalent to that from a catchment area of 300 mi<sup>2</sup>. Generally, the baseline conditions were developed from the average values of the input variables listed.

**Table 4.2-2. Data ranges of the catchment variables observed in the review of the Chesapeake Bay estuaries with the variables defined as follows; CBA the catchment basin area, TMCON the time of concentration, and CN the curve number.**

VARIABLE	CBA (mi <sup>2</sup> )	TMCON (hr)	CN
Maximum Value	1000	58	86
Average Value	300	36	78
Minimum Value	50	12	54

**Table 4.2-3. Data ranges of the estuary variables observed in the review of the Chesapeake Bay estuaries with the variables defined as follows; LW the distance between the tidal base station and the bridge station, AS the estuary plan area above the bridge location, MTR the tidal amplitude at the bridge station, LE the length of the estuary upstream of the bridge, WU the width of the estuary at the near-field Distance Above The Bridge, WD the Width of the Estuary at the Near-field Distance above the bridge, and WM the maximum width of the estuary Above the bridge.**

<b>VARIABLE</b>	<b>LW (mi)</b>	<b>AS (mi<sup>2</sup>)</b>	<b>MTR (ft)</b>	<b>LE (mi)</b>	<b>WD (mi)</b>	<b>WU (mi)</b>	<b>WM (mi)</b>
<b>Maximum Value</b>	200	18.0	1.22	20.0	2.00	2.00	4.0
<b>Average Value</b>	100	4.0	0.75	5.0	0.33	0.33	1.0
<b>Minimum Value</b>	50	1.5	0.60	0.5	0.10	0.10	0.5

**Table 4.2-4. Data Ranges of the hydraulic (cross section) variables observed in the review of the Chesapeake Bay estuaries with the variables defined as follows; WB the width of the estuary at the bridge location, XABMLE the area of the estuary cross section at the bridge location, and UESTZ the over bank side slope of the Bridge Cross Section.**

<b>VARIABLE</b>	<b>WB (mi)</b>	<b>XABMLE (ft<sup>2</sup>)</b>	<b>UESTZ</b>
<b>Maximum Value</b>	3.50	10,000	100:1
<b>Average Value</b>	0.33	17,000	200:1
<b>Minimum Value</b>	0.03	6,000	500:1

**Table 4.2-5. Data ranges of the scour variables observed in the review of the Chesapeake Bay estuaries with the variables defined as follows; D50 the estuary soil particle size for which 50% of the soil is smaller than, D16 and D84 both defined similar to D50, DMAX the maximum particle Size, PD the pier diameter, NBP the number of bridge piers in one row across the estuary, and PH the soil angle of repose.**

<b>VARIABLE</b>	<b>D50 (mm)</b>	<b>D16 (mm)</b>	<b>D84 (mm)</b>	<b>DMAX (mm)</b>	<b>PD (ft)</b>	<b>NBP</b>	<b>PH (degrees)</b>
<b>Maximum Value</b>	2.50	0.250	15.0	20.0	10.0	6	45.0
<b>Average Value</b>	0.25	0.100	2.5	3.5	5.0	9	40.0
<b>Minimum Value</b>	0.01	0.005	0.7	0.7	2.0	40	30.0

**Table 4.2-6. Data ranges of the hurricane variables observed in the review of the Chesapeake Bay estuaries with the variables defined as follows; MXSURG is the maximum expected surge at the bridge location, HRAD is the hurricane radius, HDIST is the closest distance that the hurricane approaches the bridge, HURAIN is the hurricane rainfall, and HSPEED is the hurricane travel speed.**

<b>VARIABLE</b>	<b>MXSURG (ft)</b>	<b>HRAD (mi)</b>	<b>HDIST (mi)</b>	<b>HURAIN (in.)</b>	<b>HSPEED (mph)</b>
<b>Maximum Value</b>	25	150	10.00	12	25
<b>Average Value</b>	15	100	0.50	9	12
<b>Minimum Value</b>	6	50	0.01	6	8

#### **4.2.2.4 Data Range Constraints**

The data ranges shown in Tables 4.2-2 through 4.2-6 were obtained from the review of the Chesapeake Bay data and did not necessarily reflect the ranges of the data required by the model to produce accurate and rational results. Accordingly, further constraints were placed on the data ranges shown to ensure that the input data would conform to the data ranges used in the development of the model. Ensuring that the data ranges were consistent with the ranges used in the formulation of the model assisted in improving the accuracy and rationality of the results produced. Specific discussions of the data range constraints placed on some of the critical variables and parameters are presented.

The catchment variables and parameters were constrained to ensure conformance with the SCS hydrologic data requirements. For example, the curve number was constrained to lie between 30 and 98, as these were the maximum and minimum values observed in the SCS land use tables SCS (1986). Similarly, the range of the basin areas was selected to be in conformance with ranges recommended for use in the SCS TR-55 model SCS (1986). The time of concentration was constrained based on the range of values encountered in the review of the drainage basins in the Chesapeake Bay.

In general, the data ranges of the tidal variables and parameters reflected the values encountered in the review of the Chesapeake Bay estuaries carried out during the development of the model. However, further constraints were placed on the distance between the base station and the bridge tidal station (LW), the value of the wave peakedness (PKM), and the widths of the cross sections just upstream and downstream of the bridge (UW and WD). LW was constrained to be less than 300 miles, because a greater distance would affect the accuracy of the wave distortion option used by the model. In addition, the range of PKM was selected to ensure rational values for the convex routing factor (CX), and hence, rational values of Neill's tidal discharge. UW and WD were constrained to be greater than 40% of the bridge cross section width, as smaller values affected the hydraulic assumptions used by the program in the computation of the contraction scour.

The data range of the bridge cross section observed in the review of the Chesapeake Bay estuaries was too wide to be used directly. The cross section velocity at the bridge station likewise varied from less than 1 ft/sec to as much as 30 ft/sec when the estuary cross section data range was used during the preliminary simulations. It was further determined, from the preliminary exercise, that significant scour at a controlled rate generally occurs when the cross section velocity range was between 2 ft/sec and 6 ft/sec. In order to ensure that the computed flow velocities through the bridge cross section would be realistic, rational, and produce significant but controlled scour, the width of the bridge cross section was further constrained to be between 0.25 mi and 2.5 mi.

The values assigned to the pier diameter range were based on those values observed in the literature such as Melville and Coleman (2000) and Richardson and Davis (1995). Richardson and Davis used an average pier diameter of 5 feet in the scour examples they provided while Melville and Coleman used a range of 0.5 to 3 meters. The number of bridge piers (NBP) was based on the average single bridge span used by Richardson and Davis. A maximum bridge span of 200 feet was selected because this represented the maximum values used by Richardson and Davis (1995). The data ranges of the soil particle sizes were based on the soils information provided by the Parsons Island geotechnical report by (E2CR, 2001) and the Maryland Geological Survey (2003).

The ranges of the hurricane variables were based on the National Weather Service classifications. The National Weather Service has compiled a database of the characteristics of hurricanes and has used these characteristics as the basis of classifying hurricanes. Table 4.2-7 depicts the classification of hurricanes using this method. Categories 4 and 5 were omitted from this study as the National Weather Service records indicated that a Category 3 hurricane was the largest hurricane observed over the Chesapeake Bay.

**Table 4.2-7. National Weather Service Classification of Hurricanes**

<b>Hurricane Category</b>	<b>Surge Height (ft)</b>	<b>Radius (mi)</b>	<b>Travel Speed (mph)</b>
<b>1</b>	5	75	30
<b>2</b>	7	100	25
<b>3</b>	11	150	20
<b>4</b>	16	200	15
<b>5</b>	20	250	8

## 4.3 VARIABLE AND PARAMETER SENSITIVITY ANALYSES

### 4.3.1 Method of Sensitivity Analysis

Variable and parameter sensitivity analyses were performed by determining the relative sensitivities of model predictions to the variables and parameters selected. The relative sensitivity was used as it allows the direct comparison of variables and parameters with different units and ranges. The analyses were made using three different model simulations. The continuous and hurricane analyses were done with simulations that did not consider natural armoring. In order to determine the sensitivities of D16, D84, and DMAX of the channel soil materials, simulations were done using the natural armoring method. Finally, simulations were also performed under the single-event hurricane mode using specific hurricane data to determine the relative sensitivities of the hurricane variables.

Because the relative sensitivity varied annually within the scour simulation duration, the sensitivity of a particular variable or parameter was assessed using both the sensitivity of the final 25-year scour depth and the mean sensitivity of the variable over the 25-year simulation period. The relative sensitivity (RS) of any given variable (p) was determined annually by the following equation:

$$RS_i = (dS_i/dp) * (p/S_i) \quad (4.2-1)$$

where  $RS_i$  is the relative sensitivity computed in the  $i^{th}$  year,  $dS_i$  is the difference between the baseline and test scour results in the  $i^{th}$  year,  $S_i$  is the test scour result in the  $i^{th}$  year,  $p$  is the value of the variable used in the test simulation, and  $dp$  is the difference between variable at the baseline and test condition. A review of the scour results obtained during the performance of the sensitivity analysis indicated a strong agreement between the

mean relative sensitivity of the variables tested and the average rate of scour over the 25-year simulation period. The final scour sensitivity analysis showed the impacts of the variables tested on the equilibrium scour value.

### 4.3.2 Relative Sensitivity Results

A summary of the results of the relative sensitivities determined for the selected variables and parameters are presented in Appendix B along with details of the results of the sensitivity analyses. A summary of the most sensitive variables and parameters are presented in Tables 4.3-1 and 4.3-2. Tables 4.3-3 and 4.3-4 and Figures 4.3-1 and 4.3-2 depict details of the sensitivities of the upstream pier face scour to the tide peakedness (PKM) and the sensitivity of the downstream pier face scour to the pier diameter (PD). The most sensitive variables are discussed in section 4.3.3

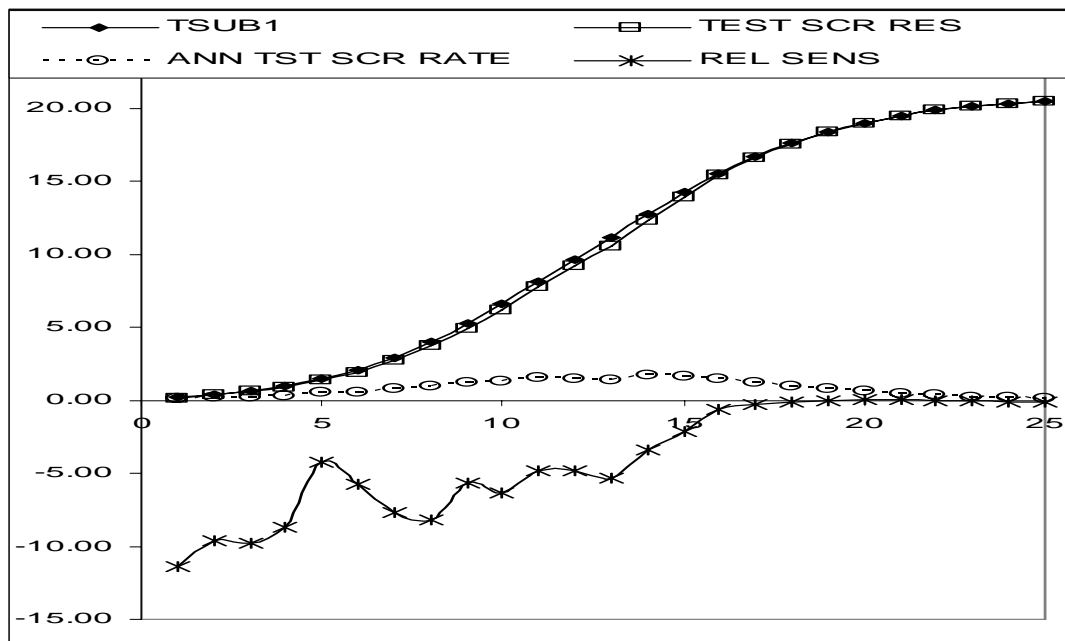


**Figure 4.3-1. Sensitivity of the upstream pier face scour to Wave Peakedness.** The x-axis represent the time in years and the y-axis represents the baseline scour (TSUB1), the scour results from the test value of the variable (TEST SCR RES), the annual test scour rate (ANN TST SCR RATE), and the relative sensitivity results (REL SENS).

**Table 4.3-1. Summary of the relative sensitivity results for the single-event hurricane. dP is the difference in the baseline and test value, TSUB and TSDB are the test scour results for the upstream and downstream pier faces, TSR is the scour result obtained with the test value of the variable, dS is the difference between the test scour and the baseline scour results, AS is the absolute sensitivity and RS is the relative sensitivity.**

Variable ABBR	Baseline Value	Test Value	dP	TSDB	P/S	TSR	dS	AS	RS
PHI (degree)	30.30	30.60	0.300	0.52	58.16	0.52	-0.001	-0.003	-0.19
HURAIN (ins.)	9	9.09	0.090	0.52	17.27	0.52	0.000	0.000	0.00
HRAD (mi.)	150	151.50	1.500	0.52	287.91	0.52	-0.004	-0.003	-0.77
HSPEED (mph.)	12	12.12	0.120	0.52	23.03	0.52	-0.002	-0.017	-0.38
MXSURG (ft.)	15	17.50	2.500	0.52	28.79	0.53	0.010	0.004	0.12
HDIST (mi.)	0.5	0.51	0.005	0.52	0.96	0.52	-0.004	-0.800	-0.77
ALPHA	5.7	5.76	0.060	0.52	10.94	0.52	0.001	0.017	0.18
MANNING'S n	0.02	0.03	0.0050	0.52	0.04	0.54	0.019	3.800	0.15
Variable ABBR	Baseline Value	Test Value	dP	TSUB	P/S	TSR	dS	AS	RS
PHI (degree)	30.30	30.60	0.300	2.89	10.47	2.89	0.00	-0.01	-0.10
HURAIN (ins.)	9.00	9.09	0.090	2.89	3.11	2.92	0.03	0.30	0.93
HRAD (mi.)	150.00	151.50	1.500	2.89	51.85	2.89	0.00	0.00	-0.03
HSPEED (mph.)	12.00	12.12	0.120	2.89	4.15	2.89	0.00	-0.01	-0.03
MXSURG (ft.)	15	17.50	2.500	2.89	5.18	2.87	-0.02	-0.01	-0.05
HDIST (mi.)	0.5	0.51	0.005	2.89	0.17	2.89	0.00	-1.00	-0.17
ALPHA	5.7	5.76	0.060	2.89	1.97	2.90	0.01	0.12	0.23
MANNING'S n	0.02	0.03	0.005	2.89	0.01	2.93	0.04	7.60	0.05

**Table 4.3-2. Summary of relative sensitivity results of 25-year simulation for the sensitive variables and parameters. dp is the baseline value less the test value, MRS is the mean relative sensitivity result, RS ms is the relative sensitivity at maximum scour, u/s is the upstream pier face, and d/s the downstream pier face.**

Variables	Baseline Values	Test Values	dp	MRS u/s	RS ms u/s	MRS d/s	RS ms d/s
Curve Number	78	78.78	0.78	1.01	0.15	-0.6	-0.01
Catchment Basin Area (sq.mi)	300	303	3	-1.02	0.23	-0.7	-0.02
Time of Concentration (hr)	36	36.36	0.36	-1.46	-0.44	-1.2	0.02
Distance from Bridge to Base Station (mi)	100	101	1	0.79	0.11	-1.2	-0.01
Wave Peakedness (ft)	0.67	0.68	0.01	-3.89	-0.09	0.3	0.01
Bridge Station Diurnal Amplitude (ft)	0.75	0.76	0.01	10.8	1.35	88.1	0.45
Pier Diameter (ft)	5	5.05	0.05	2.6	1.16	6.7	1.04
Downflow Orifice Coefficient	0.25	0.253	0.003	-3.98	-0.09	0.3	-0.01
Estuary Area (sq.mi)	4	4.04	0.04	1.03	0.56	18.7	0.21
Estuary Length above Bridge (mi)	4	4.04	0.04	-4.36	-0.13	-0.4	-0.01
Estuary Width at Bridge (mi)	1742	1759.4	17.4	-1.3	-0.58	-16.6	-0.83
Maximum Estuary Width Above Bridge (ft)	1	1.01	0.01	-7.3	-0.7	-9.6	-0.12
Bridge Cross Section Depth (ft)	10.75	10.85	0.1	-1.3	-0.58	-16.3	-0.83
Mean Soil Diameter (mm)	0.2	0.202	0.002	-7.2	-0.7	-8.8	-0.11
Maximum Soil Particle Size (mm)	0.7	0.71	0.01	-23.09	-13.57	-48.1	-84.17
Soil angle of Repose (degrees)	40	40.4	0.4	0.83	0.11	1.4	0.01



**Table 4.3-3. Annual relative sensitivity of the upstream pier face scour to Tide Peakedness (PKM). YR is the year in the simulation period, TSUB is the annual scour obtained from the baseline scenario, TSR is the annual scour obtained from the test scenario, P/S is the baseline variable value divided by the baseline scour (TSUB), ATSR is the annual test scour rate, MEAN RS is the mean relative sensitivity over the 25-year simulation period.**

YR	TSUB	TSR	P/S PKM	dS	AS	RS	ATSR
1	0.18	0.16	3.679	-0.02	-3.10	-11.42	0.16
2	0.39	0.35	1.725	-0.04	-5.57	-9.61	0.19
3	0.65	0.59	1.026	-0.06	-9.52	-9.77	0.24
4	0.95	0.87	0.707	-0.08	-12.30	-8.69	0.28
5	1.44	1.38	0.464	-0.06	-9.22	-4.28	0.52
6	2.04	1.93	0.328	-0.12	-17.49	-5.73	0.55
7	2.94	2.71	0.228	-0.23	-33.76	-7.70	0.78
8	4.03	3.70	0.166	-0.33	-49.09	-8.17	0.99
9	5.22	4.93	0.128	-0.30	-44.30	-5.68	1.23
10	6.62	6.20	0.101	-0.42	-62.97	-6.37	1.28
11	8.13	7.74	0.082	-0.39	-58.46	-4.82	1.53
12	9.65	9.18	0.069	-0.47	-69.90	-4.85	1.45
13	11.16	10.56	0.060	-0.60	-89.60	-5.38	1.38
14	12.71	12.27	0.053	-0.43	-64.58	-3.41	1.71
15	14.22	13.91	0.047	-0.31	-46.21	-2.18	1.64
16	15.49	15.39	0.043	-0.10	-15.31	-0.66	1.48
17	16.65	16.59	0.040	-0.05	-7.73	-0.31	1.21
18	17.57	17.54	0.038	-0.03	-3.97	-0.15	0.95
19	18.36	18.35	0.037	-0.01	-1.00	-0.04	0.80
20	18.97	18.98	0.035	0.01	1.07	0.04	0.63
21	19.45	19.45	0.034	0.01	0.91	0.03	0.47
22	19.86	19.85	0.034	-0.01	-0.91	-0.03	0.40
23	20.11	20.10	0.033	-0.01	-1.43	-0.05	0.24
24	20.31	20.29	0.033	-0.03	-3.79	-0.13	0.19
25	20.47	20.45	0.033	-0.02	-2.84	-0.09	0.17
				MEAN	-24.44	-3.98	

**Table 4.3-4. Annual relative sensitivity of the downstream face scour results to pier diameter (PD). YR is the year in the simulation period, TSDB is the annual scour obtained from the baseline scenario, TSR is the annual scour obtained from the test scenario, P/S is the baseline variable value divided by the baseline scour (TSDB), ATSR is the annual test scour rate, MEAN RS is the mean relative sensitivity over the 25-year simulation period.**

YR	TSDB	TSR	P/S PKM	dS	AS	RS	ATSR
1	0.07	0.07	70.22	0.00	0.06	4.07	0.07
2	0.14	0.15	34.82	0.01	0.12	4.11	0.08
3	0.22	0.23	22.23	0.01	0.19	4.22	0.08
4	0.31	0.33	16.04	0.01	0.27	4.36	0.09
5	0.41	0.43	12.26	0.02	0.37	4.51	0.10
6	0.51	0.54	9.75	0.02	0.48	4.68	0.11
7	0.63	0.66	7.93	0.03	0.62	4.90	0.12
8	0.77	0.81	6.53	0.04	0.79	5.16	0.14
9	0.92	0.97	5.42	0.05	1.01	5.49	0.17
10	1.11	1.17	4.52	0.07	1.31	5.95	0.20
11	1.32	1.41	3.78	0.09	1.75	6.60	0.24
12	1.64	1.79	3.05	0.15	2.93	8.92	0.38
13	2.26	2.54	2.21	0.28	5.52	12.20	0.75
14	3.26	3.94	1.53	0.68	13.59	20.84	1.40
15	5.29	6.32	0.94	1.03	20.56	19.41	2.38
16	8.10	9.41	0.62	1.30	26.06	16.08	3.08
17	11.16	12.60	0.45	1.44	28.79	12.90	3.19
18	14.35	15.56	0.35	1.21	24.19	8.43	2.96
19	16.59	17.53	0.30	0.94	18.83	5.67	1.97
20	18.15	18.72	0.28	0.57	11.49	3.17	1.19
21	18.80	19.22	0.27	0.42	8.39	2.23	0.50
22	19.18	19.49	0.26	0.31	6.22	1.62	0.27
23	19.33	19.55	0.26	0.22	4.32	1.12	0.06
24	19.37	19.57	0.26	0.20	4.04	1.04	0.02
25	19.39	19.59	0.26	0.20	4.02	1.04	0.02
			MEAN		7.4	6.7	

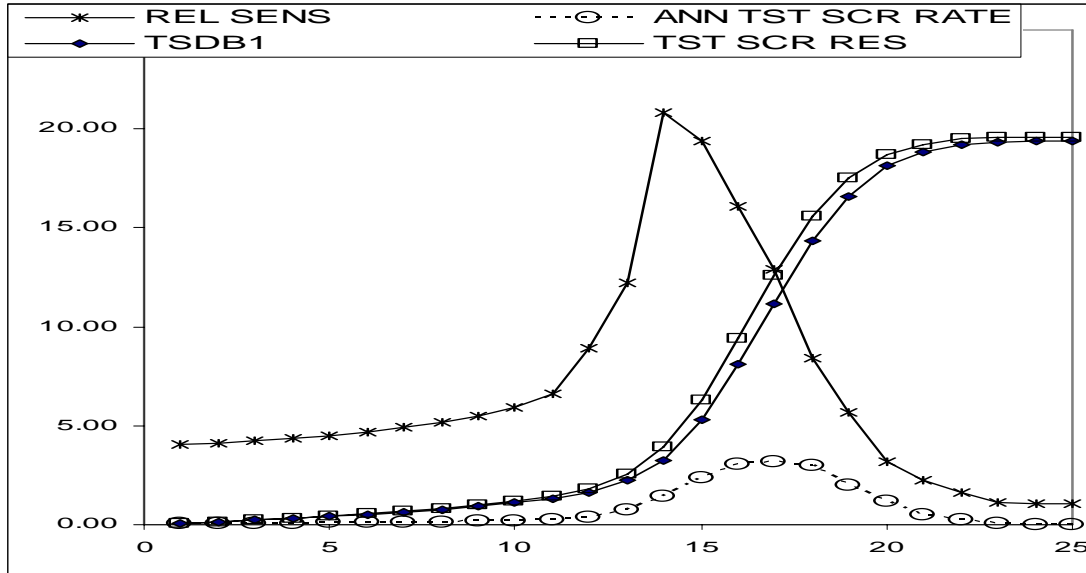


**Figure 4.3-2. Sensitivity of the downstream pier face scour to the pier diameter.** The x-axis represent the time in years and the y-axis represents the baseline scour (TSDB1), the scour results from the test value of the variable (TEST SCR RES), the annual test scour rate (ANN TST SCR RATE), and the relative sensitivity results (REL SENS).

### 4.3.3 Highly Sensitive Variables and Parameters

#### 4.3.3.1 Introduction

It will be necessary for model users to be able to identify the most sensitive variables in order to obtain reliable and accurate results. The results of the sensitivity analyses (see Tables 4.3-1 and 4.3-2) provide an indication of the importance of the variables tested and also the conditions under which these variables will be most important. Scour on the downstream and upstream faces of the piers were sensitive to different variables, as indicated by the mean relative sensitivities and the relative sensitivities shown in Tables 4.3-3 and 4.3-4. As a result, the sensitivities of scour on the upstream and downstream pier faces were assessed separately. The mean relative sensitivity and the final 25-year relative sensitivity of the variables are also discussed

along with the results of the sensitivity analyses performed on the single-event hurricane simulation.

The sign of the relative sensitivity results provides valuable insight into the rationality of the results of the model. A positive sign indicates that scour increases with an increase in the particular variable. The rationality of the model is indicated when the sign of the relative sensitivity of a given variable is positive and the theories and assumptions of the model indicate that scour should increase with an increase in the value of this variable. In all cases, the signs of the relative sensitivities of the variables reflected the changes expected and were in conformance with the theories and assumptions used in the formulation of the model.

#### **4.3.3.2 Results for the Upstream Pier Face**

As indicated earlier, the mean relative sensitivity is the sum of the relative sensitivities computed for each year of the simulation divided by the number of years. The mean relative sensitivity results obtained from the 25-year simulations indicated that scour on the upstream pier face was significantly sensitive to the 16 variables listed and ranked in Table 4.3-5. In some cases, the actual sensitivity results appeared to be appreciably high. However, these results may be explained in light of the theories employed by the WAVES program.

**Table 4.3-5. The most sensitive variables for scour on the upstream pier face ranked in order of importance. Ranking is in descending order with Rank 1 being most important.**

Mean Relative Sensitivity			Final 25-year Relative Sensitivity		
Variable	RS	Rank	Variable	RS	Rank
Maximum soil particle size (DMAX)	-23.1	1	Maximum soil particle size (DMAX)	-13.7	1
Tidal amplitude at the bridge location (MTR)	10.8	2	Tidal amplitude at the bridge (MTR)	1.35	2
Bridge cross section width (WB)	-7.31	3	Pier diameter (PD)	1.16	3
Bridge cross section depth (MDR)	-7.31	4	Maximum estuary cross section upstream of the bridge (WM)	0.70	4
Mean soil particle size (D50)	-7.20	5	Mean soil particle size (D50)	0.70	5
Length of the estuary above the bridge cross section (LE)	-4.36	6	Bridge cross section width (WB)	-0.70	6
Downflow orifice coefficient (C1)	-3.91	7	Estuary plan area (AS)	0.56	7
Wave peakedness (PKM)	-3.89	8	Catchment time of concentration (TC)	-0.44	8
Pier diameter (PD)	2.60	9			
Catchment time of concentration (TMCON)	-1.46	10			
Catchment curve number (CN)	1.00	11			
Estuary plan area (AS)	1.00	12			
Soil angle of internal friction (PHI)	0.83	13			
Distance between the bridge station and the tidal base station	0.79	14			
Maximum estuary cross section upstream of the bridge (WM)	0.73	15			
Catchment basin area (CBA)	0.70	16			

The results of the simulations indicate that scour on the upstream pier was most sensitive to the maximum soil particle size with a mean relative sensitivity of -23. This

computed value of the relative sensitivity is much higher than the values typically obtained for such studies because of the small denominator. The theoretical basis for natural armoring, which was discussed in Chapter 3, shows that the maximum particle size has an inverse relationship with the final scour results of the model. As the maximum soil particle size increases, the armoring effect increases and scour decreases. The unusually high relative sensitivity is due to a combination of a number of factors. First, it is important to discuss the results in terms of the fact that the WAVES program computes scour only when the vortex tangential velocity is greater than the incipient velocity of the bed material. Second, the armoring option increases the incipient velocity that must be surpassed in order for scouring to occur. Third, the scour rate will also depend on the value of the term  $(V_t - V_i)$  where  $V_t$  is the vortex tangential velocity and  $V_i$  is the incipient velocity of the bed material. The sensitivity analysis thus showed that natural armoring had the most significant effect on scour at the upstream pier face.

A baseline maximum sediment size of 2.0 mm was used for the analysis, while the test value was 2.02 mm. These values resulted in the prediction of 16.3 ft of scour at the end of 25 years for the baseline condition and 18.9 ft for the test condition. Appendix B shows that this difference in scour is due to the fact that the sediment value used in the test condition increased the incipient velocity and reduced the value of the  $(V_t - V_i)$  term over the duration of the simulation. This resulted in a reduction of 2.6 ft of scour over the 25-year simulation period. The magnitude of the final scour results obtained from the baseline and test simulations were reasonable, therefore, the computed value of the relative sensitivity was primarily due to the numerical range of the maximum particle sizes used in the baseline and test conditions. It should be noted that the WAVES

program used the maximum particle size only when the natural armoring option was engaged. Therefore, for simulations performed when the natural armoring option was not used, changes in the maximum soil particle did not impact the results.

The tidal amplitude at the bridge location was an important variable and had a computed mean relative sensitivity value of 10.8. The baseline tidal amplitude used was 0.75 ft with an increment of 0.008 ft. This produced a final 25-yr baseline scour of 20.4 ft and a 25-yr test scour result of 20.68 ft, which is a difference of 0.28 ft or 1.4%. The maximum annual difference in scour between the test and baseline conditions was 1.85 feet and this occurred after 15 years of simulation (see Appendix B). The sign of the mean relative sensitivity value was consistent with the theoretical predictions and real observations. The value of the mean relative sensitivity of the tidal amplitude was also higher than typically seen. However, because the baseline and test scour values were within their expected ranges, then the high mean relative sensitivity value appears to be a mathematical anomaly caused by the ranges of the baseline and test amplitude values selected.

The bridge cross section width and depth impacted the performance of the model by increasing the cross section area of the bridge section, hence reducing the flow. As expected the bridge cross section depth and width had the same mean relative sensitivity value of -7.31. The negative sign indicates that as these variables are increased the amount of scour decreases. This result is consistent with the theoretical prediction as an increase in depth or width increases the flow area and reduces the stream velocity and ultimately the tangential velocity of the vortex. The value of the mean relative sensitivity also appeared to be higher than typically expected; however, because the difference in the

25-year scour results was only 0.24 ft (see Appendix B) the magnitude of the relative sensitivity value could be considered a mathematical anomaly.

The final 25-year scour result on the upstream pier face showed significant sensitivity to eight variables. The final 25-year scour sensitivity results, shown in Table 4.3-5, provide a means of assessing the sensitivity of the equilibrium upstream pier face scour to the model variables. Table 4.3-5 indicates that the maximum soil particle size, the tidal amplitude at the bridge station, and the pier diameter had the most significant impact on the upstream face equilibrium scour.

The maximum particle size had a final 25-year relative sensitivity of -13.7. The negative sign indicates that as the particle size increases scour decreases, which is consistent with the theories used and observations made by researchers. The final 25-year scour results for the baseline and test conditions were 18.9 ft and 16.3 ft respectively indicating a difference in these values of 2.6 ft. The explanation provided for this substantial difference in the discussion of the mean relative sensitivity result is also applicable to this case. Also, as discussed earlier, the importance of the maximum soil particle size is limited only to the simulations in which the natural armoring option of the model was used.

As recorded with the mean relative sensitivity results, the diurnal tidal amplitude at the bridge station was the second most sensitive variable. The final 25-year relative sensitivity value was computed as 1.35. The positive sign indicates that scour increases as the diurnal tidal amplitude at the bridge increases. This result is consistent with the theories and observations used in the development of this model.



The pier diameter was the third most sensitive variable. The final 25-year relative sensitivity value was computed as 1.16. The sign of the computed 25-year relative sensitivity also indicated that scour increased with pier diameter as predicted by experimental observations.

The relative sensitivities for the single-event hurricane results on the upstream pier face scour are shown in Table 4.3-6. Also shown are the ranks of those variables with significant relative sensitivities. Table 4.3-6 further indicates that the most sensitive variable that affects scour on the upstream pier face due to a hurricane was the rainfall while changes in the surge height and the hurricane travel speed had little impact. These results were in agreement with the theoretical assumptions of the model. As was observed with the continuous simulations, upstream pier face scour was significantly impacted by variables, such as the hurricane rainfall, which are related to the catchment component.

**Table 4.3-6. Relative sensitivities (RS) for hurricane scour on the upstream pier face. ALPHA is a property related to the soil type. For sand ALPHA is 5.7 while for Gravel ALPHA is 7.3**

Variable	RS	RANK
Hurricane Rainfall (in.)	0.93	1
ALPHA	0.23	2
Distance of closest approach of the hurricane to the bridge (mi)	-0.17	3
Soil angle of internal friction (degree)	-0.10	4
Manning's n value	0.05	
Hurricane radius (mi)	-0.03	
Hurricane travel speed (mph)	-0.03	
Maximum surge height (ft)	-0.05	

#### **4.3.3.3 Results for the Downstream Pier Face**

The mean relative sensitivities for the 25-year simulations indicate that scour on the downstream pier face was significantly sensitive to the variables listed and ranked in Table 4.3-7. In the case of the downstream pier face scour, however, the tidal amplitude at the bridge location was found to be the variable with the greatest mean relative sensitivity. The scour rate on the downstream pier face was also very sensitive to the maximum soil particle size and the estuary plan area. As indicated earlier, the maximum soil particle size was relevant only to simulations using the natural armoring option of the model.

The tidal amplitude at the bridge location was the most sensitive variable in terms of the relative sensitivity and showed a computed value of 88. As indicated earlier, the baseline tidal amplitude used was 0.75 ft while the test value was 0.758 ft. This produced a baseline final 25-year scour result of scour of 19.38 ft and a test scour result of 19.48 ft. Appendix B also shows that the maximum difference in scour between the test and baseline conditions was 10.0 ft and this occurred after 14 years of simulation. The sign of the mean relative sensitivity value was consistent with the theoretical predictions. The value of the mean relative sensitivity was also much higher than expected. However, because the difference in the baseline and test 25-year scour values was small, the high mean relative sensitivity indicated that the change in the diurnal amplitude would significantly speed up the scour process but would have minimal impact on the equilibrium or ultimate scour value.

**Table 4.3-7. Relative Sensitivities of Model Variables (RS) on the Downstream Pier Face Ranked.**

Mean Relative Sensitivity			Final 25-year Relative Sensitivity		
Variable	RS	Rank	Variable	RS	Rank
Tidal amplitude at the bridge location (MTR)	88.0	1	Maximum soil particle size (DMAX)	-84.0	1
Maximum soil particle size (DMAX)	-48.0	2	Pier diameter (PD)	1.04	2
Estuary plan area (AS)	18.7	3	Tidal amplitude at the bridge (MTR)	0.45	3
Bridge cross section width (WB)	-9.60	4	Catchment basin area (CBA)	-0.23	4
Bridge cross section depth	-9.60	5	Estuary plan area	0.21	5
Maximum estuary cross section upstream of the bridge (WM)	9.60	6	Bridge cross section width (WB)	-0.12	6
Mean soil particle size (D50)	8.80	7	Bridge cross section depth (MDR)	-0.12	7
Pier diameter (PD)	6.70	8	Maximum estuary cross section upstream of the bridge (WM)	0.12	8
Soil angle of internal friction (PHI)	1.40	9	Mean soil particle size (D50)	-0.11	9
Catchment time of concentration (TMCON)	-1.20	10			
Distance between the bridge station and the tidal base station (LW)	-1.20	11			
Catchment basin area (CBA)	1.00	12			
Catchment curve number (CN)	0.60	13			
Length of the estuary above the bridge cross section (LE)	-0.40	14			
Downflow orifice coefficient (C1)	0.30	15			
Wave peakedness (PKM)	0.30	16			

The maximum soil particle size was also an important variable as indicated by its mean relative sensitivity result of -48. A baseline maximum sediment size of 2.0 mm was

used for the analysis, while a comparative test value of 2.02 mm was used. These values resulted in the prediction of 8.05 ft of scour at the end of 25 years for the baseline condition and 1.28 ft for the test condition. The negative value of the mean relative sensitivity is fully consistent with the observations and predictions of other researchers. The reason for the abnormally high mean sensitivity value can be explained as follows: The difference in the 25-year scour values between the baseline and test conditions is due to the fact that the value for the maximum sediment size used in the test condition increased the incipient velocity below what was required to initiate the development of the scour hole. The results of the analysis also indicate that the stream velocities, and by extension, the vortex tangential velocities generated on the downstream pier face were low. This is evident by the fact that only 8 ft of scour was generated under the baseline condition after 25 years in contrast to the 20 ft of scour generated at the upstream pier face. Therefore, because the vortex velocities were reduced, then the value of the  $(V_t - V_i)$  term over the duration of the simulation was not sufficient for the robust development of the scour hole. Increasing the maximum particle size under the test condition resulted in an increase in the incipient velocity of the material to the extent that a scour hole was not fully developed in the simulation period.

The estuary plan area is an important variable in the determination of scour on the downstream pier face as indicated by its mean relative sensitivity value of 18.7. As expected, the sign of the mean relative sensitivity value shows that scour should increase with an increase in this variable. The estuary area is important to the generation of the upstream tidal discharge and, as a consequence, should increase the vortex tangential velocities on the downstream pier face. The value of the mean relative sensitivity also

appeared to be higher than normally expected. However, the maximum difference between the scour results of the baseline and test conditions was only four feet in the seventeenth year of the simulation. In addition the final 25-year scour results for the baseline and test conditions were 19.39 ft and 19.43 ft respectively reflecting a final difference of only 0.04 ft. These results indicate that the magnitude of the mean relative sensitivity did not show a physical abnormality in the models prediction.

The equilibrium scour depth on the downstream pier face, as indicated by the final 25-year scour result shown in Table 4.3-7, showed significant sensitivity to only five variables. Table 4.3-7 indicates that the maximum soil particle size had the most significant impact on the downstream face equilibrium scour when the natural armoring option of the model is used. As was the case with the upstream pier face scour, the pier diameter, and tidal amplitude at the bridge were also very highly sensitive variables.

The maximum particle size had a final relative sensitivity of -88. The negative sign indicates that as the particle size increases scour decreases, which is consistent with the theories used and observations made by researchers. The final 25-year scour results for the baseline and test conditions were 8.05 ft and 1.28 ft respectively indicating a difference in these values of 6.77 ft. The explanation provided for this substantial difference in the discussion of the mean relative sensitivity result is also applicable in this case. Also, as discussed earlier, the importance of the maximum soil particle size is limited only to the simulations in which the natural armoring option of the model is used.

The pier diameter was the second most sensitive variable based on the 25-year scour sensitivity result. The final 25-year relative sensitivity value was computed as

1.16. The sign of the computed 25-year relative sensitivity also indicates that scour increases with pier diameter as predicted by experimental observations.

The diurnal tidal amplitude at the bridge station was the third most sensitive variable based on the 25-year scour sensitivity result. The final 25-year relative sensitivity value was computed as 0.45. The positive sign indicates that scour increases as the diurnal tidal amplitude at the bridge increases. This result is also consistent with the theories and observations used in the development of the WAVES program.

The sensitivities of the downstream pier face scour caused by the single-event hurricane are presented in Table 4.3-6. The hurricane scour on the downstream pier face was highly sensitive to the hurricane radius and the closest approach distance of the hurricane to the bridge. In general, the results also show significant sensitivity to variables, such as the hurricane travel speed, used in estimating the hurricane strength. Hurricane scour on the downstream pier face was found to be totally insensitive to the rainfall depth. This result is consistent with the previous finding that downstream face scour was not sensitive to most of the catchment variables.

**Table 4.3-8. Relative Sensitivity Results (RS) for Hurricane Scour on the Downstream Pier Face.**

Variable	RS	RANK
Hurricane radius (mi.)	-0.77	1
Distance of closest approach of the hurricane to the bridge (mi.)	-0.77	2
Hurricane travel speed (mph.)	-0.38	3
Soil angle of internal friction (degree)	-0.19	4
ALPHA	0.18	5
MANNING'S n value	0.15	6
Maximum surge height (ft.)	0.12	7
Hurricane Rainfall (ins.)	0.00	

#### **4.3.3.4 Least Sensitive Variables and Surprising Results**

The sensitivity analysis indicated that following variables did not significantly impact the scour results produced by the model; the number of bridge piers, the cross section estuary widths at the upstream and downstream near field distance from the bridge cross section, D84, and D16. A surprising result was that scour on the downstream pier face was less sensitive to the wave peakedness than what was observed for scour along the upstream pier face. However, upon further analysis, it was evident that the wave peakedness affected both the upstream and downstream tidal discharges and scour durations. Because of the distortion of the tide at the bridge station, an increase in peakedness resulted not only in an increase in the tidal discharge on the rising limb of the tide, but a shorter duration of the upstream flows in that tidal cycle when compared to the case with lower peakedness. The shortened duration acted to reduce the duration of the rising limb and also the time for scouring to occur on the downstream face of the pier. In contrast, an increase in peakedness resulted in an increase in the duration of the falling tide and an increase in the time for scouring at the upstream pier face. This translated to a reduction in the total downstream pier face scour on rising limb of the tide along with an increase in upstream pier face scour on the falling limb of the tide. A similar explanation could be provided for the significant (positive) sensitivity of scour on both the upstream and downstream pier faces to the tidal amplitude at the bridge location.

#### **4.4 PARAMETER SENSITIVITY OF MODEL COMPONENTS**

The importance of each program component was estimated by reviewing the number of sensitive parameters and variables within the component along with the degree

of the sensitivities of these parameters and variables. Tables 4.4-1 through 4.4-4 depict the sensitivities of the important variables in terms of the model components. In general, based on the aggregate of the sensitive variables and parameters presented, along with the magnitude of the relative sensitivities of these variables, the tidal, scour, and hydraulic components were the most important components, while the catchment component was the least important.

**Table 4.4-1. Mean Annual Sensitivity Results u/s Pier Face. CATCH Represents the Catchment, TID the Tidal, HX the Hydraulic Cross Section, and SCOUR the Pier and Bed Components. The Relative Sensitivities (RS) are Shown Next to the Component Variables Listed. NO VAR is the Number of Variables in the Component, SUM RS is the Sum of the Relative Sensitivities in the Component, and AVG RS is the Average Sensitivity of the Component.**

CATCH	RS	TID	RS	HX	RS	SCOUR	RS
CN	1	AMP	10.8	WB	7.3	DMAX	23
TC	1.4	PKM	3.89	MDR	7.3	D50	7.2
CBA	1	AS	1			PD	2.6
		LW	0.79			C1	3.98
		WM	0.73			PH	0.83
		LE	4.36				
<b>NO VAR.</b>	3		6		2		5
<b>SUM RS.</b>	3.4		21.57		14.6		37.61
<b>AVG RS.</b>	1.133		3.595		7.3		7.522

**Table 4.4-2. Final Scour Sensitivity Results for the u/s Pier Face**

CATCH	RS	TID	RS	HX	RS	SCOUR	RS
CBA	0.23	AMP	11.35	WD	0.58	PD	1.16
TC	0.44	AS	0.56	MDR	0.58	D50	0.7
		WM	7			DMAX	13.67
<b>NO. VAR.</b>	2		3		2		3
<b>SUM RS.</b>	0.67		18.91		1.16		15.53
<b>AVG. RS.</b>	0.335		6.3		0.58		5.18



Tables 4.4-1 and 4.4-2 show that scour on the upstream pier face was very sensitive to the variables and parameters of the tidal, hydraulic, and scour components. These tables show that the scour rates produced on the upstream pier face were most sensitive to the variables and parameters of the scour component. The overall average relative sensitivity of the scour component parameters was 7.5 for the mean annual relative sensitivity and 5.2 for the 25-year final relative sensitivity. The scour component also had five variables of mean annual relative sensitivity 0.4 or greater. Upstream pier face scour was also sensitive to the hydraulic component parameters, which had an average of the mean annual relative sensitivity of 7.3 and 0.58 for the average of the 25-year final relative sensitivity. The tables show that the tidal component was also important to scour at the upstream pier face. The tidal component parameters had an average of the mean annual relative sensitivity of 3.59 and 6.3 for the average of the 25-year final relative sensitivity. The catchment component parameters with an average of the mean annual relative sensitivity of 1.13 and 0.34 for the average of the 25-year final relative sensitivity also showed relative importance.

Tables 4.4-3 and 4.4-4 show that scour on the downstream pier face was sensitive to the variables and parameters of the tidal, hydraulic, and scour components. These tables show that the scour rates produced on the downstream pier face were most sensitive to the tidal component parameters and variables. For example, the maximum estuary cross section upstream of the bridge and the estuary plan area, were the most sensitive variables. The overall average relative sensitivity of the tidal parameters was 19.6 for the mean annual relative sensitivity and 1.51 for the 25-year final relative sensitivity. This component also had five variables of mean annual relative sensitivity

0.4 or greater. Scour on the downstream pier face was also sensitive to the parameters of the local scour component having an average of the mean annual relative sensitivity of 13.4 and 8.63 for the average of the 25-year final relative sensitivity. The tables show that the hydraulic component was also important to scour at the downstream pier face. The hydraulic component parameters had an average of the mean annual relative sensitivity of 9.6 and 1.83 for the average of the 25-year final relative sensitivity.

**Table 4.4-3. Mean Annual Sensitivity results d/s Pier Face**

CATCH	RS	TID	RS	HX	RS	SCOUR	RS
CN	0.60	AMP	88.00	WB	9.60	DMAX	48.00
TC	1.20	PKM	0.30	MDR	9.60	D50	8.80
CBA	0.70	AS	18.70			PD	6.70
		LW	1.20			C1	0.30
		WM	9.20			PHI	1.40
		LE	0.40				
<b>NO.</b>							
<b>VAR.</b>	3.00		6.00		2.00		5.00
<b>SUM</b>							
<b>RS.</b>	2.50		117.8		19.20		65.20
<b>AVG.</b>							
<b>RS.</b>	0.83		19.63		9.60		13.04

**Table 4.4-4. Final Scour Sensitivity Results d/s Pier Face**

CATCH	RS	TID	RS	HYDRAU. X-SEC	RS	SCOUR	RS
		AMP	0.45	WD	0.83	PD	1.04
		AS	0.56	MDR	0.83	DMAX	13.67
<b>NO.</b>							
<b>VAR.</b>	0		2.00		2.00		2.00
<b>SUM</b>							
<b>RS.</b>	0		3.01		3.66		16.71
<b>AVG.</b>							
<b>RS.</b>	0		1.51		1.83		8.36

## 4.5 COMPONENT UNCERTAINTY

Owing to the complexity of the WAVES program, formal component sensitivity and uncertainty analyses were not performed on all of the components. Instead, the study

focused on the sensitivities and uncertainties of the input variables. This approach may be justified for the following reasons. First, the catchment, and hydraulic cross section components were developed from models with established accuracies. Second, a tidal component did not exist with other models in the past, so the tidal component presented herein is new. Therefore, differences in scour rates, which are very dependent on the tidal component, between WAVES and other models are largely the result of the new scour model.

The sensitivity analyses carried out on the parameters of each component indicated that the scour component could be the most sensitive component. As a result, uncertainties in the scour component would impact the results of the model more than uncertainties in the other components. Therefore, in order to assess the response of the program to changes in a component, a more complex scour component was developed that included the Froude number, based on the pier diameter, raised to the power of 0.34, as used by HEC-18. The local scour model thus became:

$$d_{se} = b * \tanh(y/b) (V_t - U_i) (V / (gb)^{0.5})^{0.34} \quad (4.5-1)$$

where  $d_{se}$  is the scour depth (ft),  $y$  is the estuary depth (ft),  $V_t$  is the tangential velocity of the horseshoe vortex (ft/s),  $U_i$  is the incipient velocity of the bed sediments (ft/s),  $V$  is the mean stream velocity (ft/s),  $g$  is the acceleration due to gravity, and  $b$  is the pier diameter (ft). The baseline sensitivity data set was simulated with the adjusted model and the results were compared to the results of the baseline simulation using the unadjusted WAVES program. The results for the upstream and downstream pier faces are presented in Figures 4.5-1 and 4.5-2, respectively.

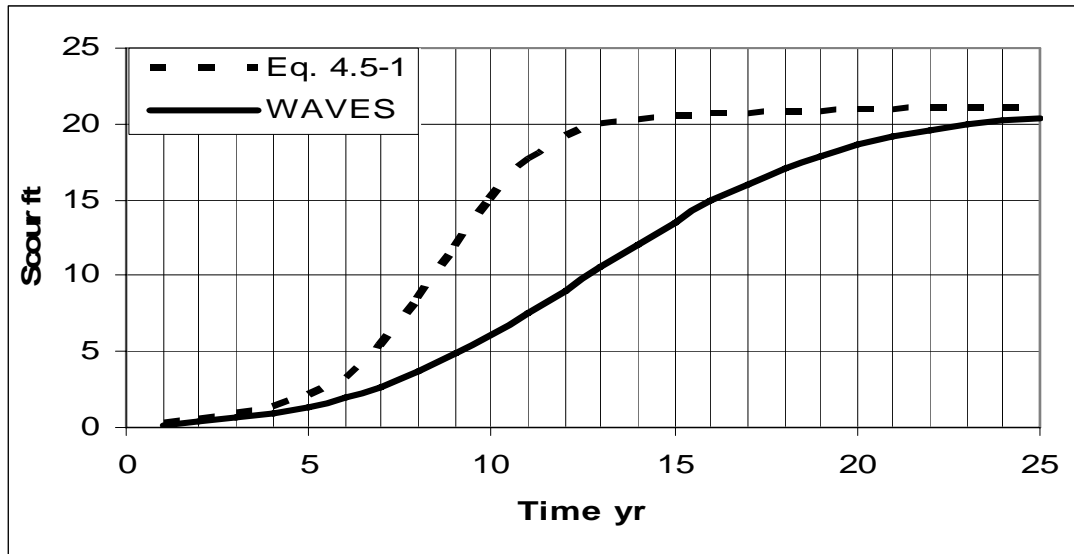


**Fig. 4.5-1. Scour at the upstream face of the pier predicted by the WAVES program with the local scour model computed with Eq. 4.5-1 compared with the scour predicted using the original WAVES algorithm.**

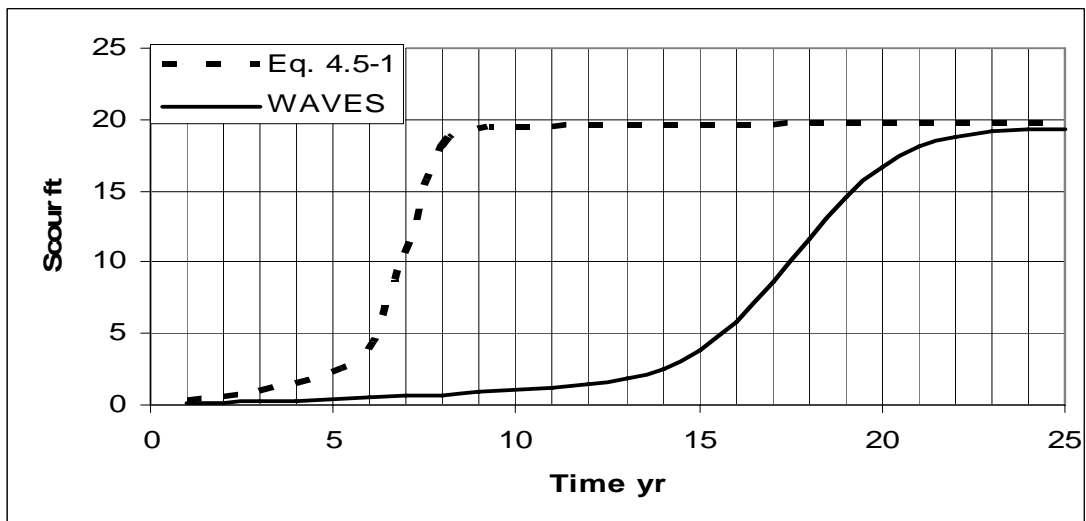


**Fig. 4.5-2. Scour at the downstream face of the pier predicted by the WAVES program with the local scour model computed with Eq. 4.5-1 compared with the scour predicted using the original WAVES algorithm.**

Figure 4.5-1 shows that the ultimate scour at the upstream pier face increased from 20.4 ft to 21.1 ft with the change to the scour component. The figure also shows that the adjusted scour component reduced the time taken to achieve ultimate scour from 24 year to 14 year. These changes represent an insignificant effect on the ultimate scour

at the upstream pier face (3%), but a very significant reduction in the time to ultimate scour (41%). Figure 4.5-2 shows that an increase in the ultimate scour at the downstream pier face of 0.3 ft (19.4 ft to 19.7 ft) was caused by the changes to the scour component. The model changes also resulted in a decrease of 14 years (23 years to 9 years) in the time required to reach ultimate scour at the downstream face of the pier. These changes represent a 1.5% increase in the ultimate scour at the downstream pier face and a 61% reduction in the time to reach the ultimate scour value. These results indicate that component uncertainties may have negligible impacts on ultimate scour values but could likely have significant effects on the time taken to reach ultimate scour.

#### **4.6 VARIABLE ERROR AND UNCERTAINTY ANALYSES**

The error propagated by each of the most sensitive variables, as indicated by the sensitivity analysis, was determined. The variable DMAX was omitted as it related only to the natural armoring scour method. The model error due to these variables was assessed through the product of the absolute variable sensitivity and the value of the error in the variable. The results of the error analysis are displayed in Table 4.6-1. The results indicate that the hydraulic (bridge cross section component) has the greatest potential for propagating errors in the final scour results. Significant errors could also be introduced with the tidal amplitude, the mean particle diameter, and the catchment time of concentration.

**Table 4.6-1. Error Analysis for the Final Scour Results.  $E_a$  is the Estimated Absolute Error of the Variable, AS is the Absolute Sensitivity, and  $E_m$  is the Estimated Model Error Due to the Error in the Variable.**

	$E_a$	U/S PIER FACE		D/S PIER FACE	
		AS	$E_m$	AS	$E_m$
<b>AMP</b>	0.05	36.8	1.84	48.7	2.44
<b>WB</b>	0.1	35.9	3.59	38	3.80
<b>MDR</b>	0.5	8.3	4.15	3.5	1.75
<b>D50</b>	0.05	71.4	3.57	1.03	0.05
<b>LE</b>	0.5	0.67	0.34	0.07	0.04
<b>C1</b>	0.01	3.98	0.04	0.72	0.01
<b>PKM</b>	0.07	2.84	0.20	0.27	0.02
<b>PD</b>	0.25	4.77	1.19	4.02	1.01
<b>TC</b>	25	0.25	6.25	0.003	0.08
<b>CN</b>	5	0.04	0.20	0.002	0.01
<b>CBA</b>	15	0.02	0.30	0.001	0.02
<b>AS</b>	0.5	1	0.50	1.03	0.52
<b>PHI</b>	2	0.11	0.22	0.003	0.01
<b>LW</b>	1	0.02	0.02	0.01	0.01
<b>WM</b>	0.5	7.3	3.65	2.4	1.20

## **CHAPTER 5**

### **DESCRIPTION OF CASE STUDY ESTUARIES AND WATERSHEDS**

#### **5.1 INTRODUCTION**

##### **5.1.1 Variations in Estuary and Watershed Conditions**

One of the objectives of this study, which has led to the development of the WAVES model, was to utilize the conceptual multi-scale framework to formulate a temporally varied multi-component model that determines the water surface elevations, flow rates, velocities, and bridge pier scour depth throughout a tidal-riverine system, and further, to compare the performance of the model with existing models. As discussed in Chapter 2, the tidal-riverine system is represented by a diverse spectrum of tidal environments that include well mixed, partially mixed, and stratified estuaries along with tidal rivers. The full tidal-riverine environmental system is adequately exhibited in the Chesapeake Bay Estuary. Many tidal experts have classified the main estuary of the Chesapeake Bay as fully mixed; however, the estuary is fed by many tidal rivers such as the Wicomico, Patuxent, and Patapsco Rivers that may be stratified or partially-mixed. In addition, the Chesapeake Bay system includes many upstream bays and inlets that may exhibit the properties of stratified and partially mixed estuaries.

The size, shape, and development conditions of the watersheds that provide fresh water to the rivers of the Chesapeake Bay also have a significant effect on the local estuaries into which they discharge. Development conditions determine the level of imperviousness of the watershed, and hence, bear a direct relationship to the volume of runoff generated by the watershed from precipitation. Similarly, runoff volumes are also

determined by the watershed area and conditions. The watershed area, topography, and shape determine the time of concentration of the watershed, which in turn controls the catchment discharge rates.

### **5.1.2 Determination of Tidal or Catchment Dominated Estuaries Using the Simmons Ratio**

The Simmons Ratio was the method used to estimate the relative dominance of the catchment (fresh water) input or tidal input at the particular bridge location.

Richardson and Davis (1995), define the Simmons Ratio ( $S_R$ ) according to Equation 5.1-1:

$$S_R = V_{\text{base}(\tau)} / V_{\Omega(\tau)} \quad (5.1-1)$$

where  $V_{\text{base}(\tau)}$  is the volume of river flow per tidal cycle and  $V_{\Omega(\tau)}$  is the volume of the tidal prism per tidal cycle. For a Simmons Ratio of 1.0 or greater, the estuary is highly stratified and dominated by the watershed. When the ratio is between 0.2 and 0.5, the estuary is partially mixed and influenced by both the catchment and tides. For ratio values 0.1 or less, a well-mixed condition exists and the tidal process dominates the estuary. Richardson and Davis (1995) indicate that conclusive classifications of estuaries could not be made for the values of the Simmons ratios from 0.5 to 1 and 0.1 to 0.2.

Implicit in the definition of the Simmons Ratio is the assumption that the catchment volume must be the volume generated by the average baseflow over one tidal cycle. If the Chesapeake Bay were used as an example, one tidal cycle is approximately 12 hours. Because of the constraints on the size of the catchment areas applicable to the WAVES model, the values of the baseflows encountered suggest that most of the test locations would be in environments that were classified as fully mixed estuaries



dominated by the tidal contributions. The results obtained from scour simulations performed using the baseline conditions discussed in Chapter 4, indicate that very low values of the Simmons Ratio, based on baseflows, in of themselves do not guarantee tidal dominance. In order to use the ratio to predict catchment or tidal dominance at the scales applicable to the model, the peak 12-hour volume obtained from the 1.25-year or 1-year storm hydrograph was used, in lieu of the baseflow, to represent the catchment input. Table 5.1-1 shows the adjusted Simmons Ratio for the case study sites along with the baseline estuary used in the sensitivity studies.

Great care must be taken in computing the 1.25-year hydrograph to ensure the proper calculation of the adjusted Simmons Ratio. The peak 1.25-year discharges shown in Table 5.1-1 were obtained for the case study sites from Moglen et al. (2006) while the SCS model was used to determine the peak 1-year discharge in the case of the baseline estuary. The freshwater volumes from the 1.25-year and 1-year hydrographs were computed assuming that they could be represented by triangular hydrographs. The adjusted Simmons Ratio indicated that for values less than 0.1 the estuary was tide dominated as observed with the Monie Bay and Baltimore Black River sites. For values from 0.1 to 0.5, inclusive, the estuary was mixed-controlled with significant inputs from both the tidal and catchment components. This condition was observed in Table 5.1-1 for the baseline estuary, the Wicomico River, and the Patuxent at Benedict sites. For values above 0.5 the estuary was catchment-controlled, as was the case with the Baltimore Patapsco site.

**Table 5.1-1. Case study site properties used to determine adjusted Simmons Ratios and the CE Ratio. Q12 is the average 12-hour discharge obtained from the 1.25-yr. runoff hydrograph. PHV is the peak 12-hr hydrograph volume based on the 1.25-yr discharge hydrograph. AHV is the 12-hr hydrograph volume based on the average 1.25-yr discharge hydrograph. SA is the adjusted Simmons Ratio based on AHV, SK is the adjusted Simmons Ratio based on PHV, and CE is the catchment area to estuary area ratio.**

	BASELINE ESTUARY	PATUXENT AT BENEDICT	WICOMICO	MONIE BAY	BALTIMORE BLACK RIVER	BALTIMORE PATAPSCO RIVER
Catchment area (mi <sup>2</sup> )	300	732	170.8	16.3	58	598.5
Curve number	78	70	79	81	84	73
Catchment length (mi)	25	94.7	33.08	14.09	19.97	69.33
1.25-yr (or 1-yr as in the case of the baseline estuary) peak discharge (cfs)	2800	5260	1170	211	1620	7310
Hydrograph time base (hr)	23.7	26.9	21.7	16.8	19.5	26.2
Hydrograph volume (1000 ac-ft)	2.74	5.85	1.05	0.13	1.31	7.92
Hydrograph time to peak (hr)	5.3	7.6	4.3	1.7	2.8	7.0
Q12 (cfs)	918	1901	343	40	429	2620
PHV (1000 ac-ft)	1.84	3.55	0.75	0.12	1.02	4.92
AHV (1000 ac-ft)	1.39	2.61	0.58	0.10	0.80	3.62
Estuary area (mi <sup>2</sup> )	4.00	9.87	3.95	2.16	9.50	3.56
Tidal range (ft)	1.5	1.2	2.38	2.38	1.87	1.87
Tidal prism volume (1000 ac-ft)	3.84	7.58	6.02	3.29	11.37	4.26
SA	0.36	0.34	0.10	0.03	0.07	0.85
SK	0.48	0.47	0.12	0.04	0.09	1.16
CE RATIO	75	73	43	7	6	168

### **5.1.3 Determination of Tidal or Catchment Dominated Estuaries Using the CE Ratio**

Though not as precise as the Simmons Ratio, the ratio of the catchment area to the associated estuary area (CE Ratio shown in Table 5.1-1) also provides a reasonable indication of the processes that will dominate pier scour in an estuary or tidal river. Through repeated simulations conducted during the sensitivity analyses by varying estuary and catchment areas, it was determined that a CE Ratio that was less than 50 indicated that the scour process would be dominated by the tidal influences and approximated the fully mixed estuary condition. A CE Ratio of 50-100 indicated that the scour process would be equally affected by the tidal and catchment inputs. A CE Ratio of 50-100 was, therefore, roughly equivalent to the partially mixed estuary condition. A CE ratio that was greater than 100 indicated that the scour process would be dominated by the catchment influences and was synonymous with the stratified estuary condition.

### **5.1.4 General Discussion of the Bridge Location Conditions**

Bridge pier scour is not only affected by the type of estuary or tidal river, but also by the configuration of the estuary or tidal river cross section at which the bridge is located. The determination of relationships between pier scour and estuary flow depths and discharges are also objectives of this study. In a completely riverine environment, a direct relationship exists between flow depth and scour. Similarly, with relatively narrow rivers, the scour depths produced are also directly dependent on discharge values. These simple relationships are used by some researchers to develop scour models. While such models may produce reasonably accurate scour estimates in a riverine environment, they do not work well with tidal rivers or estuaries. The reason can be found in the fact that,

while flow depth is usually directly related to flow velocity in non-tidal rivers, the same is not true in a tidal environment. Deep tidal rivers and estuaries typically have a damping effect on the overall estuary velocity. This is because the tide-generated discharges are created around the tidal prism only, and the water depths below the mean low-water level do not contribute to the discharge production. However, in computing the average velocity, the overall flow area is used, and this effectively reduces the flow velocity below that expected in a riverine environment. Also, estuaries tend to be significantly wider than upland rivers. As a result, predicting scour from discharges may be appropriate for narrow rivers, but this method does not produce reliable results in estuaries.

#### **5.1.5 Case Study Site Selection Rationale**

Estuary cross section sites were selected for comparative scour analyses that involved the continuous WAVES model and other single-event models currently in use. The case study sites were selected to provide scour results in diverse tidal environments that are associated with most estuaries. Scour results were required for tide dominated (well mixed) estuaries, estuaries with significant tidal and riverine inputs (partially mixed), and catchment dominated (stratified) estuaries. The sites were also selected to demonstrate the pier scour process in deep estuaries, and locations with narrow and wide cross sections. All estuary cross sections chosen were screened to ensure that the catchment area associated with a cross section conformed to the temporal and spatial scale constraints imposed by the SCS hydrologic method employed by the model. The sites were also chosen to ensure that they were sufficiently close to the tidal base station

to prevent excessive tidal distortion at the bridge location. Some of the relevant details of the five locations selected based on the criteria presented are provided in Table 5.1-1.

As indicated in Chapter 4, the baseline estuary represents the average estuary conditions found in the review of the Chesapeake Bay estuaries. The adjusted Simmons Ratio based on the peak 1-year discharge (SK) is 0.5 and represents a mixed-controlled or partially mixed estuary with significant influences from both the tidal and catchment discharges. Table 5.1-1 shows that the Patuxent River and the Wicomico River sites also represent partially mixed tidal rivers, i.e., SK values of 0.47 and 0.12, respectively. The Patuxent River site had a relatively small cross section width of 0.63 miles and tidal depth of 15 ft. The Wicomico River site appeared also to have significant tidal influences as the SK value was low. The Wicomico cross section was narrow (0.25 mi) and moderately deep (18 ft). The Baltimore Black River and Monie Bay sites with SK values of 0.09 and 0.04, respectively, represent well mixed estuaries and tide dominated sites. The Monie Bay location was relatively wide (1.1 mi) and shallow (6 ft), while the Baltimore Black River site was also wide (1.6 mi) but deeper than Monie Bay (10 ft). The Baltimore Patapsco River site had a SK value of 1.16 and was catchment dominated. The cross section was narrow (0.33 mi), but very deep (33 ft).

## **5.2 DATA COMPILATION METHODS OF THE CASE STUDY SITES**

### **5.2.1 Catchment Data**

The case study sites were selected in conformance with the applicability of the SCS hydrology. The catchment areas to the proposed bridge locations were constrained to less than 1000 square miles. The catchment areas were determined from the United

States Geological Survey (USGS) quadrangle maps based on the Maryland State plane coordinates of the proposed bridge location. The USGS quadrangle maps also provided other pertinent hydrological data such as the catchment mean channel slope, land slope, land use and land cover, the catchment length, the physiographic regions associated with the watershed, the watershed curve number (CN), and the watershed time of concentration (see Appendix C-3). Rainfall data were assumed to be similar for all of the sites selected and was based on the USGS IDF curves developed for the City of Baltimore.

## **5.2.2 Tidal Data**

### **5.2.2.1 Base Station Tidal Data**

The tidal base station used was the National Oceanographic and Atmospheric Administration (NOAA) tidal gauge at Sewell Point. The Sewell Point gauge is located along the Virginia side of the Chesapeake Bay in the Hampton Roads harbor. Sewell Point was selected for the following reasons: first, the temporal tidal profile was regular and was unaffected by fresh water inputs from the rivers and streams that discharge into the Bay. This is because Sewell Point is located sufficiently close to the mouth of the Bay to ensure that the fresh water effects remain insignificant. Second, the Sewell Point gauge is one of the few gauges located close to the mouth of the Bay that has extensive historical tidal data. This gauge has over 60 years of continuous tidal records along with other information related to the physical features of the Bay such as the tidal depth at Sewell Point. The information determined from the Sewell Point historical tidal records included the mean of the tidal depth, the mean and standard deviation of the diurnal

amplitude of the tides, the mean and standard deviation of the lunar amplitude of the tides, the mean and standard deviation of the tidal period, and the mean and standard deviation of the lunar period.

The base station tidal data also included the distance from the base station to the bridge station measured in miles, and the base station invert elevation in feet. The invert elevation of the base station was used in the determination of the mean tidal depth at the base station. The tidal depth at the base station and the distance between the base station and bridge station are critical to the determination of the factors used to adjust the tidal discharge values computed by modified Neill's method. Both the base station invert and the distance between the bridge station and base station were determined from navigational charts [Alexandria Drafting Company (ADC), 1998].

#### **5.2.2.2 Bridge Station Tidal Data**

The bridge station tidal data required by the model include the mean low water (MLW) tidal elevation, the mean diurnal tidal amplitude, the wave peakedness, and the mean tidal depth. The diurnal tidal amplitude at the bridge station was used to compute the peakedness of the tide. The mean tidal depth at the bridge station along with the MLW elevation of the tide was estimated from the closest NOAA tidal gauge with sufficient historical tidal data.

#### **5.2.3 Bridge Cross Section Data**

The bridge cross section profile is critical to the accuracy of the WAVES scour program. As indicated in the sensitivity analyses, the hydraulic component, which is

dependent on the cross section data, is the most sensitive component of the program. For the most accurate results, the cross section information should be obtained by real topographic and bathymetric surveys. For the purposes of this study, the cross section data were obtained from navigation charts [Alexandria Drafting Company (ADC), 1998]. The Manning's coefficient associated with each cross section was estimated based on the values for large natural channels determined by Chow (1959).

#### **5.2.4 Bridge Data**

The necessary bridge data consist of the number of bridge piers, the diameter of each bridge pier, and the invert elevation of the channel at the pier. The number of bridge piers, as defined for use by the program, represents the number of piers in a single row across the length of the structure. The bridge design engineer would determine these values for design simulations. When executing the program in the existing pier analysis mode, the information required could be determined from the design plans for the structure or from field measurements. The bridge data used in this study was hypothetical but the estimates were based on current bridge construction practices. The number of bridge piers was estimated from the assumption of a maximum single span length of 200 ft which, is in good agreement with the bridge data presented by Melville and Coleman (2000) and Richardson and Davis (1991). The number of piers was then computed as the total width of the bridge cross section divided by 200. The value of the pier diameter (5 ft) used in this study also represents the average pier diameter found in these sources.



### 5.2.5 Bridge Estuary Data

The bridge estuary refers to that portion of the estuary or tidal river that is located upstream of the bridge location under study. The required data are used in the tidal component of the model and are very important in the assessment of whether or not the estuary will be dominated by tidal or catchment inputs. The bridge estuary data are also important to the determination of the amount of contraction scour that may occur. The required data consist of the estuary area, the estuary length, the width of the estuary at the bridge location, the width of the estuary at the near field distance downstream of the bridge, the width of the estuary at the nearfield distance upstream of the bridge, and the maximum width of the estuary. All of the required bridge estuary data may be determined by direct measurement or from navigational charts such as ADC (1998).

In the study, the bridge location was selected so that any constriction between the bridge sections and the upstream or downstream near-field cross sections would be less than 40% of the width of the estuary at the bridge location. The bridge location was also selected to ensure that the catchment area to that location was less than 1000 mi<sup>2</sup>, as generally recommended by the SCS hydrologic model. The estuary plan area, measured in mi<sup>2</sup>, was determined based on the bridge location selected. The bridge near-field upstream and downstream distances were defined by Melville and Coleman (2000) to be the distance upstream or downstream of the bridge location equal to that distance from the bridge where the structure had no hydraulic impact on the flow. The bridge estuary widths at the upstream and downstream near-field distances were determined in miles.

The bridge estuary data also included the widths of the estuary at four elevations starting at the invert of the location and ending at the MLW elevation. This data were

used to compute the channel cross section area of the bridge location which in turn was used to compute the flow velocity rating curve for the cross section. The data were determined from the information in the bridge cross section data acquisition discussed earlier.

### **5.2.6 Soils Data**

As indicated in Chapter 4, pier scour is very sensitive to data related to the nature of the soils within the estuary channel at the location of the bridge pier. In particular, the mean soil diameter is a variable used in many scour models including the WAVES program of this study. For the most accurate results, soil data should be determined from the analysis of boring logs taken at the location of the proposed pier. A sieve analysis of the soil samples taken at 10-ft increments will provide the required soil information at various layers below the invert of the channel. Among the important data that may be obtained from the analysis of the soil boring samples are the mean particle diameter, the maximum soil particle size, the soil particle size that 16% of the sample is smaller than, and the particle size that 84% of the sample is smaller than. Other soil properties may be determined from boring samples. These properties include the specific gravity, the soil alpha property, and the soil angle of internal friction. Alternatively, as was done in the development of this study, soil information at the bridge location may be obtained from literature reports and engineering texts. The use of the engineering literature as a source of soil data is appropriate particularly for preliminary bridge design and analysis studies.

In the case of this study, the required soil information was obtained from the Parsons Island Geotechnical Report (E2CR, 2001) and the Maryland Geological Survey

(2003). These sources were discussed earlier. The soil boring data provided by the Parson Island Geotechnical Report were used to determine the required soil size properties for the case study sites located close to the main Chesapeake Bay estuary. In addition, the Maryland Geological Survey's qualitative description of the Chesapeake Bay soil was used to determine the required soil information for all of the other case study sites. The HEC-6 (1977) grain size classification table (see Appendix C-1) was also used to estimate the mean particle size of the bed sediments.

The WAVES program used the SRICOS model (Briaud et al., 1999) to compute the incipient erosive velocity during the hurricane simulation. This method requires the determination of  $\alpha$ , which is a property of the soil characterizing its grain shape and texture. The  $\alpha$  values for sand, silts, clays and gravel were also obtained from Briaud et al., (1999).

### **5.2.7 Hurricane Data**

Hurricane data are required to determine the pier scour that could be caused by a single-event hurricane that passes in the vicinity of the bridge. The required hurricane data include the hurricane travel speed, the hurricane radius, the maximum surge developed with the hurricane, and the closest approach distance of the hurricane to the bridge location. The hurricane information required may be determined from the National Weather Service (NWS). The NWS has developed a method of classifying hurricanes through the use of a system of categories to define their strengths and areas of influence. The characteristics of the NWS hurricane categories were used by this study in the execution and development of the WAVES model. In addition, the hurricane sizes

were checked against the NWS historical hurricane records. The distance of closest approach of the hurricane to the bridge may be determined from the NWS forecasting or historical tracking data.

### **5.3 THE MONIE BAY SITE**

The Monie Bay site was selected for the case study exercise because the site met the constraints of the SCS watershed hydrology and the tidal limits of the model. The Monie Bay site also displayed some of the characteristics required to ensure diversity in the overall study. The site is located along the eastern shore of the Chesapeake Bay at the location where the Monie Creek, Little Monie Creek, and Victor Creek discharge into the Chesapeake Bay estuary at Monie Bay (see Appendix C-2). The hypothetical bridge site is located at Latitude  $38^{\circ} 13.5'$  and Longitude  $75^{\circ} 50.5'$  (Maryland State Plane Easting 503147 m, Northing 62963 m) at the widest section of Monie Bay. Monie Bay at this location is approximately 5 ft deep and 1.1 miles wide. Monie Bay is surrounded by low lying tidal marshes and wildlife management areas.

#### **5.3.1 Estuary Conditions**

The Monie Bay estuary was estimated to have an area of approximately 2.16 mi<sup>2</sup>. The Bay is generally very shallow with an average depth of 5 ft below the MLW elevation. The Monie Bay estuary is widest at its entrance, and then narrows progressively to approximately 150 ft, which is the width of the tidal portion of Monie Creek. The estuary associated with Monie Bay is approximately 1.3 miles in length. However, the estuary extends up the Monie Creek for an additional two miles. NOAA

did not have tidal gauges in the Bay or creeks that drain to the Monie Bay estuary. The tidal data from the gauge located at Whitehaven on the Wicomico River were used at this location, as it represented the closest NOAA gauge to the proposed bridge location.

### **5.3.2 Watershed Conditions**

The selected bridge location across Monie Bay serves as the outlet for a watershed area of approximately 16.3 mi<sup>2</sup>. The Monie Bay watershed lies entirely within the Eastern coastal plain physiographic region and is relatively flat. The average channel slope is estimated at 1.3 ft/mi and the basin relief is only approximately 10 ft. The relatively low basin relief and channel slope contribute to ensure a time of concentration of approximately 30 hr (as predicted by the SCS lag equation). The watershed is 60% forest cover. Land use within the watershed is of low intensity, with only 3.4% urban development. In addition, the estimated amount of impervious cover is approximately 1% of the watershed area. Most of the watershed soils are of hydrologic soil group D (83%), which results in a relatively high watershed curve number of 81.

### **5.3.3 Simmons Ratio and Bridge Location Conditions**

The Monie Bay estuary at the proposed bridge location has a 1-year adjusted Simmons Ratio (SK) of 0.04, as shown in Table 5.1-1. This indicates that the Monie Bay estuary is fully mixed and should be dominated by tides. An associated watershed area of 16 mi<sup>2</sup>, an estuary area of 2.16 mi<sup>2</sup>, and a CE ratio of 7 provide further indications that pier scour within Monie Bay should be highly influenced by the tidal processes.

Not only is the type of estuary critical to the pier scour process, but the hydraulics of the cross section is of even greater importance. This fact is most applicable in the case of Monie Bay. Being relatively wide and shallow, as indicated by Figure 5.3-1, Monie Bay is subjected to two opposing hydraulic influences. The width of the Bay has the effect of reducing the average channel velocities, hence, the potential for pier scour. The Bay's shallow depth has the opposite effect. The rate of scour within Monie Bay ultimately depends on which of these influences is greater.

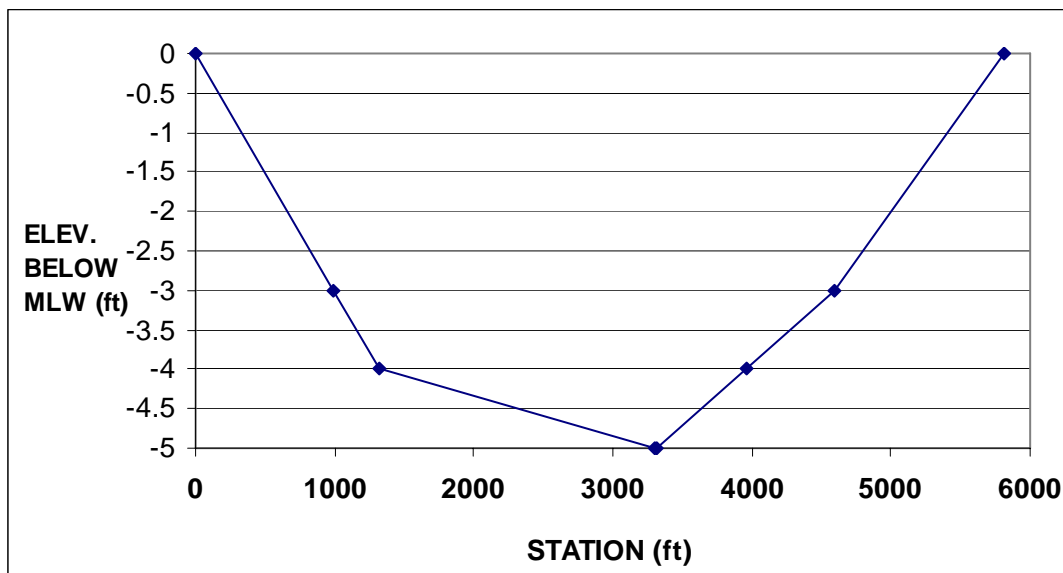


**Fig. 5.3-1. Monie Bay Cross Section Profile at the Proposed Bridge Location. MLW Refers to the Mean Low Water Elevation. The Values Along the x-Axis Represent the Horizontal Cross Section Stations in ft.**

The characteristics of the soils at the bridge cross section are also critical to the potential for pier scour. The Maryland Geological Survey (2003) indicated that the soils in the Monie Bay estuary consisted of sand and clayey sand. As a result, the mean soil particle size ( $d_{50}$ ) was estimated as 0.135 mm. The soil particle size for which 16% of the bay soils are smaller than ( $d_{16}$ ) was estimated as 0.01mm. The soil particle size for which 84% of the bay soils are smaller than ( $d_{84}$ ) was estimated as 1.75 mm, while the

maximum particle size was 2.5 mm. The estuary soils, being sand to clayey sand, were estimated to have an angle of internal friction of  $35^{\circ}$  while the soils  $\alpha$  factor was estimated as 5.7.

## **5.4 THE BLACK RIVER SITE**

The Black River Site was selected for the case study exercise because the site, like Monie Bay, met the constraints of the SCS watershed hydrology and the tidal limits of the WAVES program and represented a tide controlled (dominated) shallow estuary. The site is located along the western shore of the Chesapeake Bay at the point where the Black River discharges into the Chesapeake Bay. The proposed bridge site is located in the City of Baltimore, approximately 5 miles downstream of the existing Route 150 Black River crossing, at Latitude  $39^{\circ} 15'$  and Longitude  $76^{\circ} 25'$  (Maryland State Plane Easting 449925 m, Northing 175078 m). The Black River at this location is approximately 11 ft deep, 1.6 miles wide (see Appendix C-2).

### **5.4.1 Estuary Conditions**

The Black River estuary was estimated to have an area of  $9.5 \text{ mi}^2$ . The estuary is generally shallow with an average depth of 11 ft below the MLW elevation. The estuary is 1.4 miles wide at the upstream nearfield distance from the proposed bridge and approximately 1.75 miles wide at the downstream nearfield distance from the bridge, which should cause contraction scour along the downstream pier face. The tidal portion of the Black River extends 10 miles upstream of the proposed bridge location into the eastern part of the City of Baltimore. The closest tidal gauge operated by NOAA is

located on the Patapsco River at Fort McHenry. As a result, the tidal data from the Fort McHenry gauge, which indicated a mean tidal amplitude of 0.935 ft, was used to represent the tidal conditions at the proposed bridge location.

#### **5.4.2 Watershed Conditions**

The area of the watershed draining to the Black River bridge location is 58 mi<sup>2</sup>. The watershed lies entirely within the western coastal plain (74%) and the piedmont (26%) physiographic regions. The average channel slope is 20.5 ft/mi and the basin relief is approximately 144 ft. The basin relief and channel slope contribute to cause a low time of concentration of 9.7 hr (as predicted by the SCS lag equation). Land use within the watershed is of high intensity with 61% urban development. In addition, the estimated amount of impervious cover is approximately 38% of the watershed area. The watershed has only 14% forest cover. The watershed soils are predominantly of hydrologic soils group C (71%) and the watershed curve number is 84.

#### **5.4.3 Simmons Ratio and Bridge Location Conditions**

The Black River estuary at the proposed bridge location has an SK value of 0.09, as shown in Table 5.1-1. This indicates that the Black River estuary is fully mixed and should be dominated by tides. The watershed area of 58 mi<sup>2</sup>, along with an estuary area of 9.5 mi<sup>2</sup>, produced a CE ratio of 6 and further indicated that pier scour at the Black River location should be highly influenced by the tidal processes and that scour should be initiated from the downstream face of each pier.



The geometry of the cross section at which the proposed bridge was to be located heavily influenced the hydraulic character of the cross section. In the case of the Black River Bridge location, the estuary is wide (1.63 mi) and moderately shallow (16 ft), as indicated by Figure 5.4-1, and as a result, is subject to two opposing hydraulic influences. The width of the cross section has the effect of reducing the average channel velocities, and hence, the potential for pier scour, while the moderately shallow depth is likely to promote significant channel velocities. The rate of scour within the Black River channel should depend on which of these influences is greater.

The characteristics of the soils at the bridge cross section are also critical to the potential for pier scour. The Maryland Geological Survey (2003) indicated that the soils in the Black River at the bridge consisted of sand and clayey sand. As a result, the mean soil particle size ( $d_{50}$ ) was estimated as 0.15 mm, the soil particle size for which 16% of the soils are smaller than ( $d_{16}$ ) was estimated as 0.01mm. The soil particle size for which 84% of the soils are smaller than ( $d_{84}$ ) was estimated as 0.75 mm, while the maximum particle size was 2.0 mm. The estuary soils being sand to clayey sand was estimated to have an angle of internal friction of  $35^{\circ}$  while the  $\alpha$  property was 5.7.

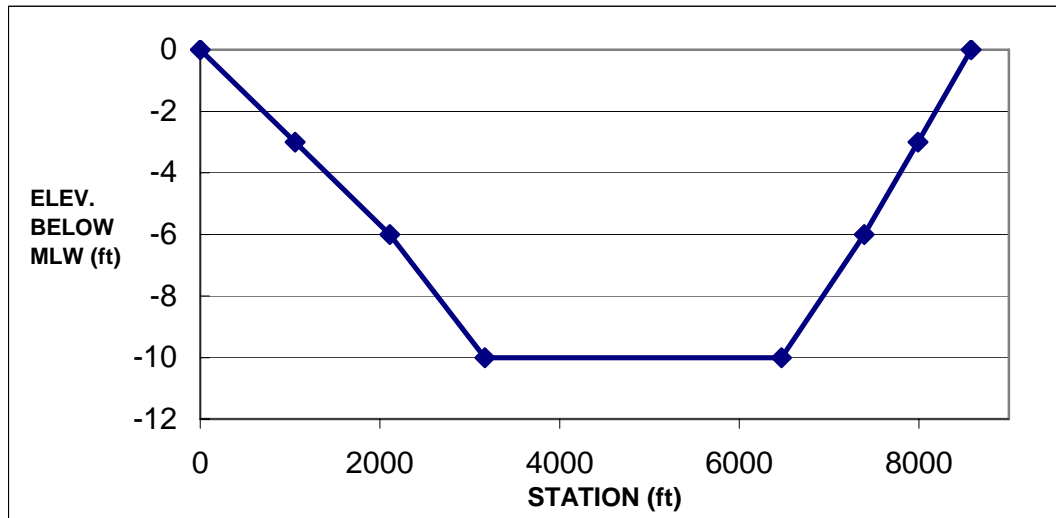


**Fig. 5.4-1. Black River Site Cross Section Profile at the Proposed Bridge Location. MLW Refers to the Mean Low Water Elevation. The Values Along the x-Axis Represent the Horizontal Cross Section Stations in ft.**

## 5.5 THE PATUXENT RIVER SITE

The Patuxent River site represented conditions that would be found in a tidal river with a large watershed. The site is located just upstream of Route 304 crossing over the Patuxent River at Benedict. The proposed bridge site is located at Latitude  $38^{\circ} 34.5'$  and Longitude  $76^{\circ} 41.5'$  (Maryland State Plane Easting 428943 m, Northing 94062 m). The Patuxent River at this location is 16 ft deep and 0.63 miles wide (see Appendix C-2).

### 5.5.1 Estuary Conditions

The estuary at the proposed bridge location is comprised of the tidal area of the river above the crossing and had an estimated area of  $9.87 \text{ mi}^2$  and an estuary length of 18 mi. The bridge location is moderately deep with an average depth of 16 ft below the MLW elevation and a width of 0.63 mi. In addition, the width of the estuary at the near-field distance upstream of the bridge cross section was 0.88 mi, which implies that there should also be contraction scour in the channel at the upstream pier face of the bridge.

The maximum width of the river upstream of the bridge location is 1.6 mi and may be found at a cross section 6 mi upstream of the proposed bridge location. The tidal data from the NOAA gauge located at Benedict on the Patuxent River were used at this location, as it represented the closest NOAA gauge to the proposed bridge. The NOAA gauge recorded an average tidal amplitude of 0.6 ft which implied that the mean low water elevation was -0.6 ft.

### **5.5.2 Watershed Conditions**

The hypothetical bridge crossing at the Patuxent at Benedict drains a total watershed area of 732 mi<sup>2</sup>. The watershed area is located in the western coastal plain (68%) and the piedmont (32%) physiographic regions. The overland slope of the watershed is predominantly mild with an average land slope of 5.9% and a basin relief of 242 ft, while the average channel slope is 5.2 ft/mi. The high basin relief, channel slope, watershed area, and a flow path of 91 mi produced an estimated time of concentration of approximately 41.8 hr (as predicted by the SCS lag equation). However, the time of concentration was increased by 20% to account for the attenuating effects produced by the Patuxent Reservoir that is located in the watershed above the proposed bridge location. The watershed is 40% forest cover and 12% impervious. Land use within the watershed is of moderate intensity, with 26% urban development. Most of the watershed soils are of hydrologic soils group B (60%), which results in a relatively low watershed curve number of 70.

### 5.5.3 Simmons Ratio and Bridge Location Conditions

The Patuxent River estuary at the proposed bridge location has an SK value of 0.47, as shown in Table 5.1-1. This indicates that the estuary is partially mixed with both tidal and riverine influences. The proposed bridge location has a CE ratio of 73 and this provides further indication that pier scour would be influenced by both the riverine and tidal processes with the riverine processes being slightly dominant.

The hydraulic effects produced by the cross section at the proposed bridge crossing are significant in terms of its impacts on flow velocities. The Patuxent River crossing is relatively wide (0.633 mi) and moderately shallow (16 ft), as indicated by Figure 5.5-1. The width of the river at the bridge location has the effect of reducing the average channel velocities, and hence, the potential for pier scour. The moderate shallowness of the river has the opposite effect. The rate of scour at the proposed cross section was dependent on which of these influences was greater.

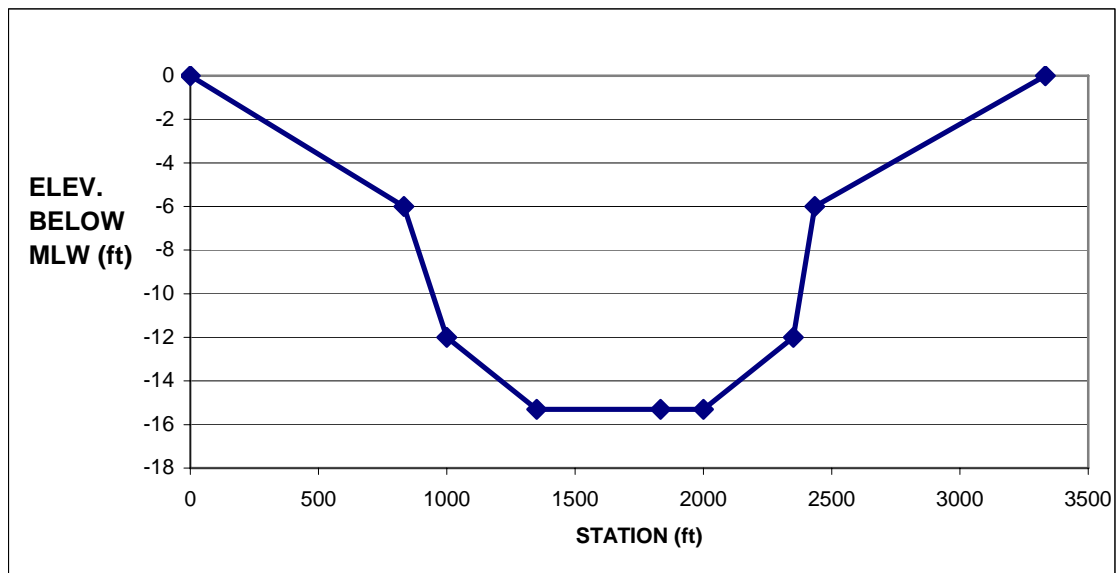


**Fig. 5.5-1. Patuxent River Cross Section Profile at the Proposed Bridge Location. MLW Refers to the Mean Low Water Elevation. The Values Along the x-Axis Represent the Horizontal Cross Section Stations in ft.**

The characteristics of the soils at the bridge cross section are also critical to the potential for pier scour. The Maryland Geological Survey (2003) indicated that the soils at the proposed Patuxent River crossing consisted of medium sized sand. As a result, the mean soil particle size ( $d_{50}$ ) was estimated as 0.25 mm. The soil particle size for which 16% of the soils are smaller than ( $d_{16}$ ) was estimated as 0.01mm. The soil particle size for which 84% of the soils are smaller than ( $d_{84}$ ) was estimated as 3.0 mm, while the maximum particle size was 3.25 mm. The estuary soils being sand was estimated to have an angle of internal friction of  $45^0$  while the  $\alpha$  property was estimated as 5.7.

## **5.6 THE WICOMICO RIVER SITE**

The Wicomico River site represented conditions that would be found in a tidal river with a small watershed. The site is located downstream of Whitehaven on the Wicomico River. The proposed bridge site is located at Latitude  $38^0 15.5'$  and Longitude  $75^0 50.5'$  (Maryland State Plane Easting 501345 m, Northing 65399 m). The Wicomico River at this location is 18 ft deep and 0.25 miles wide (see Appendix C-2).

### **5.6.1 Estuary Conditions**

The estuary at the proposed bridge location is comprised of the tidal area above the proposed bridge crossing and had an estimated area of  $3.95 \text{ mi}^2$  and an estuary length of 15 mi. The bridge location is moderately deep with an average depth of 17 ft below the MLW elevation and a width of 0.25 mi. In addition, the width of the estuary at the nearfield distance upstream and downstream of the bridge cross section was also 0.25 ft, which indicated that contraction scour should not be significant. The maximum width of

the river upstream of the bridge location is 0.35 mi and may be found at a cross section 3 mi upstream of the proposed bridge location. The tidal data from the NOAA gauge located at Whitehaven on the Wicomico River were used at this location, as it represented the closest NOAA gauge to the proposed bridge. The NOAA gauge recorded an average tidal amplitude of 1.19 ft which implied that the mean low water elevation was -1.19 ft.

### **5.6.2 Watershed Conditions**

The proposed bridge crossing drained a total watershed area of 170.8 mi<sup>2</sup>. The watershed area is fully located in the eastern coastal plain physiographic region. The overland slope of the watershed is predominantly flat with an average land slope of 0.7% and a basin relief of 31.3 ft, while the average channel slope is 1.6 ft/mi. The low basin relief, channel slope, watershed area, and a flow path of 33 mi produced an estimated time of concentration of approximately 41.8 hr (as predicted by the SCS lag equation). The watershed is 36% forest cover and 9.5% impervious. Land use within the watershed is of moderate intensity, with 20% urban development. Most of the watershed soils are of hydrologic soil group D (44%), which results in a relatively high watershed curve number of 79.

### **5.6.3 Simmons Ratio and Bridge Location Conditions**

The Wicomico River estuary at the proposed bridge location has an SK value of 0.12, as shown in Table 5.1-1. This indicates that, like the Patuxent river site, the estuary is partially mixed with both tidal and riverine influences. The proposed bridge location

has a CE ratio of 43, and this provides further indication that pier scour would be influenced by both the riverine and tidal processes, as was the case with the Patuxent River cross section. However, at this site, the tidal processes should be slightly more dominant.

The Wicomico River crossing is also relatively narrow (0.25 mi) and moderately shallow (17 ft), as indicated by Figure 5.6-1. The narrow width of the river at the bridge location has the effect of increasing the likelihood of high stream flow velocities being generated in the channel at the bridge cross section. In addition, the moderately shallow depth of the river reinforces this effect. As a result, a high rate of scour was expected at the proposed cross section.

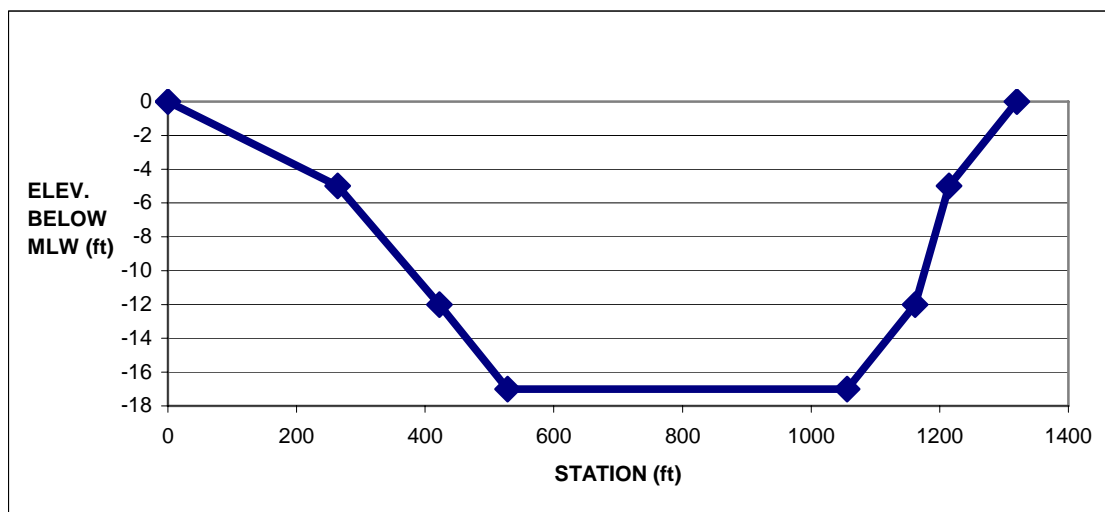


**Fig. 5.6-1. Wicomico River Cross Section Profile at the Proposed Bridge Location. MLW Refers to the Mean Low Water Elevation. The Values Along the x-Axis Represent the Horizontal Cross Section Stations in ft.**

The characteristics of the soils at the Wicomico River bridge cross section reflect a mixture of the fluvial estuarine conditions that are present there. The Maryland Geological Survey (2003) indicated that the soils at the proposed Wicomico River

crossing consisted of medium sized sand with some clayey sand present. As a result, the mean soil particle size ( $d_{50}$ ) was estimated as 0.325 mm. The soil particle size for which 16% of the bay soils are smaller than ( $d_{16}$ ) was estimated as 0.1mm. The soil particle size for which 84% of the bay soils are smaller than ( $d_{84}$ ) was estimated as 3.2 mm, while the maximum particle size was 4.25 mm. The estuary soils being sand was estimated to have an angle of internal friction of  $45^0$  while the  $\alpha$  property was estimated as 5.7.

## **5.7 THE PATAPSCO RIVER SITE**

The Patapsco River site represented conditions that would be found in a deep estuary with a large watershed. The site is located two miles downstream of the Baltimore inner harbor and immediately upstream of Fort McHenry. The hypothetical bridge site is located at Latitude  $39^0 16.5'$  and Longitude  $76^0 35.5'$  (Maryland State Plane Easting 445359 m, Northing 168475 m). The lands adjoining the estuary are comprised of commercial shipping wharves with the estuary itself containing a narrow dredged channel used by the commercial ships. As a result, the Patapsco River estuary at this location is 33 ft deep and 0.33 miles wide (see Appendix C-2).

### **5.7.1 Estuary Conditions**

The estuary at the proposed bridge location is comprised predominantly of the Baltimore Inner Harbor area estimated to be  $3.56 \text{ mi}^2$ . The estuary length is 2.56 mi. The bridge location was moderately deep with an average depth of 33 ft below the MLW elevation and a width of 0.33 mi. In addition, the width of the estuary at the nearfield distance downstream of the bridge cross section is 0.40 mi which implied that there



should also be contraction scour in the channel at the downstream pier face of the bridge. The maximum width of the river upstream of the bridge location is 0.79 mi and may be found at a cross section 1.5 mi upstream of the proposed bridge location. The tidal data from the NOAA gauge located at Fort McHenry on the Patapsco River were used at this location, as it represented the closest NOAA gauge to the proposed bridge. The NOAA gauge recorded an average tidal amplitude of 0.935 ft which implied that the mean low water elevation was  $-0.935$  ft.

### **5.7.2 Watershed Conditions**

The proposed bridge crossing drained a total watershed area of  $599 \text{ mi}^2$ . The watershed area is located in the western coastal plain (27%) and the piedmont (73%) physiographic regions. The overland slopes within watershed are predominantly mild with an average land slope of 6% and a basin relief of 428 ft, while the average channel slope is 11 ft/mi. The high basin relief, channel slope, watershed area, and a flow path of 69 mi produced an estimated time of concentration of approximately 28.2 hr (as predicted by the SCS lag equation). The watershed is 26% forest cover and 21% impervious. Land use within the watershed is very intense, with 40% urban development. Most of the watershed soils are of hydrologic soils group B (48%), which resulted in a relatively low watershed curve number of 73.

### **5.7.3 Simmons Ratio and Bridge Location Conditions**

The Patapsco River estuary at the proposed bridge location has an SK value of 1.16, as shown in Table 5.1-1. This indicates that the estuary is stratified and dominated

by the catchment and riverine influences. The proposed bridge location has a CE ratio of 168 and this provides further indication that pier scour would be influenced primarily by the riverine processes.

The hydraulic effects produced by the cross section at the proposed bridge crossing were also significant. The Patapsco River crossing is also relatively narrow (0.33 mi) but deep (33 ft), as indicated by Figure 5.4-1. The narrow width of the estuary at the bridge location should cause significant velocities to be generated in the channel and hence increase the potential for pier scour. The depth of the channel should produce the opposite effect and attenuate the rate of scour at the proposed cross section.

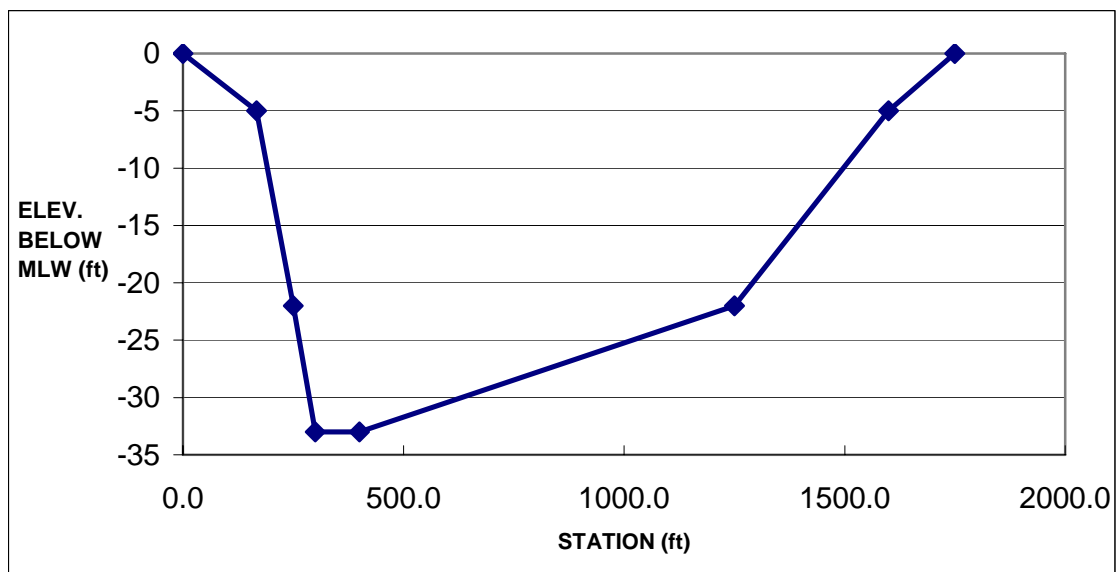


**Fig. 5.7-1. Patapsco River Cross Section Profile at the Proposed Bridge Location. MLW Refers to the Mean Low Water Elevation. The Values Along the x-Axis Represent the Horizontal Cross Section Stations in ft.**

The soil characteristics at the proposed bridge cross section displayed estuarine properties. The Maryland Geological Survey (2003) indicated that the soils at the proposed Patapsco River crossing consisted of clayey sand. As a result, the mean soil particle size ( $d_{50}$ ) was estimated as 0.15 mm. The soil particle size for which 16% of the

bay soils are smaller than ( $d_{16}$ ) was estimated as 0.01mm. The soil particle size for which 84% of the bay soils are smaller than ( $d_{84}$ ) was estimated as 0.34 mm, while the maximum particle size was 0.40 mm. The estuary soils being clayey sand was estimated to have an angle of internal friction of  $33^{\circ}$  while the  $\alpha$  property was estimated as 5.7.

## **CHAPTER 6**

### **CASE STUDIES: CONTINUOUS MODEL APPLICATION**

#### **6.1 INTRODUCTION**

Many researchers have proposed the idea that continuous pier scour models are more appropriate and beneficial than single-event pier scour models that use the design storm approach. However, it has not been conclusively shown that this is true for bridges located in tidal environments. Examining this hypothesis as it relates to pier scour within estuaries and tidal rivers is one of the primary objectives of this study and is the basis for the development of the WAVES program. Comparing the results of each model with pier scour field data from existing bridge sites could show the benefits of a continuous scour model over the design storm approach. However, since reliable pier scour field data from tidal waterways do not exist, other methods of comparing the abilities of these models were considered. In order to overcome this problem, the WAVES continuous model was compared to a number of single-event models through simulations using hypothetical bridge data at five actual estuary case study sites. The current chapter presents and discusses the results of the continuous simulations at the selected case study sites.

Some estuary locations, as is the case of the Chesapeake Bay, are frequently exposed to hurricanes and other intensely destructive weather events. It is, therefore, important to understand the impact of such individual events on bridge structures within an estuary, particularly their impacts on bridge pier scour. For the purposes of this study, hurricanes are considered to be single-events even though the magnitudes of the flow and velocity generated during the event are not constant. This is because the duration of a single hurricane is insignificant when compared to the design life of a bridge. It was

necessary to assess the scour caused by hurricane events and compare these results to the ongoing scour that occurred over the design life of the structure. An option of the WAVES model provides for single-event hurricane assessment and the use of the case study sites provided a direct means of comparing the long-term scour results with those obtained from a single hurricane event.

## **6.2 SIMULATION CONDITIONS AND ASSUMPTIONS**

### **6.2.1 Continuous Simulations**

An understanding of the options utilized in performing the continuous simulations using the WAVES program is critical to correctly interpreting the simulation results. In conducting the continuous simulations using data for the case study sites, the WAVES program was executed under a set of constant simulation conditions and assumptions. This approach was used to ensure that differences in the results would be attributed only to site specific conditions, such as channel width, channel depth, estuary, and catchment area that varied from site to site. The constant simulation conditions and assumptions included the simulation duration, the initial conditions, and the assumption that the values for  $d_{16}$ ,  $d_{50}$ ,  $d_{84}$ , and  $d_{\max}$  for the channel soil at each case study site did not vary with scour depth.

An appreciation for the considerations used to determine the simulation duration is necessary to fully understand the results produced. In determining the simulation duration, two factors were considered. First, a simulation duration long enough to provide sufficient time for a case study site to reach ultimate scour was required. Because it was thought that the typical bridge design life of 50 years would not always be sufficient for wide or deep estuaries to attain ultimate scour, a simulation duration greater

than 50 years was used. Second, the impact of the simulation duration on the total computational time was considered. The results of the WAVES program stabilized after 1000 simulations as shown in Appendix D-1. With a simulation period of 100 years, most desk top computers would be able to complete this run in four hours. Hence, a simulation duration of 100 years was selected because it was sufficient to produce ultimate scour in most cases, while maintaining a reasonable computational time.

The type of soil in the channel has a major impact on magnitude of pier scour. The channel soil conditions at each site were assumed to be constant across each cross section and with depth. Though the soil gradation and properties, such as  $d_{16}$ ,  $d_{50}$ ,  $d_{84}$ , and  $d_{\max}$  varied from site to site, these properties were assumed to be constant with depth. This simplifying assumption removed the effect of soil inhomogeneity and facilitated easier comparison of the scour results between sites. Also, a homogeneous backfill is likely to be used at the site of the pier.

The initial conditions used in the WAVES simulations had a minor impact on the scour results. The initial conditions of the simulations performed with the WAVES program were those assumed exist at the sites before the beginning of the simulations. These were the existing scour depth and the existing estuary depth. The initial estuary depths for all of the case study sites were set at the mean low water (MLW) depth for that site. Similarly, for the continuous simulations under the design mode the initial total pier scour was set at zero.

An understanding of the program execution options ensures its correct use. As defined and discussed in Chapter 3, the WAVES program was developed with a number of program execution options to provide the user with the ability to compare the results of

simulations using different tidal and contraction scour equations. The continuous simulations were made using the same program execution options for all of the sites. The program execution options used included (1) simulations in the pier design mode with and without natural armoring, (2) the determination of the contraction scour using Komura's equation, (3) the determination of the incipient scour velocity using Neill's method, (4) the use of the Brubaker-Demetrius-Neill's Modification factors, and (5) the activation of the tidal distortion option.

The analysis of existing and new bridges is an essential feature of any pier scour study. The WAVES program includes the options to perform simulations for the new bridge designs and to analyze pier scour at existing bridges. These options were described as simulation options. The execution of the program using the bridge design simulation option was termed the "pier design mode" while simulations made using the existing bridge analysis simulation option was indicated as the "existing pier analysis mode".

In making the analyses, a number of assumptions were made. Continuous simulations made under the pier design mode assumed a zero scour initial condition. The continuous simulations were also made with the program execution options for both with and without natural armoring. This enables the effects of natural armoring at each case study site to be assessed. The program execution option to employ Komura's contraction scour model was also used. This method was selected above the others because preliminary simulations showed that Komura's contraction scour equation produced more conservative results than the other available methods. The Brubaker-Demetrius-Neill's modification option was also used along with the tidal distortion option. Though these

options produced more conservative scour results, they improved the accuracy of the model results by providing more realistic estimates of the tidal generated discharges than that predicted by the Neill's equation.

### **6.2.2 Hurricane Event Simulations**

Specific assumptions and conditions were used in conducting the hurricane simulations. The hurricane was assumed to be a single event with a duration of 36 hr. The model simulation option used the existing pier analysis mode with an initial scour depth of set between 0.9 ft and 3.0 ft. The SRICOS model (Briaud et al. 1999) was used for determining the incipient scour velocity of the channel bed during the hurricane simulations. Pier scour during hurricane events was also determined without considering natural armoring. In addition, the following general hurricane conditions were used unless stated differently in the description of the conditions of each specific site. First, a hurricane of Category III strength was assumed. Second, the closest approach distance of the hurricane to the bridge was assumed to be one mile. Third, the hurricane simulations were conducted using variable rainfall amounts of 5, 8, 12, and 16 inches, while the duration of the hurricane rainfall was assumed to be 36 hours.

The pre-event scour depth for the hurricane simulation was believed to have some effect on the final hurricane scour results. Preliminary scour simulations indicated that the largest scour rates for most pier conditions occurred when the total pier scour was between 2 and 8 ft. As a result, a pre-event scour depth of between 2 and 5 ft was selected at random for the purpose of determining the effects of a hurricane under the most critical conditions. Preliminary hurricane simulations were made using the various execution options of the WAVES model. During these preliminary runs it was noticed



that the Neill's incipient velocity method did not produce the most conservative scour results. Accordingly, the SRICOS method was used. Similarly, the natural armoring option tended to significantly reduce the scour from a single-event when compared to simulations where natural armoring was not used. As a result, natural armoring was not used for the case study hurricane simulations.

The category and consequently the strength of a hurricane have a significant impact on the tidal processes in estuaries. A review of the NWS hurricane records over the past 40 years showed that the strongest hurricane to traverse the Chesapeake Bay area was a Category III event. As a result, unless stated otherwise during the specific site description, the hurricane selected for the hurricane simulation reflected the size and strength of a Category III hurricane. The approach distance of the hurricane to the bridge was selected to be close enough for the hurricane to have a very significant impact. The impact of a hurricane relative to its distance from the bridge was investigated during the performance of the sensitivity analyses and it was determined that at 1 mile the hurricane exerted a very large influence on the location. Thus, a hurricane approach distance of 1 mile was used.

## **6.3 THE MONIE BAY SITE**

### **6.3.1 Specific Modeling Assumptions and Conditions**

The summary of the important features of the Monie Bay estuary and catchment described in Chapter 5 showed that Monie Bay was a tide dominated, well-mixed estuary with very low adjusted Simmons Ratio (SK) and CE ratio. In addition, the selected bridge cross section was wide and shallow. These conditions were reflected in the inputs

of the model. Additional assumptions regarding the tidal properties, estuary overbank slopes, and soils data were also made.

Tidal and sediment properties are important to the formation of pier scour holes in tide-controlled environments like the Monie Bay site. The tidal information obtained from the NOAA gauge at Whitehaven was used to represent the tidal properties at the Monie Bay bridge cross section. From this information the diurnal tidal amplitude at the Monie Bay site was determined to be 1.19 ft. The catchment information provided by the USGS quadrangle map indicated very low basin relief and catchment slopes. As a result, the overbank channel side slope was assumed to be 1:1000 or 0.1%. The use of the Parson Island geotechnical report as a source of soil information was also discussed in Chapter 5. In the case of Monie Bay, a maximum particle diameter of 2.5 mm was assumed. This was smaller than the 10 mm indicated in the Parson Island geotechnical report. This change was made to account for the fact that Monie Bay was located further south along the shoreline of the main Chesapeake Bay estuary and was connected to a small, low-lying, flat watershed, which made it easier for the deposition of finer soils particles.

#### **6.3.1.1 Hurricane Simulations**

The tracks of historical hurricanes that affected the Chesapeake Bay area were obtained from the records of NOAA and used to estimate the possible strength of hurricanes affecting Monie Bay. It was estimated that the most critical hurricane scour impacts at Monie Bay would be due to a hurricane traveling northwards up the Chesapeake Bay with the center (or eye) being over the Chesapeake Bay just to the west of Monie Bay. This would result in the surge being directed eastward up Monie Bay just

as the center of the hurricane had passed that location. This assumed track could facilitate a hurricane of Category III strength and distance of closest approach of 1 to 5 miles. These considerations led to the modeling assumption of a Category III hurricane passing 1 mile west of the bridge.

A slow moving Category III hurricane has the potential to produce significant amounts of precipitation. However, the track of a hurricane in relation to the specific location of interest can have a significant impact on the amount of precipitation delivered to that location. It is accepted that locations east or south of the hurricane center will obtain less rainfall than locations west of the eye. As a result, it is likely that hurricane rainfall amounts could range between 5 and 8 inches. These rainfall values were within the range of rainfall depths assumed for the hurricane simulations as indicated earlier.

### **6.3.2 Continuous Simulation Results**

The continuous simulation result at Monie Bay represents long-term pier scour in a small tide-dominated estuary. Details of the continuous simulation results for Monie Bay are provided in Appendix D-3. Table 6.3-1 show a summary of the scour results and the values of important scour variables. These variables were also obtained from the detailed results of Appendix D-3, except for the armoring incipient scour velocity that was computed using Neill (1968) discussed in Chapter 3:

$$U_{iarm} = 1.328( d_{max}/1.8)^{0.33}y^{0.17} \quad (6.3-1)$$

where  $U_{iarm}$  is the incipient armoring scour velocity in ft/s,  $d_{max}$  is the maximum soil particle size in mm, and  $y$  is the maximum flow depth in the simulation.

The continuous simulation results show that scour did not occur at the upstream pier face for the entire simulation period for either an armored condition or when the natural armoring option was omitted. In the case of the downstream pier face, the continuous simulation results show that scour did not take place when natural armoring was considered. However, without natural armoring the scour hole developed to an ultimate depth of 19 ft.

The development of the scour hole is related to the maximum values of the stream velocity and tangential vortex velocity reached during the simulation. The incipient and critical armoring scour velocities are also important variables that determine whether or not scouring will occur. Low values of the maximum vortex tangential velocity suggest the incomplete development of a scour hole, and consequently significant scour will not be produced. The maximum vortex tangential velocity of the simulation being significantly greater than the maximum stream velocity is also a very good indicator of the full development of the scour hole.

Another predictor of scour is the value of the vortex tangential velocity relative to the incipient scour velocity,  $(V_t - U_i)$  or  $(V_t - U_{iarm})$ , which in turn determines the effective scour rates. When armoring is not considered, the effective scour rate is denoted by  $V_{rna}$ , while when natural armoring is considered it is denoted by  $V_{ra}$ . The effective scour rate without natural armoring ( $V_{rna}$ ) is defined as follows:

$$V_{rna} = \begin{cases} (V_t - U_i) & \text{for } V_t - U_i > 0 \\ 0 & \text{for } V_t - U_i \leq 0 \end{cases} \quad (6.3-2)$$

Similarly, the effective scour rate with natural armoring is:

$$V_{ra} = \begin{cases} (V_t - U_{iarm}) & \text{for } V_t - U_{iarm} > 0 \\ 0 & \text{for } V_t - U_{iarm} \leq 0 \end{cases} \quad (6.3-3)$$

It should be noted that  $V_{rna}$  and  $V_{ra}$  are mathematical quantities whose values indicate the likelihood of scour. A positive value for either  $V_{rna}$  or  $V_{ra}$  indicates that the vortex tangential velocity was greater than the incipient scour velocities, hence scouring of the bed material was likely.

**Table 6.3-1. Summary of Monie Bay Continuous Simulation Variables and Pier Scour Results at the Upstream (U/S) and Downstream (D/S) Pier Faces**

Scour Velocity Variables	U/S Pier Face	D/S Pier Face
Maximum discharge (cfs) $Q_{max}$	50794	50527
Maximum stream velocity w/ armoring (ft/s) $V_{maxa}$	0.72	1.52
Maximum stream velocity w/o armoring (ft/s) $V_{maxna}$	0.74	1.54
Maximum vortex tangential velocity w/ armoring (ft/s) $V_{ta}$	0.36	0.75
Maximum vortex tangential velocity w/o armoring (ft/s) $V_{tna}$	0.36	2.70
Maximum flow depth (ft) $Y$	9.5	10.0
Incipient scour velocity (ft/s) $U_i$	0.43	0.43
Maximum particle size (mm) $d_{max}$	2.5	2.5
Incipient armoring scour velocity (ft/s) $U_{iarm}$	2.17	2.19
Vortex tangential vel.— the incipient vel. w/ armoring (ft/s)	-1.81	-1.44
Vortex tangential vel.— the incipient vel. w/o armoring (ft/s)	-0.07	2.27
Effective scour rate w/armoring (ft/s) $V_{ra}$	0.0	0.0
Effective scour rate w/o armoring (ft/s) $V_{rna}$	0.0	2.72
Maximum 100-year pier scour w/ armoring (ft) $d_{sa}$	0.00	0.00
Maximum 100-year pier scour w/o armoring (ft) $d_{sna}$	0.00	19.00

### 6.3.2.1 Upstream Pier Face

The results of the simulation at Monie Bay represent the amount of scour that could be developed along the upstream face of the pier in a tide-controlled environment. Figure 6.3-1 provides a graphic view of the results of the continuous scour simulations for the upstream face of the pier at Monie Bay. The figure shows that scour did not occur at the upstream pier face with or without natural armoring being considered. Table 6.3-1

also shows that for the upstream pier face, the maximum downstream velocity of the simulation was 0.74 ft/s while the maximum vortex tangential velocity was 0.36 ft/s for both cases where armor was and was not considered. The fact that the maximum vortex tangential velocity at the upstream pier face was only half the value of the maximum stream velocity in the direction downstream indicates that a scour hole was not formed; hence, scour did not occur at the upstream pier face. Similarly, the values of the effective scour rates  $V_{ra}$  and  $V_{ma}$  indicate the incipient scour velocity was not surpassed; hence, scouring did not occur.

#### **6.3.2.2 Downstream Pier Face**

The relative amount of scour produced at the upstream and downstream faces of the pier tells whether the dominant process at Monie Bay was the catchment or tidal process. In the case of scour on the downstream pier face, Figure 6.3-1 shows that scour did not occur under the natural armoring condition; however, when the natural armoring option was not used, the scour generated by activities at the downstream pier face reached an ultimate value of approximately 19 ft over the period of simulation. When natural armoring was not considered, Figure 6.3-1 shows a relatively slow rate of scour along the downstream pier face for the first 72 years. At the end of this period the total scour had reached approximately 4.0 feet at an average rate of scour of 0.06 ft/yr. During the next 20 years the larger scour rates occurred, as the scour hole developed from 4 feet in depth to approximately 17.5 feet at an average rate of 0.68 ft/yr. The ultimate scour depth of 19 ft was reached over the next 6 years. The amount of scour produced was consistent with the fact that the maximum vortex tangential velocity on the downstream

pier face (2.70 ft/s) was significantly greater than the maximum upstream velocity of the channel (1.54 ft/s).

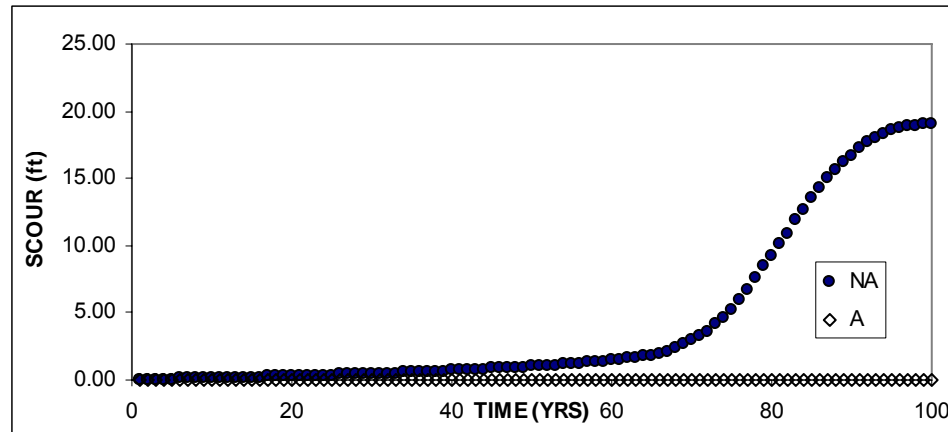


**Fig.6.3-1. Temporal variation of pier scour for the downstream face obtained from the results of the Monie Bay simulations. NA indicates that armoring was not considered, while A indicates the armoring option was used. The WAVES scour results represent the mean scour depth obtained from 1000 simulations.**

The results of the simulations performed using natural armoring at Monie Bay provides an indication of the impact that natural armoring may have on a tide-controlled site with low stream velocities. Figure 6.3-1 indicates that natural armoring had a significant effect on the pier scour process in Monie Bay. By increasing the armoring incipient scour velocity and reducing the value of  $V_{ra}$  to 0, the natural armoring process had prevented the finer particles from being detached from the bed. Thus, when natural armoring was modeled; the scour on the downstream pier face over the simulation period was 0. These results can be explained in relation to the maximum vortex tangential velocity reached during the period of simulation and the scour incipient velocity of the channel bed material. Natural armoring effectively creates a layer of larger sized particles at the surface of the channel, or scour hole, by the selective erosion of the finer sized material. This process raises the incipient scour velocity of the materials at the

surface. If the incipient velocity is raised to be approximately equal to or greater than the vortex tangential velocity, then, as is the case with the armoring option on the downstream pier face, scouring ceases.

The continuous simulation results for Monie Bay were in agreement with the hypotheses that the estuary type, as indicated by the SK and CE ratios, influences whether or not pier scour will be initiated from the downstream or upstream pier face. Monie Bay is classified as a well-mixed, tide-dominated estuary and hence the scour results are in agreement with this classification. In addition, the relatively low downstream pier face scour rate also helps to justify the assumption that pier scour is also controlled by the channel cross section width, depth, and area. Although the Monie Bay cross section is shallow, the large width of the cross section initially causes low channel velocities and consequently, a small amount of scour. However, at some point within the period of simulation, a series of tidal events occurred that initiated significant scour along the downstream pier face, and once this happened, the shallow depth of Monie Bay was able to sustain the conditions for further scour development. This resulted in the full development of the scour hole over time with scour reaching an ultimate depth of 19 ft.

### **6.3.3 Results of the Hurricane Event Simulations**

The results of the hurricane scour simulations provide an opportunity to assess bridge pier scour in a tide-controlled estuary. Details of the hurricane scour results for Monie Bay are provided in Appendix D-4. Table 6.3-2 provides a summary of the scour variables for the hurricane event simulation assuming a hurricane rainfall of 5 in. In addition, Table 6.3-3 shows the scour predicted at both the upstream and downstream



faces of the pier when hurricane rainfall depths of 5, 8, 12, and 16 inches were considered.

A small amount of pier scour was generated by the single-event hurricane at the Monie Bay site. Table 6.3-2 shows that significant pier scour did not occur on either pier face. For the upstream pier face, the maximum downstream velocity of the simulation was 2.37 ft/s while the maximum vortex tangential velocity was 0.70 ft/s. Although the maximum discharge was high, the flow depth that resulted from the surge was also high, which caused the lowering of the maximum stream velocity. This caused the maximum vortex tangential velocity at the upstream pier face to be low (0.7 ft/s) which resulted in minor scour being initiated on the pier face. Significant hurricane scour will not be produced with an increase in the amount of rainfall during a hurricane event (see Table 6.3-3).

**Table 6.3-2. Monie Bay Hurricane Scour Results for the Upstream (U/S) and Downstream (D/S) Pier Faces with 5 in. of Rainfall**

<b>Hurricane Scour Variables</b>	<b>U/S Pier Face</b>	<b>D/S Pier Face</b>
Maximum discharge (cfs) $Q_{\max}$	208193	195798
Maximum stream velocity (ft/s) $V_{\max}$	2.37	0.82
Maximum Vortex Tangential Velocity (ft/s) $V_{t\max}$	0.7	0.3
Maximum flow depth (ft) $Y$	20.29	20.19
Incipient Scour Velocity (ft/s) $U_i$	0.13	0.13
Vortex tangential vel.- The incipient vel. w/o armoring (ft/s)	0.57	0.17
Effective scour rate w/o armoring (ft/s) $V_{r\max}$	0.57	0.17
Existing scour at the start of the event (ft)	3.9	3.9
Final scour at the end of the event (ft)	4.0	4.1
Total pier scour (ft) $d_s$	0.1	0.2

**Table 6.3-3. Monie Bay Hurricane Scour Results for the Upstream (U/S) and Downstream (D/S) Pier Faces with 5, 8, 12, and 16 in. of Rainfall**

Rainfall (in)	5	8	12	16
D/S Pier Face Scour (ft)	0.2	0.1	0.03	0.02
U/S Pier Face Scour (ft)	0.1	0.3	0.4	0.6

In the case of the downstream pier face, the maximum downstream velocity of the simulation was 0.82 ft/s, while the maximum vortex tangential velocity was 0.3 ft/s. As was the case with the upstream pier face, a relatively high maximum upstream discharge along with a high flow depth caused the lowering of the maximum stream velocity. The effective scour rate at the downstream face of the pier during the hurricane event was 0.17 ft/s, and minor scouring was produced by the event. As was the case with the upstream pier face, significant hurricane scour was not produced during the hurricane event when the hurricane produced greater rainfall.

## **6.4 THE BLACK RIVER AT BALTIMORE SITE**

### **6.4.1 Specific Modeling Assumptions and Conditions**

The summary of the important features of the Black River estuary and catchment described in Chapter 5 showed that the Black River estuary was a tide dominated, well mixed estuary with very low adjusted Simmons (SK) and CE ratios. In addition, the selected bridge cross section was wide and moderately shallow. These conditions were reflected in the models input, as shown in Appendix D-2.

Scour at the Black River site was also dependent on tidal, cross section geometry, and soils properties. The tidal information obtained from the NOAA gauge at Fort

McHenry was assumed to represent the tidal properties at the bridge cross section. From this information, the diurnal tidal amplitude was determined to be 0.935 ft. The catchment information provided by the USGS quadrangle maps indicated a moderate basin relief of 143 ft and an average land slope of 4% in the catchment area. As a result, the overbank channel slope was assumed to be 1:500. The mean channel soil particle size at the proposed bridge cross section was 0.15 mm, and the maximum particle size was 2.0 mm.

#### **6.4.1.1 Hurricane Simulations**

Historical hurricane data obtained from NOAA indicated that the most critical hurricane scour impacts at the Black River watershed would be due to a hurricane traveling northwards up the Chesapeake Bay with the hurricane center (or eye) being over the Chesapeake Bay just to the west of the Black River location. This would result in the hurricane surge being directed northwards up the Black River estuary when the center of the hurricane had arrived at the same latitude as the bridge location. This track could facilitate a hurricane of Category III strength and a closest approach of 1 to 5 miles. These considerations led to the modeling assumption of a Category III hurricane passing 1 mile from the bridge.

For reasons cited in the Monie Bay discussion, it was assumed that less rain would fall than at locations to the west of the eye of the hurricane. As a result, it was assumed that less than the 8 in. of rain generally assumed for the case study sites would fall at the Black River location. However, since the Black River estuary watershed is located in the Western Coastal Plain and Piedmont physiographic regions, it was assumed that 7 in. of rainfall would accompany the hurricane event at Black River. As indicated

earlier, hurricane simulations were also made for rainfall amounts of 5, 8, 12, and 16 inches to assess the impact of significant hurricane rainfall on pier scour at this location.

#### 6.4.2 Continuous Simulation Results

The continuous simulation results show that measurable scour did not occur at the upstream pier face for the entire simulation period for either case, with or without natural armoring. Details of these are shown in Appendix D-5. Table 6.4-1 provides a summary of the scour results at both pier faces. In the case of the downstream pier face, the continuous simulation results show that scour did not occur when the site was naturally armored. However, without natural armoring the scour hole developed to an ultimate depth of 20 ft.

**Table 6.4-1. Summary of the Black River Continuous Simulation Variables and Pier Scour Results at the Upstream (U/S) and Downstream (D/S) Pier Faces**

Scour Velocity Variables	U/S Pier Face	D/S Pier Face
Maximum discharge (cfs) $Q_{\max}$	260791	271236
Maximum stream velocity w/ armoring (ft/s) $V_{\max a}$	1.48	2.22
Maximum stream velocity w/o armoring (ft/s) $V_{\max na}$	1.48	2.22
Maximum vortex tangential velocity w/armoring (ft/s) $V_{ta}$	0.66	0.94
Maximum vortex tangential velocity w/o armoring (ft/s) $V_{tna}$	0.65	3.55
Maximum flow depth (ft) $Y$	16.00	16.75
Incipient scour velocity (ft/s) $U_i$	0.51	0.51
Maximum particle size (mm) $d_{\max}$	2.75	2.75
Incipient armoring scour velocity (ft/s) $U_{iarm}$	2.45	2.46
Vortex tangential vel.— the incipient vel. w/ armoring (ft/s)	-1.79	-1.52
Vortex tangential vel.— the incipient vel. w/o armoring (ft/s)	0.14	3.04
Effective scour rate w/armoring (ft/s) $V_{ra}$	0.0	0.0
Effective scour rate w/o armoring (ft/s) $V_{rna}$	0.14	3.04
Maximum 100-year pier scour w/ armoring (ft) $d_{sa}$	0.00	0.00
Maximum 100-year pier scour w/o armoring (ft) $d_{sna}$	0.03	20.00

#### 6.4.2.1 Upstream Pier Face

A review of the velocity output variables obtained from the continuous simulation at the upstream pier face of the Black River site indicated that insignificant scour is typically generated from the upstream face of the pier in a tide-controlled estuary. Table 6.4-1 shows that the maximum downstream velocity of the simulation was 1.48 ft/s while the maximum vortex tangential velocity was 0.66 ft/s for both cases where armoring did and did not exist, respectively. The maximum vortex tangential velocity at the upstream pier face was much less than the value of the maximum stream velocity in the direction downstream, and this indicated that a scour hole was not formed.

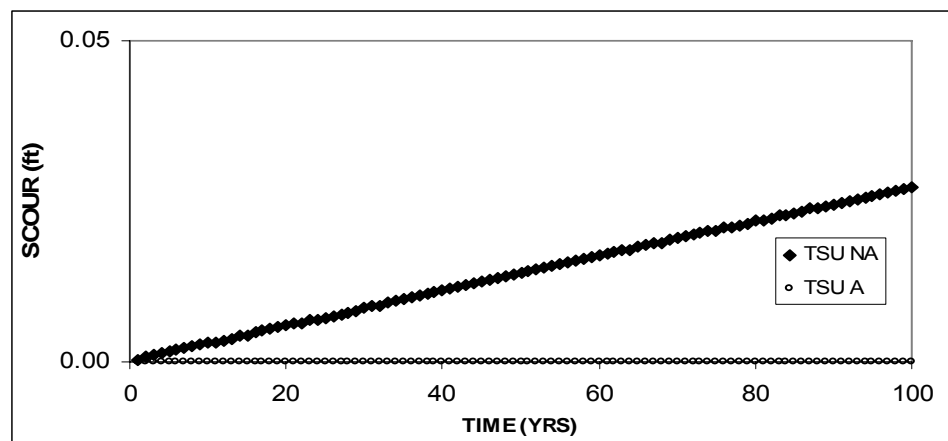


**Fig. 6.4-1. Temporal variation of pier scour for the upstream face obtained from the results of the Black River simulations. NA indicates that armoring was not considered, while A indicates that the armoring option was used. The WAVES scour results represent the mean scour depth obtained from 1000 simulations.**

It was also shown that the development of the scour hole was related to the maximum values of the effective scour rates reached during the simulation. The effective scour rate at the upstream face of the pier, when armoring was not considered ( $V_{ma} = 0.14$  ft/s), indicated that scour would be minimal. Similarly, the value of the effective scour

rate when natural armoring was considered ( $V_{ra} = 0$ ) predicted that scouring would not occur on the upstream face of the pier. Figure 6.4-1 shows that negligible scour was generated at the upstream face of the pier when natural armoring was not considered. When the natural armoring process was considered pier scour was not generated.

#### **6.4.2.2 Downstream Pier Face**

In contrast to the results obtained for the upstream pier face, it was expected that significant scour would be generated from the downstream face of the pier in a tide-controlled estuary like the Black River Site. Table 6.4-1 and Figure 6.4-2 show that scour did not occur under the natural armoring condition; however, when natural armoring did not exist, the scour generated by activities at the downstream pier face reached an ultimate value of 20 ft. Without natural armoring, a relatively slow rate of scour occurred along the downstream pier face for the first 10 years and at the end of this period the total scour had reached only 2.5 ft which is an average rate of scour of 0.25 ft/yr. The greatest scour rates occurred during the next 5 years, as the scour hole developed from 2.5 ft in depth to the ultimate scour depth of 20 ft, which is an average rate of 3.5 ft/yr. These results are in good agreement with the values indicated for the velocity of the channel in the upstream direction (2.22 ft/s) and the vortex tangential velocity on the downstream pier face (3.0 ft/s), as the maximum vortex tangential velocity was significantly greater than the maximum flow velocity upstream.

The process of natural armoring significantly affects estuary locations where the stream and vortex velocities are low. Figure 6.4-2 indicates that natural armoring had a significant impact on the pier scour process at the Black River site. In the case of the downstream pier face, natural armoring caused the incipient velocity to be raised to 2.46

ft/s and this caused the natural armoring effective scour rate to be 0. Hence no scouring occurred.

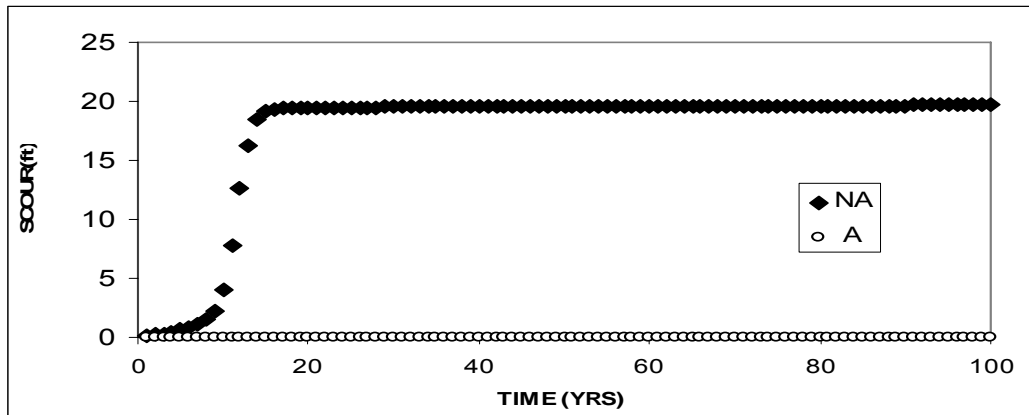


**Fig.6.4-2. Temporal variation of pier scour for the downstream face obtained from the results of the Black River simulations. NA indicating that armoring was not considered, while A indicates the armoring option was used. The WAVES scour results represent the mean scour depth obtained from 1000 simulations.**

### 6.4.3 Hurricane Event Simulation Results

The results of the hurricane scour simulations at Black River helps to provide an understanding of the process that affects pier scour during single-event storms in a tide-controlled environment. Details of the hurricane scour results for Black River are provided in Appendix D-6. Table 6.4-2 provides a summary of the scour variables produced at the upstream and downstream faces of the pier by a 7 in. hurricane event. In addition, Table 6.4-3 shows the scour predicted at both the upstream and downstream faces of the pier for hurricane rainfall depths of 5, 8, 12, and 16 inches.

The hurricane scour produced by the Black River simulation may be explained by the values of the stream flow parameters obtained during the simulation. Table 6.4-2 shows that 0.5 ft of scour was produced at the upstream pier face while 0.5 ft of scour was also generated at the downstream pier face. For the upstream pier face, the maximum downstream velocity of the simulation was 2.4 ft/s, while the maximum vortex

tangential velocity was 1.19 ft/s. Table 6.4-2 also shows that, although the maximum discharge was high, the flow depth that resulted from the surge was also high and caused the lowering of the maximum stream velocity to the value shown. Also, although the vortex tangential velocity was significant, it was still not greater than the downstream velocity thus indicating that the scour hole was not fully developed. The lack of development of the scour hole was also due to the fact that the velocities were not sustained long enough to ensure its progress.

**Table 6.4-2. Black River Hurricane Scour Results for 7 in. of Rainfall at the Upstream (U/S) and Downstream (D/S) Pier Faces**

<b>Hurricane Scour Variables</b>	<b>U/S Pier Face</b>	<b>D/S Pier Face</b>
Maximum discharge (cfs) $Q_{\max}$	893900	907615
Maximum stream velocity (ft/s) $V_{\max}$	2.40	5.36
Maximum Vortex Tangential Velocity (ft/s) $V_{t\max}$	1.19	1.94
Maximum flow depth (ft) $Y$	25.19	24.18
Incipient Scour Velocity (ft/s) $U_i$	0.20	0.20
Vortex tangential vel.- The incipient vel. w/o armoring (ft/s)	1.09	0.53
Effective scour rate w/o armoring (ft/s) $V_{ma}$	1.09	0.53
Existing scour at the start of the event (ft)	3.9	3.9
Final scour at the end of the event (ft)	4.4	4.4
Total pier scour (ft) $d_s$	0.5	0.5

**Table 6.4-3. Scour in ft Predicted for a Category III Hurricane with Variable Rainfall Amounts of 5, 8, 12, and 16 in. on the Downstream (D/S) and Upstream (U/S) Pier Faces of the Black River Case Study Sites**

Rainfall (in.)	5	8	12	16
D/S Scour (ft)	0.53	0.49	0.36	0.35
U/S Scour (ft)	0.29	0.55	0.59	0.63

The stream flow results for the downstream face also indicated that the scour generated at the downstream face of the pier would be low. In the case of the



downstream pier face, the maximum upstream velocity of the simulation was 5.36 ft/s while the maximum vortex tangential velocity was 1.94 ft/s. As was the case with the upstream pier face, the table also shows a relatively high maximum upstream discharge along with a high flow depth that caused the lowering of the maximum stream velocity. The effective scour rate without natural armoring was also significant; however, because the storm duration was relatively short, the velocities were not sustained long enough to cause significant scour. Table 6.4-3 also indicates that for hurricane rainfall greater than 7 in., pier scour at the Black River Site would remain insignificant.

## **6.5 THE PATUXENT RIVER AT BENEDICT SITE**

### **6.5.1 Specific Modeling Assumptions and Conditions**

The Patuxent River cross section at Benedict is described as a tidal river in Chapter 5, with adjusted Simmons and CE ratios of 0.47 and 73, respectively. These values indicate that the Patuxent River cross section was a partially mixed estuary with strong tidal and catchment influences. With a CE ratio value relatively close to 100, it was expected that the catchment influences may be slightly greater than the tidal influences. In addition, the selected bridge cross section was moderately narrow and shallow being 3325 ft wide and 15 ft deep. The input data that were used in the Patuxent River simulation are shown in Appendix D-2.

Assumptions were made regarding the time of concentration, tidal amplitude, over-bank slopes, and soils data used in the Patuxent River case study simulations. The time of concentration for the catchment based on the SCS Lag Equation was 40 hr. However, owing to the presence of the Patuxent Reservoir, the time of concentration was

assumed to be 55 hrs. As indicated in Chapter 5, a NOAA tidal gauge was located at the Patuxent River at the Benedict site, and this gauge was used to provide the bridge site tidal data. From this information the diurnal tidal amplitude was determined to be 0.60 ft. The catchment information provided by the USGS quadrangle maps indicated relatively high basin relief and catchment slope values. As a result, the overbank channel slope was assumed to be 1: 200. Because the Benedict site is located an appreciable distance upstream of the main Chesapeake Bay, only the soils information provided by the Maryland Geological Survey was used, which indicates a maximum channel soil particle size of 3.25 mm was estimated.

Using the Chesapeake Bay historical hurricane tracking data obtained from the NOAA records, it was estimated that the most critical hurricane scour impacts at Benedict would be caused by a Category III hurricane traveling eastwards across the Patuxent River just north of the bridge location. This would result in the surge being directed northwards up the Patuxent River just as the center of the hurricane approached the river. These considerations led to the modeling assumption of a Category III hurricane passing 1 mile north of the bridge.

The Patuxent Basin area to the Benedict site is over 700 mi<sup>2</sup> large and extends to the Western Piedmont with higher rolling terrain. A slow moving Category III hurricane could therefore cause significant amounts of precipitation. As a result, it was assumed 8 in. of rain, generally estimated for the case study sites, would fall in the Patuxent River watershed. However, hurricane simulations were also made for rainfall amounts of 5, 8, 12, and 16 inches to assess the impact of greater amounts of hurricane rainfall on pier scour at this location.

## 6.5.2 Continuous Simulation Results

The results obtained at the Patuxent River provide the basis for assessing the long-term scour mechanism in a mixed-controlled estuary. The continuous simulation results show that significant scour was generated at both pier faces during the simulations conducted without considering natural armoring. In contrast, scour was not generated at the downstream pier face when natural armoring was considered while scour at the upstream pier face took much longer to attain the ultimate depth. Details of the continuous simulation results for the Patuxent at Benedict site are provided in Appendix D-7, while Table 6.5-1 provides a summary of the scour results for the Patuxent River site. The values of the variables provide clear indications of the degree of scour that would be initiated at the pier faces.

**Table 6.5-1. Summary of Patuxent at Benedict Continuous Simulation Variables at the Upstream (U/S) and Downstream (D/S) Pier Faces**

<b>Scour Velocity Variables</b>	<b>U/S Pier Face</b>	<b>D/S Pier Face</b>
Maximum discharge (cfs) $Q_{\max}$	232629	147840
Maximum stream velocity w/ armoring (ft/s) $V_{\max a}$	5.38	2.71
Maximum stream velocity w/o armoring (ft/s) $V_{\max na}$	5.38	2.71
Maximum vortex tangential velocity w/ armoring (ft/s) $V_{ta}$	7.75	1.11
Maximum vortex tangential velocity w/o armoring (ft/s) $V_{tna}$	6.39	4.58
Maximum flow depth (ft) $Y$	19.05	20.03
Incipient scour velocity (ft/s) $U_i$	0.67	0.67
Maximum particle size (mm) $d_{\max}$	3.5	3.5
Incipient armoring scour velocity (ft/s) $U_{iarm}$	2.75	2.75
Vortex tangential vel.— the incipient vel. w/ armoring (ft/s)	5.0	-1.64
Vortex tangential vel.— the incipient vel. w/o armoring (ft/s)	5.72	3.91
Effective scour rate w/ armoring (ft/s) $V_{ra}$	5.0	0.0
Effective scour rate w/o armoring (ft/s) $V_{rna}$	5.72	3.91
Maximum 100-year pier scour w/ armoring (ft) $d_{sa}$	15.00	0.00
Maximum 100-year pier scour w/o armoring (ft) $d_{sna}$	21.70	19.00

### 6.5.2.1 Upstream Pier Face

As stated earlier, the values of the maximum downstream velocity and the maximum tangential velocity influence the amount of scour that will occur along the upstream face of a pier. Table 6.5-1 indicates that for the upstream pier face, the maximum downstream velocity was 5.38 ft/s. The maximum vortex tangential velocity was 6.39 ft/s when natural armoring was not considered and 7.75 ft/s for simulations utilizing the natural armoring option. The high values of the effective scour rates with and without natural armoring ( $V_{ra}=5.0$ ,  $V_{rna}=5.72$  ft) provide clear indications that the scour holes generated at the upstream pier face would be completely developed for both cases with and without armoring. This could be explained by the fact that the flow velocity in the upstream direction was sufficiently high (5.27 ft/s) to induce vortex tangential velocities capable of causing the scouring of the bed material.

The velocity values discussed above support the pier scour results shown in Table 6.5-1. For the simulation conducted without considering natural armoring, Table 6.5-1 and Fig. 6.5-1 indicate a relatively rapid development of the scour hole to an ultimate depth of 21 ft within 25 years. After this period some scouring occurs but at a greatly reduced rate.

Figure 6.5-1 and Table 6.5-1 also show that natural armoring has the effect of reducing the rate of scour at the upstream face. With natural armoring, scour increases steadily to a value of 15 ft after 100 years, thus not attaining ultimate scour. Projection of the curve that represents upstream pier face scour with natural armoring suggests that an ultimate scour value of approximately 18 ft would be reached in 120 years.

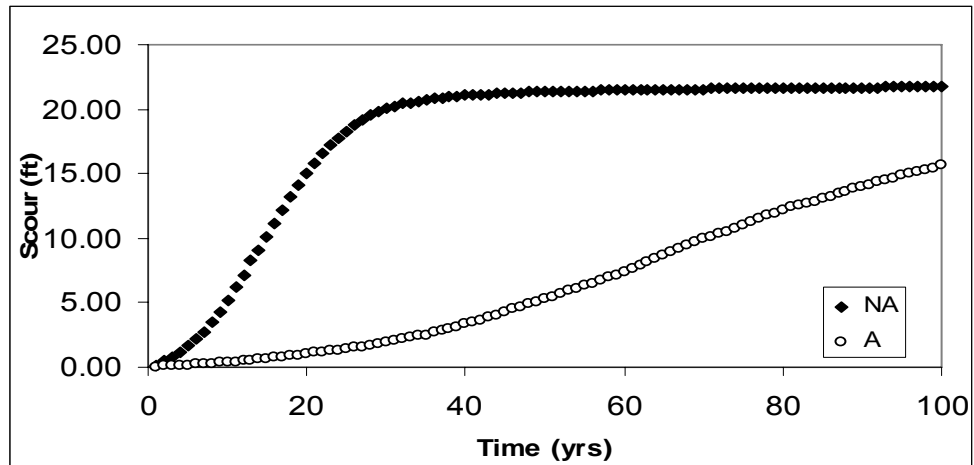


**Fig. 6.5-1. Temporal variation of pier scour for the upstream face obtained from the results of the Patuxent at Benedict Simulations. NA indicates that armoring was not considered, while A indicates the armoring option was used. The WAVES scour results represent the mean scour depth obtained from 1000 simulations.**

#### 6.5.2.2 Downstream Pier Face

Significant scour may be generated at either of the pier faces in estuaries classified as mixed-controlled. In the case of scour on the downstream pier face, Figure 6.4-2 shows that significant scour was not produced under the natural armoring condition; however, when natural armoring was neglected, the scour generated by activities at the downstream pier face reached an ultimate value of approximately 19 ft over the 100-year period. Without natural armoring, a relatively slow rate of scour along the downstream pier face occurred for the first 65 years. At the end of this period, the total scour had reached only approximately 2 feet, which is an average rate of scour of 0.03 ft/yr. The next 35 years produced the greatest scour rates, as the scour hole developed from 2 feet in depth to the ultimate scour depth of approximately 19 ft, which is an average rate of 0.54 ft/yr. The ultimate scour depth of 19 ft was reached just at the end of the 100-year simulation period.

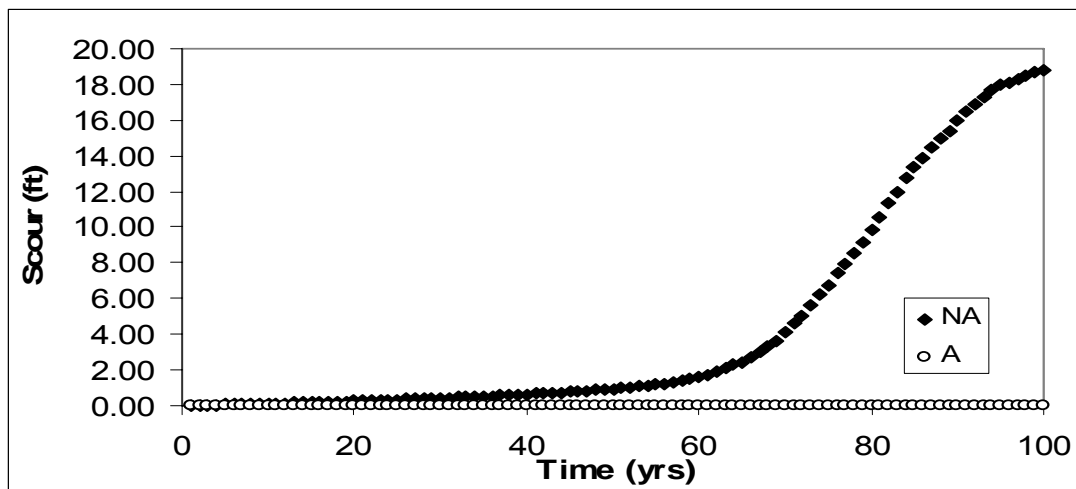


**Fig. 6.5-2. Temporal variation of pier scour for the downstream face obtained from the results of the Patuxent at Benedict simulations. NA indicates that natural armoring was not considered, while A indicates the armoring option was used. The WAVES scour results represent the mean scour depth obtained from 1000 simulations.**

The relationship between the maximum channel velocity and the maximum vortex tangential velocity, along with the effective scour rate without armoring, provide clear indications of the robust scouring that would occur at the downstream pier face of the Patuxent River site when natural armoring did not occur. The maximum channel velocity in the upstream direction, as shown in Table 6.4-1, was 2.71 ft/s, while the maximum vortex tangential velocities for the armored and unarmored conditions were 1.11 ft/s and 4.58 ft/s, respectively. These values indicate a fully developed scour hole in the unarmored case where the maximum vortex tangential velocity is greater than the maximum stream velocity. The values also indicate an undeveloped scour hole in the armored case. It can be seen that for the case without natural armoring, the effective scour rate ( $V_{ma}$ ) was significantly high (3.91 ft/s), thus predicting robust scouring. Conversely, when natural armoring of the downstream pier face was considered, the

effective scour rate ( $V_{ra}$ ) was 0, suggesting significant scour would not occur. Figure 6.5-2 also indicates that natural armoring had a significant impact on the pier scour process at the downstream face of the pier by raising the armoring incipient scour velocity sufficiently to make the effective scour rate ( $V_{ra}$ ) equal to 0.

### 6.5.3 Hurricane Event Simulation Results

The hurricane scour simulation results obtained at the Patuxent River site provides an opportunity to assess the pier scour that could be caused by a single-event storm at a mixed-controlled site. In particular, the Patuxent River site may be classified as mixed-controlled, with minor catchment dominance. Details of the hurricane scour results for the Patuxent at Benedict site are provided in Appendix D-8. Table 6.5-2 provides a summary of the scour variables produced at the upstream and downstream faces of the pier by the hurricane event assuming 8 inches of rain.

**Table 6.5-2. Patuxent at Benedict Hurricane Scour Results for Eight Inches of Rainfall**

<b>Hurricane Scour Variables</b>	<b>U/S Pier Face</b>	<b>D/S Pier Face</b>
Maximum discharge (cfs) $Q_{max}$	890967	837565
Maximum stream velocity (ft/s) $V_{max}$	12.16	5.09
Maximum Vortex Tangential Velocity (ft/s) $V_{tmax}$	5.08	2.38
Maximum flow depth (ft) $Y$	28.77	28.28
Incipient Scour Velocity (ft/s) $U_i$	1.1	1.1
The vortex tangential vel.- The incipient vel. w/o armoring (ft/s)	3.98	1.28
Effective scour rate w/o armoring (ft/s) $V_{ma}$	4.77	1.28
Existing scour at the start of the event (ft)	3.9	3.9
Final scour at the end of the event (ft)	5.03	4.75
Total pier scour (ft) $d_s$	1.1	0.85

Table 6.5-3 shows the results of the hurricane simulations made with 5, 8, 12, and 16 inches of rain. Table 6.5-2 shows that 0.85 ft of scour was produced on the

downstream pier face while 1.1 ft of scour was generated at the upstream pier face in 36 hours. Table 6.5-3 also shows that 3.7 and 4.8 ft of scour would be generated at the upstream face when the associated hurricane rainfall was 12 and 16 inches, respectively.

The values of maximum downstream velocity and vortex tangential velocity also provide a good indication of scour along the upstream pier face at a mixed-controlled site during single-event storms. Table 6.5-2 indicates that for the upstream pier face, the maximum downstream velocity of the simulation was 12.16 ft/s, while the maximum vortex tangential velocity was 5.08 ft/s. Similarly, because the incipient scour velocity was 1.1 ft/s,  $V_{ma}$  (3.98 ft/s) was significantly high. These values indicated the significant development of the scour hole in the 36-hour duration of the storm.

**Table 6.5-3. Scour in ft Predicted for a Category III Hurricane with Variable Rainfall Amounts of 5, 8, 12, and 16 in. on the Downstream (D/S) and Upstream (U/S) Pier Faces of the Patuxent River Case Study Sites.**

Rainfall (in.)	5	8	12	16
D/S Pier Face Scour (ft)	0.82	0.85	0.83	0.82
U/S Pier Face Scour (ft)	0.85	1.10	3.70	4.80

Significant scour is typically indicated when the vortex tangential velocity is greater than the maximum stream velocity. In the case of the downstream pier face, Table 6.5-2 shows the maximum upstream velocity of the simulation was 5.09 ft/s while the maximum vortex tangential velocity was 2.38 ft/s. A relatively high maximum upstream discharge occurred along with the high flow depths. These values indicate that the scour could have been greater along the downstream pier face; however, the limited duration of the storm was unable to sustain the scouring activity long enough for significant development of the scour hole.



## **6.6 THE WICOMICO RIVER SITE**

### **6.6.1 Specific Modeling Assumptions and Conditions**

The Wicomico site represented a mixed-controlled estuary, slightly dominated by its tidal processes. The Wicomico River cross section is described as a tidal river in Chapter 5 with adjusted Simmons (SK) and CE ratios of 0.12 and 43, respectively. These values indicate that the Wicomico River site was also a partially mixed estuary with strong tidal and catchment influences. However, the CE ratio indicated that the tidal processes could be slightly dominant. In addition, the selected bridge cross section was narrow and moderately deep being 1760 ft wide and 17 ft deep. The input data that were used in the Wicomico River simulation are shown in Appendix D-2.

Assumptions regarding some of the more sensitive input data, such as the wave and tide properties, over-bank slopes, and soils data, were made. As indicated in Chapter 5, a NOAA tidal gauge was located at the Whitehaven site, and this gauge was used to provide tidal information at the bridge site. From this data, the diurnal tidal amplitude was estimated as 1.19 ft. The catchment information provided by the USGS quadrangle maps indicated a relatively high basin relief and catchment slope values. As a result, the overbank channel slope was assumed to be 1: 200. Because the Wicomico site is located an appreciable distance upstream of the main Chesapeake Bay, only the soils information provided by the Maryland Geological Survey was used and a mean and maximum channel soil particle size of 0.325 mm and 4.25 mm, respectively, were estimated.

#### **6.6.1.1 Hurricane Simulations**

The location of the Wicomico site is one of the factors that determine the strength and track of potential hurricanes affecting it. The Wicomico River site is located close to

Monie Bay and just to the north east of it. Therefore, the hurricane likely to cause the most significant effects should have a track and strength similar to the hurricane discussed with Monie Bay. As was the case with Monie Bay, the most critical hurricane scour impacts at the Wicomico site should be due to a hurricane traveling northwards up the Chesapeake Bay with the hurricane center (or eye) being over the Chesapeake Bay just to the west of the Wicomico site. This would result in the surge being directed eastwards up the Wicomico River. This assumed track could facilitate a hurricane of Category III strength and distance of closest approach of 1 to 5 miles. These considerations led to the modeling assumption of a Category III hurricane passing 1 mile west of the bridge.

Since the Wicomico site is located to the east of the potential hurricane track, then it is expected that the site would receive less rainfall than locations to the west of the eye. Therefore, it was assumed that less than the eight inches of rain generally assumed for the case study sites would fall in the catchment to the Wicomico site. As a result, the total hurricane rainfall assumed at the Wicomico site was five inches. However, in order to determine the impacts of storms of greater magnitude, simulations were also made for hurricane rainfall events of 8, 12, and 16 inches of rain.

### **6.6.2 Continuous Simulation Results**

The results of the Wicomico continuous simulations may be used to assess the processes that cause long term-scour at a mixed-controlled estuary slightly dominated by tidal influences. Details of the continuous simulation results for the Wicomico River site are provided in Appendix D-9. Table 6.6-1 shows summaries of the scour 100-year

results generated at the upstream and downstream pier faces. Table 6.6-1 also provides a summary of the variables obtained from the detailed results of Appendix D-9, along with estimates of the armoring incipient scour velocity computed using Equation 6.3-1.

Values of these variables are good indicators of the amount of scour that would be generated at either of the pier faces. The continuous simulation results showed that significant scour could be generated at both pier faces during the simulations conducted without considering natural armoring. When natural armoring was considered, scour was minimized along the upstream pier. However, natural armoring appeared to have little effect on the development of scour along the downstream face of the pier.

**Table 6.6-1. Summary of the Wicomico River Continuous Simulation Variables at the Upstream (U/S) and Downstream (D/S) Pier Faces**

<b>Scour Velocity Variables</b>	<b>U/S Pier Face</b>	<b>D/S Pier Face</b>
Maximum discharge (cfs) $Q_{\max}$	100150	96922
Maximum stream velocity w/ armoring (ft/s) $V_{\max a}$	3.87	3.23
Maximum stream velocity w/o armoring (ft/s) $V_{\max na}$	3.87	3.23
Maximum vortex tangential velocity w/ armoring (ft/s) $V_{ta}$	3.56	5.75
Maximum vortex tangential velocity w/o armoring (ft/s) $V_{tna}$	4.24	5.86
Maximum flow depth (ft) $Y$	21.5	21.5
Incipient scour velocity (ft/s) $U_i$	0.75	0.75
Maximum particle size (mm) $d_{\max}$	3.5	3.5
Incipient armoring scour velocity (ft/s) $U_{iarm}$	2.75	2.75
The vortex tangential vel.— the incipient vel. w/ armoring (ft/s)	0.81	2.00
Vortex tangential vel.— the incipient vel. w/o armoring (ft/s)	3.12	5.11
Effective scour rate w/ armoring (ft/s) $V_{ra}$	0.81	2.00
Effective scour rate w/o armoring (ft/s) $V_{rna}$	3.12	5.11
Maximum 100-year pier scour w/ armoring (ft) $d_{sa}$	5.00	19.00
Maximum 100-year pier scour w/o armoring (ft) $d_{sna}$	11.00	19.00

#### **6.6.2.1 Upstream Pier Face**

Because the Wicomico site represented a mixed-controlled estuary with a slight tidal dominance, the scour generated at the upstream face of the pier was significant but

less than the scour generated at the downstream pier face. Some of the output variables obtained from the Wicomico simulation supports this result. Table 6.6-1 indicates that for the upstream pier face, the maximum downstream velocity of the simulation was 3.87 ft/s. The maximum vortex tangential velocity was 4.24 ft/s when natural armoring was not considered and 3.56 ft/s for simulations utilizing the natural armoring option. The effective scour rate without natural armoring ( $V_{ma}$ ) was 3.16 f/s and this shows that the scour hole at the upstream pier face would be completely developed. When natural armoring was considered, the effective scour rate ( $V_{ra}$ ) was reduced to 0.81 ft/s, thus indicating a less developed scour hole.

As was the case with the Patuxent River, a mixed-controlled site, the maximum tangential velocity, stream velocity, and effective scour rates may also be used as indicators of the manner in which scour will progress at the Wicomico River site. The velocity values discussed above support the results shown in Figure 6.6-1. For the simulation conducted without considering natural armoring, Figure 6.6-1 indicates a slow development of the scour hole to an ultimate depth of 10 ft over the 100-year simulation period. Figure 6.6-1 also shows that natural armoring had the effect of reducing the potential for scour at the upstream pier face as less scour was generated from that pier face when natural armoring was considered. With natural armoring, the figure shows that scour increases slowly to a value of 5 ft after 100 years, without attaining the ultimate scour depth.

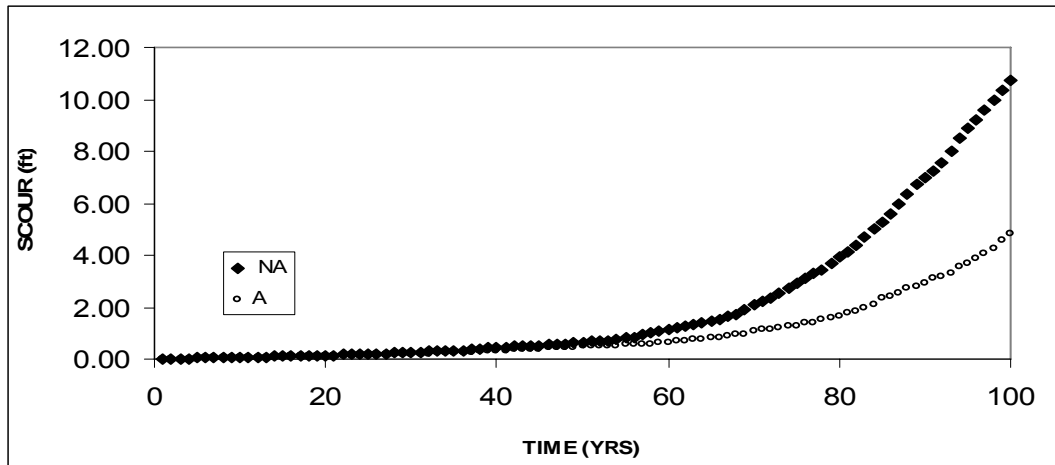


**Fig. 6.6-1. Temporal variation of pier scour for the upstream face obtained from the results of the Wicomico River Simulations. NA indicates that armoring was not considered, while A indicates the armoring option was used. The WAVES scour results represent the mean scour depth obtained from 1000 simulations.**

#### 6.6.2.2 Downstream Pier Face

Because of the slight tidal dominance, the scour generated along the downstream face of the pier at the Wicomico River site was expected to be greater than the scour generated from the upstream pier face. Figure 6.6-2 shows that the ultimate scour depth of 19 ft was achieved for both cases when natural armoring was and was not considered. When natural armoring did not occur, the figure shows a sharp increase in scour over the first six years to an ultimate scour depth of 19 ft. This resulted in a rate of scour of approximately 3 ft/yr. With natural armoring, the overall scour rate was not changed; however, scour was insignificant over the first year and then reached the ultimate value over the next five years.

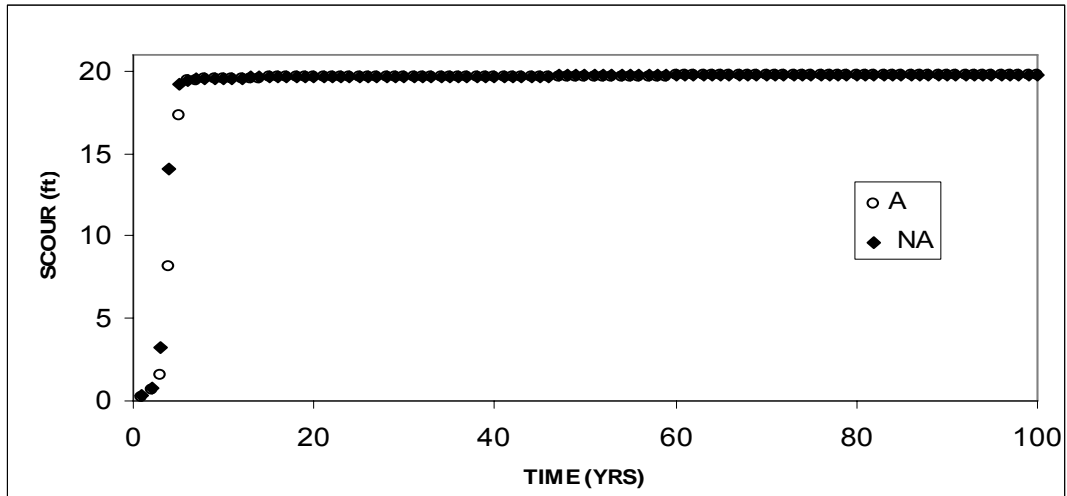


**Fig. 6.6-2. Temporal variation of pier scour for the downstream face obtained from the results of the Wicomico River Simulations. NA indicates that armoring was not considered, while A indicates the armoring option was used. The WAVES scour results represent the mean scour depth obtained from 1000 simulations.**

The results described are in agreement with the values indicated for the velocities that affect the downstream pier face. The maximum channel velocity in the upstream direction, as shown in Table 6.6-1, was 3.23 ft/s, while the maximum vortex tangential velocities for the armored and unarmored conditions were 5.75 ft/s and 5.86 ft/s, respectively. These values indicate fully developed scour holes in both the unarmored and armored cases where the maximum vortex tangential velocities were greater than the maximum stream velocity. The results also show that that for both the armored and unarmored cases the effective scour rate was 5.11 ft/s for  $V_{rna}$  and 2.00 ft/s for  $V_{ra}$ , thus, suggesting that in both cases the scour holes were fully developed.

### 6.6.3 Hurricane Event Simulation Results

The results of the hurricane scour simulation at the Wicomico site represents the scour caused by a single-event storm at a mixed-controlled site with a slight tidal dominance. Details of the scour results from a hurricane rainfall of 5 inches at the

Wicomico River are provided in Appendix D-10. Table 6.6-2 provides a summary of the scour variables produced at the upstream and downstream faces of the pier by the hurricane event simulation. The table shows that the hurricane generated 0.66 ft of scour along the downstream pier face and 0.87 ft of scour at the upstream pier face in the 36 hr event. These scour values were negligible and were primarily due to the fact that the hurricane duration was not long enough to sustain the development of the scour hole.

At the upstream pier face, moderate to low scour occurred. Table 6.6-2 also shows that the maximum downstream velocity was 8.10 ft/s, while the maximum vortex tangential velocity was 2.30 ft/s. Similarly, the low incipient scour velocity of 0.31 ft/s caused an effective scour rate ( $V_{ma}$ ) of 1.99 ft/s. These values indicate that though scouring was possible, little additional scour occurred. The table also shows that an extremely high value of the maximum discharge coupled with very high surge values resulted in moderate velocities and consequently, relatively low scour values.

**Table 6.6-2. The Wicomico River Hurricane Scour Results for 5 Inches of Rainfall. U/S Indicates Upstream and D/S Downstream**

<b>Hurricane Scour Variables</b>	<b>U/S Pier Face</b>	<b>D/S Pier Face</b>
Maximum discharge (cfs) $Q_{max}$	377347	371722
Maximum stream velocity (ft/s) $V_{max}$	8.10	2.5
Maximum Vortex Tangential Velocity (ft/s) $V_{tmax}$	2.3	1.1
Maximum flow depth (ft) $Y$	32.4	32.5
Incipient Scour Velocity (ft/s) $U_i$	0.31	0.31
The vortex tangential vel.- The incipient vel. w/o armoring (ft/s)	1.99	0.79
Effective scour rate w/o armoring (ft/s) $V_{ma}$	1.99	0.79
Existing scour at the start of the event (ft)	3.9	3.9
Final scour at the end of the event (ft)	4.77	4.56
Total pier scour (ft) $d_s$	0.87	0.66

The simulation output velocity variables at the downstream pier face indicated even less scour than that produced at the upstream face of the pier. In the case of the downstream pier face, Table 6.6-2 shows the maximum downstream velocity of the simulation was 2.5 ft/s while the maximum vortex tangential velocity was 1.1 ft/s. As was the case with the upstream pier face, the table also shows a relatively high maximum upstream discharge along with a high flow depth that caused the lowering of the maximum stream velocity. The effective scour rate at the downstream pier face ( $V_{rna}$ ) was 0.79 ft/s, which resulted in minimal scouring. The results of the hurricane simulations for 5, 8, 12, and 16 inches of rain in Table 6.6-3 show an appreciable increase in scour at the upstream face of the pier with increasing rainfall. However, the rainfall amounts appeared to have little impact on downstream pier face scour.

**Table 6.6-3. Scour in Feet Predicted for a Category III Hurricane with Variable Rainfall Amounts of 5, 8, 12, and 16 in. on the Downstream (D/S) and Upstream (U/S) Pier Face at the Wicomico Case Study Site**

Rainfall (in.)	5	8	12	16
D/S Pier Face Scour (ft)	0.66	0.56	0.54	0.53
U/S Pier Face Scour (ft)	0.87	1.18	1.65	1.97

## **6.7 BALTIMORE ON THE PATAPSCO RIVER SITE**

### **6.7.1 Specific Modeling Assumptions And Conditions**

The physical features of a catchment-controlled estuary, such as the Patapsco River site, influence the long-term scouring process. The Patapsco River cross section at the Baltimore Inner Harbor is a catchment-dominated estuary with adjusted Simmons and CE ratios of 1.16 and 168, respectively. These values indicate that the Patapsco River



cross section was a stratified estuary dominated by catchment fluvial influences. In addition, the selected bridge cross section was narrow and deep, 0.33 mi wide and 33 ft deep. The input data that were used in the Patapsco River simulation are shown in Appendix D-2.

The tidal properties, overbank slopes, and soils data represent some of the assumed input variables of the Patapsco River simulation. As indicated in Chapter 5, a NOAA tidal gauge was located at the Fort McHenry, and this gauge was used to provide the bridge site tidal information. From this information the diurnal tidal amplitude was estimated to be 0.935 ft. The catchment information, provided by the USGS quadrangle maps, indicated relatively high basin relief and catchment slope values. As a result, the estuary overbank channel slope was assumed to be 1: 200. Because the Patapsco River site was located an appreciable distance upstream of Parson Island, only the soils information provided by the Maryland Geological Survey was used, with a maximum channel soil particle size of 0.40 mm.

#### **6.7.1.1 Hurricane Simulations**

The amount of pier scour produced by a hurricane is dependent on its strength and track. Using the Chesapeake Bay historical hurricane tracking data obtained from the NOAA records, it was estimated that the most critical hurricane scour impacts at the Patapsco River site would be caused by a Category III hurricane traveling north up the Chesapeake bay just west of the bridge location. This would result in the surge being directed northwards up the Patapsco River. These considerations led to the modeling assumption of a Category III hurricane passing 1 mile west of the bridge.

The Patapsco River catchment area to the bridge site is large and extends to the Piedmont with higher rolling terrain. A slow moving Category III hurricane could, therefore, cause significant amounts of precipitation. As a result, it was assumed the 8 inches of rain, generally estimated for the case study sites, would fall in the Patapsco River watershed. In addition, rainfall amounts of 5, 12, and 16 inches were simulated with the hurricane event to determine the impact of varying the rainfall amounts on pier scour at this site.

### **6.7.2 Continuous Simulation Results**

The results of the continuous WAVES simulations at the Patapsco River site help to provide an understanding of the cause of long-term pier scour in a catchment-controlled estuary. Details of the continuous simulation results for the Patapsco River site are provided in Appendix D-11. Table 6.7-1 shows summaries of the 100-year scour results generated at the upstream and downstream pier faces. Table 6.7-1 also provides a summary of the variables obtained from the detailed results of Appendix D-11; along with estimates of the incipient scour velocity with armoring computed using Equation 6.3-1. The continuous simulation results show that significant scour was generated at the upstream pier face for both cases where natural armoring was and was not considered. In contrast, scour did not occur at the downstream pier face for either case.

#### **6.7.2.1 Upstream Pier Face**

Significant scour at the upstream face of the pier is an important characteristic of catchment-controlled estuaries. The computed velocities, as shown in Fig. 6.7-1, can also

explain the amount of scour at the upstream face of the pier at the Patapsco River site.

Table 6.7-1 indicates that the maximum downstream velocity was 4.25 ft/s. The maximum vortex tangential velocity was 6.04 ft/s when natural armoring was not considered and 4.28 ft/s for simulations utilizing the natural armoring option. The effective scour rates with and without natural armoring ( $V_{ra}$ ,  $V_{rna}$ ), were 5.15 ft/s and 5.48 ft/s, respectively, and indicated that the scour holes generated at the upstream pier face would be completely developed for both cases with and without armoring.

**Table 6.7-1. Summary of the Patapsco River Site Simulation Variables at the Upstream (U/S) and Downstream (D/S) Pier Faces**

<b>Scour Velocity Variables</b>	<b>U/S Pier Face</b>	<b>D/S Pier Face</b>
Maximum discharge (cfs) $Q_{max}$	247351	100489
Maximum stream velocity w/ armoring (ft/s) $V_{maxa}$	4.25	1.45
Maximum stream velocity w/o armoring (ft/s) $V_{maxna}$	4.25	1.45
Maximum vortex tangential velocity w/ (ft/s) $V_{ta}$	6.04	0.52
Maximum vortex tangential velocity w/o armoring (ft/s) $V_{tna}$	5.88	0.52
Maximum flow depth (ft) $Y$	42.5	42.5
Incipient scour velocity (ft/s) $U_i$	0.40	0.40
Maximum particle size (mm) $d_{max}$	2.75	2.75
Incipient armoring scour velocity (ft/s) $U_{iarm}$	2.89	2.89
Vortex tangential vel.— the incipient vel. w/ armoring (ft/s)	5.15	-2.32
Vortex tangential vel.— the incipient vel. w/o armoring (ft/s)	5.48	0.12
Effective scour rate w/ armoring (ft/s) $V_{ra}$	5.15	0.0
Effective scour rate w/o armoring (ft/s) $V_{rna}$	5.48	0.12
Maximum 100-year pier scour w/ armoring (ft) $d_{sa}$	21.0	0.00
Maximum 100-year pier scour w/o armoring (ft) $d_{sna}$	22.4	0.00

The results are shown in Figure 6.7-1. For the simulation conducted without considering natural armoring, Figure 6.7-1 indicates a relatively rapid development of the scour hole to an ultimate depth of 22 ft within 10 years. After this period some scouring occurred but at a greatly reduced rate. Figure 6.7-1 also shows that natural armoring has the effect of reducing the rate of scour at the upstream face. With natural armoring, scour

increased steadily to a value of 21 ft after 100 years without attaining the ultimate scour value. Projection of the curve representing upstream pier face scour with natural armoring suggests that an ultimate scour value of approximately 21 ft would be reached within 130 years.

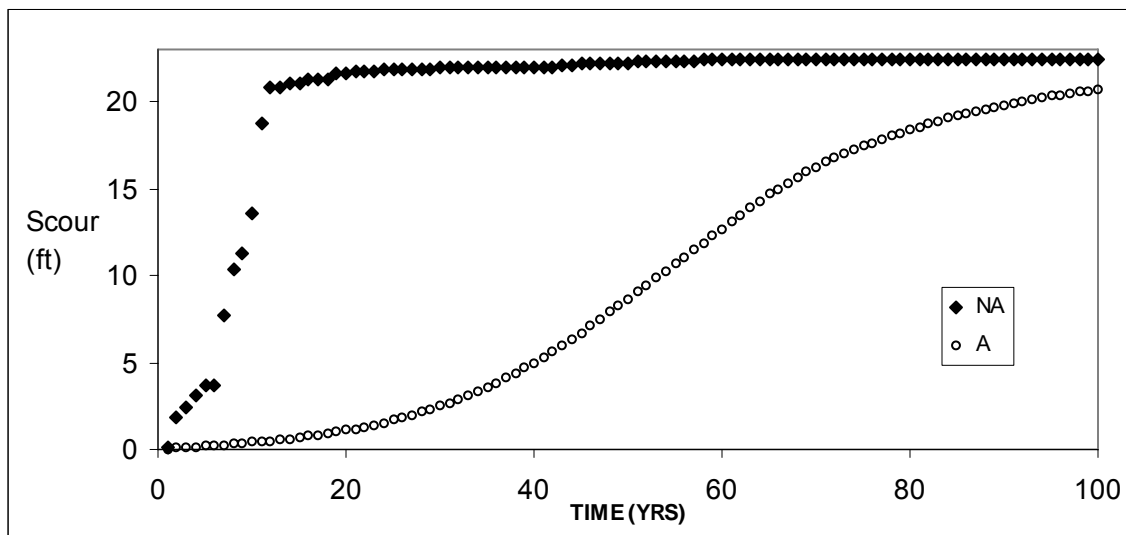


**Fig. 6.7-1. Temporal variation of pier scour for the upstream face obtained from the results of the Patapsco River Simulations. NA indicates that natural armoring was not considered, while A indicates the armoring option was used. The WAVES scour results represent the mean scour depth obtained from 1000 simulations.**

#### 6.7.2.2 Downstream Pier Face

Long-term scour generated from the downstream face of the pier was expected to be less than the scour at the upstream face of the pier at a catchment-controlled estuary such as the Patapsco River site. In the case of scour on the downstream pier face, Figure 6.7-2 shows that significant scour was not produced either with or without natural armoring. The results described are in agreement with the velocities that affect the downstream pier face. The maximum channel velocity in the upstream direction, as shown in Table 6.7-1, was 1.45 ft/s, while the maximum vortex tangential velocity both for the armored and unarmored conditions was 0.52 ft/s. These values indicate that the

scour holes did not develop in either simulation with or without natural armoring; as for both cases, the effective scour rates ( $V_{ra}$  and  $V_{ma}$ ) were 0.

### 6.7.3 Hurricane Event Simulation Results

The single-event hurricane scour simulation results provide an indication of the amount of short-term scouring that may be generated by storms in a catchment-controlled estuary. Details of the hurricane scour results for the Patapsco River are provided in Appendix D-12. Table 6.7-2 provides a summary of the scour variables produced at the upstream and downstream faces of the pier by the hurricane event simulation. The table shows that scour was not generated at the downstream pier face during the hurricane. However, significant short-term pier scour (3.45 ft) was generated at the upstream face of the pier.

**Table 6.7-2. The Patapsco River Site Hurricane Scour Results for the Upstream (U/S) and Downstream (D/S) Pier Faces with Eight Inches of Rainfall**

<b>Hurricane Scour Variables</b>	<b>U/S Pier Face</b>	<b>D/S Pier Face</b>
Maximum discharge (cfs) $Q_{max}$	337673	259690
Maximum stream velocity (ft/s) $V_{max}$	3.27	3.27
Maximum Vortex Tangential Velocity (ft/s) $V_{tmax}$	3.6	1.3
Maximum flow depth (ft) $Y$	47.32	47.18
Incipient Scour Velocity (ft/s) $U_i$	0.18	0.18
The vortex tangential vel.- The incipient vel. w/o armoring (ft/s)	3.42	1.12
Effective scour rate w/o armoring (ft/s) $V_{ma}$	3.42	1.12
Existing scour at the start of the event (ft)	3.9	3.9
Final scour at the end of the event (ft)	7.35	4.07
Total pier scour (ft) $d_s$	3.45	0.18

The velocity variables produced by the simulation may explain the scour at the upstream pier face in the single-event storm. Table 6.7-2 shows that for the upstream pier face, the maximum downstream velocity of the simulation was 3.27 ft/s while the

effective scour rate ( $V_{rna}$ ) was 3.42 ft/s. These values indicate that, though scouring was significant, the scour hole was not fully developed. This is due to the fact that the relatively short duration of the hurricane curtailed the further development of the scour hole.

The output velocity obtained from the hurricane scour simulation at the downstream face of the pier indicated that minimal scouring should be produced. Table 6.7-2 shows that the maximum upstream velocity was also 3.27 ft/s, while the maximum vortex tangential velocity was 1.3 ft/s. As was the case with the upstream pier face, the table also shows a relatively high maximum upstream discharge along with a high flow depth that caused the lowering of the maximum stream velocity. The effective scour rate was 1.12 ft/s indicating full development of the scour hole did not occur. Table 6.7-3 also shows that increasing the hurricane rainfall to 16 inches did not have an impact on the scour produced, as the scour remained insignificant at 0.15 ft.

**Table 6.7-3. Scour in ft Predicted for a Category III Hurricane with Variable Rainfall Amounts of 5, 8, 12, and 16 in. on the Upstream (U/S) and Downstream (D/S) Pier Faces at the Patapsco River Case Study Sites**

Rainfall (in.)	5	8	12	16
D/S Pier Face Scour (ft)	0.21	0.18	0.16	0.15
U/S Pier Face Scour (ft)	1.56	3.45	4.10	4.45

## 6.8 ANALYSIS OF RESULTS

### 6.8.1 Continuous Simulation Results

A common feature of the results obtained from all of the case study simulations was that the ultimate scour depths all approached an approximate value of 20 ft. This

observation can be explained by the fact that all of the case study sites were simulated with identical values for the diameter of the proposed pier (5 ft). Also, the mean bed sediment sizes were similar from site to site as that is typical for soils in the Chesapeake Bay. The pier diameter impacts the magnitude of the downflow, the horseshoe vortex, and the output of the local scour component. Similarly, the sediment sizes determine the incipient velocities of the bed sediments and ultimately impacts the output produced by the local scour component. Accordingly, since the simulations were conducted with similar pier diameters and mean sediment sizes at all sites, then the ultimate scour result from these sites should be similar.

The simulation results discussed in the prior sections of this chapter addressed the possibility of pier scour at both the upstream and downstream pier faces. Because in reality pier scour does not progress independently on either pier face, it was necessary to decide on the more likely location (upstream or the downstream pier face) from which the pier scour would be generated. For the purposes of this study, the pier face location from which scour was generated at any given time in the simulation was assumed to be the greater of the scour generated at the upstream and downstream pier faces in any given year. Accordingly, the final predicted scour results for each case study site was developed and presented below.

Modarres (1993) defines the risk of failure as:

$$R = \sum_{i=1}^n P_r C_i \quad (6.8-1)$$

in which  $R$  is the risk of failure,  $P_r$  is probability of the failure of the bridge due to the failure of the bridge pier,  $C_i$  represents the different consequences or losses due to the failure of the bridge, and  $n$  is the total number of such consequences. The consequences

of failure may be economic and defined in terms of dollars, as well as being social and defined in terms of the loss of human lives. Table 6.8-1 shows an illustrative example of the consequence analysis related to the failure of the bridge at each case study site. The information presented in the table was used to illustrate the analysis of the risk of failure at each of these sites. Engineers could also use the risks associated with failure as a part of an analysis of the structure to help policy makers determine the location of a crossing or the feasibility of the project.

In order to facilitate the determination of the temporal variation of the risks associated with the failure of the case study bridges from pier scour, the WAVES program was designed to generate as an output the probability of scour reaching a given depth at 15%, 25%, 50%, 75%, and 100% of the total simulation period. The determination of the probability of failure requires a detailed study that investigates all of the scenarios that could lead to the failure of the structure from pier failure. From such a study, the probability of failure at varying depths of scour could be determined. In reality, the probability of failure from pier scour depends on, among other things, the footing design at the actual site, and the forces that the pier would be subjected to in a given event. As a result, the development of failure scenarios is different for every structure and is beyond the scope of this study. For illustrative purposes a scour depth of 12 ft was assumed to have a 100% probability of failure. The probability of failure could then be calculated as the probability of the simulation results being greater than 12 ft.



**Table 6.8-1. Hypothetical Consequence Analysis for the Failure of the Bridge at Each Site**

	Monie Bay	Black River	Patuxent River	Wicomico River	Patapsco River
Road Class	Collector	Interstate	Major Arterial	Minor Arterial	Minor Arterial
Vehicles Per Hour (VPH)	100	1000	500	250	250
Bridge Length (mi)	1.1	1.63	0.63	0.25	0.33
Cost of Bridge Structure (millions of dollars)	20	1000	200	30	35
Bridge Failure Duration (min)	1	2	1.5	1	1
Occupants Per Vehicle (OPV)	2	3	2	2	2
Number of Vehicles Lost	2	33	13	4	4
<b>Number of Lives Lost</b>	<b>3</b>	<b>100</b>	<b>25</b>	<b>8</b>	<b>8</b>
Cost of Per Vehicle Lost (millions of dollars)	0.02	0.04	0.03	0.02	0.02
Total Cost of Vehicles Lost (millions of dollars)	0.03	1.33	0.38	0.08	0.08
Other Property Losses (millions of dollars)	0.50	30.00	1.00	0.50	5.00
<b>Total Economic Loss (millions of dollars)</b>	<b>20.53</b>	<b>1031.33</b>	<b>201.38</b>	<b>30.58</b>	<b>40.08</b>

Determination of the risks associated with the failure of a bridge requires a detailed consequence analysis that was not an objective of this research. For illustrative purposes, assumptions were made concerning the economic consequences and the losses in human life that could occur as a result of the failure of each of the case study bridges. These assumptions were used to develop the consequence of failure for each bridge site, which are presented in Table 6.8-1.

#### **6.8.1.1 Risk of Pier Failure at the Tide Controlled Sites**

Knowledge of the risks associated with the pier failure of a bridge is a powerful tool that may be used to design safer bridges. Analyses of such risks include the

determination of the final predicted ultimate pier scour at the test sites. The final predicted ultimate pier scour results for the two tide-controlled sites, Monie Bay and Black River, are shown in Figures 6.8-1 and 6.8-2. Both figures indicate that scour was initiated from the downstream face and that natural armoring prevented scour from occurring. These results were consistent with the scour mechanism present in tide-controlled estuaries, where erosion at the downstream pier face dominated that at the upstream pier face.

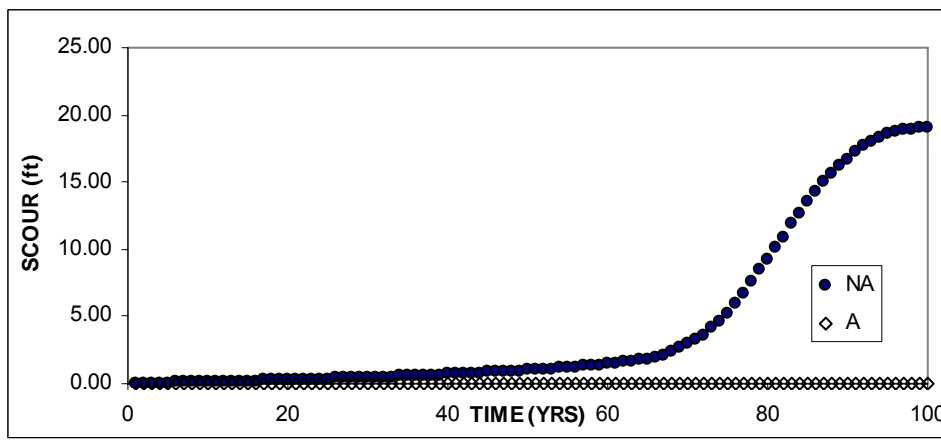


**Figure 6.8-1. Final predicted ultimate scour for Monie Bay. Scour was generated from the downstream pier face. NA indicates the simulation results without armoring while A represents the results with natural armoring. The WAVES scour results represent the mean scour depth obtained from 1000 simulations.**

Although both bridge sites were similar with regards to the process by which pier scour was initiated, they were different with respect to the time at which ultimate scour values occurred. The simulations show that the Monie Bay site took 95 years to reach its ultimate scour value, while the Black River site took only 10 years. These differences may be explained by the geometry of the cross sections of each site along with the relative sizes of their estuaries. Figures 6.4-1, and 6.5-1 show that the maximum velocity attained in the upstream direction at the Monie Bay site was 1.54 ft/s while the maximum

upstream velocity reached at the Black River site was 2.22 ft/s. By virtue of these values, the development of the downflow, and consequently the vortex velocity, would occur at a significantly faster rate at the Black River site, thus causing greater scour.

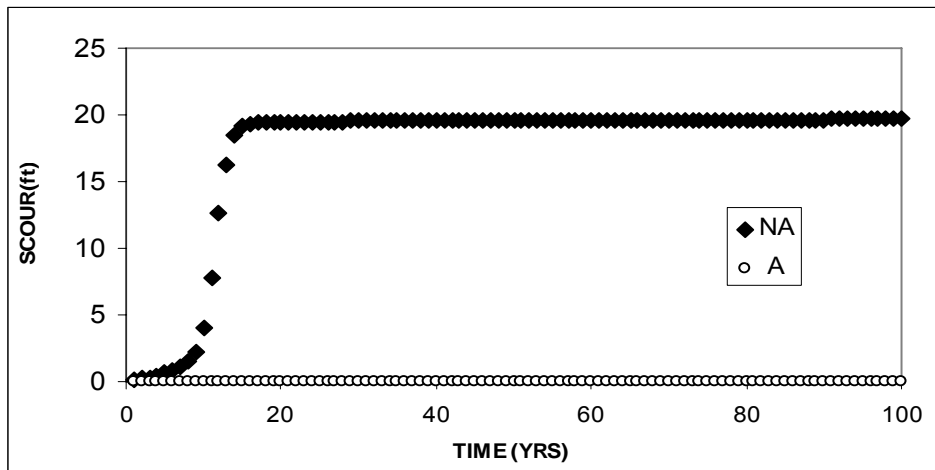


**Figure 6.8-2. Final predicted ultimate scour for Black River. Scour was generated from the downstream pier face. NA indicates the simulation results without armoring while A represents the results with natural armoring. The WAVES scour results represent the mean scour depth obtained from 1000 simulations.**

Because of its remote location, the bridge at Monie Bay was assumed to be connected to a collector highway facility with 100 vehicles per hour (see Table 6.8-1). It was also assumed that the occupants of all vehicles present on the bridge at the time of its failure would be lost. The total economic loss shown in Table 6.8-1 would be the aggregate of the loss of the structure, the damage to the surroundings caused by the failure of the structure, and the loss of the vehicles present on the structure at the time of failure. The consequences of the failure were treated separately and presented in terms of economic loss and the loss of life.

In contrast, the hypothetical Black River site was located two miles downstream of the existing I-95 crossing, and the bridge at this case study site was assumed to be used

for the realignment of the interstate highway. Table 6.8-1 shows that the total economic loss caused by the failure of the Black River bridge would be significantly greater than the losses associated with the bridge at Monie Bay. Additionally, the loss of life caused by such a failure would also be significantly greater than that caused by the failure at Monie Bay because the hourly traffic volume would be significantly greater on I-95 than on the assumed collector road at Monie Bay.

The probability of failure in any given year was estimated from the WAVES scour results. As indicated earlier, the WAVES program was designed to provide scour distributions at 15, 25, 50, 75, and 100 years. The scour at time 0 was assumed to be 0. Since a scour of 12 ft was assumed to be the condition that would cause failure, the probability of failure in any given year was calculated as 1 minus the probability that the scour would be 12 feet or less. The latter information concerning the probability of scour was obtained from the WAVES output. The computation for the probability of failure for the Monie Bay and Black River sites at the years indicated are also shown in Tables 6.8-2 and 6.8-3.

The risks associated with the failure of the Monie Bay and Black River bridges were then calculated, using Equation 6.8-1, at years 0, 15, 25, 50, 75, and 100. Tables 6.8-2, and 6.8-3 show these calculations where the risks are presented in terms of the loss of lives and the economic losses separately. Graphical representations of these results are shown in Figures 6.8-3, 6.8-4, 6.8-5, and 6.8-6.

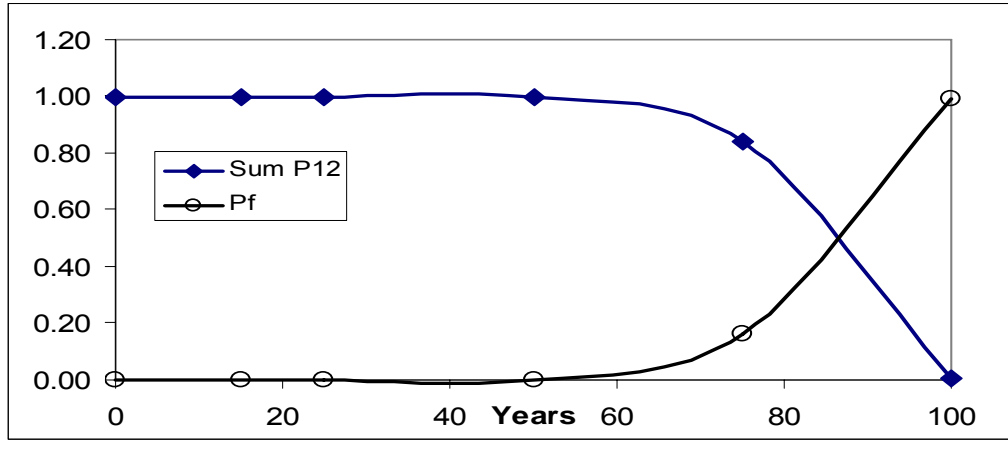


**Figure 6.8-3. Temporal Variations in the Probability of Failure of the Bridge at Monie Bay. Sum P12 is the cumulative probability that pier scour will be less than 12 ft and Pf is the probability of pier failure from scour**

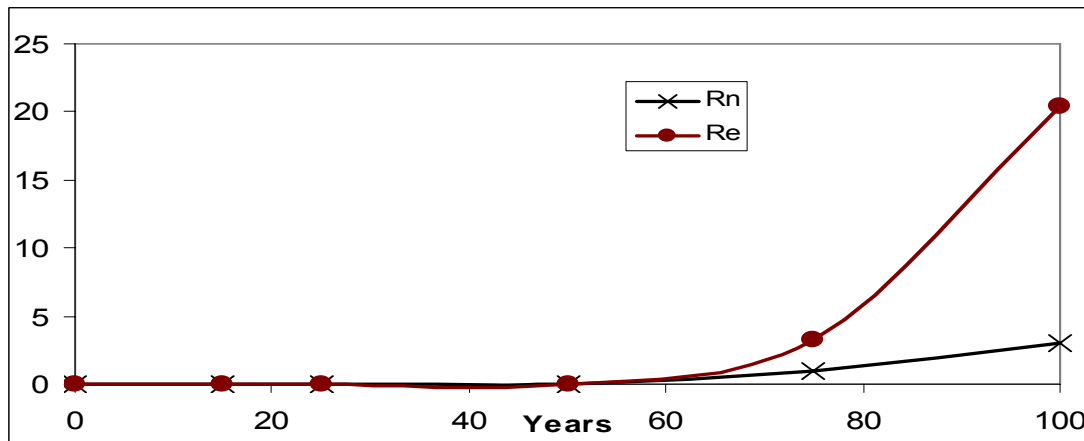


**Figure 6.8-4. Temporal Variations in the Risks of Failure for the Bridge at Monie Bay. Rn is the risk of loss of life and Re is the risk of economic loss in millions of dollars.**

The risk computations may be explained using the information presented in Table 6.8-2. The first column shows the years in the simulation at which these risks were computed. The second column shows the probability that scour would be 12 ft or less at each of these years. The information in the second column was obtained from the WAVES output. The third column contains the probability of pier failure at each of the years listed, and the values in the third column are computed as 1 minus the values in the

second column. The fourth column shows the consequence of failure in terms of the number of lives lost. The fifth column represents the risk of loss of life computed as the product of column 3 and column 4. The sixth column represents the consequence of failure in terms of economic loss, while the seventh column represents the risk of economic loss at each of the years listed, computed as the product of column 3 and column 6. The process presented could be used, in conjunction with the levels of acceptable risks set by policy makers, to determine the feasibility of the design of new projects as well as to determine the level of scour protection that should be provided for existing bridges.

**Table 6.8-2. Showing the computations of the risks associated with the failure of the bridge at Monie Bay when natural armoring was not considered. Sum P12 is the cumulative probability that pier scour will be less than 12 ft, Pf is the probability of pier failure from scour, N is the estimated number of lives lost should failure occur, Rn is the risk of loss of life, E is the economic loss due to failure in millions of dollars, and Re is the risk of economic loss in millions of dollars.**

Years	Sum P12	Pf	N	Rn	E	Re
0	1.00	0.00	3	0	20.53	0.00
15	1.00	0.00	3	0	20.53	0.00
25	1.00	0.00	3	0	20.53	0.00
50	1.00	0.00	3	0	20.53	0.00
75	0.84	0.16	3	1	20.53	3.28
100	0.01	0.99	3	3	20.53	20.41

**Table 6.8-3. Showing the computations of the risk associated with the failure of the bridge at Black River when natural armoring was not considered. Sum P12 is the cumulative probability that pier scour will be less than 12 ft, Pf is the probability of pier failure from scour, N is the estimated number of lives lost should failure occur, Rn is the risk of loss of life, E is the economic loss due to failure in millions of dollars, and Re is the risk of economic loss in millions of dollars.**

Years	Sum P12	Pf	N	Rn	E	Re
0	1.00	0.00	100	0	1031.33	0.00
15	0.01	0.99	100	99	1031.33	1021.02
25	0.00	1.00	100	100	1031.33	1031.33
50	0.00	1.00	100	100	1031.33	1031.33
75	0.00	1.00	100	100	1031.33	1031.33
100	0.00	1.00	100	100	1031.33	1031.33

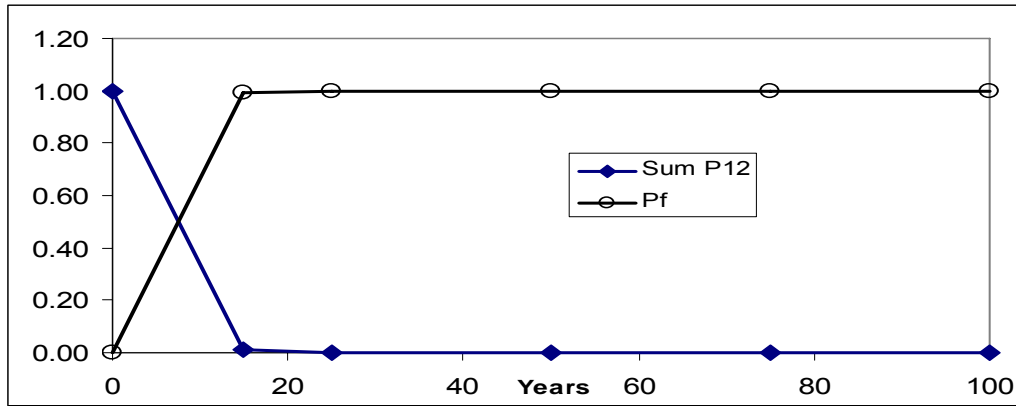


**Figure 6.8-5. Temporal Variations in the Probability of Failure of the Bridge at Black River. Sum P12 is the cumulative probability that pier scour will be less than 12 ft and Pf is the probability of pier failure from scour.**

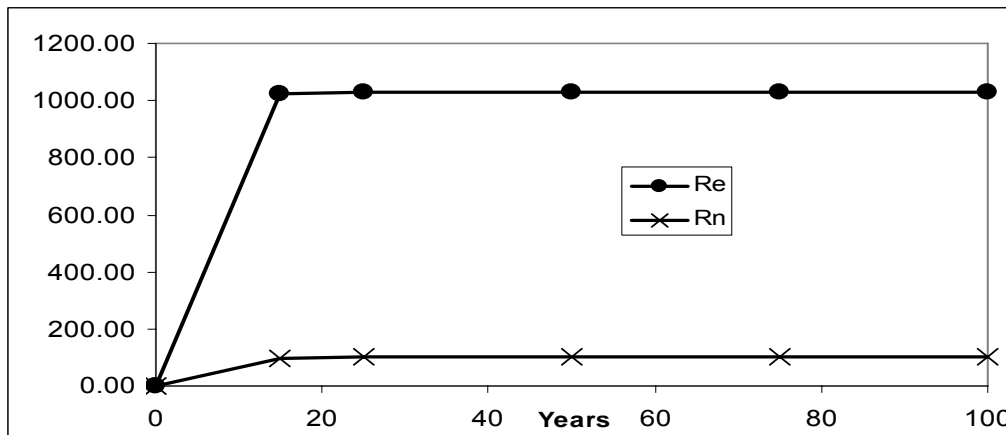


**Figure 6.8-6. Temporal Variations in the Risks of Failure for the Bridge at Black River. Rn is the risk of loss of life and Re is the risk of economic loss in millions of dollars.**

### 6.8.1.2 Risk of Pier Failure Mixed-Controlled Sites

Hypothetical risk analyses were also performed for the mixed-controlled sites commencing with the discussion of the ultimate pier scour results. The final ultimate pier scour results for the Patuxent River and Wicomico River sites are shown in Figures 6.8-7 and 6.8-8. Although scour could be initiated from the upstream or downstream pier faces in both cases, the dominant processes were found to be at the upstream pier face in the case of the Patuxent River site (see Fig. 6.8-7) and at the downstream pier face in the case

of the Wicomico River site (see Fig. 6.8-8). These results were consistent with the computed Simmons and CE ratios for both sites.

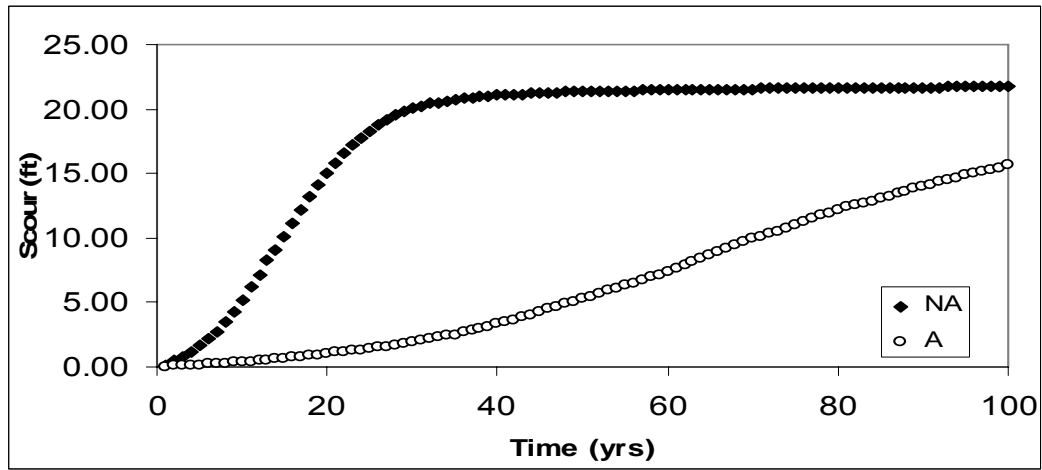


**Figure 6.8-7. Final predicted ultimate scour for the Patuxent River site. Scour was generated from the upstream pier face. NA indicates the simulation results without armoring while A represents the results with natural armoring. The WAVES scour results represent the mean scour depth obtained from 1000 simulations.**

Because the Patuxent River site was mixed-controlled with a minor catchment dominance, the results indicated that pier scour would be generated from the upstream face of the pier. Figure 6.8-7 shows that the WAVES program predicted that the Patuxent River site achieved the ultimate of 22 ft in approximately 30 years without natural armoring being considered. With natural armoring, the Patuxent River site scoured to a value of 16 ft in the 100-year simulation period.



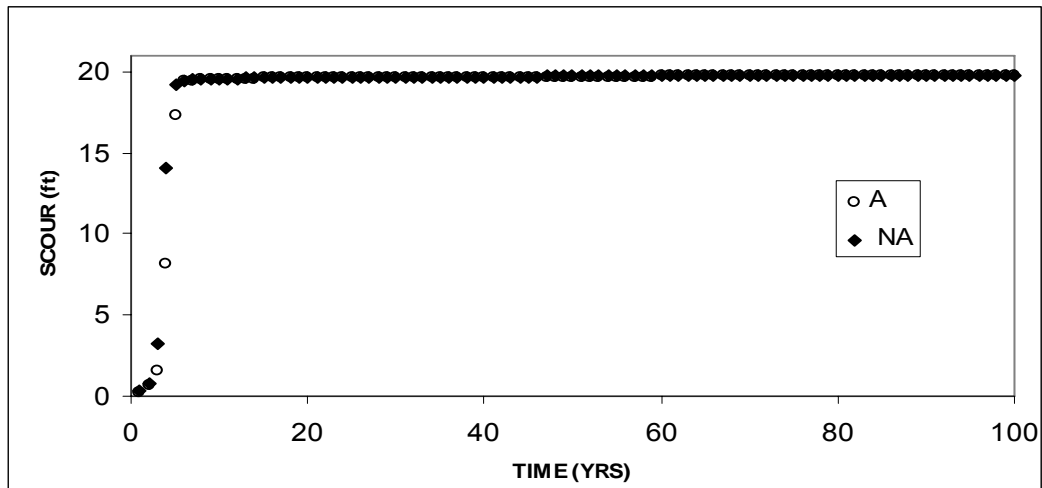


**Figure 6.8-8. Final Predicted Ultimate Scour for the Wicomico River site. Scour was generated from the downstream pier face. NA indicates the simulation results without armoring while A represents the results with natural armoring. The WAVES scour results represent the mean scour depth obtained from 1000 simulations.**

In contrast, the Wicomico site was a mixed-controlled estuary with a slight tidal dominance and this resulted in scour being generated from the downstream face of the pier. Figure 6.8-8 shows that the WAVES model predicted a more robust rate of scour at the Wicomico River site for both conditions with and without natural armoring. Ultimate scour at the Wicomico River site was achieved in approximately six years. The differences in the scour rates at both sites were primarily due to the incipient velocities of the bed materials. The Wicomico River was modeled with finer bed materials, as indicated by the soils maps for the region, and had an incipient velocity of 0.27 ft/s compared with 0.67 ft/s computed for the bed materials at the Patuxent River site.

The Patuxent River bridge was assumed to be required for the realignment of Route 304, which is a major arterial. The location of the bridge is fairly remote; however, failure of the bridge would be very costly because of the amount of traffic assumed to be conveyed by the facility. Tables 6.8-4 and 6.8-5 provide summaries of the

results of the probability of failure and the hypothetical risk analyses of the mixed control Patuxent River site for failure with and without natural armoring.

**Table 6.8-4. Showing the Computations for the Risk Analysis Associated With the Failure of the Bridge at the Patuxent River with Armoring. Sum P12 is the cumulative probability that pier scour will be less than 12 ft, Pf is the probability of pier failure from scour, N is the estimated number of lives lost should failure occur, Rn is the risk of loss of life, E is the economic loss due to failure in millions of dollars, and Re is the risk of economic loss in millions of dollars.**

Years	Sum P12	Pf	N	Rn	E	Re
0	1.00	0.00	25	0	201.38	0.00
15	0.99	0.01	25	0	201.38	2.01
25	0.97	0.03	25	1	201.38	6.04
50	0.78	0.22	25	6	201.38	44.30
75	0.48	0.52	25	13	201.38	104.72
100	0.25	0.75	25	19	201.38	151.04

**Table 6.8-5. Showing the Computations for the Risk Analysis Associated With the Failure of the Bridge at the Patuxent River without Armoring. Sum P12 is the cumulative probability that pier scour will be less than 12 ft, Pf is the probability of pier failure from scour, N is the estimated number of lives lost should failure occur, Rn is the risk of loss of life, E is the economic loss due to failure in millions of dollars, and Re is the risk of economic loss in millions of dollars.**

Years	Sum P12	Pf	N	Rn	E	Re
0	1.00	0.00	25	0	201.38	0.00
15	0.55	0.45	25	11	201.38	90.62
25	0.13	0.87	25	22	201.38	175.20
50	0.00	1.00	25	25	201.38	201.38
75	0.00	1.00	25	25	201.38	201.38
100	0.00	1.00	25	25	201.38	201.38

Figures 6.8-9 and 6.8-10 show the temporal variation of the probability of failure of the Patuxent River bridge from pier scour for both conditions with and without natural armoring. Figures 6.8-11 and 6.8-12 also provide graphical depictions of the risks associated with the failure of the Patuxent River bridges with and without natural armoring. As stated, the estimation of the variation of the failure risks with time could be

used, in conjunction with the levels of acceptable risks set by the policy makers, to determine the feasibility of the design of this bridge at its proposed location.

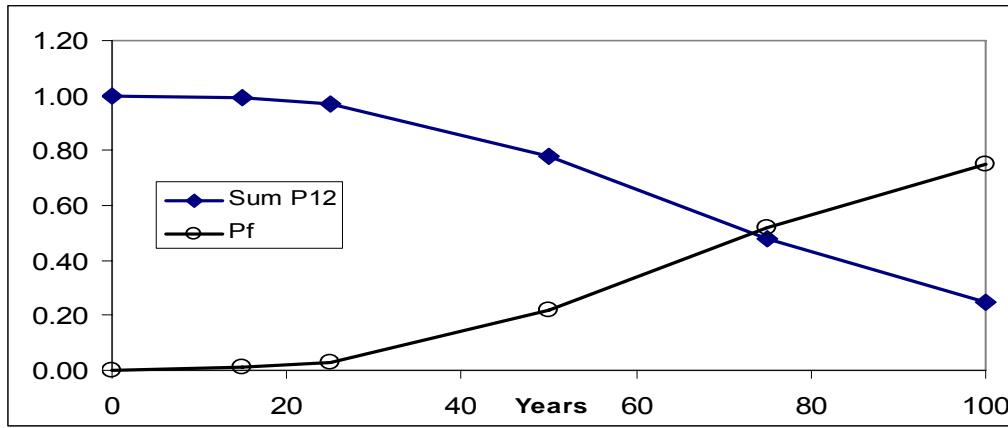


**Figure 6.8-9. Temporal variations in the probability of failure of the bridge at the Patuxent River with armoring considered. Sum P12 is the cumulative probability that pier scour will be less than 12 ft and Pf is the probability of pier failure from scour.**

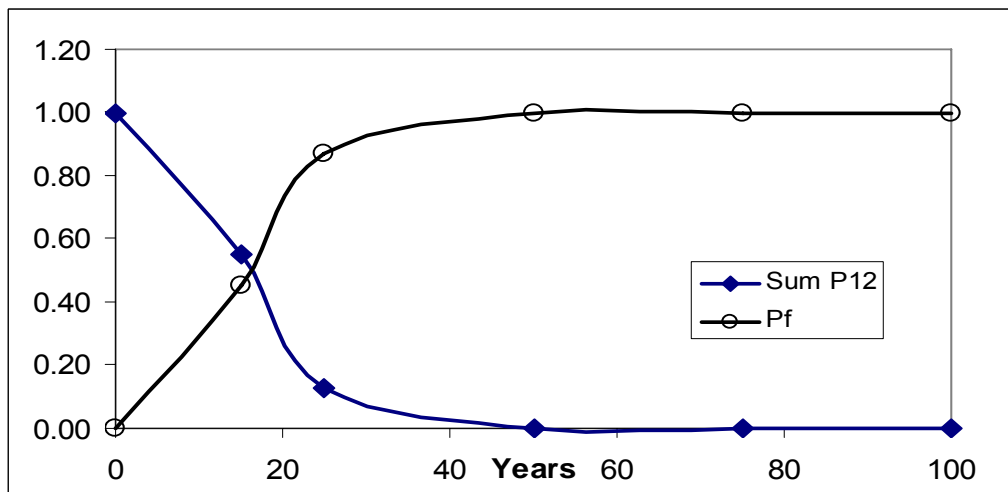


**Figure 6.8-10. Temporal variations in the probability of failure of the bridge at the Patuxent River without armoring considered. Sum P12 is the cumulative probability that pier scour will be less than 12 ft and Pf is the probability of pier failure from scour.**

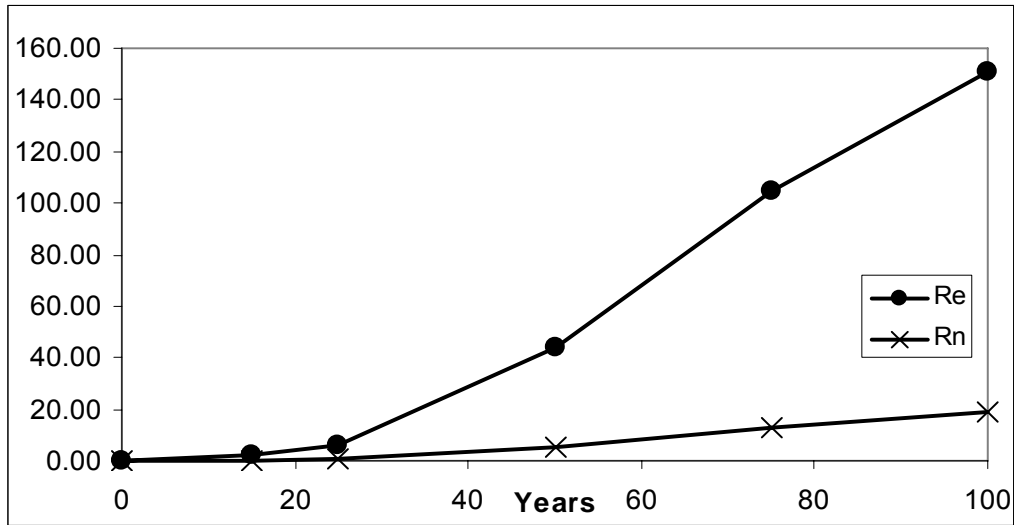


**Figure 6.8-11. Temporal variations in the risks of failure for the bridge at the Patuxent River with armoring considered. Rn is the risk of loss of life and Re is the risk of economic loss in millions of dollars.**

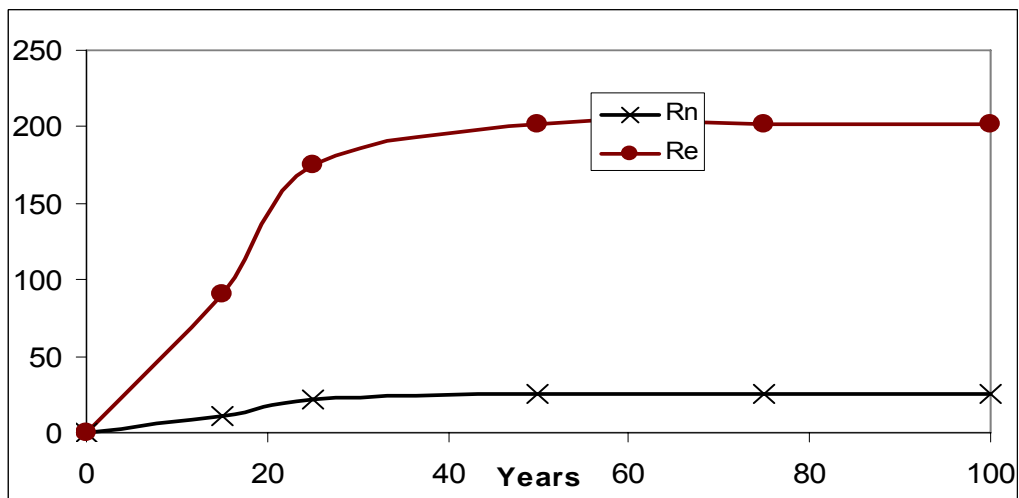


**Figure 6.8-12. Temporal variations in the risks of failure for the bridge at the Patuxent River without armoring considered. Rn is the risk of loss of life and Re is the risk of economic loss in millions of dollars.**

Table 6.8-6 summarizes the results of the hypothetical risk analyses of the Wicomico River case study site for failure with and without natural armoring. The same table was used to represent the results of both scenarios due to the similarity of the results. Table 6.8-1 also shows the assumptions and conditions used to determine the

consequences of the failure of the structure. The proposed Wicomico River bridge was assumed to be connected to a minor arterial highway facility in a moderately remote location. As a result, the tables show that the consequences and the risks of failure were not as great as at some of the other test sites.

Figure 6.8-13 shows the temporal variation of the probability of failure of the Wicomico River bridge from pier scour for both conditions with and without natural armoring. It should again be noted that Figure 6.8-13 was used to represent the probability of failure for the simulations conducted with and without considering natural armoring. Similarly, Figure 6.8-14 provides a graphical depiction of the risks associated with the failure of the Wicomico River bridge with and without considering natural armoring. The figure shows that the risks associated with the failure of the bridge, though significant, were not as costly as the other hypothetical locations.

**Table 6.8-6. Showing the computations for the risk associated with the failure of the bridge at the Wicomico River site with and without natural armoring. Sum P12 is the cumulative probability that pier scour will be less than 12 ft, Pf is the probability of pier failure from scour, N is the estimated number of lives lost should failure occur, Rn is the risk of loss of life, E is the economic loss due to failure in millions of dollars, and Re is the risk of economic loss in millions of dollars.**

Years	Sum P12	Pf	N	Rn	E	Re
0	1.00	0.00	8	0	30.58	0.00
15	0.00	1.00	8	8	30.58	30.58
25	0.00	1.00	8	8	30.58	30.58
50	0.00	1.00	8	8	30.58	30.58
75	0.00	1.00	8	8	30.58	30.58
100	0.00	1.00	8	8	30.58	30.58

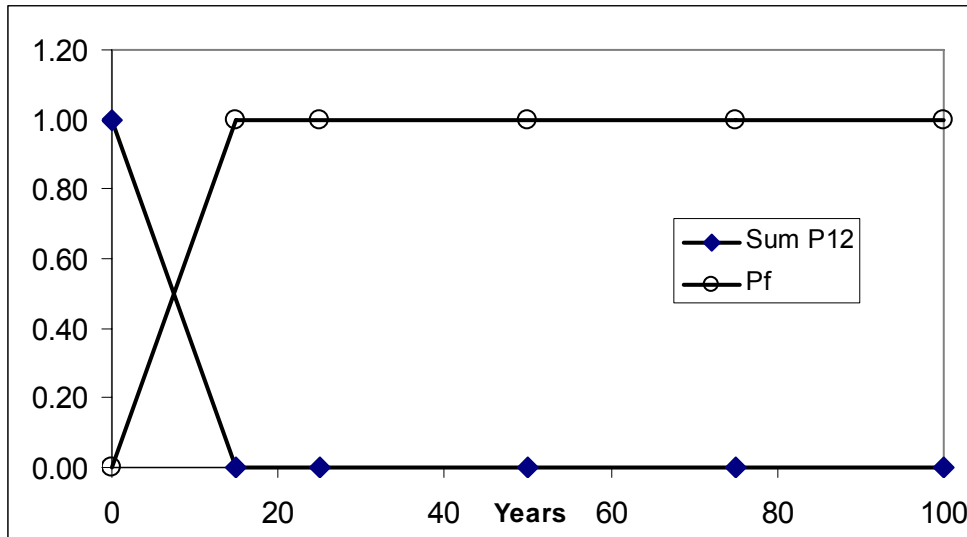


**Figure 6.8-13. Temporal variations in the probability of failure of the bridge at the Wicomico River site with and without armoring considered. Sum P12 is the cumulative probability that pier scour will be less than 12 ft and Pf is the probability of pier failure from scour.**

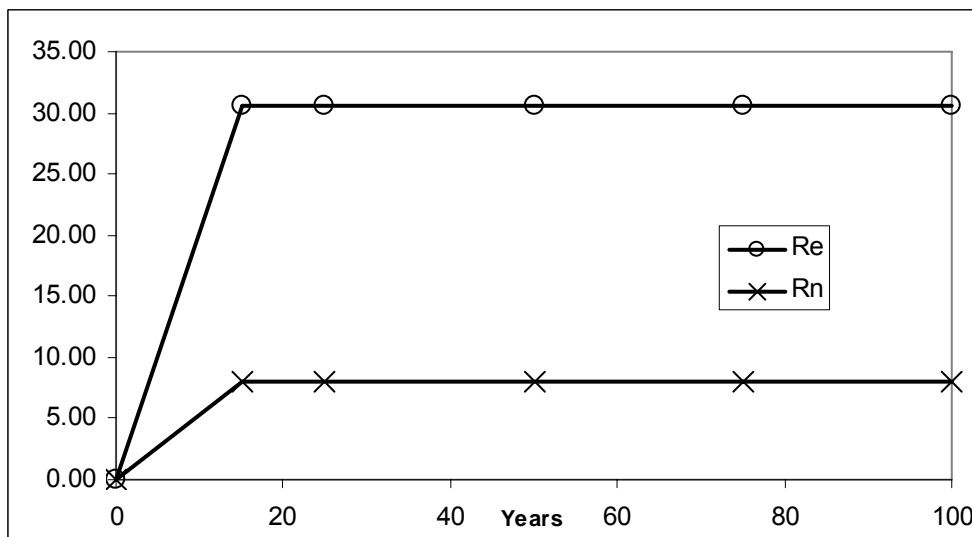


**Figure 6.8-14. Temporal Variations in the Risks of Failure for the bridge at the Wicomico River site with and without natural armoring considered. Rn is the risk of loss of life and Re is the risk of economic loss in millions of dollars.**

### 6.8.1.3 Risk of Pier Failure at a Catchment-Controlled Site

The catchment-controlled Patapsco River site showed very high estimates of failure risk. The final predicted ultimate pier scour results for this site are shown in

Figure 6.8-15. Because catchment flooding is dominant, scour was initiated from the upstream pier face. Natural armoring also significantly lowered the rate of pier scour owing to the fact that the estuary was deep. These results were also consistent with the computed Simmons and CE ratios for the site. Figure 6.8-15 shows that the WAVES program predicted that the Patapsco River site achieved the ultimate scour depth of 22 ft in approximately 15 years without natural armoring being considered. With natural armoring, the Patapsco River site scoured to a value of 21 ft in the 100-year simulation period. The probability of pier failure was also significant reaching 0.98 in 25 years when natural armoring was not considered.

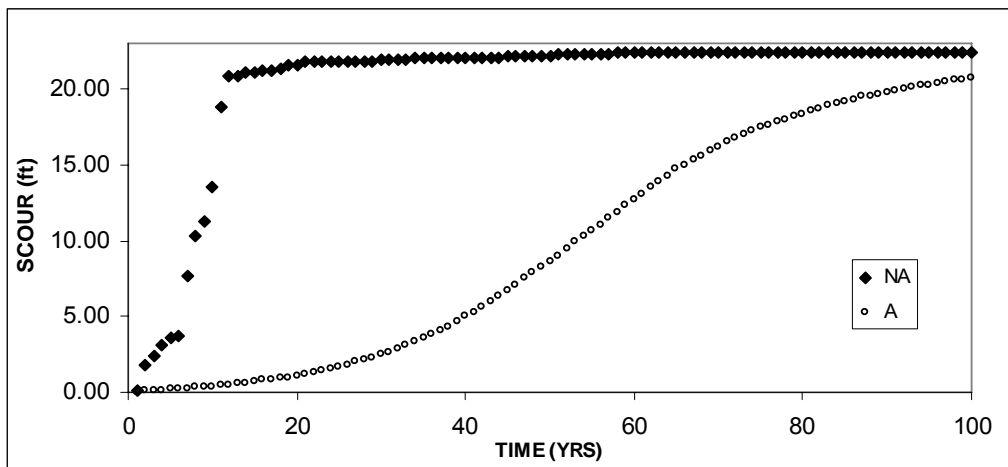


**Figure 6.8-15. Final predicted ultimate scour for the Patapsco River site. Scour was generated from the upstream pier face. NA indicates the simulation results without armoring while A represents the results with natural armoring. The WAVES scour results represent the mean scour depth obtained from 1000 simulations.**

The results of the hypothetical risk analyses of the Patapsco River site for bridge failure with and without considering natural armoring are given in Tables 6.8-7 and 6.8-8. The proposed Patapsco River bridge was assumed to be connected to a minor arterial highway facility in an urban location for the consequences analysis. It was also assumed

that the failure of the bridge would have significant economic impacts on the shipping operations conducted at the Baltimore Inner Harbor. As a result, the tables show that the economic consequence of failure was greater than most of the other test sites.

**Table 6.8-7. Showing the computations for the risk associated with the failure of the bridge at the Patapsco River site with natural armoring. Sum P12 is the cumulative probability that pier scour will be less than 12 ft, Pf is the probability of pier failure from scour, N is the estimated number of lives lost should failure occur, Rn is the risk of loss of life, E is the economic loss due to failure in millions of dollars, and Re is the risk of economic loss in millions of dollars.**

Years	Sum P12	Pf	N	Rn	E	Re
0	1.00	0.00	8	0	40.08	0.00
15	0.998	0.002	8	1	40.08	0.08
25	0.97	0.03	8	1	40.08	1.20
50	0.64	0.36	8	3	40.08	14.43
75	0.17	0.83	8	7	40.08	33.27
100	0.02	0.98	8	8	40.08	39.28

**Table 6.8-8. Showing the computations for the risk associated with the failure of the bridge at the Patapsco River site without natural armoring. Sum P12 is the cumulative probability that pier scour will be less than 12 ft, Pf is the probability of pier failure from scour, N is the estimated number of lives lost should failure occur, Rn is the risk of loss of life, E is the economic loss due to failure in millions of dollars, and Re is the risk of economic loss in millions of dollars.**

Years	Sum P12	Pf	N	Rn	E	Re
0	1.00	0.00	8	0	40.08	0.00
15	0.11	0.89	8	7	40.08	35.67
25	0.02	0.98	8	8	40.08	39.28
50	0.00	1.00	8	8	40.08	40.08
75	0.00	1.00	8	8	40.08	40.08
100	0.00	1.00	8	8	40.08	40.08

Figures 6.8-16 and 6.8-17 show the temporal variation of the probability scour of failure of the Patapsco River bridge for both conditions with and without natural armoring. Figures also 6.8-18 and 6.8-19 show the temporal variation in the risks associated with the failure of the Patapsco River bridge with and without considering natural armoring. The estimated risks were lower in the early years of the simulations when natural armoring was considered; however, the risks for both conditions were essentially the same at the end of the simulation period.



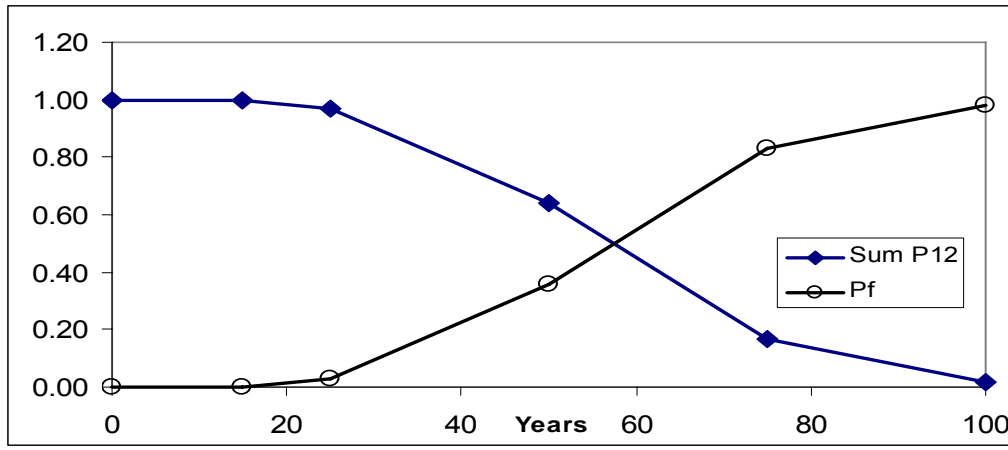


**Figure 6.8-16.** Temporal variations in the probability of failure of the bridge at the Patapsco River site with natural armoring considered. Sum P12 is the cumulative probability that pier scour will be less than 12 ft and Pf is the probability of pier failure from scour.

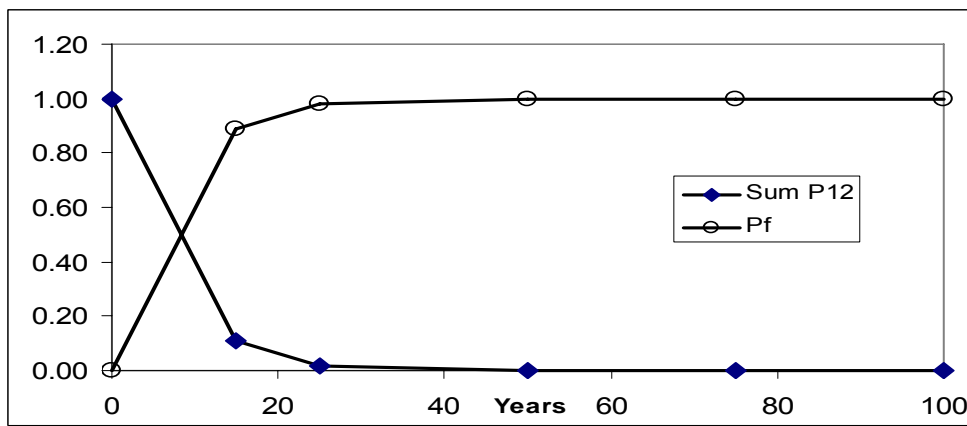


**Figure 6.8-17.** Temporal variations in the probability of failure of the bridge at the Patapsco River site without natural armoring considered. Sum P12 is the cumulative probability that pier scour will be less than 12 ft and Pf is the probability of pier failure from scour.

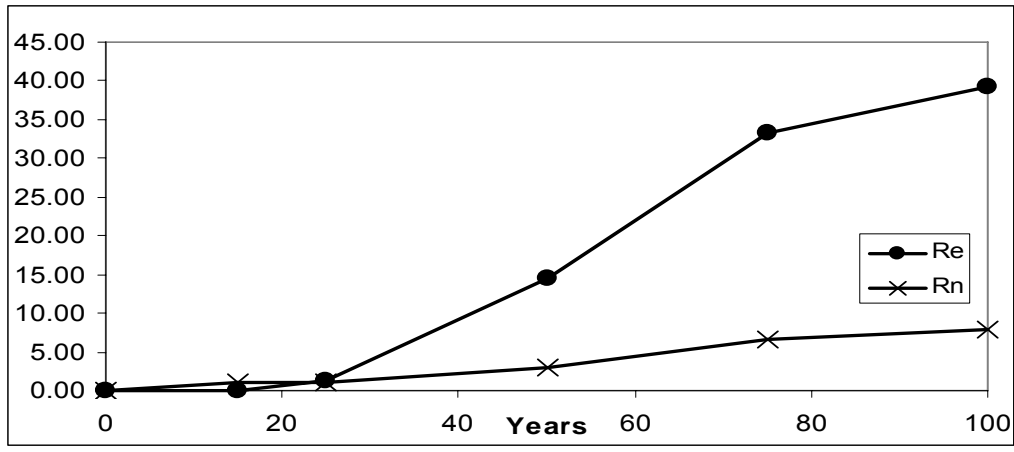


**Figure 6.8-18. Temporal Variations in the Risks of Failure for the bridge at the Patapsco River site with natural armoring considered. Rn is the risk of loss of life and Re is the risk of economic loss in millions of dollars.**

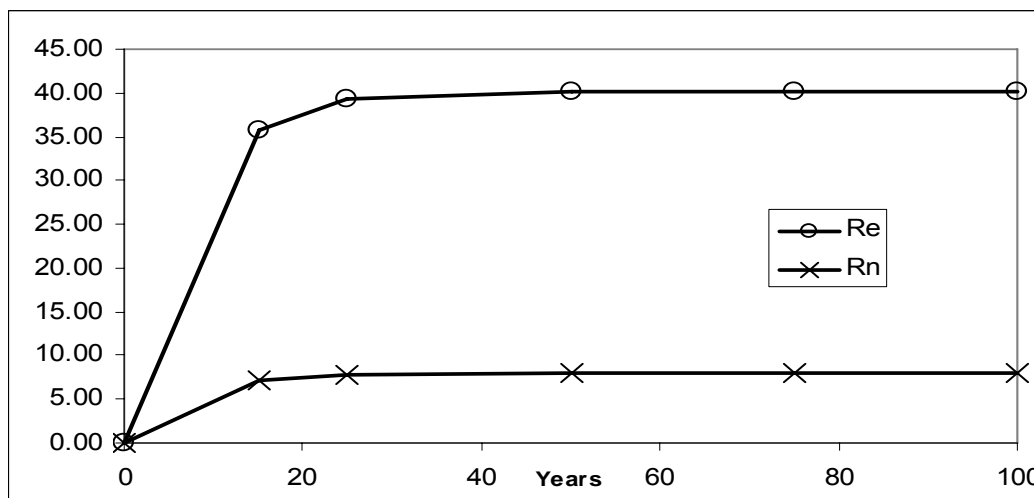


**Figure 6.8-19. Temporal Variations in the Risks of Failure for the bridge at the Patapsco River site without natural armoring considered. Rn is the risk of loss of life and Re is the risk of economic loss in millions of dollars.**

## 6.8.2 Hurricane Event Results

The assessment of the pier scour generated by single-event storms such as hurricanes in tidal rivers and estuaries is very important to the design and operation of bridge structures. Knowledge of the impacts of a hurricane on pier scour will assist engineers in the design of new bridges. Similarly, determination of the scour generated

by hurricanes will allow highway professionals to assess the safety of existing structures during and after such an event. The sites selected by this study also provide an opportunity to establish relationships between the scour generated by single-event storm and the particular type of estuary.

The results produced by the WAVES hurricane simulations are summarized in Table 6.8-9. The table shows some general characteristics of the simulations shared by all of the case study sites. First, the discharges produced were significantly higher than those produced during the 100-year simulations. Second, hurricane scour did not occur in all cases, but in the cases where scour did occur, the scour was less than that produced during the 100-year simulation. Third, the scour was generally greater at the upstream pier face than at the downstream pier face in the cases where scour occurred.

The magnitude of the discharge upstream or downstream did not have a significant effect on the amount of scour produced during a single-event storm. Table 6.8-9 shows the discharges predicted by the WAVES model during the hurricane events. In all cases, the discharges were significantly greater than the values produced in the 100-year simulations at the same sites. In addition, the discharge in the downstream direction which affected the upstream pier face, was generally greater than the discharge upstream produced by the rising surge. This result may at first appear to be inconsistent with expectations. However, the results may be explained by examining the hurricane model used in the WAVES program. The hurricane model assumed that the surge gradually increased to a maximum value when the eye of the hurricane was at its closest distance from the bridge. The eye then passes by the bridge and begins to move away from it. As this occurs, the hurricane wind reverses its direction and this results in a sharp drop in the

water surface elevation. This condition is referred to as the hurricane blow back and can cause the surge to drop 30 feet in one hour. Consequently this sharp decrease in the water surface elevation causes a sharp and very large increase in the downstream discharge.

Figure 6.8-20 shows the typical variation in the estuary discharge during the first 36 hr of a hurricane.

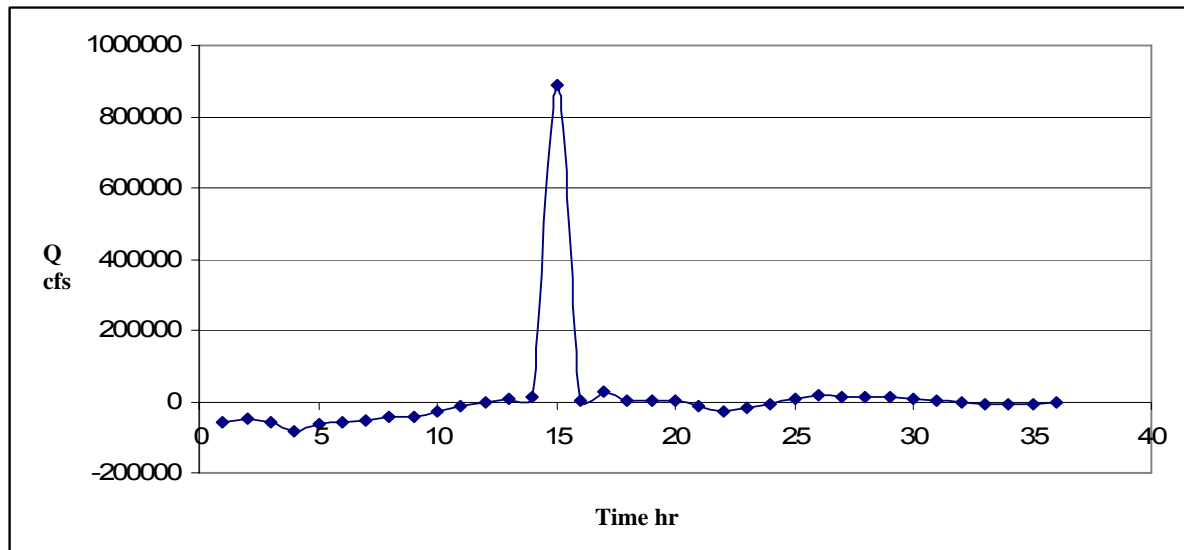


**Figure 6.8-20. Typical hurricane discharge variation with time produced by the WAVES Program. Negative discharge values indicate upstream flows.**

The factors that had the most impact on the amount of scour produced during the hurricane events were rainfall and the size of the channel sediment at the cross section of the test site. Table 6.8-9 also shows that insignificant scour was produced by the hurricanes at the Black River and Monie Bay sites, while significant hurricane scour occurred at the Patapsco and Patuxent sites. The Wicomico River site produced scour that ranged from 6 to 13 inches. The low scour can be explained by the relatively short duration of the event. Figure 6.8-16 shows that the sharp increase in the blow back

discharge lasts only two hours. As a result, the velocities developed could not be sustained long enough to cause significant scour.

**Table 6.8-9. Summary of the hurricane scour results at the upstream (U/S) and downstream (D/S) pier face. R is the assumed most likely rainfall amount that occurred with the event, V is the maximum stream velocity, and Q is the maximum discharge.**

Site	R (in.)	US Pier Face			DS Pier Face		
		Scour (ft)	Q (cfs)	V (ft/s)	Scour (ft)	Q (cfs)	V (ft/s)
<b>Monie Bay</b>	<b>5</b>	0.13	208193	2.37	0.20	195798	0.82
<b>Black River</b>	<b>7</b>	0.50	893900	2.40	0.50	907615	5.36
<b>Patuxent River</b>	<b>8</b>	1.13	890967	12.16	0.85	837565	5.09
<b>Wicomico River</b>	<b>5</b>	0.87	377347	8.10	0.66	371722	2.50
<b>Patapsco River</b>	<b>8</b>	3.45	337673	3.27	0.18	259690	3.27

Most sites tested indicated that single-event hurricane scour would be generated from the upstream face of the pier. Table 6.8-9 also shows that the hurricane scour produced at the upstream pier face was always greater than the scouring produced at the downstream pier face at the catchment-controlled and mixed-controlled sites where the catchment dominated the tidal processes. These results indicate that hurricane scour at the bridge pier was largely independent of the estuarine tidal processes, but was significantly dependent on the catchment processes. The results of the simulations further indicated that the dynamics of the hurricane had the greatest impact on pier scour, particularly with regard to the discharge and velocities generated by the hurricane blow-back.

## **CHAPTER 7**

### **COMPARISON OF EXISTING MODELS WITH THE WAVES PROGRAM**

#### **7.1 INTRODUCTION**

One objective of this study was to show that continuous simulation models produced results that were more useful and reliable than current single-event models, particularly when used to determine bridge pier scour in tidal environments. This does not mean that the use of single-event models for estimating pier scour in tidal environments is completely inappropriate, as some cases may not require precise pier scour estimates. In general, both single-event and continuous models have strengths and weaknesses that must be considered before selecting a model for bridge pier scour design or analysis.

##### **7.1.1 Benefits and Weaknesses of a Single-Event Model**

Single-event models are popular primarily because they produce single-valued estimates in minimum time and cost. Most single-event models require the minimum amount of input data to produce results. Typically, the data needed are simple and can be collected quickly and inexpensively. Single-event models usually involve simple equations that can be easily solved to produce an estimate. Though the estimate produced is sometimes imprecise, these deficiencies are typically addressed by very conservative design assumptions, such as the use of the 500-year storm to determine the expected pier scour for a bridge with a design life of 50 years. The ease and speed with which these models produce estimates provide additional cost savings to the project.

Though widely used, single-event models generally produce imprecise results, which is evident from the wide range estimates obtained from the multitude of alternative prediction equations. The model output is generally limited to a single-valued estimate of the final scour depth caused by the single-event in question. As a result, single-event models can not be used to predict the actual time of bridge failure. Also, the outputs produced by these models are not sufficiently detailed to analyze the temporal development of the scour hole. The mechanism of bridge pier scour in a tidal environment is ultimately much more complex than the scour process in upland rivers, and many of the processes that impact tidal bridge pier scour cannot be satisfactorily represented by a simple single-event pier scour model.

#### **7.1.2 Benefits and Weaknesses of Continuous Models**

Models capable of continuous pier scour simulations are generally considered to be both more structurally rational and more useful than single-event models and may be readily adapted to risk-based bridge pier designs. Continuous models provide added flexibility and the ability to analyze the effects of variables being used by the model. A continuous model can also provide an estimate of the time of pier failure. Regarding their use in the design or analysis of bridges in tidal environments, continuous pier scour models are more suited for the complexities of tidal environment and are better able to represent the complex processes that occur in this type of environment than single-event models.

### **7.1.3 Rationale for Model Comparison Exercises**

A set of experiments for various estuarine conditions at the case study sites were used to compare the final scour estimates from the WAVES continuous estuary scour program to those from 40 of the most widely used pier scour models identified in the literature. This exercise was conducted to provide information on the scour produced by the WAVES program relative to the results from most of the simple models currently in use. The models used in the comparative exercise were selected to provide a wide diversity in input data requirements and the conditions under which the models were developed.

Pier scour estimates provided by the WAVES program were compared to estimates from the most frequently used single-event models. Estimates of annual scour were obtained from the single-event models using the annual series (such as discharge, velocity, and depth) obtained from the WAVES program. The intent of these exercises was to observe the performance of the WAVES program on an annual basis in comparison with estimates from the five most widely accepted pier scour models that were not developed specifically for tidal conditions. The results were intended to assess whether or not these other models could be used in tidal environments.

## **7.2 SUMMARY DESCRIPTION OF FORTY SINGLE-EVENT MODELS**

### **7.2.1 Model Description**

Forty scour models were identified in the literature and were used in the comparative study. Details of the models are presented in Tables 7.2-1 and 7.2-2. In preparation for the comparative study, the variables, conditions, and ranges of data values



used in the development of some models were reviewed and are shown in Table 7.2-3. The models selected for the study included some developed from estuary data and those used to predict scour from wave motion. The majority of the models consisted of empirical equations developed from laboratory data and presented in the form of ratios. Notwithstanding, some of the models were also developed from field data obtained from non-tidal rivers. It is interesting to note that none of the models used in this study included the vortex, tangential, or downflow velocities as scour predictors.

One of the primary objectives of this research was the formulation of a continuous model to predict bridge pier scour in tidal rivers and estuaries, and to show, by case study simulations, that the formulated model would be more useful and appropriate for estimating pier scour in a tidal environment than the many simple models commonly used. With this objective in mind, it became necessary to identify the current models developed for estuaries and tidal rivers. Models developed by Breusers (1956) and Melville and Coleman (2000) were among the few identified. The Breusers model, identified in Table 7.2-1 as model No. 1, was developed from field data obtained from bridge piers located in estuaries. Model No. 1 was included in the study to determine if its results compared favorably with the WAVES program and the other models used in the study. The Melville and Coleman (2000) ocean wave equation, No. 27 in Table 7.2-1, was formulated to estimate scour due to oceanic wave and tidal actions.

**Table 7.2-1. Univariate and bivariate models selected for the comparison exercise. Column 2 shows the identification number assigned to each model. Column 3 shows predictor variables; b is pier diameter or width, y is flow depth, Q is discharge, q is the discharge per unit width of pier or channel, W is the width of the channel, v is velocity,  $d_{50}$  is the mean particle diameter, and  $\nu$  is the kinematic viscosity of water. A full description of the variables and constants of each model is presented in Chapter 2.**

Author	Model No.	Variables	Data Type	Equation
Breusers Eq. 1	1	B	Field	$d_s = 1.4b$
Larras	10	B	Laboratory	$d_s/b = 1.05b^{0.75}$
Basak	16	B	Laboratory	$d_{se}/b = 0.558b^{0.586}$
Neill Eq. 2	18	B	Laboratory	$d_{se}/b = 1.5b$
Chitale	22	B	Laboratory	$d_s/b = 2.5$
RDSOs	35	Y	Field	$d_s = 1.71y$
Breusers Eq. 2	2	Y, b	Laboratory	$d_s/b = 2(KS)K_\theta \tanh(y/b)$
Laursens	3	Y, b	Laboratory	$d_s/b = (1.11(y/b)^{0.5})$
Laursen & Tosh	4	Y, b	Field	$d_{se}/b = 1.5(y/b)^{0.30}$
Laursen & Neill	5	Y, b	Laboratory	$d_{se} = (b^{0.7})^*(y^{0.3})$
Inglis Eq. 1	6	Q, $d_{50}$	Field	$d_{se} = 0.47K(Q/f_1)^{0.33}$
Inglis Eq. 2	7	Q, $d_{50}$	Laboratory	$d_{se}/b = 2.32(q^{0.67}/b)^{0.78}$
Neill Eq. 3	19	Y, b	Laboratory	$d_{se}/b = 1.34(y/b)^{0.5}$
Lacy Original	28	Q, $d_{50}$	Laboratory	$d_s = 0.473(Q d_{50}^{-0.57})^{0.33}$
Lacy Revised	29	Q, $d_{50}$	Laboratory	$d_s = 0.473K(Q d_{50}^{-0.57})^{0.33}$
Railways Ministry	37	Q, $d_{50}$	Field	$d_{se} = 0.47K(Q f_1)^{0.33}$

**Table 7.2-2. Models with three or more predictor variables selected for the comparison exercise. The variables are identified as shown in Table 7.2-1. A full description of the variables and constants of each model is presented in Chapter 2.**

Author	Eqn. No.	Variables	Data Type	Equation
Sanchez	8	b, d <sub>50</sub> , v	Laboratory	$d_{se}/b = 2K_f K_5 (V^2/gb) - 30(d_{50}/b)$
Hancu Eq. 1	11	b, y, v	Laboratory	$d_s/b = 2.42[(2V/V_c)-1](y/b)^{0.33}(V_c^2/gb)^{0.33}$
Hancu Eq. 2	12	b, y, d <sub>50</sub>	Laboratory	$d_{se}/b = 3.3(d_{50}/b)^{0.20}(y/b)^{0.13}$
Coleman Eq. 1	14	b, y, v	Laboratory	$d_{se}/b = 1.49(V^2/gy)^{0.10}$
Coleman Eq. 2	15	b, y, v	Laboratory	$d_s/b = 0.54(y/b)^{0.41}(V^2/gy)^{0.6} y^{0.41}$
CSU HEC 18	23	b, y, v	Laboratory	$d_s = 2yK_1 K_2 K_3 K_4(b/y)^{0.65} Fr^{0.34}$
Richardson	24	b, y, v	Laboratory	$d_s/b = 2K_3 K_4(y/b)^{0.35} Fr^{0.43}$
Melville Eq. 1	26	b, y, d <sub>50</sub>	Laboratory	$d_s = K_{yb} K_d [(V-(V_a-V_c)/V_c]$
Mustaqs	31	Q, W, b	Field	$d_s/b = 1.468qb^{0.67}$
Blench Eq. 2	33	Q, W, b	Laboratory	$d_s/b = 1.8d_r(b/d_r)^{0.25}$
Sethis	34	Q, W, d <sub>50</sub>	Field	$d_s/b = 2.11(q_1^2/F_{fact})^{0.333}$
Izzard & Bradley	38	Q, W, b	Field Laboratory	$d_{se} = 2.15[Q/(B-b)]^{0.67}$
Shen	9	b, V, v	Laboratory Field	$d_{se} = 0.0002225R_{eb}^{0.619}$
Neill Eq. 1	17	Q, W, b, d <sub>50</sub>	Field	$d_{se}/b = 1.34K(q^2/f_1)^{0.5}$
Jain & Fischer	20	b, y, v, d <sub>50</sub>	Laboratory	$d_{se}/b = 2.0(y/b)^{0.5}[F_r - F_{rc}]^{0.25}$
Jain	21	b, y, v, d <sub>50</sub>	Laboratory	$d_{se}/b = 1.84(y/b)^{0.3} F_{rc}^{0.25}$
Gao et al.	25	b, y, d <sub>50</sub> , v	Laboratory	$d_s = 0.46Kb^{0.6} y^{0.15} d^{-0.07} [(V-V_c^*)/(V_c-V_c^*)]$
Blench Eq. 1	32	Q, y, b, W	Field	$d_s/b = 1.8(y_r/b)^{0.75} - y_r/b$ ; $y_r = 1.48(q^2/1.9d^{0.5})^{0.33}$
Arunachalams	30	Q, W, b, d <sub>50</sub>	Field	$d_s/b = (y_s/b)((1.72b^{0.05}/(y_s/b)^{0.167})-1)$ ; $y_s = 1.34*((qb)^2(d_{50}^{-0.57}))^{0.33}$
Demetrius	40	V, d <sub>50</sub> , b, y		$d_s = b \tanh(y/b)(V_t - V_i)$
Melville and Coleman	27	A, y, T, b, C		$d_s/b = 2.0[1 - \exp(-0.03\{KC-6\})]$ ; $KC = V_m T/b$
Unified Model	39	y, b, W, v, d <sub>50</sub>	Laboratory	$d_s = y(4/\alpha) n_1 n_2 n_3 n_4 F^n$

**Table 7.2-3. Data Used in the Development of Some Models**

Eqn. No.	Investigator	Channel Width m	Pier Size cm	Sediment Size mm	Flow Velocity m/s	Flow Depth cms	Froude Number	Threshold Froude Number
2	Brussers 1965	0.95	5.0	0.20	0.2 - 0.4	50	0.09 - 0.26	0.14 - 0.19
3	Laursen and Toch 1956	1.52	6.1	0.44 - 2.25	0.3 - 0.76	6.1 - 27.4	0.23 - 0.79	0.24 - 0.63
4	Laursen & Toch 1962	41.00	122.0	0.45		350.0		
6	Inglis 1962		5.4 - 17.3	0.3 - 1.3	0.18 - 0.50	11.5 - 61.0	0.17 - 0.27	0.14 - 0.36
7	Inglis 1949			0.17 - 0.39				
9	Shen et al 1966	1.83	15.2	0.24 - 0.46	0.14 - 1.02	11.4 - 26.8	0.1 - 0.95	0.19 - 0.26
10	Larras 1963							
11	Hanchu 1971		3.0 - 20.0	0.5 - 2.00	0.2 - 0.88	5 - 17.5	0.21 - 0.97	0.44 - 0.71
12	Hanchu 1971		13.0	5.00	0.5 - 0.90	6 - 16.5	0.44 - 0.93	0.11 - 0.81
14	Coleman 1 1988			0.10				
20	Jain - Fischer 1979	0.91	5.08 - 10.2	0.25 - 2.5	0.5 - 1.40	10.2 - 24.7	0.5 - 1.50	0.29 - 0.63
22	Chitale 1962	2.44	17.4	0.16 - 1.51	0.21 - 0.59	15.8 - 44.2	0.1 - 0.48	0.15 - 0.46
23	HEC 18 CSU		1.0 - 20.0	0.5 - 6.00	0.2 - 1.5	10.0 - 30.0		
26	Melville 1997		1.6 - 20.0	0.8 - 5.35	0.174 - 1.41			

The majority of the models represented in this comparative study, as shown in Table 7.2-1, were empirical relationships developed from laboratory data. Conscious attempts were made by most researchers to create simple dimensionless relationships. This resulted in most of these models being represented as dimensionless ratios. Concerns about the validity of the results obtained from ratio correlations expressed by some researchers were discussed in Chapter 2. Although the vast majority of these models were not formulated for estuarine or tidal conditions, they were included because of their overall popularity and also to assess their performance in relation to the WAVES program.

A few of the models used in the comparative study were developed from field data obtained from upland rivers. Among such models are the Neill's scour model, identified in Table 7.2-1 as model No. 17 and the Inglis model (No. 6). A few of the models were developed from riverine pier scour data obtained rivers in India. These models included the Sethi model (No. 34), the RDSO model (No. 35), the Andrus model (No. 36), and the Indian Railways Ministry model (No. 37). These models were included to assess the performance of models based on riverine field data.

The WAVES program utilizes an equation intended to estimate ultimate scour, which was developed by the author from methods discussed in Chapter 3. This equation, identified as model No. 40 in Table 7.2-2, was also included in the comparative study as it probably represents the only single-event model available that is based on the properties of the horseshoe vortex that develops around a bridge pier. Inclusion of model No. 40 also provides the opportunity to directly assess the performance of a continuous model relative to a single-event or single-event model that used the same predictors, as the WAVES program is merely the continuous form of model No. 40.

### **7.2.2 Summary of Required Inputs**

The models selected for the study reflect the diverse equations and relationships currently in use that provide single-valued estimates of pier scour from various types of input data. An important feature of the models is the wide range of input data utilized. At the low end of the range, some models used a single predictor variable while others required as many as five predictor variables.

Six of the models included in this comparison and shown in Table 7.2-1 were univariate equations. Of these, five models used the pier diameter as the predictor variable while the remaining model used the flow depth as the predictor. It was determined from the sensitivity analyses performed on the WAVES program that the pier diameter was a critical variable for the determination of pier scour in estuarine environments. This is also supported by the number of univariate models that assume pier scour depth is dependent only on the diameter of the bridge pier. In contrast, the sensitivity analyses performed on the WAVES program indicated that that estuarine pier scour shared an inverse relationship with flow depth while the univariate RDSO model that was developed from riverine data indicated a direct relationship between pier scour and flow depth. The ten bivariate models used in the comparative study are shown in Table 7.2-1. Of these models five used pier diameter and flow depth as predictors while the remaining five used stream discharge and the mean particle diameter of the channel bed material.

The model developed by Laursen and Tosh (1956), identified as model No. 4 in Table 7.2-1 has been cited by some researchers as one of the more reliable pier scour models currently in use. This model was developed from sediment data obtained from upland rivers and uses flow depth and pier diameter as predictors. However, the assumption that scour depth is directly related to the depth of flow in the channel may make it inappropriate for estuary and tidal use.

While the total discharge may be a good indicator of pier scour in narrow riverine channels, the same may not be true for wide upland rivers or estuarine environments. In an attempt to provide greater accuracy, many of the simple empirical models use the

discharge per unit channel width or the discharge per unit pier diameter as a predictor variable. A few of these models were selected for the comparison test, as indicated in Tables 7.2-1 and 7.2-2.

Many pier scour models use the flow velocity or Froude Number as predictors. Models of this type, which are shown in Table 7.2-2, include the HEC-18 (No. 23), Froelich (No. 13), Richardson and Davis (No. 24), Hancu (No. 12), and the Jain and Fischer (No. 20) models. It was thought that these models should provide more accurate results in an estuarine environment than the other models mentioned, as the velocity variable better reflected the accepted mechanism of the pier scour process than variables such as discharge and flow depth.

## **7.3 COMPARISON OF WAVES WITH FORTY SINGLE-EVENT MODELS**

### **7.3.1 Procedure**

The geometry and cross section conditions of each of the case study sites modeled in Chapter 5 were used in the comparison exercise. The mean particle size of the bed material in the WAVES simulation exercises was also used as a predictor in the selected empirical models that required this data. Similarly, test models that required the cross section width used the case study cross section width developed for the WAVES simulations. Some of the models required the definition of constants related to the pier geometry and bridge alignment. Since only circular piers were studied, all pier factors, bridge alignment factors, and all other factors related to the pier geometry were set at 1.0.

The hydrologic, hydraulic, and scour results of the last 100-year bridge scour simulation performed by the WAVES program for the case study sites, discussed in Chapter 5, were used in this comparison exercise. Specifically, the results from the 100-year simulation for each case study site used in the comparative scour exercise were the annual cumulative scour on the upstream and downstream faces of the pier, the peak annual hourly discharge in the upstream and downstream directions, the peak annual hourly flow depth in the upstream and downstream directions, and the peak annual hourly velocities of the stream in the upstream and downstream directions. The largest of the annual values of the depth, discharges, and velocities found in the WAVES output were assumed to represent the 100-yr values of these variables. Where relevant, these values were substituted for the variables of each model used in the comparative study to estimate the 100-year scour at the upstream and downstream faces of the pier. The maximum values of the vortex tangential velocity and the incipient velocity of the bed material were also obtained from the WAVES 100-year simulation and were used to compute the ultimate 100-year pier scour predicted by model No. 40, the ultimate scour model used by the WAVES program. Examples of the 100-year annual series of variables are shown in Appendix E.2. Table 7.3-1 shows the results obtained from the WAVES simulations for the upstream pier faces at the case study sites. These data were subsequently used as input to the models in this study. The scour results predicted by each model using this data were assumed to represent the scour predicted for the upstream pier face.



**Table 7.3-1. Data Obtained From the WAVES Upstream Pier Face Simulations for the Case Study Sites Used as Input Variables for the Models in the Comparative Scour Exercises**

<b>Variables</b>	<b>BLACK RIVER</b>	<b>PATUXENT RIVER</b>	<b>WICOMICO RIVER</b>	<b>PATAPSCO RIVER (BALTIMORE)</b>	<b>MONIE BAY</b>
100-yr Depth (ft)	14.75	18.1	20.8	38.8	9.2
100-yr Discharge (cfs)	211024	125435	86716	129931	50550
100-yr Velocity (f/s)	1.21	2.71	2.17	2.58	0.66
100-yr Tangential Velocity (ft/s)	0.54	1.79	.93	4.03	0.32
Mean Particle Diameter (mm)	0.15	0.25	0.325	0.15	0.135
Cross Section Width (ft)	8580	3333	1320	1750	5808

Similarly, Table 7.3-2 shows the results obtained from the WAVES simulations for the downstream stream pier faces at the case study sites. These data were also used as input to the models in this study. The scour results predicted by each model using this data were assumed to represent the scour predicted for the downstream pier face.

**7.3-2. Data Obtained From the WAVES Downstream Pier Face Simulations for the Case Study Sites Used as Input Variables for the Models in the Comparative Scour Exercises**

<b>Variables</b>	<b>BLACK RIVER</b>	<b>PATUXENT RIVER</b>	<b>WICOMICO RIVER</b>	<b>PATAPSCO RIVER (BALTIMORE)</b>	<b>MONIE BAY</b>
100-yr Depth (ft)	15.0	18.3	21.0	39.3	10.0
100-yr Discharge (cfs)	201669	106351	80450	82579	50527
100-yr Velocity (ft/s)	1.97	1.98	2.68	1.19	1.41
100-yr Tangential Velocity (f/s)	1.89	2.34	3.39	.42	2.29
Mean Particle Diameter (mm)	0.15	0.25	0.325	0.15	0.135
Cross Section Width (ft)	8580	3333	1320	1750	5808

## **7.3.2 Results of the Comparative Exercises**

### **7.3.2.1 Introduction**

One of the objectives of this study was to show, by comparison with the current single-valued models in use, that a continuous model developed specifically for estuarine environments would perform better than the single-valued empirical models. To

accomplish this objective the performance of the WAVES program was compared to the performance of 40 single-valued models. In order to evaluate and assess the performance of the WAVES program against the other models tested, it was necessary to examine and analyze the conditions and data ranges of the test models and compare these conditions with the conditions of this study. An important aspect of these analyses was to determine the reasons why some models grossly over predicted. Special treatment was given to the Breseurs model (No. 1), as this was the only model in the group that was formulated from estuary data.

Comparisons between the results of the 40 models and the WAVES program were performed through the development of histograms and curves. The mean and standard deviation of the upstream face scour, the downstream face scour, and the predicted maximum scour provided by the models were computed to show the degree of spread that was obtained from the alternative models. Results that were not close to the mean values were analyzed further to determine the reasons for their variances. In addition, the models tested were analyzed to determine their appropriateness for predicting scour in the various types of estuarine environments. To facilitate this approach, the results obtained from the case study sites were grouped in terms of the type of estuary classification made for that particular site.

#### **7.3.2.2 Summary of Results**

The WAVES program was designed to analyze scour at the upstream and downstream pier faces separately because of the need to understand the processes that caused scour in an estuarine environment. By analyzing the pier scour at each pier face,

model users would be better able to assess the causes of pier scour at that particular location. Table 7.3-3 shows the results of the upstream pier face scour for the 40-model comparative study at the case study sites.

Scour initiated at the downstream pier face is a phenomenon that is experienced only in tidal environments and not much data exist on the specifics of its mechanism. The WAVES program attempts to identify the processes that cause scour to be initiated at the downstream pier face. Table 7.3-4 shows the results of the downstream pier face scour for the 40-model comparative study at the case study sites.

Generally, three types of scour results were derived from the comparisons. The larger of the scour estimates at the upstream and downstream pier faces was used as the predicted maximum scour at the bridge pier. Since pier scour in real tidal rivers or estuaries does not progress separately or independently for both the upstream and downstream faces, it was necessary to interpret the meaning of the differences in the scour results for the upstream and downstream pier faces. This was done by defining the predicted maximum pier scour as the greater of the scour at the downstream and upstream pier faces at any given time. When only the ultimate or final scour results were considered, then the greater of the upstream or downstream pier face scour was the ultimate predicted maximum scour. The WAVES program computed the scour on both pier faces to identify which processes controlled the initiation and propagation of scour in a tidal environment. Ultimately, the design scour at a pier can be estimated as the greater of the scour initiated at the upstream and downstream pier face.

**Table 7.3-3. Results of the 40-Model comparative study for the upstream pier face. BLK, PAT, WICO, BAL, and MONIE represents the Black River, Patuxent River, Wicomico River, Baltimore Patapsco, and Monie Bay Sites, respectively. The pier scour values are recorded in feet. ARM natural indicates armoring.**

EQUATIONS	Variables	EQN	BLK.	PAT.	WICO.	BAL.	MONIE.
Breusers Eq. 1	B	1	7.0	7.0	7.0	7.0	7.0
Breusers Eq. 2	y,b	2	10.0	10.0	10.0	10.0	9.5
Laursens	y,b	3	9.5	10.6	11.3	15.4	7.5
Laursen & Tosh	y,b	4	10.4	11.1	11.5	13.8	9.0
Laursen & Neill	y,b	5	6.9	7.4	7.7	9.2	6.0
Inglis Eq. 1	Q,d <sub>50</sub>	6	15.7	19.9	26.6	27.5	9.4
Inglis Eq. 2	Q, d <sub>50</sub>	7	37.6	35.1	32.7	31.6	26.2
Sanchez	b, d <sub>50</sub> ,v	8	0.0	0.0	0.0	0.0	0.0
Shen	b,Nu,v	9	0.8	1.3	1.2	1.3	0.6
Larras	B	10	7.2	7.2	7.2	7.2	7.2
Hancu Eq. 1	b,y,v, d <sub>50</sub>	11	2.5	4.3	3.7	4.1	1.7
Hancu Eq. 2	b,y, d <sub>50</sub>	12	7.8	8.9	9.6	8.9	8.2
Froelichs	b,y,v, d <sub>50</sub>	13	6.1	7.3	7.5	11.9	4.9
Coleman Eq. 1	b,y,v	14	4.2	4.8	4.5	4.4	3.9
Coleman Eq. 2	b,y,v	15	0.4	1.1	0.9	1.6	0.1
Basak	B	16	2.3	2.3	2.3	2.3	2.3
Neill Eq. 1	Q,W,b, d <sub>50</sub>	17	7.1	12.8	24.1	20.5	3.0
Neill Eq. 2	B	18	7.5	7.5	7.5	7.5	7.5
Neill Eq. 3	b,y	19	11.5	12.8	13.7	18.6	9.1
Jain & Fischer	b,y,v, d <sub>50</sub>	20	0.0	8.4	5.6	10.8	0.0
Jain	b,y,v, d <sub>50</sub>	21	6.5	7.1	7.5	8.0	6.1
Chitale	B	22	12.5	12.5	12.5	12.5	12.5
CSU HEC-18	b,y,v, d <sub>50</sub>	23	4.3	6.1	5.7	6.6	3.0
Richardson & Davis	b,y,v, d <sub>50</sub>	24	4.3	6.1	5.7	6.6	3.0
Gao et at.	b,y, d <sub>50</sub> ,v	25	3.9	6.7	6.2	8.0	0.1
Melville Eq. 1	b,y, d <sub>50</sub>	26	5.7	9.1	7.2	9.1	0.0
Melville wave Eq. 2	A,y,T,b,C	27	0.0	0.0	0.0	0.0	0.0
Lacy Original	Q, d <sub>50</sub>	28	38.6	29.8	25.1	32.5	22.2
Lacy Revised	Q, d <sub>50</sub>	29	77.3	59.6	50.2	65.0	44.4
Arunachalams	Q,W,b, d <sub>50</sub>	30	6.7	7.4	8.4	8.9	4.5
Mustaq	Q,W,b	31	10.9	14.7	21.3	22.2	5.6
Blench Eq. 1	Q,y,b,W	32	2.6	2.0	5.1	0.0	0.8
Blench Eq. 2	Q,W,b	33	15.4	18.1	23.0	26.3	8.8
Sethis	Q,W, d <sub>50</sub>	34	16.8	20.6	28.3	34.1	7.9
RDSO	Y	35	25.2	31.3	35.6	65.8	15.7
Andrus	Q,W,b,v	36	6.9	12.1	16.4	18.0	2.9
Railways Ministry	Q, d <sub>50</sub>	37	81.7	63.0	53.1	68.7	47.0
Izzard	Q,W,b	38	12.0	16.2	23.6	24.5	6.2
Unified Model	y,b,W,v, d <sub>50</sub>	39	8.5	16.7	15.1	26.6	3.8
WAVES Ultimate Scour Equation	v,v <sub>t</sub> ,y, d <sub>50</sub> ,b	40	0.1	5.5	0.7	4.1	0.0
WAVES NO ARM		41	0.0	21.7	10.7	22.5	0.0
WAVES ARM		41	0.0	15.6	4.8	20.2	0.0

**Table 7.3-4. Results of the 40-Model comparative study for the downstream pier face. BLK, PAT, WICO, BAL, and MONIE represents the Black River, Patuxent River, Wicomico River, Baltimore Patapsco, and Monie Bay Sites, respectively. The pier scour values are recorded in feet. ARM indicates natural armoring.**

EQUATIONS	Variables	EQN	BLK.	PAT.	WICO.	BAL.	MONIE
Breusers Eq. 1	B	1	7.0	7.0	7.0	7.0	7.0
Breusers Eq. 2	y,b	2	10.0	10.0	10.0	10.0	9.6
Laursens	y,b	3	9.9	10.6	11.4	15.8	7.8
Laursen & Tosh	y,b	4	10.6	11.1	11.5	14.0	9.2
Laursen & Neill	y,b	5	7.1	7.4	7.7	9.4	6.1
Inglis Eq. 1	Q, d <sub>50</sub>	6	15.6	18.3	25.6	21.8	9.3
Inglis Eq. 2	Q, d <sub>50</sub>	7	37.4	33.3	31.9	25.3	26.1
Sanchez	b, d <sub>50</sub> , v	8	0.0	0.0	0.0	0.0	0.0
Shen	b, V, v	9	1.0	1.1	1.3	0.8	0.8
Larras	B	10	7.2	7.2	7.2	7.2	7.2
Hancu Eq. 1	b,y,v, d <sub>50</sub>	11	3.2	3.5	4.2	2.5	2.6
Hancu Eq. 2	b,y, d <sub>50</sub>	12	7.9	8.9	9.6	8.2	8.2
Froelichs	b,y,v, d <sub>50</sub>	13	6.6	7.0	7.7	11.3	5.1
Coleman Eq. 1	b,y,v	14	4.5	4.5	4.7	3.8	4.4
Coleman Eq. 2	b,y,v	15	0.6	0.8	1.2	0.7	0.3
Basak	B	16	2.3	2.3	2.3	2.3	2.3
Neill Eq. 1	Q,W,b, d <sub>50</sub>	17	7.0	10.9	22.3	11.8	3.0
Neill Eq. 2	B	18	7.5	7.5	7.5	7.5	7.5
Neill Eq. 3	b,y	19	11.9	12.8	13.7	19.0	9.4
Jain & Fischer	b,y,v, d <sub>50</sub>	20	5.9	5.5	8.1	0.0	0.0
Jain	b,y,v, d <sub>50</sub>	21	6.6	7.1	7.5	7.8	6.2
Chitale	B	22	12.5	12.5	12.5	12.5	12.5
CSU HEC-18	b,y,v	23	5.0	5.4	6.2	4.8	4.1
Richardson	b,y,v	24	5.0	5.4	6.2	4.8	4.1
Gao et al.	b,y d <sub>50</sub> , v	25	6.3	6.3	6.3	1.7	4.2
Melville Eq. 1	b,y, d <sub>50</sub>	26	8.0	7.4	8.4	5.4	4.8
Melville wave Eq. 2	A,y,T,b,C	27	0.0	0.0	0.0	0.0	0.0
Lacy Original	Q, d <sub>50</sub>	28	38.4	28.2	24.5	30.3	22.1
Lacy Revised	Q, d <sub>50</sub>	29	76.9	56.4	49.0	60.6	44.2
Arunachalams	Q,W,b, d <sub>50</sub>	30	6.7	7.0	8.2	8.3	4.4
Mustaqs	Q,W,b	31	10.7	13.1	20.3	16.5	5.5
Blench Eq. 1	Q,y,b,W	32	1.4	0.4	4.0	0.3	0.1
Blench Eq. 2	Q,W,b	33	15.3	16.6	22.2	22.2	8.7
Sethis	Q,W, d <sub>50</sub>	34	16.6	18.4	27.0	27.5	7.8
RDSOs	Y	35	26.9	31.3	35.9	68.8	16.7
Andrus	Q,W,b,v	36	7.7	9.8	16.7	10.5	3.5
Railways Ministry	Q, d <sub>50</sub>	37	81.3	59.6	51.8	64.1	46.8
Izzard&	Q,W,b	38	11.9	14.5	22.4	18.3	6.1
Unified Model	y,b,W,v, d <sub>50</sub>	39	11.5	13.3	17.7	16.3	6.4
Demetrius Ultimate Scour	v, v <sub>t</sub> , y, d <sub>50</sub> , b	40	8.5	8.3	13.0	0.0	7.2
WAVES NO ARM		42	19.5	18.8	19.8	0.0	19.2
WAVES ARM		43	0.0	0.0	19.8	0.0	0.0

A summary of the predicted maximum ultimate scour results of the 40-model comparison exercise for the predicted maximum scour is shown in Table 7.3-5. Details of the results of the simulations from the 40 models obtained from the literature are provided in Appendix E-3. The results are discussed below relative to the HEC -18 (No. 23), Froelich (No. 13), Laursen and Tosh (No. 4), Hancu (No. 11), and the Jain and Fischer (No. 20) models, as these models were identified by most researchers as the most accurate and widely used pier scour models.

### **7.3.3 Tide-Controlled Sites: Monie Bay and Black River**

#### **7.3.3.1 Upstream Pier Face**

The results presented in Table 7.3-3 show that scour was not predicted by the WAVES program at the upstream pier face for either the Monie Bay or Black River sites for the 100-year simulation period. This result was expected at these tide-controlled sites because they are dominated by the downstream processes. Most of the current equations and models used in the comparative study predicted significant scour on the upstream pier face. Notable, however, was the fact that the model developed by Jain and Fischer (No. 20), one of the five models used as a benchmark for accuracy, also did not predict scour at the upstream pier faces of the Monie Bay and Black River piers. Table 7.3-3 also shows that Hancu (No. 11) and HEC-18 (No. 23) predicted minor scour over the 100-year duration at the upstream pier face. In contrast, Froelich (No. 13) predicted scour on the upstream pier face of 4.8 and 6.1 ft, respectively, for the Monie Bay and Black River sites. Laursen and Tosh (No. 4) predicted scour at the upstream pier face of 9.0 and 10.38 feet, respectively, for these two sites. Table 7.3-3 shows that the Laursen and Tosh model (No. 4) in particular, greatly over-predicted the WAVES program.

**7.3-5. Final predicted maximum scour results determined by the 40 models tested. BLK, PAT, WICO, BAL, and MONIE represents the Black River, Patuxent, River, Wicomico River, Baltimore Patapsco, and Monie Bay Sites, respectively. The pier scour values are recorded in feet. ARM indicates natural armoring.**

EQUATIONS	Variables	EQN	BLK.	PAT.	WICO.	BAL.	MONIE.
Breusers Eq. 1	b	1	7.0	7.0	7.0	7.0	7.0
Breusers Eq. 2	y,b	2	10.0	10.0	10.0	10.0	9.6
Laursens	y,b	3	9.9	10.6	11.4	15.8	7.8
Laursen & Tosh	y,b	4	10.6	11.1	11.5	14.0	9.2
Laursen & Neill	y,b	5	7.1	7.4	7.7	9.4	6.1
Inglis Eq. 1	Q,d <sub>50</sub>	6	15.7	19.9	26.6	27.5	9.4
Inglis Eq. 2	Q, d <sub>50</sub>	7	37.6	35.1	32.7	31.6	26.2
Sanchez	B, d <sub>50</sub> ,v	8	0.0	0.0	0.0	0.0	0.0
Shen	b,Nu,v	9	1.0	1.3	1.3	1.3	0.8
Larras	b	10	7.2	7.2	7.2	7.2	7.2
Hancu Eq. 1	b,y,v, d <sub>50</sub>	11	3.2	4.3	4.2	4.1	2.6
Hancu Eq. 2	B,y, d <sub>50</sub>	12	7.9	8.9	9.6	8.9	8.2
Froelichs	b,y,v, d <sub>50</sub>	13	6.6	7.3	7.7	11.9	5.1
Coleman Eq. 1	b,y,v	14	4.5	4.8	4.7	4.4	4.4
Coleman Eq. 2	b,y,v	15	0.6	1.1	1.2	1.6	0.3
Basak	b	16	2.3	2.3	2.3	2.3	2.3
Neill Eq. 1	Q,W,b, d <sub>50</sub>	17	7.1	12.8	24.1	20.5	3.0
Neill Eq. 2	b	18	7.5	7.5	7.5	7.5	7.5
Neill Eq. 3	b,y	19	11.9	12.8	13.7	19.0	9.4
Jain & Fischer	b,y,v, d <sub>50</sub>	20	5.9	8.4	8.1	10.8	0.0
Jain	b,y,v, d <sub>50</sub>	21	6.6	7.1	7.5	8.0	6.2
Chitale	b	22	12.5	12.5	12.5	12.5	12.5
CSU HEC-18	b,y,v, d <sub>50</sub>	23	5.0	6.1	6.2	6.6	4.1
Richardson	b,y,v, d <sub>50</sub>	24	5.0	6.1	6.2	6.6	4.1
Gao et at.	b,y, d <sub>50</sub> ,v	25	6.3	6.7	6.3	8.0	4.2
Melville Eq. 1	B,y, d <sub>50</sub>	26	8.0	9.1	8.4	9.1	4.8
Melville wave Eq. 2	A,y,T,b,C	27	0.0	0.0	0.0	0.0	0.0
Lacy Original	Q, d <sub>50</sub>	28	38.6	29.8	25.1	32.5	22.2
Lacy Revised	Q, d <sub>50</sub>	29	77.3	59.6	50.2	65.0	44.4
Arunachalams	Q,W,b, d <sub>50</sub>	30	6.7	7.4	8.4	8.9	4.5
Mustaqs	Q,W,b	31	10.9	14.7	21.3	22.2	5.6
Blench Eq. 1	Q,y,b,W	32	2.6	2.0	5.1	0.3	0.8
Blench Eq. 2	Q,W,b	33	15.4	18.1	23.0	26.3	8.8
Sethis	Q,W, d <sub>50</sub>	34	16.8	20.6	28.3	34.1	7.9
RDSOs	Y	35	26.9	31.3	35.6	68.8	16.7
Andrus	Q,W,b,v	36	7.7	12.1	16.7	18.0	3.5
Railways Ministry	Q, d <sub>50</sub>	37	81.7	63.0	55.7	68.7	47.0
Izzard	Q,W,b	38	12.0	16.2	23.6	24.5	6.2
Unified Model	y,b,W,v, d <sub>50</sub>	39	11.5	16.7	17.7	26.6	6.4
WAVES Ultimate Scour	v,v <sub>t</sub> ,y, d <sub>50</sub> ,b	40	8.5	8.3	13.0	4.1	7.2
WAVES NO ARM		41	20.0	21.7	19.8	22.5	19.2
WAVES ARM		41	0.0	15.6	19.8	20.2	0.0

### **7.3.3.2 Downstream Pier Face**

The results presented in Table 7.3-4 shows that significant scour was predicted by the WAVES program at the downstream pier faces of both the Monie Bay and Black River case study sites for the 100-year simulation period. The WAVES program predicted 19 ft of scour at the downstream pier faces at both sites when natural armoring was not considered. However, when natural armoring was considered the WAVES program predicted insignificant amounts of scour at both sites. This result was expected because tide-controlled sites are dominated by downstream processes.

Most of the models used for comparison predicted insignificant downstream pier face scour at the Monie Bay and Black River sites when compared to the unarmored results predicted by the WAVES program. Jain and Fischer (No. 20) predicted zero scour initiated from the downstream pier face at the Monie Bay, and a 100-year scour of 6 feet at the Black River site. In addition, Hancu (No. 11), HEC-18 (No. 23), and Froelich (No. 13) predicted approximate scour values of 2.6, 4.0, and 5.0 feet, respectively, for the downstream pier face scour at Monie Bay, and 3.2, 5.0, and 6.6 feet, respectively, for the downstream pier face scour at Black River Bay. In contrast, Laursen and Tosh (No. 4) predicted downstream pier face scour of 9.2 and 10.6 feet at Monie Bay and Black River, respectively. This was due to the fact that the predictions of the Laursen and Tosh model was heavily dependent on the flow depth at the sites, which being estuarine, were generally high.



### **7.3.3.3 Maximum Predicted Pier Scour Results**

As indicated earlier, the Monie Bay and Black River site were classified as tide-controlled estuaries. This suggests that the scour hole development process was governed by the tidal hydrologic and hydraulic processes and initiated from the downstream face of the pier. This is the most important feature of scour in tide-controlled environments, and as a result the predicted scour at the downstream pier face was significantly greater than the scour predicted at the upstream face.

The mean and standard deviation for the scour results of the Monie Bay and Black River sites provided an indication of the consistency of the results obtained from the benchmark models and the ability of these models to identify the dominant process (tidal of catchment) at the tide-controlled sites. Table 7.3-6 shows the means and standard deviations for the five benchmark models for the downstream pier face scour, upstream pier face scour, and the maximum predicted pier scour. The mean upstream pier face scour was 4.66 ft at the Black River site and 3.69 ft at Monie Bay. The mean downstream pier face scour was 6.25 ft at Black River and 4.18 ft at Monie Bay. Comparing the upstream and downstream pier face results predicted at these two sites led to the conclusion that the mean predicted maximum scour produced by the five benchmark models was 6.25 ft at Black River and 4.18 ft at Monie Bay. The table shows that the mean scour estimates provided by the five models correctly identified the downstream pier faces at Monie Bay and Black River as the location from which the pier scour would most likely be generated. This was noted by the fact that the mean scour for the downstream pier face was greater than that of the upstream pier face at both sites. This is fully consistent with the expected scour mechanism and with the results produced

by the WAVES program. The standard deviations in the predictions of the benchmark models were 2.73 ft at the Black River site and 3.38 ft at Monie Bay. The value of the standard deviation at the Black River Site indicates some similarity in the predictions of the benchmark models. However, the spread in the predictions was greater at Monie Bay.

The mean maximum scour estimates predicted by the five benchmark models were relatively low when compared the scour predicted by the WAVES program. These models under predicted the WAVES program, which provided scour estimates of 20 ft and 19 ft, respectively, for the Black River and Monie Bay sites. These results support the hypothesis that continuous models provide more conservative predictions than single-event scour models included in the analysis. This may be attributed to the fact that continuous models account for the aggregate of all the incidences of scour during a given period.

**Table 7.3-6. Mean and standard deviation for the pier scour results provided by the five benchmark models at Black River (BLK) and Monie Bay (MONIE). US, DS, and C indicate the results for the upstream pier face, downstream pier face and the predicted maximum scour, respectively. M is the mean scour and S the standard deviation in the scour results**

		BLK.	MONIE.
<b>US</b>	M (ft)	4.66	3.69
<b>US</b>	S (ft)	3.91	3.45
<b>DS</b>	M (ft)	6.25	4.18
<b>DS</b>	S (ft)	2.73	3.38
<b>C</b>	M (ft)	6.25	4.18
<b>C</b>	S (ft)	2.73	3.38

An understanding of the mean maximum scour predicted by the test models is necessary to explain the predictions and validity of these models in tide-controlled estuarine environments. The results shown in Table 7.3-7 indicate that the mean scour at

the downstream face of the pier is the mean maximum scour for both the Black River and Monie Bay sites. These results may be interpreted as an indication that most of the 40 models tested correctly identified the downstream pier face as the location of the initiation and generation of scour in tide controlled environments. The mean maximum predicted scour values of 13.1 ft and 8.6 ft for Black River and Monie Bay, respectively, were closer to the predictions made using the WAVES than the mean scour values predicted by the benchmark models. However, the large standard deviations 17.5 ft and 10.2 ft, respectively, reflect the very large spread and variance in the predictions. The differences in the mean predictions between the benchmark models and the full 40-model set can be attributed to the predictors used by the respective models. The scour estimates produced by most of the five benchmark models were dependent on the streamflow velocity of the estuary, which are usually much lower than the streamflow velocities in riverine systems. In contrast many of the models in the set of 40 used flow depth and discharge as predictors. In estuarine systems these variables tend to be very high and this in turn leads to high scour predictions.

**Table 7.3-7. Mean and standard deviation for the pier scour results provided by the 40 models used in the comparative exercise at Black River and Monie Bay. US, DS, and C indicate the results for the upstream pier face, downstream pier face and the predicted maximum scour, respectively. M is the mean scour and S the standard deviation in the scour results.**

		BLK.	MONIE
<b>US</b>	M (ft)	12.36	7.93
<b>US</b>	S (ft)	17.81	10.46
<b>DS</b>	M (ft)	13.01	8.53
<b>DS</b>	S (ft)	17.47	10.15
<b>C</b>	M (ft)	13.08	8.57
<b>C</b>	S (ft)	17.54	10.18

Figure 7.3-1 represents the scour results predicted for the 40 models at Monie Bay. The figure shows that 75% of the models predicted that scour on the downstream face of the pier would be greater than 10 ft, compared with the 68% of the models that predicted scour on the upstream face to be greater than 10 ft. In addition, 48% of the models indicated that scour on the upstream face of the pier would be less than 10 ft as compared to 40% of the models that predicted the same for the downstream face of the pier. These results further indicate that most models correctly identified that scour would be initiated from the downstream face of the pier at the Monie Bay site.

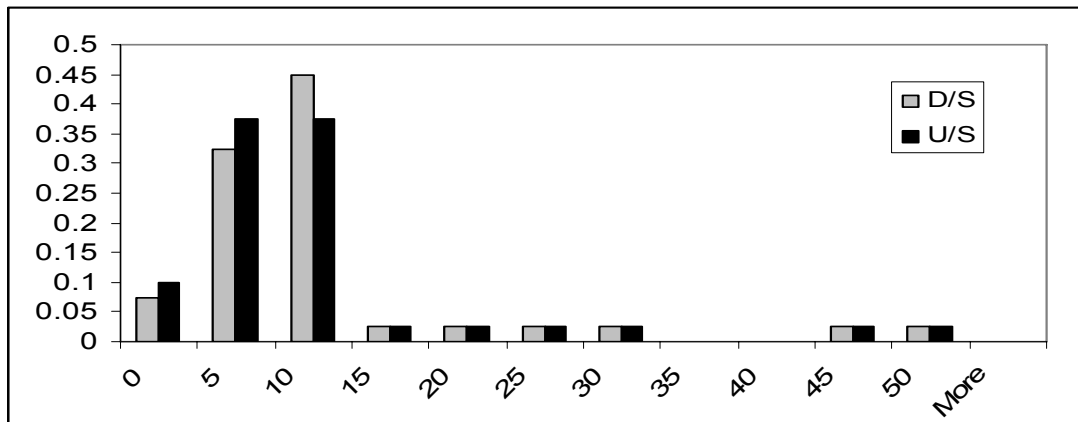


**Figure 7.3-1. Probability histogram representing the 40-Model scour results for the tide-controlled Monie Bay site. The horizontal axis represents the pier scour ranges in feet, while the vertical axis is the probability of occurrence.**

The ability to predict the downstream face of the pier as the location at which scouring would be initiated in tide control environments should be provided by all models used to predict scour in these estuarine environments. Most of the models predicted that there would be more scouring initiated at the downstream pier face of the tide-controlled sites. Figure 7.3-2 represents the predicted maximum scour results for the 40 models at the Black River site. The figure shows that 78% of the models predicted

that scour on the downstream face of the pier would be greater than 10 ft, compared with the 67% of the models that predicted scour on the upstream face to be greater than 10 ft. In addition, 32% of the models indicated that scour on the upstream face of the pier would be less than 10 ft as compared to 20% of the models that predicted the same for the downstream face of the pier. These results further indicate that most models correctly identified that scour would be initiated from the downstream face of the pier at the Black River site.

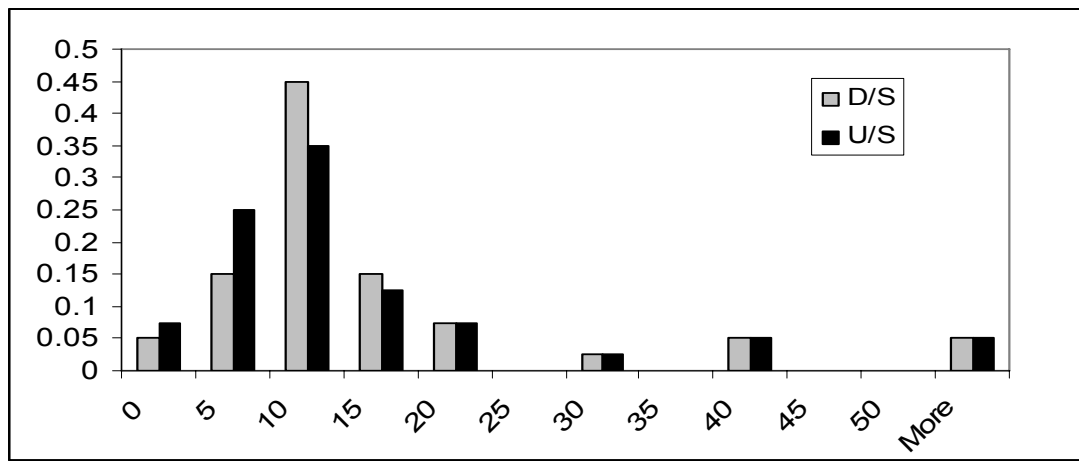


**Figure 7.3-2. Probability histogram representing the 40-Model scour results for for the tide-controlled Black River site. The horizontal axis represents the pier scour ranges in feet, while the vertical axis is the probability of occurrence.**

One of the objectives of the 40-model comparative analysis was to assess whether single-event models that were developed for scour in upland rivers would predict scour amounts that differed from the WAVES program when used in tide-controlled estuaries. Figures 7.3-3 and 7.3-4, respectively, provide summaries of the predicted maximum scour results obtained from the empirical models and the WAVES program for the Monie Bay and Black River sites. For these sites, model numbers 7, 28, 29, and 37 were the only models that produced scour results that were greater than the WAVES simulations without armoring. Table 7.2-1 indicates that models 7, 28, 29, and 37 were bivariate

models using total discharge and the mean particle diameter as predictors. In addition, model No. 35, a univariate model that depends only on flow depth, also predicted slightly larger scour at the Black River site when compared to the WAVES program without armoring. The results indicate that the five benchmark models may over-predict when used to determine pier scour in estuaries and tidal rivers. It may also be observed that armoring had a significant impact on the final scour results for these tide-dominated sites as in both cases scour was reduced to zero when natural armoring was simulated. The figures also indicate that Model No. 1, which was developed by Breseurs using field scour data from estuaries, predicted values lower than the WAVES program and most of the 40 models tested. In addition, the scour predicted by Model No. 1 was dependent on the pier diameter only and hence did not vary with site conditions. A significant feature of estuaries and tidal rivers is the complex hydraulic processes that interact to produce scour conditions. Therefore, it is unlikely the Breseurs model could provide reliable results in tidal environments by predicting scour without considering these complex hydraulic factors.

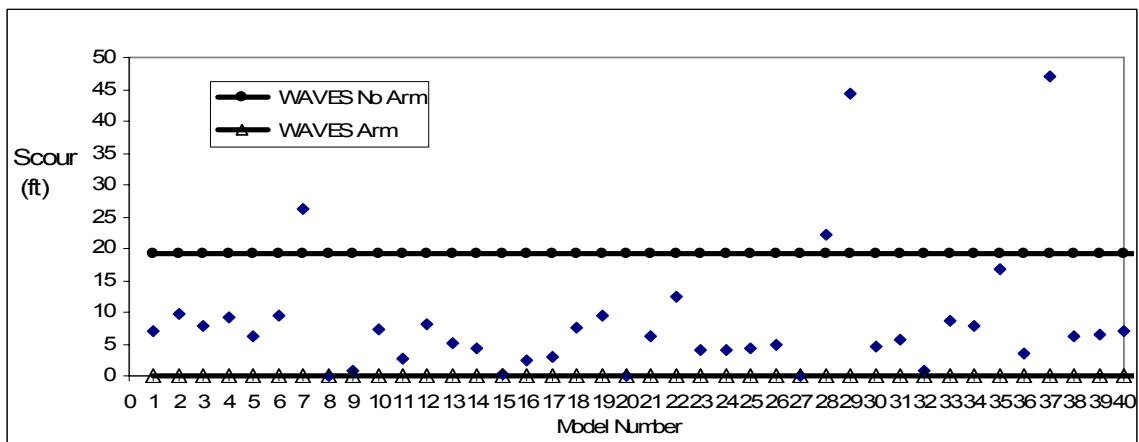


**Figure 7.3-3. Results of the 40-model study at Monie Bay in comparison to the Predicted Maximum Scour results obtained from the WAVES Program. Arm indicates the use of the natural armoring option in WAVES. No Arm indicates that natural armoring was not considered.**

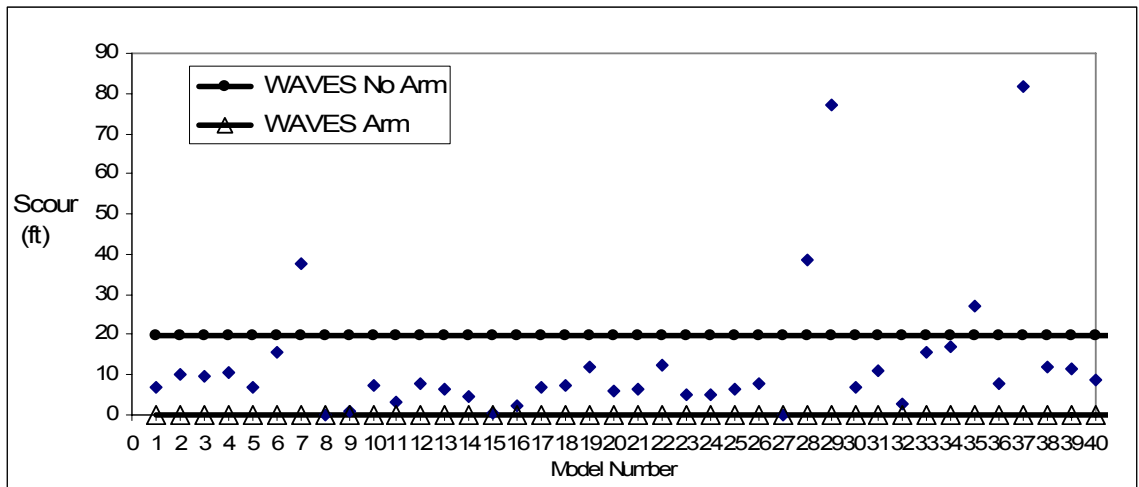


**Figure 7.3-4. Results of the 40-model study at Black River in comparison to the Predicted Maximum Scour results obtained from the WAVES Program. Arm indicates the use of the natural armoring option in WAVES. No Arm indicates that natural armoring was not considered.**

### 7.3.4 Mixed-Control Sites: Patuxent and Wicomico Rivers

#### 7.3.4.1 Upstream Pier Face

Mixed control sites are those sites that have significant tidal and catchment influences. Therefore, it is expected that pier scour could be controlled by the activities that occur at either of the pier faces, upstream or downstream. The results presented in Table 7.3-3 show that the Patuxent and Wicomico River sites had significant 100-year scour at the upstream pier face when modeled by the WAVES program. Table 7.3-3 shows a 100-year upstream pier face scour of 21 feet at the Patuxent site and 10.7 feet at the Wicomico site when armoring was not considered. With simulations including natural armoring, the upstream pier face scour results predicted by the WAVES program were 15.6 ft at the Patuxent site and 4.8 ft at the Wicomico site. The Jain and Fischer model (No. 20) predicted the scour generated from the upstream pier faces at the Patuxent and Wicomico sites to be 8.4 and 5.6 feet, respectively. In addition, Hancu (No. 11) predicted approximately 4 feet of scour for both sites, while HEC-18 (No. 23)

predicted approximately 6 feet of scour for both sites. In contrast, Froelich (No. 13) and Laursen and Tosh (No. 4) predict scour at the upstream pier face of 7.5 feet and 11 feet, respectively, for both sites. The values predicted by the Laursen and Tosh model in particular appears to be closer to the predictions of the WAVES program at these two sites.

#### **7.3.4.2 Downstream Pier Face**

The WAVES program predicted significant 100-year scour at the downstream pier faces at the Patuxent and Wicomico River sites, both of which have both tidal and catchment inputs. Table 7.3-4 shows a 100-year downstream pier face scour of 19 ft at the Patuxent site and 20 ft at the Wicomico site when armoring was not considered. With natural armoring, the WAVES program predicted zero scour at the Patuxent site, while at the Wicomico site the final 100-year scour remained at 20 feet. The WAVES program results obtained with natural armoring were significantly affected by the channel bed material at the Patuxent and Wicomico River sites. The bed material at the Patuxent River site was coarse and well graded, while in contrast the bed materials at the Wicomico River site were much finer and uniformed.

In general, the WAVES program predicted higher scour values than the five benchmark models at the downstream pier faces of the mixed-control sites. The Jain and Fischer model (No. 20) predicted scour of 5.5 and 8.1 feet on the downstream pier faces at the Patuxent and Wicomico sites, respectively. Hancu (No. 11) predicted approximately 4 feet of scour for both sites, while HEC-18 (No. 23) predicted 5.4 ft and 6.2 ft scour, respectively, for these sites. Froelich (No. 13) and Laursen and Tosh (No. 4)



predicted downstream pier face scour of approximately 7.5 feet and 11.5 feet, respectively. The lower predictions of the five benchmark models, when compared to the WAVES program, could be attributed to the fact that their predictions were based on single-value estimates of a design storm condition and did not take into consideration the continuous nature of the scour process.

#### **7.3.4.3 Maximum Predicted Pier Scour Results**

Because the Wicomico and Patuxent River sites were classified as mixed control sites, the development of scour at either site was affected by both the tidal and catchment hydrologic and hydraulic processes and could be initiated from either the downstream or upstream face of the pier. As a result, scour models should predict significant scour at both the upstream and downstream pier faces with the greater of the two scour values being considered the maximum predicted scour result. It was also expected that with a mixed-control site the resultant maximum predicted scour could be obtained from either pier face.

As was the case with tide-controlled environments, models that use the total cross section discharge and flow depth as predictor variables will most likely provide unreliable results, while models that attempt to incorporate hydraulic consideration, such as the resultant velocity of flow, will be more accurate. Table 7.3-8 shows the mean and standard deviation of the results provided by the five benchmark models for the downstream pier face scour, upstream pier face scour, and the maximum predicted pier scour for the mixed-control sites. The table shows that the mean results provided by the five benchmark models also correctly identified either pier face as the location from

which the pier scour would most likely be generated. For the Patuxent site, the table indicates the upstream pier face as the location where scour would develop, while for the Wicomico site this location was identified as the downstream pier face. This result is fully consistent with the expected scour mechanism and with the results produced by the WAVES program.

**Table 7.3-8. Mean and standard deviation for the pier scour results of the five benchmark models at the Patuxent (PAT.) and Wicomico (WICO.) Rivers. US, DS, and C represent the upstream Pier Face, Downstream Pier Face and the maximum predicted scour, respectively. M is the mean scour and S the standard deviation in the scour results**

		PAT.	WICO.
US	M (ft)	7.42	6.80
US	S (ft)	2.54	2.96
DS	M (ft)	6.48	7.57
DS	S (ft)	2.86	2.70
C	M (ft)	7.42	7.57
C	S (ft)	2.54	2.69

Table 7.3-8 also shows that the five benchmark models predicted mild to insignificant scour over the 100-year period with a mean combined scour of 7.4 and 7.6 ft at the Patuxent and Wicomico sites, respectively. These scour results produce annual scouring at a slow rate of 0.07 ft per year. The standard deviations (2.5 ft and 2.7 ft) again indicated the uniformity of the predictions of the five benchmark models. Although consistent, these models again predicted less scour than that predicted by the WAVES program, which produced 21.7 ft and 19.8 ft of scour, respectively, for the Patuxent and Wicomico River sites. These results support the hypothesis that continuous models provide more conservative predictions than single value single-event scour models.

At a mixed-control site, pier scour may be slightly dominated by the processes at either the upstream or downstream pier faces. The results shown in Table 7.3-9 indicate that most of the 40 models tested correctly identified the face of that was more influential in the initiation and generation of scour at the Patuxent and Wicomico River sites. This is determined from the fact that the table shows the maximum predicted scour as being approximately equal to the mean downstream face scour at the Wicomico River Site, while in contrast, the maximum predicted scour was approximately equal to the mean upstream face scour at the Patuxent River Site. The maximum predicted scour values of 13.2 ft and 14.2 ft for Patuxent and Wicomico sites, respectively, also appear to be more conservative than the mean scour values predicted by the benchmark models. However, the large standard deviations 13.8 ft and 12.8 ft, respectively, reflect the very large spread and variance in the results predicted.

**Table 7.3-9. Mean and standard deviation for the pier scour results of the 40 models used in the comparison exercise at the Patuxent (PAT.) and Wicomico (WICO.) Rivers. US, DS, and C represent the upstream Pier Face, Downstream Pier Face and the maximum predicted scour, respectively. M is the mean scour and S the standard deviation in the scour results.**

		PAT.	WICO.
US	M (ft)	13.17	13.63
US	S (ft)	13.76	12.86
DS	M (ft)	12.19	13.86
DS	S (ft)	13.15	12.25
C	M (ft)	13.17	14.23
C	S (ft)	13.76	12.81

The 40-model comparison study was also made to determine whether or not single-event models would predict significant scour at both the upstream and downstream pier faces in mixed-controlled sites. Figures 7.3-5 and 7.3-6 represent the scour results predicted for the 40 models at the Patuxent River and Wicomico River sites, respectively.

The figures show that 80% of the models predicted that scour on both the upstream and downstream pier faces would be greater than 10 ft. These results imply that most models identified that scour could be initiated from either the upstream or downstream face of the pier at the Patuxent River site.

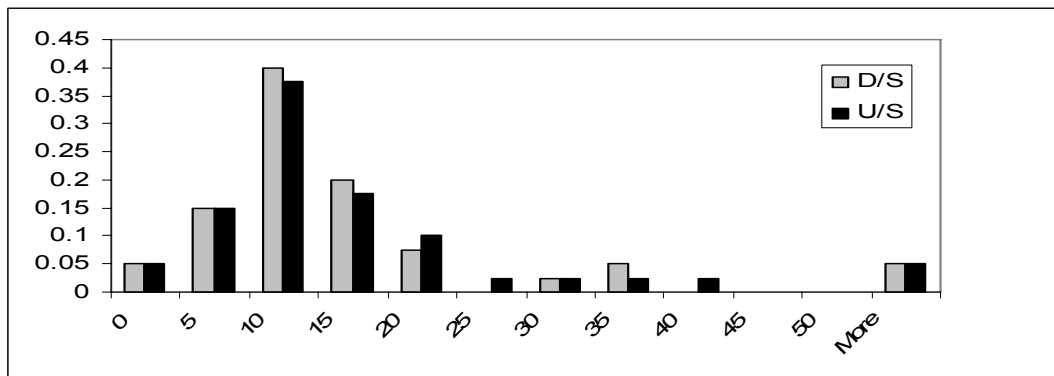


**Figure 7.3-5. Probability histogram representing the 40-Model scour results for for the mixed -control Patuxent River site. The horizontal axis represents the pier scour ranges while the vertical axis is the probability of occurrence.**

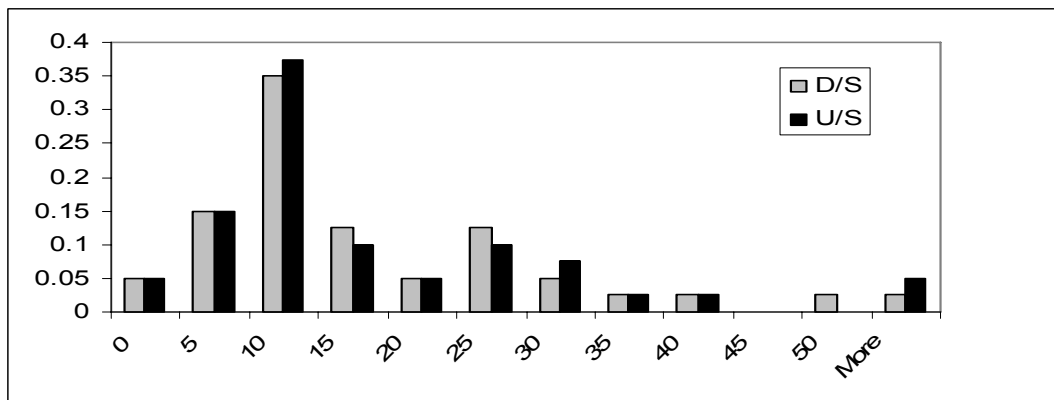


**Figure 7.3-6. Probability histogram representing the 40-Model scour results for for the mixed-control Wicomico River site. The horizontal axis represents the pier scour ranges while the vertical axis is the probability of occurrence.**

One of the objectives of the 40-model comparative analysis was to assess whether single-event models would predict scour amounts that differed from the WAVES program when used in mixed-controlled estuaries. Figures 7.3-7 and 7.3-8, respectively, provide summaries of the comparison of the results obtained from the empirical models

and the WAVES continuous model for the mixed control sites (the Patuxent and Wicomico rivers). For these sites, the bivariate and discharge dependent models (7, 28, 29, and 37 along with model No. 35) were among the models that produced greater scour estimates than the WAVES simulations without armoring. As indicated earlier, model no. 35 is a univariate model that depends on flow depth only. The results produced by these models are, therefore, likely to be unreliable when used to determine pier scour in estuaries and tidal rivers. It can also be observed that natural armoring did not have an impact on the WAVES predictions at the Wicomico site while natural armoring at the Patuxent River site caused significant scour reductions as predicted by the WAVES program.

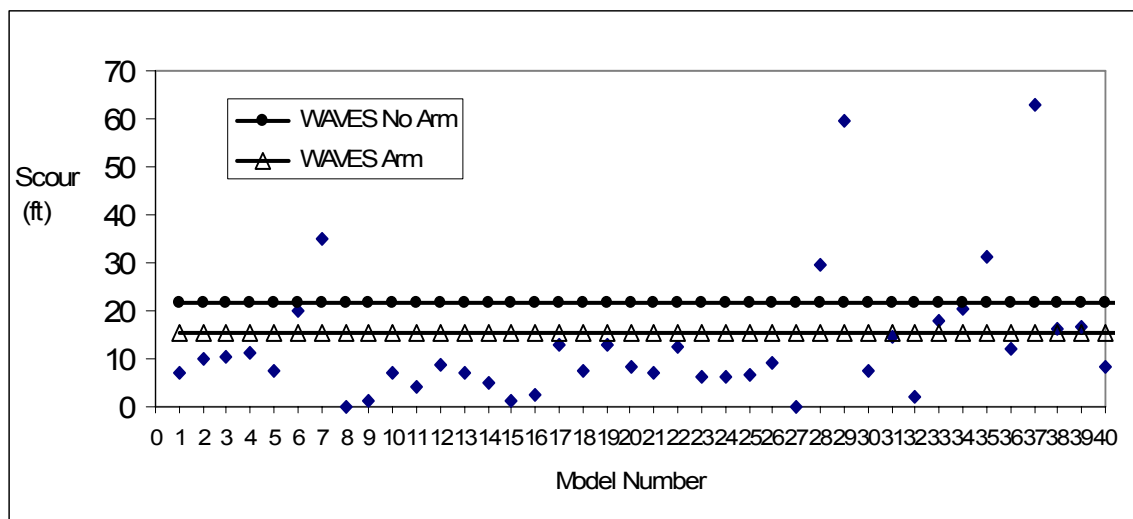


**Figure 7.3-7. Results of the 40-model study at Patuxent at Benedict in comparison to the Predicted Maximum Scour results obtained from the WAVES Program. Arm indicates the use of the natural armoring option in WAVES. No Arm indicates that natural armoring was not considered.**

Figures 7.3-7 and 7.3-8 also indicate that the Breseurs model (No. 1) again under predicted the WAVES program and most of the 40 models tested. As was the case with

the tide-controlled estuaries, the Breseur model may not provide reliable results in mixed-control estuary environments. This is due to the fact that the model uses only the pier diameter as a predictor and does not account for the complex hydraulic processes that interact to produce the typically lower stream velocities in the mixed-control estuaries.

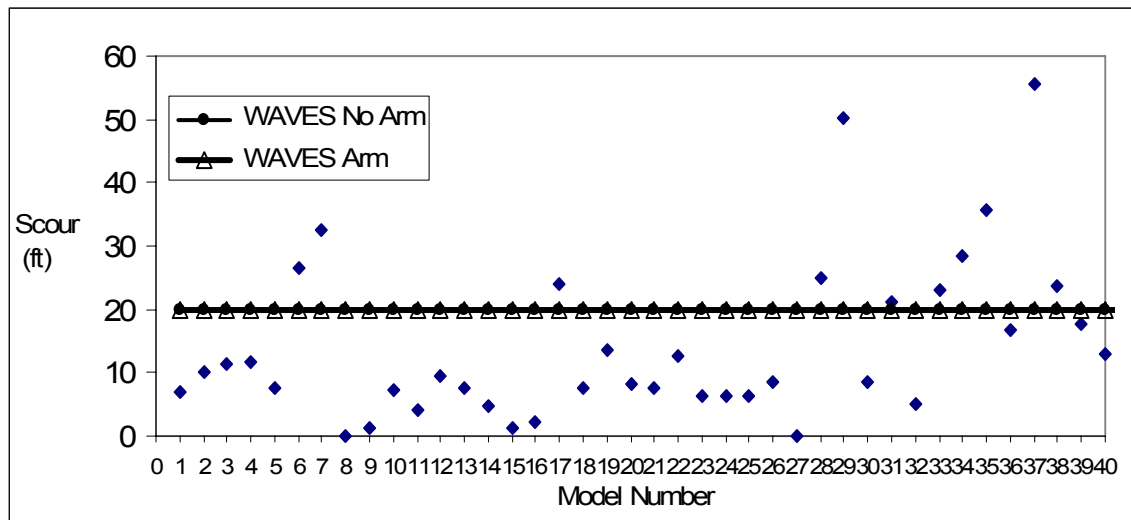


**Figure 7.3-8. Results of the 40-model study at Wicomico River in comparison to the Predicted Maximum Scour results obtained from the WAVES Program. Arm indicates the use of the natural armoring option in WAVES. No Arm indicates natural armoring was not considered.**

### 7.3.5 Catchment-Controlled Site: Baltimore Patapsco

#### 7.3.5.1 Upstream Pier Face

Table 7.3-3 shows the 100-year upstream pier face scour predicted by the WAVES program at the catchment-controlled Baltimore Patapsco site. The WAVES program estimated the 100-year upstream pier face scour of 22.5 feet without armoring and 20 feet with armoring. This result was wholly consistent with the fact that this site was catchment dominated and more subject to the upstream hydrologic processes.

Table 7.3-3 also shows the upstream pier face scour results provided by the five benchmark models at the Baltimore catchment-controlled site. Jain and Fischer (No. 20) predicted an upstream pier face scour of 10.8 feet while Hancu (No. 11) and HEC-18 (No. 23) predicted 4.1 and 6.6 feet, respectively. In contrast, Froelich (No. 13) and Laursen and Tosh (No. 4) predicted upstream pier face scour of 11.9 and 13.8 feet, respectively. All of the predictions were less than the scour predicted by the WAVES program. In particular, Hancu (No. 11) and HEC-18 (No. 23), which depended on stream velocities, predicted much lower scour values than the other benchmark models.

#### **7.3.5.2 Downstream Pier Face**

Table 7.3-4 shows the 100-year downstream pier face scour predicted by the WAVES program at the catchment-controlled Baltimore Patapsco site for simulations done with and without natural armoring. In both cases the total scour predicted by the WAVES program was zero. This result was consistent with the fact that this site was catchment dominated and more subject to the upstream hydrologic processes. Hence, as expected, the table shows that scour would not be initiated at the downstream pier face.

The downstream pier face scour for the Baltimore Patapsco site was also shown in Table 7.3-4. Jain and Fischer (No. 20) predicted scour did not occur at the downstream pier face and was in close agreement with the WAVES program. Hancu (No. 11) and HEC-18 (No. 23) predicted downstream pier face scour of 2.5 and 4.8 feet, respectively. In contrast, Froelich (No. 13) and Laursen and Tosh (No. 4) predicted upstream pier face scour of 11.3 and 14.0 feet, respectively. These results indicate that the Froelich (No. 13)

and Laursen and Tosh (No. 4) models may not provide reliable information concerning the location of the point at which pier scour is initiated in a catchment-controlled estuary.

### 7.3.5.3 Maximum Predicted Scour Results

The Patapsco River at Baltimore site is an example of a catchment-controlled site that was used to compare the scour predictions made by the benchmark models with the predictions made by the WAVES program. Table 7.3-10 shows the mean and standard deviation of the results provided by the five benchmark models for the downstream pier face scour, upstream pier face scour, and the maximum predicted pier scour at the Baltimore Patapsco site. The table shows that the mean scour provided by these models correctly identified the upstream pier face as the location from which the pier scour would most likely be generated. This was noted by the fact that the mean scour of 9.46 ft for the upstream pier face was greater than the mean scour of 6.53 ft predicted at the downstream pier face, and approximately equal to the mean maximum predicted scour of 9.49 ft. This result was again fully consistent with the expected scour mechanism and with the results produced by the WAVES program.

**Table 7.3-10. Mean and standard deviation for the pier scour results of the five benchmark models at the Baltimore (BAL) Patapsco River site. US, DS, and C represent the upstream Pier Face, Downstream Pier Face and the maximum predicted scour, respectively. M is the mean scour and S the standard deviation in the scour results.**

		BAL.
US	M (ft)	9.46
US	S (ft)	3.99
DS	M (ft)	6.53
DS	S (ft)	5.93
C	M (ft)	9.49
C	S (ft)	4.04



The comparison between the results provided by the benchmark models and those obtained from WAVES at a catchment-controlled site provides an indication of the large difference in the predictions made between continuous and single-event models. Table 7.3-10 also shows that the five benchmark models again predicted significant scour over the 100-year period with a mean maximum predicted scour of 9.5 ft. This result represents an average annual scour rate of 0.1 ft per year. The standard deviation of 4.0 ft again indicated the large spread of the predictions made by the five benchmark models. Although consistent, these models again under predicted the WAVES program, which produced 22.5 ft, and 20.5 ft of scour for the no-armoring and armoring conditions, respectively.

The predictions of the 40 test models at the Baltimore Patapsco site may be used to determine whether or not the test models will be suitable for catchment-controlled estuaries. The results shown in Table 7.3-11 indicate that most of the 40 models tested will correctly identify the upstream pier face as the location of the initiation and generation of scour in a catchment controlled environment. This is determined from the fact that the table shows the mean maximum predicted scour 16.64 ft was approximately equal to the mean upstream face scour of 16.53 ft. The mean maximum predicted scour also appeared to be closer to the 100-year scour of 20 ft predicted by the WAVES model. Again, the standard deviation of 17.5 ft, reflects the very large spread and variance in the results predicted. The magnitude of the mean scour prediction and the associated spread of the results were impacted by the very large scour results produced by those models using only total discharge and flow depth as predictors.

**Table 7.3-11. Mean and standard deviation for the pier scour results of the 40 models used in the comparison exercise at the Baltimore (BAL) Patapsco River site. US, DS, and C represent the upstream Pier Face, Downstream Pier Face and the maximum predicted scour, respectively. M is the mean scour and S the standard deviation in the scour results.**

		BAL.
<b>US</b>	M (ft)	16.53
<b>US</b>	S (ft)	17.25
<b>DS</b>	M (ft)	13.98
<b>DS</b>	S (ft)	16.68
<b>C</b>	M (ft)	16.64
<b>C</b>	S (ft)	17.47

The use of a probability histogram also provides a good method of assessing the results from the 40 single-event models at a catchment-controlled site. Figure 7.3-9 represents the scour results predicted for the 40 models at the Patapsco River site. The figure shows that 79% of the models predicted that scour on the upstream face of the pier would be greater than 10 ft, compared with the 21% of the models that predicted scour on the downstream face to be greater than 10 ft. In addition 37% of the models indicated that scour on the upstream face of the pier would be less than 10 ft as compared to 63% of the models that predicted the same for the downstream face of the pier. These results further indicate that most models correctly identified that scour would be initiated from the upstream face of the pier at the Patapsco River site.

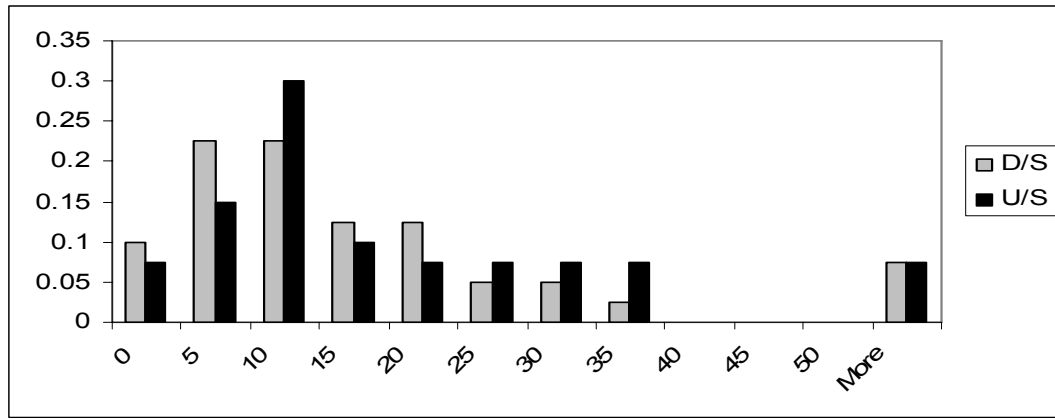


**Figure 7.3-9. Probability histogram representing the 40-model scour results for the catchment-controlled Baltimore Patapsco River site. The Horizontal Axis represents the pier scour ranges in feet while the vertical axis is the probability of occurrence.**

Comparison between the pier scour results from the 40 models tested at the Patapsco River site and those from the WAVES program provide a means of assessing the performance of a continuous model against single-event models developed for upland rivers in a catchment-controlled estuary. Figure 7.3-10 displays the maximum predicted scour results for the catchment- controlled Baltimore Patapsco River case study site. In addition to model numbers 7, 28, 29, 35, and 37, five other models also predicted greater scour than that predicted by the WAVES program. For reasons indicated earlier in Section 7.3.4.3, the results produced by the five models are likely to be unreliable when used to estimate pier scour even in catchment-controlled estuaries. Also, as was the case with the mixed control sites (Patuxent and Wicomico Rivers) natural armoring had little effect on the final scour results. This was due both to the fine nature of the bed sediments assumed to be present at the site along with the reasonably high stream velocities produced in the simulations. The figure also indicates that the Breseurs model (No. 1) under predicted the WAVES program and most of the 40 models tested. As with the other estuaries, the Breseurs model did not account for the complex hydraulic processes

that interact to produce scour conditions in tidal environments. Therefore, it is again unlikely that the Breseurs model could provide reliable results in catchment-controlled estuarine environments owing to the fact that the values predicted by the model is based only on the pier diameter while the depth, discharge, and velocity generated by the flow are not considered.

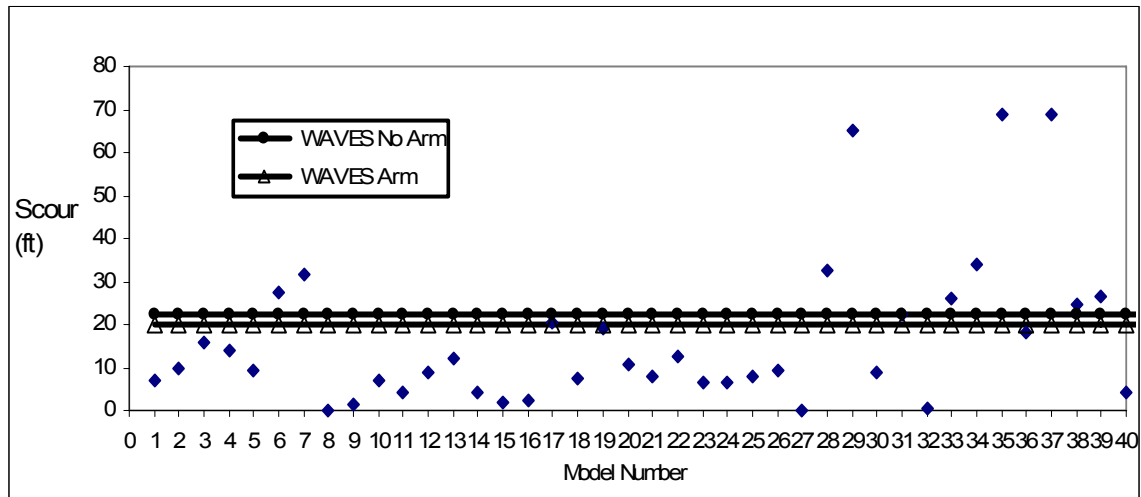


**Figure 7.3-10. Results of the 40-model study at the Baltimore Patapsco site in comparison to the Predicted Maximum Scour results obtained from the WAVES Program. Arm indicates the use of the natural armoring option in WAVES. No Arm indicates that natural armoring was not considered.**

## 7.4 COMPARISON OF THE CONTINUOUS RESULTS FROM THE FIVE BENCHMARK MODELS AND WAVES

### 7.4.1 Discussion of the Models Used

#### 7.4.1.1 Rationale of Model Selection

As discussed in Chapter 2, a number of comparative studies have been done on scour models for upland rivers by various authors. Through such studies these researchers were able to rate the accuracy of many of the empirical single-event scour models currently in use. A review of these papers indicated that there were approximately five models currently in use that consistently provided more acceptable

and reliable results than the other models. This does not mean, however, that the models identified as being among the best single-event models are themselves reliable and accurate over all conditions. The identification of these models provides only a benchmark by which other model may be assessed.

In lieu of a formal model verification, the performance of the WAVES program was assessed in comparison to the performance of the most widely accepted models currently in use. The five models identified in the literature as being the most widely used are the Laursen and Tosh (No. 4), Hancu (No. 11), Froelich (No. 13), Jain and Fischer (No. 20), and the Colorado State University HEC-18 (No. 23). In the prior sections the comparisons between the continuous simulation WAVES and single-event scour models were discussed and the inference drawn was that continuous scour models were for various reasons more useful and reliable than single-event models. The current model comparison exercise proposes to develop annual scour information from the single-event design models and use the annual series of scour data as a surrogate of actual continuous simulations. The annual scour information was then compared to the annual scour predicted by the WAVES program as a means conducting a more detailed comparison of the WAVES program in relation to the five benchmark models.

#### **7.4.1.2 Data Range Constraints of the Selected Models**

The five models selected for the continuous study were developed from both field and lab data that included varying conditions and constraints. Table 7.4-1 summarizes these conditions and constraints and helps to assess the environment for which each of these models was best suited. Note that data for Froelich's model was missing, as

information concerning the development of this equation could not be found in the literature.

**Table 7.4-1. Data ranges and constraints of models used in the continuous comparison study** W is the width of the channel, b the pier diameter,  $d_{50}$  is the mean particle diameter, V is the stream velocity, Y is the flow depth,  $F_n$  is the Froud number, and  $F_{nc}$  is the threshold Froud number of the channel soils

Model No.	Investigator	W (m)	B (cm)	$d_{50}$ (mm)	V (m/s)	Y (cm)	$F_n$	$F_{nc}$
4	Laursen & Tosh (1956)	41	122	0.45		350		
11	Hancu (1971)		3.0 – 20.0	0.5 - 2.00	0.2 - 0.88	5.0- 17.5	0.21- 0.97	0.44- 0.71
13	Froelich (1988)							
20	Fain & Fischer (1979)	0.91	5.08- 10.2	0.25- 2.50	0.5- 1.40	10.2 - 24.7	0.50 -1.50	0.29 - 0.63
23	CSU HEC-18 (1995)		10.00- 20.00	0.25- 6.00	0.2 - 1.50	10.0 - 30.0		

From a study using field data compiled different sources, Jain and Mordi (1986) identified the Laursen and Tosh (1956) model (No. 4) as the most accurate of ten models tested. The equation was developed from field data from upland rivers and showed that scour depth was dependent mainly on flow depth when the flow was transporting sediment. Hancu (1971) developed equation No. 11 from laboratory data. The use of the equation is constrained to threshold Froude numbers in the range 0.05 to 0.6. Hancu also suggested that the equation should be used only at locations where appreciable contraction scour was expected. Equation No. 13 was developed by Froelich (1988) as an empirical equation for live bed scour. Froelich utilized linear regression analyses of field scour data from published and unpublished sources to develop the equation. Equation No. 20 was developed by Jain and Fischer (1979) from laboratory data. The

equation is constrained to a difference between the Froude Number and the threshold Froude number being greater than 0.15. The authors also recommended that the equation should only be used for Froude Number values less than 1.0. Equation No. 23 was developed by the Colorado State University for the U.S Department of Transportation's Hydraulic Engineering Circular No. 18 from laboratory data. The CSU HEC-18 equation (Richardson and Davis 1995) is currently the most widely used pier scour equation and is recommended for both clear scour and live bed scour. It is recommended in HEC -18 that the limiting value of the predicted scour depths should be 2.4 times the maximum flow depth for Froude numbers less than 0.8 and 3.0 for Froude numbers greater than 0.8.

#### **7.4.2 Method of Developing Continuous Simulations from Single-Event Models**

As stated earlier, 2000 simulations, each for a duration of 100 years, were performed on the case study sites using the WAVES program. It was assumed that each 100-year simulation represented an estimate of the results that could be obtained over any given 100-year period and, therefore, could be used to provide a 100-year annual series of output variables. As a result, the WAVES program was designed to provide the maximum values calculated for the peak annual hourly depth, discharge, and velocity of the flow in both the upstream and downstream direction for each of the 100 years in the final simulation. The values were then sorted in ascending order to simulate the annual return period and used by each test model to compute the annual scour at both the upstream and downstream pier faces at the case study sites. The scour results provided by each model were also in the form of an annual series of ascending values representing the scour that was obtained each year by the test model used. Appendix E-5 shows the

annual series of input data for the test models that were developed from the WAVES program output.

### **7.4.3 Summary of Results**

#### **7.4.3.1 Tide-Controlled Estuaries Monie Bay and Black River**

The study's objective included the investigation of the continuous scour results simulated by popular single-event models in tide-controlled estuaries such as Monie Bay. Figures 7.4-1 and 7.4-2 depict the results of the comparison scour simulations conducted at Monie Bay for the upstream and downstream pier faces, respectively. Details of these results may be found in Appendix E-6. The figures show that all the test equations, except the Jain and Fischer model (No. 20), predicted that most of the scouring would occur after the first year with scour increasing gradually in succeeding years. The results also show that all the test models, except the Jain and Fischer, gave the impression that scour could be initiated from either the upstream or downstream face of the pier in tide-controlled estuaries. The Laursen and Tosh model (No. 4) predicted the highest scour values of all the test models, while Froelich (No. 13) predicted moderate scour results. Jain and Fischer No. 20, HEC-18 (No. 23), and Hancu (No. 11), predicted the smallest scour values ( 0, 3.0, and 4.0 ft, respectively) over the 100-year period.



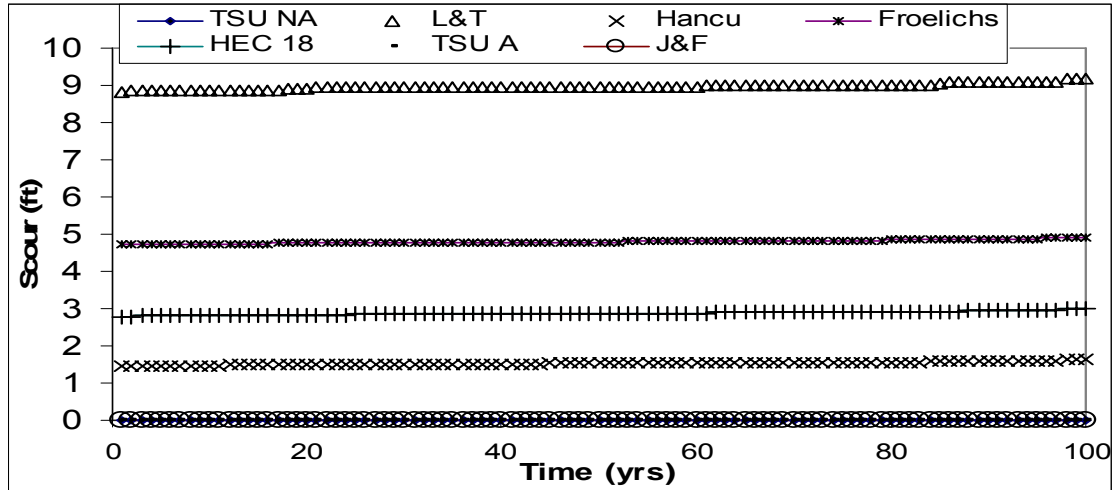


**Figure 7.4-1. Monie Bay upstream pier face. TSUNA and TSUA represent the scour results predicted by the WAVES program with and without natural armoring, respectively. L&T represents results predicted by Laursen and Tosh and J&F represents the results predicted by the Jain and Fischer Model.**

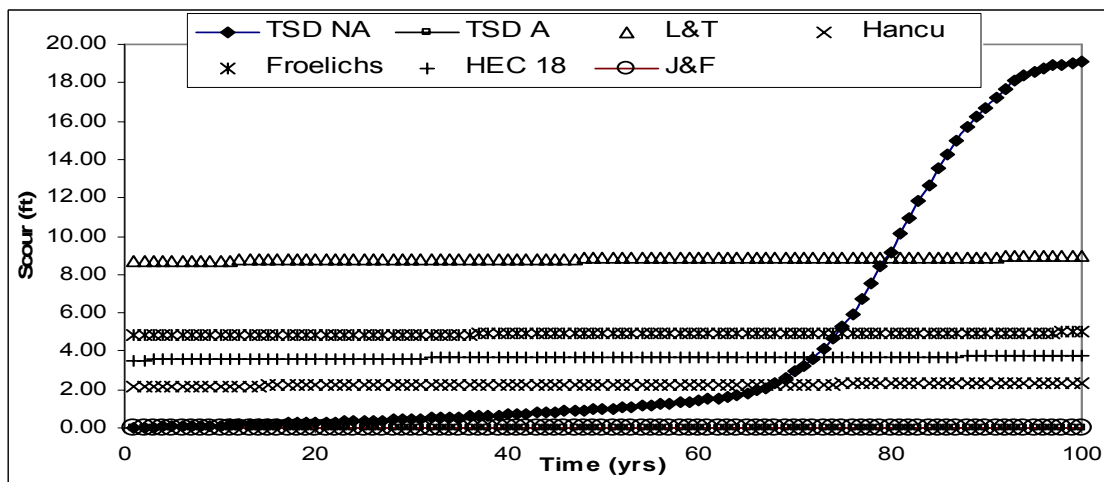


**Figure 7.4-2. Monie Bay downstream pier face. TSDNA and TSDA represent the scour results predicted by the WAVES program with and without natural armoring, respectively. L&T represents the results predicted by Laursen and Tosh and J&F represents the results predicted by the Jain and Fischer Model.**

Figures 7.4-1 and 7.4-2 also depict the results of the continuous simulations done using the WAVES program at Monie Bay for the upstream and downstream pier faces, respectively. In comparison to the results produced by the test equations, the results of

the WAVES program, without natural armoring considered, predicted scour being initiated from the downstream face only with the scour increasing to two feet over the first 60 years then increasing to a value of 19 feet over the next forty years. In the case where natural armoring was considered, the WAVES program predicted that scour would not be generated at either face over the 100-year period.

The continuous scour results simulated by popular single-event models at Black River provides an opportunity to assess whether or not inferences may be drawn regarding the ability of single-events models to simulate continuous scour in tide-controlled estuaries. Figures 7.4-3 and 7.4-4 depict the results of the comparison scour simulations conducted at the Baltimore Black River estuary location for the upstream and downstream pier faces, respectively. Again, the figures show that all the test equations, except the Jain and Fischer model (No. 20), predicted that most of the scour would occur after the first year with scour increasing gradually in succeeding years. The results also show that the test models, except the Jain and Fischer, also indicated that scour could be initiated from either the upstream or downstream pier face with the Laursen and Tosh model (No. 4) predicting the highest scour values of all the test models, while Froelich (No. 13) predicted moderate scour results. Jain and Fischer (No. 20), HEC-18 (No. 23), and Hancu (No. 11), also predicted the lowest scour. The Jain and Fischer model (No. 20) predicted that scour was not initiated at the upstream face. At the downstream pier face, the Jain and Fischer model showed that no scouring occurred after the first 75 years but gradually increased to 5 ft over the next 25 years.

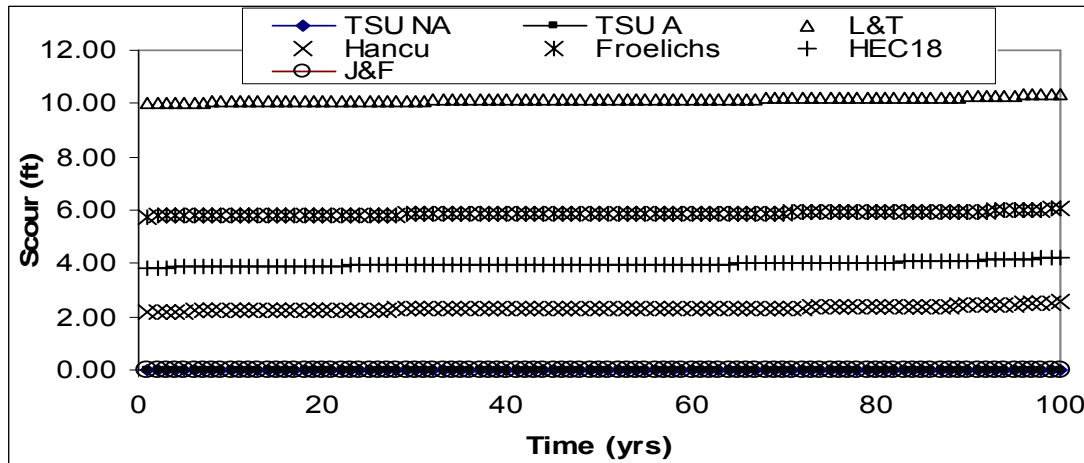


**Figure 7.4-3. Black River upstream pier face. TSUNA and TSUA represent the scour results predicted by the WAVES program with and without natural armoring, respectively. L&T represents results predicted by Laursen and Tosh and J&F represents the results predicted by the Jain and Fischer Model.**

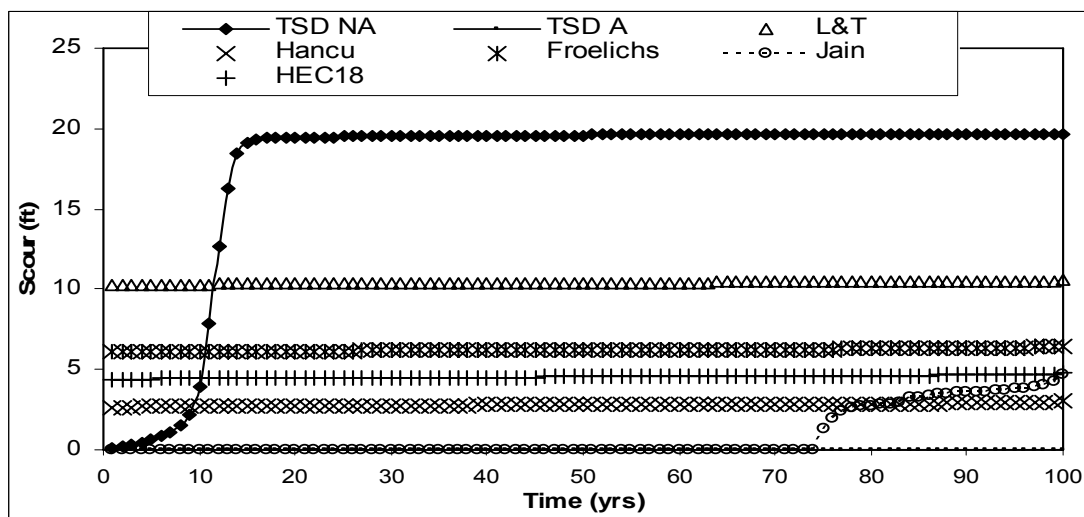


**Figure 7.4-4. Black River downstream pier face. TSDNA and TSDA represent the scour results predicted by the WAVES program with and without natural armoring, respectively. L&T represents the results predicted by Laursen and Tosh and J&F represents the results predicted by the Jain and Fischer Model.**

Figures 7.4-3 and 7.4-4 depict the results of the continuous simulations done using the WAVES program at the Black River Location for the upstream and downstream pier faces, respectively. In comparison to the results produced by the test equations, the results of the WAVES program, without natural armoring considered,

predicted scour being initiated from the downstream face only with the scour quickly increasing to three feet over the first ten years then increasing to an ultimate value of 20 feet over the next five years. In the case where natural armoring was considered, the WAVES program predicted no scour generated at either face over the 100-year period.

#### **7.4.3.2 Mixed-Control Estuaries Patuxent at Benedict and Wicomico**

The study's objective also included the investigation of the continuous scour results simulated by popular single-event models in mixed-controlled estuaries such as the Patuxent River site. Figures 7.4-5 and 7.4-6 depict the results of the comparison scour simulations conducted at the Patuxent River location for the upstream and downstream pier faces, respectively. Details of these results may be found in Appendix E-6. The figures show that the Laursen and Tosh model (No. 4) and Froelich (No. 13), predicted most of the scour after the first year, with scour increasing gradually in succeeding years. The HEC-18 (No. 23) and Hancu (No. 11) predictions showed moderate increases in scour depth on both pier faces over the 100-year period, while the Jain and Fischer Model (No. 20) predicted zero scour over the first 65 years increasing to 10 ft over the next 35 years on the upstream pier face and zero scour over the first 80 years and reaching feet of scour over the next 20 years on the downstream pier face. The results also show that all the test models indicated that scour could be initiated from either the upstream or downstream pier face with the Laursen and Tosh model (No. 4), Jain and Fischer model (No. 20), and Froelich (No. 13) predicting the highest scour values of all the test models. HEC-18 (No. 23) and Hancu (No. 11) predicted the smallest scour values at six and five feet of scour, respectively, over the 100-year period.

Figures 7.4-5 and 7.4-6 also depict the results of the continuous simulations done using the WAVES program at the Patuxent River location for the upstream and downstream pier faces, respectively. In comparison to the results produced by the test equations, the results of the WAVES program, with and without natural armoring considered, predicted scour being initiated from both the upstream and downstream faces with the greater likelihood of being initiated from the upstream pier face based on the fact that the upstream face predicted values were greater than those predicted for the downstream pier face. For the upstream pier face scour increased at an even rate to an ultimate value of 22 feet over the first 20 years when no armoring was considered, while, when natural armoring was considered, scour at the upstream pier face reached a value of 15 feet over the 100-year period.

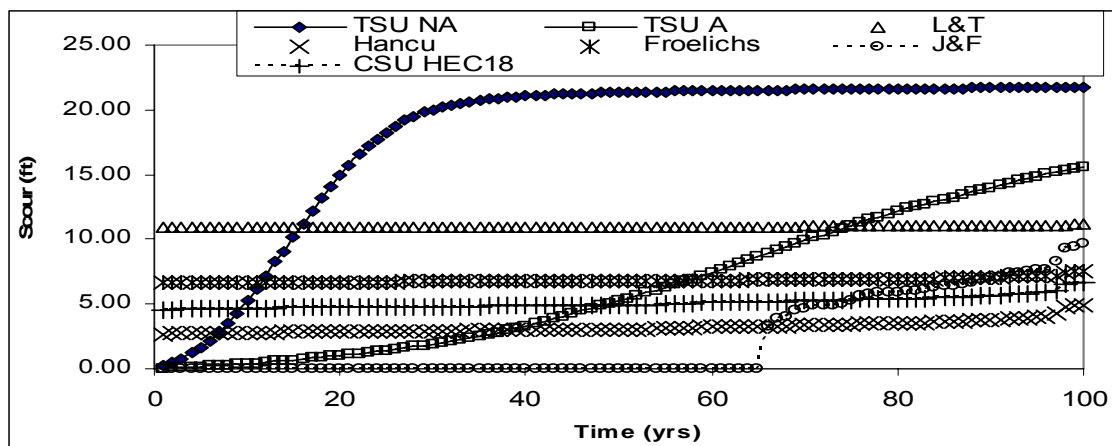


**Figure 7.4-5. Patuxent River upstream pier face. TSUNA and TSUA represent the scour results predicted by the WAVES program with and without natural armoring, respectively. L&T represents results predicted by Laursen and Tosh and J&F represents the results predicted by the Jain and Fischer Model.**

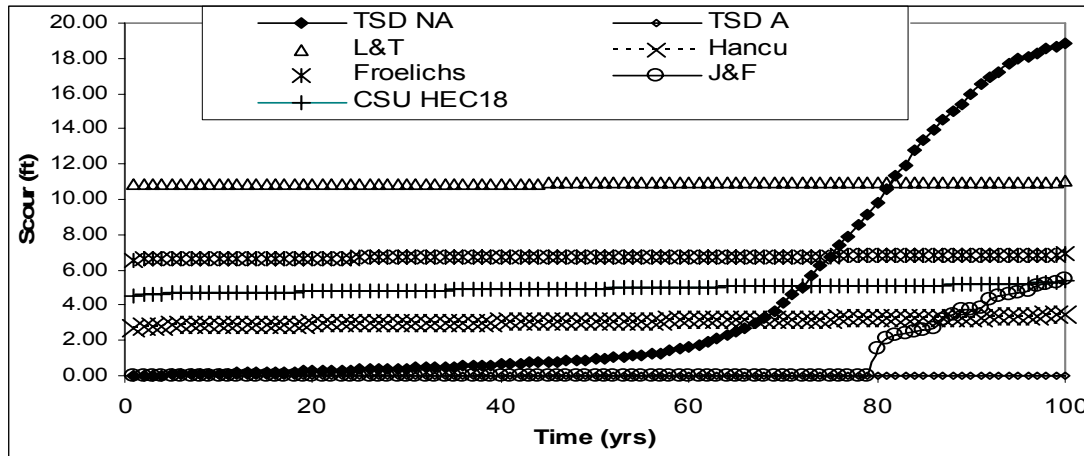


**Figure 7.4-6. Patuxent River downstream pier face. TSDNA and TSDA represent the scour results predicted by the WAVES program with and without natural armoring, respectively. L&T represents the results predicted by Laursen and Tosh and J&F represents the results predicted by the Jain and Fischer Model.**

The continuous simulations made with the benchmark models at the Wicomico River site showed similarities with, and differences from, the results obtained at the Patuxent River. Figures 7.4-7 and 7.4-8 depict the results of the comparison scour simulations conducted at the Wicomico River location for the upstream and downstream pier faces, respectively. As with the Patuxent River location, the figures show that the Laursen and Tosh model (No. 4) and Froelich (No. 13) predicted most of the scour after the first year with scour increasing gradually in succeeding years. The HEC-18 (No. 23) and Hancu (No. 11) predictions also showed moderate increases in scour depth on both pier faces over the 100-year period. In the case of the downstream pier face results the Jain and Fischer Model (No. 20) also predicted significant scour over the first year with the scour hole increasing to eight feet at the end of the 100-year simulation period. The results also indicated that although the test models showed that scour could be initiated from either the upstream or downstream pier face, it would be more likely that scour would be caused by activities at the downstream pier face by virtue of the fact that the

predicted scour along the down stream pier face was in general higher than that generated along the upstream pier face. The Laursen and Tosh model (No. 4), Jain and Fischer (No. 20), and Froelich (No. 13) predicted the highest scour values of all the test models. HEC-18 (No. 23) and Hancu (No. 11) predicted the lowest scour (five and three feet of scour , respectively) over the 100-year period.

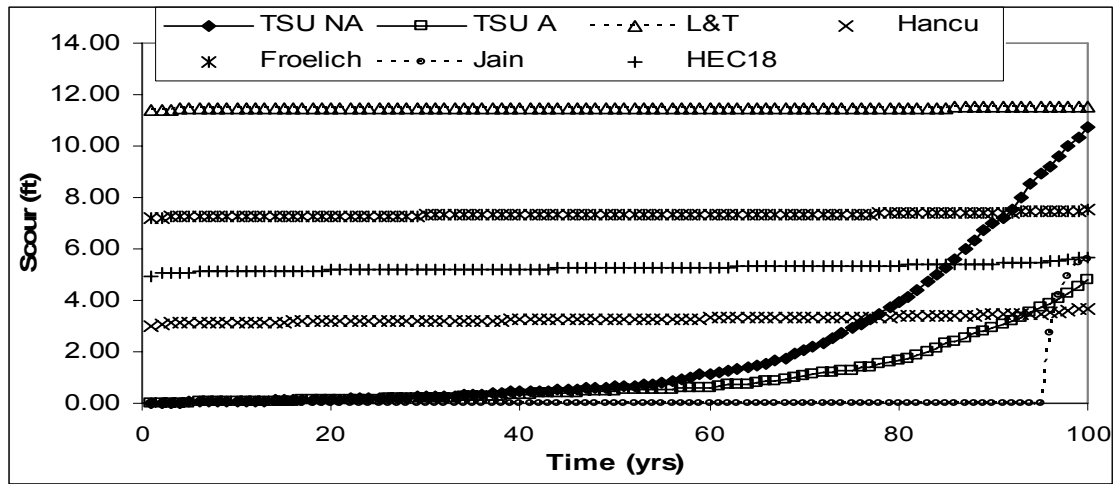


**Figure 7.4-7. Wicomico River upstream pier face. TSUNA and TSUA represent the scour results predicted by the WAVES program with and without natural armoring, respectively. L&T represents results predicted by Laursen and Tosh and J&F represents the results predicted by the Jain and Fischer Model.**

Figures 7.4-7 and 7.4-8 also include the results of the continuous simulations done using the WAVES program at the Wicomico River location for the upstream and downstream pier faces, respectively. In comparison to the results produced by the test equations, the results of the WAVES program, with and without natural armoring considered, also predicted scour being initiated from both the upstream and downstream faces with the greater likelihood of being initiated from the downstream pier face based on the fact that the downstream face predicted values were greater than those predicted for the upstream pier face. For the downstream pier face scour increased at an even rate

to an ultimate value of 20 feet over the first three years when no armoring was considered, while, when natural armoring was considered, scour at the downstream pier face reached a value of 10 feet over the 100-year period.

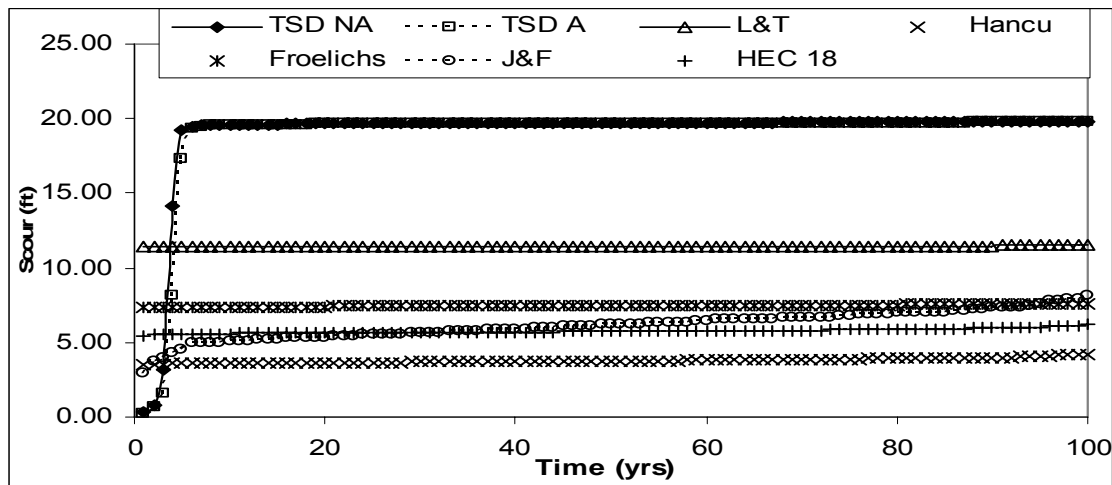


**Figure 7.4-8. Wicomico River downstream pier face. TSDNA and TSDA represent the scour results predicted by the WAVES program with and without natural armoring, respectively. L&T represents the results predicted by Laursen and Tosh and J&F represents the results predicted by the Jain and Fischer Model.**

#### 7.4.3.3 Catchment-Controlled Estuary Baltimore at the Patapsco

Because the benchmark models were developed for upland rivers, catchment-controlled environments provide the best opportunity for these models to produce continuous scour results comparable to the WAVES program. Figures 7.4-9 and 7.4-10 depict the results of the comparison scour simulations conducted at the Patapsco River location for the upstream and downstream pier faces, respectively. Details of these results may be found in Appendix E-6. The figures again show that the Laursen and Tosh model (No. 4) and Froelich (No. 13) predicted most of the scour after the first year with scour increasing gradually in succeeding years. The HEC-18 (No. 23) and Hancu (No. 11) predictions also showed moderate increases in scour depth on both pier faces over the 100-year period. In the case of the upstream pier face results the Jain and



Fischer Model (No. 20) also predicted significant scour but indicated that the development of the scour hole was delayed for 75 years after which scour developed to a maximum of 11 feet over the next 25 years. The results also indicated that although most of the test models showed that scour could be initiated from either the upstream or downstream pier face, it would be more likely that scour would be caused by activities at the upstream pier face by virtue of the fact that the predicted scour along the downstream pier face was in general less than that generated along the upstream pier face. The Jain and Fischer model (No. 20) presented an exception to this general observation, as the model predicted zero scour over the 100-year simulation period at the downstream pier face. The Laursen and Tosh model (No. 4), Jain and Fischer (No. 20), and Froelich (No. 13) again predicted the highest scour values of all the test models. HEC-18 (No. 23) and Hancu (No. 11) predicted the lowest over the 100-year period.

Figures 7.5-9 and 7.5-10 also include the results of the continuous simulations done using the WAVES program at the Patapsco River location for the upstream and downstream pier faces, respectively. In comparison to the results produced by the test equations, the results of the WAVES program, with and without natural armoring considered, also predicted scour being initiated from only the upstream pier face. For the upstream pier face scour increased at an even rate to an ultimate value of 22 feet over the first ten years when armoring was not considered, while, when natural armoring was considered, scour at the upstream pier face reached a value of 15 feet over the 100-year period. The WAVES program results indicated that scour would not be initiated from the downstream pier face.

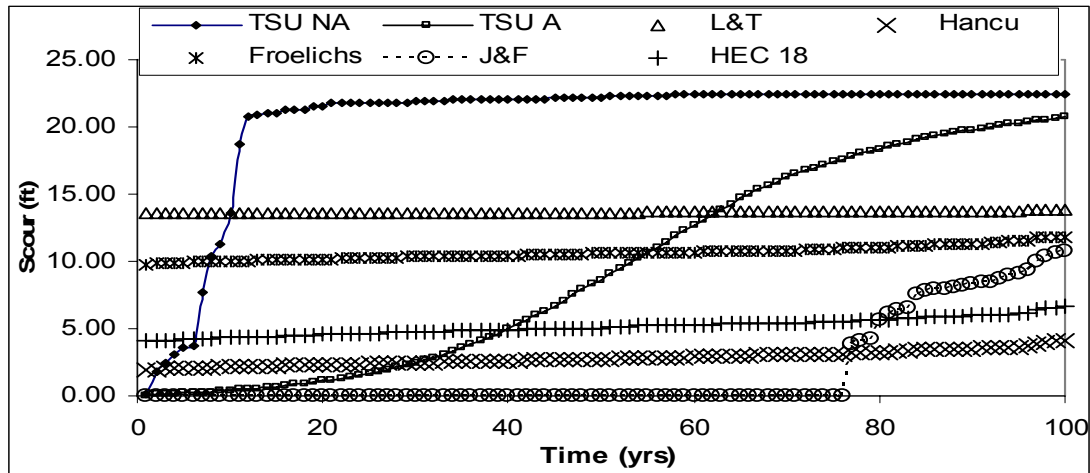


**Figure 7.4-9. Baltimore Patapsco River upstream pier face. TSUNA and TSUA represent the scour results predicted by the WAVES program with and without natural armoring, respectively. L&T represents results predicted by Laursen and Tosh and J&F represents the results predicted by the Jain and Fischer Model.**

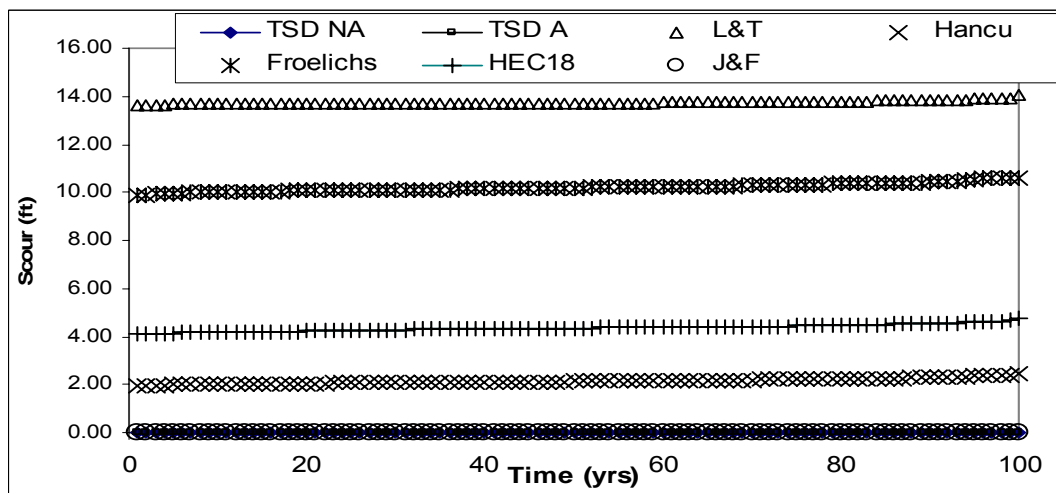


**Figure 7.4-10. Baltimore Patapsco River downstream pier face. TSDNA and TSDA represent the scour results predicted by the WAVES program with and without natural armoring, respectively. L&T represents the results predicted by Laursen and Tosh and J&F represents the results predicted by the Jain and Fischer Model.**

#### 7.4.4 Discussion of Results

##### 7.4.4.1 Tide-Controlled Estuaries Monie Bay and Black River

All models tested indicated scour would be initiated from the downstream pier face in tide-controlled estuaries by predicting higher scour values along the downstream

face of the pier. A review of the results obtained along the downstream pier faces of both Monie Bay and Black River showed that Laursen and Tosh (No. 4) predicted scour increasing from eight feet, at the first year to nine feet at the end of the 100-year simulation period at Monie Bay and 9 to 11 feet of scour at Black River. Froelich (No. 13) predicted scour starting at 5 ft after the first year while increasing to 6.5 feet over the 100-year simulation period. Reasons for the slow increase in scour predicted by these models were discussed in section 7.4.1.

The Hancu (No.11) and CSU HEC-18 (No. 23) model predicted relatively low scour for the tide-controlled sites. These values ranged in general from three feet of scour over the first year to five feet of scour at the end of the 100-year simulation period. As indicated earlier, the low scour values could be attributed to the relatively low annual velocities, computed at these locations by the WAVES program, that were used by the benchmark models for the continuous scour simulations.

The behavior of the Jain and Fischer equation (No. 20) is of particular interest. The Jain and Fischer results are in many ways similar to the results predicted by the WAVES program. Figures 7.4-1 and 7.4-3 show that, unlike the other equations tested, the Jain and Fischer and WAVES programs predicted that zero scour would be initiated from the upstream pier faces of the tidal controlled estuaries. In addition, the Jain and Fischer model also predicted zero scour along the downstream pier face at Monie Bay (see Fig. 7.4-2), while the WAVES program predicted low or insignificant scour initiated during the first 60 years of the simulation period with scour increasing to 19 feet over the next 40 years. At the Black River Site, the Jain and Fischer model exhibited a similar scour profile along the downstream pier face to what was observed with the WAVES

results (see Fig. 7.4-4). However, with the Jain and Fischer predictions, significant scour was delayed until after 75 years of simulation then increased to 5 feet over the remaining 25 years. With the WAVES program the ultimate scour depth was reached in five years. The behavior of the Jain and Fischer model may be attributed to the high threshold scour condition imposed by both the way in which the critical scour velocity was calculated and the fact that the model used the difference between the Froude number of the stream flow and the threshold Froude number of the bed material as a predictor. As a result, in estuarine situations with low annual velocities this difference will tend to the value of zero hence no significant scour for most years was the result obtained.

#### **7.4.4.2 Mixed-Control Estuaries Patuxent at Benedict and Wicomico**

The models tested at the mixed-controlled estuaries showed that scour could be initiated at either the upstream or downstream pier face. The Patuxent River results showed that scour was initiated at the upstream pier face, while the Wicomico results indicate that scour at the downstream pier face predominated. A review of the results obtained along the downstream pier face of the Wicomico River site showed that Laursen and Tosh (No. 4) predicted scour increasing from 11 ft, at the first year to 11.5 ft at the end of the 100-year simulation period (see Fig. 7.4-8). At the Patuxent River site upstream pier face (see Fig. 7.4-5), Laursen and Tosh (No. 4) predicted scour increasing from 11 ft, at the first year to 12 ft at the end of the 100-year simulation period. Froelich (No. 13) predicted scour in the range starting at seven feet after the first year while increasing to eight feet over the 100-year simulation period for both the Wicomico downstream pier face and the Patuxent River upstream pier face. The relatively small increase in scour after the first year was again due to the fact that the flat slopes and wide

floodplains associated with estuaries caused minor changes in the annual series of flow depths used in estimating the scour variation with time.

The Hancu model (No.11) and CSU HEC-18 model (No. 23) again predicted relatively low scour values for the mixed control sites (see Fig. 7.4-5 and 7.4-8). However the values predicted were slightly higher than what these models indicated for the tide-controlled sites. The HEC-18 predictions ranged in general from four feet of scour over the first year to five and a half feet of scour at the end of the 100-year simulation period for both the Patuxent River site (Fig. 7.4-5) and the Wicomico River Site (Fig. 7.4-8). As indicated earlier, the low scour values may be attributed to the relatively low annual velocities computed at these locations by the WAVES program. However, because these sites displayed more of a riverine characteristic than the tide-controlled sites, the annual series of velocity results was somewhat greater than those produced by the tidal sites, hence slightly greater scour results were produced by these models.

At the mixed-control sites Jain and Fischer (No. 20) predicted greater scour values than what they predicted at the tide controlled sites. Figures 7.4-5 and 7.4-8 show that Jain and Fischer predicted no scour at the Patuxent river site over the first 65 years with scour increasing to ten feet over the next 35 years, while at the Wicomico River site three feet of scour was predicted after the first year gradually increasing to eight feet of scour at the end of the 100-year simulation period. In comparison, the WAVES program predicted a steady increase in scour from 0 to 22 ft (without natural armoring) at the Patuxent site over the simulation period, while predicting a high scour rate of 0 to 20 ft of scour over the first three years at the Wicomico site with or without armoring. The delay

in scour exhibited by the Jain and Fischer model was still evident in the Patuxent River results and this may be attributed to the high threshold scour velocity caused by the large relatively mean particle size used at the Patuxent site. A small mean particle size was estimated for the bed material at the Wicomico site and this resulted in the prediction of a faster rate of scour over the first year by Jain and Fischer (1979).

#### **7.4.4.3 Catchment-Controlled Estuary the Patapsco at Baltimore**

The models tested indicated scour would be initiated from the upstream pier face in the catchment-controlled site at Patapsco River in Baltimore by predicting higher scour values along the upstream face of the pier. A review of the results obtained along the upstream pier face at the Baltimore Patapsco site (see Fig. 7.4-9) showed that Laursen and Tosh (No. 4) predicted scour increasing from slowly from 14 ft, at the first year, to 14.5 ft at the end of the 100-year simulation period, while Froelich (No. 13) predicted scour in the range starting at ten feet after the first year increasing to twelve feet over the 100-year simulation period. Reasons for the slow increase in scour predicted by these models were discussed in Section 7.4.1. Of note however, is the fact that both models predicted higher scour values than they did for the other test sites. This is due to the fact that the Patapsco River estuary is relatively deep (35 ft) hence these depth dependent models would then to predict higher scour results at this location.

The Hancu (No.11) and CSU HEC-18 (No. 23) model predicted relatively low scour values for the catchment controlled site; however, these values were higher than what was predicted by the models at the other test sites. Hancu No. 11 predicted scour two feet of scour over the first year increasing to four feet of scour at the end of the 100-

year simulation period, while HEC-18 (No. 23) predicted four feet of scour at the end of the first year increasing to seven feet of scour at the end of the simulation period. As indicated earlier, the low scour values may be attributed to the relatively low annual velocities computed at these locations by the WAVES program. There was however greater variations in the annual scour predictions at the catchment-controlled site than observed at all the other sites excluding the Patuxent site. The Patuxent River site, though not formally classified as catchment controlled, still caused scour to be initiated at the upstream pier face, which is a characteristic shared by the Patapsco site.

The results predicted by the Jain and Fischer equation (No. 20) were similar to the predictions made by Jain and Fischer at the upstream pier face of the Patuxent River site. Figure 7.4-9 shows that the Jain and Fischer model also predicted significant scour being delayed until after 75 years of simulation then increased to ten feet over the remaining 25 years. In comparison the WAVES program predicted that the ultimate scour depth of 22 ft would be reached in 10 years when no armoring was considered, while with natural armoring a scour depth of 19 ft would be achieved over the 100-year simulation period. The results predicted by the Jain and Fischer model may again be attributed to the high threshold scour condition imposed by both the way in which the critical scour velocity was calculated and the fact that the model used the difference between the Froude number of the stream flow and the threshold Froude number of the bed material as a predictor resulting in no significant scour for most years.

## **7.5 CONCLUSIONS**

### **7.5.1 Forty Model Comparison**

The appropriateness of the models tested were assessed by comparing the results they produce at the case study sites with the results obtained from the five most widely used models and the continuous WAVES program. In all but a few cases, the continuous WAVES program provided estimates that were more conservative than the single event models tested. In contrast, most of the models used in the test produced scour estimates that were greater than those produced by the five benchmark models.

It was also expected that in estuarine environments most pier scour empirical equations, developed from data collected from upstream rivers, would not provide the most accurate predictions. Specifically, models using the total cross section discharge as a predictor variable were most likely to provide misleading results. In contrast, models that attempt to incorporate hydraulic consideration, as is the case with four of the five benchmark models, should be more accurate. The results also show that the univariate and bivariate models produced estimates that did not vary significantly from site to site, and hence were probably not as precise as the models using three or more predictor variables.

The ultimate scour equation used by the WAVES program is a multivariate that uses the tangential vortex velocity as one of its variables. The equation produced 100-year scour results that compared favorably with the benchmark models. The results produced by the WAVES ultimate scour equation also appeared to be slightly more conservative than those provided by Model Numbers 11, 13, 20, and 23.



Models that used total discharge as a predictor also appeared to over predict the amount of scour that was produced at all of the case study site, while equations that used the discharge per unit width and velocity as predictors produced results that were comparable to the results produced by the benchmark models. While the total discharge may be a good indicator of pier scour in narrow riverine channels, the same may not be true for estuarine environments because the discharge immediately around the pier in a wide estuary will be a small fraction of the total discharge across the estuary cross section. As a result, models using discharge as a predictor may also be inappropriate for use in estuaries.

#### **7.5.2 Continuous Simulations Comparison**

A review of the results of the continuous comparative study showed some general trends, which were apparent regardless of the type of estuarine environments that were used in the study. The trends observed were: (1) the models tested correctly identified the most likely side of the pier from which scour should be initiated, (2) the similarity of the values predicted for the upstream and downstream pier faces, (3) the sharp early scour predicted by most of the test models over the first year, (4) the comparatively high predictions made by the models using flow depth as a predictor, and (5) the comparatively low predictions of the models using velocity as a predictor.

A common observation made with the models tested, and also with the results predicted by the WAVES program, was that in all the test cases each model correctly identified the location along the pier face, whether upstream or down stream, from which scour should be initiated. The pier face location from which pier scour was generated

was taken as the location (upstream or downstream pier face) that produced the greater of the pier scour result at the end of any given year. This result could in part be attributed to the fact that the continuous scour using the test models were generated from ranked annual series of the hydraulic data generated from the WAVES program and as a result, the scour results predicted should conform to the data obtained from the WAVES program.

The results also showed that the differences in scour predicted by the test models at the upstream and down stream pier faces was always relatively small. This was the case even though the higher of the two was always located at the pier face from which the initiation of scour was expected. This result indicates the imprecision in the five benchmark models tested when used in tidal environments.

Most of the models appeared to over predict pier scour over the first year. This effect may be attributed to the small range in the annual hydraulic values observed in estuaries. This resulted in relatively minor differences between the lowest and highest values in the annual series of data produced by the WAVES simulations, which in turn caused relatively small annual differences between the scour results produced by the test models.

Models, such as Laursen and Tosh (No. 4) and Froelich (No. 13), that depended directly on the value of flow depth predicted higher scour values than the other test models used, underscores the care that must be used when selecting empirical scour equations to predict scour in tidal environments. Because all estuaries and tidal rivers have minimum depths that are not hydraulically active, models developed from upland rivers using flow depth as a predictor cannot adequately address the inactive water depths

in estuaries and therefore will not provide accurate results particularly in deep estuaries. As a result, the predictions made by the Laursen and Tosh (No. 4) and Froelich (No. 13) models, though closer to the WAVES predictions, could not be fully trusted.

Models such as HEC-18 (No. 23) and Hancu (No. 11), that used velocity as a predictor, provided lower scour estimates. Again, this could be attributed to the generally low annual velocities produced in estuaries and tidal rivers. As indicated earlier, estuaries typically have larger widths, depths, and flood plain areas than upland rivers and these features work together to reduce the estuarine flow velocities.

## **CHAPTER 8**

### **CONCLUSIONS**

#### **8.1 INTRODUCTION**

The goal of this study was to develop a multi-component, time dependent model that could predict bridge pier scour in tidal environments and be used as part of a methodology for bridge pier designs in these environments. In general, the currently available pier scour design equations were developed from laboratory models and field data to predict scour in upland rivers, and do not include the considerations necessary to design bridge piers in tidal and estuarine environments. Additionally, these equations are lumped (i.e., static) in that they do not account for the time dependence of the pier scour process. At the other end of the spectrum of pier scour models are the multi-dimensional hydrodynamic models that include the tidal processes; however, these models require extensive and costly data inputs and are characteristically computationally intensive and very complex.

One objective of this study was to develop a pier scour model that was relatively easy to apply and did not require extensively detailed data input. At the same time, the model should provide time varying scour and hydraulic output that could be used by engineers to analyze the scour estimates important for the safety of bridges. Through the performance of this study, several conclusions related to the goal of this study were drawn and are discussed in detail below.

## **8.2 THE THEORETICAL BASIS OF THE WAVES PROGRAM**

The theoretical basis of the of the multi-component WAVES scour program is sound and governs the characteristics of the program. The program was formulated from accepted fluid dynamics, hydrologic, tidal, and hydraulic theories along with the empirical relationships developed from field and laboratory studies. The model includes four components: tidal, catchment, hydraulic, and scour.

The hydraulic component incorporates well known tidal and stream hydraulic theories with the formulation of the downflow model. In addition, the model links the formation of the horseshoe vortex to the downflow and quantified the size and velocity of the vortex using available research findings and theoretical considerations. The tangential vortex velocity was assumed to be the agent that caused bed erosion thus leading to the development of a local scour model, which incorporated the vortex tangential velocity.

Sensitivity and uncertainty analyses were conducted primarily to determine the sensitivity of the WAVES model input variables. Parameter sensitivity analyses were also conducted on each component, to estimate the relative importance of the parameters. These parameter sensitivity studies indicated that the local scour component would likely be the most sensitive component. In order to estimate the uncertainty in the results of the model arising from uncertainties in the components, the sensitivity and uncertainty of the local scour component was analyzed. The analysis indicated that uncertainties in the model components could have a significant effect on the time to reach ultimate scour but a negligible effect on the magnitude of the ultimate scour value. While one example of

component sensitivity was determined, it must be stated that the focus of the sensitivity analyses was on the sensitivity of input variables and how these variables could impact the model results. This information is important to design engineers.

The local scour model utilized both the tangential vortex velocity and two incipient erosion equations. The Neill's version of the incipient erosion model was used primarily in the continuous simulations. However, when modeling hurricanes, the SRICOS model was the alternative used. This approach is justified because Neill's incipient scour velocity is a function of flow depth. As a result, the Neill model was believed to over predict the incipient velocities during hurricanes, which generated very large flow depths caused by the hurricane surges. The WAVES program also incorporated contraction scour where applicable for greater accuracy.

### **8.3 DATA INPUT NEEDED FOR THE MULTI-SCALE FRAMEWORK**

The development of the WAVES program from a conceptual temporal, multi-scale framework enables all scales to be considered in a design, but ultimately, only data for the scales to which the particular design is sensitive would be required. This approach may reduce the overall complexity and cost of bridge pier designs by requiring complex analyses only in situations where they are needed. This assertion is justified by the input data required by the WAVES program. Much of the data utilized by the model are routinely required for other aspects of bridge designs such as the structural, geotechnical, or highway requirements. In addition, the level of detail required for hydrologic, tidal, channel geometry, and hydraulic information to be used by the program greatly depends on the scale at which the information is being used. By utilizing data

that are readily available and easily collected, the multi-scale methodology employed by WAVES will allow bridge engineers and policy makers to economically improve the safety of bridges. Table 8.3-1 shows the WAVES model input variables as a function of scales.

**Table 8.3-1. WAVES Model Variable Input as a Function of Scales**

<b>Open Ocean</b>	<b>Catchment</b>	<b>Tidal Estuary</b>	<b>Bridge Far-field</b>	<b>Bridge Near-field</b>	<b>Bridge Local</b>
Tidal periods	Time of concentration	Tidal periods	Maximum Estuary width	Estuary width upstream of bridge cross section	Bridge cross section depth
Tidal amplitude	Catchment area	Mean diurnal amplitude	Estuary plan area	Estuary width downstream of bridge cross section	Bridge cross section width
Distance from tidal base station to bridge station	Curve number	Estuary plan area			Pier geometry
	Catchment length	Estuary geometry		Sediment properties	Sediment properties
	Synthetic rainfall				

The model uses the SCS synthetic hydrograph approach at the catchment scale. The important variables required by the SCS model include the rainfall amounts, basin curve numbers, basin areas, and times of concentration. Rainfall data may be obtained from existing IDF curves. The other hydrologic data listed may be determined from field measurements and existing databases.

The data and parameters used at the tidal scale may be obtained from NOAA historical records from gauged locations. The mean tidal amplitude at the bridge site is needed for the model simulations. If the site is ungauged, this information may be easily estimated with the use of simple instruments such as tide poles.

The hydraulic process in tidal environments is significantly more complex than that found in upland rivers as it involves the combined effects of both the tidal and catchment influences. As a result, the accuracy of the data used in the hydraulic component is critical to the accuracy of scour predictions in estuaries. The hydraulic data include the information used at the local and bridge near-field scales and typically include the bridge cross section geometry of the estuary, the geometry of the near field cross sections, the properties of the soils found in the channel at that location, and hydraulic parameters such as Manning's coefficient. The geometric data are important as they determine the hydraulic outputs at the cross section upon which the scour process depends. The soil properties of the cross section are equally important as they define the incipient erosion velocities that must be exceeded in order that scour may be initiated. Hydraulic parameters, such as Manning's coefficient, also need to be accurately estimated from literature values. Much of the data described are also required for other aspects of the bridge design (i.e., the structural and the geometric designs). As a result, the local bridge and near-field data needed for the hydraulic component may be acquired without additional costs.

#### **8.4 ESTUARY PIER SCOUR DATA FOR MODEL VALIDATION**

Development of the WAVES program did not include a formal validation process because of the total lack of quality field pier scour data in estuaries and tidal rivers. Many researchers and bridge designers cite the lack of adequate pier scour data as a challenge that must be overcome if the science of pier scour prediction is to be improved. The concerns about current field data for pier scour are based on the fact that standard



protocols for the collection of these data were only recently developed. As a result, the integrity of most of the existing data cannot be guaranteed. Adding to the problem is the time at which pier scour data are typically collected. Pier scour measurements were, until recently, not made during the peak of storms because of the hazard that this would pose to scuba divers who collected the data. This resulted in a loss of accuracy in the measurements as the data were collected after storm events when the scour holes were partially filled in by unconsolidated material.

In order to formally validate a continuous model such as the WAVES program, 15 to 25 years of annual pier scour data would be required. This is particularly problematic because of the lack of the integrity of the data that were collected as recently as five years ago. Current efforts at collecting data by use of remote sensing techniques will correct this problem; however, the benefits of these developments are still several years away from being realized.

## **8.5 THE BENEFITS OF A TIME DEPENDENT SCOUR MODEL**

The results of this study also indicate that a temporal model for tidal environment that provides a time history of scour could significantly improve the usefulness of scour predictions. The methodology employed by the WAVES program provides these improvements at reasonable costs. A time varying pier scour model that was formulated specifically for estuarine conditions, easy to use, and did not require a large amount of field data that was difficult to obtain was considered necessary for several reasons. First, actual bridge failures from pier scour, such as the Schoharie Creek Bridge, showed that temporal variation in discharges and velocities determined the depth to which the scour

hole developed. The peak flow rate in a single storm would generally not be sustained long enough for the complete penetration of the scour hole. A number of storms are almost always required to reach ultimate scour. Second, the outputs provided by time varying models, such as the WAVES program, will better help engineers and bridge designers to analyze and interpret the hydrologic, hydraulic, and sediment conditions that may lead to bridge failure. Third, a time dependent pier scour model forms the basis of computing the probability and risk of failure annually. Bridge engineers and policy makers could use this methodology to improve bridge designs, and the overall safety of bridges.

## **8.6 BENEFITS OF A RISK-BASED DESIGN APPROACH**

The WAVES program facilitates a risk-based design approach by yielding estimates of the probability of scour depths over time. Because of the uncertainty in the results produced by most scour equations and models, information such as a distribution of the probability or failure risk at any given time would be more useful than absolute scour predictions provided by available models. The output from the WAVES program includes the cumulative probability of scour depths at 0.5 ft increments at 0, 15, 25, 50, 75, and 100 years. The scour depth that would possibly cause the failure of a bridge structure may be determined independently using structural analyses. As was shown in Chapter 6, the scour depth at which a bridge is expected to fail could be used by design engineers, in conjunction with the probabilities of scour depth at points in time, to estimate the variation of the probability of failure of the structure with time. By evaluating the probability of failure associated with various configurations of bridge pier

sizes and foundation depths, the designer would be able to maximize the safety of the bridge design within the budget appropriated.

Information about the risks of failure may be more useful than the probability of failure for setting policies that govern the design of new bridges and the operation and maintenance of existing bridges. This is because by definition, the risk of failure considers not only the probability of failure, but also incorporates the consequences of failure (Modarres 1993). This is particularly true for bridges over tidal waterways, as these structures are generally much longer and more expensive than bridges over upland rivers. The following discussion provides examples of how the WAVES output could be used to assist bridge engineers and policy makers to decide whether or not to design a new bridge or continue to operate an existing one.

Generally, the decisions about the construction of bridges are based on the long-term cost of the structure weighed against its benefits. The cost of the structure generally includes the design and maintenance costs; however, the cost of failure plays a prominent role in the decision making process and must be included in the analysis. To ensure that the risks of failure, in terms of economic and human consequences, are kept below levels decided by the policy makers, it may be necessary to improve the safety of the structure by increasing its maintenance and design costs. These additional costs must then be included in the overall cost of the structure and compared to the benefits. If the comparison does not meet specific criteria set by the decision makers, it may be necessary to shelve the design project. The hypothetical case study exercises presented in Chapter 6 shows how engineers may use the WAVES program to analyze the risk of bridge failure.

The analyses of the risks associated with bridge failure due to pier scour are also very important to making decisions regarding the use of existing bridges. The risk analyses in the design phase are usually performed to select appropriate crossings and to determine the sizes of the bridge piers and are based on conditions existing at the time that the structures are being designed. However, many factors are considered during the design phase that will progressively change during the life of the structure. These factors include traffic volumes, land use changes within the watershed, and the cost of maintenance and remedial construction. To account for these changes, it is necessary to repeat the risk analysis at regular intervals over the life of a structure to re-evaluate the costs necessary to ensure that the risk of failure remains below the accepted level in relation to the benefits accrued by keeping the bridges open. If remediation costs exceed the benefits of the structure, then the decision may be to close or decommission a structure. The WAVES program will help bridge engineers to perform these analyses by providing estimates of the annual probability of failure due to changing conditions. These new revised probabilities of failure may then be incorporated with the revised consequences to determine the new failure risks.

## **8.7 THE USE OF CURRENT SCOUR EQUATIONS FOR ESTUARIES**

The results of the comparative study described in Chapter 7 indicate that some simple scour equations currently in use may not accurately model scour in estuaries and tidal rivers. Such equations include those models that utilize only the pier diameter, flow depth, and total channel discharges as predictor variables. It was generally found that models that did not use the stream velocity, the critical or incipient velocity, and the bed

sediment sizes typically provided unrealistic estimates of the depth of the pier scour in estuaries.

The most limited models were those that utilized only the pier diameter as a predictor variable. The drawbacks of using these equations included their inability to provide results that varied with catchment and tidal conditions, and consequently the inability of such models to produce results that varied with time. Because these equations depended on pier diameters only, the hydraulic results of the combination of the tidal and riverine process were not considered, thus possibly leading to unreliable predictions. Also, the results produced by these models remained constant with time and did not vary between different estuaries, which is unrealistic. In addition, these models could not be used for risk-based designs as the scour results produced did not vary with time. This is a significant disadvantage as the risk or probability-based designs could not be used to provide a method of minimizing the imprecise effects of these equations.

Models that used flow depth and pier diameter or flow depth only provided very little improvement over models using only pier diameter as a predictor and are probably inappropriate for use in tidal environments. Though these equations have the ability to produce time variant conditions and scour results, the disadvantage of using them is that flow depth is a very inaccurate predictor of scour in tidal environments. As discussed earlier, the most hydraulically active flow area in estuaries is the tidal prism. Estuary waters below the tidal prism remain largely hydraulically inactive and do not participate in the development of the estuary discharges. As a result, the hydraulic relationship that exists between flow depth, discharge, and velocity in upland rivers does not exist in

estuaries. Consequently, the use of flow depth as a predictor of pier scour, though valid for upland rivers, may be totally inappropriate for estuaries.

Scour equations that use estuary discharge as a predictor, as opposed to discharge per unit width, usually produce unrealistically high scour values. These equations overestimate scour in estuaries and tidal environments owing to the very high discharges generated in these environments. This discrepancy is due to the fact that these models were developed from upland rivers, which were relatively narrow, and where the hydraulic conditions could be adequately represented by discharge values. A much better predictor is the discharge per unit width of the estuary as this takes into account the attenuating effects of the widths of large estuaries.

## **8.8 HURRICANE SCOUR**

The results of this study show that scour over the life of a bridge structure will be significantly greater than the scour produced by single-event storms such as hurricanes. The analysis of the scour produced by hurricanes within the tidal environment presents a special case. One of the most prominent scour generating features accompanying hurricanes is the wind driven surge that occurs in waterways along the hurricane path. Researchers such as the U.S. Army Corps of Engineers (1991) and Richardson and Edge (1997) have maintained that surge heights increase gradually as a hurricane approaches a location but falls sharply soon after the eye of the storm passes the location in question. This is caused by the blow-back phenomena discussed in Chapters 2 and 3. This sharp fall in the water-surface elevation generates very strong tidal discharges in the

downstream direction, which in turns generates a downstream velocity and scour on the upstream pier face. Results of the current study show that for most estuaries or tidal rivers, hurricane scour was generally generated from the upstream pier face.

This study showed that when hurricane scour did occur, the scour rates were comparable to, and in most cases greater than, the rates of scour generated over the life of the structure. On the other hand, the magnitude of the pier scour over the life of the bridge was much greater than the amount of scour that was caused by a single hurricane event. Many researchers ascribe this difference to the fact that sustained scour activity is necessary for the complete development of a scour hole, and the duration of a hurricane and other single-event storm is not sufficient to facilitate the full development of new scour holes or the further development of existing scour.

## **8.9 IMPORTANT FEATURES OF PIER SCOUR IN ESTUARIES**

The pier scour process in tidal waterways exhibits some distinctly different features from the process observed with upland or fluvial rivers. A somewhat surprising result is the realization that for tidal rivers or estuaries, pier scour may be initiated at either the upstream or downstream face of the bridge pier depending on whether the crossing is dominated by the catchment or tidal processes. It was assumed by many tidal researchers that the combined effect of the catchment discharges and the discharges generated by the falling tides would always out-weigh the tidal discharges generated by the rising tides. This study indicates that the dominant discharge direction, upstream or downstream, depends on the relative sizes of the catchment and estuary areas. This can be explained by the fact that tidal waterways are affected by a finite number of storms

annually and during these periods the downstream flows are favored. Between storms, however, discharges are generated by tidal variations only. In addition, researchers have determined that in a tidal environment the rising tide tends to generate significantly greater discharges than the falling tide (Demetrius et al. 2002). Hence, this leads to the result that if an estuary is very large compared to its catchment area; scour will likely be initiated from the downstream pier face.

Another feature of pier scour in estuaries is the attenuating effects that the typically wide estuary cross section has on flow velocities. Preliminary simulations indicated that in many cases, significant scour would not develop over the life of the bridge. In addition, estuaries with deep channels and significant inactive flow depths also produce much lower flow velocities when compared to upland rivers. It was also observed that estuarine channel depth bore an inverse relationship with flow velocities which is in sharp contrast to the relationship between depths and flow velocities in upland rivers where a direct relationship usually exists.

The impact of the geometry of the bridge cross section is, therefore, quite significant. If the cross section is deep (greater than 20 ft) and wide (greater than 1 mi), then significant pier scour may not develop over the life of the structure. This finding suggests that bridges across estuaries or tidal rivers should be located at the widest cross sections for maximum safety against bridge failure from pier scour. However, such a design consideration would lead to greater design, construction, maintenance, and operation costs. The implication of this finding is that a process that optimizes the cost of constructing bridges of a given length against bridge safety must be incorporated in the design analyses of new bridges.



## **CHAPTER 9**

### **RECOMMENDATIONS**

#### **9.1 INTRODUCTION**

This study involved the development of a program that could be used to provide time varying estimates of scour induced at circular bridge piers in estuaries and tidal rivers. As a result of the limitations of the scope of this study, the applicability of the program presented here is constrained to specific situations and conditions. A clear understanding of the WAVES program will allow bridge design engineers to use the model under the appropriate conditions for its intended purpose. Also, because of the imprecision of most pier scour models, knowledge of the limitations associated with the methods currently used to design bridges against scouring are important. Development of risk-based design methodologies would improve the design of bridges by eliminating the dependence of such designs on unreliable estimates of pier scour. Adoption of these measures will in turn lead to the construction of safer bridges over tidal waterways.

#### **9.2 THE NEED FOR A RISK-BASED DESIGN METHODOLOGY**

The current state of the science of pier scour prediction makes it difficult for most scour models to produce reliable and precise results. The uncertainties in scour predictions may cause the design of bridge piers using these estimates to be flawed. This problem is further compounded when bridges are to be designed over estuaries and tidal waterways because most available models are based on upland riverine conditions and do not consider the complex processes of the estuarine environment. In addition, current design procedures typically use these scour estimates as absolute values where

uncertainties in these are addressed by the application of safety factors to the final design. This study shows that a risk-based design procedure has the potential of better handling the uncertainties of current scour estimations, particularly in estuarine environments. With a risk-based analysis, the bridge design is not based totally on an absolute scour value, but incorporates the probability of occurrence of various scour depths over time. Also, a risk-based approach incorporates the consequences of failure and this further reduces the impacts of the uncertainties in scour estimation on bridge design. For these reasons, a risk-based process would improve the design of bridges.

### **9.3 IMPROVING THE SCIENCE OF PIER SCOUR PREDICTIONS**

#### **9.3.1 Further Research into the Scour Process**

Researchers of bridge pier scour unanimously agree that a much deeper understanding of the processes and mechanisms involved is needed to improve the state of the science. Specifically, greater research in specific areas of the scour mechanism such as the development of the downflow, horseshoe vortex, and scour hole are needed. The WAVES program was developed based on the conceptual considerations of the roles of the downflow, horseshoe vortex, and the erosion mechanisms governing the formation of the scour hole. The accuracy of the program could be improved by a more complete understanding of the changes that occur in the downflow at all stages of the development of scour hole. Similarly, the predictions of the program will be improved by the knowledge of the relationship between the downflow and horseshoe vortex and the properties of the vortex. Finally, the predictions of the WAVES program could be improved with the further clarification of the role of the vortex in the erosion process.

Much research has been done regarding the development of the downflow at the base of a bridge pier placed in the path of the stream flow. The extensive work done by Ettema (1984) was used as a part of this study to formulate a conceptual equation for the development of the downflow. While the development of the downflow to its maximum value has been well researched, studies have not been performed to investigate its properties and further development after it has reached its maximum value of 2.3 times the pier diameter. In addition, studies have not been done to determine the properties of the downflow from field measurements. As a result, much work is needed to determine the decay of the downflow after the maximum value is reached and the scour hole is fully developed.

Many researchers cite the horseshoe vortex as playing the most critical role in the development of the scour hole; however, enough studies have not been done to quantify its properties. As a result, studies that quantitatively model the development of the horseshoe vortex are needed. While there is wide acceptance of the mechanism involved in the formation of the vortex, more research needs to be undertaken to develop the relationships between the vortex properties and the hydraulic properties of the tidal environment. In addition, further research is needed to determine the quantitative relationship between the horseshoe vortex and the downflow.

The scientific community is split on the issue of the process that actually causes the erosion that leads to bridge pier scour. One school of thought believes that the downflow is the actual agent of erosion and the other supports the idea that the horseshoe vortex, either via its tangential velocity, negative pressure, or both, is the cause. Further

research is needed to verify whether the downflow or the horseshoe vortex is the cause of erosion.

The WAVES program reasonably assumes that estuary soils are predominantly alluvial and, therefore, cohesionless. It has been shown, however, that the soil strata of the estuary channel at the lowest horizons may indeed contain cohesive clays. Further, current research suggests that the mechanism of erosion is different for cohesive and cohesionless soils. In the case of cohesionless soils, the erosion mechanism requires the exceedence of some threshold condition, such as velocity, or discharge. Scour in cohesive soils is affected by the weak Van der Waals attractions between the particles that resist scour and the extremely low diameter and weight of the soil particles that do not provide much gravitational resistance to erosion. Research suggests that erosion in cohesive soils occur at all values of velocity or discharge. However, the scientific community accepts that the threshold condition, used for the determination of scour in granular materials, may still be applied to cohesive soils because the scour of cohesive soils at low velocities may be relatively insignificant. As a result, more research involving pier scour in cohesive sediments is needed to formulate a method of determining the effective threshold condition at which scour will become significant.

### **9.3.2 The Importance of Reliable Pier Scour Field Data**

Improving the quality of scour data collected in the field would enhance the understanding of the scour mechanism and the quantitative modeling of the scour process. Most of the scour research undertaken has been based on laboratory data that, though useful, cannot satisfy the need for field data. Though some field data exists, the

integrity and quality of the data cannot be assured. The survey of local transportation departments conducted as a part of this study indicated that a primary concern was that most scour data collected in the field were done after the recession of the channel floods. The result was that this data represented conditions after the scour hole had been partially filled in by unconsolidated deposition brought down by the floods and did not reflect the maximum scour depth reached during the peak of the flood.

In order to improve the quality of scour data collected in the field, methods of conducting the real-time monitoring of scour at piers need to be developed. The available technology in the areas of telecommunications and systems engineering could also be used to transfer real-time scour measurements to central locations where the data could be analyzed and stored. In addition, consistent protocols are needed to address the equipment and process used to define the dimensions of the scour hole with regard to the location of the consolidated and unconsolidated soil interface.

## **9.4 IMPROVING THE WAVES PROGRAM**

### **9.4.1 Pier Geometry**

The WAVES program was developed specifically for circular piers and piers with semicircular leading edges oriented parallel to the direction of flow. In contrast, a wide and diverse range of pier shapes is actually used in bridge designs. In order to improve the applicability of the model, further research is needed to investigate the effects of piers of other shapes on the models results. This information could then be used to develop shape coefficients to modify the results of the program for the given pier geometry.

### **9.4.2 Pier Type**

Melville and Coleman (2000) identified three types of pier configurations used typically in bridge designs and construction. In the first configuration, the pier footing, caisson, or pile cap is set below the invert of the channel. Failure in this case occurs when scour progresses to an elevation lower than the elevation of the pile footing, pile cap, or caisson. The second configuration is applicable only to pile and caisson foundations. In this case the bottom of the pile cap is located at the invert of the channel with the piles driven into the ground. Also, where caisson foundations are used, the caisson is partly driven into the channel bed with a portion of it remaining above the invert of the channel. Pier failure in the second configuration is believed to occur when scour progresses below the bottom of the caisson or pile foundation. The third configuration is again applicable only to pile and caisson foundations. Here the top of the caisson is set at the water surface or above. Where piles are used, the top of the pile cap is set at or above the water surface while the bottom of the pile cap is set at an elevation greater than the invert of the channel. Partially buried piles are then used to support the pile cap. Pier failure in the third configuration is believed to occur when the piles or caisson are undermined.

The WAVES program is directly applicable to piers designed with foundations using the first configuration. The program may also be applied to circular caissons in the third configuration. Uncertainties exist regarding the applicability of the program to piers supported by piles and piers designed with caissons using the second configuration. To improve the program's applicability, adjustments should be made to the algorithms to

allow the modeling of piers both with the caissons described in the second configuration and with circular piles discussed in the third configuration.

#### **9.4.3 Modeling Pressure Flow**

Bridge piers are usually subjected to pressure flow when flooding levels rise to or above the elevation of the bridge deck. Pressure flows have the impact of increasing the stream flow velocities around the bridge pier thus generating greater scouring when compared to non-pressurized flow conditions. The WAVES program assumes that the deck of the bridge being modeled will always be greater than the flooding levels and, as a result, the program assumes that pressure flow will never be encountered. This assumption may be true for bridges over most wide estuaries; however, bridge deck overtopping may occur in small tidal rivers. The accuracy and range of applicability of the model could, therefore, be improved by adding an option for the consideration of pressure flows.

#### **9.4.4 Improving the Hydraulic Component**

The accuracy of the scour results predicted by the WAVES program depends greatly on the hydraulic component method used to convert flow discharges to stream velocities. This is because the downflow and vortex development are also dependent on stream velocities. The WAVES program currently uses the steady-flow continuity equation to compute stream velocities at each computational time step. The accuracy of the model could be improved if the hydraulic component was developed to utilize the

one-dimensional unsteady-flow (Saint Venant) equations for the computation of velocities.

#### **9.4.5 Model Calibration and Verification**

Owing to the difficulties involved in obtaining real pier scour data from estuaries, and the unreliability of scour data in general, the WAVES program was not formally calibrated and verified. Components of the program, such as the hydrologic, downflow, and vortex components were individually calibrated either by the author of this dissertation or by other independent sources. It is, therefore, important to collect reliable temporally varied estuarine scour data for the calibration of the WAVES program. This would result in the improvement of the accuracy of the model's predictions.



## APPENDIX A-1

### COMPREHENSIVE SCOUR MODEL LIST OF ALL VARIABLES August 9, 2004

AI	in.	R	amount rainfall excess
AFD		R	'a' factor for the computation of the tangential velocity on the downstream face of the pier
AFU		R	'a' factor for the computation of the tangential velocity on the upstream face of the pier
ALPHA( )		R	Array of soil alpha properties ( used in calculation soil incipient velocities
ALPHAU		R	alpha property pointer upstream face
ALPHAD		R	alpha property pointer downstream face
AS	Sq miles	R	Surface area of tidal estuary upstream of bridge location
ASD		R	annual storm distribution U( MNS, SDS)
AMT		R	the factor used to normalize the total direct runoff volume.
AX( )	Sq. ft.	R	cross sectional area of the estuary at bridge location b
B18		R	Gamma variate constant B for duration 18hrs.
B24		R	Gamma variate constant B for duration 24 hrs
B36		R	Gamma variate constant B for duration 36 hrs
CBA	Sq. miles	R	catchment area
CBAMIN,	sq.mi.	R	minimum catchment area
CN		R	basin curve number
CSD	ft.	R	computed scour depth downstream face
CSU	ft.	R	computed scour depth upstream face
CX		R	the convex routing factor
C1		R	downflow orifice constant
C18		I	Gamma variate constant C for duration 18 hrs
C24		I	Gamma variate constant C for duration 24 hrs
C36		I	Gamma variate constant C for duration 36 hrs
CHY18( )	cfs.	R	catchment hydrograph 18 hr storm
CHY24( )	cfs.	R	catchment hydrograph 24 hr storm
CHY36( )	cfs.	R	catchment hydrograph 36 hr storm
D18	hrs	I	duration of 18 hr storm
D24	hrs	I	duration of 24 hr storm
D36	hrs	I	duration of 36 hr storm

DA	ft.	R	diurnal amplitude
DED	ft.	R	equilibrium scour depth downstream face
DEU( )	ft.	R	equilibrium or ultimate local scour depth upstream face
DIM		R	the ratio of estuary length upstream of bridge to tidal wavelength
DLT	hrs.	R	computational time step
DPTH( )	ft.	R	array of soil depth at bridge station
DPTHD	ft.	R	depth pointer at downstream face
DPTHU	ft.	R	depth pointer at upstream face
DRO18( )	cfs.	R	freshwater hydrograph discharge value 18 hr storm
DRO24( )	cfs.	R	freshwater hydrograph discharge value 24 hr storm
DRO36( )	cfs.	R	freshwater hydrograph discharge value 36 hr storm
DSD( )		R	ratio of scour depth to pier diameter at downstream face
DSU		R	ratio of scour depth to pier diameter at upstream face
DT	hrs.	R	diurnal period
DU	hrs.	R	unit hydrograph duration
DUH( )	cfs.	R	DIMHYD contains dimensionless discharge array
D50( )	mm.	R	Array of mean particle diameter in mm varying with depth
D50D	mm.	R	Mean particle diameter downstream face of pier
D50U	mm.	R	Mean particle diameter upstream face of pier
F18		R	proportion of scour producing storm with duration 18 hrs
F24		R	proportion of scour producing storm with duration 24 hrs
F36		R	proportion of scour producing storm with duration 36 hrs
GR	f/s <sup>2</sup>	R	acceleration due to gravity
GAMMAS		R	specific weight of soil
GW		R	the specific weight of water
HF		R	Tidal depth factor for the modification of Neill's eqn.
IA	in.	R	initial abstraction
IBR	ft.	R	invert of bridge station
IBS	ft.	R	invert of tidal base station

KT		R	contraction scour factor
LA	ft.	R	lunar amplitude
LC	miles	R	length of catchment flowpath in miles
LE	miles	R	Length of estuary upstream of bridge station
LT	hrs	R	lunar period
LW	miles.	R	distance from base station to bridge station in feet
MAS		I	mean number of scour producing storms per year
MDA	ft.	R	mean diurnal amplitude at base station
MDR	ft.	R	mean depth of bridge station
MLA	ft.	R	mean lunar amplitude at base station
MLT	ft.	R	the mean low tide depth at bridge station
MNS		I	mean number of scour producing storms in the simulation period
MTL	hrs	R	the mean tidal lag time in moving from base station B to bridge station b.
MTR	ft.	R	mean tidal amplitude at bridge station
MUW	ft <sup>2</sup> /sec.	R	kinematic viscosity of water
NBP		I	number of bridge piers in a straight line across channel
ND		I	number of diurnal variates
NO		I	number of dimensionless unit hydrograph ordinates
NU		I	number of unit hydrograph ordinates
N18		I	number of 18 hr scour producing storm in simul. period
N24		I	number of 24 hr scour producing storm in simul. period
N36		I	number of 36 hr scour producing storm in simul. period
NMFF		R	Neill's modification factor falling limb of tide
NMFR		R	Neill's modification factor rising limb of tide
NP18		I	number of rainfall ordinates 18 hr storm
NP24		I	number of rainfall ordinates 24 hr storm
NP36		I	number of rainfall ordinates 36 hr storm
NR18		I	number of runoff ordinates 18 hr storm
NR24		I	number of runoff ordinates 24 hr storm
NR36		I	number of runoff ordinates 36 hr storm

PD	ft.	R	bridge pier diameter
PE18( )	ins.	R	array of cumulated excess runoff 18 hr storm
PE24( )	ins.	R	array of cumulated excess runoff 24 hr storm
PE36( )	ins.	R	array of cumulated excess runoff 36 hr storm
PEI18( )	ins.	R	array of discrete excess runoff values 18 hr storm
PEI24( )	ins.	R	array of discrete excess runoff values 24 hr storm
PEI36( )	ins.	R	array of discrete excess runoff values 36 hr storm
PI		R	3.142
PH( )	deg.	R	array of the soil angle of repose
PHI	deg.	R	initial soil phi angle
PHD	rad.	R	phase angle of the diurnal wave
PHDD	deg	R	pointer for soil phi angle downstream face
PHL	rad.	R	phase angle of the lunar wave
PHU	deg	R	pointer for soil phi angle upstream face
PKM	ft. per ft.	R	mean peakedness of the base station tides
PP18	in.	R	total inches of rainfall in a 18 hr. event
PP24	in.	R	total inches of rainfall in a 24 hr. event
PP36	in.	R	total inches of rainfall in a 36 hr. event
QBF	cfs.	R	catchment base flow
QTF( )	cfs.	R	array of tidal discharge produced by the falling limb
QTR( )	cfs.	R	array of tidal discharge produced by the rising limb
QNF( )	cfs	R	array of Neill's tidal discharge falling limb
QNR( )	cfs	R	array of Neill's tidal discharge rising limb
QNFM( )	cfs	R	array of modified Neill's tidal discharge falling limb
QNRM( )	cfs	R	array of modified Neill's tidal discharge rising limb
QT( )	cfs.	R	array of total resultant discharge at bridge station
RHW	lb/cuft.	R	density of water
RLU	fps.	R	the rate of local scour upstream face of the pier
RLD	fps.	R	the rate of local scour downstream face of the pier
SC		R	soil infiltration potential
SDS		R	standard deviation in the annual scour producing storms
SDA		R	standard deviation in the diurnal amplitude
SDI	ft.	R	initial scour depth at downstream face
SF	cuft.	R	the volume of fresh water entering the estuary over one hydrograph step
SG		R	specific gravity
SLA	ft.	R	standard deviation in the lunar amplitude
S18(18)		R	array with SCS type II storm with duration 18 hrs

S24(24)	R	array with SCS type II.storm with duration 24 hrs
S36(36)	R	array with SCS type II storm with duration 36 hrs
SOL(30, 4)	R	array with soil mean particle diam (mm,), D50, phi angle PH and soil property alpha with ALPHA
SQ cuft	R	fresh water storage
ST cuft	R	total volumetric storage
SUI ft.	R	initial scour depth at upstream face
TAF	R	tide attenuation factor
TB hrs.	R	hydrograph time base
TBR( ) hrs.	R	array of arrival time of each point on the tide at the
TC hrs.	R	time of concentration
TDI ft.	R	initial scour at downstream face of pier
TE hrs.	R	time to reach equilibrium scour depth (ft)
TEB( ) ft.	R	tidal elevations at base station
TER( ) ft.	R	tidal elevations at bridge station
THU( )deg.	R	scour angle at upstream face of pier
THD( )deg.	R	scour angle at downstream face of pier
THUI deg..	R	initial scour upstream face
THDI deg.	R	initial scour angle downstream face
TMS	I	the number of times simulations are repeated
TNR	R	array of normalized wave arrival times at bridge
TNRI	R	array of normalized interpolated wave arrival times at bridge
TO ( ) hrs.	R	contains dimensionless time array
TP hrs.	R	time to peak
TR ft.	R	mean tidal range at bridge station
TS cuft.	R	tidal storage
TSU ft.	R	total scour depth on the upstream face of the pier
TSD ft.	R	total scour on the downstream face of the pier
UVA	R	uniformed variates used to determine the gamma variate representing rainfall amount
UVAR	R	pointer for multiplying uniform variates
UC fps.	R	critical mean stream velocity that causes bedload movement
UID( ) fps.	R	velocity causing incipient motion of a given bed particle size at downstream face
UIU( ) fps.	R	velocity causing incipient motion of a given bed particle size at upstream face
VDU fps.	R	maximum downflow on the upstream face of the pier
VDD fps.	R	maximum downflow on the downstream face of the

VMD	fps.	R	pier maximum tangential velocity along downstream pier face
VMU	fps.	R	maximum tangential velocity along upstream pier face
VNU	fps.	R	net velocity up directed up the estuary
VND( )	fps.	R	net velocity down the estuary
VTU( )	fps.	R	tangential velocity on the upstream pier face
VTD( )	fps.	R	tangential velocity on the downstream pier face
VNT( )	fps.	R	net velocity at bridge station between tidal and riverine flows
VNU( )	fps.	R	net velocity up the estuary
WB	miles	R	width of estuary channel at bridge location
WBE	miles	R	the effective bottom width of the channel at the bridge location
WD	miles	R	width of channel at near field downstream of bridge
WF		R	estuary width factor for the modification of Neill's eqn.
WM	miles	R	the maximum width of the estuary upstream of location b
WU	miles	R	width of channel at near field upstream of bridge
YAT( )	ft	R	attenuated time varying tidal depth at b
YATI( )	ft	R	interpolated attenuated tidal depths
YB ( )	ft	R	tidal depth at base station
YRS	yrs.	I	length of a full simulation yrs
YSU	ft	R	total contraction scour on upstream face of the pier
YSD	ft	R	total contraction scour on downstream face of the pier
YT	ft	R	the total water depth at the bridge location
YTM	ft	R	maximum total water depth
YMI	ft	R	initial maximum depth

## APPENDIX A-2

PROGRAM WAVES2  
C WAVES2 Version 3)                      march 17, 2005  
C **W**atershed **I**nvested **E**stuary **S**cour

C     OPTION ADDED FOR CRITICAL VELOCITY CALCULATION  
C     IMPROVED ROUTING  
C     Surge formula adjusted to start from zero  
C     USE UNIFORMED DIMENSION SIZES FOR HYDROGRAPH AND TIDAL SERIES  
C     RE-CONFIGURE TIDAL SERIES BASED ON TIDE DEPTH.  
C     \*  
C     TIDE DISTORTION OPTION IS PROVIDED ALONG WITH THE OPTION TO  
C     BYPASS THE NEILL'S MODIFICATION FACTOR. PROGRAM INCLUDES  
C     HISTOGRAM FOR SCOUR SIMULATIONS  
C     \*  
C     \*  
C     YT SEPARATED TO COMPUTE U/S, AND D/S CONTRACTION SCOUR.  
C     CORRECTIONS MADE TO THE COMPUTATION OF YT.  
C     \*  
C     TIDAL DEPTHS CONSTRAINED TO BE GREATER THAN MLW  
C     \*  
C     FEATURE ADDED TO TRACK THE ANNUAL SCOUR RESULTS OVER YRS  
C     \*  
C     OPTION FOR THE ANALYSIS OF EXISTING BRIDGES ADDED  
C     \*  
C     FEATURE TO ANALYZE A DESCRETE HURRICANE EVENT ADDED  
C     \*  
C     AVERAGE VELOCITY OVER 1 HOUR USED TO COMPUTE SCOUR  
C     \*  
C     Scour coefficients adjusted  
C     Recordation of annual maximum Q, V and YT included  
C     \*  
C     Contraction scour computed hourly using Straub's equation  
C     Bed level adjusted hourly  
C     \*  
C     Critical velocity modified by Donlounig initiation factor  
C     \*  
C     Armouring option provided  
C     \*  
C     Correction made to the hurricane option  
C     \*  
C     Model improved to accept specific hurricane information as an  
C     option  
C     Estuary cross sectional area adjustment factor, and flowdepth  
C     factor added.  
C     Full simulation of all storms

C     Estuary volume routing included  
C     Over bank flow area adjusted  
C     User friendly additions  
C     Latest changes made to the pier analysis option and the single  
event model

IMPLICIT NONE

C

```
DIMENSION S18(18), S24(24), S36(36), TO(36), DUH(36),
S6(6)
DIMENSION QU(200), T(200), DRO18(300), DRO6(300)
DIMENSION DRO24(300),DRO36(300),PEI18(18), PEI24(24), PEI6(6)
DIMENSION PEI36(36), CHY18(300),CHY24(300),CHY36(300),CHY6(300)
DIMENSION DPTH(30), D50(30), PH(30), ALPHA(30),P18(18)
DIMENSION P24(24), P36(36), PE18(18), PE24(24), PE36(36)

DIMENSION P6(6), PE6(6)

DIMENSION TBR(400), TER(400),YATI(300),TNRI(300),TERS(400)
DIMENSION YAT(400), YB(400), TEB(400), TNR(400), TERI(300)

DIMENSION QN(300), YTR(300), YTF(300), YT(300), VITID(300)
DIMENSION QT(300), VNU(300), VND(300), VNT(300), VITOT(300)
DIMENSION QNM(300), QROUT(300),VOUT(300),VICAT(300),VBAL(300)

DIMENSION DSU(300),CSU(300),VDU(300),VDD(300),THU(300),THD(300)
DIMENSION VMU(300),VMD(300),AFU(300),AFD(300),VTU(300),VTD(300)
DIMENSION DSD(300),CSD(300),VNUIN(300), VNDIN(300), VCRINU(300)
DIMENSION VCRIND(300)

REAL YTSU(100), YMNTSU(100),YSMTSU(100),YSTTSU(100),YSMUSQ(100)
REAL YTSD(100), YMNTSD(100),YSMTSD(100),YSTTSD(100),YSMDSQ(100)
REAL YYSUIN(100),YYSUIN(100),SMYYSU(100)
REAL SMYYSU(100),MNYYSU(100),MNYYSU(100), MNLSU(100), MNLSU(100)

DIMENSION DEU(300), TEU(300), DED(300), TED(300), UIU(300)
DIMENSION K1U(300), K2U(300), RLU(300), RLD(300), UID(300)
DIMENSION K1D(300), K2D(300), K3U(300), K3D(300), VARMU(300)
DIMENSION VARMD(300)

DIMENSION B(100), FU(100), FD(100), PRU(100), PRD(100)
DIMENSION CPRU(100), CPRD(100), FHD(100), FHU(100), PRHU(100)
DIMENSION PRHD(100), CPRHU(100),CPRHD(100)

REAL FU15(100), FU25(100), FU50(100), FU75(100)
REAL FD15(100), FD25(100), FD50(100), FD75(100)
REAL PRU15(100), PRU25(100), PRU50(100), PRU75(100)
REAL PRD15(100), PRD25(100), PRD50(100), PRD75(100)
REAL CPRU15(100),CPRU25(100),CPRU50(100),CPRU75(100)
REAL CPRD15(100),CPRD25(100),CPRD50(100),CPRD75(100)

REAL S18, S24, S36, TO, DUH, QU, T, IA
REAL C18, C24, C36, C6, S6
REAL DPTH, D50, PH, ALPHA, DPTHD, D50D, PHD
REAL DPTHU, ALPHAU, D50U,PHU, ALPHAD, VCUF, VCDF
```

C

```
REAL GR, SWW, MUW, MAN, PI, RHW, SWS, CN
REAL CBA, CBAMIN, LC, DU, SDS, B18, B24, B36
REAL FQ18, FQ24, FQ36, PPT18,PPT24, PPT36, MLA, SDA
REAL UVAR18, UVAR24, UVAR36, UVA, MDA, CX, LEW, PHL
```



```

REAL IBS,      DT,      LT,      LW,      PD,      C1,      TER,      TERS
REAL SLA,      SC,      TAF,      PKM,      MLT,      DA,      TMCON, AFACT
REAL UESTZ,    PPT6,    B6,      FQ6,      UVAR6,    ENS

```

```

REAL CS,      IRS,      MDR,      MTR,      MTL,      YTMR,      COFU,      COFD
REAL AS,      LE,      WB,      WD,      WU,      WM,      KT,      SS
REAL YMIF,    TDI,      TUI,      MAS,      NMFF,      NMFR,      QNM,      TEB
REAL PHDD,    K1U,      K2U,      K3U,      K1D,      K2D,      K3D,      DLT
REAL YMIR,    YTMF,      YTR,      YTF,      VOUT,      QROUT,    VICAT,    VBAL
REAL VITOT,    HITIDE,    HIBASE, THSD,      THSU,      LA

```

```

REAL HPRM,    MAXSRG,    MXSRG1,    MXSRG2, MXSRG3, MXSRG4, MXSRG5, HRAD
REAL HDIST,    HSPEED,    HSPED1,    HSPED2, HSPED3, HSPED4, HSPED5, JIN
REAL HRAD1,    HRAD2,    HRAD3,    HRAD4, HRAD5, HURPPT
REAL HURAIN,    MXSRGI,    HRADI,    HSPEDI,    BLOCON

```

```

REAL HTER(300), HYAT(300), HSURGE(300)

```

C        REAL VARIABLES USED TO COMPUTE THE HURRICANE SCOUR STATISTICS

```

REAL STDHSD, SSQHSD, MNTHSD, SQTHSD, SMTHSD
REAL STDHSU, SSQHSU, MNTHSU, SQTHSU, SMTHSU

```

```

REAL VUPMSM(100), VDNMSM(100), YTRYRS(100)
REAL AVDNYR(100), AVUPYR(100), VUPYR(100), VDNYR(100)
REAL QUPYR(100), QDNYR(100), YTFYRS(100), YTYRS(100)

```

```

REAL SUMYSD, SUMYSU, SIGMAU, SIGMAD, D16D, D84D, D16U, D84U
REAL YUINMX, YDINMX, DMAXU, DMAXD

```

C        YUINMX, YDINMX are the maximum contraction scour indicator values  
of YSUIN and YSDIN

```

REAL D16(30), D84(30), YTRF(300), YTFF(300), YSU(300), YSD(300)
REAL YSDIN, YSUIN, DMAX(30)

```

C        VUPM and VDOWNM are the holding places for the maximum annual stream  
velocities

C        VUPMSM and VDNMSM are the sum of the annual velocities over "TMS"

C        in the upstream and downstream directions. AVDNYR and AVUPYR are the  
average annual

C        upstream and downstream maximum velocities

C        EPI is the existing pair invert

C        THSD, THSU are the total hurricane scour upstream and downstream  
face

```

REAL VCRINU, VCRIND, VARMU, VARMD
REAL DEL,      B,      PRD,      CPRD
REAL FD,      FU,      PRU,      CPRU, TDRO, TINF

```

```

REAL QTUMAX, QTRMAX, QTFMAX, SUMQTU, QTRMX, QTFMX
REAL YTMAX, YTRMX, YTFMX, SUMYT, YTRMAX, YTFMAX
REAL VNUMAX, SUMVNU, VNDMAX, SUMVND
REAL CONQTU, CONYT, CONVNU, CONVND, VUPM, VDOWNM

```

```

REAL VTUMX, VTDMX, UIUMIN, UIDMIN, VUPMS, VDOWNMS
REAL VTUMXS, VTDMXS

```

```

REAL COFUF, COFUS, COFDF, COFDS, VNDNAM, VNUPAM, YTMRF, YTMFF

REAL VNUA(300), VNDA(300), TAUDD(300), TAUCD(300), TAUDU(300)
REAL TAUCU(300), VNDAYR(100), VNUAYR(100), YTRFYR(100),
YTFFYR(100)
REAL QTR(300), QTF(300), QPK18(100), QPK24(100), QPK36(100)
REAL QPK6(100)

REAL QP18MX, QP24MX, QP36MX, QP6MX, ASUM6, ASUM18, ASUM24, ASUM36

REAL QTRMXS, QTFMXS

C

C      Declare routing variables and arrays

REAL EBMLT(4), TWBMLT(4), XABMLT(3), SUMXAB(3), XADJAD(150)
REAL XAAML(150), XADJAU(150), XABMLE, ELAML(150), TWAML(150)
REAL MLTE, SXAML(150), PLANA(150), ESVOL(150), SESVOL(150)
REAL YTAML(150), XATOT(300)

REAL FREX, INDX, TC, TP, AI, QP, QBF, TR, WBE, DIM, WF, HF, TT, SUM, AMT
REAL TSU, TSD, HIELE, PPTMAX, SUM6, P6, PE6, DRO6, CHY6, YB, QN, QT, YAT
REAL CHY18, YT, YTMX, YTFMXS, YTRMXS, TBR, YATI, TERI, DPTHCU, D16CU
REAL D50CU, D84CU, SIGMCU, DPTHCD, SP, D16CD, D50CD, D84CD, SIGMCD
REAL VNT, VNUIN, VNU, CSD, DSD, VDD, THD, AFD, VMD, UID, VTD, TED, DED, RLD
REAL VNDIN, VND, CSU, DSU, VDU, THU, AFU, VMU, UIU, VTU, TEU, DEU, RLU, SUM18
REAL P18, PE18, DRO18, SUM24, P24, PE24, DRO24, CHY24, SUM36, P36, PE36
REAL DRO36, CHY36, HDUR, FHD, FHU, PRHD, PRHU, CPRHD, CPRHU, PEI6, PEI24
REAL PEI36, TNR, TNRI, RANNO, PEI18, BNDX, VFACT, VITID, NMFRF, NMFFF
REAL NMFRH, RADCON

C      Declare integers
INTEGER IERROR, NU, TMS, YRS, NO, NBP, D18, D24, D36
INTEGER NR18, NR24, NR36, TB, NORNG, DISCON, NORUN, YR(100)
INTEGER HCAT, CONTRA, ARMVEL, YEAR, D6, NR6, ACTNM
INTEGER I, J, K, L, M, NP6, NP18, NP24, NP36, NS, ARR, N6, N18
INTEGER N24, N36, JINMAX, VINCIP, HCVIND, CONROUT

C      HCAT is the Hurricane category(1,2,3,4,5)

CHARACTER*50 FILE1, FILE2, DATE, TITLE
CHARACTER*6 DESIN, ANALIN, DATUM

C      OPEN INPUT FILE AND READ IN DATA
C
WRITE(*,*) 'ENTER THE NAME OF THE INPUT FILE'
READ(*,*) FILE1

OPEN (6, FILE= FILE1, STATUS = 'OLD', IOSTAT = IERROR)

C      CREATE AND OPEN OUTPUT FILE

WRITE(*,*) 'ENTER THE NAME OF THE OUTPUT FILE'
READ(*,*) FILE2

```

```

      OPEN (12, FILE = FILE2, STATUS = 'UNKNOWN')
C
C      ENGINEERING CONSTANTS
C
      READ (6,*)
      READ (6,*)
      READ (6,*)
      READ (6,*)
      READ (6,*)
      READ (6,*)
      READ (6,*)
      READ (6,*) GR, SWW, MUW, MAN, PI, RHW, SWS
      READ (6,*)

C
C      SIMULATION DATA
C
      READ (6,*)
      READ (6,*)
      READ (6,*)
      READ (6,*) DLT, TMS, YRS
      READ (6,*)

      IF(TMS.LT.2)WRITE(*,*) 'NUMBER OF SIMULATIONS MUST BE 2 OR
GREATER'
      IF(TMS.LT.2) GO TO 2000
C
C      CATCHMENT BAIN HYDROLOGIC DATA
C
      READ (6,*)
      READ (6,*)
      READ (6,*)
      READ (6,*) CN, CBA, CBAMIN, LC, DU, NO,TMCON
      READ (6,*)

C
C      STORM (RAINFALL)DATA
C
      READ (6,*)
      READ (6,*)
      READ (6,*)
      READ (6,*) FQ6, FQ18, FQ24, FQ36, MAS, SDS
      READ (6,*)
      READ (6,*)
      READ (6,*) B6, B18, B24, B36, C6, C18, C24, C36
      READ (6,*)

C
C      SCS TYPE II STORM DISTRIBUTION FOR 18, 24,36 HRS
C
      READ (6,*)
      READ (6,*)
      READ (6,*)
      READ (6,*) (S18(I),I=1,18)

```

```

      READ (6,*)
      READ (6,*)
      READ (6,*) (S24(I),I=1,24)
      READ (6,*)
      READ (6,*)
      READ (6,*) (S36(I),I=1,36)
      READ (6,*)
      READ (6,*) (S6(I),I=1,6)
C
C      SCS DIMENSIONLESS UNIT HYDROGRAPH
C
C      READ (6,*)
      READ (6,*)
      READ (6,*) (TO(I),I=1,36)
      READ (6,*)
      READ (6,*) (DUH(I),I=1,36)
C
C      BASE STATION TIDAL DATA
C
C      READ (6,*)
      READ (6,*)
      READ (6,*)
      READ (6,*) IBS, DT, LT, LW, MDA, MLA, SDA, SLA
      READ (6,*)
C
C      BRIDGE STATION TIDAL DATA
C
C      READ (6,*)
      READ (6,*)
      READ (6,*)
      READ (6,*) DATUM, CS, MTR, PKM
      READ (6,*)
      READ (6,*)
      READ (6,*)
      IF(DATUM.NE.'MSL') WRITE(*,*)'ELEVATION DATUM MUST BE MSL'
      IF(DATUM.NE.'MSL') GO TO 2000
C
C      BRIDGE DATA
C
C      READ (6,*)
      READ (6,*) NBP, PD, C1
      READ (6,*)
C
C      BRIDGE ESTUARY DATA
C
C      READ (6,*)
      READ (6,*)
      READ (6,*)
      READ (6,*)
      READ (6,*) AS, LE, WB, WD, WU, WM, AFACT, UESTZ
      READ (6,*)

```

```

C          ESTUARY CROSS SECTION DATA
C
      READ (6,*)
      READ (6,*) (EBMLT(I),I=1,4)
      READ (6,*)
      READ (6,*) (TWBMLT(I),I=1,4)

C
C          SOIL DATA
C
      READ (6,*)
      READ (6,*)
      READ (6,*)
      READ (6,*) KT, SS
      READ (6,*)

C
C          ARRAYS WITH DEPTH RELATED SOIL PROPERTIES
C

      READ (6,*)
      READ (6,*)
      READ (6,*) (DPTH(I),I=1,30)
      READ (6,*)
      READ (6,*) (D50(I),I=1,30)
      READ (6,*)
      READ (6,*) (D16(I),I=1,30)
      READ (6,*)
      READ (6,*) (D84(I),I=1,30)
      READ (6,*)
      READ (6,*) (DMAX(I),I=1,30)
      READ (6,*)
      READ (6,*) (PH(I),I=1,30)
      READ (6,*)
      READ (6,*) (ALPHA(I),I=1,30)

C
C          INITIAL CONDITIONS
C

      READ (6,*)
      READ (6,*)
      READ (6,*)
      READ (6,*) YMIF, YMIR, TDI, TUI
      READ (6,*)

C
C          HURRICANE DATA
C

      READ (6,*)
      READ (6,*)
      READ (6,*)
      READ (6,*)
      READ (6,*) HRAD1, HRAD2, HRAD3, HRAD4, HRAD5, HDIST
      READ (6,*)
      READ (6,*)
      READ (6,*) HSPED1, HSPED2, HSPED3, HSPED4, HSPED5
      READ (6,*)

```

```

READ (6,*)
READ (6,*)  MXSRG1, MXSRG2, MXSRG3, MXSRG4, MXSRG5
READ (6,*)
READ (6,*)
READ (6,*)
READ (6,*)  HURAIN, MXSRGI, HSPEDI, HRADI

C      SELECT PROGRAM EXECUTION AND CONTROL OPTIONS

      IF(YRS.EQ.0) WRITE(*,*)'SINGLE EVENT HURRICANE SIMULATION'

      IF(TDI.NE.0.00.OR.TUI.NE.0.0) THEN
        WRITE(*,*)'THE PROGRAM IS BEING EXECUTED IN THE EXISTING PIER
ANA  `LYSIS MODE. DO YOU WISH TO CONTINUE? ENTER y FOR YES OR n FOR NO'
        READ(*,*)ANALIN
        IF(ANALIN.EQ.'y') THEN
          GO TO 11
        ELSE
C      Go to the end of the program
          GO TO 2000
        END IF

      ELSE

        WRITE(*,*)'THE PROGRAM IS BEING EXECUTED IN THE PIER DESIGN MODE
        `DO YOU WISH TO CONTINUE? ENTER Y FOR YES OR N FOR NO'
        READ(*,*)DESIN
        IF(DESIN.EQ.'y') THEN
          GO TO 11
        ELSE
C      Go to the end of the program
          GO TO 2000
        END IF
      END IF

11 CONTINUE

C      Record date of the run

C      Record Run title
      WRITE(*,*)'RECORD RUN TITLE'
      READ(*,*)TITLE
      WRITE(*,*)'RECORD DATE OF THE RUN'
      READ(*,*)DATE

C      SELECT MODEL ALGORITHM CONTROL OPTIONS

      WRITE(*,*)'TO COMPUTE SCOUR USING NEILLS CRITICAL VELOCITY ENTER
I  `NTEGER 1 (ONE), TO USE SRICOS CRITICAL VELOCITY ENTER INTEGER
2(TW `O) TO USE GKY CRITICAL VELOCITY ENTER INTEGER 3(THREE)'

```

```

        READ(*,*)VINCIP

        WRITE(*,*)'CONTRACTION SCOUR METHOD, ENTER INTEGER 1(ONE) FOR
STRA      `BS EQUATION, ENTER 2(TWO)FOR KOMURAS EQN ENTER 3(THREE) FOR
HEC18'
        READ(*,*)CONTRA

        WRITE(*,*)'TO COMPUTE LOCAL SCOUR CONSIDERING ARMOURING ENTER AN
I          `NTEGER GREATER THAN 0 (ZERO), OTHERWISE ENTER 0 (ZERO)'
        READ(*,*)ARMVEL

        WRITE(*,*)'ENTER THE HURRICANE CATEGORY(1-5)IF YOU WISH TO DETERM
        `INE THE SCOUR FROM A HURRICANE EVENT AT THE END OF THE CONTINUOUS
        `SIMULATION. ENTER 99 IF THE SIMULATION IS TO BE DONE WITH
        `SPECIFIC HURRICANE INFORMATION, OTHERWISE ENTER ZERO (0) FOR NO
HU
        `RRICANE SIMULATATION'
        READ(*,*)HCAT

        IF(HCAT.EQ.1) THEN

            HRAD    = HRAD1
            HSPEED  = HSPED1
            MAXSRG  = MXSRG1

        ELSE IF(HCAT.EQ.2) THEN

            HRAD    = HRAD2
            HSPEED  = HSPED2
            MAXSRG  = MXSRG2

        ELSE IF(HCAT.EQ.3) THEN

            HRAD    = HRAD3
            HSPEED  = HSPED3
            MAXSRG  = MXSRG3

        ELSE IF(HCAT.EQ.4) THEN

            HRAD    = HRAD4
            HSPEED  = HSPED4

            MAXSRG  = MXSRG4

        ELSE IF (HCAT.EQ.5) THEN

            HRAD    = HRAD5
            HSPEED  = HSPED5
            MAXSRG  = MXSRG5

        ELSE      IF(HCAT.EQ.99) THEN

            HRAD = HRADI
            HSPEED =HSPEDI

```

```

        MAXSRG =MXSRGI

        END IF

        IF(HCAT.NE.0) THEN
        WRITE(*,*)'HURRICANE CRITICAL VELOCITY METHOD, ENTER INTEGER
1(ONE
  `) FOR NEILLS, ENTER 2(TWO)FOR SRICOS, ENTER 3(THREE) FOR GKY'
  READ(*,*)HCVIND
  END IF

        WRITE(*,*)'ENTER AN INTEGER GREATER THAN ZERO (0)TO DETERMINE
BRID  `GE STATION TIDAL PROFILE USING CONVEX ROUTING,ELSE ENTER ZERO
(0)'
        READ(*,*)CONROUT

        WRITE(*,*)'ENTER "AN INTEGER" GREATER THAN ZERO TO ACTIVATE THE
BR   `UBAKER-DEMETRIUS NEILLS MODIFICATION FACTOR'
        READ(*,*)ACTNM

        WRITE(*,*)'ENTER "AN INTEGER" GREATER THAN ZERO TO ACTIVATE THE
  `TIDE DISTORTION OPTION. OTHERWISE ENTER ZERO'
        READ(*,*)DISCON

C      DEVELOPE HISTOGRAM

C      Number of histogram ranges
        NORNG = 100
C      Width of each histogram range is DEL
        DEL =0.5
C      First bound value of the histogram is B(1)

        B(1) = 1.0
C      Last bound value of the histogram is B(100)

        B(100) =(NORNG -1)*DEL + B(1)

C      SET UP HISTOGRAM BOUND RANGES B1, B2 B3 ETC...

        DO 1 I = 2,99
          B(I) = B(I-1) + DEL
1 CONTINUE

C      INITIALIZE SCOUR FREQUENCY ARRAYS
        Do 2 I=1,100
          FU(I)=0
          FD(I)=0
2 CONTINUE

        IF(HCAT.NE.0) THEN

          DO 3 I= 1,100
            FHD(I) = 0
            FHU(I) = 0
          3 CONTINUE

```



```

        ELSE
C      Continue to the computation of constant parameters
        GO TO 4
      END IF
4 CONTINUE

C*****
*****      COMPUTE CONSTANT PARAMETERS
*****
C*****

C      COMPUTE NUMBER OF COMPUTATIONAL TIME STEPS IN HRS BASED ON
CONTINUOUS
C      ANNUAL SIMULATION
C      COMPUTATIONAL ARRAY SIZE (I)= ARR

C      FREX is the exponent of the Froude Number term in the scour
equation
C      INDX is the exponent of the velocity term in the scour equation
C      BLOCON is the constant related to the duration of hurricane
tidal blow-
C      back
C      VFACT = OVERBANK DEAD STORAGE FACTOR
C      RADCON is the conversion factor for degrees to radians

C      MSL = 0
C      MDR = MEAN TIDAL DEPTH
C      IRS = INVERT OF THE CROSS SECTION  (EBMLT(1))

      IRS = EBMLT(1)
      MDR = 0 -IRS

C      MEAN LOW TIDE DEPTH(MLT) = MEAN DEPTH(MDR) - TIDAL AMPLITUDE AT
THE
C      BRIDGE XSEC.(MTR)

      MLT = MDR - MTR

C      MEAN LOW TIDE ELEV(MLTE) = MSL - MTR

      MLTE = 0 - MTR

      VFACT = 0.0007*UESTZ
      IF(VFACT.GT.0.85) VFACT = 0.85

      RADCON = 2.0*PI/360.0
      BLOCON = 0.15
      BNDX =1
      FREX= 0
      INDX =1
      D 6=6
      D18=18
      D24=24

```

```

D36=36
LW = 5280*LW
LE = 5280*LE
WM = 5280*WM
WB = 5280*WB
AS = AS*(5280**2)
WU= 5280*WU
WD= 5280*WD

TC = TMCON
IF(TMCON.EQ.0) TC = 0.61*CBA**0.4

TP = 0.67*TC

C    Compute ENS the real value of TMS
    ENS = TMS

C    CBAMIN is computed based on a minimum TP of 3 hrs
C    CBAMIN = 150 sq miles

    IF(CBA.LT.CBAMIN) WRITE(*,*)'WARNING CBA OUTSIDE ACCEPTABLE
RANGE'

SC = ((1000/CN) -10.)
IA = 0.2 * SC
AI = 0.8 * SC
NU = 5*TP
QP = 484*CBA/TP
QBF = 1.02*CBA**0.91
TAF = MTR/MDA
MTL = 3.694+19.164*PKM - 21.247*TAF
CX = DLT/MTL
IF(MTL.LE.DLT) CX = 1.0
TR = 2*MTR

C    Determine geometric properties of the estuary

    Do 5, I=1,3
        XABMLT(I)=0.5*ABS((TWBMLT(I)+TWBMLT(I+1))*
        (EBMLT(I)-EBMLT(I+1)))
5    CONTINUE

    SUMXAB(1) = XABMLT(1)
    Do 7, I = 2,3
        SUMXAB(I) = SUMXAB(I-1) + XABMLT(I)
7    CONTINUE

    XABMLE = SUMXAB(3)
    XABMLE = AFACT*XABMLE

    ELAMLT(1) = MLTE +0.25
    TWAMLT(1) = 0.25*2*UESTZ +WB

    XAAMLT(1) = 0.5*ABS((TWAMLT(1)+ WB)*(ELAMLT(1)-MLTE))

```

```

      SXAMLT(1) = XAAMLT(1)
      PLANA(1)  = AS*(TWAMLT(1)/WB)
      ESVOL(1)  = 0.5*ABS((PLANA(1)+ AS)*(ELAMLT(1)-MLTE))
      SESVOL(1) = ESVOL(1)
      YTAMLT(1) = ABS(ELAMLT(1)-MLTE)

      Do 8, I=2,150

      ELAMLT(I) = ELAMLT(I-1) + 0.25
      TWAMLT(I) = 0.25*2*UESTZ +TWAMLT(I-1)

      YTAMLT(I)= ABS(ELAMLT(I)-MLTE)
      XAAMLT(I)=0.5*ABS((TWAMLT(I)+ TWAMLT(I-1))*
      (ELAMLT(I)-ELAMLT(I-1)))

      ESVOL(I)  = 0.5*ABS((PLANA(I)+ PLANA(I-1))*
      (ELAMLT(I)-ELAMLT(I-1)))

      SXAMLT(I) = SXAMLT(I-1) + XAAMLT(I)
      PLANA(I)  = AS*(TWAMLT(I)/WB)

      SESVOL(I) = ESVOL(I) + SESVOL(I-1)
8 CONTINUE

C DETERMINE NP THE NUMBER OF RAINFALL ORDINATES FOR EACH STORM
DURATION.
C DETERMINE NR THE NUMBER OF ORDINATES IN THE CATCHMENT HYDROGRAPH FOR
EACH STORM DURATION.
C (where NU is equal to 5*TP)

      NP6 = INT(D6/DLT)
      NR6 = INT(NP6 +NU -1)

      NP18 = INT(D18/DLT)
      NR18 = INT(NP18+NU -1)

      NP24 = INT(D24/DLT)
      NR24 = INT(NP24+NU -1)

      NP36 = INT(D36/DLT)
      NR36 = INT(NP36+NU -1)

C
C DETERMINE THE EFFECTIVE BRIDGE WIDTH
C
      WBE = WB - (NBP *PD)
      IF(WBE.LE.0) WRITE(12,*) 'ERROR IN EFFECTIVE BRIDGE WIDTH'
      *****
      *****
C          SET UP DECISIONS FOR THE COMPUTATION OF CONTRACTION SCOUR
C          CONTRACTION SCOUR COMPUTATIONS PRODUCE UNSTABLE RESULTS
C          FOR ESTUARY WIDTH REDUCTIONS GREATER THAN 40% OF THE
C          BRIDGE CROSS SECTION
      *****
      *****

```

```

COFU = ((WU/WBE)**0.67)

COFUF = 0
IF (COFU.GT.1) COFUF = COFU**1.6

COFUS = 0
IF (COFU.GT.1) COFUS = 1

COFD = ((WD/WBE)**0.67)

COFDF = 0
IF (COFD.GT.1) COFDF = COFD**1.6
COFDS = 0
IF(COFD.GT.1) COFDS = 1

*****
*****

DIM = LE / ( (32.2*MDR)**0.5 * (3600*DT) )
IF(MDR.LE.0.0) DIM=0.005

WF = WM / WB
HF = TR / MDR

C COMPUTE BRUBAKER-DEMETRIUS NEILL'S MODIFICATION FACTORS
NMFRF =0.8

NMFFF= 0.8

IF(DISCON.LE.0) THEN

NMFF=1
IF(ACTNM.GT.0) NMFF = DIM**0.09* HF**0.256

NMFR =1
IF(DIM.GT.0.01.AND.ACTNM.GT.0) NMFR = (1+SIN((DIM-0.01)**1.04 *
\
WF**0.58 * HF**(-1.13)))

ELSE

NMFF=1
IF(ACTNM.GT.0) NMFF = DIM**0.09* HF**0.256
IF(NMFF.LT.NMFFF) NMFF = NMFFF

NMFR =1
IF(DIM.GT.0.01.AND.ACTNM.GT.0) NMFR = (1+SIN((DIM-0.01)**1.04 *
\
WF**0.58 * HF**(-1.13)))

IF(NMFR.GT.NMFRF) NMFR = NMFRF

END IF

NMFRH =1
IF(DIM.GT.0.01.AND.ACTNM.GT.0) NMFRH = (1+SIN((DIM-0.01)**1.04 *
\
WF**0.58 * HF**(-1.13)))

```

```

        IF(NMFRH.GT.1.25) NMFRH = 1.25

C*****
C*****
C                                     COMPUTE BASIN UNIT HYDROGRAPH
C*****
        DO 10 I=1, NO
            TO(I)= TO(I)*TP
            DUH(I)= DUH(I)*QP
10     CONTINUE

        DO 30 I=1, NU
            TT =I
            T(I) =I
            DO 20 J= 2, NO
                IF(TT.GT.TO(J)) GO TO 20
                QU(I)=DUH(J-1)+(DUH(J)-DUH(J-1))*(TT-TO(J-1))/(TO(J)-TO(J-
1))
                GO TO 30
            20     CONTINUE
            30     CONTINUE

C
C NORMALIZE UNIT HYDROGRAPH WITH FACTOR AMT TO MAKE THE TOTAL RUNOFF 1
INCH
C
        SUM = 0.0
        DO 40 I=1, NU
            SUM = SUM + QU(I)
40     CONTINUE
        AMT = 0.001549587*SUM/CBA

        DO 50 I=1, NU
            QU(I) =QU(I)/AMT
50     CONTINUE

C      Debug 51
        WRITE(*,51)
51     FORMAT(' RUNNING')

C*****
C*****
C                                     SET THE DO LOOP FOR THE TOTAL NUMBER OF
SIMULATIONS
C*****
C Repeat Overall Simulation (TMS)

        DO 1500 I=1,TMS

C Set initial conditions for each simulation

```

```

      YTMF = YMIF
      YTMR = YMIR

      TSU = TUI
      TSD = TDI

      SUMYSU =0
      SUMYSD =0

      YUINMX =0
      YDINMX =0

      VNUMAX = 0
      VNDMAX = 0

      QTUMAX =0
      QTRMAX =0
      QTFMAX =0

      YTMAX =0
      YTRMAX =0
      YTFMAX =0

      UIUMIN =20
      UIDMIN =20

      VTUMX = 0
      VTDMX = 0

DO 55 J = 1, 100
      YSD(J) = 0
      YSU(J) = 0

      CSU(J) = 0
      CSD(J) = 0

      VNDAYR(J) = 0
      VNUAYR(J) = 0

      YTRYRS(J) = 0

      YTFYRS(J) = 0

      YTRFYR(J) = 0

      YTFFYR(J) = 0

      QUPYR(J) = 0
      QDNYR(J) = 0

      QPK6(J)   = 0
      QPK18(J)  = 0
      QPK24(J)  = 0
      QPK36(J)  = 0

55 CONTINUE

```

```

C      Bypass continuous simulations if only a single event hurricane
C      simulation is desired ( i.e. if YRS =0)

C DO  LOOP FOR DESIGN LIFE CYCLE
      HIELE =0
      HIBASE= 0
      HITIDE =0

      IF(YRS.EQ.0) GO TO 1106
*****
*****

C      SET YEARS OF SIMULATION LOOP
*****
*****

      DO 1100 J=1, YRS

C Initialize maximum annual velocities and annual maximum flow depth

      VUPM = 0
      VDWNM = 0

      VNDNAM= 0
      VNUPAM= 0

      YTMAX = 0
      YTRMX = 0
      YTFMX = 0

      YTMRF = 0

      YTMFF = 0

      QTRMX = 0
      QTFMX = 0

      QP24MX= 0
      QP18MX= 0
      QP36MX= 0
      QP6MX = 0
C Generate a random number to determine total number of scour storms
for each year

      NS=RANNO(2, MAS, SDS)
C Ensure that NS remains positive

      NS=ABS(NS)
      NS=INT(NS)
      ARR = INT(8766/(NS*DLT))
      IF(ARR.GT.300) WRITE(*,*)'ARRAY SIZE OUTSIDE OF ACCEPTABLE RANGE'

```

```

C      If array size is greater than 300 go to the end of the program,
abort.
      IF(ARR.GT.300) GO TO 2000

C Compute the number of 6, 18, 24 and 36 hour storms in each year
      N6 = INT(FQ6*NS)
      N18= INT(FQ18*NS)
      N24 =INT(FQ24*NS)
      N36 =INT(NS - (N6 + N18 + N24))

*****
*****
C                                  DO LOOP FOR ALL 6 HR STORMS IN A GIVEN YEAR
C
*****
*****
C      Previous location of code debug 451

      Do 4500 K = 1, N6

C Initialize UVAR
      UVA=0
      UVAR6 = 1

      Do 4060 L = 1,INT(C6)

C Generate uniform variate UVA from RANNO

      UVA =RANNO(1,0.0,1.0)
      UVAR6 = UVAR6*UVA

4060    CONTINUE

      PPT6 = -B6*LOG(UVAR6)

C      Store the largest rainfall event in the simulation

      IF(PPT6.GT.PPTMAX) PPTMAX = PPT6

      SUM6 = SUM6 + PPT6

C Compute the total direct runoff (TDRO) and total expected
infiltration
C (TINF) from each storm

      TDRO = 0
      IF( PPT6.GT.IA) TDRO = (PPT6 - IA) ** 2/ (PPT6 + AI)
      IF(TDRO.LE.0.0) NORUN = NORUN + 1

C      DETERMINE CATCHMENT HYDROGRAPH

C      Convert rainfall from dimensionless cumulative hyetograph to a
C      cumulative depth hyetograph

      Do 4070 L = 1, NP6

```



```

        P6(L) = S6(L) * PPT6
4070    CONTINUE

        Do 4080 L = 1, NP6
            SP = P6(L)
            PE6(L) = 0.0
            IF(SP.GT.IA) PE6(L) = (SP - IA) ** 2/ (SP + AI)
4080    CONTINUE

            PEI6(1) =PE6(1)
        Do 4090 L = 2, NP6
            PEI6(L) = PE6(L) - PE6(L -1)
4090    CONTINUE

C      Convolve unit hydrographs convolve sub routine

        CALL CONVOL(QU, PEI6, DRO6, NU, NP6, NR6, 36, 6, 300)

C      Add base flow to direct runoff hydrograph.  Final output is
CHY(NR), NR

        Do 4100 L = 1, ARR
            CHY6(L) = DRO6(L) + QBF

            IF (CHY6(L).GT.QP6MX) QP6MX = CHY6(L)

4100    CONTINUE

C*****
C      SYNTHESIZE TIDAL SERIES AT BASE STATION B.
C*****
C      Compute array of tidal depths, TEB(ARR) to cover twice the number
of
C      runoff ordinates
C      Generate uniform variates between 0.0 and 2*Pi to represent
diurnal and
C      Lunar cycle
C      Phase angles.  Generate normal variates to represent the Lunar
amplitude

        PHD = RANNO(1, 0.0, 6.284)
        PHL = RANNO(1, 0.0, 6.284)

        LA= RANNO( 2, MLA, SLA)
        LA=ABS(LA)

C
C      Generate normal variates that change with every diurnal cycle to
represent
C      the diurnal amplitude
        TB = 0
        DO 4120 L =1, 400
            IF(TB.EQ.0) THEN

```

```

        DA= RANNO(2, MDA, SDA)
        DA=ABS(DA)
        ELSE
        GO TO 4110
        END IF
4110      CONTINUE

C      Create array of MSL water surface elevations TEB(300) varying
hourly with
C      time
        LEW = L
        TB=TB+1

        TEB(L)= DA*SIN(2*PI*(LEW/DT)+
PHD)+LA*SIN(2*PI*(LEW/LT)+PHL)
        IF(TB.EQ.INT(DT)) TB=0

4120      CONTINUE
C      ADD A CONDITION TO ENSURE TIDE DOES NOT DECREASE BELOW MEAN
LOW WATER

        DO 4125 L=1,400
        IF(TEB(L).LT.(IBS +1.0)) TEB(L) = (IBS+1.0)
4125      CONTINUE

C      DETERMINE TIDAL ELEVATIONS AT THE BRIDGE STATION
C      by convex routing or otherwise

        TER(1)=TAF*TEB(1)

        IF(CONROUT.EQ.0) THEN

        Do 4127 L=2, 400
        TER(L)= TAF*TEB(L)
        IF(TER(L).GT.HIELE) HIELE = TER(L)

4127      CONTINUE

        ELSE IF(CONROUT.NE.0) THEN

        Do 4130 L=2, 400
        TER(L)= CX*TEB(L-1) + (1.0 - CX)*TER(L-1)
        IF(TER(L).GT.HIELE) HIELE = TER(L)

4130      CONTINUE

        END IF

C      Compute array for base station depth YB(150) by subtracting
C      channel invert elev. at the base station (or adding the
C      absolute value of (IBS) the array of tidal elevations

        Do 4135 L= 1, 400
        YB(L) = TEB(L) + ABS(IBS)
        IF(YB(L).GT.HIBASE) HIBASE = YB(L)
4135      CONTINUE

```

```

      IF(DISCON.EQ.0) THEN
C
      Do 4140 L = 1, ARR
        QN(L) = AS * ( (TER(L) - TER(L+1)))/(3600*DLT)

C      Modify the Neill's discharges with modification factors NMFR,
NMFF
C      developed by Brubaker and Demetrius.

        QNM(L)= NMFF*QN(L)
        IF (QN(L).LT.0) QNM(L)= NMFR*QN(L)

C      DETERMINE THE COMBINED TIDAL AND RIVERINE DISCHARGES BY
C      VECTOR ADDITION OF TIDAL AND RIVERINE DISCHARGES
C
        QT(L)= CHY6(L) + QNM(L)

        IF(QT(L).LE.0) THEN
          QTR(L) = ABS(QT(L))

          ELSE IF(QT(L).GT.0) THEN
            QTF(L) = ABS(QT(L))

C      Determine the maximum discharge values in the last run

          IF((QTR(L)).GT.QTRMAX) QTRMAX = QTR(L)
          IF((QTF(L)).GT.QTFMAX) QTFMAX = QTF(L)

          IF((QTR(L)).GT.QTRMX) QTRMX = QTR(L)
          IF((QTF(L)).GT.QTFMX) QTFMX = QTF(L)

C      Determine the maximum discharges in the full simulation

          IF((QTR(L)).GT.QTRMXS) QTRMXS = QTR(L)
          IF((QTF(L)).GT.QTFMXS) QTFMXS = QTF(L)

          IF(ABS(QT(L)).GT.QTUMAX) QTUMAX = ABS(QT(L))

          SUMQTU = SUMQTU + ABS(QT(L))

          CONQTU = CONQTU + 1

        END IF

C      DETERMINE THE COMBINED DEPTH YT
C
        YAT(L) = TER(L) + ABS(IRS)
        IF(YAT(L).LE.MLT) YAT(L)= MLT
        IF(YAT(L).GE.HITIDE) HITIDE = YAT(L)

4140      CONTINUE

      Do 4150 L =1,ARR

```

```

        IF(QT(L).GT.0)  QROUT(L) = QT(L)
        IF(QT(L).LE.0)  QROUT(L)= 0

4150      CONTINUE

        VOUT(1) = 3600*0.5*(QROUT(1))
        VITID(1)= 0.5*(YAT(1)-MLT)*AS
        VICAT(1)= 3600*(QBF)
        VITOT(1)= VICAT(1)+ VITID(1)

        Do 4160 l=2, ARR
            VICAT(L)=0.5*(CHY6(L)+CHY6(L-1))*3600
            VITID(L)=(YAT(L) - YAT(L-1))*AS
            VITOT(L)=VICAT(L) + VITID(L)
            VOUT(L) =3600*0.5*(QROUT(L)+QROUT(L-1))
4160      CONTINUE

        VBAL(1) = VITOT(1) - VOUT(1)
        IF(VBAL(1).LE.0) VBAL(1) = 0
            IF(VBAL(1).LE.0) YT(1)= MLT
            IF(VBAL(1).GT.0.AND.VBAL(1).LE.SESVOL(1))
YT(1)=
            MLT + YTAMLT(1)

        Do 4170 L=2,ARR
            VBAL(L) =VITOT(L-1) + VITOT(L)-VOUT(L)
            IF (VBAL(L).LE.0) VBAL(L) = 0
            IF (VBAL(L).LE.0) YT(L) = MLT

            IF(VBAL(L).GT.0.AND.VBAL(L).LE.SESVOL(1)) YT(L)=
            MLT + YTAMLT(1)

        Do 4165 M =2, 150

            IF(VBAL(L).GT.SESVOL(M-
1).AND.VBAL(L).LE.SESVOL(M))
            YT(L) = MLT + YTAMLT(M)
4165      CONTINUE
4170      CONTINUE

        Do 4180 L=1,ARR

            IF(YT(L).LT.YAT(L)) YT(L) = YAT(L)

4180      CONTINUE

        IF(YT(1).LT.YT(2)) YTR(1) = YT(1)
        IF(YT(1).GE.YT(2)) YTR(1) = MLT

            IF(YT(1).GE.YT(2)) YTF(1) = YT(1)
            IF(YT(1).LT.YT(2)) YTF(1) = MLT

        Do 4185 L= 1,ARR

            IF(YT(L+1).GT.YT(L)) YTR(L+1) = YT(L+1)
            IF(YT(L+1).LE.YT(L)) YTR(L+1) = MLT

```

```

                                IF(YT(L+1).LE.YT(L)) YTF(L+1) = YT(L+1)
                                IF(YT(L+1).GT.YT(L)) YTF(L+1) = MLT

                                IF(YT(L).GT.YTMAX) YTMAX = YT(L)
                                SUMYT = SUMYT + YT(L)
                                CONYT = CONYT + 1

C      Record annual maximum depth at bridge station
                                IF(YT(L).GT.YTMX) YTMX = YT(L)

C      Record maximum depth at bridge station last run

                                IF(YTF(L).GT.YTFMX) YTFMX = YTF(L)
                                IF(YTR(L).GT.YTRMX) YTRMX = YTR(L)

                                IF(YTF(L).GT.YTFMAX) YTFMAX = YTF(L)
                                IF(YTR(L).GT.YTRMAX) YTRMAX = YTR(L)

C      Record maximum depth at bridge station in the full simulation

                                IF(YTFMX.GT.YTFMXS) YTFMXS = YTFMX
                                IF(YTRMX.GT.YTRMXS) YTRMXS = YTRMX

4185                                CONTINUE

                                ELSE

                                Do 4190 L= 1, 400
                                    TERS(L)=TER(L)
                                LEW =L
                                    TBR(L) = LEW + (LW/(1800*32.2*(YB(L) + MDR))**0.5)
4190                                CONTINUE

C      Sort array TBR(400) in ascending order also sort array  TERS(300)
C      based on the order of array TBR(400).

                                CALL SORT2(400,TBR, TERS)

C      Normalize the array TBR(300) by subtracting TBR(1) and adding
1.00 to
C      all elements in the array.  Also determine corresponding tidal
depths (YAT(L))

                                Do 4200 L=1, 400
                                    TNR(L) = TBR(L) +1-TBR(1)

                                    YAT(L) = TERS(L) + ABS(IRS)
                                    IF(YAT(L).LT.MLT) YAT(L)=MLT
4200                                CONTINUE

```

```

C Determine the array of the interpolated tidal depths at the bridge
location

      CALL INTERP(TNR, YAT, TNRI, YATI, 400, 300,400, 300)

C Determine the tidal discharges at the bridge location using the
Neill's Equation
C QN(NR18) represents an array of computed Neill's discharges with
negative
C and positive values. The negative values represents the discharges
C produced by the rising tide directed up the estuary. While the
positive values
C represents the discharges directed downstream. In the algorithm QNR
represents
C Neill's discharges due to the rising limb and QNF represents
Neill's
C discharges due to the falling limb.

      Do 4210 L= 1, (ARR+1)
      IF(YATI(L).LE.0.5*MLT) YATI(L) = 0.5*MLT
      TERI(L) = YATI(L)+IRS
4210      CONTINUE

C
      Do 4220 L = 1, ARR
      QN(L) = AS * ( (TERI(L) - TERI(L+1)))/(3600*DLT)

C Modify the Neill's discharges with modification factors NMFR,
NMFF
C developed by Brubaker and Demetrius.

      QNM(L)= NMFF*QN(L)
      IF (QN(L).LT.0) QNM(L)= NMFR*QN(L)

C DETERMINE THE COMBINED TIDAL AND RIVERINE DISCHARGES BY
C VECTOR ADDITION OF TIDAL AND RIVERINE DISCHARGES
C

      QT(L)= CHY6(L) + QNM(L)

      IF(QT(L).LE.0) THEN
      QTR(L) = ABS(QT(L))

      ELSE IF(QT(L).GT.0) THEN
      QTF(L) = ABS(QT(L))

      IF((QTR(L)).GT.QTRMAX) QTRMAX = QTR(L)
      IF((QTF(L)).GT.QTFMAX) QTFMAX = QTF(L)

      IF((QTR(L)).GT.QTRMX) QTRMX = QTR(L)
      IF((QTF(L)).GT.QTFMX) QTFMX = QTF(L)

      IF((QTR(L)).GT.QTRMXS) QTRMXS = QTR(L)
      IF((QTF(L)).GT.QTFMXS) QTFMXS = QTF(L)

      IF(ABS(QT(L)).GT.QTUMAX) QTUMAX = ABS(QT(L))

```

```

        SUMQTU = SUMQTU + ABS(QT(L))

        CONQTU = CONQTU + 1

    END IF

    IF(YATI(L).GE.HITIDE) HITIDE = YATI(L)

4220        CONTINUE

C
C        DETERMINE THE COMBINED DEPTH YT
C

        Do 4230 L =1,ARR

C        Falling limb combined with catchment discharge

                IF(QT(L).GT.0) QROUT(L) = QT(L)
                IF(QT(L).LE.0) QROUT(L)= 0

4230        CONTINUE

                VOUT(1) = 3600*0.5*(QROUT(1))
                VITID(1)= 0.5*(YATI(1)-MLT)*AS
                VICAT(1)= 3600*(QBF)
                VITOT(1)= VICAT(1)+ VITID(1)

                Do 4240 l=2, ARR
                        VICAT(L)=0.5*(CHY6(L)+CHY6(L-1))*3600
                        VITID(L)=(YATI(L) - YATI(L-1))*AS
                        VITOT(L)=VICAT(L) + VITID(L)
                        VOUT(L) =3600*0.5*(QROUT(L)+QROUT(L-1))
4240        CONTINUE

                VBAL(1) = VITOT(1) - VOUT(1)
                IF(VBAL(1).LE.0) VBAL(1) = 0
                IF(VBAL(1).LE.0) YT(1)= MLT
                IF(VBAL(1).GT.0.AND.VBAL(1).LE.SESVOL(1))
YT(1)=
                MLT + YTAMLT(1)

                Do 4250 L=2,ARR
                        VBAL(L) =VITOT(L-1) + VITOT(L)-VOUT(L)
                        IF (VBAL(L).LE.0) VBAL(L) = 0
                        IF (VBAL(L).LE.0) YT(L) = MLT

                        IF(VBAL(L).GT.0.AND.VBAL(L).LE.SESVOL(1)) YT(L)=
                MLT + YTAMLT(1)

                Do 4245 M =2, 150

                        IF(VBAL(L).GT.SESVOL(M-
1).AND.VBAL(L).LE.SESVOL(M))
                YT(L) = MLT + YTAMLT(M)
4245        CONTINUE
4250        CONTINUE

```

```

Do 4260 L=1,ARR
IF(YT(L).LT.YATI(L)) YT(L) = YATI(L)
4260 CONTINUE

IF(YT(1).LT.YT(2)) YTR(1) = YT(1)
IF(YT(1).GE.YT(2)) YTR(1) = MLT

IF(YT(1).GE.YT(2)) YTF(1) = YT(1)
IF(YT(1).LT.YT(2)) YTF(1) = MLT

Do 4270 L= 1,ARR

IF(YT(L+1).GT.YT(L)) YTR(L+1) = YT(L+1)
IF(YT(L+1).LE.YT(L)) YTR(L+1) = MLT

IF(YT(L+1).LE.YT(L)) YTF(L+1) = YT(L+1)
IF(YT(L+1).GT.YT(L)) YTF(L+1) = MLT

SUMYT = SUMYT + YT(L)
CONYT = CONYT + 1

IF(YT(L).GT.YTMAX) YTMAX = YT(L)

C      Record annual maximum depth at bridge station
IF(YT(L).GT.YTMX) YTMX = YT(L)

IF(YTF(L).GT.YTFMX) YTFMX = YTF(L)
IF(YTR(L).GT.YTRMX) YTRMX = YTR(L)

IF(YTF(L).GT.YTFMAX) YTFMAX = YTF(L)
IF(YTR(L).GT.YTRMAX) YTRMAX = YTR(L)

IF(YTFMX.GT.YTFMXS) YTFMXS = YTFMX
IF(YTRMX.GT.YTRMXS) YTRMXS = YTRMX

4270 CONTINUE
END IF

C
C DETERMINE COMBINED VELOCITY AT BRIDGE STATION
C
C The inputs required for this step are the time varying tidal
discharges at
C location b QT(ARR) flow depth YT(ARR) and the
C cross section area of the estuary at bridge location b. The net
velocity VNT(L)
C is computed as { QT(L)/(YT*WB)}

C Compute the array of velocity directed up the channel
C Ensure the array of resultant velocities directed down the
channel

Do 4280 L=1,ARR

```



```

      IF(YT(L).LE.MLT) VNT(L) = QT(L)/XABMLE

      IF(YT(L).LE.MLT) XATOT(L) = XABMLE

      IF(YT(L).GT.MLT.AND.YT(L).LE.(MLT+YTAMLT(1)))
        VNT(L) = QT(L)/(XABMLE+SXAMLT(1)-VFACT*UESTZ*(YT(L)-
MLT)**2)

      IF(YT(L).GT.MLT.AND.YT(L).LE.(MLT+YTAMLT(1)))
        XATOT(L)=(XABMLE + SXAMLT(1)-VFACT*UESTZ*(YT(L)-MLT)**2)

      Do 4275 M= 2, 150
      IF(YT(L).GT.(MLT+YTAMLT(M-1)).AND.YT(L).LE.(MLT+YTAMLT(M)))
        VNT(L)=QT(L)/(XABMLE+ SXAMLT(M)-VFACT*UESTZ*(YT(L)-
MLT)**2)

      IF(YT(L).GT.(MLT+YTAMLT(M-1)).AND.YT(L).LE.(MLT+YTAMLT(M)))
        XATOT(L) =(XABMLE+SXAMLT(M)-VFACT*UESTZ*(YT(L)-MLT)**2)

4275  CONTINUE
4280  CONTINUE
*****
C      INITIALIZE SOIL SCOUR VARIABLES FOR EACH STORM
C      INITIALIZE CSU, AND CSD

DO 4282 L=1, ARR
  CSD(L) =TSD - SUMYSD
  IF (SUMYSD.GT.TSD) CSD(L) = 0

  CSU(L) = TSU - SUMYSU
  IF (SUMYSU.GT.TSU) CSU(L) = 0

  YTFF(L) = YTF(L) + SUMYSU

  YTRF(L) = YTR(L) + SUMYSD
4282  CONTINUE

Do 4285 L =1,30

  DPTHU =TSU
  IF(DPTHU.GE.DPTH(L).AND. DPTHU.LE.DPTH(L+1)) THEN
    ALPHAU = ALPHA(L)
    D16U   = D16(L)
    D50U   = D50(L)
    D84U   = D84(L)
    DMAXU  = DMAX(L)
    VCUF   = 0.476*(D50U/PD)**0.053
    SIGMAU = (D84U/D16U)**0.5
    PHU    = PH(L)
  END IF

```

```

      DPTHHD = TSD
      IF(DPTHHD.GE.DPTH(L).AND. DPTHHD.LE.DPTH(L+1)) THEN
        ALPHAD = ALPHA(L)
        D16D   = D16(L)
        D50D   = D50(L)
        D84D   = D84(L)
        DMAXD  = DMAX(L)
        VCDF   = 0.476*(D50D/PD)**0.053
        SIGMAD = (D84D/D16D)**0.5
        PHDD   = PH(L)
      END IF

      DPTHCU = SUMYSU
      IF(DPTHCU.GE.DPTH(L).AND. DPTHCU.LE.DPTH(L+1)) THEN

        D16CU   = D16(L)
        D50CU   = D50(L)
        D84CU   = D84(L)
        SIGMCU  = (D84CU/D16CU)**0.5

      END IF

      DPTHCD = SUMYSD
      IF(DPTHCD.GE.DPTH(L).AND. DPTHCD.LE.DPTH(L+1)) THEN

        D16CD   = D16(L)
        D50CD   = D50(L)
        D84CD   = D84(L)
        SIGMCD  = (D84CD/D16CD)**0.5

      END IF

4285    CONTINUE

C      DETERMINE FLOW VELOCITY DOWNFLOW,VORTEX VELOCITY VECTORS, AND
C      SCOUR FOR

C      EACH HOUR OF STORM
C
C      The required inputs are the net edutary velocity (VNU,VND),
C      the total flow depth (YT), the bridge pier diameter (PD),
C      the existing scour depth at the beginning of the process (TSU,
C      TSD),
C      the soils property at the invert of the estuary channel
C      ( D50, PH,) as a function of local scour depth (TSU, TCD)

C      Determine ratio of scour to bridge diameter along the upstream
C      and downstream face of the pier

C      Set up downflow, Tangential velocity and scour algorithms
C      The process involves the computation of the total local scour
C      depth over each storm event and summing over the full simulation.

```

C     The contraction scour will then be computed for each storm but  
will  
C     be based successively on the highest value of YT in YRS and added  
to the  
C     total scour at the upstream and downstream faces of the pier.

```

      Do 4290 L=1,ARR
        VNUIN(L) = 0
        IF(VNT(L).LT.0) VNUIN(L) = ABS(VNT(L))

        VNU(1) = 0.5*VNUIN(1)
        Do 4286 M=2, ARR
          VNU(M) = 0.5*(VNUIN(M)+ VNUIN(M-1))
4286      CONTINUE

```

```

      IF(VNU(L).LE.0) VNU(L)= 0
      IF(VNU(L).GT.0) THEN
        IF(VNU(L).GT.VNUMAX) VNUMAX = VNU(L)
        SUMVNU = SUMVNU + VNU(L)
        CONVNU = CONVNU + 1
      END IF

```

C Place maximum storm velocity in all simulations VUPM

```

      IF(VNU(L).GT.VUPM) VUPM = VNU(L)
      IF(VUPM.GT.VUPMS) VUPMS = VUPM
*****
*****

```

C     Compute incremental contraction scour over time DLT           and  
adjust flow depth to include the  
C     lowering of the bed

```

      IF(CONTRA.EQ.1) THEN

```

C     Compute contraction scour using Straub's eqn

C      $q_s = (g \cdot (S_s - 1) \cdot d_{50}^{*3})^{*0.5} \cdot ((T/T_c) - 1)^{*2}$  English units,  
d50 in feet

C     Converting the equations so that D50 is in mm and solving for  
scour depth gives

```

C     YS =           (0.67/PD)*DLT*d50mm**1.5*[(T/Tc)-1]**2

```

```

C     T =           28.11*(Q/WB)**2* [n**2/YTFF**2.33]

```

```

C     If D50mm <0.065 then
C         Tc = 4.84*D50mm
C     Else
C         Tc = 0.8d50^.67*Y^.33

```

```

      IF ( D50CD.LT.0.065) THEN
        TAUCD(L) = 4.84*D50CD
      ELSE

```

```

        TAUCD(L) = 0.84*D50CD**0.67*YTRF(L)**0.33
    END IF

    TAUDD(L)= 28.11*(QTR(L)/WB)**2*(MAN**2/YTRF(L)**2.33)

    YSD(L) = 0
    IF ((TAUDD(L)/TAUCD(L)).GT.1) YSD(L) = COFDS*(0.67/PD)
    \ *DLT*D50CD**1.5*((TAUDD(L)/TAUCD(L))-1)**1.5

    ELSE IF (CONTRA.EQ.2) THEN

        YSDIN=YTR(L)*(1.45*(VNU(L)/(32.2*YTR(L))**0.5)**0.2
        \ *COFDF*(1/SIGMCD**0.2)-1)

        IF(YSDIN.LE.0) YSDIN = 0

        YSD(L) = 0
        IF(YSDIN.GT.YDINMX) YSD(L) = YSDIN - YDINMX

        IF(YSDIN.GT.YDINMX) YDINMX = YSDIN

    ELSE

        YSDIN = 0
        IF(COFD.GT.1) YSDIN = YTR(L)*(COFD - 1)

        YSD(L) = 0
        IF(YSDIN.GT.YDINMX) YSD(L) = YSDIN - YDINMX

        IF(YSDIN.GT.YDINMX) YDINMX = YSDIN

    END IF

    SUMYSD= SUMYSD + YSD(L)

    YTRF(L) = YTR(L) + SUMYSD

    XADJAD(L) = 0.5*(TWBMLT(4)+TWBMLT(3))*SUMYSD

    VNUA(L) = VNU(L)*XATOT(L)/(XATOT(L) + XADJAD(L))
    IF(VNUA(L).GT.VNUPAM) VNUPAM = VNUA(L)

C      Recompute flowdepth and velocity, and computed local scour dept
to adjust for contraction
C      scour

        CSD(L) = CSD(L) - YSD(L)
        IF (YSD(L).GT.CSD(L)) CSD(L) = 0
        IF(CSD(L)+SUMYSD.LT.TSD) CSD(L) = TSD - SUMYSD

        LEW =L
        T(L)=LEW*DLT

        DSD(L) = CSD(L)/PD
C      Compute the scour angles along the downstream(THD) pier face

```

```

      THD(L) = PHDD
      IF (31*DSD(L)**2.LT.PHDD) THD(L) =31*DSD(L)**2

*****
*****

C      Compute downflow velocity on  downstream faces of the pier

      IF(DSD(L).GT.100) THEN
        VDD(L) = 0

        ELSE IF (DSD(L).LE.2.3.AND.YTRF(L).GT.MLT) THEN
          VDD(L) = VNUA(L)* (0.15*(DSD(L))
            + 0.24* PD **0.18/(YTRF(L)**0.18 * C1**0.5))

        ELSE IF (DSD(L).GT.2.3) THEN
          VDD(L) = VNUA(L)*(0.40/EXP(1+(3*(DSD(L)-4)) + 0.4))

      END IF

      IF(VDD(L).GT.0.8*VNUA(L)) VDD(L) = 0.8*VNUA(L)

C      Compute the maximum tangential velocities along the upstream(VMU)
and downstream
C      (VMD) pier faces

      VMD(L) = 2.7* VDD(L)
      IF(31*DSD(L)**2.LE.PHDD) VMD(L) = 2.24*C1**0.5*VDD(L)

C      Compute the A factors and tangential velocities (VTU)
C      along the upstream and downstream (VTD) pier faces

      AFD(L)=-0.0002*THD(L)**2+0.012*THD(L)+0.80

      VTD(L)=0
      IF(AFD(L).GT.0) VTD(L)=1.4*AFD(L)*VMD(L)*
        (1-EXP(-1.25*(1/AFD(L)**2)))

*****
*****

C      SELECT CRITICAL VELOCITY MERHOD

      UID(L)=0

      IF(YTRF(L).GT.0.AND.VINCIP.EQ.1) UID(L)=
        VCDF*(1.66*D50D**0.333*YTRF(L)**0.167)

      IF(YTRF(L).GT.0.AND.VINCIP.EQ.2) UID(L)= VCDF*0.09*
        (D50D*Tan(PHDD*RADCON)* YTRF(L)**0.33/(ALPHAD*MAN**2))**0.5

      IF(YTRF(L).GT.0.AND.VINCIP.EQ.3) UID(L)= VCDF*(0.024/MAN)*
        (D50D**0.5)*(YTRF(L)**0.167)

```

```

*****
*****
C      Compute armouring velocity

      VARMD(L)=0
      IF(ARMVEL.GT.0.AND.SIGMAD.GT.1.3) VARMD(L)=1.328*(DMAXD/1.8)**
      0.333*YTRF(L)**0.167

      IF(VARMD(L).LE.0) THEN
        VCRIND(L) = UID(L)

      ELSE IF(VTD(L).LE.VARMD(L).AND.VARMD(L).GT.0) THEN

        VCRIND(L) = VARMD(L)-(UID(L)/VCDF)

      ELSE IF (VTD(L).GT.VARMD(L).AND.VARMD(L).GT.0) THEN

        VCRIND(L) = VARMD(L)

      END IF

      IF(VCRIND(L).LT.UID(L)) VCRIND(L)= UID(L)

*****
*****

      DED(L) =0
      IF(VTD(L).GT.VCRIND(L)) DED(L)=(PD**BNDX)*TANH(YTRF(L)/PD)
      *((VTD(L)-VCRIND(L))**INDX)*(VNUA(L)/(32.2*PD)**0.5)**FREX

      TED(L)=0
      IF(VCRIND(L).GT.0.0.AND.(VTD(L)/UID(L)).GT.VCDF) THEN

        TED(L) = 24*30.89*(PD/VTD(L))*((VTD(L)/VCRIND(L))-0.4)*
        (YTRF(L)/PD)**0.25

      ELSE IF(YTRF(L)-6.0*PD.GT.0.AND.((VTD(L)/VCRIND(L))
      -VCDF).GT.0.0) THEN

        TED(L)= 24*48.26*(PD/VTD(L))*((VTD(L)/VCRIND(L))-0.4)
      END IF

*****
*****

      K1D(L)=0
      IF(TED(L).GT.0.001.AND.VTD(L).GT.0.03) K1D(L)= EXP(-0.08*
      (ABS((VCRIND(L)/VTD(L))*LOG(DLT/TED(L))))**1.2)

      K2D(L)=0
      IF(TED(L).GT.0.001) K2D(L)=(ABS(LOG(DLT/TED(L))))**0.2

      K3D(L)=0
      IF(VTD(L).GT.0.03) K3D(L) = 0.1*(DED(L)/DLT)
      *(ABS(VCRIND(L)/VTD(L))**1.2)

```

```

      RLD(L)= K1D(L)* K2D(L)* K3D(L)

      CSD(L+1) = CSD(L) + (RLD(L)*DLT)
      IF(CSD(L+1).LT.CSD(L)) CSD(L+1) =CSD(L)

*****
*****
C                                     Repeat process for upstream pier
face
*****
*****

      VNDIN(L) =0
      IF(VNT(L).GT.0)   VNDIN(L) = ABS(VNT(L))

      VND(1) = 0.5*VNDIN(1)
      Do 4288 M=2, ARR
      VND(M) = 0.5*(VNDIN(M)+ VNDIN(M-1))
4288      CONTINUE

      IF(VND(L).LE.0) VND(L)= 0
      IF(VND(L).GT.0) THEN
      IF(VND(L).GT.VNDMAX) VNDMAX = VND(L)
      SUMVND = SUMVND + VND(L)
      CONVND = CONVND + 1
      END IF

C Place maximum storm velocity in annual holding location VDWNM

      IF(VND(L).GT.VDWNM) VDWNM = VND(L)
      IF(VDWNM.GT.VDWNMS) VDWNMS = VDWNM

*****
*****

C      Compute incremental contraction scour over time DLT      and
adjust flow depth to include the
C      lowering of the bed

      IF(CONTRA.EQ.1) THEN

C      Compute contraction scour using Straub's eqn
C      qs = (g*(Ss-1)*d50**3)**0.5 * ((T/Tc) - 1)**2 English units,
d50 in feet
C      Converting the equations so that D50 is in mm and solving for
scour depth
C      gives
C      YS =(0.67/PD)*DLT*d50mm**1.5*[(T/Tc)-1]**2
C      T = 28.11*(Q/WB)**2* [n**2/YTFF**2.33]
C      If D50mm <0.065 then
C      Tc = 4.84*D50mm
C      Else
C      Tc = 0.8d50^.67*Y^.33

      IF ( D50CU.LT.0.065) THEN

```

```

        TAUCU(L) = 4.84*D50CU
        ELSE
        TAUCU(L) = 0.84*D50CU**0.67*YTFF(L)**0.33
    END IF

    TAUDU(L) = 28.11*(QTF(L)/WB)**2*(MAN**2/YTFF(L)**2.33)

    YSU(L) = 0
    IF((TAUDU(L)/TAUCU(L)).GT.1) YSU(L) = COFUS*(0.67/PD)*
    DLT*D50CU**1.5*((TAUDU(L)/TAUCU(L))-1)**1.5

    ELSE IF (CONTRA.EQ.2) THEN

        YSUIN =YTFF(L)*(1.45*(VND(L)/(32.2*YTFF(L))**0.5)**0.2
        *COFUF*(1/SIGMCU**0.2)-1)

        IF(YSUIN.LE.0) YSUIN = 0

        YSU(L) = 0
        IF(YSUIN.GT.YUINMX) YSU(L) = YSUIN - YUINMX

        IF(YSUIN.GT.YUINMX) YUINMX = YSUIN

    ELSE

        YSUIN = 0
        IF(COFU.GT.1) YSUIN = YTFF(L)*(COFU - 1)

        YSU(L) = 0
        IF(YSUIN.GT.YUINMX) YSU(L) = YSUIN - YUINMX

        IF(YSUIN.GT.YUINMX) YUINMX = YSUIN

    END IF

    SUMYSU= SUMYSU + YSU(L)
    YTFF(L) = YTFF(L) + SUMYSU

    XADJAU(L) = 0.5*(TWBMLT(4)+TWBMLT(3))*SUMYSU

    VNDA(L) = VND(L)*XATOT(L)/(XATOT(L) + XADJAU(L))
    IF(VNDA(L).GT.VNDNAM) VNDNAM = VNDA(L)

C      Recompute flowdepth and velocity, and computed local scour dept
to adjust
C      for contraction
C      scour

    CSU(L) = CSU(L) - YSU(L)
    IF (YSU(L).GT.CSU(L)) CSU(L) = 0
    IF(CSU(L)+SUMYSU.LT.TSU) CSU(L) = TSU - SUMYSU

    LEW =L
    T(L)=LEW*DLT

```



```

DSU(L) = CSU(L)/PD

C      Compute the scour angles along the upstream(THU) pier face

      THU(L) = PHU
      IF (31*DSU(L)**2.LT.PHU) THU(L) = 31*DSU(L)**2

C      Compute downflow velocity on upstream face of the pier

      IF(DSU(L).GT.100) THEN
        VDU(L) = 0

        ELSE IF (DSU(L).LE.2.3.AND.YTFF(L).GT.MLT) THEN
          VDU(L)= VNDA(L)*(0.15 * (DSU(L))
            + 0.24*PD ** 0.18/(YTFF(L)**0.18* C1**0.5))

        ELSE IF (DSU(L).GT.2.3) THEN
          VDU(L) = VNDA(L)*(0.40/(1+EXP(3*(DSU(L)-4)) + 0.4))

      END IF

      IF(VDU(L).GT.0.8*VNDA(L)) VDU(L) = 0.8*VNDA(L)

*****
*****
C
C
      VMU(L) = 2.7* VDU(L)
      IF(31*DSU(L)**2.LE.PHU) VMU(L) = 2.24*C1**0.5*VDU(L)

      AFU(L) = -0.0002*THU(L)**2+0.012*THU(L)+0.80

      VTU(L)=0
      IF(AFU(L).GT.0) VTU(L)=1.4*AFU(L)*VMU(L)*
        (1-EXP(-1.25*(1/AFU(L)**2)))

*****
*****

      UIU(L)=0

      IF(YTFF(L).GT.0.AND.VINCIP.EQ.1) UIU(L)=
        VCUF*(1.66*D50U**0.333*YTFF(L)**0.167)

      IF(YTFF(L).GT.0.AND.VINCIP.EQ.2) UIU(L)= VCUF*0.09*
        (D50U*Tan(PHU*RADCON)* YTFF(L)**0.33/(ALPHAU*MAN**2))**0.5

      IF(YTFF(L).GT.0.AND.VINCIP.EQ.3) UIU(L)= VCUF*(0.024/MAN)*
        (D50U**0.5)*(YTFF(L)**0.167)

*****
*****

```

```

C      Compute armouring velocity

      VARMU(L)=0
      IF(ARMVEL.GT.0.AND.SIGMAU.GT.1.3) VARMU(L)=1.328*(DMAXU/1.8)**
      0.333*YTFF(L)**0.167

      IF(VARMU(L).LE.0) THEN
        VCRINU(L) = UIU(L)

      ELSE IF(VTU(L).LE.VARMU(L).AND.VARMU(L).GT.0) THEN

        VCRINU(L) = VARMU(L)-(UIU(L)/VCUF)

      ELSE IF (VTU(L).GT.VARMU(L).AND.VARMU(L).GT.0) THEN

        VCRINU(L) = VARMU(L)

      END IF

      IF(VCRINU(L).LT.UIU(L)) VCRINU(L)= UIU(L)

*****
*****

      DEU(L) =0
      IF(VTU(L).GT.VCRINU(L)) DEU(L)=(PD**BNDX)*TANH(YTFF(L)/PD)
      *((VTU(L)-VCRINU(L))**INDX)*(VNDA(L)/(32.2*PD)**0.5)**FREX

      TEU(L)=0
      IF(VCRINU(L).GT.0.0.AND.(VTU(L)/UIU(L)).GT.VCUF) THEN

      TEU(L) = 24*30.89*(PD/VTU(L))*((VTU(L)/VCRINU(L))-0.4)*
      (YTFF(L)/PD)**0.25

      ELSE IF(YTFF(L)-6.0*PD.GT.0.AND.((VTU(L)/VCRINU(L))
      -VCUF).GT.0.0) THEN

      TEU(L)= 24*48.26*(PD/VTU(L))*((VTU(L)/VCRINU(L))-0.4)
      END IF

*****
*****

      K1U(L)=0
      IF(TEU(L).GT.0.001.AND.VTU(L).GT.0.03) K1U(L)= EXP(-0.08
      *(ABS((VCRINU(L)/VTU(L))*LOG(DLT/TEU(L))))**1.2)

      K2U(L)=0
      IF(TEU(L).GT.0.001) K2U(L)= (ABS(LOG(DLT/TEU(L))))**0.2

      K3U(L)=0
      IF(VTU(L).GT.0.03) K3U(L) = 0.1*(DEU(L)/DLT)
      *(ABS(VCRINU(L)/VTU(L)))*1.2

```

```

*****
*****
      RLU(L)= K1U(L)* K2U(L)* K3U(L)

      CSU(L+1) = CSU(L) + (RLU(L)*DLT)
      IF(CSU(L+1).LT.CSU(L)) CSU(L+1) = CSU(L)

      IF(YTRF(L).GT.YTMRF) YTMRF= YTRF(L)
      IF(YTFF(L).GT.YTMFF) YTMFF= YTFF(L)

      IF(VTD(L).GT.VTDMX) VTDMX= VTD(L)
      IF(VTU(L).GT.VTUMX) VTUMX= VTU(L)

      IF(VTD(L).GT.VTDMX) VTDMX= VTD(L)
      IF(VTU(L).GT.VTUMX) VTUMX= VTU(L)

      IF(UIU(L).LT.UIUMIN) UIUMIN= UIU(L)
      IF(UID(L).LT.UIDMIN) UIDMIN= UID(L)

4290  CONTINUE

*****
*****
      TSD=CSD(ARR) + SUMYSD

C      Compute Contraction scour and sum to local scour to obtain total
scour for
C      downstream face for each storm

      TSU=CSU(ARR) + SUMYSU
*****
*****
4500  CONTINUE

*****
*****
C      DO LOOP FOR ALL 18 HR STORMS IN A GIVEN YEAR
C
*****
*****
      Do 400 K = 1, N18

C Initialize UVAR
      UVA=0
      UVAR18 = 1

      Do 60 L = 1,INT(C18)

C Generate uniform variate UVA from RANNO

      UVA =RANNO(1,0.0,1.0)
      UVAR18 = UVAR18*UVA

```

```

60      CONTINUE

          PPT18 = -B18*LOG(UVAR18)

C      Store the largest rainfall event in the simulation

          IF(PPT18.GT.PPTMAX) PPTMAX = PPT18

          SUM18 = SUM18 + PPT18

C Compute the total direct runoff (TDRO) and total expected
infiltration
C (TINF) from each storm

          TDRO = 0
          IF( PPT18.GT.IA) TDRO = (PPT18 - IA) ** 2/ (PPT18 + AI)

          IF(TDRO.LE.0.0) NORUN = NORUN + 1

C      DETERMINE CATCHMENT HYDROGRAPH

C      Convert rainfall from dimensionless cumulative hyetograph to a
C      cumulative depth hyetograph

          Do 70 L = 1, NP18
              P18(L) = S18(L) * PPT18
70      CONTINUE

          Do 80 L = 1, NP18
              SP = P18(L)
              PE18(L) = 0.0
              IF(SP.GT.IA) PE18(L) = (SP - IA) ** 2/ (SP + AI)
80      CONTINUE

              PEI18(1) =PE18(1)
              Do 90 L = 2, NP18
                  PEI18(L) = PE18(L) - PE18(L -1)
90      CONTINUE

C      Convolve unit hydrographs convolve sub routine

          CALL CONVOL(QU, PEI18, DRO18, NU, NP18, NR18, 36, 18, 300)

C      Add base flow to direct runoff hydrograph. Final output is
CHY(NR), NR

          Do 100 L = 1, ARR
              CHY18(L) = DRO18(L) + QBF

          IF (CHY18(L).GT.QP18MX) QP18MX = CHY18(L)

100     CONTINUE

```

```

C*****
C      SYNTHESIZE TIDAL SERIES AT BASE STATION B.
C*****
C      Compute array of tidal depths, TEB(ARR) to cover twice the number
of runoff ordinates
C      Generate uniform variates between 0.0 and 2*Pi to represent
diurnal and Lunar cycle
C      Phase angles. Generate normal variates to represent the Lunar
amplitude

          PHD = RANNO(1, 0.0, 6.284)
          PHL = RANNO(1, 0.0, 6.284)

          LA= RANNO( 2, MLA, SLA)
          LA=ABS(LA)
C
C      Generate normal variates that change with every diurnal cycle to
represent
C      the diurnal amplitude
          TB = 0
          DO 120 L =1, 400
              IF(TB.EQ.0) THEN
                  DA= RANNO(2, MDA, SDA)
                  DA=ABS(DA)
              ELSE
                  GO TO 110
              END IF
110          CONTINUE

C      Create array of MSL water surface elevations TEB(300) varying
hourly with
C      time
          LEW = L
          TB=TB+1

          TEB(L)= DA*SIN(2*PI*(LEW/DT))+
PHD)+LA*SIN(2*PI*(LEW/LT)+PHL)
          IF(TB.EQ.INT(DT)) TB=0

120          CONTINUE
C      ADD A CONDITION TO ENSURE TIDE DOES NOT DECREASE BELOW MEAN
LOW WATER

          DO 125 L=1,400
              IF(TEB(L).LT.(IBS +1.0)) TEB(L) = (IBS+1.0)
125          CONTINUE

C      DETERMINE TIDAL ELEVATIONS AT THE BRIDGE STATION
C      by convex routing and wave distortion

          TER(1)=TAF*TEB(1)

          IF(CONROUT.EQ.0) THEN

```

```

      Do 127 L=2, 400
      TER(L)= TAF*TEB(L)
      IF(TER(L).GT.HIELE) HIELE = TER(L)

127    CONTINUE

      ELSE IF(CONROUT.NE.0) THEN

      Do 130 L=2, 400
      TER(L)= CX*TEB(L-1) + (1.0 - CX)*TER(L-1)
      IF(TER(L).GT.HIELE) HIELE = TER(L)

130    CONTINUE

      END IF

C      Compute array for base station depth YB(150) by subtracting
C      channel invert elev. at the base station (or adding the
C      absolute value of (IBS) the array of tidal elevations

      Do 135 L= 1, 400
      YB(L) = TEB(L) + ABS(IBS)
      IF(YB(L).GT.HIBASE) HIBASE = YB(L)
135    CONTINUE

      IF(DISCON.EQ.0) THEN

C
      Do 140 L = 1, ARR
      QN(L) = AS * ( (TER(L) - TER(L+1)))/(3600*DLT)

C      Modify the Neill's discharges with modification factors NMFR,
NMFF
C      developed by Brubaker and Demetrius.

      QNM(L)= NMFF*QN(L)
      IF (QN(L).LT.0) QNM(L)= NMFR*QN(L)

C      DETERMINE THE COMBINED TIDAL AND RIVERINE DISCHARGES BY
C      VECTOR ADDITION OF TIDAL AND RIVERINE DISCHARGES
C

      QT(L)= CHY18(L) + QNM(L)

      IF(QT(L).LE.0) THEN
      QTR(L) = ABS(QT(L))

      ELSE IF(QT(L).GT.0) THEN
      QTF(L) = ABS(QT(L))

      IF(ABS(QT(L)).GT.QTUMAX) QTUMAX = ABS(QT(L))

      IF((QTR(L)).GT.QTRMAX) QTRMAX = QTR(L)
      IF((QTF(L)).GT.QTFMAX) QTFMAX = QTF(L)

```

```

IF((QTR(L)).GT.QTRMX) QTRMX = QTR(L)
IF((QTF(L)).GT.QTFMX) QTFMX = QTF(L)

IF((QTR(L)).GT.QTRMXS) QTRMXS = QTR(L)
IF((QTF(L)).GT.QTFMXS) QTFMXS = QTF(L)

SUMQTU = SUMQTU + ABS(QT(L))

CONQTU = CONQTU + 1

END IF

C      DETERMINE THE COMBINED DEPTH YT
C

YAT(L) = TER(L) +ABS(IRS)
      IF(YAT(L).LT.MLT) YAT(L) = MLT
      IF(YAT(L).GE.HITIDE) HITIDE = YAT(L)

140      CONTINUE

      Do 150 L =1,ARR

          IF(QT(L).GT.0) QROUT(L) = QT(L)

          IF(QT(L).LE.0) QROUT(L)= 0

150      CONTINUE

          VOUT(1) = 3600*0.5*(QROUT(1))
          VITID(1)= 0.5*(YAT(1)-MLT)*AS
          VICAT(1)= 3600*(QBF)
          VITOT(1)= VICAT(1)+ VITID(1)

          Do 160 l=2, ARR
              VICAT(L)=0.5*(CHY18(L)+CHY18(L-1))*3600
              VITID(L)=(YAT(L) - YAT(L-1))*AS
              VITOT(L)=VICAT(L) + VITID(L)
              VOUT(L) =3600*0.5*(QROUT(L)+QROUT(L-1))
160      CONTINUE

          VBAL(1) = VITOT(1) - VOUT(1)
          IF(VBAL(1).LE.0) VBAL(1) = 0
          IF(VBAL(1).LE.0) YT(1)= MLT
          IF(VBAL(1).GT.0.AND.VBAL(1).LE.SESVOL(1))
YT(1)=
          MLT + YTAMLT(1)

          Do 170 L=2,ARR
              VBAL(L) =VITOT(L-1) + VITOT(L)-VOUT(L)

```

```

        IF (VBAL(L).LE.0) VBAL(L) = 0
        IF (VBAL(L).LE.0) YT(L) = MLT

        IF(VBAL(L).GT.0.AND.VBAL(L).LE.SESVOL(1)) YT(L)=
            MLT + YTAMLT(1)

        Do 165 M =2, 150

            IF(VBAL(L).GT.SESVOL(M-
1) .AND.VBAL(L).LE.SESVOL(M))
                YT(L) = MLT + YTAMLT(M)
165             CONTINUE
170             CONTINUE

        Do 180 L=1,ARR

        IF(YT(L).LT.YAT(L)) YT(L) = YAT(L)
180     CONTINUE

        IF(YT(1).LT.YT(2)) YTR(1) = YT(1)
        IF(YT(1).GE.YT(2)) YTR(1) = MLT

            IF(YT(1).GE.YT(2)) YTF(1) = YT(1)
            IF(YT(1).LT.YT(2)) YTF(1) = MLT

        Do 185 L= 1,ARR

            IF(YT(L+1).GT.YT(L)) YTR(L+1) = YT(L+1)
            IF(YT(L+1).LE.YT(L)) YTR(L+1) = MLT

            IF(YT(L+1).LE.YT(L)) YTF(L+1) = YT(L+1)
            IF(YT(L+1).GT.YT(L)) YTF(L+1) = MLT

            IF(YT(L).GT.YTMAX) YTMAX = YT(L)
            SUMYT = SUMYT + YT(L)
            CONYT = CONYT + 1

C      Record annual maximum depth at bridge station
            IF(YT(L).GT.YTMX) YTMX = YT(L)

            IF(YTF(L).GT.YTFMX) YTFMX = YTF(L)
            IF(YTR(L).GT.YTRMX) YTRMX = YTR(L)

            IF(YTF(L).GT.YTFMAX) YTFMAX = YTF(L)
            IF(YTR(L).GT.YTRMAX) YTRMAX = YTR(L)

            IF(YTFMX.GT.YTFMXS) YTFMXS = YTFMX
            IF(YTRMX.GT.YTRMXS) YTRMXS = YTRMX

185             CONTINUE

            ELSE

        Do 190 L= 1, 400

```



```

        TERS(L)=TER(L)
        LEW =L
        TBR(L) = LEW + (LW/(1800*32.2*(YB(L) + MDR))**0.5)
190      CONTINUE

C      Sort array TBR(300) in ascending order also sort array  TERS(300)
C      based on the order of array TBR(300).

        CALL SORT2(400,TBR, TERS)

C      Normalize the array TBR(300) by subtracting TBR(1) and adding
C      1.00 to
C      all elements in the array.  Also determine corresponding tidal
C      depths (YAT(L))

        Do 200 L=1, 400
            TNR(L) = TBR(L) +1-TBR(1)

            YAT(L) = TERS(L) + ABS(IRS)
            IF(YAT(L).LT.MLT) YAT(L)=MLT
200      CONTINUE

C Determine the array of the interpolated tidal depths at the bridge
C location

        CALL INTERP(TNR, YAT, TNRI, YATI, 400, 300,400, 300)

C Determine the tidal discharges at the bridge location using the
C Neill's Equation
C QN(NR18) represents an array of computed Neill's discharges with
C negative
C and positive values. The negative values represents the discharges
C produced by the rising tide directed up the estuary. While the
C positive values
C represents the discharges directed downstream. In the algorithm QNR
C represents
C Neill's discharges due to the rising limb and QNF represents
C Neill's
C discharges due to the falling limb.

        Do 210 L= 1, (ARR+1)
            TERI(L) = YATI(L)+IRS
210      CONTINUE

C

        Do 220 L = 1, ARR

            QN(L) = AS * ( (TERI(L) - TERI(L+1)))/(3600*DLT)
C      Modify the Neill's discharges with modification factors NMFR,
C      NMFF
C      developed by Brubaker and Demetrius.

            QNM(L)= NMFF*QN(L)
            IF (QN(L).LT.0) QNM(L)= NMFR*QN(L)

```

```

C      DETERMINE THE COMBINED TIDAL AND RIVERINE DISCHARGES BY
C      VECTOR ADDITION OF TIDAL AND RIVERINE DISCHARGES
C
      QT(L)= CHY18(L) + QNM(L)

      IF(QT(L).LE.0) THEN
        QTR(L) = ABS(QT(L))

      ELSE IF(QT(L).GT.0) THEN
        QTF(L) = ABS(QT(L))

      IF(ABS(QT(L)).GT.QTUMAX) QTUMAX = ABS(QT(L))

      IF((QTR(L)).GT.QTRMAX) QTRMAX = QTR(L)
      IF((QTF(L)).GT.QTFMAX) QTFMAX = QTF(L)

      IF((QTR(L)).GT.QTRMX) QTRMX = QTR(L)
      IF((QTF(L)).GT.QTFMX) QTFMX = QTF(L)

      IF((QTR(L)).GT.QTRMXS) QTRMXS = QTR(L)
      IF((QTF(L)).GT.QTFMXS) QTFMXS = QTF(L)

      SUMQTU = SUMQTU + ABS(QT(L))

      CONQTU = CONQTU + 1

      END IF

      IF(YATI(L).GE.HITIDE) HITIDE = YATI(L)

220      CONTINUE

C
C      DETERMINE THE COMBINED DEPTH YT
C
      IF(QT(L).GT.0) QROUT(L) = QT(L)
      IF(QT(L).LE.0) QROUT(L)= 0

230      CONTINUE

      VOUT(1) = 3600*0.5*(QROUT(1))
      VITID(1)= 0.5*(YATI(1)-MLT)*AS
      VICAT(1)= 3600*(QBF)
      VITOT(1)= VICAT(1)+ VITID(1)

      Do 240 l=2, ARR
        VICAT(L)=0.5*(CHY18(L)+CHY18(L-1))*3600
        VITID(L)=(YATI(L) - YATI(L-1))*AS
        VITOT(L)=VICAT(L) + VITID(L)
        VOUT(L) =3600*0.5*(QROUT(L)+QROUT(L-1))
240      CONTINUE

      VBAL(1) = VITOT(1) - VOUT(1)
      IF(VBAL(1).LE.0) VBAL(1) = 0
      IF(VBAL(1).LE.0) YT(1)= MLT

```

```

                                IF(VBAL(1).GT.0.AND.VBAL(1).LE.SESVOL(1))
YT(1)=
                                MLT + YTAMLT(1)

                                Do 250 L=2,ARR
                                VBAL(L) =VITOT(L-1) + VITOT(L)-VOUT(L)
                                IF (VBAL(L).LE.0) VBAL(L) = 0
                                IF (VBAL(L).LE.0) YT(L) = MLT

                                IF(VBAL(L).GT.0.AND.VBAL(L).LE.SESVOL(1)) YT(L)=
                                MLT + YTAMLT(1)

                                Do 245 M =2, 150

                                IF(VBAL(L).GT.SESVOL(M-
1).AND.VBAL(L).LE.SESVOL(M))
                                YT(L) = MLT + YTAMLT(M)
245                                CONTINUE
250                                CONTINUE

                                Do 260 L=1,ARR
                                IF(YT(L).LT.YATI(L)) YT(L) = YATI(L)
260                                CONTINUE

*****
*****

                                IF(YT(1).LT.YT(2)) YTR(1) = YT(1)
                                IF(YT(1).GE.YT(2)) YTR(1) = MLT

                                IF(YT(1).GE.YT(2)) YTF(1) = YT(1)
                                IF(YT(1).LT.YT(2)) YTF(1) = MLT

                                Do 270 L= 1,ARR

                                IF(YT(L+1).GT.YT(L)) YTR(L+1) = YT(L+1)
                                IF(YT(L+1).LE.YT(L)) YTR(L+1) = MLT

                                IF(YT(L+1).LE.YT(L)) YTF(L+1) = YT(L+1)
                                IF(YT(L+1).GT.YT(L)) YTF(L+1) = MLT

                                SUMYT = SUMYT + YT(L)
                                CONYT = CONYT + 1

                                IF(YT(L).GT.YTMAX) YTMAX = YT(L)

C      Record annual maximum depth at bridge station
                                IF(YT(L).GT.YTMX) YTMX = YT(L)

                                IF(YTF(L).GT.YTFMX) YTFMX = YTF(L)
                                IF(YTR(L).GT.YTRMX) YTRMX = YTR(L)

                                IF(YTF(L).GT.YTFMAX) YTFMAX = YTF(L)

```

```

        IF(YTR(L).GT.YTRMAX) YTRMAX = YTR(L)

        IF(YTFMX.GT.YTFMXS) YTFMXS = YTFMX
        IF(YTRMX.GT.YTRMXS) YTRMXS = YTRMX

270          CONTINUE
          END IF

C
C DETERMINE COMBINED VELOCITY AT BRIDGE STATION
C
C   The inputs required for this step are the time varying tidal
discharges at
C   location b QT(ARR) flow depth YT(ARR) and the
C   cross section area of the estuary at bridge location b. The net
velocity VNT(L)
C   is computed as { QT(L)/(YT*WB)}

C   Compute the array of velocity directed up the channel
C   Ensure the array of resultant velocities directed down the
channel

      Do 280 L=1,ARR

        IF(YT(L).LE.MLT) VNT(L) = QT(L)/XABMLE

        IF(YT(L).LE.MLT) XATOT(L) = XABMLE

        IF(YT(L).GT.MLT.AND.YT(L).LE.(MLT+YTAMLT(1)))
          VNT(L) = QT(L)/(XABMLE+SXAMLT(1)-VFACT*UESTZ*(YT(L)-
MLT)**2)

        IF(YT(L).GT.MLT.AND.YT(L).LE.(MLT+YTAMLT(1)))
          XATOT(L)=(XABMLE + SXAMLT(1)-VFACT*UESTZ*(YT(L)-MLT)**2)

      Do 275 M= 2, 150
        IF(YT(L).GT.(MLT+YTAMLT(M-1)).AND.YT(L).LE.(MLT+YTAMLT(M)))
          VNT(L)=QT(L)/(XABMLE+ SXAMLT(M)-VFACT*UESTZ*(YT(L)-
MLT)**2)

        IF(YT(L).GT.(MLT+YTAMLT(M-1)).AND.YT(L).LE.(MLT+YTAMLT(M)))
          XATOT(L) =(XABMLE+SXAMLT(M)-VFACT*UESTZ*(YT(L)-MLT)**2)

275  CONTINUE
280  CONTINUE
*****

C   INITIALIZE SOIL SCOUR VARIABLES FOR EACH STORM
C   INITIALIZE CSU, AND CSD

      DO 282 L=1, ARR
        CSD(L) =TSD - SUMYSD
        IF (SUMYSD.GT.TSD) CSD(L) = 0

```

```

      CSU(L) = TSU - SUMYSU
      IF (SUMYSU.GT.TSU) CSU(L) = 0

      YTFF(L) = YTF(L) + SUMYSU

      YTRF(L) = YTR(L) + SUMYSD
282  CONTINUE

      Do 285 L =1,30

          DPTHU =TSU
          IF(DPTHU.GE.DPTH(L).AND. DPTHU.LE.DPTH(L+1)) THEN
              ALPHAU = ALPHA(L)
              D16U   = D16(L)
              D50U   = D50(L)
              D84U   = D84(L)
              DMAXU  = DMAX(L)
              VCUF   = 0.476*(D50U/PD)**0.053
              SIGMAU = (D84U/D16U)**0.5
              PHU    = PH(L)
          END IF

          DPTHU = TSD
          IF(DPTHU.GE.DPTH(L).AND. DPTHU.LE.DPTH(L+1)) THEN
              ALPHAD = ALPHA(L)
              D16D   = D16(L)
              D50D   = D50(L)
              D84D   = D84(L)
              DMAXD  = DMAX(L)
              VCDF   = 0.476*(D50D/PD)**0.053
              SIGMAD = (D84D/D16D)**0.5
              PHDD   = PH(L)
          END IF

          DPTHCU = SUMYSU
          IF(DPTHCU.GE.DPTH(L).AND. DPTHCU.LE.DPTH(L+1)) THEN

              D16CU   = D16(L)
              D50CU   = D50(L)
              D84CU   = D84(L)
              SIGMCU  = (D84CU/D16CU)**0.5

          END IF

          DPTHCD = SUMYSD
          IF(DPTHCD.GE.DPTH(L).AND. DPTHCD.LE.DPTH(L+1)) THEN

              D16CD   = D16(L)
              D50CD   = D50(L)
              D84CD   = D84(L)
              SIGMCD  = (D84CD/D16CD)**0.5

          END IF

285  CONTINUE

```

```

C      DETERMINE FLOW VELOCITY DOWNFLOW,VORTEX VELOCITY VECTORS, AND
SCOUR FOR EACH HOUR OF STORM
C
C      The required inputs are the net edutary velocity (VNU,VND),
C      the total flow depth (YT), the bridge pier diameter (PD),
C      the existing scour depth at the beginning of the process (TSU,
TSD),
C      the soils property at the invert of the estuary channel
C      ( D50, PH,) as a function of local scour depth (TSU, TCD)

C      Determine ratio of scour to bridge diameter along the upstream
C      and downstream face of the pier

C      Set up downflow, Tangential velocity and scour algorithms
C      The process involves the computation of the total local scour
C      depth over each storm event and summing over the full simulation.
C      The contraction scour will then be computed for each storm but
will
C      be based successively on the highest value of YT in YRS and added
to the
C      total scour at the upstream and downstream faces of the pier.

      Do 290 L=1,ARR
        VNUIN(L) = 0
        IF(VNT(L).LT.0) VNUIN(L) = ABS(VNT(L))

        VNU(1) = 0.5*VNUIN(1)
        Do 286 M=2, ARR
          VNU(M) = 0.5*(VNUIN(M)+ VNUIN(M-1))
286      CONTINUE

        IF(VNU(L).LE.0) VNU(L)= 0
        IF(VNU(L).GT.0) THEN
          IF(VNU(L).GT.VNUMAX) VNUMAX = VNU(L)
          SUMVNU = SUMVNU + VNU(L)
          CONVNU = CONVNU + 1
        END IF

C Place maximum storm velocity in annual holding location VUPM

        IF(VNU(L).GT.VUPM) VUPM = VNU(L)
        IF(VUPM.GT.VUPMS) VUPMS = VUPM
*****
*****

C      Compute incremental contraction scour over time DLT      and
adjust flow depth to include the
C      lowering of the bed

      IF(CONTRA.EQ.1) THEN

C      Compute contraction scour using Straub's eqn

```

```

C      qs = (g*(Ss-1)*d50**3)**0.5 * ((T/Tc) - 1)**2 English units,
d50 in
C      feet

C      Converting the equations so that D50 is in mm and solving for
scour depth
C      gives

C      YS =      (0.67/PD)*DLT*d50mm**1.5*[(T/Tc)-1]**2

C      T =      28.11*(Q/WB)**2* [n**2/YTFF**2.33]

C      If D50mm <0.065 then
C          Tc = 4.84*D50mm
C      Else
C          Tc = 0.8d50^.67*Y^.33

          IF ( D50CD.LT.0.065) THEN
            TAUCD(L) = 4.84*D50CD
          ELSE
            TAUCD(L) = 0.84*D50CD**0.67*YTRF(L)**0.33
          END IF

          TAUDD(L)= 28.11*(QTR(L)/WB)**2*(MAN**2/YTRF(L)**2.33)

          YSD(L) = 0
          IF ((TAUDD(L)/TAUCD(L)).GT.1) YSD(L) = COFDS*(0.67/PD)
            *DLT*D50CD**1.5*((TAUDD(L)/TAUCD(L))-1)**1.5
*****
          ELSE IF (CONTRA.EQ.2) THEN

            YSDIN=YTR(L)*(1.45*(VNU(L)/(32.2*YTR(L))**0.5)**0.2
            *COFDF*(1/SIGMCD**0.2)-1)

            IF(YSDIN.LE.0) YSDIN = 0

            YSD(L) = 0
            IF(YSDIN.GT.YDINMX) YSD(L) = YSDIN - YDINMX

            IF(YSDIN.GT.YDINMX) YDINMX = YSDIN

          ELSE

            YSDIN = 0
            IF(COFD.GT.1) YSDIN = YTR(L)*(COFD - 1)

            YSD(L) = 0
            IF(YSDIN.GT.YDINMX) YSD(L) = YSDIN - YDINMX

            IF(YSDIN.GT.YDINMX) YDINMX = YSDIN

          END IF

          SUMYSD= SUMYSD + YSD(L)

```

```

YTRF(L) = YTR(L) + SUMYSD

XADJAD(L) = 0.5*(TWBMLT(4)+TWBMLT(3))*SUMYSD

VNUA(L) = VNU(L)*XATOT(L)/(XATOT(L) + XADJAD(L))
IF(VNUA(L).GT.VNUPAM) VNUPAM = VNUA(L)

C      Recompute flowdepth and velocity, and computed local scour dept
to adjust
C      for contraction
C      scour

CSD(L) = CSD(L) - YSD(L)
IF (YSD(L).GT.CSD(L)) CSD(L) = 0
IF(CSD(L)+SUMYSD.LT.TSD) CSD(L) = TSD - SUMYSD

LEW =L
T(L)=LEW*DLT

DSD(L) = CSD(L)/PD
C      Compute the scour angles along the downstream(THD) pier face

THD(L) = PHDD
IF (31*DSD(L)**2.LT.PHDD) THD(L) =31*DSD(L)**2

*****
*****

C      Compute downflow velocity on downstream faces of the pier

IF(DSD(L).GT.100) THEN
VDD(L) = 0

ELSE IF (DSD(L).LE.2.3.AND.YTRF(L).GT.MLT) THEN
VDD(L) = VNUA(L)* (0.15*(DSD(L))
+ 0.24* PD **0.18/(YTRF(L)**0.18 * C1**0.5))

ELSE IF (DSD(L).GT.2.3) THEN
VDD(L) = VNUA(L)*(0.40/EXP(1+(3*(DSD(L)-4)) + 0.4))

END IF

IF(VDD(L).GT.0.8*VNUA(L)) VDD(L) = 0.8*VNUA(L)

C      Compute the maximum tangential velocities along the upstream(VMU)
and downstream
C      (VMD) pier faces

VMD(L) = 2.7* VDD(L)
IF(31*DSD(L)**2.LE.PHDD) VMD(L) = 2.24*C1**0.5*VDD(L)

C      Compute the A factors and tangential velocities (VTU)

```



```

C      along the upstream and downstream (VTD) pier faces

      AFD(L)=-0.0002*THD(L)**2+0.012*THD(L)+0.80

      VTD(L)=0
      IF(AFD(L).GT.0) VTD(L)=1.4*AFD(L)*VMD(L)*
      (1-EXP(-1.25*(1/AFD(L)**2)))

*****
*****
C      SELECT CRITICAL VELOCITY MERHOD

      UID(L)=0

      IF(YTRF(L).GT.0.AND.VINCIP.EQ.1) UID(L)=
      VCDF*(1.66*D50D**0.333*YTRF(L)**0.167)

      IF(YTRF(L).GT.0.AND.VINCIP.EQ.2) UID(L)= VCDF*0.09*
      (D50D*Tan(PHDD*RADCON)* YTRF(L)**0.33/(ALPHAD*MAN**2))**0.5

      IF(YTRF(L).GT.0.AND.VINCIP.EQ.3) UID(L)= VCDF*(0.024/MAN)*
      (D50D**0.5)*(YTRF(L)**0.167)

*****
*****
C      Compute armouring velocity

      VARMD(L)=0
      IF(ARMVEL.GT.0.AND.SIGMAD.GT.1.3) VARMD(L)=1.328*(DMAXD/1.8)**
      0.333*YTRF(L)**0.167

      IF(VARMD(L).LE.0) THEN
        VCRIND(L) = UID(L)

      ELSE IF(VTD(L).LE.VARMD(L).AND.VARMD(L).GT.0) THEN

        VCRIND(L) = VARMD(L)-(UID(L)/VCDF)

      ELSE IF (VTD(L).GT.VARMD(L).AND.VARMD(L).GT.0) THEN

        VCRIND(L) = VARMD(L)

      END IF

      IF(VCRIND(L).LT.UID(L)) VCRIND(L)= UID(L)

*****
*****

      DED(L) =0

```

```

IF(VTD(L).GT.VCRIND(L)) DED(L)=(PD**BNDX)*TANH(YTRF(L)/PD)
  *((VTD(L)-VCRIND(L))**INDX)*(VNUA(L)/(32.2*PD)**0.5)**FREX

TED(L)=0
IF(VCRIND(L).GT.0.0.AND.(VTD(L)/UID(L)).GT.VCDF) THEN

TED(L) = 24*30.89*(PD/VTD(L))*((VTD(L)/VCRIND(L))-0.4)*
  (YTRF(L)/PD)**0.25

ELSE IF(YTRF(L)-6.0*PD.GT.0.AND.((VTD(L)/VCRIND(L))
  -VCDF).GT.0.0) THEN

TED(L)= 24*48.26*(PD/VTD(L))*((VTD(L)/VCRIND(L))-0.4)
END IF

*****
*****

K1D(L)=0
IF(TED(L).GT.0.001.AND.VTD(L).GT.0.03) K1D(L)= EXP(-0.08*
  (ABS((VCRIND(L)/VTD(L))*LOG(DLT/TED(L))))**1.2)

K2D(L)=0
IF(TED(L).GT.0.001) K2D(L)=(ABS(LOG(DLT/TED(L))))**0.2

K3D(L)=0
IF(VTD(L).GT.0.03) K3D(L) = 0.1*(DED(L)/DLT)
  *(VCRIND(L)/VTD(L))**1.2

RLD(L)= K1D(L)* K2D(L)* K3D(L)

CSD(L+1) = CSD(L) + (RLD(L)*DLT)
IF(CSD(L+1).LT.CSD(L)) CSD(L+1) =CSD(L)

*****
*****
C Repeat process for upstream pier face
*****
*****

VNDIN(L) =0
IF(VNT(L).GT.0) VNDIN(L) = ABS(VNT(L))

VND(1) = 0.5*VNDIN(1)
Do 288 M=2, ARR
  VND(M) = 0.5*(VNDIN(M)+ VNDIN(M-1))
288 CONTINUE

IF(VND(L).LE.0) VND(L)= 0
IF(VND(L).GT.0) THEN
IF(VND(L).GT.VNDMAX) VNDMAX = VND(L)
SUMVND = SUMVND + VND(L)
CONVND = CONVND + 1
END IF

```

```

C Place maximum storm velocity in annual holding location VDWNM

      IF(VND(L).GT.VDWNM) VDWNM = VND(L)
      IF(VDWNM.GT.VDWNMS) VDWNMS = VDWNM

*****
*****

C      Compute incremental contraction scour over time DLT      and
adjust flow depth to include the
C      lowering of the bed

      IF(CONTRA.EQ.1) THEN

C      Compute contraction scour using Straub's eqn
C       $qs = (g \cdot (Ss - 1) \cdot d50^3)^{0.5} \cdot ((T/Tc) - 1)^2$  English units,
d50 in feet
C      Converting the equations so that D50 is in mm and solving for
scour depth
C      gives
C       $YS = (0.67/PD) \cdot DLT \cdot d50^{1.5} \cdot [(T/Tc) - 1]^2$ 
C       $T = 28.11 \cdot (Q/WB)^{0.5} \cdot [n^2/YTFF^{2.33}]$ 
C      If D50mm < 0.065 then
C       $Tc = 4.84 \cdot D50$ 
C      Else
C       $Tc = 0.8 \cdot d50^{0.67} \cdot Y^{0.33}$ 

      IF ( D50CU.LT.0.065) THEN
        TAUCU(L) = 4.84*D50CU
      ELSE
        TAUCU(L) = 0.84*D50CU**0.67*YTFF(L)**0.33
      END IF

      TAUDU(L) = 28.11*(QTF(L)/WB)**0.5*(MAN**2/YTFF(L)**2.33)

      YSU(L) = 0
      IF((TAUDU(L)/TAUCU(L)).GT.1) YSU(L) = COFUS*(0.67/PD)*
      DLT*D50CU**1.5*((TAUDU(L)/TAUCU(L))-1)**1.5

    ELSE IF (CONTRA.EQ.2) THEN

      YSUIN = YTF(L)*(1.45*(VND(L)/(32.2*YTF(L))**0.5)**0.2
      *COFUF*(1/SIGMCU**0.2)-1)

      IF(YSUIN.LE.0) YSUIN = 0

      YSU(L) = 0
      IF(YSUIN.GT.YUINMX) YSU(L) = YSUIN - YUINMX

      IF(YSUIN.GT.YUINMX) YUINMX = YSUIN

    ELSE

      YSUIN = 0

```

```

        IF(COFU.GT.1) YSUIN = YTF(L)*(COFU - 1)

        YSU(L) = 0
        IF(YSUIN.GT.YUINMX) YSU(L) = YSUIN - YUINMX

        IF(YSUIN.GT.YUINMX) YUINMX = YSUIN

    END IF

    SUMYSU= SUMYSU + YSU(L)

    YTFF(L) = YTF(L) + SUMYSU

    XADJAU(L) = 0.5*(TWBMLT(4)+TWBMLT(3))*SUMYSU

    VNDA(L) = VND(L)*XATOT(L)/(XATOT(L) + XADJAU(L))
    IF(VNDA(L).GT.VNDNAM) VNDNAM = VNDA(L)

C      Recompute flowdepth and velocity, and computed local scour dept
to adjust
C      for contraction
C      scour

        CSU(L) = CSU(L) - YSU(L)
        IF (YSU(L).GT.CSU(L)) CSU(L) = 0
        IF(CSU(L)+SUMYSU.LT.TSU) CSU(L) = TSU - SUMYSU

        LEW =L
        T(L)=LEW*DLT

        DSU(L) = CSU(L)/PD

C      Compute the scour angles along the upstream(THU) pier face

        THU(L) = PHU
        IF (31*DSU(L)**2.LT.PHU) THU(L) = 31*DSU(L)**2

C      Compute downflow velocity on upstream face of the pier

        IF(DSU(L).GT.100) THEN
            VDU(L) = 0

        ELSE IF (DSU(L).LE.2.3.AND.YTFF(L).GT.MLT) THEN
            VDU(L)= VNDA(L)*(0.15 * (DSU(L))
            + 0.24*PD ** 0.18/(YTFF(L)**0.18* C1**0.5))

        ELSE IF (DSU(L).GT.2.3) THEN
            VDU(L) = VNDA(L)*(0.40/(1+EXP(3*(DSU(L)-4)) + 0.4))

        END IF

        IF(VDU(L).GT.0.8*VNDA(L)) VDU(L) = 0.8*VNDA(L)

```

```
*****
*****
```

```
C
C
```

```
VMU(L) = 2.7* VDU(L)
IF(31*DSU(L)**2.LE.PHU) VMU(L) = 2.24*C1**0.5*VDU(L)
```

```
AFU(L) = -0.0002*THU(L)**2+0.012*THU(L)+0.80
```

```
VTU(L)=0
IF(AFU(L).GT.0) VTU(L)=1.4*AFU(L)*VMU(L)*
(1-EXP(-1.25*(1/AFU(L)**2)))
```

```
*****
*****
*****
```

```
UIU(L)=0
```

```
IF(YTFF(L).GT.0.AND.VINCIP.EQ.1) UIU(L)=
VCUF*(1.66*D50U**0.333*YTFF(L)**0.167)
```

```
IF(YTFF(L).GT.0.AND.VINCIP.EQ.2) UIU(L)= VCUF*0.09*
(D50U*Tan(PHU*RADCON)* YTFF(L)**0.33/(ALPHAU*MAN**2))**0.5
```

```
IF(YTFF(L).GT.0.AND.VINCIP.EQ.3) UIU(L)= VCUF*(0.024/MAN)*
(D50U**0.5)*(YTFF(L)**0.167)
```

```
*****
*****
```

```
C      Compute armouring velocity
```

```
VARMU(L)=0
IF(ARMVEL.GT.0.AND.SIGMAU.GT.1.3) VARMU(L)=1.328*(DMAXU/1.8)**
0.333*YTFF(L)**0.167
```

```
IF(VARMU(L).LE.0) THEN
VCRINU(L) = UIU(L)
```

```
ELSE IF(VTU(L).LE.VARMU(L).AND.VARMU(L).GT.0) THEN

VCRINU(L) = VARMU(L)-(UIU(L)/VCUF)
```

```
ELSE IF (VTU(L).GT.VARMU(L).AND.VARMU(L).GT.0) THEN

VCRINU(L) = VARMU(L)
```

```
END IF
```

```
IF(VCRINU(L).LT.UIU(L)) VCRINU(L)= UIU(L)
```

```
*****
*****
```

```

      DEU(L) =0
      IF(VTU(L).GT.VCRINU(L)) DEU(L)=(PD**BNDX)*TANH(YTFF(L)/PD)
      *((VTU(L)-VCRINU(L))**INDX)*(VNDA(L)/(32.2*PD)**0.5)**FREX

      TEU(L)=0
      IF(VCRINU(L).GT.0.0.AND.(VTU(L)/UIU(L)).GT.VCUF) THEN

      TEU(L) = 24*30.89*(PD/VTU(L))*((VTU(L)/VCRINU(L))-0.4)*
      * (YTFF(L)/PD)**0.25

      ELSE IF(YTFF(L)-6.0*PD.GT.0.AND.((VTU(L)/VCRINU(L))
      -VCUF).GT.0.0) THEN

      TEU(L)= 24*48.26*(PD/VTU(L))*((VTU(L)/VCRINU(L))-0.4)
      END IF

```

```
*****
*****
```

```

      K1U(L)=0
      IF(TEU(L).GT.0.001.AND.VTU(L).GT.0.03) K1U(L)= EXP(-0.08
      *(ABS((VCRINU(L)/VTU(L))*LOG(DLT/TEU(L))))**1.2)

      K2U(L)=0
      IF(TEU(L).GT.0.001) K2U(L)= (ABS(LOG(DLT/TEU(L))))**0.2

      K3U(L)=0
      IF(VTU(L).GT.0.03) K3U(L) = 0.1*(DEU(L)/DLT)
      * (ABS(VCRINU(L)/VTU(L)))*1.2

```

```
*****
*****
```

```

      RLU(L)= K1U(L)* K2U(L)* K3U(L)

      CSU(L+1) = CSU(L) + (RLU(L)*DLT)
      IF(CSU(L+1).LT.CSU(L)) CSU(L+1) = CSU(L)

      IF(YTRF(L).GT.YTMRF) YTMRF= YTRF(L)
      IF(YTFF(L).GT.YTMFF) YTMFF= YTFF(L)

      IF(VTD(L).GT.VTDMX) VTDMX= VTD(L)
      IF(VTU(L).GT.VTUMX) VTUMX= VTU(L)

      IF(VTDMX.GT.VTDMXS) VTDMXS= VTDMX
      IF(VTUMX.GT.VTUMXS) VTUMXS= VTUMX

      IF(UIU(L).LT.UIUMIN) UIUMIN= UIU(L)
      IF(UID(L).LT.UIDMIN) UIDMIN= UID(L)

```

```

290  CONTINUE

*****
*****
      TSD=CSD(ARR) + SUMYSD

C Compute Contraction scour and sum to local scour to obtain total
scour for
C  downstream face for each storm

      TSU=CSU(ARR) + SUMYSU
*****
*****

400  CONTINUE

C
*****
*****
C  REPEAT PROCESS FOR THE SCOUR SIMULATION FROM ALL 24 HR STORMS
C
      Do 700 K = 1, N24
C      Initialize UVAR
      UVA=0
      UVAR24 = 1

      Do 410  L = 1, INT(C24)

C Generate uniform variate UVR from RANNO

      UVA=RANNO(1,0.0,1.0)
      UVAR24 = UVAR24*UVA
410    CONTINUE

      PPT24 = -B24*LOG(UVAR24)

      IF(PPT24.GT.PPTMAX) PPTMAX =PPT24

      SUM24 = SUM24 + PPT24

      TDRO = 0
      IF( PPT24.GT.IA) TDRO = (PPT24 - IA) ** 2/ (PPT24 + AI)
      IF(TDRO.LE.0.0) NORUN = NORUN + 1

C      Determine catchment hydrograph

C      Convert rainfall from dimensionless cumulative hyetograph to a
cumulative depth hyetograph

      Do 420  L = 1, NP24
      P24(L) = S24(L) * PPT24
420    CONTINUE

      Do 430  L = 1, NP24
      SP = P24(L)
      PE24(L) = 0.0
      IF(SP.GT.IA) PE24(L) = (SP - IA) ** 2/ (SP + AI)

```

```

430      CONTINUE

      PEI24(1) = PE24(1)

      Do 440 L = 2, NP24
        PEI24(L) = PE24(L) - PE24(L-1)
440      CONTINUE

C      Convolve unit hydrographs convolve sub routine

      CALL CONVOL(QU, PEI24, DRO24, NU, NP24, NR24, 36, 24, 300)

C      Add base flow to direct runoff hydrograph.  Final output is
DRO(NR), NR

      Do 450 L = 1, ARR
        CHY24(L) = DRO24(L) + QBF

        IF (CHY24(L).GT.QP24MX) QP24MX = CHY24(L)

450      CONTINUE

C
C      SYNTHESIZE TIDAL SERIES AT BASE STATION B.

      PHD = RANNO(1, 0.0, 6.284)
      PHL = RANNO(1, 0.0, 6.284)

      LA= RANNO( 2, MLA, SLA)
      LA=ABS(LA)

C
C      Generate normal variates that change with every diurnal cycle to
represent
C      the diurnal amplitude
C
      TB = 0
      DO 470 L =1, 400
        IF(TB.EQ.0) THEN
          DA= RANNO(2, MDA, SDA)
          DA=ABS(DA)
        ELSE
          GO TO 460
        END IF
460      CONTINUE

C      Create array of MSL water surface elevations TEB(300) varying
hourly with
C      time

      LEW = L
      TB=TB+1

      TEB(L)=DA*SIN(2*PI*(LEW/DT))+
PHD)+LA*SIN(2*PI*(LEW/LT)+PHL)
      IF(TB.EQ.INT(DT)) TB=0
470      CONTINUE

```



```

DO 475 L=1,400
  IF(TEB(L).LT.(IBS + 1.0)) TEB(L) = (IBS + 1.0)
475  CONTINUE

C
C  DETERMINE TIDAL ELEVATIONS AT THE BRIDGE STATION
C    by convex routing or otherwise

      TER(1)=TAF*TEB(1)

      IF(CONROUT.EQ.0) THEN

        Do 478 L=2, 400
          TER(L)= TAF*TEB(L)
          IF(TER(L).GT.HIELE) HIELE = TER(L)

478    CONTINUE

      ELSE IF(CONROUT.NE.0) THEN

        Do 480 L=2, 400
          TER(L)= CX*TEB(L-1) + (1.0 - CX)*TER(L-1)
          IF(TER(L).GT.HIELE) HIELE = TER(L)

480    CONTINUE

      END IF

C    Compute array for base station depth YB(300) by subtracting
C    channel invert elev. at the base station (or adding the
C    absolute value of (IBS) the array of tidal elevations

      Do 485 L= 1, 400
        YB(L) = TEB(L) + ABS(IBS)
        IF(YB(L).GT.HIBASE) HIBASE = YB(L)

485    CONTINUE

      IF(DISCON.EQ.0) THEN

C
        Do 490 L = 1, ARR
          QN(L) = AS * ( (TER(L) - TER(L+1)))/(3600*DLT)

C      Modify the Neill's discharges with modification factors NMFR,
NMFF
C      developed by Brubaker and Demetrius.

          QNM(L)= NMFF*QN(L)
          IF (QN(L).LT.0) QNM(L)= NMFR*QN(L)

C
C      DETERMINE THE COMBINED TIDAL AND RIVERINE DISCHARGES BY
C      VECTOR ADDITION OF TIDAL AND RIVERINE DISCHARGES
C

          QT(L)= CHY24(L) + QNM(L)

          IF(QT(L).LE.0) THEN

```

```

        QTR(L) = ABS(QT(L))

        ELSE IF(QT(L).GT.0) THEN
            QTF(L) = ABS(QT(L))

            IF(ABS(QT(L)).GT.QTUMAX) QTUMAX = ABS(QT(L))

            IF((QTR(L)).GT.QTRMAX) QTRMAX = QTR(L)
            IF((QTF(L)).GT.QTFMAX) QTFMAX = QTF(L)

            IF((QTR(L)).GT.QTRMX) QTRMX = QTR(L)
            IF((QTF(L)).GT.QTFMX) QTFMX = QTF(L)

            IF((QTR(L)).GT.QTRMXS) QTRMXS = QTR(L)
            IF((QTF(L)).GT.QTFMXS) QTFMXS = QTF(L)

            SUMQTU = SUMQTU + ABS(QT(L))

            CONQTU = CONQTU + 1

        END IF

C      DETERMINE THE COMBINED DEPTH YT

        YAT(L) = TER(L) +ABS(IRS)
        IF(YAT(L).LE.MLT) YAT(L) = MLT
        IF(YAT(L).GE.HITIDE) HITIDE = YAT(L)

490      CONTINUE

        Do 495 L =1,ARR

            IF(QT(L).GT.0) QROUT(L) = QT(L)
            IF(QT(L).LE.0) QROUT(L)= 0

495      CONTINUE

        VOUT(1) = 3600*0.5*(QROUT(1))
        VITID(1)= 0.5*(YAT(1)-MLT)*AS
        VICAT(1)= 3600*(QBF)
        VITOT(1)= VICAT(1)+ VITID(1)

        Do 500 l=2, ARR
            VICAT(L)=0.5*(CHY24(L)+CHY24(L-1))*3600
            VITID(L)=(YAT(L) - YAT(L-1))*AS
            VITOT(L)=VICAT(L) + VITID(L)
            VOUT(L) =3600*0.5*(QROUT(L)+QROUT(L-1))
500      CONTINUE

        VBAL(1) = VITOT(1) - VOUT(1)
        IF(VBAL(1).LE.0) VBAL(1) = 0
        IF(VBAL(1).LE.0) YT(1)= MLT
        IF(VBAL(1).GT.0.AND.VBAL(1).LE.SESVOL(1))
YT(1)=
        MLT + YTAMLT(1)

```

```

      Do 510 L=2,ARR
      VBAL(L) =VITOT(L-1) + VITOT(L)-VOUT(L)

      IF (VBAL(L).LE.0) VBAL(L) = 0
      IF (VBAL(L).LE.0) YT(L) = MLT

      IF(VBAL(L).GT.0.AND.VBAL(L).LE.SESVOL(1)) YT(L)=
        MLT + YTAMLT(1)

      Do 505 M =2, 150

          IF(VBAL(L).GT.SESVOL(M-
1).AND.VBAL(L).LE.SESVOL(M))
              YT(L) = MLT + YTAMLT(M)
505          CONTINUE
510          CONTINUE

      Do 520 L=1,ARR
      IF(YT(L).LT.YAT(L)) YT(L) = YAT(L)
520      CONTINUE

*****
*****

      IF(YT(1).LT.YT(2)) YTR(1) = YT(1)
      IF(YT(1).GE.YT(2)) YTR(1) = MLT

      IF(YT(1).GE.YT(2)) YTF(1) = YT(1)
      IF(YT(1).LT.YT(2)) YTF(1) = MLT

      Do 530 L= 1,ARR

      IF(YT(L+1).GT.YT(L)) YTR(L+1) = YT(L+1)
      IF(YT(L+1).LE.YT(L)) YTR(L+1) = MLT

      IF(YT(L+1).LE.YT(L)) YTF(L+1) = YT(L+1)
      IF(YT(L+1).GT.YT(L)) YTF(L+1) = MLT

      IF(YT(L).GT.YTMAX) YTMAX = YT(L)
      SUMYT = SUMYT + YT(L)
      CONYT = CONYT + 1

C      Record annual maximum depth at bridge station

      IF(YT(L).GT.YTMX) YTMX = YT(L)

      IF(YTF(L).GT.YTFMX) YTFMX = YTF(L)
      IF(YTR(L).GT.YTRMX) YTRMX = YTR(L)

      IF(YTF(L).GT.YTFMAX) YTFMAX = YTF(L)
      IF(YTR(L).GT.YTRMAX) YTRMAX = YTR(L)

      IF(YTFMX.GT.YTFMXS) YTFMXS = YTFMX
      IF(YTRMX.GT.YTRMXS) YTRMXS = YTRMX

```

```

530             CONTINUE

                ELSE

                    Do 540 L= 1, 400

                        TERS(L)= TER(L)

                        LEW =L
                        TBR(L) = LEW + (LW/(1800*32.2*(YB(L) + MDR))**0.5)
540             CONTINUE

C      Sort array TBR(300) in ascending order also sort array  TER(300)
C      based on the order of array TBR(300).

                CALL SORT2(400,TBR, TERS)

C      Normalize the array TBR(300) by subtracting TBR(1) and adding
C      1.00 to
C      all elements in the array.  Also determine corresponding tidal
C      depths (YAT(L))

                Do 550 L=1, 400
                    TNR(L) = TBR(L) +1-TBR(1)

                    YAT(L) = TERS(L) + ABS(IRS)
                    IF(YAT(L).LT.MLT) YAT(L)=MLT
550             CONTINUE

C Determine the array of the interpolated tidal depths at the bridge
C location

                CALL INTERP(TNR, YAT, TNRI, YATI, 400, 300,400, 300)

C Determine the tidal discharges at the bridge location using the
C Neill's Equation
C QN(NR18) represents an array of computed Neill's discharges with
C negative
C and positive values. The negative values represents the discharges
C produced by the rising tide directed up the estuary. While the
C positive values
C represents the discharges directed downstream. In the algorithm QNR
C represents
C Neill's discharges due to the rising limb and QNF represents
C Neill's
C discharges due to the falling limb.

                Do 560 L= 1, (ARR+1)
                    TERI(L) = YATI(L)+IRS
560             CONTINUE

C

```

```

Do 570 L = 1, ARR
    QN(L) = AS * ( (TERI(L) - TERI(L+1)))/(3600*DLT)

C    Modify the Neill's discharges with modification factors NMFR,
NMFF
C    developed by Brubaker and Demetrius.

    QNM(L)= NMFF*QN(L)
    IF (QN(L).LT.0) QNM(L)= NMFR*QN(L)

C    DETERMINE THE COMBINED TIDAL AND RIVERINE DISCHARGES BY
C    VECTOR ADDITION OF TIDAL AND RIVERINE DISCHARGES
C

    QT(L)= CHY24(L) + QNM(L)

    IF(QT(L).LE.0) THEN
        QTR(L) = ABS(QT(L))

        ELSE IF(QT(L).GT.0) THEN
            QTF(L) = ABS(QT(L))

            IF(ABS(QT(L)).GT.QTUMAX) QTUMAX = ABS(QT(L))

            IF((QTR(L)).GT.QTRMAX) QTRMAX = QTR(L)
            IF((QTF(L)).GT.QTFMAX) QTFMAX = QTF(L)

            IF((QTR(L)).GT.QTRMX) QTRMX = QTR(L)
            IF((QTF(L)).GT.QTFMX) QTFMX = QTF(L)

            IF((QTR(L)).GT.QTRMXS) QTRMXS = QTR(L)
            IF((QTF(L)).GT.QTFMXS) QTFMXS = QTF(L)

            SUMQTU = SUMQTU + ABS(QT(L))

            CONQTU = CONQTU + 1

        END IF

        IF(YATI(L).GE.HITIDE) HITIDE = YATI(L)

570    CONTINUE

C
C    DETERMINE THE COMBINED DEPTH YT
C

    Do 595 L =1,ARR

        IF(QT(L).GT.0) QROUT(L) = QT(L)
        IF(QT(L).LE.0) QROUT(L)= 0

595    CONTINUE

    VOUT(1) = 3600*0.5*(QROUT(1))
    VITID(1)= 0.5*(YATI(1)-MLT)*AS
    VICAT(1)= 3600*(QBF)
    VITOT(1)= VICAT(1)+ VITID(1)

    Do 600 l=2, ARR

```

```

        VICAT(L)=0.5*(CHY24(L)+CHY24(L-1))*3600
VITID(L)=(YATI(L) - YATI(L-1))*AS
        VITOT(L)=VICAT(L) + VITID(L)
VOUT(L) =3600*0.5*(QROUT(L)+QROUT(L-1))
600      CONTINUE

        VBAL(1) = VITOT(1) - VOUT(1)
        IF(VBAL(1).LE.0) VBAL(1) = 0
            IF(VBAL(1).LE.0) YT(1)= MLT
            IF(VBAL(1).GT.0.AND.VBAL(1).LE.SESVOL(1))
YT(1)=
        MLT + YTAMLT(1)

        Do 610 L=2,ARR
            VBAL(L) =VITOT(L-1) + VITOT(L)-VOUT(L)
            IF (VBAL(L).LE.0) VBAL(L) = 0
            IF (VBAL(L).LE.0) YT(L) = MLT

            IF(VBAL(L).GT.0.AND.VBAL(L).LE.SESVOL(1)) YT(L)=
        MLT + YTAMLT(1)

        Do 605 M =2, 150

            IF(VBAL(L).GT.SESVOL(M-
1).AND.VBAL(L).LE.SESVOL(M))
        MLT + YTAMLT(M)
605      CONTINUE
610      CONTINUE

        Do 615 L=1,ARR
            IF(YT(L).LT.YATI(L)) YT(L) = YATI(L)
615      CONTINUE

*****
*****

        IF(YT(1).LT.YT(2)) YTR(1) = YT(1)
        IF(YT(1).GE.YT(2)) YTR(1) = MLT

        IF(YT(1).GE.YT(2)) YTF(1) = YT(1)
        IF(YT(1).LT.YT(2)) YTF(1) = MLT

        Do 620 L= 1,ARR

            IF(YT(L+1).GT.YT(L)) YTR(L+1) = YT(L+1)
            IF(YT(L+1).LE.YT(L)) YTR(L+1) = MLT

            IF(YT(L+1).LE.YT(L)) YTF(L+1) = YT(L+1)
            IF(YT(L+1).GT.YT(L)) YTF(L+1) = MLT

        IF(YT(L).GT.YTMAX) YTMAX = YT(L)
        SUMYT = SUMYT + YT(L)
        CONYT = CONYT + 1

```

```

C      Record annual maximum depth at bridge station
      IF(YT(L).GT.YTMX) YTMX = YT(L)

      IF(YTF(L).GT.YTFMX) YTFMX = YTF(L)
      IF(YTR(L).GT.YTRMX) YTRMX = YTR(L)

      IF(YTF(L).GT.YTFMAX) YTFMAX = YTF(L)
      IF(YTR(L).GT.YTRMAX) YTRMAX = YTR(L)

      IF(YTFMX.GT.YTFMXS) YTFMXS = YTFMX
      IF(YTRMX.GT.YTRMXS) YTRMXS = YTRMX
620      CONTINUE

      END IF

C
C DETERMINE COMBINED VELOCITY AT BRIDGE STATION
C
      DO 630 L =1,ARR

      IF(YT(L).LE.MLT) VNT(L) = QT(L)/XABMLE

      IF(YT(L).LE.MLT) XATOT(L) = XABMLE

      IF(YT(L).GT.MLT.AND.YT(L).LE.(MLT+YTAMLT(1)))
      VNT(L) = QT(L)/(XABMLE+SXAMLT(1)-VFACT*UESTZ*(YT(L)-
MLT)**2)

      IF(YT(L).GT.MLT.AND.YT(L).LE.(MLT+YTAMLT(1)))
      XATOT(L)=(XABMLE + SXAMLT(1)-VFACT*UESTZ*(YT(L)-MLT)**2)

      DO 625 M= 2, 150
      IF(YT(L).GT.(MLT+YTAMLT(M-1)).AND.YT(L).LE.(MLT+YTAMLT(M)))
      VNT(L)=QT(L)/(XABMLE+ SXAMLT(M)-VFACT*UESTZ*(YT(L)-
MLT)**2)

      IF(YT(L).GT.(MLT+YTAMLT(M-1)).AND.YT(L).LE.(MLT+YTAMLT(M)))
      XATOT(L) =(XABMLE+SXAMLT(M)-VFACT*UESTZ*(YT(L)-MLT)**2)

625      CONTINUE
630      CONTINUE

*****
*****
*****
*****

C      INITIALIZE SOIL SCOUR VARIABLES FOR EACH STORM
C      INITIALIZE CSU, AND CSD

      DO 632 L=1, ARR
      CSD(L) =TSD - SUMYSD

```

```

        IF (SUMYSD.GT.TSD) CSD(L) = 0

        CSU(L) = TSU - SUMYSU
        IF (SUMYSU.GT.TSU) CSU(L) = 0

        YTFF(L) = YTF(L) + SUMYSU

        YTRF(L) = YTR(L) + SUMYSD
632  CONTINUE

        Do 635 L =1,30

            DPTHU =TSU
            IF(DPTHU.GE.DPTH(L).AND. DPTHU.LE.DPTH(L+1)) THEN
                ALPHAU = ALPHA(L)
                D16U   = D16(L)
                D50U   = D50(L)
                D84U   = D84(L)
                DMAXU  = DMAX(L)
                VCUF   = 0.476*(D50U/PD)**0.053
                SIGMAU = (D84U/D16U)**0.5
                PHU    = PH(L)
            END IF

            DPTHU = TSD
            IF(DPTHU.GE.DPTH(L).AND. DPTHU.LE.DPTH(L+1)) THEN
                ALPHAD = ALPHA(L)
                D16D   = D16(L)
                D50D   = D50(L)
                D84D   = D84(L)
                DMAXD  = DMAX(L)
                VCDF   = 0.476*(D50D/PD)**0.053
                SIGMAD = (D84D/D16D)**0.5
                PHDD   = PH(L)
            END IF

            DPTHCU = SUMYSU
            IF(DPTHCU.GE.DPTH(L).AND. DPTHCU.LE.DPTH(L+1)) THEN

                D16CU   = D16(L)
                D50CU   = D50(L)
                D84CU   = D84(L)
                SIGMCU  = (D84CU/D16CU)**0.5

            END IF

            DPTHCD = SUMYSD
            IF(DPTHCD.GE.DPTH(L).AND. DPTHCD.LE.DPTH(L+1)) THEN

                D16CD   = D16(L)
                D50CD   = D50(L)
                D84CD   = D84(L)
                SIGMCD  = (D84CD/D16CD)**0.5

            END IF

```



```

635      CONTINUE

C          DETERMINE FLOW VELOCITY DOWNFLOW,VORTEX VELOCITY VECTORS, AND
SCOUR FOR EACH HOUR OF STORM
C
C          The required inputs are the net edutary velocity (VNU,VND),
C          the total flow depth (YT), the bridge pier diameter (PD),
C          the existing scour depth at the beginning of the process (TSU,
TSD),
C          the soils property at the invert of the estuary channel
C          ( D50, PH,) as a function of local scour depth (TSU, TCD)

C          Determine ratio of scour to bridge diameter along the upstream
C          and downstream face of the pier

C          Set up downflow, Tangential velocity and scour algorithms
C          The process involves the computation of the total local scour
C          depth over each storm event and summing over the full simulation.
C          The contraction scour will then be computed for each storm but
will
C          be based successively on the highest value of YT in YRS and added
to the
C          total scour at the upstream and downstream faces of the pier.

      Do 690 L=1,ARR
        VNUIN(L) = 0
        IF(VNT(L).LT.0) VNUIN(L) =  ABS(VNT(L))

        VNU(1) = 0.5*VNUIN(1)
        Do 686 M=2, ARR
          VNU(M) = 0.5*(VNUIN(M)+ VNUIN(M-1))
686      CONTINUE

        IF(VNU(L).LE.0) VNU(L)= 0
        IF(VNU(L).GT.0) THEN
          IF(VNU(L).GT.VNUMAX) VNUMAX = VNU(L)
          SUMVNU = SUMVNU + VNU(L)
          CONVNU = CONVNU + 1
        END IF

C Place maximum storm velocity in annual holding location VUPM

        IF(VNU(L).GT.VUPM) VUPM = VNU(L)
        IF(VUPM.GT.VUPMS) VUPMS = VUPM
*****
*****

C          Compute incremental contraction scour over time DLT          and
adjust flow depth to include the
C          lowering of the bed

      IF(CONTRA.EQ.1) THEN

```

```

C      Compute contraction scour using Straub's eqn

C       $q_s = (g \cdot (S_s - 1) \cdot d_{50}^3)^{0.5} \cdot ((T/T_c) - 1)^2$  English units,
d50 in feet

C      Converting the equations so that D50 is in mm and solving for
scour depth
C      gives

C       $Y_S = (0.67/PD) \cdot DLT \cdot d_{50}^{1.5} \cdot [(T/T_c) - 1]^2$ 

C       $T = 28.11 \cdot (Q/WB)^{0.5} \cdot [n^2/YTFF^{2.33}]$ 

C      If D50mm < 0.065 then
C           $T_c = 4.84 \cdot D50_{mm}$ 
C      Else
C           $T_c = 0.8 d_{50}^{0.67} \cdot Y^{0.33}$ 

      IF ( D50CD.LT.0.065) THEN
      TAUCD(L) = 4.84*D50CD
      ELSE
      TAUCD(L) = 0.84*D50CD**0.67*YTRF(L)**0.33
      END IF

      TAUDD(L) = 28.11*(QTR(L)/WB)**2*(MAN**2/YTRF(L)**2.33)

      YSD(L) = 0
      IF ((TAUDD(L)/TAUCD(L)).GT.1) YSD(L) = COFDS*(0.67/PD)
      *DLT*D50CD**1.5*((TAUDD(L)/TAUCD(L))-1)**1.5

      ELSE IF (CONTRA.EQ.2) THEN

      YSDIN=YTR(L)*(1.45*(VNU(L)/(32.2*YTR(L))**0.5)**0.2
      *COFDF*(1/SIGMCD**0.2)-1)

      IF(YSDIN.LE.0) YSDIN = 0

      YSD(L) = 0
      IF(YSDIN.GT.YDINMX) YSD(L) = YSDIN - YDINMX

      IF(YSDIN.GT.YDINMX) YDINMX = YSDIN

      ELSE

      YSDIN = 0
      IF(COFD.GT.1) YSDIN = YTR(L)*(COFD - 1)

      YSD(L) = 0
      IF(YSDIN.GT.YDINMX) YSD(L) = YSDIN - YDINMX

      IF(YSDIN.GT.YDINMX) YDINMX = YSDIN

      END IF

      SUMYSD= SUMYSD + YSD(L)

```

```

YTRF(L) = YTR(L) + SUMYSD

XADJAD(L) = 0.5*(TWBMLT(4)+TWBMLT(3))*SUMYSD

VNUA(L) = VNU(L)*XATOT(L)/(XATOT(L) + XADJAD(L))
IF(VNUA(L).GT.VNUPAM) VNUPAM = VNUA(L)

C      Recompute flowdepth and velocity, and computed local scour dept
to adjust
C      for contraction
C      scour

      CSD(L) = CSD(L) - YSD(L)
      IF (YSD(L).GT.CSD(L)) CSD(L) = 0
      IF(CSD(L)+SUMYSD.LT.TSD) CSD(L) = TSD - SUMYSD

      LEW =L
      T(L)=LEW*DLT

      DSD(L) = CSD(L)/PD
C      Compute the scour angles along the downstream(THD) pier face

      THD(L) = PHDD
      IF (31*DSD(L)**2.LT.PHDD) THD(L) =31*DSD(L)**2

*****
*****
C      Compute downflow velocity on downstream faces of the pier

      IF(DSD(L).GT.100) THEN
        VDD(L) = 0

      ELSE IF (DSD(L).LE.2.3.AND.YTRF(L).GT.MLT) THEN
        VDD(L) = VNUA(L)* (0.15*(DSD(L))
          + 0.24* PD **0.18/(YTRF(L)**0.18 * C1**0.5))

      ELSE IF (DSD(L).GT.2.3) THEN
        VDD(L) = VNUA(L)*(0.40/EXP(1+(3*(DSD(L)-4)) + 0.4))

      END IF

      IF(VDD(L).GT.0.8*VNUA(L)) VDD(L) = 0.8*VNUA(L)

C      Compute the maximum tangential velocities along the upstream(VMU)
and downstream
C      (VMD) pier faces

      VMD(L) = 2.7* VDD(L)
      IF(31*DSD(L)**2.LE.PHDD) VMD(L) = 2.24*C1**0.5*VDD(L)

C      Compute the A factors and tangential velocities (VTU)
C      along the upstream and downstream (VTD) pier faces

```

```

AFD(L)=-0.0002*THD(L)**2+0.012*THD(L)+0.80

VTD(L)=0
IF (AFD(L).GT.0) VTD(L)=1.4*AFD(L)*VMD(L)*
~ (1-EXP(-1.25*(1/AFD(L)**2)))

*****
*****
C      SELECT CRITICAL VELOCITY MERHOD

UID(L)=0

IF (YTRF(L).GT.0.AND.VINCIP.EQ.1) UID(L)=
~ VCDF*(1.66*D50D**0.333*YTRF(L)**0.167)

IF (YTRF(L).GT.0.AND.VINCIP.EQ.2) UID(L)= VCDF*0.09*
~ (D50D*Tan(PHDD*RADCON)* YTRF(L)**0.33/(ALPHAD*MAN**2))**0.5

IF (YTRF(L).GT.0.AND.VINCIP.EQ.3) UID(L)= VCDF*(0.024/MAN)*
~ (D50D**0.5)*(YTRF(L)**0.167)

*****
*****
C      Compute armouring velocity

VARMD(L)=0
IF (ARMVEL.GT.0.AND.SIGMAD.GT.1.3) VARMD(L)=1.328*(DMAXD/1.8)**
~ 0.333*YTRF(L)**0.167

IF (VARMD(L).LE.0) THEN
    VCRIND(L) = UID(L)

ELSE IF (VTD(L).LE.VARMD(L).AND.VARMD(L).GT.0) THEN

    VCRIND(L) = VARMD(L)-(UID(L)/VCDF)

ELSE IF (VTD(L).GT.VARMD(L).AND.VARMD(L).GT.0) THEN

    VCRIND(L) = VARMD(L)

END IF

IF (VCRIND(L).LT.UID(L)) VCRIND(L)= UID(L)

*****
*****

DED(L) =0
IF (VTD(L).GT.VCRIND(L)) DED(L)=(PD**BNDX)*TANH(YTRF(L)/PD)
~ *((VTD(L)-VCRIND(L))**INDX)*(VNUA(L)/(32.2*PD)**0.5)**FREX

```

```

      TED(L)=0
      IF(VCRIND(L).GT.0.0.AND.(VTD(L)/UID(L)).GT.VCDF) THEN

      TED(L) = 24*30.89*(PD/VTD(L))*((VTD(L)/VCRIND(L))-0.4)*
      (YTRF(L)/PD)**0.25

      ELSE IF(YTRF(L)-6.0*PD.GT.0.AND.((VTD(L)/VCRIND(L))
      -VCDF).GT.0.0) THEN

      TED(L)= 24*48.26*(PD/VTD(L))*((VTD(L)/VCRIND(L))-0.4)
      END IF

*****
*****

      K1D(L)=0
      IF(TED(L).GT.0.001.AND.VTD(L).GT.0.03) K1D(L)= EXP(-0.08*
      (ABS((VCRIND(L)/VTD(L))*LOG(DLT/TED(L))))**1.2)

      K2D(L)=0
      IF(TED(L).GT.0.001) K2D(L)=(ABS(LOG(DLT/TED(L))))**0.2

      K3D(L)=0
      IF(VTD(L).GT.0.03) K3D(L) = 0.1*(DED(L)/DLT)
      *(VCRIND(L)/VTD(L))**1.2

      RLD(L)= K1D(L)* K2D(L)* K3D(L)

      CSD(L+1) = CSD(L) + (RLD(L)*DLT)
      IF(CSD(L+1).LT.CSD(L)) CSD(L+1) =CSD(L)

*****
*****
C Repeat process for upstream pier face
*****
*****

      VNDIN(L) =0
      IF(VNT(L).GT.0) VNDIN(L) = ABS(VNT(L))

      VND(1) = 0.5*VNDIN(1)
      Do 688 M=2, ARR
      VND(M) = 0.5*(VNDIN(M)+ VNDIN(M-1))
688 CONTINUE

      IF(VND(L).LE.0) VND(L)= 0
      IF(VND(L).GT.0) THEN
      IF(VND(L).GT.VNDMAX) VNDMAX = VND(L)
      SUMVND = SUMVND + VND(L)
      CONVND = CONVND + 1
      END IF

C Place maximum storm velocity in annual holding location VDWNM

      IF(VND(L).GT.VDWNM) VDWNM = VND(L)

```

```

      IF(VDWNM.GT.VDWNMS) VDWNMS = VDWNM

*****
*****

C      Compute incremental contraction scour over time DLT and adjust
flow
C      depth to include the
C      lowering of the bed

      IF(CONTRA.EQ.1) THEN

C      Compute contraction scour using Straub's eqn

C       $qs = (g \cdot (Ss-1) \cdot d50^{*3})^{*0.5} \cdot ((T/Tc) - 1)^{*2}$  English units,
d50 in
C      feet

C      Converting the equations so that D50 is in mm and solving for
scour depth
C      gives

C       $YS = (0.67/PD) \cdot DLT \cdot d50mm^{*1.5} \cdot ((T/Tc)-1)^{*2}$ 
C       $T = 28.11 \cdot (Q/WB)^{*2} \cdot [n^{*2}/YTFF^{*2.33}]$ 

C      If D50mm < 0.065 then
C       $Tc = 4.84 \cdot D50mm$ 
C      Else
C       $Tc = 0.8d50^{*.67} \cdot Y^{*.33}$ 

      IF ( D50CU.LT.0.065) THEN
        TAUCU(L) = 4.84*D50CU
      ELSE
        TAUCU(L) = 0.84*D50CU**0.67*YTFF(L)**0.33
      END IF

      TAUDU(L) = 28.11*(QTF(L)/WB)**2*(MAN**2/YTFF(L)**2.33)

      YSU(L) = 0
      IF((TAUDU(L)/TAUCU(L)).GT.1) YSU(L) = COFUS*(0.67/PD)*
      DLT*D50CU**1.5*((TAUDU(L)/TAUCU(L))-1)**1.5

    ELSE IF (CONTRA.EQ.2) THEN

      YSUIN =YTFF(L)*(1.45*(VND(L)/(32.2*YTFF(L))**0.5)**0.2
      *COFUF*(1/SIGMCU**0.2)-1)

      IF(YSUIN.LE.0) YSUIN = 0

      YSU(L) = 0
      IF(YSUIN.GT.YUINMX) YSU(L) = YSUIN - YUINMX

      IF(YSUIN.GT.YUINMX) YUINMX = YSUIN

    ELSE

```

```

        YSUIN = 0
        IF(COFU.GT.1) YSUIN = YTF(L)*(COFU - 1)

        YSU(L) = 0
        IF(YSUIN.GT.YUINMX) YSU(L) = YSUIN - YUINMX

        IF(YSUIN.GT.YUINMX) YUINMX = YSUIN

END IF

SUMYSU= SUMYSU + YSU(L)

YTFF(L) = YTF(L) + SUMYSU

XADJAU(L) = 0.5*(TWBMLT(4)+TWBMLT(3))*SUMYSU

VNDA(L) = VND(L)*XATOT(L)/(XATOT(L) + XADJAU(L))
IF(VNDA(L).GT.VNDNAM) VNDNAM = VNDA(L)

C      Recompute flowdepth and velocity, and computed local scour dept
to adjust
C      for contraction
C      scour

        CSU(L) = CSU(L) - YSU(L)
        IF (YSU(L).GT.CSU(L)) CSU(L) = 0
        IF(CSU(L)+SUMYSU.LT.TSU) CSU(L) = TSU - SUMYSU

        LEW =L
        T(L)=LEW*DLT

        DSU(L) = CSU(L)/PD

C      Compute the scour angles along the upstream(THU) pier face

        THU(L) = PHU
        IF (31*DSU(L)**2.LT.PHU) THU(L) = 31*DSU(L)**2

C      Compute downflow velocity on upstream face of the pier

        IF(DSU(L).GT.100) THEN
            VDU(L) = 0

            ELSE IF (DSU(L).LE.2.3.AND.YTFF(L).GT.MLT) THEN
                VDU(L)= VNDA(L)*(0.15 * (DSU(L))
                + 0.24*PD ** 0.18/(YTFF(L)**0.18* C1**0.5))

            ELSE IF (DSU(L).GT.2.3) THEN
                VDU(L) = VNDA(L)*(0.40/(1+EXP(3*(DSU(L)-4)) + 0.4))

        END IF

```

```

      IF(VDU(L).GT.0.8*VNDA(L)) VDU(L) = 0.8*VNDA(L)

*****
*****
C
C
      VMU(L) = 2.7* VDU(L)
      IF(31*DSU(L)**2.LE.PHU) VMU(L) = 2.24*C1**0.5*VDU(L)

      AFU(L) = -0.0002*THU(L)**2+0.012*THU(L)+0.80

      VTU(L)=0
      IF(AFU(L).GT.0) VTU(L)=1.4*AFU(L)*VMU(L)*
      (1-EXP(-1.25*(1/AFU(L)**2)))

*****
*****

      UIU(L)=0

      IF(YTFF(L).GT.0.AND.VINCIP.EQ.1) UIU(L)=
      VCUF*(1.66*D50U**0.333*YTFF(L)**0.167)

      IF(YTFF(L).GT.0.AND.VINCIP.EQ.2) UIU(L)= VCUF*0.09*
      (D50U*Tan(PHU*RADCON)* YTFF(L)**0.33/(ALPHAU*MAN**2))**0.5

      IF(YTFF(L).GT.0.AND.VINCIP.EQ.3) UIU(L)= VCUF*(0.024/MAN)*
      (D50U**0.5)*(YTFF(L)**0.167)

*****
*****

C      Compute armouring velocity

      VARMU(L)=0
      IF(ARMVEL.GT.0.AND.SIGMAU.GT.1.3) VARMU(L)=1.328*(DMAXU/1.8)**
      0.333*YTFF(L)**0.167

      IF(VARMU(L).LE.0) THEN
        VCRINU(L) = UIU(L)

      ELSE IF(VTU(L).LE.VARMU(L).AND.VARMU(L).GT.0) THEN

        VCRINU(L) = VARMU(L)-(UIU(L)/VCUF)

      ELSE IF (VTU(L).GT.VARMU(L).AND.VARMU(L).GT.0) THEN

        VCRINU(L) = VARMU(L)

      END IF

      IF(VCRINU(L).LT.UIU(L)) VCRINU(L)= UIU(L)

```



```
*****
*****
```

```
      DEU(L) =0
      IF(VTU(L).GT.VCRINU(L)) DEU(L)=(PD**BNDX)*TANH(YTFF(L)/PD)
      *((VTU(L)-VCRINU(L))**INDX)*(VNDA(L)/(32.2*PD)**0.5)**FREX

      TEU(L)=0
      IF(VCRINU(L).GT.0.0.AND.(VTU(L)/UIU(L)).GT.VCUF) THEN

      TEU(L) = 24*30.89*(PD/VTU(L))*((VTU(L)/VCRINU(L))- 0.4)*
      (YTFF(L)/PD)**0.25

      ELSE IF(YTFF(L)-6.0*PD.GT.0.AND.((VTU(L)/VCRINU(L))
      -VCUF).GT.0.0) THEN

      TEU(L)= 24*48.26*(PD/VTU(L))*((VTU(L)/VCRINU(L))-0.4)
      END IF
```

```
*****
*****
```

```
      K1U(L)=0
      IF(TEU(L).GT.0.001.AND.VTU(L).GT.0.03) K1U(L)= EXP(-0.08
      *(ABS((VCRINU(L)/VTU(L))*LOG(DLT/TEU(L))))**1.2)

      K2U(L)=0
      IF(TEU(L).GT.0.001) K2U(L)= (ABS(LOG(DLT/TEU(L))))**0.2

      K3U(L)=0
      IF(VTU(L).GT.0.03) K3U(L) = 0.1*(DEU(L)/DLT)
      *(ABS(VCRINU(L)/VTU(L)))*1.2
```

```
*****
*****
```

```
      RLU(L)= K1U(L)* K2U(L)* K3U(L)

      CSU(L+1) = CSU(L) + (RLU(L)*DLT)
      IF(CSU(L+1).LT.CSU(L)) CSU(L+1) = CSU(L)

      IF(YTRF(L).GT.YTMRFF) YTMRFF= YTRF(L)
      IF(YTFF(L).GT.YTMFF) YTMFF= YTFF(L)

      IF(VTD(L).GT.VTDMX) VTDMX= VTD(L)
      IF(VTU(L).GT.VTUMX) VTUMX= VTU(L)

      IF(VTD(L).GT.VTDMX) VTDMX= VTD(L)
      IF(VTU(L).GT.VTUMX) VTUMX= VTU(L)

      IF(UIU(L).LT.UIUMIN) UIUMIN= UIU(L)
      IF(UID(L).LT.UIDMIN) UIDMIN= UID(L)
```

```
690 CONTINUE
```

```
*****
*****
```

```
TSD=CSD(ARR) + SUMYSD
```

```
C Compute Contraction scour and sum to local scour to obtain total
scour for
C downstream face for each storm
```

```
TSU=CSU(ARR) + SUMYSU
```

```
*****
*****
```

```
700 CONTINUE
```

```
*****
*****
```

```
C*****
*****
```

```
C REPEAT PROCESS FOR THE SCOUR SIMULATION FROM ALL 36 HR STORMS IN
EACH
```

```
C YEAR
```

```
C*****
*****
```

```
Do 1000 K = 1, N36
```

```
C Initialize Scour parameters for each Storm
```

```
C
```

```
C Initialize UVAR
```

```
UVA=0
```

```
UVAR36 = 1
```

```
Do 710 L = 1, INT(C36)
```

```
C Generate uniform variate UVR from RANNO
```

```
UVA=RANNO(1,0.0, 1.0)
```

```
UVAR36 = UVAR36*UVA
```

```
710 CONTINUE
```

```
PPT36 = -B36*LOG(UVAR36)
```

```
IF(PPT36.GT.PPTMAX) PPTMAX =PPT36
```

```
SUM36 = SUM36 + PPT36
```

```
TDRO = 0
```

```
IF( PPT36.GT.IA) TDRO = (PPT36 - IA) ** 2/(PPT36 + AI)
```

```
IF(TDRO.LE.0.0) NORUN = NORUN + 1
```

```
C Determine catchment hydrograph
```

C Convert rainfall from dimensionless cumulative hyetograph to a cumulative depth hyetograph

```

      Do 720 L = 1, NP36
        P36(L) = S36(L) * PPT36
720    CONTINUE

      Do 730 L = 1, NP36
        SP = P36(L)
        PE36(L) = 0.0
        IF(SP.GT.IA) PE36(L) = (SP - IA) ** 2 / (SP + IA)
730    CONTINUE

      PEI36(1) = PE36(1)

      Do 740 L = 2, NP36
        PEI36(L) = P36(L) - P36(L -1)
740    CONTINUE

```

C Convolve unit hydrographs convolve sub routine

```
CALL CONVOL(QU, PEI36, DRO36, NU, NP36, NR36, 36, 36, 300)
```

C Add base flow to direct runoff hydrograph. Final output is CHY(NR), NR

```

      Do 750 L = 1, ARR
        CHY36(L) = DRO36(L) + QBF
        IF (CHY36(L).GT.QP36MX) QP36MX = CHY36(L)
750    CONTINUE

```

C SYNTHESIZE TIDAL SERIES AT BASE STATION B.

```

      PHD = RANNO(1, 0.0, 6.284)
      PHL = RANNO(1, 0.0, 6.284)

      LA= RANNO( 2, MLA, SLA)
      LA=ABS(LA)

      TB = 0
      DO 770 L =1, 400
        IF(TB.EQ.0) THEN
          DA= RANNO(2, MDA, SDA)
          DA=ABS(DA)
        ELSE
          GO TO 760
        END IF
770    CONTINUE

```

C Create array of MSL water surface elevations TEB(300) varying hourly with

```

C time
      LEW = L

```

```

        TB=TB+1

        TEB(L) = DA*SIN(2*PI*(LEW/DT)+ PHD)+LA*SIN(2*PI*(LEW/LT)+PHL)
        IF(TB.EQ.INT(DT)) TB=0
770  CONTINUE

        DO 775 L=1,400
        IF(TEB(L).LT.(IBS + 1.0)) TEB(L) = (IBS +1.0)
775  CONTINUE

C   DETERMINE TIDAL ELEVATIONS AT THE BRIDGE STATION
C   by convex routing or otherwise

        TER(1)=TAF*TEB(1)

        IF(CONROUT.EQ.0) THEN

            DO 778 L=2, 400
            TER(L)= TAF*TEB(L)
            IF(TER(L).GT.HIELE) HIELE = TER(L)

778    CONTINUE

        ELSE IF(CONROUT.NE.0) THEN

            DO 780 L=2, 400
            TER(L)= CX*TEB(L-1) + (1.0 - CX)*TER(L-1)
            IF(TER(L).GT.HIELE) HIELE = TER(L)

780    CONTINUE

        END IF

        DO 785 L= 1, 400
        YB(L) = TEB(L) + ABS(IBS)
        IF(YB(L).GT.HIBASE) HIBASE = YB(L)

785    CONTINUE

        IF(DISCON.EQ.0) THEN
C
            DO 790 L = 1, ARR
            QN(L) = AS * ( (TER(L) - TER(L+1)))/(3600*DLT)

C   Modify the Neill's discharges with modification factors NMFR,
NMFF
C   developed by Brubaker and Demetrius.

            QNM(L)= NMFF*QN(L)
            IF (QN(L).LT.0) QNM(L)= NMFR*QN(L)

```

```

C      DETERMINE THE COMBINED TIDAL AND RIVERINE DISCHARGES BY
C      VECTOR ADDITION OF TIDAL AND RIVERINE DISCHARGES
C
      QT(L)= CHY36(L) + QNM(L)

      IF(QT(L).LE.0) THEN
        QTR(L) = ABS(QT(L))

      ELSE IF(QT(L).GT.0) THEN
        QTF(L) = ABS(QT(L))

      IF(ABS(QT(L)).GT.QTUMAX) QTUMAX = ABS(QT(L))

      IF((QTR(L)).GT.QTRMAX) QTRMAX = QTR(L)
      IF((QTF(L)).GT.QTFMAX) QTFMAX = QTF(L)

      IF((QTR(L)).GT.QTRMX) QTRMX = QTR(L)
      IF((QTF(L)).GT.QTFMX) QTFMX = QTF(L)

      IF((QTR(L)).GT.QTRMXS) QTRMXS = QTR(L)
      IF((QTF(L)).GT.QTFMXS) QTFMXS = QTF(L)

      SUMQTU = SUMQTU + ABS(QT(L))

      CONQTU = CONQTU + 1

      END IF

C      DETERMINE THE COMBINED DEPTH YT
C

      YAT(L) = TER(L) +ABS(IRS)
      IF(YAT(L).LT.MLT) YAT(L) = MLT
      IF(YAT(L).GE.HITIDE) HITIDE = YAT(L)

790      CONTINUE

      Do 795 L =1,ARR

      IF(QT(L).GT.0) QROUT(L) = QT(L)
      IF(QT(L).LE.0) QROUT(L)= 0

795      CONTINUE

      VOUT(1) = 3600*0.5*(QROUT(1))
      VITID(1)= 0.5*(YAT(1)-MLT)*AS
      VICAT(1)= 3600*(QBF)
      VITOT(1)= VICAT(1)+ VITID(1)

      Do 800 l=2, ARR
        VICAT(L)=0.5*(CHY36(L)+CHY36(L-1))*3600
        VITID(L)=(YAT(L) - YAT(L-1))*AS
        VITOT(L)=VICAT(L) + VITID(L)
        VOUT(L) =3600*0.5*(QROUT(L)+QROUT(L-1))

```

```

800          CONTINUE

          VBAL(1) = VITOT(1) - VOUT(1)
          IF(VBAL(1).LE.0) VBAL(1) = 0
            IF(VBAL(1).LE.0) YT(1)= MLT
              IF(VBAL(1).GT.0.AND.VBAL(1).LE.SESVOL(1))
YT(1)=
                MLT + YTAMLT(1)

                Do 810 L=2,ARR
                  VBAL(L) =VITOT(L-1) + VITOT(L)-VOUT(L)

                  IF (VBAL(L).LE.0) VBAL(L) = 0
                  IF (VBAL(L).LE.0) YT(L) = MLT

                  IF(VBAL(L).GT.0.AND.VBAL(L).LE.SESVOL(1)) YT(L)=
                    MLT + YTAMLT(1)

                Do 805 M =2, 150

                    IF(VBAL(L).GT.SESVOL(M-
1).AND.VBAL(L).LE.SESVOL(M))
                    YT(L) = MLT + YTAMLT(M)
805          CONTINUE
810          CONTINUE

                Do 820 L=1,ARR
                  IF(YT(L).LT.YAT(L)) YT(L) = YAT(L)
820          CONTINUE

*****
*****

          IF(YT(1).LT.YT(2)) YTR(1) = YT(1)
          IF(YT(1).GE.YT(2)) YTR(1) = MLT

          IF(YT(1).GE.YT(2)) YTF(1) = YT(1)
          IF(YT(1).LT.YT(2)) YTF(1) = MLT

          Do 830 L= 1,ARR

              IF(YT(L+1).GT.YT(L)) YTR(L+1) = YT(L+1)
              IF(YT(L+1).LE.YT(L)) YTR(L+1) = MLT

              IF(YT(L+1).LE.YT(L)) YTF(L+1) = YT(L+1)
              IF(YT(L+1).GT.YT(L)) YTF(L+1) = MLT

              SUMYT = SUMYT + YT(L)
              CONYT = CONYT + 1

              IF(YT(L).GT.YTMAX) YTMAX = YT(L)

C          Record annual maximum depth at bridge station
          IF(YT(L).GT.YTMX) YTMX = YT(L)

```

```

      IF(YTF(L).GT.YTFMX) YTFMX = YTF(L)
      IF(YTR(L).GT.YTRMX) YTRMX = YTR(L)

      IF(YTF(L).GT.YTFMAX) YTFMAX = YTF(L)
      IF(YTR(L).GT.YTRMAX) YTRMAX = YTR(L)

      IF(YTFMX.GT.YTFMXS) YTFMXS = YTFMX
      IF(YTRMX.GT.YTRMXS) YTRMXS = YTRMX

830          CONTINUE
      ELSE

      Do 835 L= 1, 400

      TERS(L)=TER(L)

      LEW=L
      TBR(L) = LEW + (LW/(1800*32.2*(YB(L) + MDR))**0.5)
835          CONTINUE

C      Sort array TBR(150) in ascending order also sort array TER(150)
C      based on the order of array TBR(150).

      CALL SORT2(400,TBR, TERS)

C      Normalize the array TBR(300) by subtracting TBR(1) and adding
C      1.00 to
C      all elements in the array. Also determine corresponding tidal
C      depths (YAT(L))

      Do 840 L=1, 400
      TNR(L) = TBR(L) +1-TBR(1)

      YAT(L) = TERS(L) + ABS(IRS)
      IF(YAT(L).LT.MLT) YAT(L)=MLT

840          CONTINUE

C Determine the array of the interpolated tidal depths at the bridge
C location

      CALL INTERP(TNR, YAT, TNRI, YATI, 400, 300,400, 300)

C Determine the tidal discharges at the bridge location using the
C Neill's Equation
C QN(NR18) represents an array of computed Neill's discharges with
C negative
C and positive values. The negative values represents the discharges
C produced by the rising tide directed up the estuary. While the
C positive values
C represents the discharges directed downstream. In the algorithm QNR
C represents
C Neill's discharges due to the rising limb and QNF represents
C Neill's
C discharges due to the falling limb.

```

```

      Do 850 L= 1, (ARR+1)
      TERI(L) = YATI(L)+IRS
850      CONTINUE

      Do 860 L = 1, ARR

      QN(L) = AS * ( (TERI(L) - TERI(L+1)))/(3600*DLT)

C      Modify the Neill's discharges with modification factors NMFR,
NMFF
C      developed by Brubaker and Demetrius.

      QNM(L)= NMFF*QN(L)
      IF (QN(L).LT.0) QNM(L)= NMFR*QN(L)

C      DETERMINE THE COMBINED TIDAL AND RIVERINE DISCHARGES BY
C      VECTOR ADDITION OF TIDAL AND RIVERINE DISCHARGES
C

      QT(L)= CHY36(L) + QNM(L)

      IF(QT(L).LE.0) THEN
        QTR(L) = ABS(QT(L))

        ELSE IF(QT(L).GT.0) THEN
          QTF(L) = ABS(QT(L))

          IF(ABS(QT(L)).GT.QTUMAX) QTUMAX = ABS(QT(L))

          IF((QTR(L)).GT.QTRMAX) QTRMAX = QTR(L)
          IF((QTF(L)).GT.QTFMAX) QTFMAX = QTF(L)

          IF((QTR(L)).GT.QTRMX) QTRMX = QTR(L)
          IF((QTF(L)).GT.QTFMX) QTFMX = QTF(L)

          IF((QTR(L)).GT.QTRMXS) QTRMXS = QTR(L)
          IF((QTF(L)).GT.QTFMXS) QTFMXS = QTF(L)

          SUMQTU = SUMQTU + ABS(QT(L))

          CONQTU = CONQTU + 1

        END IF

      IF(YATI(L).GE.HITIDE) HITIDE = YATI(L)

860      CONTINUE

C      DETERMINE THE COMBINED DEPTH YT
C

      Do 870 L =1,ARR

```



```

            IF(QT(L).GT.0) QROUT(L) = QT(L)
            IF(QT(L).LE.0) QROUT(L)= 0

870          CONTINUE

            VOUT(1) = 3600*0.5*(QROUT(1))
            VITID(1)= 0.5*(YATI(1)-MLT)*AS
            VICAT(1)= 3600*(QBF)
            VITOT(1)= VICAT(1)+ VITID(1)

            Do 880 l=2, ARR
                VICAT(L)=0.5*(CHY36(L)+CHY36(L-1))*3600
                VITID(L)=(YATI(L) - YATI(L-1))*AS
                VITOT(L)=VICAT(L) + VITID(L)
                VOUT(L) =3600*0.5*(QROUT(L)+QROUT(L-1))
880          CONTINUE

            VBAL(1) = VITOT(1) - VOUT(1)
            IF(VBAL(1).LE.0) VBAL(1) = 0
            IF(VBAL(1).LE.0) YT(1)= MLT
            IF(VBAL(1).GT.0.AND.VBAL(1).LE.SESVOL(1))
YT(1)=
            MLT + YTAMLT(1)

            Do 890 L=2,ARR
                VBAL(L) =VITOT(L-1) + VITOT(L)-VOUT(L)

            IF (VBAL(L).LE.0) VBAL(L) = 0
            IF (VBAL(L).LE.0) YT(L) = MLT

            IF(VBAL(L).GT.0.AND.VBAL(L).LE.SESVOL(1)) YT(L)=
            MLT + YTAMLT(1)

            Do 885 M =2, 150

                IF(VBAL(L).GT.SESVOL(M-
1).AND.VBAL(L).LE.SESVOL(M))
            YT(L) = MLT + YTAMLT(M)
885          CONTINUE
890          CONTINUE

            Do 900 L=1,ARR
                IF(YT(L).LT.YATI(L)) YT(L) = YATI(L)
900          CONTINUE

*****
*****

            IF(YT(1).LT.YT(2)) YTR(1) = YT(1)
            IF(YT(1).GE.YT(2)) YTR(1) = MLT

            IF(YT(1).GE.YT(2)) YTF(1) = YT(1)
            IF(YT(1).LT.YT(2)) YTF(1) = MLT

```

```

      Do 910 L= 1,ARR

      IF(YT(L+1).GT.YT(L)) YTR(L+1) = YT(L+1)
      IF(YT(L+1).LE.YT(L)) YTR(L+1) = MLT

      IF(YT(L+1).LE.YT(L)) YTF(L+1) = YT(L+1)
      IF(YT(L+1).GT.YT(L)) YTF(L+1) = MLT

      SUMYT = SUMYT + YT(L)
      CONYT = CONYT + 1

      IF(YT(L).GT.YTMX) YTMX = YT(L)

C      Record annual maximum depth at bridge station
      IF(YT(L).GT.YTMX) YTMX = YT(L)

      IF(YTF(L).GT.YTFMX) YTFMX = YTF(L)
      IF(YTR(L).GT.YTRMX) YTRMX = YTR(L)

      IF(YTF(L).GT.YTFMAX) YTFMAX = YTF(L)
      IF(YTR(L).GT.YTRMAX) YTRMAX = YTR(L)

      IF(YTFMX.GT.YTFMXS) YTFMXS = YTFMX
      IF(YTRMX.GT.YTRMXS) YTRMXS = YTRMX

910      CONTINUE
      END IF

C
C DETERMINE COMBINED VELOCITY AT BRIDGE STATION
C
      Do 920 L=1,ARR
      IF(YT(L).LE.MLT) VNT(L) = QT(L)/XABMLE

      IF(YT(L).LE.MLT) XATOT(L) = XABMLE

      IF(YT(L).GT.MLT.AND.YT(L).LE.(MLT+YTAMLT(1)))
      VNT(L) = QT(L)/(XABMLE+SXAMLT(1)-VFACT*UESTZ*(YT(L)-
MLT)**2)

      IF(YT(L).GT.MLT.AND.YT(L).LE.(MLT+YTAMLT(1)))
      XATOT(L)=(XABMLE + SXAMLT(1)-VFACT*UESTZ*(YT(L)-MLT)**2)

      Do 915 M= 2, 150
      IF(YT(L).GT.(MLT+YTAMLT(M-1)).AND.YT(L).LE.(MLT+YTAMLT(M)))
      VNT(L)=QT(L)/(XABMLE+ SXAMLT(M)-VFACT*UESTZ*(YT(L)-
MLT)**2)

      IF(YT(L).GT.(MLT+YTAMLT(M-1)).AND.YT(L).LE.(MLT+YTAMLT(M)))
      XATOT(L) =(XABMLE+SXAMLT(M)-VFACT*UESTZ*(YT(L)-MLT)**2)

```

```

915          CONTINUE
920          CONTINUE
*****
*****
*****

C          INITIALIZE SOIL SCOUR VARIABLES FOR EACH STORM
C          INITIALIZE CSU, AND CSD

DO 922 L=1, ARR

    CSD(L) =TSD - SUMYSD
    IF (SUMYSD.GT.TSD) CSD(L) = 0

    CSU(L) = TSU - SUMYSU
    IF (SUMYSU.GT.TSU) CSU(L) = 0

    YTFF(L) = YTF(L) + SUMYSU

    YTRF(L) = YTR(L) + SUMYSD
922 CONTINUE

    Do 925 L =1,30

        DPTHU =TSU
        IF(DPTHU.GE.DPTH(L).AND. DPTHU.LE.DPTH(L+1)) THEN
            ALPHAU = ALPHA(L)
            D16U   = D16(L)
            D50U   = D50(L)
            D84U   = D84(L)
            DMAXU  = DMAX(L)
            VCUF   = 0.476*(D50U/PD)**0.053
            SIGMAU = (D84U/D16U)**0.5
            PHU    = PH(L)
        END IF

        DPTHU = TSD
        IF(DPTHU.GE.DPTH(L).AND. DPTHU.LE.DPTH(L+1)) THEN
            ALPHAD = ALPHA(L)
            D16D   = D16(L)
            D50D   = D50(L)
            D84D   = D84(L)
            DMAXD  = DMAX(L)
            VCDF   = 0.476*(D50D/PD)**0.053
            SIGMAD = (D84D/D16D)**0.5
            PHDD   = PH(L)
        END IF

        DPTHCU = SUMYSU
        IF(DPTHCU.GE.DPTH(L).AND. DPTHCU.LE.DPTH(L+1)) THEN

            D16CU   = D16(L)

```

```

        D50CU   = D50(L)
        D84CU   = D84(L)
        SIGMCU  = (D84CU/D16CU)**0.5

END IF

        DPTHCD = SUMYSD
        IF(DPTHCD.GE.DPTH(L).AND. DPTHCD.LE.DPTH(L+1)) THEN

                D16CD   = D16(L)
                D50CD   = D50(L)
                D84CD   = D84(L)
                SIGMCD  = (D84CD/D16CD)**0.5

        END IF

925    CONTINUE

C      DETERMINE FLOW VELOCITY DOWNFLOW,VORTEX VELOCITY VECTORS, AND
SCOUR FOR EACH HOUR OF STORM
C
        Do 990 L=1,ARR

                VNUIN(L) = 0
                IF(VNT(L).LT.0) VNUIN(L) = ABS(VNT(L))

                VNU(1) = 0.5*VNUIN(1)
                Do 986 M=2, ARR

                        VNU(M) = 0.5*(VNUIN(M)+ VNUIN(M-1))
986        CONTINUE

                IF(VNU(L).LE.0) VNU(L)= 0
                IF(VNU(L).GT.0) THEN
                IF(VNU(L).GT.VNUMAX) VNUMAX = VNU(L)
                SUMVNU  = SUMVNU + VNU(L)
                CONVNU  = CONVNU + 1
                END IF

C Place maximum storm velocity in annual holding location VUPM

                IF(VNU(L).GT.VUPM) VUPM = VNU(L)
                IF(VUPM.GT.VUPMS) VUPMS = VUPM
*****
*****

C      Compute incremental contraction scour over time DLT      and
adjust flow depth to include the
C      lowering of the bed

                IF(CONTRA.EQ.1) THEN

C      Compute contraction scour using Straub's eqn

```

C         $qs = (g \cdot (Ss - 1) \cdot d50^{*3})^{*0.5} \cdot ((T/Tc) - 1)^{*2}$  English units,  
d50 in feet

C        Converting the equations so that D50 is in mm and solving for  
scour depth gives

C         $YS = (0.67/PD) \cdot DLT \cdot d50mm^{*1.5} \cdot [(T/Tc) - 1]^{*2}$

C         $T = 28.11 \cdot (Q/WB)^{*2} \cdot [n^{*2}/YTFF^{*2.33}]$

C        If D50mm < 0.065 then

C                 $Tc = 4.84 \cdot D50mm$

C        Else

C                 $Tc = 0.8d50^{*.67} \cdot Y^{*.33}$

          IF ( D50CD.LT.0.065) THEN

$TAUCD(L) = 4.84 \cdot D50CD$

          ELSE

$TAUCD(L) = 0.84 \cdot D50CD^{*0.67} \cdot YTRF(L)^{*0.33}$

          END IF

$TAUDD(L) = 28.11 \cdot (QTR(L)/WB)^{*2} \cdot (MAN^{*2}/YTRF(L)^{*2.33})$

$YSD(L) = 0$

IF ((TAUDD(L)/TAUCD(L)).GT.1)  $YSD(L) = COFDS \cdot (0.67/PD)$

$\cdot DLT \cdot D50CD^{*1.5} \cdot ((TAUDD(L)/TAUCD(L)) - 1)^{*1.5}$

ELSE IF (CONTRA.EQ.2) THEN

$YSDIN = YTR(L) \cdot (1.45 \cdot (VNU(L)/(32.2 \cdot YTR(L))^{*0.5})^{*0.2}$   
           $\cdot COFDF \cdot (1/SIGMCD^{*0.2}) - 1)$

          IF(YSDIN.LE.0)  $YSDIN = 0$

$YSD(L) = 0$

          IF(YSDIN.GT.YDINMX)  $YSD(L) = YSDIN - YDINMX$

          IF(YSDIN.GT.YDINMX)  $YDINMX = YSDIN$

ELSE

$YSDIN = 0$

          IF(COFD.GT.1)  $YSDIN = YTR(L) \cdot (COFD - 1)$

$YSD(L) = 0$

          IF(YSDIN.GT.YDINMX)  $YSD(L) = YSDIN - YDINMX$

          IF(YSDIN.GT.YDINMX)  $YDINMX = YSDIN$

END IF

$SUMYSD = SUMYSD + YSD(L)$

$YTRF(L) = YTR(L) + SUMYSD$

$XADJAD(L) = 0.5 \cdot (TWBMLT(4) + TWBMLT(3)) \cdot SUMYSD$

```

        VNUA(L) = VNU(L)*XATOT(L)/(XATOT(L) + XADJAD(L))
        IF(VNUA(L).GT.VNUPAM) VNUPAM = VNUA(L)

C      Recompute flowdepth and velocity, and computed local scour dept
to adjust for contraction
C      scour

        CSD(L) = CSD(L) - YSD(L)
        IF (YSD(L).GT.CSD(L)) CSD(L) = 0
        IF(CSD(L)+SUMYSD.LT.TSD) CSD(L) = TSD - SUMYSD

        LEW =L
        T(L)=LEW*DLT

        DSD(L) = CSD(L)/PD
C      Compute the scour angles along the downstream(THD) pier face

        THD(L) = PHDD
        IF (31*DSD(L)**2.LT.PHDD) THD(L) =31*DSD(L)**2

*****
*****

C      Compute downflow velocity on downstream faces of the pier

        IF(DSD(L).GT.100) THEN
            VDD(L) = 0

            ELSE IF (DSD(L).LE.2.3.AND.YTRF(L).GT.MLT) THEN
                VDD(L) = VNUA(L)* (0.15*(DSD(L))
                + 0.24* PD **0.18/(YTRF(L)**0.18 * C1**0.5))

            ELSE IF (DSD(L).GT.2.3) THEN
                VDD(L) = VNUA(L)*(0.40/EXP(1+(3*(DSD(L)-4)) + 0.4))

        END IF

        IF(VDD(L).GT.0.8*VNUA(L)) VDD(L) = 0.8*VNUA(L)

C      Compute the maximum tangential velocities along the upstream(VMU)
and downstream
C      (VMD) pier faces

        VMD(L) = 2.7* VDD(L)
        IF(31*DSD(L)**2.LE.PHDD) VMD(L) = 2.24*C1**0.5*VDD(L)

C      Compute the A factors and tangential velocities (VTU)
C      along the upstream and downstream (VTD) pier faces

        AFD(L)=-0.0002*THD(L)**2+0.012*THD(L)+0.80

        VTD(L)=0

```

```

        IF (AFD(L).GT.0) VTD(L)=1.4*AFD(L)*VMD(L)*
        (1-EXP(-1.25*(1/AFD(L)**2)))

*****
*****
C      SELECT CRITICAL VELOCITY MERHOD

        UID(L)=0

        IF (YTRF(L).GT.0.AND.VINCIP.EQ.1) UID(L)=
        VCDF*(1.66*D50D**0.333*YTRF(L)**0.167)

        IF (YTRF(L).GT.0.AND.VINCIP.EQ.2) UID(L)= VCDF*0.09*
        (D50D*Tan(PHDD*RADCON)* YTRF(L)**0.33/(ALPHAD*MAN**2))**0.5

        IF (YTRF(L).GT.0.AND.VINCIP.EQ.3) UID(L)= VCDF*(0.024/MAN)*
        (D50D**0.5)*(YTRF(L)**0.167)

*****
*****
C      Compute armouring velocity

        VARMD(L)=0
        IF (ARMVEL.GT.0.AND.SIGMAD.GT.1.3) VARMD(L)=1.328*(DMAXD/1.8)**
        0.333*YTRF(L)**0.167

        IF (VARMD(L).LE.0) THEN
            VCRIND(L) = UID(L)

        ELSE IF (VTD(L).LE.VARMD(L).AND.VARMD(L).GT.0) THEN

            VCRIND(L) = VARMD(L)-(UID(L)/VCDF)

        ELSE IF (VTD(L).GT.VARMD(L).AND.VARMD(L).GT.0) THEN

            VCRIND(L) = VARMD(L)

        END IF

        IF (VCRIND(L).LT.UID(L)) VCRIND(L)= UID(L)

*****
*****

        DED(L) =0
        IF (VTD(L).GT.VCRIND(L)) DED(L)=(PD**BNDX)*TANH(YTRF(L)/PD)
        *((VTD(L)-VCRIND(L))**INDX)*(VNUA(L)/(32.2*PD)**0.5)**FREX

        TED(L)=0
        IF (VCRIND(L).GT.0.0.AND.(VTD(L)/UID(L)).GT.VCDF) THEN

            TED(L) = 24*30.89*(PD/VTD(L))*((VTD(L)/VCRIND(L))-0.4)*

```

```

      (YTRF(L)/PD)**0.25

      ELSE IF(YTRF(L)-6.0*PD.GT.0.AND.((VTD(L)/VCRIND(L))
      -VCDF).GT.0.0) THEN

      TED(L)= 24*48.26*(PD/VTD(L))*((VTD(L)/VCRIND(L))-0.4)
      END IF

*****
*****

      K1D(L)=0
      IF(TED(L).GT.0.001.AND.VTD(L).GT.0.03) K1D(L)= EXP(-0.08*
      (ABS((VCRIND(L)/VTD(L))*LOG(DLT/TED(L))))**1.2)

      K2D(L)=0
      IF(TED(L).GT.0.001) K2D(L)=(ABS(LOG(DLT/TED(L))))**0.2

      K3D(L)=0
      IF(VTD(L).GT.0.03) K3D(L) = 0.1*(DED(L)/DLT)
      *(VCRIND(L)/VTD(L))**1.2

      RLD(L)= K1D(L)* K2D(L)* K3D(L)

      CSD(L+1) = CSD(L) + (RLD(L)*DLT)
      IF(CSD(L+1).LT.CSD(L)) CSD(L+1) =CSD(L)

*****
*****
C Repeat process for upstream pier face
*****
*****

      VNDIN(L) =0
      IF(VNT(L).GT.0) VNDIN(L) = ABS(VNT(L))

      VND(1) = 0.5*VNDIN(1)
      DO 988 M=2, ARR

      VND(M) = 0.5*(VNDIN(M)+ VNDIN(M-1))
988      CONTINUE

      IF(VND(L).LE.0) VND(L)= 0
      IF(VND(L).GT.0) THEN
      IF(VND(L).GT.VNDMAX) VNDMAX = VND(L)
      SUMVND = SUMVND + VND(L)
      CONVND = CONVND + 1
      END IF

C Place maximum storm velocity in annual holding location VDWNM

      IF(VND(L).GT.VDWNM) VDWNM = VND(L)
      IF(VDWNM.GT.VDWNMS) VDWNMS = VDWNM

*****
*****

```



```

C      Compute incremental contraction scour over time DLT      and
adjust flow depth to include the
C      lowering of the bed

      IF(CONTRA.EQ.1) THEN

C      Compute contraction scour using Straub's eqn

C       $q_s = (g \cdot (S_s - 1) \cdot d_{50}^3)^{0.5} \cdot ((T/T_c) - 1)^2$  English units,
d50 in feet

C      Converting the equations so that D50 is in mm and solving for
scour depth gives

C       $Y_S = (0.67/PD) \cdot DLT \cdot d_{50}^{1.5} \cdot [(T/T_c) - 1]^2$ 
C       $T = 28.11 \cdot (Q/WB)^{0.5} \cdot [n^2/YTFF^{2.33}]$ 
C      If D50mm < 0.065 then
C       $T_c = 4.84 \cdot D50_{mm}$ 
C      Else
C       $T_c = 0.8 \cdot d_{50}^{0.67} \cdot Y^{0.33}$ 

      IF ( D50CU.LT.0.065) THEN
      TAUCU(L) = 4.84*D50CU
      ELSE
      TAUCU(L) = 0.84*D50CU**0.67*YTFF(L)**0.33
      END IF

      TAUDU(L) = 28.11*(QTF(L)/WB)**2*(MAN**2/YTFF(L)**2.33)

      YSU(L) = 0
      IF((TAUDU(L)/TAUCU(L)).GT.1) YSU(L) = COFUS*(0.67/PD)*
      DLT*D50CU**1.5*((TAUDU(L)/TAUCU(L))-1)**1.5

ELSE IF (CONTRA.EQ.2) THEN

      YSUIN =YTF(L)*(1.45*(VND(L)/(32.2*YTF(L))**0.5)**0.2
      *COFUF*(1/SIGMCU**0.2)-1)

      IF(YSUIN.LE.0) YSUIN = 0

      YSU(L) = 0
      IF(YSUIN.GT.YUINMX) YSU(L) = YSUIN - YUINMX

      IF(YSUIN.GT.YUINMX) YUINMX = YSUIN

ELSE

      YSUIN = 0
      IF(COFU.GT.1) YSUIN = YTF(L)*(COFU - 1)

      YSU(L) = 0
      IF(YSUIN.GT.YUINMX) YSU(L) = YSUIN - YUINMX

      IF(YSUIN.GT.YUINMX) YUINMX = YSUIN

```

```

END IF

SUMYSU= SUMYSU + YSU(L)

YTFF(L) = YTF(L) + SUMYSU

XADJAU(L) = 0.5*(TWBMLT(4)+TWBMLT(3))*SUMYSU

VNDA(L) = VND(L)*XATOT(L)/(XATOT(L) + XADJAU(L))
IF(VNDA(L).GT.VNDNAM) VNDNAM = VNDA(L)

C      Recompute flowdepth and velocity, and computed local scour dept
to adjust for contraction
C      scour

CSU(L) = CSU(L) - YSU(L)
IF (YSU(L).GT.CSU(L)) CSU(L) = 0
IF(CSU(L)+SUMYSU.LT.TSU) CSU(L) = TSU - SUMYSU

LEW =L
T(L)=LEW*DLT

DSU(L) = CSU(L)/PD

C      Compute the scour angles along the upstream(THU) pier face

THU(L) = PHU
IF (31*DSU(L)**2.LT.PHU) THU(L) = 31*DSU(L)**2

C      Compute downflow velocity on upstream face of the pier

IF(DSU(L).GT.100) THEN
VDU(L) = 0

ELSE IF (DSU(L).LE.2.3.AND.YTFF(L).GT.MLT) THEN
VDU(L)= VNDA(L)*(0.15 * (DSU(L))
+ 0.24*PD ** 0.18/(YTFF(L)**0.18* C1**0.5))

ELSE IF (DSU(L).GT.2.3) THEN
VDU(L) = VNDA(L)*(0.40/(1+EXP(3*(DSU(L)-4)) + 0.4))

END IF

IF(VDU(L).GT.0.8*VNDA(L)) VDU(L) = 0.8*VNDA(L)

*****
*****
C
C
VMU(L) = 2.7* VDU(L)
IF(31*DSU(L)**2.LE.PHU) VMU(L) = 2.24*C1**0.5*VDU(L)

```

```

      AFU(L) = -0.0002*THU(L)**2+0.012*THU(L)+0.80

      VTU(L)=0
      IF (AFU(L).GT.0) VTU(L)=1.4*AFU(L)*VMU(L)*
      (1-EXP(-1.25*(1/AFU(L)**2)))

*****
*****

      UIU(L)=0

      IF (YTFF(L).GT.0.AND.VINCIP.EQ.1) UIU(L)=
      VCUF*(1.66*D50U**0.333*YTFF(L)**0.167)

      IF (YTFF(L).GT.0.AND.VINCIP.EQ.2) UIU(L)= VCUF*0.09*
      (D50U*Tan(PHU*RADCON)* YTFF(L)**0.33/(ALPHAU*MAN**2))**0.5

      IF (YTFF(L).GT.0.AND.VINCIP.EQ.3) UIU(L)= VCUF*(0.024/MAN)*
      (D50U**0.5)*(YTFF(L)**0.167)

*****
*****

C      Compute armouring velocity

      VARMU(L)=0
      IF (ARMVEL.GT.0.AND.SIGMAU.GT.1.3) VARMU(L)=1.328*(DMAXU/1.8)**
      0.333*YTFF(L)**0.167

      IF (VARMU(L).LE.0) THEN
        VCRINU(L) = UIU(L)

      ELSE IF (VTU(L).LE.VARMU(L).AND.VARMU(L).GT.0) THEN

        VCRINU(L) = VARMU(L)-(UIU(L)/VCUF)

      ELSE IF (VTU(L).GT.VARMU(L).AND.VARMU(L).GT.0) THEN

        VCRINU(L) = VARMU(L)

      END IF

      IF (VCRINU(L).LT.UIU(L)) VCRINU(L)= UIU(L)

*****
*****

      DEU(L) =0
      IF (VTU(L).GT.VCRINU(L)) DEU(L)=(PD**BNDX)*TANH(YTFF(L)/PD)
      *((VTU(L)-VCRINU(L))**INDX)*(VNDA(L)/(32.2*PD)**0.5)**FREX

```

```

      TEU(L)=0
      IF(VCRINU(L).GT.0.0.AND.(VTU(L)/UIU(L)).GT.VCUF) THEN

      TEU(L) = 24*30.89*(PD/VTU(L))*((VTU(L)/VCRINU(L))- 0.4)*
      ` (YTFF(L)/PD)**0.25

      ELSE IF(YTFF(L)-6.0*PD.GT.0.AND.((VTU(L)/VCRINU(L))
      ` -VCUF).GT.0.0) THEN

      TEU(L)= 24*48.26*(PD/VTU(L))*((VTU(L)/VCRINU(L))-0.4)
      END IF

*****
*****

      K1U(L)=0
      IF(TEU(L).GT.0.001.AND.VTU(L).GT.0.03) K1U(L)= EXP(-0.08
      ` *(ABS((VCRINU(L)/VTU(L))*LOG(DLT/TEU(L))))**1.2)

      K2U(L)=0
      IF(TEU(L).GT.0.001) K2U(L)= (ABS(LOG(DLT/TEU(L))))**0.2

      K3U(L)=0
      IF(VTU(L).GT.0.03) K3U(L) = 0.1*(DEU(L)/DLT)
      ` *(ABS(VCRINU(L)/VTU(L)))*1.2

*****
*****

      RLU(L)= K1U(L)* K2U(L)* K3U(L)

      CSU(L+1) = CSU(L) + (RLU(L)*DLT)
      IF(CSU(L+1).LT.CSU(L)) CSU(L+1) = CSU(L)

      IF(YTRF(L).GT.YTMRF) YTMRF= YTRF(L)
      IF(YTFF(L).GT.YTMFF) YTMFF= YTFF(L)

      IF(VTD(L).GT.VTDMX) VTDMX= VTD(L)
      IF(VTU(L).GT.VTUMX) VTUMX= VTU(L)

      IF(VTD(L).GT.VTDMX) VTDMX= VTD(L)
      IF(VTU(L).GT.VTUMX) VTUMX= VTU(L)

      IF(UIU(L).LT.UIUMIN) UIUMIN= UIU(L)
      IF(UID(L).LT.UIDMIN) UIDMIN= UID(L)

990  CONTINUE

*****
*****

      TSD=CSD(ARR) + SUMYSD

```

```

C Compute Contraction scour and sum to local scour to obtain total
scour for
C downstream face for each storm

      TSU=CSU(ARR) + SUMYSU
*****
*****

1000  CONTINUE

C      DETERMINE AVERAGE ANNUAL RAINFALL

      ASUM6 = SUM6/(TMS*YRS)
      ASUM18= SUM18/(TMS*YRS)
      ASUM24 =SUM24/(TMS*YRS)
      ASUM36= SUM36/(TMS*YRS)

C      SET UP ARRAYS TO RECORD THE MAXIMUM ANNUAL VELOCIES IN THE
UPSTREAM AND DOWNSTREAM
C      DIRECTION

      VUPYR(J) = VUPM
      VUPMSM(J) = VUPMSM(J) + VUPYR(J)

      VDNYR(J) = VDWNM
      VDNMSM(J) = VDNMSM(J) + VDNYR(J)

      VNDAYR(J) = VNDNAM

      VNUAYR(J) = VNUPAM

C      SET UP ARRAYS TO RECORD THE MAXIMUM ANNUAL FLOW DEPTHS

      YTYRS (J) = YTMAX

      YTRYRS(J) = YTRMX

      YTFYRS(J) = YTFMX

      YTRFYR(J) = YTMRF

      YTFFYR(J) = YTMFF

C      SET UP ARRAY TO RECORD THE PEAK ANNUAL RIVERINE 6, 18, 24,36 HR
DISCHARGES
      QPK      6(J) = QP6MX
      QPK18(J) = QP18MX
      QPK24(J) = QP24MX
      QPK36(J) = QP36MX

C      SET UP ARRAYS TO RECORD THE MAXIMUM ANNUAL DISCHARGE IN THE
UPSTREAM AND
C      DOWNSTREAM DIRECTION

```

```

      QUPYR(J) = QTRMX
      QDNYR(J) = QTFMX

C      SET UP ARRAYS TO RECORD THE SCOUR VALUE AT THE END OF EACH YR
C      UPSTREAM PIER FACE

      YYSUIN(J)=SUMYSU
      SMYYSU(J) = SMYYSU(J)+ YYSUIN(J)

      YTSU(J)= TSU
      YSMTSU(J) = YSMTSU(J) + YTSU(J)

      YSMUSQ(J) = YSMUSQ(J) + (YTSU(J))**2

C      DOWNSTREAM PIER FACE

      YYSDIN(J)= SUMYSD
      SMYYSD(J) = SMYYSD(J) +YYSDIN(J)

      YTSD(J)= TSD

      YSMTSD(J) = YSMTSD(J) + YTSD(J)

      YSMDSQ(J) = YSMDSQ(J) + (YTSD(J))**2

C*****
C*****

C      DETERMINE DISTRIBUTION FOR SCOUR RESULTS AT 15%TMS, 25%TMS,
50%TMS AND 75% TMS

C*****
C*****

      YEAR = J

      IF(YEAR.EQ.INT(0.15*YRS)) THEN

C      PLACE INPUTS IN THE FIRST RANGE
      IF(TSD.LT.B(1)) FD15(1)=FD15(1) + 1
      IF(TSU.LT.B(1)) FU15(1)=FU15(1) + 1

C      PLACE INPUTS IN THE INTERIOR AND LAST RANGE

      DO 1015 K = 1, 99
        IF(TSD.GE.B(K).AND.TSD.LT.B(K+1)) FD15(K+1) =FD15(K+1) + 1

```

```

        IF(TSU.GE.B(K).AND.TSU.LT.B(K+1)) FU15(K+1) =FU15(K+1) + 1
1015  CONTINUE

      END IF

      IF(YEAR.EQ.INT(0.25*YRS)) THEN

C      PLACE INPUTS IN THE FIRST RANGE
      IF(TSD.LT.B(1)) FD25(1)=FD25(1) + 1
      IF(TSU.LT.B(1)) FU25(1)=FU25(1) + 1

C      PLACE INPUTS IN THE INTERIOR AND LAST RANGE

      DO 1025 K = 1, 99
        IF(TSD.GE.B(K).AND.TSD.LT.B(K+1)) FD25(K+1) =FD25(K+1) + 1
        IF(TSU.GE.B(K).AND.TSU.LT.B(K+1)) FU25(K+1) =FU25(K+1) + 1
1025  CONTINUE

      END IF

      IF(YEAR.EQ.INT(0.50*YRS)) THEN

C      PLACE INPUTS IN THE FIRST RANGE
      IF(TSD.LT.B(1)) FD50(1)=FD50(1) + 1
      IF(TSU.LT.B(1)) FU50(1)=FU50(1) + 1

C      PLACE INPUTS IN THE INTERIOR AND LAST RANGE

      DO 1050 K = 1, 99
        IF(TSD.GE.B(K).AND.TSD.LT.B(K+1)) FD50(K+1) =FD50(K+1) + 1
        IF(TSU.GE.B(K).AND.TSU.LT.B(K+1)) FU50(K+1) =FU50(K+1) + 1
1050  CONTINUE

      END IF

      IF(YEAR.EQ.INT(0.75*YRS)) THEN

C      PLACE INPUTS IN THE FIRST RANGE
      IF(TSD.LT.B(1)) FD75(1)=FD75(1) + 1
      IF(TSU.LT.B(1)) FU75(1)=FU75(1) + 1

C      PLACE INPUTS IN THE INTERIOR AND LAST RANGE

      DO 1075 K = 1, 99
        IF(TSD.GE.B(K).AND.TSD.LT.B(K+1)) FD75(K+1) =FD75(K+1) + 1
        IF(TSU.GE.B(K).AND.TSU.LT.B(K+1)) FU75(K+1) =FU75(K+1) + 1
1075  CONTINUE

      END IF

1100  CONTINUE

C      COMPUTE THE MEAN UPSTREAM AND DOWNSTREAM AVERAGE MAXIMUM
      VELOCITIES EACH YEAR

      Do 1104 J =1, YRS

```

```

          AVUPYR(J) = VUPMSM(J)/ENS

          AVDNYR(J) = VDNMSM(J)/ENS

1104      CONTINUE

C          COMPUTE THE MEAN AND STANDARD DEVIATION FOR THE SCOUR EACH YEAR

          Do 1105 J=1,YRS

C          UPSTREAM PIER FACE

          MNYYSU(J) = SMYYSU(J)/ENS

          YMNTSU(J) = (YSMTSU(J)/ENS)

          YSTTSU(J) = SQRT(ABS((YSMUSQ(J) - YSMTSU(J)**2/ENS)
            /(ENS-1)))

          MNLSU(J) = YMNTSU(J)- MNYYSU(J)

C          DOWNSTREAM PIER FACE

          MNYYSD(J) = SMYYSU(J)/ENS

          YMNTSD(J) = (YSMTSD(J)/ENS)

          YSTTSD(J) = SQRT(ABS((YSMDSQ(J) - YSMTSD(J)**2/ENS)
            /(ENS-1)))

          MNLSD(J) = YMNTSD(J)- MNYYSD(J)

1105      CONTINUE

          Do 1108 J=2,YRS

          IF(MNLSD(J).LE.MNLSD(J-1)) MNLSD(J) = MNLSD(J-1)
          IF(MNLSU(J).LE.MNLSU(J-1)) MNLSU(J) = MNLSU(J-1)

1108      CONTINUE

*****
*****
*                                     SINGLE EVENT HURRICANE MODEL
*
*****
*****

```



```

C      GO TO 1106(line 460) used to bypass the continuous simulations
when a
C      single hurricane simulation is desired

1106 CONTINUE
C      REPEAT PROCESS FOR THE SCOUR SIMULATION FROM 36 HR HURRICANE
C
      IF (HCAT.EQ.0) GO TO 1435

C      Select the type of hurricane information to be used

C
C      Initialize Scour parameters for each Storm
C
      IF ( HCAT.LE.5.AND.HCAT.GT.0) THEN

C      Initialize UVAR

      UVA=0
      UVAR36 = 1

      Do 1110  L = 1, INT(C36)

C Generate uniform variate UVR from RANNO

      UVA=RANNO(1,0.0, 1.0)
      UVAR36 = UVAR36*UVA
1110    CONTINUE

      PPT36 = -B36*LOG(UVAR36)

      HURPPT = PPT36

      IF(PPT36.GT.PPTMAX) PPTMAX =PPT36

      TDRO = (PPT36 - IA) ** 2/ (PPT36 + AI)
      TINF = (PPT36 - TDRO)

      IF(PPT36-TINF.LE.0.0) NORUN = NORUN + 1

C      Determine catchment hydrograph

C      Convert rainfall from dimensionless cumulative hyetograph to a
cumulative
C      depth hyetograph

      Do 1120  L = 1, NP36
      P36(L) = S36(L) * PPT36
1120    CONTINUE

      Do 1130  L = 1, NP36
      SP = P36(L)
      PE36(L) = 0.0
      IF(SP.GT.IA) PE36(L) = (SP - IA) ** 2/ (SP + AI)
1130    CONTINUE

```

```

        PEI36(1) = PE36(1)

        Do 1140 L = 2, NP36
            PEI36(L) = P36(L) - P36(L-1)
1140      CONTINUE

C      Convolve unit hydrographs convolve sub routine

        CALL CONVOL(QU, PEI36, DRO36, NU, NP36, NR36, 36, 36, 300)

C      Add base flow to direct runoff hydrograph.  Final output is
CHY(NR), NR

        Do 1150 L = 1, 120

            CHY36(L) = DRO36(L) + QBF
1150      CONTINUE

C      SYNTHESIZE TIDAL SERIES AT BASE STATION B.

        PHD = RANNO(1, 0.0, 6.284)

        PHL = RANNO(1, 0.0, 6.284)

        LA= RANNO( 2, MLA, SLA)
        LA=ABS(LA)

        TB = 0
        DO 1170  L =1, 400
            IF(TB.EQ.0) THEN
                DA= RANNO(2, 1.42, 0.64)
                DA=ABS(DA)
            ELSE
                GO TO 1160
            END IF
1160      CONTINUE

C      Create array of MSL water surface elevations TEB(150) varying
hourly with
C      time

        LEW = L
        TB=TB+1
C      TEB is the normal base line tide

        TEB(L) = DA*SIN(2*PI*(LEW/DT)+ PHD)+LA*SIN(2*PI*(LEW/LT)+PHL)
        IF(TB.EQ.INT(DT)) TB=0
1170 CONTINUE

C      Synthesize hurricane surge

        HDUR = HRAD/HSPEED

        IF (HDIST.GE.HRAD) HPRM = 0
        IF (HDIST.LT.HRAD) HPRM = (HRAD - HDIST)

```

```

DO 1180 L = 1, 120
    JIN=L

    IF (ABS(JIN-HDUR).GE.1.0) HSURGE(L)= MAXSRG*(HPRM/HRAD)*
    \ (1-EXP(-(MAXSRG*(HPRM/HRAD))/HRAD)*(ABS(JIN/(HDUR-JIN))))

    IF (ABS(JIN-HDUR).LT.1.0) HSURGE(L)= MAXSRG*(HPRM/HRAD)

    IF (HSURGE(L).EQ.MAXSRG*(HPRM/HRAD)) JINMAX = L
    IF (L.EQ.JINMAX+1) HSURGE(L)= 0.95*MAXSRG*(HPRM/HRAD)

    IF ((JIN-HDUR).GT.3.0) HSURGE(L)= - MAXSRG*(HPRM/HRAD)*
    \ (1-EXP(-(HRAD/(HSPEED*JIN))))

1180 CONTINUE

ELSE

*****
*****
    PPT36 = HURAIN

    HURPPT = PPT36

    IF (PPT36.GT.PPTMAX) PPTMAX =PPT36

    TDRO=0
    IF (PPT36.GT.IA) TDRO = (PPT36 - IA) ** 2/ (PPT36 + AI)
    TINF = (PPT36 - TDRO)

    IF (PPT36-TINF.LE.0.0) NORUN = NORUN + 1

C    Determine catchment hydrograph

C    Convert rainfall from dimensionless cumulative hyetograph to a
cumulative depth hyetograph

    Do 1182 L = 1, NP36
        P36(L) = S36(L) * PPT36
1182    CONTINUE

    Do 1183 L = 1, NP36
        SP = P36(L)
        PE36(L) = 0.0
        IF (SP.GT.IA) PE36(L) = (SP - IA) ** 2/ (SP + AI)
1183    CONTINUE

    PEI36(1) = PE36(1)

    Do 1184 L = 2, NP36
        PEI36(L) = P36(L) - P36(L-1)
1184    CONTINUE

```

```

C      Convolve unit hydrographs convolve sub routine

      CALL CONVOL(QU, PEI36, DRO36, NU, NP36, NR36, 36, 36, 300)

C      Add base flow to direct runoff hydrograph.  Final output is
CHY(NR), NR

      DO 1185 L = 1, 120

      CHY36(L) = DRO36(L) + QBF
1185      CONTINUE

C      SYNTHESIZE TIDAL SERIES AT BASE STATION B.

      PHD = RANNO(1, 0.0, 6.284)
      PHL = RANNO(1, 0.0, 6.284)

      LA= RANNO( 2, MLA, SLA)
      LA=ABS(LA)

      TB = 0
      DO 1187 L =1, 400
      IF(TB.EQ.0) THEN
      DA= RANNO(2, 1.42, 0.64)
      DA=ABS(DA)
      ELSE
      GO TO 1186
      END IF
1186      CONTINUE

C      Create array of MSL water surface elevations TEB(150) varying
hourly with
C      time
      LEW = L
      TB=TB+1
C      TEB is the normal base line tide

      TEB(L) = DA*SIN(2*PI*(LEW/DT)+ PHD)+LA*SIN(2*PI*(LEW/LT)+PHL)
      IF(TB.EQ.INT(DT)) TB=0
1187 CONTINUE

C      Synthesize hurricane surge

      HDUR = HRAD/HSPEED

      IF (HDIST.GE.HRAD) HPRM = 0
      IF (HDIST.LT.HRAD) HPRM = (HRAD - HDIST)

      DO 1188 L = 1, 120
      JIN=L

      IF(ABS(JIN-HDUR).GE.1.0) HSURGE(L)= MAXSRG*(HPRM/HRAD)*
      (1-EXP(-(MAXSRG*(HPRM/HRAD))/HRAD)*(ABS(JIN/(HDUR-JIN))))

      IF(ABS(JIN-HDUR).LT.1.0) HSURGE(L)= MAXSRG*(HPRM/HRAD)

```

```

        IF(HSURGE(L).EQ.MAXSRG*(HPRM/HRAD)) JINMAX = L
        IF(L.EQ.JINMAX+1) HSURGE(L)= 0.95*MAXSRG*(HPRM/HRAD)

        IF((JIN-HDUR).GT.3.0) HSURGE(L)= - MAXSRG*(HPRM/HRAD)*
            (1-EXP(-(HRAD/(HSPEED*JIN))))

1188 CONTINUE

        END IF
*****
*****

C      COMPUTE RESULTANT TIDAL PROFILE

        DO 1190 L=1,400
        IF(TEB(L).LT.(IBS + 1.0)) TEB(L) = (IBS +1.0)
1190 CONTINUE

C DETERMINE TIDAL ELEVATIONS AT THE BRIDGE STATION
C   by convex routing or otherwise

        TER(1)=TAF*TEB(1)

        IF(CONROUT.EQ.0) THEN

            Do 1192 L=2, 400
            TER(L)= TAF*TEB(L)

1192 CONTINUE

            ELSE IF(CONROUT.NE.0) THEN

                Do 1195 L=2, 400
                TER(L)= CX*TEB(L-1) + (1.0 - CX)*TER(L-1)

1195 CONTINUE

            END IF

        IF(DISCON.EQ.0) THEN

C      Add surge to routed tide elevation

            Do 1205 L=1,120
            HTER(L) = HSURGE(L) +TER(L)

            IF(HTER(L).LT.(MLT+IRS)) HTER(L)=0.2*(MLT+IRS)

            IF(L.GE.INT((BLOCON+1)*HDUR)) HTER(L) = TER(L)

            IF(HTER(L).GT.HIELE) HIELE = HTER(L)

1205 CONTINUE

```

```

      Do 1210 L= 1, 120
        YB(L) = TEB(L) + ABS(IRS)
        IF(YB(L).GT.HIBASE) HIBASE = YB(L)

1210    CONTINUE

      Do 1220 L = 1, 120
        QN(L) = AS * ( (HTER(L) - HTER(L+1)))/(3600*DLT)

C      Modify the Neill's discharges with modification factors NMFR,
NMFF
C      developed by Brubaker and Demetrius.

        QNM(L)= NMFRH*QN(L)
        IF(QN(L).GT.0) QNM(L) = QN(L)
C      DETERMINE THE COMBINED TIDAL AND RIVERINE DISCHARGES BY
C      VECTOR ADDITION OF TIDAL AND RIVERINE DISCHARGES
C
        QT(L)= CHY36(L) + QNM(L)

        QTR(L) = 0
        IF(QT(L).LE.0) QTR(L) = ABS(QT(L))

        QTF(L) = 0
        IF(QT(L).GT.0) QTF(L) = ABS(QT(L))

        IF(ABS(QT(L)).GT.QTUMAX) QTUMAX = ABS(QT(L))

        IF((QTR(L)).GT.QTRMAX) QTRMAX = QTR(L)
        IF((QTF(L)).GT.QTFMAX) QTFMAX = QTF(L)

        IF((QTR(L)).GT.QTRMX) QTRMX = QTR(L)
        IF((QTF(L)).GT.QTFMX) QTFMX = QTF(L)

        IF((QTR(L)).GT.QTRMXS) QTRMXS = QTR(L)
        IF((QTF(L)).GT.QTFMXS) QTFMXS = QTF(L)

        SUMQTU = SUMQTU + ABS(QT(L))

        CONQTU = CONQTU + 1

C      DETERMINE THE COMBINED DEPTH YT
C
        HYAT(L) = HTER(L) +ABS(IRS)

        IF(HYAT(L).GE.HITIDE) HITIDE = HYAT(L)

1220    CONTINUE

      Do 1230 L =1,ARR

```

```

                IF(QT(L).GT.0)      QROUT(L) = QT(L)
                IF(QT(L).LE.0)      QROUT(L) = 0
1230      CONTINUE

                VOUT(1) = 3600*0.5*(QROUT(1))
                VITID(1)= 0.5*(HYAT(1)-MLT)*AS
                VICAT(1)= 3600*(QBF)
                VITOT(1)= VICAT(1)+ VITID(1)

                Do 1240 l=2, ARR
                VICAT(L)=0.5*(CHY36(L)+CHY36(L-1))*3600
                VITID(L)=(HYAT(L) - HYAT(L-1))*AS
                VITOT(L)=VICAT(L) + VITID(L)
                VOUT(L) =3600*0.5*(QROUT(L)+QROUT(L-1))
1240      CONTINUE

                VBAL(1) = VITOT(1) - VOUT(1)
                IF(VBAL(1).LE.0) VBAL(1) = 0
                IF(VBAL(1).LE.0) YT(1)= MLT
                IF(VBAL(1).GT.0.AND.VBAL(1).LE.SESVOL(1))
YT(1)=
                MLT + YTAMLT(1)

                Do 1250 L=2,ARR
                VBAL(L) =VITOT(L-1) + VITOT(L)-VOUT(L)

                IF (VBAL(L).LE.0) VBAL(L) = 0
                IF (VBAL(L).LE.0) YT(L) = MLT

                IF(VBAL(L).GT.0.AND.VBAL(L).LE.SESVOL(1)) YT(L)=
                MLT + YTAMLT(1)

                Do 1245 M =2, 150

                IF(VBAL(L).GT.SESVOL(M-
1) .AND.VBAL(L).LE.SESVOL(M))
                YT(L) = MLT + YTAMLT(M)
1245      CONTINUE
1250      CONTINUE

*****
*****

                Do 1260 L=1,120

                IF(YT(L).LT.HYAT(L)) YT(L) = HYAT(L)
1260      CONTINUE

                IF(YT(1).LT.YT(2)) YTR(1) = YT(1)
                IF(YT(1).GE.YT(2)) YTR(1) = MLT

                IF(YT(1).GE.YT(2)) YTF(1) = YT(1)
                IF(YT(1).LT.YT(2)) YTF(1) = MLT

                Do 1270 L= 1,120

```

```

        IF(YT(L+1).GT.YT(L)) YTR(L+1) = YT(L+1)
        IF(YT(L+1).LE.YT(L)) YTR(L+1) = MLT

        IF(YT(L+1).LE.YT(L)) YTF(L+1) = YT(L+1)
        IF(YT(L+1).GT.YT(L)) YTF(L+1) = MLT

        SUMYT = SUMYT + YT(L)
        CONYT = CONYT + 1

        IF(YT(L).GT.YTMAX) YTMAX = YT(L)

        IF(YTF(L).GT.YTFMX) YTFMX = YTF(L)
        IF(YTR(L).GT.YTRMX) YTRMX = YTR(L)

        IF(YTF(L).GT.YTFMAX) YTFMAX = YTF(L)
        IF(YTR(L).GT.YTRMAX) YTRMAX = YTR(L)

        IF(YTFMX.GT.YTFMXS) YTFMXS = YTFMX
        IF(YTRMX.GT.YTRMXS) YTRMXS = YTRMX
1270      CONTINUE

        ELSE

        Do 1280 L= 1, 400

        TERS(L)=TER(L)

        LEW=L
        TBR(L) = LEW + (LW/(1800*32.2*(YB(L) + MDR))**0.5)
1280      CONTINUE

C      Sort array TBR(300) in ascending order also sort array  TER(300)
C      based on the order of array TBR(300).

        CALL SORT2(400,TBR, TERS)

C      Normalize the array TBR(150) by subtracting TBR(1) and adding
C      1.00 to
C      all elements in the array.  Also determine corresponding tidal
C      depths
C      (YAT(L))

        Do 1290 L=1, 400
        TNR(L) = TBR(L) +1-TBR(1)

        YAT(L) = TERS(L) + ABS(IRS)
        IF(YAT(L).LT.MLT) YAT(L)=MLT

1290      CONTINUE

C Determine the array of the interpolated tidal depths at the bridge
location

```



```

CALL INTERP(TNR, YAT, TNRI, YATI, 400, 300,400, 300)

C Determine the tidal discharges at the bridge location using the
C Neill's
C Equation
C QN(NR18) represents an array of computed Neill's discharges with
C negative
C and positive values. The negative values represents the discharges
C produced by the rising tide directed up the estuary. While the
C positive
C values
C represents the discharges directed downstream. In the algorithm QNR
C represents
C Neill's discharges due to the rising limb and QNF represents
C Neill's
C discharges due to the falling limb.

      Do 1300 L= 1, 120 + 1
        TERI(L) = YATI(L)+IRS
C Add storm surge to routed tide elevations
      HTER(L) = TERI(L) + HSURGE(L)

      IF(L.GE.INT((BLOCON+1)*HDUR)) HTER(L) = TERI(L)

      IF(HTER(L).LT.(MLT+IRS)) HTER(L)=0.2*(MLT+IRS)

      HYAT(L) = HTER(L) - IRS
1300      CONTINUE

      Do 1310 L = 1, 120
        QN(L) = AS * ( (HTER(L)- HTER(L+1)))/(3600*DLT)

C Modify the Neill's discharges with modification factors NMFR,
C NMFF
C developed by Brubaker and Demetrius.

      QNM(L)= NMFRH*QN(L)
      IF(QN(L).GT.0) QNM(L) = QN(L)

C DETERMINE THE COMBINED TIDAL AND RIVERINE DISCHARGES BY
C VECTOR ADDITION OF TIDAL AND RIVERINE DISCHARGES
C
      QT(L)= CHY36(L) + QNM(L)

      QTR(L) = 0
      IF(QT(L).LT.0) QTR(L) = ABS(QT(L))

      QTF(L)= 0
      IF(QT(L).GT.0) QTF(L) = ABS(QT(L))

      IF(ABS(QT(L)).GT.QTUMAX) QTUMAX = ABS(QT(L))

      IF((QTR(L)).GT.QTRMAX) QTRMAX = QTR(L)
      IF((QTF(L)).GT.QTFMAX) QTFMAX = QTF(L)

```

```

      IF((QTR(L)).GT.QTRMX) QTRMX = QTR(L)
      IF((QTF(L)).GT.QTFMX) QTFMX = QTF(L)

      IF((QTR(L)).GT.QTRMXS) QTRMXS = QTR(L)
      IF((QTF(L)).GT.QTFMXS) QTFMXS = QTF(L)

      SUMQTU = SUMQTU + ABS(QT(L))

      CONQTU = CONQTU + 1

      IF(HYAT(L).GE.HITIDE) HITIDE = HYAT(L)

1310      CONTINUE

C      DETERMINE THE COMBINED DEPTH YT
C
      Do 1320 L =1,120

          IF(QT(L).GT.0) QROUT(L) = QT(L)
          IF(QT(L).LE.0) QROUT(L)= 0

1320      CONTINUE

      VOUT(1) = 3600*0.5*(QROUT(1))
      VITID(1)= 0.5*(HYAT(1)-MLT)*AS
      VICAT(1)= 3600*(QBF)
      VITOT(1)= VICAT(1)+ VITID(1)

      Do 1330 l=2, ARR
          VICAT(L)=0.5*(CHY36(L)+CHY36(L-1))*3600
          VITID(L)=(HYAT(L) - HYAT(L-1))*AS
          VITOT(L)=VICAT(L) + VITID(L)
          VOUT(L) =3600*0.5*(QROUT(L)+QROUT(L-1))
1330      CONTINUE

      VBAL(1) = VITOT(1) - VOUT(1)
      IF(VBAL(1).LE.0) VBAL(1) = 0
      IF(VBAL(1).LE.0) YT(1)= MLT
      IF(VBAL(1).GT.0.AND.VBAL(1).LE.SESVOL(1))
YT(1)=
      MLT + YTAMLT(1)

      Do 1340 L=2,ARR
          VBAL(L) =VITOT(L)-VOUT(L)
          IF (VBAL(L).LE.0) VBAL(L) = 0
          IF (VBAL(L).LE.0) YT(L) = MLT

      IF(VBAL(L).GT.0.AND.VBAL(L).LE.SESVOL(1)) YT(L)=
      MLT + YTAMLT(1)

      Do 1335 M =2, 150

```

```

                                IF(VBAL(L).GT.SESVOL(M-
1).AND.VBAL(L).LE.SESVOL(M))
                                YT(L) = MLT + YTAMLT(M)
1335                                CONTINUE
1340                                CONTINUE

*****
*****

                                Do 1350 L=1,120

                                IF(YT(L).LT.HYAT(L)) YT(L) = HYAT(L)
1350                                CONTINUE

                                IF(YT(1).LT.YT(2)) YTR(1) = YT(1)
                                IF(YT(1).GE.YT(2)) YTR(1) = MLT

                                IF(YT(1).GE.YT(2)) YTF(1) = YT(1)
                                IF(YT(1).LT.YT(2)) YTF(1) = MLT

                                Do 1360 L= 1,120

                                IF(YT(L+1).GT.YT(L)) YTR(L+1) = YT(L+1)
                                IF(YT(L+1).LE.YT(L)) YTR(L+1) = MLT

                                IF(YT(L+1).LE.YT(L)) YTF(L+1) = YT(L+1)
                                IF(YT(L+1).GT.YT(L)) YTF(L+1) = MLT

                                SUMYT = SUMYT + YT(L)
                                CONYT = CONYT + 1

                                IF(YT(L).GT.YTMAX) YTMAX = YT(L)

                                IF(YTF(L).GT.YTFMX) YTFMX = YTF(L)
                                IF(YTR(L).GT.YTRMX) YTRMX = YTR(L)

                                IF(YTF(L).GT.YTFMAX) YTFMAX = YTF(L)
                                IF(YTR(L).GT.YTRMAX) YTRMAX = YTR(L)

                                IF(YTFMX.GT.YTFMXS) YTFMXS = YTFMX
                                IF(YTRMX.GT.YTRMXS) YTRMXS = YTRMX

1360                                CONTINUE
                                END IF

C
C DETERMINE COMBINED VELOCITY AT BRIDGE STATION
C
                                Do 1370 L=1,120

                                IF(YT(L).LE.MLT) VNT(L) = QT(L)/XABMLE

                                IF(YT(L).LE.MLT) XATOT(L) = XABMLE

```

```

      IF(YT(L).GT.MLT.AND.YT(L).LE.(MLT+YTAMLT(1)))
      VNT(L) = QT(L)/(XABMLE+SXAMLT(1)-VFACT*UESTZ*(YT(L)-
MLT)**2)

      IF(YT(L).GT.MLT.AND.YT(L).LE.(MLT+YTAMLT(1)))
      XATOT(L)=(XABMLE + SXAMLT(1)-VFACT*UESTZ*(YT(L)-MLT)**2)

      Do 1365 M= 2, 150
      IF(YT(L).GT.(MLT+YTAMLT(M-1)).AND.YT(L).LE.(MLT+YTAMLT(M)))
      VNT(L)=QT(L)/(XABMLE+ SXAMLT(M)-VFACT*UESTZ*(YT(L)-
MLT)**2)

      IF(YT(L).GT.(MLT+YTAMLT(M-1)).AND.YT(L).LE.(MLT+YTAMLT(M)))
      XATOT(L) =(XABMLE+SXAMLT(M)-VFACT*UESTZ*(YT(L)-MLT)**2)

1365      CONTINUE
1370      CONTINUE

*****
*****

C      INITIALIZE SOIL SCOUR VARIABLES FOR EACH STORM
C      INITIALIZE CSU, AND CSD

DO 1390 L=1, 120
  CSD(L) =TSD - SUMYSD
  IF (SUMYSD.GT.TSD) CSD(L) = 0

  CSU(L) = TSU - SUMYSU
  IF (SUMYSU.GT.TSU) CSU(L) = 0

  YTFF(L) = YTF(L) + SUMYSU

  YTRF(L) = YTR(L) + SUMYSD

  Do 1375 M =1,30

    DPTHU =TSU
    IF(DPTHU.GE.DPTH(M).AND. DPTHU.LE.DPTH(M+1)) THEN
      ALPHAU = ALPHA(M)
      D16U   = D16(M)
      D50U   = D50(M)
      D84U   = D84(M)
      DMAXU  = DMAX(L)
      VCUF   = 0.476*(D50U/PD)**0.053
      SIGMAU = (D84U/D16U)**0.5
      PHU    = PH(M)
    END IF

    DPTHU = TSD
    IF(DPTHU.GE.DPTH(M).AND. DPTHU.LE.DPTH(M+1)) THEN
      ALPHAD = ALPHA(M)

```

```

D16D    = D16(M)
D50D    = D50(M)
D84D    = D84(M)
DMAXD   = DMAX(M)
VCDF    = 0.476*(D50D/PD)**0.053
SIGMAD  = (D84D/D16D)**0.5
PHDD    = PH(M)
END IF

DPTHCU = SUMYSU
IF(DPTHCU.GE.DPTH(M).AND. DPTHCU.LE.DPTH(M+1)) THEN

D16CU   = D16(M)
D50CU   = D50(M)
D84CU   = D84(M)
SIGMCU  = (D84CU/D16CU)**0.5

END IF

DPTHCD = SUMYSD
IF(DPTHCD.GE.DPTH(M).AND. DPTHCD.LE.DPTH(M+1)) THEN

D16CD   = D16(M)
D50CD   = D50(M)
D84CD   = D84(M)
SIGMCD  = (D84CD/D16CD)**0.5

END IF

1375  CONTINUE

C      DETERMINE FLOW VELOCITY DOWNFLOW,VORTEX VELOCITY VECTORS, AND
SCOUR FOR EACH HOUR OF STORM
C

VNUIN(L) = 0
IF(VNT(L).LT.0) VNUIN(L) = ABS(VNT(L))

VNU(1) = 0.5*VNUIN(1)
Do 1386 M=2, 120
VNU(M) = 0.5*(VNUIN(M)+ VNUIN(M-1))
1386  CONTINUE

IF(VNU(L).LT.0.1) VNU(L)= 0
IF(VNU(L).GT.0) THEN
IF(VNU(L).GT.VNUMAX) VNUMAX = VNU(L)
SUMVNU = SUMVNU + VNU(L)
CONVNU = CONVNU + 1
END IF

C Place maximum storm velocity in annual holding location VUPM

IF(VNU(L).GT.VUPM) VUPM = VNU(L)
IF(VUPM.GT.VUPMS) VUPMS = VUPM

```

```

*****
*****

```

```

C      Compute incremental contraction scour over time DLT      and
adjust flow depth to include the
C      lowering of the bed

      IF(CONTRA.EQ.1) THEN

C      Compute contraction scour using Straub's eqn

C       $q_s = (g*(S_s-1)*d_{50}^{*3})^{*0.5} * ((T/T_c) - 1)^{*2}$  English units,
d50 in feet

C      Converting the equations so that D50 is in mm and solving for
scour depth gives

C       $Y_S = (0.67/PD)*DLT*d_{50mm}^{*1.5}[(T/T_c)-1]^{*2}$ 

C       $T = 28.11*(Q/WB)^{*2} * [n^{*2}/Y_{TFF}^{*2.33}]$ 

C      If D50mm <0.065 then
C       $T_c = 4.84*D_{50mm}$ 
C      Else
C       $T_c = 0.8d_{50}^{*.67}*Y^{*.33}$ 

      IF ( D50CD.LT.0.065) THEN
        TAUCD(L) = 4.84*D50CD
      ELSE
        TAUCD(L) = 0.84*D50CD**0.67*YTRF(L)**0.33
      END IF

      TAUDD(L) = 28.11*(QTR(L)/WB)**2*(MAN**2/YTRF(L)**2.33)

      YSD(L) = 0
      IF ((TAUDD(L)/TAUCD(L)).GT.1) YSD(L) = COFDS*(0.67/PD)
      *DLT*D50CD**1.5*((TAUDD(L)/TAUCD(L))-1)**1.5

ELSE IF (CONTRA.EQ.2) THEN

      YSDIN=YTR(L)*(1.45*(VNU(L)/(32.2*YTR(L))**0.5)**0.2
      *COFDF*(1/SIGMCD**0.2)-1)

      IF(YSDIN.LE.0) YSDIN = 0

      YSD(L) = 0
      IF(YSDIN.GT.YDINMX) YSD(L) = YSDIN - YDINMX

      IF(YSDIN.GT.YDINMX) YDINMX = YSDIN
ELSE

      YSDIN = 0
      IF(COFD.GT.1) YSDIN = YTR(L)*(COFD - 1)

      YSD(L) = 0
      IF(YSDIN.GT.YDINMX) YSD(L) = YSDIN - SUMYSD

```

```

        IF(YSDIN.GT.YDINMX) YDINMX = YSDIN

END IF

SUMYSD= SUMYSD + YSD(L)

YTRF(L) = YTR(L) + SUMYSD

XADJAD(L) = 0.5*(TWBMLT(4)+TWBMLT(3))*SUMYSD

VNUA(L) = VNU(L)*XATOT(L)/(XATOT(L) + XADJAD(L))
IF(VNUA(L).GT.VNUPAM) VNUPAM = VNUA(L)

C      Recompute flowdepth and velocity, and computed local scour dept
to adjust for contraction
C      scour

        CSD(L) = CSD(L) - YSD(L)
        IF (YSD(L).GT.CSD(L)) CSD(L) = 0
        IF(CSD(L)+SUMYSD.LT.TSD) CSD(L) = TSD - SUMYSD

        LEW =L
        T(L)=LEW*DLT

        DSD(L) = CSD(L)/PD
C      Compute the scour angles along the downstream(THD) pier face

        THD(L) = PHDD
        IF (31*DSD(L)**2.LT.PHDD) THD(L) =31*DSD(L)**2

*****
*****

C      Compute downflow velocity on downstream faces of the pier

        IF(DSD(L).GT.100.OR.VNUA(L).LT.0.01) THEN
            VDD(L) = 0

            ELSE IF (DSD(L).LE.2.3.AND.YTRF(L).GT.MLT) THEN
                VDD(L) = VNUA(L)* (0.15*(DSD(L))
                + 0.24* PD **0.18/(YTRF(L)**0.18 * C1**0.5))

            ELSE IF (DSD(L).GT.2.3) THEN
                VDD(L) = VNUA(L)*(0.40/EXP(1+(3*(DSD(L)-4)) + 0.4))

        END IF

        IF(VDD(L).GT.0.8*VNUA(L)) VDD(L) = 0.8*VNUA(L)

C      Compute the maximum tangential velocities along the upstream(VMU)
and downstream
C      (VMD) pier faces

        VMD(L) = 2.7* VDD(L)
        IF(31*DSD(L)**2.LE.PHDD) VMD(L) = 2.24*C1**0.5*VDD(L)

```

```

C      Compute the A factors and tangential velocities (VTU)
C      along the upstream and downstream (VTD) pier faces

```

```

      AFD(L)=-0.0002*THD(L)**2+0.012*THD(L)+0.80

```

```

      VTD(L)=0

```

```

      IF(AFD(L).GT.0) VTD(L)=1.4*AFD(L)*VMD(L)*
      (1-EXP(-1.25*(1/AFD(L)**2)))

```

```

*****
*****

```

```

      UID(L)=0

```

```

      IF(YTRF(L).GT.0.AND.HCVIND.EQ.1) UID(L)=
      VCDF*(1.66*D50D**0.333*YTRF(L)**0.167)

```

```

      IF(YTRF(L).GT.0.AND.HCVIND.EQ.2) UID(L)= VCDF*0.09*
      (D50D*Tan(PHDD*RADCON)* YTRF(L)**0.33/(ALPHAD*MAN**2))**0.5

```

```

      IF(YTRF(L).GT.0.AND.HCVIND.EQ.3) UID(L)= VCDF*(0.024/MAN)*
      (D50D**0.5)*(YTRF(L)**0.167)

```

```

*****
*****

```

```

C      Compute armouring velocity

```

```

      VARMD(L)=0

```

```

      IF(ARMVEL.GT.0.AND.SIGMAD.GT.1.3) VARMD(L)=1.328*(D50D/1.8)**
      0.333*YTRF(L)**0.167

```

```

      IF(VARMD(L).LE.0) THEN
        VCRIND(L) = UID(L)

```

```

      ELSE IF(VTD(L).LE.VARMD(L).AND.VARMD(L).GT.0) THEN

```

```

        VCRIND(L) = VARMD(L)-(UID(L)/VCDF)

```

```

      ELSE IF (VTD(L).GT.VARMD(L).AND.VARMD(L).GT.0) THEN

```

```

        VCRIND(L) = VARMD(L)

```

```

      END IF

```

```

      IF(VCRIND(L).LT.UID(L)) VCRIND(L)= UID(L)

```

```

*****
*****

```

```

      DED(L) =0

```



```

      IF(VTD(L).GT.VCRIND(L)) DED(L)=(PD**BNDX)*TANH(YTRF(L)/PD)
      *((VTD(L)-VCRIND(L))**INDX)*(VNUA(L)/(32.2*PD)**0.5)**FREX

      TED(L)=0
      IF(VCRIND(L).GT.0.0.AND.(VTD(L)/UID(L)).GT.VCDF) THEN

      TED(L) = 24*30.89*(PD/VTD(L))*((VTD(L)/VCRIND(L))-0.4)*
      (YTRF(L)/PD)**0.25

      ELSE IF(YTRF(L)-6.0*PD.GT.0.AND.((VTD(L)/VCRIND(L))
      -VCDF).GT.0.0) THEN

      TED(L)= 24*48.26*(PD/VTD(L))*((VTD(L)/VCRIND(L))-0.4)
      END IF

*****
*****

      K1D(L)=0
      IF(TED(L).GE.0.001.AND.VTD(L).GT.0.03) K1D(L)= EXP(-0.08*
      (ABS((VCRIND(L)/VTD(L))*LOG(DLT/TED(L))))**1.2)

      K2D(L)=0
      IF(TED(L).GT.0.001) K2D(L)=(ABS(LOG(DLT/TED(L))))**0.2

      K3D(L)=0
      IF(VTD(L).GT.0.03) K3D(L) = 0.1*(DED(L)/DLT)
      *(VCRIND(L)/VTD(L))**1.2

      RLD(L)= K1D(L)* K2D(L)* K3D(L)

      CSD(L+1) = CSD(L) + (RLD(L)*DLT)
      IF(CSD(L+1).LT.CSD(L)) CSD(L+1) =CSD(L)

      TSD = CSD(L+1) + SUMYSD

*****
*****
C Repeat process for upstream pier face
*****
*****

      VNDIN(L) =0
      IF(VNT(L).GT.0) VNDIN(L) = ABS(VNT(L))

      VND(1) = 0.5*VNDIN(1)
      Do 1388 M=2, 120
      VND(M) = 0.5*(VNDIN(M)+ VNDIN(M-1))
1388 CONTINUE

      IF(VND(L).LT.0.1) VND(L)= 0
      IF(VND(L).GT.0) THEN
      IF(VND(L).GT.VNDMAX) VNDMAX = VND(L)
      SUMVND = SUMVND + VND(L)
      CONVND = CONVND + 1
      END IF

```

```

C Place maximum storm velocity in annual holding location VDWNM

      IF(VND(L).GT.VDWNM) VDWNM = VND(L)
      IF(VDWNM.GT.VDWNMS) VDWNMS = VDWNM

*****
*****

C      Compute incremental contraction scour over time DLT      and
adjust flow depth to include the
C      lowering of the bed

      IF(CONTRA.EQ.1) THEN

C      Compute contraction scour using Straub's eqn

C       $q_s = (g \cdot (S_s - 1) \cdot d_{50}^{*3})^{*0.5} \cdot ((T/T_c) - 1)^{*2}$  English units,
d50 in feet

C      Converting the equations so that D50 is in mm and solving for
scour depth
C      gives

C       $Y_S = (0.67/PD) \cdot DLT \cdot d_{50mm}^{*1.5} \cdot [(T/T_c) - 1]^{*2}$ 

C       $T = 28.11 \cdot (Q/WB)^{*2} \cdot [n^{*2}/YTFF^{*2.33}]$ 

C      If D50mm < 0.065 then
C       $T_c = 4.84 \cdot D50mm$ 
C      Else
C       $T_c = 0.8d_{50}^{*.67} \cdot Y^{*.33}$ 

      IF ( D50CU.LT.0.065) THEN
        TAUCU(L) = 4.84*D50CU
      ELSE
        TAUCU(L) = 0.84*D50CU**0.67*YTFF(L)**0.33
      END IF

      TAUDU(L) = 28.11*(QTF(L)/WB)**2*(MAN**2/YTFF(L)**2.33)

      YSU(L) = 0
      IF((TAUDU(L)/TAUCU(L)).GT.1) YSU(L) = COFUS*(0.67/PD)*
      DLT*D50CU**1.5*((TAUDU(L)/TAUCU(L))-1)**1.5

ELSE IF (CONTRA.EQ.2) THEN

      YSUIN =YTF(L)*(1.45*(VND(L)/(32.2*YTF(L))**0.5)**0.2
      *COFUF*(1/SIGMCU**0.2)-1)

      IF(YSUIN.LE.0) YSUIN = 0

      YSU(L) = 0
      IF(YSUIN.GT.YUINMX) YSU(L) = YSUIN - YUINMX

      IF(YSUIN.GT.YUINMX) YUINMX = YSUIN

```

```

ELSE

    YSUIN = 0

    IF(COFU.GT.1) YSUIN = YTF(L)*(COFU - 1)

    YSU(L) = 0
    IF(YSUIN.GT.YUINMX) YSU(L) = YSUIN - YUINMX

    IF(YSUIN.GT.YUINMX) YUINMX = YSUIN
    END IF

    SUMYSU= SUMYSU + YSU(L)

    YTFF(L) = YTF(L) + SUMYSU

    XADJAU(L) = 0.5*(TWBMLT(4)+TWBMLT(3))*SUMYSU

    VNDA(L) = VND(L)*XATOT(L)/(XATOT(L) + XADJAU(L))
    IF(VNDA(L).GT.VNDNAM) VNDNAM = VNDA(L)

C      Recompute flowdepth and velocity, and computed local scour dept
to adjust
C      for contraction
C      scour

    CSU(L) = CSU(L) - YSU(L)

    IF (YSU(L).GT.CSU(L)) CSU(L) = 0
    IF(CSU(L)+SUMYSU.LT.TSU) CSU(L) = TSU - SUMYSU

    LEW =L
    T(L)=LEW*DLT

    DSU(L) = CSU(L)/PD

C      Compute the scour angles along the upstream(THU) pier face

    THU(L) = PHU
    IF (31*DSU(L)**2.LT.PHU) THU(L) = 31*DSU(L)**2

C      Compute downflow velocity on upstream face of the pier

    IF(DSU(L).GT.100.OR.VNDA(L).LT.0.10) THEN
        VDU(L) = 0

    ELSE IF (DSU(L).LE.2.3.AND.YTFF(L).GT.MLT) THEN
        VDU(L)= VNDA(L)*(0.15 * (DSU(L))
        + 0.24*PD ** 0.18/(YTFF(L)**0.18* C1**0.5))

    ELSE IF (DSU(L).GT.2.3) THEN
        VDU(L) = VNDA(L)*(0.40/(1+EXP(3*(DSU(L)-4)) + 0.4))

```

```

      END IF

      IF(VDU(L).GT.0.8*VNDA(L)) VDU(L) = 0.8*VNDA(L)

*****
*****

C
C
      VMU(L) = 2.7* VDU(L)
      IF(31*DSU(L)**2.LE.PHU) VMU(L) = 2.24*C1**0.5*VDU(L)

      AFU(L) = -0.0002*THU(L)**2+0.012*THU(L)+0.80

      VTU(L)=0
      IF(AFU(L).GT.0) VTU(L)=1.4*AFU(L)*VMU(L)*
      (1-EXP(-1.25*(1/AFU(L)**2)))

*****
*****

      UIU(L)=0

      IF(YTFF(L).GT.0.AND.HCVIND.EQ.1) UIU(L)=
      VCUF*(1.66*D50U**0.333*YTFF(L)**0.167)

      IF(YTFF(L).GT.0.AND.HCVIND.EQ.2) UIU(L)= VCUF*0.09*
      (D50U*Tan(PHU*RADCON)* YTFF(L)**0.33/(ALPHAU*MAN**2))**0.5

      IF(YTFF(L).GT.0.AND.HCVIND.EQ.3) UIU(L)= VCUF*(0.024/MAN)*
      (D50U**0.5)*(YTFF(L)**0.167)

*****
*****

C      Compute armouring velocity

      VARMU(L)=0
      IF(ARMVEL.GT.0.AND.SIGMAU.GT.1.3) VARMU(L)=1.328*(DMAXU/1.8)**
      0.333*YTFF(L)**0.167

      IF(VARMU(L).LE.0) THEN
        VCRINU(L) = UIU(L)

      ELSE IF(VTU(L).LE.VARMU(L).AND.VARMU(L).GT.0) THEN

        VCRINU(L) = VARMU(L)-(UIU(L)/VCUF)

      ELSE IF (VTU(L).GT.VARMU(L).AND.VARMU(L).GT.0) THEN

        VCRINU(L) = VARMU(L)

      END IF

      IF(VCRINU(L).LT.UIU(L)) VCRINU(L)= UIU(L)

```

```
*****
*****
```

```

      DEU(L) =0
      IF(VTU(L).GT.VCRINU(L)) DEU(L)=(PD**BNDX)*TANH(YTFF(L)/PD)
      *((VTU(L)-VCRINU(L))**INDX)*(VNDA(L)/(32.2*PD)**0.5)**FREX

      TEU(L)=0
      IF(VCRINU(L).GT.0.0.AND.(VTU(L)/UIU(L)).GT.VCUF) THEN

      TEU(L) = 24*30.89*(PD/VTU(L))*((VTU(L)/VCRINU(L))- 0.4)*
      * (YTFF(L)/PD)**0.25

      ELSE IF(YTFF(L)-6.0*PD.GT.0.AND.((VTU(L)/VCRINU(L))
      -VCUF).GT.0.0) THEN

      TEU(L)= 24*48.26*(PD/VTU(L))*((VTU(L)/VCRINU(L))-0.4)
      END IF

```

```
*****
*****
```

```

      K1U(L)=0
      IF(TEU(L).GT.0.001.AND.VTU(L).GT.0.03) K1U(L)= EXP(-0.08
      *(ABS((VCRINU(L)/VTU(L))*LOG(DLT/TEU(L))))**1.2)

      K2U(L)=0
      IF(TEU(L).GT.0.001) K2U(L)= (ABS(LOG(DLT/TEU(L))))**0.2

      K3U(L)=0
      IF(VTU(L).GT.0.03) K3U(L) = 0.1*(DEU(L)/DLT)
      *(ABS(VCRINU(L)/VTU(L)))*1.2

```

```
*****
*****
```

```

      RLU(L)= K1U(L)* K2U(L)* K3U(L)

      CSU(L+1) = CSU(L) + (RLU(L)*DLT)
      IF(CSU(L+1).LT.CSU(L)) CSU(L+1) = CSU(L)
      TSU = CSU(L+1) +SUMYSU

      IF(YTRF(L).GT.YTMRF) YTMRF= YTRF(L)
      IF(YTFF(L).GT.YTMFF) YTMFF= YTFF(L)

      IF(VTD(L).GT.VTDMX) VTDMX= VTD(L)
      IF(VTU(L).GT.VTUMX) VTUMX= VTU(L)

      IF(VTD(L).GT.VTDMX) VTDMX= VTD(L)
      IF(VTU(L).GT.VTUMX) VTUMX= VTU(L)

      IF(UIU(L).LT.UIUMIN) UIUMIN= UIU(L)
      IF(UID(L).LT.UIDMIN) UIDMIN= UID(L)

```

```

1390  CONTINUE

*****
*****

      THSD=TSD

C Compute Contraction scour and sum to local scour to obtain total
scour for
C  downstream face for each storm

      THSU=TSU

*****
*****
*****

C Compute Contraction scour and sum to local scour to obtain total
scour for
C  downstream face for each storm

      SMTHSD = SMTHSD + THSD

C      SQTHSD is the square of THSD

C      SSQHSD is the sum of the squares of THSD

      SQTHSD = THSD**2

      SSQHSD = SSQHSD + SQTHSD

C Compute Contraction scour and sum to local scour to obtain total
scour for
C  downstream face for each storm

      SMTHSU = SMTHSU + THSU

C      SSQHSU is the sum of the squares of THSU

      SQTHSU = THSU**2

      SSQHSU = SSQHSU + SQTHSU

*****
*****
*****

1435  CONTINUE

      IF(YRS.EQ.0) GO TO 1445

C      COMPUTE PARAMETERS TO DETERMINE MEAN AND STANDARD DEVIATION
C      IN THE RESULTS OF THE SCOUR SIMULATIONS

C      DEVELOPE HISTOGRAM FOR THE CONTINUOUS SIMULATION

```

```

C      PLACE INPUTS IN THE FIRST RANGE
      IF(TSD.LT.B(1)) FD(1)=FD(1) + 1
      IF(TSU.LT.B(1)) FU(1)=FU(1) + 1

C      PLACE INPUTS IN THE INTERIOR AND LAST RANGE

      DO 1440 J = 1, 99
        IF(TSD.GE.B(J).AND.TSD.LT.B(J+1)) FD(J+1) =FD(J+1) + 1
        IF(TSU.GE.B(J).AND.TSU.LT.B(J+1)) FU(J+1) =FU(J+1) + 1
1440    CONTINUE
C      Continue 1445 to match GO TO statement 1445

1445 CONTINUE
C      DEVELOPE HISTOGRAM FOR THE HURRICANE SIMULATION

C      PLACE INPUTS IN THE FIRST RANGE

      IF (HCAT.EQ.0) GO TO 1460

      IF(THSD.LT.B(1)) FHD(1)=FHD(1) + 1
      IF(THSU.LT.B(1)) FHU(1)=FHU(1) + 1

C      PLACE INPUTS IN THE INTERIOR AND LAST RANGE

      DO 1450 J = 1, 99
        IF(THSD.GE.B(J).AND.THSD.LT.B(J+1)) FHD(J+1) =FHD(J+1) + 1
        IF(THSU.GE.B(J).AND.THSU.LT.B(J+1)) FHU(J+1) =FHU(J+1) + 1
1450    CONTINUE

1460    CONTINUE

1500 CONTINUE

C      MNTHSD is the mean hurricane scour on the downstream pier face

      MNTHSD = SMTHSD/ENS
C      STDHSD is the standard deviation in the hurricane scour on the
C      downstream face
C
      STDHSD = SQRT(ABS((SSQHSD - SMTHSD**2/ENS)/(ENS-1.0)))

C      MNTHSU is the mean hurricane scour on the upstream pier face

      MNTHSU = SMTHSU/TMS

C      STDHSD is the standard deviation in the hurricane scour on the
upstream
C      face

      STDHSU = SQRT(ABS((SSQHSU - SMTHSU**2/ENS)/(ENS-1.0)))

C      DIVIDE THE COUNT IN EACH BOUND RANGE BY THE NUMBER OF
C      SIMULATIONS TO GET THE PROBABILITY OF EACH RANGE
      IF(YRS.EQ.0) GO TO 1503
      PRD(1) = FD(1) / TMS

```

```

        PRU(1) = FU(1) / TMS
1503 CONTINUE

        IF (HCAT.EQ.0) GO TO 1504

        PRHD(1) = FHD(1) / TMS
        PRHU(1) = FHU(1) / TMS

1504 CONTINUE

        IF(YRS.EQ.0) GO TO 1506

        DO 1505 I = 2, 100
            PRD(I) =FD(I)/TMS
            PRU(I) =FU(I)/TMS
1505 CONTINUE

1506 CONTINUE
        IF (HCAT.EQ.0) GO TO 1510

        DO 1508 I =2, 100
            PRHD(I) =FHD(I)/TMS
            PRHU(I) =FHU(I)/TMS
1508 CONTINUE
1510 CONTINUE


        IF(YRS.EQ.0) GO TO 1512

        CPRD(1) = PRD(1)
        CPRU(1) = PRU(1)
1512 CONTINUE

        IF (HCAT.EQ.0) GO TO 1515
        CPRHD(1) = PRHD(1)
        CPRHU(1) = PRHU(1)
1515 CONTINUE

        IF(YRS.EQ.0) GO TO 1517

        Do 1516 I=2, 100
            CPRD(I) = CPRD(I-1)+ PRD(I)
            CPRU(I) = CPRU(I-1)+ PRU(I)

1516 CONTINUE
1517 CONTINUE


        IF (HCAT.EQ.0) GO TO 1520

        DO 1518 I= 2, 100
            CPRHD(I) = CPRHD(I-1)+ PRHD(I)
            CPRHU(I) = CPRHU(I-1)+ PRHU(I)
1518 CONTINUE
1520 CONTINUE

```



```

IF(YRS.EQ.0) GO TO 5300

PRD15(1) = FD15(1) / TMS
PRU15(1) = FU15(1) / TMS

CPRD15(1) = PRD15(1)
CPRU15(1) = PRU15(1)

Do 5000 I=2, 100
PRD15(I) =FD15(I)/TMS
PRU15(I) =FU15(I)/TMS

CPRD15(I) = CPRD15(I-1)+ PRD15(I)
CPRU15(I) = CPRU15(I-1)+ PRU15(I)
5000 CONTINUE


PRD25(1) = FD25(1) / TMS
PRU25(1) = FU25(1) / TMS

CPRD25(1) = PRD25(1)
CPRU25(1) = PRU25(1)

Do 5100 I=2, 100
PRD25(I) =FD25(I)/TMS
PRU25(I) =FU25(I)/TMS

CPRD25(I) = CPRD25(I-1)+ PRD25(I)
CPRU25(I) = CPRU25(I-1)+ PRU25(I)
5100 CONTINUE


PRD50(1) = FD50(1) / TMS
PRU50(1) = FU50(1) / TMS

CPRD50(1) = PRD50(1)
CPRU50(1) = PRU50(1)

Do 5200 I=2, 100
PRD50(I) =FD50(I)/TMS
PRU50(I) =FU50(I)/TMS

CPRD50(I) = CPRD50(I-1)+ PRD50(I)
CPRU50(I) = CPRU50(I-1)+ PRU50(I)
5200 CONTINUE


PRD75(1) = FD75(1) / TMS
PRU75(1) = FU75(1) / TMS

CPRD75(1) = PRD75(1)
CPRU75(1) = PRU75(1)

Do 5250 I=2, 100
PRD75(I) =FD75(I)/TMS
PRU75(I) =FU75(I)/TMS

```

```

        CPRD75(I) = CPRD75(I-1)+ PRD75(I)
        CPRU75(I) = CPRU75(I-1)+ PRU75(I)

5250 CONTINUE

C        5300 connected to above go to statement
5300 CONTINUE

C        DISPLAY RESULTS

        WRITE(12,*)'RUN TITLE IS',TITLE
        WRITE(12,*)'RUN DATE IS',DATE
        IF(TUI.NE.0.00.OR.TDI.NE.0) THEN
        WRITE(12,*)'THE PROGRAM WAS EXECUTED IN THE EXISTING PIER ANALYSI
        `S MODE.'
        ELSE
        WRITE(12,*)'THE PROGRAM WAS EXECUTED IN PIER DESIGN MODE.'
        END IF

        IF ( CONTRA.EQ.1) THEN
        WRITE(12,*)'CONTRACTION SCOUR METHOD IS STRABS EQUATION'
        ELSE IF(CONTRA.EQ.2) THEN
        WRITE(12,*)'CONTRACTION SCOUR METHOD IS KOMURAS EQN'
        ELSE IF (CONTRA.EQ.3) THEN
        WRITE(12,*)'CONTRACTION SCOUR METHOD IS HEC18'
        END IF

        IF(ARMVEL.GT.0) THEN
        WRITE(12,*)' SCOUR COMPUTED CONSIDERING ARMOURING'
        ELSE
        WRITE(12,*)' SCOUR COMPUTED WITHOUT ARMOURING'
        END IF

        IF(ACTNM.LE.1) THEN
        WRITE(12,*)'BRUBAKER-DEMETRIUS NEILLS MODIFICATION FACTOR NOT
USED `
        ELSE
        WRITE(12,*)'BRUBAKER-DEMETRIUS NEILLS MODIFICATION FACTOR
ACTIVATE `D'
        END IF

        IF(DISCON.LE.1) THEN
        WRITE(12,*)'TIDE DISTORTION OPTION NOT USED'
        ELSE
        WRITE(12,*)'TIDE DISTORTION OPTION ACTIVATED'
        END IF

        WRITE(12,*)'MEAN TIDAL DEPTH MDR is =',MDR
        WRITE(12,*)'MEAN LOW TIDAL DEPTH MLT is =',MLT
        WRITE(12,*)'MEAN LOW TIDE ELEVATION MLTE is =',MLTE
        WRITE(12,*)'TIDAL AMP. AT BRIDGE XSEC MTR is =',MTR
        WRITE(12,*)'CHANNEL INVERT AT BRIDGE IRS is =',IRS
        WRITE(12,*)

```

```

WRITE(12,*)
WRITE(12,*) 'Estuary in bank area is =',XABMLE
WRITE(12,*)
WRITE(12,*)
WRITE(12,*) 'Maximum tide in the simulation HITIDE is =',HITIDE
WRITE(12,*) 'Maximum u/s flow depth in sim. YTRMXS is =',YTRMXS
WRITE(12,*) 'Maximum d/s flow depth in sim. YTFMXS is =',YTFMXS

WRITE(12,*) 'Maximum u/s disch. in sim. QTRMXS is =',QTRMXS
WRITE(12,*) 'Maximum d/s disch. in sim. QTFMXS is =',QTFMXS

WRITE(12,*) 'Maximum u/s vel.in sim. VUPMS is =',VUPMS
WRITE(12,*) 'Maximum d/s vel.in sim. VDOWNMS is =',VDWNMS

IF(YRS.GT.0) WRITE(12,*) 'Maximum u/s face tang.vel.in sim.
VTUMXS
`is =',VTUMXS

IF(YRS.GT.0) WRITE(12,*) 'Maximum d/s face tang.vel.in sim.
VTDMXS
`is =',VTDMXS

WRITE(12,*)
WRITE(12,*)
WRITE(12,*) 'Maximum u/s flow depth last run YTRMAX is =',YTRMAX
WRITE(12,*) 'Maximum d/s flow depth last run YTFMAX is =',YTFMAX

WRITE(12,*) 'Maximum u/s discharge last run QTRMAX is =',QTRMAX
WRITE(12,*) 'Maximum d/s discharge last run QTFMAX is =',QTFMAX

WRITE(12,*) 'Maximum u/s velocity last run VNUMAX is =',VNUMAX
WRITE(12,*) 'Maximum d/s velocity last run VNDMAX is =',VNDMAX

WRITE(12,*) 'Maximum tangential vel d/s face last run VTDMX is ='
`,VTDMX
WRITE(12,*) 'Maximum tangential vel u/s face last run VTUMX is ='
`,VTUMX

WRITE(12,*) 'critical vel u/s face last run UIUMIN is ='
`,UIUMIN
WRITE(12,*) 'critical vel d/s face last run UIDMIN is ='
`,UIDMIN

WRITE(12,*)
WRITE (12,*) 'Time of concentration = ', TC,'hrs'
WRITE (12,*) 'Time to peak = ', TP,'hrs'
WRITE (12,*) 'Number of unit hydrograph ordinates = ', NU
WRITE (12,*) 'Soil infiltration potential = ', SC
WRITE (12,*) 'Peak discharge of the UHG = ', QP,'cfs'
WRITE (12,*) 'Initial abstractions IA = ', IA, 'in'

WRITE (12,*) 'UNIT HYDROGRAPH INFORMATION'
WRITE (12,*) 'TIME ORDINATES'

```

```

WRITE (12,*) (T(I),I=1,NU)

WRITE (12,*) 'DISCHARGE ORDINATES'
WRITE (12,*) (QU(I), I=1,NU)

WRITE (12,*) 'Catchment base flow = ', QBF,'cfs'
WRITE (12,*) 'Tide attenuation factor TAF = ', TAF
WRITE (12,*) 'Tidal lag MTL= ', MTL,'hrs'
WRITE (12,*) 'Tidal routing constant CX = ', CX
WRITE (12,*) 'Bridge station tidal range TR = ', TR,'ft'
WRITE (12,*) 'Effective bottom channel width at brdg.WBE = ', WBE,
`'ft'
WRITE (12,*) 'Estuary Area', AS

WRITE (12,*) 'Contraction scour factor u/s face= ',COFU
WRITE (12,*) 'Contraction scour factor d/s face= ',COFD

WRITE (12,*) 'Estuary to wavelength ratio DIM = ', DIM
WRITE (12,*) 'Estuary width factor WF = ', WF
WRITE (12,*) 'Tidal range factor HF = ', HF
WRITE (12,*) 'Neill Mod. factor rising limb.NMRF = ',NMFR
WRITE (12,*) 'Neill Mod. factor falling limb.NMFF = ',NMFF
WRITE (12,*)
WRITE (12,*)

WRITE (12,*) 'The maximum storm event in the simulation
is',PPTMAX,
`'ins'

IF(YRS.GT.0) THEN

WRITE(12,*) 'ANNUAL MAX UPSTREAM VELOCITY LAST RUN =',VUPYR
WRITE(12,*) 'ANNUAL MAX DWNSTREAM VELOCITY LAST RUN =',VDNYR

WRITE(12,*) 'ANNUAL MAX US ADJUSTED VELOCITY LAST RUN =',VNUAYR
WRITE(12,*) 'ANNUAL MAX DS ADJUSTED VELOCITY LAST RUN =',VNDAYR

WRITE(12,*) 'ANNUAL MAX UPSTREAM DISCHARGE LAST RUN =',QUPYR
WRITE(12,*) 'ANNUAL MAX DWNSTREAM DISCHARGE LAST RUN =',QDNYR

WRITE(12,*) 'ANNUAL PK DISCHARGE FROM 6 HR STORM (L.R) =',QPK6
WRITE(12,*) 'ANNUAL PK DISCHARGE FROM 18 HR STORM (L.R) =',QPK18
WRITE(12,*) 'ANNUAL PK DISCHARGE FROM 24 HR STORM (L.R) =',QPK24
WRITE(12,*) 'ANNUAL PK DISCHARGE FROM 36 HR STORM (L.R) =',QPK36

WRITE(12,*) 'ANNUAL MAX FLOW DEPTH LAST RUN = YTYRS(J)',YTYRS

WRITE(12,*) 'ANNUAL MAX UPSTREAM FLOW DEPTH LAST RUN =',YTRYRS
WRITE(12,*) 'ANNUAL MAX DWNTREAM FLOW DEPTH LAST RUN =',YTFYRS

WRITE(12,*) 'ANNUAL MAX US ADJ. FLOW DEPTH LAST RUN =',YTRFYR
WRITE(12,*) 'ANNUAL MAX DS ADJ. FLOW DEPTH LAST RUN =',YTFFYR

WRITE(12,*) 'ANNUAL AVG MAX UPSTREAM VELOCITY =',AVUPYR
WRITE(12,*) 'ANNUAL AVG MAX DWNSTREAM VELOCITY =',AVDNYR

```

```

WRITE (12,*)'The no.of storms in the last.NS= ',NS
WRITE (12,*)'The no.of storms producing no runoff over the simula
`tion.NORUN= ',NORUN

WRITE(12,*)

WRITE (12,*)'The number of 6 hr storms in YRS is = ',N6
WRITE (12,*)'The number of 18 hr storms in YRS is = ',N18
WRITE (12,*)'The number of 24 hr storms in YRS is = ',N24
WRITE (12,*)'The number of 36 hr storms in YRS is = ',N36

WRITE (12,*)'The number of 6 hr runoff hyd.ordinates is = ',NR6
WRITE (12,*)'The number of 18 hr runoff hyd.ordinates is = ',NR18
WRITE (12,*)'The number of 24 hr runoff hyd,ordinates is = ',NR24
WRITE (12,*)'The number of 36 hr runoff hyd.ordinates is = ',NR36

WRITE (12,*)'UVAR6 last run is = ',UVAR6
WRITE (12,*)'UVAR18 last run is = ',UVAR18
WRITE (12,*)'UVAR24 last run is = ',UVAR24
WRITE (12,*)'UVAR36 last run is = ',UVAR36

WRITE (12,*)'The avg. 6hr. annual rainfall amt. is = ',ASUM6,'in'
WRITE (12,*)'The avg. 18hr.annual rainfall amt. is =
',ASUM18,'in'
WRITE (12,*)'The avg. 24hr.annual rainfall amt. is =
',ASUM24,'in'
WRITE (12,*)'The avg. 36hr.annual rainfall amt. is =
',ASUM36,'in'

WRITE (12,*)'The 6hr. rainfall amt.last run is = ',PPT6,'in'
WRITE (12,*)'The 18hr. rainfall amt.last run is = ',PPT18,'in'
WRITE (12,*)'The 24hr. rainfall amt.last run is = ',PPT24,'in'
WRITE (12,*)'The 36hr. rainfall amt.last run is = ',PPT36,'in'

WRITE (12,*)'The hrly. rainfall for 6hr storm last run is = ',P6
WRITE (12,*)'The hrly. rainfall for 18hr storm last run is =
',P18
WRITE (12,*)'The hrly. rainfall fot 24hr storm last run is =
',P24
WRITE (12,*)'The hrly. rainfall fot 36hr storm last run is =
',P36

WRITE (12,*)'The 6 hr.storm direct runoff array is = ',PE6
WRITE (12,*)'The 18 hr.storm direct runoff array is = ',PE18
WRITE (12,*)'The 24 hr.storm direct runoff array is = ',PE24
WRITE (12,*)'The 36 hr.storm direct runoff array is = ',PE36

WRITE (12,*)'The 6 hr incremental runoff array is = ',PEI6
WRITE (12,*)'The 18 hr incremental runoff array is = ',PEI18
WRITE (12,*)'The 24 hr incremental runoff array is = ',PEI24
WRITE (12,*)'The 36 hr incremental runoff array is = ',PEI36

WRITE (12,*)'The 6 hr DRO hydrograph last run is = ' ,
`(DRO6(I), I=1,ARR)
WRITE (12,*)'The 18 hr DRO hydrograph last run is = ' ,
`(DRO18(I), I=1,ARR)

```

```

WRITE (12,*)'The 24 hr DRO hydrograph last run is = ' ,
` (DRO24(I), I=1,ARR)
WRITE (12,*)'The 36 hr DRO hydrograph last run is = ' ,
` (DRO36(I), I=1,ARR)

WRITE (12,*)'The 6 hr Catchment hydrograph is = ' ,
` (CHY6(I), I=1,ARR)
WRITE (12,*)'The 18 hr Catchment hydrograph is = ' ,
` (CHY18(I), I=1,ARR)
WRITE (12,*)'The 24 hr Catchment hydrograph is = ' ,
` (CHY24(I), I=1,ARR)
WRITE (12,*)'The 36 hr Catchment hydrograph is = ' ,
` (CHY36(I), I=1,ARR)

C*****
*****

IF(HCAT.GT.0) THEN

WRITE (12,*)'The hurricane normal tide elevation at bridge is
` ' ,TER,'ft'

WRITE (12,*)'The hurricane rainfall is' ,HURPPT,'ins'
WRITE (12,*)'The hurricane surge is' ,
` (HSURGE(I),I=1,120),'ft'
WRITE (12,*)'The total hurricane elev at bridge is ' ,
` (HTER(I),I=1,120),'ft'
WRITE (12,*)'The total hurricane depth at bridge is ' ,
` (HYAT(I),I=1,120),'ft'
ELSE

GO TO 1522
END IF
C*****
*****
1522 CONTINUE

WRITE (12,*)'Highest base sta. tidal depth ',HIBASE
WRITE (12,*)'Highest bridge sta. tidal elev ',HIELE

WRITE (12,*)'Array of base sta. tidal elev TEB= ' ,
` (TEB(I),I=1,ARR),'ft'
WRITE (12,*)'Array of base sta. tidal depths is YB= ' ,
` (YB(I),I=1,ARR),'ft'

IF(DISCON.EQ.0) THEN
WRITE (12,*)'Array of brdg.sta.tide elev is TER, ='
WRITE (12,*)(TER(I), I=1,ARR)
WRITE (12,*)'Array routed dpths. at bridge sta.is YAT= '
WRITE (12,*)(YAT(I), I=1,ARR)
WRITE (12,*)'Maximum tidal depth at bridge sta. is ',HITIDE
ELSE
GO TO 1600
END IF

1600 CONTINUE

```

```

      IF(DISCON.GT.0) WRITE (12,*)'Array of norm.wave arrival time at
`bridge is TNR= ',(TNR(I), I=1,ARR)
      IF(DISCON.GT.0) WRITE (12,*)'Array of interpolated arrival time
`is TNRI= ',(TNRI(I), I=1,ARR)
      IF(DISCON.GT.0) WRITE (12,*)'Array of interpolated routed bridge
`elev is TERI= ',(TERI(I), I=1,ARR)
      IF(DISCON.GT.0) WRITE (12,*)'Array of interpolated routed depths
`is YATI= ',(YATI(I), I=1,ARR)

      IF(DISCON.GT.0) WRITE (12,*)'Maximum tidal depth at bridge sta.
`is ',HITIDE

      WRITE (12,*)'Array of Neills discharge is QN= ',(QN(I),I=1,ARR)
      WRITE (12,*)'Array of mod Neills disch.is QNM =
',(QNM(I),I=1,ARR)
      WRITE (12,*)'Array of total combined depth at bridge is YT= ',
`(YT(I), I=1,ARR)

      WRITE (12,*)'Array of total combined depth at bridge d/s face is
`YTR= ',(YTR(I), I=1,ARR)
      WRITE (12,*)'Array of total combined depth at bridge u/s face is
`YTF= ',(YTF(I), I=1,ARR)

      WRITE (12,*)'Array of total adjusted depth at bridge d/s face is
`YTRF= ',(YTRF(I), I=1,ARR)
      WRITE (12,*)'Array of total adjusted depth at bridge u/s face is
`YTFF= ',(YTFF(I), I=1,ARR)

      WRITE (12,*)'Array total net disch. value at bridge is QT= ',
'(QT(I), I=1,ARR)
      WRITE (12,*)'Array of total net velocity at bridge is VNT = ',
`(VNT(I), I=1,ARR)
      WRITE (12,*)'Array of net adjusted vel.upstream is VNUA = ',
`(VNUA(I), I=1,ARR)
      WRITE (12,*)'Array of net adjusted vel.downstream is VNDA= ',
`(VNDA(I), I=1,ARR)
      WRITE (12,*)'Array of net vel.u/stream is VNU =
',(VNU(I),I=1,ARR)
      WRITE (12,*)'Array of net vel.d/stream is VND= ',(VND(I),
I=1,ARR)

      WRITE (12,*)'Array of downflow velocity d/s face is VDD= ',
`(VDD(I), I=1,ARR)
      WRITE (12,*)'Array of downflow velocity u/s face is VDU= ',
`(VDU(I), I=1,ARR)

      WRITE (12,*)'Array of tangential velocity d/s face is VTD= ',
`(VTD(I), I=1,ARR)
      WRITE (12,*)'Array of tangential velocity u/s face is VTU= ',
`(VTU(I), I=1,ARR)

      WRITE (12,*)'Total scour d/s face last run is TSD = ',TSD
      WRITE (12,*)'Total scour u/s face last run is TSU = ',TSU

      WRITE (12,*)'Total scour local d/s face last run is CSD = ',

```

```

      `(CSD(I), I=1,ARR)
      WRITE (12,*)'Total scour local u/s face last run is CSU = ',
      `(CSU(I), I=1,ARR)

      WRITE (12,*)'Total contraction scour d/s face is YSD',
      `(YSD(I), I=1,ARR)
      WRITE (12,*)'Total contraction scour u/s face is',
      `(YSU(I), I=1,ARR)

      WRITE (12,*)'          B          FD          PRD          CPRD'
      Do 1650 I = 1,100
      WRITE (12,1640)B(I), FD(I), PRD(I), CPRD(I)
1640  FORMAT(1X,4F12.4)
1650 CONTINUE

      WRITE (12,*)'          B          FU          PRU          CPRU'
      Do 1660 I = 1,100
      WRITE (12,1655)B(I), FU(I), PRU(I), CPRU(I)
1655  FORMAT(1X,4F12.4)
1660 CONTINUE

C*****
*****

      WRITE (12,*)'15 PERCENT TMS SCOUR RESULTS'
      WRITE (12,*)'          B          FD15          PRD15
CPRD15'
      Do 5500 I = 1,100
      WRITE (12,5450)B(I), FD15(I), PRD15(I), CPRD15(I)
5450  FORMAT(1X,4F12.4)
5500 CONTINUE

      WRITE (12,*)'          B          FU15          PRU15
CPRU15'
      Do 5600 I = 1,100
      WRITE (12,5550)B(I), FU15(I), PRU15(I), CPRU15(I)
5550  FORMAT(1X,4F12.4)
5600 CONTINUE

      WRITE (12,*)'25 PERCENT SCOUR RESULTS'
      WRITE (12,*)'          B          FD25          PRD25
CPRD25'
      Do 5700 I = 1,100
      WRITE (12,5650)B(I), FD25(I), PRD25(I), CPRD25(I)
5650  FORMAT(1X,4F12.4)
5700 CONTINUE

      WRITE (12,*)'          B          FU25          PRU25
CPRU25'
      Do 5800 I = 1,100
      WRITE (12,5750)B(I), FU25(I), PRU25(I), CPRU25(I)
5750  FORMAT(1X,4F12.4)
5800 CONTINUE

```



```

        WRITE (12,*)'50 PERCENT TMS SCOUR RESULTS'
        WRITE (12,*)'          B          FD50          PRD50
CPRD50'
        Do 5900 I = 1,100
        WRITE (12,5850)B(I),  FD50(I),  PRD50(I), CPRD50(I)
5850  FORMAT(1X,4F12.4)
5900  CONTINUE

        WRITE (12,*)'          B          FU50          PRU50
CPRU50'
        Do 6000 I = 1,100
        WRITE (12,5950)B(I),  FU50(I),  PRU50(I), CPRU50(I)
5950  FORMAT(1X,4F12.4)
6000  CONTINUE

        WRITE (12,*)'75 PERCENT TMS SCOUR RESULTS'
        WRITE (12,*)'          B          FD75          PRD75
CPRD75'
        Do 6100 I = 1,100
        WRITE (12,6050)B(I),  FD75(I),  PRD75(I), CPRD75(I)
6050  FORMAT(1X,4F12.4)
6100  CONTINUE

        WRITE (12,*)'          B          FU75          PRU75
CPRU75'
        Do 6200 I = 1,100
        WRITE (12,6150)B(I),  FU75(I),  PRU75(I), CPRU75(I)
6150  FORMAT(1X,4F12.4)
6200  CONTINUE

        WRITE (12,*)'The mean annual contraction scour d/s face is
MNYYSO'
        WRITE (12,*)'The mean annual scour value d/s face is MNLTSD'
        WRITE (12,*)'The mean annual total scour d/s face is YMNTSD'
        WRITE (12,*)'The standard dev in annual scour d/s face is YSTTSD'

        Do 1665 I=1,YRS
        YR(I) = I
1665  CONTINUE

        WRITE (12,*)'YR          MNYYSO          MNLSO          YMNTSD
YSTTSD'

        Do 1680 I = 1, YRS
        WRITE (12,1675)YR(I), MNYYSO(I),  MNLSO(I), YMNTSD(I), YSTTSD(I)
1675  FORMAT(1X,I3.3,4F12.4)
1680  CONTINUE

        WRITE (12,*)'The annual contraction scour u/s face is MNYYSU'
        WRITE (12,*)'The mean annual local scour value u/s face is MNLSU'
        WRITE (12,*)'The mean annual total scour value u/s face is
YMNTSU'
        WRITE (12,*)'The standard dev in annual scour u/s face is YSTTSU'

```

```

WRITE (12,*)'YR          MNYYSU          MNLSU          YMNTSU          YSTTSU'

  Do 1690 I = 1,YRS
    WRITE (12,1685)YR(I), MNYYSU(I), MNLSU(I), YMNTSU(I), YSTTSU(I)
1685  FORMAT(1X,I3.3,4F12.4)
1690 CONTINUE

  IF(HCAT.NE.0) THEN
    WRITE (12,*)'The mean hurricane scour u/s face is MNTHSU',MNTHSU
    WRITE (12,*)'The std.dev.in hurricane scour u/s face is
STDHSU',ST
    `DHSU

    WRITE (12,*)'The mean hurricane scour d/s face is MNTHSD',MNTHSD
    WRITE (12,*)'The std.dev.in hurricane scour d/s face is
STDHSD',ST
    `DHSD

    WRITE (12,*)'          B          FHU          PRHU          CPRHU'
    Do 1700 I = 1,100
      WRITE (12,1695)B(I), FHU(I), PRHU(I), CPRHU(I)
1695  FORMAT(1X,4F12.4)
1700 CONTINUE

    WRITE (12,*)'          B          FHD          PRHD          CPRHD'
    Do 1710 I = 1,100
      WRITE (12,1705)B(I), FHD(I), PRHD(I), CPRHD(I)
1705  FORMAT(1X,4F12.4)
1710 CONTINUE
    END IF

  ELSE

    GO TO 7000
  END IF

7000 CONTINUE

  IF (HCAT.NE.0.AND.YRS.EQ.0) THEN

    WRITE (12,*)'Array of total SURGRE at bridge is HSURGE= ',
    `(HSURGE(I), I=1,120)

    WRITE (12,*)'Array of total combined depth at bridge is YT= ',
    `(YT(I), I=1,120)

    WRITE (12,*)'Array of total combined depth at bridge d/s face is
`YTR= ',(YTR(I), I=1,120)
    WRITE (12,*)'Array of total combined depth at bridge u/s face is
`YTF= ',(YTF(I), I=1,120)

    WRITE (12,*)'Array of Neills discharge is QN= ', (QN(I),I=1,120)
    WRITE (12,*)'Array of mod Neills disch.is QNM =
', (QNM(I),I=1,120)

```

```

        WRITE (12,*)'Array of Catch.disch.is  CHY36 =
', (CHY36(I), I=1,120)

        WRITE (12,*)'Array total net disch. value at bridge is QT= ',
'(QT(I), I=1,120)
        WRITE (12,*)'Array of total net velocity at bridge is VNT = ',
`(VNT(I), I=1,120)
        WRITE (12,*)'Array of net adjusted vel.upstream is VNUA = ',
`(VNUA(I), I=1,120)
        WRITE (12,*)'Array of net adjusted vel.downstream is VNDA= ',
`(VNDA(I), I=1,120)
        WRITE (12,*)'Array of net vel.u/stream is VNU =
', (VNU(I), I=1,120)
        WRITE (12,*)'Array of net vel.d/stream is VND= ', (VND(I),
I=1,120)

        WRITE (12,*)'Array of downflow velocity d/s face is VDD= ',
`(VDD(I), I=1,120)
        WRITE (12,*)'Array of downflow velocity u/s face is VDU= ',
`(VDU(I), I=1,120)

        WRITE (12,*)'Array of tangential velocity d/s face is VTD= ',
`(VTD(I), I=1,120)
        WRITE (12,*)'Array of tangential velocity u/s face is VTU= ',
`(VTU(I), I=1,120)

        WRITE (12,*)'The mean hurricane scour u/s face is MNTHSU', MNTHSU
        WRITE (12,*)'The std.dev.in hurricane scour u/s face is
STDHSU', ST
        `DHSU

        WRITE (12,*)'The mean hurricane scour d/s face is MNTHSD', MNTHSD
        WRITE (12,*)'The std.dev.in hurricane scour d/s face is
STDHSD', ST
        `DHSD

        WRITE (12,*)'
                B                FHU                PRHU                CPRHU '
        Do 7020 I = 1,100
        WRITE (12,7010)B(I),  FHU(I),  PRHU(I),  CPRHU(I)
7010  FORMAT(1X,4F12.4)
7020  CONTINUE

        WRITE (12,*)'
                B                FHD                PRHD                CPRHD '
        Do 7040 I = 1,100
        WRITE (12,7030)B(I),  FHD(I),  PRHD(I),  CPRHD(I)
7030  FORMAT(1X,4F12.4)
7040  CONTINUE

        ELSE
        GO TO 7100
        END IF

7100  CONTINUE

C      GO TO END OF PROGRAM STATEMENT FROM RUN OPTIONS

```

```

2000 CONTINUE
      WRITE(*,*) 'END OF RUN'
      CLOSE (12, STATUS = 'KEEP')
      CLOSE (6, STATUS = 'KEEP')
      END

      FUNCTION RANNO(MODNO, PAR1, PAR2)
C
C
      *****
C
      SUBPROGRAM: RANDOM NUMBER GENERATION
      Programmed by Richard H. McCuen
      Updated March 3, 1996
C
      *****
C
      MODNO      DISTRIBUTION      PAR1      PAR2
C      -----      -
C      1      uniform      lower X      upper X
C      2      normal      mean      std. dev.
C      3      Log normal      log mean      log sd
C
      *****
C
      IF(IND1.EQ.1) GO TO 20
      IND1 = 1
      ISEED = 2345679
C      eliminate first ten generated values
      XXX = RAND(ISEED)
      DO 10 I = 1,10
        J = INT(XXX)
        XXX = RAND(J)
      10 CONTINUE
      20 CONTINUE
      GO TO (100, 200, 300), MODNO
      100 CONTINUE
C
C      enter for uniform variates
C
      J = INT(XXX)
      XXX = RAND(J)
      RANNO = PAR1 + (PAR2 - PAR1) * XXX
      RETURN
      200 CONTINUE
C
C      enter for normal variates
C
      SUM = 0.0
      DO 210 JJK = 1, 12
        J = INT(XXX)
        XXX = RAND(J)

```

```

        SUM = SUM + XXX
210    CONTINUE
        SUM = SUM - 6.
        RANNO = PAR1 + PAR2 * SUM
        RETURN
300 CONTINUE
        RETURN
C
        END
*
*
*
        FUNCTION RAND(K)
C
        INTEGER K, M, CONST1
        PARAMETER (CONST1 = 2147483647, CONST2 = .4656613E-9)
        SAVE
        DATA M /0/
C
        IF (M .EQ. 0) M=K
        M = M*65539
        IF (M .LT. 0) M= (M+1) + CONST1
        RAND = M*CONST2
        END
*
*
        SUBROUTINE CONVOL(U, P, R, NU, NP, NR, M1, M2, M3)
C
C      CONVOLUTION OF P (PE) WITH U (UH) TO GET R (DRO)
C      INPUT  P,U,NP,NU,M1,M2,M3
C      OUTPUT R,NR
C
        DIMENSION U(M1), P(M2), R(M3)
C
        NR = NP + NU - 1
        DO 2 I = 1, NR
            R(I) = 0.0
            DO 1 J = 1, NP
                K = I - J + 1
                IF(K.LT.1.OR.K.GT.NU) GO TO 1
                R(I) = R(I) + P(J) * U(K)
1          CONTINUE
2        CONTINUE
        RETURN
        END

        SUBROUTINE sort2(n,arr,brr)
        INTEGER n,M,NSTACK
        REAL arr(n),brr(n)
        PARAMETER (M=7,NSTACK=150)
        INTEGER i,ir,j,jstack,k,l,istack(NSTACK)
        REAL a,b,temp
        jstack=0
        l=1
        ir=n
1      if(ir-l.lt.M)then
            do 12 j=l+1,ir

```

```

        a=arr(j)
        b=brr(j)
        do 11 i=j-1,1,-1
            if(arr(i).le.a)goto 2
            arr(i+1)=arr(i)
            brr(i+1)=brr(i)
11      continue
        i=l-1
        2   arr(i+1)=a
            brr(i+1)=b
12      continue
        if(jstack.eq.0)return
        ir=istack(jstack)
        l=istack(jstack-1)
        jstack=jstack-2
    else
        k=(l+ir)/2
        temp=arr(k)

        arr(k)=arr(l+1)
        arr(l+1)=temp
        temp=brr(k)
        brr(k)=brr(l+1)
        brr(l+1)=temp
        if(arr(l).gt.arr(ir))then
            temp=arr(l)
            arr(l)=arr(ir)
            arr(ir)=temp
            temp=brr(l)
            brr(l)=brr(ir)
            brr(ir)=temp
        endif
        if(arr(l+1).gt.arr(ir))then
            temp=arr(l+1)
            arr(l+1)=arr(ir)
            arr(ir)=temp
            temp=brr(l+1)
            brr(l+1)=brr(ir)
            brr(ir)=temp
        endif
        if(arr(l).gt.arr(l+1))then
            temp=arr(l)
            arr(l)=arr(l+1)
            arr(l+1)=temp

            temp=brr(l)
            brr(l)=brr(l+1)
            brr(l+1)=temp
        endif
        i=l+1
        j=ir
        a=arr(l+1)
        b=brr(l+1)
        3   continue
            i=i+1
            if(arr(i).lt.a)goto 3
        4   continue

```

```

        j=j-1
        if(arr(j).gt.a)goto 4
        if(j.lt.i)goto 5
        temp=arr(i)
        arr(i)=arr(j)
        arr(j)=temp
        temp=brr(i)
        brr(i)=brr(j)
        brr(j)=temp
        goto 3
5      arr(l+1)=arr(j)
        arr(j)=a
        brr(l+1)=brr(j)
        brr(j)=b

        jstack=jstack+2
        if(jstack.gt.NSTACK)pause
        if(ir-i+1.ge.j-1)then
            istack(jstack)=ir
            istack(jstack-1)=i
            ir=j-1
        else
            istack(jstack)=j-1
            istack(jstack-1)=l
            l=i
        endif
    endif
    goto 1
END

```

```

SUBROUTINE INTERP(T, X, B, Y, N, M, IAD1, IAD2)
C      Using IAD (Integer Adjustment Dimension)in the subroutine
C      dimensions make it possible to vary the dimensions of
C      arguement arrays in the main program

DIMENSION T(IAD1), X(IAD1), Y(IAD2), B(IAD2)

C      T= array of time values at unequal intervals (TNR)
C      X=array of values of tides depths at unequal time (YAT)
C      B= array of equal time intervals(TNRI)
C      Y= array of tide depths on equal time intervals (YATI)
C      N = number of values in TNR = 150
C      M =Number of interpolated time intervals ( NR18, NR24, or NR36)

DO 50 I = 1, M
    A = I
    DO 30 J = 1, N
        IF(A.LT.T(J).OR.A.GE.T(J+1)) GO TO 30
        Y(I) = X(J) + (A - T(J)) / (T(J+1) - T(J)) * (X(J+1) -
X(J))
        IF(Y(I).LT.0.0) Y(I)= 0.0

        B(I) = A
    GO TO 50
30    CONTINUE

```

```

1))      Y(I) = X(N-1) + (A - T(N-1)) / (T(N) - T(N-1)) * (X(N) -X(N-
          IF(Y(I).LT.0.0) Y(I)= 0.0
          B(I) = A
50      CONTINUE
          RETURN
      END

```



# APPENDIX B-1

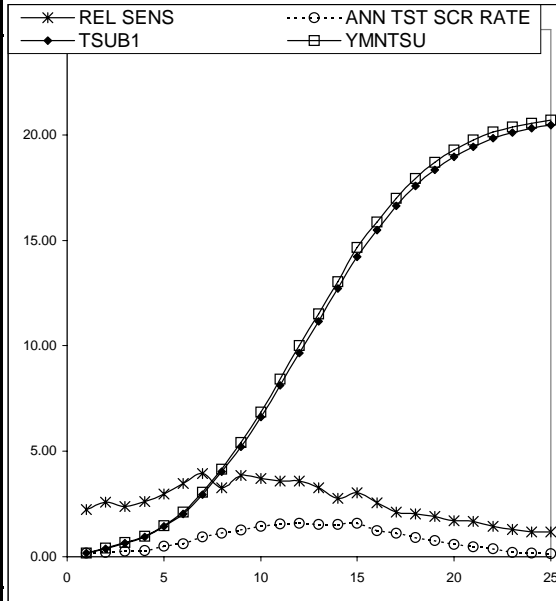
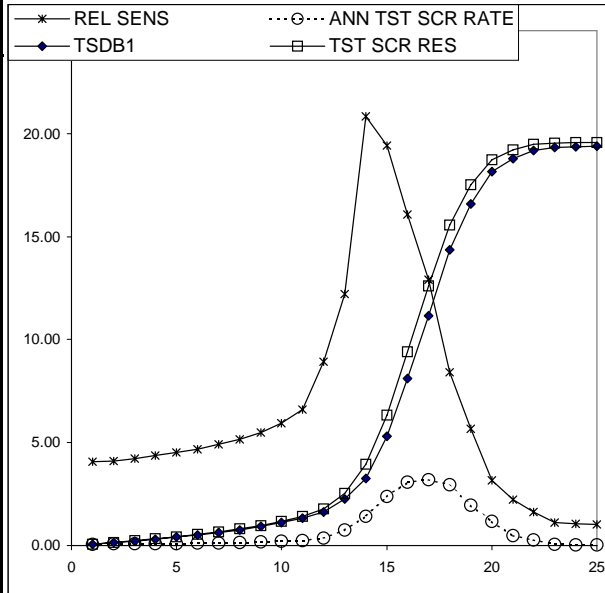
## BASELINE CONDITIONS AND RESULTS

Variable	ABBR.	Baseline Values 1	Max Value	Min Value	YRS	TSUB1
Curve Number	CN	78	70	88	1	0.16
Catchment Basin Area sq. mi.	CBA	300	1200	75	2	0.34
gamma b					3	0.57
	B6	0.1	0.4	0.03	4	0.84
	B18	0.4	1.6	0.10	5	1.29
	B24	0.8	3.2	0.20	6	1.84
	B36	1.35	5.4	0.34	7	2.53
gamma c					8	3.51
	C6	3.0	12	0.75	9	4.66
	C18	2.0	8	0.5	10	5.86
	C24	1.0	4	0.25	11	7.29
	C36	1.0	4	0.25	12	8.69
					13	10.09
Base station invert ft	IBS	-28.01	-112.04	-7.00	14	11.62
Base station diurnal period hrs.	DT	12.31			15	13.32
Base station lunar period hrs.	LT	356			16	14.79
Distance between bridge and base station mi.	LW	100	400	25	17	16.11
Base station diurnal amplitude ft.	MDA	1.22			18	17.15
Base station lunar amplitude ft.	MLA	0.36			19	18.01
Stdv. In base station diurnal amplitude ft.	SDA	0.56			20	18.63
Stdv. In base station lunar amplitude ft.	SLA	0.18			21	19.16
Base station wave peakedness amplitude ft.	PKM	0.67	2.68	0.17	22	19.61
					23	19.95
Bridge station invert ft	IRS	-10.75	-43	-2.6875	24	20.18
Bridge station mean depth ft	MDR	10.75	43	2.6875	25	20.33
Bridge station diurnal amplitude ft.	MTR	0.75	3	0.1875		
Bridge station mean low tide depth ft.	MLT	10.00	40	2.5		
Bridge station mean low tide elevation ft.	MLTE	-0.75	-3	-0.1875	YRS	TSDB1
					1	0.07
Number of bridge piers	NBP	9	36	2.25	2	0.13
Pier diameter ft	PD	5.0	20	1.25	3	0.21
Orifice factor for downflow computation	C1	0.25	1	0.06	4	0.29
					5	0.38
Estuary plan area Sq.mi.	AS	4	16	1.00	6	0.48
Estuary length above bridge station mi.	LE	4	16	1.00	7	0.59
Estuary width at bridge station mi.	WB	0.33	1.32	0.08	8	0.71
Estuary width at bridge station ft.	WTBMLT	1742	10454	436	9	0.85
Estuary width at nearfield distance below bridge station mi.	WD	0.33	1.32	0.0825	10	1.02
Estuary width at nearfield distance above bridge station mi.	WU	0.33	1.32	0.0825	11	1.20
Maximum estuary width above bridge station mi.	WM	1.00	4	0.25	12	1.47
Estuary overbank side slope UESTZ:1	UESTZ	200	800	50	13	1.80
Estuary in bank area at bridge cross section sq ft.	XABMLE	17420	69680	4355	14	2.67
					15	4.06
Soils gradation data d50, 50% finer than. mm.	D50	0.20	0.8	0.05	16	6.24
Soils gradation data d16, 16% finer than. mm.	D16	0.05	0.2	0.01	17	8.93
Soils gradation data d84, 84% finer than. mm.	D84	0.40	1.6	0.10	18	11.82
Soils gradation data maximum particle size. mm.	DMAX	0.70	2.8	0.18	19	14.66
Soil phi angle	PHI	40.00	75	30	20	16.66
<b>Hurricane Data</b>					21	17.98
Hurricane Rainfall ins.	HURAIN	6	18	1.5	22	18.68
Hurricane Radius Mi.	HRAD	150	300	50	23	19.11
Hurricane translation speed mph.	HSPEED	20	30	6.67	24	19.34
Hurricane surge ft	MXSURG	11	25	3	25	19.36
Closest distance of approach to the bridge mi	HDIST	10	30	0.05		

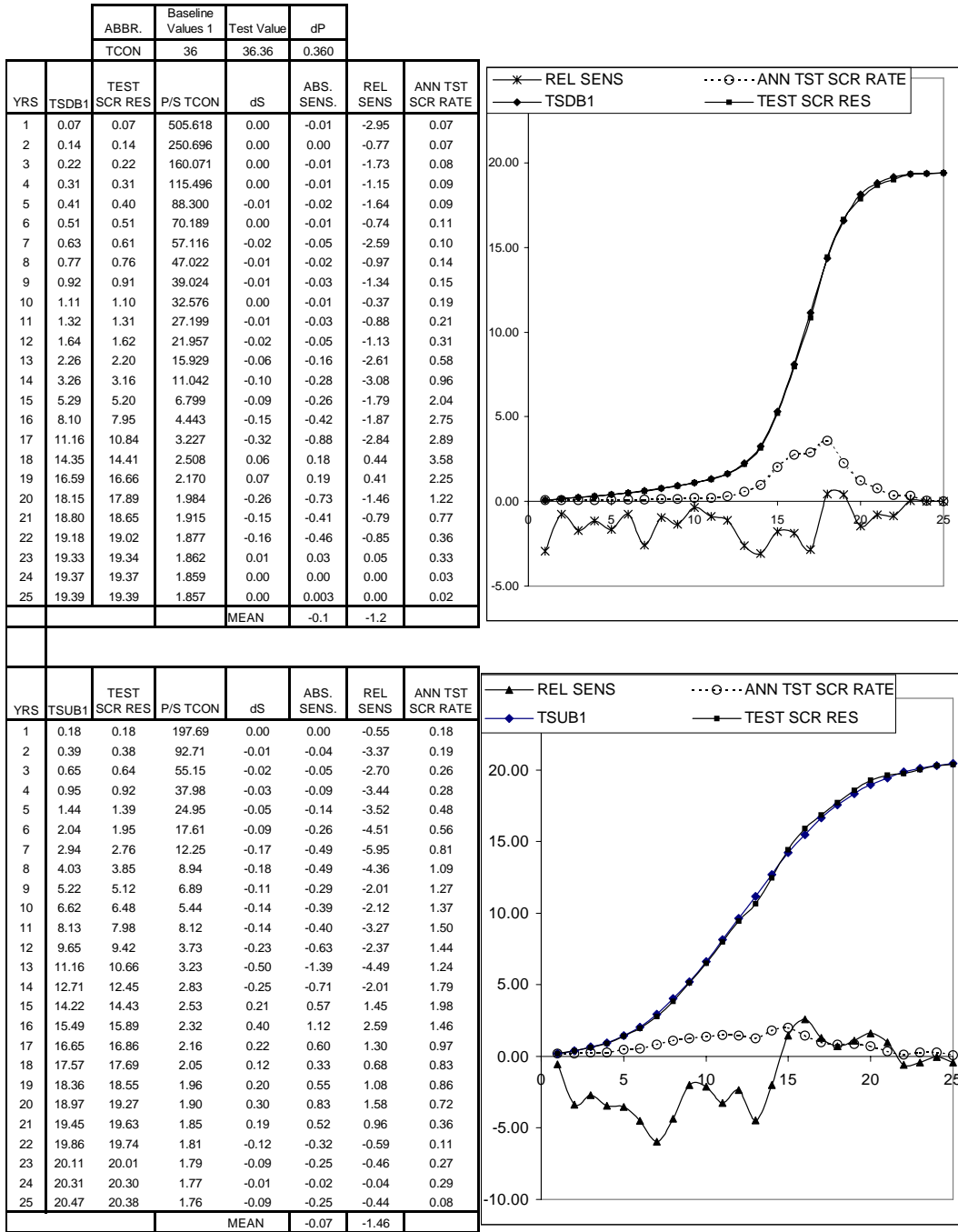
## APPENDIX B-2

RELATIVE SENSITIVITY RESULTS FOR PIER DIAMETER

ABBR.	Baseline Values 1	Test Value	dP				
PD	5.0	5.05	0.050				
YRS	TSDB1	TST SCR RES	P/S PD	dS	ABS. SENS.	REL SENS	ANN TST SCR RATE
1	0.07	0.07	70.22	0.00	0.06	4.07	0.07
2	0.14	0.15	34.82	0.01	0.12	4.11	0.08
3	0.22	0.23	22.23	0.01	0.19	4.22	0.08
4	0.31	0.33	16.04	0.01	0.27	4.36	0.09
5	0.41	0.43	12.26	0.02	0.37	4.51	0.10
6	0.51	0.54	9.75	0.02	0.48	4.68	0.11
7	0.63	0.66	7.93	0.03	0.62	4.90	0.12
8	0.77	0.81	6.53	0.04	0.79	5.16	0.14
9	0.92	0.97	5.42	0.05	1.01	5.49	0.17
10	1.11	1.17	4.52	0.07	1.31	5.95	0.20
11	1.32	1.41	3.78	0.09	1.75	6.60	0.24
12	1.64	1.79	3.05	0.15	2.93	8.92	0.38
13	2.26	2.54	2.21	0.28	5.52	12.20	0.75
14	3.26	3.94	1.53	0.68	13.59	20.84	1.40
15	5.29	6.32	0.94	1.03	20.56	19.41	2.38
16	8.10	9.41	0.62	1.30	26.06	16.08	3.08
17	11.16	12.60	0.45	1.44	28.79	12.90	3.19
18	14.35	15.56	0.35	1.21	24.19	8.43	2.96
19	16.59	17.53	0.30	0.94	18.83	5.67	1.97
20	18.15	18.72	0.28	0.57	11.49	3.17	1.19
21	18.80	19.22	0.27	0.42	8.39	2.23	0.50
22	19.18	19.49	0.26	0.31	6.22	1.62	0.27
23	19.33	19.55	0.26	0.22	4.32	1.12	0.06
24	19.37	19.57	0.26	0.20	4.04	1.04	0.02
25	19.39	19.59	0.26	0.20	4.02	1.04	0.02
		MEAN			7.4	6.7	
YRS	TSUB1	YMNTSU	P/S PD	dS	ABS. SENS.	REL SENS	ANN TST SCR RATE
1	0.18	0.19	27.46	0.00	0.08	2.25	0.19
2	0.39	0.40	12.88	0.01	0.20	2.60	0.21
3	0.65	0.67	7.66	0.02	0.31	2.37	0.27
4	0.95	0.97	5.28	0.02	0.50	2.63	0.30
5	1.44	1.49	3.47	0.04	0.86	2.98	0.51
6	2.04	2.12	2.45	0.07	1.42	3.46	0.63
7	2.94	3.05	1.70	0.12	2.32	3.94	0.94
8	4.03	4.16	1.24	0.13	2.64	3.27	1.11
9	5.22	5.42	0.96	0.20	4.03	3.86	1.27
10	6.62	6.87	0.75	0.25	4.91	3.70	1.44
11	8.13	8.42	0.62	0.29	5.82	3.58	1.55
12	9.65	10.00	0.52	0.35	6.93	3.59	1.58
13	11.16	11.53	0.45	0.37	7.31	3.27	1.53
14	12.71	13.06	0.39	0.35	7.02	2.76	1.53
15	14.22	14.65	0.35	0.43	8.64	3.04	1.60
16	15.49	15.89	0.32	0.40	7.91	2.55	1.23
17	16.65	17.00	0.30	0.35	7.06	2.12	1.11
18	17.57	17.93	0.28	0.35	7.10	2.02	0.93
19	18.36	18.71	0.27	0.35	7.01	1.91	0.78
20	18.97	19.30	0.26	0.33	6.51	1.72	0.59
21	19.45	19.77	0.26	0.33	6.53	1.68	0.48
22	19.86	20.15	0.25	0.29	5.77	1.45	0.37
23	20.11	20.36	0.25	0.26	5.16	1.28	0.22
24	20.31	20.55	0.25	0.24	4.77	1.17	0.19
25	20.47	20.71	0.24	0.24	4.77	1.16	0.16
		MEAN			4.6	2.6	



RELATIVE SENSITIVITY RESULTS FOR TIME OF CONCENTRATION



# RELATIVE SENSITIVITY RESULTS FOR CATCHMENT AREA

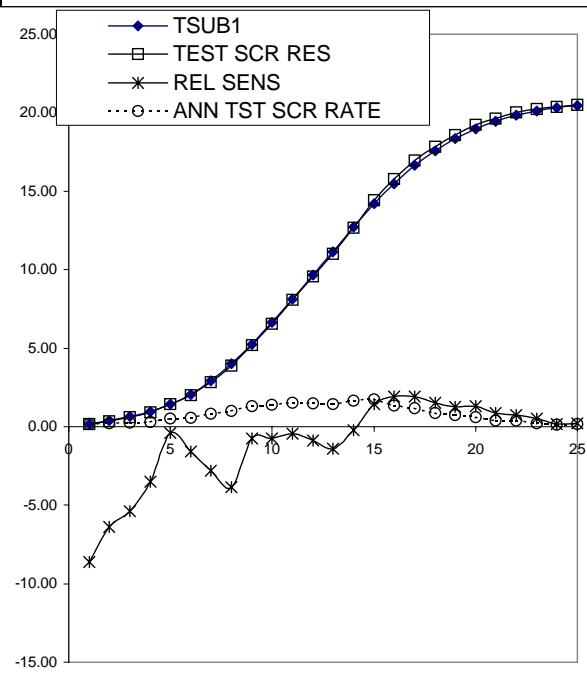
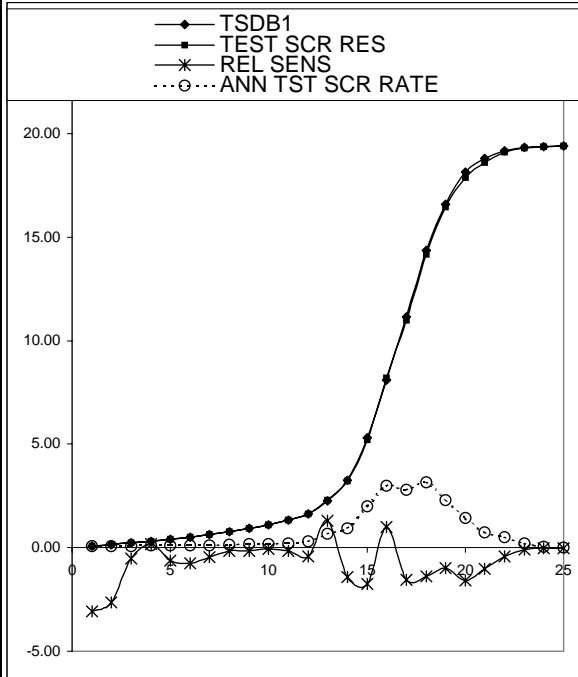
P= Predictor variable

S= Baseline scour

	ABBR.	Baseline Values 1	Test Value	dP			
	CBA	300	303.00	3.000			
YRS	TSDB1	TEST SCR RES	P/S CBA	dS	ABS. SENS.	REL SENS	ANN TST SCR RATE
1	0.07	0.07	4213.5	0.00	0.00	-3.09	0.07
2	0.14	0.14	2089.14	0.00	0.00	-2.65	0.07
3	0.22	0.22	1333.93	0.00	0.00	-0.53	0.08
4	0.31	0.31	962.46	0.00	0.00	0.16	0.09
5	0.41	0.41	735.84	0.00	0.00	-0.64	0.09
6	0.51	0.51	584.91	0.00	0.00	-0.76	0.10
7	0.63	0.63	475.96	0.00	0.00	-0.44	0.12
8	0.77	0.76	391.85	0.00	0.00	-0.14	0.14
9	0.92	0.92	325.20	0.00	0.00	-0.16	0.16
10	1.11	1.10	271.47	0.00	0.00	-0.05	0.18
11	1.32	1.32	226.65	0.00	0.00	-0.17	0.22
12	1.64	1.63	182.97	-0.01	0.00	-0.42	0.31
13	2.26	2.29	132.74	0.03	0.01	1.29	0.66
14	3.26	3.21	92.01	-0.05	-0.02	-1.43	0.92
15	5.29	5.20	56.66	-0.09	-0.03	-1.76	1.99
16	8.10	8.18	37.03	0.08	0.03	0.99	2.98
17	11.16	10.98	26.89	-0.17	-0.06	-1.55	2.80
18	14.35	14.15	20.90	-0.20	-0.07	-1.39	3.17
19	16.59	16.43	18.08	-0.16	-0.05	-0.98	2.28
20	18.15	17.86	16.53	-0.29	-0.10	-1.59	1.43
21	18.80	18.61	15.96	-0.19	-0.06	-1.03	0.75
22	19.18	19.10	15.64	-0.08	-0.03	-0.42	0.49
23	19.33	19.31	15.52	-0.02	-0.01	-0.10	0.22
24	19.37	19.37	15.49	0.00	0.00	-0.02	0.05
25	19.39	19.38	15.48	0.00	-0.001	-0.02	0.02
MEAN					-0.016	-0.7	

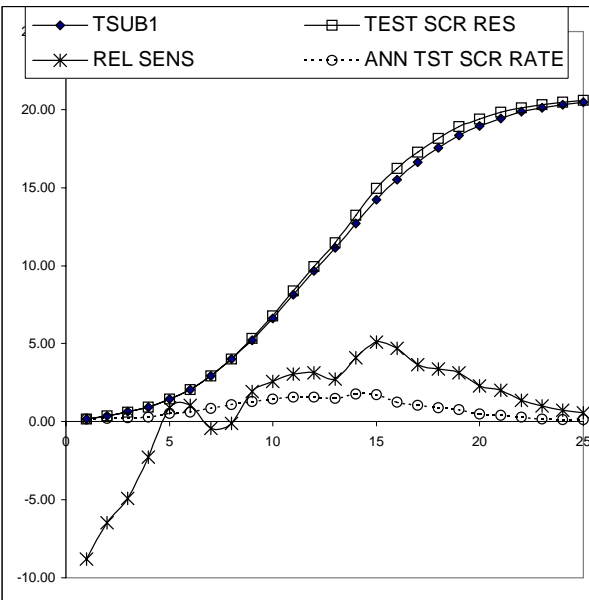
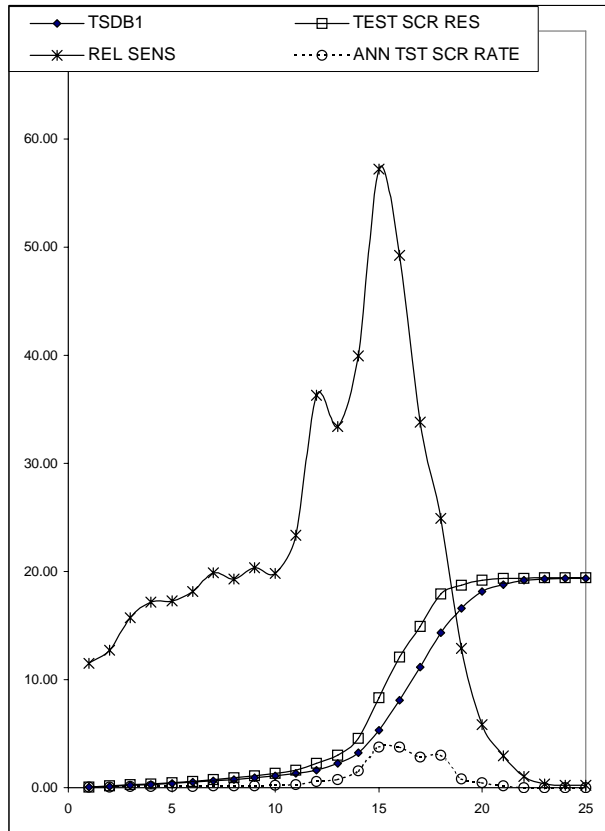
  

YRS	TSUB1	TEST SCR RES	P/S CBA	dS	ABS. SENS.	REL SENS	ANN TST SCR RATE
1	0.18	0.17	1647.45	-0.02	-0.01	-8.62	0.17
2	0.39	0.36	772.60	-0.02	-0.01	-6.39	0.20
3	0.65	0.62	459.56	-0.04	-0.01	-5.38	0.25
4	0.95	0.91	316.52	-0.03	-0.01	-3.50	0.30
5	1.44	1.44	207.93	-0.01	0.00	-0.40	0.52
6	2.04	2.01	146.76	-0.03	-0.01	-1.59	0.57
7	2.94	2.86	102.11	-0.08	-0.03	-2.82	0.84
8	4.03	3.87	74.48	-0.16	-0.05	-3.85	1.02
9	5.22	5.18	57.43	-0.04	-0.01	-0.75	1.31
10	6.62	6.57	45.29	-0.05	-0.02	-0.77	1.39
11	8.13	8.09	36.91	-0.04	-0.01	-0.43	1.52
12	9.65	9.57	31.08	-0.08	-0.03	-0.88	1.48
13	11.16	11.01	26.88	-0.16	-0.05	-1.40	1.44
14	12.71	12.68	23.61	-0.03	-0.01	-0.20	1.67
15	14.22	14.43	21.09	0.20	0.07	1.43	1.75
16	15.49	15.79	19.37	0.30	0.10	1.93	1.36
17	16.65	16.97	18.02	0.32	0.11	1.93	1.18
18	17.57	17.84	17.07	0.27	0.09	1.54	0.87
19	18.36	18.59	16.34	0.23	0.08	1.27	0.75
20	18.97	19.21	15.81	0.24	0.08	1.29	0.63
21	19.45	19.61	15.43	0.17	0.06	0.86	0.40
22	19.86	20.00	15.11	0.14	0.05	0.72	0.39
23	20.11	20.21	14.92	0.11	0.04	0.54	0.21
24	20.31	20.35	14.77	0.04	0.01	0.17	0.13
25	20.47	20.52	14.66	0.05	0.02	0.23	0.17
MEAN					0.017	-1.0	



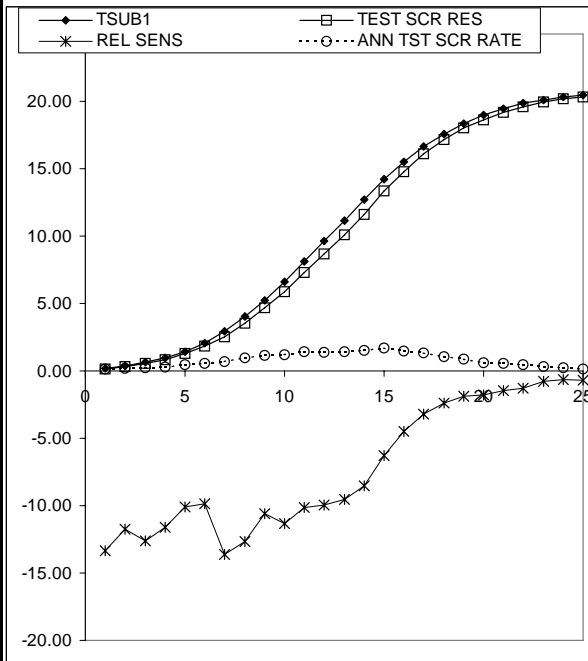
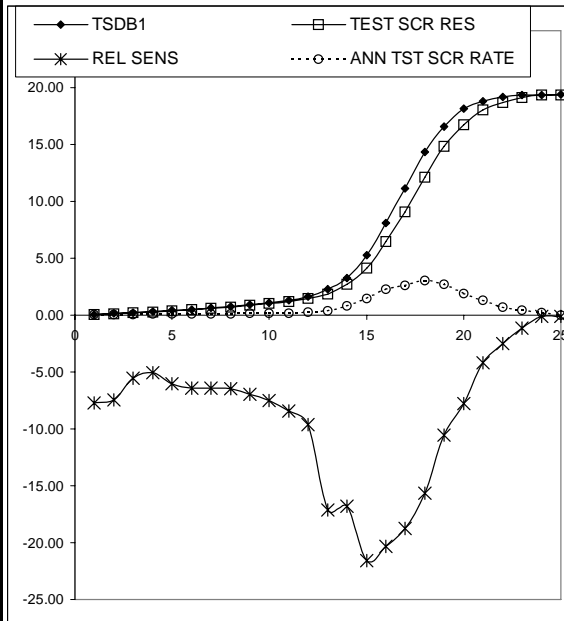
RELATIVE SENSITIVITY RESULTS FOR ESTUARY AREA  
P= Predictor variable S= Baseline scour

ABBR.	Baseline Values 1	Test Value	dP				
AS	4	4.04	0.040				
YRS	TSDB1	TEST SCR RES	P/S AS	dS	ABS. SENS.	REL SENS	ANN TST SCR RATE
1	0.07	0.08	56.18	0.01	0.21	11.52	0.08
2	0.14	0.16	27.86	0.02	0.46	12.74	0.08
3	0.22	0.26	17.79	0.04	0.88	15.74	0.10
4	0.31	0.37	12.83	0.05	1.34	17.20	0.11
5	0.41	0.48	9.81	0.07	1.76	17.29	0.11
6	0.51	0.61	7.80	0.09	2.33	18.13	0.13
7	0.63	0.76	6.35	0.13	3.13	19.86	0.15
8	0.77	0.91	5.22	0.15	3.69	19.28	0.16
9	0.92	1.11	4.34	0.19	4.69	20.33	0.20
10	1.11	1.32	3.62	0.22	5.48	19.83	0.21
11	1.32	1.63	3.02	0.31	7.72	23.35	0.31
12	1.64	2.23	2.44	0.60	14.88	36.30	0.60
13	2.26	3.01	1.77	0.75	18.86	33.38	0.78
14	3.26	4.56	1.23	1.30	32.57	39.96	1.55
15	5.29	8.33	0.76	3.03	75.77	57.24	3.76
16	8.10	12.09	0.49	3.99	99.81	49.28	3.77
17	11.16	14.93	0.36	3.78	94.38	33.84	2.84
18	14.35	17.92	0.28	3.57	89.34	24.90	2.99
19	16.59	18.74	0.24	2.14	53.58	12.92	0.81
20	18.15	19.21	0.22	1.06	26.43	5.83	0.47
21	18.80	19.36	0.21	0.56	13.92	2.96	0.15
22	19.18	19.38	0.21	0.20	5.04	1.05	0.02
23	19.33	19.40	0.21	0.07	1.66	0.34	0.02
24	19.37	19.42	0.21	0.05	1.16	0.24	0.02
25	19.39	19.43	0.21	0.04	1.03	0.21	0.01
			MEAN		22.4	19.7	
YRS	TSUB1	TEST SCR RES	P/S AS	dS	ABS. SENS.	REL SENS	ANN TST SCR RATE
1	0.18	0.17	21.97	-0.02	-0.40	-8.79	0.17
2	0.39	0.36	10.30	-0.03	-0.63	-6.49	0.20
3	0.65	0.62	6.13	-0.03	-0.80	-4.93	0.26
4	0.95	0.93	4.22	-0.02	-0.53	-2.26	0.31
5	1.44	1.46	2.77	0.01	0.32	0.89	0.53
6	2.04	2.07	1.96	0.02	0.53	1.04	0.61
7	2.94	2.93	1.36	-0.01	-0.33	-0.44	0.86
8	4.03	4.02	0.99	0.00	-0.10	-0.10	1.10
9	5.22	5.32	0.77	0.10	2.52	1.93	1.30
10	6.62	6.79	0.60	0.17	4.29	2.59	1.47
11	8.13	8.38	0.49	0.25	6.19	3.05	1.58
12	9.65	9.95	0.41	0.30	7.55	3.13	1.58
13	11.16	11.47	0.36	0.30	7.60	2.72	1.51
14	12.71	13.23	0.31	0.52	12.99	4.09	1.76
15	14.22	14.95	0.28	0.72	18.12	5.10	1.72
16	15.49	16.22	0.26	0.73	18.18	4.70	1.27
17	16.65	17.26	0.24	0.61	15.25	3.67	1.04
18	17.57	18.16	0.23	0.59	14.80	3.37	0.91
19	18.36	18.93	0.22	0.57	14.34	3.13	0.77
20	18.97	19.41	0.21	0.44	10.96	2.31	0.48
21	19.45	19.84	0.21	0.39	9.83	2.02	0.43
22	19.86	20.13	0.20	0.27	6.87	1.38	0.29
23	20.11	20.31	0.20	0.20	5.04	1.00	0.18
24	20.31	20.46	0.20	0.15	3.69	0.73	0.15
25	20.47	20.59	0.20	0.12	2.89	0.56	0.13
			MEAN		6.4	1.0	



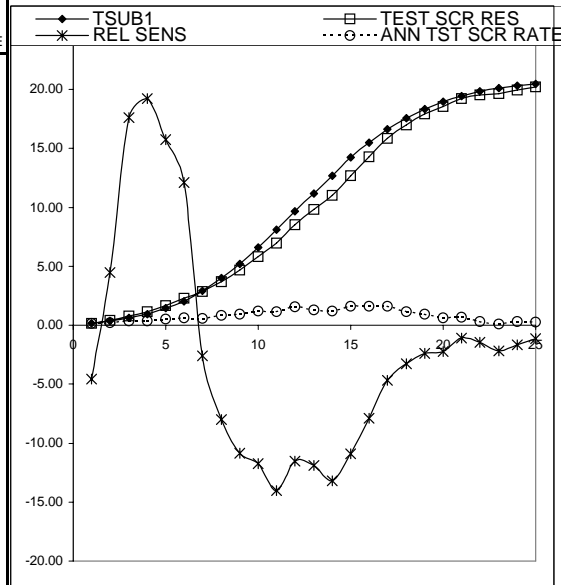
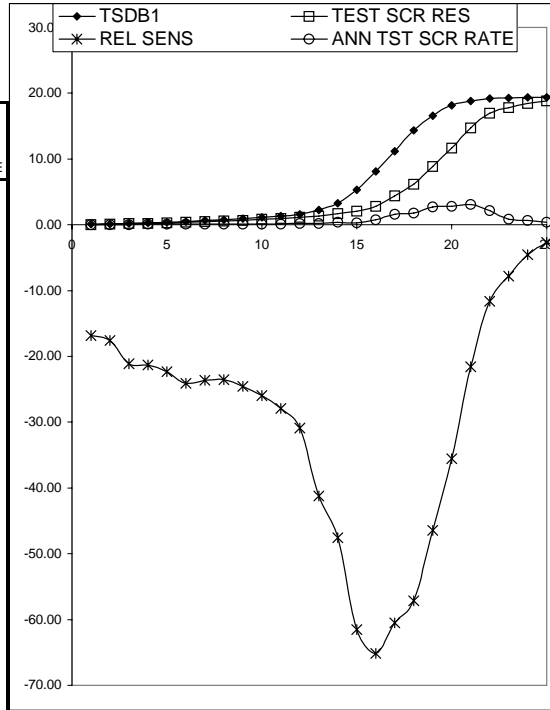
RELATIVE SENSITIVITY RESULTS FOR D50  
P= Predictor variable S= Baseline scour

		ABBR.	Baseline Values 1	Test Value	dP			
		D50	0.200	0.202	0.002			
		TEST SCR RES	P/S D50	dS	ABS. SENS.	REL SENS	ANN TST SCR RATE	
YRS	TSDB1							
1	0.07	0.07	2.81	-0.01	-2.75	-7.72	0.07	
2	0.14	0.13	1.39	-0.01	-5.35	-7.45	0.07	
3	0.22	0.21	0.89	-0.01	-6.25	-5.56	0.08	
4	0.31	0.30	0.64	-0.02	-7.90	-5.07	0.08	
5	0.41	0.38	0.49	-0.02	-12.30	-6.03	0.09	
6	0.51	0.48	0.39	-0.03	-16.45	-6.41	0.10	
7	0.63	0.59	0.32	-0.04	-20.20	-6.41	0.11	
8	0.77	0.72	0.26	-0.05	-24.80	-6.48	0.13	
9	0.92	0.86	0.22	-0.06	-32.15	-6.97	0.14	
10	1.11	1.02	0.18	-0.08	-41.30	-7.47	0.16	
11	1.32	1.21	0.15	-0.11	-55.85	-8.44	0.19	
12	1.64	1.48	0.12	-0.16	-78.85	-9.62	0.27	
13	2.26	1.87	0.09	-0.39	-193.55	-17.13	0.39	
14	3.26	2.71	0.06	-0.55	-273.70	-16.79	0.84	
15	5.29	4.15	0.04	-1.14	-570.70	-21.56	1.44	
16	8.10	6.46	0.02	-1.65	-822.60	-20.31	2.30	
17	11.16	9.06	0.02	-2.09	-1047.45	-18.78	2.61	
18	14.35	12.10	0.01	-2.25	-1123.90	-15.66	3.04	
19	16.59	14.84	0.01	-1.75	-875.95	-10.56	2.74	
20	18.15	16.73	0.01	-1.42	-707.70	-7.80	1.89	
21	18.80	18.02	0.01	-0.78	-392.30	-4.17	1.28	
22	19.18	18.71	0.01	-0.47	-237.25	-2.47	0.69	
23	19.33	19.12	0.01	-0.22	-108.60	-1.12	0.41	
24	19.37	19.34	0.01	-0.03	-13.00	-0.13	0.23	
25	19.39	19.36	0.01	-0.02	-11.10	-0.11	0.02	
MEAN					-267.3	-8.8		
YRS	TSUB1	TEST SCR RES	P/S D50	dS	ABS. SENS.	REL SENS	ANN TST SCR RATE	
1	0.18	0.16	1.10	-0.02	-12.15	-13.34	0.16	
2	0.39	0.34	0.52	-0.05	-22.80	-11.74	0.18	
3	0.65	0.57	0.31	-0.08	-41.10	-12.59	0.23	
4	0.95	0.84	0.21	-0.11	-55.05	-11.62	0.27	
5	1.44	1.30	0.14	-0.15	-72.95	-10.11	0.46	
6	2.04	1.84	0.10	-0.20	-100.90	-9.87	0.55	
7	2.94	2.54	0.07	-0.40	-199.80	-13.60	0.70	
8	4.03	3.52	0.05	-0.51	-254.75	-12.65	0.98	
9	5.22	4.67	0.04	-0.55	-277.20	-10.61	1.15	
10	6.62	5.87	0.03	-0.75	-374.85	-11.32	1.20	
11	8.13	7.31	0.02	-0.82	-411.05	-10.12	1.43	
12	9.65	8.69	0.02	-0.96	-479.90	-9.94	1.39	
13	11.16	10.10	0.02	-1.06	-531.85	-9.53	1.41	
14	12.71	11.62	0.02	-1.09	-543.45	-8.55	1.52	
15	14.22	13.33	0.01	-0.89	-445.50	-6.27	1.71	
16	15.49	14.79	0.01	-0.70	-349.80	-4.52	1.46	
17	16.65	16.11	0.01	-0.53	-266.00	-3.20	1.32	
18	17.57	17.15	0.01	-0.42	-208.90	-2.38	1.04	
19	18.36	18.01	0.01	-0.34	-170.60	-1.86	0.86	
20	18.97	18.63	0.01	-0.34	-171.05	-1.80	0.61	
21	19.45	19.16	0.01	-0.29	-142.50	-1.47	0.53	
22	19.86	19.61	0.01	-0.25	-125.45	-1.26	0.45	
23	20.11	19.95	0.01	-0.16	-78.40	-0.78	0.34	
24	20.31	20.18	0.01	-0.13	-66.90	-0.66	0.23	
25	20.47	20.33	0.01	-0.14	-71.40	-0.70	0.15	
MEAN				-219.0	-7.2			



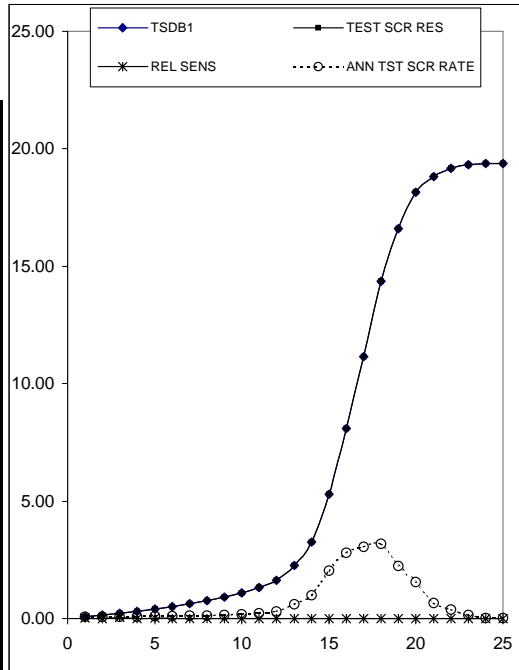
RELATIVE SENSITIVITY RESULTS FOR CROSS SECTION AREA  
P= Predictor variable S= Baseline scour

	ABBR.	Baseline Values1	Test Value	dP			
	XABMLE	17420	17594	174.2			
YRS	TSDB1	TEST SCR RES	P/S XAREA	dS	ABS. SENS.	REL SENS	ANN TST SCR RATE
1	0.07	0.06	244663	-0.01	-0.0001	-16.85	0.06
2	0.14	0.12	121309	-0.03	-0.0001	-17.62	0.06
3	0.22	0.18	77457	-0.05	-0.0003	-21.08	0.06
4	0.31	0.25	55887	-0.07	-0.0004	-21.30	0.07
5	0.41	0.32	42727	-0.09	-0.0005	-22.34	0.07
6	0.51	0.39	33964	-0.12	-0.0007	-24.08	0.07
7	0.63	0.48	27638	-0.15	-0.0009	-23.66	0.09
8	0.77	0.59	22753	-0.18	-0.0010	-23.51	0.10
9	0.92	0.70	18883	-0.23	-0.0013	-24.54	0.11
10	1.11	0.82	15763	-0.29	-0.0016	-25.98	0.12
11	1.32	0.95	13161	-0.37	-0.0021	-27.92	0.14
12	1.64	1.13	10625	-0.51	-0.0029	-30.86	0.18
13	2.26	1.33	7708	-0.93	-0.0053	-41.20	0.20
14	3.26	1.71	5343	-1.55	-0.0089	-47.58	0.38
15	5.29	2.04	3290	-3.26	-0.0187	-61.53	0.33
16	8.10	2.82	2150	-5.28	-0.0303	-65.16	0.79
17	11.16	4.41	1561	-6.75	-0.0387	-60.49	1.59
18	14.35	6.15	1214	-8.20	-0.0471	-57.13	1.75
19	16.59	8.88	1050	-7.71	-0.0443	-46.49	2.73
20	18.15	11.69	960	-6.46	-0.0371	-35.59	2.81
21	18.80	14.75	927	-4.05	-0.0233	-21.55	3.06
22	19.18	16.95	908	-2.23	-0.0128	-11.63	2.20
23	19.33	17.83	901	-1.51	-0.0087	-7.80	0.88
24	19.37	18.50	899	-0.87	-0.0050	-4.50	0.67
25	19.39	18.87	899	-0.52	-0.0030	-2.68	0.37
			MEAN		-0.012	-29.7	
YRS	TSUB1	TEST SCR RES	P/S XAREA	dS	ABS. SENS.	REL SENS	ANN TST SCR RATE
1	0.18	0.17	95662	-0.01	0.0000	-4.56	0.17
2	0.39	0.41	44862	0.02	0.0001	4.46	0.23
3	0.65	0.77	26685	0.12	0.0007	17.63	0.36
4	0.95	1.13	18379	0.18	0.0010	19.21	0.36
5	1.44	1.67	12074	0.23	0.0013	15.77	0.54
6	2.04	2.29	8522	0.25	0.0014	12.13	0.62
7	2.94	2.86	5929	-0.08	-0.0004	-2.60	0.57
8	4.03	3.71	4325	-0.32	-0.0018	-8.00	0.84
9	5.22	4.66	3335	-0.57	-0.0033	-10.84	0.95
10	6.62	5.85	2630	-0.78	-0.0045	-11.71	1.19
11	8.13	6.99	2143	-1.14	-0.0065	-14.02	1.14
12	9.65	8.54	1805	-1.11	-0.0064	-11.53	1.55
13	11.16	9.84	1561	-1.33	-0.0076	-11.88	1.30
14	12.71	11.03	1371	-1.68	-0.0096	-13.19	1.19
15	14.22	12.67	1225	-1.55	-0.0089	-10.93	1.64
16	15.49	14.27	1125	-1.22	-0.0070	-7.87	1.60
17	16.65	15.86	1047	-0.78	-0.0045	-4.69	1.59
18	17.57	17.00	991	-0.57	-0.0033	-3.27	1.13
19	18.36	17.92	949	-0.43	-0.0025	-2.36	0.92
20	18.97	18.54	918	-0.43	-0.0025	-2.25	0.62
21	19.45	19.23	896	-0.21	-0.0012	-1.09	0.69
22	19.86	19.57	877	-0.29	-0.0017	-1.47	0.33
23	20.11	19.67	866	-0.43	-0.0025	-2.15	0.11
24	20.31	19.97	858	-0.34	-0.0019	-1.65	0.30
25	20.47	20.23	851	-0.24	-0.0014	-1.15	0.26
			MEAN REL SENS.		-0.003	-2.3	

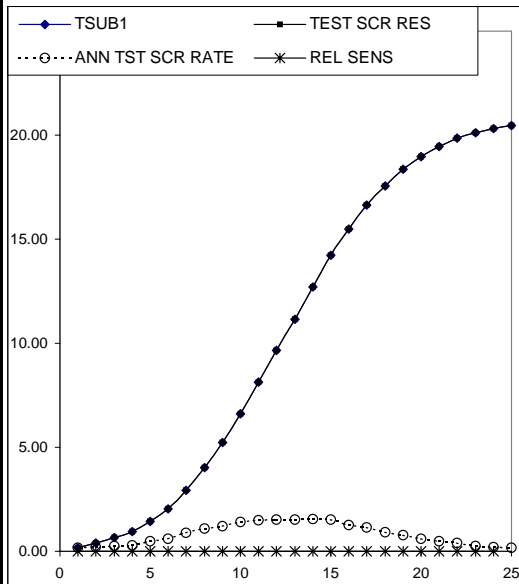


RELATIVE SENSIVITY RESULTS FOR NUMBER OF BRIDGE PIERS

	Baseline		Test Value	dP			
	ABBR.	Values 1					
	NBP	9					
YRS	TSDB1	TEST SCR RES	P/S NBP	dS	ABS. SENS.	REL SENS	ANN TST SCR RATE
1	0.07	0.07	126.404	0.00	0.00	0.03	0.07
2	0.14	0.14	62.674	0.00	0.00	0.01	0.07
3	0.22	0.23	40.018	0.00	0.00	0.04	0.08
4	0.31	0.31	28.874	0.00	0.00	0.01	0.09
5	0.41	0.41	22.075	0.00	0.00	0.02	0.10
6	0.51	0.51	17.547	0.00	0.00	0.01	0.11
7	0.63	0.63	14.279	0.00	0.00	0.00	0.12
8	0.77	0.77	11.755	0.00	0.00	0.01	0.13
9	0.92	0.92	9.756	0.00	0.00	0.01	0.16
10	1.11	1.11	8.144	0.00	0.00	0.00	0.18
11	1.32	1.32	6.800	0.00	0.00	0.00	0.22
12	1.64	1.64	5.489	0.00	0.00	0.00	0.32
13	2.26	2.26	3.982	0.00	0.00	0.00	0.62
14	3.26	3.26	2.760	0.00	0.00	0.00	1.00
15	5.29	5.29	1.700	0.00	0.00	0.00	2.03
16	8.10	8.10	1.111	0.00	0.00	0.00	2.81
17	11.16	11.16	0.807	0.00	0.00	0.00	3.05
18	14.35	14.35	0.627	0.00	0.00	0.00	3.19
19	16.59	16.59	0.542	0.00	0.00	0.00	2.24
20	18.15	18.15	0.496	0.00	0.00	0.00	1.56
21	18.80	18.80	0.479	0.00	0.00	0.00	0.65
22	19.18	19.18	0.469	0.00	0.00	0.00	0.38
23	19.33	19.33	0.466	0.00	0.00	0.00	0.15
24	19.37	19.37	0.465	0.00	0.00	0.00	0.04
25	19.39	19.39	0.464	0.00	0.00	0.00	0.02
				MEAN REL SENS.		0.0	

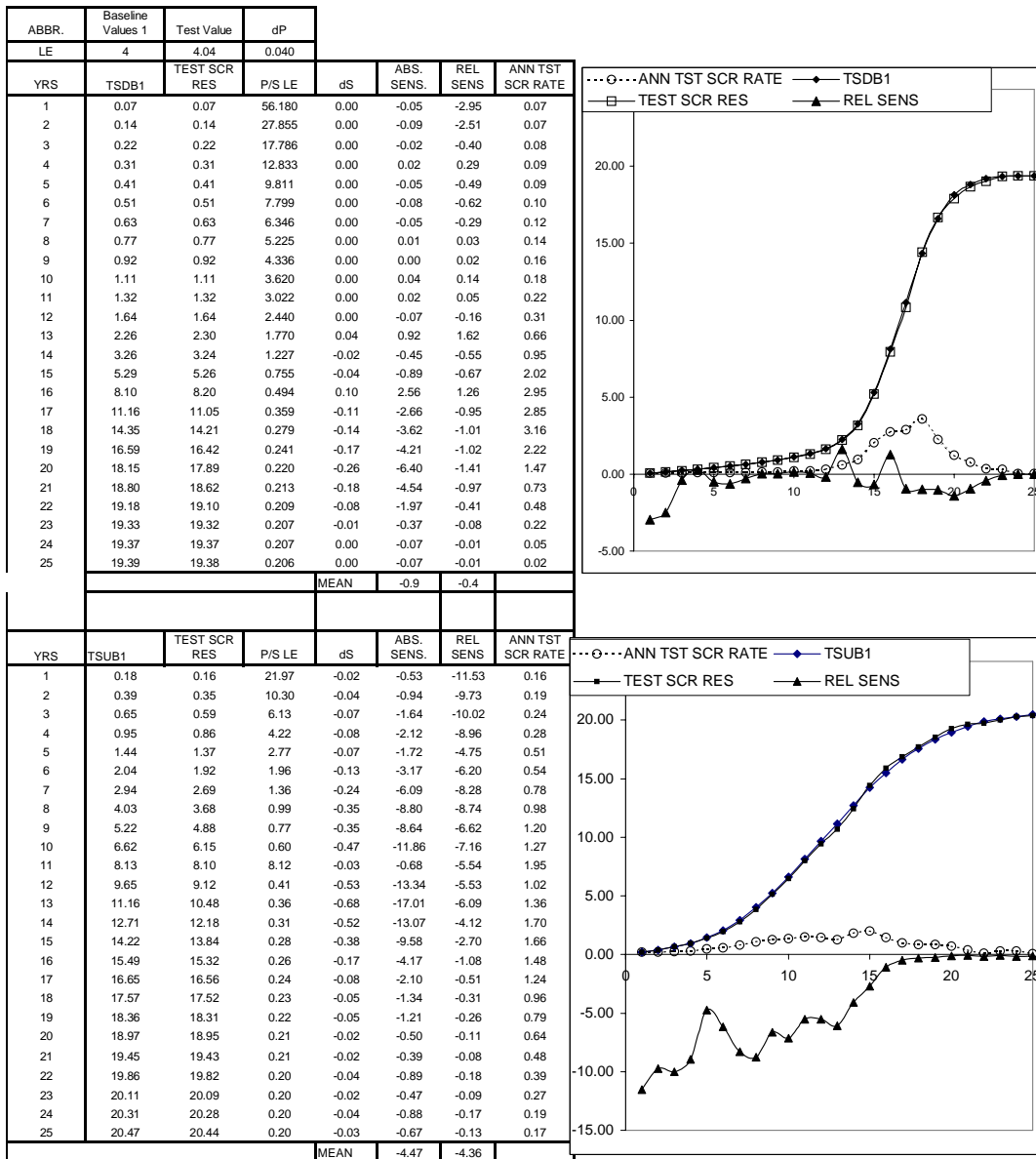


	Baseline Values 1			ABS. SENS.	REL SENS	ANN TST SCR RATE
YRS	TSUB1	TEST	P/S NBP			
		SCR RES				
1	0.18	0.18	49.42	0.00	0.00	0.18
2	0.39	0.39	23.18	0.00	0.00	0.21
3	0.65	0.65	13.79	0.00	0.00	0.26
4	0.95	0.95	9.50	0.00	0.00	0.30
5	1.44	1.44	6.24	0.00	0.00	0.50
6	2.04	2.04	4.40	0.00	0.00	0.60
7	2.94	2.94	3.06	0.00	0.00	0.89
8	4.03	4.03	2.23	0.00	0.00	1.09
9	5.22	5.22	1.72	0.00	0.00	1.20
10	6.62	6.62	1.36	0.00	0.00	1.40
11	8.13	8.13	1.11	0.00	0.00	1.50
12	9.65	9.65	0.93	0.00	0.00	1.52
13	11.16	11.16	0.81	0.00	0.00	1.51
14	12.71	12.71	0.71	0.00	0.00	1.54
15	14.22	14.22	0.63	0.00	0.00	1.52
16	15.49	15.49	0.58	0.00	0.00	1.27
17	16.65	16.65	0.54	0.00	0.00	1.16
18	17.57	17.57	0.51	0.00	0.00	0.92
19	18.36	18.36	0.49	0.00	0.00	0.78
20	18.97	18.97	0.47	0.00	0.00	0.62
21	19.45	19.45	0.46	0.00	0.00	0.48
22	19.86	19.86	0.45	0.00	0.00	0.41
23	20.11	20.11	0.45	0.00	0.00	0.25
24	20.31	20.31	0.44	0.00	0.00	0.20
25	20.47	20.47	0.44	0.00	0.00	0.16
			MEAN REL SENS.		0.00	



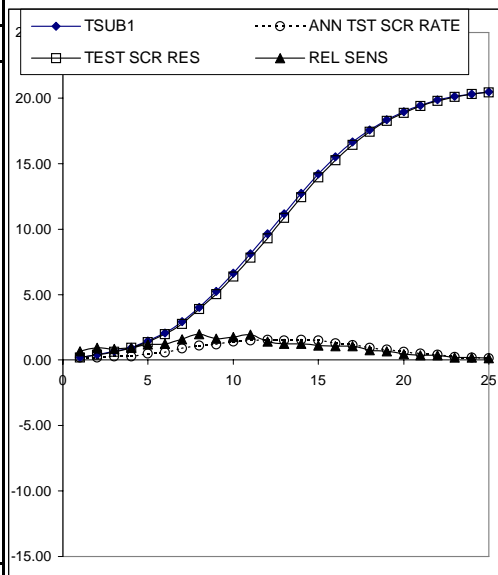
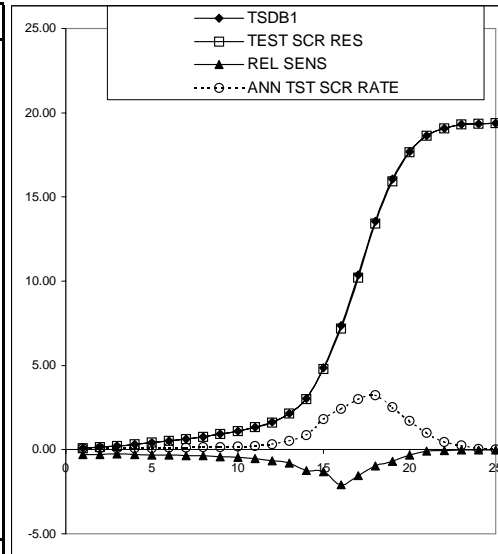


RELATIVE SENSITIVITY RESULTS FOR ESTUARY LENGTH



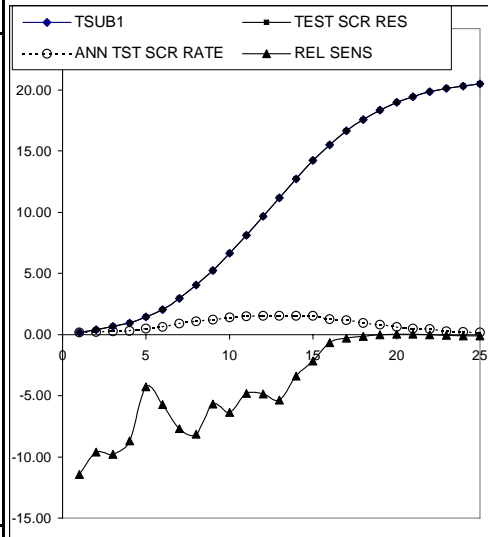
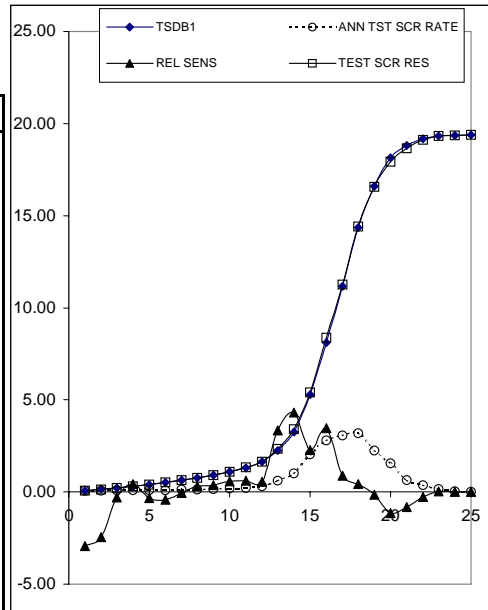
RELATIVE SENSIVITY RESULTS FOR CURVE NUMBER

		ABBR.	Baseline Values 1	Test Value	dP			
		CN	78	78.78	0.780			
YRS	TSDB1	TEST SCR RES	P/S CN	dS	ABS. SENS.	REL SENS	ANN TST SCR RATE	
1	0.07	0.07	1095.506	0.00	0.00	-0.28	0.07	
2	0.14	0.14	543.175	0.00	0.00	-0.28	0.07	
3	0.22	0.22	346.821	0.00	0.00	-0.27	0.08	
4	0.31	0.31	250.241	0.00	0.00	-0.29	0.09	
5	0.41	0.41	191.317	0.00	0.00	-0.32	0.10	
6	0.51	0.51	152.076	0.00	0.00	-0.33	0.10	
7	0.63	0.63	123.751	0.00	0.00	-0.35	0.12	
8	0.77	0.76	101.881	0.00	0.00	-0.37	0.13	
9	0.92	0.92	84.553	0.00	-0.01	-0.42	0.16	
10	1.11	1.10	70.582	-0.01	-0.01	-0.47	0.18	
11	1.32	1.32	58.930	-0.01	-0.01	-0.54	0.22	
12	1.63	1.62	47.944	-0.01	-0.01	-0.68	0.30	
13	2.15	2.13	36.331	-0.02	-0.02	-0.81	0.51	
14	3.03	2.99	25.737	-0.04	-0.05	-1.25	0.86	
15	4.85	4.79	16.076	-0.06	-0.08	-1.30	1.80	
16	7.35	7.20	10.613	-0.15	-0.20	-2.09	2.41	
17	10.36	10.20	7.529	-0.16	-0.20	-1.54	3.00	
18	13.56	13.42	5.754	-0.13	-0.17	-0.97	3.22	
19	16.06	15.94	4.858	-0.12	-0.15	-0.72	2.52	
20	17.69	17.64	4.408	-0.06	-0.07	-0.33	1.70	
21	18.65	18.64	4.182	-0.01	-0.02	-0.08	1.00	
22	19.08	19.07	4.087	-0.01	-0.01	-0.06	0.44	
23	19.32	19.32	4.037	0.00	0.00	-0.01	0.25	
24	19.36	19.36	4.029	0.00	0.00	-0.01	0.04	
25	19.38	19.38	4.025	0.00	-0.002	-0.01	0.02	
MEAN					-0.041	-0.6		
YRS	TSUB1	TEST SCR RES	P/S CN	dS	ABS. SENS.	REL SENS	ANN TST SCR RATE	
1	0.18	0.18	428.34	0.00	0.00	0.66	0.18	
2	0.38	0.39	202.86	0.00	0.00	0.91	0.20	
3	0.64	0.65	121.74	0.01	0.01	0.86	0.26	
4	0.92	0.93	84.81	0.01	0.01	0.91	0.28	
5	1.37	1.38	57.08	0.02	0.02	1.19	0.45	
6	1.96	1.99	39.76	0.02	0.03	1.25	0.60	
7	2.74	2.78	28.52	0.04	0.06	1.60	0.79	
8	3.80	3.87	20.53	0.08	0.10	1.98	1.09	
9	4.94	5.02	15.80	0.08	0.10	1.64	1.14	
10	6.25	6.36	12.47	0.11	0.14	1.74	1.35	
11	7.66	7.81	10.18	0.15	0.19	1.93	1.44	
12	9.17	9.30	8.50	0.13	0.16	1.39	1.49	
13	10.73	10.87	7.27	0.13	0.17	1.25	1.57	
14	12.27	12.43	6.35	0.15	0.19	1.23	1.56	
15	13.79	13.94	5.66	0.15	0.20	1.12	1.52	
16	15.11	15.27	5.16	0.16	0.21	1.07	1.33	
17	16.25	16.42	4.80	0.17	0.22	1.07	1.16	
18	17.29	17.42	4.51	0.13	0.17	0.75	0.99	
19	18.11	18.23	4.31	0.12	0.16	0.69	0.82	
20	18.77	18.85	4.16	0.09	0.11	0.46	0.62	
21	19.31	19.38	4.04	0.07	0.09	0.37	0.53	
22	19.72	19.79	3.96	0.08	0.10	0.38	0.41	
23	20.02	20.06	3.90	0.04	0.05	0.21	0.27	
24	20.25	20.28	3.85	0.04	0.05	0.18	0.22	
25	20.40	20.43	3.82	0.03	0.04	0.15	0.15	
MEAN					0.10	1.00		



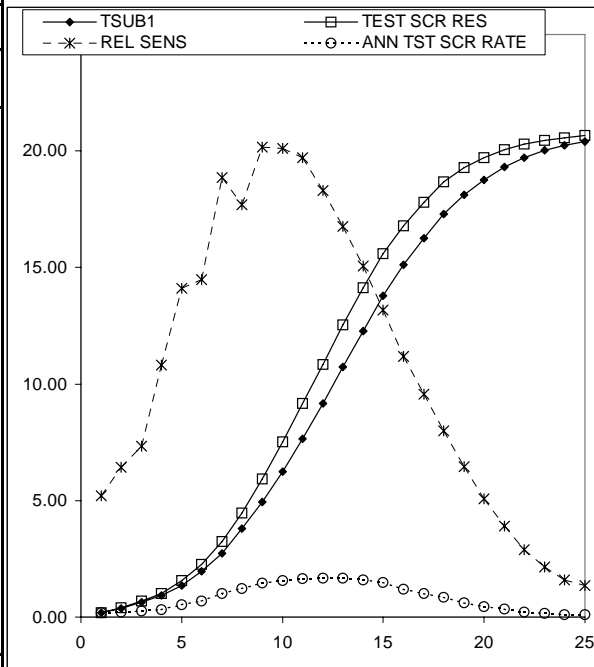
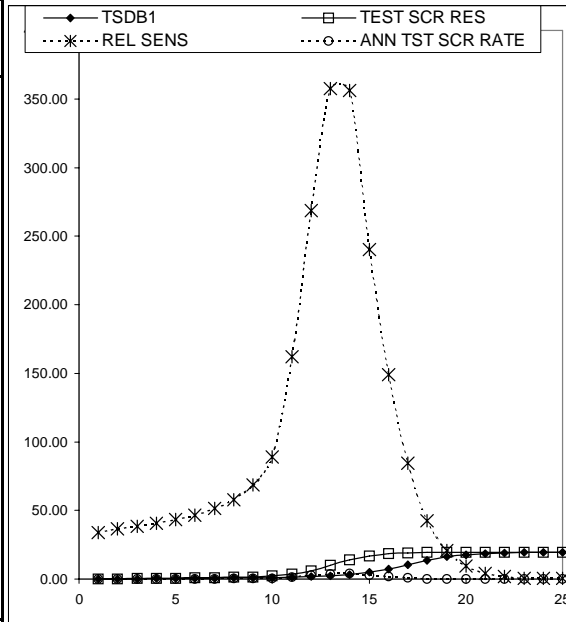
RELATIVE SENSIVITY RESULTS FOR C1

		ABBR.	Baseline Values 1	Test Value	dP			
		C1	0.25	0.253	0.003			
YRS	TSDB1	TEST SCR RES	P/S C1	dS	ABS. SENS.	REL SENS	ANN TST SCR RATE	
1	0.07	0.07	3.511	0.00	-0.84	-2.95	0.07	
2	0.14	0.14	1.741	0.00	-1.40	-2.44	0.07	
3	0.22	0.22	1.112	0.00	-0.28	-0.31	0.08	
4	0.31	0.31	0.802	0.00	0.52	0.42	0.09	
5	0.41	0.41	0.613	0.00	-0.56	-0.34	0.09	
6	0.51	0.51	0.487	0.00	-0.88	-0.43	0.10	
7	0.63	0.63	0.397	0.00	-0.16	-0.06	0.12	
8	0.77	0.77	0.327	0.00	0.96	0.31	0.14	
9	0.92	0.93	0.271	0.00	1.36	0.37	0.16	
10	1.11	1.11	0.226	0.01	2.56	0.58	0.19	
11	1.32	1.33	0.189	0.01	3.28	0.62	0.22	
12	1.64	1.65	0.152	0.01	3.68	0.56	0.32	
13	2.26	2.34	0.111	0.08	30.16	3.34	0.69	
14	3.26	3.40	0.077	0.14	56.24	4.31	1.07	
15	5.29	5.42	0.047	0.12	48.28	2.28	2.01	
16	8.10	8.38	0.031	0.28	111.84	3.45	2.97	
17	11.16	11.26	0.022	0.10	40.12	0.90	2.88	
18	14.35	14.41	0.017	0.06	23.80	0.41	3.15	
19	16.59	16.57	0.015	-0.02	-9.16	-0.14	2.16	
20	18.15	17.94	0.014	-0.21	-82.28	-1.13	1.37	
21	18.80	18.65	0.013	-0.15	-60.92	-0.81	0.71	
22	19.18	19.13	0.013	-0.05	-21.40	-0.28	0.48	
23	19.33	19.34	0.013	0.01	2.32	0.03	0.21	
24	19.37	19.37	0.013	0.00	-0.60	-0.01	0.03	
25	19.39	19.38	0.013	0.00	-0.72	-0.01	0.02	
				MEAN	5.8	0.3		
YRS	TSUB1	TEST SCR RES	P/S C1	dS	ABS. SENS.	REL SENS	ANN TST SCR RATE	
1	0.18	0.16	1.37	-0.02	-8.32	-11.42	0.16	
2	0.39	0.35	0.64	-0.04	-14.92	-9.61	0.19	
3	0.65	0.59	0.38	-0.06	-25.52	-9.77	0.24	
4	0.95	0.87	0.26	-0.08	-32.96	-8.69	0.28	
5	1.44	1.38	0.17	-0.06	-24.72	-4.28	0.52	
6	2.04	1.93	0.12	-0.12	-46.88	-5.73	0.55	
7	2.94	2.71	0.09	-0.23	-90.48	-7.70	0.78	
8	4.03	3.70	0.06	-0.33	-131.56	-8.17	0.99	
9	5.22	4.93	0.05	-0.30	-118.72	-5.68	1.23	
10	6.62	6.20	0.04	-0.42	-168.76	-6.37	1.28	
11	8.13	7.74	0.03	-0.39	-156.68	-4.82	1.53	
12	9.65	9.18	0.03	-0.47	-187.32	-4.85	1.45	
13	11.16	10.56	0.02	-0.60	-240.12	-5.38	1.38	
14	12.71	12.27	0.02	-0.43	-173.08	-3.41	1.71	
15	14.22	13.91	0.02	-0.31	-123.84	-2.18	1.64	
16	15.49	15.39	0.02	-0.10	-41.04	-0.66	1.48	
17	16.65	16.59	0.02	-0.05	-20.72	-0.31	1.21	
18	17.57	17.54	0.01	-0.03	-10.64	-0.15	0.95	
19	18.36	18.35	0.01	-0.01	-2.68	-0.04	0.80	
20	18.97	18.98	0.01	0.01	2.88	0.04	0.63	
21	19.45	19.45	0.01	0.01	2.44	0.03	0.47	
22	19.86	19.85	0.01	-0.01	-2.44	-0.03	0.40	
23	20.11	20.10	0.01	-0.01	-3.84	-0.05	0.24	
24	20.31	20.29	0.01	-0.03	-10.16	-0.13	0.19	
25	20.47	20.45	0.01	-0.02	-7.60	-0.09	0.17	
				MEAN	-65.51	-3.98		



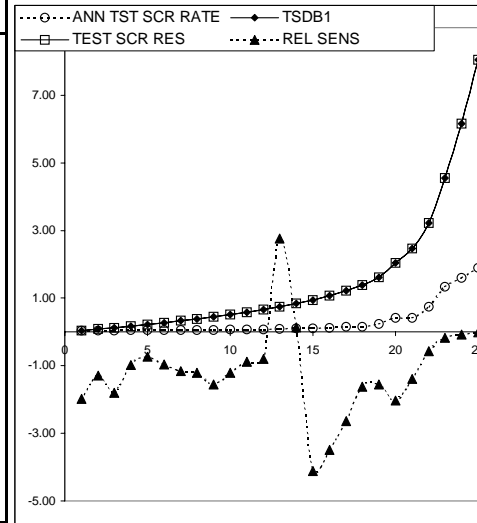
RELATIVE SENSITIVITY TIDAL AMPLITUDE BRIDGE STATION  
P= Predictor variable S= Baseline scour

	ABBR.	Baseline Values 1	Test Value	dP			
	MDA	1.22	1.23	0.012			
YRS	TSDB1	TEST SCR RES	P/S MTR	dS	ABS. SENS.	REL SENS	ANN TST SCR RATE
1	0.07	0.10	10.53	0.02	3.21	33.85	0.10
2	0.14	0.20	5.22	0.05	6.96	36.35	0.10
3	0.22	0.31	3.33	0.09	11.45	38.19	0.12
4	0.31	0.44	2.41	0.13	16.81	40.46	0.13
5	0.41	0.58	1.84	0.18	23.57	43.37	0.15
6	0.51	0.75	1.46	0.24	31.95	46.71	0.17
7	0.63	0.95	1.19	0.32	43.21	51.42	0.20
8	0.77	1.21	0.98	0.44	58.89	57.69	0.25
9	0.92	1.55	0.81	0.63	84.19	68.44	0.35
10	1.11	2.09	0.68	0.98	131.16	89.01	0.53
11	1.32	3.47	0.57	2.14	285.68	161.88	1.38
12	1.63	6.00	0.46	4.37	582.80	268.67	2.53
13	2.15	9.82	0.35	7.68	1023.33	357.49	3.82
14	3.03	13.82	0.25	10.79	1439.08	356.14	4.00
15	4.85	16.50	0.15	11.65	1553.59	240.15	2.68
16	7.35	18.31	0.10	10.96	1460.80	149.07	1.80
17	10.36	19.12	0.07	8.76	1168.37	84.58	0.82
18	13.56	19.28	0.06	5.73	763.43	42.24	0.16
19	16.06	19.38	0.05	3.32	442.92	20.69	0.10
20	17.69	19.40	0.04	1.71	227.48	9.64	0.02
21	18.65	19.42	0.04	0.77	102.28	4.11	0.02
22	19.08	19.43	0.04	0.35	46.51	1.83	0.01
23	19.32	19.45	0.04	0.12	16.65	0.65	0.01
24	19.36	19.46	0.04	0.10	12.89	0.50	0.01
25	19.38	19.47	0.04	0.09	11.73	0.45	0.01
MEAN R					382.0	88.1	
YRS	TSUB1	TEST SCR RES	P/S MTR	dS	ABS. SENS.	REL SENS	ANN TST SCR RATE
1	0.18	0.19	4.12	0.01	1.27	5.22	0.19
2	0.38	0.41	1.95	0.02	3.29	6.42	0.22
3	0.64	0.69	1.17	0.05	6.27	7.34	0.28
4	0.92	1.02	0.82	0.10	13.25	10.81	0.33
5	1.37	1.56	0.55	0.19	25.68	14.10	0.54
6	1.96	2.25	0.38	0.28	37.88	14.48	0.69
7	2.74	3.25	0.27	0.52	68.77	18.86	1.01
8	3.80	4.47	0.20	0.67	89.57	17.68	1.22
9	4.94	5.93	0.15	1.00	132.75	20.17	1.46
10	6.25	7.51	0.12	1.26	167.73	20.11	1.58
11	7.66	9.17	0.10	1.51	201.23	19.70	1.66
12	9.17	10.85	0.08	1.68	223.76	18.29	1.68
13	10.73	12.53	0.07	1.80	240.07	16.77	1.68
14	12.27	14.12	0.06	1.85	246.69	15.07	1.59
15	13.79	15.60	0.05	1.82	242.07	13.17	1.48
16	15.11	16.80	0.05	1.69	225.25	11.18	1.19
17	16.25	17.80	0.05	1.56	207.45	9.58	1.01
18	17.29	18.67	0.04	1.38	184.07	7.99	0.86
19	18.11	19.28	0.04	1.17	155.79	6.45	0.61
20	18.77	19.72	0.04	0.95	126.85	5.07	0.44
21	19.31	20.07	0.04	0.75	100.47	3.90	0.35
22	19.72	20.29	0.04	0.57	76.23	2.90	0.23
23	20.02	20.45	0.04	0.43	57.47	2.15	0.16
24	20.25	20.57	0.04	0.32	42.88	1.59	0.11
25	20.40	20.68	0.04	0.28	36.81	1.35	0.11
MEAN					116.5	10.8	

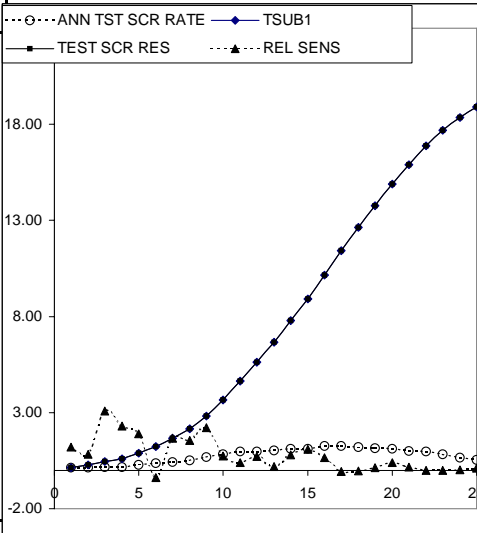


RELATIVE SENSITIVITY RESULTS FOR DISTANCE FROM BRIDGE TO BASE STATION(LW)

	ABBR.	Baseline Values 1	Test Value	dP			
	CN	78	78.78	0.780			
YRS	TSDB1	TEST SCR RES	P/S LE	dS	ABS. SENS.	REL SENS	ANN TST SCR RATE
1	0.07	0.06	1526.718	0.00	0.00	-1.98	0.06
2	0.13	0.13	755.287	0.00	0.00	-1.28	0.07
3	0.21	0.21	472.813	0.00	0.00	-1.80	0.08
4	0.29	0.29	339.443	0.00	0.00	-0.98	0.08
5	0.38	0.38	262.329	0.00	0.00	-0.73	0.09
6	0.48	0.47	209.380	0.00	0.00	-0.96	0.09
7	0.59	0.58	170.416	-0.01	-0.01	-1.16	0.11
8	0.71	0.70	140.469	-0.01	-0.01	-1.21	0.12
9	0.85	0.84	117.247	-0.01	-0.01	-1.56	0.14
10	1.02	1.00	98.464	-0.01	-0.01	-1.21	0.16
11	1.20	1.19	83.153	-0.01	-0.01	-0.88	0.19
12	1.47	1.46	68.064	-0.01	-0.01	-0.80	0.27
13	1.80	1.85	55.423	0.05	0.05	2.76	0.40
14	2.67	2.68	37.421	0.00	0.00	0.14	0.82
15	4.06	3.90	24.604	-0.17	-0.17	-4.11	1.22
16	6.24	6.02	16.026	-0.22	-0.22	-3.48	2.13
17	8.93	8.70	11.194	-0.24	-0.24	-2.64	2.68
18	11.82	11.63	8.460	-0.19	-0.19	-1.62	2.93
19	14.66	14.43	6.822	-0.23	-0.23	-1.55	2.80
20	16.66	16.32	6.003	-0.34	-0.34	-2.04	1.89
21	17.98	17.73	5.562	-0.25	-0.25	-1.38	1.41
22	18.68	18.58	5.353	-0.11	-0.11	-0.57	0.84
23	19.11	19.08	5.233	-0.03	-0.03	-0.17	0.50
24	19.34	19.33	5.170	-0.02	-0.02	-0.08	0.25
25	19.36	19.36	5.165	0.00	0.00	-0.01	0.04
				MEAN	-0.1	-1.2	
YRS	TSUB1	TEST SCR RES	P/S LE	dS	ABS. SENS.	REL SENS	ANN TST SCR RATE
1	0.16	0.16	634.52	0.00	0.00	1.21	0.16
2	0.34	0.35	292.23	0.00	0.00	0.82	0.19
3	0.57	0.59	175.50	0.02	0.02	3.09	0.24
4	0.84	0.86	119.60	0.02	0.02	2.31	0.27
5	1.29	1.32	77.42	0.02	0.02	1.90	0.46
6	1.84	1.83	54.43	-0.01	-0.01	-0.38	0.51
7	2.53	2.57	39.49	0.04	0.04	1.68	0.74
8	3.51	3.56	28.51	0.05	0.05	1.56	0.99
9	4.66	4.76	21.45	0.10	0.10	2.21	1.20
10	5.86	5.91	17.05	0.04	0.04	0.75	1.14
11	7.29	7.34	8.12	0.05	0.05	0.39	1.43
12	8.69	8.75	11.51	0.06	0.06	0.70	1.41
13	10.09	10.11	9.91	0.02	0.02	0.19	1.36
14	11.62	11.71	8.61	0.09	0.09	0.80	1.60
15	13.32	13.47	7.51	0.14	0.14	1.08	1.76
16	14.79	14.89	6.76	0.10	0.10	0.66	1.42
17	16.11	16.10	6.21	-0.01	-0.01	-0.07	1.21
18	17.15	17.15	5.83	0.00	0.00	-0.03	1.05
19	18.01	18.04	5.55	0.02	0.02	0.13	0.89
20	18.63	18.70	5.37	0.07	0.07	0.39	0.67
21	19.16	19.20	5.22	0.03	0.03	0.18	0.49
22	19.61	19.61	5.10	0.00	0.00	0.00	0.41
23	19.95	19.95	5.01	0.00	0.00	0.00	0.34
24	20.18	20.18	4.96	0.01	0.01	0.03	0.23
25	20.33	20.35	4.92	0.02	0.02	0.11	0.17
				MEAN	0.04	0.79	

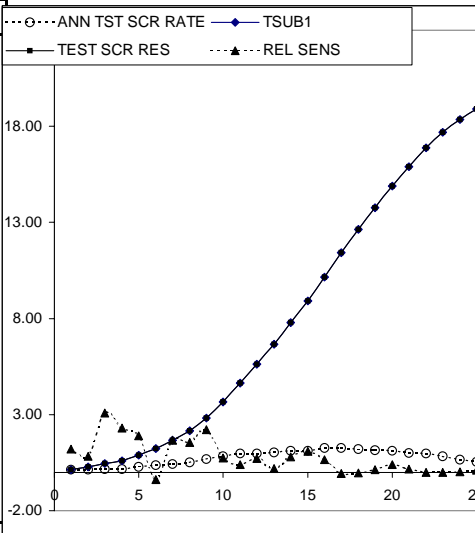
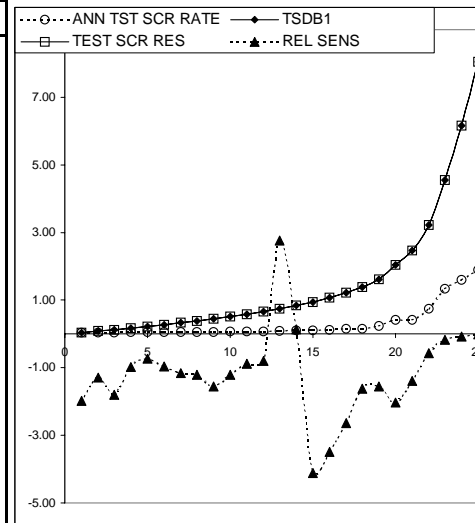


17.4 18.3



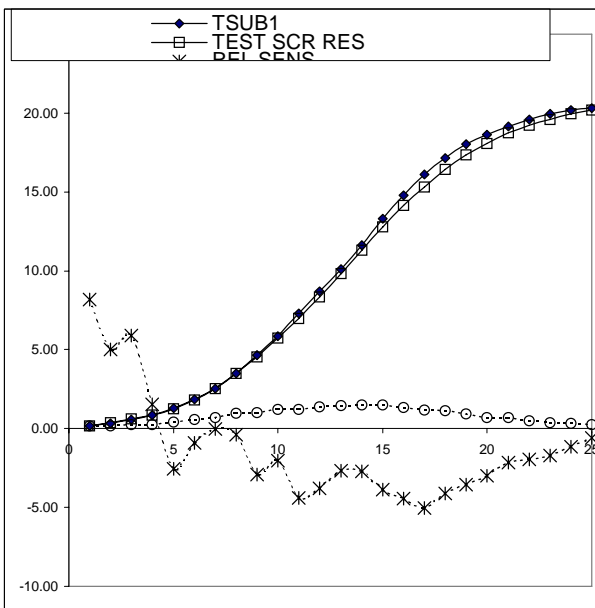
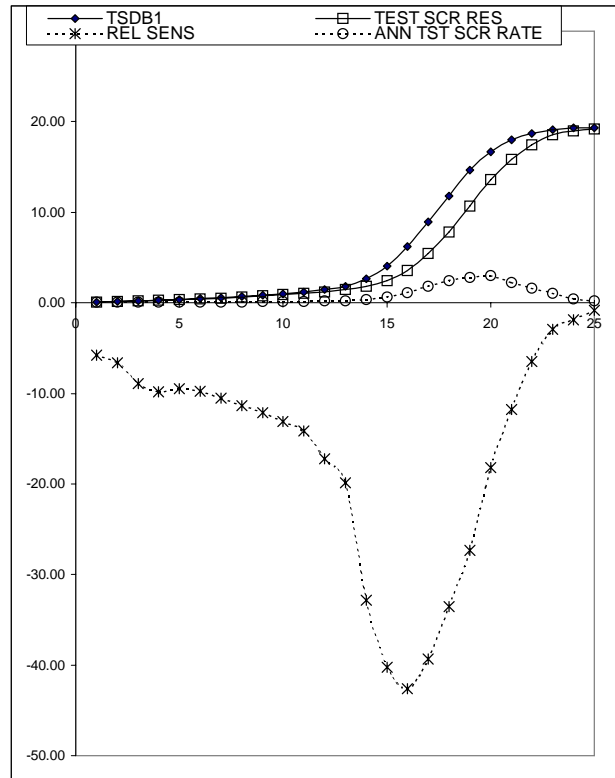
RELATIVE SENSITIVITY RESULTS FOR DISTANCE FROM BRIDGE TO BASE STATION(LW)

	ABBR.	Baseline Values 1	Test Value	dP			
	LW	100	101.00	1.000			
YRS	TSDB1	TEST SCR RES	P/S LE	dS	ABS. SENS.	REL SENS	ANN TST SCR RATE
1	0.07	0.06	1526.718	0.00	0.00	-1.98	0.06
2	0.13	0.13	755.287	0.00	0.00	-1.28	0.07
3	0.21	0.21	472.813	0.00	0.00	-1.80	0.08
4	0.29	0.29	339.443	0.00	0.00	-0.98	0.08
5	0.38	0.38	262.329	0.00	0.00	-0.73	0.09
6	0.48	0.47	209.380	0.00	0.00	-0.96	0.09
7	0.59	0.58	170.416	-0.01	-0.01	-1.16	0.11
8	0.71	0.70	140.469	-0.01	-0.01	-1.21	0.12
9	0.85	0.84	117.247	-0.01	-0.01	-1.56	0.14
10	1.02	1.00	98.464	-0.01	-0.01	-1.21	0.16
11	1.20	1.19	83.153	-0.01	-0.01	-0.88	0.19
12	1.47	1.46	68.064	-0.01	-0.01	-0.80	0.27
13	1.80	1.85	55.423	0.05	0.05	2.76	0.40
14	2.67	2.68	37.421	0.00	0.00	0.14	0.82
15	4.06	3.90	24.604	-0.17	-0.17	-4.11	1.22
16	6.24	6.02	16.026	-0.22	-0.22	-3.48	2.13
17	8.93	8.70	11.194	-0.24	-0.24	-2.64	2.68
18	11.82	11.63	8.460	-0.19	-0.19	-1.62	2.93
19	14.66	14.43	6.822	-0.23	-0.23	-1.55	2.80
20	16.66	16.32	6.003	-0.34	-0.34	-2.04	1.89
21	17.98	17.73	5.562	-0.25	-0.25	-1.38	1.41
22	18.68	18.58	5.353	-0.11	-0.11	-0.57	0.84
23	19.11	19.08	5.233	-0.03	-0.03	-0.17	0.50
24	19.34	19.33	5.170	-0.02	-0.02	-0.08	0.25
25	19.36	19.36	5.165	0.00	0.00	-0.01	0.04
				MEAN	-0.1	-1.2	
YRS	TSUB1	TEST SCR RES	P/S LE	dS	ABS. SENS.	REL SENS	ANN TST SCR RATE
1	0.16	0.16	634.52	0.00	0.00	1.21	0.16
2	0.34	0.35	292.23	0.00	0.00	0.82	0.19
3	0.57	0.59	175.50	0.02	0.02	3.09	0.24
4	0.84	0.86	119.60	0.02	0.02	2.31	0.27
5	1.29	1.32	77.42	0.02	0.02	1.90	0.46
6	1.84	1.83	54.43	-0.01	-0.01	-0.38	0.51
7	2.53	2.57	39.49	0.04	0.04	1.68	0.74
8	3.51	3.56	28.51	0.05	0.05	1.56	0.99
9	4.66	4.76	21.45	0.10	0.10	2.21	1.20
10	5.86	5.91	17.05	0.04	0.04	0.75	1.14
11	7.29	7.34	8.12	0.05	0.05	0.39	1.43
12	8.69	8.75	11.51	0.06	0.06	0.70	1.41
13	10.09	10.11	9.91	0.02	0.02	0.19	1.36
14	11.62	11.71	8.61	0.09	0.09	0.80	1.60
15	13.32	13.47	7.51	0.14	0.14	1.08	1.76
16	14.79	14.89	6.76	0.10	0.10	0.66	1.42
17	16.11	16.10	6.21	-0.01	-0.01	-0.07	1.21
18	17.15	17.15	5.83	0.00	0.00	-0.03	1.05
19	18.01	18.04	5.55	0.02	0.02	0.13	0.89
20	18.63	18.70	5.37	0.07	0.07	0.39	0.67
21	19.16	19.20	5.22	0.03	0.03	0.18	0.49
22	19.61	19.61	5.10	0.00	0.00	0.00	0.41
23	19.95	19.95	5.01	0.00	0.00	0.00	0.34
24	20.18	20.18	4.96	0.01	0.01	0.03	0.23
25	20.33	20.35	4.92	0.02	0.02	0.11	0.17
				MEAN	0.04	0.79	



RELATIVE SENSITIVITY RESULTS FOR ESTUARY WIDTH AT BRIDGE CROSS SECTION  
P= Predictor variable S= Baseline scour

	ABBR.	Baseline Values 1	Test Value	dP			
	WB	0.33	0.33	0.003			
YRS	TSDB1	TEST SCR RES	P/S WB	dS	ABS. SENS.	REL SENS	ANN TST SCR RATE
1	0.07	0.06	5.04	0.00	-1.2	-5.80	0.06
2	0.13	0.12	2.49	-0.01	-2.7	-6.65	0.06
3	0.21	0.19	1.56	-0.02	-5.7	-8.94	0.07
4	0.29	0.27	1.12	-0.03	-8.8	-9.84	0.07
5	0.38	0.35	0.87	-0.04	-10.9	-9.47	0.08
6	0.48	0.43	0.69	-0.05	-14.1	-9.74	0.09
7	0.59	0.52	0.56	-0.06	-18.8	-10.55	0.09
8	0.71	0.63	0.46	-0.08	-24.6	-11.39	0.11
9	0.85	0.75	0.39	-0.10	-31.3	-12.11	0.12
10	1.02	0.88	0.32	-0.13	-40.3	-13.11	0.13
11	1.20	1.03	0.27	-0.17	-51.7	-14.18	0.15
12	1.47	1.22	0.22	-0.25	-76.5	-17.19	0.18
13	1.80	1.45	0.18	-0.36	-108.5	-19.85	0.23
14	2.67	1.79	0.12	-0.88	-266.2	-32.87	0.35
15	4.06	2.43	0.08	-1.63	-495.2	-40.21	0.64
16	6.24	3.58	0.05	-2.66	-806.2	-42.64	1.15
17	8.93	5.42	0.04	-3.52	-1065.4	-39.36	1.84
18	11.82	7.85	0.03	-3.97	-1202.1	-33.56	2.44
19	14.66	10.65	0.02	-4.01	-1215.6	-27.37	2.79
20	16.66	13.62	0.02	-3.04	-920.1	-18.23	2.98
21	17.98	15.87	0.02	-2.11	-639.9	-11.75	2.25
22	18.68	17.47	0.02	-1.21	-366.2	-6.47	1.61
23	19.11	18.55	0.02	-0.56	-170.8	-2.95	1.07
24	19.34	18.97	0.02	-0.37	-111.4	-1.90	0.43
25	19.36	19.20	0.02	-0.16	-48.7	-0.83	0.23
MEAN					-308.1	-16.3	
YRS	TSUB1	TEST SCR RES	P/S WB	dS	ABS. SENS.	REL SENS	ANN TST SCR RATE
1	0.16	0.17	2.09	0.01	3.91	8.19	0.17
2	0.34	0.36	0.96	0.02	5.21	5.03	0.19
3	0.57	0.60	0.58	0.03	10.18	5.90	0.24
4	0.84	0.85	0.39	0.01	3.85	1.52	0.25
5	1.29	1.26	0.26	-0.03	-10.00	-2.55	0.41
6	1.84	1.82	0.18	-0.02	-4.97	-0.89	0.56
7	2.53	2.53	0.13	0.00	-0.18	-0.02	0.71
8	3.51	3.50	0.09	-0.01	-3.94	-0.37	0.96
9	4.66	4.53	0.07	-0.14	-41.15	-2.91	1.03
10	5.86	5.74	0.06	-0.12	-36.09	-2.03	1.22
11	7.29	6.97	0.05	-0.32	-97.00	-4.39	1.23
12	8.69	8.36	0.04	-0.33	-99.36	-3.78	1.39
13	10.09	9.82	0.03	-0.27	-81.85	-2.68	1.46
14	11.62	11.30	0.03	-0.31	-95.39	-2.71	1.48
15	13.32	12.81	0.02	-0.52	-157.00	-3.89	1.50
16	14.79	14.13	0.02	-0.66	-199.48	-4.45	1.32
17	16.11	15.30	0.02	-0.81	-246.00	-5.04	1.17
18	17.15	16.45	0.02	-0.70	-213.27	-4.10	1.15
19	18.01	17.37	0.02	-0.64	-194.88	-3.57	0.92
20	18.63	18.07	0.02	-0.56	-169.73	-3.01	0.70
21	19.16	18.75	0.02	-0.41	-125.73	-2.17	0.68
22	19.61	19.23	0.02	-0.38	-115.55	-1.94	0.48
23	19.95	19.61	0.02	-0.34	-102.45	-1.69	0.39
24	20.18	19.94	0.02	-0.23	-70.82	-1.16	0.33
25	20.33	20.21	0.02	-0.12	-35.91	-0.58	0.27
MEAN					-83.1	-1.3	

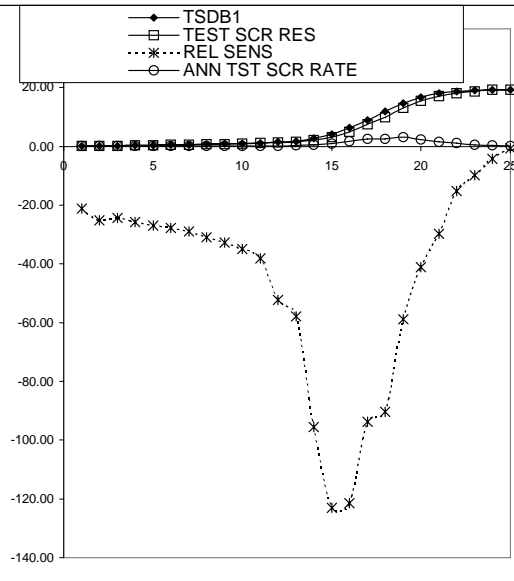


RELATIVE SENSIVITY RESULTS FOR MEAN DIURNAL AMP AT THE BASE STA.

P= Predictor variable

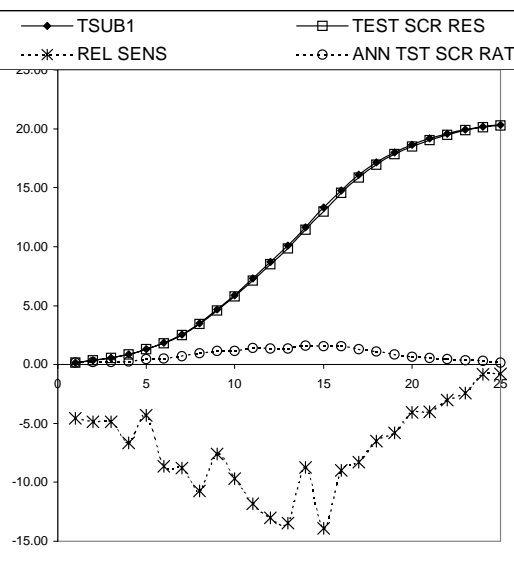
S= Baseline scour

YRS	TSDB1	TEST SCR RES	P/S XAREA	dS	ABS. SENS.	REL SENS	ANN TST SCR RATE
1	0.07	0.06	19	0.00	-1	-21.17	0.06
2	0.13	0.13	9	-0.01	-3	-25.13	0.06
3	0.21	0.20	6	-0.01	-4	-24.38	0.08
4	0.29	0.28	4	-0.01	-6	-25.79	0.08
5	0.38	0.36	3	-0.02	-8	-26.91	0.08
6	0.48	0.45	3	-0.02	-11	-27.75	0.09
7	0.59	0.56	2	-0.03	-14	-28.92	0.10
8	0.71	0.67	2	-0.04	-18	-30.92	0.12
9	0.85	0.80	1	-0.05	-23	-32.70	0.13
10	1.02	0.95	1	-0.06	-29	-35.00	0.15
11	1.20	1.12	1	-0.08	-38	-38.04	0.17
12	1.47	1.33	1	-0.14	-63	-52.31	0.21
13	1.80	1.62	1	-0.19	-86	-57.87	0.29
14	2.67	2.21	0	-0.46	-209	-95.48	0.60
15	4.06	3.16	0	-0.90	-410	-122.96	0.95
16	6.24	4.87	0	-1.37	-621	-121.43	1.71
17	8.93	7.42	0	-1.51	-687	-93.83	2.55
18	11.82	9.89	0	-1.93	-876	-90.39	2.47
19	14.66	13.10	0	-1.56	-708	-58.92	3.21
20	16.66	15.43	0	-1.23	-561	-41.05	2.33
21	17.98	17.02	0	-0.96	-438	-29.71	1.59
22	18.68	18.17	0	-0.51	-232	-15.16	1.15
23	19.11	18.77	0	-0.34	-154	-9.83	0.60
24	19.34	19.20	0	-0.15	-66	-4.16	0.43
25	19.36	19.34	0	-0.02	-10	-0.62	0.14



				MEAN REL SENS	-44.4	
--	--	--	--	---------------	-------	--

YRS	TSUB1	TEST SCR RES	P/S XAREA	dS	ABS. SENS.	REL SENS	ANN TST SCR RATE
1	0.16	0.16	8	0.00	-1	-4.57	0.16
2	0.34	0.34	4	0.00	-1	-4.86	0.18
3	0.57	0.56	2	-0.01	-2	-4.87	0.23
4	0.84	0.83	1	-0.01	-5	-6.63	0.26
5	1.29	1.28	1	-0.01	-5	-4.34	0.46
6	1.84	1.81	1	-0.03	-13	-8.66	0.53
7	2.53	2.49	0	-0.04	-18	-8.80	0.68
8	3.51	3.44	0	-0.07	-31	-10.72	0.95
9	4.66	4.60	0	-0.06	-29	-7.58	1.16
10	5.86	5.76	0	-0.10	-47	-9.67	1.16
11	7.29	7.13	0	-0.16	-71	-11.82	1.37
12	8.69	8.48	0	-0.20	-93	-13.03	1.35
13	10.09	9.84	0	-0.24	-111	-13.46	1.36
14	11.62	11.43	0	-0.18	-83	-8.76	1.59
15	13.32	12.99	0	-0.33	-152	-13.91	1.56
16	14.79	14.55	0	-0.24	-109	-9.00	1.56
17	16.11	15.87	0	-0.24	-109	-8.28	1.32
18	17.15	16.95	0	-0.20	-91	-6.49	1.08
19	18.01	17.83	0	-0.19	-85	-5.78	0.88
20	18.63	18.50	0	-0.14	-62	-4.06	0.67
21	19.16	19.02	0	-0.14	-63	-4.02	0.53
22	19.61	19.50	0	-0.11	-49	-3.02	0.48
23	19.95	19.86	0	-0.09	-40	-2.44	0.36
24	20.18	20.15	0	-0.03	-14	-0.86	0.28
25	20.33	20.30	0	-0.03	-13	-0.81	0.15

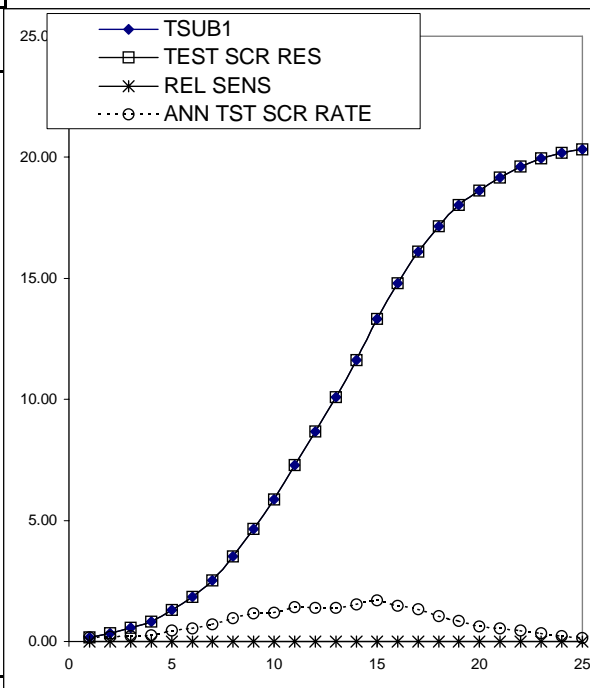
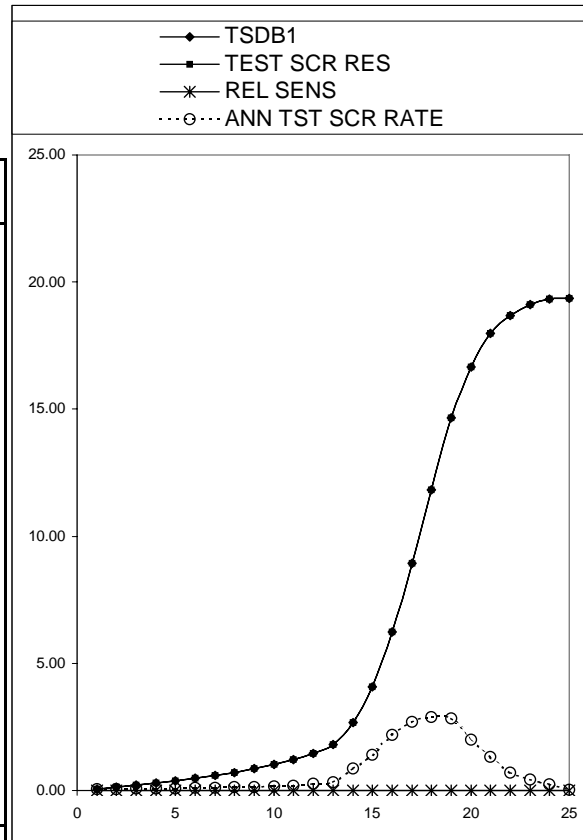


				MEAN REL SENS.	-7.1	
--	--	--	--	----------------	------	--

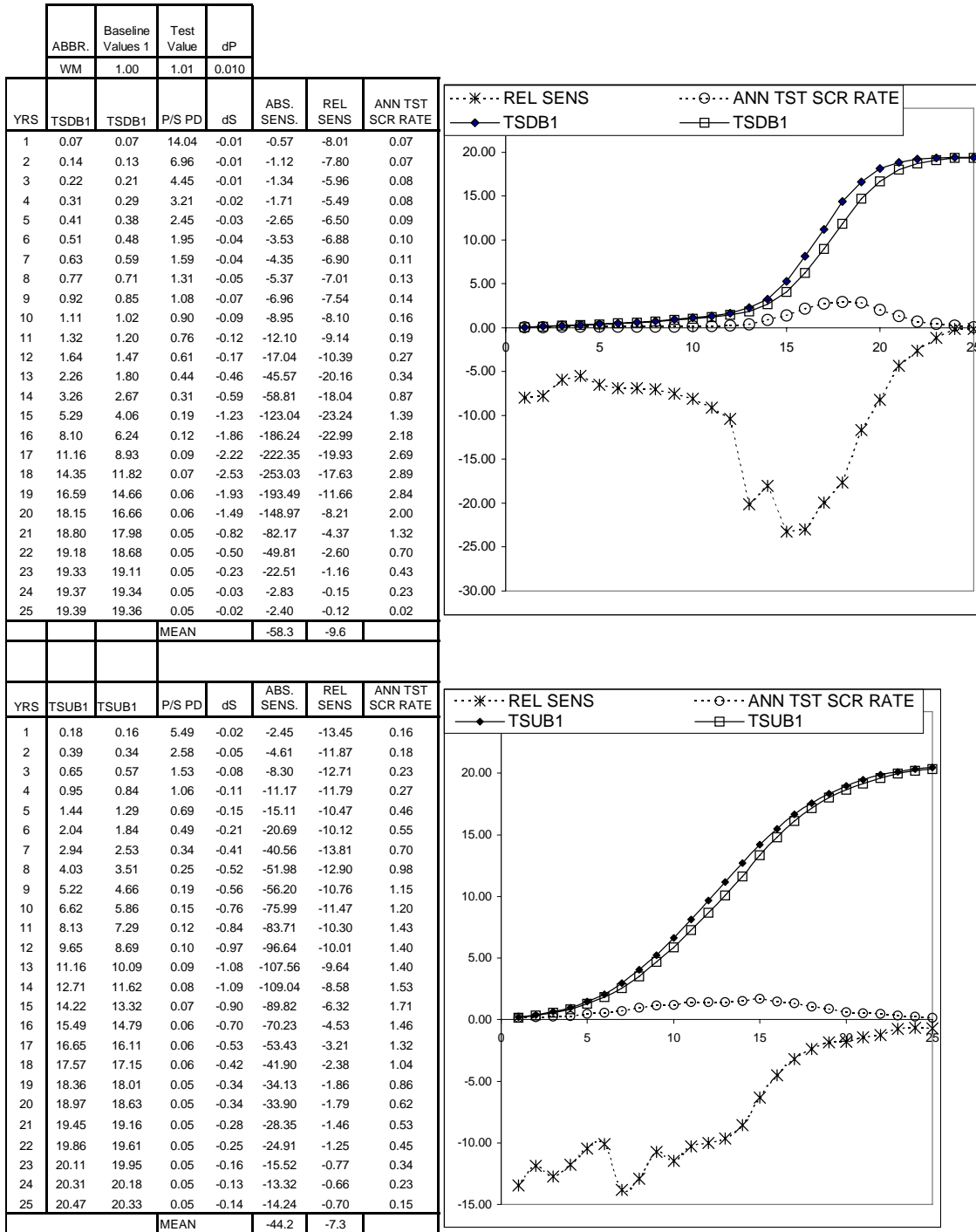


RELATIVE SENSITIVITY RESULTS FOR UPSTREAM WIDTH  
P= Predictor variable S= Baseline scour

	ABBR.	Baseline Values 1	Test Value	dP			
	WU	0.33	0.33	0.003			
YRS	TSDB1	TEST SCR RES	P/S WU	dS	ABS. SENS.	REL SENS	ANN TST SCR RATE
1	0.07	0.07	4580.2	0.00	0.00	0.00	0.07
2	0.13	0.13	2265.86	0.00	0.00	0.00	0.07
3	0.21	0.21	1418.44	0.00	0.00	0.00	0.08
4	0.29	0.29	1018.33	0.00	0.00	0.00	0.08
5	0.38	0.38	786.99	0.00	0.00	0.00	0.09
6	0.48	0.48	628.14	0.00	0.00	0.00	0.10
7	0.59	0.59	511.25	0.00	0.00	0.00	0.11
8	0.71	0.71	421.41	0.00	0.00	0.00	0.13
9	0.85	0.85	351.74	0.00	0.00	0.00	0.14
10	1.02	1.02	295.39	0.00	0.00	0.00	0.16
11	1.20	1.20	249.46	0.00	0.00	0.00	0.19
12	1.47	1.47	204.19	0.00	0.00	0.00	0.27
13	1.80	1.80	166.27	0.00	0.00	0.00	0.34
14	2.67	2.67	112.26	0.00	0.00	0.00	0.87
15	4.06	4.06	73.81	0.00	0.00	0.00	1.39
16	6.24	6.24	48.08	0.00	0.00	0.00	2.18
17	8.93	8.93	33.58	0.00	0.00	0.00	2.69
18	11.82	11.82	25.38	0.00	0.00	0.00	2.89
19	14.66	14.66	20.47	0.00	0.00	0.00	2.84
20	16.66	16.66	18.01	0.00	0.00	0.00	2.00
21	17.98	17.98	16.69	0.00	0.00	0.00	1.32
22	18.68	18.68	16.06	0.00	0.00	0.00	0.70
23	19.11	19.11	15.70	0.00	0.00	0.00	0.43
24	19.34	19.34	15.51	0.00	0.00	0.00	0.23
25	19.36	19.36	15.49	0.00	0.00	0.00	0.02
			MEAN REL SENS.			0.0	
YRS	TSUB1	TEST SCR RES	P/S WU	dS	ABS. SENS.	REL SENS	ANN TST SCR RATE
1	0.16	0.16	1903.55	0.00	0.00	0.00	0.16
2	0.34	0.34	876.68	0.00	0.00	0.00	0.18
3	0.57	0.57	526.50	0.00	0.00	0.00	0.23
4	0.84	0.84	358.81	0.00	0.00	0.00	0.27
5	1.29	1.29	232.25	0.00	0.00	0.00	0.46
6	1.84	1.84	163.28	0.00	0.00	0.00	0.55
7	2.53	2.53	118.46	0.00	0.00	0.00	0.70
8	3.51	3.51	85.52	0.00	0.00	0.00	0.98
9	4.66	4.66	64.36	0.00	0.00	0.00	1.15
10	5.86	5.86	51.16	0.00	0.00	0.00	1.20
11	7.29	7.29	41.15	0.00	0.00	0.00	1.43
12	8.69	8.69	34.54	0.00	0.00	0.00	1.40
13	10.09	10.09	29.74	0.00	0.00	0.00	1.40
14	11.62	11.62	25.83	0.00	0.00	0.00	1.53
15	13.32	13.32	22.52	0.00	0.00	0.00	1.71
16	14.79	14.79	20.29	0.00	0.00	0.00	1.46
17	16.11	16.11	18.62	0.00	0.00	0.00	1.32
18	17.15	17.15	17.49	0.00	0.00	0.00	1.04
19	18.01	18.01	16.65	0.00	0.00	0.00	0.86
20	18.63	18.63	16.10	0.00	0.00	0.00	0.62
21	19.16	19.16	15.66	0.00	0.00	0.00	0.53
22	19.61	19.61	15.30	0.00	0.00	0.00	0.45
23	19.95	19.95	15.04	0.00	0.00	0.00	0.34
24	20.18	20.18	14.87	0.00	0.00	0.00	0.23
25	20.33	20.33	14.76	0.00	0.00	0.00	0.15
			MEAN REL SENS.			0.0	

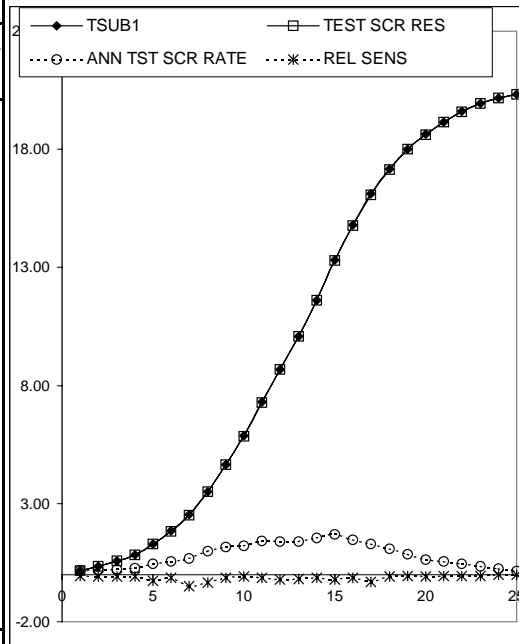
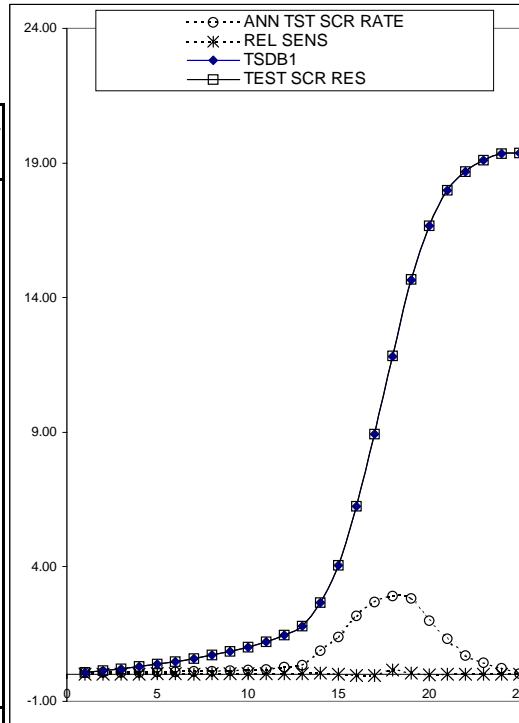


RELATIVE SENSITIVITY RESULTS FOR MAX ESTUARY WIDTH



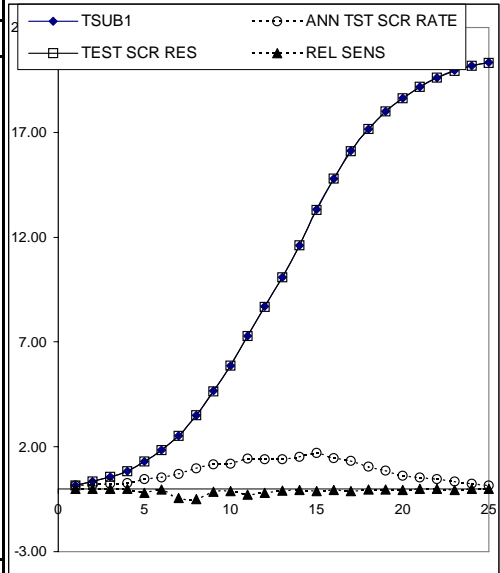
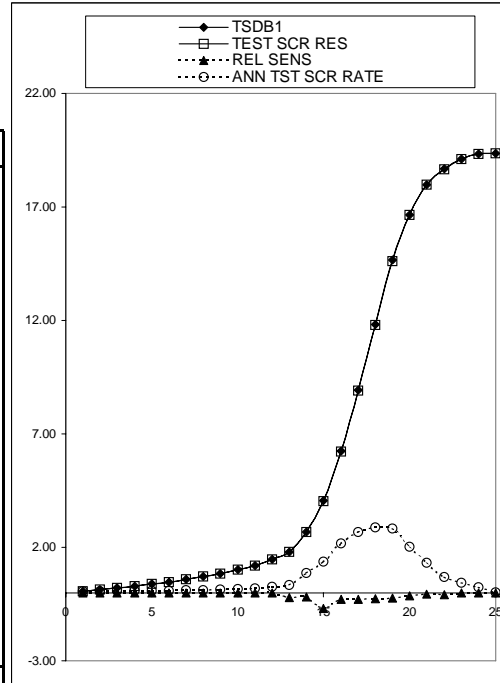
RELATIVE SENSIVITY RESULTS FOR OVERBANK SLOPE

	ABBR.	Baseline Values 1	Test Value	dP			
	UESTZ	200	202.00	2.000			
		TEST SCR RES	P/S UESTZ		ABS. SENS.	REL SENS	ANN TST SCR RATE
YRS	TSDB1			dS			
1	0.07	0.07	3053.435	0.000	0.00	0.00	0.07
2	0.13	0.13	1510.574	0.000	0.00	0.00	0.07
3	0.21	0.21	945.626	0.000	0.00	0.00	0.08
4	0.29	0.29	678.887	0.000	0.00	0.00	0.08
5	0.38	0.38	524.659	0.000	0.00	0.03	0.09
6	0.48	0.48	418.760	0.000	0.00	0.02	0.10
7	0.59	0.59	340.832	0.000	0.00	0.02	0.11
8	0.71	0.71	280.938	0.000	0.00	0.03	0.13
9	0.85	0.85	234.494	0.000	0.00	0.02	0.14
10	1.02	1.02	196.928	0.000	0.00	0.02	0.16
11	1.20	1.20	166.306	0.000	0.00	0.02	0.19
12	1.47	1.47	136.129	0.000	0.00	0.03	0.27
13	1.80	1.80	110.846	0.000	0.00	0.03	0.34
14	2.67	2.67	74.842	0.001	0.00	0.04	0.87
15	4.06	4.06	49.209	0.000	0.00	0.00	1.39
16	6.24	6.24	32.053	-0.002	0.00	-0.03	2.17
17	8.93	8.93	22.388	-0.004	0.00	-0.04	2.69
18	11.82	11.84	16.919	0.020	0.01	0.17	2.91
19	14.66	14.67	13.644	0.009	0.00	0.06	2.83
20	16.66	16.66	12.005	-0.003	0.00	-0.02	1.99
21	17.98	17.98	11.123	0.000	0.00	0.00	1.32
22	18.68	18.68	10.705	0.001	0.00	0.01	0.70
23	19.11	19.11	10.466	0.000	0.00	0.00	0.43
24	19.34	19.34	10.341	0.000	0.00	0.00	0.23
25	19.36	19.36	10.330	0.000	0.00	0.00	0.02
				MEAN REL SENS.		0.0	
YRS	TSUB1	TEST SCR RES	P/S PKM	dS	ABS. SENS.	REL SENS	ANN TST SCR RATE
1	0.16	0.16	1269.036	0.00	0.00	-0.06	0.16
2	0.34	0.34	584.454	0.00	0.00	-0.09	0.18
3	0.57	0.57	351.000	0.00	0.00	-0.09	0.23
4	0.84	0.84	239.206	0.00	0.00	-0.08	0.27
5	1.29	1.29	154.835	0.00	0.00	-0.26	0.45
6	1.84	1.83	108.855	0.00	0.00	-0.14	0.55
7	2.53	2.52	78.976	-0.01	-0.01	-0.50	0.69
8	3.51	3.50	57.011	-0.01	-0.01	-0.34	0.98
9	4.66	4.66	42.906	-0.01	0.00	-0.13	1.16
10	5.86	5.86	34.109	-0.01	0.00	-0.10	1.20
11	7.29	7.28	27.434	-0.01	0.00	-0.14	1.42
12	8.69	8.67	23.028	-0.02	-0.01	-0.22	1.39
13	10.09	10.07	19.828	-0.02	-0.01	-0.19	1.40
14	11.62	11.60	17.218	-0.02	-0.01	-0.15	1.53
15	13.32	13.29	15.011	-0.03	-0.02	-0.23	1.69
16	14.79	14.77	13.525	-0.02	-0.01	-0.14	1.47
17	16.11	16.06	12.414	-0.05	-0.03	-0.32	1.29
18	17.15	17.14	11.661	-0.02	-0.01	-0.09	1.08
19	18.01	18.00	11.103	-0.01	-0.01	-0.07	0.87
20	18.63	18.62	10.735	-0.02	-0.01	-0.08	0.61
21	19.16	19.15	10.437	-0.01	-0.01	-0.05	0.54
22	19.61	19.60	10.200	-0.01	-0.01	-0.06	0.44
23	19.95	19.94	10.025	-0.01	-0.01	-0.07	0.34
24	20.18	20.17	9.912	0.00	0.00	-0.02	0.24
25	20.33	20.32	9.839	0.00	0.00	-0.01	0.15
			MEAN REL SENS.		-0.15		



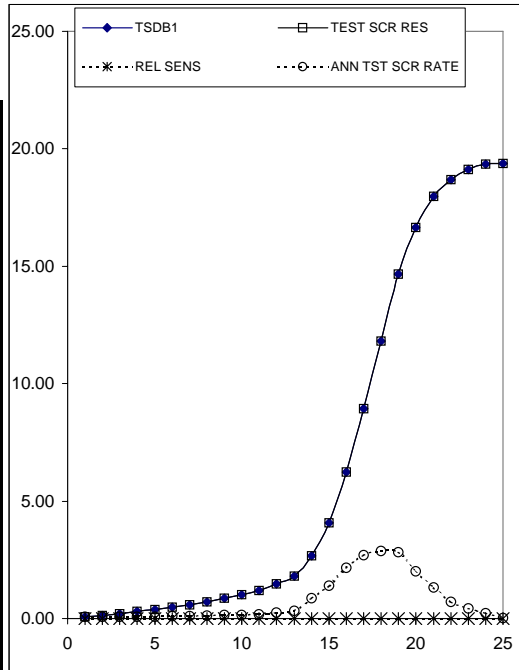
RELATIVE SENSIVITY RESULTS FOR PHI ANGLE

		ABBR.	Baseline Values 1	Test Value	dP			
		PHI	40.00	40.40	0.400			
YRS	TSDB1	TEST SCR RES	P/S CN	dS	ABS. SENS.	REL SENS	ANN TST SCR RATE	
1	0.07	0.07	1190.840	0.00	0.00	0.00	0.07	
2	0.13	0.13	589.124	0.00	0.00	0.00	0.07	
3	0.21	0.21	368.794	0.00	0.00	0.00	0.08	
4	0.29	0.29	264.766	0.00	0.00	0.00	0.08	
5	0.38	0.38	204.617	0.00	0.00	0.00	0.09	
6	0.48	0.48	163.317	0.00	0.00	0.00	0.10	
7	0.59	0.59	132.924	0.00	0.00	0.00	0.11	
8	0.71	0.71	109.566	0.00	0.00	0.00	0.13	
9	0.85	0.85	91.453	0.00	0.00	0.00	0.14	
10	1.02	1.02	76.802	0.00	0.00	0.00	0.16	
11	1.20	1.20	64.859	0.00	0.00	0.00	0.19	
12	1.47	1.47	53.090	0.00	0.00	0.00	0.27	
13	1.80	1.80	43.230	0.00	0.00	-0.21	0.33	
14	2.67	2.67	29.188	-0.01	-0.01	-0.19	0.87	
15	4.06	4.04	19.191	-0.03	-0.04	-0.69	1.37	
16	6.24	6.22	12.501	-0.02	-0.02	-0.29	2.19	
17	8.93	8.91	8.731	-0.03	-0.03	-0.30	2.69	
18	11.82	11.79	6.598	-0.03	-0.04	-0.26	2.88	
19	14.66	14.62	5.321	-0.04	-0.05	-0.25	2.83	
20	16.66	16.64	4.682	-0.02	-0.03	-0.12	2.02	
21	17.98	17.97	4.338	-0.01	-0.01	-0.06	1.33	
22	18.68	18.67	4.175	-0.01	-0.02	-0.07	0.70	
23	19.11	19.11	4.082	0.00	0.00	-0.01	0.44	
24	19.34	19.34	4.033	0.00	0.00	0.00	0.23	
25	19.36	19.36	4.029	0.00	0.00	0.00	0.02	
				MEAN REL SENS.		-0.1		
YRS	TSUB1	TEST SCR RES	P/S CN	dS	ABS. SENS.	REL SENS	ANN TST SCR RATE	
1	0.16	0.16	494.92	0.00	0.00	0.00	0.16	
2	0.34	0.34	227.94	0.00	0.00	0.00	0.18	
3	0.57	0.57	136.89	0.00	0.00	0.00	0.23	
4	0.84	0.84	93.29	0.00	0.00	-0.01	0.27	
5	1.29	1.29	60.39	0.00	0.00	-0.20	0.45	
6	1.84	1.84	42.45	0.00	0.00	-0.04	0.55	
7	2.53	2.52	30.80	-0.01	-0.01	-0.43	0.68	
8	3.51	3.49	22.23	-0.02	-0.02	-0.48	0.97	
9	4.66	4.65	16.73	-0.01	-0.01	-0.14	1.16	
10	5.86	5.86	13.30	-0.01	-0.01	-0.12	1.20	
11	7.29	7.27	10.70	-0.02	-0.03	-0.28	1.41	
12	8.69	8.67	8.98	-0.02	-0.02	-0.19	1.40	
13	10.09	10.08	7.73	-0.01	-0.01	-0.10	1.41	
14	11.62	11.61	6.71	-0.01	-0.01	-0.06	1.53	
15	13.32	13.31	5.85	-0.02	-0.02	-0.11	1.70	
16	14.79	14.78	5.27	-0.01	-0.01	-0.07	1.47	
17	16.11	16.09	4.84	-0.02	-0.02	-0.12	1.31	
18	17.15	17.14	4.55	-0.01	-0.01	-0.04	1.05	
19	18.01	18.01	4.33	-0.01	-0.01	-0.04	0.86	
20	18.63	18.62	4.19	-0.01	-0.02	-0.06	0.61	
21	19.16	19.16	4.07	0.00	0.00	-0.02	0.54	
22	19.61	19.61	3.98	0.00	0.00	-0.02	0.45	
23	19.95	19.94	3.91	-0.01	-0.01	-0.05	0.34	
24	20.18	20.18	3.87	0.00	0.00	-0.01	0.23	
25	20.33	20.33	3.84	0.00	0.00	-0.01	0.15	
				MEAN REL SENS.		-0.10		

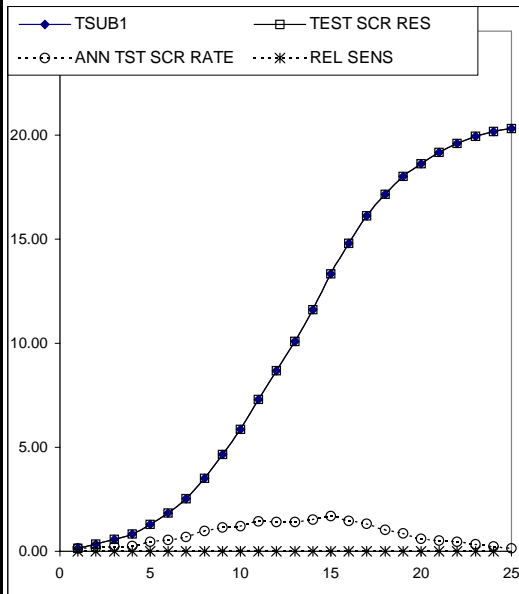


RELATIVE SENSITIVITY RESULTS FOR YTRI

	ABBR.	Baseline Values 1	Test Value	dP			
	YTRI	5	5.05	0.050			
YRS	TSDB1	TEST SCR RES	P/S NBP	dS	ABS. SENS.	REL SENS	ANN TST SCR RATE
1	0.07	0.0655	76.336	0.00	0.00	0.00	0.07
2	0.13	0.1324	37.764	0.00	0.00	0.00	0.07
3	0.21	0.2115	23.641	0.00	0.00	0.00	0.08
4	0.29	0.2946	16.972	0.00	0.00	0.00	0.08
5	0.38	0.3812	13.116	0.00	0.00	0.00	0.09
6	0.48	0.4776	10.469	0.00	0.00	0.00	0.10
7	0.59	0.5868	8.521	0.00	0.00	0.00	0.11
8	0.71	0.7119	7.023	0.00	0.00	0.00	0.13
9	0.85	0.8529	5.862	0.00	0.00	0.00	0.14
10	1.02	1.0156	4.923	0.00	0.00	0.00	0.16
11	1.20	1.2026	4.158	0.00	0.00	0.00	0.19
12	1.47	1.4692	3.403	0.00	0.00	0.00	0.27
13	1.80	1.8043	2.771	0.00	0.00	0.00	0.34
14	2.67	2.6723	1.871	0.00	0.00	0.00	0.87
15	4.06	4.0643	1.230	0.00	0.00	0.00	1.39
16	6.24	6.2397	0.801	0.00	0.00	0.00	2.18
17	8.93	8.9333	0.560	0.00	0.00	0.00	2.69
18	11.82	11.821	0.423	0.00	0.00	0.00	2.89
19	14.66	14.658	0.341	0.00	0.00	0.00	2.84
20	16.66	16.66	0.300	0.00	0.00	0.00	2.00
21	17.98	17.98	0.278	0.00	0.00	0.00	1.32
22	18.68	18.682	0.268	0.00	0.00	0.00	0.70
23	19.11	19.109	0.262	0.00	0.00	0.00	0.43
24	19.34	19.341	0.259	0.00	0.00	0.00	0.23
25	19.36	19.362	0.258	0.00	0.00	0.00	0.02
				MEAN REL SENS.		0.0	

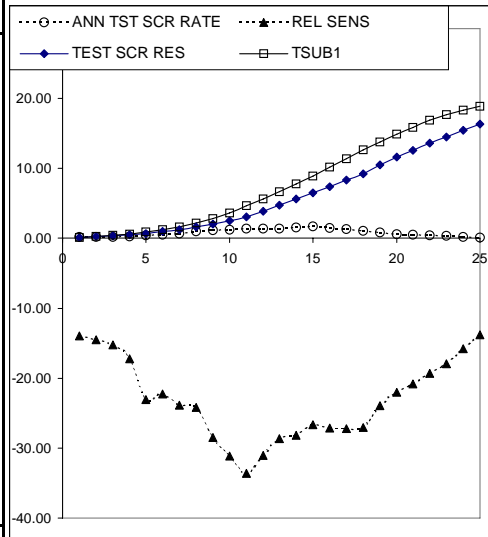
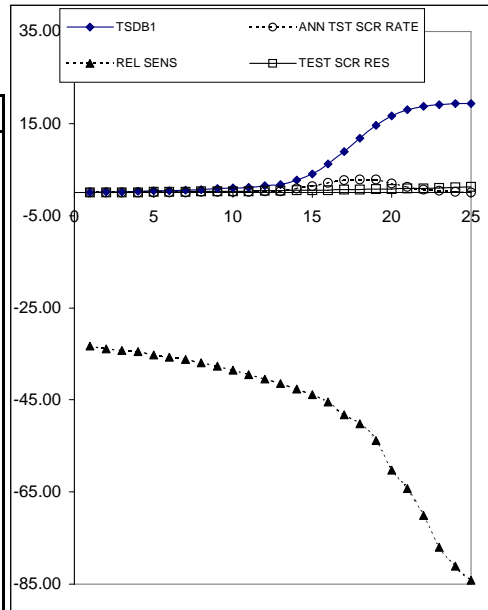


YRS	TSUB1	TEST SCR RES	P/S NBP	dS	ABS. SENS.	REL SENS	ANN TST SCR RATE
1	0.16	0.1576	31.73	0.00	0.00	0.00	0.16
2	0.34	0.3422	14.61	0.00	0.00	0.00	0.18
3	0.57	0.5698	8.78	0.00	0.00	0.00	0.23
4	0.84	0.8361	5.98	0.00	0.00	0.00	0.27
5	1.29	1.2917	3.87	0.00	0.00	0.00	0.46
6	1.84	1.8373	2.72	0.00	0.00	0.00	0.55
7	2.53	2.5324	1.97	0.00	0.00	0.00	0.70
8	3.51	3.5081	1.43	0.00	0.00	0.00	0.98
9	4.66	4.6613	1.07	0.00	0.00	0.00	1.15
10	5.86	5.8636	0.85	0.00	0.00	0.00	1.20
11	7.29	7.2902	0.69	0.00	0.00	0.00	1.43
12	8.69	8.6852	0.58	0.00	0.00	0.00	1.40
13	10.09	10.087	0.50	0.00	0.00	0.00	1.40
14	11.62	11.616	0.43	0.00	0.00	0.00	1.53
15	13.32	13.324	0.38	0.00	0.00	0.00	1.71
16	14.79	14.788	0.34	0.00	0.00	0.00	1.46
17	16.11	16.111	0.31	0.00	0.00	0.00	1.32
18	17.15	17.152	0.29	0.00	0.00	0.00	1.04
19	18.01	18.014	0.28	0.00	0.00	0.00	0.86
20	18.63	18.631	0.27	0.00	0.00	0.00	0.62
21	19.16	19.163	0.26	0.00	0.00	0.00	0.53
22	19.61	19.609	0.25	0.00	0.00	0.00	0.45
23	19.95	19.951	0.25	0.00	0.00	0.00	0.34
24	20.18	20.177	0.25	0.00	0.00	0.00	0.23
25	20.33	20.328	0.25	0.00	0.00	0.00	0.15
				MEAN REL SENS.		0.00	



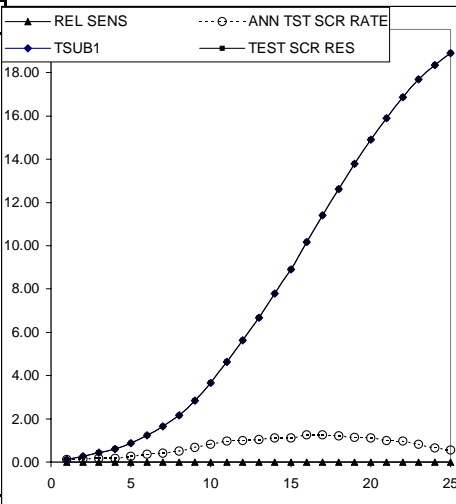
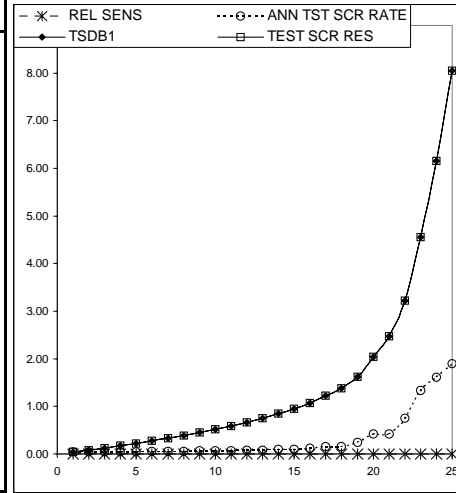
RELATIVE SENSITIVITY RESULTS FOR DMAX

	ABBR.	Baseline Values 1	Test Value	dP			
	DMAX	0.70	0.71	0.007			
YRS	TSDB1	TEST SCR RES	P/S C1	dS	ABS. SENS.	REL SENS	ANN TST SCR RATE
1	0.04	0.03	49.751	-0.01	-0.67	-33.33	0.03
2	0.08	0.05	25.031	-0.03	-1.36	-33.92	0.03
3	0.13	0.08	15.860	-0.04	-2.16	-34.26	0.03
4	0.17	0.11	11.494	-0.06	-3.01	-34.54	0.03
5	0.22	0.14	9.054	-0.08	-3.89	-35.22	0.03
6	0.27	0.17	7.356	-0.10	-4.86	-35.75	0.03
7	0.33	0.21	6.109	-0.12	-5.94	-36.26	0.03
8	0.39	0.24	5.164	-0.14	-7.14	-36.90	0.04
9	0.45	0.28	4.441	-0.17	-8.49	-37.71	0.04
10	0.52	0.32	3.862	-0.20	-9.97	-38.53	0.04
11	0.59	0.35	3.411	-0.23	-11.58	-39.50	0.04
12	0.67	0.40	3.004	-0.27	-13.46	-40.42	0.04
13	0.75	0.44	2.674	-0.31	-15.52	-41.50	0.04
14	0.85	0.49	2.366	-0.36	-18.01	-42.61	0.05
15	0.95	0.53	2.110	-0.42	-20.80	-43.90	0.05
16	1.07	0.58	1.876	-0.48	-24.21	-45.41	0.05
17	1.22	0.63	1.633	-0.59	-29.57	-48.29	0.05
18	1.38	0.69	1.447	-0.69	-34.65	-50.15	0.06
19	1.62	0.75	1.233	-0.87	-43.69	-53.87	0.06
20	2.04	0.81	0.978	-1.23	-61.60	-60.25	0.06
21	2.47	0.88	0.810	-1.59	-79.26	-64.24	0.07
22	3.22	0.96	0.622	-2.25	-112.66	-70.08	0.08
23	4.55	1.05	0.439	-3.51	-175.28	-77.01	0.08
24	6.16	1.16	0.325	-5.00	-249.82	-81.14	0.11
25	8.05	1.28	0.248	-6.78	-338.91	-84.17	0.11
			MEAN		-51.1	-48.0	
YRS	TSUB1	TEST SCR RES	P/S C1	dS	ABS. SENS.	REL SENS	ANN TST SCR RATE
1	0.13	0.11	15.56	-0.02	-0.89	-13.93	0.11
2	0.28	0.24	7.23	-0.04	-2.01	-14.50	0.13
3	0.44	0.37	4.53	-0.07	-3.37	-15.23	0.14
4	0.61	0.51	3.27	-0.11	-5.26	-17.24	0.13
5	0.88	0.68	2.27	-0.20	-10.17	-23.06	0.17
6	1.24	0.96	1.61	-0.28	-13.80	-22.27	0.29
7	1.66	1.26	1.21	-0.40	-19.75	-23.86	0.30
8	2.16	1.63	0.93	-0.52	-26.06	-24.17	0.37
9	2.83	2.02	0.71	-0.81	-40.34	-28.51	0.39
10	3.67	2.52	0.55	-1.14	-57.03	-31.12	0.50
11	4.64	3.08	0.43	-1.56	-77.96	-33.60	0.56
12	5.63	3.88	0.36	-1.75	-87.34	-31.05	0.80
13	6.67	4.75	0.30	-1.91	-95.57	-28.67	0.88
14	7.79	5.60	0.26	-2.20	-109.78	-28.18	0.84
15	8.91	6.53	0.22	-2.38	-118.78	-26.67	0.93
16	10.17	7.41	0.20	-2.76	-137.98	-27.14	0.88
17	11.42	8.31	0.18	-3.10	-155.19	-27.18	0.91
18	12.63	9.21	0.16	-3.42	-170.96	-27.08	0.89
19	13.78	10.48	0.15	-3.30	-164.97	-23.95	1.27
20	14.90	11.62	0.13	-3.28	-164.13	-22.03	1.14
21	15.90	12.59	0.13	-3.31	-165.49	-20.82	0.97
22	16.87	13.61	0.12	-3.26	-163.13	-19.34	1.02
23	17.70	14.52	0.11	-3.18	-159.09	-17.98	0.91
24	18.35	15.45	0.11	-2.90	-145.08	-15.81	0.93
25	18.90	16.30	0.11	-2.60	-130.01	-13.76	0.85
			MEAN		-88.96	-23.09	



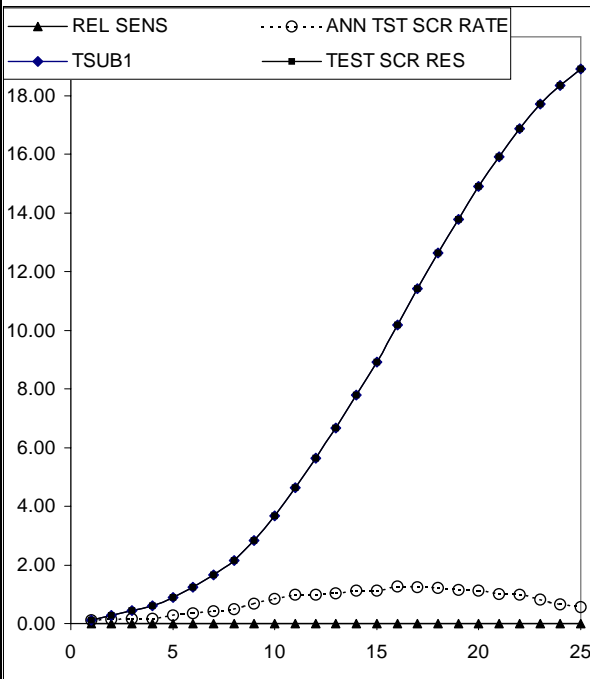
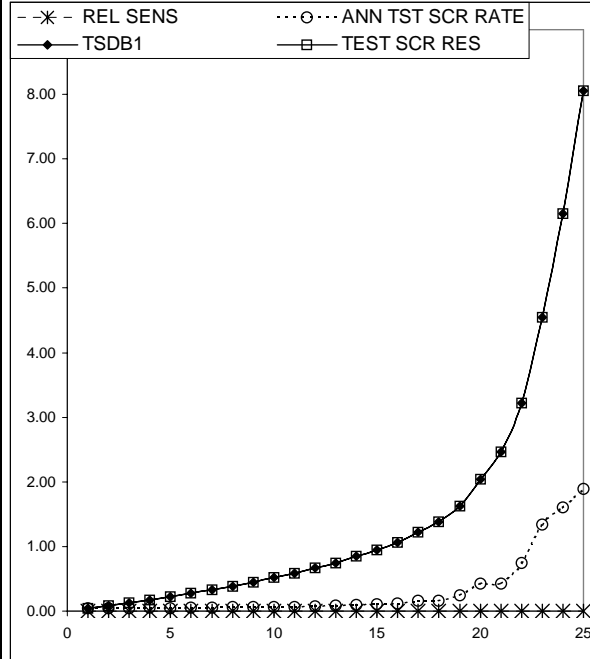
RELATIVE SENSIVITY RESULTS FOR D84

YRS	ABBR.	Baseline Values 1	Test Value	dP			
	CN	78	78.78	0.780			
	TSDB1	TEST SCR RES	P/S TCON	dS	ABS. SENS.	REL SENS	ANN TST SCR RATE
1	0.04	0.04	9.950	0.00	0.00	0.00	0.04
2	0.08	0.08	5.006	0.00	0.00	0.00	0.04
3	0.13	0.13	3.172	0.00	0.00	0.00	0.05
4	0.17	0.17	2.299	0.00	0.00	0.00	0.05
5	0.22	0.22	1.811	0.00	0.00	0.00	0.05
6	0.27	0.27	1.471	0.00	0.00	0.00	0.05
7	0.33	0.33	1.222	0.00	0.00	0.00	0.06
8	0.39	0.39	1.033	0.00	0.00	0.00	0.06
9	0.45	0.45	0.888	0.00	0.00	0.00	0.06
10	0.52	0.52	0.772	0.00	0.00	0.00	0.07
11	0.59	0.59	0.682	0.00	0.00	0.00	0.07
12	0.67	0.67	0.601	0.00	0.00	0.00	0.08
13	0.75	0.75	0.535	0.00	0.00	0.00	0.08
14	0.85	0.85	0.473	0.00	0.00	0.00	0.10
15	0.95	0.95	0.422	0.00	0.00	0.00	0.10
16	1.07	1.07	0.375	0.00	0.00	0.00	0.12
17	1.22	1.22	0.327	0.00	0.00	0.00	0.16
18	1.38	1.38	0.289	0.00	0.00	0.00	0.16
19	1.62	1.62	0.247	0.00	0.00	0.00	0.24
20	2.04	2.04	0.196	0.00	0.00	0.00	0.42
21	2.47	2.47	0.162	0.00	0.00	0.00	0.42
22	3.22	3.22	0.124	0.00	0.00	0.00	0.75
23	4.55	4.55	0.088	0.00	0.00	0.00	1.34
24	6.16	6.16	0.065	0.00	0.00	0.00	1.61
25	8.05	8.05	0.050	0.00	0.00	0.00	1.90
MEAN REL. SENS.					0.0		
YRS	TSUB1	TEST SCR RES	P/S TCON	dS	ABS. SENS.	REL SENS	ANN TST SCR RATE
1	0.13	0.13	3.11	0.00	0.00	0.00	0.13
2	0.28	0.28	1.45	0.00	0.00	0.00	0.15
3	0.44	0.44	0.91	0.00	0.00	0.00	0.17
4	0.61	0.61	0.65	0.00	0.00	0.00	0.17
5	0.88	0.88	0.45	0.00	0.00	0.00	0.27
6	1.24	1.24	0.32	0.00	0.00	0.00	0.36
7	1.66	1.66	0.24	0.00	0.00	0.00	0.42
8	2.16	2.16	0.19	0.00	0.00	0.00	0.50
9	2.83	2.83	0.14	0.00	0.00	0.00	0.67
10	3.67	3.67	0.11	0.00	0.00	0.00	0.84
11	4.64	4.64	8.12	0.00	0.00	0.00	0.98
12	5.63	5.63	0.07	0.00	0.00	0.00	0.99
13	6.67	6.67	0.06	0.00	0.00	0.00	1.04
14	7.79	7.79	0.05	0.00	0.00	0.00	1.13
15	8.91	8.91	0.04	0.00	0.00	0.00	1.11
16	10.17	10.17	0.04	0.00	0.00	0.00	1.26
17	11.42	11.42	0.04	0.00	0.00	0.00	1.25
18	12.63	12.63	0.03	0.00	0.00	0.00	1.21
19	13.78	13.78	0.03	0.00	0.00	0.00	1.15
20	14.90	14.90	0.03	0.00	0.00	0.00	1.12
21	15.90	15.90	0.03	0.00	0.00	0.00	1.00
22	16.87	16.87	0.02	0.00	0.00	0.00	0.98
23	17.70	17.70	0.02	0.00	0.00	0.00	0.83
24	18.35	18.35	0.02	0.00	0.00	0.00	0.65
25	18.90	18.90	0.02	0.00	0.00	0.00	0.55
MEAN REL. SENS.					0.00		



RELATIVE SENSITIVITY RESULTS FOR D16

	ABBR.	Baseline Values 1	Test Value	dP			
	D16	0.05	0.06	0.005			
YRS	TSDB1	TEST SCR RES	P/S TCON	dS	ABS. SENS.	REL SENS	ANN TST SCR RATE
1	0.04	0.04	1.244	0.00	0.00	0.00	0.04
2	0.08	0.08	0.626	0.00	0.00	0.00	0.04
3	0.13	0.13	0.397	0.00	0.00	0.00	0.05
4	0.17	0.17	0.287	0.00	0.00	0.00	0.05
5	0.22	0.22	0.226	0.00	0.00	0.00	0.05
6	0.27	0.27	0.184	0.00	0.00	0.00	0.05
7	0.33	0.33	0.153	0.00	0.00	0.00	0.06
8	0.39	0.39	0.129	0.00	0.00	0.00	0.06
9	0.45	0.45	0.111	0.00	0.00	0.00	0.06
10	0.52	0.52	0.097	0.00	0.00	0.00	0.07
11	0.59	0.59	0.085	0.00	0.00	0.00	0.07
12	0.67	0.67	0.075	0.00	0.00	0.00	0.08
13	0.75	0.75	0.067	0.00	0.00	0.00	0.08
14	0.85	0.85	0.059	0.00	0.00	0.00	0.10
15	0.95	0.95	0.053	0.00	0.00	0.00	0.10
16	1.07	1.07	0.047	0.00	0.00	0.00	0.12
17	1.22	1.22	0.041	0.00	0.00	0.00	0.16
18	1.38	1.38	0.036	0.00	0.00	0.00	0.16
19	1.62	1.62	0.031	0.00	0.00	0.00	0.24
20	2.04	2.04	0.024	0.00	0.00	0.00	0.42
21	2.47	2.47	0.020	0.00	0.00	0.00	0.42
22	3.22	3.22	0.016	0.00	0.00	0.00	0.75
23	4.55	4.55	0.011	0.00	0.00	0.00	1.34
24	6.16	6.16	0.008	0.00	0.00	0.00	1.61
25	8.05	8.05	0.006	0.00	0.00	0.00	1.90
				MEAN REL SENS.		0.0	
YRS	TSUB1	TEST SCR RES	P/S TCON	dS	ABS. SENS.	REL SENS	ANN TST SCR RATE
1	0.13	0.13	0.39	0.00	0.00	0.00	0.13
2	0.28	0.28	0.18	0.00	0.00	0.00	0.15
3	0.44	0.44	0.11	0.00	0.00	0.00	0.17
4	0.61	0.61	0.08	0.00	0.00	0.00	0.17
5	0.88	0.88	0.06	0.00	0.00	0.00	0.27
6	1.24	1.24	0.04	0.00	0.00	0.00	0.36
7	1.66	1.66	0.03	0.00	0.00	0.00	0.42
8	2.16	2.16	0.02	0.00	0.00	0.00	0.50
9	2.83	2.83	0.02	0.00	0.00	0.00	0.67
10	3.67	3.67	0.01	0.00	0.00	0.00	0.84
11	4.64	4.64	8.12	0.00	0.00	0.00	0.98
12	5.63	5.63	0.01	0.00	0.00	0.00	0.99
13	6.67	6.67	0.01	0.00	0.00	0.00	1.04
14	7.79	7.79	0.01	0.00	0.00	0.00	1.13
15	8.91	8.91	0.01	0.00	0.00	0.00	1.11
16	10.17	10.17	0.00	0.00	0.00	0.00	1.26
17	11.42	11.42	0.00	0.00	0.00	0.00	1.25
18	12.63	12.63	0.00	0.00	0.00	0.00	1.21
19	13.78	13.78	0.00	0.00	0.00	0.00	1.15
20	14.90	14.90	0.00	0.00	0.00	0.00	1.12
21	15.90	15.90	0.00	0.00	0.00	0.00	1.00
22	16.87	16.87	0.00	0.00	0.00	0.00	0.98
23	17.70	17.70	0.00	0.00	0.00	0.00	0.83
24	18.35	18.35	0.00	0.00	0.00	0.00	0.65
25	18.90	18.90	0.00	0.00	0.00	0.00	0.55
			MEAN REL. SENS.			0.00	



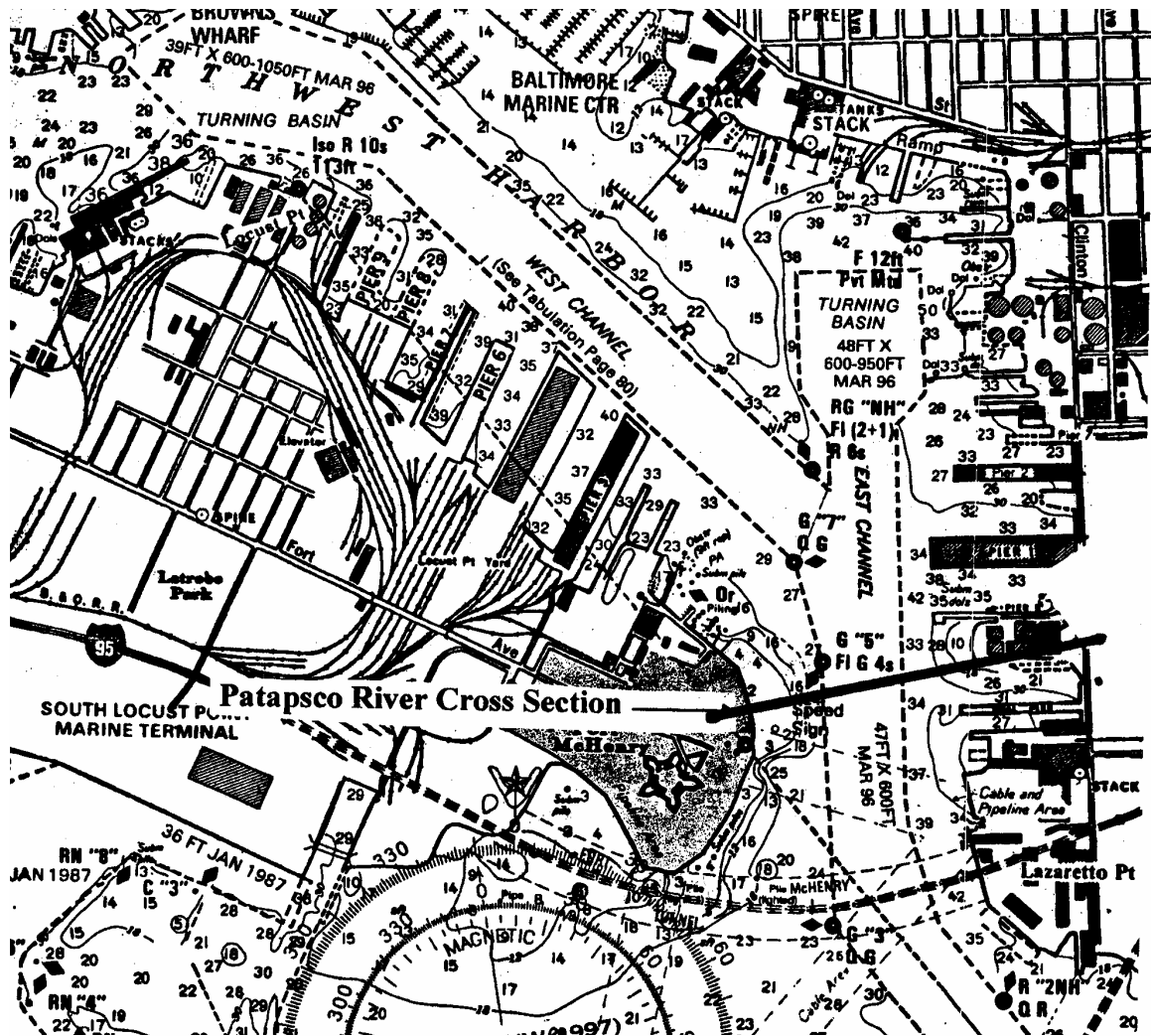


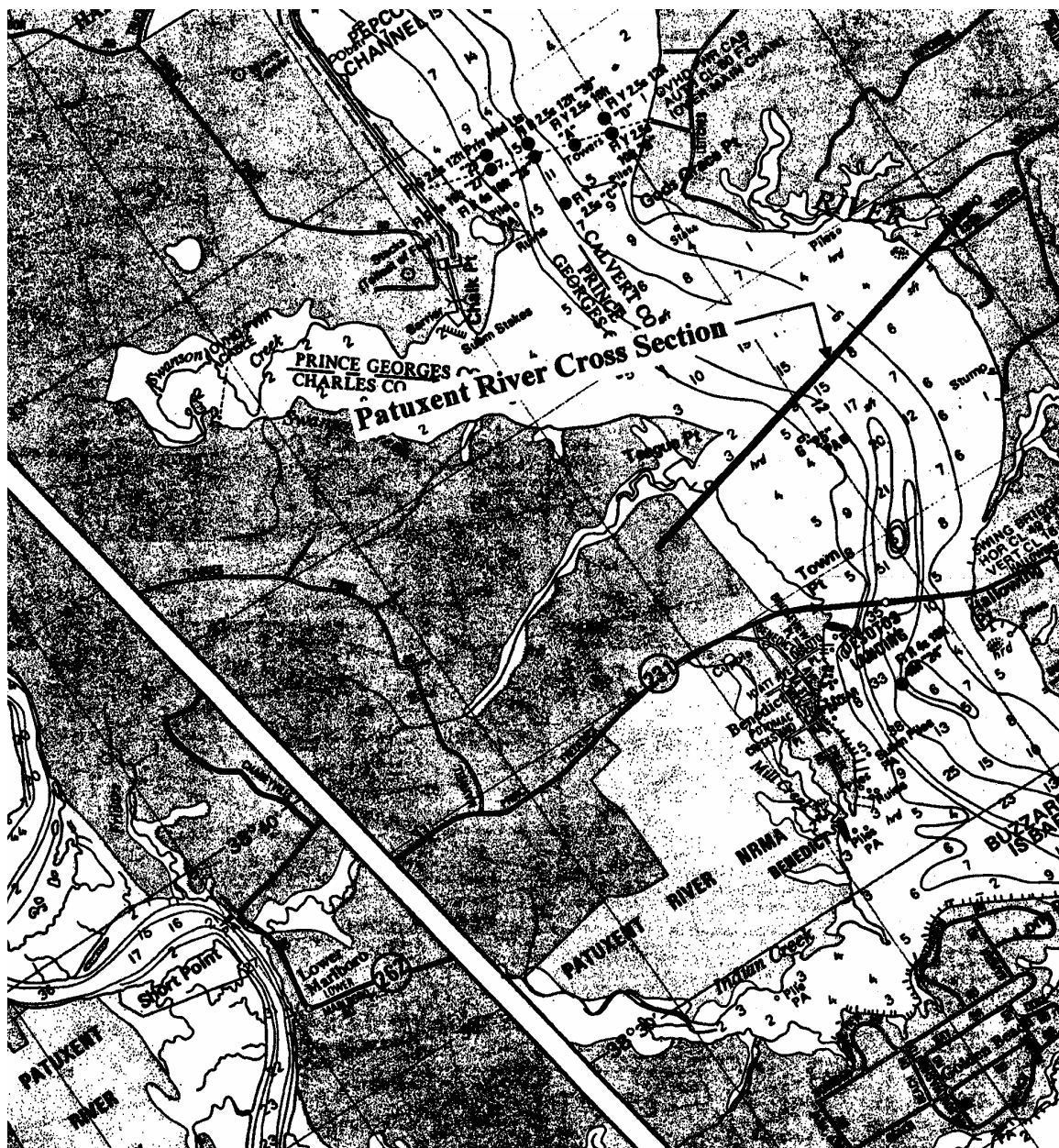
## APPENDIX C-1

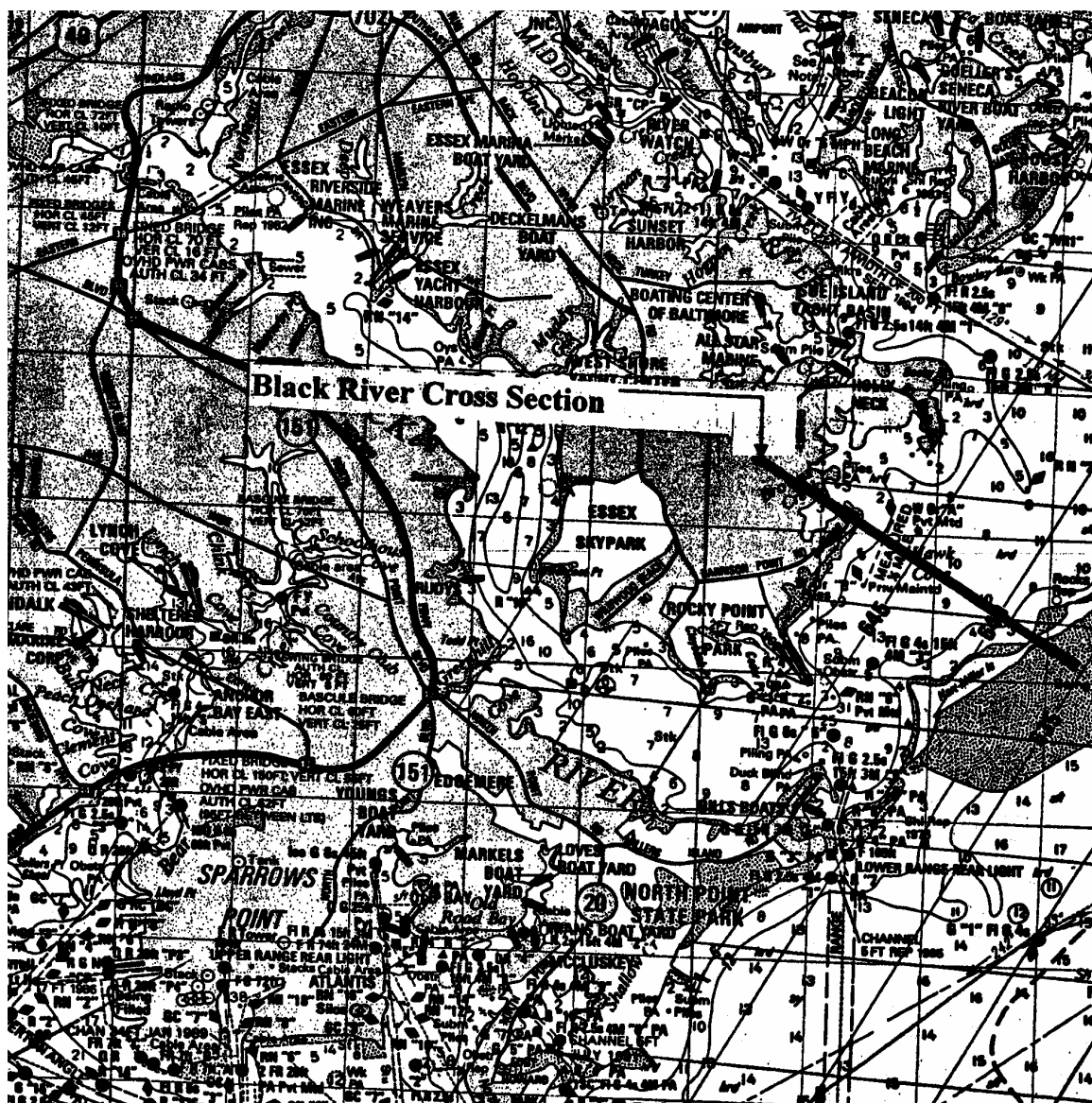
**Grain Size Classification of Sediment Material**

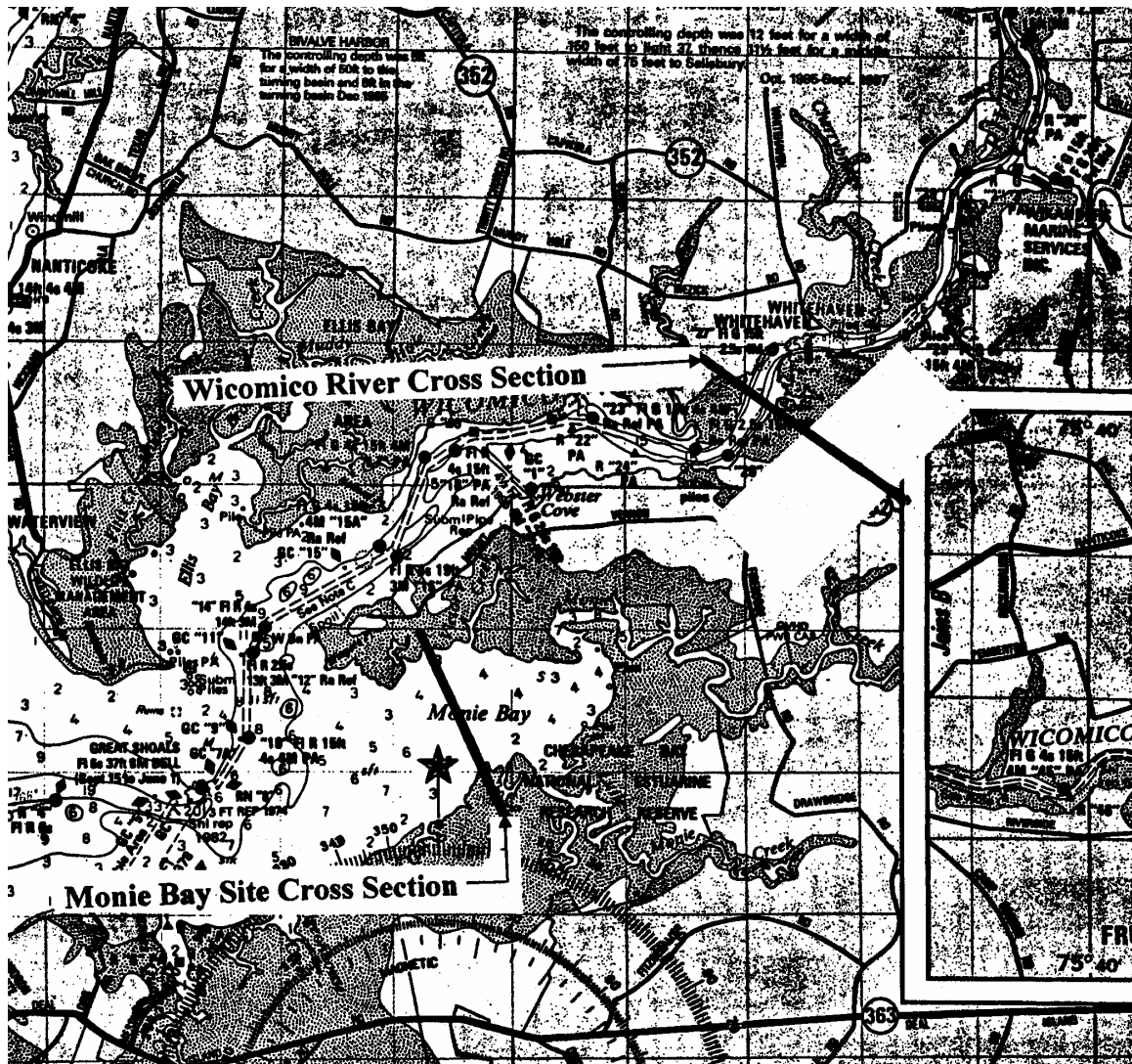
<b>Class Size Number Used in HEC-6</b>	<b>Sediment Material</b>	<b>Grain Diameter (mm)</b>
1	Clay	0.002 - 0.004
1	Very Fine Silt	0.004 - 0.008
2	Fine Silt	0.008 - 0.016
3	Medium Silt	0.016 - 0.032
4	Coarse Silt	0.032 - 0.0625
1	Very Fine Sand (VFS)	0.0625 - 0.125
2	Fine Sand (FS)	0.125 - 0.250
3	Medium Sand (MS)	0.25 - 0.50
4	Coarse Sand (CS)	0.5 - 1.0
5	Very Coarse Sand (VCS)	1 - 2
6	Very Fine Gravel (VFG)	2 - 4
7	Fine Gravel (FG)	4 - 8
8	Medium Gravel (MG)	8 - 16
9	Coarse Gravel (CG)	16 - 32
10	Very Coarse Gravel (VCG)	32 - 64
11	Small Cobbles (SC)	64 - 128
12	Large Cobbles (LC)	128 - 256
13	Small Boulders (SB)	256 - 512
14	Medium Boulders (MB)	512 - 1024
15	Large Boulders (LB)	1024 - 2048

## APPENDIX C-2









### APPENDIX C-3

#### MONIE BAY SITE CATCHMENT HYDROLOGIC INFORMATION

##### Watershed Statistics for:

GISHydro Release Version Date: October 20, 2004

Hydro Extension Version Date: October 15, 2004

Analysis Date: January 20, 2005

##### Data Selected:

Quadrangles Used: wetipquin, monie, princess\_anne, eden, dividing\_creek, salisbury, delmar, hebron, pittsville, wango

DEM Coverage: NED DEMs

Land Use Coverage: 2000 MOP Landuse

Soil Coverage: Ragan Soils

Hydrologic Condition: (see Lookup Table)

Impose NHD stream Locations: Yes

Outlet Easting: 503147 m. (MD Stateplane, NAD 1983)

Outlet Northing: 62963 m. (MD Stateplane, NAD 1983)

##### Findings:

Outlet Location: Eastern Coastal Plain

Outlet State: Maryland

Drainage Area 16.3 square miles

-Eastern Coastal Plain (100.0% of area)

Channel Slope: 1.3 feet/mile

Land Slope: 0.003 ft/ft

Urban Area: 3.4%

Impervious Area: 1.0%

Time of Concentration: 47.4 hours [W.O. Thomas, Jr. Equation]

Time of Concentration: 29.6 hours [From SCS Lag Equation \* 1.67]

Longest Flow Path: 14.09 miles

Basin Relief: 10.0 feet

Average CN: 81

% Forest Cover: 59.6

% Storage: 12.6

% Limestone: 0.0

% A Soils: 0.1

% B Soils: 7.7

% C Soils: 7.3

% D Soils: 83.3

2-Year,24-hour Prec.: 3.32 inches

##### .S.G.S. Peak Flow Estimates for:

GISHydro Release Version Date: October 20, 2004

Hydro Extension Version Date: October 15, 2004

Analysis Date: January 20, 2005

##### Geographic Province(s):

-Eastern Coastal Plain (100.0% of area)

Q(2): 168 cfs

Q(5): 208 cfs

Q(10): 241 cfs

Q(25): 292 cfs

Q(50): 335 cfs

Q(100): 384 cfs

Q(500): 509 cfs

Area Weighted Prediction Intervals (from Tasker)

Return	50 PERCENT		67 PERCENT		90 PERCENT		95 PERCENT	
Period	lower	upper	lower	upper	lower	upper	lower	upper
2	117	241	99	285	68	413	57	494
5	144	300	122	356	84	517	70	621
10	166	349	140	414	96	606	80	729
25	199	426	167	508	113	750	94	906
50	227	495	190	593	127	883	105	1070
100	257	573	213	690	142	1040	116	1270
500	328	790	268	968	171	1520	137	1890

Individual Province Tasker Analyses Follow:

Flood frequency estimates for

REGION; Eastern Coastal Plain region

area= 16.30: curve = 81.00: storage = 12.60

: forest = 59.60 : relief = 10.00 :skew= 0.67

Return	Discharge	Standard	Equivalent	Standard
Period	(cfs)	Error of	Years of	Error of
		Prediction	Record	Prediction
		(percent)		(logs)
2	168.	56.9	1.50	0.2301
5	208.	57.7	3.05	0.2329
10	241.	58.6	4.69	0.2358
25	292.	60.1	7.10	0.2413
50	335.	61.9	8.93	0.2473
100	384.	64.1	10.66	0.2548
500	509.	71.5	13.82	0.2791

P R E D I C T I O N I N T E R V A L S								
Return	50 PERCENT		67 PERCENT		90 PERCENT		95 PERCENT	
Period	lower	upper	lower	upper	lower	upper	lower	upper
2	117.	241.	99.	285.	68.	413.	57.	494.
5	144.	300.	122.	356.	84.	517.	70.	621.
10	166.	349.	140.	414.	96.	606.	80.	729.
25	199.	426.	167.	508.	113.	750.	94.	906.
50	227.	495.	190.	593.	127.	883.	105.	1070.
100	257.	573.	213.	690.	142.	1040.	116.	1270.
500	328.	790.	268.	968.	171.	1520.	137.	1890.
500	328.	790.	268.	968.	171.	1520.	137.	1890.

Fixed Region Peak Flow Estimates for:

GISHydro Release Version Date: October 20, 2004

Hydro Extension Version Date: October 15, 2004

Analysis Date: January 20, 2005

Overall Weighted Fixed Region Estimated Discharges

Q(1.25): 211 cfs  
 Q(1.50): 267 cfs  
 Q(1.75): 301 cfs  
 Q(2): 325 cfs  
 Q(5): 543 cfs  
 Q(10): 737 cfs  
 Q(25): 1040 cfs  
 Q(50): 1340 cfs  
 Q(100): 1700 cfs  
 Q(200): 2130 cfs  
 Q(500): 2850 cfs

Individual Province Predictions Follow:

Fixed Region Estimated Discharges for: Eastern Coastal Plain region

Q(1.25): 211 cfs  
Q(1.50): 267 cfs  
Q(1.75): 301 cfs  
Q(2): 325 cfs  
Q(5): 543 cfs  
Q(10): 737 cfs  
Q(25): 1040 cfs  
Q(50): 1340 cfs  
Q(100): 1700 cfs  
Q(200): 2130 cfs  
Q(500): 2850 cfs

#### BLACK RIVER SITE CATCHMENT HYDROLOGIC INFORMATION

Watershed Statistics for:

GISHydro Release Version Date: October 20, 2004

Hydro Extension Version Date: October 15, 2004

Analysis Date: January 20, 2005

Data Selected:

Quadrangles Used: middle\_river, sparrows\_point, baltimore\_east, towson  
DEM Coverage: NED DEMs  
Land Use Coverage: 2000 MOP Landuse  
Soil Coverage: Ragan Soils  
Hydrologic Condition: (see Lookup Table)  
Impose NHD stream Locations: Yes  
Outlet Easting: 449925 m. (MD Stateplane, NAD 1983)  
Outlet Northing: 175078 m. (MD Stateplane, NAD 1983)

Findings:

Outlet Location: Western Coastal Plain  
Outlet State: Maryland  
Drainage Area 58.3 square miles  
-Piedmont (26.0% of area)  
-Western Coastal Plain (74.0% of area)  
Channel Slope: 20.5 feet/mile  
Land Slope: 0.040 ft/ft  
Urban Area: 60.9%  
Impervious Area: 37.8%

\*\*\*\*\*

URBAN DEVELOPMENT IN WATERSHED EXCEEDS 15%.  
Calculated discharges from USGS Regression  
Equations may not be appropriate.

\*\*\*\*\*

Time of Concentration: 16.8 hours [W.O. Thomas, Jr. Equation]  
Time of Concentration: 9.7 hours [From SCS Lag Equation \* 1.67]  
Longest Flow Path: 19.97 miles  
Basin Relief: 143.7 feet  
Average CN: 84  
% Forest Cover: 14.2  
% Storage: 10.2  
% Limestone: 0.0  
% A Soils: 0.9



% B Soils: 17.5  
 % C Soils: 71.0  
 % D Soils: 2.8  
 2-Year,24-hour Prec.: 3.31 inches

U.S.G.S. Peak Flow Estimates for:  
 GISHydro Release Version Date: October 20, 2004  
 Hydro Extension Version Date: October 15, 2004  
 Analysis Date: January 20, 2005

Geographic Province(s):  
 -Piedmont (26.0% of area)  
 -Western Coastal Plain (74.0% of area)

Q(2): 2557 cfs  
 Q(5): 4522 cfs  
 Q(10): 6202 cfs  
 Q(25): 8814 cfs  
 Q(50): 11148 cfs  
 Q(100): 13996 cfs  
 Q(500): 22710 cfs

Area Weighted Prediction Intervals (from Tasker)								
Return	50 PERCENT		67 PERCENT		90 PERCENT		95 PERCENT	
Period	lower	upper	lower	upper	lower	upper	lower	upper
2	1667	3973	1380	4870	895	7896	724	10078
5	3007	6869	2511	8335	1669	13229	1367	16674
10	4098	9489	3403	11571	2249	18571	1844	23671
25	5649	13986	4635	17311	2985	28826	2415	37512
50	6927	18370	5606	23131	3507	40312	2799	53574
100	8328	23995	6623	30861	4000	56552	3146	77082
500	12096	43940	9204	59771	5073	125865	3832	183711

Individual Province Tasker Analyses Follow:

Flood frequency estimates for

REGION: Piedmont region  
 area= 58.30: forest = 14.20 :skew= 0.53

Return	Discharge	Standard	Equivalent	Standard
Period	(cfs)	Error of	Years of	Error of
		Prediction	Record	Prediction
		(percent)		(logs)
2	2550.	39.2	2.43	0.1644
5	4470.	35.4	5.60	0.1493
10	6150.	35.0	8.70	0.1475
25	8740.	36.7	12.23	0.1543
50	11000.	39.2	14.05	0.1640
100	13700.	42.4	15.16	0.1764
500	21600.	51.9	15.88	0.2123

P R E D I C T I O N I N T E R V A L S								
Return	50 PERCENT		67 PERCENT		90 PERCENT		95 PERCENT	
Period	lower	upper	lower	upper	lower	upper	lower	upper
2	1970.	3300.	1750.	3730.	1360.	4780.	1190.	5460.
5	3540.	5640.	3170.	6300.	2520.	7900.	2240.	8910.
10	4890.	7750.	4380.	8640.	3500.	10800.	3110.	12200.
25	6870.	11100.	6130.	12500.	4850.	15800.	4280.	17900.
50	8540.	14300.	7560.	16100.	5890.	20700.	5160.	23600.
100	10400.	18000.	9110.	20500.	6960.	26800.	6040.	30900.

500	15500.	30100.	13200.	35200.	9580.	48600.	8080.	57600.
500	15500.	30100.	13200.	35200.	9580.	48600.	8080.	57600.

Flood frequency estimates for

REGION: Western Coastal Plain region  
area= 58.30: forest = 14.20 :skew= 0.69

Return Period	Discharge (cfs)	Standard Error of Prediction (percent)	Equivalent Years of Record	Standard Error of Prediction (logs)
2	2560.	82.5	1.06	0.3130
5	4540.	78.0	2.46	0.2993
10	6220.	80.6	3.70	0.3074
25	8840.	89.2	5.04	0.3322
50	11200.	98.8	5.74	0.3584
100	14100.	110.9	6.18	0.3890
500	23100.	150.0	6.57	0.4715

P R E D I C T I O N I N T E R V A L S								
Return Period	50 PERCENT		67 PERCENT		90 PERCENT		95 PERCENT	
	lower	upper	lower	upper	lower	upper	lower	upper
2	1560.	4210.	1250.	5270.	732.	8990.	560.	11700.
5	2820.	7300.	2280.	9050.	1370.	15100.	1060.	19400.
10	3820.	10100.	3060.	12600.	1810.	21300.	1400.	27700.
25	5220.	15000.	4110.	19000.	2330.	33400.	1760.	44400.
50	6360.	19800.	4920.	25600.	2670.	47200.	1970.	64100.
100	7600.	26100.	5750.	34500.	2960.	67000.	2130.	93300.
500	10900.	48800.	7800.	68400.	3490.	153000.	2340.	228000.
500	10900.	48800.	7800.	68400.	3490.	153000.	2340.	228000.

WARNING -- Prediction beyond observed data

Fixed Region Peak Flow Estimates for:  
GISHydro Release Version Date: October 20, 2004  
Hydro Extension Version Date: October 15, 2004  
Analysis Date: January 20, 2005

Overall Weighted Fixed Region Estimated Discharges

Q(1.25): 1620 cfs  
Q(1.50): 2030 cfs  
Q(1.75): 2280 cfs  
Q(2): 2440 cfs  
Q(5): 4010 cfs  
Q(10): 5400 cfs  
Q(25): 7430 cfs  
Q(50): 9480 cfs  
Q(100): 12100 cfs  
Q(200): 15000 cfs  
Q(500): 19700 cfs

Individual Province Predictions Follow:

Fixed Region Estimated Discharges for: Piedmont region

Q(1.25): 2580 cfs  
 Q(1.50): 3450 cfs  
 Q(1.75): 3930 cfs  
 Q(2): 4200 cfs  
 Q(5): 7430 cfs  
 Q(10): 10400 cfs  
 Q(25): 15100 cfs  
 Q(50): 19700 cfs  
 Q(100): 25100 cfs  
 Q(200): 31700 cfs  
 Q(500): 42500 cfs

Fixed Region Estimated Discharges for: Western Coastal Plain region

Q(1.25): 1290 cfs  
 Q(1.50): 1540 cfs  
 Q(1.75): 1700 cfs  
 Q(2): 1830 cfs  
 Q(5): 2810 cfs  
 Q(10): 3640 cfs  
 Q(25): 4730 cfs  
 Q(50): 5900 cfs  
 Q(100): 7500 cfs  
 Q(200): 9100 cfs  
 Q(500): 11700 cfs

#### PATUXENT RIVER SITE CATCHMENT HYDROLOGIC INFORMATION

##### Watershed Statistics for:

GISHydro Release Version Date: October 20, 2004

Hydro Extension Version Date: October 15, 2004

Analysis Date: January 20, 2005

##### Data Selected:

Quadrangles Used: hughesville, benedict, prince\_frederick, north\_beach,  
 lower\_marlboro, brandywine, upper\_marlboro, bristol, deale, deale\_oe\_e,  
 south\_river, bowie, lanham, washington\_east, laurel\_md, beltsville, odenton,  
 relay, savage, clarksville, sandy\_spring, gaithersburg, damascus, woodbine,  
 sykesville, ellicott\_city

DEM Coverage: NED DEMs

Land Use Coverage: 2000 MOP Landuse

Soil Coverage: Ragan Soils

Hydrologic Condition: (see Lookup Table)

Impose NHD stream Locations: Yes

Outlet Easting: 428943 m. (MD Stateplane, NAD 1983)

Outlet Northing: 94062.2 m. (MD Stateplane, NAD 1983)

##### Findings:

Outlet Location: Western Coastal Plain

Outlet State: Maryland

Drainage Area 732.0 square miles

-Piedmont (31.6% of area)

-Western Coastal Plain (68.4% of area)

Channel Slope: 5.2 feet/mile

Land Slope: 0.059 ft/ft

Urban Area: 25.5%

Impervious Area: 11.8%

\*\*\*\*\*

URBAN DEVELOPMENT IN WATERSHED EXCEEDS 15%.

Calculated discharges from USGS Regression

Equations may not be appropriate.

\*\*\*\*\*

Time of Concentration: 53.0 hours [W.O. Thomas, Jr. Equation]  
Time of Concentration: 41.8 hours [From SCS Lag Equation \* 1.67]  
Longest Flow Path: 94.72 miles  
Basin Relief: 241.4 feet  
Average CN: 70  
% Forest Cover: 39.9  
% Storage: 3.1  
% Limestone: 0.0  
% A Soils: 8.5  
% B Soils: 59.8  
% C Soils: 19.1  
% D Soils: 11.5  
2-Year,24-hour Prec.: 3.21 inches

U.S.G.S. Peak Flow Estimates for:  
GISHydro Release Version Date: October 20, 2004  
Hydro Extension Version Date: October 15, 2004  
Analysis Date: January 20, 2005

Geographic Province(s):  
-Piedmont (31.6% of area)  
-Western Coastal Plain (68.4% of area)

Q(2): 10144 cfs  
Q(5): 18668 cfs  
Q(10): 26457 cfs  
Q(25): 39199 cfs  
Q(50): 51219 cfs  
Q(100): 65813 cfs  
Q(500): 112824 cfs

# Area Weighted Prediction Intervals (from Tasker)

Return	50 PERCENT		67 PERCENT		90 PERCENT		95 PERCENT	
Period	lower	upper	lower	upper	lower	upper	lower	upper
2	6821	15273	5707	18373	3830	28688	3144	36035
5	12779	27510	10732	32946	7349	50360	6078	62532
10	17963	39361	15105	47208	10225	72916	8424	91245
25	25800	60107	21458	73179	14090	117358	11467	148586
50	32642	81321	26679	100813	17016	166973	13595	216188
100	40325	108645	32405	137483	19874	238375	15648	316280
500	62193	209455	47683	278078	26248	549460	19675	773374

Individual Province Tasker Analyses Follow:

Flood frequency estimates for

REGION: Piedmont region  
area= 732.00: forest = 39.90 :skew= 0.53

Return Period	Discharge (cfs)	Standard Error of Prediction (percent)	Equivalent Years of Record	Standard Error of Prediction (logs)
2	10500.	40.3	1.79	0.1683
5	17300.	36.4	4.11	0.1532
10	22900.	36.0	6.38	0.1515
25	31400.	37.8	8.94	0.1587
50	38700.	40.4	10.25	0.1688
100	47000.	43.7	11.05	0.1817
500	71300.	53.8	11.54	0.2189

P R E D I C T I O N I N T E R V A L S								
Return	50 PERCENT		67 PERCENT		90 PERCENT		95 PERCENT	
Period	lower	upper	lower	upper	lower	upper	lower	upper
2	8080.	13700.	7130.	15500.	5520.	20000.	4820.	22900.
5	13600.	21900.	12100.	24600.	9620.	31000.	8500.	35100.
10	18100.	29100.	16200.	32500.	12900.	40900.	11400.	46300.
25	24500.	40200.	21800.	45200.	17100.	57500.	15100.	65400.
50	29700.	50400.	26200.	57100.	20300.	73800.	17700.	84500.
100	35400.	62400.	30900.	71400.	23500.	94100.	20300.	109000.
500	50700.	100000.	43100.	118000.	30900.	165000.	25900.	196000.
500	50700.	100000.	43100.	118000.	30900.	165000.	25900.	196000.

WARNING - Drainage area out of range of observed data

Flood frequency estimates for

REGION: Western Coastal Plain region

GISHydro Release Version Date: October 20, 2004  
 Hydro Extension Version Date: October 15, 2004  
 Analysis Date: January 20, 2005

Overall Weighted Fixed Region Estimated Discharges

Q(1.25): 5260 cfs  
 Q(1.50): 6960 cfs  
 Q(1.75): 7980 cfs  
 Q(2): 8650 cfs  
 Q(5): 15700 cfs  
 Q(10): 22500 cfs  
 Q(25): 32400 cfs  
 Q(50): 44400 cfs  
 Q(100): 59400 cfs  
 Q(200): 77400 cfs  
 Q(500): 108000 cfs

Individual Province Predictions Follow:

Fixed Region Estimated Discharges for: Piedmont region

Q(1.25): 6630 cfs  
 Q(1.50): 8840 cfs  
 Q(1.75): 10200 cfs  
 Q(2): 10900 cfs  
 Q(5): 20700 cfs  
 Q(10): 31000 cfs  
 Q(25): 49200 cfs  
 Q(50): 68800 cfs  
 Q(100): 93800 cfs  
 Q(200): 128000 cfs  
 Q(500): 188000 cfs

Fixed Region Estimated Discharges for: Western Coastal Plain region

Q(1.25): 4620 cfs  
 Q(1.50): 6090 cfs  
 Q(1.75): 6970 cfs  
 Q(2): 7610 cfs  
 Q(5): 13400 cfs  
 Q(10): 18500 cfs  
 Q(25): 24600 cfs  
 Q(50): 33100 cfs

Q(100): 43500 cfs  
Q(200): 54100 cfs  
Q(500): 71600 cfs

#### WICOMICO RIVER SITE CATCHMENT HYDROLOGIC INFORMATION

##### Watershed Statistics for:

GISHydro Release Version Date: October 20, 2004  
Hydro Extension Version Date: October 15, 2004  
Analysis Date: January 20, 2005

##### Data Selected:

Quadrangles Used: wetipquin, monie, princess\_anne, eden, dividing\_creek,  
salisbury, delmar, hebron, pittsville, wango  
DEM Coverage: NED DEMs  
Land Use Coverage: 2000 MOP Landuse  
Soil Coverage: Ragan Soils  
Hydrologic Condition: (see Lookup Table)  
Impose NHD stream Locations: Yes  
Outlet Easting: 501345 m. (MD Stateplane, NAD 1983)  
Outlet Northing: 65399.1 m. (MD Stateplane, NAD 1983)

##### Findings:

Outlet Location: Eastern Coastal Plain  
Outlet State: Maryland  
Drainage Area: 170.8 square miles  
-Eastern Coastal Plain (100.0% of area)  
Channel Slope: 1.6 feet/mile  
Land Slope: 0.007 ft/ft  
Urban Area: 20.0%  
Impervious Area: 9.5%

\*\*\*\*\*

URBAN DEVELOPMENT IN WATERSHED EXCEEDS 15%.  
Calculated discharges from USGS Regression  
Equations may not be appropriate.

\*\*\*\*\*

Time of Concentration: 54.2 hours [W.O. Thomas, Jr. Equation]  
Time of Concentration: 41.8 hours [From SCS Lag Equation \* 1.67]  
Longest Flow Path: 33.08 miles  
Basin Relief: 31.3 feet  
Average CN: 79  
% Forest Cover: 35.7  
% Storage: 6.5  
% Limestone: 0.0  
% A Soils: 8.8  
% B Soils: 19.1  
% C Soils: 24.8  
% D Soils: 43.5  
2-Year,24-hour Prec.: 3.41 inches

##### U.S.G.S. Peak Flow Estimates for:

GISHydro Release Version Date: October 20, 2004  
Hydro Extension Version Date: October 15, 2004  
Analysis Date: January 20, 2005

Geographic Province(s):  
 -Eastern Coastal Plain (100.0% of area)

Q(2): 1140 cfs  
 Q(5): 1850 cfs  
 Q(10): 2470 cfs  
 Q(25): 3410 cfs  
 Q(50): 4210 cfs  
 Q(100): 5110 cfs  
 Q(500): 7540 cfs

Area Weighted Prediction Intervals (from Tasker)

Return	50 PERCENT		67 PERCENT		90 PERCENT		95 PERCENT	
Period	lower	upper	lower	upper	lower	upper	lower	upper
2	817	1580	701	1840	501	2570	425	3030
5	1340	2560	1150	2980	828	4150	705	4880
10	1790	3400	1550	3940	1120	5460	952	6400
25	2480	4670	2150	5400	1550	7460	1330	8730
50	3070	5770	2650	6680	1920	9230	1640	10800
100	3720	7010	3210	8130	2320	11300	1980	13200
500	5400	10500	4620	12300	3280	17300	2780	20500

Individual Province Tasker Analyses Follow:

Flood frequency estimates for

REGION; Eastern Coastal Plain region  
 area= 170.80: curve = 79.00: storage = 6.50  
 : forest = 35.70 : relief = 31.30 :skew= 0.67

Return	Discharge	Standard	Equivalent	Standard
Period	(cfs)	Error of	Years of	Error of
		Prediction	Record	Prediction
		(percent)		(logs)
2	1140.	51.1	1.65	0.2092
5	1850.	50.2	3.54	0.2060
10	2470.	49.4	5.76	0.2029
25	3410.	48.7	9.36	0.2004
50	4210.	48.7	12.35	0.2005
100	5110.	49.1	15.42	0.2020
500	7540.	52.0	21.69	0.2124

P R E D I C T I O N I N T E R V A L S								
Return	50 PERCENT		67 PERCENT		90 PERCENT		95 PERCENT	
Period	lower	upper	lower	upper	lower	upper	lower	upper
2	817.	1580.	701.	1840.	501.	2570.	425.	3030.
5	1340.	2560.	1150.	2980.	828.	4150.	705.	4880.
10	1790.	3400.	1550.	3940.	1120.	5460.	952.	6400.
25	2480.	4670.	2150.	5400.	1550.	7460.	1330.	8730.
50	3070.	5770.	2650.	6680.	1920.	9230.	1640.	10800.
100	3720.	7010.	3210.	8130.	2320.	11300.	1980.	13200.
500	5400.	10500.	4620.	12300.	3280.	17300.	2780.	20500.
500	5400.	10500.	4620.	12300.	3280.	17300.	2780.	20500.

WARNING - Drainage area out of range of observed data

GISHydro Release Version Date: October 20, 2004  
 Hydro Extension Version Date: October 15, 2004  
 Analysis Date: January 20, 2005

Overall Weighted Fixed Region Estimated Discharges

Q(1.25): 1170 cfs  
 Q(1.50): 1520 cfs  
 Q(1.75): 1790 cfs  
 Q(2): 2010 cfs  
 Q(5): 3500 cfs  
 Q(10): 4700 cfs  
 Q(25): 6390 cfs  
 Q(50): 7860 cfs  
 Q(100): 9430 cfs  
 Q(200): 11100 cfs  
 Q(500): 13700 cfs

Individual Province Predictions Follow:

Fixed Region Estimated Discharges for: Eastern Coastal Plain region

Q(1.25): 1170 cfs  
 Q(1.50): 1520 cfs  
 Q(1.75): 1790 cfs  
 Q(2): 2010 cfs  
 Q(5): 3500 cfs  
 Q(10): 4700 cfs  
 Q(25): 6390 cfs  
 Q(50): 7860 cfs  
 Q(100): 9430 cfs  
 Q(200): 11100 cfs  
 Q(500): 13700 cfs

#### PATAPSCO RIVER SITE CATCHMENT HYDROLOGIC INFORMATION

Watershed Statistics for:

GISHydro Release Version Date: October 20, 2004

Hydro Extension Version Date: October 15, 2004

Analysis Date: January 20, 2005

Data Selected:

Quadrangles Used: sparrows\_point, middle\_river, curtis\_bay, baltimore\_east,  
 savage, round\_bay, relay, odenton, baltimore\_west, cockeysville, towson,  
 reisterstown, ellicott\_city, sykesville, finksburg, woodbine, damascus,  
 libertytown, winfield, westminister, hampstead, new\_windsor, manchester,  
 lineboro

DEM Coverage: 30m DEMs

Land Use Coverage: 2000 MOP Landuse

Soil Coverage: Ragan Soils

Hydrologic Condition: (see Lookup Table)

Impose NHD stream Locations: Yes

Outlet Easting: 445359 m. (MD Stateplane, NAD 1983)

Outlet Northing: 168475 m. (MD Stateplane, NAD 1983)

Findings:

Outlet Location: Western Coastal Plain

Outlet State: Maryland

Drainage Area 598.5 square miles

-Piedmont (73.3% of area)

-Western Coastal Plain (26.7% of area)

Channel Slope: 10.9 feet/mile

Land Slope: 0.067 ft/ft



Urban Area: 39.8%  
 Impervious Area: 21.4%  
 \*\*\*\*\*  
 URBAN DEVELOPMENT IN WATERSHED EXCEEDS 15%.  
 Calculated discharges from USGS Regression  
 Equations may not be appropriate.  
 \*\*\*\*\*  
 Time of Concentration: 26.9 hours [W.O. Thomas, Jr. Equation]  
 Time of Concentration: 28.2 hours [From SCS Lag Equation \* 1.67]  
 Longest Flow Path: 69.33 miles  
 Basin Relief: 428.4 feet  
 Average CN: 73  
 % Forest Cover: 26.0  
 % Storage: 5.7  
 % Limestone: 0.0  
 % A Soils: 13.9  
 % B Soils: 47.7  
 % C Soils: 28.9  
 % D Soils: 5.1  
 2-Year,24-hour Prec.: 3.18 inches

U.S.G.S. Peak Flow Estimates for:  
 GISHydro Release Version Date: October 20, 2004  
 Hydro Extension Version Date: October 15, 2004  
 Analysis Date: January 20, 2005

Geographic Province(s):  
 -Piedmont (73.3% of area)  
 -Western Coastal Plain (26.7% of area)

Q(2): 10367 cfs  
 Q(5): 17694 cfs  
 Q(10): 24047 cfs  
 Q(25): 33721 cfs  
 Q(50): 42448 cfs  
 Q(100): 52629 cfs  
 Q(500): 83891 cfs

Area Weighted Prediction Intervals (from Tasker)								
Return	50 PERCENT		67 PERCENT		90 PERCENT		95 PERCENT	
Period	lower	upper	lower	upper	lower	upper	lower	upper
2	7469	14487	6439	16987	4715	24668	4029	29956
5	13020	24334	11327	28401	8423	40396	7265	48724
10	17560	33262	15280	38856	11357	56025	9805	67694
25	24133	48009	20787	56837	15140	84562	12929	104466
50	29607	62284	25240	74739	17973	115546	15185	145772
100	35607	79959	29920	97808	20726	158073	17379	204496
500	51807	141039	41900	181686	27086	333918	21839	462080

Individual Province Tasker Analyses Follow:

Flood frequency estimates for

REGION: Piedmont region  
 area= 598.50: forest = 26.00 :skew= 0.53

Return Period	Discharge (cfs)	Standard Error of Prediction (percent)	Equivalent Years of Record	Standard Error of Prediction (logs)
2	10100.	40.1	1.84	0.1678
5	16600.	36.3	4.22	0.1526

10	22100.	35.8	6.56	0.1510
25	30200.	37.7	9.19	0.1581
50	37300.	40.2	10.53	0.1682
100	45400.	43.6	11.35	0.1811
500	69300.	53.6	11.86	0.2182

P R E D I C T I O N I N T E R V A L S

Return	50 PERCENT		67 PERCENT		90 PERCENT		95 PERCENT	
Period	lower	upper	lower	upper	lower	upper	lower	upper
2	7760.	13100.	6850.	14800.	5310.	19200.	4640.	21900.
5	13100.	21000.	11700.	23600.	9250.	29700.	8180.	33600.
10	17400.	27900.	15600.	31200.	12400.	39300.	11000.	44300.
25	23600.	38700.	21000.	43500.	16500.	55300.	14500.	62800.
50	28700.	48600.	25400.	55000.	19600.	71000.	17100.	81300.
100	34300.	60300.	30000.	69000.	22700.	90800.	19700.	105000.
500	49300.	97400.	41900.	115000.	30100.	160000.	25200.	190000.
500	49300.	97400.	41900.	115000.	30100.	160000.	25200.	190000.

WARNING - Drainage area out of range of observed data

Flood frequency estimates for

REGION: Western Coastal Plain region  
area= 598.50: forest = 26.00 :skew= 0.69

Return	Discharge	Standard	Equivalent	Standard
Period	(cfs)	Error of	Years of	Error of
		Prediction	Record	Prediction
		(percent)		(logs)
2	11100.	84.5	1.16	0.3188
5	20700.	79.2	2.72	0.3031
10	29400.	81.4	4.13	0.3097
25	43400.	89.5	5.70	0.3330
50	56600.	98.7	6.52	0.3582
100	72500.	110.6	7.05	0.3882
500	124000.	149.1	7.51	0.4698

P R E D I C T I O N I N T E R V A L S

Return	50 PERCENT		67 PERCENT		90 PERCENT		95 PERCENT	
Period	lower	upper	lower	upper	lower	upper	lower	upper
2	6670.	18300.	5310.	23000.	3080.	39700.	2350.	52100.
5	12800.	33500.	10300.	41600.	6150.	69800.	4750.	90300.
10	18000.	48000.	14400.	59900.	8490.	102000.	6520.	132000.
25	25600.	73600.	20200.	93500.	11400.	165000.	8610.	219000.
50	32100.	99900.	24800.	129000.	13500.	238000.	9920.	323000.
100	39200.	134000.	29700.	177000.	15300.	343000.	11000.	478000.
500	58700.	261000.	41900.	365000.	18800.	812000.	12600.	1210000.
500	58700.	261000.	41900.	365000.	18800.	812000.	12600.	1210000.

Fixed Region Peak Flow Estimates for:  
GISHydro Release Version Date: October 20, 2004  
Hydro Extension Version Date: October 15, 2004  
Analysis Date: January 20, 2005

Overall Weighted Fixed Region Estimated Discharges

Q(1.25): 7310 cfs  
Q(1.50): 9620 cfs  
Q(1.75): 10900 cfs  
Q(2): 11600 cfs  
Q(5): 20700 cfs  
Q(10): 29600 cfs

Q(25): 43800 cfs  
Q(50): 58800 cfs  
Q(100): 77300 cfs  
Q(200): 101000 cfs  
Q(500): 141000 cfs

Individual Province Predictions Follow:

Fixed Region Estimated Discharges for: Piedmont region

Q(1.25): 8300 cfs  
Q(1.50): 11000 cfs  
Q(1.75): 12600 cfs  
Q(2): 13300 cfs  
Q(5): 24200 cfs  
Q(10): 34900 cfs  
Q(25): 52800 cfs  
Q(50): 71200 cfs  
Q(100): 93800 cfs  
Q(200): 123000 cfs  
Q(500): 174000 cfs

Fixed Region Estimated Discharges for: Western Coastal Plain region

Q(1.25): 4590 cfs  
Q(1.50): 5720 cfs  
Q(1.75): 6430 cfs  
Q(2): 6950 cfs  
Q(5): 11200 cfs  
Q(10): 14900 cfs  
Q(25): 19100 cfs  
Q(50): 24700 cfs  
Q(100): 31900 cfs  
Q(200): 38900 cfs  
Q(500): 50100 cfs

## APPENDIX D-1

**Table D-1-1. Results of Exercise to Determine the Number Simulations**

Number of Simulations	Simulaion Duration (yrs)	Mean Final Scour Depth Upstream Face (ft)	Standard Deviation in Final Scour Result Upstream Face (ft)	Mean Final Scour Depth Downstream Face (ft)	Standard Deviation in Final Scour Result Downstream Face (ft)
10	100	22.52	0.1647	19.92	0.0571
100	100	22.51	0.1956	19.92	0.0615
200	100	22.53	0.2053	19.92	0.0559
500	100	22.52	0.2134	19.92	0.0573
800	100	22.52	0.2053	19.92	0.0565
1000	100	22.52	0.2045	19.92	0.0559
2000	100	22.51	0.2043	19.93	0.0438
5000	100	22.51	0.2043	19.93	0.0337

## APPENDIX D-2

**TITLE: COMPREHENSIVE ESTUARY SCOUR INPUT FILE Continuous Simulations**

**PROJECT NAME: MONIE RIVER OUTLET**

**DATE: 3/15/05**

**BRIDGE LOCATION: MONIE BAY**

**BASE STATION LOCATION:**

**ENGINEERING CONSTANTS**

grav	spgw	visc	n val		rho w	spg soil
GR	GW	MUW	MAN	PI	RHW	SG
32.2	62.4	0.0000205	0.045	3.142	1.94	165.3
ft/s-2	lb/cuf	lb.s/sqft			s/cuf	lb/cuf

**SIMULATION DATA**

**step no sym brg. life**

**DLT TMS YRS**

1.0 1000 100

hr yr

**CATCHMENT BASIN HYDROLOGY**

cv.no	basin	min BA	ca.length	uhg dur	no duh	
CN	CBA	CBAMIN	LC	DU	NO	TMCON
81	16.0	150	14.09	36	36	30.5
	sqmi	sqmi.	mi	hr		

**STORM (RAINFALL) DATA**

**pr.dur 6,18,24,36 mean std**

**F6 F18 F24 F36 MAS SDS**

0.775 0.088 0.075 0.063 80 0.50

**All variables in this set are dimensionless**

**gamma b const gamma c consts**

**B6 B18 B24 B36 C6 C18 C24 C36**

0.10 0.40 0.83 1.35 3.0 2.0 2.0 1.0

**All variables in this set are dimensionless**

**SCS STORM DISTRIBUTION FOR 6, 18, 24 AND 36 HR TYPE II STORMS**

**DISTRIBUTION ARRAY FOR 18 HR STORM**

**S18**

0.014 0.030 0.050 0.060 0.089 0.116

0.156 0.213 0.657 0.786 0.843 0.886

0.911 0.930 0.949 0.971 0.986 1.000

**DISTRIBUTION ARRAY FOR 24 HR STORM**

**S24**

0.011 0.023 0.035 0.048 0.063 0.080

0.098 0.120 0.148 0.181 0.235 0.663

0.772 0.820 0.854 0.880 0.902 0.921

0.938 0.953 0.965 0.977 0.990 1.000

**DISTRIBUTION ARRAY FOR 36 HR STORM**

**S36**

0.007 0.014 0.030 0.032 0.036 0.050

0.057 0.060 0.080 0.089 0.107 0.115

0.140 0.156 0.179 0.213 0.279 0.657

0.742 0.786 0.817 0.843 0.871 0.886

0.900 0.911 0.917 0.930 0.943 0.949

0.960 0.971 0.974 0.986 0.994 1.000

**S6**

0.048 0.12 0.663 0.880 0.953 1.00

**SCS DIMENSIONLESS UNIT HYDROGRAPH**

**TO - DIMENSIONLESS TIME T/Tp**

0.0 0.1 0.2 0.3 0.4 0.5

0.6 0.7 0.8 0.9 1.0 1.1

1.2 1.3 1.4 1.5 1.6 1.7

```

1.8 1.9 2.0 2.2 2.4 2.6
2.8 3.0 3.2 3.4 3.6 3.8
4.0 4.2 4.4 4.6 4.8 5.0
DUH- DIMENSIONLESS DISCHARGE Q/Qp
0.000 0.030 0.100 0.190 0.310 0.470
0.660 0.820 0.930 0.990 1.000 0.990
0.930 0.860 0.780 0.680 0.560 0.460
0.390 0.330 0.280 0.207 0.147 0.107
0.077 0.055 0.040 0.029 0.021 0.015
0.011 0.008 0.006 0.004 0.002 0.000
BASE STATION TIDAL DATA
inv      di.per lu per dist md amp ml amp std  std
IBS      DT      LT      LW      MDA      MLA      SDA      SLA
-28.01   12.31   356.   187     1.22   0.36   0.56   .18
ft       hr       hr       mi       ft       ft       ft       ft
BRIDGE STATION TIDAL DATA
  DATUM          slope amp      peaked
  CHAR          CS      MTR      PKM
  MSL           .0002   1.19   0.67
  ft              ft
BRIDGE DATA
no piers pier diam const
NBP      PD      C1
30        5.0      0.25
          ft
BRIDGE ESTUARY DATA
area  est l est w  wdnf  wupf  maxw  X-area  Upr-est
          adj-fac s-slp
AS      LE      WB      WD      WU      WM      AFACT  UESTZ(Z:1)
2.16    10      1.13   1.13   1.0    1.13  1.0    500.0
Sqmi    mi      mi      mi      mi      mi
Estuary elev below mean low tide (ft) EBMTL(1)-EBMTL(4)
-5.935  -4.935  -3.935  -0.935
Associated top widths in feet TWBMTL(1)-TWBMTL(4)
10.0    2700.0  3600.0  5808.0
SOIL DATA
cont coef  spg
KT         SS
0.3256     2.65

ARRAY WITH SOIL PROPERTIES
DEPTH (DPTH) ft
0.0  2.0  4.0  6.0  8.0  10.0 12.0 14.0 16.0 18.0
20.0 22.0 24.0 26.0 28.0 30.0 32.0 34.0 36.0 38.0
40.0 42.0 44.0 46.0 48.0 50.0 52.0 54.0 56.0 58.0
D50 mm
.135 .135 .135 .135 .135 .135 .135 .135 .135 .135
.135 .135 .135 .135 .135 .135 .135 .135 .135 .135
.135 .135 .135 .135 .135 .135 .135 .135 .135 .135
D16mm
0.01 0.01 0.01 0.01 0.01 0.01 0.01 0.01 0.01 0.01
0.01 0.01 0.01 0.01 0.01 0.01 0.01 0.01 0.01 0.01
0.01 0.01 0.01 0.01 0.01 0.01 100. 100. 100. 100.
D84mm
1.75 1.75 1.75 1.75 1.75 1.75 1.75 1.75 1.75 1.75
1.75 1.75 1.75 1.75 1.75 1.75 1.75 1.75 1.75 1.75
1.75 1.75 1.75 1.75 1.75 1.75 1.75 1.75 1.75 1.75

```

**DMAX**

2.5	2.5	2.5	2.5	2.5	2.5	2.5	2.5	2.5	2.5
2.5	2.5	2.5	2.5	2.5	2.5	2.5	2.5	2.5	2.5
2.5	2.5	2.5	2.5	2.5	2.5	2.5	2.5	2.5	2.5

**PHI deg**

35.	35.	35.	35.	35.	35.	35.	35.	35.	35.
35.	35.	35.	35.	35.	35.	35.	35.	35.	35.
35.	35.	35.	35.	35.	35.	35.	35.	35.	35.

**ALPHA**

5.7	5.7	5.7	5.7	5.7	5.7	5.7	5.7	5.7	5.7
5.7	5.7	5.7	5.7	5.7	5.7	5.7	5.7	5.7	5.7
5.7	5.7	5.7	5.7	5.7	5.7	5.7	5.7	5.7	5.7

**INITIAL CONDITIONS****water d scr d scr u**

YMIF	YMIR	TDI	TUI
5.00	5.0	0.00	0.00
ft	ft	ft	ft

**HURRICANE DATA**

**HURRICANE RADIUS FOR CATEGORY 1-5 IN MILES, AND CLOSEST  
DISTANCE OF THE BRIDGE LOCATION FROM THE CENTER**

HRAD1	HRAD2	HRAD3	HRAD4	HRAD5	HDIST
75.	100.	150.	200.	250.	0.1

**HURRICANE SPEED CATEGORY 1-5**

HSPED1	HSPED2	HSPED3	HSPED4	HSPED5
30.	25.	20.	15.	10.

**HURRICANE MAXIMUM SURGE (FT) CATEGORY 1-5**

MXSRG1	MXSRG2	MXSRG3	MXSRG4	MXSRG5
5.	7.	11.	16.	20.

**SPECIFIC HURRICANE INFO.**

**Rainfall ins, Max surge ft, System speed mph, hurricane radius miles**

HURAIN	MXSRGI	HSPEDI	HRADI
--------	--------	--------	-------

**TITLE: COMPREHENSIVE ESTUARY SCOUR INPUT FILE Hurricane Simulation**

**PROJECT NAME: MONIE RIVER OUTLET** **DATE: 3/15/05**

**BRIDGE LOCATION: MONIE BAY**

**BASE STATION LOCATION:**

**ENGINEERING CONSTANTS**

grav	spgw	visc	n val	rho w	spg soil	
GR	GW	MUW	MAN	PI	RHW	SG
32.2	62.4	0.0000205	0.045	3.142	1.94	165.3
ft/s-2	lb/cuf	lb.s/sqft		s/cuf	lb/cuf	

**SIMULATION DATA**

step	no sym	brg. life
------	--------	-----------

DLT	TMS	YRS
-----	-----	-----

1.0	10000	0
-----	-------	---

hr	yr
----	----

**CATCHMENT BASIN HYDROLOGY**

cv no	basin	min BA	ca.lngth	uhg dur	no duh	
CN	CBA	CBAMIN	LC	DU	NO	TMCON
81	16.0	150	14.09	36	36	30.5
	sqmi	sqmi.	mi	hr		

**STORM (RAINFALL) DATA**

pr.dur	6,18,24,36	mean	std		
F6	F18	F24	F36	MAS	SDS
0.775	0.088	0.075	0.063	80	0.50

All variables in this set are dimensionless  
gamma b const gamma c consts  
B6 B18 B24 B36 C6 C18 C24 C36  
0.10 0.40 0.83 1.35 3.0 2.0 2.0 1.0  
All variables in this set are dimensionless  
SCS STORM DISTRIBUTION FOR 6, 18, 24 AND 36 HR TYPE II STORMS  
DISTRIBUTION ARRAY FOR 18 HR STORM  
S18  
0.014 0.030 0.050 0.060 0.089 0.116  
0.156 0.213 0.657 0.786 0.843 0.886  
0.911 0.930 0.949 0.971 0.986 1.000  
DISTRIBUTION ARRAY FOR 24 HR STORM  
S24  
0.011 0.023 0.035 0.048 0.063 0.080  
0.098 0.120 0.148 0.181 0.235 0.663  
0.772 0.820 0.854 0.880 0.902 0.921  
0.938 0.953 0.965 0.977 0.990 1.000  
DISTRIBUTION ARRAY FOR 36 HR STORM  
S36  
0.007 0.014 0.030 0.032 0.036 0.050  
0.057 0.060 0.080 0.089 0.107 0.115  
0.140 0.156 0.179 0.213 0.279 0.657  
0.742 0.786 0.817 0.843 0.871 0.886  
0.900 0.911 0.917 0.930 0.943 0.949  
0.960 0.971 0.974 0.986 0.994 1.000  
S6  
0.048 0.12 0.663 0.880 0.953 1.00  
SCS DIMENSIONLESS UNIT HYDROGRAPH  
TO - DIMENSIONLESS TIME T/Tp  
0.0 0.1 0.2 0.3 0.4 0.5  
0.6 0.7 0.8 0.9 1.0 1.1  
1.2 1.3 1.4 1.5 1.6 1.7  
1.8 1.9 2.0 2.2 2.4 2.6  
2.8 3.0 3.2 3.4 3.6 3.8  
4.0 4.2 4.4 4.6 4.8 5.0  
DUH- DIMENSIONLESS DISCHARGE Q/Qp  
0.000 0.030 0.100 0.190 0.310 0.470  
0.660 0.820 0.930 0.990 1.000 0.990  
0.930 0.860 0.780 0.680 0.560 0.460  
0.390 0.330 0.280 0.207 0.147 0.107  
0.077 0.055 0.040 0.029 0.021 0.015  
0.011 0.008 0.006 0.004 0.002 0.000  
BASE STATION TIDAL DATA  
inv di.per lu per dist md amp ml amp std std  
IBS DT LT LW MDA MLA SDA SLA  
-28.01 12.31 356. 187 1.22 0.36 0.56 .18  
ft hr hr mi ft ft ft ft  
BRIDGE STATION TIDAL DATA  
DATUM slope amp peaked  
CHAR CS MTR PKM  
MSL .0002 1.19 0.67  
ft ft  
BRIDGE DATA  
no piers pier diam const  
NBP PD C1  
30 5.0 0.25  
ft



## BRIDGE ESTUARY DATA

area	est l	est w	wnf	wupf	maxw	X-area	Upr-est
						adj-fac	s-slp
AS	LE	WB	WD	WU	WM	AFACT	UESTZ(Z:1)
2.16	10	1.13	1.13	1.0	1.13	1.0	500.0
Sqmi	mi	mi	mi	mi	mi		
Estuary elev below mean low tide (ft) EBMTL(1)-EBMTL(4)							
-5.935	-4.935	-3.935	-0.935				
Associated top widths in feet TWBMTL(1)-TWBMTL(4)							
10.0	2700.0	3600.0	5808.0				

SOIL DATA

cont coef	spg
KT	SS
0.3256	2.65

## ARRAY WITH SOIL PROPERTIES

DEPTH (DPTH) ft

0.0	2.0	4.0	6.0	8.0	10.0	12.0	14.0	16.0	18.0
20.0	22.0	24.0	26.0	28.0	30.0	32.0	34.0	36.0	38.0
40.0	42.0	44.0	46.0	48.0	50.0	52.0	54.0	56.0	58.0

D50 mm

.135	.135	.135	.135	.135	.135	.135	.135	.135	.135
.135	.135	.135	.135	.135	.135	.135	.135	.135	.135
.135	.135	.135	.135	.135	.135	.135	.135	.135	.135

D16mm

0.01	0.01	0.01	0.01	0.01	0.01	0.01	0.01	0.01	0.01
0.01	0.01	0.01	0.01	0.01	0.01	0.01	0.01	0.01	0.01
0.01	0.01	0.01	0.01	0.01	0.01	0.01	100.	100.	100.

D84mm

1.75	1.75	1.75	1.75	1.75	1.75	1.75	1.75	1.75	1.75
1.75	1.75	1.75	1.75	1.75	1.75	1.75	1.75	1.75	1.75
1.75	1.75	1.75	1.75	1.75	1.75	1.75	1.75	1.75	1.75

DMAX

2.5	2.5	2.5	2.5	2.5	2.5	2.5	2.5	2.5	2.5
2.5	2.5	2.5	2.5	2.5	2.5	2.5	2.5	2.5	2.5
2.5	2.5	2.5	2.5	2.5	2.5	2.5	2.5	2.5	2.5

PHI deg

35.	35.	35.	35.	35.	35.	35.	35.	35.	35.
35.	35.	35.	35.	35.	35.	35.	35.	35.	35.
35.	35.	35.	35.	35.	35.	35.	35.	35.	35.

ALPHA

5.7	5.7	5.7	5.7	5.7	5.7	5.7	5.7	5.7	5.7
5.7	5.7	5.7	5.7	5.7	5.7	5.7	5.7	5.7	5.7
5.7	5.7	5.7	5.7	5.7	5.7	5.7	5.7	5.7	5.7

INITIAL CONDITIONS

water d	scr d	scr u
YMIF	YMIR	TDI
5.00	5.0	3.9
ft	ft	ft

HURRICANE DATA

HURRICANE RADIUS FOR CATEGORY 1-5 IN MILES, AND CLOSEST DISTANCE OF THE BRIDGE LOCATION FROM THE CENTER

HRAD1	HRAD2	HRAD3	HRAD4	HRAD5	HDIST
75.	100.	150.	200.	250.	1.0

HURRICANE SPEED CATEGORY 1-5

HSPED1	HSPED2	HSPED3	HSPED4	HSPED5
30.	25.	20.	15.	10.

HURRICANE MAXIMUM SURGE (FT) CATEGORY 1-5  
 MXSRG1      MXSRG2      MXSRG3      MXSRG4      MXSRG5  
 5.            7.            11.           16.           20.  
 SPECIFIC HURRICANE INFO.  
 Rainfall ins, Max surge ft, System speed mph, hurricane radius miles  
 HURAIN      MXSRGI      HSPEDI      HRADI  
 5.            11.           20.           150.

-----  
 -----  
 TITLE: COMPREHENSIVE ESTUARY SCOUR INPUT FILE Continuous Simulations  
 PROJECT NAME: EAST BALTIMORE BLACK RIVER      DATE: 3/27/05

BRIDGE LOCATION: STONY POINT

BASE STATION LOCATION:

ENGINEERING CONSTANTS

grav	spgw	visc	n val		rho w	spg soil
GR	GW	MUW	MAN	PI	RHW	SG
32.2	62.4	0.0000205	0.035	3.142	1.94	165.3
ft/s-2	lb/cuf	lb.s/sqft			s/cuf	lb/cuf

SIMULATION DATA

step no sym brg. life

DLT TMS YRS

1.0 1000 100

hr yr

CATCHMENT BASIN HYDROLOGY

cv no	basin	min BA	ca.length	uhg	dur	no	duh
CN	CBA	CBAMIN	LC	DU	NO	TMCON	
84	58.0	150	19.97	36	36	9.7	
	sqmi	sqmi.	mi	hr			

STORM (RAINFALL) DATA

pr.dur	6,18,24,36	mean	std
F6	F18	F24	F36
0.775	0.088	0.075	0.063
			80
			0.50

All variables in this set are dimensionless

gamma b const gamma c consts

B6	B18	B24	B36	C6	C18	C24	C36
0.10	0.40	0.83	1.35	3.0	2.0	2.0	1.0

All variables in this set are dimensionless

SCS STORM DISTRIBUTION FOR 18, 24 AND 36 HR TYPE II STORMS

DISTRIBUTION ARRAY FOR 18 HR STORM

S18

0.014	0.030	0.050	0.060	0.089	0.116
0.156	0.213	0.657	0.786	0.843	0.886
0.911	0.930	0.949	0.971	0.986	1.000

DISTRIBUTION ARRAY FOR 24 HR STORM

S24

0.011	0.023	0.035	0.048	0.063	0.080
0.098	0.120	0.148	0.181	0.235	0.663
0.772	0.820	0.854	0.880	0.902	0.921
0.938	0.953	0.965	0.977	0.990	1.000

DISTRIBUTION ARRAY FOR 36 HR STORM

S36

0.007	0.014	0.030	0.032	0.036	0.050
0.057	0.060	0.080	0.089	0.107	0.115
0.140	0.156	0.179	0.213	0.279	0.657
0.742	0.786	0.817	0.843	0.871	0.886

0.900 0.911 0.917 0.930 0.943 0.949  
 0.960 0.971 0.974 0.986 0.994 1.000  
 S6  
 0.048 0.12 0.663 0.880 0.953 1.00  
 SCS DIMENSIONLESS UNIT HYDROGRAPH  
 TO - DIMENSIONLESS TIME T/Tp  
 0.0 0.1 0.2 0.3 0.4 0.5  
 0.6 0.7 0.8 0.9 1.0 1.1  
 1.2 1.3 1.4 1.5 1.6 1.7  
 1.8 1.9 2.0 2.2 2.4 2.6  
 2.8 3.0 3.2 3.4 3.6 3.8  
 4.0 4.2 4.4 4.6 4.8 5.0  
 DUH- DIMENSIONLESS DISCHARGE Q/Qp  
 0.000 0.030 0.100 0.190 0.310 0.470  
 0.660 0.820 0.930 0.990 1.000 0.990  
 0.930 0.860 0.780 0.680 0.560 0.460  
 0.390 0.330 0.280 0.207 0.147 0.107  
 0.077 0.055 0.040 0.029 0.021 0.015  
 0.011 0.008 0.006 0.004 0.002 0.000  
 BASE STATION TIDAL DATA  
 inv di.per lu per dist md amp ml amp std std  
 IBS DT LT LW MDA MLA SDA SLA  
 -28.01 12.31 356. 187 1.22 0.36 0.56 .18  
 ft hr hr mi ft ft ft ft  
 BRIDGE STATION TIDAL DATA  
 DATUM slope amp peaked  
 CHAR CS MTR PKM  
 MSL .0002 0.935 0.67  
 ft ft  
 BRIDGE DATA  
 no piers pier diam const  
 NBP PD C1  
 40 5.0 0.25  
 ft  
 BRIDGE ESTUARY DATA  
 area est l est w wdnf wupf maxw X-area Upr-est  
 adj-fac s-slp  
 AS LE WB WD WU WM AFACT UESTZ(Z:1)  
 9.5 10.00 1.63 1.75 1.4 1.63 1.00 300.0  
 Sqmi mi mi mi mi mi  
 Estuary elev below mean low tide (ft) EBMTL(1)-EBMTL(4)  
 -10.935 -6.935 -3.935 -.935  
 Associated top widths in feet TWBMTL(1)-TWBMTL(4)  
 3300.0 5280.0 6930.0 8580.0  
 SOIL DATA  
 cont coef spg  
 KT SS  
 0.3256 2.65  
 ARRAY WITH SOIL PROPERTIES  
 DEPTH (DPTH) ft  
 0.0 2.0 4.0 6.0 8.0 10.0 12.0 14.0 16.0 18.0  
 20.0 22.0 24.0 26.0 28.0 30.0 32.0 34.0 36.0 38.0  
 40.0 42.0 44.0 46.0 48.0 50.0 52.0 54.0 56.0 58.0  
 D50 mm  
 0.15 0.15 0.15 0.15 0.15 0.15 0.15 0.15 0.15 0.15  
 0.15 0.15 0.15 0.15 0.15 0.15 0.15 0.15 0.15 0.15

0.15 0.15 0.15 0.15 0.15 0.15 0.15 0.15 0.15 0.15  
 D16mm  
 0.01 0.01 0.01 0.01 0.01 0.01 0.01 0.01 0.01 0.01  
 0.01 0.01 0.01 0.01 0.01 0.01 0.01 0.01 0.01 0.01  
 0.01 0.01 0.01 0.01 0.01 0.01 0.01 0.01 0.01 0.01  
 D84mm  
 0.75 0.75 0.75 0.75 0.75 0.75 0.75 0.75 0.75 0.75  
 0.75 0.75 0.75 0.75 0.75 0.75 0.75 0.75 0.75 0.75  
 0.75 0.75 0.75 0.75 0.75 0.75 0.75 0.75 0.75 0.75  
 DMAX  
 2.0 2.0 2.0 2.0 2.0 2.0 2.0 2.0 2.0 2.0  
 2.0 2.0 2.0 2.0 2.0 2.0 2.0 2.0 2.0 2.0  
 2.0 2.0 2.0 2.0 2.0 2.0 2.0 2.0 2.0 2.0  
 PHI deg  
 35. 35. 35. 35. 35. 35. 35. 35. 35. 35.  
 35. 35. 35. 35. 35. 35. 35. 35. 35. 35.  
 35. 35. 35. 35. 35. 35. 35. 35. 35. 35.  
 ALPHA  
 5.7 5.7 5.7 5.7 5.7 5.7 5.7 5.7 5.7 5.7  
 5.7 5.7 5.7 5.7 5.7 5.7 5.7 5.7 5.7 5.7  
 5.7 5.7 5.7 5.7 5.7 5.7 5.7 5.7 5.7 5.7  
 INITIAL CONDITIONS  
 water d scr d scr u  
 YMIF YMIR TDI TUI  
 5.00 5.0 0 0  
 ft ft ft ft  
 HURRICANE DATA  
 HURRICANE RADIUS FOR CATEGORY 1-5 IN MILES, AND CLOSEST  
 DISTANCE OF THE BRIDGE LOCATION FROM THE CENTER  
 HRAD1 HRAD2 HRAD3 HRAD4 HRAD5 HDIST  
 75. 100. 150. 200. 250. 0.1  
 HURRICANE SPEED CATEGORY 1-5  
 HSPED1 HSPED2 HSPED3 HSPED4 HSPED5  
 30. 25. 20. 15. 10.  
 HURRICANE MAXIMUM SURGE (FT) CATEGORY 1-5  
 MXSRG1 MXSRG2 MXSRG3 MXSRG4 MXSRG5  
 5. 7. 11. 16. 20.  
 SPECIFIC HURRICANE INFO.  
 Rainfall ins, Max surge ft, System speed mph, hurricane radius miles  
 HURAIN MXSRGI HSPEDI HRADI

TITLE: COMPREHENSIVE ESTUARY SCOUR INPUT FILE Hurricane Simulation  
 PROJECT NAME: EAST BALTIMORE BLACK RIVER DATE: 3/27/05  
 BRIDGE LOCATION: STONY POINT  
 BASE STATION LOCATION:  
 ENGINEERING CONSTANTS  

grav	spgw	visc	n val		rho w	spg soil
GR	GW	MUW	MAN	PI	RHW	SG
32.2	62.4	0.0000205	0.035	3.142	1.94	165.3
ft/s-2	lb/cuf	lb.s/sqft			s/cuf	lb/cuf

 SIMULATION DATA  

step	no sym	brg. life
DLT	TMS	YRS
1.0	2000	0
hr		yr

CATCHMENT BASIN HYDROLOGY

cv no	basin	min BA	ca.lngth	uhg dur	no duh
CN	CBA	CBAMIN	LC	DU	NO TMCON
84	58.0	150	19.97	36	36 9.7
	sqmi	sqmi.	mi	hr	

STORM (RAINfall) DATA

pr.dur	6,18,24,36	mean	std
F6	F18	F24	F36
MAS	SDS		
0.775	0.088	0.075	0.063
80	0.50		

All variables in this set are dimensionless

gamma b	const	gamma c	consts
B6	B18	B24	B36
C6	C18	C24	C36
0.10	0.40	0.83	1.35
3.0	2.0	2.0	1.0

All variables in this set are dimensionless

SCS STORM DISTRIBUTION FOR 18, 24 AND 36 HR TYPE II STORMS

DISTRIBUTION ARRAY FOR 18 HR STORM

S18

0.014	0.030	0.050	0.060	0.089	0.116
0.156	0.213	0.657	0.786	0.843	0.886
0.911	0.930	0.949	0.971	0.986	1.000

DISTRIBUTION ARRAY FOR 24 HR STORM

S24

0.011	0.023	0.035	0.048	0.063	0.080
0.098	0.120	0.148	0.181	0.235	0.663
0.772	0.820	0.854	0.880	0.902	0.921
0.938	0.953	0.965	0.977	0.990	1.000

DISTRIBUTION ARRAY FOR 36 HR STORM

S36

0.007	0.014	0.030	0.032	0.036	0.050
0.057	0.060	0.080	0.089	0.107	0.115
0.140	0.156	0.179	0.213	0.279	0.657
0.742	0.786	0.817	0.843	0.871	0.886
0.900	0.911	0.917	0.930	0.943	0.949
0.960	0.971	0.974	0.986	0.994	1.000

S6

0.048	0.12	0.663	0.880	0.953	1.00
-------	------	-------	-------	-------	------

SCS DIMENSIONLESS UNIT HYDROGRAPH

TO - DIMENSIONLESS TIME T/Tp

0.0	0.1	0.2	0.3	0.4	0.5
0.6	0.7	0.8	0.9	1.0	1.1
1.2	1.3	1.4	1.5	1.6	1.7
1.8	1.9	2.0	2.2	2.4	2.6
2.8	3.0	3.2	3.4	3.6	3.8
4.0	4.2	4.4	4.6	4.8	5.0

DUH- DIMENSIONLESS DISCHARGE Q/Qp

0.000	0.030	0.100	0.190	0.310	0.470
0.660	0.820	0.930	0.990	1.000	0.990
0.930	0.860	0.780	0.680	0.560	0.460
0.390	0.330	0.280	0.207	0.147	0.107
0.077	0.055	0.040	0.029	0.021	0.015
0.011	0.008	0.006	0.004	0.002	0.000

BASE STATION TIDAL DATA

inv	di.per	lu per	dist	md amp	ml amp	std	std
IBS	DT	LT	LW	MDA	MLA	SDA	SLA
-28.01	12.31	356.	187	1.22	0.36	0.56	.18
ft	hr	hr	mi	ft	ft	ft	ft

BRIDGE STATION TIDAL DATA

DATUM	slope	amp	peaked
CHAR	CS	MTR	PKM
MSL	.0002	0.935	0.67
ft		ft	

BRIDGE DATA

no piers	pier	diam	const
NBP	PD		C1
40	5.0		0.25
	ft		

BRIDGE ESTUARY DATA

area	est l	est w	wdnf	wupf	maxw	X-area	Upr-est
						adj-fac	s-slp
AS	LE	WB	WD	WU	WM	AFACT	UESTZ(Z:1)
9.5	10.00	1.63	1.75	1.4	1.63	1.00	300.0
Sqmi	mi	mi	mi	mi	mi		
Estuary elev below mean low tide (ft) EBMTL(1)-EBMTL(4)							
-10.935	-6.935	-3.935		-.935			
Associated top widths in feet TWBMTL(1)-TWBMTL(4)							
3300.0	5280.0	6930.0	8580.0				

SOIL DATA

cont coef	spg
KT	SS
0.3256	2.65

ARRAY WITH SOIL PROPERTIES

DEPTH (DPTH) ft

0.0	2.0	4.0	6.0	8.0	10.0	12.0	14.0	16.0	18.0
20.0	22.0	24.0	26.0	28.0	30.0	32.0	34.0	36.0	38.0
40.0	42.0	44.0	46.0	48.0	50.0	52.0	54.0	56.0	58.0

D50 mm

0.15	0.15	0.15	0.15	0.15	0.15	0.15	0.15	0.15	0.15
0.15	0.15	0.15	0.15	0.15	0.15	0.15	0.15	0.15	0.15
0.15	0.15	0.15	0.15	0.15	0.15	0.15	0.15	0.15	0.15

D16mm

0.01	0.01	0.01	0.01	0.01	0.01	0.01	0.01	0.01	0.01
0.01	0.01	0.01	0.01	0.01	0.01	0.01	0.01	0.01	0.01
0.01	0.01	0.01	0.01	0.01	0.01	100.	100.	100.	100.

D84mm

0.75	0.75	0.75	0.75	0.75	0.75	0.75	0.75	0.75	0.75
0.75	0.75	0.75	0.75	0.75	0.75	0.75	0.75	0.75	0.75
0.75	0.75	0.75	0.75	0.75	0.75	0.75	0.75	0.75	0.75

DMAX

2.0	2.0	2.0	2.0	2.0	2.0	2.0	2.0	2.0	2.0
2.0	2.0	2.0	2.0	2.0	2.0	2.0	2.0	2.0	2.0
2.0	2.0	2.0	2.0	2.0	2.0	2.0	2.0	2.0	2.0

PHI deg

35.	35.	35.	35.	35.	35.	35.	35.	35.	35.
35.	35.	35.	35.	35.	35.	35.	35.	35.	35.
35.	35.	35.	35.	35.	35.	35.	35.	35.	35.

ALPHA

5.7	5.7	5.7	5.7	5.7	5.7	5.7	5.7	5.7	5.7
5.7	5.7	5.7	5.7	5.7	5.7	5.7	5.7	5.7	5.7
5.7	5.7	5.7	5.7	5.7	5.7	5.7	5.7	5.7	5.7

INITIAL CONDITIONS

water d	scr d	scr u	
YMIF	YMIR	TDI	TUI
5.00	5.0	3.9	3.9

```

ft      ft      ft      ft
HURRICANE DATA
HURRICANE RADIUS FOR CATEGORY 1-5 IN MILES, AND CLOSEST
DISTANCE OF THE BRIDGE LOCATION FROM THE CENTER
HRAD1   HRAD2       HRAD3   HRAD4   HRAD5   HDIST
75.      100.      150.    200.    250.    1.0
HURRICANE SPEED CATEGORY 1-5
HSPED1       HSPED2   HSPED3       HSPED4       HSPED5
30.      25.      20.      15.      10.
HURRICANE MAXIMUM SURGE (FT) CATEGORY 1-5
MXSRG1      MXSRG2      MXSRG3      MXSRG4      MXSRG5
5.      7.      11.      16.      20.
SPECIFIC HURRICANE INFO.
Rainfall ins, Max surge ft, System speed mph, hurricane radius miles
HURAIN      MXSRGI      HSPEDI      HRADI
7      11      20      150

```

```

-----
TITLE: COMPREHENSIVE ESTUARY SCOUR INPUT FILE Continuous Simulations
PROJECT NAME: PATUXENT RIVER, BENEDICT NO ARMOURING DATE: 3/27/05
BRIDGE LOCATION: RTE 231 CROSSING AT BENEDICT
BASE STATION LOCATION: HAMPTON ROAD NORFOLK
ENGINEERING CONSTANTS

```

```

grav      spgw      visc      n val      rho w      spg soil
GR      GW      MUW      MAN      PI      RHW      SG
32.2      62.4      0.0000205      0.045      3.142      1.94      165.3
ft/s-2      lb/cuf      lb.s/sqft      s/cuf      lb/cuf

```

```

SIMULATION DATA
step no sym brg. life
DLT TMS YRS
1.0 1000 100
hr yr

```

```

CATCHMENT BASIN HYDROLOGY
cv no basin min BA ca.lngth uhg dur no duh
CN CBA CBAMIN LC DU NO TMCON
70 723 150 33.08 36 36 50.0
sqmi sqmi. mi hr hr

```

```

STORM (RAINFALL) DATA
pr.dur6,18,24,36 mean std
F6 F18 F24 F36 MAS SDS
0.775 0.088 0.075 0.063 80 0.50
All variables in this set are dimensionless
gamma b const gamma c consts
B6 B18 B24 B36 C6 C18 C24 C36
0.10 0.40 0.83 1.35 3.0 2.0 2.0 1.0
All variables in this set are dimensionless

```

```

SCS STORM DISTRIBUTION FOR 6, 18, 24 AND 36 HR TYPE II STORMS
DISTRIBUTION ARRAY FOR 18 HR STORM
S18
0.014 0.030 0.050 0.060 0.089 0.116
0.156 0.213 0.657 0.786 0.843 0.886
0.911 0.930 0.949 0.971 0.986 1.000
DISTRIBUTION ARRAY FOR 24 HR STORM
S24

```

0.011 0.023 0.035 0.048 0.063 0.080  
 0.098 0.120 0.148 0.181 0.235 0.663  
 0.772 0.820 0.854 0.880 0.902 0.921  
 0.938 0.953 0.965 0.977 0.990 1.000  
 DISTRIBUTION ARRAY FOR 36 HR STORM  
 S36  
 0.007 0.014 0.030 0.032 0.036 0.050  
 0.057 0.060 0.080 0.089 0.107 0.115  
 0.140 0.156 0.179 0.213 0.279 0.657  
 0.742 0.786 0.817 0.843 0.871 0.886  
 0.900 0.911 0.917 0.930 0.943 0.949  
 0.960 0.971 0.974 0.986 0.994 1.000  
 S6  
 0.048 0.12 0.663 0.880 0.953 1.00  
 SCS DIMENSIONLESS UNIT HYDROGRAPH  
 TO - DIMENSIONLESS TIME T/Tp  
 0.0 0.1 0.2 0.3 0.4 0.5  
 0.6 0.7 0.8 0.9 1.0 1.1  
 1.2 1.3 1.4 1.5 1.6 1.7  
 1.8 1.9 2.0 2.2 2.4 2.6  
 2.8 3.0 3.2 3.4 3.6 3.8  
 4.0 4.2 4.4 4.6 4.8 5.0  
 DUH- DIMENSIONLESS DISCHARGE Q/Qp  
 0.000 0.030 0.100 0.190 0.310 0.470  
 0.660 0.820 0.930 0.990 1.000 0.990  
 0.930 0.860 0.780 0.680 0.560 0.460  
 0.390 0.330 0.280 0.207 0.147 0.107  
 0.077 0.055 0.040 0.029 0.021 0.015  
 0.011 0.008 0.006 0.004 0.002 0.000  
 BASE STATION TIDAL DATA  

inv	di.per	lu per	dist	md amp	ml amp	std	std
IBS	DT	LT	LW	MDA	MLA	SDA	SLA
-28.01	12.31	356.	130	1.22	0.6	0.56	.15
ft	hr	hr	mi	ft	ft	ft	ft

 BRIDGE STATION TIDAL DATA  

DATUM	slope	amp	peaked
CHAR	CS	MTR	PKM
MSL	.0002	0.6	0.67
ft		ft	

 BRIDGE DATA  

no piers	pier	diam	const
NBP	PD		C1
16	5.0		0.25
	ft		

 BRIDGE ESTUARY DATA  

area	est l	est w	wnf	wupf	maxw	X-area	upr-est
						adj-fact	side-slope
AS	LE	WB	WD	WU	WM	AFACT	UESTZ(Z:1)
9.87	18.52	0.633	0.633	0.88	1.58	0.96	200.
Sqmi	mi	mi	mi	mi	mi		
Estuary elev below mean low tide (ft) EBMTL(1)-EBMTL(4)							
-15.9	-12.6	-6.6	-0.6				
Associated top widths in feet TWBMTL(1)-TWBMTL(4)							
1000.	1350.0	1600.0	3333.33				

 SOIL DATA  

cont	coef	spg
KT		SS



0.3256        2.65

ARRAY WITH SOIL PROPERTIES

DEPTH (DPTH) ft

0.0	2.0	4.0	6.0	8.0	10.0	12.0	14.0	16.0	18.0
20.0	22.0	24.0	26.0	28.0	30.0	32.0	34.0	36.0	38.0
40.0	42.0	44.0	46.0	48.0	50.0	52.0	54.0	56.0	58.0

D50 mm

.25	.25	.25	.25	.25	.25	.25	.25	.25	.25
.25	.25	.25	.25	.25	.25	.25	.25	.25	.25
.25	.25	.25	.25	.25	.25	.25	.25	.25	.25

D16mm

0.01	0.01	0.01	0.01	0.01	0.01	0.01	0.01	0.01	0.01
0.01	0.01	0.01	0.01	0.01	0.01	0.01	0.01	0.01	0.01
0.01	0.01	0.01	0.01	0.01	0.01	100.	100.	100.	100.

D84mm

3.0	3.0	3.0	3.0	3.0	3.0	3.0	3.0	3.0	3.0
3.0	3.0	3.0	3.0	3.0	3.0	3.0	3.0	3.0	3.0
3.0	3.0	3.0	3.0	3.0	3.0	3.0	3.0	3.0	3.0

DMAX

3.25	3.25	3.25	3.25	3.25	3.25	3.25	3.25	3.25	3.25
3.25	3.25	3.25	3.25	3.25	3.25	3.25	3.25	3.25	3.25
3.25	3.25	3.25	3.25	3.25	3.25	3.25	3.25	3.25	3.25

PHI deg

45.	45.	45.	45.	45.	45.	45.	45.	45.	45.
45.	45.	45.	45.	45.	45.	45.	45.	45.	45.
45.	45.	45.	45.	45.	45.	45.	45.	45.	45.

ALPHA

5.7	5.7	5.7	5.7	5.7	5.7	5.7	5.7	5.7	5.7
5.7	5.7	5.7	5.7	5.7	5.7	5.7	5.7	5.7	5.7
5.7	5.7	5.7	5.7	5.7	5.7	5.7	5.7	5.7	5.7

INITIAL CONDITIONS

water d scr d scr u

YMIF	YMIR	TDI	TUI
5.00	5.0	0.00	0.00
ft	ft	ft	ft

HURRICANE DATA

HURRICANE RADIUS FOR CATEGORY 1-5 IN MILES, AND CLOSEST  
DISTANCE OF THE BRIDGE LOCATION FROM THE CENTER

HRAD1	HRAD2	HRAD3	HRAD4	HRAD5	HDIST
75.	100.	150.	200.	250.	1.

HURRICANE SPEED CATEGORY 1-5

HSPED1	HSPED2	HSPED3	HSPED4	HSPED5
30.	25.	20.	15.	10.

HURRICANE MAXIMUM SURGE (FT) CATEGORY 1-5

MXSRG1	MXSRG2	MXSRG3	MXSRG4	MXSRG5
5.	7.	11.	16.	20.

SPECIFIC HURRICANE INFO.

Rainfall ins, Max surge ft, System speed mph, hurricane radius miles

HURAIN	MXSRGI	HSPEDI	HRADI
--------	--------	--------	-------

TITLE: COMPREHENSIVE ESTUARY SCOUR Continuous PROJECT NAME: WICOMICO  
RIVER OUTLET                      DATE: 3/15/05  
BRIDGE LOCATION: WICOMICO RIVER OUTLET  
BASE STATION LOCATION: HAMPTON ROAD NORFOLK  
ENGINEERING CONSTANTS



```

0.390 0.330 0.280 0.207 0.147 0.107
0.077 0.055 0.040 0.029 0.021 0.015
0.011 0.008 0.006 0.004 0.002 0.000
BASE STATION TIDAL DATA
inv      di.per lu per dist md amp ml amp std  std
IBS      DT      LT      LW      MDA      MLA      SDA      SLA
-28.01 12.31 356. 116 1.22 0.56 0.36 .18
ft      hr      hr      mi      ft      ft      ft      ft
BRIDGE STATION TIDAL DATA
DATUM      slope amp peaked
CHAR      CS      MTR      PKM
MSL      .0002 1.19 0.67
ft      ft
BRIDGE DATA
no piers pier diam const
NBP      PD      C1
23      5.0      0.25
ft
BRIDGE ESTUARY DATA
area est l est w wdnf wupf maxw X-area- Upr-est
adj-fact. Side-slope
AS      LE      WB      WD      WU      WM      AFACT      UESTZ(Z:1)
3.95 15.88 0.25 0.25 0.25 0.35 1.00 500.
Sqmi mi mi mi mi mi
Estuary elev below mean low tide (ft) EBMTL(1)-EBMTL(4)
-18.19 -12.69 -6.19 -1.19
Associated top widths in feet TWBMTL(1)-TWBMTL(4)
528.0 739.0 950.4 1320.0
SOIL DATA
cont coef spg
KT      SS
0.3256 2.65

ARRAY WITH SOIL PROPERTIES
DEPTH (DPTH) ft
0.0 2.0 4.0 6.0 8.0 10.0 12.0 14.0 16.0 18.0
20.0 22.0 24.0 26.0 28.0 30.0 32.0 34.0 36.0 38.0
40.0 42.0 44.0 46.0 48.0 50.0 52.0 54.0 56.0 58.0
D50 mm
0.325 0.325 0.325 0.325 0.325 0.325 0.325 0.325 0.325 0.325
0.325 0.325 0.325 0.325 0.325 0.325 0.325 0.325 0.325 0.325
0.325 0.325 0.325 0.325 0.325 0.325 0.325 0.325 0.325 0.325
D16mm
0.1 0.1 0.1 0.1 0.1 0.1 0.1 0.1 0.1 0.1
0.1 0.1 0.1 0.1 0.1 0.1 0.1 0.1 0.1 0.1
0.1 0.1 0.1 0.1 0.1 0.1 0.1 0.1 0.1 0.1
D84mm
3.2 3.2 3.2 3.2 3.2 3.2 3.2 3.2 3.2 3.2
3.2 3.2 3.2 3.2 3.2 3.2 3.2 3.2 3.2 3.2
3.2 3.2 3.2 3.2 3.2 3.2 3.2 3.2 3.2 3.2
DMAX
4.25 4.25 4.25 4.25 4.25 4.25 4.25 4.25 4.25 4.25
4.25 4.25 4.25 4.25 4.25 4.25 4.25 4.25 4.25 4.25
4.25 4.25 4.25 4.25 4.25 4.25 4.25 4.25 4.25 4.25
PHI deg
45. 45. 45. 45. 45. 45. 45. 45. 45. 45.
45. 45. 45. 45. 45. 45. 45. 45. 45. 45.

```

```

45. 45. 45. 45. 45. 45. 45. 45. 45. 45.
ALPHA
5.7 5.7 5.7 5.7 5.7 5.7 5.7 5.7 5.7 5.7
5.7 5.7 5.7 5.7 5.7 5.7 5.7 5.7 5.7 5.7
5.7 5.7 5.7 5.7 5.7 5.7 5.7 5.7 5.7 5.7
INITIAL CONDITIONS
water d scr d scr u
YMIF  YMIR      TDI   TUI
5.00  5.0      0      0
ft      ft      ft      ft
HURRICANE DATA
HURRICANE RADIUS FOR CATEGORY 1-5 IN MILES, AND CLOSEST
DISTANCE OF THE BRIDGE LOCATION FROM THE CENTER
HRAD1  HRAD2      HRAD3  HRAD4      HRAD5      HDIST
75.    100.    150.    200.    250.    60.
HURRICANE SPEED CATEGORY 1-5
HSPED1      HSPED2  HSPED3      HSPED4      HSPED5
30.    25.    20.    15.    10.
HURRICANE MAXIMUM SURGE (FT) CATEGORY 1-5
MXSRG1      MXSRG2      MXSRG3      MXSRG4      MXSRG5
5.    7.    11.    16.    20.
SPECIFIC HURRICANE INFO.
Rainfall ins, Max surge ft, System speed mph, hurricane radius miles
HURAIN      MXSRGI      HSPEDI      HRADI
6      14      12      150

```

```

-----
TITLE: COMPREHENSIVE ESTUARY SCOUR Hurricane Simulation
PROJECT NAME: WICOMICO RIVER OUTLET          DATE: 3/15/05
BRIDGE LOCATION: WICOMICO RIVER OUTLET
BASE STATION LOCATION: HAMPTON ROAD NORFOLK

```

```

ENGINEERING CONSTANTS
grav      spgw      visc      n val      rho w      spg soil
GR      GW      MUW      MAN      PI      RHW      SG
32.2    62.4    0.0000205    0.045    3.142    1.94    165.3
ft/s-2  lb/cuf  lb.s/sqft      s/cuf  lb/cuf

```

```

SIMULATION DATA
step no sym brg. life
DLT  TMS  YRS
1.0  2000  0
hr      yr

```

```

CATCHMENT BASIN HYDROLOGY
cv no basin min BA      ca.lngth uhg dur no duh
CN  CBA  CBAMIN  LC      DU      NO      TMCON
79  170.8  150      33.08  36      36      42.0
      sqmi  sqmi.      mi      hr      hrs

```

```

STORM (RAINFALL) DATA
pr.dur 6,18,24,36      mean std
F6      F18      F24      F36      MAS  SDS
0.775  0.088  0.075  0.063  80    0.50
All variables in this set are dimensionless
gamma b const  gamma c consts
B6      B18      B24  B36  C6  C18      C24      C36
0.10  0.40  0.83  1.35  3.0  2.0      2.0      1.0
All variables in this set are dimensionless

```

SCS STORM DISTRIBUTION FOR 6, 18, 24 AND 36 HR TYPE II STORMS  
DISTRIBUTION ARRAY FOR 18 HR STORM

S18

0.014 0.030 0.050 0.060 0.089 0.116  
0.156 0.213 0.657 0.786 0.843 0.886  
0.911 0.930 0.949 0.971 0.986 1.000

DISTRIBUTION ARRAY FOR 24 HR STORM

S24

0.011 0.023 0.035 0.048 0.063 0.080  
0.098 0.120 0.148 0.181 0.235 0.663  
0.772 0.820 0.854 0.880 0.902 0.921  
0.938 0.953 0.965 0.977 0.990 1.000

DISTRIBUTION ARRAY FOR 36 HR STORM

S36

0.007 0.014 0.030 0.032 0.036 0.050  
0.057 0.060 0.080 0.089 0.107 0.115  
0.140 0.156 0.179 0.213 0.279 0.657  
0.742 0.786 0.817 0.843 0.871 0.886  
0.900 0.911 0.917 0.930 0.943 0.949  
0.960 0.971 0.974 0.986 0.994 1.000

S6

0.048 0.12 0.663 0.880 0.953 1.00

SCS DIMENSIONLESS UNIT HYDROGRAPH

TO - DIMENSIONLESS TIME T/Tp

0.0 0.1 0.2 0.3 0.4 0.5  
0.6 0.7 0.8 0.9 1.0 1.1  
1.2 1.3 1.4 1.5 1.6 1.7  
1.8 1.9 2.0 2.2 2.4 2.6  
2.8 3.0 3.2 3.4 3.6 3.8  
4.0 4.2 4.4 4.6 4.8 5.0

DUH- DIMENSIONLESS DISCHARGE Q/Qp

0.000 0.030 0.100 0.190 0.310 0.470  
0.660 0.820 0.930 0.990 1.000 0.990  
0.930 0.860 0.780 0.680 0.560 0.460  
0.390 0.330 0.280 0.207 0.147 0.107  
0.077 0.055 0.040 0.029 0.021 0.015  
0.011 0.008 0.006 0.004 0.002 0.000

BASE STATION TIDAL DATA

inv	di.per	lu per	dist	md amp	ml amp	std	std
IBS	DT	LT	LW	MDA	MLA	SDA	SLA
-28.01	12.31	356.	116	1.22	0.56	0.36	.18
ft	hr	hr	mi	ft	ft	ft	ft

BRIDGE STATION TIDAL DATA

DATUM	slope	amp	peaked
CHAR	CS	MTR	PKM
MSL	.0002	1.19	0.67
ft		ft	

BRIDGE DATA

no piers	pier diam	const
NBP	PD	C1
23	5.0	0.25
	ft	

BRIDGE ESTUARY DATA

area	est l	est w	wnf	wupf	maxw	X-area-	Upr-est
						adj-fact.	Side-slope
AS	LE	WB	WD	WU	WM	AFACT	UESTZ(Z:1)
3.95	15.88	0.25	0.25	0.25	0.35	1.00	500.

```

Sqmi    mi    mi    mi    mi    mi
Estuary elev below mean low tide (ft) EBMTL(1)-EBMTL(4)
-18.19 -12.69 -6.19 -1.19
Associated top widths in feet TWBMTL(1)-TWBMTL(4)
528.0 739.0 950.4 1320.0
SOIL DATA
cont coef spg
KT SS
0.3256 2.65

ARRAY WITH SOIL PROPERTIES
DEPTH (DPTH) ft
0.0 2.0 4.0 6.0 8.0 10.0 12.0 14.0 16.0 18.0
20.0 22.0 24.0 26.0 28.0 30.0 32.0 34.0 36.0 38.0
40.0 42.0 44.0 46.0 48.0 50.0 52.0 54.0 56.0 58.0
D50 mm
.325 .325 .325 .325 .325 .325 .325 .325 .325 .325
.325 .325 .325 .325 .325 .325 .325 .325 .325 .325
.325 .325 .325 .325 .325 .325 .325 .325 .325 .325
D16mm
0.1 0.1 0.1 0.1 0.1 0.1 0.1 0.1 0.1 0.1
0.1 0.1 0.1 0.1 0.1 0.1 0.1 0.1 0.1 0.1
0.1 0.1 0.1 0.1 0.1 0.1 0.1 0.1 0.1 0.1
D84mm
3.2 3.2 3.2 3.2 3.2 3.2 3.2 3.2 3.2 3.2
3.2 3.2 3.2 3.2 3.2 3.2 3.2 3.2 3.2 3.2
3.2 3.2 3.2 3.2 3.2 3.2 3.2 3.2 3.2 3.2
DMAX
4.25 4.25 4.25 4.25 4.25 4.25 4.25 4.25 4.25 4.25
4.25 4.25 4.25 4.25 4.25 4.25 4.25 4.25 4.25 4.25
4.25 4.25 4.25 4.25 4.25 4.25 4.25 4.25 4.25 4.25
PHI deg
45. 45. 45. 45. 45. 45. 45. 45. 45. 45.
45. 45. 45. 45. 45. 45. 45. 45. 45. 45.
45. 45. 45. 45. 45. 45. 45. 45. 45. 45.
ALPHA
5.7 5.7 5.7 5.7 5.7 5.7 5.7 5.7 5.7 5.7
5.7 5.7 5.7 5.7 5.7 5.7 5.7 5.7 5.7 5.7
5.7 5.7 5.7 5.7 5.7 5.7 5.7 5.7 5.7 5.7
INITIAL CONDITIONS
water d scr d scr u
YMIF YMIR TDI TUI
5.00 5.0 3.9 3.9
ft ft ft ft
HURRICANE DATA
HURRICANE RADIUS FOR CATEGORY 1-5 IN MILES, AND CLOSEST
DISTANCE OF THE BRIDGE LOCATION FROM THE CENTER
HRAD1 HRAD2 HRAD3 HRAD4 HRAD5 HDIST
75. 100. 150. 200. 250. 1.
HURRICANE SPEED CATEGORY 1-5
HSPED1 HSPED2 HSPED3 HSPED4 HSPED5
30. 25. 20. 15. 10.
HURRICANE MAXIMUM SURGE (FT) CATEGORY 1-5
MXSRG1 MXSRG2 MXSRG3 MXSRG4 MXSRG5
5. 7. 11. 16. 20.
SPECIFIC HURRICANE INFO.
Rainfall ins, Max surge ft, System speed mph, hurricane radius miles

```

HURAIN	MXSRGI	HSPEDI	HRADI
5	11	20	150

-----  
 -----  
 TITLE: COMPREHENSIVE ESTUARY SCOUR Continuous Simulations  
 PROJECT NAME: BALTIMORE AT THE PATAPSCO                      DATE: 3/27/05  
 BRIDGE LOCATION: STONY POINT  
 BASE STATION LOCATION:

ENGINEERING CONSTANTS

grav	spgw	visc	n val		rho w	spg soil
GR	GW	MUW	MAN	PI	RHW	SG
32.2	62.4	0.0000205	0.045	3.142	1.94	165.3
ft/s-2	lb/cuf	lb.s/sqft			s/cuf	lb/cuf

SIMULATION DATA

step	no sym	brg. life
DLT	TMS	YRS
1.0	1000	100
hr		yr

CATCHMENT BASIN HYDROLOGY

cv no	basin	min BA	ca.lngth	uhg dur	no duh	Time of conc
CN	CBA	CBAMIN	LC	DU	NO	TMCON
70	598.0	150	69.33	36	36	28.2
	sqmi	sqmi.	mi	hr		

STORM (RAINFALL) DATA

pr.dur	6,18,24,36	mean	std
F6	F18 F24 F36	MAS	SDS
0.775	0.088 0.075 0.063	80	0.50

All variables in this set are dimensionless

gamma b const	gamma c const
B6 B18 B24 B36 C6 C18 C24 C36	
0.10 0.40 0.83 1.35 3.0 2.0 2.0 1.0	

All variables in this set are dimensionless  
 SCS STORM DISTRIBUTION FOR 6,18, 24 AND 36 HR TYPE II STORMS

DISTRIBUTION ARRAY FOR 18 HR STORM  
 S18

0.014	0.030	0.050	0.060	0.089	0.116
0.156	0.213	0.657	0.786	0.843	0.886
0.911	0.930	0.949	0.971	0.986	1.000

DISTRIBUTION ARRAY FOR 24 HR STORM  
 S24

0.011	0.023	0.035	0.048	0.063	0.080
0.098	0.120	0.148	0.181	0.235	0.663
0.772	0.820	0.854	0.880	0.902	0.921
0.938	0.953	0.965	0.977	0.990	1.000

DISTRIBUTION ARRAY FOR 36 HR STORM  
 S36

0.007	0.014	0.030	0.032	0.036	0.050
0.057	0.060	0.080	0.089	0.107	0.115
0.140	0.156	0.179	0.213	0.279	0.657
0.742	0.786	0.817	0.843	0.871	0.886
0.900	0.911	0.917	0.930	0.943	0.949
0.960	0.971	0.974	0.986	0.994	1.000

S6  
 0.048 0.12 0.663 0.880 0.953 1.00

SCS DIMENSIONLESS UNIT HYDROGRAPH  
 TO - DIMENSIONLESS TIME T/Tp

```

0.0 0.1 0.2 0.3 0.4 0.5
0.6 0.7 0.8 0.9 1.0 1.1
1.2 1.3 1.4 1.5 1.6 1.7
1.8 1.9 2.0 2.2 2.4 2.6
2.8 3.0 3.2 3.4 3.6 3.8
4.0 4.2 4.4 4.6 4.8 5.0
DUH- DIMENSIONLESS DISCHARGE Q/Qp
0.000 0.030 0.100 0.190 0.310 0.470
0.660 0.820 0.930 0.990 1.000 0.990
0.930 0.860 0.780 0.680 0.560 0.460
0.390 0.330 0.280 0.207 0.147 0.107
0.077 0.055 0.040 0.029 0.021 0.015
0.011 0.008 0.006 0.004 0.002 0.000
BASE STATION TIDAL DATA
inv      di.per lu per dist md amp ml amp std  std
IBS      DT      LT      LW      MDA      MLA      SDA      SLA
-28.01   12.31   356.    187    1.41    0.6     0.64    .35
ft       hr       hr       mi       ft       ft       ft       ft
BRIDGE STATION TIDAL DATA
  DATUM          slope amp      peaked
  CHAR          CS      MTR      PKM
  MSL           .0002   0.935  0.67
  ft              ft
BRIDGE DATA
no piers pier diam const
NBP      PD      C1
9        5.0     0.25
          ft
BRIDGE ESTUARY DATA
area  est l est w  wdnf  wupf  maxw  X-area  upr-est
                        adj-fct.side slope
AS     LE     WB     WD     WU     WM     AFACT  UESTZ(Z:1)
3.56   2.67   0.33   0.41   0.30   0.79   1.00    200.
Sqmi   mi     mi     mi     mi     mi
Estuary elev below mean low tide (ft) EBMTL(1)-EBMTL(4)
-33.935 -22.935 -5.935  -0.935
Associated top widths in feet TWBMTL(1)-TWBMTL(4)
0.5    1000.0  1430.0    1750.0
SOIL DATA
cont coef  spg
KT         SS
0.3256     2.65

ARRAY WITH SOIL PROPERTIES
DEPTH (DPTH) ft
0.0  2.0  4.0  6.0  8.0  10.0  12.0  14.0  16.0  18.0
20.0 22.0 24.0 26.0 28.0 30.0 32.0 34.0 36.0 38.0
40.0 42.0 44.0 46.0 48.0 50.0 52.0 54.0 56.0 58.0
D50 mm
0.15  0.15  0.15  0.15  0.15  0.15  0.15  0.15  0.15  0.15
0.15  0.15  0.15  0.15  0.15  0.15  0.15  0.15  0.15  0.15
0.15  0.15  0.15  0.15  0.15  0.15  0.15  0.15  0.15  0.15
D16mm
0.01  0.01  0.01  0.01  0.01  0.01  0.01  0.01  0.01  0.01
0.01  0.01  0.01  0.01  0.01  0.01  0.01  0.01  0.01  0.01
0.01  0.01  0.01  0.01  0.01  0.01  100. 100. 100. 100.
D84mm

```



```

0.34 0.34 0.34 0.34 0.34 0.34 0.34 0.34 0.34 0.34
0.34 0.34 0.34 0.34 0.34 0.34 0.34 0.34 0.34 0.34
0.34 0.34 0.34 0.34 0.34 0.34 0.34 0.34 0.34 0.34
DMAX
0.4 0.4 0.4 0.4 0.4 0.4 0.4 0.4 0.4 0.4
0.4 0.4 0.4 0.4 0.4 0.4 0.4 0.4 0.4 0.4
0.4 0.4 0.4 0.4 0.4 0.4 0.4 0.4 0.4 0.4
PHI deg
33. 33. 33. 33. 33. 33. 33. 33. 33. 33.
33. 33. 33. 33. 33. 33. 33. 33. 33. 33.
33. 33. 33. 33. 33. 33. 33. 33. 33. 33.
ALPHA
5.7 5.7 5.7 5.7 5.7 5.7 5.7 5.7 5.7 5.7
5.7 5.7 5.7 5.7 5.7 5.7 5.7 5.7 5.7 5.7
5.7 5.7 5.7 5.7 5.7 5.7 5.7 5.7 5.7 5.7
INITIAL CONDITIONS
water d scr d scr u
YMIF YMIR TDI TUI
5.00 5.0 0.0 0.00
ft ft ft ft
HURRICANE DATA
HURRICANE RADIUS FOR CATEGORY 1-5 IN MILES, AND CLOSEST
DISTANCE OF THE BRIDGE LOCATION FROM THE CENTER
HRAD1 HRAD2 HRAD3 HRAD4 HRAD5 HDIST
75. 100. 150. 200. 250. 1.
HURRICANE SPEED CATEGORY 1-5
HSPED1 HSPED2 HSPED3 HSPED4 HSPED5
30. 25. 20. 15. 10.
HURRICANE MAXIMUM SURGE (FT) CATEGORY 1-5
MXSRG1 MXSRG2 MXSRG3 MXSRG4 MXSRG5
5. 7. 11. 16. 20.
SPECIFIC HURRICANE INFO.
Rainfall ins, Max surge ft, System speed mph, hurricane radius miles
HURAIN MXSRGI HSPEDI HRADI

TITLE: COMPREHENSIVE ESTUARY SCOUR Hurricane Simulations
PROJECT NAME: BALTIMORE AT THE PATAPSCO DATE: 3/27/05
BRIDGE LOCATION: STONY POINT
BASE STATION LOCATION:
ENGINEERING CONSTANTS
grav spgw visc n val rho w spg soil
GR GW MUW MAN PI RHW SG
32.2 62.4 0.0000205 0.045 3.142 1.94 165.3
ft/s-2 lb/cuf lb.s/sqft s/cuf lb/cuf
SIMULATION DATA
step no sym brg. life
DLT TMS YRS
1.0 5000 0
hr yr
CATCHMENT BASIN HYDROLOGY
cv no basin min BA ca.lngth uhg dur no duh Time of conc
CN CBA CBAMIN LC DU NO TMCON
70 598.0 150 69.33 36 36 28.2
sqmi sqmi. mi hr
STORM (RAINFALL) DATA
pr.dur 6,18,24,36 mean std
F6 F18 F24 F36 MAS SDS

```

```

0.775 0.088 0.075 0.063 80 0.50
All variables in this set are dimensionless
gamma b const gamma c consts
B6 B18 B24 B36 C6 C18 C24 C36
0.10 0.40 0.83 1.35 3.0 2.0 2.0 1.0
All variables in this set are dimensionless
SCS STORM DISTRIBUTION FOR 6,18, 24 AND 36 HR TYPE II STORMS
DISTRIBUTION ARRAY FOR 18 HR STORM
S18
0.014 0.030 0.050 0.060 0.089 0.116
0.156 0.213 0.657 0.786 0.843 0.886
0.911 0.930 0.949 0.971 0.986 1.000
DISTRIBUTION ARRAY FOR 24 HR STORM
S24
0.011 0.023 0.035 0.048 0.063 0.080
0.098 0.120 0.148 0.181 0.235 0.663
0.772 0.820 0.854 0.880 0.902 0.921
0.938 0.953 0.965 0.977 0.990 1.000
DISTRIBUTION ARRAY FOR 36 HR STORM
S36
0.007 0.014 0.030 0.032 0.036 0.050
0.057 0.060 0.080 0.089 0.107 0.115
0.140 0.156 0.179 0.213 0.279 0.657
0.742 0.786 0.817 0.843 0.871 0.886
0.900 0.911 0.917 0.930 0.943 0.949
0.960 0.971 0.974 0.986 0.994 1.000
S6
0.048 0.12 0.663 0.880 0.953 1.00
SCS DIMENSIONLESS UNIT HYDROGRAPH
TO - DIMENSIONLESS TIME T/Tp
0.0 0.1 0.2 0.3 0.4 0.5
0.6 0.7 0.8 0.9 1.0 1.1
1.2 1.3 1.4 1.5 1.6 1.7
1.8 1.9 2.0 2.2 2.4 2.6
2.8 3.0 3.2 3.4 3.6 3.8
4.0 4.2 4.4 4.6 4.8 5.0
DUH- DIMENSIONLESS DISCHARGE Q/Qp
0.000 0.030 0.100 0.190 0.310 0.470
0.660 0.820 0.930 0.990 1.000 0.990
0.930 0.860 0.780 0.680 0.560 0.460
0.390 0.330 0.280 0.207 0.147 0.107
0.077 0.055 0.040 0.029 0.021 0.015
0.011 0.008 0.006 0.004 0.002 0.000
BASE STATION TIDAL DATA
inv di.per lu per dist md amp ml amp std std
IBS DT LT LW MDA MLA SDA SLA
-28.01 12.31 356. 187 1.41 0.6 0.64 .35
ft hr mi ft ft ft ft
BRIDGE STATION TIDAL DATA
DATUM slope amp peaked
CHAR CS MTR PKM
MSL .0002 0.935 0.67
ft ft
BRIDGE DATA
no piers pier diam const
NBP PD C1
9 5.0 0.25

```

```

ft
BRIDGE ESTUARY DATA
area  est l  est w  wdnf  wupf  maxw  X-area  upr-est
                                adj-fct.side slope
AS      LE      WB      WD      WU      WM      AFACT  UESTZ(Z:1)
3.56    2.67    0.33    0.41    0.30    0.79    1.00    200.
Sqmi    mi      mi      mi      mi      mi
Estuary elev below mean low tide (ft) EBMTL(1)-EBMTL(4)
-33.935 -22.935 -5.935 -0.935
Associated top widths in feet TWBMTL(1)-TWBMTL(4)
0.5     1000.0  1430.0   1750.0
SOIL DATA
cont coef  spg
KT          SS
0.3256     2.65

ARRAY WITH SOIL PROPERTIES
DEPTH (DPTH) ft
0.0  2.0  4.0  6.0  8.0  10.0  12.0  14.0  16.0  18.0
20.0 22.0 24.0 26.0 28.0 30.0 32.0 34.0 36.0 38.0
40.0 42.0 44.0 46.0 48.0 50.0 52.0 54.0 56.0 58.0
D50 mm
0.15  0.15  0.15  0.15  0.15  0.15  0.15  0.15  0.15  0.15
0.15  0.15  0.15  0.15  0.15  0.15  0.15  0.15  0.15  0.15
0.15  0.15  0.15  0.15  0.15  0.15  0.15  0.15  0.15  0.15
D16mm
0.01  0.01  0.01  0.01  0.01  0.01  0.01  0.01  0.01  0.01
0.01  0.01  0.01  0.01  0.01  0.01  0.01  0.01  0.01  0.01
0.01  0.01  0.01  0.01  0.01  0.01  100. 100. 100. 100.
D84mm
0.34  03.4  0.34  0.34  0.34  0.34  0.34  0.34  0.34  0.34
0.34  03.4  0.34  0.34  0.34  0.34  0.34  0.34  0.34  0.34
0.34  03.4  0.34  0.34  0.34  0.34  0.34  0.34  0.34  0.34
DMAX
0.4  0.4  0.4  0.4  0.4  0.4  0.4  0.4  0.4  0.4
0.4  0.4  0.4  0.4  0.4  0.4  0.4  0.4  0.4  0.4
0.4  0.4  0.4  0.4  0.4  0.4  0.4  0.4  0.4  0.4
PHI deg
33. 33. 33. 33. 33. 33. 33. 33. 33. 33.
33. 33. 33. 33. 33. 33. 33. 33. 33. 33.
33. 33. 33. 33. 33. 33. 33. 33. 33. 33.
ALPHA
5.7 5.7 5.7 5.7 5.7 5.7 5.7 5.7 5.7 5.7
5.7 5.7 5.7 5.7 5.7 5.7 5.7 5.7 5.7 5.7
5.7 5.7 5.7 5.7 5.7 5.7 5.7 5.7 5.7 5.7
INITIAL CONDITIONS
water d scr d scr u
YMIF  YMIR      TDI  TUI
5.00  5.0      3.9   3.9
ft     ft      ft    ft
HURRICANE DATA
HURRICANE RADIUS FOR CATEGORY 1-5 IN MILES, AND CLOSEST
DISTANCE OF THE BRIDGE LOCATION FROM THE CENTER
HRAD1  HRAD2      HRAD3  HRAD4      HRAD5      HDIST
75.     100.     150.    200.     250.      1.
HURRICANE SPEED CATEGORY 1-5
HSPED1      HSPED2  HSPED3      HSPED4      HSPED5

```

30.	25.	20.	15.	10.
HURRICANE MAXIMUM SURGE (FT) CATEGORY 1-5				
MXSRG1	MXSRG2	MXSRG3	MXSRG4	MXSRG5
5.	7.	11.	16.	20.

SPECIFIC HURRICANE INFO.

Rainfall ins, Max surge ft, System speed mph, hurricane radius miles

HURAIN	MXSRGI	HSPEDI	HRADI
8	11	20	150

-----

-----

### APPENDIX D-3

RUN TITLE **Monie Bay** Continuous simulations  
 RUN DATE 4/08/05  
 THE PROGRAM WAS EXECUTED IN PIER DESIGN MODE.  
 CONTRACTION SCOUR METHOD IS KOMURAS EQN  
 SCOUR COMPUTED WITHOUT ARMOURING  
 BRUBAKER-DEMETRIUS NEILLS MODIFICATION FACTOR ACTIVATED  
 TIDE DISTORTION OPTION ACTIVATED  
 MEAN TIDAL DEPTH MDR is = 5.935000  
 MEAN LOW TIDAL DEPTH MLT is = 4.745000  
 MEAN LOW TIDE ELEVATION MLTE is = -1.190000  
 TIDAL AMP. AT BRIDGE XSEC MTR is = 1.190000  
 CHANNEL INVERT AT BRIDGE IRS is = -5.935000  
  
 Estuary in bank area is = 18617.000000  
  
 Maximum tide in the simulation HITIDE is = 9.173283  
 Maximum u/s flow depth in sim. YTRMXS is = 9.995000  
 Maximum d/s flow depth in sim. YTFMXS is = 9.545000  
 Maximum u/s disch. in sim. QTRMXS is = 50527.050000  
 Maximum d/s disch. in sim. QTFMXS is = 50794.130000  
 Maximum u/s vel.in sim. VUPMS is = 1.538754  
 Maximum d/s vel.in sim. VDOWNMS is = 7.415236E-01  
 Maximum u/s face tang.vel.in sim. VTUMXSis = 3.620554E-01  
 Maximum d/s face tang.vel.in sim. VTDMSis = 2.695128  
  
 Maximum u/s flow depth last run YTRMAX is = 9.995000  
 Maximum d/s flow depth last run YTFMAX is = 9.245000  
 Maximum u/s discharge last run QTRMAX is = 50527.050000  
 Maximum d/s discharge last run QTFMAX is = 50550.990000  
 Maximum u/s velocity last run VNUMAX is = 1.408754  
 Maximum d/s velocity last run VNDMAX is = 6.615236E-01  
 Maximum tangential vel d/s face last run VTDMS is = 2.290317  
 Maximum tangential vel u/s face last run VTUMX is = 3.220554E-01  
 critical vel u/s face last run UIUMIN is = 4.344201E-01  
 critical vel d/s face last run UIDMIN is = 4.344201E-01  
  
 Time of concentration = 38.500000hrs  
 Time to peak = 25.795000hrs  
 Number of unit hydrograph ordinates = 128  
 Soil infiltration potential = 2.345679  
 Peak discharge of the UHG = 300.213200cfs  
 Initial abstractions IA = 4.691358E-01in  
  
 Catchment base flow = 12.715970cfs  
 Tide attenuation factor TAF = 9.754099E-01  
 Tidal lag MTL= -4.190653hrs  
 Tidal routing constant CX = 7.000000E-01  
 Bridge station tidal range TR = 2.380000ft  
 Effective bottom channel width at brdg.WBE = 5216.400000ft  
 Estuary Area 6.021735E+07  
 Contraction scour factor u/s face= 1.008152  
 Contraction scour factor d/s face= 1.094180

Estuary to wavelength ratio DIM = 8.618567E-02  
 Estuary width factor WF = 1.000000  
 Tidal range factor HF = 4.010110E-01  
 Neill Mod. factor rising limb.NMRF = 8.000000E-01  
 Neill Mod. factor falling limb.NMFF = 8.000000E-01

The maximum storm event in the simulation is 9.900685ins  
 ANNUAL MAX UPSTREAM VELOCITY LAST RUN = 1.065757 1.242033

1.096860	1.016291	9.927958E-01	9.111453E-01
1.017369	1.115101	1.091918	1.107990
1.143996	9.912748E-01	9.297574E-01	1.150177
1.005615	1.014722	1.091742	9.716369E-01
9.646621E-01	9.471502E-01	1.085657	1.084739
9.294004E-01	9.491114E-01	1.052660	1.013822
1.084523	9.794714E-01	1.050517	1.105743
1.041013	1.108922	8.889236E-01	1.081407
1.134108	1.026132	1.084295	1.118204
9.550909E-01	9.373394E-01	1.015939	1.042482
8.510341E-01	1.066193	9.571586E-01	1.180248
1.103804	1.150056	1.007385	1.248806
1.044277	1.071354	1.011807	9.877745E-01
1.008518	9.609995E-01	1.146057	1.151071
1.101770	1.111636	9.940314E-01	1.112264
9.393173E-01	1.408754	1.032768	9.111736E-01
1.093367	1.220187	1.026058	1.063695
9.850203E-01	1.105063	1.058946	9.502029E-01
1.056969	1.015734	1.030061	1.251362
1.102096	1.206404	1.066230	1.022726
1.079199	9.270074E-01	9.697666E-01	9.636766E-01
9.878467E-01	1.059033	1.254408	9.738631E-01
1.075373	9.417990E-01	9.368961E-01	9.740301E-01
1.133360	1.045197	1.082743	8.815030E-01
1.046169	1.029162		

ANNUAL MAX DWNSTREAM VELOCITY LAST RUN = 5.905355E-01 6.177908E-01

5.878229E-01	5.512557E-01	6.251256E-01	6.171355E-01
6.009783E-01	6.035676E-01	6.137961E-01	5.659245E-01
6.159304E-01	5.853845E-01	5.426438E-01	5.862695E-01
5.879153E-01	5.700608E-01	5.698293E-01	5.610082E-01
5.965563E-01	5.649116E-01	6.160181E-01	5.974163E-01
6.024175E-01	5.794241E-01	5.754811E-01	5.595501E-01
5.791355E-01	5.496882E-01	6.065647E-01	5.898461E-01
5.686995E-01	5.637906E-01	5.711054E-01	5.795109E-01
6.018610E-01	5.774754E-01	6.266273E-01	5.618666E-01
5.779951E-01	5.952319E-01	5.417353E-01	5.950171E-01
5.772915E-01	5.721473E-01	5.989382E-01	6.137170E-01
5.726511E-01	5.509964E-01	5.699242E-01	5.649636E-01
5.932547E-01	5.748895E-01	5.913566E-01	5.867468E-01
5.690062E-01	5.437918E-01	6.615236E-01	5.710542E-01
5.768998E-01	6.101898E-01	6.399040E-01	6.011847E-01
5.809631E-01	5.615147E-01	5.636551E-01	5.957874E-01
5.409352E-01	5.842665E-01	5.652792E-01	5.724488E-01
5.625614E-01	6.121222E-01	5.815270E-01	5.580202E-01
6.007769E-01	6.170388E-01	5.756883E-01	6.030960E-01
5.530685E-01	5.614761E-01	5.576924E-01	5.507864E-01
6.327173E-01	5.812076E-01	5.953085E-01	6.442097E-01

5.842042E-01	5.863311E-01	5.789304E-01	5.561932E-01
5.531400E-01	5.757112E-01	5.661561E-01	5.763102E-01
5.998825E-01	5.616366E-01	5.675319E-01	5.661818E-01
6.021416E-01	5.773752E-01		
ANNUAL MAX US ADJUSTED VELOCITY LAST RUN =			1.065757
1.242033			
1.096860	1.016291	9.927958E-01	9.111453E-01
1.017369	1.115101	1.091918	1.107990
1.143996	9.912748E-01	9.297574E-01	1.150177
1.005615	1.014722	1.091742	9.716369E-01
9.646621E-01	9.471502E-01	1.085657	1.084739
9.294004E-01	9.491114E-01	1.052660	1.013822
1.084523	9.794714E-01	1.050517	1.105743
1.041013	1.108922	8.889236E-01	1.081407
1.134108	1.026132	1.084295	1.118204
9.550909E-01	9.373394E-01	1.015939	1.042482
8.510341E-01	1.066193	9.571586E-01	1.180248
1.103804	1.150056	1.007385	1.248806
1.044277	1.071354	1.011807	9.877745E-01
1.008518	9.609995E-01	1.146057	1.151071
1.101770	1.111636	9.940314E-01	1.112264
9.393173E-01	1.408754	1.032768	9.111736E-01
1.093367	1.220187	1.026058	1.063695
9.850203E-01	1.105063	1.058946	9.502029E-01
1.056969	1.015734	1.030061	1.251362
1.102096	1.206404	1.066230	1.022726
1.079199	9.270074E-01	9.697666E-01	9.636766E-01
9.878467E-01	1.059033	1.254408	9.738631E-01
1.075373	9.417990E-01	9.368961E-01	9.740301E-01
1.133360	1.045197	1.082743	8.815030E-01
1.046169	1.029162		
ANNUAL MAX DS ADJUSTED VELOCITY LAST RUN =			5.905355E-01
6.177908E-01			
5.878229E-01	5.512557E-01	6.251256E-01	6.171355E-01
6.009783E-01	6.035676E-01	6.137961E-01	5.659245E-01
6.159304E-01	5.853845E-01	5.426438E-01	5.862695E-01
5.879153E-01	5.700608E-01	5.698293E-01	5.610082E-01
5.965563E-01	5.649116E-01	6.160181E-01	5.974163E-01
6.024175E-01	5.794241E-01	5.754811E-01	5.595501E-01
5.791355E-01	5.496882E-01	6.065647E-01	5.898461E-01
5.686995E-01	5.637906E-01	5.711054E-01	5.795109E-01
6.018610E-01	5.774754E-01	6.266273E-01	5.618666E-01
5.779951E-01	5.952319E-01	5.417353E-01	5.950171E-01
5.772915E-01	5.721473E-01	5.989382E-01	6.137170E-01
5.726511E-01	5.509964E-01	5.699242E-01	5.649636E-01
5.932547E-01	5.748895E-01	5.913566E-01	5.867468E-01
5.690062E-01	5.437918E-01	6.615236E-01	5.710542E-01
5.768998E-01	6.101898E-01	6.399040E-01	6.011847E-01
5.809631E-01	5.615147E-01	5.636551E-01	5.957874E-01
5.409352E-01	5.842665E-01	5.652792E-01	5.724488E-01
5.625614E-01	6.121222E-01	5.815270E-01	5.580202E-01
6.007769E-01	6.170388E-01	5.756883E-01	6.030960E-01
5.530685E-01	5.614761E-01	5.576924E-01	5.507864E-01
6.327173E-01	5.812076E-01	5.953085E-01	6.442097E-01
5.842042E-01	5.863311E-01	5.789304E-01	5.561932E-01
5.531400E-01	5.757112E-01	5.661561E-01	5.763102E-01
5.998825E-01	5.616366E-01	5.675319E-01	5.661818E-01

6.021416E-01	5.773752E-01		
ANNUAL MAX UPSTREAM DISCHARGE LAST RUN =		38153.320000	
36247.680000			
44181.130000	40013.980000	39989.510000	40196.160000
40965.180000	44915.560000	43982.100000	44293.310000
46072.500000	39927.250000	36176.960000	46328.020000
37001.330000	37755.020000	35393.060000	39121.630000
38855.370000	36704.820000	40191.920000	41416.060000
37415.640000	38648.340000	38008.010000	33793.230000
38251.300000	38345.520000	45582.750000	36600.710000
41931.360000	38334.090000	36028.250000	43558.490000
42573.480000	41332.240000	39670.800000	35744.990000
38465.000000	37740.670000	43849.810000	39288.420000
32514.440000	39698.610000	36239.620000	38273.780000
41099.040000	37072.810000	40021.040000	43272.600000
42051.950000	39704.330000	40343.160000	39672.310000
41289.760000	35781.860000	46155.250000	46361.590000
44155.710000	44775.870000	40017.540000	42456.630000
37820.870000	44841.440000	44377.740000	38177.930000
40710.420000	37266.040000	43547.880000	42838.450000
37080.180000	41145.910000	44556.070000	38273.710000
42574.390000	35274.710000	40929.000000	40959.880000
38340.290000	42965.260000	39102.070000	36493.270000
43469.790000	35043.200000	39061.770000	38802.070000
39780.000000	40713.550000	50527.050000	41476.210000
43315.590000	40930.940000	39278.940000	36563.270000
45651.320000	40742.810000	39773.370000	34777.730000
41766.860000	41450.060000		
ANNUAL MAX DWNSTREAM DISCHARGE LAST RUN =		42260.360000	
46294.350000			
39052.300000	38336.210000	37122.910000	46120.300000
40900.280000	39417.710000	39495.010000	41446.280000
44743.130000	40732.450000	38975.200000	41123.180000
40065.100000	39780.430000	43761.570000	38918.530000
38466.910000	37476.450000	46476.340000	39971.160000
40856.950000	42989.710000	38730.840000	39490.440000
39941.790000	40277.840000	48205.020000	39240.370000
38818.900000	50310.730000	45380.140000	43482.230000
41444.170000	38137.000000	39815.410000	42885.430000
39249.690000	36437.070000	41748.240000	45222.660000
43947.140000	38526.940000	40144.940000	46450.780000
45254.520000	42240.390000	42708.150000	44584.510000
39084.580000	48614.580000	45936.610000	42806.260000
40580.690000	40832.010000	45412.540000	44164.660000
37221.000000	39774.620000	46403.720000	45263.160000
44099.450000	50550.990000	43612.590000	46703.000000
41031.530000	42483.130000	42433.430000	45847.930000
40207.440000	41969.850000	47465.260000	36405.490000
39522.370000	43367.290000	42157.160000	38177.070000
35529.040000	38673.780000	38242.650000	45145.970000
43383.730000	38605.820000	41419.160000	40127.180000
39367.160000	43866.840000	38574.390000	38117.390000
42014.850000	39717.740000	39910.520000	45257.870000
41601.530000	48060.140000	36925.500000	45117.640000
40001.260000	42598.130000		



ANNUAL MAX UPSTREAM FLOW DEPTH LAST RUN =		8.657200	
8.657200			
9.245000	8.745000	8.657200	8.685199
8.657200	8.657200	8.995000	8.995000
8.657200	8.495000	8.405587	9.098116
9.098116	9.098116	9.098116	9.098116
9.098116	9.098116	9.098116	9.098116
9.098116	9.098116	9.098116	9.098116
9.098116	9.098116	9.098116	9.098116
9.098116	9.098116	9.098116	9.098116
9.245000	9.098116	9.098116	9.098116
9.098116	9.098116	9.098116	9.098116
9.098116	8.459832	8.473576	8.995000
8.745000	8.712579	8.712579	8.712579
8.712579	8.712579	8.712579	8.712579
8.745000	8.712579	8.712579	9.245000
8.712579	8.712579	8.803782	8.803782
8.803782	8.803782	8.807333	8.807333
8.495000	8.245000	8.419100	8.433814
8.403076	8.495000	8.606614	8.403076
8.403076	8.745000	8.745000	8.403076
8.438987	8.415760	8.415760	8.495000
8.415760	8.624671	8.624671	8.768705
8.729970	8.729970	8.729970	8.729970
8.729970	8.729970	8.729970	8.729970
8.745000	8.729970	8.729970	8.729970
8.219649	8.495000		

ANNUAL MAX DWTREAME FLOW DEPTH LAST RUN =		9.245000	
8.995000			
9.245000	8.773869	8.995000	9.173283
9.245000	9.745000	9.495000	9.495000
9.495000	8.995000	8.995000	9.152212
8.995000	9.245000	9.245000	8.745000
8.995000	9.245000	9.245000	9.745000
8.995000	9.245000	9.745000	8.646978
8.995000	8.895731	8.745000	9.245000
9.495000	9.245000	8.995000	9.245000
9.495000	9.245000	8.995000	9.245000
8.745000	8.995000	8.995000	8.995000
9.245000	9.495000	8.995000	8.995000
9.245000	8.758671	8.995000	9.245000
9.495000	9.745000	8.995000	9.245000
9.245000	8.995000	9.072608	9.245000
8.995000	9.495000	8.995000	9.245000
8.745000	9.245000	9.745000	9.495000
9.245000	8.995000	8.995000	9.245000
9.495000	8.745000	9.745000	8.745000
8.745000	9.245000	8.995000	9.745000
9.245000	8.995000	8.745000	8.995000
8.745000	8.745000	9.245000	8.772450
8.995000	9.245000	9.995000	9.245000
9.245000	8.745000	8.995000	8.995000
8.995000	8.995000	9.245000	8.995000
9.245000	8.995000		

ANNUAL MAX US ADJ. FLOW DEPTH LAST RUN =		8.657200	
8.657200			
9.245000	8.745000	8.657200	8.685199

8.657200	8.657200	8.995000	8.995000
8.657200	8.495000	8.405587	9.098116
9.098116	9.098116	9.098116	9.098116
9.098116	9.098116	9.098116	9.098116
9.098116	9.098116	9.098116	9.098116
9.098116	9.098116	9.098116	9.098116
9.098116	9.098116	9.098116	9.098116
9.245000	9.098116	9.098116	9.098116
9.098116	9.098116	9.098116	9.098116
9.098116	8.459832	8.473576	8.995000
8.745000	8.712579	8.712579	8.712579
8.712579	8.712579	8.712579	8.712579
8.745000	8.712579	8.712579	9.245000
8.712579	8.712579	8.803782	8.803782
8.803782	8.803782	8.807333	8.807333
8.495000	8.245000	8.419100	8.433814
8.403076	8.495000	8.606614	8.403076
8.403076	8.745000	8.745000	8.403076
8.438987	8.415760	8.415760	8.495000
8.415760	8.624671	8.624671	8.768705
8.729970	8.729970	8.729970	8.729970
8.729970	8.729970	8.729970	8.729970
8.745000	8.729970	8.729970	8.729970
8.219649	8.495000		

ANNUAL MAX DS ADJ. FLOW DEPTH LAST RUN = 9.245000  
8.995000

9.245000	8.773869	8.995000	9.173283
9.245000	9.745000	9.495000	9.495000
9.495000	8.995000	8.995000	9.152212
8.995000	9.245000	9.245000	8.745000
8.995000	9.245000	9.245000	9.745000
8.995000	9.245000	9.745000	8.646978
8.995000	8.895731	8.745000	9.245000
9.495000	9.245000	8.995000	9.245000
9.495000	9.245000	8.995000	9.245000
8.745000	8.995000	8.995000	8.995000
9.245000	9.495000	8.995000	8.995000
9.245000	8.758671	8.995000	9.245000
9.495000	9.745000	8.995000	9.245000
9.245000	8.995000	9.072608	9.245000
8.995000	9.495000	8.995000	9.245000
8.745000	9.245000	9.745000	9.495000
9.245000	8.995000	8.995000	9.245000
9.495000	8.745000	9.745000	8.745000
8.745000	9.245000	8.995000	9.745000
9.245000	8.995000	8.745000	8.995000
8.745000	8.745000	9.245000	8.772450
8.995000	9.245000	9.995000	9.245000
9.245000	8.745000	8.995000	8.995000
8.995000	8.995000	9.245000	8.995000
9.245000	8.995000		

The no.of storms in the last run NS= 81  
The no.of storms producing no runoff over the simulation.NORUN= 11220

The number of 6 hr storms in YRS is = 62





[illegible]

20.0000	.0000	.0000	1.0000
20.5000	.0000	.0000	1.0000
21.0000	.0000	.0000	1.0000
21.5000	.0000	.0000	1.0000
22.0000	.0000	.0000	1.0000
22.5000	.0000	.0000	1.0000
23.0000	.0000	.0000	1.0000
23.5000	.0000	.0000	1.0000
24.0000	.0000	.0000	1.0000
24.5000	.0000	.0000	1.0000
25.0000	.0000	.0000	1.0000
25.5000	.0000	.0000	1.0000
26.0000	.0000	.0000	1.0000
26.5000	.0000	.0000	1.0000
27.0000	.0000	.0000	1.0000
27.5000	.0000	.0000	1.0000
28.0000	.0000	.0000	1.0000
28.5000	.0000	.0000	1.0000
29.0000	.0000	.0000	1.0000
29.5000	.0000	.0000	1.0000
30.0000	.0000	.0000	1.0000
30.5000	.0000	.0000	1.0000
31.0000	.0000	.0000	1.0000
31.5000	.0000	.0000	1.0000
32.0000	.0000	.0000	1.0000
32.5000	.0000	.0000	1.0000
33.0000	.0000	.0000	1.0000
33.5000	.0000	.0000	1.0000
34.0000	.0000	.0000	1.0000
34.5000	.0000	.0000	1.0000
35.0000	.0000	.0000	1.0000
35.5000	.0000	.0000	1.0000
36.0000	.0000	.0000	1.0000
36.5000	.0000	.0000	1.0000
37.0000	.0000	.0000	1.0000
37.5000	.0000	.0000	1.0000
38.0000	.0000	.0000	1.0000
38.5000	.0000	.0000	1.0000
39.0000	.0000	.0000	1.0000
39.5000	.0000	.0000	1.0000
40.0000	.0000	.0000	1.0000
40.5000	.0000	.0000	1.0000
41.0000	.0000	.0000	1.0000
41.5000	.0000	.0000	1.0000
42.0000	.0000	.0000	1.0000
42.5000	.0000	.0000	1.0000
43.0000	.0000	.0000	1.0000
43.5000	.0000	.0000	1.0000
44.0000	.0000	.0000	1.0000
44.5000	.0000	.0000	1.0000
45.0000	.0000	.0000	1.0000
45.5000	.0000	.0000	1.0000
46.0000	.0000	.0000	1.0000
46.5000	.0000	.0000	1.0000
47.0000	.0000	.0000	1.0000
47.5000	.0000	.0000	1.0000
48.0000	.0000	.0000	1.0000

48.5000	.0000	.0000	1.0000
49.0000	.0000	.0000	1.0000
49.5000	.0000	.0000	1.0000
50.0000	.0000	.0000	1.0000
50.5000	.0000	.0000	1.0000
B	FU	PRU	CPRU
1.0000	2.0000	1.0000	1.0000
1.5000	.0000	.0000	1.0000
2.0000	.0000	.0000	1.0000
2.5000	.0000	.0000	1.0000
3.0000	.0000	.0000	1.0000
3.5000	.0000	.0000	1.0000
4.0000	.0000	.0000	1.0000
4.5000	.0000	.0000	1.0000
5.0000	.0000	.0000	1.0000
5.5000	.0000	.0000	1.0000
6.0000	.0000	.0000	1.0000
6.5000	.0000	.0000	1.0000
7.0000	.0000	.0000	1.0000
7.5000	.0000	.0000	1.0000
8.0000	.0000	.0000	1.0000
8.5000	.0000	.0000	1.0000
9.0000	.0000	.0000	1.0000
9.5000	.0000	.0000	1.0000
10.0000	.0000	.0000	1.0000
10.5000	.0000	.0000	1.0000
11.0000	.0000	.0000	1.0000
11.5000	.0000	.0000	1.0000
12.0000	.0000	.0000	1.0000
12.5000	.0000	.0000	1.0000
13.0000	.0000	.0000	1.0000
13.5000	.0000	.0000	1.0000
14.0000	.0000	.0000	1.0000
14.5000	.0000	.0000	1.0000
15.0000	.0000	.0000	1.0000
15.5000	.0000	.0000	1.0000
16.0000	.0000	.0000	1.0000
16.5000	.0000	.0000	1.0000
17.0000	.0000	.0000	1.0000
17.5000	.0000	.0000	1.0000
18.0000	.0000	.0000	1.0000
18.5000	.0000	.0000	1.0000
19.0000	.0000	.0000	1.0000
19.5000	.0000	.0000	1.0000
20.0000	.0000	.0000	1.0000
20.5000	.0000	.0000	1.0000
21.0000	.0000	.0000	1.0000
21.5000	.0000	.0000	1.0000
22.0000	.0000	.0000	1.0000
22.5000	.0000	.0000	1.0000
23.0000	.0000	.0000	1.0000
23.5000	.0000	.0000	1.0000
24.0000	.0000	.0000	1.0000
24.5000	.0000	.0000	1.0000
25.0000	.0000	.0000	1.0000
25.5000	.0000	.0000	1.0000
26.0000	.0000	.0000	1.0000

26.5000	.0000	.0000	1.0000
27.0000	.0000	.0000	1.0000
27.5000	.0000	.0000	1.0000
28.0000	.0000	.0000	1.0000
28.5000	.0000	.0000	1.0000
29.0000	.0000	.0000	1.0000
29.5000	.0000	.0000	1.0000
30.0000	.0000	.0000	1.0000
30.5000	.0000	.0000	1.0000
31.0000	.0000	.0000	1.0000
31.5000	.0000	.0000	1.0000
32.0000	.0000	.0000	1.0000
32.5000	.0000	.0000	1.0000
33.0000	.0000	.0000	1.0000
33.5000	.0000	.0000	1.0000
34.0000	.0000	.0000	1.0000
34.5000	.0000	.0000	1.0000
35.0000	.0000	.0000	1.0000
35.5000	.0000	.0000	1.0000
36.0000	.0000	.0000	1.0000
36.5000	.0000	.0000	1.0000
37.0000	.0000	.0000	1.0000
37.5000	.0000	.0000	1.0000
38.0000	.0000	.0000	1.0000
38.5000	.0000	.0000	1.0000
39.0000	.0000	.0000	1.0000
39.5000	.0000	.0000	1.0000
40.0000	.0000	.0000	1.0000
40.5000	.0000	.0000	1.0000
41.0000	.0000	.0000	1.0000
41.5000	.0000	.0000	1.0000
42.0000	.0000	.0000	1.0000
42.5000	.0000	.0000	1.0000
43.0000	.0000	.0000	1.0000
43.5000	.0000	.0000	1.0000
44.0000	.0000	.0000	1.0000
44.5000	.0000	.0000	1.0000
45.0000	.0000	.0000	1.0000
45.5000	.0000	.0000	1.0000
46.0000	.0000	.0000	1.0000
46.5000	.0000	.0000	1.0000
47.0000	.0000	.0000	1.0000
47.5000	.0000	.0000	1.0000
48.0000	.0000	.0000	1.0000
48.5000	.0000	.0000	1.0000
49.0000	.0000	.0000	1.0000
49.5000	.0000	.0000	1.0000
50.0000	.0000	.0000	1.0000
50.5000	.0000	.0000	1.0000

15 PERCENT TMS SCOUR RESULTS

B	FD15	PRD15	CPRD15
1.0000	2.0000	1.0000	1.0000
1.5000	.0000	.0000	1.0000
2.0000	.0000	.0000	1.0000
2.5000	.0000	.0000	1.0000
3.0000	.0000	.0000	1.0000
3.5000	.0000	.0000	1.0000



4.0000	.0000	.0000	1.0000
4.5000	.0000	.0000	1.0000
5.0000	.0000	.0000	1.0000
5.5000	.0000	.0000	1.0000
6.0000	.0000	.0000	1.0000
6.5000	.0000	.0000	1.0000
7.0000	.0000	.0000	1.0000
7.5000	.0000	.0000	1.0000
8.0000	.0000	.0000	1.0000
8.5000	.0000	.0000	1.0000
9.0000	.0000	.0000	1.0000
9.5000	.0000	.0000	1.0000
10.0000	.0000	.0000	1.0000
10.5000	.0000	.0000	1.0000
11.0000	.0000	.0000	1.0000
11.5000	.0000	.0000	1.0000
12.0000	.0000	.0000	1.0000
12.5000	.0000	.0000	1.0000
13.0000	.0000	.0000	1.0000
13.5000	.0000	.0000	1.0000
14.0000	.0000	.0000	1.0000
14.5000	.0000	.0000	1.0000
15.0000	.0000	.0000	1.0000
15.5000	.0000	.0000	1.0000
16.0000	.0000	.0000	1.0000
16.5000	.0000	.0000	1.0000
17.0000	.0000	.0000	1.0000
17.5000	.0000	.0000	1.0000
18.0000	.0000	.0000	1.0000
18.5000	.0000	.0000	1.0000
19.0000	.0000	.0000	1.0000
19.5000	.0000	.0000	1.0000
20.0000	.0000	.0000	1.0000
20.5000	.0000	.0000	1.0000
21.0000	.0000	.0000	1.0000
21.5000	.0000	.0000	1.0000
22.0000	.0000	.0000	1.0000
22.5000	.0000	.0000	1.0000
23.0000	.0000	.0000	1.0000
23.5000	.0000	.0000	1.0000
24.0000	.0000	.0000	1.0000
24.5000	.0000	.0000	1.0000
25.0000	.0000	.0000	1.0000
25.5000	.0000	.0000	1.0000
26.0000	.0000	.0000	1.0000
26.5000	.0000	.0000	1.0000
27.0000	.0000	.0000	1.0000
27.5000	.0000	.0000	1.0000
28.0000	.0000	.0000	1.0000
28.5000	.0000	.0000	1.0000
29.0000	.0000	.0000	1.0000
29.5000	.0000	.0000	1.0000
30.0000	.0000	.0000	1.0000
30.5000	.0000	.0000	1.0000
31.0000	.0000	.0000	1.0000
31.5000	.0000	.0000	1.0000
32.0000	.0000	.0000	1.0000

32.5000	.0000	.0000	1.0000
33.0000	.0000	.0000	1.0000
33.5000	.0000	.0000	1.0000
34.0000	.0000	.0000	1.0000
34.5000	.0000	.0000	1.0000
35.0000	.0000	.0000	1.0000
35.5000	.0000	.0000	1.0000
36.0000	.0000	.0000	1.0000
36.5000	.0000	.0000	1.0000
37.0000	.0000	.0000	1.0000
37.5000	.0000	.0000	1.0000
38.0000	.0000	.0000	1.0000
38.5000	.0000	.0000	1.0000
39.0000	.0000	.0000	1.0000
39.5000	.0000	.0000	1.0000
40.0000	.0000	.0000	1.0000
40.5000	.0000	.0000	1.0000
41.0000	.0000	.0000	1.0000
41.5000	.0000	.0000	1.0000
42.0000	.0000	.0000	1.0000
42.5000	.0000	.0000	1.0000
43.0000	.0000	.0000	1.0000
43.5000	.0000	.0000	1.0000
44.0000	.0000	.0000	1.0000
44.5000	.0000	.0000	1.0000
45.0000	.0000	.0000	1.0000
45.5000	.0000	.0000	1.0000
46.0000	.0000	.0000	1.0000
46.5000	.0000	.0000	1.0000
47.0000	.0000	.0000	1.0000
47.5000	.0000	.0000	1.0000
48.0000	.0000	.0000	1.0000
48.5000	.0000	.0000	1.0000
49.0000	.0000	.0000	1.0000
49.5000	.0000	.0000	1.0000
50.0000	.0000	.0000	1.0000
50.5000	.0000	.0000	1.0000
B	FU15	PRU15	CPRU15
1.0000	2.0000	1.0000	1.0000
1.5000	.0000	.0000	1.0000
2.0000	.0000	.0000	1.0000
2.5000	.0000	.0000	1.0000
3.0000	.0000	.0000	1.0000
3.5000	.0000	.0000	1.0000
4.0000	.0000	.0000	1.0000
4.5000	.0000	.0000	1.0000
5.0000	.0000	.0000	1.0000
5.5000	.0000	.0000	1.0000
6.0000	.0000	.0000	1.0000
6.5000	.0000	.0000	1.0000
7.0000	.0000	.0000	1.0000
7.5000	.0000	.0000	1.0000
8.0000	.0000	.0000	1.0000
8.5000	.0000	.0000	1.0000
9.0000	.0000	.0000	1.0000
9.5000	.0000	.0000	1.0000
10.0000	.0000	.0000	1.0000

10.5000	.0000	.0000	1.0000
11.0000	.0000	.0000	1.0000
11.5000	.0000	.0000	1.0000
12.0000	.0000	.0000	1.0000
12.5000	.0000	.0000	1.0000
13.0000	.0000	.0000	1.0000
13.5000	.0000	.0000	1.0000
14.0000	.0000	.0000	1.0000
14.5000	.0000	.0000	1.0000
15.0000	.0000	.0000	1.0000
15.5000	.0000	.0000	1.0000
16.0000	.0000	.0000	1.0000
16.5000	.0000	.0000	1.0000
17.0000	.0000	.0000	1.0000
17.5000	.0000	.0000	1.0000
18.0000	.0000	.0000	1.0000
18.5000	.0000	.0000	1.0000
19.0000	.0000	.0000	1.0000
19.5000	.0000	.0000	1.0000
20.0000	.0000	.0000	1.0000
20.5000	.0000	.0000	1.0000
21.0000	.0000	.0000	1.0000
21.5000	.0000	.0000	1.0000
22.0000	.0000	.0000	1.0000
22.5000	.0000	.0000	1.0000
23.0000	.0000	.0000	1.0000
23.5000	.0000	.0000	1.0000
24.0000	.0000	.0000	1.0000
24.5000	.0000	.0000	1.0000
25.0000	.0000	.0000	1.0000
25.5000	.0000	.0000	1.0000
26.0000	.0000	.0000	1.0000
26.5000	.0000	.0000	1.0000
27.0000	.0000	.0000	1.0000
27.5000	.0000	.0000	1.0000
28.0000	.0000	.0000	1.0000
28.5000	.0000	.0000	1.0000
29.0000	.0000	.0000	1.0000
29.5000	.0000	.0000	1.0000
30.0000	.0000	.0000	1.0000
30.5000	.0000	.0000	1.0000
31.0000	.0000	.0000	1.0000
31.5000	.0000	.0000	1.0000
32.0000	.0000	.0000	1.0000
32.5000	.0000	.0000	1.0000
33.0000	.0000	.0000	1.0000
33.5000	.0000	.0000	1.0000
34.0000	.0000	.0000	1.0000
34.5000	.0000	.0000	1.0000
35.0000	.0000	.0000	1.0000
35.5000	.0000	.0000	1.0000
36.0000	.0000	.0000	1.0000
36.5000	.0000	.0000	1.0000
37.0000	.0000	.0000	1.0000
37.5000	.0000	.0000	1.0000
38.0000	.0000	.0000	1.0000
38.5000	.0000	.0000	1.0000

39.0000	.0000	.0000	1.0000
39.5000	.0000	.0000	1.0000
40.0000	.0000	.0000	1.0000
40.5000	.0000	.0000	1.0000
41.0000	.0000	.0000	1.0000
41.5000	.0000	.0000	1.0000
42.0000	.0000	.0000	1.0000
42.5000	.0000	.0000	1.0000
43.0000	.0000	.0000	1.0000
43.5000	.0000	.0000	1.0000
44.0000	.0000	.0000	1.0000
44.5000	.0000	.0000	1.0000
45.0000	.0000	.0000	1.0000
45.5000	.0000	.0000	1.0000
46.0000	.0000	.0000	1.0000
46.5000	.0000	.0000	1.0000
47.0000	.0000	.0000	1.0000
47.5000	.0000	.0000	1.0000
48.0000	.0000	.0000	1.0000
48.5000	.0000	.0000	1.0000
49.0000	.0000	.0000	1.0000
49.5000	.0000	.0000	1.0000
50.0000	.0000	.0000	1.0000
50.5000	.0000	.0000	1.0000

25 PERCENT SCOUR RESULTS

B	FD25	PRD25	CPRD25
1.0000	2.0000	1.0000	1.0000
1.5000	.0000	.0000	1.0000
2.0000	.0000	.0000	1.0000
2.5000	.0000	.0000	1.0000
3.0000	.0000	.0000	1.0000
3.5000	.0000	.0000	1.0000
4.0000	.0000	.0000	1.0000
4.5000	.0000	.0000	1.0000
5.0000	.0000	.0000	1.0000
5.5000	.0000	.0000	1.0000
6.0000	.0000	.0000	1.0000
6.5000	.0000	.0000	1.0000
7.0000	.0000	.0000	1.0000
7.5000	.0000	.0000	1.0000
8.0000	.0000	.0000	1.0000
8.5000	.0000	.0000	1.0000
9.0000	.0000	.0000	1.0000
9.5000	.0000	.0000	1.0000
10.0000	.0000	.0000	1.0000
10.5000	.0000	.0000	1.0000
11.0000	.0000	.0000	1.0000
11.5000	.0000	.0000	1.0000
12.0000	.0000	.0000	1.0000
12.5000	.0000	.0000	1.0000
13.0000	.0000	.0000	1.0000
13.5000	.0000	.0000	1.0000
14.0000	.0000	.0000	1.0000
14.5000	.0000	.0000	1.0000
15.0000	.0000	.0000	1.0000
15.5000	.0000	.0000	1.0000
16.0000	.0000	.0000	1.0000

16.5000	.0000	.0000	1.0000
17.0000	.0000	.0000	1.0000
17.5000	.0000	.0000	1.0000
18.0000	.0000	.0000	1.0000
18.5000	.0000	.0000	1.0000
19.0000	.0000	.0000	1.0000
19.5000	.0000	.0000	1.0000
20.0000	.0000	.0000	1.0000
20.5000	.0000	.0000	1.0000
21.0000	.0000	.0000	1.0000
21.5000	.0000	.0000	1.0000
22.0000	.0000	.0000	1.0000
22.5000	.0000	.0000	1.0000
23.0000	.0000	.0000	1.0000
23.5000	.0000	.0000	1.0000
24.0000	.0000	.0000	1.0000
24.5000	.0000	.0000	1.0000
25.0000	.0000	.0000	1.0000
25.5000	.0000	.0000	1.0000
26.0000	.0000	.0000	1.0000
26.5000	.0000	.0000	1.0000
27.0000	.0000	.0000	1.0000
27.5000	.0000	.0000	1.0000
28.0000	.0000	.0000	1.0000
28.5000	.0000	.0000	1.0000
29.0000	.0000	.0000	1.0000
29.5000	.0000	.0000	1.0000
30.0000	.0000	.0000	1.0000
30.5000	.0000	.0000	1.0000
31.0000	.0000	.0000	1.0000
31.5000	.0000	.0000	1.0000
32.0000	.0000	.0000	1.0000
32.5000	.0000	.0000	1.0000
33.0000	.0000	.0000	1.0000
33.5000	.0000	.0000	1.0000
34.0000	.0000	.0000	1.0000
34.5000	.0000	.0000	1.0000
35.0000	.0000	.0000	1.0000
35.5000	.0000	.0000	1.0000
36.0000	.0000	.0000	1.0000
36.5000	.0000	.0000	1.0000
37.0000	.0000	.0000	1.0000
37.5000	.0000	.0000	1.0000
38.0000	.0000	.0000	1.0000
38.5000	.0000	.0000	1.0000
39.0000	.0000	.0000	1.0000
39.5000	.0000	.0000	1.0000
40.0000	.0000	.0000	1.0000
40.5000	.0000	.0000	1.0000
41.0000	.0000	.0000	1.0000
41.5000	.0000	.0000	1.0000
42.0000	.0000	.0000	1.0000
42.5000	.0000	.0000	1.0000
43.0000	.0000	.0000	1.0000
43.5000	.0000	.0000	1.0000
44.0000	.0000	.0000	1.0000
44.5000	.0000	.0000	1.0000

45.0000	.0000	.0000	1.0000
45.5000	.0000	.0000	1.0000
46.0000	.0000	.0000	1.0000
46.5000	.0000	.0000	1.0000
47.0000	.0000	.0000	1.0000
47.5000	.0000	.0000	1.0000
48.0000	.0000	.0000	1.0000
48.5000	.0000	.0000	1.0000
49.0000	.0000	.0000	1.0000
49.5000	.0000	.0000	1.0000
50.0000	.0000	.0000	1.0000
50.5000	.0000	.0000	1.0000
B	FU25	PRU25	CPRU25
1.0000	2.0000	1.0000	1.0000
1.5000	.0000	.0000	1.0000
2.0000	.0000	.0000	1.0000
2.5000	.0000	.0000	1.0000
3.0000	.0000	.0000	1.0000
3.5000	.0000	.0000	1.0000
4.0000	.0000	.0000	1.0000
4.5000	.0000	.0000	1.0000
5.0000	.0000	.0000	1.0000
5.5000	.0000	.0000	1.0000
6.0000	.0000	.0000	1.0000
6.5000	.0000	.0000	1.0000
7.0000	.0000	.0000	1.0000
7.5000	.0000	.0000	1.0000
8.0000	.0000	.0000	1.0000
8.5000	.0000	.0000	1.0000
9.0000	.0000	.0000	1.0000
9.5000	.0000	.0000	1.0000
10.0000	.0000	.0000	1.0000
10.5000	.0000	.0000	1.0000
11.0000	.0000	.0000	1.0000
11.5000	.0000	.0000	1.0000
12.0000	.0000	.0000	1.0000
12.5000	.0000	.0000	1.0000
13.0000	.0000	.0000	1.0000
13.5000	.0000	.0000	1.0000
14.0000	.0000	.0000	1.0000
14.5000	.0000	.0000	1.0000
15.0000	.0000	.0000	1.0000
15.5000	.0000	.0000	1.0000
16.0000	.0000	.0000	1.0000
16.5000	.0000	.0000	1.0000
17.0000	.0000	.0000	1.0000
17.5000	.0000	.0000	1.0000
18.0000	.0000	.0000	1.0000
18.5000	.0000	.0000	1.0000
19.0000	.0000	.0000	1.0000
19.5000	.0000	.0000	1.0000
20.0000	.0000	.0000	1.0000
20.5000	.0000	.0000	1.0000
21.0000	.0000	.0000	1.0000
21.5000	.0000	.0000	1.0000
22.0000	.0000	.0000	1.0000
22.5000	.0000	.0000	1.0000

23.0000	.0000	.0000	1.0000
23.5000	.0000	.0000	1.0000
24.0000	.0000	.0000	1.0000
24.5000	.0000	.0000	1.0000
25.0000	.0000	.0000	1.0000
25.5000	.0000	.0000	1.0000
26.0000	.0000	.0000	1.0000
26.5000	.0000	.0000	1.0000
27.0000	.0000	.0000	1.0000
27.5000	.0000	.0000	1.0000
28.0000	.0000	.0000	1.0000
28.5000	.0000	.0000	1.0000
29.0000	.0000	.0000	1.0000
29.5000	.0000	.0000	1.0000
30.0000	.0000	.0000	1.0000
30.5000	.0000	.0000	1.0000
31.0000	.0000	.0000	1.0000
31.5000	.0000	.0000	1.0000
32.0000	.0000	.0000	1.0000
32.5000	.0000	.0000	1.0000
33.0000	.0000	.0000	1.0000
33.5000	.0000	.0000	1.0000
34.0000	.0000	.0000	1.0000
34.5000	.0000	.0000	1.0000
35.0000	.0000	.0000	1.0000
35.5000	.0000	.0000	1.0000
36.0000	.0000	.0000	1.0000
36.5000	.0000	.0000	1.0000
37.0000	.0000	.0000	1.0000
37.5000	.0000	.0000	1.0000
38.0000	.0000	.0000	1.0000
38.5000	.0000	.0000	1.0000
39.0000	.0000	.0000	1.0000
39.5000	.0000	.0000	1.0000
40.0000	.0000	.0000	1.0000
40.5000	.0000	.0000	1.0000
41.0000	.0000	.0000	1.0000
41.5000	.0000	.0000	1.0000
42.0000	.0000	.0000	1.0000
42.5000	.0000	.0000	1.0000
43.0000	.0000	.0000	1.0000
43.5000	.0000	.0000	1.0000
44.0000	.0000	.0000	1.0000
44.5000	.0000	.0000	1.0000
45.0000	.0000	.0000	1.0000
45.5000	.0000	.0000	1.0000
46.0000	.0000	.0000	1.0000
46.5000	.0000	.0000	1.0000
47.0000	.0000	.0000	1.0000
47.5000	.0000	.0000	1.0000
48.0000	.0000	.0000	1.0000
48.5000	.0000	.0000	1.0000
49.0000	.0000	.0000	1.0000
49.5000	.0000	.0000	1.0000
50.0000	.0000	.0000	1.0000
50.5000	.0000	.0000	1.0000

50 PERCENT TMS SCOUR RESULTS

B	FD50	PRD50	CPRD50
1.0000	1.0000	.5000	.5000
1.5000	1.0000	.5000	1.0000
2.0000	.0000	.0000	1.0000
2.5000	.0000	.0000	1.0000
3.0000	.0000	.0000	1.0000
3.5000	.0000	.0000	1.0000
4.0000	.0000	.0000	1.0000
4.5000	.0000	.0000	1.0000
5.0000	.0000	.0000	1.0000
5.5000	.0000	.0000	1.0000
6.0000	.0000	.0000	1.0000
6.5000	.0000	.0000	1.0000
7.0000	.0000	.0000	1.0000
7.5000	.0000	.0000	1.0000
8.0000	.0000	.0000	1.0000
8.5000	.0000	.0000	1.0000
9.0000	.0000	.0000	1.0000
9.5000	.0000	.0000	1.0000
10.0000	.0000	.0000	1.0000
10.5000	.0000	.0000	1.0000
11.0000	.0000	.0000	1.0000
11.5000	.0000	.0000	1.0000
12.0000	.0000	.0000	1.0000
12.5000	.0000	.0000	1.0000
13.0000	.0000	.0000	1.0000
13.5000	.0000	.0000	1.0000
14.0000	.0000	.0000	1.0000
14.5000	.0000	.0000	1.0000
15.0000	.0000	.0000	1.0000
15.5000	.0000	.0000	1.0000
16.0000	.0000	.0000	1.0000
16.5000	.0000	.0000	1.0000
17.0000	.0000	.0000	1.0000
17.5000	.0000	.0000	1.0000
18.0000	.0000	.0000	1.0000
18.5000	.0000	.0000	1.0000
19.0000	.0000	.0000	1.0000
19.5000	.0000	.0000	1.0000
20.0000	.0000	.0000	1.0000
20.5000	.0000	.0000	1.0000
21.0000	.0000	.0000	1.0000
21.5000	.0000	.0000	1.0000
22.0000	.0000	.0000	1.0000
22.5000	.0000	.0000	1.0000
23.0000	.0000	.0000	1.0000
23.5000	.0000	.0000	1.0000
24.0000	.0000	.0000	1.0000
24.5000	.0000	.0000	1.0000
25.0000	.0000	.0000	1.0000
25.5000	.0000	.0000	1.0000
26.0000	.0000	.0000	1.0000
26.5000	.0000	.0000	1.0000
27.0000	.0000	.0000	1.0000
27.5000	.0000	.0000	1.0000
28.0000	.0000	.0000	1.0000
28.5000	.0000	.0000	1.0000



29.0000	.0000	.0000	1.0000
29.5000	.0000	.0000	1.0000
30.0000	.0000	.0000	1.0000
30.5000	.0000	.0000	1.0000
31.0000	.0000	.0000	1.0000
31.5000	.0000	.0000	1.0000
32.0000	.0000	.0000	1.0000
32.5000	.0000	.0000	1.0000
33.0000	.0000	.0000	1.0000
33.5000	.0000	.0000	1.0000
34.0000	.0000	.0000	1.0000
34.5000	.0000	.0000	1.0000
35.0000	.0000	.0000	1.0000
35.5000	.0000	.0000	1.0000
36.0000	.0000	.0000	1.0000
36.5000	.0000	.0000	1.0000
37.0000	.0000	.0000	1.0000
37.5000	.0000	.0000	1.0000
38.0000	.0000	.0000	1.0000
38.5000	.0000	.0000	1.0000
39.0000	.0000	.0000	1.0000
39.5000	.0000	.0000	1.0000
40.0000	.0000	.0000	1.0000
40.5000	.0000	.0000	1.0000
41.0000	.0000	.0000	1.0000
41.5000	.0000	.0000	1.0000
42.0000	.0000	.0000	1.0000
42.5000	.0000	.0000	1.0000
43.0000	.0000	.0000	1.0000
43.5000	.0000	.0000	1.0000
44.0000	.0000	.0000	1.0000
44.5000	.0000	.0000	1.0000
45.0000	.0000	.0000	1.0000
45.5000	.0000	.0000	1.0000
46.0000	.0000	.0000	1.0000
46.5000	.0000	.0000	1.0000
47.0000	.0000	.0000	1.0000
47.5000	.0000	.0000	1.0000
48.0000	.0000	.0000	1.0000
48.5000	.0000	.0000	1.0000
49.0000	.0000	.0000	1.0000
49.5000	.0000	.0000	1.0000
50.0000	.0000	.0000	1.0000
50.5000	.0000	.0000	1.0000
B	FU50	PRU50	CPRU50
1.0000	2.0000	1.0000	1.0000
1.5000	.0000	.0000	1.0000
2.0000	.0000	.0000	1.0000
2.5000	.0000	.0000	1.0000
3.0000	.0000	.0000	1.0000
3.5000	.0000	.0000	1.0000
4.0000	.0000	.0000	1.0000
4.5000	.0000	.0000	1.0000
5.0000	.0000	.0000	1.0000
5.5000	.0000	.0000	1.0000
6.0000	.0000	.0000	1.0000
6.5000	.0000	.0000	1.0000

7.0000	.0000	.0000	1.0000
7.5000	.0000	.0000	1.0000
8.0000	.0000	.0000	1.0000
8.5000	.0000	.0000	1.0000
9.0000	.0000	.0000	1.0000
9.5000	.0000	.0000	1.0000
10.0000	.0000	.0000	1.0000
10.5000	.0000	.0000	1.0000
11.0000	.0000	.0000	1.0000
11.5000	.0000	.0000	1.0000
12.0000	.0000	.0000	1.0000
12.5000	.0000	.0000	1.0000
13.0000	.0000	.0000	1.0000
13.5000	.0000	.0000	1.0000
14.0000	.0000	.0000	1.0000
14.5000	.0000	.0000	1.0000
15.0000	.0000	.0000	1.0000
15.5000	.0000	.0000	1.0000
16.0000	.0000	.0000	1.0000
16.5000	.0000	.0000	1.0000
17.0000	.0000	.0000	1.0000
17.5000	.0000	.0000	1.0000
18.0000	.0000	.0000	1.0000
18.5000	.0000	.0000	1.0000
19.0000	.0000	.0000	1.0000
19.5000	.0000	.0000	1.0000
20.0000	.0000	.0000	1.0000
20.5000	.0000	.0000	1.0000
21.0000	.0000	.0000	1.0000
21.5000	.0000	.0000	1.0000
22.0000	.0000	.0000	1.0000
22.5000	.0000	.0000	1.0000
23.0000	.0000	.0000	1.0000
23.5000	.0000	.0000	1.0000
24.0000	.0000	.0000	1.0000
24.5000	.0000	.0000	1.0000
25.0000	.0000	.0000	1.0000
25.5000	.0000	.0000	1.0000
26.0000	.0000	.0000	1.0000
26.5000	.0000	.0000	1.0000
27.0000	.0000	.0000	1.0000
27.5000	.0000	.0000	1.0000
28.0000	.0000	.0000	1.0000
28.5000	.0000	.0000	1.0000
29.0000	.0000	.0000	1.0000
29.5000	.0000	.0000	1.0000
30.0000	.0000	.0000	1.0000
30.5000	.0000	.0000	1.0000
31.0000	.0000	.0000	1.0000
31.5000	.0000	.0000	1.0000
32.0000	.0000	.0000	1.0000
32.5000	.0000	.0000	1.0000
33.0000	.0000	.0000	1.0000
33.5000	.0000	.0000	1.0000
34.0000	.0000	.0000	1.0000
34.5000	.0000	.0000	1.0000
35.0000	.0000	.0000	1.0000

35.5000	.0000	.0000	1.0000
36.0000	.0000	.0000	1.0000
36.5000	.0000	.0000	1.0000
37.0000	.0000	.0000	1.0000
37.5000	.0000	.0000	1.0000
38.0000	.0000	.0000	1.0000
38.5000	.0000	.0000	1.0000
39.0000	.0000	.0000	1.0000
39.5000	.0000	.0000	1.0000
40.0000	.0000	.0000	1.0000
40.5000	.0000	.0000	1.0000
41.0000	.0000	.0000	1.0000
41.5000	.0000	.0000	1.0000
42.0000	.0000	.0000	1.0000
42.5000	.0000	.0000	1.0000
43.0000	.0000	.0000	1.0000
43.5000	.0000	.0000	1.0000
44.0000	.0000	.0000	1.0000
44.5000	.0000	.0000	1.0000
45.0000	.0000	.0000	1.0000
45.5000	.0000	.0000	1.0000
46.0000	.0000	.0000	1.0000
46.5000	.0000	.0000	1.0000
47.0000	.0000	.0000	1.0000
47.5000	.0000	.0000	1.0000
48.0000	.0000	.0000	1.0000
48.5000	.0000	.0000	1.0000
49.0000	.0000	.0000	1.0000
49.5000	.0000	.0000	1.0000
50.0000	.0000	.0000	1.0000
50.5000	.0000	.0000	1.0000

75 PERCENT TMS SCOUR RESULTS

B	FD75	PRD75	CPRD75
1.0000	.0000	.0000	.0000
1.5000	.0000	.0000	.0000
2.0000	.0000	.0000	.0000
2.5000	.0000	.0000	.0000
3.0000	.0000	.0000	.0000
3.5000	.0000	.0000	.0000
4.0000	.0000	.0000	.0000
4.5000	1.0000	.5000	.5000
5.0000	.0000	.0000	.5000
5.5000	.0000	.0000	.5000
6.0000	.0000	.0000	.5000
6.5000	.0000	.0000	.5000
7.0000	.0000	.0000	.5000
7.5000	.0000	.0000	.5000
8.0000	.0000	.0000	.5000
8.5000	.0000	.0000	.5000
9.0000	.0000	.0000	.5000
9.5000	.0000	.0000	.5000
10.0000	.0000	.0000	.5000
10.5000	.0000	.0000	.5000
11.0000	.0000	.0000	.5000
11.5000	.0000	.0000	.5000
12.0000	.0000	.0000	.5000
12.5000	.0000	.0000	.5000

13.0000	.0000	.0000	.5000
13.5000	.0000	.0000	.5000
14.0000	.0000	.0000	.5000
14.5000	.0000	.0000	.5000
15.0000	.0000	.0000	.5000
15.5000	.0000	.0000	.5000
16.0000	.0000	.0000	.5000
16.5000	.0000	.0000	.5000
17.0000	.0000	.0000	.5000
17.5000	.0000	.0000	.5000
18.0000	.0000	.0000	.5000
18.5000	.0000	.0000	.5000
19.0000	1.0000	.5000	1.0000
19.5000	.0000	.0000	1.0000
20.0000	.0000	.0000	1.0000
20.5000	.0000	.0000	1.0000
21.0000	.0000	.0000	1.0000
21.5000	.0000	.0000	1.0000
22.0000	.0000	.0000	1.0000
22.5000	.0000	.0000	1.0000
23.0000	.0000	.0000	1.0000
23.5000	.0000	.0000	1.0000
24.0000	.0000	.0000	1.0000
24.5000	.0000	.0000	1.0000
25.0000	.0000	.0000	1.0000
25.5000	.0000	.0000	1.0000
26.0000	.0000	.0000	1.0000
26.5000	.0000	.0000	1.0000
27.0000	.0000	.0000	1.0000
27.5000	.0000	.0000	1.0000
28.0000	.0000	.0000	1.0000
28.5000	.0000	.0000	1.0000
29.0000	.0000	.0000	1.0000
29.5000	.0000	.0000	1.0000
30.0000	.0000	.0000	1.0000
30.5000	.0000	.0000	1.0000
31.0000	.0000	.0000	1.0000
31.5000	.0000	.0000	1.0000
32.0000	.0000	.0000	1.0000
32.5000	.0000	.0000	1.0000
33.0000	.0000	.0000	1.0000
33.5000	.0000	.0000	1.0000
34.0000	.0000	.0000	1.0000
34.5000	.0000	.0000	1.0000
35.0000	.0000	.0000	1.0000
35.5000	.0000	.0000	1.0000
36.0000	.0000	.0000	1.0000
36.5000	.0000	.0000	1.0000
37.0000	.0000	.0000	1.0000
37.5000	.0000	.0000	1.0000
38.0000	.0000	.0000	1.0000
38.5000	.0000	.0000	1.0000
39.0000	.0000	.0000	1.0000
39.5000	.0000	.0000	1.0000
40.0000	.0000	.0000	1.0000
40.5000	.0000	.0000	1.0000
41.0000	.0000	.0000	1.0000

41.5000	.0000	.0000	1.0000
42.0000	.0000	.0000	1.0000
42.5000	.0000	.0000	1.0000
43.0000	.0000	.0000	1.0000
43.5000	.0000	.0000	1.0000
44.0000	.0000	.0000	1.0000
44.5000	.0000	.0000	1.0000
45.0000	.0000	.0000	1.0000
45.5000	.0000	.0000	1.0000
46.0000	.0000	.0000	1.0000
46.5000	.0000	.0000	1.0000
47.0000	.0000	.0000	1.0000
47.5000	.0000	.0000	1.0000
48.0000	.0000	.0000	1.0000
48.5000	.0000	.0000	1.0000
49.0000	.0000	.0000	1.0000
49.5000	.0000	.0000	1.0000
50.0000	.0000	.0000	1.0000
50.5000	.0000	.0000	1.0000
B	FU75	PRU75	CPRU75
1.0000	2.0000	1.0000	1.0000
1.5000	.0000	.0000	1.0000
2.0000	.0000	.0000	1.0000
2.5000	.0000	.0000	1.0000
3.0000	.0000	.0000	1.0000
3.5000	.0000	.0000	1.0000
4.0000	.0000	.0000	1.0000
4.5000	.0000	.0000	1.0000
5.0000	.0000	.0000	1.0000
5.5000	.0000	.0000	1.0000
6.0000	.0000	.0000	1.0000
6.5000	.0000	.0000	1.0000
7.0000	.0000	.0000	1.0000
7.5000	.0000	.0000	1.0000
8.0000	.0000	.0000	1.0000
8.5000	.0000	.0000	1.0000
9.0000	.0000	.0000	1.0000
9.5000	.0000	.0000	1.0000
10.0000	.0000	.0000	1.0000
10.5000	.0000	.0000	1.0000
11.0000	.0000	.0000	1.0000
11.5000	.0000	.0000	1.0000
12.0000	.0000	.0000	1.0000
12.5000	.0000	.0000	1.0000
13.0000	.0000	.0000	1.0000
13.5000	.0000	.0000	1.0000
14.0000	.0000	.0000	1.0000
14.5000	.0000	.0000	1.0000
15.0000	.0000	.0000	1.0000
15.5000	.0000	.0000	1.0000
16.0000	.0000	.0000	1.0000
16.5000	.0000	.0000	1.0000
17.0000	.0000	.0000	1.0000
17.5000	.0000	.0000	1.0000
18.0000	.0000	.0000	1.0000
18.5000	.0000	.0000	1.0000
19.0000	.0000	.0000	1.0000

19.5000	.0000	.0000	1.0000
20.0000	.0000	.0000	1.0000
20.5000	.0000	.0000	1.0000
21.0000	.0000	.0000	1.0000
21.5000	.0000	.0000	1.0000
22.0000	.0000	.0000	1.0000
22.5000	.0000	.0000	1.0000
23.0000	.0000	.0000	1.0000
23.5000	.0000	.0000	1.0000
24.0000	.0000	.0000	1.0000
24.5000	.0000	.0000	1.0000
25.0000	.0000	.0000	1.0000
25.5000	.0000	.0000	1.0000
26.0000	.0000	.0000	1.0000
26.5000	.0000	.0000	1.0000
27.0000	.0000	.0000	1.0000
27.5000	.0000	.0000	1.0000
28.0000	.0000	.0000	1.0000
28.5000	.0000	.0000	1.0000
29.0000	.0000	.0000	1.0000
29.5000	.0000	.0000	1.0000
30.0000	.0000	.0000	1.0000
30.5000	.0000	.0000	1.0000
31.0000	.0000	.0000	1.0000
31.5000	.0000	.0000	1.0000
32.0000	.0000	.0000	1.0000
32.5000	.0000	.0000	1.0000
33.0000	.0000	.0000	1.0000
33.5000	.0000	.0000	1.0000
34.0000	.0000	.0000	1.0000
34.5000	.0000	.0000	1.0000
35.0000	.0000	.0000	1.0000
35.5000	.0000	.0000	1.0000
36.0000	.0000	.0000	1.0000
36.5000	.0000	.0000	1.0000
37.0000	.0000	.0000	1.0000
37.5000	.0000	.0000	1.0000
38.0000	.0000	.0000	1.0000
38.5000	.0000	.0000	1.0000
39.0000	.0000	.0000	1.0000
39.5000	.0000	.0000	1.0000
40.0000	.0000	.0000	1.0000
40.5000	.0000	.0000	1.0000
41.0000	.0000	.0000	1.0000
41.5000	.0000	.0000	1.0000
42.0000	.0000	.0000	1.0000
42.5000	.0000	.0000	1.0000
43.0000	.0000	.0000	1.0000
43.5000	.0000	.0000	1.0000
44.0000	.0000	.0000	1.0000
44.5000	.0000	.0000	1.0000
45.0000	.0000	.0000	1.0000
45.5000	.0000	.0000	1.0000
46.0000	.0000	.0000	1.0000
46.5000	.0000	.0000	1.0000
47.0000	.0000	.0000	1.0000
47.5000	.0000	.0000	1.0000

48.0000	.0000	.0000	1.0000
48.5000	.0000	.0000	1.0000
49.0000	.0000	.0000	1.0000
49.5000	.0000	.0000	1.0000
50.0000	.0000	.0000	1.0000
50.5000	.0000	.0000	1.0000

The mean annual contraction scour d/s face is MNYYS

The mean annual scour value d/s face is MNLTSD

The mean annual total scour d/s face is YMNTSD

The standard dev in annual scour d/s face is YSTTSD

YR	MNYYS	MNLTSD	YMNTSD	YSTTSD
001	.0000	.0127	.0127	.0093
002	.0000	.0328	.0328	.0169
003	.0000	.0426	.0426	.0285
004	.0000	.0476	.0476	.0214
005	.0000	.0559	.0559	.0240
006	.0000	.0571	.0571	.0243
007	.0000	.0765	.0765	.0250
008	.0000	.0854	.0854	.0376
009	.0000	.1247	.1247	.0419
010	.0000	.1438	.1438	.0689
011	.0000	.1616	.1616	.0941
012	.0000	.1726	.1726	.1000
013	.0000	.1803	.1803	.0897
014	.0000	.2069	.2069	.0790
015	.0000	.2166	.2166	.0928
016	.0000	.2263	.2263	.0967
017	.0000	.2509	.2509	.0727
018	.0000	.2600	.2600	.0855
019	.0000	.3044	.3044	.0314
020	.0000	.3310	.3310	.0199
021	.0000	.3399	.3399	.0324
022	.0000	.3746	.3746	.0557
023	.0000	.3878	.3878	.0371
024	.0000	.3984	.3984	.0382
025	.0000	.4206	.4206	.0490
026	.0000	.4334	.4334	.0395
027	.0000	.4578	.4578	.0365
028	.0000	.4700	.4700	.0400
029	.0000	.4943	.4943	.0198
030	.0000	.5177	.5177	.0323
031	.0000	.5324	.5324	.0260
032	.0000	.5670	.5670	.0091
033	.0000	.5670	.5670	.0091
034	.0000	.5846	.5846	.0136
035	.0000	.6143	.6143	.0475
036	.0000	.6366	.6366	.0285
037	.0000	.6585	.6585	.0363
038	.0000	.7069	.7069	.0072
039	.0000	.7121	.7121	.0053
040	.0000	.7363	.7363	.0013
041	.0000	.7537	.7537	.0120
042	.0000	.7882	.7882	.0203
043	.0000	.8019	.8019	.0019
044	.0000	.8184	.8184	.0024
045	.0000	.8214	.8214	.0058
046	.0000	.8484	.8484	.0440

047	.0000	.8703	.8703	.0467
048	.0000	.8987	.8987	.0582
049	.0000	.9636	.9636	.0369
050	.0000	1.0362	1.0362	.1107
051	.0000	1.0885	1.0885	.0719
052	.0000	1.1313	1.1313	.1209
053	.0000	1.1849	1.1849	.1311
054	.0000	1.2222	1.2222	.1222
055	.0000	1.2793	1.2793	.1213
056	.0000	1.3244	1.3244	.0899
057	.0000	1.3765	1.3765	.1329
058	.0000	1.5061	1.5061	.0838
059	.0000	1.5626	1.5626	.0923
060	.0000	1.6395	1.6395	.0633
061	.0000	1.7673	1.7673	.0226
062	.0000	1.8796	1.8796	.0083
063	.0000	1.9671	1.9671	.0345
064	.0000	2.1160	2.1160	.0483
065	.0000	2.2165	2.2165	.0101
066	.0000	2.3116	2.3116	.0319
067	.0000	2.5192	2.5192	.1004
068	.0000	2.7323	2.7323	.1427
069	.0000	2.9251	2.9251	.2325
070	.0000	3.1248	3.1248	.2786
071	.0000	3.3143	3.3143	.3104
072	.0000	3.4822	3.4822	.2562
073	.0000	3.9452	3.9452	.4321
074	.0000	4.4000	4.4000	.6703
075	.0000	11.3925	11.3925	10.2605
076	.0000	11.6631	11.6631	10.1156
077	.0000	11.8997	11.8997	9.8930
078	.0000	18.8561	18.8561	.1723
079	.0000	18.9377	18.9377	.0648
080	.0000	19.0110	19.0110	.0475
081	.0000	19.0278	19.0278	.0216
082	.0000	19.0473	19.0473	.0296
083	.0000	19.0724	19.0724	.0296
084	.0000	19.0728	19.0728	.0301
085	.0000	19.0749	19.0749	.0260
086	.0000	19.0778	19.0778	.0249
087	.0000	19.0946	19.0946	.0385
088	.0000	19.1095	19.1095	.0306
089	.0000	19.1356	19.1356	.0093
090	.0000	19.1386	19.1386	.0084
091	.0000	19.1474	19.1474	.0038
092	.0000	19.1474	19.1474	.0038
093	.0000	19.1624	19.1624	.0199
094	.0000	19.1624	19.1624	.0199
095	.0000	19.1813	19.1813	.0087
096	.0000	19.1844	19.1844	.0041
097	.0000	19.1977	19.1977	.0091
098	.0000	19.1977	19.1977	.0091
099	.0000	19.2044	19.2044	.0081
100	.0000	19.2053	19.2053	.0049

The annual contraction scour u/s face is MNYYSU

The mean annual local scour value u/s face is MNLSU

The mean annual total scour value u/s face is YMNTSU



The standard dev in annual scour u/s face is YSTTSU				
YR	MNYYSU	MNLSU	YMNTSU	YSTTSU
001	.0000	.0000	.0000	.0000
002	.0000	.0000	.0000	.0000
003	.0000	.0000	.0000	.0000
004	.0000	.0000	.0000	.0000
005	.0000	.0000	.0000	.0000
006	.0000	.0000	.0000	.0000
007	.0000	.0000	.0000	.0000
008	.0000	.0000	.0000	.0000
009	.0000	.0000	.0000	.0000
010	.0000	.0000	.0000	.0000
011	.0000	.0000	.0000	.0000
012	.0000	.0000	.0000	.0000
013	.0000	.0000	.0000	.0000
014	.0000	.0000	.0000	.0000
015	.0000	.0000	.0000	.0000
016	.0000	.0000	.0000	.0000
017	.0000	.0000	.0000	.0000
018	.0000	.0000	.0000	.0000
019	.0000	.0000	.0000	.0000
020	.0000	.0000	.0000	.0000
021	.0000	.0000	.0000	.0000
022	.0000	.0000	.0000	.0000
023	.0000	.0000	.0000	.0000
024	.0000	.0000	.0000	.0000
025	.0000	.0000	.0000	.0000
026	.0000	.0000	.0000	.0000
027	.0000	.0000	.0000	.0000
028	.0000	.0000	.0000	.0000
029	.0000	.0000	.0000	.0000
030	.0000	.0000	.0000	.0000
031	.0000	.0000	.0000	.0000
032	.0000	.0000	.0000	.0000
033	.0000	.0000	.0000	.0000
034	.0000	.0000	.0000	.0000
035	.0000	.0000	.0000	.0000
036	.0000	.0000	.0000	.0000
037	.0000	.0000	.0000	.0000
038	.0000	.0000	.0000	.0000
039	.0000	.0000	.0000	.0000
040	.0000	.0000	.0000	.0000
041	.0000	.0000	.0000	.0000
042	.0000	.0000	.0000	.0000
043	.0000	.0000	.0000	.0000
044	.0000	.0000	.0000	.0000
045	.0000	.0000	.0000	.0000
046	.0000	.0000	.0000	.0000
047	.0000	.0000	.0000	.0000
048	.0000	.0000	.0000	.0000
049	.0000	.0000	.0000	.0000
050	.0000	.0000	.0000	.0000
051	.0000	.0000	.0000	.0000
052	.0000	.0000	.0000	.0000
053	.0000	.0000	.0000	.0000
054	.0000	.0000	.0000	.0000
055	.0000	.0000	.0000	.0000

056	.0000	.0000	.0000	.0000
057	.0000	.0000	.0000	.0000
058	.0000	.0000	.0000	.0000
059	.0000	.0000	.0000	.0000
060	.0000	.0000	.0000	.0000
061	.0000	.0000	.0000	.0000
062	.0000	.0000	.0000	.0000
063	.0000	.0000	.0000	.0000
064	.0000	.0000	.0000	.0000
065	.0000	.0000	.0000	.0000
066	.0000	.0000	.0000	.0000
067	.0000	.0000	.0000	.0000
068	.0000	.0000	.0000	.0000
069	.0000	.0000	.0000	.0000
070	.0000	.0000	.0000	.0000
071	.0000	.0000	.0000	.0000
072	.0000	.0000	.0000	.0000
073	.0000	.0000	.0000	.0000
074	.0000	.0000	.0000	.0000
075	.0000	.0000	.0000	.0000
076	.0000	.0000	.0000	.0000
077	.0000	.0000	.0000	.0000
078	.0000	.0000	.0000	.0000
079	.0000	.0000	.0000	.0000
080	.0000	.0000	.0000	.0000
081	.0000	.0000	.0000	.0000
082	.0000	.0000	.0000	.0000
083	.0000	.0000	.0000	.0000
084	.0000	.0000	.0000	.0000
085	.0000	.0000	.0000	.0000
086	.0000	.0000	.0000	.0000
087	.0000	.0000	.0000	.0000
088	.0000	.0000	.0000	.0000
089	.0000	.0000	.0000	.0000
090	.0000	.0000	.0000	.0000
091	.0000	.0000	.0000	.0000
092	.0000	.0000	.0000	.0000
093	.0000	.0000	.0000	.0000
094	.0000	.0000	.0000	.0000
095	.0000	.0000	.0000	.0000
096	.0000	.0000	.0000	.0000
097	.0000	.0000	.0000	.0000
098	.0000	.0000	.0000	.0000
099	.0000	.0000	.0000	.0000
100	.0000	.0000	.0000	.0000

#### APPENDIX D-4

RUN TITLE IS Monie Bay Hurricane simulation  
RUN DATE IS 10/9/05  
THE PROGRAM WAS EXECUTED IN THE EXISTING PIER ANALYSIS MODE.  
CONTRACTION SCOUR METHOD IS KOMURAS EQN  
SCOUR COMPUTED WITHOUT ARMOURING  
BRUBAKER-DEMETRIUS NEILLS MODIFICATION FACTOR ACTIVATED  
TIDE DISTORTION OPTION ACTIVATED  
MEAN TIDAL DEPTH MDR is = 5.935000  
MEAN LOW TIDAL DEPTH MLT is = 4.745000  
MEAN LOW TIDE ELEVATION MLTE is = -1.190000  
TIDAL AMP. AT BRIDGE XSEC MTR is = 1.190000  
CHANNEL INVERT AT BRIDGE IRS is = -5.935000

Estuary in bank area is = 18617.000000

Maximum tide in the simulation HITIDE is = 17.075690  
Maximum u/s flow depth in sim. YTRMXS is = 20.291940  
Maximum d/s flow depth in sim. YTFMXS is = 20.161010  
Maximum u/s disch. in sim. QTRMXS is = 195798.700000  
Maximum d/s disch. in sim. QTFMXS is = 208193.000000  
Maximum u/s vel.in sim. VUPMS is = 8.230374E-01  
Maximum d/s vel.in sim. VDOWNMS is = 2.371017

Maximum u/s flow depth last run YTRMAX is = 20.291940  
Maximum d/s flow depth last run YTFMAX is = 19.116360  
Maximum u/s discharge last run QTRMAX is = 170834.700000  
Maximum d/s discharge last run QTFMAX is = 174499.500000  
Maximum u/s velocity last run VNUMAX is = 1.256297  
Maximum d/s velocity last run VNDMAX is = 5.133153E-01  
Maximum tangential vel d/s face last run VTDMX is = 3.097629E-01  
Maximum tangential vel u/s face last run VTUMX is = 7.307125E-01  
critical vel u/s face last run UIUMIN is = 1.309054E-01  
critical vel d/s face last run UIDMIN is = 1.309054E-01

Time of concentration = 38.500000hrs  
Time to peak = 25.795000hrs  
Number of unit hydrograph ordinates = 128  
Soil infiltration potential = 2.345679  
Peak discharge of the UHG = 300.213200cfs  
Initial abstractions IA = 4.691358E-01in

Catchment base flow = 12.715970cfs  
Tide attenuation factor TAF = 9.754099E-01  
Tidal lag MTL= -4.190653hrs  
Tidal routing constant CX = 1.000000  
Bridge station tidal range TR = 2.380000ft  
Effective bottom channel width at brdg.WBE = 5216.400000ft  
Estuary Area 6.021735E+07  
Contraction scour factor u/s face= 1.008152  
Contraction scour factor d/s face= 1.094180  
Estuary to wavelength ratio DIM = 8.618567E-02  
Estuary width factor WF = 1.000000

Tidal range factor HF = 4.010110E-01  
 Neill Mod. factor rising limb.NMRF = 8.000000E-01  
 Neill Mod. factor falling limb.NMFF = 8.000000E-01

The maximum storm event in the simulation is 5.000000ins  
 Array of total SURGRE at bridge is HSURGE= 10.380330  
 2.856355E-01

5.179529E-01	8.728182E-01	1.481365	2.761897
10.926670	10.926670	3.868823	2.761897
-5.401087	-5.078043	-4.789991	-4.531823
-4.299308	-4.088933	-3.897769	-3.723364
-3.563652	-3.416886	-3.281578	-3.156457
-3.040428	-2.932547	-2.831993	-2.738052
-2.650098	-2.567580	-2.490014	-2.416970
-2.348066	-2.282962	-2.221354	-2.162968
-2.107560	-2.054909	-2.004814	-1.957096
-1.911588	-1.868142	-1.826621	-1.786900
-1.748865	-1.712412	-1.677443	-1.643871
-1.611613	-1.580593	-1.550743	-1.521997
-1.494296	-1.467583	-1.441807	-1.416919
-1.392874	-1.369630	-1.347148	-1.325391
-1.304325	-1.283917	-1.264137	-1.244957
-1.226349	-1.208288	-1.190751	-1.173715
-1.157160	-1.141064	-1.125410	-1.110179
-1.095354	-1.080919	-1.066860	-1.053161
-1.039810	-1.026792	-1.014096	-1.001710
-9.896228E-01	-9.778234E-01	-9.663019E-01	-9.550486E-01
-9.440541E-01	-9.333097E-01	-9.228069E-01	-9.125378E-01
-9.024945E-01	-8.926698E-01	-8.830566E-01	-8.736480E-01
-8.644378E-01	-8.554195E-01	-8.465874E-01	-8.379357E-01
-8.294590E-01	-8.211520E-01	-8.130096E-01	-8.050270E-01
-7.971996E-01	-7.895228E-01	-7.819924E-01	-7.746043E-01
-7.673544E-01	-7.602389E-01	-7.532541E-01	-7.463963E-01
-7.396623E-01	-7.330486E-01	-7.265522E-01	-7.201698E-01
-7.138985E-01	-7.077355E-01	-7.016779E-01	-6.957231E-01
-6.898685E-01	-6.841115E-01	-6.784499E-01	-6.728811E-01
-6.674029E-01	-6.620133E-01		

Array of total combined depth at bridge is YT= 19.116360  
 10.163270

10.346110	10.157900	10.750770	12.095030
20.291940	9.360037	9.582955	9.622069
9.385002	9.590307	9.317761	9.784895
9.578135	9.321850	9.756060	9.645088
10.116590	9.820195	9.458979	9.225802
10.082640	10.110900	9.520922	9.590406
9.294579	9.579410	9.271439	9.659349
9.867636	9.747543	9.333932	9.320117
9.648362	9.561447	9.196396	9.352130
9.430647	9.597586	9.904292	9.518978
9.466090	9.274731	9.272921	9.504324
9.514458	9.660125	9.402449	9.531334
9.343533	9.514418	9.249331	9.144859
9.509972	9.818240	9.723592	9.465555
9.547260	9.511665	9.234170	9.622461
9.339378	9.451406	9.611336	9.506972
9.215064	9.532695	9.637154	9.364924

9.222733	9.333730	9.704607	9.442145
9.253599	9.905503	9.978102	9.444235
9.208185	9.145417	9.396202	9.638000
9.668593	9.398315	9.215653	9.228976
9.590085	9.637198	9.346807	9.516125
9.382147	9.436987	9.362576	9.155539
9.551835	9.574038	9.780535	9.648170
9.536007	9.360473	9.719770	9.553011
9.484163	9.474613	9.420713	9.493007
9.427571	9.655191	9.987129	9.479844
9.727008	9.475186	9.458727	9.751261
9.564009	9.559904	9.449709	9.507874
9.306983	9.453148		

Array of total combined depth at bridge d/s face is YTR=  
4.745000

4.745000	10.346110	4.745000	10.750770
12.095030	20.291940	4.745000	9.582955
9.622069	4.745000	9.590307	4.745000
9.784895	4.745000	4.745000	9.756060
4.745000	10.116590	4.745000	4.745000
4.745000	10.082640	10.110900	4.745000
9.590406	4.745000	9.579410	4.745000
9.659349	9.867636	4.745000	4.745000
4.745000	9.648362	4.745000	4.745000
9.352130	9.430647	9.597586	9.904292
4.745000	4.745000	4.745000	4.745000
9.504324	9.514458	9.660125	4.745000
9.531334	4.745000	9.514418	4.745000
4.745000	9.509972	9.818240	4.745000
4.745000	9.547260	4.745000	4.745000
9.622461	4.745000	9.451406	9.611336
4.745000	4.745000	9.532695	9.637154
4.745000	4.745000	9.333730	9.704607
4.745000	4.745000	9.905503	9.978102
4.745000	4.745000	4.745000	9.396202
9.638000	9.668593	4.745000	4.745000
9.228976	9.590085	9.637198	4.745000
9.516125	4.745000	9.436987	4.745000
4.745000	9.551835	9.574038	9.780535
4.745000	4.745000	4.745000	9.719770
4.745000	4.745000	4.745000	4.745000
9.493007	4.745000	9.655191	9.987129
4.745000	9.727008	4.745000	4.745000
9.751261	4.745000	4.745000	4.745000
9.507874	4.745000	9.453148	

Array of total combined depth at bridge u/s face is YTF=  
19.116360

10.163270	4.745000	10.157900	4.745000
4.745000	4.745000	9.360037	4.745000
4.745000	9.385002	4.745000	9.317761
4.745000	9.578135	9.321850	4.745000
9.645088	4.745000	9.820195	9.458979
9.225802	4.745000	4.745000	9.520922
4.745000	9.294579	4.745000	9.271439
4.745000	4.745000	9.747543	9.333932
9.320117	4.745000	9.561447	9.196396
4.745000	4.745000	4.745000	4.745000

9.518978	9.466090	9.274731	9.272921
4.745000	4.745000	4.745000	9.402449
4.745000	9.343533	4.745000	9.249331
9.144859	4.745000	4.745000	9.723592
9.465555	4.745000	9.511665	9.234170
4.745000	9.339378	4.745000	4.745000
9.506972	9.215064	4.745000	4.745000
9.364924	9.222733	4.745000	4.745000
9.442145	9.253599	4.745000	4.745000
9.444235	9.208185	9.145417	4.745000
4.745000	4.745000	9.398315	9.215653
4.745000	4.745000	4.745000	9.346807
4.745000	9.382147	4.745000	9.362576
9.155539	4.745000	4.745000	4.745000
9.648170	9.536007	9.360473	4.745000
9.553011	9.484163	9.474613	9.420713
4.745000	9.427571	4.745000	4.745000
9.479844	4.745000	9.475186	9.458727
4.745000	9.564009	9.559904	9.449709
4.745000	9.306983	4.745000	
Array of Neills discharge is QN= 168710.400000 3523.424000			
Array total net disch. value at bridge is QT= 168723.100000			
3536.262000			
-1590.221000	-11402.260000	-29735.240000	-170834.700000
174499.500000	-9134.451000	-6069.092000	-1445.346000
2991.715000	6443.000000	8926.379000	12840.500000
9154.396000	3158.708000	-4322.432000	-11255.170000
-15276.730000	-15352.300000	-11453.140000	-4566.985000
3034.360000	9177.455000	13559.780000	11179.720000
9023.600000	4717.819000	-866.941800	-6839.720000
-10857.560000	-11880.000000	-9628.457000	-4657.315000
1676.710000	6959.548000	12575.360000	8513.996000
7620.642000	5135.075000	1693.029000	-2426.948000
-5619.565000	-7003.608000	-6222.534000	-3481.066000
521.849700	4210.202000	4981.313000	11071.170000
10528.360000	7641.739000	3139.819000	-2407.415000
-7403.740000	-10205.210000	-10110.700000	-7154.252000
-2099.733000	3275.477000	8219.831000	9616.727000
9828.358000	7743.649000	3884.551000	-1030.263000
-6122.646000	-9472.432000	-10231.900000	-8214.023000
-3941.109000	1314.425000	4259.209000	9688.916000
10758.940000	9210.722000	5434.109000	387.645000
-5586.138000	-10040.890000	-11823.590000	-10483.230000
-6364.686000	-521.088900	-4019.637000	12953.930000
15775.270000	14657.940000	2057.794000	134.054600
126.741700	-7753.921000	-17876.040000	-17294.020000
-12223.580000	-3959.172000	25767.790000	2449.071000
3228.863000	3248.953000	2503.105000	1180.196000
-469.799600	-2145.890000	-3208.600000	-3387.836000
-2639.011000	-1153.967000	-9348.512000	4735.315000
7177.593000	7841.862000	6557.980000	3652.585000
-167.227600	-4580.538000	-7769.849000	-8922.725000
-7745.922000	-4540.217000		
Array of total net velocity at bridge is VNT = 9.690552E-01			
5.757545E-02			
-2.486084E-02	-1.856145E-01	-4.301592E-01	-2.082436
8.980001E-01	-1.675696E-01	-1.067506E-01	-2.545229E-02

5.492312E-02	1.133522E-01	1.635486E-01	2.166195E-01
1.609956E-01	5.788061E-02	-7.285716E-02	-1.983392E-01
-2.483708E-01	-2.592670E-01	-2.107299E-01	-8.769642E-02
4.928198E-02	1.491822E-01	2.380690E-01	1.966863E-01
1.652178E-01	8.297402E-02	-1.586262E-02	-1.205819E-01
-1.836230E-01	-2.001941E-01	-1.764959E-01	-8.533695E-02
2.954999E-02	1.223349E-01	2.412624E-01	1.561509E-01
1.400944E-01	9.036144E-02	2.866448E-02	-4.260748E-02
-1.034185E-01	-1.281587E-01	-1.138599E-01	-6.108736E-02
9.160377E-03	7.422616E-02	9.149663E-02	1.944361E-01
1.930462E-01	1.341404E-01	5.741323E-02	-4.611639E-02
-1.299457E-01	-1.723336E-01	-1.785984E-01	-1.316596E-01
-3.689360E-02	5.749194E-02	1.578791E-01	1.693509E-01
1.801891E-01	1.424451E-01	6.838422E-02	-1.808093E-02
-1.175307E-01	-1.663650E-01	-1.802638E-01	-1.507064E-01
-7.567119E-02	2.409412E-02	7.519206E-02	1.781785E-01
1.967570E-01	1.559515E-01	9.221387E-02	7.129213E-03
-1.072097E-01	-1.923463E-01	-2.171348E-01	-1.846964E-01
-1.122387E-01	-9.570166E-03	-7.716253E-02	2.487685E-01
2.775338E-01	2.582414E-01	3.773502E-02	2.353266E-03
2.326577E-03	-1.425718E-01	-3.279569E-01	-3.313884E-01
-2.148048E-01	-6.962030E-02	4.346468E-01	4.316166E-02
5.671429E-02	5.960211E-02	4.421037E-02	2.074029E-02
-8.650619E-03	-3.950166E-02	-5.896781E-02	-6.239853E-02
-4.850989E-02	-2.034147E-02	-1.586837E-01	8.718187E-02
1.268004E-01	1.443560E-01	1.206614E-01	6.155777E-02
-2.939748E-03	-8.051297E-02	-1.429197E-01	-1.565964E-01
-1.418755E-01	-8.352208E-02		
Array of net adjusted vel.upstream is VNUA = 0.000000E+00			
0.000000E+00			
0.000000E+00	1.052377E-01	3.078868E-01	1.256297
1.041218	0.000000E+00	1.371601E-01	0.000000E+00
0.000000E+00	0.000000E+00	0.000000E+00	0.000000E+00
0.000000E+00	0.000000E+00	0.000000E+00	1.355982E-01
2.233550E-01	2.538189E-01	2.349984E-01	1.492132E-01
0.000000E+00	0.000000E+00	0.000000E+00	0.000000E+00
0.000000E+00	0.000000E+00	0.000000E+00	0.000000E+00
1.521025E-01	1.919085E-01	1.883450E-01	1.309164E-01
0.000000E+00	0.000000E+00	0.000000E+00	0.000000E+00
0.000000E+00	0.000000E+00	0.000000E+00	0.000000E+00
0.000000E+00	1.157886E-01	1.210093E-01	0.000000E+00
0.000000E+00	0.000000E+00	0.000000E+00	0.000000E+00
0.000000E+00	0.000000E+00	0.000000E+00	0.000000E+00
0.000000E+00	1.511396E-01	1.754660E-01	1.551290E-01
0.000000E+00	0.000000E+00	0.000000E+00	0.000000E+00
0.000000E+00	0.000000E+00	0.000000E+00	0.000000E+00
0.000000E+00	1.419478E-01	1.733144E-01	1.654851E-01
1.131888E-01	0.000000E+00	0.000000E+00	0.000000E+00
0.000000E+00	0.000000E+00	0.000000E+00	0.000000E+00
0.000000E+00	1.497780E-01	2.047406E-01	2.009156E-01
1.484676E-01	0.000000E+00	0.000000E+00	0.000000E+00
0.000000E+00	0.000000E+00	0.000000E+00	0.000000E+00
0.000000E+00	0.000000E+00	2.352644E-01	3.296727E-01
2.730966E-01	1.422126E-01	0.000000E+00	0.000000E+00
0.000000E+00	0.000000E+00	0.000000E+00	0.000000E+00
0.000000E+00	0.000000E+00	0.000000E+00	0.000000E+00
0.000000E+00	0.000000E+00	0.000000E+00	0.000000E+00

0.000000E+00	0.000000E+00	0.000000E+00	0.000000E+00
0.000000E+00	0.000000E+00	1.117163E-01	1.497580E-01
1.492359E-01	1.126988E-01		
Array of net adjusted vel.downstream is VNDA=			4.845276E-01
5.133153E-01			
0.000000E+00	0.000000E+00	0.000000E+00	0.000000E+00
4.490000E-01	4.490000E-01	0.000000E+00	0.000000E+00
0.000000E+00	0.000000E+00	1.384504E-01	1.900840E-01
1.888076E-01	1.094381E-01	0.000000E+00	0.000000E+00
0.000000E+00	0.000000E+00	0.000000E+00	0.000000E+00
0.000000E+00	0.000000E+00	1.936256E-01	2.173776E-01
1.809520E-01	1.240959E-01	0.000000E+00	0.000000E+00
0.000000E+00	0.000000E+00	0.000000E+00	0.000000E+00
0.000000E+00	0.000000E+00	1.817986E-01	1.987066E-01
1.481226E-01	1.152279E-01	0.000000E+00	0.000000E+00
0.000000E+00	0.000000E+00	0.000000E+00	0.000000E+00
0.000000E+00	0.000000E+00	0.000000E+00	1.429663E-01
1.937411E-01	1.635933E-01	0.000000E+00	0.000000E+00
0.000000E+00	0.000000E+00	0.000000E+00	0.000000E+00
0.000000E+00	0.000000E+00	1.076855E-01	1.636150E-01
1.747700E-01	1.613171E-01	1.054146E-01	0.000000E+00
0.000000E+00	0.000000E+00	0.000000E+00	0.000000E+00
0.000000E+00	0.000000E+00	0.000000E+00	1.266853E-01
1.874677E-01	1.763542E-01	1.240827E-01	0.000000E+00
0.000000E+00	0.000000E+00	0.000000E+00	0.000000E+00
0.000000E+00	0.000000E+00	0.000000E+00	1.243843E-01
2.631512E-01	2.678876E-01	1.479882E-01	0.000000E+00
0.000000E+00	0.000000E+00	0.000000E+00	0.000000E+00
0.000000E+00	0.000000E+00	2.173234E-01	2.389042E-01
0.000000E+00	0.000000E+00	0.000000E+00	0.000000E+00
0.000000E+00	0.000000E+00	0.000000E+00	0.000000E+00
1.069912E-01	1.355782E-01	1.325087E-01	0.000000E+00
0.000000E+00	0.000000E+00	0.000000E+00	0.000000E+00
0.000000E+00	0.000000E+00		
Array of net vel.u/stream is VNU =		0.000000E+00	0.000000E+00
1.243042E-02	1.052377E-01	3.078868E-01	1.256297
1.041218	8.378478E-02	1.371601E-01	6.610146E-02
1.272614E-02	0.000000E+00	0.000000E+00	0.000000E+00
0.000000E+00	0.000000E+00	3.642858E-02	1.355982E-01
2.233550E-01	2.538189E-01	2.349984E-01	1.492132E-01
4.384821E-02	0.000000E+00	0.000000E+00	0.000000E+00
0.000000E+00	0.000000E+00	7.931309E-03	6.822227E-02
1.521025E-01	1.919085E-01	1.883450E-01	1.309164E-01
4.266848E-02	0.000000E+00	0.000000E+00	0.000000E+00
0.000000E+00	0.000000E+00	0.000000E+00	2.130374E-02
7.301297E-02	1.157886E-01	1.210093E-01	8.747364E-02
3.054368E-02	0.000000E+00	0.000000E+00	0.000000E+00
0.000000E+00	0.000000E+00	0.000000E+00	2.305819E-02
8.803105E-02	1.511396E-01	1.754660E-01	1.551290E-01
8.427660E-02	1.844680E-02	0.000000E+00	0.000000E+00
0.000000E+00	0.000000E+00	0.000000E+00	9.040464E-03
6.780579E-02	1.419478E-01	1.733144E-01	1.654851E-01
1.131888E-01	3.783559E-02	0.000000E+00	0.000000E+00
0.000000E+00	0.000000E+00	0.000000E+00	0.000000E+00
5.360484E-02	1.497780E-01	2.047406E-01	2.009156E-01
1.484676E-01	6.090444E-02	4.336635E-02	3.858127E-02



0.000000E+00	0.000000E+00	0.000000E+00	0.000000E+00
0.000000E+00	7.128592E-02	2.352644E-01	3.296727E-01
2.730966E-01	1.422126E-01	3.481015E-02	0.000000E+00
0.000000E+00	0.000000E+00	0.000000E+00	0.000000E+00
4.325309E-03	2.407614E-02	4.923473E-02	6.068317E-02
5.545421E-02	3.442568E-02	8.951259E-02	7.934185E-02
0.000000E+00	0.000000E+00	0.000000E+00	0.000000E+00
1.469874E-03	4.172636E-02	1.117163E-01	1.497580E-01
1.492359E-01	1.126988E-01		
Array of net vel.d/stream is VND=		4.845276E-01	5.133153E-01
2.878772E-02	0.000000E+00	0.000000E+00	0.000000E+00
4.490000E-01	4.490000E-01	0.000000E+00	0.000000E+00
2.746156E-02	8.413766E-02	1.384504E-01	1.900840E-01
1.888076E-01	1.094381E-01	2.894030E-02	0.000000E+00
0.000000E+00	0.000000E+00	0.000000E+00	0.000000E+00
2.464099E-02	9.923208E-02	1.936256E-01	2.173776E-01
1.809520E-01	1.240959E-01	4.148701E-02	0.000000E+00
0.000000E+00	0.000000E+00	0.000000E+00	0.000000E+00
1.477499E-02	7.594243E-02	1.817986E-01	1.987066E-01
1.481226E-01	1.152279E-01	5.951296E-02	1.433224E-02
0.000000E+00	0.000000E+00	0.000000E+00	0.000000E+00
4.580189E-03	4.169327E-02	8.286139E-02	1.429663E-01
1.937411E-01	1.635933E-01	9.577681E-02	2.870661E-02
0.000000E+00	0.000000E+00	0.000000E+00	0.000000E+00
0.000000E+00	2.874597E-02	1.076855E-01	1.636150E-01
1.747700E-01	1.613171E-01	1.054146E-01	3.419211E-02
0.000000E+00	0.000000E+00	0.000000E+00	0.000000E+00
0.000000E+00	1.204706E-02	4.964309E-02	1.266853E-01
1.874677E-01	1.763542E-01	1.240827E-01	4.967154E-02
3.564607E-03	0.000000E+00	0.000000E+00	0.000000E+00
0.000000E+00	0.000000E+00	0.000000E+00	1.243843E-01
2.631512E-01	2.678876E-01	1.479882E-01	2.004414E-02
2.339921E-03	1.163289E-03	0.000000E+00	0.000000E+00
0.000000E+00	0.000000E+00	2.173234E-01	2.389042E-01
4.993798E-02	5.815820E-02	5.190624E-02	3.247533E-02
1.037015E-02	0.000000E+00	0.000000E+00	0.000000E+00
0.000000E+00	0.000000E+00	0.000000E+00	4.359094E-02
1.069912E-01	1.355782E-01	1.325087E-01	9.110957E-02
3.077888E-02	0.000000E+00	0.000000E+00	0.000000E+00
0.000000E+00	0.000000E+00		
Array of tangential velocity d/s face is VTD=		0.000000E+00	
0.000000E+00			
0.000000E+00	0.000000E+00	1.840916E-01	7.391909E-01
5.723632E-01	0.000000E+00	8.392598E-02	0.000000E+00
0.000000E+00	0.000000E+00	0.000000E+00	0.000000E+00
0.000000E+00	0.000000E+00	0.000000E+00	0.000000E+00
1.356328E-01	0.000000E+00	0.000000E+00	0.000000E+00
0.000000E+00	0.000000E+00	0.000000E+00	0.000000E+00
0.000000E+00	0.000000E+00	0.000000E+00	0.000000E+00
9.268757E-02	0.000000E+00	0.000000E+00	0.000000E+00
0.000000E+00	0.000000E+00	0.000000E+00	0.000000E+00
0.000000E+00	0.000000E+00	0.000000E+00	0.000000E+00
0.000000E+00	0.000000E+00	0.000000E+00	0.000000E+00
0.000000E+00	0.000000E+00	0.000000E+00	0.000000E+00
0.000000E+00	0.000000E+00	0.000000E+00	0.000000E+00
0.000000E+00	0.000000E+00	0.000000E+00	0.000000E+00
0.000000E+00	0.000000E+00	0.000000E+00	0.000000E+00
0.000000E+00	9.216567E-02	0.000000E+00	0.000000E+00
0.000000E+00	0.000000E+00	0.000000E+00	0.000000E+00

0.000000E+00	0.000000E+00	0.000000E+00	0.000000E+00
0.000000E+00	8.691966E-02	1.059643E-01	0.000000E+00
0.000000E+00	0.000000E+00	0.000000E+00	0.000000E+00
0.000000E+00	0.000000E+00	0.000000E+00	0.000000E+00
0.000000E+00	0.000000E+00	1.256240E-01	1.228382E-01
9.073149E-02	0.000000E+00	0.000000E+00	0.000000E+00
0.000000E+00	0.000000E+00	0.000000E+00	0.000000E+00
0.000000E+00	0.000000E+00	0.000000E+00	0.000000E+00
1.671796E-01	8.705133E-02	0.000000E+00	0.000000E+00
0.000000E+00	0.000000E+00	0.000000E+00	0.000000E+00
0.000000E+00	0.000000E+00	0.000000E+00	0.000000E+00
0.000000E+00	0.000000E+00	0.000000E+00	0.000000E+00
0.000000E+00	0.000000E+00	0.000000E+00	0.000000E+00
0.000000E+00	0.000000E+00	0.000000E+00	0.000000E+00
0.000000E+00	0.000000E+00	0.000000E+00	9.175932E-02
0.000000E+00	6.910849E-02		
Array of tangential velocity u/s face is VTU=			2.674294E-01
3.097629E-01			
0.000000E+00	0.000000E+00	0.000000E+00	0.000000E+00
0.000000E+00	2.745922E-01	0.000000E+00	0.000000E+00
0.000000E+00	0.000000E+00	8.484714E-02	0.000000E+00
1.152597E-01	6.706328E-02	0.000000E+00	0.000000E+00
0.000000E+00	0.000000E+00	0.000000E+00	0.000000E+00
0.000000E+00	0.000000E+00	1.183006E-01	0.000000E+00
1.109325E-01	0.000000E+00	0.000000E+00	0.000000E+00
0.000000E+00	0.000000E+00	0.000000E+00	0.000000E+00
0.000000E+00	0.000000E+00	1.116184E-01	0.000000E+00
0.000000E+00	0.000000E+00	0.000000E+00	0.000000E+00
0.000000E+00	0.000000E+00	0.000000E+00	0.000000E+00
0.000000E+00	0.000000E+00	0.000000E+00	0.000000E+00
1.186850E-01	0.000000E+00	0.000000E+00	0.000000E+00
0.000000E+00	0.000000E+00	0.000000E+00	0.000000E+00
0.000000E+00	0.000000E+00	6.607719E-02	0.000000E+00
1.070701E-01	0.000000E+00	0.000000E+00	0.000000E+00
0.000000E+00	0.000000E+00	0.000000E+00	0.000000E+00
0.000000E+00	0.000000E+00	0.000000E+00	7.749223E-02
1.149985E-01	0.000000E+00	0.000000E+00	0.000000E+00
0.000000E+00	0.000000E+00	0.000000E+00	0.000000E+00
0.000000E+00	0.000000E+00	0.000000E+00	0.000000E+00
0.000000E+00	0.000000E+00	9.065247E-02	0.000000E+00
0.000000E+00	0.000000E+00	0.000000E+00	0.000000E+00
0.000000E+00	0.000000E+00	0.000000E+00	1.456924E-01
0.000000E+00	0.000000E+00	0.000000E+00	0.000000E+00
0.000000E+00	0.000000E+00	0.000000E+00	0.000000E+00
0.000000E+00	0.000000E+00	0.000000E+00	0.000000E+00
0.000000E+00	8.289120E-02	8.103434E-02	0.000000E+00
0.000000E+00	0.000000E+00	0.000000E+00	0.000000E+00
0.000000E+00	0.000000E+00		
The mean hurricane scour u/s face is MNTHSU			4.030408
The std.dev.in hurricane scour u/s face is STDHSU			2.309076E-02
The mean hurricane scour d/s face is MNTHSD			4.067635
The std.dev.in hurricane scour d/s face is STDHSD			3.681452E-02
B	FHU	PRHU	CPRHU
1.0000	.0000	.0000	.0000
1.5000	.0000	.0000	.0000
2.0000	.0000	.0000	.0000
2.5000	.0000	.0000	.0000
3.0000	.0000	.0000	.0000

3.5000	.0000	.0000	.0000
4.0000	886.0000	.0886	.0886
4.5000	9114.0000	.9114	1.0000
5.0000	.0000	.0000	1.0000
5.5000	.0000	.0000	1.0000
6.0000	.0000	.0000	1.0000
6.5000	.0000	.0000	1.0000
7.0000	.0000	.0000	1.0000
7.5000	.0000	.0000	1.0000
8.0000	.0000	.0000	1.0000
8.5000	.0000	.0000	1.0000
9.0000	.0000	.0000	1.0000
9.5000	.0000	.0000	1.0000
10.0000	.0000	.0000	1.0000
10.5000	.0000	.0000	1.0000
11.0000	.0000	.0000	1.0000
11.5000	.0000	.0000	1.0000
12.0000	.0000	.0000	1.0000
12.5000	.0000	.0000	1.0000
13.0000	.0000	.0000	1.0000
13.5000	.0000	.0000	1.0000
14.0000	.0000	.0000	1.0000
14.5000	.0000	.0000	1.0000
15.0000	.0000	.0000	1.0000
15.5000	.0000	.0000	1.0000
16.0000	.0000	.0000	1.0000
16.5000	.0000	.0000	1.0000
17.0000	.0000	.0000	1.0000
17.5000	.0000	.0000	1.0000
18.0000	.0000	.0000	1.0000
18.5000	.0000	.0000	1.0000
19.0000	.0000	.0000	1.0000
19.5000	.0000	.0000	1.0000
20.0000	.0000	.0000	1.0000
20.5000	.0000	.0000	1.0000
21.0000	.0000	.0000	1.0000
21.5000	.0000	.0000	1.0000
22.0000	.0000	.0000	1.0000
22.5000	.0000	.0000	1.0000
23.0000	.0000	.0000	1.0000
23.5000	.0000	.0000	1.0000
24.0000	.0000	.0000	1.0000
24.5000	.0000	.0000	1.0000
25.0000	.0000	.0000	1.0000
25.5000	.0000	.0000	1.0000
26.0000	.0000	.0000	1.0000
26.5000	.0000	.0000	1.0000
27.0000	.0000	.0000	1.0000
27.5000	.0000	.0000	1.0000
28.0000	.0000	.0000	1.0000
28.5000	.0000	.0000	1.0000
29.0000	.0000	.0000	1.0000
29.5000	.0000	.0000	1.0000
30.0000	.0000	.0000	1.0000
30.5000	.0000	.0000	1.0000
31.0000	.0000	.0000	1.0000
31.5000	.0000	.0000	1.0000

32.0000	.0000	.0000	1.0000
32.5000	.0000	.0000	1.0000
33.0000	.0000	.0000	1.0000
33.5000	.0000	.0000	1.0000
34.0000	.0000	.0000	1.0000
34.5000	.0000	.0000	1.0000
35.0000	.0000	.0000	1.0000
35.5000	.0000	.0000	1.0000
36.0000	.0000	.0000	1.0000
36.5000	.0000	.0000	1.0000
37.0000	.0000	.0000	1.0000
37.5000	.0000	.0000	1.0000
38.0000	.0000	.0000	1.0000
38.5000	.0000	.0000	1.0000
39.0000	.0000	.0000	1.0000
39.5000	.0000	.0000	1.0000
40.0000	.0000	.0000	1.0000
40.5000	.0000	.0000	1.0000
41.0000	.0000	.0000	1.0000
41.5000	.0000	.0000	1.0000
42.0000	.0000	.0000	1.0000
42.5000	.0000	.0000	1.0000
43.0000	.0000	.0000	1.0000
43.5000	.0000	.0000	1.0000
44.0000	.0000	.0000	1.0000
44.5000	.0000	.0000	1.0000
45.0000	.0000	.0000	1.0000
45.5000	.0000	.0000	1.0000
46.0000	.0000	.0000	1.0000
46.5000	.0000	.0000	1.0000
47.0000	.0000	.0000	1.0000
47.5000	.0000	.0000	1.0000
48.0000	.0000	.0000	1.0000
48.5000	.0000	.0000	1.0000
49.0000	.0000	.0000	1.0000
49.5000	.0000	.0000	1.0000
50.0000	.0000	.0000	1.0000
50.5000	.0000	.0000	1.0000
B	FHD	PRHD	CPRHD
1.0000	.0000	.0000	.0000
1.5000	.0000	.0000	.0000
2.0000	.0000	.0000	.0000
2.5000	.0000	.0000	.0000
3.0000	.0000	.0000	.0000
3.5000	.0000	.0000	.0000
4.0000	3.0000	.0003	.0003
4.5000	9996.0000	.9996	.9999
5.0000	1.0000	.0001	1.0000
5.5000	.0000	.0000	1.0000
6.0000	.0000	.0000	1.0000
6.5000	.0000	.0000	1.0000
7.0000	.0000	.0000	1.0000
7.5000	.0000	.0000	1.0000
8.0000	.0000	.0000	1.0000
8.5000	.0000	.0000	1.0000
9.0000	.0000	.0000	1.0000
9.5000	.0000	.0000	1.0000

10.0000	.0000	.0000	1.0000
10.5000	.0000	.0000	1.0000
11.0000	.0000	.0000	1.0000
11.5000	.0000	.0000	1.0000
12.0000	.0000	.0000	1.0000
12.5000	.0000	.0000	1.0000
13.0000	.0000	.0000	1.0000
13.5000	.0000	.0000	1.0000
14.0000	.0000	.0000	1.0000
14.5000	.0000	.0000	1.0000
15.0000	.0000	.0000	1.0000
15.5000	.0000	.0000	1.0000
16.0000	.0000	.0000	1.0000
16.5000	.0000	.0000	1.0000
17.0000	.0000	.0000	1.0000
17.5000	.0000	.0000	1.0000
18.0000	.0000	.0000	1.0000
18.5000	.0000	.0000	1.0000
19.0000	.0000	.0000	1.0000
19.5000	.0000	.0000	1.0000
20.0000	.0000	.0000	1.0000
20.5000	.0000	.0000	1.0000
21.0000	.0000	.0000	1.0000
21.5000	.0000	.0000	1.0000
22.0000	.0000	.0000	1.0000
22.5000	.0000	.0000	1.0000
23.0000	.0000	.0000	1.0000
23.5000	.0000	.0000	1.0000
24.0000	.0000	.0000	1.0000
24.5000	.0000	.0000	1.0000
25.0000	.0000	.0000	1.0000
25.5000	.0000	.0000	1.0000
26.0000	.0000	.0000	1.0000
26.5000	.0000	.0000	1.0000
27.0000	.0000	.0000	1.0000
27.5000	.0000	.0000	1.0000
28.0000	.0000	.0000	1.0000
28.5000	.0000	.0000	1.0000
29.0000	.0000	.0000	1.0000
29.5000	.0000	.0000	1.0000
30.0000	.0000	.0000	1.0000
30.5000	.0000	.0000	1.0000
31.0000	.0000	.0000	1.0000
31.5000	.0000	.0000	1.0000
32.0000	.0000	.0000	1.0000
32.5000	.0000	.0000	1.0000
33.0000	.0000	.0000	1.0000
33.5000	.0000	.0000	1.0000
34.0000	.0000	.0000	1.0000
34.5000	.0000	.0000	1.0000
35.0000	.0000	.0000	1.0000
35.5000	.0000	.0000	1.0000
36.0000	.0000	.0000	1.0000
36.5000	.0000	.0000	1.0000
37.0000	.0000	.0000	1.0000
37.5000	.0000	.0000	1.0000
38.0000	.0000	.0000	1.0000

38.5000	.0000	.0000	1.0000
39.0000	.0000	.0000	1.0000
39.5000	.0000	.0000	1.0000
40.0000	.0000	.0000	1.0000
40.5000	.0000	.0000	1.0000
41.0000	.0000	.0000	1.0000
41.5000	.0000	.0000	1.0000
42.0000	.0000	.0000	1.0000
42.5000	.0000	.0000	1.0000
43.0000	.0000	.0000	1.0000
43.5000	.0000	.0000	1.0000
44.0000	.0000	.0000	1.0000
44.5000	.0000	.0000	1.0000
45.0000	.0000	.0000	1.0000
45.5000	.0000	.0000	1.0000
46.0000	.0000	.0000	1.0000
46.5000	.0000	.0000	1.0000
47.0000	.0000	.0000	1.0000
47.5000	.0000	.0000	1.0000
48.0000	.0000	.0000	1.0000
48.5000	.0000	.0000	1.0000
49.0000	.0000	.0000	1.0000
49.5000	.0000	.0000	1.0000
50.0000	.0000	.0000	1.0000
50.5000	.0000	.0000	1.0000

## Appendix D-5

RUN TITLE Black River Continuous Simulation  
RUN DATE 3/27/06  
THE PROGRAM WAS EXECUTED IN PIER DESIGN MODE.  
CONTRACTION SCOUR METHOD IS KOMURAS EQN  
SCOUR COMPUTED WITHOUT ARMOURING  
BRUBAKER-DEMETRIUS NEILLS MODIFICATION FACTOR ACTIVATED  
TIDE DISTORTION OPTION ACTIVATED  
MEAN TIDAL DEPTH MDR is = 10.935000  
MEAN LOW TIDAL DEPTH MLT is = 10.000000  
MEAN LOW TIDE ELEVATION MLTE is = -9.350000E-01  
TIDAL AMP. AT BRIDGE XSEC MTR is = 9.350000E-01  
CHANNEL INVERT AT BRIDGE IRS is = -10.935000

Estuary in bank area is = 58740.000000

Maximum tide in the simulation HITIDE is = 14.081680  
Maximum u/s flow depth in sim. YTRMXS is = 16.750000  
Maximum d/s flow depth in sim. YTFMXS is = 16.000000  
Maximum u/s disch. in sim. QTRMXS is = 271236.200000  
Maximum d/s disch. in sim. QTFMXS is = 260791.400000  
Maximum u/s vel.in sim. VUPMS is = 2.226527  
Maximum d/s vel.in sim. VDOWNMS is = 1.478876  
Maximum u/s face tang.vel.in sim. VTUMXSis = 6.588506E-01  
Maximum d/s face tang.vel.in sim. VTDMXSis = 3.552769

Maximum u/s flow depth last run YTRMAX is = 15.500000  
Maximum d/s flow depth last run YTFMAX is = 15.000000  
Maximum u/s discharge last run QTRMAX is = 201669.900000  
Maximum d/s discharge last run QTFMAX is = 211024.000000  
Maximum u/s velocity last run VNUMAX is = 1.968874  
Maximum d/s velocity last run VNDMAX is = 1.209202  
Maximum tangential vel d/s face last run VTDMX is = 1.893825  
Maximum tangential vel u/s face last run VTUMX is = 5.398135E-01  
critical vel u/s face last run UIUMIN is = 5.124375E-01  
critical vel d/s face last run UIDMIN is = 5.124375E-01

Time of concentration = 13.250000hrs  
Time to peak = 8.877501hrs  
Number of unit hydrograph ordinates = 44  
Soil infiltration potential = 1.904762  
Peak discharge of the UHG = 3162.151000cfs  
Initial abstractions IA = 3.809524E-01in

Catchment base flow = 41.050620cfs  
Tide attenuation factor TAF = 7.663934E-01  
Tidal lag MTL= 2.503192E-01hrs  
Tidal routing constant CX = 7.000000E-01  
Bridge station tidal range TR = 1.870000ft  
Effective bottom channel width at brdg.WBE = 8406.400000ft  
Estuary Area 2.648448E+08  
Contraction scour factor u/s face= 9.174486E-01  
Contraction scour factor d/s face= 1.065397

Estuary to wavelength ratio DIM = 6.349449E-02  
 Estuary width factor WF = 1.000000  
 Tidal range factor HF = 1.710105E-01  
 Neill Mod. factor rising limb.NMRF = 8.000000E-01  
 Neill Mod. factor falling limb.NMFF = 8.000000E-01

The maximum storm event in the simulation is 17.540860ins  
 ANNUAL MAX UPSTREAM VELOCITY LAST RUN = 1.359432 1.508331

1.424561	1.531120	1.337672	1.315226
1.341980	1.243831	1.371419	1.533581
1.374736	1.436547	1.300901	1.615046
1.537985	1.345207	1.558331	1.581566
1.371512	1.597703	1.384094	1.511501
1.587445	1.341504	1.320199	1.450077
1.391628	1.449286	1.368573	1.626851
1.371205	1.386672	1.501420	1.565648
1.485469	1.270007	1.471844	1.307586
1.410293	1.562620	1.386015	1.432727
1.288257	1.525587	1.302753	1.435589
1.417276	1.380431	1.464552	1.390948
1.324835	1.541474	1.747105	1.479736
1.518512	1.403571	1.503291	1.512363
1.478217	1.458973	1.379576	1.411471
1.358255	1.495390	1.345740	1.381623
1.283140	1.417771	1.450821	1.586354
1.496821	1.458416	1.242488	1.334101
1.436632	1.407714	1.583390	1.533863
1.346003	1.281022	1.390143	1.508234
1.347024	1.398928	1.968874	1.361775
1.440047	1.501706	1.664297	1.302159
1.355824	1.322184	1.534005	1.459441
1.386060	1.350760	1.453740	1.629114
1.500762	1.452992		

ANNUAL MAX DWNSTREAM VELOCITY LAST RUN = 1.076251  
 1.100536

1.083966	1.067267	1.060633	1.044742
1.172818	1.055049	1.118029	1.114566
1.058959	1.082243	1.069519	1.054579
1.066565	1.020598	1.085199	1.047609
1.030108	1.125532	1.170992	1.029543
1.096134	1.139649	9.671694E-01	1.045652
1.039393	1.037774	1.079204	1.060638
1.084756	1.085083	1.162544	1.070577
1.084399	1.008123	1.053244	1.098652
1.121133	1.139383	1.067886	1.036920
1.030201	1.136870	1.067541	1.031031
1.072946	1.091731	1.206410	1.017204
1.038495	1.084033	1.061325	1.129092
1.122931	1.111003	9.928966E-01	1.125171
1.155915	1.140743	1.026227	1.124109
1.093720	9.939406E-01	1.065292	1.028262
1.038539	1.152570	1.144485	1.085982
1.068316	1.052236	1.088445	1.052743
1.078273	1.049927	1.014927	1.132474
1.091274	1.117049	1.121627	1.096303
1.109313	1.112770	1.118885	1.055501



1.019678	1.027945	1.076688	1.145859
1.209202	9.937201E-01	1.117168	1.099066
1.067919	1.193063	9.653108E-01	1.175126
1.086160	1.040010		
ANNUAL MAX US ADJUSTED VELOCITY LAST RUN =			1.359432
1.508331			
1.424561	1.531120	1.337672	1.315226
1.341980	1.243831	1.371419	1.533581
1.374736	1.436547	1.300901	1.615046
1.537985	1.345207	1.558331	1.581566
1.371512	1.597703	1.384094	1.511501
1.587445	1.341504	1.320199	1.450077
1.391628	1.449286	1.368573	1.626851
1.371205	1.386672	1.501420	1.565648
1.485469	1.270007	1.471844	1.307586
1.410293	1.562620	1.386015	1.432727
1.288257	1.525587	1.302753	1.435589
1.417276	1.380431	1.464552	1.390948
1.324835	1.541474	1.747105	1.479736
1.518512	1.403571	1.503291	1.512363
1.478217	1.458973	1.379576	1.411471
1.358255	1.495390	1.345740	1.381623
1.283140	1.417771	1.450821	1.586354
1.496821	1.458416	1.242488	1.334101
1.436632	1.407714	1.583390	1.533863
1.346003	1.281022	1.390143	1.508234
1.347024	1.398928	1.968874	1.361775
1.440047	1.501706	1.664297	1.302159
1.355824	1.322184	1.534005	1.459441
1.386060	1.350760	1.453740	1.629114
1.500762	1.452992		
ANNUAL MAX DS ADJUSTED VELOCITY LAST RUN =			1.076251
1.100536			
1.083966	1.067267	1.060633	1.044742
1.172818	1.055049	1.118029	1.114566
1.058959	1.082243	1.069519	1.054579
1.066565	1.020598	1.085199	1.047609
1.030108	1.125532	1.170992	1.029543
1.096134	1.139649	9.671694E-01	1.045652
1.039393	1.037774	1.079204	1.060638
1.084756	1.085083	1.162544	1.070577
1.084399	1.008123	1.053244	1.098652
1.121133	1.139383	1.067886	1.036920
1.030201	1.136870	1.067541	1.031031
1.072946	1.091731	1.206410	1.017204
1.038495	1.084033	1.061325	1.129092
1.122931	1.111003	9.928966E-01	1.125171
1.155915	1.140743	1.026227	1.124109
1.093720	9.939406E-01	1.065292	1.028262
1.038539	1.152570	1.144485	1.085982
1.068316	1.052236	1.088445	1.052743
1.078273	1.049927	1.014927	1.132474
1.091274	1.117049	1.121627	1.096303
1.109313	1.112770	1.118885	1.055501
1.019678	1.027945	1.076688	1.145859
1.209202	9.937201E-01	1.117168	1.099066
1.067919	1.193063	9.653108E-01	1.175126

1.086160	1.040010		
ANNUAL MAX UPSTREAM DISCHARGE LAST RUN = 168718.900000			
168469.100000			
172411.800000	181716.900000	162947.700000	160218.300000
156320.100000	156990.500000	155620.100000	180691.500000
167471.300000	163707.000000	150757.300000	196746.000000
183788.700000	166130.700000	162270.300000	192664.700000
153764.100000	201669.900000	153404.000000	167332.500000
176479.700000	160804.600000	157356.800000	176649.400000
148858.600000	173534.000000	151301.700000	191122.500000
167041.100000	168920.500000	175107.800000	183932.300000
180960.100000	153710.800000	153378.900000	151216.800000
171802.800000	180439.000000	168844.900000	180831.400000
149138.700000	147156.000000	158702.200000	180633.600000
175237.600000	168159.200000	178409.300000	165845.100000
159199.300000	187783.500000	158894.200000	180260.900000
169255.800000	170983.000000	179399.400000	164515.000000
171253.000000	164247.700000	174139.600000	169100.300000
156644.400000	182169.000000	162621.400000	153408.300000
154365.700000	157306.100000	166521.300000	186364.900000
182343.500000	167571.700000	148450.700000	156995.300000
149865.300000	171486.700000	170438.100000	186855.600000
164504.800000	158882.700000	155233.700000	183728.100000
155151.800000	155001.500000	178533.900000	165892.200000
181763.300000	161988.400000	178935.700000	163215.500000
153674.000000	161069.300000	163229.100000	184221.700000
166750.800000	156234.900000	183499.800000	187543.200000
170409.400000	153057.100000		
ANNUAL MAX DWNSTREAM DISCHARGE LAST RUN = 165773.000000			
167696.200000			
177459.100000	166158.500000	200283.900000	170374.500000
168939.700000	178733.500000	177786.600000	176563.200000
169417.500000	200280.000000	179151.000000	179332.900000
177346.300000	181356.700000	180127.100000	186925.200000
168306.400000	175002.500000	177814.500000	174446.500000
179683.300000	176718.900000	156416.000000	186593.300000
172212.300000	166493.400000	168926.000000	164891.800000
180778.300000	178967.200000	187892.600000	171078.800000
185138.100000	167545.400000	172365.700000	157013.700000
151401.400000	176306.800000	180839.300000	181036.200000
178908.000000	176872.400000	159074.100000	172348.800000
169600.600000	173774.700000	163148.300000	174265.100000
166705.600000	154806.500000	158873.400000	157185.500000
176675.500000	164076.700000	168220.100000	206526.800000
167154.600000	169632.800000	178822.900000	174422.200000
206457.500000	157730.800000	172431.600000	182212.400000
160759.000000	211024.000000	170237.200000	177922.900000
157548.100000	168808.500000	161342.800000	179240.000000
196824.700000	198290.400000	177784.000000	189105.900000
153694.700000	159845.700000	171449.200000	155912.900000
183224.800000	181967.700000	176804.000000	157184.600000
173345.800000	171945.400000	154879.500000	168332.600000
166539.800000	182220.700000	188590.700000	176143.200000
188165.900000	169542.500000	164638.600000	178708.000000
171794.400000	172166.200000		

ANNUAL MAX UPSTREAM FLOW DEPTH LAST RUN = 13.500000  
13.750000

13.591020	13.750000	13.390770	13.500000
13.750000	13.500000	14.500000	13.500000
13.250000	13.750000	14.000000	13.750000
13.500000	13.750000	13.750000	13.250000
13.750000	13.750000	14.000000	14.250000
15.000000	14.000000	13.500000	13.500000
14.000000	14.000000	13.500000	14.250000
13.750000	13.750000	13.500000	13.750000
13.750000	13.750000	14.000000	13.750000
13.750000	13.750000	13.750000	14.000000
13.750000	14.000000	13.500000	13.750000
13.781830	13.250000	14.250000	14.000000
13.500000	14.750000	14.000000	14.000000
14.000000	13.750000	14.000000	14.250000
14.000000	14.500000	13.750000	13.750000
14.000000	13.500000	14.000000	14.000000
13.750000	14.000000	13.750000	14.000000
14.000000	14.000000	13.628000	13.628000
13.750000	14.002110	14.250000	13.750000
14.000000	13.750000	14.000000	13.750000
14.000000	13.273480	13.250000	13.750000
13.001940	14.250000	13.750000	13.250000
14.250000	13.250000	13.189790	13.500000
13.423270	13.747820	13.750000	15.000000
13.750000	13.750000		

ANNUAL MAX DWTREEM FLOW DEPTH LAST RUN = 14.750000  
14.750000

14.500000	14.750000	14.250000	14.250000
14.750000	14.250000	14.750000	14.500000
14.750000	14.750000	14.750000	14.750000
15.250000	15.250000	15.500000	14.250000
14.750000	14.750000	15.000000	14.500000
15.250000	14.750000	15.000000	14.500000
14.500000	14.500000	14.500000	15.000000
14.750000	15.000000	14.750000	14.500000
14.500000	14.500000	14.750000	14.500000
14.750000	15.000000	14.500000	14.500000
14.250000	14.750000	14.500000	14.500000
14.500000	14.250000	14.750000	14.750000
15.000000	15.000000	15.500000	14.250000
14.750000	14.750000	15.000000	14.750000
14.500000	15.250000	14.750000	14.500000
14.500000	15.000000	14.750000	14.750000
14.500000	15.000000	14.750000	15.000000
14.500000	14.750000	14.250000	15.000000
14.250000	15.000000	14.750000	14.750000
14.750000	14.000000	14.750000	15.000000
15.000000	15.250000	14.750000	14.250000
14.500000	15.000000	15.000000	14.000000
14.500000	14.500000	14.750000	14.500000
14.250000	14.500000	15.000000	15.000000
15.000000	15.250000		

ANNUAL MAX US ADJ. FLOW DEPTH LAST RUN = 13.500000  
13.750000

13.591020	13.750000	13.390770	13.500000
-----------	-----------	-----------	-----------

13.750000	13.500000	14.500000	13.500000
13.250000	13.750000	14.000000	13.750000
13.500000	13.750000	13.750000	13.250000
13.750000	13.750000	14.000000	14.250000
15.000000	14.000000	13.500000	13.500000
14.000000	14.000000	13.500000	14.250000
13.750000	13.750000	13.500000	13.750000
13.750000	13.750000	14.000000	13.750000
13.750000	13.750000	13.750000	14.000000
13.750000	14.000000	13.500000	13.750000
13.781830	13.250000	14.250000	14.000000
13.500000	14.750000	14.000000	14.000000
14.000000	13.750000	14.000000	14.250000
14.000000	14.500000	13.750000	13.750000
14.000000	13.500000	14.000000	14.000000
13.750000	14.000000	13.750000	14.000000
14.000000	14.000000	13.628000	13.628000
13.750000	14.002110	14.250000	13.750000
14.000000	13.750000	14.000000	13.750000
14.000000	13.273480	13.250000	13.750000
13.001940	14.250000	13.750000	13.250000
14.250000	13.250000	13.189790	13.500000
13.423270	13.747820	13.750000	15.000000
13.750000	13.750000		

ANNUAL MAX DS ADJ. FLOW DEPTH LAST RUN = 14.750000  
14.750000

14.500000	14.750000	14.250000	14.250000
14.750000	14.250000	14.750000	14.500000
14.750000	14.750000	14.750000	14.750000
15.250000	15.250000	15.500000	14.250000
14.750000	14.750000	15.000000	14.500000
15.250000	14.750000	15.000000	14.500000
14.500000	14.500000	14.500000	15.000000
14.750000	15.000000	14.750000	14.500000
14.500000	14.500000	14.750000	14.500000
14.750000	15.000000	14.500000	14.500000
14.250000	14.750000	14.500000	14.500000
14.500000	14.250000	14.750000	14.750000
15.000000	15.000000	15.500000	14.250000
14.750000	14.750000	15.000000	14.750000
14.500000	15.250000	14.750000	14.500000
14.500000	15.000000	14.750000	14.750000
14.500000	15.000000	14.750000	15.000000
14.500000	14.750000	14.250000	15.000000
14.250000	15.000000	14.750000	14.750000
14.750000	14.000000	14.750000	15.000000
15.000000	15.250000	14.750000	14.250000
14.500000	15.000000	15.000000	14.000000
14.500000	14.500000	14.750000	14.500000
14.250000	14.500000	15.000000	15.000000
15.000000	15.250000		

The no.of storms in the last.NS= 79  
The no.of storms producing no runoff over the simula tion.NORUN=  
4828219

The number of 6 hr storms in YRS is = 61

643



[illegible]

B	FD	PRD	CPRD
1.0000	.0000	.0000	.0000
1.5000	.0000	.0000	.0000
2.0000	.0000	.0000	.0000
2.5000	.0000	.0000	.0000
3.0000	.0000	.0000	.0000
3.5000	.0000	.0000	.0000
4.0000	.0000	.0000	.0000
4.5000	.0000	.0000	.0000
5.0000	.0000	.0000	.0000
5.5000	.0000	.0000	.0000
6.0000	.0000	.0000	.0000
6.5000	.0000	.0000	.0000
7.0000	.0000	.0000	.0000
7.5000	.0000	.0000	.0000
8.0000	.0000	.0000	.0000
8.5000	.0000	.0000	.0000
9.0000	.0000	.0000	.0000
9.5000	.0000	.0000	.0000
10.0000	.0000	.0000	.0000
10.5000	.0000	.0000	.0000
11.0000	.0000	.0000	.0000
11.5000	.0000	.0000	.0000
12.0000	.0000	.0000	.0000
12.5000	.0000	.0000	.0000
13.0000	.0000	.0000	.0000
13.5000	.0000	.0000	.0000
14.0000	.0000	.0000	.0000
14.5000	.0000	.0000	.0000
15.0000	.0000	.0000	.0000
15.5000	.0000	.0000	.0000
16.0000	.0000	.0000	.0000
16.5000	.0000	.0000	.0000
17.0000	.0000	.0000	.0000
17.5000	.0000	.0000	.0000

18.0000	.0000	.0000	.0000
18.5000	.0000	.0000	.0000
19.0000	.0000	.0000	.0000
19.5000	.0000	.0000	.0000
20.0000	1000.0000	1.0000	1.0000
20.5000	.0000	.0000	1.0000
21.0000	.0000	.0000	1.0000
21.5000	.0000	.0000	1.0000
22.0000	.0000	.0000	1.0000
22.5000	.0000	.0000	1.0000
23.0000	.0000	.0000	1.0000
23.5000	.0000	.0000	1.0000
24.0000	.0000	.0000	1.0000
24.5000	.0000	.0000	1.0000
25.0000	.0000	.0000	1.0000
25.5000	.0000	.0000	1.0000
26.0000	.0000	.0000	1.0000
26.5000	.0000	.0000	1.0000
27.0000	.0000	.0000	1.0000
27.5000	.0000	.0000	1.0000
28.0000	.0000	.0000	1.0000
28.5000	.0000	.0000	1.0000
29.0000	.0000	.0000	1.0000
29.5000	.0000	.0000	1.0000
30.0000	.0000	.0000	1.0000
30.5000	.0000	.0000	1.0000
31.0000	.0000	.0000	1.0000
31.5000	.0000	.0000	1.0000
32.0000	.0000	.0000	1.0000
32.5000	.0000	.0000	1.0000
33.0000	.0000	.0000	1.0000
33.5000	.0000	.0000	1.0000
34.0000	.0000	.0000	1.0000
34.5000	.0000	.0000	1.0000
35.0000	.0000	.0000	1.0000
35.5000	.0000	.0000	1.0000
36.0000	.0000	.0000	1.0000
36.5000	.0000	.0000	1.0000
37.0000	.0000	.0000	1.0000
37.5000	.0000	.0000	1.0000
38.0000	.0000	.0000	1.0000
38.5000	.0000	.0000	1.0000
39.0000	.0000	.0000	1.0000
39.5000	.0000	.0000	1.0000
40.0000	.0000	.0000	1.0000
40.5000	.0000	.0000	1.0000
41.0000	.0000	.0000	1.0000
41.5000	.0000	.0000	1.0000
42.0000	.0000	.0000	1.0000
42.5000	.0000	.0000	1.0000
43.0000	.0000	.0000	1.0000
43.5000	.0000	.0000	1.0000
44.0000	.0000	.0000	1.0000
44.5000	.0000	.0000	1.0000
45.0000	.0000	.0000	1.0000
45.5000	.0000	.0000	1.0000
46.0000	.0000	.0000	1.0000



46.5000	.0000	.0000	1.0000
47.0000	.0000	.0000	1.0000
47.5000	.0000	.0000	1.0000
48.0000	.0000	.0000	1.0000
48.5000	.0000	.0000	1.0000
49.0000	.0000	.0000	1.0000
49.5000	.0000	.0000	1.0000
50.0000	.0000	.0000	1.0000
50.5000	.0000	.0000	1.0000
B	FU	PRU	CPRU
1.0000	1000.0000	1.0000	1.0000
1.5000	.0000	.0000	1.0000
2.0000	.0000	.0000	1.0000
2.5000	.0000	.0000	1.0000
3.0000	.0000	.0000	1.0000
3.5000	.0000	.0000	1.0000
4.0000	.0000	.0000	1.0000
4.5000	.0000	.0000	1.0000
5.0000	.0000	.0000	1.0000
5.5000	.0000	.0000	1.0000
6.0000	.0000	.0000	1.0000
6.5000	.0000	.0000	1.0000
7.0000	.0000	.0000	1.0000
7.5000	.0000	.0000	1.0000
8.0000	.0000	.0000	1.0000
8.5000	.0000	.0000	1.0000
9.0000	.0000	.0000	1.0000
9.5000	.0000	.0000	1.0000
10.0000	.0000	.0000	1.0000
10.5000	.0000	.0000	1.0000
11.0000	.0000	.0000	1.0000
11.5000	.0000	.0000	1.0000
12.0000	.0000	.0000	1.0000
12.5000	.0000	.0000	1.0000
13.0000	.0000	.0000	1.0000
13.5000	.0000	.0000	1.0000
14.0000	.0000	.0000	1.0000
14.5000	.0000	.0000	1.0000
15.0000	.0000	.0000	1.0000
15.5000	.0000	.0000	1.0000
16.0000	.0000	.0000	1.0000
16.5000	.0000	.0000	1.0000
17.0000	.0000	.0000	1.0000
17.5000	.0000	.0000	1.0000
18.0000	.0000	.0000	1.0000
18.5000	.0000	.0000	1.0000
19.0000	.0000	.0000	1.0000
19.5000	.0000	.0000	1.0000
20.0000	.0000	.0000	1.0000
20.5000	.0000	.0000	1.0000
21.0000	.0000	.0000	1.0000
21.5000	.0000	.0000	1.0000
22.0000	.0000	.0000	1.0000
22.5000	.0000	.0000	1.0000
23.0000	.0000	.0000	1.0000
23.5000	.0000	.0000	1.0000
24.0000	.0000	.0000	1.0000

24.5000	.0000	.0000	1.0000
25.0000	.0000	.0000	1.0000
25.5000	.0000	.0000	1.0000
26.0000	.0000	.0000	1.0000
26.5000	.0000	.0000	1.0000
27.0000	.0000	.0000	1.0000
27.5000	.0000	.0000	1.0000
28.0000	.0000	.0000	1.0000
28.5000	.0000	.0000	1.0000
29.0000	.0000	.0000	1.0000
29.5000	.0000	.0000	1.0000
30.0000	.0000	.0000	1.0000
30.5000	.0000	.0000	1.0000
31.0000	.0000	.0000	1.0000
31.5000	.0000	.0000	1.0000
32.0000	.0000	.0000	1.0000
32.5000	.0000	.0000	1.0000
33.0000	.0000	.0000	1.0000
33.5000	.0000	.0000	1.0000
34.0000	.0000	.0000	1.0000
34.5000	.0000	.0000	1.0000
35.0000	.0000	.0000	1.0000
35.5000	.0000	.0000	1.0000
36.0000	.0000	.0000	1.0000
36.5000	.0000	.0000	1.0000
37.0000	.0000	.0000	1.0000
37.5000	.0000	.0000	1.0000
38.0000	.0000	.0000	1.0000
38.5000	.0000	.0000	1.0000
39.0000	.0000	.0000	1.0000
39.5000	.0000	.0000	1.0000
40.0000	.0000	.0000	1.0000
40.5000	.0000	.0000	1.0000
41.0000	.0000	.0000	1.0000
41.5000	.0000	.0000	1.0000
42.0000	.0000	.0000	1.0000
42.5000	.0000	.0000	1.0000
43.0000	.0000	.0000	1.0000
43.5000	.0000	.0000	1.0000
44.0000	.0000	.0000	1.0000
44.5000	.0000	.0000	1.0000
45.0000	.0000	.0000	1.0000
45.5000	.0000	.0000	1.0000
46.0000	.0000	.0000	1.0000
46.5000	.0000	.0000	1.0000
47.0000	.0000	.0000	1.0000
47.5000	.0000	.0000	1.0000
48.0000	.0000	.0000	1.0000
48.5000	.0000	.0000	1.0000
49.0000	.0000	.0000	1.0000
49.5000	.0000	.0000	1.0000
50.0000	.0000	.0000	1.0000
50.5000	.0000	.0000	1.0000

15 PERCENT TMS SCOUR RESULTS

B	FD15	PRD15	CPRD15
1.0000	.0000	.0000	.0000
1.5000	.0000	.0000	.0000

2.0000	.0000	.0000	.0000
2.5000	1.0000	.0010	.0010
3.0000	1.0000	.0010	.0020
3.5000	1.0000	.0010	.0030
4.0000	5.0000	.0050	.0080
4.5000	.0000	.0000	.0080
5.0000	.0000	.0000	.0080
5.5000	1.0000	.0010	.0090
6.0000	3.0000	.0030	.0120
6.5000	.0000	.0000	.0120
7.0000	.0000	.0000	.0120
7.5000	.0000	.0000	.0120
8.0000	.0000	.0000	.0120
8.5000	.0000	.0000	.0120
9.0000	.0000	.0000	.0120
9.5000	.0000	.0000	.0120
10.0000	.0000	.0000	.0120
10.5000	.0000	.0000	.0120
11.0000	.0000	.0000	.0120
11.5000	.0000	.0000	.0120
12.0000	.0000	.0000	.0120
12.5000	.0000	.0000	.0120
13.0000	.0000	.0000	.0120
13.5000	.0000	.0000	.0120
14.0000	.0000	.0000	.0120
14.5000	.0000	.0000	.0120
15.0000	1.0000	.0010	.0130
15.5000	.0000	.0000	.0130
16.0000	.0000	.0000	.0130
16.5000	.0000	.0000	.0130
17.0000	.0000	.0000	.0130
17.5000	.0000	.0000	.0130
18.0000	.0000	.0000	.0130
18.5000	2.0000	.0020	.0150
19.0000	5.0000	.0050	.0200
19.5000	977.0000	.9770	.9970
20.0000	3.0000	.0030	1.0000
20.5000	.0000	.0000	1.0000
21.0000	.0000	.0000	1.0000
21.5000	.0000	.0000	1.0000
22.0000	.0000	.0000	1.0000
22.5000	.0000	.0000	1.0000
23.0000	.0000	.0000	1.0000
23.5000	.0000	.0000	1.0000
24.0000	.0000	.0000	1.0000
24.5000	.0000	.0000	1.0000
25.0000	.0000	.0000	1.0000
25.5000	.0000	.0000	1.0000
26.0000	.0000	.0000	1.0000
26.5000	.0000	.0000	1.0000
27.0000	.0000	.0000	1.0000
27.5000	.0000	.0000	1.0000
28.0000	.0000	.0000	1.0000
28.5000	.0000	.0000	1.0000
29.0000	.0000	.0000	1.0000
29.5000	.0000	.0000	1.0000
30.0000	.0000	.0000	1.0000

30.5000	.0000	.0000	1.0000
31.0000	.0000	.0000	1.0000
31.5000	.0000	.0000	1.0000
32.0000	.0000	.0000	1.0000
32.5000	.0000	.0000	1.0000
33.0000	.0000	.0000	1.0000
33.5000	.0000	.0000	1.0000
34.0000	.0000	.0000	1.0000
34.5000	.0000	.0000	1.0000
35.0000	.0000	.0000	1.0000
35.5000	.0000	.0000	1.0000
36.0000	.0000	.0000	1.0000
36.5000	.0000	.0000	1.0000
37.0000	.0000	.0000	1.0000
37.5000	.0000	.0000	1.0000
38.0000	.0000	.0000	1.0000
38.5000	.0000	.0000	1.0000
39.0000	.0000	.0000	1.0000
39.5000	.0000	.0000	1.0000
40.0000	.0000	.0000	1.0000
40.5000	.0000	.0000	1.0000
41.0000	.0000	.0000	1.0000
41.5000	.0000	.0000	1.0000
42.0000	.0000	.0000	1.0000
42.5000	.0000	.0000	1.0000
43.0000	.0000	.0000	1.0000
43.5000	.0000	.0000	1.0000
44.0000	.0000	.0000	1.0000
44.5000	.0000	.0000	1.0000
45.0000	.0000	.0000	1.0000
45.5000	.0000	.0000	1.0000
46.0000	.0000	.0000	1.0000
46.5000	.0000	.0000	1.0000
47.0000	.0000	.0000	1.0000
47.5000	.0000	.0000	1.0000
48.0000	.0000	.0000	1.0000
48.5000	.0000	.0000	1.0000
49.0000	.0000	.0000	1.0000
49.5000	.0000	.0000	1.0000
50.0000	.0000	.0000	1.0000
50.5000	.0000	.0000	1.0000
B	FU15	PRU15	CPRU15
1.0000	1000.0000	1.0000	1.0000
1.5000	.0000	.0000	1.0000
2.0000	.0000	.0000	1.0000
2.5000	.0000	.0000	1.0000
3.0000	.0000	.0000	1.0000
3.5000	.0000	.0000	1.0000
4.0000	.0000	.0000	1.0000
4.5000	.0000	.0000	1.0000
5.0000	.0000	.0000	1.0000
5.5000	.0000	.0000	1.0000
6.0000	.0000	.0000	1.0000
6.5000	.0000	.0000	1.0000
7.0000	.0000	.0000	1.0000
7.5000	.0000	.0000	1.0000
8.0000	.0000	.0000	1.0000

8.5000	.0000	.0000	1.0000
9.0000	.0000	.0000	1.0000
9.5000	.0000	.0000	1.0000
10.0000	.0000	.0000	1.0000
10.5000	.0000	.0000	1.0000
11.0000	.0000	.0000	1.0000
11.5000	.0000	.0000	1.0000
12.0000	.0000	.0000	1.0000
12.5000	.0000	.0000	1.0000
13.0000	.0000	.0000	1.0000
13.5000	.0000	.0000	1.0000
14.0000	.0000	.0000	1.0000
14.5000	.0000	.0000	1.0000
15.0000	.0000	.0000	1.0000
15.5000	.0000	.0000	1.0000
16.0000	.0000	.0000	1.0000
16.5000	.0000	.0000	1.0000
17.0000	.0000	.0000	1.0000
17.5000	.0000	.0000	1.0000
18.0000	.0000	.0000	1.0000
18.5000	.0000	.0000	1.0000
19.0000	.0000	.0000	1.0000
19.5000	.0000	.0000	1.0000
20.0000	.0000	.0000	1.0000
20.5000	.0000	.0000	1.0000
21.0000	.0000	.0000	1.0000
21.5000	.0000	.0000	1.0000
22.0000	.0000	.0000	1.0000
22.5000	.0000	.0000	1.0000
23.0000	.0000	.0000	1.0000
23.5000	.0000	.0000	1.0000
24.0000	.0000	.0000	1.0000
24.5000	.0000	.0000	1.0000
25.0000	.0000	.0000	1.0000
25.5000	.0000	.0000	1.0000
26.0000	.0000	.0000	1.0000
26.5000	.0000	.0000	1.0000
27.0000	.0000	.0000	1.0000
27.5000	.0000	.0000	1.0000
28.0000	.0000	.0000	1.0000
28.5000	.0000	.0000	1.0000
29.0000	.0000	.0000	1.0000
29.5000	.0000	.0000	1.0000
30.0000	.0000	.0000	1.0000
30.5000	.0000	.0000	1.0000
31.0000	.0000	.0000	1.0000
31.5000	.0000	.0000	1.0000
32.0000	.0000	.0000	1.0000
32.5000	.0000	.0000	1.0000
33.0000	.0000	.0000	1.0000
33.5000	.0000	.0000	1.0000
34.0000	.0000	.0000	1.0000
34.5000	.0000	.0000	1.0000
35.0000	.0000	.0000	1.0000
35.5000	.0000	.0000	1.0000
36.0000	.0000	.0000	1.0000
36.5000	.0000	.0000	1.0000

37.0000	.0000	.0000	1.0000
37.5000	.0000	.0000	1.0000
38.0000	.0000	.0000	1.0000
38.5000	.0000	.0000	1.0000
39.0000	.0000	.0000	1.0000
39.5000	.0000	.0000	1.0000
40.0000	.0000	.0000	1.0000
40.5000	.0000	.0000	1.0000
41.0000	.0000	.0000	1.0000
41.5000	.0000	.0000	1.0000
42.0000	.0000	.0000	1.0000
42.5000	.0000	.0000	1.0000
43.0000	.0000	.0000	1.0000
43.5000	.0000	.0000	1.0000
44.0000	.0000	.0000	1.0000
44.5000	.0000	.0000	1.0000
45.0000	.0000	.0000	1.0000
45.5000	.0000	.0000	1.0000
46.0000	.0000	.0000	1.0000
46.5000	.0000	.0000	1.0000
47.0000	.0000	.0000	1.0000
47.5000	.0000	.0000	1.0000
48.0000	.0000	.0000	1.0000
48.5000	.0000	.0000	1.0000
49.0000	.0000	.0000	1.0000
49.5000	.0000	.0000	1.0000
50.0000	.0000	.0000	1.0000
50.5000	.0000	.0000	1.0000

25 PERCENT SCOUR RESULTS

B	FD25	PRD25	CPRD25
1.0000	.0000	.0000	.0000
1.5000	.0000	.0000	.0000
2.0000	.0000	.0000	.0000
2.5000	.0000	.0000	.0000
3.0000	.0000	.0000	.0000
3.5000	.0000	.0000	.0000
4.0000	.0000	.0000	.0000
4.5000	.0000	.0000	.0000
5.0000	.0000	.0000	.0000
5.5000	.0000	.0000	.0000
6.0000	.0000	.0000	.0000
6.5000	.0000	.0000	.0000
7.0000	.0000	.0000	.0000
7.5000	.0000	.0000	.0000
8.0000	.0000	.0000	.0000
8.5000	.0000	.0000	.0000
9.0000	.0000	.0000	.0000
9.5000	.0000	.0000	.0000
10.0000	.0000	.0000	.0000
10.5000	.0000	.0000	.0000
11.0000	.0000	.0000	.0000
11.5000	.0000	.0000	.0000
12.0000	.0000	.0000	.0000
12.5000	.0000	.0000	.0000
13.0000	.0000	.0000	.0000
13.5000	.0000	.0000	.0000
14.0000	.0000	.0000	.0000

14.5000	.0000	.0000	.0000
15.0000	.0000	.0000	.0000
15.5000	.0000	.0000	.0000
16.0000	.0000	.0000	.0000
16.5000	.0000	.0000	.0000
17.0000	.0000	.0000	.0000
17.5000	.0000	.0000	.0000
18.0000	.0000	.0000	.0000
18.5000	.0000	.0000	.0000
19.0000	.0000	.0000	.0000
19.5000	593.0000	.5930	.5930
20.0000	407.0000	.4070	1.0000
20.5000	.0000	.0000	1.0000
21.0000	.0000	.0000	1.0000
21.5000	.0000	.0000	1.0000
22.0000	.0000	.0000	1.0000
22.5000	.0000	.0000	1.0000
23.0000	.0000	.0000	1.0000
23.5000	.0000	.0000	1.0000
24.0000	.0000	.0000	1.0000
24.5000	.0000	.0000	1.0000
25.0000	.0000	.0000	1.0000
25.5000	.0000	.0000	1.0000
26.0000	.0000	.0000	1.0000
26.5000	.0000	.0000	1.0000
27.0000	.0000	.0000	1.0000
27.5000	.0000	.0000	1.0000
28.0000	.0000	.0000	1.0000
28.5000	.0000	.0000	1.0000
29.0000	.0000	.0000	1.0000
29.5000	.0000	.0000	1.0000
30.0000	.0000	.0000	1.0000
30.5000	.0000	.0000	1.0000
31.0000	.0000	.0000	1.0000
31.5000	.0000	.0000	1.0000
32.0000	.0000	.0000	1.0000
32.5000	.0000	.0000	1.0000
33.0000	.0000	.0000	1.0000
33.5000	.0000	.0000	1.0000
34.0000	.0000	.0000	1.0000
34.5000	.0000	.0000	1.0000
35.0000	.0000	.0000	1.0000
35.5000	.0000	.0000	1.0000
36.0000	.0000	.0000	1.0000
36.5000	.0000	.0000	1.0000
37.0000	.0000	.0000	1.0000
37.5000	.0000	.0000	1.0000
38.0000	.0000	.0000	1.0000
38.5000	.0000	.0000	1.0000
39.0000	.0000	.0000	1.0000
39.5000	.0000	.0000	1.0000
40.0000	.0000	.0000	1.0000
40.5000	.0000	.0000	1.0000
41.0000	.0000	.0000	1.0000
41.5000	.0000	.0000	1.0000
42.0000	.0000	.0000	1.0000
42.5000	.0000	.0000	1.0000

43.0000	.0000	.0000	1.0000
43.5000	.0000	.0000	1.0000
44.0000	.0000	.0000	1.0000
44.5000	.0000	.0000	1.0000
45.0000	.0000	.0000	1.0000
45.5000	.0000	.0000	1.0000
46.0000	.0000	.0000	1.0000
46.5000	.0000	.0000	1.0000
47.0000	.0000	.0000	1.0000
47.5000	.0000	.0000	1.0000
48.0000	.0000	.0000	1.0000
48.5000	.0000	.0000	1.0000
49.0000	.0000	.0000	1.0000
49.5000	.0000	.0000	1.0000
50.0000	.0000	.0000	1.0000
50.5000	.0000	.0000	1.0000
B	FU25	PRU25	CPRU25
1.0000	1000.0000	1.0000	1.0000
1.5000	.0000	.0000	1.0000
2.0000	.0000	.0000	1.0000
2.5000	.0000	.0000	1.0000
3.0000	.0000	.0000	1.0000
3.5000	.0000	.0000	1.0000
4.0000	.0000	.0000	1.0000
4.5000	.0000	.0000	1.0000
5.0000	.0000	.0000	1.0000
5.5000	.0000	.0000	1.0000
6.0000	.0000	.0000	1.0000
6.5000	.0000	.0000	1.0000
7.0000	.0000	.0000	1.0000
7.5000	.0000	.0000	1.0000
8.0000	.0000	.0000	1.0000
8.5000	.0000	.0000	1.0000
9.0000	.0000	.0000	1.0000
9.5000	.0000	.0000	1.0000
10.0000	.0000	.0000	1.0000
10.5000	.0000	.0000	1.0000
11.0000	.0000	.0000	1.0000
11.5000	.0000	.0000	1.0000
12.0000	.0000	.0000	1.0000
12.5000	.0000	.0000	1.0000
13.0000	.0000	.0000	1.0000
13.5000	.0000	.0000	1.0000
14.0000	.0000	.0000	1.0000
14.5000	.0000	.0000	1.0000
15.0000	.0000	.0000	1.0000
15.5000	.0000	.0000	1.0000
16.0000	.0000	.0000	1.0000
16.5000	.0000	.0000	1.0000
17.0000	.0000	.0000	1.0000
17.5000	.0000	.0000	1.0000
18.0000	.0000	.0000	1.0000
18.5000	.0000	.0000	1.0000
19.0000	.0000	.0000	1.0000
19.5000	.0000	.0000	1.0000
20.0000	.0000	.0000	1.0000
20.5000	.0000	.0000	1.0000



21.0000	.0000	.0000	1.0000
21.5000	.0000	.0000	1.0000
22.0000	.0000	.0000	1.0000
22.5000	.0000	.0000	1.0000
23.0000	.0000	.0000	1.0000
23.5000	.0000	.0000	1.0000
24.0000	.0000	.0000	1.0000
24.5000	.0000	.0000	1.0000
25.0000	.0000	.0000	1.0000
25.5000	.0000	.0000	1.0000
26.0000	.0000	.0000	1.0000
26.5000	.0000	.0000	1.0000
27.0000	.0000	.0000	1.0000
27.5000	.0000	.0000	1.0000
28.0000	.0000	.0000	1.0000
28.5000	.0000	.0000	1.0000
29.0000	.0000	.0000	1.0000
29.5000	.0000	.0000	1.0000
30.0000	.0000	.0000	1.0000
30.5000	.0000	.0000	1.0000
31.0000	.0000	.0000	1.0000
31.5000	.0000	.0000	1.0000
32.0000	.0000	.0000	1.0000
32.5000	.0000	.0000	1.0000
33.0000	.0000	.0000	1.0000
33.5000	.0000	.0000	1.0000
34.0000	.0000	.0000	1.0000
34.5000	.0000	.0000	1.0000
35.0000	.0000	.0000	1.0000
35.5000	.0000	.0000	1.0000
36.0000	.0000	.0000	1.0000
36.5000	.0000	.0000	1.0000
37.0000	.0000	.0000	1.0000
37.5000	.0000	.0000	1.0000
38.0000	.0000	.0000	1.0000
38.5000	.0000	.0000	1.0000
39.0000	.0000	.0000	1.0000
39.5000	.0000	.0000	1.0000
40.0000	.0000	.0000	1.0000
40.5000	.0000	.0000	1.0000
41.0000	.0000	.0000	1.0000
41.5000	.0000	.0000	1.0000
42.0000	.0000	.0000	1.0000
42.5000	.0000	.0000	1.0000
43.0000	.0000	.0000	1.0000
43.5000	.0000	.0000	1.0000
44.0000	.0000	.0000	1.0000
44.5000	.0000	.0000	1.0000
45.0000	.0000	.0000	1.0000
45.5000	.0000	.0000	1.0000
46.0000	.0000	.0000	1.0000
46.5000	.0000	.0000	1.0000
47.0000	.0000	.0000	1.0000
47.5000	.0000	.0000	1.0000
48.0000	.0000	.0000	1.0000
48.5000	.0000	.0000	1.0000
49.0000	.0000	.0000	1.0000

49.5000	.0000	.0000	1.0000
50.0000	.0000	.0000	1.0000
50.5000	.0000	.0000	1.0000
50 PERCENT TMS SCOUR RESULTS			
B	FD50	PRD50	CPRD50
1.0000	.0000	.0000	.0000
1.5000	.0000	.0000	.0000
2.0000	.0000	.0000	.0000
2.5000	.0000	.0000	.0000
3.0000	.0000	.0000	.0000
3.5000	.0000	.0000	.0000
4.0000	.0000	.0000	.0000
4.5000	.0000	.0000	.0000
5.0000	.0000	.0000	.0000
5.5000	.0000	.0000	.0000
6.0000	.0000	.0000	.0000
6.5000	.0000	.0000	.0000
7.0000	.0000	.0000	.0000
7.5000	.0000	.0000	.0000
8.0000	.0000	.0000	.0000
8.5000	.0000	.0000	.0000
9.0000	.0000	.0000	.0000
9.5000	.0000	.0000	.0000
10.0000	.0000	.0000	.0000
10.5000	.0000	.0000	.0000
11.0000	.0000	.0000	.0000
11.5000	.0000	.0000	.0000
12.0000	.0000	.0000	.0000
12.5000	.0000	.0000	.0000
13.0000	.0000	.0000	.0000
13.5000	.0000	.0000	.0000
14.0000	.0000	.0000	.0000
14.5000	.0000	.0000	.0000
15.0000	.0000	.0000	.0000
15.5000	.0000	.0000	.0000
16.0000	.0000	.0000	.0000
16.5000	.0000	.0000	.0000
17.0000	.0000	.0000	.0000
17.5000	.0000	.0000	.0000
18.0000	.0000	.0000	.0000
18.5000	.0000	.0000	.0000
19.0000	.0000	.0000	.0000
19.5000	.0000	.0000	.0000
20.0000	1000.0000	1.0000	1.0000
20.5000	.0000	.0000	1.0000
21.0000	.0000	.0000	1.0000
21.5000	.0000	.0000	1.0000
22.0000	.0000	.0000	1.0000
22.5000	.0000	.0000	1.0000
23.0000	.0000	.0000	1.0000
23.5000	.0000	.0000	1.0000
24.0000	.0000	.0000	1.0000
24.5000	.0000	.0000	1.0000
25.0000	.0000	.0000	1.0000
25.5000	.0000	.0000	1.0000
26.0000	.0000	.0000	1.0000
26.5000	.0000	.0000	1.0000

27.0000	.0000	.0000	1.0000
27.5000	.0000	.0000	1.0000
28.0000	.0000	.0000	1.0000
28.5000	.0000	.0000	1.0000
29.0000	.0000	.0000	1.0000
29.5000	.0000	.0000	1.0000
30.0000	.0000	.0000	1.0000
30.5000	.0000	.0000	1.0000
31.0000	.0000	.0000	1.0000
31.5000	.0000	.0000	1.0000
32.0000	.0000	.0000	1.0000
32.5000	.0000	.0000	1.0000
33.0000	.0000	.0000	1.0000
33.5000	.0000	.0000	1.0000
34.0000	.0000	.0000	1.0000
34.5000	.0000	.0000	1.0000
35.0000	.0000	.0000	1.0000
35.5000	.0000	.0000	1.0000
36.0000	.0000	.0000	1.0000
36.5000	.0000	.0000	1.0000
37.0000	.0000	.0000	1.0000
37.5000	.0000	.0000	1.0000
38.0000	.0000	.0000	1.0000
38.5000	.0000	.0000	1.0000
39.0000	.0000	.0000	1.0000
39.5000	.0000	.0000	1.0000
40.0000	.0000	.0000	1.0000
40.5000	.0000	.0000	1.0000
41.0000	.0000	.0000	1.0000
41.5000	.0000	.0000	1.0000
42.0000	.0000	.0000	1.0000
42.5000	.0000	.0000	1.0000
43.0000	.0000	.0000	1.0000
43.5000	.0000	.0000	1.0000
44.0000	.0000	.0000	1.0000
44.5000	.0000	.0000	1.0000
45.0000	.0000	.0000	1.0000
45.5000	.0000	.0000	1.0000
46.0000	.0000	.0000	1.0000
46.5000	.0000	.0000	1.0000
47.0000	.0000	.0000	1.0000
47.5000	.0000	.0000	1.0000
48.0000	.0000	.0000	1.0000
48.5000	.0000	.0000	1.0000
49.0000	.0000	.0000	1.0000
49.5000	.0000	.0000	1.0000
50.0000	.0000	.0000	1.0000
50.5000	.0000	.0000	1.0000
B	FU50	PRU50	CPRU50
1.0000	1000.0000	1.0000	1.0000
1.5000	.0000	.0000	1.0000
2.0000	.0000	.0000	1.0000
2.5000	.0000	.0000	1.0000
3.0000	.0000	.0000	1.0000
3.5000	.0000	.0000	1.0000
4.0000	.0000	.0000	1.0000
4.5000	.0000	.0000	1.0000

5.0000	.0000	.0000	1.0000
5.5000	.0000	.0000	1.0000
6.0000	.0000	.0000	1.0000
6.5000	.0000	.0000	1.0000
7.0000	.0000	.0000	1.0000
7.5000	.0000	.0000	1.0000
8.0000	.0000	.0000	1.0000
8.5000	.0000	.0000	1.0000
9.0000	.0000	.0000	1.0000
9.5000	.0000	.0000	1.0000
10.0000	.0000	.0000	1.0000
10.5000	.0000	.0000	1.0000
11.0000	.0000	.0000	1.0000
11.5000	.0000	.0000	1.0000
12.0000	.0000	.0000	1.0000
12.5000	.0000	.0000	1.0000
13.0000	.0000	.0000	1.0000
13.5000	.0000	.0000	1.0000
14.0000	.0000	.0000	1.0000
14.5000	.0000	.0000	1.0000
15.0000	.0000	.0000	1.0000
15.5000	.0000	.0000	1.0000
16.0000	.0000	.0000	1.0000
16.5000	.0000	.0000	1.0000
17.0000	.0000	.0000	1.0000
17.5000	.0000	.0000	1.0000
18.0000	.0000	.0000	1.0000
18.5000	.0000	.0000	1.0000
19.0000	.0000	.0000	1.0000
19.5000	.0000	.0000	1.0000
20.0000	.0000	.0000	1.0000
20.5000	.0000	.0000	1.0000
21.0000	.0000	.0000	1.0000
21.5000	.0000	.0000	1.0000
22.0000	.0000	.0000	1.0000
22.5000	.0000	.0000	1.0000
23.0000	.0000	.0000	1.0000
23.5000	.0000	.0000	1.0000
24.0000	.0000	.0000	1.0000
24.5000	.0000	.0000	1.0000
25.0000	.0000	.0000	1.0000
25.5000	.0000	.0000	1.0000
26.0000	.0000	.0000	1.0000
26.5000	.0000	.0000	1.0000
27.0000	.0000	.0000	1.0000
27.5000	.0000	.0000	1.0000
28.0000	.0000	.0000	1.0000
28.5000	.0000	.0000	1.0000
29.0000	.0000	.0000	1.0000
29.5000	.0000	.0000	1.0000
30.0000	.0000	.0000	1.0000
30.5000	.0000	.0000	1.0000
31.0000	.0000	.0000	1.0000
31.5000	.0000	.0000	1.0000
32.0000	.0000	.0000	1.0000
32.5000	.0000	.0000	1.0000
33.0000	.0000	.0000	1.0000

33.5000	.0000	.0000	1.0000
34.0000	.0000	.0000	1.0000
34.5000	.0000	.0000	1.0000
35.0000	.0000	.0000	1.0000
35.5000	.0000	.0000	1.0000
36.0000	.0000	.0000	1.0000
36.5000	.0000	.0000	1.0000
37.0000	.0000	.0000	1.0000
37.5000	.0000	.0000	1.0000
38.0000	.0000	.0000	1.0000
38.5000	.0000	.0000	1.0000
39.0000	.0000	.0000	1.0000
39.5000	.0000	.0000	1.0000
40.0000	.0000	.0000	1.0000
40.5000	.0000	.0000	1.0000
41.0000	.0000	.0000	1.0000
41.5000	.0000	.0000	1.0000
42.0000	.0000	.0000	1.0000
42.5000	.0000	.0000	1.0000
43.0000	.0000	.0000	1.0000
43.5000	.0000	.0000	1.0000
44.0000	.0000	.0000	1.0000
44.5000	.0000	.0000	1.0000
45.0000	.0000	.0000	1.0000
45.5000	.0000	.0000	1.0000
46.0000	.0000	.0000	1.0000
46.5000	.0000	.0000	1.0000
47.0000	.0000	.0000	1.0000
47.5000	.0000	.0000	1.0000
48.0000	.0000	.0000	1.0000
48.5000	.0000	.0000	1.0000
49.0000	.0000	.0000	1.0000
49.5000	.0000	.0000	1.0000
50.0000	.0000	.0000	1.0000
50.5000	.0000	.0000	1.0000

75 PERCENT TMS SCOUR RESULTS

B	FD75	PRD75	CPRD75
1.0000	.0000	.0000	.0000
1.5000	.0000	.0000	.0000
2.0000	.0000	.0000	.0000
2.5000	.0000	.0000	.0000
3.0000	.0000	.0000	.0000
3.5000	.0000	.0000	.0000
4.0000	.0000	.0000	.0000
4.5000	.0000	.0000	.0000
5.0000	.0000	.0000	.0000
5.5000	.0000	.0000	.0000
6.0000	.0000	.0000	.0000
6.5000	.0000	.0000	.0000
7.0000	.0000	.0000	.0000
7.5000	.0000	.0000	.0000
8.0000	.0000	.0000	.0000
8.5000	.0000	.0000	.0000
9.0000	.0000	.0000	.0000
9.5000	.0000	.0000	.0000
10.0000	.0000	.0000	.0000
10.5000	.0000	.0000	.0000

11.0000	.0000	.0000	.0000
11.5000	.0000	.0000	.0000
12.0000	.0000	.0000	.0000
12.5000	.0000	.0000	.0000
13.0000	.0000	.0000	.0000
13.5000	.0000	.0000	.0000
14.0000	.0000	.0000	.0000
14.5000	.0000	.0000	.0000
15.0000	.0000	.0000	.0000
15.5000	.0000	.0000	.0000
16.0000	.0000	.0000	.0000
16.5000	.0000	.0000	.0000
17.0000	.0000	.0000	.0000
17.5000	.0000	.0000	.0000
18.0000	.0000	.0000	.0000
18.5000	.0000	.0000	.0000
19.0000	.0000	.0000	.0000
19.5000	.0000	.0000	.0000
20.0000	1000.0000	1.0000	1.0000
20.5000	.0000	.0000	1.0000
21.0000	.0000	.0000	1.0000
21.5000	.0000	.0000	1.0000
22.0000	.0000	.0000	1.0000
22.5000	.0000	.0000	1.0000
23.0000	.0000	.0000	1.0000
23.5000	.0000	.0000	1.0000
24.0000	.0000	.0000	1.0000
24.5000	.0000	.0000	1.0000
25.0000	.0000	.0000	1.0000
25.5000	.0000	.0000	1.0000
26.0000	.0000	.0000	1.0000
26.5000	.0000	.0000	1.0000
27.0000	.0000	.0000	1.0000
27.5000	.0000	.0000	1.0000
28.0000	.0000	.0000	1.0000
28.5000	.0000	.0000	1.0000
29.0000	.0000	.0000	1.0000
29.5000	.0000	.0000	1.0000
30.0000	.0000	.0000	1.0000
30.5000	.0000	.0000	1.0000
31.0000	.0000	.0000	1.0000
31.5000	.0000	.0000	1.0000
32.0000	.0000	.0000	1.0000
32.5000	.0000	.0000	1.0000
33.0000	.0000	.0000	1.0000
33.5000	.0000	.0000	1.0000
34.0000	.0000	.0000	1.0000
34.5000	.0000	.0000	1.0000
35.0000	.0000	.0000	1.0000
35.5000	.0000	.0000	1.0000
36.0000	.0000	.0000	1.0000
36.5000	.0000	.0000	1.0000
37.0000	.0000	.0000	1.0000
37.5000	.0000	.0000	1.0000
38.0000	.0000	.0000	1.0000
38.5000	.0000	.0000	1.0000
39.0000	.0000	.0000	1.0000

39.5000	.0000	.0000	1.0000
40.0000	.0000	.0000	1.0000
40.5000	.0000	.0000	1.0000
41.0000	.0000	.0000	1.0000
41.5000	.0000	.0000	1.0000
42.0000	.0000	.0000	1.0000
42.5000	.0000	.0000	1.0000
43.0000	.0000	.0000	1.0000
43.5000	.0000	.0000	1.0000
44.0000	.0000	.0000	1.0000
44.5000	.0000	.0000	1.0000
45.0000	.0000	.0000	1.0000
45.5000	.0000	.0000	1.0000
46.0000	.0000	.0000	1.0000
46.5000	.0000	.0000	1.0000
47.0000	.0000	.0000	1.0000
47.5000	.0000	.0000	1.0000
48.0000	.0000	.0000	1.0000
48.5000	.0000	.0000	1.0000
49.0000	.0000	.0000	1.0000
49.5000	.0000	.0000	1.0000
50.0000	.0000	.0000	1.0000
50.5000	.0000	.0000	1.0000
B	FU75	PRU75	CPRU75
1.0000	1000.0000	1.0000	1.0000
1.5000	.0000	.0000	1.0000
2.0000	.0000	.0000	1.0000
2.5000	.0000	.0000	1.0000
3.0000	.0000	.0000	1.0000
3.5000	.0000	.0000	1.0000
4.0000	.0000	.0000	1.0000
4.5000	.0000	.0000	1.0000
5.0000	.0000	.0000	1.0000
5.5000	.0000	.0000	1.0000
6.0000	.0000	.0000	1.0000
6.5000	.0000	.0000	1.0000
7.0000	.0000	.0000	1.0000
7.5000	.0000	.0000	1.0000
8.0000	.0000	.0000	1.0000
8.5000	.0000	.0000	1.0000
9.0000	.0000	.0000	1.0000
9.5000	.0000	.0000	1.0000
10.0000	.0000	.0000	1.0000
10.5000	.0000	.0000	1.0000
11.0000	.0000	.0000	1.0000
11.5000	.0000	.0000	1.0000
12.0000	.0000	.0000	1.0000
12.5000	.0000	.0000	1.0000
13.0000	.0000	.0000	1.0000
13.5000	.0000	.0000	1.0000
14.0000	.0000	.0000	1.0000
14.5000	.0000	.0000	1.0000
15.0000	.0000	.0000	1.0000
15.5000	.0000	.0000	1.0000
16.0000	.0000	.0000	1.0000
16.5000	.0000	.0000	1.0000
17.0000	.0000	.0000	1.0000

17.5000	.0000	.0000	1.0000
18.0000	.0000	.0000	1.0000
18.5000	.0000	.0000	1.0000
19.0000	.0000	.0000	1.0000
19.5000	.0000	.0000	1.0000
20.0000	.0000	.0000	1.0000
20.5000	.0000	.0000	1.0000
21.0000	.0000	.0000	1.0000
21.5000	.0000	.0000	1.0000
22.0000	.0000	.0000	1.0000
22.5000	.0000	.0000	1.0000
23.0000	.0000	.0000	1.0000
23.5000	.0000	.0000	1.0000
24.0000	.0000	.0000	1.0000
24.5000	.0000	.0000	1.0000
25.0000	.0000	.0000	1.0000
25.5000	.0000	.0000	1.0000
26.0000	.0000	.0000	1.0000
26.5000	.0000	.0000	1.0000
27.0000	.0000	.0000	1.0000
27.5000	.0000	.0000	1.0000
28.0000	.0000	.0000	1.0000
28.5000	.0000	.0000	1.0000
29.0000	.0000	.0000	1.0000
29.5000	.0000	.0000	1.0000
30.0000	.0000	.0000	1.0000
30.5000	.0000	.0000	1.0000
31.0000	.0000	.0000	1.0000
31.5000	.0000	.0000	1.0000
32.0000	.0000	.0000	1.0000
32.5000	.0000	.0000	1.0000
33.0000	.0000	.0000	1.0000
33.5000	.0000	.0000	1.0000
34.0000	.0000	.0000	1.0000
34.5000	.0000	.0000	1.0000
35.0000	.0000	.0000	1.0000
35.5000	.0000	.0000	1.0000
36.0000	.0000	.0000	1.0000
36.5000	.0000	.0000	1.0000
37.0000	.0000	.0000	1.0000
37.5000	.0000	.0000	1.0000
38.0000	.0000	.0000	1.0000
38.5000	.0000	.0000	1.0000
39.0000	.0000	.0000	1.0000
39.5000	.0000	.0000	1.0000
40.0000	.0000	.0000	1.0000
40.5000	.0000	.0000	1.0000
41.0000	.0000	.0000	1.0000
41.5000	.0000	.0000	1.0000
42.0000	.0000	.0000	1.0000
42.5000	.0000	.0000	1.0000
43.0000	.0000	.0000	1.0000
43.5000	.0000	.0000	1.0000
44.0000	.0000	.0000	1.0000
44.5000	.0000	.0000	1.0000
45.0000	.0000	.0000	1.0000
45.5000	.0000	.0000	1.0000



46.0000	.0000	.0000	1.0000
46.5000	.0000	.0000	1.0000
47.0000	.0000	.0000	1.0000
47.5000	.0000	.0000	1.0000
48.0000	.0000	.0000	1.0000
48.5000	.0000	.0000	1.0000
49.0000	.0000	.0000	1.0000
49.5000	.0000	.0000	1.0000
50.0000	.0000	.0000	1.0000
50.5000	.0000	.0000	1.0000

The mean annual contraction scour d/s face is MNYYS

The mean annual scour value d/s face is MNLTS

The mean annual total scour d/s face is YMNTS

The standard dev in annual scour d/s face is YSTTS

YR	MNYYS	MNLTS	YMNTS	YSTTS
001	.0000	.1002	.1002	.0534
002	.0000	.2092	.2092	.0807
003	.0000	.3336	.3336	.1140
004	.0000	.4779	.4779	.1479
005	.0000	.6462	.6462	.1957
006	.0000	.8498	.8498	.2596
007	.0000	1.1107	1.1107	.3654
008	.0000	1.4815	1.4815	.7579
009	.0000	2.2031	2.2031	2.0973
010	.0000	3.9685	3.9685	4.5648
011	.0000	7.8372	7.8372	7.2271
012	.0000	12.6505	12.6505	7.6422
013	.0000	16.2876	16.2876	5.9488
014	.0000	18.4215	18.4215	3.4426
015	.0000	19.1307	19.1307	1.6714
016	.0000	19.3191	19.3191	.7409
017	.0000	19.3874	19.3874	.0597
018	.0000	19.4089	19.4089	.0500
019	.0000	19.4257	19.4257	.0511
020	.0000	19.4410	19.4410	.0465
021	.0000	19.4535	19.4535	.0409
022	.0000	19.4649	19.4649	.0464
023	.0000	19.4747	19.4747	.0370
024	.0000	19.4838	19.4838	.0414
025	.0000	19.4917	19.4917	.0397
026	.0000	19.4994	19.4994	.0436
027	.0000	19.5065	19.5065	.0463
028	.0000	19.5133	19.5133	.0430
029	.0000	19.5193	19.5193	.0352
030	.0000	19.5248	19.5248	.0384
031	.0000	19.5300	19.5300	.0373
032	.0000	19.5346	19.5346	.0377
033	.0000	19.5389	19.5389	.0374
034	.0000	19.5433	19.5433	.0327
035	.0000	19.5472	19.5472	.0394
036	.0000	19.5509	19.5509	.0402
037	.0000	19.5549	19.5549	.0314
038	.0000	19.5587	19.5587	.0330
039	.0000	19.5623	19.5623	.0316
040	.0000	19.5657	19.5657	.0339
041	.0000	19.5691	19.5691	.0322
042	.0000	19.5728	19.5728	.0319

043	.0000	19.5755	19.5755	.0312
044	.0000	19.5787	19.5787	.0326
045	.0000	19.5816	19.5816	.0335
046	.0000	19.5844	19.5844	.0372
047	.0000	19.5871	19.5871	.0371
048	.0000	19.5898	19.5898	.0367
049	.0000	19.5921	19.5921	.0368
050	.0000	19.5943	19.5943	.0364
051	.0000	19.5968	19.5968	.0340
052	.0000	19.5990	19.5990	.0321
053	.0000	19.6009	19.6009	.0331
054	.0000	19.6029	19.6029	.0339
055	.0000	19.6051	19.6051	.0368
056	.0000	19.6070	19.6070	.0392
057	.0000	19.6090	19.6090	.0406
058	.0000	19.6107	19.6107	.0410
059	.0000	19.6126	19.6126	.0360
060	.0000	19.6144	19.6144	.0370
061	.0000	19.6164	19.6164	.0297
062	.0000	19.6182	19.6182	.0280
063	.0000	19.6199	19.6199	.0316
064	.0000	19.6214	19.6214	.0344
065	.0000	19.6230	19.6230	.0295
066	.0000	19.6246	19.6246	.0300
067	.0000	19.6260	19.6260	.0304
068	.0000	19.6276	19.6276	.0250
069	.0000	19.6289	19.6289	.0367
070	.0000	19.6302	19.6302	.0390
071	.0000	19.6315	19.6315	.0364
072	.0000	19.6329	19.6329	.0357
073	.0000	19.6342	19.6342	.0367
074	.0000	19.6356	19.6356	.0392
075	.0000	19.6368	19.6368	.0368
076	.0000	19.6381	19.6381	.0384
077	.0000	19.6392	19.6392	.0360
078	.0000	19.6404	19.6404	.0346
079	.0000	19.6417	19.6417	.0348
080	.0000	19.6429	19.6429	.0369
081	.0000	19.6444	19.6444	.0367
082	.0000	19.6453	19.6453	.0318
083	.0000	19.6465	19.6465	.0305
084	.0000	19.6476	19.6476	.0317
085	.0000	19.6488	19.6488	.0278
086	.0000	19.6498	19.6498	.0306
087	.0000	19.6512	19.6512	.0330
088	.0000	19.6523	19.6523	.0302
089	.0000	19.6536	19.6536	.0297
090	.0000	19.6547	19.6547	.0243
091	.0000	19.6559	19.6559	.0262
092	.0000	19.6571	19.6571	.0129
093	.0000	19.6580	19.6580	.0099
094	.0000	19.6591	19.6591	.0214
095	.0000	19.6601	19.6601	.0262
096	.0000	19.6612	19.6612	.0224
097	.0000	19.6621	19.6621	.0283
098	.0000	19.6629	19.6629	.0294
099	.0000	19.6639	19.6639	.0232

100	.0000	19.6649	19.6649	.0334
The annual contraction scour u/s face is MNYYSU				
The mean annual local scour value u/s face is MNLSU				
The mean annual total scour value u/s face is YMNTSU				
The standard dev in annual scour u/s face is YSTTSU				
YR	MNYYSU	MNLSU	YMNTSU	YSTTSU
001	.0000	.0004	.0004	.0020
002	.0000	.0007	.0007	.0025
003	.0000	.0010	.0010	.0029
004	.0000	.0013	.0013	.0033
005	.0000	.0015	.0015	.0035
006	.0000	.0018	.0018	.0038
007	.0000	.0022	.0022	.0043
008	.0000	.0024	.0024	.0045
009	.0000	.0027	.0027	.0048
010	.0000	.0029	.0029	.0049
011	.0000	.0031	.0031	.0050
012	.0000	.0033	.0033	.0051
013	.0000	.0036	.0036	.0054
014	.0000	.0040	.0040	.0057
015	.0000	.0042	.0042	.0058
016	.0000	.0045	.0045	.0060
017	.0000	.0048	.0048	.0062
018	.0000	.0051	.0051	.0063
019	.0000	.0054	.0054	.0065
020	.0000	.0056	.0056	.0066
021	.0000	.0059	.0059	.0068
022	.0000	.0061	.0061	.0070
023	.0000	.0064	.0064	.0070
024	.0000	.0065	.0065	.0071
025	.0000	.0068	.0068	.0072
026	.0000	.0071	.0071	.0072
027	.0000	.0074	.0074	.0074
028	.0000	.0077	.0077	.0076
029	.0000	.0080	.0080	.0078
030	.0000	.0083	.0083	.0078
031	.0000	.0086	.0086	.0079
032	.0000	.0088	.0088	.0080
033	.0000	.0092	.0092	.0082
034	.0000	.0094	.0094	.0084
035	.0000	.0097	.0097	.0086
036	.0000	.0101	.0101	.0088
037	.0000	.0104	.0104	.0090
038	.0000	.0107	.0107	.0092
039	.0000	.0110	.0110	.0094
040	.0000	.0112	.0112	.0094
041	.0000	.0114	.0114	.0095
042	.0000	.0117	.0117	.0096
043	.0000	.0119	.0119	.0097
044	.0000	.0122	.0122	.0098
045	.0000	.0125	.0125	.0099
046	.0000	.0128	.0128	.0101
047	.0000	.0130	.0130	.0103
048	.0000	.0133	.0133	.0103
049	.0000	.0135	.0135	.0104
050	.0000	.0138	.0138	.0104
051	.0000	.0142	.0142	.0107

052	.0000	.0145	.0145	.0107
053	.0000	.0147	.0147	.0107
054	.0000	.0149	.0149	.0109
055	.0000	.0152	.0152	.0109
056	.0000	.0154	.0154	.0110
057	.0000	.0157	.0157	.0111
058	.0000	.0160	.0160	.0112
059	.0000	.0162	.0162	.0112
060	.0000	.0165	.0165	.0113
061	.0000	.0168	.0168	.0115
062	.0000	.0171	.0171	.0116
063	.0000	.0173	.0173	.0117
064	.0000	.0175	.0175	.0117
065	.0000	.0179	.0179	.0118
066	.0000	.0182	.0182	.0120
067	.0000	.0184	.0184	.0121
068	.0000	.0186	.0186	.0121
069	.0000	.0189	.0189	.0123
070	.0000	.0192	.0192	.0124
071	.0000	.0195	.0195	.0125
072	.0000	.0198	.0198	.0127
073	.0000	.0201	.0201	.0127
074	.0000	.0203	.0203	.0128
075	.0000	.0205	.0205	.0129
076	.0000	.0208	.0208	.0130
077	.0000	.0210	.0210	.0131
078	.0000	.0212	.0212	.0131
079	.0000	.0215	.0215	.0132
080	.0000	.0219	.0219	.0133
081	.0000	.0221	.0221	.0134
082	.0000	.0224	.0224	.0135
083	.0000	.0227	.0227	.0136
084	.0000	.0229	.0229	.0137
085	.0000	.0232	.0232	.0138
086	.0000	.0234	.0234	.0138
087	.0000	.0238	.0238	.0139
088	.0000	.0240	.0240	.0140
089	.0000	.0242	.0242	.0140
090	.0000	.0245	.0245	.0141
091	.0000	.0247	.0247	.0141
092	.0000	.0250	.0250	.0143
093	.0000	.0253	.0253	.0144
094	.0000	.0255	.0255	.0145
095	.0000	.0258	.0258	.0145
096	.0000	.0261	.0261	.0146
097	.0000	.0264	.0264	.0146
098	.0000	.0267	.0267	.0146
099	.0000	.0269	.0269	.0146
100	.0000	.0271	.0271	.0146

## Appendix D-6

RUN TITLE IS Black River Hurricane Simulation  
RUN DATE IS 109/05  
THE PROGRAM WAS EXECUTED IN THE EXISTING PIER ANALYSIS MODE.  
CONTRACTION SCOUR METHOD IS KOMURAS EQN  
SCOUR COMPUTED WITHOUT ARMOURING  
BRUBAKER-DEMETRIUS NEILLS MODIFICATION FACTOR ACTIVATED  
TIDE DISTORTION OPTION ACTIVATED  
MEAN TIDAL DEPTH MDR is = 10.935000  
MEAN LOW TIDAL DEPTH MLT is = 10.000000  
MEAN LOW TIDE ELEVATION MLTE is = -9.350000E-01  
TIDAL AMP. AT BRIDGE XSEC MTR is = 9.350000E-01  
CHANNEL INVERT AT BRIDGE IRS is = -10.935000

Estuary in bank area is = 58740.000000

Maximum tide in the simulation HITIDE is = 21.876030  
Maximum u/s flow depth in sim. YTRMXS is = 25.186090  
Maximum d/s flow depth in sim. YTFMXS is = 24.179480  
Maximum u/s disch. in sim. QTRMXS is = 907615.000002  
Maximum d/s disch. in sim. QTFMXS is = 893900.900000  
Maximum u/s vel.in sim. VUPMS is = 5.366290  
Maximum d/s vel.in sim. VDOWNMS is = 2.460412

Maximum u/s flow depth last run YTRMAX is = 25.186090  
Maximum d/s flow depth last run YTFMAX is = 21.876030  
Maximum u/s discharge last run QTRMAX is = 750528.400000  
Maximum d/s discharge last run QTFMAX is = 802566.300000  
Maximum u/s velocity last run VNUMAX is = 3.458784  
Maximum d/s velocity last run VNDMAX is = 2.090724  
Maximum tangential vel d/s face last run VTDMX is = 1.949851  
Maximum tangential vel u/s face last run VTUMX is = 1.199898  
critical vel u/s face last run UIUMIN is = 2.017563E-01  
critical vel d/s face last run UIDMIN is = 2.017563E-01

Time of concentration = 13.250000hrs  
Time to peak = 8.877501hrs  
Number of unit hydrograph ordinates = 44  
Soil infiltration potential = 1.904762  
Peak discharge of the UHG = 3162.151000cfs  
Initial abstractions IA = 3.809524E-01in

Catchment base flow = 41.050620cfs  
Tide attenuation factor TAF = 7.663934E-01  
Tidal lag MTL= 2.503192E-01hrs  
Tidal routing constant CX = 1.000000  
Bridge station tidal range TR = 1.870000ft  
Effective bottom channel width at brdg.WBE = 8406.400000ft  
Estuary Area 2.648448E+08  
Contraction scour factor u/s face= 9.174486E-01  
Contraction scour factor d/s face= 1.065397  
Estuary to wavelength ratio DIM = 6.349449E-02

Estuary width factor WF = 1.000000  
Tidal range factor HF = 1.710105E-01  
Neill Mod. factor rising limb.NMRF = 8.000000E-01  
Neill Mod. factor falling limb.NMFF = 8.000000E-01

The maximum storm event in the simulation is 7.000000ins  
Array of total SURGRE at bridge is HSURGE= 10.380330  
2.856355E-01

5.179529E-01	8.728182E-01	1.481365	2.761897
10.926670	10.926670	3.868823	2.761897
-5.401087	-5.078043	-4.789991	-4.531823
-4.299308	-4.088933	-3.897769	-3.723364
-3.563652	-3.416886	-3.281578	-3.156457
-3.040428	-2.932547	-2.831993	-2.738052
-2.650098	-2.567580	-2.490014	-2.416970
-2.348066	-2.282962	-2.221354	-2.162968
-2.107560	-2.054909	-2.004814	-1.957096
-1.911588	-1.868142	-1.826621	-1.786900
-1.748865	-1.712412	-1.677443	-1.643871
-1.611613	-1.580593	-1.550743	-1.521997
-1.494296	-1.467583	-1.441807	-1.416919
-1.392874	-1.369630	-1.347148	-1.325391
-1.304325	-1.283917	-1.264137	-1.244957
-1.226349	-1.208288	-1.190751	-1.173715
-1.157160	-1.141064	-1.125410	-1.110179
-1.095354	-1.080919	-1.066860	-1.053161
-1.039810	-1.026792	-1.014096	-1.001710
-9.896228E-01	-9.778234E-01	-9.663019E-01	-9.550486E-01
-9.440541E-01	-9.333097E-01	-9.228069E-01	-9.125378E-01
-9.024945E-01	-8.926698E-01	-8.830566E-01	-8.736480E-01
-8.644378E-01	-8.554195E-01	-8.465874E-01	-8.379357E-01
-8.294590E-01	-8.211520E-01	-8.130096E-01	-8.050270E-01
-7.971996E-01	-7.895228E-01	-7.819924E-01	-7.746043E-01
-7.673544E-01	-7.602389E-01	-7.532541E-01	-7.463963E-01
-7.396623E-01	-7.330486E-01	-7.265522E-01	-7.201698E-01
-7.138985E-01	-7.077355E-01	-7.016779E-01	-6.957231E-01
-6.898685E-01	-6.841115E-01	-6.784499E-01	-6.728811E-01
-6.674029E-01	-6.620133E-01		

Array of total combined depth at bridge d/s face is YTR=  
10.000000

10.000000	15.039670	10.000000	15.470560
16.729010	25.186090	10.000000	14.582960
10.000000	14.385000	10.000000	10.000000
14.784890	10.000000	10.000000	10.000000
14.645090	10.000000	14.707890	10.000000
10.000000	14.184980	10.000000	10.000000
14.198090	10.000000	14.209360	10.000000
14.659350	10.000000	10.000000	10.000000
14.112890	10.000000	14.006710	10.000000
14.236720	10.000000	10.000000	14.105720
14.138330	10.000000	10.000000	13.900850
13.985430	14.138450	14.660130	10.000000
10.000000	10.000000	14.192270	14.249330
10.000000	14.226590	10.000000	14.264440
14.465560	14.547260	10.000000	14.234170

10.000000	10.000000	10.000000	14.611340
10.000000	10.000000	14.532700	10.000000
10.000000	10.000000	10.000000	14.264290
10.000000	10.000000	10.000000	14.492050
10.000000	10.000000	13.963600	14.062360
14.108420	14.668590	10.000000	10.000000
14.228980	14.590090	10.000000	10.000000
10.000000	14.223800	14.399590	10.000000
10.000000	14.015800	14.574040	14.780540
10.000000	10.000000	10.000000	14.522660
10.000000	14.484160	10.000000	10.000000
14.273580	14.427570	14.655190	14.987130
10.000000	10.000000	10.000000	10.000000
14.294150	10.000000	10.000000	10.000000
14.360550	10.000000	10.000000	

Array of total combined depth at bridge u/s face is YTF=  
21.876030

14.957810	10.000000	14.951920	10.000000
10.000000	10.000000	14.165810	10.000000
14.208010	10.000000	14.236200	14.081190
10.000000	14.578130	14.321850	14.296100
10.000000	14.186210	10.000000	14.458980
14.144640	10.000000	14.095440	13.927890
10.000000	14.133890	10.000000	14.180200
10.000000	14.604270	14.602800	14.107070
10.000000	13.889630	10.000000	13.874310
10.000000	13.886380	13.790330	10.000000
10.000000	13.980400	13.888660	10.000000
10.000000	10.000000	10.000000	14.356190
14.275770	14.087640	10.000000	10.000000
14.010700	10.000000	14.224820	10.000000
10.000000	10.000000	14.099860	10.000000
14.121210	14.030980	13.985670	10.000000
14.506970	14.148430	10.000000	14.413890
14.364930	14.171120	14.074330	10.000000
14.165660	14.129740	14.093010	10.000000
14.259830	13.910890	10.000000	10.000000
10.000000	10.000000	14.398320	14.150630
10.000000	10.000000	14.433940	14.226340
14.206260	10.000000	10.000000	14.362580
13.813990	10.000000	10.000000	10.000000
14.319880	14.273900	14.154690	10.000000
14.184860	10.000000	14.474610	14.239440
10.000000	10.000000	10.000000	10.000000
14.333370	14.312080	14.134010	13.924200
10.000000	14.008180	14.008160	13.894680
10.000000	14.271460	13.829610	

Array total net disch. value at bridge is QT= 730114.500000  
49839.450000

29692.100000	-55839.420000	-117564.100000	-750528.400000
802566.300000	-82484.080000	-82377.480000	-61172.000000
-24232.070000	15532.120000	24781.300000	84595.160000
86762.130000	2346.977000	2687.478000	3412.592000
4584.496000	-50557.300000	-101918.100000	-80417.740000
-35930.660000	19180.620000	74460.010000	85489.460000
94809.360000	48515.960000	14326.570000	13083.230000

11563.020000	-25480.030000	-90417.140000	-81783.220000
-50238.560000	-4068.796000	-24831.610000	96207.800000
118042.500000	57530.480000	3631.149000	3190.397000
2785.888000	2403.389000	-110308.800000	-136242.300000
-98767.150000	-35793.230000	103714.200000	50359.670000
69318.880000	70741.470000	19696.790000	434.868100
369.029100	-250.885000	-83809.100000	-89324.730000
-72081.310000	-36484.510000	-58308.720000	57211.430000
90356.630000	100432.600000	25575.250000	67.242390
61.964860	57.808520	-40875.730000	-126047.400000
-111410.000000	-68408.700000	93393.920000	21281.600000
40304.430000	49022.860000	45215.310000	28596.490000
41.108470	-12305.870000	-47673.560000	-60819.960000
-58482.400000	-41255.160000	-88429.200000	22789.070000
57172.760000	76969.630000	77133.670000	13510.070000
41.050620	41.050620	-2480.847000	-93938.950000
-98080.580000	-77210.540000	-14144.580000	9404.382000
42357.370000	64521.520000	70247.130000	42523.440000
41.050620	41.050620	41.050620	-71034.630000
-88001.660000	-76106.400000	10791.510000	-1253.838000
21630.940000	38772.900000	46062.020000	41641.250000
26639.660000	3997.649000	-21499.710000	-45495.100000
-56731.210000	-53448.780000		
Array of net adjusted vel.upstream is VNUA = 0.000000E+00			
0.000000E+00			
0.000000E+00	2.591706E-01	7.781494E-01	3.458784
2.939805	4.138995E-01	8.059270E-01	6.990530E-01
4.254243E-01	1.183988E-01	0.000000E+00	0.000000E+00
0.000000E+00	0.000000E+00	0.000000E+00	0.000000E+00
0.000000E+00	2.407656E-01	7.389417E-01	9.016620E-01
5.838017E-01	1.803158E-01	0.000000E+00	0.000000E+00
0.000000E+00	0.000000E+00	0.000000E+00	0.000000E+00
0.000000E+00	1.212706E-01	5.748382E-01	8.638366E-01
6.691973E-01	2.793286E-01	1.483718E-01	1.279716E-01
0.000000E+00	0.000000E+00	0.000000E+00	0.000000E+00
0.000000E+00	0.000000E+00	5.685613E-01	1.271095
1.198069	6.659455E-01	1.704099E-01	0.000000E+00
0.000000E+00	0.000000E+00	0.000000E+00	0.000000E+00
0.000000E+00	0.000000E+00	4.104910E-01	8.458672E-01
7.795975E-01	5.259756E-01	4.757091E-01	2.926954E-01
0.000000E+00	0.000000E+00	0.000000E+00	0.000000E+00
0.000000E+00	0.000000E+00	1.997516E-01	8.155571E-01
1.174869	9.021701E-01	3.431066E-01	0.000000E+00
0.000000E+00	0.000000E+00	0.000000E+00	0.000000E+00
0.000000E+00	0.000000E+00	3.025421E-01	5.441928E-01
5.835439E-01	4.800339E-01	6.452850E-01	4.436962E-01
0.000000E+00	0.000000E+00	0.000000E+00	0.000000E+00
0.000000E+00	0.000000E+00	0.000000E+00	4.960961E-01
9.757560E-01	8.592005E-01	4.330066E-01	0.000000E+00
0.000000E+00	0.000000E+00	0.000000E+00	0.000000E+00
0.000000E+00	0.000000E+00	0.000000E+00	3.468718E-01
7.769504E-01	7.924076E-01	3.623290E-01	0.000000E+00
0.000000E+00	0.000000E+00	0.000000E+00	0.000000E+00
0.000000E+00	0.000000E+00	1.108118E-01	3.330733E-01
4.992846E-01	5.524141E-01		
Array of net adjusted vel.downstream is VNDA= 1.859394			
2.090724			



3.655718E-01	1.342413E-01	0.000000E+00	0.000000E+00
1.636371	1.636371	0.000000E+00	0.000000E+00
0.000000E+00	0.000000E+00	2.022643E-01	5.165592E-01
8.051459E-01	4.243463E-01	0.000000E+00	0.000000E+00
0.000000E+00	0.000000E+00	0.000000E+00	0.000000E+00
0.000000E+00	0.000000E+00	4.800514E-01	8.128932E-01
9.047207E-01	7.191731E-01	3.154011E-01	1.341836E-01
1.173223E-01	0.000000E+00	0.000000E+00	0.000000E+00
0.000000E+00	0.000000E+00	0.000000E+00	4.829461E-01
1.091324	9.047423E-01	3.145791E-01	0.000000E+00
0.000000E+00	0.000000E+00	0.000000E+00	0.000000E+00
0.000000E+00	0.000000E+00	5.066727E-01	7.525887E-01
5.936115E-01	7.027210E-01	4.539065E-01	1.010614E-01
0.000000E+00	0.000000E+00	0.000000E+00	0.000000E+00
0.000000E+00	0.000000E+00	0.000000E+00	2.870160E-01
7.401028E-01	9.709684E-01	6.396111E-01	1.220494E-01
0.000000E+00	0.000000E+00	0.000000E+00	0.000000E+00
0.000000E+00	0.000000E+00	4.560330E-01	5.628225E-01
3.089961E-01	4.481065E-01	4.669529E-01	3.606835E-01
1.398424E-01	0.000000E+00	0.000000E+00	0.000000E+00
0.000000E+00	0.000000E+00	0.000000E+00	1.143923E-01
3.864834E-01	6.482674E-01	7.633523E-01	4.549829E-01
0.000000E+00	0.000000E+00	0.000000E+00	0.000000E+00
0.000000E+00	0.000000E+00	0.000000E+00	0.000000E+00
2.527713E-01	5.305828E-01	6.579359E-01	5.475913E-01
2.136019E-01	0.000000E+00	0.000000E+00	0.000000E+00
0.000000E+00	0.000000E+00	0.000000E+00	0.000000E+00
1.056483E-01	3.001756E-01	4.319715E-01	4.408062E-01
3.369291E-01	1.536108E-01	0.000000E+00	0.000000E+00
0.000000E+00	0.000000E+00		
Array of net vel.u/stream is VNU =		0.000000E+00	0.000000E+00
0.000000E+00	2.591706E-01	7.781494E-01	3.458784
2.939805	4.138995E-01	8.059270E-01	6.990530E-01
4.254243E-01	1.183988E-01	0.000000E+00	0.000000E+00
0.000000E+00	0.000000E+00	0.000000E+00	0.000000E+00
0.000000E+00	2.407656E-01	7.389417E-01	9.016620E-01
5.838017E-01	1.803158E-01	0.000000E+00	0.000000E+00
0.000000E+00	0.000000E+00	0.000000E+00	0.000000E+00
0.000000E+00	1.212706E-01	5.748382E-01	8.638366E-01
6.691973E-01	2.793286E-01	1.483718E-01	1.279716E-01
0.000000E+00	0.000000E+00	0.000000E+00	0.000000E+00
0.000000E+00	0.000000E+00	5.685613E-01	1.271095
1.198069	6.659455E-01	1.704099E-01	0.000000E+00
0.000000E+00	0.000000E+00	0.000000E+00	0.000000E+00
0.000000E+00	1.259318E-03	4.104910E-01	8.458672E-01
7.795975E-01	5.259756E-01	4.757091E-01	2.926954E-01
0.000000E+00	0.000000E+00	0.000000E+00	0.000000E+00
0.000000E+00	0.000000E+00	1.997516E-01	8.155571E-01
1.174869	9.021701E-01	3.431066E-01	0.000000E+00
0.000000E+00	0.000000E+00	0.000000E+00	0.000000E+00
0.000000E+00	6.344808E-02	3.025421E-01	5.441928E-01
5.835439E-01	4.800339E-01	6.452850E-01	4.436962E-01
0.000000E+00	0.000000E+00	0.000000E+00	0.000000E+00
0.000000E+00	0.000000E+00	1.212005E-02	4.960961E-01
9.757560E-01	8.592005E-01	4.330066E-01	6.558605E-02
0.000000E+00	0.000000E+00	0.000000E+00	0.000000E+00
0.000000E+00	0.000000E+00	0.000000E+00	3.468718E-01

7.769504E-01	7.924076E-01	3.623290E-01	6.124603E-03
6.124603E-03	0.000000E+00	0.000000E+00	0.000000E+00
0.000000E+00	0.000000E+00	1.108118E-01	3.330733E-01
4.992846E-01	5.524141E-01		
Array of net vel.d/stream is VND=		1.859394	2.090724
3.655718E-01	1.342413E-01	0.000000E+00	0.000000E+00
1.636371	1.636371	0.000000E+00	0.000000E+00
0.000000E+00	7.796825E-02	2.022643E-01	5.165592E-01
8.051459E-01	4.243463E-01	2.458842E-02	2.937071E-02
3.925299E-02	2.300717E-02	0.000000E+00	0.000000E+00
0.000000E+00	9.621168E-02	4.800514E-01	8.128932E-01
9.047207E-01	7.191731E-01	3.154011E-01	1.341836E-01
1.173223E-01	5.503391E-02	0.000000E+00	0.000000E+00
0.000000E+00	0.000000E+00	0.000000E+00	4.829461E-01
1.091324	9.047423E-01	3.145791E-01	3.422201E-02
3.037195E-02	2.675202E-02	1.238695E-02	0.000000E+00
0.000000E+00	0.000000E+00	5.066727E-01	7.525887E-01
5.936115E-01	7.027210E-01	4.539065E-01	1.010614E-01
4.032750E-03	1.852360E-03	0.000000E+00	0.000000E+00
0.000000E+00	0.000000E+00	0.000000E+00	2.870160E-01
7.401028E-01	9.709684E-01	6.396111E-01	1.220494E-01
6.307755E-04	5.859373E-04	2.750304E-04	0.000000E+00
0.000000E+00	0.000000E+00	4.560330E-01	5.628225E-01
3.089961E-01	4.481065E-01	4.669529E-01	3.606835E-01
1.398424E-01	2.118949E-04	0.000000E+00	0.000000E+00
0.000000E+00	0.000000E+00	0.000000E+00	1.143923E-01
3.864834E-01	6.482674E-01	7.633523E-01	4.549829E-01
6.801318E-02	4.066432E-04	2.005907E-04	0.000000E+00
0.000000E+00	0.000000E+00	0.000000E+00	4.593413E-02
2.527713E-01	5.305828E-01	6.579359E-01	5.475913E-01
2.136019E-01	4.013564E-04	4.067427E-04	2.060698E-04
0.000000E+00	0.000000E+00	5.009750E-02	5.009750E-02
1.056483E-01	3.001756E-01	4.319715E-01	4.408062E-01
3.369291E-01	1.536108E-01	2.004360E-02	0.000000E+00
0.000000E+00	0.000000E+00		
Array of tangential velocity d/s face is VTD=		0.000000E+00	
0.000000E+00	0.000000E+00	4.422162E-01	1.949851
1.576523	0.000000E+00	4.682607E-01	0.000000E+00
2.483509E-01	0.000000E+00	0.000000E+00	0.000000E+00
0.000000E+00	0.000000E+00	0.000000E+00	0.000000E+00
0.000000E+00	1.401939E-01	0.000000E+00	0.000000E+00
3.416247E-01	0.000000E+00	0.000000E+00	0.000000E+00
0.000000E+00	0.000000E+00	0.000000E+00	0.000000E+00
0.000000E+00	0.000000E+00	0.000000E+00	5.066910E-01
0.000000E+00	1.645164E-01	0.000000E+00	7.520454E-02
0.000000E+00	0.000000E+00	0.000000E+00	0.000000E+00
0.000000E+00	0.000000E+00	3.352125E-01	7.499818E-01
7.087488E-01	3.935885E-01	0.000000E+00	0.000000E+00
0.000000E+00	0.000000E+00	0.000000E+00	0.000000E+00
0.000000E+00	0.000000E+00	2.440277E-01	5.021092E-01
4.637991E-01	0.000000E+00	2.846020E-01	0.000000E+00
0.000000E+00	0.000000E+00	0.000000E+00	0.000000E+00
0.000000E+00	0.000000E+00	0.000000E+00	0.000000E+00
0.000000E+00	0.000000E+00	2.054044E-01	0.000000E+00
0.000000E+00	0.000000E+00	0.000000E+00	0.000000E+00

0.000000E+00	0.000000E+00	1.814656E-01	3.262657E-01
3.485448E-01	0.000000E+00	0.000000E+00	2.665356E-01
0.000000E+00	0.000000E+00	0.000000E+00	0.000000E+00
0.000000E+00	0.000000E+00	0.000000E+00	0.000000E+00
5.877444E-01	5.165990E-01	2.606448E-01	0.000000E+00
0.000000E+00	0.000000E+00	0.000000E+00	0.000000E+00
0.000000E+00	0.000000E+00	0.000000E+00	2.098884E-01
4.694579E-01	4.790926E-01	2.190212E-01	0.000000E+00
0.000000E+00	0.000000E+00	0.000000E+00	0.000000E+00
0.000000E+00	0.000000E+00	0.000000E+00	2.024781E-01
0.000000E+00	0.000000E+00		
Array of tangential velocity u/s face is VTU=			1.007489
1.199898			
0.000000E+00	7.744161E-02	0.000000E+00	0.000000E+00
0.000000E+00	9.510370E-01	0.000000E+00	0.000000E+00
0.000000E+00	0.000000E+00	1.182004E-01	0.000000E+00
4.682845E-01	2.481107E-01	0.000000E+00	0.000000E+00
0.000000E+00	0.000000E+00	0.000000E+00	0.000000E+00
0.000000E+00	0.000000E+00	2.818879E-01	0.000000E+00
5.306922E-01	0.000000E+00	1.855226E-01	0.000000E+00
6.873424E-02	0.000000E+00	0.000000E+00	0.000000E+00
0.000000E+00	0.000000E+00	0.000000E+00	0.000000E+00
6.437629E-01	5.362024E-01	0.000000E+00	0.000000E+00
0.000000E+00	0.000000E+00	0.000000E+00	0.000000E+00
0.000000E+00	0.000000E+00	2.996107E-01	4.458741E-01
3.532310E-01	0.000000E+00	0.000000E+00	6.028650E-02
0.000000E+00	0.000000E+00	0.000000E+00	0.000000E+00
0.000000E+00	0.000000E+00	0.000000E+00	1.710337E-01
4.414099E-01	5.808233E-01	0.000000E+00	7.289785E-02
0.000000E+00	0.000000E+00	0.000000E+00	0.000000E+00
0.000000E+00	0.000000E+00	0.000000E+00	3.372348E-01
1.854966E-01	2.691009E-01	0.000000E+00	2.164211E-01
8.419032E-02	0.000000E+00	0.000000E+00	0.000000E+00
0.000000E+00	0.000000E+00	0.000000E+00	0.000000E+00
0.000000E+00	3.883642E-01	4.591365E-01	2.744316E-01
0.000000E+00	0.000000E+00	0.000000E+00	0.000000E+00
0.000000E+00	0.000000E+00	0.000000E+00	0.000000E+00
1.524895E-01	3.204413E-01	0.000000E+00	3.310670E-01
0.000000E+00	0.000000E+00	0.000000E+00	0.000000E+00
0.000000E+00	0.000000E+00	0.000000E+00	0.000000E+00
6.389184E-02	1.818350E-01	2.621905E-01	0.000000E+00
2.044724E-01	9.322188E-02	0.000000E+00	0.000000E+00
0.000000E+00	0.000000E+00		
The mean hurricane scour u/s face is MNTHSU			4.392889
The std.dev.in hurricane scour u/s face is STDHSU			1.021582E-01
The mean hurricane scour d/s face is MNTHSD			4.447548
The std.dev.in hurricane scour d/s face is STDHSD			1.411031E-01
B	FHU	PRHU	CPRHU
1.0000	.0000	.0000	.0000
1.5000	.0000	.0000	.0000
2.0000	.0000	.0000	.0000
2.5000	.0000	.0000	.0000
3.0000	.0000	.0000	.0000
3.5000	.0000	.0000	.0000
4.0000	.0000	.0000	.0000
4.5000	1709.0000	.8545	.8545
5.0000	289.0000	.1445	.9990

5.5000	2.0000	.0010	1.0000
6.0000	.0000	.0000	1.0000
6.5000	.0000	.0000	1.0000
7.0000	.0000	.0000	1.0000
7.5000	.0000	.0000	1.0000
8.0000	.0000	.0000	1.0000
8.5000	.0000	.0000	1.0000
9.0000	.0000	.0000	1.0000
9.5000	.0000	.0000	1.0000
10.0000	.0000	.0000	1.0000
10.5000	.0000	.0000	1.0000
11.0000	.0000	.0000	1.0000
11.5000	.0000	.0000	1.0000
12.0000	.0000	.0000	1.0000
12.5000	.0000	.0000	1.0000
13.0000	.0000	.0000	1.0000
13.5000	.0000	.0000	1.0000
14.0000	.0000	.0000	1.0000
14.5000	.0000	.0000	1.0000
15.0000	.0000	.0000	1.0000
15.5000	.0000	.0000	1.0000
16.0000	.0000	.0000	1.0000
16.5000	.0000	.0000	1.0000
17.0000	.0000	.0000	1.0000
17.5000	.0000	.0000	1.0000
18.0000	.0000	.0000	1.0000
18.5000	.0000	.0000	1.0000
19.0000	.0000	.0000	1.0000
19.5000	.0000	.0000	1.0000
20.0000	.0000	.0000	1.0000
20.5000	.0000	.0000	1.0000
21.0000	.0000	.0000	1.0000
21.5000	.0000	.0000	1.0000
22.0000	.0000	.0000	1.0000
22.5000	.0000	.0000	1.0000
23.0000	.0000	.0000	1.0000
23.5000	.0000	.0000	1.0000
24.0000	.0000	.0000	1.0000
24.5000	.0000	.0000	1.0000
25.0000	.0000	.0000	1.0000
25.5000	.0000	.0000	1.0000
26.0000	.0000	.0000	1.0000
26.5000	.0000	.0000	1.0000
27.0000	.0000	.0000	1.0000
27.5000	.0000	.0000	1.0000
28.0000	.0000	.0000	1.0000
28.5000	.0000	.0000	1.0000
29.0000	.0000	.0000	1.0000
29.5000	.0000	.0000	1.0000
30.0000	.0000	.0000	1.0000
30.5000	.0000	.0000	1.0000
31.0000	.0000	.0000	1.0000
31.5000	.0000	.0000	1.0000
32.0000	.0000	.0000	1.0000
32.5000	.0000	.0000	1.0000
33.0000	.0000	.0000	1.0000
33.5000	.0000	.0000	1.0000

34.0000	.0000	.0000	1.0000
34.5000	.0000	.0000	1.0000
35.0000	.0000	.0000	1.0000
35.5000	.0000	.0000	1.0000
36.0000	.0000	.0000	1.0000
36.5000	.0000	.0000	1.0000
37.0000	.0000	.0000	1.0000
37.5000	.0000	.0000	1.0000
38.0000	.0000	.0000	1.0000
38.5000	.0000	.0000	1.0000
39.0000	.0000	.0000	1.0000
39.5000	.0000	.0000	1.0000
40.0000	.0000	.0000	1.0000
40.5000	.0000	.0000	1.0000
41.0000	.0000	.0000	1.0000
41.5000	.0000	.0000	1.0000
42.0000	.0000	.0000	1.0000
42.5000	.0000	.0000	1.0000
43.0000	.0000	.0000	1.0000
43.5000	.0000	.0000	1.0000
44.0000	.0000	.0000	1.0000
44.5000	.0000	.0000	1.0000
45.0000	.0000	.0000	1.0000
45.5000	.0000	.0000	1.0000
46.0000	.0000	.0000	1.0000
46.5000	.0000	.0000	1.0000
47.0000	.0000	.0000	1.0000
47.5000	.0000	.0000	1.0000
48.0000	.0000	.0000	1.0000
48.5000	.0000	.0000	1.0000
49.0000	.0000	.0000	1.0000
49.5000	.0000	.0000	1.0000
50.0000	.0000	.0000	1.0000
50.5000	.0000	.0000	1.0000
B	FHD	PRHD	CPRHD
1.0000	.0000	.0000	.0000
1.5000	.0000	.0000	.0000
2.0000	.0000	.0000	.0000
2.5000	.0000	.0000	.0000
3.0000	.0000	.0000	.0000
3.5000	.0000	.0000	.0000
4.0000	.0000	.0000	.0000
4.5000	1366.0000	.6830	.6830
5.0000	632.0000	.3160	.9990
5.5000	1.0000	.0005	.9995
6.0000	1.0000	.0005	1.0000
6.5000	.0000	.0000	1.0000
7.0000	.0000	.0000	1.0000
7.5000	.0000	.0000	1.0000
8.0000	.0000	.0000	1.0000
8.5000	.0000	.0000	1.0000
9.0000	.0000	.0000	1.0000
9.5000	.0000	.0000	1.0000
10.0000	.0000	.0000	1.0000
10.5000	.0000	.0000	1.0000
11.0000	.0000	.0000	1.0000
11.5000	.0000	.0000	1.0000

12.0000	.0000	.0000	1.0000
12.5000	.0000	.0000	1.0000
13.0000	.0000	.0000	1.0000
13.5000	.0000	.0000	1.0000
14.0000	.0000	.0000	1.0000
14.5000	.0000	.0000	1.0000
15.0000	.0000	.0000	1.0000
15.5000	.0000	.0000	1.0000
16.0000	.0000	.0000	1.0000
16.5000	.0000	.0000	1.0000
17.0000	.0000	.0000	1.0000
17.5000	.0000	.0000	1.0000
18.0000	.0000	.0000	1.0000
18.5000	.0000	.0000	1.0000
19.0000	.0000	.0000	1.0000
19.5000	.0000	.0000	1.0000
20.0000	.0000	.0000	1.0000
20.5000	.0000	.0000	1.0000
21.0000	.0000	.0000	1.0000
21.5000	.0000	.0000	1.0000
22.0000	.0000	.0000	1.0000
22.5000	.0000	.0000	1.0000
23.0000	.0000	.0000	1.0000
23.5000	.0000	.0000	1.0000
24.0000	.0000	.0000	1.0000
24.5000	.0000	.0000	1.0000
25.0000	.0000	.0000	1.0000
25.5000	.0000	.0000	1.0000
26.0000	.0000	.0000	1.0000
26.5000	.0000	.0000	1.0000
27.0000	.0000	.0000	1.0000
27.5000	.0000	.0000	1.0000
28.0000	.0000	.0000	1.0000
28.5000	.0000	.0000	1.0000
29.0000	.0000	.0000	1.0000
29.5000	.0000	.0000	1.0000
30.0000	.0000	.0000	1.0000
30.5000	.0000	.0000	1.0000
31.0000	.0000	.0000	1.0000
31.5000	.0000	.0000	1.0000
32.0000	.0000	.0000	1.0000
32.5000	.0000	.0000	1.0000
33.0000	.0000	.0000	1.0000
33.5000	.0000	.0000	1.0000
34.0000	.0000	.0000	1.0000
34.5000	.0000	.0000	1.0000
35.0000	.0000	.0000	1.0000
35.5000	.0000	.0000	1.0000
36.0000	.0000	.0000	1.0000
36.5000	.0000	.0000	1.0000
37.0000	.0000	.0000	1.0000
37.5000	.0000	.0000	1.0000
38.0000	.0000	.0000	1.0000
38.5000	.0000	.0000	1.0000
39.0000	.0000	.0000	1.0000
39.5000	.0000	.0000	1.0000
40.0000	.0000	.0000	1.0000

40.5000	.0000	.0000	1.0000
41.0000	.0000	.0000	1.0000
41.5000	.0000	.0000	1.0000
42.0000	.0000	.0000	1.0000
42.5000	.0000	.0000	1.0000
43.0000	.0000	.0000	1.0000
43.5000	.0000	.0000	1.0000
44.0000	.0000	.0000	1.0000
44.5000	.0000	.0000	1.0000
45.0000	.0000	.0000	1.0000
45.5000	.0000	.0000	1.0000
46.0000	.0000	.0000	1.0000
46.5000	.0000	.0000	1.0000
47.0000	.0000	.0000	1.0000
47.5000	.0000	.0000	1.0000
48.0000	.0000	.0000	1.0000
48.5000	.0000	.0000	1.0000
49.0000	.0000	.0000	1.0000
49.5000	.0000	.0000	1.0000
50.0000	.0000	.0000	1.0000
50.5000	.0000	.0000	1.0000

## Appendix D-7

RUN TITLE Patuxent River Continuous Simulation

RUN DATE 3/31/05

THE PROGRAM WAS EXECUTED IN PIER DESIGN MODE.

CONTRACTION SCOUR METHOD IS KOMURAS EQN

SCOUR COMPUTED WITHOUT ARMOURING

BRUBAKER-DEMETRIUS NEILLS MODIFICATION FACTOR ACTIVATED

TIDE DISTORTION OPTION ACTIVATED

MEAN TIDAL DEPTH MDR is = 15.900000

MEAN LOW TIDAL DEPTH MLT is = 15.300000

MEAN LOW TIDE ELEVATION MLTE is = -6.000000E-01

TIDAL AMP. AT BRIDGE XSEC MTR is = 6.000000E-01

CHANNEL INVERT AT BRIDGE IRS is = -15.900000

Estuary in bank area is = 26426.390000

Maximum tide in the simulation HITIDE is = 18.144820

Maximum u/s flow depth in sim. YTRMXS is = 20.050000

Maximum d/s flow depth in sim. YTFMXS is = 19.800000

Maximum u/s disch. in sim. QTRMXS is = 147839.700000

Maximum d/s disch. in sim. QTFMXS is = 232629.000000

Maximum u/s vel.in sim. VUPMS is = 2.710341

Maximum d/s vel.in sim. VDOWNMS is = 5.388817

Maximum u/s face tang.vel.in sim. VTUMXSis = 6.385844

Maximum d/s face tang.vel.in sim. VTDMXSis = 4.582942

Maximum u/s flow depth last run YTRMAX is = 18.300000

Maximum d/s flow depth last run YTFMAX is = 18.050000

Maximum u/s discharge last run QTRMAX is = 106351.200000

Maximum d/s discharge last run QTFMAX is = 125435.500000

Maximum u/s velocity last run VNUMAX is = 1.980304

Maximum d/s velocity last run VNDMAX is = 2.711949

Maximum tangential vel d/s face last run VTDMX is = 2.345420

Maximum tangential vel u/s face last run VTUMX is = 1.794748

critical vel u/s face last run UIUMIN is = 6.700665E-01

critical vel d/s face last run UIDMIN is = 6.700665E-01

Time of concentration = 53.000000hrs

Time to peak = 35.510000hrs

Number of unit hydrograph ordinates = 177

Soil infiltration potential = 4.285714

Peak discharge of the UHG = 9854.463000cfs

Initial abstractions IA = 8.571429E-01in

Catchment base flow = 407.770800cfs

Tide attenuation factor TAF = 4.918033E-01

Tidal lag MTL= 6.084536hrs

Tidal routing constant CX = 1.643511E-01

Bridge station tidal range TR = 1.200000ft

Effective bottom channel width at brdg.WBE = 3262.240000ft

Estuary Area 2.751598E+08

Contraction scour factor u/s face= 1.267396

Contraction scour factor d/s face= 1.016365



Estuary to wavelength ratio DIM = 9.751869E-02  
 Estuary width factor WF = 2.496051  
 Tidal range factor HF = 7.547170E-02  
 Neill Mod. factor rising limb.NMRF = 8.000000E-01  
 Neill Mod. factor falling limb.NMFF = 8.000000E-01

The maximum storm event in the simulation is 17.540860ins  
 ANNUAL MAX UPSTREAM VELOCITY LAST RUN = 1.567170 1.884795

1.741027	1.563060	1.488132	1.732842
1.781514	1.769986	1.733798	1.630951
1.554986	1.644161	1.583825	1.584878
1.511380	1.612089	1.588335	1.586137
1.801724	1.833766	1.438960	1.735371
1.605883	1.689497	1.477512	1.838591
1.692273	1.499201	1.752849	1.655729
1.650799	1.727695	1.809078	1.879026
1.821498	1.647550	1.811663	1.644336
1.777379	1.585487	1.471010	1.751842
1.750343	1.334382	1.936495	1.804598
1.900772	1.621735	1.806643	1.500918
1.586794	1.489300	1.653678	1.524542
1.866763	1.740348	1.671500	1.809932
1.688887	1.516733	1.780856	1.515332
1.949662	1.610359	1.716997	1.641194
1.769831	1.942062	1.594874	1.451216
1.766730	1.692337	1.538771	1.514773
1.743561	1.766951	1.646306	1.837900
1.568531	1.769240	1.624406	1.754077
1.430896	1.493503	1.604264	1.770634
1.902038	1.672451	1.843853	1.503074
1.980304	1.575525	1.583574	1.808084
1.633552	1.566845	1.498644	1.616985
1.587658	1.792825		

ANNUAL MAX DWNSTREAM VELOCITY LAST RUN = 1.464173  
 1.476181

1.999984	1.946745	2.688903	2.490155
1.564070	1.563139	1.459940	1.498440
1.904922	1.505974	1.608830	2.410543
1.435449	1.430291	1.661848	1.956090
2.078062	1.834023	2.036304	1.618747
1.874203	1.585056	1.880477	1.780695
1.459238	1.380437	1.856357	1.387382
1.818105	2.146832	1.562753	1.809073
2.096366	2.531136	1.588615	1.415374
1.449562	1.414503	1.553368	1.372086
1.954260	2.059736	1.701590	1.661102
1.404088	1.942392	1.483912	1.683647
1.451882	1.550318	1.583688	2.711949
1.902168	1.500196	2.289214	1.735584
2.194894	1.614069	1.549613	1.566894
1.685224	1.765664	1.634830	1.631412
2.364820	1.663724	1.881617	1.577147
1.687603	1.679485	2.188611	1.680995
1.403233	1.514496	1.722323	1.520904
1.362301	1.552143	2.156016	1.899855
1.441149	1.432899	1.691357	1.923167

1.576486	2.327169	1.490382	2.571936
1.690863	1.730314	2.072342	1.593996
1.613682	1.558330	1.602563	2.640761
1.675236	1.370121		
ANNUAL MAX US ADJUSTED VELOCITY LAST RUN =			1.567170
1.884795			
1.741027	1.563060	1.488132	1.732842
1.781514	1.769986	1.733798	1.630951
1.554986	1.644161	1.583825	1.584878
1.511380	1.612089	1.588335	1.586137
1.801724	1.833766	1.438960	1.735371
1.605883	1.689497	1.477512	1.838591
1.692273	1.499201	1.752849	1.655729
1.650799	1.727695	1.809078	1.879026
1.821498	1.647550	1.811663	1.644336
1.777379	1.585487	1.471010	1.751842
1.750343	1.334382	1.936495	1.804598
1.900772	1.621735	1.806643	1.500918
1.586794	1.489300	1.653678	1.524542
1.866763	1.740348	1.671500	1.809932
1.688887	1.516733	1.780856	1.515332
1.949662	1.610359	1.716997	1.641194
1.769831	1.942062	1.594874	1.451216
1.766730	1.692337	1.538771	1.514773
1.743561	1.766951	1.646306	1.837900
1.568531	1.769240	1.624406	1.754077
1.430896	1.493503	1.604264	1.770634
1.902038	1.672451	1.843853	1.503074
1.980304	1.575525	1.583574	1.808084
1.633552	1.566845	1.498644	1.616985
1.587658	1.792825		
ANNUAL MAX DS ADJUSTED VELOCITY LAST RUN =			1.464173
1.476181			
1.999984	1.946745	2.688903	2.490155
1.564070	1.563139	1.459940	1.498440
1.904922	1.505974	1.608830	2.410543
1.435449	1.430291	1.661848	1.956090
2.078062	1.834023	2.036304	1.618747
1.874203	1.585056	1.880477	1.780695
1.459238	1.380437	1.856357	1.387382
1.818105	2.146832	1.562753	1.809073
2.096366	2.531136	1.588615	1.415374
1.449562	1.414503	1.553368	1.372086
1.954260	2.059736	1.701590	1.661102
1.404088	1.942392	1.483912	1.683647
1.451882	1.550318	1.583688	2.711949
1.902168	1.500196	2.289214	1.735584
2.194894	1.614069	1.549613	1.566894
1.685224	1.765664	1.634830	1.631412
2.364820	1.663724	1.881617	1.577147
1.687603	1.679485	2.188611	1.680995
1.403233	1.514496	1.722323	1.520904
1.362301	1.552143	2.156016	1.899855
1.441149	1.432899	1.691357	1.923167
1.576486	2.327169	1.490382	2.571936
1.690863	1.730314	2.072342	1.593996
1.613682	1.558330	1.602563	2.640761

1.675236	1.370121		
ANNUAL MAX UPSTREAM DISCHARGE LAST RUN =		87157.880000	
106094.900000			
79727.400000	87983.480000	76674.880000	70394.590000
94157.970000	85754.730000	88232.610000	94702.070000
87525.600000	84704.440000	81984.840000	84718.550000
77276.140000	74656.300000	72663.800000	86520.680000
84547.850000	87233.450000	78493.700000	68199.840000
84456.230000	79789.270000	85797.700000	90727.910000
81027.310000	81027.310000	85633.980000	90318.090000
81066.870000	91508.050000	98677.390000	102497.800000
99356.750000	81576.300000	98823.590000	82662.690000
89502.740000	90991.430000	77001.690000	83560.720000
92510.520000	77380.280000	105632.300000	98436.450000
84078.200000	79292.660000	78006.930000	81871.930000
69115.980000	81234.890000	84544.770000	81818.480000
73273.670000	91795.820000	84250.810000	95808.200000
80896.530000	81559.680000	97137.500000	87999.310000
106351.200000	83278.960000	93217.340000	78567.650000
87194.670000	105937.200000	105937.200000	79124.250000
87999.640000	87763.880000	79040.630000	82412.900000
94499.020000	83668.720000	89804.160000	78609.400000
74976.790000	85580.280000	84820.300000	75050.670000
75653.340000	69394.630000	83879.350000	76865.410000
89899.700000	89945.930000	94122.010000	74733.850000
84687.740000	69446.700000	83958.590000	88987.660000
89107.840000	84805.380000	76299.470000	82495.500000
83249.240000	79349.280000		
ANNUAL MAX DWNSTREAM DISCHARGE LAST RUN =		79161.950000	
88153.960000			
106844.400000	92259.420000	93468.190000	88192.940000
90017.660000	76578.520000	79571.480000	101360.400000
91641.430000	88352.810000	83317.870000	94273.980000
93274.920000	78764.690000	94026.500000	88145.920000
105925.400000	101187.600000	98754.040000	100933.900000
100770.400000	86391.080000	92192.330000	100297.600000
82737.700000	85998.210000	81889.880000	83491.770000
125435.500000	109593.400000	86992.830000	78994.300000
94823.330000	114850.500000	93556.890000	97543.170000
79705.310000	89045.950000	85721.580000	80730.420000
98219.420000	98747.830000	81804.410000	103093.100000
83246.900000	87923.680000	87191.780000	93343.550000
77715.410000	92859.380000	88731.390000	102512.200000
88970.480000	97059.090000	93883.950000	99081.650000
88267.850000	82854.630000	98887.410000	89644.800000
95116.190000	109906.500000	95088.250000	102234.700000
89547.730000	98817.210000	90044.630000	87576.540000
86876.380000	96361.300000	83110.530000	84806.490000
91436.480000	83718.430000	87106.410000	92753.540000
80499.910000	95264.410000	92159.450000	100096.500000
85120.060000	91211.360000	90805.070000	83943.880000
88511.660000	90779.170000	87210.950000	113414.200000
96593.080000	89590.530000	90497.060000	90408.090000
90107.480000	97568.230000	115020.500000	109018.400000
93293.640000	89909.560000		

ANNUAL MAX UPSTREAM FLOW DEPTH LAST RUN =			17.527210
17.332160			
17.714210	17.950450	17.550000	17.471910
17.604190	17.406810	17.300000	17.509870
17.419050	17.550000	17.552330	17.550000
17.399100	17.397650	17.452770	17.345190
17.266800	17.692980	17.374260	17.721910
17.446550	17.368180	17.339370	17.344870
17.550000	17.482780	17.550000	17.372360
17.550000	17.592870	17.369020	17.415830
17.550000	18.050000	17.550000	17.550000
17.444080	17.688170	17.590290	17.585780
17.550000	17.550000	17.433400	17.607270
17.525250	17.432220	17.407400	17.544880
17.295400	17.501800	17.397220	17.386160
17.439330	17.391480	17.800000	17.550000
17.800000	17.408920	17.800000	17.403270
17.515290	17.522340	17.550000	17.474210
17.295790	17.375390	17.300000	17.358520
17.427340	17.735000	17.308380	17.419150
17.645870	17.804540	17.544580	17.387470
17.497510	17.421670	17.387580	17.521650
17.556740	17.233510	17.579030	17.476660
17.208370	17.800000	17.587650	17.800000
17.727440	17.445990	17.335350	17.550000
17.401180	17.456740	17.662330	17.550000
17.550000	17.484650		
ANNUAL MAX DWTNTEAM FLOW DEPTH LAST RUN =			17.800000
17.800000			
17.872540	17.951540	17.721280	17.800000
17.800000	17.800000	17.800000	17.732740
17.550000	17.800000	17.557800	18.050000
17.800000	17.550000	17.550000	17.550000
17.800000	18.050000	17.550000	18.050000
17.800000	17.550000	18.050000	17.800000
17.800000	17.550000	18.050000	17.550000
18.050000	17.847600	17.550000	18.050000
18.050000	18.300000	17.800000	17.800000
18.050000	17.800000	17.800000	17.846730
17.800000	18.050000	17.800000	17.858470
18.050000	17.800000	17.800000	17.594640
17.550000	17.550000	17.550000	18.300000
18.050000	18.050000	17.800000	17.800000
18.050000	17.467900	18.050000	17.800000
17.800000	17.800000	17.800000	17.800000
18.050000	17.550000	17.550000	17.800000
18.050000	18.050000	18.300000	17.800000
17.754200	18.144820	17.630890	17.800000
17.499710	18.050000	17.750140	17.800000
17.565610	17.800000	17.800000	17.800000
17.800000	17.800000	18.300000	17.800000
18.050000	18.050000	17.800000	17.800000
17.800000	17.629910	17.800000	18.050000
17.568650	17.550000		
ANNUAL MAX US ADJ. FLOW DEPTH LAST RUN =			17.527210
17.332160			
17.714210	17.950450	17.550000	17.471910

17.604190	17.406810	17.300000	17.509870
17.419050	17.550000	17.552330	17.550000
17.399100	17.397650	17.452770	17.345190
17.266800	17.692980	17.374260	17.721910
17.446550	17.368180	17.339370	17.344870
17.550000	17.482780	17.550000	17.372360
17.550000	17.592870	17.369020	17.415830
17.550000	18.050000	17.550000	17.550000
17.444080	17.688170	17.590290	17.585780
17.550000	17.550000	17.433400	17.607270
17.525250	17.432220	17.407400	17.544880
17.295400	17.501800	17.397220	17.386160
17.439330	17.391480	17.800000	17.550000
17.800000	17.408920	17.800000	17.403270
17.515290	17.522340	17.550000	17.474210
17.295790	17.375390	17.300000	17.358520
17.427340	17.735000	17.308380	17.419150
17.645870	17.804540	17.544580	17.387470
17.497510	17.421670	17.387580	17.521650
17.556740	17.233510	17.579030	17.476660
17.208370	17.800000	17.587650	17.800000
17.727440	17.445990	17.335350	17.550000
17.401180	17.456740	17.662330	17.550000
17.550000	17.484650		
ANNUAL MAX DS ADJ. FLOW DEPTH LAST RUN =		17.800000	
17.800000			
17.872540	17.951540	17.721280	17.800000
17.800000	17.800000	17.800000	17.732740
17.550000	17.800000	17.557800	18.050000
17.800000	17.550000	17.550000	17.550000
17.800000	18.050000	17.550000	18.050000
17.800000	17.550000	18.050000	17.800000
17.800000	17.550000	18.050000	17.550000
18.050000	17.847600	17.550000	18.050000
18.050000	18.300000	17.800000	17.800000
18.050000	17.800000	17.800000	17.846730
17.800000	18.050000	17.800000	17.858470
18.050000	17.800000	17.800000	17.594640
17.550000	17.550000	17.550000	18.300000
18.050000	18.050000	17.800000	17.800000
18.050000	17.467900	18.050000	17.800000
17.800000	17.800000	17.800000	17.800000
18.050000	17.550000	17.550000	17.800000
18.050000	18.050000	18.300000	17.800000
17.754200	18.144820	17.630890	17.800000
17.499710	18.050000	17.750140	17.800000
17.565610	17.800000	17.800000	17.800000
17.800000	17.800000	18.300000	17.800000
18.050000	18.050000	17.800000	17.800000
17.800000	17.629910	17.800000	18.050000
17.568650	17.550000		
ANNUAL AVG MAX UPSTREAM VELOCITY =		1.673776	1.677651
1.673942	1.674013	1.674422	1.676951
1.675654	1.677357	1.667293	1.673356
1.676524	1.677484	1.681247	1.682921
1.680292	1.667587	1.679042	1.673949
1.679621	1.671179	1.674301	1.683845

```

The no.of storms in the last.NS=          79
The no.of storms producing no runoff over the simula tion.NORUN=
6913951

```

```

Total scour d/s face last run is TSD =      19.304180
Total scour u/s face last run is TSU =      21.341390
Total scour local d/s face last run is CSD =      19.304180
19.304180

```

684

[illegible]





7.0000	.0000	.0000	.0330
7.5000	.0000	.0000	.0330
8.0000	.0000	.0000	.0330
8.5000	.0000	.0000	.0330
9.0000	.0000	.0000	.0330
9.5000	.0000	.0000	.0330
10.0000	.0000	.0000	.0330
10.5000	.0000	.0000	.0330
11.0000	.0000	.0000	.0330
11.5000	.0000	.0000	.0330
12.0000	.0000	.0000	.0330
12.5000	.0000	.0000	.0330
13.0000	.0000	.0000	.0330
13.5000	.0000	.0000	.0330
14.0000	.0000	.0000	.0330
14.5000	.0000	.0000	.0330
15.0000	.0000	.0000	.0330
15.5000	.0000	.0000	.0330
16.0000	.0000	.0000	.0330
16.5000	.0000	.0000	.0330
17.0000	.0000	.0000	.0330
17.5000	.0000	.0000	.0330
18.0000	.0000	.0000	.0330
18.5000	1.0000	.0010	.0340
19.0000	8.0000	.0080	.0420
19.5000	935.0000	.9350	.9770
20.0000	23.0000	.0230	1.0000
20.5000	.0000	.0000	1.0000
21.0000	.0000	.0000	1.0000
21.5000	.0000	.0000	1.0000
22.0000	.0000	.0000	1.0000
22.5000	.0000	.0000	1.0000
23.0000	.0000	.0000	1.0000
23.5000	.0000	.0000	1.0000
24.0000	.0000	.0000	1.0000
24.5000	.0000	.0000	1.0000
25.0000	.0000	.0000	1.0000
25.5000	.0000	.0000	1.0000
26.0000	.0000	.0000	1.0000
26.5000	.0000	.0000	1.0000
27.0000	.0000	.0000	1.0000
27.5000	.0000	.0000	1.0000
28.0000	.0000	.0000	1.0000
28.5000	.0000	.0000	1.0000
29.0000	.0000	.0000	1.0000
29.5000	.0000	.0000	1.0000
30.0000	.0000	.0000	1.0000
30.5000	.0000	.0000	1.0000
31.0000	.0000	.0000	1.0000
31.5000	.0000	.0000	1.0000
32.0000	.0000	.0000	1.0000
32.5000	.0000	.0000	1.0000
33.0000	.0000	.0000	1.0000
33.5000	.0000	.0000	1.0000
34.0000	.0000	.0000	1.0000
34.5000	.0000	.0000	1.0000
35.0000	.0000	.0000	1.0000

35.5000	.0000	.0000	1.0000
36.0000	.0000	.0000	1.0000
36.5000	.0000	.0000	1.0000
37.0000	.0000	.0000	1.0000
37.5000	.0000	.0000	1.0000
38.0000	.0000	.0000	1.0000
38.5000	.0000	.0000	1.0000
39.0000	.0000	.0000	1.0000
39.5000	.0000	.0000	1.0000
40.0000	.0000	.0000	1.0000
40.5000	.0000	.0000	1.0000
41.0000	.0000	.0000	1.0000
41.5000	.0000	.0000	1.0000
42.0000	.0000	.0000	1.0000
42.5000	.0000	.0000	1.0000
43.0000	.0000	.0000	1.0000
43.5000	.0000	.0000	1.0000
44.0000	.0000	.0000	1.0000
44.5000	.0000	.0000	1.0000
45.0000	.0000	.0000	1.0000
45.5000	.0000	.0000	1.0000
46.0000	.0000	.0000	1.0000
46.5000	.0000	.0000	1.0000
47.0000	.0000	.0000	1.0000
47.5000	.0000	.0000	1.0000
48.0000	.0000	.0000	1.0000
48.5000	.0000	.0000	1.0000
49.0000	.0000	.0000	1.0000
49.5000	.0000	.0000	1.0000
50.0000	.0000	.0000	1.0000
50.5000	.0000	.0000	1.0000
B	FU	PRU	CPRU
1.0000	.0000	.0000	.0000
1.5000	.0000	.0000	.0000
2.0000	.0000	.0000	.0000
2.5000	.0000	.0000	.0000
3.0000	.0000	.0000	.0000
3.5000	.0000	.0000	.0000
4.0000	.0000	.0000	.0000
4.5000	.0000	.0000	.0000
5.0000	.0000	.0000	.0000
5.5000	.0000	.0000	.0000
6.0000	.0000	.0000	.0000
6.5000	.0000	.0000	.0000
7.0000	.0000	.0000	.0000
7.5000	.0000	.0000	.0000
8.0000	.0000	.0000	.0000
8.5000	.0000	.0000	.0000
9.0000	.0000	.0000	.0000
9.5000	.0000	.0000	.0000
10.0000	.0000	.0000	.0000
10.5000	.0000	.0000	.0000
11.0000	.0000	.0000	.0000
11.5000	.0000	.0000	.0000
12.0000	.0000	.0000	.0000
12.5000	.0000	.0000	.0000
13.0000	.0000	.0000	.0000

13.5000	.0000	.0000	.0000
14.0000	.0000	.0000	.0000
14.5000	.0000	.0000	.0000
15.0000	.0000	.0000	.0000
15.5000	.0000	.0000	.0000
16.0000	.0000	.0000	.0000
16.5000	.0000	.0000	.0000
17.0000	.0000	.0000	.0000
17.5000	.0000	.0000	.0000
18.0000	.0000	.0000	.0000
18.5000	.0000	.0000	.0000
19.0000	.0000	.0000	.0000
19.5000	.0000	.0000	.0000
20.0000	.0000	.0000	.0000
20.5000	.0000	.0000	.0000
21.0000	.0000	.0000	.0000
21.5000	231.0000	.2310	.2310
22.0000	593.0000	.5930	.8240
22.5000	145.0000	.1450	.9690
23.0000	26.0000	.0260	.9950
23.5000	5.0000	.0050	1.0000
24.0000	.0000	.0000	1.0000
24.5000	.0000	.0000	1.0000
25.0000	.0000	.0000	1.0000
25.5000	.0000	.0000	1.0000
26.0000	.0000	.0000	1.0000
26.5000	.0000	.0000	1.0000
27.0000	.0000	.0000	1.0000
27.5000	.0000	.0000	1.0000
28.0000	.0000	.0000	1.0000
28.5000	.0000	.0000	1.0000
29.0000	.0000	.0000	1.0000
29.5000	.0000	.0000	1.0000
30.0000	.0000	.0000	1.0000
30.5000	.0000	.0000	1.0000
31.0000	.0000	.0000	1.0000
31.5000	.0000	.0000	1.0000
32.0000	.0000	.0000	1.0000
32.5000	.0000	.0000	1.0000
33.0000	.0000	.0000	1.0000
33.5000	.0000	.0000	1.0000
34.0000	.0000	.0000	1.0000
34.5000	.0000	.0000	1.0000
35.0000	.0000	.0000	1.0000
35.5000	.0000	.0000	1.0000
36.0000	.0000	.0000	1.0000
36.5000	.0000	.0000	1.0000
37.0000	.0000	.0000	1.0000
37.5000	.0000	.0000	1.0000
38.0000	.0000	.0000	1.0000
38.5000	.0000	.0000	1.0000
39.0000	.0000	.0000	1.0000
39.5000	.0000	.0000	1.0000
40.0000	.0000	.0000	1.0000
40.5000	.0000	.0000	1.0000
41.0000	.0000	.0000	1.0000
41.5000	.0000	.0000	1.0000

42.0000	.0000	.0000	1.0000
42.5000	.0000	.0000	1.0000
43.0000	.0000	.0000	1.0000
43.5000	.0000	.0000	1.0000
44.0000	.0000	.0000	1.0000
44.5000	.0000	.0000	1.0000
45.0000	.0000	.0000	1.0000
45.5000	.0000	.0000	1.0000
46.0000	.0000	.0000	1.0000
46.5000	.0000	.0000	1.0000
47.0000	.0000	.0000	1.0000
47.5000	.0000	.0000	1.0000
48.0000	.0000	.0000	1.0000
48.5000	.0000	.0000	1.0000
49.0000	.0000	.0000	1.0000
49.5000	.0000	.0000	1.0000
50.0000	.0000	.0000	1.0000
50.5000	.0000	.0000	1.0000

15 PERCENT TMS SCOUR RESULTS

B	FD15	PRD15	CPRD15
1.0000	1000.0000	1.0000	1.0000
1.5000	.0000	.0000	1.0000
2.0000	.0000	.0000	1.0000
2.5000	.0000	.0000	1.0000
3.0000	.0000	.0000	1.0000
3.5000	.0000	.0000	1.0000
4.0000	.0000	.0000	1.0000
4.5000	.0000	.0000	1.0000
5.0000	.0000	.0000	1.0000
5.5000	.0000	.0000	1.0000
6.0000	.0000	.0000	1.0000
6.5000	.0000	.0000	1.0000
7.0000	.0000	.0000	1.0000
7.5000	.0000	.0000	1.0000
8.0000	.0000	.0000	1.0000
8.5000	.0000	.0000	1.0000
9.0000	.0000	.0000	1.0000
9.5000	.0000	.0000	1.0000
10.0000	.0000	.0000	1.0000
10.5000	.0000	.0000	1.0000
11.0000	.0000	.0000	1.0000
11.5000	.0000	.0000	1.0000
12.0000	.0000	.0000	1.0000
12.5000	.0000	.0000	1.0000
13.0000	.0000	.0000	1.0000
13.5000	.0000	.0000	1.0000
14.0000	.0000	.0000	1.0000
14.5000	.0000	.0000	1.0000
15.0000	.0000	.0000	1.0000
15.5000	.0000	.0000	1.0000
16.0000	.0000	.0000	1.0000
16.5000	.0000	.0000	1.0000
17.0000	.0000	.0000	1.0000
17.5000	.0000	.0000	1.0000
18.0000	.0000	.0000	1.0000
18.5000	.0000	.0000	1.0000
19.0000	.0000	.0000	1.0000

19.5000	.0000	.0000	1.0000
20.0000	.0000	.0000	1.0000
20.5000	.0000	.0000	1.0000
21.0000	.0000	.0000	1.0000
21.5000	.0000	.0000	1.0000
22.0000	.0000	.0000	1.0000
22.5000	.0000	.0000	1.0000
23.0000	.0000	.0000	1.0000
23.5000	.0000	.0000	1.0000
24.0000	.0000	.0000	1.0000
24.5000	.0000	.0000	1.0000
25.0000	.0000	.0000	1.0000
25.5000	.0000	.0000	1.0000
26.0000	.0000	.0000	1.0000
26.5000	.0000	.0000	1.0000
27.0000	.0000	.0000	1.0000
27.5000	.0000	.0000	1.0000
28.0000	.0000	.0000	1.0000
28.5000	.0000	.0000	1.0000
29.0000	.0000	.0000	1.0000
29.5000	.0000	.0000	1.0000
30.0000	.0000	.0000	1.0000
30.5000	.0000	.0000	1.0000
31.0000	.0000	.0000	1.0000
31.5000	.0000	.0000	1.0000
32.0000	.0000	.0000	1.0000
32.5000	.0000	.0000	1.0000
33.0000	.0000	.0000	1.0000
33.5000	.0000	.0000	1.0000
34.0000	.0000	.0000	1.0000
34.5000	.0000	.0000	1.0000
35.0000	.0000	.0000	1.0000
35.5000	.0000	.0000	1.0000
36.0000	.0000	.0000	1.0000
36.5000	.0000	.0000	1.0000
37.0000	.0000	.0000	1.0000
37.5000	.0000	.0000	1.0000
38.0000	.0000	.0000	1.0000
38.5000	.0000	.0000	1.0000
39.0000	.0000	.0000	1.0000
39.5000	.0000	.0000	1.0000
40.0000	.0000	.0000	1.0000
40.5000	.0000	.0000	1.0000
41.0000	.0000	.0000	1.0000
41.5000	.0000	.0000	1.0000
42.0000	.0000	.0000	1.0000
42.5000	.0000	.0000	1.0000
43.0000	.0000	.0000	1.0000
43.5000	.0000	.0000	1.0000
44.0000	.0000	.0000	1.0000
44.5000	.0000	.0000	1.0000
45.0000	.0000	.0000	1.0000
45.5000	.0000	.0000	1.0000
46.0000	.0000	.0000	1.0000
46.5000	.0000	.0000	1.0000
47.0000	.0000	.0000	1.0000
47.5000	.0000	.0000	1.0000

48.0000	.0000	.0000	1.0000
48.5000	.0000	.0000	1.0000
49.0000	.0000	.0000	1.0000
49.5000	.0000	.0000	1.0000
50.0000	.0000	.0000	1.0000
50.5000	.0000	.0000	1.0000
B	FU15	PRU15	CPRU15
1.0000	140.0000	.1400	.1400
1.5000	86.0000	.0860	.2260
2.0000	54.0000	.0540	.2800
2.5000	63.0000	.0630	.3430
3.0000	45.0000	.0450	.3880
3.5000	48.0000	.0480	.4360
4.0000	30.0000	.0300	.4660
4.5000	37.0000	.0370	.5030
5.0000	24.0000	.0240	.5270
5.5000	1.0000	.0010	.5280
6.0000	.0000	.0000	.5280
6.5000	.0000	.0000	.5280
7.0000	.0000	.0000	.5280
7.5000	1.0000	.0010	.5290
8.0000	.0000	.0000	.5290
8.5000	1.0000	.0010	.5300
9.0000	.0000	.0000	.5300
9.5000	.0000	.0000	.5300
10.0000	.0000	.0000	.5300
10.5000	2.0000	.0020	.5320
11.0000	.0000	.0000	.5320
11.5000	.0000	.0000	.5320
12.0000	13.0000	.0130	.5450
12.5000	4.0000	.0040	.5490
13.0000	5.0000	.0050	.5540
13.5000	2.0000	.0020	.5560
14.0000	8.0000	.0080	.5640
14.5000	4.0000	.0040	.5680
15.0000	.0000	.0000	.5680
15.5000	3.0000	.0030	.5710
16.0000	10.0000	.0100	.5810
16.5000	4.0000	.0040	.5850
17.0000	6.0000	.0060	.5910
17.5000	5.0000	.0050	.5960
18.0000	12.0000	.0120	.6080
18.5000	16.0000	.0160	.6240
19.0000	31.0000	.0310	.6550
19.5000	53.0000	.0530	.7080
20.0000	69.0000	.0690	.7770
20.5000	91.0000	.0910	.8680
21.0000	91.0000	.0910	.9590
21.5000	33.0000	.0330	.9920
22.0000	6.0000	.0060	.9980
22.5000	2.0000	.0020	1.0000
23.0000	.0000	.0000	1.0000
23.5000	.0000	.0000	1.0000
24.0000	.0000	.0000	1.0000
24.5000	.0000	.0000	1.0000
25.0000	.0000	.0000	1.0000
25.5000	.0000	.0000	1.0000

26.0000	.0000	.0000	1.0000
26.5000	.0000	.0000	1.0000
27.0000	.0000	.0000	1.0000
27.5000	.0000	.0000	1.0000
28.0000	.0000	.0000	1.0000
28.5000	.0000	.0000	1.0000
29.0000	.0000	.0000	1.0000
29.5000	.0000	.0000	1.0000
30.0000	.0000	.0000	1.0000
30.5000	.0000	.0000	1.0000
31.0000	.0000	.0000	1.0000
31.5000	.0000	.0000	1.0000
32.0000	.0000	.0000	1.0000
32.5000	.0000	.0000	1.0000
33.0000	.0000	.0000	1.0000
33.5000	.0000	.0000	1.0000
34.0000	.0000	.0000	1.0000
34.5000	.0000	.0000	1.0000
35.0000	.0000	.0000	1.0000
35.5000	.0000	.0000	1.0000
36.0000	.0000	.0000	1.0000
36.5000	.0000	.0000	1.0000
37.0000	.0000	.0000	1.0000
37.5000	.0000	.0000	1.0000
38.0000	.0000	.0000	1.0000
38.5000	.0000	.0000	1.0000
39.0000	.0000	.0000	1.0000
39.5000	.0000	.0000	1.0000
40.0000	.0000	.0000	1.0000
40.5000	.0000	.0000	1.0000
41.0000	.0000	.0000	1.0000
41.5000	.0000	.0000	1.0000
42.0000	.0000	.0000	1.0000
42.5000	.0000	.0000	1.0000
43.0000	.0000	.0000	1.0000
43.5000	.0000	.0000	1.0000
44.0000	.0000	.0000	1.0000
44.5000	.0000	.0000	1.0000
45.0000	.0000	.0000	1.0000
45.5000	.0000	.0000	1.0000
46.0000	.0000	.0000	1.0000
46.5000	.0000	.0000	1.0000
47.0000	.0000	.0000	1.0000
47.5000	.0000	.0000	1.0000
48.0000	.0000	.0000	1.0000
48.5000	.0000	.0000	1.0000
49.0000	.0000	.0000	1.0000
49.5000	.0000	.0000	1.0000
50.0000	.0000	.0000	1.0000
50.5000	.0000	.0000	1.0000
25 PERCENT SCOUR RESULTS			
B	FD25	PRD25	CPRD25
1.0000	1000.0000	1.0000	1.0000
1.5000	.0000	.0000	1.0000
2.0000	.0000	.0000	1.0000
2.5000	.0000	.0000	1.0000
3.0000	.0000	.0000	1.0000

3.5000	.0000	.0000	1.0000
4.0000	.0000	.0000	1.0000
4.5000	.0000	.0000	1.0000
5.0000	.0000	.0000	1.0000
5.5000	.0000	.0000	1.0000
6.0000	.0000	.0000	1.0000
6.5000	.0000	.0000	1.0000
7.0000	.0000	.0000	1.0000
7.5000	.0000	.0000	1.0000
8.0000	.0000	.0000	1.0000
8.5000	.0000	.0000	1.0000
9.0000	.0000	.0000	1.0000
9.5000	.0000	.0000	1.0000
10.0000	.0000	.0000	1.0000
10.5000	.0000	.0000	1.0000
11.0000	.0000	.0000	1.0000
11.5000	.0000	.0000	1.0000
12.0000	.0000	.0000	1.0000
12.5000	.0000	.0000	1.0000
13.0000	.0000	.0000	1.0000
13.5000	.0000	.0000	1.0000
14.0000	.0000	.0000	1.0000
14.5000	.0000	.0000	1.0000
15.0000	.0000	.0000	1.0000
15.5000	.0000	.0000	1.0000
16.0000	.0000	.0000	1.0000
16.5000	.0000	.0000	1.0000
17.0000	.0000	.0000	1.0000
17.5000	.0000	.0000	1.0000
18.0000	.0000	.0000	1.0000
18.5000	.0000	.0000	1.0000
19.0000	.0000	.0000	1.0000
19.5000	.0000	.0000	1.0000
20.0000	.0000	.0000	1.0000
20.5000	.0000	.0000	1.0000
21.0000	.0000	.0000	1.0000
21.5000	.0000	.0000	1.0000
22.0000	.0000	.0000	1.0000
22.5000	.0000	.0000	1.0000
23.0000	.0000	.0000	1.0000
23.5000	.0000	.0000	1.0000
24.0000	.0000	.0000	1.0000
24.5000	.0000	.0000	1.0000
25.0000	.0000	.0000	1.0000
25.5000	.0000	.0000	1.0000
26.0000	.0000	.0000	1.0000
26.5000	.0000	.0000	1.0000
27.0000	.0000	.0000	1.0000
27.5000	.0000	.0000	1.0000
28.0000	.0000	.0000	1.0000
28.5000	.0000	.0000	1.0000
29.0000	.0000	.0000	1.0000
29.5000	.0000	.0000	1.0000
30.0000	.0000	.0000	1.0000
30.5000	.0000	.0000	1.0000
31.0000	.0000	.0000	1.0000
31.5000	.0000	.0000	1.0000



32.0000	.0000	.0000	1.0000
32.5000	.0000	.0000	1.0000
33.0000	.0000	.0000	1.0000
33.5000	.0000	.0000	1.0000
34.0000	.0000	.0000	1.0000
34.5000	.0000	.0000	1.0000
35.0000	.0000	.0000	1.0000
35.5000	.0000	.0000	1.0000
36.0000	.0000	.0000	1.0000
36.5000	.0000	.0000	1.0000
37.0000	.0000	.0000	1.0000
37.5000	.0000	.0000	1.0000
38.0000	.0000	.0000	1.0000
38.5000	.0000	.0000	1.0000
39.0000	.0000	.0000	1.0000
39.5000	.0000	.0000	1.0000
40.0000	.0000	.0000	1.0000
40.5000	.0000	.0000	1.0000
41.0000	.0000	.0000	1.0000
41.5000	.0000	.0000	1.0000
42.0000	.0000	.0000	1.0000
42.5000	.0000	.0000	1.0000
43.0000	.0000	.0000	1.0000
43.5000	.0000	.0000	1.0000
44.0000	.0000	.0000	1.0000
44.5000	.0000	.0000	1.0000
45.0000	.0000	.0000	1.0000
45.5000	.0000	.0000	1.0000
46.0000	.0000	.0000	1.0000
46.5000	.0000	.0000	1.0000
47.0000	.0000	.0000	1.0000
47.5000	.0000	.0000	1.0000
48.0000	.0000	.0000	1.0000
48.5000	.0000	.0000	1.0000
49.0000	.0000	.0000	1.0000
49.5000	.0000	.0000	1.0000
50.0000	.0000	.0000	1.0000
50.5000	.0000	.0000	1.0000
B	FU25	PRU25	CPRU25
1.0000	8.0000	.0080	.0080
1.5000	14.0000	.0140	.0220
2.0000	7.0000	.0070	.0290
2.5000	18.0000	.0180	.0470
3.0000	15.0000	.0150	.0620
3.5000	17.0000	.0170	.0790
4.0000	13.0000	.0130	.0920
4.5000	15.0000	.0150	.1070
5.0000	9.0000	.0090	.1160
5.5000	1.0000	.0010	.1170
6.0000	.0000	.0000	.1170
6.5000	1.0000	.0010	.1180
7.0000	1.0000	.0010	.1190
7.5000	1.0000	.0010	.1200
8.0000	.0000	.0000	.1200
8.5000	.0000	.0000	.1200
9.0000	.0000	.0000	.1200
9.5000	.0000	.0000	.1200

10.0000	.0000	.0000	.1200
10.5000	.0000	.0000	.1200
11.0000	.0000	.0000	.1200
11.5000	.0000	.0000	.1200
12.0000	6.0000	.0060	.1260
12.5000	8.0000	.0080	.1340
13.0000	2.0000	.0020	.1360
13.5000	.0000	.0000	.1360
14.0000	1.0000	.0010	.1370
14.5000	2.0000	.0020	.1390
15.0000	.0000	.0000	.1390
15.5000	2.0000	.0020	.1410
16.0000	6.0000	.0060	.1470
16.5000	3.0000	.0030	.1500
17.0000	3.0000	.0030	.1530
17.5000	3.0000	.0030	.1560
18.0000	7.0000	.0070	.1630
18.5000	10.0000	.0100	.1730
19.0000	15.0000	.0150	.1880
19.5000	34.0000	.0340	.2220
20.0000	72.0000	.0720	.2940
20.5000	210.0000	.2100	.5040
21.0000	267.0000	.2670	.7710
21.5000	170.0000	.1700	.9410
22.0000	48.0000	.0480	.9890
22.5000	9.0000	.0090	.9980
23.0000	.0000	.0000	.9980
23.5000	2.0000	.0020	1.0000
24.0000	.0000	.0000	1.0000
24.5000	.0000	.0000	1.0000
25.0000	.0000	.0000	1.0000
25.5000	.0000	.0000	1.0000
26.0000	.0000	.0000	1.0000
26.5000	.0000	.0000	1.0000
27.0000	.0000	.0000	1.0000
27.5000	.0000	.0000	1.0000
28.0000	.0000	.0000	1.0000
28.5000	.0000	.0000	1.0000
29.0000	.0000	.0000	1.0000
29.5000	.0000	.0000	1.0000
30.0000	.0000	.0000	1.0000
30.5000	.0000	.0000	1.0000
31.0000	.0000	.0000	1.0000
31.5000	.0000	.0000	1.0000
32.0000	.0000	.0000	1.0000
32.5000	.0000	.0000	1.0000
33.0000	.0000	.0000	1.0000
33.5000	.0000	.0000	1.0000
34.0000	.0000	.0000	1.0000
34.5000	.0000	.0000	1.0000
35.0000	.0000	.0000	1.0000
35.5000	.0000	.0000	1.0000
36.0000	.0000	.0000	1.0000
36.5000	.0000	.0000	1.0000
37.0000	.0000	.0000	1.0000
37.5000	.0000	.0000	1.0000
38.0000	.0000	.0000	1.0000

38.5000	.0000	.0000	1.0000
39.0000	.0000	.0000	1.0000
39.5000	.0000	.0000	1.0000
40.0000	.0000	.0000	1.0000
40.5000	.0000	.0000	1.0000
41.0000	.0000	.0000	1.0000
41.5000	.0000	.0000	1.0000
42.0000	.0000	.0000	1.0000
42.5000	.0000	.0000	1.0000
43.0000	.0000	.0000	1.0000
43.5000	.0000	.0000	1.0000
44.0000	.0000	.0000	1.0000
44.5000	.0000	.0000	1.0000
45.0000	.0000	.0000	1.0000
45.5000	.0000	.0000	1.0000
46.0000	.0000	.0000	1.0000
46.5000	.0000	.0000	1.0000
47.0000	.0000	.0000	1.0000
47.5000	.0000	.0000	1.0000
48.0000	.0000	.0000	1.0000
48.5000	.0000	.0000	1.0000
49.0000	.0000	.0000	1.0000
49.5000	.0000	.0000	1.0000
50.0000	.0000	.0000	1.0000
50.5000	.0000	.0000	1.0000

50 PERCENT TMS SCOUR RESULTS

B	FD50	PRD50	CPRD50
1.0000	644.0000	.6440	.6440
1.5000	295.0000	.2950	.9390
2.0000	45.0000	.0450	.9840
2.5000	13.0000	.0130	.9970
3.0000	2.0000	.0020	.9990
3.5000	.0000	.0000	.9990
4.0000	.0000	.0000	.9990
4.5000	1.0000	.0010	1.0000
5.0000	.0000	.0000	1.0000
5.5000	.0000	.0000	1.0000
6.0000	.0000	.0000	1.0000
6.5000	.0000	.0000	1.0000
7.0000	.0000	.0000	1.0000
7.5000	.0000	.0000	1.0000
8.0000	.0000	.0000	1.0000
8.5000	.0000	.0000	1.0000
9.0000	.0000	.0000	1.0000
9.5000	.0000	.0000	1.0000
10.0000	.0000	.0000	1.0000
10.5000	.0000	.0000	1.0000
11.0000	.0000	.0000	1.0000
11.5000	.0000	.0000	1.0000
12.0000	.0000	.0000	1.0000
12.5000	.0000	.0000	1.0000
13.0000	.0000	.0000	1.0000
13.5000	.0000	.0000	1.0000
14.0000	.0000	.0000	1.0000
14.5000	.0000	.0000	1.0000
15.0000	.0000	.0000	1.0000
15.5000	.0000	.0000	1.0000

16.0000	.0000	.0000	1.0000
16.5000	.0000	.0000	1.0000
17.0000	.0000	.0000	1.0000
17.5000	.0000	.0000	1.0000
18.0000	.0000	.0000	1.0000
18.5000	.0000	.0000	1.0000
19.0000	.0000	.0000	1.0000
19.5000	.0000	.0000	1.0000
20.0000	.0000	.0000	1.0000
20.5000	.0000	.0000	1.0000
21.0000	.0000	.0000	1.0000
21.5000	.0000	.0000	1.0000
22.0000	.0000	.0000	1.0000
22.5000	.0000	.0000	1.0000
23.0000	.0000	.0000	1.0000
23.5000	.0000	.0000	1.0000
24.0000	.0000	.0000	1.0000
24.5000	.0000	.0000	1.0000
25.0000	.0000	.0000	1.0000
25.5000	.0000	.0000	1.0000
26.0000	.0000	.0000	1.0000
26.5000	.0000	.0000	1.0000
27.0000	.0000	.0000	1.0000
27.5000	.0000	.0000	1.0000
28.0000	.0000	.0000	1.0000
28.5000	.0000	.0000	1.0000
29.0000	.0000	.0000	1.0000
29.5000	.0000	.0000	1.0000
30.0000	.0000	.0000	1.0000
30.5000	.0000	.0000	1.0000
31.0000	.0000	.0000	1.0000
31.5000	.0000	.0000	1.0000
32.0000	.0000	.0000	1.0000
32.5000	.0000	.0000	1.0000
33.0000	.0000	.0000	1.0000
33.5000	.0000	.0000	1.0000
34.0000	.0000	.0000	1.0000
34.5000	.0000	.0000	1.0000
35.0000	.0000	.0000	1.0000
35.5000	.0000	.0000	1.0000
36.0000	.0000	.0000	1.0000
36.5000	.0000	.0000	1.0000
37.0000	.0000	.0000	1.0000
37.5000	.0000	.0000	1.0000
38.0000	.0000	.0000	1.0000
38.5000	.0000	.0000	1.0000
39.0000	.0000	.0000	1.0000
39.5000	.0000	.0000	1.0000
40.0000	.0000	.0000	1.0000
40.5000	.0000	.0000	1.0000
41.0000	.0000	.0000	1.0000
41.5000	.0000	.0000	1.0000
42.0000	.0000	.0000	1.0000
42.5000	.0000	.0000	1.0000
43.0000	.0000	.0000	1.0000
43.5000	.0000	.0000	1.0000
44.0000	.0000	.0000	1.0000

44.5000	.0000	.0000	1.0000
45.0000	.0000	.0000	1.0000
45.5000	.0000	.0000	1.0000
46.0000	.0000	.0000	1.0000
46.5000	.0000	.0000	1.0000
47.0000	.0000	.0000	1.0000
47.5000	.0000	.0000	1.0000
48.0000	.0000	.0000	1.0000
48.5000	.0000	.0000	1.0000
49.0000	.0000	.0000	1.0000
49.5000	.0000	.0000	1.0000
50.0000	.0000	.0000	1.0000
50.5000	.0000	.0000	1.0000
B	FU50	PRU50	CPRU50
1.0000	.0000	.0000	.0000
1.5000	.0000	.0000	.0000
2.0000	.0000	.0000	.0000
2.5000	.0000	.0000	.0000
3.0000	.0000	.0000	.0000
3.5000	.0000	.0000	.0000
4.0000	.0000	.0000	.0000
4.5000	.0000	.0000	.0000
5.0000	.0000	.0000	.0000
5.5000	.0000	.0000	.0000
6.0000	.0000	.0000	.0000
6.5000	.0000	.0000	.0000
7.0000	.0000	.0000	.0000
7.5000	.0000	.0000	.0000
8.0000	.0000	.0000	.0000
8.5000	.0000	.0000	.0000
9.0000	.0000	.0000	.0000
9.5000	.0000	.0000	.0000
10.0000	.0000	.0000	.0000
10.5000	.0000	.0000	.0000
11.0000	.0000	.0000	.0000
11.5000	.0000	.0000	.0000
12.0000	.0000	.0000	.0000
12.5000	.0000	.0000	.0000
13.0000	.0000	.0000	.0000
13.5000	.0000	.0000	.0000
14.0000	.0000	.0000	.0000
14.5000	.0000	.0000	.0000
15.0000	.0000	.0000	.0000
15.5000	.0000	.0000	.0000
16.0000	.0000	.0000	.0000
16.5000	.0000	.0000	.0000
17.0000	.0000	.0000	.0000
17.5000	.0000	.0000	.0000
18.0000	.0000	.0000	.0000
18.5000	.0000	.0000	.0000
19.0000	.0000	.0000	.0000
19.5000	1.0000	.0010	.0010
20.0000	1.0000	.0010	.0020
20.5000	5.0000	.0050	.0070
21.0000	153.0000	.1530	.1600
21.5000	527.0000	.5270	.6870
22.0000	250.0000	.2500	.9370

22.5000	52.0000	.0520	.9890
23.0000	8.0000	.0080	.9970
23.5000	3.0000	.0030	1.0000
24.0000	.0000	.0000	1.0000
24.5000	.0000	.0000	1.0000
25.0000	.0000	.0000	1.0000
25.5000	.0000	.0000	1.0000
26.0000	.0000	.0000	1.0000
26.5000	.0000	.0000	1.0000
27.0000	.0000	.0000	1.0000
27.5000	.0000	.0000	1.0000
28.0000	.0000	.0000	1.0000
28.5000	.0000	.0000	1.0000
29.0000	.0000	.0000	1.0000
29.5000	.0000	.0000	1.0000
30.0000	.0000	.0000	1.0000
30.5000	.0000	.0000	1.0000
31.0000	.0000	.0000	1.0000
31.5000	.0000	.0000	1.0000
32.0000	.0000	.0000	1.0000
32.5000	.0000	.0000	1.0000
33.0000	.0000	.0000	1.0000
33.5000	.0000	.0000	1.0000
34.0000	.0000	.0000	1.0000
34.5000	.0000	.0000	1.0000
35.0000	.0000	.0000	1.0000
35.5000	.0000	.0000	1.0000
36.0000	.0000	.0000	1.0000
36.5000	.0000	.0000	1.0000
37.0000	.0000	.0000	1.0000
37.5000	.0000	.0000	1.0000
38.0000	.0000	.0000	1.0000
38.5000	.0000	.0000	1.0000
39.0000	.0000	.0000	1.0000
39.5000	.0000	.0000	1.0000
40.0000	.0000	.0000	1.0000
40.5000	.0000	.0000	1.0000
41.0000	.0000	.0000	1.0000
41.5000	.0000	.0000	1.0000
42.0000	.0000	.0000	1.0000
42.5000	.0000	.0000	1.0000
43.0000	.0000	.0000	1.0000
43.5000	.0000	.0000	1.0000
44.0000	.0000	.0000	1.0000
44.5000	.0000	.0000	1.0000
45.0000	.0000	.0000	1.0000
45.5000	.0000	.0000	1.0000
46.0000	.0000	.0000	1.0000
46.5000	.0000	.0000	1.0000
47.0000	.0000	.0000	1.0000
47.5000	.0000	.0000	1.0000
48.0000	.0000	.0000	1.0000
48.5000	.0000	.0000	1.0000
49.0000	.0000	.0000	1.0000
49.5000	.0000	.0000	1.0000
50.0000	.0000	.0000	1.0000
50.5000	.0000	.0000	1.0000

75 PERCENT TMS SCOUR RESULTS

B	FD75	PRD75	CPRD75
1.0000	16.0000	.0160	.0160
1.5000	122.0000	.1220	.1380
2.0000	187.0000	.1870	.3250
2.5000	148.0000	.1480	.4730
3.0000	111.0000	.1110	.5840
3.5000	58.0000	.0580	.6420
4.0000	45.0000	.0450	.6870
4.5000	27.0000	.0270	.7140
5.0000	26.0000	.0260	.7400
5.5000	.0000	.0000	.7400
6.0000	.0000	.0000	.7400
6.5000	.0000	.0000	.7400
7.0000	.0000	.0000	.7400
7.5000	.0000	.0000	.7400
8.0000	.0000	.0000	.7400
8.5000	.0000	.0000	.7400
9.0000	1.0000	.0010	.7410
9.5000	.0000	.0000	.7410
10.0000	.0000	.0000	.7410
10.5000	.0000	.0000	.7410
11.0000	.0000	.0000	.7410
11.5000	.0000	.0000	.7410
12.0000	.0000	.0000	.7410
12.5000	.0000	.0000	.7410
13.0000	.0000	.0000	.7410
13.5000	.0000	.0000	.7410
14.0000	.0000	.0000	.7410
14.5000	.0000	.0000	.7410
15.0000	.0000	.0000	.7410
15.5000	.0000	.0000	.7410
16.0000	.0000	.0000	.7410
16.5000	.0000	.0000	.7410
17.0000	.0000	.0000	.7410
17.5000	.0000	.0000	.7410
18.0000	.0000	.0000	.7410
18.5000	3.0000	.0030	.7440
19.0000	36.0000	.0360	.7800
19.5000	220.0000	.2200	1.0000
20.0000	.0000	.0000	1.0000
20.5000	.0000	.0000	1.0000
21.0000	.0000	.0000	1.0000
21.5000	.0000	.0000	1.0000
22.0000	.0000	.0000	1.0000
22.5000	.0000	.0000	1.0000
23.0000	.0000	.0000	1.0000
23.5000	.0000	.0000	1.0000
24.0000	.0000	.0000	1.0000
24.5000	.0000	.0000	1.0000
25.0000	.0000	.0000	1.0000
25.5000	.0000	.0000	1.0000
26.0000	.0000	.0000	1.0000
26.5000	.0000	.0000	1.0000
27.0000	.0000	.0000	1.0000
27.5000	.0000	.0000	1.0000
28.0000	.0000	.0000	1.0000

28.5000	.0000	.0000	1.0000
29.0000	.0000	.0000	1.0000
29.5000	.0000	.0000	1.0000
30.0000	.0000	.0000	1.0000
30.5000	.0000	.0000	1.0000
31.0000	.0000	.0000	1.0000
31.5000	.0000	.0000	1.0000
32.0000	.0000	.0000	1.0000
32.5000	.0000	.0000	1.0000
33.0000	.0000	.0000	1.0000
33.5000	.0000	.0000	1.0000
34.0000	.0000	.0000	1.0000
34.5000	.0000	.0000	1.0000
35.0000	.0000	.0000	1.0000
35.5000	.0000	.0000	1.0000
36.0000	.0000	.0000	1.0000
36.5000	.0000	.0000	1.0000
37.0000	.0000	.0000	1.0000
37.5000	.0000	.0000	1.0000
38.0000	.0000	.0000	1.0000
38.5000	.0000	.0000	1.0000
39.0000	.0000	.0000	1.0000
39.5000	.0000	.0000	1.0000
40.0000	.0000	.0000	1.0000
40.5000	.0000	.0000	1.0000
41.0000	.0000	.0000	1.0000
41.5000	.0000	.0000	1.0000
42.0000	.0000	.0000	1.0000
42.5000	.0000	.0000	1.0000
43.0000	.0000	.0000	1.0000
43.5000	.0000	.0000	1.0000
44.0000	.0000	.0000	1.0000
44.5000	.0000	.0000	1.0000
45.0000	.0000	.0000	1.0000
45.5000	.0000	.0000	1.0000
46.0000	.0000	.0000	1.0000
46.5000	.0000	.0000	1.0000
47.0000	.0000	.0000	1.0000
47.5000	.0000	.0000	1.0000
48.0000	.0000	.0000	1.0000
48.5000	.0000	.0000	1.0000
49.0000	.0000	.0000	1.0000
49.5000	.0000	.0000	1.0000
50.0000	.0000	.0000	1.0000
50.5000	.0000	.0000	1.0000
B	FU75	PRU75	CPRU75
1.0000	.0000	.0000	.0000
1.5000	.0000	.0000	.0000
2.0000	.0000	.0000	.0000
2.5000	.0000	.0000	.0000
3.0000	.0000	.0000	.0000
3.5000	.0000	.0000	.0000
4.0000	.0000	.0000	.0000
4.5000	.0000	.0000	.0000
5.0000	.0000	.0000	.0000
5.5000	.0000	.0000	.0000
6.0000	.0000	.0000	.0000



6.5000	.0000	.0000	.0000
7.0000	.0000	.0000	.0000
7.5000	.0000	.0000	.0000
8.0000	.0000	.0000	.0000
8.5000	.0000	.0000	.0000
9.0000	.0000	.0000	.0000
9.5000	.0000	.0000	.0000
10.0000	.0000	.0000	.0000
10.5000	.0000	.0000	.0000
11.0000	.0000	.0000	.0000
11.5000	.0000	.0000	.0000
12.0000	.0000	.0000	.0000
12.5000	.0000	.0000	.0000
13.0000	.0000	.0000	.0000
13.5000	.0000	.0000	.0000
14.0000	.0000	.0000	.0000
14.5000	.0000	.0000	.0000
15.0000	.0000	.0000	.0000
15.5000	.0000	.0000	.0000
16.0000	.0000	.0000	.0000
16.5000	.0000	.0000	.0000
17.0000	.0000	.0000	.0000
17.5000	.0000	.0000	.0000
18.0000	.0000	.0000	.0000
18.5000	.0000	.0000	.0000
19.0000	.0000	.0000	.0000
19.5000	.0000	.0000	.0000
20.0000	.0000	.0000	.0000
20.5000	.0000	.0000	.0000
21.0000	8.0000	.0080	.0080
21.5000	415.0000	.4150	.4230
22.0000	458.0000	.4580	.8810
22.5000	98.0000	.0980	.9790
23.0000	18.0000	.0180	.9970
23.5000	3.0000	.0030	1.0000
24.0000	.0000	.0000	1.0000
24.5000	.0000	.0000	1.0000
25.0000	.0000	.0000	1.0000
25.5000	.0000	.0000	1.0000
26.0000	.0000	.0000	1.0000
26.5000	.0000	.0000	1.0000
27.0000	.0000	.0000	1.0000
27.5000	.0000	.0000	1.0000
28.0000	.0000	.0000	1.0000
28.5000	.0000	.0000	1.0000
29.0000	.0000	.0000	1.0000
29.5000	.0000	.0000	1.0000
30.0000	.0000	.0000	1.0000
30.5000	.0000	.0000	1.0000
31.0000	.0000	.0000	1.0000
31.5000	.0000	.0000	1.0000
32.0000	.0000	.0000	1.0000
32.5000	.0000	.0000	1.0000
33.0000	.0000	.0000	1.0000
33.5000	.0000	.0000	1.0000
34.0000	.0000	.0000	1.0000
34.5000	.0000	.0000	1.0000

35.0000	.0000	.0000	1.0000
35.5000	.0000	.0000	1.0000
36.0000	.0000	.0000	1.0000
36.5000	.0000	.0000	1.0000
37.0000	.0000	.0000	1.0000
37.5000	.0000	.0000	1.0000
38.0000	.0000	.0000	1.0000
38.5000	.0000	.0000	1.0000
39.0000	.0000	.0000	1.0000
39.5000	.0000	.0000	1.0000
40.0000	.0000	.0000	1.0000
40.5000	.0000	.0000	1.0000
41.0000	.0000	.0000	1.0000
41.5000	.0000	.0000	1.0000
42.0000	.0000	.0000	1.0000
42.5000	.0000	.0000	1.0000
43.0000	.0000	.0000	1.0000
43.5000	.0000	.0000	1.0000
44.0000	.0000	.0000	1.0000
44.5000	.0000	.0000	1.0000
45.0000	.0000	.0000	1.0000
45.5000	.0000	.0000	1.0000
46.0000	.0000	.0000	1.0000
46.5000	.0000	.0000	1.0000
47.0000	.0000	.0000	1.0000
47.5000	.0000	.0000	1.0000
48.0000	.0000	.0000	1.0000
48.5000	.0000	.0000	1.0000
49.0000	.0000	.0000	1.0000
49.5000	.0000	.0000	1.0000
50.0000	.0000	.0000	1.0000
50.5000	.0000	.0000	1.0000

The mean annual contraction scour d/s face is MNYYS

The mean annual scour value d/s face is MNLTS

The mean annual total scour d/s face is YMNTS

The standard dev in annual scour d/s face is YSTTS

YR	MNYYS	MNLTS	YMNTS	YSTTS
001	.0000	.0113	.0113	.0180
002	.0000	.0226	.0226	.0257
003	.0000	.0342	.0342	.0319
004	.0000	.0456	.0456	.0368
005	.0000	.0575	.0575	.0415
006	.0000	.0694	.0694	.0457
007	.0000	.0815	.0815	.0490
008	.0000	.0938	.0938	.0535
009	.0000	.1056	.1056	.0578
010	.0000	.1183	.1183	.0620
011	.0000	.1313	.1313	.0664
012	.0000	.1446	.1446	.0698
013	.0000	.1593	.1593	.0746
014	.0000	.1739	.1739	.0787
015	.0000	.1885	.1885	.0812
016	.0000	.2016	.2016	.0844
017	.0000	.2173	.2173	.0894
018	.0000	.2315	.2315	.0928
019	.0000	.2470	.2470	.0972
020	.0000	.2620	.2620	.1019

021	.0000	.2773	.2773	.1052
022	.0000	.2948	.2948	.1096
023	.0000	.3102	.3102	.1143
024	.0000	.3264	.3264	.1194
025	.0000	.3417	.3417	.1237
026	.0000	.3582	.3582	.1301
027	.0000	.3749	.3749	.1353
028	.0000	.3922	.3922	.1398
029	.0000	.4094	.4094	.1444
030	.0000	.4284	.4284	.1506
031	.0000	.4473	.4473	.1550
032	.0000	.4660	.4660	.1608
033	.0000	.4870	.4870	.1655
034	.0000	.5072	.5072	.1715
035	.0000	.5284	.5284	.1790
036	.0000	.5501	.5501	.1849
037	.0000	.5720	.5720	.1916
038	.0000	.5946	.5946	.1988
039	.0000	.6180	.6180	.2056
040	.0000	.6421	.6421	.2134
041	.0000	.6682	.6682	.2248
042	.0000	.6934	.6934	.2341
043	.0000	.7212	.7212	.2461
044	.0000	.7499	.7499	.2578
045	.0000	.7787	.7787	.2708
046	.0000	.8081	.8081	.2824
047	.0000	.8391	.8391	.2991
048	.0000	.8711	.8711	.3136
049	.0000	.9061	.9061	.3344
050	.0000	.9445	.9445	.3602
051	.0000	.9898	.9898	.5516
052	.0000	1.0339	1.0339	.6883
053	.0000	1.0749	1.0749	.7054
054	.0000	1.1210	1.1210	.7226
055	.0000	1.1678	1.1678	.7447
056	.0000	1.2305	1.2305	.9446
057	.0000	1.2849	1.2849	.9761
058	.0000	1.4130	1.4130	1.5580
059	.0000	1.5462	1.5462	1.9866
060	.0000	1.6278	1.6278	2.0928
061	.0000	1.7543	1.7543	2.3585
062	.0000	1.9112	1.9112	2.6828
063	.0000	2.0937	2.0937	3.0532
064	.0000	2.2804	2.2804	3.3673
065	.0000	2.4617	2.4617	3.6147
066	.0000	2.6876	2.6876	3.9296
067	.0000	2.9953	2.9953	4.3808
068	.0000	3.2905	3.2905	4.7270
069	.0000	3.6565	3.6565	5.1536
070	.0000	4.1014	4.1014	5.6195
071	.0000	4.5784	4.5784	6.0622
072	.0000	5.0475	5.0475	6.4225
073	.0000	5.6739	5.6739	6.8763
074	.0000	6.2390	6.2390	7.2182
075	.0000	6.7003	6.7003	7.4204
076	.0000	7.3880	7.3880	7.7230
077	.0000	7.9009	7.9009	7.8713

078	.0000	8.5696	8.5696	8.0599
079	.0000	9.1710	9.1710	8.1525
080	.0000	9.8411	9.8411	8.2276
081	.0000	10.5933	10.5933	8.2692
082	.0000	11.3444	11.3444	8.2409
083	.0000	11.9690	11.9690	8.1779
084	.0000	12.7678	12.7678	8.0376
085	.0000	13.3471	13.3471	7.8701
086	.0000	13.9115	13.9115	7.6853
087	.0000	14.4845	14.4845	7.4355
088	.0000	14.9732	14.9732	7.1754
089	.0000	15.3894	15.3894	6.9148
090	.0000	15.9911	15.9911	6.5127
091	.0000	16.5156	16.5156	6.0995
092	.0000	16.9326	16.9326	5.7136
093	.0000	17.2459	17.2459	5.3738
094	.0000	17.6716	17.6716	4.8920
095	.0000	17.9518	17.9518	4.5144
096	.0000	18.0762	18.0762	4.3134
097	.0000	18.3131	18.3131	3.9293
098	.0000	18.5129	18.5129	3.5698
099	.0000	18.6936	18.6936	3.1970
100	.0000	18.8296	18.8296	2.8849
The annual contraction scour u/s face is MNYYSU				
The mean annual local scour value u/s face is MNLSU				
The mean annual total scour value u/s face is YMNTSU				
The standard dev in annual scour u/s face is YSTTSU				
YR	MNYYSU	MNLSU	YMNTSU	YSTTSU
001	.0023	.1863	.1886	.7292
002	.0036	.4867	.4903	1.5719
003	.0041	.8063	.8104	2.3655
004	.0053	1.1947	1.2000	3.0305
005	.0054	1.6327	1.6381	3.7613
006	.0056	2.1349	2.1405	4.4861
007	.0060	2.7290	2.7349	5.1985
008	.0070	3.4809	3.4879	5.9222
009	.0092	4.2928	4.3019	6.5639
010	.0097	5.2298	5.2395	7.1769
011	.0099	6.1944	6.2042	7.7154
012	.0111	7.1675	7.1786	8.1239
013	.0119	8.2188	8.2307	8.4633
014	.0125	9.0925	9.1049	8.6398
015	.0149	10.1086	10.1235	8.7163
016	.0175	11.1171	11.1346	8.7307
017	.0184	12.1571	12.1755	8.6584
018	.0202	13.1688	13.1891	8.5089
019	.0203	14.1016	14.1219	8.2528
020	.0235	14.9675	14.9910	7.9231
021	.0239	15.7318	15.7556	7.6356
022	.0248	16.4963	16.5210	7.1852
023	.0252	17.1404	17.1656	6.7915
024	.0262	17.6754	17.7016	6.3706
025	.0282	18.1952	18.2234	5.8493
026	.0293	18.7268	18.7561	5.2787
027	.0305	19.1474	19.1779	4.7968
028	.0316	19.5003	19.5319	4.3310
029	.0322	19.7793	19.8115	3.9470

030	.0331	19.9942	20.0273	3.6012
031	.0338	20.1986	20.2324	3.1795
032	.0371	20.3703	20.4074	2.8480
033	.0384	20.4775	20.5159	2.7193
034	.0388	20.5669	20.6057	2.5454
035	.0395	20.6627	20.7021	2.3019
036	.0408	20.7529	20.7937	2.1120
037	.0414	20.8564	20.8978	1.7656
038	.0422	20.9280	20.9701	1.5222
039	.0437	20.9796	21.0232	1.4228
040	.0440	21.0185	21.0625	1.3669
041	.0442	21.0605	21.1047	1.1665
042	.0449	21.0972	21.1421	1.0099
043	.0459	21.1264	21.1723	.9679
044	.0476	21.1540	21.2015	.9313
045	.0483	21.1856	21.2340	.7643
046	.0487	21.2132	21.2619	.7023
047	.0504	21.2425	21.2929	.5013
048	.0534	21.2684	21.3218	.4029
049	.0546	21.2842	21.3388	.3984
050	.0563	21.2982	21.3545	.3979
051	.0566	21.3106	21.3672	.3895
052	.0590	21.3214	21.3804	.3901
053	.0597	21.3335	21.3932	.3853
054	.0602	21.3446	21.4048	.3835
055	.0612	21.3551	21.4162	.3768
056	.0633	21.3670	21.4302	.3766
057	.0639	21.3777	21.4416	.3731
058	.0651	21.3901	21.4552	.3722
059	.0661	21.3986	21.4647	.3702
060	.0677	21.4088	21.4765	.3678
061	.0691	21.4176	21.4867	.3626
062	.0692	21.4253	21.4945	.3592
063	.0699	21.4347	21.5046	.3559
064	.0702	21.4414	21.5116	.3547
065	.0713	21.4499	21.5213	.3549
066	.0720	21.4569	21.5289	.3536
067	.0721	21.4642	21.5363	.3501
068	.0736	21.4710	21.5446	.3498
069	.0749	21.4807	21.5555	.3483
070	.0768	21.4875	21.5643	.3519
071	.0784	21.4942	21.5726	.3510
072	.0795	21.4999	21.5793	.3499
073	.0797	21.5038	21.5835	.3476
074	.0806	21.5084	21.5890	.3467
075	.0808	21.5136	21.5944	.3459
076	.0834	21.5208	21.6041	.3485
077	.0845	21.5263	21.6108	.3486
078	.0849	21.5312	21.6161	.3479
079	.0858	21.5363	21.6221	.3476
080	.0858	21.5409	21.6267	.3461
081	.0865	21.5445	21.6310	.3454
082	.0868	21.5497	21.6365	.3436
083	.0889	21.5549	21.6438	.3455
084	.0899	21.5604	21.6503	.3446
085	.0911	21.5654	21.6565	.3434
086	.0921	21.5699	21.6620	.3418

087	.0935	21.5744	21.6679	.3421
088	.0944	21.5782	21.6726	.3409
089	.0953	21.5813	21.6766	.3399
090	.0972	21.5834	21.6806	.3424
091	.0988	21.5893	21.6881	.3437
092	.0992	21.5940	21.6932	.3418
093	.1010	21.5983	21.6993	.3411
094	.1018	21.6025	21.7044	.3421
095	.1023	21.6074	21.7097	.3416
096	.1046	21.6129	21.7175	.3429
097	.1048	21.6159	21.7207	.3410
098	.1055	21.6191	21.7246	.3393
099	.1056	21.6212	21.7269	.3380
100	.1060	21.6248	21.7308	.3362

## Appendix D-8

RUN TITLE IS Patuxent Hurricane Simulation Results  
RUN DATE is 10/9/05  
THE PROGRAM WAS EXECUTED IN THE EXISTING PIER ANALYSIS MODE.  
CONTRACTION SCOUR METHOD IS KOMURAS EQN  
SCOUR COMPUTED WITHOUT ARMOURING  
BRUBAKER-DEMETRIUS NEILLS MODIFICATION FACTOR ACTIVATED  
TIDE DISTORTION OPTION ACTIVATED  
MEAN TIDAL DEPTH MDR is = 15.900000  
MEAN LOW TIDAL DEPTH MLT is = 15.300000  
MEAN LOW TIDE ELEVATION MLTE is = -6.000000E-01  
TIDAL AMP. AT BRIDGE XSEC MTR is = 6.000000E-01  
CHANNEL INVERT AT BRIDGE IRS is = -15.900000

Estuary in bank area is = 26426.390000

Maximum tide in the simulation HITIDE is = 26.998300  
Maximum u/s flow depth in sim. YTRMXS is = 28.773230  
Maximum d/s flow depth in sim. YTFMXS is = 28.287450  
Maximum u/s disch. in sim. QTRMXS is = 890967.700000  
Maximum d/s disch. in sim. QTFMXS is = 837565.700000  
Maximum u/s vel.in sim. VUPMS is = 5.093286  
Maximum d/s vel.in sim. VDOWNMS is = 12.165770

Maximum u/s flow depth last run YTRMAX is = 28.773230  
Maximum d/s flow depth last run YTFMAX is = 26.631380  
Maximum u/s discharge last run QTRMAX is = 784214.600000  
Maximum d/s discharge last run QTFMAX is = 826394.200000  
Maximum u/s velocity last run VNUMAX is = 9.135580  
Maximum d/s velocity last run VNDMAX is = 4.380194  
Maximum tangential vel d/s face last run VTDMX is = 2.38878  
Maximum tangential vel u/s face last run VTUMX is = 5.08503  
critical vel u/s face last run UIUMIN is = 1.108954  
critical vel d/s face last run UIDMIN is = 1.108954

Time of concentration = 53.000000hrs  
Time to peak = 35.510000hrs  
Number of unit hydrograph ordinates = 177  
Soil infiltration potential = 4.285714  
Peak discharge of the UHG = 9854.463000cfs  
Initial abstractions IA = 8.571429E-01in

Catchment base flow = 407.770800cfs  
Tide attenuation factor TAF = 4.918033E-01  
Tidal lag MTL= 6.084536hrs  
Tidal routing constant CX = 1.643511E-01  
Bridge station tidal range TR = 1.200000ft  
Effective bottom channel width at brdg.WBE = 3262.240000ft  
Estuary Area 2.751598E+08  
Contraction scour factor u/s face= 1.267396  
Contraction scour factor d/s face= 1.016365  
Estuary to wavelength ratio DIM = 9.751869E-02

Estuary width factor WF = 2.496051  
 Tidal range factor HF = 7.547170E-02  
 Neill Mod. factor rising limb.NMRF = 8.000000E-01  
 Neill Mod. factor falling limb.NMFF = 8.000000E-01

The maximum storm event in the simulation is 8.000000ins  
 Array of total SURGRE at bridge is HSURGE= 10.380330  
 2.856355E-01

5.179529E-01	8.728182E-01	1.481365	2.761897
10.926670	10.926670	3.868823	2.761897
-5.401087	-5.078043	-4.789991	-4.531823
-4.299308	-4.088933	-3.897769	-3.723364
-3.563652	-3.416886	-3.281578	-3.156457
-3.040428	-2.932547	-2.831993	-2.738052
-2.650098	-2.567580	-2.490014	-2.416970
-2.348066	-2.282962	-2.221354	-2.162968
-2.107560	-2.054909	-2.004814	-1.957096
-1.911588	-1.868142	-1.826621	-1.786900
-1.748865	-1.712412	-1.677443	-1.643871
-1.611613	-1.580593	-1.550743	-1.521997
-1.494296	-1.467583	-1.441807	-1.416919
-1.392874	-1.369630	-1.347148	-1.325391
-1.304325	-1.283917	-1.264137	-1.244957
-1.226349	-1.208288	-1.190751	-1.173715
-1.157160	-1.141064	-1.125410	-1.110179
-1.095354	-1.080919	-1.066860	-1.053161
-1.039810	-1.026792	-1.014096	-1.001710
-9.896228E-01	-9.778234E-01	-9.663019E-01	-9.550486E-01
-9.440541E-01	-9.333097E-01	-9.228069E-01	-9.125378E-01
-9.024945E-01	-8.926698E-01	-8.830566E-01	-8.736480E-01
-8.644378E-01	-8.554195E-01	-8.465874E-01	-8.379357E-01
-8.294590E-01	-8.211520E-01	-8.130096E-01	-8.050270E-01
-7.971996E-01	-7.895228E-01	-7.819924E-01	-7.746043E-01
-7.673544E-01	-7.602389E-01	-7.532541E-01	-7.463963E-01
-7.396623E-01	-7.330486E-01	-7.265522E-01	-7.201698E-01
-7.138985E-01	-7.077355E-01	-7.016779E-01	-6.957231E-01
-6.898685E-01	-6.841115E-01	-6.784499E-01	-6.728811E-01
-6.674029E-01	-6.620133E-01		

Array of total combined depth at bridge is YT= 26.631380  
 18.533620

19.026730	19.473850	19.901720	20.780950
28.773230	17.528480	17.484750	17.413660
17.309800	17.312590	17.440700	17.396320
17.619430	17.803580	17.781990	17.917400
18.027880	17.865010	17.949100	17.823970
17.597560	17.529560	17.776270	17.624640
17.444630	17.589770	17.806980	17.829930
17.749020	17.825080	17.919130	17.769460
17.592140	17.517060	17.585290	17.476580
17.520000	17.587800	17.742000	17.874100
17.956100	17.843620	17.541560	17.562850
17.541980	17.521480	17.441620	17.447570
17.517740	17.742160	17.756330	17.641470
17.665890	17.730360	17.610210	17.828250
17.838640	17.593550	17.513710	17.473930
17.519760	17.536920	17.629360	17.827640



17.946170	17.871930	17.714320	17.730450
17.607990	17.547920	17.507780	17.472790
17.586540	17.695860	18.051600	18.262950
18.196640	17.856000	17.685190	17.556340
17.607180	17.681350	17.575760	17.559750
17.577810	17.673920	17.839420	17.771830
17.765940	17.606400	17.583570	17.602280
17.574480	17.494740	17.542180	17.504810
17.487250	17.686220	17.724170	17.775130
17.846750	17.769110	17.649420	17.740180
17.676460	17.627860	17.608140	17.566510
17.603040	17.877440	18.000790	17.863040
17.916220	17.920370	17.740880	17.680710
17.642880	17.503170		

Array of total combined depth at bridge d/s face is YTR=  
15.300000

15.300000	19.026730	19.473850	19.901720
20.780950	28.773230	15.300000	15.300000
15.300000	15.300000	17.312590	17.440700
15.300000	17.619430	17.803580	15.300000
17.917400	18.027880	15.300000	17.949100
15.300000	15.300000	15.300000	17.776270
15.300000	15.300000	17.589770	17.806980
17.829930	15.300000	17.825080	17.919130
15.300000	15.300000	15.300000	17.585290
15.300000	17.520000	17.587800	17.742000
17.874100	17.956100	15.300000	15.300000
17.562850	15.300000	15.300000	15.300000
17.447570	17.517740	17.742160	17.756330
15.300000	17.665890	17.730360	15.300000
17.828250	17.838640	15.300000	15.300000
15.300000	17.519760	17.536920	17.629360
17.827640	17.946170	15.300000	15.300000
17.730450	15.300000	15.300000	15.300000
15.300000	17.586540	17.695860	18.051600
18.262950	15.300000	15.300000	15.300000
15.300000	17.607180	17.681350	15.300000
15.300000	17.577810	17.673920	17.839420
15.300000	15.300000	15.300000	15.300000
17.602280	15.300000	15.300000	17.542180
15.300000	15.300000	17.686220	17.724170
17.775130	17.846750	15.300000	15.300000
17.740180	15.300000	15.300000	15.300000
15.300000	17.603040	17.877440	18.000790
15.300000	17.916220	17.920370	15.300000
15.300000	15.300000	15.300000	

Array of total combined depth at bridge u/s face is YTF=  
26.631380

18.533620	15.300000	15.300000	15.300000
15.300000	15.300000	17.528480	17.484750
17.413660	17.309800	15.300000	15.300000
17.396320	15.300000	15.300000	17.781990
15.300000	15.300000	17.865010	15.300000
17.823970	17.597560	17.529560	15.300000
17.624640	17.444630	15.300000	15.300000
15.300000	17.749020	15.300000	15.300000
17.769460	17.592140	17.517060	15.300000

17.476580	15.300000	15.300000	15.300000
15.300000	15.300000	17.843620	17.541560
15.300000	17.541980	17.521480	17.441620
15.300000	15.300000	15.300000	15.300000
17.641470	15.300000	15.300000	17.610210
15.300000	15.300000	17.593550	17.513710
17.473930	15.300000	15.300000	15.300000
15.300000	15.300000	17.871930	17.714320
15.300000	17.607990	17.547920	17.507780
17.472790	15.300000	15.300000	15.300000
15.300000	18.196640	17.856000	17.685190
17.556340	15.300000	15.300000	17.575760
17.559750	15.300000	15.300000	15.300000
17.771830	17.765940	17.606400	17.583570
15.300000	17.574480	17.494740	15.300000
17.504810	17.487250	15.300000	15.300000
15.300000	15.300000	17.769110	17.649420
15.300000	17.676460	17.627860	17.608140
17.566510	15.300000	15.300000	15.300000
17.863040	15.300000	15.300000	17.740880
17.680710	17.642880	17.503170	

Array total net disch. value at bridge is QT= 768434.300000 -  
18531.820000

-26450.950000	-51262.110000	-119823.900000	-784214.600000
826394.200000	-16329.260000	-18253.220000	-16184.790000
-10480.440000	-2439.331000	5589.230000	14709.540000
19623.180000	19314.740000	14098.890000	5707.434000
-5521.414000	-15298.650000	-20046.910000	-18178.270000
-9904.406000	3071.737000	17182.660000	26342.970000
32736.170000	35275.860000	33924.890000	29465.210000
23159.040000	16404.320000	13105.820000	14760.980000
21775.320000	33278.490000	47886.520000	56220.370000
62864.250000	66932.700000	68142.160000	66830.980000
63774.180000	59545.690000	56602.200000	56329.940000
59281.040000	65198.830000	70955.330000	79691.160000
86253.700000	89552.750000	88835.070000	84374.880000
77404.020000	68490.090000	60079.210000	55138.420000
54772.480000	58825.400000	66582.160000	72925.940000
77650.380000	79703.850000	78228.270000	73208.080000
65452.250000	55972.450000	46009.660000	38930.720000
35927.300000	37289.090000	40835.850000	47971.880000
53382.120000	56456.540000	55922.910000	51558.000000
43986.070000	34649.750000	23681.850000	15382.270000
11507.800000	12690.200000	10778.930000	24350.440000
35548.300000	43619.020000	46732.570000	43802.990000
35369.100000	23377.130000	8545.428000	-4187.205000
-10938.420000	-10132.850000	17418.240000	18327.430000
19579.300000	20547.390000	20706.710000	19765.730000
17782.490000	15019.440000	11978.350000	8878.037000
6663.774000	5920.792000	-1213.087000	4594.155000
11093.440000	16231.660000	19512.980000	20025.240000
17562.320000	12679.360000	6541.729000	-718.553700
-5893.224000	-7727.006000		

Array of total net velocity at bridge is VNT = 8.760387 -  
4.738578E-01

-6.391680E-01	-1.171555	-2.592378	-15.678780
---------------	-----------	-----------	------------





0.000000E+00	0.000000E+00	0.000000E+00	0.000000E+00
0.000000E+00	0.000000E+00	0.000000E+00	0.000000E+00
0.000000E+00	0.000000E+00	0.000000E+00	5.834431E-02
2.107445E-01	2.978866E-01	1.454863E-01	0.000000E+00
0.000000E+00	0.000000E+00	0.000000E+00	0.000000E+00
0.000000E+00	0.000000E+00	0.000000E+00	0.000000E+00
0.000000E+00	0.000000E+00	1.690345E-02	1.690345E-02
0.000000E+00	0.000000E+00	0.000000E+00	0.000000E+00
0.000000E+00	0.000000E+00	0.000000E+00	1.001516E-02
9.214314E-02	1.930748E-01		
Array of net vel.d/stream is VND=		4.380194	4.380194
0.000000E+00	0.000000E+00	0.000000E+00	0.000000E+00
4.014980	4.014980	0.000000E+00	0.000000E+00
0.000000E+00	0.000000E+00	8.023445E-02	2.913607E-01
4.845716E-01	5.347763E-01	4.579161E-01	2.738416E-01
7.725646E-02	0.000000E+00	0.000000E+00	0.000000E+00
0.000000E+00	4.410913E-02	2.836869E-01	6.066691E-01
8.370314E-01	9.614502E-01	9.505242E-01	8.577225E-01
7.215810E-01	5.448435E-01	3.993739E-01	3.832099E-01
5.092121E-01	7.812520E-01	1.145055	1.474362
1.709833	1.835268	1.882570	1.854459
1.767866	1.669173	1.618608	1.597612
1.636082	1.787501	1.954787	2.162589
2.382531	2.486992	2.487002	2.414374
2.254636	2.033583	1.791954	1.583265
1.487279	1.560823	1.775688	2.003030
2.161981	2.259546	2.234687	2.080741
1.876677	1.643584	1.398875	1.184076
1.043335	1.036114	1.121838	1.275066
1.432504	1.530715	1.521965	1.413297
1.256752	1.047397	7.989918E-01	5.443826E-01
3.746528E-01	3.372278E-01	3.270546E-01	4.894253E-01
8.345314E-01	1.103229	1.240329	1.243119
1.103866	8.188722E-01	4.448043E-01	1.190636E-01
0.000000E+00	0.000000E+00	2.501315E-01	5.132841E-01
5.442625E-01	5.675044E-01	5.750504E-01	5.642483E-01
5.162315E-01	4.500495E-01	3.763446E-01	2.907037E-01
2.166471E-01	1.753855E-01	8.250766E-02	6.400657E-02
2.185825E-01	3.742548E-01	4.838977E-01	5.352248E-01
5.087305E-01	4.093556E-01	2.628301E-01	9.119892E-02
0.000000E+00	0.000000E+00		
The mean hurricane scour u/s face is MNTHSU		5.034045	
The std.dev.in hurricane scour u/s face is STDHSU		2.439838E-01	
The mean hurricane scour d/s face is MNTHSD		4.751547	
The std.dev.in hurricane scour d/s face is STDHSD		3.317009E-02	
B	FHU	PRHU	CPRHU
1.0000	.0000	.0000	.0000
1.5000	.0000	.0000	.0000
2.0000	.0000	.0000	.0000
2.5000	.0000	.0000	.0000
3.0000	.0000	.0000	.0000
3.5000	.0000	.0000	.0000
4.0000	.0000	.0000	.0000
4.5000	.0000	.0000	.0000
5.0000	5030.0000	.5030	.5030
5.5000	4778.0000	.4778	.9808
6.0000	181.0000	.0181	.9989

6.5000	1.0000	.0001	.9990
7.0000	1.0000	.0001	.9991
7.5000	1.0000	.0001	.9992
8.0000	.0000	.0000	.9992
8.5000	1.0000	.0001	.9993
9.0000	.0000	.0000	.9993
9.5000	2.0000	.0002	.9995
10.0000	1.0000	.0001	.9996
10.5000	1.0000	.0001	.9997
11.0000	.0000	.0000	.9997
11.5000	1.0000	.0001	.9998
12.0000	2.0000	.0002	1.0000
12.5000	.0000	.0000	1.0000
13.0000	.0000	.0000	1.0000
13.5000	.0000	.0000	1.0000
14.0000	.0000	.0000	1.0000
14.5000	.0000	.0000	1.0000
15.0000	.0000	.0000	1.0000
15.5000	.0000	.0000	1.0000
16.0000	.0000	.0000	1.0000
16.5000	.0000	.0000	1.0000
17.0000	.0000	.0000	1.0000
17.5000	.0000	.0000	1.0000
18.0000	.0000	.0000	1.0000
18.5000	.0000	.0000	1.0000
19.0000	.0000	.0000	1.0000
19.5000	.0000	.0000	1.0000
20.0000	.0000	.0000	1.0000
20.5000	.0000	.0000	1.0000
21.0000	.0000	.0000	1.0000
21.5000	.0000	.0000	1.0000
22.0000	.0000	.0000	1.0000
22.5000	.0000	.0000	1.0000
23.0000	.0000	.0000	1.0000
23.5000	.0000	.0000	1.0000
24.0000	.0000	.0000	1.0000
24.5000	.0000	.0000	1.0000
25.0000	.0000	.0000	1.0000
25.5000	.0000	.0000	1.0000
26.0000	.0000	.0000	1.0000
26.5000	.0000	.0000	1.0000
27.0000	.0000	.0000	1.0000
27.5000	.0000	.0000	1.0000
28.0000	.0000	.0000	1.0000
28.5000	.0000	.0000	1.0000
29.0000	.0000	.0000	1.0000
29.5000	.0000	.0000	1.0000
30.0000	.0000	.0000	1.0000
30.5000	.0000	.0000	1.0000
31.0000	.0000	.0000	1.0000
31.5000	.0000	.0000	1.0000
32.0000	.0000	.0000	1.0000
32.5000	.0000	.0000	1.0000
33.0000	.0000	.0000	1.0000
33.5000	.0000	.0000	1.0000
34.0000	.0000	.0000	1.0000
34.5000	.0000	.0000	1.0000

35.0000	.0000	.0000	1.0000
35.5000	.0000	.0000	1.0000
36.0000	.0000	.0000	1.0000
36.5000	.0000	.0000	1.0000
37.0000	.0000	.0000	1.0000
37.5000	.0000	.0000	1.0000
38.0000	.0000	.0000	1.0000
38.5000	.0000	.0000	1.0000
39.0000	.0000	.0000	1.0000
39.5000	.0000	.0000	1.0000
40.0000	.0000	.0000	1.0000
40.5000	.0000	.0000	1.0000
41.0000	.0000	.0000	1.0000
41.5000	.0000	.0000	1.0000
42.0000	.0000	.0000	1.0000
42.5000	.0000	.0000	1.0000
43.0000	.0000	.0000	1.0000
43.5000	.0000	.0000	1.0000
44.0000	.0000	.0000	1.0000
44.5000	.0000	.0000	1.0000
45.0000	.0000	.0000	1.0000
45.5000	.0000	.0000	1.0000
46.0000	.0000	.0000	1.0000
46.5000	.0000	.0000	1.0000
47.0000	.0000	.0000	1.0000
47.5000	.0000	.0000	1.0000
48.0000	.0000	.0000	1.0000
48.5000	.0000	.0000	1.0000
49.0000	.0000	.0000	1.0000
49.5000	.0000	.0000	1.0000
50.0000	.0000	.0000	1.0000
50.5000	.0000	.0000	1.0000
B	FHD	PRHD	CPRHD
1.0000	.0000	.0000	.0000
1.5000	.0000	.0000	.0000
2.0000	.0000	.0000	.0000
2.5000	.0000	.0000	.0000
3.0000	.0000	.0000	.0000
3.5000	.0000	.0000	.0000
4.0000	.0000	.0000	.0000
4.5000	.0000	.0000	.0000
5.0000	10000.0000	1.0000	1.0000
5.5000	.0000	.0000	1.0000
6.0000	.0000	.0000	1.0000
6.5000	.0000	.0000	1.0000
7.0000	.0000	.0000	1.0000
7.5000	.0000	.0000	1.0000
8.0000	.0000	.0000	1.0000
8.5000	.0000	.0000	1.0000
9.0000	.0000	.0000	1.0000
9.5000	.0000	.0000	1.0000
10.0000	.0000	.0000	1.0000
10.5000	.0000	.0000	1.0000
11.0000	.0000	.0000	1.0000
11.5000	.0000	.0000	1.0000
12.0000	.0000	.0000	1.0000
12.5000	.0000	.0000	1.0000

13.0000	.0000	.0000	1.0000
13.5000	.0000	.0000	1.0000
14.0000	.0000	.0000	1.0000
14.5000	.0000	.0000	1.0000
15.0000	.0000	.0000	1.0000
15.5000	.0000	.0000	1.0000
16.0000	.0000	.0000	1.0000
16.5000	.0000	.0000	1.0000
17.0000	.0000	.0000	1.0000
17.5000	.0000	.0000	1.0000
18.0000	.0000	.0000	1.0000
18.5000	.0000	.0000	1.0000
19.0000	.0000	.0000	1.0000
19.5000	.0000	.0000	1.0000
20.0000	.0000	.0000	1.0000
20.5000	.0000	.0000	1.0000
21.0000	.0000	.0000	1.0000
21.5000	.0000	.0000	1.0000
22.0000	.0000	.0000	1.0000
22.5000	.0000	.0000	1.0000
23.0000	.0000	.0000	1.0000
23.5000	.0000	.0000	1.0000
24.0000	.0000	.0000	1.0000
24.5000	.0000	.0000	1.0000
25.0000	.0000	.0000	1.0000
25.5000	.0000	.0000	1.0000
26.0000	.0000	.0000	1.0000
26.5000	.0000	.0000	1.0000
27.0000	.0000	.0000	1.0000
27.5000	.0000	.0000	1.0000
28.0000	.0000	.0000	1.0000
28.5000	.0000	.0000	1.0000
29.0000	.0000	.0000	1.0000
29.5000	.0000	.0000	1.0000
30.0000	.0000	.0000	1.0000
30.5000	.0000	.0000	1.0000
31.0000	.0000	.0000	1.0000
31.5000	.0000	.0000	1.0000
32.0000	.0000	.0000	1.0000
32.5000	.0000	.0000	1.0000
33.0000	.0000	.0000	1.0000
33.5000	.0000	.0000	1.0000
34.0000	.0000	.0000	1.0000
34.5000	.0000	.0000	1.0000
35.0000	.0000	.0000	1.0000
35.5000	.0000	.0000	1.0000
36.0000	.0000	.0000	1.0000
36.5000	.0000	.0000	1.0000
37.0000	.0000	.0000	1.0000
37.5000	.0000	.0000	1.0000
38.0000	.0000	.0000	1.0000
38.5000	.0000	.0000	1.0000
39.0000	.0000	.0000	1.0000
39.5000	.0000	.0000	1.0000
40.0000	.0000	.0000	1.0000
40.5000	.0000	.0000	1.0000
41.0000	.0000	.0000	1.0000



41.5000	.0000	.0000	1.0000
42.0000	.0000	.0000	1.0000
42.5000	.0000	.0000	1.0000
43.0000	.0000	.0000	1.0000
43.5000	.0000	.0000	1.0000
44.0000	.0000	.0000	1.0000
44.5000	.0000	.0000	1.0000
45.0000	.0000	.0000	1.0000
45.5000	.0000	.0000	1.0000
46.0000	.0000	.0000	1.0000
46.5000	.0000	.0000	1.0000
47.0000	.0000	.0000	1.0000
47.5000	.0000	.0000	1.0000
48.0000	.0000	.0000	1.0000
48.5000	.0000	.0000	1.0000
49.0000	.0000	.0000	1.0000
49.5000	.0000	.0000	1.0000
50.0000	.0000	.0000	1.0000
50.5000	.0000	.0000	1.0000

## Appendix D-9

RUN TITLE IS WICOMICO RIER CONTINUOUS SIMULATIONS  
RUN DATE IS.....3/30/05.....  
THE PROGRAM WAS EXECUTED IN PIER DESIGN MODE.  
CONTRACTION SCOUR METHOD IS KOMURAS EQN  
SCOUR COMPUTED WITHOUT ARMOURING  
BRUBAKER-DEMETRIUS NEILLS MODIFICATION FACTOR ACTIVATED  
TIDE DISTORTION OPTION ACTIVATED  
MEAN TIDAL DEPTH MDR is = 18.190000  
MEAN LOW TIDAL DEPTH MLT is = 17.000000  
MEAN LOW TIDE ELEVATION MLTE is = -1.190000  
TIDAL AMP. AT BRIDGE XSEC MTR is = 1.190000  
CHANNEL INVERT AT BRIDGE IRS is = -18.190000

Estuary in bank area is = 14650.800000

Maximum tide in the simulation HITIDE is = 20.999290  
Maximum u/s flow depth in sim. YTRMXS is = 21.549780  
Maximum d/s flow depth in sim. YTFMXS is = 21.530130  
Maximum u/s disch. in sim. QTRMXS is = 96921.630000  
Maximum d/s disch. in sim. QTFMXS is = 100149.600000  
Maximum u/s vel.in sim. VUPMS is = 3.228127  
Maximum d/s vel.in sim. VDOWNMS is = 3.877909  
Maximum u/s face tang.vel.in sim. VTUMXSis = 4.241842  
Maximum d/s face tang.vel.in sim. VTDMXSis = 5.860367

Maximum u/s flow depth last run YTRMAX is = 20.999290  
Maximum d/s flow depth last run YTFMAX is = 20.839950  
Maximum u/s discharge last run QTRMAX is = 80450.060000  
Maximum d/s discharge last run QTFMAX is = 86716.800000  
Maximum u/s velocity last run VNUMAX is = 2.679556  
Maximum d/s velocity last run VNDMAX is = 2.169101  
Maximum tangential vel d/s face last run VTDMX is = 3.388780  
Maximum tangential vel u/s face last run VTUMX is = 9.256863E-01  
critical vel u/s face last run UIUMIN is = 7.546430E-01  
critical vel d/s face last run UIDMIN is = 7.546430E-01

Time of concentration = 48.000000hrs  
Time to peak = 32.160000hrs  
Number of unit hydrograph ordinates = 160  
Soil infiltration potential = 2.658228  
Peak discharge of the UHG = 2570.498000cfs  
Initial abstractions IA = 5.316456E-01in

Catchment base flow = 109.689300cfs  
Tide attenuation factor TAF = 9.754099E-01  
Tidal lag MTL= -4.190653hrs  
Tidal routing constant CX = 7.000000E-01  
Bridge station tidal range TR = 2.380000ft  
Effective bottom channel width at brdg.WBE = 1205.000000ft  
Estuary Area 1.101197E+08  
Contraction scour factor u/s face= 1.062975

Contraction scour factor d/s face= 1.062975  
 Estuary to wavelength ratio DIM = 7.817710E-02  
 Estuary width factor WF = 1.400000  
 Tidal range factor HF = 1.308411E-01  
 Neill Mod. factor rising limb.NMRF = 8.000000E-01  
 Neill Mod. factor falling limb.NMFF = 8.000000E-01

The maximum storm event in the simulation is 17.540860ins  
 ANNUAL MAX UPSTREAM VELOCITY LAST RUN = 2.257031 2.157247

2.452946	2.305281	2.572725	2.136336
2.390796	2.452071	2.206610	2.366519
2.177101	2.154559	2.469816	2.511524
2.146433	2.306036	2.210821	2.166484
2.451684	2.296778	2.205621	2.171070
2.133322	2.345441	2.134962	2.643292
2.156808	2.390297	2.315309	2.117939
2.112857	2.387876	2.176033	2.227109
2.107565	2.190026	2.314231	2.371798
2.473184	2.381320	2.235625	2.456764
2.165903	2.321932	2.126019	2.080171
2.123820	2.069941	2.265144	2.126837
2.309554	2.322697	2.228547	2.207768
2.375772	2.250506	2.299999	2.405754
2.116410	2.297915	2.109399	2.167768
2.392966	2.192100	2.054062	2.139870
2.189528	2.024424	2.141492	2.147034
2.226782	2.189152	2.259224	2.403189
2.346864	2.116083	2.325758	2.205940
2.209811	2.287028	2.490083	2.162787
2.131427	2.242718	2.276067	2.204160
2.265275	2.679556	2.369963	2.601057
2.250819	2.046666	2.241501	2.377903
2.268325	2.315300	2.308720	2.247273
2.212940	2.606858		

ANNUAL MAX DWNSTREAM VELOCITY LAST RUN = 1.821532  
 1.816269

1.851572	1.994957	2.169101	1.830860
1.713217	1.781865	1.789728	1.977430
1.791858	1.815240	1.904375	1.862026
1.703549	1.751860	1.710914	1.722576
2.156173	1.763084	1.737903	1.775806
1.860806	1.868693	1.725446	2.067293
1.768930	1.712817	1.740279	1.773467
1.776126	1.913507	1.752242	1.826217
2.000971	2.031474	1.886993	1.803148
1.952907	1.940556	1.782908	1.778918
1.751305	1.875536	1.708586	1.857862
1.869472	1.965102	1.856906	1.845039
1.697770	1.894582	1.889264	1.747865
1.926507	1.863116	1.977738	1.860720
1.823056	1.823082	1.917357	1.917076
1.579566	1.754919	1.790583	1.771878
1.664985	1.682107	1.718342	1.761162
1.921671	1.794858	1.968936	1.803161
1.821153	1.830766	1.897418	1.754951
1.696062	1.822237	1.702986	1.739395

1.775386	1.786921	1.885039	1.768051
1.838659	1.970756	1.876183	1.873237
1.840946	1.733713	1.827370	1.852940
1.762858	1.901042	1.840441	2.107810
1.885355	1.812340		
ANNUAL MAX US ADJUSTED VELOCITY LAST RUN =			2.257031
2.157247			
2.452946	2.305281	2.572725	2.136336
2.390796	2.452071	2.206610	2.366519
2.177101	2.154559	2.469816	2.511524
2.146433	2.306036	2.210821	2.166484
2.451684	2.296778	2.205621	2.171070
2.133322	2.345441	2.134962	2.643292
2.156808	2.390297	2.315309	2.117939
2.112857	2.387876	2.176033	2.227109
2.107565	2.190026	2.314231	2.371798
2.473184	2.381320	2.235625	2.456764
2.165903	2.321932	2.126019	2.080171
2.123820	2.069941	2.265144	2.126837
2.309554	2.322697	2.228547	2.207768
2.375772	2.250506	2.299999	2.405754
2.116410	2.297915	2.109399	2.167768
2.392966	2.192100	2.054062	2.139870
2.189528	2.024424	2.141492	2.147034
2.226782	2.189152	2.259224	2.403189
2.346864	2.116083	2.325758	2.205940
2.209811	2.287028	2.490083	2.162787
2.131427	2.242718	2.276067	2.204160
2.265275	2.679556	2.369963	2.601057
2.250819	2.046666	2.241501	2.377903
2.268325	2.315300	2.308720	2.247273
2.212940	2.606858		
ANNUAL MAX DS ADJUSTED VELOCITY LAST RUN =			1.821532
1.816269			
1.851572	1.994957	2.169101	1.830860
1.713217	1.781865	1.789728	1.977430
1.791858	1.815240	1.904375	1.862026
1.703549	1.751860	1.710914	1.722576
2.156173	1.763084	1.737903	1.775806
1.860806	1.868693	1.725446	2.067293
1.768930	1.712817	1.740279	1.773467
1.776126	1.913507	1.752242	1.826217
2.000971	2.031474	1.886993	1.803148
1.952907	1.940556	1.782908	1.778918
1.751305	1.875536	1.708586	1.857862
1.869472	1.965102	1.856906	1.845039
1.697770	1.894582	1.889264	1.747865
1.926507	1.863116	1.977738	1.860720
1.823056	1.823082	1.917357	1.917076
1.579566	1.754919	1.790583	1.771878
1.664985	1.682107	1.718342	1.761162
1.921671	1.794858	1.968936	1.803161
1.821153	1.830766	1.897418	1.754951
1.696062	1.822237	1.702986	1.739395
1.775386	1.786921	1.885039	1.768051
1.838659	1.970756	1.876183	1.873237
1.840946	1.733713	1.827370	1.852940

1.762858	1.901042	1.840441	2.107810
1.885355	1.812340		

ANNUAL MAX UPSTREAM DISCHARGE LAST RUN = 67747.320000  
62789.140000

73646.020000	63035.070000	77233.630000	62687.900000
71781.360000	73616.830000	66825.710000	71043.340000
65361.340000	61498.260000	69200.210000	75406.180000
70957.570000	67570.540000	67093.520000	67093.520000
66520.630000	62152.640000	64878.470000	63609.030000
64869.110000	70419.300000	64094.680000	58432.160000
64711.260000	70378.790000	67842.270000	62656.340000
60547.450000	64382.080000	67121.480000	65403.910000
63032.900000	63551.890000	67006.260000	71188.970000
74254.330000	65643.770000	63229.610000	71987.120000
64731.140000	69504.480000	62605.570000	62003.600000
64653.380000	61337.280000	67998.470000	62319.730000
67673.620000	61061.710000	66864.800000	64691.140000
66974.000000	67566.380000	67899.980000	70492.450000
61050.640000	63379.480000	62710.210000	65084.980000
61823.160000	64232.040000	63276.520000	65885.590000
67044.110000	59234.160000	66041.720000	64418.840000
66856.240000	62292.710000	67829.550000	72151.360000
70446.870000	63977.290000	62992.020000	69949.370000
64907.920000	70523.290000	62205.990000	64925.910000
58179.640000	67298.570000	64334.300000	64651.230000
69827.280000	80450.060000	63176.530000	63754.750000
67577.340000	63064.580000	67289.950000	64550.050000
69276.470000	69512.090000	59231.030000	67429.310000
62996.960000	78261.610000		

ANNUAL MAX DWNSTREAM DISCHARGE LAST RUN = 75404.000000  
71152.150000

67198.410000	72515.700000	64939.280000	67117.960000
80195.630000	71642.740000	73545.800000	68491.520000
73038.410000	81578.510000	77736.660000	74027.740000
71285.830000	76870.330000	67759.800000	68295.040000
73683.680000	71842.340000	71137.810000	69789.340000
63338.700000	69344.340000	67412.240000	76155.900000
71528.250000	70723.130000	71955.030000	70085.660000
83066.780000	69741.250000	74797.870000	72512.160000
75105.720000	65197.180000	81657.340000	68959.350000
70695.840000	72345.520000	71020.240000	68569.300000
67158.000000	68579.020000	69902.980000	74145.400000
71802.280000	63697.570000	68141.670000	67792.910000
69447.000000	69470.930000	74570.880000	62660.290000
66453.070000	71021.320000	70064.910000	71807.470000
72305.440000	80219.850000	80873.130000	77533.990000
67276.460000	72339.950000	72845.030000	72763.300000
71595.960000	74607.150000	69254.940000	68653.740000
70008.990000	86716.800000	73134.050000	71175.430000
77669.480000	76620.710000	70989.850000	70097.710000
72950.940000	77613.090000	67404.590000	70318.500000
71313.940000	74493.330000	75085.890000	74469.300000
62397.550000	82732.330000	66392.210000	66888.500000
78352.200000	70234.170000	73190.250000	82189.740000
68382.950000	80541.040000	68555.500000	68258.920000
67394.860000	69608.800000		

ANNUAL MAX DWNTREAM FLOW DEPTH LAST RUN = 20.493580  
20.537200

20.920080	20.784440	20.562890	20.701020
20.587550	20.409530	20.593820	20.729630
20.903150	20.789530	20.999290	20.664220
20.620850	20.620330	20.685360	20.711070
20.837940	20.689450	20.463340	20.698000
20.594460	20.556350	20.556820	20.639030
20.464930	20.507210	20.487610	20.392380
20.544240	20.796930	20.692760	20.500520
20.732520	20.784030	20.566070	20.856640
20.380820	20.808230	20.539900	20.826490
20.706870	20.462740	20.742400	20.758190
20.902800	20.479220	20.730380	20.472640
20.368260	20.498170	20.468250	20.521700
20.596840	20.425190	20.426270	20.741470
20.833040	20.624640	20.479880	20.636960
20.458120	20.619460	20.781830	20.642930
20.506300	20.482030	20.567930	20.572010
20.445600	20.539170	20.422910	20.631080
20.668990	20.855750	20.794540	20.583310
20.574660	20.622640	20.781080	20.521410
20.412460	20.875220	20.529480	20.456050
20.499200	20.918500	20.785180	20.376270
20.706360	20.502290	20.513850	20.567130
20.647720	20.553000	20.499280	20.640130
20.522770	20.649360		

ANNUAL MAX US ADJ. FLOW DEPTH LAST RUN = 20.486830  
20.346900

20.839950	20.755460	20.573200	20.306630
20.473560	20.314040	20.145000	20.696520
20.162380	20.414500	20.275210	20.536290
20.290500	20.252690	20.520040	20.363770
20.395940	20.530700	20.253780	20.632050
20.225840	20.465400	20.404150	20.192320
20.064920	20.456220	20.405500	20.365410
20.314670	20.795080	20.409210	20.471390
20.417240	20.612220	20.478430	20.569610
20.569610	20.688110	20.506020	20.730080
20.585560	20.229530	20.328770	20.530270
20.602810	20.335460	20.689490	20.381230
20.183600	20.274610	20.305950	20.423090
20.409470	20.279480	20.394530	20.303630
20.456850	20.440370	20.479070	20.351370
20.396400	20.252140	20.402320	20.343310
20.233570	20.169360	20.076940	20.376320
20.360290	20.248750	20.313690	20.349400
20.586030	20.766530	20.604860	20.455870
20.288320	20.438450	20.669140	20.356510
20.392380	20.423620	20.489960	20.254130
20.254730	20.428440	20.699280	20.332670
20.677570	20.303160	20.287120	20.355340
20.142970	20.525550	20.490360	20.556580
20.506690	20.360810		

ANNUAL MAX DS ADJ. FLOW DEPTH LAST RUN = 20.493580  
20.537200

20.920080	20.784440	20.562890	20.701020
-----------	-----------	-----------	-----------

20.587550	20.409530	20.593820	20.729630
20.903150	20.789530	20.999290	20.664220
20.620850	20.620330	20.685360	20.711070
20.837940	20.689450	20.463340	20.698000
20.594460	20.556350	20.556820	20.639030
20.464930	20.507210	20.487610	20.392380
20.544240	20.796930	20.692760	20.500520
20.732520	20.784030	20.566070	20.856640
20.380820	20.808230	20.539900	20.826490
20.706870	20.462740	20.742400	20.758190
20.902800	20.479220	20.730380	20.472640
20.368260	20.498170	20.468250	20.521700
20.596840	20.425190	20.426270	20.741470
20.833040	20.624640	20.479880	20.636960
20.458120	20.619460	20.781830	20.642930
20.506300	20.482030	20.567930	20.572010
20.445600	20.539170	20.422910	20.631080
20.668990	20.855750	20.794540	20.583310
20.574660	20.622640	20.781080	20.521410
20.412460	20.875220	20.529480	20.456050
20.499200	20.918500	20.785180	20.376270
20.706360	20.502290	20.513850	20.567130
20.647720	20.553000	20.499280	20.640130
20.522770	20.649360		

The no.of storms in the last.NS= 79  
The no.of storms producing no runoff over the simula tion.NORUN= 6022723

The number of 6 hr storms in YRS is = 61  
The number of 18 hr storms in YRS is = 6  
The number of 24 hr storms in YRS is = 5  
The number of 36 hr storms in YRS is = 7  
The number of 6 hr runoff hyd.ordinates is = 165  
The number of 18 hr runoff hyd.ordinates is = 177  
The number of 24 hr runoff hyd,ordinates is = 183  
The number of 36 hr runoff hyd.ordinates is = 195  
UVAR6 last run is = 2.873612E-01  
UVAR18 last run is = 6.304253E-02  
UVAR24 last run is = 8.351123E-01  
UVAR36 last run is = 7.747977E-01  
The avg. 6hr. annual rainfall amt. is = 18.307650in  
The avg. 18hr.annual rainfall amt. is = 5.199970in  
The avg. 24hr.annual rainfall amt. is = 9.131759in  
The avg. 36hr.annual rainfall amt. is = 8.778363in  
The 6hr. rainfall amt.last run is = 1.247015E-01in

Total scour d/s face last run is TSD = 19.794800  
Total scour u/s face last run is TSU = 9.030800E-01  
Total scour local d/s face last run is CSD = 19.794800  
19.794800

19.794800	19.794800	19.794800	19.794800
19.794800	19.794800	19.794800	19.794800
19.794800	19.794800	19.794800	19.794800
19.794800	19.794800	19.794800	19.794800
19.794800	19.794800	19.794800	19.794800
19.794800	19.794800	19.794800	19.794800

[illegible]





4.5000	.0000	.0000	.0000
5.0000	.0000	.0000	.0000
5.5000	.0000	.0000	.0000
6.0000	.0000	.0000	.0000
6.5000	.0000	.0000	.0000
7.0000	.0000	.0000	.0000
7.5000	.0000	.0000	.0000
8.0000	.0000	.0000	.0000
8.5000	.0000	.0000	.0000
9.0000	.0000	.0000	.0000
9.5000	.0000	.0000	.0000
10.0000	.0000	.0000	.0000
10.5000	.0000	.0000	.0000
11.0000	.0000	.0000	.0000
11.5000	.0000	.0000	.0000
12.0000	.0000	.0000	.0000
12.5000	.0000	.0000	.0000
13.0000	.0000	.0000	.0000
13.5000	.0000	.0000	.0000
14.0000	.0000	.0000	.0000
14.5000	.0000	.0000	.0000
15.0000	.0000	.0000	.0000
15.5000	.0000	.0000	.0000
16.0000	.0000	.0000	.0000
16.5000	.0000	.0000	.0000
17.0000	.0000	.0000	.0000
17.5000	.0000	.0000	.0000
18.0000	.0000	.0000	.0000
18.5000	.0000	.0000	.0000
19.0000	.0000	.0000	.0000
19.5000	.0000	.0000	.0000
20.0000	1000.0000	1.0000	1.0000
20.5000	.0000	.0000	1.0000
21.0000	.0000	.0000	1.0000
21.5000	.0000	.0000	1.0000
22.0000	.0000	.0000	1.0000
22.5000	.0000	.0000	1.0000
23.0000	.0000	.0000	1.0000
23.5000	.0000	.0000	1.0000
24.0000	.0000	.0000	1.0000
24.5000	.0000	.0000	1.0000
25.0000	.0000	.0000	1.0000
25.5000	.0000	.0000	1.0000
26.0000	.0000	.0000	1.0000
26.5000	.0000	.0000	1.0000
27.0000	.0000	.0000	1.0000
27.5000	.0000	.0000	1.0000
28.0000	.0000	.0000	1.0000
28.5000	.0000	.0000	1.0000
29.0000	.0000	.0000	1.0000
29.5000	.0000	.0000	1.0000
30.0000	.0000	.0000	1.0000
30.5000	.0000	.0000	1.0000
31.0000	.0000	.0000	1.0000
31.5000	.0000	.0000	1.0000
32.0000	.0000	.0000	1.0000
32.5000	.0000	.0000	1.0000

33.0000	.0000	.0000	1.0000
33.5000	.0000	.0000	1.0000
34.0000	.0000	.0000	1.0000
34.5000	.0000	.0000	1.0000
35.0000	.0000	.0000	1.0000
35.5000	.0000	.0000	1.0000
36.0000	.0000	.0000	1.0000
36.5000	.0000	.0000	1.0000
37.0000	.0000	.0000	1.0000
37.5000	.0000	.0000	1.0000
38.0000	.0000	.0000	1.0000
38.5000	.0000	.0000	1.0000
39.0000	.0000	.0000	1.0000
39.5000	.0000	.0000	1.0000
40.0000	.0000	.0000	1.0000
40.5000	.0000	.0000	1.0000
41.0000	.0000	.0000	1.0000
41.5000	.0000	.0000	1.0000
42.0000	.0000	.0000	1.0000
42.5000	.0000	.0000	1.0000
43.0000	.0000	.0000	1.0000
43.5000	.0000	.0000	1.0000
44.0000	.0000	.0000	1.0000
44.5000	.0000	.0000	1.0000
45.0000	.0000	.0000	1.0000
45.5000	.0000	.0000	1.0000
46.0000	.0000	.0000	1.0000
46.5000	.0000	.0000	1.0000
47.0000	.0000	.0000	1.0000
47.5000	.0000	.0000	1.0000
48.0000	.0000	.0000	1.0000
48.5000	.0000	.0000	1.0000
49.0000	.0000	.0000	1.0000
49.5000	.0000	.0000	1.0000
50.0000	.0000	.0000	1.0000
50.5000	.0000	.0000	1.0000
B	FU	PRU	CPRU
1.0000	133.0000	.1330	.1330
1.5000	151.0000	.1510	.2840
2.0000	102.0000	.1020	.3860
2.5000	44.0000	.0440	.4300
3.0000	21.0000	.0210	.4510
3.5000	16.0000	.0160	.4670
4.0000	15.0000	.0150	.4820
4.5000	10.0000	.0100	.4920
5.0000	6.0000	.0060	.4980
5.5000	2.0000	.0020	.5000
6.0000	6.0000	.0060	.5060
6.5000	.0000	.0000	.5060
7.0000	1.0000	.0010	.5070
7.5000	.0000	.0000	.5070
8.0000	.0000	.0000	.5070
8.5000	.0000	.0000	.5070
9.0000	.0000	.0000	.5070
9.5000	.0000	.0000	.5070
10.0000	.0000	.0000	.5070
10.5000	.0000	.0000	.5070

11.0000	.0000	.0000	.5070
11.5000	.0000	.0000	.5070
12.0000	1.0000	.0010	.5080
12.5000	.0000	.0000	.5080
13.0000	1.0000	.0010	.5090
13.5000	1.0000	.0010	.5100
14.0000	.0000	.0000	.5100
14.5000	1.0000	.0010	.5110
15.0000	.0000	.0000	.5110
15.5000	1.0000	.0010	.5120
16.0000	.0000	.0000	.5120
16.5000	.0000	.0000	.5120
17.0000	.0000	.0000	.5120
17.5000	1.0000	.0010	.5130
18.0000	2.0000	.0020	.5150
18.5000	.0000	.0000	.5150
19.0000	9.0000	.0090	.5240
19.5000	15.0000	.0150	.5390
20.0000	100.0000	.1000	.6390
20.5000	351.0000	.3510	.9900
21.0000	10.0000	.0100	1.0000
21.5000	.0000	.0000	1.0000
22.0000	.0000	.0000	1.0000
22.5000	.0000	.0000	1.0000
23.0000	.0000	.0000	1.0000
23.5000	.0000	.0000	1.0000
24.0000	.0000	.0000	1.0000
24.5000	.0000	.0000	1.0000
25.0000	.0000	.0000	1.0000
25.5000	.0000	.0000	1.0000
26.0000	.0000	.0000	1.0000
26.5000	.0000	.0000	1.0000
27.0000	.0000	.0000	1.0000
27.5000	.0000	.0000	1.0000
28.0000	.0000	.0000	1.0000
28.5000	.0000	.0000	1.0000
29.0000	.0000	.0000	1.0000
29.5000	.0000	.0000	1.0000
30.0000	.0000	.0000	1.0000
30.5000	.0000	.0000	1.0000
31.0000	.0000	.0000	1.0000
31.5000	.0000	.0000	1.0000
32.0000	.0000	.0000	1.0000
32.5000	.0000	.0000	1.0000
33.0000	.0000	.0000	1.0000
33.5000	.0000	.0000	1.0000
34.0000	.0000	.0000	1.0000
34.5000	.0000	.0000	1.0000
35.0000	.0000	.0000	1.0000
35.5000	.0000	.0000	1.0000
36.0000	.0000	.0000	1.0000
36.5000	.0000	.0000	1.0000
37.0000	.0000	.0000	1.0000
37.5000	.0000	.0000	1.0000
38.0000	.0000	.0000	1.0000
38.5000	.0000	.0000	1.0000
39.0000	.0000	.0000	1.0000

39.5000	.0000	.0000	1.0000
40.0000	.0000	.0000	1.0000
40.5000	.0000	.0000	1.0000
41.0000	.0000	.0000	1.0000
41.5000	.0000	.0000	1.0000
42.0000	.0000	.0000	1.0000
42.5000	.0000	.0000	1.0000
43.0000	.0000	.0000	1.0000
43.5000	.0000	.0000	1.0000
44.0000	.0000	.0000	1.0000
44.5000	.0000	.0000	1.0000
45.0000	.0000	.0000	1.0000
45.5000	.0000	.0000	1.0000
46.0000	.0000	.0000	1.0000
46.5000	.0000	.0000	1.0000
47.0000	.0000	.0000	1.0000
47.5000	.0000	.0000	1.0000
48.0000	.0000	.0000	1.0000
48.5000	.0000	.0000	1.0000
49.0000	.0000	.0000	1.0000
49.5000	.0000	.0000	1.0000
50.0000	.0000	.0000	1.0000
50.5000	.0000	.0000	1.0000

15 PERCENT TMS SCOUR RESULTS

B	FD15	PRD15	CPRD15
1.0000	.0000	.0000	.0000
1.5000	.0000	.0000	.0000
2.0000	.0000	.0000	.0000
2.5000	.0000	.0000	.0000
3.0000	.0000	.0000	.0000
3.5000	.0000	.0000	.0000
4.0000	.0000	.0000	.0000
4.5000	.0000	.0000	.0000
5.0000	.0000	.0000	.0000
5.5000	.0000	.0000	.0000
6.0000	.0000	.0000	.0000
6.5000	.0000	.0000	.0000
7.0000	.0000	.0000	.0000
7.5000	.0000	.0000	.0000
8.0000	.0000	.0000	.0000
8.5000	.0000	.0000	.0000
9.0000	.0000	.0000	.0000
9.5000	.0000	.0000	.0000
10.0000	.0000	.0000	.0000
10.5000	.0000	.0000	.0000
11.0000	.0000	.0000	.0000
11.5000	.0000	.0000	.0000
12.0000	.0000	.0000	.0000
12.5000	.0000	.0000	.0000
13.0000	.0000	.0000	.0000
13.5000	.0000	.0000	.0000
14.0000	.0000	.0000	.0000
14.5000	.0000	.0000	.0000
15.0000	.0000	.0000	.0000
15.5000	.0000	.0000	.0000
16.0000	.0000	.0000	.0000
16.5000	.0000	.0000	.0000

17.0000	.0000	.0000	.0000
17.5000	.0000	.0000	.0000
18.0000	.0000	.0000	.0000
18.5000	.0000	.0000	.0000
19.0000	.0000	.0000	.0000
19.5000	.0000	.0000	.0000
20.0000	1000.0000	1.0000	1.0000
20.5000	.0000	.0000	1.0000
21.0000	.0000	.0000	1.0000
21.5000	.0000	.0000	1.0000
22.0000	.0000	.0000	1.0000
22.5000	.0000	.0000	1.0000
23.0000	.0000	.0000	1.0000
23.5000	.0000	.0000	1.0000
24.0000	.0000	.0000	1.0000
24.5000	.0000	.0000	1.0000
25.0000	.0000	.0000	1.0000
25.5000	.0000	.0000	1.0000
26.0000	.0000	.0000	1.0000
26.5000	.0000	.0000	1.0000
27.0000	.0000	.0000	1.0000
27.5000	.0000	.0000	1.0000
28.0000	.0000	.0000	1.0000
28.5000	.0000	.0000	1.0000
29.0000	.0000	.0000	1.0000
29.5000	.0000	.0000	1.0000
30.0000	.0000	.0000	1.0000
30.5000	.0000	.0000	1.0000
31.0000	.0000	.0000	1.0000
31.5000	.0000	.0000	1.0000
32.0000	.0000	.0000	1.0000
32.5000	.0000	.0000	1.0000
33.0000	.0000	.0000	1.0000
33.5000	.0000	.0000	1.0000
34.0000	.0000	.0000	1.0000
34.5000	.0000	.0000	1.0000
35.0000	.0000	.0000	1.0000
35.5000	.0000	.0000	1.0000
36.0000	.0000	.0000	1.0000
36.5000	.0000	.0000	1.0000
37.0000	.0000	.0000	1.0000
37.5000	.0000	.0000	1.0000
38.0000	.0000	.0000	1.0000
38.5000	.0000	.0000	1.0000
39.0000	.0000	.0000	1.0000
39.5000	.0000	.0000	1.0000
40.0000	.0000	.0000	1.0000
40.5000	.0000	.0000	1.0000
41.0000	.0000	.0000	1.0000
41.5000	.0000	.0000	1.0000
42.0000	.0000	.0000	1.0000
42.5000	.0000	.0000	1.0000
43.0000	.0000	.0000	1.0000
43.5000	.0000	.0000	1.0000
44.0000	.0000	.0000	1.0000
44.5000	.0000	.0000	1.0000
45.0000	.0000	.0000	1.0000

45.5000	.0000	.0000	1.0000
46.0000	.0000	.0000	1.0000
46.5000	.0000	.0000	1.0000
47.0000	.0000	.0000	1.0000
47.5000	.0000	.0000	1.0000
48.0000	.0000	.0000	1.0000
48.5000	.0000	.0000	1.0000
49.0000	.0000	.0000	1.0000
49.5000	.0000	.0000	1.0000
50.0000	.0000	.0000	1.0000
50.5000	.0000	.0000	1.0000
B	FU15	PRU15	CPRU15
1.0000	999.0000	.9990	.9990
1.5000	1.0000	.0010	1.0000
2.0000	.0000	.0000	1.0000
2.5000	.0000	.0000	1.0000
3.0000	.0000	.0000	1.0000
3.5000	.0000	.0000	1.0000
4.0000	.0000	.0000	1.0000
4.5000	.0000	.0000	1.0000
5.0000	.0000	.0000	1.0000
5.5000	.0000	.0000	1.0000
6.0000	.0000	.0000	1.0000
6.5000	.0000	.0000	1.0000
7.0000	.0000	.0000	1.0000
7.5000	.0000	.0000	1.0000
8.0000	.0000	.0000	1.0000
8.5000	.0000	.0000	1.0000
9.0000	.0000	.0000	1.0000
9.5000	.0000	.0000	1.0000
10.0000	.0000	.0000	1.0000
10.5000	.0000	.0000	1.0000
11.0000	.0000	.0000	1.0000
11.5000	.0000	.0000	1.0000
12.0000	.0000	.0000	1.0000
12.5000	.0000	.0000	1.0000
13.0000	.0000	.0000	1.0000
13.5000	.0000	.0000	1.0000
14.0000	.0000	.0000	1.0000
14.5000	.0000	.0000	1.0000
15.0000	.0000	.0000	1.0000
15.5000	.0000	.0000	1.0000
16.0000	.0000	.0000	1.0000
16.5000	.0000	.0000	1.0000
17.0000	.0000	.0000	1.0000
17.5000	.0000	.0000	1.0000
18.0000	.0000	.0000	1.0000
18.5000	.0000	.0000	1.0000
19.0000	.0000	.0000	1.0000
19.5000	.0000	.0000	1.0000
20.0000	.0000	.0000	1.0000
20.5000	.0000	.0000	1.0000
21.0000	.0000	.0000	1.0000
21.5000	.0000	.0000	1.0000
22.0000	.0000	.0000	1.0000
22.5000	.0000	.0000	1.0000
23.0000	.0000	.0000	1.0000

23.5000	.0000	.0000	1.0000
24.0000	.0000	.0000	1.0000
24.5000	.0000	.0000	1.0000
25.0000	.0000	.0000	1.0000
25.5000	.0000	.0000	1.0000
26.0000	.0000	.0000	1.0000
26.5000	.0000	.0000	1.0000
27.0000	.0000	.0000	1.0000
27.5000	.0000	.0000	1.0000
28.0000	.0000	.0000	1.0000
28.5000	.0000	.0000	1.0000
29.0000	.0000	.0000	1.0000
29.5000	.0000	.0000	1.0000
30.0000	.0000	.0000	1.0000
30.5000	.0000	.0000	1.0000
31.0000	.0000	.0000	1.0000
31.5000	.0000	.0000	1.0000
32.0000	.0000	.0000	1.0000
32.5000	.0000	.0000	1.0000
33.0000	.0000	.0000	1.0000
33.5000	.0000	.0000	1.0000
34.0000	.0000	.0000	1.0000
34.5000	.0000	.0000	1.0000
35.0000	.0000	.0000	1.0000
35.5000	.0000	.0000	1.0000
36.0000	.0000	.0000	1.0000
36.5000	.0000	.0000	1.0000
37.0000	.0000	.0000	1.0000
37.5000	.0000	.0000	1.0000
38.0000	.0000	.0000	1.0000
38.5000	.0000	.0000	1.0000
39.0000	.0000	.0000	1.0000
39.5000	.0000	.0000	1.0000
40.0000	.0000	.0000	1.0000
40.5000	.0000	.0000	1.0000
41.0000	.0000	.0000	1.0000
41.5000	.0000	.0000	1.0000
42.0000	.0000	.0000	1.0000
42.5000	.0000	.0000	1.0000
43.0000	.0000	.0000	1.0000
43.5000	.0000	.0000	1.0000
44.0000	.0000	.0000	1.0000
44.5000	.0000	.0000	1.0000
45.0000	.0000	.0000	1.0000
45.5000	.0000	.0000	1.0000
46.0000	.0000	.0000	1.0000
46.5000	.0000	.0000	1.0000
47.0000	.0000	.0000	1.0000
47.5000	.0000	.0000	1.0000
48.0000	.0000	.0000	1.0000
48.5000	.0000	.0000	1.0000
49.0000	.0000	.0000	1.0000
49.5000	.0000	.0000	1.0000
50.0000	.0000	.0000	1.0000
50.5000	.0000	.0000	1.0000

25 PERCENT SCOUR RESULTS

B

FD25

PRD25

CPRD25



1.0000	.0000	.0000	.0000
1.5000	.0000	.0000	.0000
2.0000	.0000	.0000	.0000
2.5000	.0000	.0000	.0000
3.0000	.0000	.0000	.0000
3.5000	.0000	.0000	.0000
4.0000	.0000	.0000	.0000
4.5000	.0000	.0000	.0000
5.0000	.0000	.0000	.0000
5.5000	.0000	.0000	.0000
6.0000	.0000	.0000	.0000
6.5000	.0000	.0000	.0000
7.0000	.0000	.0000	.0000
7.5000	.0000	.0000	.0000
8.0000	.0000	.0000	.0000
8.5000	.0000	.0000	.0000
9.0000	.0000	.0000	.0000
9.5000	.0000	.0000	.0000
10.0000	.0000	.0000	.0000
10.5000	.0000	.0000	.0000
11.0000	.0000	.0000	.0000
11.5000	.0000	.0000	.0000
12.0000	.0000	.0000	.0000
12.5000	.0000	.0000	.0000
13.0000	.0000	.0000	.0000
13.5000	.0000	.0000	.0000
14.0000	.0000	.0000	.0000
14.5000	.0000	.0000	.0000
15.0000	.0000	.0000	.0000
15.5000	.0000	.0000	.0000
16.0000	.0000	.0000	.0000
16.5000	.0000	.0000	.0000
17.0000	.0000	.0000	.0000
17.5000	.0000	.0000	.0000
18.0000	.0000	.0000	.0000
18.5000	.0000	.0000	.0000
19.0000	.0000	.0000	.0000
19.5000	.0000	.0000	.0000
20.0000	1000.0000	1.0000	1.0000
20.5000	.0000	.0000	1.0000
21.0000	.0000	.0000	1.0000
21.5000	.0000	.0000	1.0000
22.0000	.0000	.0000	1.0000
22.5000	.0000	.0000	1.0000
23.0000	.0000	.0000	1.0000
23.5000	.0000	.0000	1.0000
24.0000	.0000	.0000	1.0000
24.5000	.0000	.0000	1.0000
25.0000	.0000	.0000	1.0000
25.5000	.0000	.0000	1.0000
26.0000	.0000	.0000	1.0000
26.5000	.0000	.0000	1.0000
27.0000	.0000	.0000	1.0000
27.5000	.0000	.0000	1.0000
28.0000	.0000	.0000	1.0000
28.5000	.0000	.0000	1.0000
29.0000	.0000	.0000	1.0000

29.5000	.0000	.0000	1.0000
30.0000	.0000	.0000	1.0000
30.5000	.0000	.0000	1.0000
31.0000	.0000	.0000	1.0000
31.5000	.0000	.0000	1.0000
32.0000	.0000	.0000	1.0000
32.5000	.0000	.0000	1.0000
33.0000	.0000	.0000	1.0000
33.5000	.0000	.0000	1.0000
34.0000	.0000	.0000	1.0000
34.5000	.0000	.0000	1.0000
35.0000	.0000	.0000	1.0000
35.5000	.0000	.0000	1.0000
36.0000	.0000	.0000	1.0000
36.5000	.0000	.0000	1.0000
37.0000	.0000	.0000	1.0000
37.5000	.0000	.0000	1.0000
38.0000	.0000	.0000	1.0000
38.5000	.0000	.0000	1.0000
39.0000	.0000	.0000	1.0000
39.5000	.0000	.0000	1.0000
40.0000	.0000	.0000	1.0000
40.5000	.0000	.0000	1.0000
41.0000	.0000	.0000	1.0000
41.5000	.0000	.0000	1.0000
42.0000	.0000	.0000	1.0000
42.5000	.0000	.0000	1.0000
43.0000	.0000	.0000	1.0000
43.5000	.0000	.0000	1.0000
44.0000	.0000	.0000	1.0000
44.5000	.0000	.0000	1.0000
45.0000	.0000	.0000	1.0000
45.5000	.0000	.0000	1.0000
46.0000	.0000	.0000	1.0000
46.5000	.0000	.0000	1.0000
47.0000	.0000	.0000	1.0000
47.5000	.0000	.0000	1.0000
48.0000	.0000	.0000	1.0000
48.5000	.0000	.0000	1.0000
49.0000	.0000	.0000	1.0000
49.5000	.0000	.0000	1.0000
50.0000	.0000	.0000	1.0000
50.5000	.0000	.0000	1.0000
B	FU25	PRU25	CPRU25
1.0000	997.0000	.9970	.9970
1.5000	2.0000	.0020	.9990
2.0000	.0000	.0000	.9990
2.5000	1.0000	.0010	1.0000
3.0000	.0000	.0000	1.0000
3.5000	.0000	.0000	1.0000
4.0000	.0000	.0000	1.0000
4.5000	.0000	.0000	1.0000
5.0000	.0000	.0000	1.0000
5.5000	.0000	.0000	1.0000
6.0000	.0000	.0000	1.0000
6.5000	.0000	.0000	1.0000
7.0000	.0000	.0000	1.0000

7.5000	.0000	.0000	1.0000
8.0000	.0000	.0000	1.0000
8.5000	.0000	.0000	1.0000
9.0000	.0000	.0000	1.0000
9.5000	.0000	.0000	1.0000
10.0000	.0000	.0000	1.0000
10.5000	.0000	.0000	1.0000
11.0000	.0000	.0000	1.0000
11.5000	.0000	.0000	1.0000
12.0000	.0000	.0000	1.0000
12.5000	.0000	.0000	1.0000
13.0000	.0000	.0000	1.0000
13.5000	.0000	.0000	1.0000
14.0000	.0000	.0000	1.0000
14.5000	.0000	.0000	1.0000
15.0000	.0000	.0000	1.0000
15.5000	.0000	.0000	1.0000
16.0000	.0000	.0000	1.0000
16.5000	.0000	.0000	1.0000
17.0000	.0000	.0000	1.0000
17.5000	.0000	.0000	1.0000
18.0000	.0000	.0000	1.0000
18.5000	.0000	.0000	1.0000
19.0000	.0000	.0000	1.0000
19.5000	.0000	.0000	1.0000
20.0000	.0000	.0000	1.0000
20.5000	.0000	.0000	1.0000
21.0000	.0000	.0000	1.0000
21.5000	.0000	.0000	1.0000
22.0000	.0000	.0000	1.0000
22.5000	.0000	.0000	1.0000
23.0000	.0000	.0000	1.0000
23.5000	.0000	.0000	1.0000
24.0000	.0000	.0000	1.0000
24.5000	.0000	.0000	1.0000
25.0000	.0000	.0000	1.0000
25.5000	.0000	.0000	1.0000
26.0000	.0000	.0000	1.0000
26.5000	.0000	.0000	1.0000
27.0000	.0000	.0000	1.0000
27.5000	.0000	.0000	1.0000
28.0000	.0000	.0000	1.0000
28.5000	.0000	.0000	1.0000
29.0000	.0000	.0000	1.0000
29.5000	.0000	.0000	1.0000
30.0000	.0000	.0000	1.0000
30.5000	.0000	.0000	1.0000
31.0000	.0000	.0000	1.0000
31.5000	.0000	.0000	1.0000
32.0000	.0000	.0000	1.0000
32.5000	.0000	.0000	1.0000
33.0000	.0000	.0000	1.0000
33.5000	.0000	.0000	1.0000
34.0000	.0000	.0000	1.0000
34.5000	.0000	.0000	1.0000
35.0000	.0000	.0000	1.0000
35.5000	.0000	.0000	1.0000

36.0000	.0000	.0000	1.0000
36.5000	.0000	.0000	1.0000
37.0000	.0000	.0000	1.0000
37.5000	.0000	.0000	1.0000
38.0000	.0000	.0000	1.0000
38.5000	.0000	.0000	1.0000
39.0000	.0000	.0000	1.0000
39.5000	.0000	.0000	1.0000
40.0000	.0000	.0000	1.0000
40.5000	.0000	.0000	1.0000
41.0000	.0000	.0000	1.0000
41.5000	.0000	.0000	1.0000
42.0000	.0000	.0000	1.0000
42.5000	.0000	.0000	1.0000
43.0000	.0000	.0000	1.0000
43.5000	.0000	.0000	1.0000
44.0000	.0000	.0000	1.0000
44.5000	.0000	.0000	1.0000
45.0000	.0000	.0000	1.0000
45.5000	.0000	.0000	1.0000
46.0000	.0000	.0000	1.0000
46.5000	.0000	.0000	1.0000
47.0000	.0000	.0000	1.0000
47.5000	.0000	.0000	1.0000
48.0000	.0000	.0000	1.0000
48.5000	.0000	.0000	1.0000
49.0000	.0000	.0000	1.0000
49.5000	.0000	.0000	1.0000
50.0000	.0000	.0000	1.0000
50.5000	.0000	.0000	1.0000

50 PERCENT TMS SCOUR RESULTS

B	FD50	PRD50	CPRD50
1.0000	.0000	.0000	.0000
1.5000	.0000	.0000	.0000
2.0000	.0000	.0000	.0000
2.5000	.0000	.0000	.0000
3.0000	.0000	.0000	.0000
3.5000	.0000	.0000	.0000
4.0000	.0000	.0000	.0000
4.5000	.0000	.0000	.0000
5.0000	.0000	.0000	.0000
5.5000	.0000	.0000	.0000
6.0000	.0000	.0000	.0000
6.5000	.0000	.0000	.0000
7.0000	.0000	.0000	.0000
7.5000	.0000	.0000	.0000
8.0000	.0000	.0000	.0000
8.5000	.0000	.0000	.0000
9.0000	.0000	.0000	.0000
9.5000	.0000	.0000	.0000
10.0000	.0000	.0000	.0000
10.5000	.0000	.0000	.0000
11.0000	.0000	.0000	.0000
11.5000	.0000	.0000	.0000
12.0000	.0000	.0000	.0000
12.5000	.0000	.0000	.0000
13.0000	.0000	.0000	.0000

13.5000	.0000	.0000	.0000
14.0000	.0000	.0000	.0000
14.5000	.0000	.0000	.0000
15.0000	.0000	.0000	.0000
15.5000	.0000	.0000	.0000
16.0000	.0000	.0000	.0000
16.5000	.0000	.0000	.0000
17.0000	.0000	.0000	.0000
17.5000	.0000	.0000	.0000
18.0000	.0000	.0000	.0000
18.5000	.0000	.0000	.0000
19.0000	.0000	.0000	.0000
19.5000	.0000	.0000	.0000
20.0000	1000.0000	1.0000	1.0000
20.5000	.0000	.0000	1.0000
21.0000	.0000	.0000	1.0000
21.5000	.0000	.0000	1.0000
22.0000	.0000	.0000	1.0000
22.5000	.0000	.0000	1.0000
23.0000	.0000	.0000	1.0000
23.5000	.0000	.0000	1.0000
24.0000	.0000	.0000	1.0000
24.5000	.0000	.0000	1.0000
25.0000	.0000	.0000	1.0000
25.5000	.0000	.0000	1.0000
26.0000	.0000	.0000	1.0000
26.5000	.0000	.0000	1.0000
27.0000	.0000	.0000	1.0000
27.5000	.0000	.0000	1.0000
28.0000	.0000	.0000	1.0000
28.5000	.0000	.0000	1.0000
29.0000	.0000	.0000	1.0000
29.5000	.0000	.0000	1.0000
30.0000	.0000	.0000	1.0000
30.5000	.0000	.0000	1.0000
31.0000	.0000	.0000	1.0000
31.5000	.0000	.0000	1.0000
32.0000	.0000	.0000	1.0000
32.5000	.0000	.0000	1.0000
33.0000	.0000	.0000	1.0000
33.5000	.0000	.0000	1.0000
34.0000	.0000	.0000	1.0000
34.5000	.0000	.0000	1.0000
35.0000	.0000	.0000	1.0000
35.5000	.0000	.0000	1.0000
36.0000	.0000	.0000	1.0000
36.5000	.0000	.0000	1.0000
37.0000	.0000	.0000	1.0000
37.5000	.0000	.0000	1.0000
38.0000	.0000	.0000	1.0000
38.5000	.0000	.0000	1.0000
39.0000	.0000	.0000	1.0000
39.5000	.0000	.0000	1.0000
40.0000	.0000	.0000	1.0000
40.5000	.0000	.0000	1.0000
41.0000	.0000	.0000	1.0000
41.5000	.0000	.0000	1.0000

42.0000	.0000	.0000	1.0000
42.5000	.0000	.0000	1.0000
43.0000	.0000	.0000	1.0000
43.5000	.0000	.0000	1.0000
44.0000	.0000	.0000	1.0000
44.5000	.0000	.0000	1.0000
45.0000	.0000	.0000	1.0000
45.5000	.0000	.0000	1.0000
46.0000	.0000	.0000	1.0000
46.5000	.0000	.0000	1.0000
47.0000	.0000	.0000	1.0000
47.5000	.0000	.0000	1.0000
48.0000	.0000	.0000	1.0000
48.5000	.0000	.0000	1.0000
49.0000	.0000	.0000	1.0000
49.5000	.0000	.0000	1.0000
50.0000	.0000	.0000	1.0000
50.5000	.0000	.0000	1.0000
B	FU50	PRU50	CPRU50
1.0000	939.0000	.9390	.9390
1.5000	33.0000	.0330	.9720
2.0000	14.0000	.0140	.9860
2.5000	4.0000	.0040	.9900
3.0000	2.0000	.0020	.9920
3.5000	.0000	.0000	.9920
4.0000	.0000	.0000	.9920
4.5000	.0000	.0000	.9920
5.0000	.0000	.0000	.9920
5.5000	.0000	.0000	.9920
6.0000	1.0000	.0010	.9930
6.5000	.0000	.0000	.9930
7.0000	.0000	.0000	.9930
7.5000	.0000	.0000	.9930
8.0000	.0000	.0000	.9930
8.5000	.0000	.0000	.9930
9.0000	.0000	.0000	.9930
9.5000	.0000	.0000	.9930
10.0000	.0000	.0000	.9930
10.5000	.0000	.0000	.9930
11.0000	.0000	.0000	.9930
11.5000	.0000	.0000	.9930
12.0000	.0000	.0000	.9930
12.5000	.0000	.0000	.9930
13.0000	.0000	.0000	.9930
13.5000	.0000	.0000	.9930
14.0000	.0000	.0000	.9930
14.5000	.0000	.0000	.9930
15.0000	.0000	.0000	.9930
15.5000	.0000	.0000	.9930
16.0000	.0000	.0000	.9930
16.5000	.0000	.0000	.9930
17.0000	.0000	.0000	.9930
17.5000	.0000	.0000	.9930
18.0000	.0000	.0000	.9930
18.5000	.0000	.0000	.9930
19.0000	.0000	.0000	.9930
19.5000	.0000	.0000	.9930

20.0000	2.0000	.0020	.9950
20.5000	5.0000	.0050	1.0000
21.0000	.0000	.0000	1.0000
21.5000	.0000	.0000	1.0000
22.0000	.0000	.0000	1.0000
22.5000	.0000	.0000	1.0000
23.0000	.0000	.0000	1.0000
23.5000	.0000	.0000	1.0000
24.0000	.0000	.0000	1.0000
24.5000	.0000	.0000	1.0000
25.0000	.0000	.0000	1.0000
25.5000	.0000	.0000	1.0000
26.0000	.0000	.0000	1.0000
26.5000	.0000	.0000	1.0000
27.0000	.0000	.0000	1.0000
27.5000	.0000	.0000	1.0000
28.0000	.0000	.0000	1.0000
28.5000	.0000	.0000	1.0000
29.0000	.0000	.0000	1.0000
29.5000	.0000	.0000	1.0000
30.0000	.0000	.0000	1.0000
30.5000	.0000	.0000	1.0000
31.0000	.0000	.0000	1.0000
31.5000	.0000	.0000	1.0000
32.0000	.0000	.0000	1.0000
32.5000	.0000	.0000	1.0000
33.0000	.0000	.0000	1.0000
33.5000	.0000	.0000	1.0000
34.0000	.0000	.0000	1.0000
34.5000	.0000	.0000	1.0000
35.0000	.0000	.0000	1.0000
35.5000	.0000	.0000	1.0000
36.0000	.0000	.0000	1.0000
36.5000	.0000	.0000	1.0000
37.0000	.0000	.0000	1.0000
37.5000	.0000	.0000	1.0000
38.0000	.0000	.0000	1.0000
38.5000	.0000	.0000	1.0000
39.0000	.0000	.0000	1.0000
39.5000	.0000	.0000	1.0000
40.0000	.0000	.0000	1.0000
40.5000	.0000	.0000	1.0000
41.0000	.0000	.0000	1.0000
41.5000	.0000	.0000	1.0000
42.0000	.0000	.0000	1.0000
42.5000	.0000	.0000	1.0000
43.0000	.0000	.0000	1.0000
43.5000	.0000	.0000	1.0000
44.0000	.0000	.0000	1.0000
44.5000	.0000	.0000	1.0000
45.0000	.0000	.0000	1.0000
45.5000	.0000	.0000	1.0000
46.0000	.0000	.0000	1.0000
46.5000	.0000	.0000	1.0000
47.0000	.0000	.0000	1.0000
47.5000	.0000	.0000	1.0000
48.0000	.0000	.0000	1.0000

48.5000	.0000	.0000	1.0000
49.0000	.0000	.0000	1.0000
49.5000	.0000	.0000	1.0000
50.0000	.0000	.0000	1.0000
50.5000	.0000	.0000	1.0000
75 PERCENT TMS SCOUR RESULTS			
B	FD75	PRD75	CPRD75
1.0000	.0000	.0000	.0000
1.5000	.0000	.0000	.0000
2.0000	.0000	.0000	.0000
2.5000	.0000	.0000	.0000
3.0000	.0000	.0000	.0000
3.5000	.0000	.0000	.0000
4.0000	.0000	.0000	.0000
4.5000	.0000	.0000	.0000
5.0000	.0000	.0000	.0000
5.5000	.0000	.0000	.0000
6.0000	.0000	.0000	.0000
6.5000	.0000	.0000	.0000
7.0000	.0000	.0000	.0000
7.5000	.0000	.0000	.0000
8.0000	.0000	.0000	.0000
8.5000	.0000	.0000	.0000
9.0000	.0000	.0000	.0000
9.5000	.0000	.0000	.0000
10.0000	.0000	.0000	.0000
10.5000	.0000	.0000	.0000
11.0000	.0000	.0000	.0000
11.5000	.0000	.0000	.0000
12.0000	.0000	.0000	.0000
12.5000	.0000	.0000	.0000
13.0000	.0000	.0000	.0000
13.5000	.0000	.0000	.0000
14.0000	.0000	.0000	.0000
14.5000	.0000	.0000	.0000
15.0000	.0000	.0000	.0000
15.5000	.0000	.0000	.0000
16.0000	.0000	.0000	.0000
16.5000	.0000	.0000	.0000
17.0000	.0000	.0000	.0000
17.5000	.0000	.0000	.0000
18.0000	.0000	.0000	.0000
18.5000	.0000	.0000	.0000
19.0000	.0000	.0000	.0000
19.5000	.0000	.0000	.0000
20.0000	1000.0000	1.0000	1.0000
20.5000	.0000	.0000	1.0000
21.0000	.0000	.0000	1.0000
21.5000	.0000	.0000	1.0000
22.0000	.0000	.0000	1.0000
22.5000	.0000	.0000	1.0000
23.0000	.0000	.0000	1.0000
23.5000	.0000	.0000	1.0000
24.0000	.0000	.0000	1.0000
24.5000	.0000	.0000	1.0000
25.0000	.0000	.0000	1.0000
25.5000	.0000	.0000	1.0000



26.0000	.0000	.0000	1.0000
26.5000	.0000	.0000	1.0000
27.0000	.0000	.0000	1.0000
27.5000	.0000	.0000	1.0000
28.0000	.0000	.0000	1.0000
28.5000	.0000	.0000	1.0000
29.0000	.0000	.0000	1.0000
29.5000	.0000	.0000	1.0000
30.0000	.0000	.0000	1.0000
30.5000	.0000	.0000	1.0000
31.0000	.0000	.0000	1.0000
31.5000	.0000	.0000	1.0000
32.0000	.0000	.0000	1.0000
32.5000	.0000	.0000	1.0000
33.0000	.0000	.0000	1.0000
33.5000	.0000	.0000	1.0000
34.0000	.0000	.0000	1.0000
34.5000	.0000	.0000	1.0000
35.0000	.0000	.0000	1.0000
35.5000	.0000	.0000	1.0000
36.0000	.0000	.0000	1.0000
36.5000	.0000	.0000	1.0000
37.0000	.0000	.0000	1.0000
37.5000	.0000	.0000	1.0000
38.0000	.0000	.0000	1.0000
38.5000	.0000	.0000	1.0000
39.0000	.0000	.0000	1.0000
39.5000	.0000	.0000	1.0000
40.0000	.0000	.0000	1.0000
40.5000	.0000	.0000	1.0000
41.0000	.0000	.0000	1.0000
41.5000	.0000	.0000	1.0000
42.0000	.0000	.0000	1.0000
42.5000	.0000	.0000	1.0000
43.0000	.0000	.0000	1.0000
43.5000	.0000	.0000	1.0000
44.0000	.0000	.0000	1.0000
44.5000	.0000	.0000	1.0000
45.0000	.0000	.0000	1.0000
45.5000	.0000	.0000	1.0000
46.0000	.0000	.0000	1.0000
46.5000	.0000	.0000	1.0000
47.0000	.0000	.0000	1.0000
47.5000	.0000	.0000	1.0000
48.0000	.0000	.0000	1.0000
48.5000	.0000	.0000	1.0000
49.0000	.0000	.0000	1.0000
49.5000	.0000	.0000	1.0000
50.0000	.0000	.0000	1.0000
50.5000	.0000	.0000	1.0000
B	FU75	PRU75	CPRU75
1.0000	588.0000	.5880	.5880
1.5000	175.0000	.1750	.7630
2.0000	78.0000	.0780	.8410
2.5000	25.0000	.0250	.8660
3.0000	13.0000	.0130	.8790
3.5000	9.0000	.0090	.8880

4.0000	2.0000	.0020	.8900
4.5000	4.0000	.0040	.8940
5.0000	1.0000	.0010	.8950
5.5000	2.0000	.0020	.8970
6.0000	1.0000	.0010	.8980
6.5000	.0000	.0000	.8980
7.0000	.0000	.0000	.8980
7.5000	.0000	.0000	.8980
8.0000	.0000	.0000	.8980
8.5000	.0000	.0000	.8980
9.0000	.0000	.0000	.8980
9.5000	.0000	.0000	.8980
10.0000	.0000	.0000	.8980
10.5000	.0000	.0000	.8980
11.0000	.0000	.0000	.8980
11.5000	.0000	.0000	.8980
12.0000	.0000	.0000	.8980
12.5000	.0000	.0000	.8980
13.0000	.0000	.0000	.8980
13.5000	.0000	.0000	.8980
14.0000	.0000	.0000	.8980
14.5000	.0000	.0000	.8980
15.0000	.0000	.0000	.8980
15.5000	.0000	.0000	.8980
16.0000	.0000	.0000	.8980
16.5000	.0000	.0000	.8980
17.0000	.0000	.0000	.8980
17.5000	1.0000	.0010	.8990
18.0000	1.0000	.0010	.9000
18.5000	1.0000	.0010	.9010
19.0000	1.0000	.0010	.9020
19.5000	14.0000	.0140	.9160
20.0000	35.0000	.0350	.9510
20.5000	49.0000	.0490	1.0000
21.0000	.0000	.0000	1.0000
21.5000	.0000	.0000	1.0000
22.0000	.0000	.0000	1.0000
22.5000	.0000	.0000	1.0000
23.0000	.0000	.0000	1.0000
23.5000	.0000	.0000	1.0000
24.0000	.0000	.0000	1.0000
24.5000	.0000	.0000	1.0000
25.0000	.0000	.0000	1.0000
25.5000	.0000	.0000	1.0000
26.0000	.0000	.0000	1.0000
26.5000	.0000	.0000	1.0000
27.0000	.0000	.0000	1.0000
27.5000	.0000	.0000	1.0000
28.0000	.0000	.0000	1.0000
28.5000	.0000	.0000	1.0000
29.0000	.0000	.0000	1.0000
29.5000	.0000	.0000	1.0000
30.0000	.0000	.0000	1.0000
30.5000	.0000	.0000	1.0000
31.0000	.0000	.0000	1.0000
31.5000	.0000	.0000	1.0000
32.0000	.0000	.0000	1.0000

32.5000	.0000	.0000	1.0000
33.0000	.0000	.0000	1.0000
33.5000	.0000	.0000	1.0000
34.0000	.0000	.0000	1.0000
34.5000	.0000	.0000	1.0000
35.0000	.0000	.0000	1.0000
35.5000	.0000	.0000	1.0000
36.0000	.0000	.0000	1.0000
36.5000	.0000	.0000	1.0000
37.0000	.0000	.0000	1.0000
37.5000	.0000	.0000	1.0000
38.0000	.0000	.0000	1.0000
38.5000	.0000	.0000	1.0000
39.0000	.0000	.0000	1.0000
39.5000	.0000	.0000	1.0000
40.0000	.0000	.0000	1.0000
40.5000	.0000	.0000	1.0000
41.0000	.0000	.0000	1.0000
41.5000	.0000	.0000	1.0000
42.0000	.0000	.0000	1.0000
42.5000	.0000	.0000	1.0000
43.0000	.0000	.0000	1.0000
43.5000	.0000	.0000	1.0000
44.0000	.0000	.0000	1.0000
44.5000	.0000	.0000	1.0000
45.0000	.0000	.0000	1.0000
45.5000	.0000	.0000	1.0000
46.0000	.0000	.0000	1.0000
46.5000	.0000	.0000	1.0000
47.0000	.0000	.0000	1.0000
47.5000	.0000	.0000	1.0000
48.0000	.0000	.0000	1.0000
48.5000	.0000	.0000	1.0000
49.0000	.0000	.0000	1.0000
49.5000	.0000	.0000	1.0000
50.0000	.0000	.0000	1.0000
50.5000	.0000	.0000	1.0000

The mean annual contraction scour d/s face is MNYYS

The mean annual scour value d/s face is MNLTS

The mean annual total scour d/s face is YMNTS

The standard dev in annual scour d/s face is YSTTS

YR	MNYYS	MNLTS	YMNTS	YSTTS
001	.0000	.3072	.3072	.1317
002	.0000	.8181	.8181	.3376
003	.0000	3.2199	3.2199	4.4190
004	.0000	14.1008	14.1008	7.4410
005	.0000	19.1787	19.1787	1.9296
006	.0000	19.4886	19.4886	.0408
007	.0000	19.5230	19.5230	.0375
008	.0000	19.5487	19.5487	.0366
009	.0000	19.5669	19.5669	.0469
010	.0000	19.5807	19.5807	.0460
011	.0000	19.5928	19.5928	.0324
012	.0000	19.6031	19.6031	.0316
013	.0000	19.6113	19.6113	.0398
014	.0000	19.6191	19.6191	.0411
015	.0000	19.6266	19.6266	.0390

016	.0000	19.6324	19.6324	.0320
017	.0000	19.6372	19.6372	.0356
018	.0000	19.6422	19.6422	.0310
019	.0000	19.6470	19.6470	.0219
020	.0000	19.6517	19.6517	.0226
021	.0000	19.6562	19.6562	.0235
022	.0000	19.6599	19.6599	.0246
023	.0000	19.6638	19.6638	.0292
024	.0000	19.6675	19.6675	.0266
025	.0000	19.6706	19.6706	.0279
026	.0000	19.6735	19.6735	.0326
027	.0000	19.6762	19.6762	.0339
028	.0000	19.6792	19.6792	.0328
029	.0000	19.6817	19.6817	.0296
030	.0000	19.6848	19.6848	.0347
031	.0000	19.6870	19.6870	.0381
032	.0000	19.6895	19.6895	.0402
033	.0000	19.6921	19.6921	.0370
034	.0000	19.6946	19.6946	.0303
035	.0000	19.6967	19.6967	.0271
036	.0000	19.6984	19.6984	.0276
037	.0000	19.7006	19.7006	.0293
038	.0000	19.7027	19.7027	.0269
039	.0000	19.7045	19.7045	.0186
040	.0000	19.7061	19.7061	.0227
041	.0000	19.7079	19.7079	.0217
042	.0000	19.7095	19.7095	.0250
043	.0000	19.7109	19.7109	.0204
044	.0000	19.7121	19.7121	.0255
045	.0000	19.7135	19.7135	.0273
046	.0000	19.7151	19.7151	.0307
047	.0000	19.7167	19.7167	.0322
048	.0000	19.7183	19.7183	.0316
049	.0000	19.7195	19.7195	.0302
050	.0000	19.7209	19.7209	.0358
051	.0000	19.7224	19.7224	.0322
052	.0000	19.7236	19.7236	.0318
053	.0000	19.7249	19.7249	.0341
054	.0000	19.7264	19.7264	.0283
055	.0000	19.7273	19.7273	.0275
056	.0000	19.7287	19.7287	.0263
057	.0000	19.7296	19.7296	.0265
058	.0000	19.7307	19.7307	.0275
059	.0000	19.7322	19.7322	.0350
060	.0000	19.7332	19.7332	.0322
061	.0000	19.7342	19.7342	.0353
062	.0000	19.7352	19.7352	.0316
063	.0000	19.7359	19.7359	.0296
064	.0000	19.7370	19.7370	.0334
065	.0000	19.7380	19.7380	.0348
066	.0000	19.7389	19.7389	.0344
067	.0000	19.7397	19.7397	.0372
068	.0000	19.7407	19.7407	.0329
069	.0000	19.7418	19.7418	.0351
070	.0000	19.7427	19.7427	.0395
071	.0000	19.7436	19.7436	.0370
072	.0000	19.7443	19.7443	.0353

073	.0000	19.7453	19.7453	.0336
074	.0000	19.7462	19.7462	.0345
075	.0000	19.7470	19.7470	.0342
076	.0000	19.7476	19.7476	.0345
077	.0000	19.7485	19.7485	.0329
078	.0000	19.7494	19.7494	.0321
079	.0000	19.7501	19.7501	.0281
080	.0000	19.7510	19.7510	.0292
081	.0000	19.7518	19.7518	.0245
082	.0000	19.7525	19.7525	.0237
083	.0000	19.7532	19.7532	.0264
084	.0000	19.7540	19.7540	.0281
085	.0000	19.7549	19.7549	.0289
086	.0000	19.7557	19.7557	.0276
087	.0000	19.7562	19.7562	.0307
088	.0000	19.7568	19.7568	.0329
089	.0000	19.7574	19.7574	.0317
090	.0000	19.7582	19.7582	.0335
091	.0000	19.7589	19.7589	.0329
092	.0000	19.7594	19.7594	.0311
093	.0000	19.7600	19.7600	.0287
094	.0000	19.7609	19.7609	.0307
095	.0000	19.7614	19.7614	.0301
096	.0000	19.7619	19.7619	.0256
097	.0000	19.7626	19.7626	.0285
098	.0000	19.7633	19.7633	.0289
099	.0000	19.7640	19.7640	.0320
100	.0000	19.7645	19.7645	.0315

The annual contraction scour u/s face is MNYYSU

The mean annual local scour value u/s face is MNLSU

The mean annual total scour value u/s face is YMNTSU

The standard dev in annual scour u/s face is YSTTSU

YR	MNYYSU	MNLSU	YMNTSU	YSTTSU
001	.0000	.0076	.0076	.0233
002	.0000	.0156	.0156	.0357
003	.0000	.0213	.0213	.0402
004	.0000	.0289	.0289	.0523
005	.0000	.0359	.0359	.0573
006	.0000	.0418	.0418	.0600
007	.0000	.0484	.0484	.0628
008	.0000	.0557	.0557	.0665
009	.0000	.0633	.0633	.0715
010	.0000	.0706	.0706	.0752
011	.0000	.0776	.0776	.0774
012	.0000	.0843	.0843	.0798
013	.0000	.0926	.0926	.0845
014	.0000	.1003	.1003	.0886
015	.0000	.1091	.1091	.0931
016	.0000	.1174	.1174	.1012
017	.0000	.1250	.1250	.1049
018	.0000	.1342	.1342	.1109
019	.0000	.1416	.1416	.1146
020	.0000	.1500	.1500	.1191
021	.0000	.1579	.1579	.1236
022	.0000	.1672	.1672	.1287
023	.0000	.1758	.1758	.1324
024	.0000	.1855	.1855	.1409

025	.0000	.1957	.1957	.1518
026	.0000	.2065	.2065	.1605
027	.0000	.2178	.2178	.1814
028	.0000	.2294	.2294	.1986
029	.0000	.2501	.2501	.5308
030	.0000	.2639	.2639	.6274
031	.0000	.2752	.2752	.6360
032	.0000	.2875	.2875	.6482
033	.0000	.2995	.2995	.6543
034	.0000	.3106	.3106	.6627
035	.0000	.3227	.3227	.6694
036	.0000	.3390	.3390	.6907
037	.0000	.3682	.3682	.9013
038	.0000	.4091	.4091	1.2084
039	.0000	.4379	.4379	1.3626
040	.0000	.4517	.4517	1.3840
041	.0000	.4647	.4647	1.3919
042	.0000	.4784	.4784	1.3965
043	.0000	.4923	.4923	1.4030
044	.0000	.5083	.5083	1.4087
045	.0000	.5338	.5338	1.4869
046	.0000	.5525	.5525	1.5304
047	.0000	.5701	.5701	1.5436
048	.0000	.5960	.5960	1.5937
049	.0000	.6198	.6198	1.6566
050	.0000	.6393	.6393	1.6696
051	.0000	.6704	.6704	1.7671
052	.0000	.6894	.6894	1.7784
053	.0000	.7128	.7128	1.7929
054	.0000	.7616	.7616	1.9417
055	.0000	.8164	.8164	2.1411
056	.0000	.8480	.8480	2.1725
057	.0000	.9313	.9313	2.4505
058	.0000	1.0276	1.0276	2.7423
059	.0000	1.1009	1.1009	2.9615
060	.0000	1.1438	1.1438	3.0229
061	.0000	1.2046	1.2046	3.1434
062	.0000	1.2652	1.2652	3.2549
063	.0000	1.3399	1.3399	3.3905
064	.0000	1.4010	1.4010	3.5126
065	.0000	1.4639	1.4639	3.6006
066	.0000	1.5463	1.5463	3.7333
067	.0000	1.6633	1.6633	3.9454
068	.0000	1.7436	1.7436	4.0541
069	.0000	1.9188	1.9188	4.3524
070	.0000	2.0709	2.0709	4.6133
071	.0000	2.2016	2.2016	4.7956
072	.0000	2.3466	2.3466	4.9841
073	.0000	2.5329	2.5329	5.2423
074	.0000	2.7370	2.7370	5.5057
075	.0000	2.9213	2.9213	5.7483
076	.0000	3.0965	3.0965	5.9212
077	.0000	3.2863	3.2863	6.1120
078	.0000	3.4569	3.4569	6.2694
079	.0000	3.7070	3.7070	6.5041
080	.0000	3.9584	3.9584	6.7446
081	.0000	4.1573	4.1573	6.9103

082	.0000	4.3879	4.3879	7.0592
083	.0000	4.7294	4.7294	7.3314
084	.0000	4.9977	4.9977	7.5186
085	.0000	5.2659	5.2659	7.6739
086	.0000	5.6089	5.6089	7.8710
087	.0000	5.9746	5.9746	8.0963
088	.0000	6.3279	6.3279	8.2527
089	.0000	6.7035	6.7035	8.4512
090	.0000	6.9981	6.9981	8.5781
091	.0000	7.2322	7.2322	8.6360
092	.0000	7.5493	7.5493	8.7191
093	.0000	8.0150	8.0150	8.8543
094	.0000	8.5336	8.5336	9.0046
095	.0000	8.9088	8.9088	9.1018
096	.0000	9.2124	9.2124	9.1430
097	.0000	9.5721	9.5721	9.1703
098	.0000	9.9834	9.9834	9.1955
099	.0000	10.3237	10.3237	9.2111
100	.0000	10.7172	10.7172	9.2117

## Appendix D-10

RUN TITLE IS Wicomico Hurricane Simulation  
RUN DATE IS 10/9/05  
THE PROGRAM WAS EXECUTED IN THE EXISTING PIER ANALYSIS MODE.  
CONTRACTION SCOUR METHOD IS KOMURAS EQN  
SCOUR COMPUTED WITHOUT ARMOURING  
BRUBAKER-DEMETRIUS NEILLS MODIFICATION FACTOR ACTIVATED  
TIDE DISTORTION OPTION ACTIVATED  
MEAN TIDAL DEPTH MDR is = 18.190000  
MEAN LOW TIDAL DEPTH MLT is = 17.000000  
MEAN LOW TIDE ELEVATION MLTE is = -1.190000  
TIDAL AMP. AT BRIDGE XSEC MTR is = 1.190000  
CHANNEL INVERT AT BRIDGE IRS is = -18.190000

Estuary in bank area is = 14650.800000

Maximum tide in the simulation HITIDE is = 29.256680  
Maximum u/s flow depth in sim. YTRMXS is = 32.512250  
Maximum d/s flow depth in sim. YTFMXS is = 32.401840  
Maximum u/s disch. in sim. QTRMXS is = 371722.800000  
Maximum d/s disch. in sim. QTFMXS is = 377347.000000  
Maximum u/s vel.in sim. VUPMS is = 2.589252  
Maximum d/s vel.in sim. VDOWNMS is = 8.124564

Maximum u/s flow depth last run YTRMAX is = 32.512250  
Maximum d/s flow depth last run YTFMAX is = 29.904540  
Maximum u/s discharge last run QTRMAX is = 312059.200000  
Maximum d/s discharge last run QTFMAX is = 326059.100000  
Maximum u/s velocity last run VNUMAX is = 4.465335  
Maximum d/s velocity last run VNDMAX is = 2.093080  
Maximum tangential vel d/s face last run VTDMX is = 1.104595  
Maximum tangential vel u/s face last run VTUMX is = 2.394595

critical vel u/s face last run UIUMIN is = 3.139019E-01  
critical vel d/s face last run UIDMIN is = 3.139019E-01

Time of concentration = 48.000000hrs  
Time to peak = 32.160000hrs  
Number of unit hydrograph ordinates = 160  
Soil infiltration potential = 2.658228  
Peak discharge of the UHG = 2570.498000cfs  
Initial abstractions IA = 5.316456E-01in

Catchment base flow = 109.689300cfs  
Tide attenuation factor TAF = 9.754099E-01  
Tidal lag MTL= -4.190653hrs  
Tidal routing constant CX = 1.000000  
Bridge station tidal range TR = 2.380000ft  
Effective bottom channel width at brdg.WBE = 1205.000000ft  
Estuary Area 1.101197E+08  
Contraction scour factor u/s face= 1.062975  
Contraction scour factor d/s face= 1.062975  
Estuary to wavelength ratio DIM = 7.817710E-02



Estuary width factor WF = 1.400000  
 Tidal range factor HF = 1.308411E-01  
 Neill Mod. factor rising limb.NMRF = 8.000000E-01  
 Neill Mod. factor falling limb.NMFF = 8.000000E-01

The maximum storm event in the simulation is 5.000000ins  
 Array of total SURGRE at bridge is HSURGE= 10.380330  
 2.856355E-01

5.179529E-01	8.728182E-01	1.481365	2.761897
10.926670	10.926670	3.868823	2.761897
-5.401087	-5.078043	-4.789991	-4.531823
-4.299308	-4.088933	-3.897769	-3.723364
-3.563652	-3.416886	-3.281578	-3.156457
-3.040428	-2.932547	-2.831993	-2.738052
-2.650098	-2.567580	-2.490014	-2.416970
-2.348066	-2.282962	-2.221354	-2.162968
-2.107560	-2.054909	-2.004814	-1.957096
-1.911588	-1.868142	-1.826621	-1.786900
-1.748865	-1.712412	-1.677443	-1.643871
-1.611613	-1.580593	-1.550743	-1.521997
-1.494296	-1.467583	-1.441807	-1.416919
-1.392874	-1.369630	-1.347148	-1.325391
-1.304325	-1.283917	-1.264137	-1.244957
-1.226349	-1.208288	-1.190751	-1.173715
-1.157160	-1.141064	-1.125410	-1.110179
-1.095354	-1.080919	-1.066860	-1.053161
-1.039810	-1.026792	-1.014096	-1.001710
-9.896228E-01	-9.778234E-01	-9.663019E-01	-9.550486E-01
-9.440541E-01	-9.333097E-01	-9.228069E-01	-9.125378E-01
-9.024945E-01	-8.926698E-01	-8.830566E-01	-8.736480E-01
-8.644378E-01	-8.554195E-01	-8.465874E-01	-8.379357E-01
-8.294590E-01	-8.211520E-01	-8.130096E-01	-8.050270E-01
-7.971996E-01	-7.895228E-01	-7.819924E-01	-7.746043E-01
-7.673544E-01	-7.602389E-01	-7.532541E-01	-7.463963E-01
-7.396623E-01	-7.330486E-01	-7.265522E-01	-7.201698E-01
-7.138985E-01	-7.077355E-01	-7.016779E-01	-6.957231E-01
-6.898685E-01	-6.841115E-01	-6.784499E-01	-6.728811E-01
-6.674029E-01	-6.620133E-01		

Array of total combined depth at bridge d/s face is YTR=  
 17.000000

17.000000	22.478510	17.000000	22.923680
24.155860	32.512250	17.000000	22.023550
17.000000	21.829160	17.000000	17.000000
22.231070	17.000000	17.000000	17.000000
22.096740	17.000000	22.056710	17.000000
17.000000	21.639580	17.000000	17.000000
21.598520	17.000000	21.663800	17.000000
22.108660	17.000000	22.054110	17.000000
21.567630	17.000000	21.394050	17.000000
21.688710	17.000000	17.000000	21.557660
21.589640	17.000000	17.000000	21.238030
21.414890	21.581960	22.104780	17.000000
17.000000	17.000000	21.573240	21.676120
17.000000	21.513090	17.000000	21.691130
21.894030	21.959660	17.000000	21.665220
17.000000	17.000000	21.420890	22.047760

17.000000	17.000000	21.887970	17.000000
17.000000	17.000000	17.000000	21.637520
17.000000	21.528520	17.000000	21.946280
17.000000	17.000000	17.000000	21.288840
21.548640	22.085110	17.000000	17.000000
21.638450	22.042280	17.000000	17.000000
17.000000	17.000000	21.853770	17.000000
17.000000	21.379700	22.027370	22.233380
17.000000	17.000000	17.000000	21.960540
17.000000	21.928910	17.000000	17.000000
21.708730	21.881690	22.097260	22.430420
17.000000	17.000000	17.000000	17.000000
21.686330	17.000000	21.459330	17.000000
21.768150	17.000000	17.000000	

Array of total combined depth at bridge u/s face is YTF=  
29.904540

22.403730	17.000000	22.206190	17.000000
17.000000	17.000000	21.605060	17.000000
21.649890	17.000000	21.634080	21.534700
17.000000	22.023240	21.776610	21.748440
17.000000	21.630450	17.000000	21.912640
21.598490	17.000000	21.544410	21.367790
17.000000	21.582940	17.000000	21.618070
17.000000	21.985170	17.000000	21.559020
17.000000	21.329270	17.000000	21.237190
17.000000	21.295210	21.192880	17.000000
17.000000	21.426150	21.155230	17.000000
17.000000	17.000000	17.000000	21.782280
21.721820	21.540570	17.000000	17.000000
21.425130	17.000000	21.507830	17.000000
17.000000	17.000000	21.422780	17.000000
21.574860	21.263130	17.000000	17.000000
21.944850	21.597150	17.000000	21.830410
21.771470	21.597520	21.466680	17.000000
21.527470	17.000000	21.506460	17.000000
21.683060	21.346430	21.132800	17.000000
17.000000	17.000000	21.816890	21.408090
17.000000	17.000000	21.885520	21.661160
21.654530	21.506690	17.000000	21.817050
21.260910	17.000000	17.000000	17.000000
21.774850	21.728780	21.593970	17.000000
21.639270	17.000000	21.920440	21.638770
17.000000	17.000000	17.000000	17.000000
21.782780	21.648820	21.473960	21.313780
17.000000	21.338800	17.000000	21.344150
17.000000	21.681320	21.273920	

Array total net disch. value at bridge is QT= 308365.100000  
20706.590000

15854.140000	-18619.430000	-48841.790000	-312059.200000
326059.100000	-34536.380000	-34547.840000	-25789.450000
-10489.190000	6015.286000	9805.841000	34617.640000
36148.580000	8189.221000	494.743800	620.412200
768.548000	-33865.270000	-44716.690000	-36500.840000
-18678.340000	3831.760000	26693.590000	31470.020000
35774.050000	27041.320000	3944.752000	4409.032000
4931.353000	-22099.750000	-35399.550000	-30793.010000

-16718.300000	3379.980000	-4414.292000	46721.700000
56536.160000	43032.290000	10324.900000	10712.770000
11057.900000	8907.314000	-47015.630000	-45696.250000
-29871.830000	-3491.563000	54692.140000	32606.470000
40545.420000	41155.790000	31972.020000	11835.830000
11666.040000	-4157.260000	-23790.960000	-26299.230000
-19362.530000	-4818.970000	-14164.660000	33597.610000
47053.930000	50905.320000	32344.990000	8509.220000
8117.013000	7723.572000	-26094.040000	-45511.450000
-39776.980000	-22227.320000	44765.500000	14498.230000
22134.450000	25504.160000	23673.380000	17046.360000
7261.975000	-5123.851000	-15838.690000	-21491.940000
-20693.370000	-13696.950000	-33472.950000	12620.860000
26767.180000	34855.250000	34791.750000	22069.460000
2502.228000	2380.665000	-16153.930000	-36936.800000
-38755.460000	-30167.210000	-4030.945000	5677.368000
19297.930000	28435.570000	30743.240000	25616.180000
8848.695000	1348.855000	-13392.540000	-30967.330000
-35418.930000	-30522.090000	5557.580000	509.186600
9974.790000	17059.720000	20049.740000	18174.670000
11903.820000	2826.143000	-8626.487000	-18172.370000
-22872.400000	-21534.530000		
Array of total net velocity at bridge is VNT =			3.537574
6.485859E-01			
4.988193E-01	-6.081051E-01	-1.418580	-7.512090
2.778239	-1.212190	-1.116401	-9.074948E-01
-3.535326E-01	2.114783E-01	3.428203E-01	1.132282
1.168107	2.751939E-01	1.750921E-02	2.013271E-02
2.701412E-02	-1.096416	-1.514416	-1.280664
-6.568774E-01	1.340338E-01	9.750289E-01	1.104155
1.254065	9.523059E-01	1.385586E-01	1.431745E-01
1.677234E-01	-7.153909E-01	-1.239274	-1.078527
-6.093597E-01	1.236414E-01	-1.688057E-01	1.647750
2.056813	1.641483	3.614289E-01	3.756793E-01
4.052381E-01	3.390613E-01	-1.797997	-1.673559
-1.047104	-1.133559E-01	1.838483	1.152159
1.417964	1.441938	1.126748	4.337217E-01
4.073672E-01	-1.451255E-01	-8.391613E-01	-8.897115E-01
-6.575580E-01	-1.765668E-01	-4.988733E-01	1.177236
1.708858	1.864967	1.046659	2.887244E-01
2.847712E-01	2.611993E-01	-8.795481E-01	-1.528944
-1.395534	-8.164506E-01	1.574121	5.066671E-01
7.735740E-01	8.902559E-01	8.033234E-01	6.009830E-01
2.649408E-01	-1.948007E-01	-5.760188E-01	-7.519585E-01
-6.710600E-01	-4.613261E-01	-1.225427	4.438199E-01
8.658945E-01	1.178583	1.225065	7.767998E-01
8.734463E-02	8.035196E-02	-5.440844E-01	-1.341273
-1.416553	-9.750538E-01	-1.318634E-01	1.907658E-01
6.821750E-01	9.974332E-01	1.044105	9.008505E-01
2.999626E-01	4.570232E-02	-4.709651E-01	-1.093405
-1.197379	-9.904885E-01	1.743547E-01	1.711685E-02
3.509775E-01	6.268973E-01	7.301627E-01	6.408837E-01
4.341071E-01	1.037657E-01	-3.146829E-01	-6.103819E-01
-8.063042E-01	-7.825279E-01		
Array of net adjusted vel.upstream is VNUA =			0.000000E+00
0.000000E+00			
0.000000E+00	3.040526E-01	1.013343	4.465335

3.756045	6.060950E-01	1.164295	1.011948
6.305137E-01	1.767663E-01	0.000000E+00	0.000000E+00
0.000000E+00	0.000000E+00	0.000000E+00	0.000000E+00
0.000000E+00	5.482081E-01	1.305416	1.397540
9.687708E-01	3.284387E-01	0.000000E+00	0.000000E+00
0.000000E+00	0.000000E+00	0.000000E+00	0.000000E+00
0.000000E+00	3.576954E-01	9.773326E-01	1.158900
8.439432E-01	3.046798E-01	0.000000E+00	0.000000E+00
0.000000E+00	0.000000E+00	0.000000E+00	0.000000E+00
0.000000E+00	0.000000E+00	8.989987E-01	1.735778
1.360332	5.802302E-01	0.000000E+00	0.000000E+00
0.000000E+00	0.000000E+00	0.000000E+00	0.000000E+00
0.000000E+00	0.000000E+00	4.921434E-01	8.644364E-01
7.736348E-01	4.170624E-01	3.377200E-01	2.494366E-01
0.000000E+00	0.000000E+00	0.000000E+00	0.000000E+00
0.000000E+00	0.000000E+00	4.397741E-01	1.204246
1.462239	1.105993	4.082253E-01	0.000000E+00
0.000000E+00	0.000000E+00	0.000000E+00	0.000000E+00
0.000000E+00	0.000000E+00	3.854097E-01	6.639886E-01
7.115093E-01	5.661931E-01	8.433767E-01	6.127136E-01
0.000000E+00	0.000000E+00	0.000000E+00	0.000000E+00
0.000000E+00	0.000000E+00	2.720422E-01	9.426787E-01
1.378913	1.195803	5.534586E-01	0.000000E+00
0.000000E+00	0.000000E+00	0.000000E+00	0.000000E+00
0.000000E+00	0.000000E+00	2.354826E-01	7.821849E-01
1.145392	1.093934	4.952443E-01	0.000000E+00
0.000000E+00	0.000000E+00	0.000000E+00	0.000000E+00
0.000000E+00	0.000000E+00	1.573415E-01	4.625324E-01
7.083430E-01	7.944161E-01		
Array of net adjusted vel.downstream is VNDA=			1.768787
2.093080			
5.737026E-01	2.494096E-01	0.000000E+00	0.000000E+00
1.389119	1.389119	0.000000E+00	0.000000E+00
0.000000E+00	1.057392E-01	2.771493E-01	7.375511E-01
1.150194	7.216505E-01	1.463516E-01	0.000000E+00
0.000000E+00	0.000000E+00	0.000000E+00	0.000000E+00
0.000000E+00	0.000000E+00	5.545313E-01	1.039592
1.179110	1.103185	5.454323E-01	1.408665E-01
1.554489E-01	0.000000E+00	0.000000E+00	0.000000E+00
0.000000E+00	0.000000E+00	0.000000E+00	8.238750E-01
1.852282	1.849148	1.001456	3.685541E-01
3.904587E-01	3.721497E-01	1.695306E-01	0.000000E+00
0.000000E+00	0.000000E+00	9.192413E-01	1.495321
1.285062	1.429951	1.284343	7.802349E-01
4.205445E-01	2.036836E-01	0.000000E+00	0.000000E+00
0.000000E+00	0.000000E+00	0.000000E+00	5.886179E-01
1.443047	1.786913	1.455813	6.676919E-01
2.867478E-01	2.729852E-01	1.305996E-01	0.000000E+00
0.000000E+00	0.000000E+00	7.870607E-01	1.040394
6.401206E-01	8.319149E-01	8.467897E-01	7.021532E-01
4.329619E-01	1.324704E-01	0.000000E+00	0.000000E+00
0.000000E+00	0.000000E+00	0.000000E+00	2.219100E-01
6.548572E-01	1.022239	1.201824	1.000932
4.320722E-01	0.000000E+00	0.000000E+00	0.000000E+00
0.000000E+00	0.000000E+00	0.000000E+00	0.000000E+00
4.364704E-01	8.398041E-01	1.020769	9.724778E-01
6.004065E-01	1.728324E-01	0.000000E+00	0.000000E+00

0.000000E+00	0.000000E+00	0.000000E+00	0.000000E+00
1.840471E-01	4.889374E-01	6.785300E-01	6.855232E-01
5.374954E-01	2.689364E-01	0.000000E+00	0.000000E+00
0.000000E+00	0.000000E+00		
Array of net vel.u/stream is VNU =		0.000000E+00	0.000000E+00
0.000000E+00	3.040526E-01	1.013343	4.465335
3.756045	6.060950E-01	1.164295	1.011948
6.305137E-01	1.767663E-01	0.000000E+00	0.000000E+00
0.000000E+00	0.000000E+00	0.000000E+00	0.000000E+00
0.000000E+00	5.482081E-01	1.305416	1.397540
9.687708E-01	3.284387E-01	0.000000E+00	0.000000E+00
0.000000E+00	0.000000E+00	0.000000E+00	0.000000E+00
0.000000E+00	3.576954E-01	9.773326E-01	1.158900
8.439432E-01	3.046798E-01	8.440285E-02	8.440285E-02
0.000000E+00	0.000000E+00	0.000000E+00	0.000000E+00
0.000000E+00	0.000000E+00	8.989987E-01	1.735778
1.360332	5.802302E-01	5.667797E-02	0.000000E+00
0.000000E+00	0.000000E+00	0.000000E+00	0.000000E+00
0.000000E+00	7.256275E-02	4.921434E-01	8.644364E-01
7.736348E-01	4.170624E-01	3.377200E-01	2.494366E-01
0.000000E+00	0.000000E+00	0.000000E+00	0.000000E+00
0.000000E+00	0.000000E+00	4.397741E-01	1.204246
1.462239	1.105993	4.082253E-01	0.000000E+00
0.000000E+00	0.000000E+00	0.000000E+00	0.000000E+00
0.000000E+00	9.740036E-02	3.854097E-01	6.639886E-01
7.115093E-01	5.661931E-01	8.433767E-01	6.127136E-01
0.000000E+00	0.000000E+00	0.000000E+00	0.000000E+00
0.000000E+00	0.000000E+00	2.720422E-01	9.426787E-01
1.378913	1.195803	5.534586E-01	6.593168E-02
0.000000E+00	0.000000E+00	0.000000E+00	0.000000E+00
0.000000E+00	0.000000E+00	2.354826E-01	7.821849E-01
1.145392	1.093934	4.952443E-01	0.000000E+00
0.000000E+00	0.000000E+00	0.000000E+00	0.000000E+00
0.000000E+00	0.000000E+00	1.573415E-01	4.625324E-01
7.083430E-01	7.944161E-01		
Array of net vel.d/stream is VND=		1.768787	2.093080
5.737026E-01	2.494096E-01	0.000000E+00	0.000000E+00
1.389119	1.389119	0.000000E+00	0.000000E+00
0.000000E+00	1.057392E-01	2.771493E-01	7.375511E-01
1.150194	7.216505E-01	1.463516E-01	1.882096E-02
2.357342E-02	1.350706E-02	0.000000E+00	0.000000E+00
0.000000E+00	6.701689E-02	5.545313E-01	1.039592
1.179110	1.103185	5.454323E-01	1.408665E-01
1.554489E-01	8.386168E-02	0.000000E+00	0.000000E+00
0.000000E+00	6.182072E-02	6.182072E-02	8.238750E-01
1.852282	1.849148	1.001456	3.685541E-01
3.904587E-01	3.721497E-01	1.695306E-01	0.000000E+00
0.000000E+00	0.000000E+00	9.192413E-01	1.495321
1.285062	1.429951	1.284343	7.802349E-01
4.205445E-01	2.036836E-01	0.000000E+00	0.000000E+00
0.000000E+00	0.000000E+00	0.000000E+00	5.886179E-01
1.443047	1.786913	1.455813	6.676919E-01
2.867478E-01	2.729852E-01	1.305996E-01	0.000000E+00
0.000000E+00	0.000000E+00	7.870607E-01	1.040394
6.401206E-01	8.319149E-01	8.467897E-01	7.021532E-01
4.329619E-01	1.324704E-01	0.000000E+00	0.000000E+00
0.000000E+00	0.000000E+00	0.000000E+00	2.219100E-01

6.548572E-01	1.022239	1.201824	1.000932
4.320722E-01	8.384830E-02	4.017598E-02	0.000000E+00
0.000000E+00	0.000000E+00	0.000000E+00	9.538288E-02
4.364704E-01	8.398041E-01	1.020769	9.724778E-01
6.004065E-01	1.728324E-01	2.285116E-02	0.000000E+00
0.000000E+00	0.000000E+00	8.717733E-02	9.573575E-02
1.840471E-01	4.889374E-01	6.785300E-01	6.855232E-01
5.374954E-01	2.689364E-01	5.188284E-02	0.000000E+00
0.000000E+00	0.000000E+00		
Array of downflow velocity d/s face is VDD=			0.000000E+00
0.000000E+00			
0.000000E+00	0.000000E+00	4.883561E-01	2.143161
1.747301	0.000000E+00	5.753934E-01	0.000000E+00
3.131963E-01	0.000000E+00	0.000000E+00	0.000000E+00
0.000000E+00	0.000000E+00	0.000000E+00	0.000000E+00
0.000000E+00	2.720303E-01	0.000000E+00	0.000000E+00
4.819463E-01	0.000000E+00	0.000000E+00	0.000000E+00
0.000000E+00	0.000000E+00	0.000000E+00	0.000000E+00
0.000000E+00	1.780090E-01	0.000000E+00	5.784461E-01
0.000000E+00	1.528381E-01	0.000000E+00	0.000000E+00
0.000000E+00	0.000000E+00	0.000000E+00	0.000000E+00
0.000000E+00	0.000000E+00	4.514073E-01	8.727656E-01
6.873328E-01	2.936608E-01	0.000000E+00	0.000000E+00
0.000000E+00	0.000000E+00	0.000000E+00	0.000000E+00
0.000000E+00	0.000000E+00	2.496971E-01	4.380527E-01
3.927673E-01	0.000000E+00	1.720331E-01	0.000000E+00
0.000000E+00	0.000000E+00	0.000000E+00	0.000000E+00
0.000000E+00	0.000000E+00	0.000000E+00	0.000000E+00
0.000000E+00	0.000000E+00	2.079828E-01	0.000000E+00
0.000000E+00	0.000000E+00	0.000000E+00	0.000000E+00
0.000000E+00	0.000000E+00	1.967749E-01	3.384707E-01
3.618105E-01	0.000000E+00	0.000000E+00	3.127484E-01
0.000000E+00	0.000000E+00	0.000000E+00	0.000000E+00
0.000000E+00	0.000000E+00	0.000000E+00	0.000000E+00
7.051808E-01	6.121516E-01	2.841577E-01	0.000000E+00
0.000000E+00	0.000000E+00	0.000000E+00	0.000000E+00
0.000000E+00	0.000000E+00	0.000000E+00	4.028271E-01
5.902963E-01	5.652770E-01	2.563612E-01	0.000000E+00
0.000000E+00	0.000000E+00	0.000000E+00	0.000000E+00
0.000000E+00	0.000000E+00	0.000000E+00	2.403447E-01
0.000000E+00	0.000000E+00		
Array of tangential velocity d/s face is VTD=			0.000000E+00
0.000000E+00			
0.000000E+00	0.000000E+00	5.455736E-01	2.394595
1.952939	0.000000E+00	6.432749E-01	0.000000E+00
3.501790E-01	0.000000E+00	0.000000E+00	0.000000E+00
0.000000E+00	0.000000E+00	0.000000E+00	0.000000E+00
0.000000E+00	3.041544E-01	0.000000E+00	0.000000E+00
5.388595E-01	0.000000E+00	0.000000E+00	0.000000E+00
0.000000E+00	0.000000E+00	0.000000E+00	0.000000E+00
0.000000E+00	1.990423E-01	0.000000E+00	6.467944E-01
0.000000E+00	1.709096E-01	0.000000E+00	0.000000E+00
0.000000E+00	0.000000E+00	0.000000E+00	0.000000E+00
0.000000E+00	0.000000E+00	5.047814E-01	9.759995E-01
7.686927E-01	3.284369E-01	0.000000E+00	0.000000E+00
0.000000E+00	0.000000E+00	0.000000E+00	0.000000E+00
0.000000E+00	0.000000E+00	2.792670E-01	4.899282E-01

4.392876E-01	0.000000E+00	1.924112E-01	0.000000E+00
0.000000E+00	0.000000E+00	0.000000E+00	0.000000E+00
0.000000E+00	0.000000E+00	0.000000E+00	0.000000E+00
0.000000E+00	0.000000E+00	2.326194E-01	0.000000E+00
0.000000E+00	0.000000E+00	0.000000E+00	0.000000E+00
0.000000E+00	0.000000E+00	2.200838E-01	3.785641E-01
4.046705E-01	0.000000E+00	0.000000E+00	3.497987E-01
0.000000E+00	0.000000E+00	0.000000E+00	0.000000E+00
0.000000E+00	0.000000E+00	0.000000E+00	0.000000E+00
7.887228E-01	6.846862E-01	3.178305E-01	0.000000E+00
0.000000E+00	0.000000E+00	0.000000E+00	0.000000E+00
0.000000E+00	0.000000E+00	0.000000E+00	4.505623E-01
6.602473E-01	6.322613E-01	2.867367E-01	0.000000E+00
0.000000E+00	0.000000E+00	0.000000E+00	0.000000E+00
0.000000E+00	0.000000E+00	0.000000E+00	2.688224E-01
0.000000E+00	0.000000E+00		
Array of tangential velocity u/s face is VTU=			9.186042E-01
1.137457			
0.000000E+00	1.366479E-01	0.000000E+00	0.000000E+00
0.000000E+00	7.639000E-01	0.000000E+00	0.000000E+00
0.000000E+00	5.843119E-02	1.532467E-01	0.000000E+00
6.340753E-01	4.000084E-01	8.122654E-02	0.000000E+00
0.000000E+00	0.000000E+00	0.000000E+00	0.000000E+00
0.000000E+00	0.000000E+00	3.084973E-01	0.000000E+00
6.550856E-01	0.000000E+00	3.042101E-01	0.000000E+00
8.650629E-02	0.000000E+00	0.000000E+00	0.000000E+00
0.000000E+00	0.000000E+00	0.000000E+00	0.000000E+00
1.035166	1.040583	0.000000E+00	0.000000E+00
2.207788E-01	2.107788E-01	0.000000E+00	0.000000E+00
0.000000E+00	0.000000E+00	5.186455E-01	8.462036E-01
7.318770E-01	0.000000E+00	0.000000E+00	4.466966E-01
0.000000E+00	1.167525E-01	0.000000E+00	0.000000E+00
0.000000E+00	0.000000E+00	0.000000E+00	3.372626E-01
8.285201E-01	0.000000E+00	0.000000E+00	3.837442E-01
1.652770E-01	0.000000E+00	7.517156E-02	0.000000E+00
0.000000E+00	0.000000E+00	0.000000E+00	5.999172E-01
0.000000E+00	4.813910E-01	0.000000E+00	4.067342E-01
2.515884E-01	7.707604E-02	0.000000E+00	0.000000E+00
0.000000E+00	0.000000E+00	0.000000E+00	0.000000E+00
0.000000E+00	5.921164E-01	6.993448E-01	5.848954E-01
2.535039E-01	0.000000E+00	0.000000E+00	0.000000E+00
0.000000E+00	0.000000E+00	0.000000E+00	0.000000E+00
2.557515E-01	4.924743E-01	0.000000E+00	5.713733E-01
0.000000E+00	1.016876E-01	0.000000E+00	0.000000E+00
0.000000E+00	0.000000E+00	0.000000E+00	0.000000E+00
1.084559E-01	2.884173E-01	4.006331E-01	0.000000E+00
3.176401E-01	0.000000E+00	0.000000E+00	0.000000E+00
0.000000E+00	0.000000E+00		
The mean hurricane scour u/s face is MNTHSU			4.774221
The std.dev.in hurricane scour u/s face is STDHSU			2.017122E-01
The mean hurricane scour d/s face is MNTHSD			4.564212
The std.dev.in hurricane scour d/s face is STDHSD			1.856906E-01
B	FHU	PRHU	CPRHU
1.0000	.0000	.0000	.0000
1.5000	.0000	.0000	.0000
2.0000	.0000	.0000	.0000
2.5000	.0000	.0000	.0000

3.0000	.0000	.0000	.0000
3.5000	.0000	.0000	.0000
4.0000	.0000	.0000	.0000
4.5000	116.0000	.0580	.0580
5.0000	1621.0000	.8105	.8685
5.5000	259.0000	.1295	.9980
6.0000	2.0000	.0010	.9990
6.5000	1.0000	.0005	.9995
7.0000	.0000	.0000	.9995
7.5000	1.0000	.0005	1.0000
8.0000	.0000	.0000	1.0000
8.5000	.0000	.0000	1.0000
9.0000	.0000	.0000	1.0000
9.5000	.0000	.0000	1.0000
10.0000	.0000	.0000	1.0000
10.5000	.0000	.0000	1.0000
11.0000	.0000	.0000	1.0000
11.5000	.0000	.0000	1.0000
12.0000	.0000	.0000	1.0000
12.5000	.0000	.0000	1.0000
13.0000	.0000	.0000	1.0000
13.5000	.0000	.0000	1.0000
14.0000	.0000	.0000	1.0000
14.5000	.0000	.0000	1.0000
15.0000	.0000	.0000	1.0000
15.5000	.0000	.0000	1.0000
16.0000	.0000	.0000	1.0000
16.5000	.0000	.0000	1.0000
17.0000	.0000	.0000	1.0000
17.5000	.0000	.0000	1.0000
18.0000	.0000	.0000	1.0000
18.5000	.0000	.0000	1.0000
19.0000	.0000	.0000	1.0000
19.5000	.0000	.0000	1.0000
20.0000	.0000	.0000	1.0000
20.5000	.0000	.0000	1.0000
21.0000	.0000	.0000	1.0000
21.5000	.0000	.0000	1.0000
22.0000	.0000	.0000	1.0000
22.5000	.0000	.0000	1.0000
23.0000	.0000	.0000	1.0000
23.5000	.0000	.0000	1.0000
24.0000	.0000	.0000	1.0000
24.5000	.0000	.0000	1.0000
25.0000	.0000	.0000	1.0000
25.5000	.0000	.0000	1.0000
26.0000	.0000	.0000	1.0000
26.5000	.0000	.0000	1.0000
27.0000	.0000	.0000	1.0000
27.5000	.0000	.0000	1.0000
28.0000	.0000	.0000	1.0000
28.5000	.0000	.0000	1.0000
29.0000	.0000	.0000	1.0000
29.5000	.0000	.0000	1.0000
30.0000	.0000	.0000	1.0000
30.5000	.0000	.0000	1.0000
31.0000	.0000	.0000	1.0000



31.5000	.0000	.0000	1.0000
32.0000	.0000	.0000	1.0000
32.5000	.0000	.0000	1.0000
33.0000	.0000	.0000	1.0000
33.5000	.0000	.0000	1.0000
34.0000	.0000	.0000	1.0000
34.5000	.0000	.0000	1.0000
35.0000	.0000	.0000	1.0000
35.5000	.0000	.0000	1.0000
36.0000	.0000	.0000	1.0000
36.5000	.0000	.0000	1.0000
37.0000	.0000	.0000	1.0000
37.5000	.0000	.0000	1.0000
38.0000	.0000	.0000	1.0000
38.5000	.0000	.0000	1.0000
39.0000	.0000	.0000	1.0000
39.5000	.0000	.0000	1.0000
40.0000	.0000	.0000	1.0000
40.5000	.0000	.0000	1.0000
41.0000	.0000	.0000	1.0000
41.5000	.0000	.0000	1.0000
42.0000	.0000	.0000	1.0000
42.5000	.0000	.0000	1.0000
43.0000	.0000	.0000	1.0000
43.5000	.0000	.0000	1.0000
44.0000	.0000	.0000	1.0000
44.5000	.0000	.0000	1.0000
45.0000	.0000	.0000	1.0000
45.5000	.0000	.0000	1.0000
46.0000	.0000	.0000	1.0000
46.5000	.0000	.0000	1.0000
47.0000	.0000	.0000	1.0000
47.5000	.0000	.0000	1.0000
48.0000	.0000	.0000	1.0000
48.5000	.0000	.0000	1.0000
49.0000	.0000	.0000	1.0000
49.5000	.0000	.0000	1.0000
50.0000	.0000	.0000	1.0000
50.5000	.0000	.0000	1.0000
B	FHD	PRHD	CPRHD
1.0000	.0000	.0000	.0000
1.5000	.0000	.0000	.0000
2.0000	.0000	.0000	.0000
2.5000	.0000	.0000	.0000
3.0000	.0000	.0000	.0000
3.5000	.0000	.0000	.0000
4.0000	.0000	.0000	.0000
4.5000	827.0000	.4135	.4135
5.0000	1130.0000	.5650	.9785
5.5000	41.0000	.0205	.9990
6.0000	1.0000	.0005	.9995
6.5000	1.0000	.0005	1.0000
7.0000	.0000	.0000	1.0000
7.5000	.0000	.0000	1.0000
8.0000	.0000	.0000	1.0000
8.5000	.0000	.0000	1.0000
9.0000	.0000	.0000	1.0000

9.5000	.0000	.0000	1.0000
10.0000	.0000	.0000	1.0000
10.5000	.0000	.0000	1.0000
11.0000	.0000	.0000	1.0000
11.5000	.0000	.0000	1.0000
12.0000	.0000	.0000	1.0000
12.5000	.0000	.0000	1.0000
13.0000	.0000	.0000	1.0000
13.5000	.0000	.0000	1.0000
14.0000	.0000	.0000	1.0000
14.5000	.0000	.0000	1.0000
15.0000	.0000	.0000	1.0000
15.5000	.0000	.0000	1.0000
16.0000	.0000	.0000	1.0000
16.5000	.0000	.0000	1.0000
17.0000	.0000	.0000	1.0000
17.5000	.0000	.0000	1.0000
18.0000	.0000	.0000	1.0000
18.5000	.0000	.0000	1.0000
19.0000	.0000	.0000	1.0000
19.5000	.0000	.0000	1.0000
20.0000	.0000	.0000	1.0000
20.5000	.0000	.0000	1.0000
21.0000	.0000	.0000	1.0000
21.5000	.0000	.0000	1.0000
22.0000	.0000	.0000	1.0000
22.5000	.0000	.0000	1.0000
23.0000	.0000	.0000	1.0000
23.5000	.0000	.0000	1.0000
24.0000	.0000	.0000	1.0000
24.5000	.0000	.0000	1.0000
25.0000	.0000	.0000	1.0000
25.5000	.0000	.0000	1.0000
26.0000	.0000	.0000	1.0000
26.5000	.0000	.0000	1.0000
27.0000	.0000	.0000	1.0000
27.5000	.0000	.0000	1.0000
28.0000	.0000	.0000	1.0000
28.5000	.0000	.0000	1.0000
29.0000	.0000	.0000	1.0000
29.5000	.0000	.0000	1.0000
30.0000	.0000	.0000	1.0000
30.5000	.0000	.0000	1.0000
31.0000	.0000	.0000	1.0000
31.5000	.0000	.0000	1.0000
32.0000	.0000	.0000	1.0000
32.5000	.0000	.0000	1.0000
33.0000	.0000	.0000	1.0000
33.5000	.0000	.0000	1.0000
34.0000	.0000	.0000	1.0000
34.5000	.0000	.0000	1.0000
35.0000	.0000	.0000	1.0000
35.5000	.0000	.0000	1.0000
36.0000	.0000	.0000	1.0000
36.5000	.0000	.0000	1.0000
37.0000	.0000	.0000	1.0000
37.5000	.0000	.0000	1.0000

38.0000	.0000	.0000	1.0000
38.5000	.0000	.0000	1.0000
39.0000	.0000	.0000	1.0000
39.5000	.0000	.0000	1.0000
40.0000	.0000	.0000	1.0000
40.5000	.0000	.0000	1.0000
41.0000	.0000	.0000	1.0000
41.5000	.0000	.0000	1.0000
42.0000	.0000	.0000	1.0000
42.5000	.0000	.0000	1.0000
43.0000	.0000	.0000	1.0000
43.5000	.0000	.0000	1.0000
44.0000	.0000	.0000	1.0000
44.5000	.0000	.0000	1.0000
45.0000	.0000	.0000	1.0000
45.5000	.0000	.0000	1.0000
46.0000	.0000	.0000	1.0000
46.5000	.0000	.0000	1.0000
47.0000	.0000	.0000	1.0000
47.5000	.0000	.0000	1.0000
48.0000	.0000	.0000	1.0000
48.5000	.0000	.0000	1.0000
49.0000	.0000	.0000	1.0000
49.5000	.0000	.0000	1.0000
50.0000	.0000	.0000	1.0000
50.5000	.0000	.0000	1.0000

## Appendix D-11

RUN TITLE IS: PATAPSCO RIVER CONTINUOUS SIMULATIONS  
RUN DATE IS;  
THE PROGRAM WAS EXECUTED IN PIER DESIGN MODE.  
CONTRACTION SCOUR METHOD IS KOMURAS EQN  
SCOUR COMPUTED WITHOUT ARMOURING  
BRUBAKER-DEMETRIUS NEILLS MODIFICATION FACTOR ACTIVATED  
TIDE DISTORTION OPTION ACTIVATED  
MEAN TIDAL DEPTH MDR is = 33.935000  
MEAN LOW TIDAL DEPTH MLT is = 33.000000  
MEAN LOW TIDE ELEVATION MLTE is = -9.350000E-01  
TIDAL AMP. AT BRIDGE XSEC MTR is = 9.350000E-01  
CHANNEL INVERT AT BRIDGE IRS is = -33.935000

Estuary in bank area is = 34107.750000

Maximum tide in the simulation HITIDE is = 37.514030  
Maximum u/s flow depth in sim. YTRMXS is = 42.750000  
Maximum d/s flow depth in sim. YTFMXS is = 42.250000  
Maximum u/s disch. in sim. QTRMXS is = 100489.100000  
Maximum d/s disch. in sim. QTFMXS is = 247351.500000  
Maximum u/s vel.in sim. VUPMS is = 1.454013  
Maximum d/s vel.in sim. VDOWNMS is = 4.253708  
Maximum u/s face tang.vel.in sim. VTUMXSis = 5.887701  
Maximum d/s face tang.vel.in sim. VTDMXSis = 5.224584E-01

Maximum u/s flow depth last run YTRMAX is = 39.250000  
Maximum d/s flow depth last run YTFMAX is = 38.750000  
Maximum u/s discharge last run QTRMAX is = 82579.710000  
Maximum d/s discharge last run QTFMAX is = 129931.500000  
Maximum u/s velocity last run VNUMAX is = 1.194882  
Maximum d/s velocity last run VNDMAX is = 2.580252  
Maximum tangential vel d/s face last run VTDMX is = 4.296002E-01  
Maximum tangential vel u/s face last run VTUMX is = 4.026459  
critical vel u/s face last run UIUMIN is = 6.255078E-01  
critical vel d/s face last run UIDMIN is = 6.255078E-01

Time of concentration = 27.600000hrs  
Time to peak = 18.492000hrs  
Number of unit hydrograph ordinates = 92  
Soil infiltration potential = 4.285714  
Peak discharge of the UHG = 15651.740000cfs  
Initial abstractions IA = 8.571429E-01in

Catchment base flow = 343.082300cfs  
Tide attenuation factor TAF = 6.631206E-01  
Tidal lag MTL= 2.444557hrs  
Tidal routing constant CX = 4.090720E-01  
Bridge station tidal range TR = 1.870000ft  
Effective bottom channel width at brdg.WBE = 1697.400000ft  
Estuary Area 9.924710E+07

Contraction scour factor u/s face= 9.547300E-01  
 Contraction scour factor d/s face= 1.176995  
 Estuary to wavelength ratio DIM = 9.623493E-03  
 Estuary width factor WF = 2.393939  
 Tidal range factor HF = 5.510535E-02  
 Neill Mod. factor rising limb.NMRF = 8.000000E-01  
 Neill Mod. factor falling limb.NMFF = 8.000000E-01

The maximum storm event in the simulation is 17.540860ins  
 ANNUAL MAX UPSTREAM VELOCITY LAST RUN = 1.042961 1.015477

9.462508E-01	9.464179E-01	8.246149E-01	8.852946E-01
9.748330E-01	1.068496	9.554860E-01	8.905261E-01
9.229528E-01	1.015435	1.040308	9.520143E-01
1.009560	1.025659	9.633124E-01	1.007240
1.009279	1.050810	9.462192E-01	8.287537E-01
9.827309E-01	1.026613	9.436362E-01	9.876090E-01
8.879385E-01	8.798143E-01	9.592052E-01	9.489326E-01
9.581022E-01	9.529543E-01	9.379629E-01	9.495699E-01
1.011150	9.510589E-01	8.877410E-01	9.160058E-01
9.031009E-01	9.251480E-01	9.028993E-01	1.059280
8.883025E-01	8.906776E-01	1.139979	9.430666E-01
1.017978	8.565441E-01	1.111339	9.509873E-01
9.395388E-01	9.953431E-01	9.576279E-01	8.312370E-01
1.001465	1.016914	9.104413E-01	1.194882
9.322065E-01	8.782240E-01	1.059895	9.037853E-01
1.021940	1.007887	9.544667E-01	9.044439E-01
9.441676E-01	1.174592	9.803725E-01	9.750562E-01
9.532123E-01	9.598794E-01	8.738623E-01	9.369457E-01
1.018518	9.508025E-01	8.865155E-01	9.753418E-01
9.559017E-01	1.111661	9.826078E-01	1.020182
8.949619E-01	1.006080	9.069943E-01	9.927385E-01
1.079597	9.135489E-01	1.016304	9.497236E-01
8.771642E-01	9.281113E-01	9.031460E-01	9.534972E-01
9.713302E-01	8.803160E-01	8.991486E-01	1.009521
8.872234E-01	1.153860		

ANNUAL MAX DWNSTREAM VELOCITY LAST RUN = 1.238974  
 1.371984

1.965574	1.777336	2.580252	1.783640
1.114192	1.212872	1.108562	1.181335
1.820592	1.289675	1.292715	2.502550
1.007562	1.247173	1.022056	2.100950
1.742546	2.004594	1.820264	1.402171
1.428923	7.909279E-01	1.485274	1.551212
8.543501E-01	1.065620	1.529689	1.113761
8.070495E-01	1.869717	1.359676	1.651781
1.728025	2.054943	1.292238	9.769673E-01
9.021355E-01	1.238472	1.542575	9.711797E-01
1.386620	1.782023	1.622180	1.253182
1.112272	1.906992	8.172714E-01	1.726371
1.322417	9.102172E-01	1.363127	2.219834
1.906485	1.259358	2.070082	1.675835
1.903465	1.203892	1.124138	1.184530
1.135547	1.321566	1.716703	1.326909
2.263973	1.349324	2.073964	1.303249
1.092813	9.069383E-01	1.881641	1.657262
1.156878	1.526664	1.341791	1.098983

1.188592	1.195654	1.773570	1.419667
9.900039E-01	9.459242E-01	1.565590	1.976120
1.026446	1.456572	1.041493	2.415179
1.619750	1.170977	1.778872	1.691023
8.795996E-01	1.313238	1.112654	2.555676
1.306080	1.171398		
ANNUAL MAX US ADJUSTED VELOCITY LAST RUN =			1.042961
1.015477			
9.462508E-01	9.464179E-01	8.246149E-01	8.852946E-01
9.748330E-01	1.068496	9.554860E-01	8.905261E-01
9.229528E-01	1.015435	1.040308	9.520143E-01
1.009560	1.025659	9.633124E-01	1.007240
1.009279	1.050810	9.462192E-01	8.287537E-01
9.827309E-01	1.026613	9.436362E-01	9.876090E-01
8.879385E-01	8.798143E-01	9.592052E-01	9.489326E-01
9.581022E-01	9.529543E-01	9.379629E-01	9.495699E-01
1.011150	9.510589E-01	8.877410E-01	9.160058E-01
9.031009E-01	9.251480E-01	9.028993E-01	1.059280
8.883025E-01	8.906776E-01	1.139979	9.430666E-01
1.017978	8.565441E-01	1.111339	9.509873E-01
9.395388E-01	9.953431E-01	9.576279E-01	8.312370E-01
1.001465	1.016914	9.104413E-01	1.194882
9.322065E-01	8.782240E-01	1.059895	9.037853E-01
1.021940	1.007887	9.544667E-01	9.044439E-01
9.441676E-01	1.174592	9.803725E-01	9.750562E-01
9.532123E-01	9.598794E-01	8.738623E-01	9.369457E-01
1.018518	9.508025E-01	8.865155E-01	9.753418E-01
9.559017E-01	1.111661	9.826078E-01	1.020182
8.949619E-01	1.006080	9.069943E-01	9.927385E-01
1.079597	9.135489E-01	1.016304	9.497236E-01
8.771642E-01	9.281113E-01	9.031460E-01	9.534972E-01
9.713302E-01	8.803160E-01	8.991486E-01	1.009521
8.872234E-01	1.153860		
ANNUAL MAX DS ADJUSTED VELOCITY LAST RUN =			1.238974
1.371984			
1.965574	1.777336	2.580252	1.783640
1.114192	1.212872	1.108562	1.181335
1.820592	1.289675	1.292715	2.502550
1.007562	1.247173	1.022056	2.100950
1.742546	2.004594	1.820264	1.402171
1.428923	7.909279E-01	1.485274	1.551212
8.543501E-01	1.065620	1.529689	1.113761
8.070495E-01	1.869717	1.359676	1.651781
1.728025	2.054943	1.292238	9.769673E-01
9.021355E-01	1.238472	1.542575	9.711797E-01
1.386620	1.782023	1.622180	1.253182
1.112272	1.906992	8.172714E-01	1.726371
1.322417	9.102172E-01	1.363127	2.219834
1.906485	1.259358	2.070082	1.675835
1.903465	1.203892	1.124138	1.184530
1.135547	1.321566	1.716703	1.326909
2.263973	1.349324	2.073964	1.303249
1.092813	9.069383E-01	1.881641	1.657262
1.156878	1.526664	1.341791	1.098983
1.188592	1.195654	1.773570	1.419667
9.900039E-01	9.459242E-01	1.565590	1.976120
1.026446	1.456572	1.041493	2.415179

1.619750	1.170977	1.778872	1.691023
8.795996E-01	1.313238	1.112654	2.555676
1.306080	1.171398		
ANNUAL MAX UPSTREAM DISCHARGE LAST RUN = 72080.800000			
62550.910000			
63603.070000	65408.390000	55927.660000	60000.680000
62844.090000	73845.560000	66035.050000	53809.260000
65556.720000	70223.560000	70555.800000	58270.650000
69768.910000	63019.640000	67290.240000	69609.480000
65633.950000	74646.430000	66281.270000	57018.670000
67918.110000	71915.050000	66097.610000	60897.140000
61560.700000	60805.460000	67194.590000	65143.040000
62704.110000	65860.160000	54381.200000	65625.590000
70834.200000	55900.210000	61086.660000	60288.740000
61555.870000	60131.480000	59086.070000	64734.820000
61391.410000	62776.910000	78784.160000	65173.640000
70351.110000	59197.120000	54254.070000	65722.730000
58924.350000	58924.350000	64981.250000	57250.790000
62601.050000	65396.360000	64577.840000	82579.710000
66211.520000	60692.830000	62296.490000	61728.300000
72582.650000	59910.890000	63646.740000	56931.600000
61361.100000	58255.770000	54943.960000	58543.830000
65874.910000	62545.860000	58853.770000	59407.390000
70390.640000	60335.770000	59600.630000	67407.470000
65207.320000	76828.780000	67909.360000	67910.220000
61471.250000	69531.660000	60211.140000	68608.550000
75625.810000	63136.890000	65012.360000	62587.760000
58705.700000	63496.390000	61574.880000	65889.610000
59811.620000	56819.950000	58471.730000	71702.450000
60449.980000	60244.410000		
ANNUAL MAX DWNSTREAM DISCHARGE LAST RUN = 69359.780000			
70384.750000			
85428.480000	72355.230000	128380.300000	81406.340000
67928.010000	62545.160000	72016.200000	74108.050000
81994.550000	65098.840000	92550.460000	128609.000000
67476.610000	66371.840000	74996.100000	90670.270000
76761.450000	89339.340000	78906.750000	73337.240000
73155.010000	62889.940000	68943.090000	86301.360000
63984.850000	64959.950000	80379.270000	61317.500000
60824.140000	92691.780000	77742.890000	82489.300000
88007.500000	98426.950000	80751.460000	71797.900000
66950.420000	62003.840000	80053.030000	62381.270000
67999.840000	100210.500000	73925.590000	73703.030000
66898.870000	88358.390000	66186.140000	74933.470000
71600.720000	79067.510000	63090.090000	109376.500000
89750.790000	74718.730000	114865.600000	81788.640000
80371.810000	62889.770000	63858.810000	64572.220000
68698.480000	70631.630000	89248.010000	69728.960000
102987.100000	68370.690000	106630.100000	74198.620000
67487.520000	70064.450000	90776.750000	67853.300000
66336.020000	70505.390000	60361.820000	69530.800000
65925.120000	75637.910000	79168.710000	72955.430000
66246.590000	73700.840000	85769.910000	92997.700000
73752.400000	76660.290000	62931.380000	129931.500000
75174.190000	69996.440000	87583.160000	74075.980000
74564.890000	75550.390000	67803.700000	119192.300000
63080.890000	67732.130000		

ANNUAL MAX UPSTREAM FLOW DEPTH LAST RUN = 37.000000  
 36.750000

37.750000	37.072270	38.500000	37.000000
36.750000	36.521670	37.000000	36.848270
37.250000	36.577110	36.750000	38.750000
36.442030	36.750000	36.750000	37.750000
37.750000	37.005220	37.250000	36.886850
36.531910	36.750000	37.000000	36.750000
36.478960	37.000000	37.000000	37.000000
36.750000	37.136490	37.250000	36.579070
36.750000	37.500000	36.750000	36.648090
36.248020	36.770110	37.250000	37.007350
36.581620	37.250000	36.750000	37.000000
36.500000	36.750000	36.678760	36.608150
36.417620	36.420900	36.500000	38.250000
37.750000	36.750000	37.250000	37.250000
37.000000	36.509580	36.767600	36.750000
36.696990	37.000000	36.742070	36.500000
37.500000	36.295560	38.000000	36.750000
36.718870	37.025590	37.750000	37.250000
36.929230	37.176140	36.978160	36.507170
37.000000	36.770600	36.750000	37.500000
36.596460	36.552930	37.000000	37.500000
36.500000	37.000000	36.860860	37.250000
36.873590	36.750000	37.750000	37.750000
36.990760	36.737800	36.527760	38.500000
36.397140	36.429580		

ANNUAL MAX DWTREEM FLOW DEPTH LAST RUN = 37.750000  
 37.750000

38.500000	38.750000	39.250000	38.500000
37.000000	37.000000	37.000000	37.000000
38.250000	37.250000	37.250000	39.250000
37.000000	36.750000	37.000000	39.000000
37.750000	39.250000	37.750000	37.000000
37.750000	37.000000	38.000000	37.250000
36.750000	37.000000	37.750000	37.500000
37.000000	38.000000	38.000000	37.750000
38.000000	38.250000	38.250000	37.250000
36.750000	37.000000	37.500000	37.250000
37.000000	37.500000	38.250000	37.500000
36.750000	38.500000	37.250000	38.250000
37.000000	37.000000	37.000000	38.750000
38.250000	37.250000	38.750000	37.750000
37.500000	36.750000	37.750000	37.750000
37.035150	37.500000	38.250000	37.000000
38.500000	37.000000	39.250000	38.250000
37.000000	37.116000	37.750000	37.500000
36.966450	37.250000	37.250000	37.250000
37.000000	37.000000	37.250000	38.250000
37.000000	37.137940	37.250000	39.000000
36.820180	37.514030	37.500000	38.750000
37.250000	37.000000	37.750000	38.250000
37.250000	37.500000	36.750000	39.000000
37.250000	36.805500		

ANNUAL MAX US ADJ. FLOW DEPTH LAST RUN = 37.000000  
 36.750000

37.750000	37.072270	38.500000	37.000000
-----------	-----------	-----------	-----------



36.750000	36.521670	37.000000	36.848270
37.250000	36.577110	36.750000	38.750000
36.442030	36.750000	36.750000	37.750000
37.750000	37.005220	37.250000	36.886850
36.531910	36.750000	37.000000	36.750000
36.478960	37.000000	37.000000	37.000000
36.750000	37.136490	37.250000	36.579070
36.750000	37.500000	36.750000	36.648090
36.248020	36.770110	37.250000	37.007350
36.581620	37.250000	36.750000	37.000000
36.500000	36.750000	36.678760	36.608150
36.417620	36.420900	36.500000	38.250000
37.750000	36.750000	37.250000	37.250000
37.000000	36.509580	36.767600	36.750000
36.696990	37.000000	36.742070	36.500000
37.500000	36.295560	38.000000	36.750000
36.718870	37.025590	37.750000	37.250000
36.929230	37.176140	36.978160	36.507170
37.000000	36.770600	36.750000	37.500000
36.596460	36.552930	37.000000	37.500000
36.500000	37.000000	36.860860	37.250000
36.873590	36.750000	37.750000	37.750000
36.990760	36.737800	36.527760	38.500000
36.397140	36.429580		

ANNUAL MAX DS ADJ. FLOW DEPTH LAST RUN = 37.750000  
37.750000

38.500000	38.750000	39.250000	38.500000
37.000000	37.000000	37.000000	37.000000
38.250000	37.250000	37.250000	39.250000
37.000000	36.750000	37.000000	39.000000
37.750000	39.250000	37.750000	37.000000
37.750000	37.000000	38.000000	37.250000
36.750000	37.000000	37.750000	37.500000
37.000000	38.000000	38.000000	37.750000
38.000000	38.250000	38.250000	37.250000
36.750000	37.000000	37.500000	37.250000
37.000000	37.500000	38.250000	37.500000
36.750000	38.500000	37.250000	38.250000
37.000000	37.000000	37.000000	38.750000
38.250000	37.250000	38.750000	37.750000
37.500000	36.750000	37.750000	37.750000
37.035150	37.500000	38.250000	37.000000
38.500000	37.000000	39.250000	38.250000
37.000000	37.116000	37.750000	37.500000
36.966450	37.250000	37.250000	37.250000
37.000000	37.000000	37.250000	38.250000
37.000000	37.137940	37.250000	39.000000
36.820180	37.514030	37.500000	38.750000
37.250000	37.000000	37.750000	38.250000
37.250000	37.500000	36.750000	39.000000
37.250000	36.805500		

The no.of storms in the last.NS= 79  
The no.of storms producing no runoff over the simula tion.NORUN= 6913951

The number of 6 hr storms in YRS is = 61



[illegible]

[illegible]

20.0000	.0000	.0000	1.0000
20.5000	.0000	.0000	1.0000
21.0000	.0000	.0000	1.0000
21.5000	.0000	.0000	1.0000
22.0000	.0000	.0000	1.0000
22.5000	.0000	.0000	1.0000
23.0000	.0000	.0000	1.0000
23.5000	.0000	.0000	1.0000
24.0000	.0000	.0000	1.0000
24.5000	.0000	.0000	1.0000
25.0000	.0000	.0000	1.0000
25.5000	.0000	.0000	1.0000
26.0000	.0000	.0000	1.0000
26.5000	.0000	.0000	1.0000
27.0000	.0000	.0000	1.0000
27.5000	.0000	.0000	1.0000
28.0000	.0000	.0000	1.0000
28.5000	.0000	.0000	1.0000
29.0000	.0000	.0000	1.0000
29.5000	.0000	.0000	1.0000
30.0000	.0000	.0000	1.0000
30.5000	.0000	.0000	1.0000
31.0000	.0000	.0000	1.0000
31.5000	.0000	.0000	1.0000
32.0000	.0000	.0000	1.0000
32.5000	.0000	.0000	1.0000
33.0000	.0000	.0000	1.0000
33.5000	.0000	.0000	1.0000
34.0000	.0000	.0000	1.0000
34.5000	.0000	.0000	1.0000
35.0000	.0000	.0000	1.0000
35.5000	.0000	.0000	1.0000
36.0000	.0000	.0000	1.0000
36.5000	.0000	.0000	1.0000
37.0000	.0000	.0000	1.0000
37.5000	.0000	.0000	1.0000
38.0000	.0000	.0000	1.0000
38.5000	.0000	.0000	1.0000
39.0000	.0000	.0000	1.0000
39.5000	.0000	.0000	1.0000
40.0000	.0000	.0000	1.0000
40.5000	.0000	.0000	1.0000
41.0000	.0000	.0000	1.0000
41.5000	.0000	.0000	1.0000
42.0000	.0000	.0000	1.0000
42.5000	.0000	.0000	1.0000
43.0000	.0000	.0000	1.0000
43.5000	.0000	.0000	1.0000
44.0000	.0000	.0000	1.0000
44.5000	.0000	.0000	1.0000
45.0000	.0000	.0000	1.0000
45.5000	.0000	.0000	1.0000
46.0000	.0000	.0000	1.0000
46.5000	.0000	.0000	1.0000
47.0000	.0000	.0000	1.0000
47.5000	.0000	.0000	1.0000
48.0000	.0000	.0000	1.0000

48.5000	.0000	.0000	1.0000
49.0000	.0000	.0000	1.0000
49.5000	.0000	.0000	1.0000
50.0000	.0000	.0000	1.0000
50.5000	.0000	.0000	1.0000
B	FU	PRU	CPRU
1.0000	.0000	.0000	.0000
1.5000	1.0000	.0010	.0010
2.0000	.0000	.0000	.0010
2.5000	1.0000	.0010	.0020
3.0000	4.0000	.0040	.0060
3.5000	2.0000	.0020	.0080
4.0000	2.0000	.0020	.0100
4.5000	3.0000	.0030	.0130
5.0000	.0000	.0000	.0130
5.5000	1.0000	.0010	.0140
6.0000	.0000	.0000	.0140
6.5000	.0000	.0000	.0140
7.0000	.0000	.0000	.0140
7.5000	1.0000	.0010	.0150
8.0000	.0000	.0000	.0150
8.5000	1.0000	.0010	.0160
9.0000	.0000	.0000	.0160
9.5000	.0000	.0000	.0160
10.0000	.0000	.0000	.0160
10.5000	.0000	.0000	.0160
11.0000	1.0000	.0010	.0170
11.5000	.0000	.0000	.0170
12.0000	4.0000	.0040	.0210
12.5000	.0000	.0000	.0210
13.0000	1.0000	.0010	.0220
13.5000	5.0000	.0050	.0270
14.0000	2.0000	.0020	.0290
14.5000	.0000	.0000	.0290
15.0000	2.0000	.0020	.0310
15.5000	.0000	.0000	.0310
16.0000	2.0000	.0020	.0330
16.5000	.0000	.0000	.0330
17.0000	4.0000	.0040	.0370
17.5000	2.0000	.0020	.0390
18.0000	3.0000	.0030	.0420
18.5000	4.0000	.0040	.0460
19.0000	2.0000	.0020	.0480
19.5000	6.0000	.0060	.0540
20.0000	15.0000	.0150	.0690
20.5000	35.0000	.0350	.1040
21.0000	207.0000	.2070	.3110
21.5000	491.0000	.4910	.8020
22.0000	192.0000	.1920	.9940
22.5000	6.0000	.0060	1.0000
23.0000	.0000	.0000	1.0000
23.5000	.0000	.0000	1.0000
24.0000	.0000	.0000	1.0000
24.5000	.0000	.0000	1.0000
25.0000	.0000	.0000	1.0000
25.5000	.0000	.0000	1.0000
26.0000	.0000	.0000	1.0000

26.5000	.0000	.0000	1.0000
27.0000	.0000	.0000	1.0000
27.5000	.0000	.0000	1.0000
28.0000	.0000	.0000	1.0000
28.5000	.0000	.0000	1.0000
29.0000	.0000	.0000	1.0000
29.5000	.0000	.0000	1.0000
30.0000	.0000	.0000	1.0000
30.5000	.0000	.0000	1.0000
31.0000	.0000	.0000	1.0000
31.5000	.0000	.0000	1.0000
32.0000	.0000	.0000	1.0000
32.5000	.0000	.0000	1.0000
33.0000	.0000	.0000	1.0000
33.5000	.0000	.0000	1.0000
34.0000	.0000	.0000	1.0000
34.5000	.0000	.0000	1.0000
35.0000	.0000	.0000	1.0000
35.5000	.0000	.0000	1.0000
36.0000	.0000	.0000	1.0000
36.5000	.0000	.0000	1.0000
37.0000	.0000	.0000	1.0000
37.5000	.0000	.0000	1.0000
38.0000	.0000	.0000	1.0000
38.5000	.0000	.0000	1.0000
39.0000	.0000	.0000	1.0000
39.5000	.0000	.0000	1.0000
40.0000	.0000	.0000	1.0000
40.5000	.0000	.0000	1.0000
41.0000	.0000	.0000	1.0000
41.5000	.0000	.0000	1.0000
42.0000	.0000	.0000	1.0000
42.5000	.0000	.0000	1.0000
43.0000	.0000	.0000	1.0000
43.5000	.0000	.0000	1.0000
44.0000	.0000	.0000	1.0000
44.5000	.0000	.0000	1.0000
45.0000	.0000	.0000	1.0000
45.5000	.0000	.0000	1.0000
46.0000	.0000	.0000	1.0000
46.5000	.0000	.0000	1.0000
47.0000	.0000	.0000	1.0000
47.5000	.0000	.0000	1.0000
48.0000	.0000	.0000	1.0000
48.5000	.0000	.0000	1.0000
49.0000	.0000	.0000	1.0000
49.5000	.0000	.0000	1.0000
50.0000	.0000	.0000	1.0000
50.5000	.0000	.0000	1.0000

15 PERCENT TMS SCOUR RESULTS

B	FD15	PRD15	CPRD15
1.0000	1000.0000	1.0000	1.0000
1.5000	.0000	.0000	1.0000
2.0000	.0000	.0000	1.0000
2.5000	.0000	.0000	1.0000
3.0000	.0000	.0000	1.0000
3.5000	.0000	.0000	1.0000

4.0000	.0000	.0000	1.0000
4.5000	.0000	.0000	1.0000
5.0000	.0000	.0000	1.0000
5.5000	.0000	.0000	1.0000
6.0000	.0000	.0000	1.0000
6.5000	.0000	.0000	1.0000
7.0000	.0000	.0000	1.0000
7.5000	.0000	.0000	1.0000
8.0000	.0000	.0000	1.0000
8.5000	.0000	.0000	1.0000
9.0000	.0000	.0000	1.0000
9.5000	.0000	.0000	1.0000
10.0000	.0000	.0000	1.0000
10.5000	.0000	.0000	1.0000
11.0000	.0000	.0000	1.0000
11.5000	.0000	.0000	1.0000
12.0000	.0000	.0000	1.0000
12.5000	.0000	.0000	1.0000
13.0000	.0000	.0000	1.0000
13.5000	.0000	.0000	1.0000
14.0000	.0000	.0000	1.0000
14.5000	.0000	.0000	1.0000
15.0000	.0000	.0000	1.0000
15.5000	.0000	.0000	1.0000
16.0000	.0000	.0000	1.0000
16.5000	.0000	.0000	1.0000
17.0000	.0000	.0000	1.0000
17.5000	.0000	.0000	1.0000
18.0000	.0000	.0000	1.0000
18.5000	.0000	.0000	1.0000
19.0000	.0000	.0000	1.0000
19.5000	.0000	.0000	1.0000
20.0000	.0000	.0000	1.0000
20.5000	.0000	.0000	1.0000
21.0000	.0000	.0000	1.0000
21.5000	.0000	.0000	1.0000
22.0000	.0000	.0000	1.0000
22.5000	.0000	.0000	1.0000
23.0000	.0000	.0000	1.0000
23.5000	.0000	.0000	1.0000
24.0000	.0000	.0000	1.0000
24.5000	.0000	.0000	1.0000
25.0000	.0000	.0000	1.0000
25.5000	.0000	.0000	1.0000
26.0000	.0000	.0000	1.0000
26.5000	.0000	.0000	1.0000
27.0000	.0000	.0000	1.0000
27.5000	.0000	.0000	1.0000
28.0000	.0000	.0000	1.0000
28.5000	.0000	.0000	1.0000
29.0000	.0000	.0000	1.0000
29.5000	.0000	.0000	1.0000
30.0000	.0000	.0000	1.0000
30.5000	.0000	.0000	1.0000
31.0000	.0000	.0000	1.0000
31.5000	.0000	.0000	1.0000
32.0000	.0000	.0000	1.0000



32.5000	.0000	.0000	1.0000
33.0000	.0000	.0000	1.0000
33.5000	.0000	.0000	1.0000
34.0000	.0000	.0000	1.0000
34.5000	.0000	.0000	1.0000
35.0000	.0000	.0000	1.0000
35.5000	.0000	.0000	1.0000
36.0000	.0000	.0000	1.0000
36.5000	.0000	.0000	1.0000
37.0000	.0000	.0000	1.0000
37.5000	.0000	.0000	1.0000
38.0000	.0000	.0000	1.0000
38.5000	.0000	.0000	1.0000
39.0000	.0000	.0000	1.0000
39.5000	.0000	.0000	1.0000
40.0000	.0000	.0000	1.0000
40.5000	.0000	.0000	1.0000
41.0000	.0000	.0000	1.0000
41.5000	.0000	.0000	1.0000
42.0000	.0000	.0000	1.0000
42.5000	.0000	.0000	1.0000
43.0000	.0000	.0000	1.0000
43.5000	.0000	.0000	1.0000
44.0000	.0000	.0000	1.0000
44.5000	.0000	.0000	1.0000
45.0000	.0000	.0000	1.0000
45.5000	.0000	.0000	1.0000
46.0000	.0000	.0000	1.0000
46.5000	.0000	.0000	1.0000
47.0000	.0000	.0000	1.0000
47.5000	.0000	.0000	1.0000
48.0000	.0000	.0000	1.0000
48.5000	.0000	.0000	1.0000
49.0000	.0000	.0000	1.0000
49.5000	.0000	.0000	1.0000
50.0000	.0000	.0000	1.0000
50.5000	.0000	.0000	1.0000
B	FU15	PRU15	CPRU15
1.0000	784.0000	.7840	.7840
1.5000	115.0000	.1150	.8990
2.0000	47.0000	.0470	.9460
2.5000	24.0000	.0240	.9700
3.0000	8.0000	.0080	.9780
3.5000	6.0000	.0060	.9840
4.0000	8.0000	.0080	.9920
4.5000	3.0000	.0030	.9950
5.0000	2.0000	.0020	.9970
5.5000	.0000	.0000	.9970
6.0000	.0000	.0000	.9970
6.5000	.0000	.0000	.9970
7.0000	1.0000	.0010	.9980
7.5000	.0000	.0000	.9980
8.0000	.0000	.0000	.9980
8.5000	.0000	.0000	.9980
9.0000	.0000	.0000	.9980
9.5000	.0000	.0000	.9980
10.0000	.0000	.0000	.9980

10.5000	.0000	.0000	.9980
11.0000	.0000	.0000	.9980
11.5000	.0000	.0000	.9980
12.0000	.0000	.0000	.9980
12.5000	.0000	.0000	.9980
13.0000	.0000	.0000	.9980
13.5000	.0000	.0000	.9980
14.0000	.0000	.0000	.9980
14.5000	.0000	.0000	.9980
15.0000	1.0000	.0010	.9990
15.5000	.0000	.0000	.9990
16.0000	.0000	.0000	.9990
16.5000	.0000	.0000	.9990
17.0000	.0000	.0000	.9990
17.5000	.0000	.0000	.9990
18.0000	.0000	.0000	.9990
18.5000	.0000	.0000	.9990
19.0000	1.0000	.0010	1.0000
19.5000	.0000	.0000	1.0000
20.0000	.0000	.0000	1.0000
20.5000	.0000	.0000	1.0000
21.0000	.0000	.0000	1.0000
21.5000	.0000	.0000	1.0000
22.0000	.0000	.0000	1.0000
22.5000	.0000	.0000	1.0000
23.0000	.0000	.0000	1.0000
23.5000	.0000	.0000	1.0000
24.0000	.0000	.0000	1.0000
24.5000	.0000	.0000	1.0000
25.0000	.0000	.0000	1.0000
25.5000	.0000	.0000	1.0000
26.0000	.0000	.0000	1.0000
26.5000	.0000	.0000	1.0000
27.0000	.0000	.0000	1.0000
27.5000	.0000	.0000	1.0000
28.0000	.0000	.0000	1.0000
28.5000	.0000	.0000	1.0000
29.0000	.0000	.0000	1.0000
29.5000	.0000	.0000	1.0000
30.0000	.0000	.0000	1.0000
30.5000	.0000	.0000	1.0000
31.0000	.0000	.0000	1.0000
31.5000	.0000	.0000	1.0000
32.0000	.0000	.0000	1.0000
32.5000	.0000	.0000	1.0000
33.0000	.0000	.0000	1.0000
33.5000	.0000	.0000	1.0000
34.0000	.0000	.0000	1.0000
34.5000	.0000	.0000	1.0000
35.0000	.0000	.0000	1.0000
35.5000	.0000	.0000	1.0000
36.0000	.0000	.0000	1.0000
36.5000	.0000	.0000	1.0000
37.0000	.0000	.0000	1.0000
37.5000	.0000	.0000	1.0000
38.0000	.0000	.0000	1.0000
38.5000	.0000	.0000	1.0000

39.0000	.0000	.0000	1.0000
39.5000	.0000	.0000	1.0000
40.0000	.0000	.0000	1.0000
40.5000	.0000	.0000	1.0000
41.0000	.0000	.0000	1.0000
41.5000	.0000	.0000	1.0000
42.0000	.0000	.0000	1.0000
42.5000	.0000	.0000	1.0000
43.0000	.0000	.0000	1.0000
43.5000	.0000	.0000	1.0000
44.0000	.0000	.0000	1.0000
44.5000	.0000	.0000	1.0000
45.0000	.0000	.0000	1.0000
45.5000	.0000	.0000	1.0000
46.0000	.0000	.0000	1.0000
46.5000	.0000	.0000	1.0000
47.0000	.0000	.0000	1.0000
47.5000	.0000	.0000	1.0000
48.0000	.0000	.0000	1.0000
48.5000	.0000	.0000	1.0000
49.0000	.0000	.0000	1.0000
49.5000	.0000	.0000	1.0000
50.0000	.0000	.0000	1.0000
50.5000	.0000	.0000	1.0000

25 PERCENT SCOUR RESULTS

B	FD25	PRD25	CPRD25
1.0000	1000.0000	1.0000	1.0000
1.5000	.0000	.0000	1.0000
2.0000	.0000	.0000	1.0000
2.5000	.0000	.0000	1.0000
3.0000	.0000	.0000	1.0000
3.5000	.0000	.0000	1.0000
4.0000	.0000	.0000	1.0000
4.5000	.0000	.0000	1.0000
5.0000	.0000	.0000	1.0000
5.5000	.0000	.0000	1.0000
6.0000	.0000	.0000	1.0000
6.5000	.0000	.0000	1.0000
7.0000	.0000	.0000	1.0000
7.5000	.0000	.0000	1.0000
8.0000	.0000	.0000	1.0000
8.5000	.0000	.0000	1.0000
9.0000	.0000	.0000	1.0000
9.5000	.0000	.0000	1.0000
10.0000	.0000	.0000	1.0000
10.5000	.0000	.0000	1.0000
11.0000	.0000	.0000	1.0000
11.5000	.0000	.0000	1.0000
12.0000	.0000	.0000	1.0000
12.5000	.0000	.0000	1.0000
13.0000	.0000	.0000	1.0000
13.5000	.0000	.0000	1.0000
14.0000	.0000	.0000	1.0000
14.5000	.0000	.0000	1.0000
15.0000	.0000	.0000	1.0000
15.5000	.0000	.0000	1.0000
16.0000	.0000	.0000	1.0000

16.5000	.0000	.0000	1.0000
17.0000	.0000	.0000	1.0000
17.5000	.0000	.0000	1.0000
18.0000	.0000	.0000	1.0000
18.5000	.0000	.0000	1.0000
19.0000	.0000	.0000	1.0000
19.5000	.0000	.0000	1.0000
20.0000	.0000	.0000	1.0000
20.5000	.0000	.0000	1.0000
21.0000	.0000	.0000	1.0000
21.5000	.0000	.0000	1.0000
22.0000	.0000	.0000	1.0000
22.5000	.0000	.0000	1.0000
23.0000	.0000	.0000	1.0000
23.5000	.0000	.0000	1.0000
24.0000	.0000	.0000	1.0000
24.5000	.0000	.0000	1.0000
25.0000	.0000	.0000	1.0000
25.5000	.0000	.0000	1.0000
26.0000	.0000	.0000	1.0000
26.5000	.0000	.0000	1.0000
27.0000	.0000	.0000	1.0000
27.5000	.0000	.0000	1.0000
28.0000	.0000	.0000	1.0000
28.5000	.0000	.0000	1.0000
29.0000	.0000	.0000	1.0000
29.5000	.0000	.0000	1.0000
30.0000	.0000	.0000	1.0000
30.5000	.0000	.0000	1.0000
31.0000	.0000	.0000	1.0000
31.5000	.0000	.0000	1.0000
32.0000	.0000	.0000	1.0000
32.5000	.0000	.0000	1.0000
33.0000	.0000	.0000	1.0000
33.5000	.0000	.0000	1.0000
34.0000	.0000	.0000	1.0000
34.5000	.0000	.0000	1.0000
35.0000	.0000	.0000	1.0000
35.5000	.0000	.0000	1.0000
36.0000	.0000	.0000	1.0000
36.5000	.0000	.0000	1.0000
37.0000	.0000	.0000	1.0000
37.5000	.0000	.0000	1.0000
38.0000	.0000	.0000	1.0000
38.5000	.0000	.0000	1.0000
39.0000	.0000	.0000	1.0000
39.5000	.0000	.0000	1.0000
40.0000	.0000	.0000	1.0000
40.5000	.0000	.0000	1.0000
41.0000	.0000	.0000	1.0000
41.5000	.0000	.0000	1.0000
42.0000	.0000	.0000	1.0000
42.5000	.0000	.0000	1.0000
43.0000	.0000	.0000	1.0000
43.5000	.0000	.0000	1.0000
44.0000	.0000	.0000	1.0000
44.5000	.0000	.0000	1.0000

45.0000	.0000	.0000	1.0000
45.5000	.0000	.0000	1.0000
46.0000	.0000	.0000	1.0000
46.5000	.0000	.0000	1.0000
47.0000	.0000	.0000	1.0000
47.5000	.0000	.0000	1.0000
48.0000	.0000	.0000	1.0000
48.5000	.0000	.0000	1.0000
49.0000	.0000	.0000	1.0000
49.5000	.0000	.0000	1.0000
50.0000	.0000	.0000	1.0000
50.5000	.0000	.0000	1.0000
B	FU25	PRU25	CPRU25
1.0000	515.0000	.5150	.5150
1.5000	180.0000	.1800	.6950
2.0000	105.0000	.1050	.8000
2.5000	62.0000	.0620	.8620
3.0000	43.0000	.0430	.9050
3.5000	27.0000	.0270	.9320
4.0000	14.0000	.0140	.9460
4.5000	8.0000	.0080	.9540
5.0000	7.0000	.0070	.9610
5.5000	4.0000	.0040	.9650
6.0000	.0000	.0000	.9650
6.5000	.0000	.0000	.9650
7.0000	1.0000	.0010	.9660
7.5000	1.0000	.0010	.9670
8.0000	.0000	.0000	.9670
8.5000	.0000	.0000	.9670
9.0000	.0000	.0000	.9670
9.5000	.0000	.0000	.9670
10.0000	.0000	.0000	.9670
10.5000	.0000	.0000	.9670
11.0000	1.0000	.0010	.9680
11.5000	1.0000	.0010	.9690
12.0000	6.0000	.0060	.9750
12.5000	1.0000	.0010	.9760
13.0000	.0000	.0000	.9760
13.5000	1.0000	.0010	.9770
14.0000	.0000	.0000	.9770
14.5000	.0000	.0000	.9770
15.0000	.0000	.0000	.9770
15.5000	2.0000	.0020	.9790
16.0000	1.0000	.0010	.9800
16.5000	3.0000	.0030	.9830
17.0000	2.0000	.0020	.9850
17.5000	2.0000	.0020	.9870
18.0000	1.0000	.0010	.9880
18.5000	1.0000	.0010	.9890
19.0000	1.0000	.0010	.9900
19.5000	1.0000	.0010	.9910
20.0000	3.0000	.0030	.9940
20.5000	4.0000	.0040	.9980
21.0000	2.0000	.0020	1.0000
21.5000	.0000	.0000	1.0000
22.0000	.0000	.0000	1.0000
22.5000	.0000	.0000	1.0000

23.0000	.0000	.0000	1.0000
23.5000	.0000	.0000	1.0000
24.0000	.0000	.0000	1.0000
24.5000	.0000	.0000	1.0000
25.0000	.0000	.0000	1.0000
25.5000	.0000	.0000	1.0000
26.0000	.0000	.0000	1.0000
26.5000	.0000	.0000	1.0000
27.0000	.0000	.0000	1.0000
27.5000	.0000	.0000	1.0000
28.0000	.0000	.0000	1.0000
28.5000	.0000	.0000	1.0000
29.0000	.0000	.0000	1.0000
29.5000	.0000	.0000	1.0000
30.0000	.0000	.0000	1.0000
30.5000	.0000	.0000	1.0000
31.0000	.0000	.0000	1.0000
31.5000	.0000	.0000	1.0000
32.0000	.0000	.0000	1.0000
32.5000	.0000	.0000	1.0000
33.0000	.0000	.0000	1.0000
33.5000	.0000	.0000	1.0000
34.0000	.0000	.0000	1.0000
34.5000	.0000	.0000	1.0000
35.0000	.0000	.0000	1.0000
35.5000	.0000	.0000	1.0000
36.0000	.0000	.0000	1.0000
36.5000	.0000	.0000	1.0000
37.0000	.0000	.0000	1.0000
37.5000	.0000	.0000	1.0000
38.0000	.0000	.0000	1.0000
38.5000	.0000	.0000	1.0000
39.0000	.0000	.0000	1.0000
39.5000	.0000	.0000	1.0000
40.0000	.0000	.0000	1.0000
40.5000	.0000	.0000	1.0000
41.0000	.0000	.0000	1.0000
41.5000	.0000	.0000	1.0000
42.0000	.0000	.0000	1.0000
42.5000	.0000	.0000	1.0000
43.0000	.0000	.0000	1.0000
43.5000	.0000	.0000	1.0000
44.0000	.0000	.0000	1.0000
44.5000	.0000	.0000	1.0000
45.0000	.0000	.0000	1.0000
45.5000	.0000	.0000	1.0000
46.0000	.0000	.0000	1.0000
46.5000	.0000	.0000	1.0000
47.0000	.0000	.0000	1.0000
47.5000	.0000	.0000	1.0000
48.0000	.0000	.0000	1.0000
48.5000	.0000	.0000	1.0000
49.0000	.0000	.0000	1.0000
49.5000	.0000	.0000	1.0000
50.0000	.0000	.0000	1.0000
50.5000	.0000	.0000	1.0000

50 PERCENT TMS SCOUR RESULTS

B	FD50	PRD50	CPRD50
1.0000	1000.0000	1.0000	1.0000
1.5000	.0000	.0000	1.0000
2.0000	.0000	.0000	1.0000
2.5000	.0000	.0000	1.0000
3.0000	.0000	.0000	1.0000
3.5000	.0000	.0000	1.0000
4.0000	.0000	.0000	1.0000
4.5000	.0000	.0000	1.0000
5.0000	.0000	.0000	1.0000
5.5000	.0000	.0000	1.0000
6.0000	.0000	.0000	1.0000
6.5000	.0000	.0000	1.0000
7.0000	.0000	.0000	1.0000
7.5000	.0000	.0000	1.0000
8.0000	.0000	.0000	1.0000
8.5000	.0000	.0000	1.0000
9.0000	.0000	.0000	1.0000
9.5000	.0000	.0000	1.0000
10.0000	.0000	.0000	1.0000
10.5000	.0000	.0000	1.0000
11.0000	.0000	.0000	1.0000
11.5000	.0000	.0000	1.0000
12.0000	.0000	.0000	1.0000
12.5000	.0000	.0000	1.0000
13.0000	.0000	.0000	1.0000
13.5000	.0000	.0000	1.0000
14.0000	.0000	.0000	1.0000
14.5000	.0000	.0000	1.0000
15.0000	.0000	.0000	1.0000
15.5000	.0000	.0000	1.0000
16.0000	.0000	.0000	1.0000
16.5000	.0000	.0000	1.0000
17.0000	.0000	.0000	1.0000
17.5000	.0000	.0000	1.0000
18.0000	.0000	.0000	1.0000
18.5000	.0000	.0000	1.0000
19.0000	.0000	.0000	1.0000
19.5000	.0000	.0000	1.0000
20.0000	.0000	.0000	1.0000
20.5000	.0000	.0000	1.0000
21.0000	.0000	.0000	1.0000
21.5000	.0000	.0000	1.0000
22.0000	.0000	.0000	1.0000
22.5000	.0000	.0000	1.0000
23.0000	.0000	.0000	1.0000
23.5000	.0000	.0000	1.0000
24.0000	.0000	.0000	1.0000
24.5000	.0000	.0000	1.0000
25.0000	.0000	.0000	1.0000
25.5000	.0000	.0000	1.0000
26.0000	.0000	.0000	1.0000
26.5000	.0000	.0000	1.0000
27.0000	.0000	.0000	1.0000
27.5000	.0000	.0000	1.0000
28.0000	.0000	.0000	1.0000
28.5000	.0000	.0000	1.0000

29.0000	.0000	.0000	1.0000
29.5000	.0000	.0000	1.0000
30.0000	.0000	.0000	1.0000
30.5000	.0000	.0000	1.0000
31.0000	.0000	.0000	1.0000
31.5000	.0000	.0000	1.0000
32.0000	.0000	.0000	1.0000
32.5000	.0000	.0000	1.0000
33.0000	.0000	.0000	1.0000
33.5000	.0000	.0000	1.0000
34.0000	.0000	.0000	1.0000
34.5000	.0000	.0000	1.0000
35.0000	.0000	.0000	1.0000
35.5000	.0000	.0000	1.0000
36.0000	.0000	.0000	1.0000
36.5000	.0000	.0000	1.0000
37.0000	.0000	.0000	1.0000
37.5000	.0000	.0000	1.0000
38.0000	.0000	.0000	1.0000
38.5000	.0000	.0000	1.0000
39.0000	.0000	.0000	1.0000
39.5000	.0000	.0000	1.0000
40.0000	.0000	.0000	1.0000
40.5000	.0000	.0000	1.0000
41.0000	.0000	.0000	1.0000
41.5000	.0000	.0000	1.0000
42.0000	.0000	.0000	1.0000
42.5000	.0000	.0000	1.0000
43.0000	.0000	.0000	1.0000
43.5000	.0000	.0000	1.0000
44.0000	.0000	.0000	1.0000
44.5000	.0000	.0000	1.0000
45.0000	.0000	.0000	1.0000
45.5000	.0000	.0000	1.0000
46.0000	.0000	.0000	1.0000
46.5000	.0000	.0000	1.0000
47.0000	.0000	.0000	1.0000
47.5000	.0000	.0000	1.0000
48.0000	.0000	.0000	1.0000
48.5000	.0000	.0000	1.0000
49.0000	.0000	.0000	1.0000
49.5000	.0000	.0000	1.0000
50.0000	.0000	.0000	1.0000
50.5000	.0000	.0000	1.0000
B	FU50	PRU50	CPRU50
1.0000	73.0000	.0730	.0730
1.5000	91.0000	.0910	.1640
2.0000	77.0000	.0770	.2410
2.5000	88.0000	.0880	.3290
3.0000	73.0000	.0730	.4020
3.5000	59.0000	.0590	.4610
4.0000	50.0000	.0500	.5110
4.5000	45.0000	.0450	.5560
5.0000	42.0000	.0420	.5980
5.5000	19.0000	.0190	.6170
6.0000	.0000	.0000	.6170
6.5000	.0000	.0000	.6170



7.0000	1.0000	.0010	.6180
7.5000	.0000	.0000	.6180
8.0000	1.0000	.0010	.6190
8.5000	1.0000	.0010	.6200
9.0000	.0000	.0000	.6200
9.5000	2.0000	.0020	.6220
10.0000	.0000	.0000	.6220
10.5000	1.0000	.0010	.6230
11.0000	2.0000	.0020	.6250
11.5000	.0000	.0000	.6250
12.0000	12.0000	.0120	.6370
12.5000	7.0000	.0070	.6440
13.0000	2.0000	.0020	.6460
13.5000	6.0000	.0060	.6520
14.0000	10.0000	.0100	.6620
14.5000	6.0000	.0060	.6680
15.0000	6.0000	.0060	.6740
15.5000	5.0000	.0050	.6790
16.0000	11.0000	.0110	.6900
16.5000	10.0000	.0100	.7000
17.0000	7.0000	.0070	.7070
17.5000	12.0000	.0120	.7190
18.0000	10.0000	.0100	.7290
18.5000	16.0000	.0160	.7450
19.0000	20.0000	.0200	.7650
19.5000	25.0000	.0250	.7900
20.0000	40.0000	.0400	.8300
20.5000	43.0000	.0430	.8730
21.0000	81.0000	.0810	.9540
21.5000	40.0000	.0400	.9940
22.0000	6.0000	.0060	1.0000
22.5000	.0000	.0000	1.0000
23.0000	.0000	.0000	1.0000
23.5000	.0000	.0000	1.0000
24.0000	.0000	.0000	1.0000
24.5000	.0000	.0000	1.0000
25.0000	.0000	.0000	1.0000
25.5000	.0000	.0000	1.0000
26.0000	.0000	.0000	1.0000
26.5000	.0000	.0000	1.0000
27.0000	.0000	.0000	1.0000
27.5000	.0000	.0000	1.0000
28.0000	.0000	.0000	1.0000
28.5000	.0000	.0000	1.0000
29.0000	.0000	.0000	1.0000
29.5000	.0000	.0000	1.0000
30.0000	.0000	.0000	1.0000
30.5000	.0000	.0000	1.0000
31.0000	.0000	.0000	1.0000
31.5000	.0000	.0000	1.0000
32.0000	.0000	.0000	1.0000
32.5000	.0000	.0000	1.0000
33.0000	.0000	.0000	1.0000
33.5000	.0000	.0000	1.0000
34.0000	.0000	.0000	1.0000
34.5000	.0000	.0000	1.0000
35.0000	.0000	.0000	1.0000

35.5000	.0000	.0000	1.0000
36.0000	.0000	.0000	1.0000
36.5000	.0000	.0000	1.0000
37.0000	.0000	.0000	1.0000
37.5000	.0000	.0000	1.0000
38.0000	.0000	.0000	1.0000
38.5000	.0000	.0000	1.0000
39.0000	.0000	.0000	1.0000
39.5000	.0000	.0000	1.0000
40.0000	.0000	.0000	1.0000
40.5000	.0000	.0000	1.0000
41.0000	.0000	.0000	1.0000
41.5000	.0000	.0000	1.0000
42.0000	.0000	.0000	1.0000
42.5000	.0000	.0000	1.0000
43.0000	.0000	.0000	1.0000
43.5000	.0000	.0000	1.0000
44.0000	.0000	.0000	1.0000
44.5000	.0000	.0000	1.0000
45.0000	.0000	.0000	1.0000
45.5000	.0000	.0000	1.0000
46.0000	.0000	.0000	1.0000
46.5000	.0000	.0000	1.0000
47.0000	.0000	.0000	1.0000
47.5000	.0000	.0000	1.0000
48.0000	.0000	.0000	1.0000
48.5000	.0000	.0000	1.0000
49.0000	.0000	.0000	1.0000
49.5000	.0000	.0000	1.0000
50.0000	.0000	.0000	1.0000
50.5000	.0000	.0000	1.0000

75 PERCENT TMS SCOUR RESULTS

B	FD75	PRD75	CPRD75
1.0000	1000.0000	1.0000	1.0000
1.5000	.0000	.0000	1.0000
2.0000	.0000	.0000	1.0000
2.5000	.0000	.0000	1.0000
3.0000	.0000	.0000	1.0000
3.5000	.0000	.0000	1.0000
4.0000	.0000	.0000	1.0000
4.5000	.0000	.0000	1.0000
5.0000	.0000	.0000	1.0000
5.5000	.0000	.0000	1.0000
6.0000	.0000	.0000	1.0000
6.5000	.0000	.0000	1.0000
7.0000	.0000	.0000	1.0000
7.5000	.0000	.0000	1.0000
8.0000	.0000	.0000	1.0000
8.5000	.0000	.0000	1.0000
9.0000	.0000	.0000	1.0000
9.5000	.0000	.0000	1.0000
10.0000	.0000	.0000	1.0000
10.5000	.0000	.0000	1.0000
11.0000	.0000	.0000	1.0000
11.5000	.0000	.0000	1.0000
12.0000	.0000	.0000	1.0000
12.5000	.0000	.0000	1.0000

13.0000	.0000	.0000	1.0000
13.5000	.0000	.0000	1.0000
14.0000	.0000	.0000	1.0000
14.5000	.0000	.0000	1.0000
15.0000	.0000	.0000	1.0000
15.5000	.0000	.0000	1.0000
16.0000	.0000	.0000	1.0000
16.5000	.0000	.0000	1.0000
17.0000	.0000	.0000	1.0000
17.5000	.0000	.0000	1.0000
18.0000	.0000	.0000	1.0000
18.5000	.0000	.0000	1.0000
19.0000	.0000	.0000	1.0000
19.5000	.0000	.0000	1.0000
20.0000	.0000	.0000	1.0000
20.5000	.0000	.0000	1.0000
21.0000	.0000	.0000	1.0000
21.5000	.0000	.0000	1.0000
22.0000	.0000	.0000	1.0000
22.5000	.0000	.0000	1.0000
23.0000	.0000	.0000	1.0000
23.5000	.0000	.0000	1.0000
24.0000	.0000	.0000	1.0000
24.5000	.0000	.0000	1.0000
25.0000	.0000	.0000	1.0000
25.5000	.0000	.0000	1.0000
26.0000	.0000	.0000	1.0000
26.5000	.0000	.0000	1.0000
27.0000	.0000	.0000	1.0000
27.5000	.0000	.0000	1.0000
28.0000	.0000	.0000	1.0000
28.5000	.0000	.0000	1.0000
29.0000	.0000	.0000	1.0000
29.5000	.0000	.0000	1.0000
30.0000	.0000	.0000	1.0000
30.5000	.0000	.0000	1.0000
31.0000	.0000	.0000	1.0000
31.5000	.0000	.0000	1.0000
32.0000	.0000	.0000	1.0000
32.5000	.0000	.0000	1.0000
33.0000	.0000	.0000	1.0000
33.5000	.0000	.0000	1.0000
34.0000	.0000	.0000	1.0000
34.5000	.0000	.0000	1.0000
35.0000	.0000	.0000	1.0000
35.5000	.0000	.0000	1.0000
36.0000	.0000	.0000	1.0000
36.5000	.0000	.0000	1.0000
37.0000	.0000	.0000	1.0000
37.5000	.0000	.0000	1.0000
38.0000	.0000	.0000	1.0000
38.5000	.0000	.0000	1.0000
39.0000	.0000	.0000	1.0000
39.5000	.0000	.0000	1.0000
40.0000	.0000	.0000	1.0000
40.5000	.0000	.0000	1.0000
41.0000	.0000	.0000	1.0000

41.5000	.0000	.0000	1.0000
42.0000	.0000	.0000	1.0000
42.5000	.0000	.0000	1.0000
43.0000	.0000	.0000	1.0000
43.5000	.0000	.0000	1.0000
44.0000	.0000	.0000	1.0000
44.5000	.0000	.0000	1.0000
45.0000	.0000	.0000	1.0000
45.5000	.0000	.0000	1.0000
46.0000	.0000	.0000	1.0000
46.5000	.0000	.0000	1.0000
47.0000	.0000	.0000	1.0000
47.5000	.0000	.0000	1.0000
48.0000	.0000	.0000	1.0000
48.5000	.0000	.0000	1.0000
49.0000	.0000	.0000	1.0000
49.5000	.0000	.0000	1.0000
50.0000	.0000	.0000	1.0000
50.5000	.0000	.0000	1.0000
B	FU75	PRU75	CPRU75
1.0000	4.0000	.0040	.0040
1.5000	12.0000	.0120	.0160
2.0000	18.0000	.0180	.0340
2.5000	20.0000	.0200	.0540
3.0000	17.0000	.0170	.0710
3.5000	29.0000	.0290	.1000
4.0000	19.0000	.0190	.1190
4.5000	19.0000	.0190	.1380
5.0000	15.0000	.0150	.1530
5.5000	8.0000	.0080	.1610
6.0000	.0000	.0000	.1610
6.5000	.0000	.0000	.1610
7.0000	.0000	.0000	.1610
7.5000	.0000	.0000	.1610
8.0000	2.0000	.0020	.1630
8.5000	.0000	.0000	.1630
9.0000	1.0000	.0010	.1640
9.5000	.0000	.0000	.1640
10.0000	.0000	.0000	.1640
10.5000	1.0000	.0010	.1650
11.0000	.0000	.0000	.1650
11.5000	1.0000	.0010	.1660
12.0000	8.0000	.0080	.1740
12.5000	2.0000	.0020	.1760
13.0000	4.0000	.0040	.1800
13.5000	3.0000	.0030	.1830
14.0000	5.0000	.0050	.1880
14.5000	8.0000	.0080	.1960
15.0000	3.0000	.0030	.1990
15.5000	4.0000	.0040	.2030
16.0000	4.0000	.0040	.2070
16.5000	.0000	.0000	.2070
17.0000	9.0000	.0090	.2160
17.5000	8.0000	.0080	.2240
18.0000	7.0000	.0070	.2310
18.5000	10.0000	.0100	.2410
19.0000	13.0000	.0130	.2540

19.5000	24.0000	.0240	.2780
20.0000	53.0000	.0530	.3310
20.5000	119.0000	.1190	.4500
21.0000	254.0000	.2540	.7040
21.5000	238.0000	.2380	.9420
22.0000	58.0000	.0580	1.0000
22.5000	.0000	.0000	1.0000
23.0000	.0000	.0000	1.0000
23.5000	.0000	.0000	1.0000
24.0000	.0000	.0000	1.0000
24.5000	.0000	.0000	1.0000
25.0000	.0000	.0000	1.0000
25.5000	.0000	.0000	1.0000
26.0000	.0000	.0000	1.0000
26.5000	.0000	.0000	1.0000
27.0000	.0000	.0000	1.0000
27.5000	.0000	.0000	1.0000
28.0000	.0000	.0000	1.0000
28.5000	.0000	.0000	1.0000
29.0000	.0000	.0000	1.0000
29.5000	.0000	.0000	1.0000
30.0000	.0000	.0000	1.0000
30.5000	.0000	.0000	1.0000
31.0000	.0000	.0000	1.0000
31.5000	.0000	.0000	1.0000
32.0000	.0000	.0000	1.0000
32.5000	.0000	.0000	1.0000
33.0000	.0000	.0000	1.0000
33.5000	.0000	.0000	1.0000
34.0000	.0000	.0000	1.0000
34.5000	.0000	.0000	1.0000
35.0000	.0000	.0000	1.0000
35.5000	.0000	.0000	1.0000
36.0000	.0000	.0000	1.0000
36.5000	.0000	.0000	1.0000
37.0000	.0000	.0000	1.0000
37.5000	.0000	.0000	1.0000
38.0000	.0000	.0000	1.0000
38.5000	.0000	.0000	1.0000
39.0000	.0000	.0000	1.0000
39.5000	.0000	.0000	1.0000
40.0000	.0000	.0000	1.0000
40.5000	.0000	.0000	1.0000
41.0000	.0000	.0000	1.0000
41.5000	.0000	.0000	1.0000
42.0000	.0000	.0000	1.0000
42.5000	.0000	.0000	1.0000
43.0000	.0000	.0000	1.0000
43.5000	.0000	.0000	1.0000
44.0000	.0000	.0000	1.0000
44.5000	.0000	.0000	1.0000
45.0000	.0000	.0000	1.0000
45.5000	.0000	.0000	1.0000
46.0000	.0000	.0000	1.0000
46.5000	.0000	.0000	1.0000
47.0000	.0000	.0000	1.0000
47.5000	.0000	.0000	1.0000

48.0000	.0000	.0000	1.0000
48.5000	.0000	.0000	1.0000
49.0000	.0000	.0000	1.0000
49.5000	.0000	.0000	1.0000
50.0000	.0000	.0000	1.0000
50.5000	.0000	.0000	1.0000

The mean annual contraction scour d/s face is MNYYS

The mean annual scour value d/s face is MNLTS

The mean annual total scour d/s face is YMNTS

The standard dev in annual scour d/s face is YSTS

YR	MNYYS	MNLTS	YMNTS	YSTS
001	.0000	.0000	.0000	.0000
002	.0000	.0000	.0000	.0000
003	.0000	.0000	.0000	.0000
004	.0000	.0000	.0000	.0000
005	.0000	.0000	.0000	.0000
006	.0000	.0000	.0000	.0000
007	.0000	.0000	.0000	.0000
008	.0000	.0000	.0000	.0000
009	.0000	.0000	.0000	.0000
010	.0000	.0000	.0000	.0000
011	.0000	.0000	.0000	.0000
012	.0000	.0000	.0000	.0000
013	.0000	.0000	.0000	.0000
014	.0000	.0000	.0000	.0000
015	.0000	.0000	.0000	.0000
016	.0000	.0000	.0000	.0000
017	.0000	.0000	.0000	.0000
018	.0000	.0000	.0000	.0000
019	.0000	.0000	.0000	.0000
020	.0000	.0000	.0000	.0000
021	.0000	.0000	.0000	.0000
022	.0000	.0000	.0000	.0000
023	.0000	.0000	.0000	.0000
024	.0000	.0000	.0000	.0000
025	.0000	.0000	.0000	.0000
026	.0000	.0000	.0000	.0000
027	.0000	.0000	.0000	.0000
028	.0000	.0000	.0000	.0000
029	.0000	.0000	.0000	.0000
030	.0000	.0000	.0000	.0000
031	.0000	.0000	.0000	.0000
032	.0000	.0000	.0000	.0000
033	.0000	.0000	.0000	.0000
034	.0000	.0000	.0000	.0000
035	.0000	.0000	.0000	.0000
036	.0000	.0000	.0000	.0000
037	.0000	.0000	.0000	.0000
038	.0000	.0000	.0000	.0000
039	.0000	.0000	.0000	.0000
040	.0000	.0000	.0000	.0000
041	.0000	.0000	.0000	.0000
042	.0000	.0000	.0000	.0000
043	.0000	.0000	.0000	.0000
044	.0000	.0000	.0000	.0000
045	.0000	.0000	.0000	.0000
046	.0000	.0000	.0000	.0000

047	.0000	.0000	.0000	.0000
048	.0000	.0000	.0000	.0000
049	.0000	.0000	.0000	.0000
050	.0000	.0000	.0000	.0000
051	.0000	.0000	.0000	.0000
052	.0000	.0000	.0000	.0000
053	.0000	.0000	.0000	.0000
054	.0000	.0000	.0000	.0000
055	.0000	.0000	.0000	.0000
056	.0000	.0000	.0000	.0000
057	.0000	.0000	.0000	.0000
058	.0000	.0000	.0000	.0000
059	.0000	.0000	.0000	.0000
060	.0000	.0000	.0000	.0000
061	.0000	.0000	.0000	.0000
062	.0000	.0000	.0000	.0000
063	.0000	.0000	.0000	.0000
064	.0000	.0000	.0000	.0000
065	.0000	.0000	.0000	.0000
066	.0000	.0000	.0000	.0000
067	.0000	.0000	.0000	.0000
068	.0000	.0000	.0000	.0000
069	.0000	.0000	.0000	.0000
070	.0000	.0000	.0000	.0000
071	.0000	.0000	.0000	.0000
072	.0000	.0000	.0000	.0000
073	.0000	.0000	.0000	.0000
074	.0000	.0000	.0000	.0000
075	.0000	.0000	.0000	.0000
076	.0000	.0000	.0000	.0000
077	.0000	.0000	.0000	.0000
078	.0000	.0000	.0000	.0000
079	.0000	.0000	.0000	.0000
080	.0000	.0000	.0000	.0000
081	.0000	.0000	.0000	.0000
082	.0000	.0000	.0000	.0000
083	.0000	.0000	.0000	.0000
084	.0000	.0000	.0000	.0000
085	.0000	.0000	.0000	.0000
086	.0000	.0000	.0000	.0000
087	.0000	.0000	.0000	.0000
088	.0000	.0000	.0000	.0000
089	.0000	.0000	.0000	.0000
090	.0000	.0000	.0000	.0000
091	.0000	.0000	.0000	.0000
092	.0000	.0000	.0000	.0000
093	.0000	.0000	.0000	.0000
094	.0000	.0000	.0000	.0000
095	.0000	.0000	.0000	.0000
096	.0000	.0000	.0000	.0000
097	.0000	.0000	.0000	.0000
098	.0000	.0000	.0000	.0000
099	.0000	.0000	.0000	.0000
100	.0000	.0000	.0000	.0000

The annual contraction scour u/s face is MNYYSU

The mean annual local scour value u/s face is MNLSU

The mean annual total scour value u/s face is YMNTSU

YR	MNYYSU	MNLSU	YMNTSU	YSTTSU
001	.0000	.0364	.0364	.1321
002	.0000	.0818	.0818	.2019
003	.0000	.1186	.1186	.2490
004	.0000	.1613	.1613	.3132
005	.0000	.1942	.1942	.3462
006	.0000	.2310	.2310	.3781
007	.0000	.2711	.2711	.4221
008	.0000	.3205	.3205	.4601
009	.0000	.3764	.3764	.6029
010	.0000	.4184	.4184	.6261
011	.0000	.4618	.4618	.6682
012	.0000	.5130	.5130	.7153
013	.0000	.5767	.5767	.8069
014	.0000	.6301	.6301	.9052
015	.0000	.6953	.6953	1.0381
016	.0000	.7804	.7804	1.3356
017	.0000	.8424	.8424	1.4073
018	.0000	.9148	.9148	1.5072
019	.0000	1.0019	1.0019	1.6822
020	.0000	1.1002	1.1002	1.8887
021	.0000	1.2053	1.2053	2.1085
022	.0000	1.3119	1.3119	2.2762
023	.0000	1.4213	1.4213	2.4771
024	.0000	1.5359	1.5359	2.6565
025	.0000	1.6994	1.6994	2.9354
026	.0000	1.8317	1.8317	3.1559
027	.0000	1.9889	1.9889	3.3863
028	.0000	2.1500	2.1500	3.6156
029	.0000	2.3229	2.3229	3.8512
030	.0000	2.4923	2.4923	4.0652
031	.0000	2.6627	2.6627	4.2563
032	.0000	2.8609	2.8609	4.4805
033	.0000	3.0916	3.0916	4.7394
034	.0000	3.3295	3.3295	4.9955
035	.0000	3.5599	3.5599	5.2328
036	.0000	3.8089	3.8089	5.4627
037	.0000	4.1241	4.1241	5.7417
038	.0000	4.3787	4.3787	5.9545
039	.0000	4.6681	4.6681	6.1603
040	.0000	4.9865	4.9865	6.3689
041	.0000	5.3424	5.3424	6.6166
042	.0000	5.6847	5.6847	6.8243
043	.0000	5.9870	5.9870	7.0016
044	.0000	6.3193	6.3193	7.1691
045	.0000	6.7275	6.7275	7.3417
046	.0000	7.1022	7.1022	7.5107
047	.0000	7.5245	7.5245	7.6640
048	.0000	7.9483	7.9483	7.8436
049	.0000	8.2896	8.2896	7.9676
050	.0000	8.6595	8.6595	8.0687
051	.0000	9.0612	9.0612	8.1435
052	.0000	9.4683	9.4683	8.2313
053	.0000	9.9393	9.9393	8.3158
054	.0000	10.3188	10.3188	8.3598
055	.0000	10.6825	10.6825	8.4077



056	.0000	11.0695	11.0695	8.4242
057	.0000	11.4813	11.4813	8.4055
058	.0000	11.9069	11.9069	8.4109
059	.0000	12.3424	12.3424	8.3661
060	.0000	12.7396	12.7396	8.2939
061	.0000	13.1040	13.1040	8.2447
062	.0000	13.5404	13.5404	8.1471
063	.0000	13.9358	13.9358	8.0612
064	.0000	14.3084	14.3084	7.9599
065	.0000	14.7185	14.7185	7.8750
066	.0000	15.0185	15.0185	7.7932
067	.0000	15.3578	15.3578	7.6550
068	.0000	15.6592	15.6592	7.5313
069	.0000	15.9694	15.9694	7.3978
070	.0000	16.2530	16.2530	7.2652
071	.0000	16.5271	16.5271	7.1351
072	.0000	16.7834	16.7834	6.9823
073	.0000	16.9865	16.9865	6.8702
074	.0000	17.2228	17.2228	6.7012
075	.0000	17.4569	17.4569	6.5631
076	.0000	17.6383	17.6383	6.4585
077	.0000	17.8415	17.8415	6.2874
078	.0000	18.0370	18.0370	6.1426
079	.0000	18.2134	18.2134	5.9872
080	.0000	18.3962	18.3962	5.8437
081	.0000	18.5459	18.5459	5.7346
082	.0000	18.7253	18.7253	5.5247
083	.0000	18.9109	18.9109	5.2959
084	.0000	19.0584	19.0584	5.1332
085	.0000	19.1943	19.1943	4.9719
086	.0000	19.3445	19.3445	4.7943
087	.0000	19.4793	19.4793	4.6439
088	.0000	19.5875	19.5875	4.5144
089	.0000	19.6962	19.6962	4.3656
090	.0000	19.7927	19.7927	4.2310
091	.0000	19.9083	19.9083	4.0614
092	.0000	20.0029	20.0029	3.9377
093	.0000	20.1193	20.1193	3.7267
094	.0000	20.2183	20.2183	3.5229
095	.0000	20.3076	20.3076	3.3852
096	.0000	20.3869	20.3869	3.2621
097	.0000	20.4820	20.4820	3.0589
098	.0000	20.5685	20.5685	2.8404
099	.0000	20.6322	20.6322	2.6894
100	.0000	20.7125	20.7125	2.4669

## Appendix D-12

RUN TITLE IS Patapasco River Hurricane Simulation  
RUN DATE IS  
THE PROGRAM WAS EXECUTED IN THE EXISTING PIER ANALYSIS MODE.  
CONTRACTION SCOUR METHOD IS KOMURAS EQN  
SCOUR COMPUTED WITHOUT ARMOURING  
BRUBAKER-DEMETRIUS NEILLS MODIFICATION FACTOR ACTIVATED  
TIDE DISTORTION OPTION ACTIVATE  
MEAN TIDAL DEPTH MDR is = 33.935000  
MEAN LOW TIDAL DEPTH MLT is = 33.000000  
MEAN LOW TIDE ELEVATION MLTE is = -9.350000E-01  
TIDAL AMP. AT BRIDGE XSEC MTR is = 9.350000E-01  
CHANNEL INVERT AT BRIDGE IRS is = -33.935000

Estuary in bank area is = 34107.750000

Maximum tide in the simulation HITIDE is = 45.580940  
Maximum u/s flow depth in sim. YTRMXS is = 47.752080  
Maximum d/s flow depth in sim. YTFMXS is = 47.036070  
Maximum u/s disch. in sim. QTRMXS is = 259690.900000  
Maximum d/s disch. in sim. QTFMXS is = 337632.900000  
Maximum u/s vel.in sim. VUPMS is = 3.274987  
Maximum d/s vel.in sim. VDOWNMS is = 3.278295

Maximum u/s flow depth last run YTRMAX is = 47.752080  
Maximum d/s flow depth last run YTFMAX is = 43.684090  
Maximum u/s discharge last run QTRMAX is = 231099.000000  
Maximum d/s discharge last run QTFMAX is = 300859.600000  
Maximum u/s velocity last run VNUMAX is = 2.601955  
Maximum d/s velocity last run VNDMAX is = 2.670653  
Maximum tangential vel d/s face last run VTDMX is = 1.305721  
Maximum tangential vel u/s face last run VTUMX is = 3.620485  
critical vel u/s face last run UIUMIN is = 1.840270E-01  
critical vel d/s face last run UIDMIN is = 1.840270E-01

Time of concentration = 27.600000hrs  
Time to peak = 18.492000hrs  
Number of unit hydrograph ordinates = 92  
Soil infiltration potential = 4.285714  
Peak discharge of the UHG = 15651.740000cfs  
Initial abstractions IA = 8.571429E-01in

Catchment base flow = 343.082300cfs  
Tide attenuation factor TAF = 6.631206E-01  
Tidal lag MTL= 2.444557hrs  
Tidal routing constant CX = 4.090720E-01  
Bridge station tidal range TR = 1.870000ft  
Effective bottom channel width at brdg.WBE = 1697.400000ft  
Estuary Area 9.924710E+07  
Contraction scour factor u/s face= 9.547300E-01  
Contraction scour factor d/s face= 1.176995  
Estuary to wavelength ratio DIM = 9.623493E-03

Estuary width factor WF = 2.393939  
Tidal range factor HF = 5.510535E-02  
Neill Mod. factor rising limb.NMRF = 8.000000E-01  
Neill Mod. factor falling limb.NMFF = 8.000000E-01

The maximum storm event in the simulation is 8.000000ins  
Array of total SURGRE at bridge is HSURGE= 10.380330  
2.856355E-01

5.179529E-01	8.728182E-01	1.481365	2.761897
10.926670	10.926670	3.868823	2.761897
-5.401087	-5.078043	-4.789991	-4.531823
-4.299308	-4.088933	-3.897769	-3.723364
-3.563652	-3.416886	-3.281578	-3.156457
-3.040428	-2.932547	-2.831993	-2.738052
-2.650098	-2.567580	-2.490014	-2.416970
-2.348066	-2.282962	-2.221354	-2.162968
-2.107560	-2.054909	-2.004814	-1.957096
-1.911588	-1.868142	-1.826621	-1.786900
-1.748865	-1.712412	-1.677443	-1.643871
-1.611613	-1.580593	-1.550743	-1.521997
-1.494296	-1.467583	-1.441807	-1.416919
-1.392874	-1.369630	-1.347148	-1.325391
-1.304325	-1.283917	-1.264137	-1.244957
-1.226349	-1.208288	-1.190751	-1.173715
-1.157160	-1.141064	-1.125410	-1.110179
-1.095354	-1.080919	-1.066860	-1.053161
-1.039810	-1.026792	-1.014096	-1.001710
-9.896228E-01	-9.778234E-01	-9.663019E-01	-9.550486E-01
-9.440541E-01	-9.333097E-01	-9.228069E-01	-9.125378E-01
-9.024945E-01	-8.926698E-01	-8.830566E-01	-8.736480E-01
-8.644378E-01	-8.554195E-01	-8.465874E-01	-8.379357E-01
-8.294590E-01	-8.211520E-01	-8.130096E-01	-8.050270E-01
-7.971996E-01	-7.895228E-01	-7.819924E-01	-7.746043E-01
-7.673544E-01	-7.602389E-01	-7.532541E-01	-7.463963E-01
-7.396623E-01	-7.330486E-01	-7.265522E-01	-7.201698E-01
-7.138985E-01	-7.077355E-01	-7.016779E-01	-6.957231E-01
-6.898685E-01	-6.841115E-01	-6.784499E-01	-6.728811E-01
-6.674029E-01	-6.620133E-01		

Array of total combined depth at bridge d/s face is YTR=  
33.000000

33.000000	37.978260	38.067190	38.585970
39.630120	47.752080	33.000000	33.000000
37.126950	33.000000	37.010950	33.000000
33.000000	37.108810	33.000000	33.000000
37.246300	33.000000	33.000000	33.000000
37.045910	33.000000	37.501770	37.564300
33.000000	36.834310	33.000000	36.831270
37.097090	37.352810	33.000000	37.196860
33.000000	33.000000	37.130700	33.000000
33.000000	36.693630	36.799760	36.891960
37.323700	33.000000	33.000000	36.939290
33.000000	36.913040	33.000000	37.034740
33.000000	36.938480	33.000000	33.000000
36.858730	33.000000	36.838880	37.462400
37.549610	33.000000	33.000000	33.000000

36.813310	33.000000	33.000000	37.137820
37.528770	33.000000	33.000000	37.222810
33.000000	33.000000	33.000000	37.140440
33.000000	36.837510	33.000000	37.010310
37.288250	33.000000	33.000000	33.000000
36.814020	33.000000	37.131380	33.000000
33.000000	33.000000	37.029400	33.000000
37.060930	33.000000	36.929130	36.956720
36.957700	33.000000	36.847700	37.378920
33.000000	36.990480	37.014060	37.019050
37.235470	33.000000	33.000000	36.898300
33.000000	37.199440	33.000000	37.206990
33.000000	36.981310	33.000000	36.904050
37.047580	37.344180	33.000000	37.113240
33.000000	33.000000	33.000000	

Array of total combined depth at bridge u/s face is YTF=  
43.684090

37.506790	33.000000	33.000000	33.000000
33.000000	33.000000	36.999480	36.973370
33.000000	36.946780	33.000000	37.006790
36.751840	33.000000	37.067200	36.952850
33.000000	37.096720	36.976150	36.872890
33.000000	36.946540	33.000000	33.000000
36.572370	33.000000	36.830220	33.000000
33.000000	33.000000	37.096050	33.000000
37.035260	36.953200	33.000000	37.097240
36.457370	33.000000	33.000000	33.000000
33.000000	37.193620	36.763830	33.000000
36.877740	33.000000	36.781330	33.000000
36.617220	33.000000	36.883430	36.744540
33.000000	36.650380	33.000000	33.000000
33.000000	37.077960	36.868200	36.761410
33.000000	36.693180	36.645130	33.000000
33.000000	37.462390	37.121410	33.000000
36.928240	36.882100	36.847290	33.000000
36.758800	33.000000	36.797210	33.000000
33.000000	37.200440	36.930670	36.714820
33.000000	36.798530	33.000000	36.974280
36.924990	36.611930	33.000000	36.927060
33.000000	36.881760	33.000000	33.000000
33.000000	36.672030	33.000000	33.000000
36.789050	33.000000	33.000000	33.000000
33.000000	37.170360	36.897930	33.000000
36.823260	33.000000	37.104230	33.000000
36.907140	33.000000	36.804240	33.000000
33.000000	33.000000	37.061830	33.000000
37.058900	36.824030	36.693880	

Array total net disch. value at bridge is QT= 282256.700000 -  
9654.068000

-18213.280000	-27506.200000	-45100.420000	-231099.000000
300859.600000	5681.355000	10685.440000	13432.110000
13384.440000	10677.010000	8965.732000	5391.878000
-593.168000	-17038.810000	-16034.480000	-6942.692000
7830.638000	25621.820000	42283.590000	54717.230000
61056.040000	45052.010000	47793.360000	53892.050000
53221.230000	60465.680000	68660.620000	78461.430000
88646.440000	98943.200000	107524.500000	113615.800000

116145.600000	115346.600000	123151.700000	108229.800000
96341.700000	84400.260000	77934.560000	76493.270000
79511.370000	84852.220000	90165.710000	92732.770000
91023.870000	84313.720000	58337.490000	53268.280000
47071.660000	41076.300000	36464.250000	33680.640000
32962.980000	33554.880000	34624.190000	35279.130000
34758.260000	32497.070000	34452.330000	26175.930000
17477.580000	9766.966000	4435.210000	2445.157000
3811.543000	7813.275000	13134.500000	18169.280000
21327.460000	21569.170000	23401.360000	15753.390000
6410.690000	-2554.448000	-9064.067000	-11667.830000
-9860.116000	-4226.433000	3701.214000	11778.990000
17859.370000	20319.840000	14387.520000	10100.730000
3779.856000	-2929.961000	-8331.252000	-11070.230000
-10473.510000	-6713.942000	-787.472300	5766.339000
11253.920000	14252.670000	11768.040000	8856.674000
3979.411000	-1633.106000	-6562.859000	-9567.804000
-9897.564000	-7483.310000	-2955.210000	2518.204000
7526.283000	10779.550000	15996.900000	13138.570000
6906.437000	-1055.806000	-8682.240000	-14006.960000
-15659.980000	-13212.840000	-7285.725000	612.511400
8468.927000	14281.580000		
Array of total net velocity at bridge is VNT =			3.879558 -
2.083855E-01			
-3.864820E-01	-5.724625E-01	-9.044439E-01	-4.299467
3.034379	1.296241E-01	2.437633E-01	3.008407E-01
3.052936E-01	2.389930E-01	2.006838E-01	1.228688E-01
-1.328402E-02	-3.815035E-01	-3.657513E-01	-1.555939E-01
1.753565E-01	5.845104E-01	9.641160E-01	1.225001
1.392662	9.724322E-01	1.031957	1.250485
1.213277	1.378400	1.565223	1.757041
1.949643	2.215692	2.409120	2.543475
2.649321	2.583483	2.757822	2.557327
2.236747	1.923737	1.777168	1.682091
1.781447	1.933703	2.056566	2.114468
2.075866	1.921593	1.305976	1.236270
1.073641	9.366373E-01	8.467919E-01	7.679048E-01
7.651372E-01	7.649629E-01	7.619596E-01	7.616873E-01
7.782894E-01	7.409545E-01	7.851273E-01	5.966677E-01
4.057726E-01	2.267053E-01	9.934161E-02	5.278566E-02
8.387896E-02	1.749900E-01	2.943229E-01	4.143953E-01
4.863136E-01	4.917406E-01	5.241601E-01	3.589964E-01
1.461459E-01	-5.822286E-02	-2.028884E-01	-2.565279E-01
-2.209232E-01	-9.639543E-02	8.593914E-02	2.684973E-01
4.070664E-01	4.551168E-01	3.282193E-01	2.303683E-01
8.772214E-02	-6.559002E-02	-1.900137E-01	-2.478573E-01
-2.388189E-01	-1.531287E-01	-1.796283E-02	1.315351E-01
2.612531E-01	3.249374E-01	2.588564E-01	2.018599E-01
9.078887E-02	-3.655583E-02	-1.469083E-01	-2.144134E-01
-2.217272E-01	-1.706495E-01	-6.739078E-02	5.740403E-02
1.686310E-01	2.414027E-01	3.584347E-01	2.996260E-01
1.575606E-01	-2.406552E-02	-1.979960E-01	-3.135883E-01
-3.444014E-01	-2.958309E-01	-1.631678E-01	1.371371E-02
1.930552E-01	3.315730E-01		
Array of net adjusted vel.upstream is VNUA =			0.000000E+00
1.041927E-01			
2.974337E-01	4.794723E-01	7.384531E-01	2.601955



[illegible]

1.590452E-01	4.386107E-02	0.000000E+00	0.000000E+00
0.000000E+00	0.000000E+00	0.000000E+00	6.576756E-02
1.963941E-01	2.930953E-01	2.918969E-01	2.303581E-01
1.463244E-01	4.539444E-02	0.000000E+00	0.000000E+00
0.000000E+00	0.000000E+00	0.000000E+00	2.870201E-02
1.130175E-01	2.050169E-01	2.999187E-01	3.290304E-01
2.285933E-01	7.878030E-02	0.000000E+00	0.000000E+00
0.000000E+00	0.000000E+00	0.000000E+00	6.856855E-03
1.033845E-01	2.623141E-01		

The mean hurricane scour u/s face is MNTHSU 7.352936  
 The std.dev.in hurricane scour u/s face is STDHSU 1.346727E-01  
 The mean hurricane scour d/s face is MNTHSD 4.079572  
 The std.dev.in hurricane scour d/s face is STDHSD 2.413366E-02

B	FHU	PRHU	CPRHU
1.0000	.0000	.0000	.0000
1.5000	.0000	.0000	.0000
2.0000	.0000	.0000	.0000
2.5000	.0000	.0000	.0000
3.0000	.0000	.0000	.0000
3.5000	.0000	.0000	.0000
4.0000	.0000	.0000	.0000
4.5000	.0000	.0000	.0000
5.0000	.0000	.0000	.0000
5.5000	.0000	.0000	.0000
6.0000	.0000	.0000	.0000
6.5000	.0000	.0000	.0000
7.0000	19.0000	.0038	.0038
7.5000	4303.0000	.8606	.8644
8.0000	678.0000	.1356	1.0000
8.5000	.0000	.0000	1.0000
9.0000	.0000	.0000	1.0000
9.5000	.0000	.0000	1.0000
10.0000	.0000	.0000	1.0000
10.5000	.0000	.0000	1.0000
11.0000	.0000	.0000	1.0000
11.5000	.0000	.0000	1.0000
12.0000	.0000	.0000	1.0000
12.5000	.0000	.0000	1.0000
13.0000	.0000	.0000	1.0000
13.5000	.0000	.0000	1.0000
14.0000	.0000	.0000	1.0000
14.5000	.0000	.0000	1.0000
15.0000	.0000	.0000	1.0000
15.5000	.0000	.0000	1.0000
16.0000	.0000	.0000	1.0000
16.5000	.0000	.0000	1.0000
17.0000	.0000	.0000	1.0000
17.5000	.0000	.0000	1.0000
18.0000	.0000	.0000	1.0000
18.5000	.0000	.0000	1.0000
19.0000	.0000	.0000	1.0000
19.5000	.0000	.0000	1.0000
20.0000	.0000	.0000	1.0000
20.5000	.0000	.0000	1.0000
21.0000	.0000	.0000	1.0000
21.5000	.0000	.0000	1.0000



22.0000	.0000	.0000	1.0000
22.5000	.0000	.0000	1.0000
23.0000	.0000	.0000	1.0000
23.5000	.0000	.0000	1.0000
24.0000	.0000	.0000	1.0000
24.5000	.0000	.0000	1.0000
25.0000	.0000	.0000	1.0000
25.5000	.0000	.0000	1.0000
26.0000	.0000	.0000	1.0000
26.5000	.0000	.0000	1.0000
27.0000	.0000	.0000	1.0000
27.5000	.0000	.0000	1.0000
28.0000	.0000	.0000	1.0000
28.5000	.0000	.0000	1.0000
29.0000	.0000	.0000	1.0000
29.5000	.0000	.0000	1.0000
30.0000	.0000	.0000	1.0000
30.5000	.0000	.0000	1.0000
31.0000	.0000	.0000	1.0000
31.5000	.0000	.0000	1.0000
32.0000	.0000	.0000	1.0000
32.5000	.0000	.0000	1.0000
33.0000	.0000	.0000	1.0000
33.5000	.0000	.0000	1.0000
34.0000	.0000	.0000	1.0000
34.5000	.0000	.0000	1.0000
35.0000	.0000	.0000	1.0000
35.5000	.0000	.0000	1.0000
36.0000	.0000	.0000	1.0000
36.5000	.0000	.0000	1.0000
37.0000	.0000	.0000	1.0000
37.5000	.0000	.0000	1.0000
38.0000	.0000	.0000	1.0000
38.5000	.0000	.0000	1.0000
39.0000	.0000	.0000	1.0000
39.5000	.0000	.0000	1.0000
40.0000	.0000	.0000	1.0000
40.5000	.0000	.0000	1.0000
41.0000	.0000	.0000	1.0000
41.5000	.0000	.0000	1.0000
42.0000	.0000	.0000	1.0000
42.5000	.0000	.0000	1.0000
43.0000	.0000	.0000	1.0000
43.5000	.0000	.0000	1.0000
44.0000	.0000	.0000	1.0000
44.5000	.0000	.0000	1.0000
45.0000	.0000	.0000	1.0000
45.5000	.0000	.0000	1.0000
46.0000	.0000	.0000	1.0000
46.5000	.0000	.0000	1.0000
47.0000	.0000	.0000	1.0000
47.5000	.0000	.0000	1.0000
48.0000	.0000	.0000	1.0000
48.5000	.0000	.0000	1.0000
49.0000	.0000	.0000	1.0000
49.5000	.0000	.0000	1.0000
50.0000	.0000	.0000	1.0000

50.5000	.0000	.0000	1.0000
B	FHD	PRHD	CPRHD
1.0000	.0000	.0000	.0000
1.5000	.0000	.0000	.0000
2.0000	.0000	.0000	.0000
2.5000	.0000	.0000	.0000
3.0000	.0000	.0000	.0000
3.5000	.0000	.0000	.0000
4.0000	.0000	.0000	.0000
4.5000	5000.0000	1.0000	1.0000
5.0000	.0000	.0000	1.0000
5.5000	.0000	.0000	1.0000
6.0000	.0000	.0000	1.0000
6.5000	.0000	.0000	1.0000
7.0000	.0000	.0000	1.0000
7.5000	.0000	.0000	1.0000
8.0000	.0000	.0000	1.0000
8.5000	.0000	.0000	1.0000
9.0000	.0000	.0000	1.0000
9.5000	.0000	.0000	1.0000
10.0000	.0000	.0000	1.0000
10.5000	.0000	.0000	1.0000
11.0000	.0000	.0000	1.0000
11.5000	.0000	.0000	1.0000
12.0000	.0000	.0000	1.0000
12.5000	.0000	.0000	1.0000
13.0000	.0000	.0000	1.0000
13.5000	.0000	.0000	1.0000
14.0000	.0000	.0000	1.0000
14.5000	.0000	.0000	1.0000
15.0000	.0000	.0000	1.0000
15.5000	.0000	.0000	1.0000
16.0000	.0000	.0000	1.0000
16.5000	.0000	.0000	1.0000
17.0000	.0000	.0000	1.0000
17.5000	.0000	.0000	1.0000
18.0000	.0000	.0000	1.0000
18.5000	.0000	.0000	1.0000
19.0000	.0000	.0000	1.0000
19.5000	.0000	.0000	1.0000
20.0000	.0000	.0000	1.0000
20.5000	.0000	.0000	1.0000
21.0000	.0000	.0000	1.0000
21.5000	.0000	.0000	1.0000
22.0000	.0000	.0000	1.0000
22.5000	.0000	.0000	1.0000
23.0000	.0000	.0000	1.0000
23.5000	.0000	.0000	1.0000
24.0000	.0000	.0000	1.0000
24.5000	.0000	.0000	1.0000
25.0000	.0000	.0000	1.0000
25.5000	.0000	.0000	1.0000
26.0000	.0000	.0000	1.0000
26.5000	.0000	.0000	1.0000
27.0000	.0000	.0000	1.0000
27.5000	.0000	.0000	1.0000
28.0000	.0000	.0000	1.0000

28.5000	.0000	.0000	1.0000
29.0000	.0000	.0000	1.0000
29.5000	.0000	.0000	1.0000
30.0000	.0000	.0000	1.0000
30.5000	.0000	.0000	1.0000
31.0000	.0000	.0000	1.0000
31.5000	.0000	.0000	1.0000
32.0000	.0000	.0000	1.0000
32.5000	.0000	.0000	1.0000
33.0000	.0000	.0000	1.0000
33.5000	.0000	.0000	1.0000
34.0000	.0000	.0000	1.0000
34.5000	.0000	.0000	1.0000
35.0000	.0000	.0000	1.0000
35.5000	.0000	.0000	1.0000
36.0000	.0000	.0000	1.0000
36.5000	.0000	.0000	1.0000
37.0000	.0000	.0000	1.0000
37.5000	.0000	.0000	1.0000
38.0000	.0000	.0000	1.0000
38.5000	.0000	.0000	1.0000
39.0000	.0000	.0000	1.0000
39.5000	.0000	.0000	1.0000
40.0000	.0000	.0000	1.0000
40.5000	.0000	.0000	1.0000
41.0000	.0000	.0000	1.0000
41.5000	.0000	.0000	1.0000
42.0000	.0000	.0000	1.0000
42.5000	.0000	.0000	1.0000
43.0000	.0000	.0000	1.0000
43.5000	.0000	.0000	1.0000
44.0000	.0000	.0000	1.0000
44.5000	.0000	.0000	1.0000
45.0000	.0000	.0000	1.0000
45.5000	.0000	.0000	1.0000
46.0000	.0000	.0000	1.0000
46.5000	.0000	.0000	1.0000
47.0000	.0000	.0000	1.0000
47.5000	.0000	.0000	1.0000
48.0000	.0000	.0000	1.0000
48.5000	.0000	.0000	1.0000
49.0000	.0000	.0000	1.0000
49.5000	.0000	.0000	1.0000
50.0000	.0000	.0000	1.0000
50.5000	.0000	.0000	1.0000

## APPENDIX E-1

```

PROGRAM CSPFIN
C
C      COMPARATIVE SCOUR PROGRAM :Comparisom with detailed estuary
results
C      2/10/05
C
C      d, D,  b, L = pier diameter
C      ds      = scour depth for live bed or clear water scour
C      dse     = equilibrium scour depth for live bed scour
C      f       = bed factor
C      fn      = pier shape factor
C      F,      = Froud number based on pier diameter
C      g       = acceleration due to gravity
C      B, C    = constant
C      Kyb    =  $y/b$ 
C      KI     =  $[V-(V_a-V_c)]/V_c$ 
C      Kd     =  $b/d50$ 
C      Ks     = ratio of scour depth for a particular pier shape to the
scour
C      depth for a circular
C      pier
C      KG     = approach channel geometry factor used with bridge
abutments only
C      Kt     = time factor; ratio of the local scour depth at a
particular time
C      to the equilibrium
C      local scour depth
C      K?     = bridge alignment factor used with non cylindrical piers
only
C      K1, K2 , K5      = scour factors that are functions of g, and y/b
C      K, K3, K4= other scour factors
C      Q, q      = discharge
C      R         = channel hydraulic radius
C      Re       = Reynolds number
C      U        = mean free stream horizontal velocity (ft/s)
C      u        = horizontal component of the estuary velocity that
varies
C                  vertically according to the turbulent flow profile
(ft/s)
C
C      V       = mean free stream horizontal velocity (ft/s)
C      Va     = stream velocity where scouring begins to transition from
clear
C                  water to live bed
C      Vc     = critical velocity for bed movement
C      x      = the distance along the horizontal axis measured from the
center
C                  of the pier
C      y      = vertical displacement from estuary bed
C      Ym     = flow depth
C      VOR    = vorticity ft/sec per ft
C      RHO    = water density
C      MU     = viscosity
C      GAMMA  = specific weight of water =*g

```

```

C      K      = von Karman constant
C      PI      = 3.142
C      Vd      = the downflow velocity
C      Vt      = vortex tangential velocity at any given distance from
the
C              center (ft/s)
C      f      = the angle of internal friction of the bed material.

REAL b,  B1, YRS,  KTM,  VM,  KC,  K3,  K4
REAL T,  g,  PI,  AMP,  K,  KS,  KTHET, KI, KNEIL
REAL ESTWID, TIME, TEMAX, KYBMAX,  KD
REAL VCRITM, F1,  FRMAX, FRCMAX, ALPHA
REAL QMAX,  VMAX,  YTMAX,  D50M
REAL VCSM,  nMAX,  KGAO, NU, N, N1, N2, N3, N4
REAL DSJAIM, VT, VCRIN, INDX, DEME

C
C

CHARACTER*50 FILE1, FILE2

C      OPEN INPUT FILE AND READ IN DATA
C

WRITE(*,*) 'ENTER THE NAME OF THE INPUT FILE'
READ(*,*) FILE1

OPEN (6, FILE= FILE1, STATUS = 'OLD', IOSTAT = IERROR)

C      CREATE AND OPEN OUTPUT FILE

WRITE(*,*) 'ENTER THE NAME OF THE OUTPUT FILE'
READ(*,*) FILE2

OPEN (12, FILE = FILE2, STATUS = 'UNKNOWN')

READ(6,*)
READ(6,*)
READ(6,*)
READ(6,*) b, YRS, QMAX, VMAX, YTMAX, VT
READ(6,*)
READ(6,*)
READ(6,*) D50M, AMP, ESTWID

C
C
C      COMPUTATION INPUT DATA DATA  for 100 yr events

C      CONVER is the conversion factor from meters to feet
C      PARAMETERS
      CONVER = 3.28
      g = 32.2
      PI = 3.142

```

```

C      COMPUTED VARIABLES
      WRITE(*,8)
8      FORMAT('debug 8')

C      CHANGE COMPUTED VARIABLES TO S I UNITS

      gm = 9.81
      bm = 0.3048*b

      QMMAX = 0.028*QMAX
      VMMAX = 0.3048*VMAX

      YMMAX = 0.3048*YTMAX
      D50MET= D50M/1000
      AMPM  = 0.3048*AMP
      ESTWM = 0.3048*ESTWID
C      Kinematic viscosity for water NU = 10**(-6) m**2/s

      NU = 0.000001

C      COMPUTE VARIABLE TO BE USED

      TIME =      YRS*365.25

C      f1 is Lacey's silt factor

      F1      =  D50M**(-0.57)

      B1      =  ESTWM
C      B1 is the estuary width in meters

      ALPHA = (ESTWM - bm)/ESTWM

      N      = -0.0094*D50M**2 + 0.109*D50M + 0.711
      IF (D50M.GE.16.2) N=0

      N1     = 1.13*EXP(-0.07*D50M)
      IF (D50M.GE.133.32) N1=0

      N2     = 1
      N3     = 1.15
      N4     = 0.90

      WRITE(*,9)
9      FORMAT('debug 9')

      VCRIN  = (0.476*(D50M/b)**0.053)*(1.66*D50M**0.333*YTMAX**0.167)

      FRMAX   =      VMAX/(g*YTMAX)**0.5

      FbMAX   =      VMAX/(g*b)**0.5

      q1MAX    =      QMMAX/(ESTWM)

      qbMAX    =      QMMAX/(ESTWM/bm)

```

```

FbMMAX = VMMAX/(gm*bm)**0.5

YRMAX = 1.48*(qbMAX**2/(1.9*D50M**0.5))**0.33

FRMMAX = VMMAX/(gm*YMMAX)**0.5

YARUM = 1.34*((qbMAX)**2*D50M**(-0.57))**0.33

VCRITM = 1.75*(D50M)**0.33*(YTMAX)**0.17

FRCMAX = VCRITM/(g*YTMAX)**0.5

IF(YTMAX/b.GT.6.AND.VMAX/VCRITM.GT.0.4) THEN
  TEMAX = 48.26*(b/VMAX)*(VMAX/VCRITM - 0.4)

ELSE IF(YTMAX/b.LE.6.AND.VMAX/VCRITM.GT.0.4) THEN
  TEMAX = 30.89*(b/VMAX)*(VMAX/VCRITM - 0.4)*(YTMAX/b)**0.25

ELSE

  TEMAX = 1
END IF

WRITE(*,11)
11 FORMAT('debug 11')

IF ( b/YTMAX.LT.0.7) KYBMAX = 2.4*b
IF ( b/YTMAX.GE.0.7.AND. b/YTMAX.LT.5) KYBMAX = 2*(b*YTMAX)**0.5
IF ( b/YTMAX.GE.5) KYBMAX = 4.5*YTMAX

C KS and KTHETA is 1 for cylindrical piers

K = 1
KNEIL = 1.25
KS = 1
KTHET = 1
KI = 1
KMUS = 1.9
KTM = exp(-0.03*ABS((VCRITM/VMAX)*LOG(TIME/TEMAX))**1.6)

T = 12
VM = 2*PI*AMP/T
KC = VM*T/b
KF = 1

KD = 1
IF((bm/D50MET).LE.25) KD= 0.57*log10(2.24*(bm/D50MET))
WRITE(*,12)
12 FORMAT('debug 12')

K1 = 1
K2 = 1

```

```

K3      = 1
K4      = 1
K5      = 1
KFMMAX  = 1.0
K5MMAX  = 3.5
KLAC    = 2.09
KIND    = 1.92
KING    = 2

VCRTGM= (YMMAX/(D50M/1000))**0.14*(17.6*1.65*D50M/1000 +
`      (6.05/10000000)*( (10+YMMAX)/(D50M/1000)**0.72) )**0.5

VCSM   = 0.645*((D50M/1000)/(bm))**0.053*VCRTGM
nMAX   = (VCRTGM/(VMMAX))** (9.35+2.23*log10(D50M/1000))

KGAO   = 1

Fd     = D50M**(0.526)

drMAX  = (qbMAX**2/Fd)**(0.333)

Ffact  = D50M**(0.568)

WRITE(*,13)
13 FORMAT('debug 13')

RebmM  =      VMMAX*bm/NU

INDX   = 1.0

*****
*****
C                               SCOUR EQUATIONS
*****
*****
C
C      2      Breusers           EstuaryScour  ds =1.4b
C      3      Englis             dse/b=2.32(q**0.67/b)**0.78
C      4      Englis             dse=0.47K(Q/ f1)**0.33
C      5      Laursen &Toch      dse/b=1.5(y/b)**0.30
C      6      Hancu              dse/b=3.3(d/b)**0.20(y/b)**0.13
C      7      Coleman            dse/b=1.49(U**2/gy)**0.10
C      8      Basak et al        dse=0.558b**0.586
C      9      Neill              dse=1.34K(q**2/ f1)**0.5
C     10      Andru              dseFb**0.33 =2.67[Q/(B-b)]**0.67
C     11      Railways Ministry, India  dse=0.47K(Q f1)**0.33
C     12      Izzard& Bradley      dse =2.15[Q/(B-b)]**0.67
C     13      Jain & Fischer        dse/b=2.0(y/b)**0.5[Fr -Frc]**0.25
C                                     ; Frc is the Froud number at the critical
velocity
C     14      HEC18              ds=2yK1 K2 K3 K4[b/y]**0.65 Fr**0.34
C                                     Terms are defined in the HEC 18 manual.
C                                     These terms are equivalent to Ks, KI , KG ,
Ktheta

```



```

C      15   Laursen 1958      dse/y=0.182(b/y){[( dse/11.5y)+1]**1.7-
1}**-1
C      16   Laursen 1958      dse/b=1.11(y/b)**0.5
C      17   Larras      1963   ds/b=1.05b**0.75 for circular piers
C      18   Blench      1969   ds/b=1.8(yr/b)**0.75-y/b; yr =
1.48(q**2/1.9d**0.5)**0.33
C      19   Coleman      1971   ds/b=0.54(y/b)**0.41(U**2/gy)**0.6y**0.41
C      20   Hancu 1971   ds/b=2.42[(2V/Vc)-1](y/b)**0.33(Vc**2/gb)**0.33
C                                     (2V/Vc)-1=1 for live bed
C      21   Chitale 1988      ds=2.5b
C      22   Melville 1997      ds=Kyb Kd [(V-(Va-Vc)/Vc] ;
C                                     Kyb =2.4b for b/y<0.7, 2(by)0.5 for
0.7<b/y<5,4.5y for b/y>5
C                                     Kd= 0.057log(2.44b/ d50) for B/d50<=25,1for
B/d50>25
C      23   Gao et al      ds=0.46Kb**0.6 y**0.15 d**-0.07[(V-
V*c)/(Vc-V*c]**n ;      n=1
C      24   Richardson & Davis 1995      ds/b=2K3 K4[y/b]*0.35* Fr
0.43
C      25   Lacey      ds=K(0.473)(Q d50**-0.57)**0.33
C      26   Maza & Sanchez      dse/b=2Kf K5 (V**2/gb)- 30(d/b)
C      27   Garde      ds/y=4nln2n3(1/a) Frn
C      28   Froelich      dse/L=2.27KsKtheta(y/L)**0.57 Fr**0.61
C      29   Melville      ds/b=2.0[1-exp(-0.03{KC-6})]; KC = VmT/b
C                                     ; Vm = maximum oscillatory flow; T=s the
wave period
C      30   The Demetruis model: ds= Tanh (y/b)*(Vt-Vc)**0.5*Vt**2/2g
C      SCOUR EQUATIONS COMPUTATION

*****
*****
C                                     Rational formulas
*****
*****
C      DSB2 is Breusers eqn (independent of Q or V)

      DSB2 = CONVER*(1.4*bm)

C      DSLAR      Laursen 1958      dse/b=1.11(y/b)**0.5. Dimensionless
ratio - eqn

      DSLARM= b*(1.11*(YTMAX/b)**0.5)

C      Laursen Toch and Neill ds = 1.35*b**0.7*y**0.3

      DSLTNM = CONVER*(bm**0.7)*(YMMAX**0.3)

C      DSENG is the Inglis eqn 1      determined from field data

      DSINGM = CONVER*bm*2.32*(qbMAX**0.67/bm)**0.78

      WRITE(*,14)
14 FORMAT('debug 14')

C      DSIN2 is Inglis eqn 2      determined from river data

      DSIN2M =CONVER*(0.47*KING*(QMMAX/ F1)**0.33 )

```

C DSE31 Breusers  $ds/b = (2.0 * \tanh(y/b)) * KS * KTHET$ . Dimensionless  
eqn

$$DSBREM = b * KS * KTHET^2 * \tanh(YTMAX/b)$$

C Sanchez and Maza  $ds/b = KF * K5 * Fb^{**2} - (30 * D50 \text{ in cms/b}) * KTHET$ . Dimensionless eqn

$$DSMSM = 0$$

$$IF (KFMMAX * K5MMAX * (FbMMAX^{**2}) .GT. (30 * (D50M/10) / bm)) DSMSM =$$

$$CONVER * bm * (KFMMAX * K5MMAX * (FbMMAX^{**2}) - (30 * (D50M/10) / bm))$$

C Shen et al.  $ds = 0.0002225 * Rebm^{**0.619}$  wher Rebm is the pier  
reynolds number in meters

$$DSSM = 0.0002225 * Rebm^{**0.619}$$

C Larras 1963  $ds/b = 1.05b^{**0.75}$  for circular piers

$$DSLARR = CONVER * bm * (1.05 * bm^{**0.75})$$

C DSE5 Laursen & Toch  $dse/b = 1.5(y/b)^{**0.30}$  independent of Q, V  
C Dimensionless ratio-equation

$$DSLTM = b * 1.5 * (YTMAX/b)^{**0.30}$$

WRITE(\*,15)  
15 FORMAT('debug 15')

C DSE6 Hancu  $dse/b = 2.42(y/b)^{**0.33} * Fr^{**0.67}$  Dimensionless ratio  
eqn

$$DSHANM = b * 2.42 * (YTMAX/b)^{**0.33} * FRMAX^{**0.67}$$

C Hancu eq 1971  $ds/b = 2.42[(2V/Vc) - 1](Vc^{**2}/gb)$  For  
0.05 < Vc/bg < 0.6

$$DSHAM = b * 2.42 * ((2 * VMAX / VCRITM) - 1) * (VCRITM^{**2} / (g * b))$$

C Hanchu eq 3 Unknown paper

$$DSHA2M = CONVER * 3.3 * (D50M/bm)^{**0.2} * (YMMAX/bm)^{**0.13}$$

C Froelich's eqn 1988 with adjustments for circular piers  
C Ref Peggy Johnson's Dissertation  
C  $ds = b * 0.32K1(b'/b)^{**0.62} * (y/b)^{**0.46} * F^{**0.2} * (b/d50)^{**0.08} + 1$

$$DSFROM = CONVER * bm * 0.32 * (YMMAX/bm)^{**0.46} * (VMMAX / (gm * bm))^{**0.5} * 0.2 * (bm/D50MET)^{**0.08} + CONVER$$

C DSE7 Coleman  $dse/b = 1.49(U^{**2}/gy)^{**0.10}$  dimensionless

$$DSCOLM = b * 1.49 * (FRMAX^{**2})^{**0.10}$$

C Second Coleman equation  $ds = b * 0.54 * (y/b)^{**0.19} * Fr^{**1.19} * Y^{**0.41}$

```

DSCO2M
=CONVER*bm*0.54*(YMMAX/bm)**0.19*FbMMAX**1.19*YMMAX**0.41
WRITE(*,17)
17 FORMAT('debug 17')

C      DSE8 Basak et al      dse=0.558b**0.586

      DSBASA = CONVER*(0.558*bm**0.586)

C      DSE9 Neill dse=1.34K(q**2/ f1)**0.5      Field data

      DSNELM= CONVER*1.34*KNEIL* (q1MAX**2/ F1)**0.5

      WRITE(*,18)
18 FORMAT('debug 18')

C      Neill second eqn DSE = 1.5b for circular piers

      DSNEI2 = CONVER*(1.5*bm)

C      Second form of Neils eq1 Dimensionless

      DSNE3M = 1.34*b*(YTMAX/b)**0.5

C      Jain & Fischer      dse/b=2.0(y/b)**0.5[Fr - Frc]**0.25
Dimensionless

      DSJFM = 0
      IF(FRMAX.GT.FRCMAX) DSJFM = b*2.0*(YTMAX/b)**0.5*
      (FRMAX - FRCMAX)**0.25

C      Jain dse/b=1.84(y/b)**0.3*Frc**0.25 Dimensionless

      DSJAIM = b*1.84*(YTMAX/b)**0.3*FRCMAX**0.25

C      DSCHIT      Chitale 1988      ds=2.5b
      DSCHIT = CONVER*2.5*bm

C      Colorado state University HEC18 ds=2yK1 K2[b/y]**0.65 Fr**0.43
dimensionless

      DSCSUM = 2*YTMAX*K1*K2*(b/YTMAX)**0.65*FRMAX**0.43

C      Richardson and Davis HEC18 1995 ds=2KSKTHETK3K4[b/y]**0.65
Fr**0.43      dimensionless

      RADSUM = 2*YTMAX*KS*KTHET*K3*K4*(b/YTMAX)**0.65*FRMAX**0.43

C      Gao et al ds=0.46Kb**0.6 y**0.15 d**-0.07[(V-V*c)/(Vc-V*c)]**n ;
      WRITE(*,19)
19 FORMAT('debug 19')

```

```

        DSGAOM = 0
        IF(VMMAX.GT.VCSM) DSGAOM =CONVER*0.46*KGAO*(bm)**0.6*(YMMAX)**
        ` 0.15*(D50M/1000)**(-0.07)*((VMMAX -VCSM)/(VCRTGM -VCSM))**nMAX

C      DSE22      Melville 1997      ds=Kyb Kd Ki Kt;

        DSMELM  = KYBMAX* KD *KI*KTM

        WRITE(*,20)
20  FORMAT('debug 20')

C      DSMELW      Melville ds/b=2.0[1-exp(-0.03{KC-6})];  KC = VmT/b
        DSMELW = 0
        IF(KC.GT.6.0)  DSMELW = b*(2.0*(1-exp(-0.03*(KC-6))))

        WRITE(*,21)
21  FORMAT('debug 21')

*****
*****
C      Regime formulas
*****
*****

C      original Lacy      ds=(0.473)(Q d50**-0.57)**0.33

        DSLAOM = CONVER*(0.473)*(QMMAX*(D50M**(-0.57)))**0.33

C      DLAC Lacey ds=K(0.473)(Q d50**-0.57)**0.33

        DSLACM = CONVER*KLAC*(0.473)*(QMMAX*(D50M**(-0.57)))**0.33

C      Arunachalam's formula

        DSARUM =CONVER*bm*(YARUM/bm)*((1.72*bm**0.05/(YARUM/bm)**0.167)-
1)

C      Mustaq Formula

        DSMUSM = CONVER*1.468*KMUS*qbMAX**.67

C      Blench      1969 first formula      ds/b=1.8(yr/b)**0.75-y/b;  yr
= 1.48(q**2/1.9d**0.5)**0.33

        DSBL1M = 0
        IF(1.8*(YRMAX/bm)**0.75 - (YMMAX/bm).GT.0) DSBL1M= CONVER*bm*
        ` (1.8*(YRMAX/bm)**0.75 - (YMMAX/bm))

C      Blenches second formula

        DSBL2M =      CONVER*1.8*drMAX*(bm/drMAX)**0.25

C      Sethi's formula

```

```

DSSETM = CONVER* 2.11*(q1MAX**2/ Ffact)**0.333

C      RDSO's Formula

DSRDM = CONVER*1.71*(YMMAX)

*****
*****
C
Additional Models
*****
*****

C      Andru      dseFb**0.33 =2.67[Q/(B-b)]**0.67

DSANDM = CONVER*(FbmMAX**0.33)*2.67*(QMMAX/(ESTWM-bm))**0.67

C      11      Railways Ministry, India      dse=0.47K(Q f1)**0.33. Real data
from Indian rivers

DSINDM = CONVER*KIND*(QMMAX*F1)**0.33

C      12      Izzard& Bradley      dse =2.15[Q/(B-b)]**0.67

DSIZBM = CONVER*2.15*(QMMAX/(ESTWM-bm))**0.67

C      d = Y *(4/ALPHA)n*n1*n2*n3*n4F**n      Unified model from paper
with unknown reference

DSUNIM = CONVER*YMMAX*(4/ALPHA)*N1*N2*N3*N4*FRMMAX**N

C      The Demetrius ultimate scour model

DEME = 0
IF(VT.GT.VCRIN) DEME =b*(TANH(YTMAX/b))*((VT - VCRIN)**INDX))

*****
*****
C
DISPLAY RESULTS
C
*****
*****
WRITE(12,*) 'b =',b
WRITE(12,*) 'YRS =',YRS
WRITE(12,*) 'VMAX =',VMAX
WRITE(12,*) 'QMAX =',QMAX

```

```

WRITE(12,*) 'YTMAX =',YTMAX
WRITE(12,*) 'VT =',VT

WRITE(12,*)
WRITE(12,*) 'YMMAX =', YMMAX
WRITE(12,*) 'N =', N
WRITE(12,*) 'N1 =', N1
WRITE(12,*) 'N2 =', N2
WRITE(12,*) 'N3 =', N3
WRITE(12,*) 'N4 =', N4
WRITE(12,*) 'ALPHA =', ALPHA
WRITE(12,*) 'FRMMAX =',FRMMAX
WRITE(12,*) 'VCRIN =',VCRIN
WRITE(12,*)
WRITE(12,*)
WRITE(12,*) 'M indicate maximum conditions (V,Q, Y)'
WRITE(12,*)
WRITE(12,*)
WRITE(12,*) 'Breusers eq1. based on estuary data = ', DSBR2

WRITE(12,*) 'Breusers eqn2 f(y/b) (M) = ',DSBREM

WRITE(12,*) 'Laursens equation (M) =',DSLARM

WRITE(12,*) 'Laursen &Toch (M)= ', DSLTM

WRITE(12,*) 'Lauresn Neills Toch (M) = ',DSLTNM

WRITE(12,*) 'Inglis eqn lab data(M) = ',DSINGM

WRITE(12,*) 'Inglis eqn2 field data (M) = ',DSIN2M

WRITE(12,*) 'Sanchez and Maza (M) = ',DSMSM

WRITE(12,*) 'Shen et al. (M) = ',DSSM

WRITE(12,*) 'Larras 1963 for circular piers = ',DSLARR

WRITE(12,*) 'Hancu eq1-Dimensionless ratio (M)= ',DSHANM

WRITE(12,*) 'Hancu eq2 paper unknown ref.(M)= ',DSHA2M

WRITE(12,*) 'Froelichs eqn 1988 for circular piers(M)= ',DSFROM

WRITE(12,*) 'Coleman eq 1 dimensionless (M)= ',DSCOLM

```

```

WRITE(12,*)'Coleman      eq 2 dimensionless (M)= ',DSCO2M

WRITE(12,*)'Basak et al = ',DSBASA

WRITE(12,*)'Neill eq1, field data (M)= ',DSNELM

WRITE(12,*)'Neill eq2, field data = ',DSNEI2

WRITE(12,*)'Neill eq3, field data (M)= ',DSNE3M

WRITE(12,*)'Jain & Fischer,Dimensionless(M)= ',DSJFM

WRITE(12,*)'Jain ,Dimensionless(M)= ',DSJAIM

WRITE(12,*)'Chitale 1988      = ',DSCHIT

WRITE(12,*)'Colorado state University HEC18 (M)= ',DSCSUM

WRITE(12,*)'Richardson and Davis HEC18 1995 (M)= ',RADSUM

WRITE(12,*)'Gao et al, (M)= ',DSGAOM

WRITE(12,*)'Melville Eq 1 1997(M)= ',DSMELM

WRITE(12,*)'Melville Eq 2 for waves= ',DSMELW

WRITE(12,*)'original Lacy, Field data (M)= ',DSL AOM

WRITE(12,*)'Lacy revised by others, Field data (M)= ',DSLACM

WRITE(12,*)'Arunachalams formula (M)= ',DSARUM

WRITE(12,*)'Mustaqs formula (M)= ',DSMUSM

WRITE(12,*)'Blench Eq 1 1969 (M)= ',DSBL1M

WRITE(12,*)'Blench Eq 2 (M)= ',DSBL2M

WRITE(12,*)'Sethis formula (M)= ',DSSETM

```

```

WRITE(12,*)'RDSOs Formula (M)= ',DSRDM

WRITE(12,*)'Andrus Formula (A)= ',DSANDM

WRITE(12,*)'Railways Ministry, India (M)= ',DSINDM

WRITE(12,*)'Izzard& Bradley (A)= ',DSIZBM

WRITE(12,*)'Unified model unknown reference (M)= ',DSUNIM

WRITE(12,*)'The Demetrius ultimate scour model (M)= ',DEME

CLOSE (12, STATUS = 'REPLACE')

END

```



## Appendix E-2

TITLE: COMPARITIVE SCOUR INPUT FILE NAME: CSPMONU.DAT  
PROJECT NAME: MONIE BAY U/STREAM PIER FACE DATE: 4/09/05  
Pier diam(b) Time(YRS) QMAX VMAX YTMAX VT  
5.0 100 50550 0.66 9.24 0.32

D50M AMP ESTWID  
0.135 1.19 5808

TITLE: COMPARITIVE SCOUR INPUT FILE NAME: CSMOND.DAT  
PROJECT NAME: MONIE BAY D/STREAM PIER FACE DATE: 4/09/05  
Pier diam(b) Time(YRS) QMAX VMAX YTMAX VT  
5.0 100 50527 1.41 10.00 2.29

D50M AMP ESTWID  
0.135 1.19 5808

TITLE: COMPARITIVE SCOUR INPUT FILE NAME: CSPBLKU.DAT  
PROJECT NAME: BLACK RIVER UPSTREAM PIER FACE DATE: 2/15/05  
Pier diam(b) Time(YRS) QMAX VMAX YTMAX VT  
5.0 100 211024 1.21 14.75 0.54

D50M AMP ESTWID  
0.15 0.935 8580

TITLE: COMPARITIVE SCOUR INPUT FILE NAME: CSPBLKD.DAT  
PROJECT NAME: BLACK RIVER D/STREAM PIER FACE DATE: 4/09/05  
Pier diam(b) Time(YRS) QMAX VMAX YTMAX VT  
5.0 100 201669 1.97 15.0 1.89

D50M AMP ESTWID  
0.15 0.935 8580

TITLE: COMPARITIVE SCOUR INPUT FILE NAME: CPX30105.DAT  
PROJECT NAME: PATUXENT RIVER UPSTREAMS PIER FACE DATE:  
3/13/05  
Pier diam(b) Time(YRS) QMAX VMAX YTMAX VT  
5.0 100 125435 2.71 18.05 1.79

D50M AMP ESTWID  
0.25 0.935 3333

TITLE: COMPARITIVE SCOUR INPUT FILE NAME: Csptxd.DAT  
PROJECT NAME: PATUXENT RIVER D/STREAMS PIER FACE DATE: 3/13/05  
Pierd(b) Time(YRS) QMAX VMAX YTMAX VT  
5.0 100 106351 1.98 18.3 2.34

D50M AMP ESTWID  
0.25 0.935 3333

TITLE: COMPARITIVE SCOUR INPUT FILE NAME: CSPWICU.DAT  
PROJECT NAME: WICOMICO RIVER U/STREAM PIER FACE DATE:  
4/06/05  
Pier diam(b) Time(YRS) QMAX VMAX YTMAX VT

5.0                    100            86716        2.17        20.83    0.93

D50M    AMP        ESTWID  
0.325   1.19       1320

TITLE: COMPARITIVE SCOUR INPUT FILE NAME: CSPWICU.DAT

PROJECT NAME: WICOMICO RIVER D/STREAM PIER FACE

DATE:

4/06/05

Pier diam(b)	Time(YRS)	QMAX	VMAX	YTMAX	VT
5.0	100	80450	2.68	21.0	3.39

D50M    AMP        ESTWID  
0.325   1.19       1320

TITLE: COMPARITIVE SCOUR INPUT FILE NAME: CSPBAL.DAT

PROJECT NAME: PATAPSCO RIVER UPSTREAM CONDITIONS

DATE:

3/21/05

Pier diam(b)	Time(YRS)	QMAX	VMAX	YTMAX	VT
5.0	100	129931	2.58	38.75	4.03

D50M    AMP        ESTWID  
0.15    0.935       1750

TITLE: COMPARITIVE SCOUR INPUT FILE NAME: CSPBALD.DAT

PROJECT NAME: PATAPSCO RIVER D/STREAM PIER FACE

DATE:

3/21/05

Pier diam(b)	Time(YRS)	QMAX	VMAX	YTMAX	VT
5.0	100	82579	1.19	39.25	0.42

D50M    AMP        ESTWID  
0.15    0.935       1750

### APPENDIX E-3

Monie Bay Upstream Pier Face

b = 5.000000  
 YRS = 100.000000  
 VMAX = 6.600000E-01  
 QMAX = 50555.000000  
 YTMAX = 9.240000  
 VT = 3.200000E-01  
  
 YMMAX = 2.798064  
 N = 7.376626E-01  
 N1 = 1.110397  
 N2 = 1.000000  
 N3 = 1.150000  
 N4 = 9.000000E-01  
 ALPHA = 9.991391E-01  
 FRMMAX = 3.781508E-02  
 VCRIN = 6.152749E-01

M indicate maximum conditions (V,Q, Y)

Breusers eq1. based on estuary data = 6.998208  
 Breusers eqn2 f(y/b) (M) = 9.504097  
 Laursens equation (M) = 7.520199  
 Laursen & Toch (M)= 8.999598  
 Laursen Neills Toch (M) = 5.998196  
 Inglis eqn lab data(M) = 9.351477  
 Inglis eqn2 field data (M) = 26.201710  
 Sanchez and Maza (M) = 0.000000E+00  
 Shen et al. (M) = 5.487777E-01  
 Larras 1963 for circular piers = 7.199243  
 Hancu eq1-Dimensionless ratio (M)= 1.647522  
 Hancu eq2 paper unknown ref.(M)= 8.159851  
 Froelichs eqn 1988 for circular piers(M)= 4.777487  
 Coleman eq 1 dimensionless (M)= 3.869627  
 Coleman eq 2 dimensionless (M)= 1.345939E-01  
 Basak et al = 2.342811  
 Neill eq1, field data (M)= 3.017028  
 Neill eq2, field data = 7.498080  
 Neill eq3, field data (M)= 9.078439  
 Jain & Fischer, Dimensionless(M)= 0.000000E+00  
 Jain ,Dimensionless(M)= 6.111146  
 Chitale 1988 = 12.496800  
 Colorado state University HEC18 (M)= 3.024879  
 Richardson and Davis HEC18 1995 (M)= 3.024879  
 Gao et al, (M)= 1.063566E-01  
 Melville Eq 1 1997(M)= 3.551483E-02  
 Melville Eq 2 for waves= 0.000000E+00  
 original Lacy, Field data (M)= 22.210480  
 Lacy revised by others, Field data (M)= 44.420950  
 Arunachalams formula (M)= 4.461293

Mustags formula (M)= 5.568727  
 Blench Eq 1 1969 (M)= 7.480761E-01  
 Blench Eq 2 (M)= 8.771392  
 Sethis formula (M)= 7.851331  
 RDSOs Formula (M)= 15.693780  
 Andrus Formula (A)= 2.866554  
 Railways Ministry, India (M)= 46.956610  
 Izzard& Bradley (A)= 6.153455  
 Unified model unknown reference (M)= 3.770343  
 The Demetrius ultimate scour model (M)= 0.000000E+00

Monie Bay Downstream Pier Face

b = 5.000000  
 YRS = 100.000000  
 VMAX = 1.260000  
 QMAX = 50916.000000  
 YTMAX = 10.000000  
 VT = 2.110000  
  
 YMMAX = 2.971800  
 N = 7.376626E-01  
 N1 = 1.110397  
 N2 = 1.000000  
 N3 = 1.150000  
 N4 = 9.000000E-01  
 ALPHA = 9.991391E-01  
 FRMMAX = 7.112810E-02  
 VCRIN = 6.214958E-01

M indicate maximum conditions (V,Q, Y)

Breusers eq1. based on estuary data = 6.998208  
 Breusers eqn2 f(y/b) (M) = 9.603194  
 Laursens equation (M) = 7.750154  
 Laursen & Toch (M)= 9.163716  
 Laursen Neills Toch (M) = 6.107581  
 Inglis eqn lab data(M) = 9.291948  
 Inglis eqn2 field data (M) = 26.096260  
 Sanchez and Maza (M) = 0.000000E+00  
 Shen et al. (M) = 8.266705E-01  
 Larras 1963 for circular piers = 7.199243  
 Hancu eq1-Dimensionless ratio (M)= 2.566237  
 Hancu eq2 paper unknown ref.(M)= 8.224003  
 Froelichs eqn 1988 for circular piers(M)= 5.095585  
 Coleman eq 1 dimensionless (M)= 4.390807  
 Coleman eq 2 dimensionless (M)= 3.067586E-01  
 Basak et al = 2.342811  
 Neill eq1, field data (M)= 2.980385  
 Neill eq2, field data = 7.498080  
 Neill eq3, field data (M)= 9.356041  
 Jain & Fischer, Dimensionless(M)= 0.000000E+00  
 Jain ,Dimensionless(M)= 6.191743  
 Chitale 1988 = 12.496800  
 Colorado state University HEC18 (M)= 4.053652

Richardson and Davis HEC18 1995 (M)= 4.053652  
 Gao et al, (M)= 4.192363  
 Melville Eq 1 1997(M)= 4.830154  
 Melville Eq 2 for waves= 0.000000E+00  
 original Lacy, Field data (M)= 22.121090  
 Lacy revised by others, Field data (M)= 44.242180  
 Arunachalams formula (M)= 4.440223  
 Mustags formula (M)= 5.523321  
 Blench Eq 1 1969 (M)= 1.183653E-01  
 Blench Eq 2 (M)= 8.718017  
 Sethis formula (M)= 7.787693  
 RDSOs Formula (M)= 16.668230  
 Andrus Formula (A)= 3.537247  
 Railways Ministry, India (M)= 46.767640  
 Izzard& Bradley (A)= 6.103281  
 Unified model unknown reference (M)= 6.381751  
 The Demetrius ultimate scour model (M)= 7.147196

-----  
 -----  
 -----

#### Black River Upstream Pier Face

b = 5  
 YRS = 100  
 VMAX = 1.21  
 QMAX = 211024  
 YTMAX = 15.5  
 VT = 5.40E-01  
  
 YMMAX = 4.4958  
 N = 7.27E-01  
 N1 = 1.118197  
 N2 = 1  
 N3 = 1.15  
 N4 = 9.00E-01  
 ALPHA = 9.99E-01  
 FRMMAX = 5.69E-02  
 VCRIN = 5.47E-01

M indicate maximum conditions "(V,Q," Y)

Breusers eq1. based on estuary 7.00 =  
 Breusers eqn2 f(y/b) (M) = 9.95  
 Laursens equation (M) = 9.53  
 Laursen &Toch (M)= 10.38  
 Lauresn Neills Toch (M) = 6.92  
 Inglis eqn lab data(M) = 15.73  
 Inglis eqn2 field data (M) 37.60  
 Sanchez and Maza (M) = 0.00  
 Shen et al. (M) = 0.82  
 Larras 1963 for circular piers 7.20  
 Hancu eq1-Dimensionless ratio (M)= 2.53  
 Hancu eq2 paper unknown ref.(M)= 7.84

Froelichs	eqn	1988	for circular	6.13	
Coleman	eq	1	dimensionless	(M)=	4.20
Coleman	eq	2	dimensionless	(M)=	0.39
Basak et	al	=	2.34		
Neill	"eq1,"	field data	(M)=	7.06	
Neill	"eq2,"	field data	=	7.50	
Neill	"eq3,"	field data	(M)=	11.51	
Jain &	"Fischer,Dimensionless(M)="				0.00
Jain	" ,Dimensionless(M)="				6.50
Chitale	1988	=	12.50		
Colorado	state University	HEC18	(M)=	4.26	
Richardson	and Davis	HEC18	1995	4.26	
Gao et	"al,"	(M)=	3.91		
Melville	Eq	1	1997(M)=	5.71	
Melville	Eq	2	for waves=	0.00	
original	"Lacy,"	Field data	(M)=	38.63	
Lacy revised	by	"others,"	Field	77.25	(M)=
Arunachalams	formula	(M)=		6.70	
Mustaqs	formula	(M)=		10.85	
Blench	Eq	1	1969 (M)=	2.56	
Blench	Eq	2	(M)=	15.42	
Sethis	formula	(M)=		16.78	
RDSOs Formula	(M)=		25.22		
Andrus	Formula	(A)=		6.91	
Railways	"Ministry,"	India (M)=		81.66	
Izzard&	Bradley	(A)=		11.99	
Unified	model unknown	reference	(M)=	8.50	
The Demetrius	ultimate	scour model		0.07	

#### Black river Downstream Pier Face

b = 5.000000  
 YRS = 100.000000  
 VMAX = 1.970000  
 QMAX = 201669.000000  
 YTMAX = 15.750000  
 VT = 1.890000  
  
 YMMAX = 4.800600  
 N = 7.271385E-01  
 N1 = 1.118197  
 N2 = 1.000000  
 N3 = 1.150000  
 N4 = 9.000000E-01  
 ALPHA = 9.994172E-01  
 FRMMAX = 7.861510E-02  
 VCRIN = 5.528238E-01

M indicate maximum conditions (V,Q, Y)

Breusers eq1. based on estuary data =	6.998208
Breusers eqn2 f(y/b) (M) =	9.963341
Laursens equation (M) =	9.850273
Laursen &Toch (M)=	10.581680
Lauresn Neills Toch (M) =	7.052644

Inglis eqn lab data(M) = 15.613450  
 Inglis eqn2 field data (M) = 37.419360  
 Sanchez and Maza (M) = 0.000000E+00  
 Shen et al. (M) = 1.020231  
 Larras 1963 for circular piers = 7.199243  
 Hancu eq1-Dimensionless ratio (M)= 3.214765  
 Hancu eq2 paper unknown ref.(M)= 7.902953  
 Froelichs eqn 1988 for circular piers(M)= 6.550099  
 Coleman eq 1 dimensionless (M)= 4.479580  
 Coleman eq 2 dimensionless (M)= 6.129282E-01  
 Basak et al = 2.342811  
 Neill eq1, field data (M)= 6.955616  
 Neill eq2, field data = 7.498080  
 Neill eq3, field data (M)= 11.891320  
 Jain & Fischer,Dimensionless(M)= 5.899098  
 Jain ,Dimensionless(M)= 6.588862  
 Chitale 1988 = 12.496800  
 Colorado state University HEC18 (M)= 5.005332  
 Richardson and Davis HEC18 1995 (M)= 5.005332  
 Gao et al, (M)= 6.301048  
 Melville Eq 1 1997(M)= 8.028263  
 Melville Eq 2 for waves= 0.000000E+00  
 original Lacy, Field data (M)= 38.440060  
 Lacy revised by others, Field data (M)= 76.880130  
 Arunachalams formula (M)= 6.670786  
 Mustags formula (M)= 10.743970  
 Blench Eq 1 1969 (M)= 1.436194  
 Blench Eq 2 (M)= 15.310560  
 Sethis formula (M)= 16.619170  
 RDSOs Formula (M)= 26.925610  
 Andrus Formula (A)= 7.695870  
 Railways Ministry, India (M)= 81.268640  
 Izzard& Bradley (A)= 11.869890  
 Unified model unknown reference (M)= 11.476810  
 The Demetrius ultimate scour model (M)= 8.504589

-----  
 -----  
 -----

#### Patuxent River Upstream Pier Face

b = 5  
 YRS = 100  
 VMAX = 2.71  
 QMAX = 125435  
 YTMAX = 18.03  
 VT = 1.79  
  
 YMMAX = 5.57784  
 N = 7.38E-01  
 N1 = 1.110397  
 N2 = 1  
 N3 = 1.15  
 N4 = 9.00E-01

ALPHA = 9.98E-01  
 FRMMAX = 1.12E-01  
 VCRIN = 6.90E-01

M indicate maximum conditions "(V,Q," Y)

Breusers eq1. based on estuary 7.00 =  
 Breusers eqn2 f(y/b) (M) = 9.99  
 Laursens equation (M) = 10.62  
 Laursen &Toch (M)= 11.07  
 Lauresn Neills Toch (M) = 7.38  
 Inglis eqn lab data(M) = 19.90  
 Inglis eqn2 field data (M) 35.14  
 Sanchez and Maza (M) = 0.00  
 Shen et al. (M) = 1.33  
 Larras 1963 for circular piers 7.20  
 Hancu eq1-Dimensionless ratio (M)= 4.27  
 Hancu eq2 paper unknown ref.(M)= 8.93  
 Froelichs eqn 1988 for circular 7.25  
 Coleman eq 1 dimensionless (M)= 4.81  
 Coleman eq 2 dimensionless (M)= 1.11  
 Basak et al = 2.34  
 Neill "eq1," field data (M)= 12.79  
 Neill "eq2," field data = 7.50  
 Neill "eq3," field data (M)= 12.82  
 Jain & "Fischer,Dimensionless(M)=" 8.38  
 Jain ",Dimensionless(M)=" 7.10  
 Chitale 1988 = 12.50  
 Colorado state University HEC18 (M)= 6.13  
 Richardson and Davis HEC18 1995 6.13  
 Gao et "al," (M)= 6.68  
 Melville Eq 1 1997(M)= 9.06  
 Melville Eq 2 for waves= 0.00  
 original "Lacy," Field data (M)= 29.79  
 Lacy revised by "others," Field 59.57 (M)=  
 Arunachalams formula (M)= 7.36  
 Mustags formula (M)= 14.66  
 Blench Eq 1 1969 (M)= 2.00  
 Blench Eq 2 (M)= 18.05  
 Sethis formula (M)= 20.55  
 RDSOs Formula (M)= 31.28  
 Andrus Formula (A)= 12.09  
 Railways "Ministry," India (M)= 62.97  
 Izzard& Bradley (A)= 16.21  
 Unified model unknown reference (M)= 16.72  
 The Demetrius ultimate scour model 5.49

Patuxent River Downstream Pier Face

b = 5.000000  
 YRS = 100.000000  
 VMAX = 1.980000  
 QMAX = 106351.000000  
 YTMAX = 18.300000  
 VT = 1.790000



YMMAX = 5.577840  
 N = 7.376626E-01  
 N1 = 1.110397  
 N2 = 1.000000  
 N3 = 1.150000  
 N4 = 9.000000E-01  
 ALPHA = 9.984999E-01  
 FRMMAX = 8.158543E-02  
 VCRIN = 6.904048E-01

M indicate maximum conditions (V,Q, Y)

Breusers eq1. based on estuary data = 6.998208  
 Breusers eqn2 f(y/b) (M) = 9.986766  
 Laursens equation (M) = 10.617770  
 Laursen & Toch (M)= 11.068930  
 Laursen Neills Toch (M) = 7.377397  
 Inglis eqn lab data(M) = 18.252670  
 Inglis eqn2 field data (M) = 33.276770  
 Sanchez and Maza (M) = 0.000000E+00  
 Shen et al. (M) = 1.093551  
 Larras 1963 for circular piers = 7.199243  
 Hancu eq1-Dimensionless ratio (M)= 3.462956  
 Hancu eq2 paper unknown ref.(M)= 8.925474  
 Froelichs eqn 1988 for circular piers(M)= 7.010112  
 Coleman eq 1 dimensionless (M)= 4.512930  
 Coleman eq 2 dimensionless (M)= 7.663996E-01  
 Basak et al = 2.342811  
 Neill eq1, field data (M)= 10.848030  
 Neill eq2, field data = 7.498080  
 Neill eq3, field data (M)= 12.817850  
 Jain & Fischer, Dimensionless(M)= 5.489750  
 Jain ,Dimensionless(M)= 7.100477  
 Chitale 1988 = 12.496800  
 Colorado state University HEC18 (M)= 5.360045  
 Richardson and Davis HEC18 1995 (M)= 5.360045  
 Gao et al, (M)= 6.292767  
 Melville Eq 1 1997(M)= 7.402301  
 Melville Eq 2 for waves= 0.000000E+00  
 original Lacy, Field data (M)= 28.207810  
 Lacy revised by others, Field data (M)= 56.415620  
 Arunachalams formula (M)= 7.000618  
 Mustaq's formula (M)= 13.125710  
 Blench Eq 1 1969 (M)= 4.058765E-01  
 Blench Eq 2 (M)= 16.621740  
 Sethis formula (M)= 18.411420  
 RDSOs Formula (M)= 31.284990  
 Andrus Formula (A)= 9.762286  
 Railways Ministry, India (M)= 59.635960  
 Izzard & Bradley (A)= 14.510160  
 Unified model unknown reference (M)= 13.261960  
 The Demetrius ultimate scour model (M)= 8.29

-----  
 -----  
 -----

# Wicomico River Upstream Pier Face

```

b =          5.000000
YRS =        100.000000
VMAX =         2.170000
QMAX =      86717.000000
YTMAX =         20.840000
VT =         9.200000E-01

YMMAX =         6.352032
N =       7.454321E-01
N1 =         1.104583
N2 =         1.000000
N3 =         1.150000
N4 =       9.000000E-01
ALPHA =       9.962121E-01
FRMMAX =       8.378839E-02
VCRIN =       7.807509E-01

```

M indicate maximum conditions (V,Q, Y)

```

Breusers eq1. based on estuary data =          6.998208
Breusers eqn2 f(y/b) (M) =          9.995207
Laursens equation (M) =          11.330700
Laursen & Toch (M)=          11.509050
Laursen Neills Toch (M) =          7.670738
Inglis eqn lab data(M) =          26.621120
Inglis eqn2 field data (M) =          32.683120
Sanchez and Maza (M) =          0.000000E+00
Shen et al. (M) =          1.157369
Larras 1963 for circular piers =          7.199243
Hancu eq1-Dimensionless ratio (M)=          3.679824
Hancu eq2 paper unknown ref.(M)=          9.566609
Froelichs eqn 1988 for circular piers(M)=          7.516547
Coleman eq 1 dimensionless (M)=          4.537043
Coleman eq 2 dimensionless (M)=          9.240146E-01
Basak et al =          2.342811
Neill eq1, field data (M)=          24.068490
Neill eq2, field data =          7.498080
Neill eq3, field data (M)=          13.678510
Jain & Fischer,Dimensionless(M)=          5.595523
Jain ,Dimensionless(M)=          7.463886
Chitale 1988 =          12.496800
Colorado state University HEC18 (M)=          5.674144
Richardson and Davis HEC18 1995 (M)=          5.674144
Gao et al, (M)=          6.203473
Melville Eq 1 1997(M)=          7.223472
Melville Eq 2 for waves=          0.000000E+00
original Lacy, Field data (M)=          25.100730
Lacy revised by others, Field data (M)=          50.201460
Arunachalams formula (M)=          8.375849
Mustaqs formula (M)=          21.293700
Blench Eq 1 1969 (M)=          5.048223

```

Blench Eq 2 (M)= 23.033670  
 Sethis formula (M)= 28.340600  
 RDSOs Formula (M)= 35.627280  
 Andrus Formula (A)= 16.348550  
 Railways Ministry, India (M)= 53.067080  
 Izzard& Bradley (A)= 23.575870  
 Unified model unknown reference (M)= 15.063990  
 The Demetrius ultimate scour model (M)= 6.959117E-01

#### Wicomico River Downstream Pier Face

b = 5  
 YRS = 100  
 VMAX = 2.67  
 QMAX = 80450  
 YTMAX = 21.0  
 VT = 3.39  
  
 YMMAX = 6.397752  
 N = 7.45E-01  
 N1 = 1.104583  
 N2 = 1  
 N3 = 1.15  
 N4 = 9.00E-01  
 ALPHA = 9.96E-01  
 FRMMAX = 1.03E-01  
 VCRIN = 7.82E-01

M indicate maximum conditions "(V,Q," Y)

Breusers eq1. based on estuary 7.00 =  
 Breusers eqn2 f(y/b) (M) = 10.00  
 Laursens equation (M) = 11.37  
 Laursen &Toch (M)= 11.53  
 Lauresn Neills Toch (M) = 7.69  
 Inglis eqn lab data(M) = 25.60  
 Inglis eqn2 field data (M) 31.88  
 Sanchez and Maza (M) = 0.00  
 Shen et al. (M) = 1.32  
 Larras 1963 for circular piers 7.20  
 Hancu eq1-Dimensionless ratio (M)= 4.23  
 Hancu eq2 paper unknown ref.(M)= 9.58  
 Froelichs eqn 1988 for circular 7.73  
 Coleman eq 1 dimensionless (M)= 4.73  
 Coleman eq 2 dimensionless (M)= 1.19  
 Basak et al = 2.34  
 Neill "eq1," field data (M)= 22.33  
 Neill "eq2," field data = 7.50  
 Neill "eq3," field data (M)= 13.73  
 Jain & "Fischer,Dimensionless(M)=" 8.13  
 Jain ",Dimensionless(M)=" 7.48  
 Chitale 1988 = 12.50  
 Colorado state University HEC18 (M)= 6.21  
 Richardson and Davis HEC18 1995 6.21  
 Gao et "al," (M)= 6.33

Melville	Eq	1	1997(M)=	8.41
Melville	Eq	2	for waves=	0.00
original	"Lacy,"		Field data (M)=	24.49
Lacy revised	by	"others,"	Field	48.97
Arunachalams	formula	(M)=		8.22
Mustaqs	formula	(M)=		20.25
Blench	Eq	1	1969 (M)=	3.95
Blench	Eq	2	(M)=	22.19
Sethis	formula	(M)=		26.96
RDSOs Formula	(M)=			35.88
Andrus	Formula	(A)=		16.65
Railways	"Ministry,"	India (M)=		51.77
Izzard&	Bradley	(A)=		22.42
Unified	model unknown	reference (M)=		17.66
The Demetrius	ultimate	scour model		12.99

Patapsco River Upstream Pier Face

b = 5.000000  
 YRS = 100.000000  
 VMAX = 2.580000  
 QMAX = 129931.000000  
 YTMAX = 38.750000  
 VT = 4.030000  
  
 YMMAX = 11.734800  
 N = 7.271385E-01  
 N1 = 1.118197  
 N2 = 1.000000  
 N3 = 1.150000  
 N4 = 9.000000E-01  
 ALPHA = 9.971429E-01  
 FRMMAX = 7.272480E-02  
 VCRIN = 6.418194E-01

M indicate maximum conditions (V,Q, Y)

Breusers eq1. based on estuary data =	6.998208
Breusers eqn2 f(y/b) (M) =	9.999996
Laursens equation (M) =	15.400630
Laursen &Toch (M)=	13.835930
Lauresn Neills Toch (M) =	9.221595
Inglis eqn lab data(M) =	27.469810
Inglis eqn2 field data (M) =	31.635920
Sanchez and Maza (M) =	0.000000E+00
Shen et al. (M) =	1.282046
Larras 1963 for circular piers =	7.199243
Hancu eq1-Dimensionless ratio (M)=	4.098142
Hancu eq2 paper unknown ref.(M)=	8.876726
Froelichs eqn 1988 for circular piers(M)=	11.885860
Coleman eq 1 dimensionless (M)=	4.410346

Coleman eq 2 dimensionless (M)= 1.625680  
 Basak et al = 2.342811  
 Neill eq1, field data (M)= 20.503490  
 Neill eq2, field data = 7.498080  
 Neill eq3, field data (M)= 18.591750  
 Jain & Fischer, Dimensionless(M)= 10.838440  
 Jain ,Dimensionless(M)= 8.002757  
 Chitale 1988 = 12.496800  
 Colorado state University HEC18 (M)= 6.618382  
 Richardson and Davis HEC18 1995 (M)= 6.618382  
 Gao et al, (M)= 7.960562  
 Melville Eq 1 1997(M)= 9.103172  
 Melville Eq 2 for waves= 0.000000E+00  
 original Lacy, Field data (M)= 32.498870  
 Lacy revised by others, Field data (M)= 64.997740  
 Arunachalams formula (M)= 8.911863  
 Mustaq's formula (M)= 22.167890  
 Blench Eq 1 1969 (M)= 0.000000E+00  
 Blench Eq 2 (M)= 26.272560  
 Sethis formula (M)= 34.142180  
 RDSOs Formula (M)= 65.818150  
 Andrus Formula (A)= 17.962570  
 Railways Ministry, India (M)= 68.707980  
 Izzard & Bradley (A)= 24.528410  
 Unified model unknown reference (M)= 26.570300  
 The Demetrius ultimate scour model (M)= 4.090902

#### Patapsco River Downstream Pier Face

b = 5.000000  
 YRS = 100.000000  
 VMAX = 1.190000  
 QMAX = 82579.000000  
 YTMAX = 39.250000  
 VT = 6.200000E-01  
  
 YMMAX = 12.268200  
 N = 7.218060E-01  
 N1 = 1.122118  
 N2 = 1.000000  
 N3 = 1.150000  
 N4 = 9.000000E-01  
 ALPHA = 9.971429E-01  
 FRMMAX = 3.389611E-02  
 VCRIN = 5.529241E-01

M indicate maximum conditions (V, Q, Y)

Breusers eq1. based on estuary data = 6.998208  
 Breusers eqn2 f(y/b) (M) = 9.999998  
 Laursens equation (M) = 15.746750  
 Laursen & Toch (M)= 14.021680  
 Laursen Neills Toch (M) = 9.345393  
 Inglis eqn lab data(M) = 21.813320  
 Inglis eqn2 field data (M) = 25.341220

Sanchez and Maza (M) = 0.000000E+00  
 Shen et al. (M) = 8.103261E-01  
 Larras 1963 for circular piers = 7.199243  
 Hancu eq1-Dimensionless ratio (M)= 2.493623  
 Hancu eq2 paper unknown ref.(M)= 8.232737  
 Froelichs eqn 1988 for circular piers(M)= 11.293290  
 Coleman eq 1 dimensionless (M)= 3.785873  
 Coleman eq 2 dimensionless (M)= 6.911635E-01  
 Basak et al = 2.342811  
 Neill eq1, field data (M)= 11.749920  
 Neill eq2, field data = 7.498080  
 Neill eq3, field data (M)= 19.009590  
 Jain & Fischer,Dimensionless(M)= 0.000000E+00  
 Jain ,Dimensionless(M)= 7.814675  
 Chitale 1988 = 12.496800  
 Colorado state University HEC18 (M)= 4.841162  
 Richardson and Davis HEC18 1995 (M)= 4.841162  
 Gao et al, (M)= 1.737150  
 Melville Eq 1 1997(M)= 5.441085  
 Melville Eq 2 for waves= 0.000000E+00  
 original Lacy, Field data (M)= 30.322200  
 Lacy revised by others, Field data (M)= 60.644410  
 Arunachalams formula (M)= 8.284074  
 Mustaq's formula (M)= 16.494830  
 Blench Eq 1 1969 (M)= 0.000000E+00  
 Blench Eq 2 (M)= 22.229390  
 Sethis formula (M)= 27.478160  
 RDSOs Formula (M)= 68.809880  
 Andrus Formula (A)= 10.465770  
 Railways Ministry, India (M)= 64.106140  
 Izzard& Bradley (A)= 18.251260  
 Unified model unknown reference (M)= 16.292560  
 The Demetrius ultimate scour model (M)= 0.000000E+00

-----  
 -----  
 -----

# APPENDIX E-4

```

PROGRAM Sc5m
C
C DETAILED COMPARATIVE SCOUR PROGRAM :      2/10/05
C ANNUAL SERIES DATA

REAL b, K1, K2, K3, K4, K5
REAL g, PI, KTHET, KI, K, KS
REAL CONVER, D50MET, D50M

REAL QMM500,QM500,VMM500, VM500, YMM500,YTM500
REAL FRM500,VCR500, FRC500

REAL DSH500, DSF500, DSJ500, DSC500, DSL500

REAL VCRITM(100), FRMAX(100), FRCMAX(100)
REAL QMAX(100), VMAX(100), YTMAX(100)
REAL QMMAX(100), VMMAX(100), YMMAX(100), DSLTM(100)
REAL DSHA1M(100), DSFROM(100), DSJFM(100), DSCSUM(100)

CHARACTER*50 FILE1, FILE2

C OPEN INPUT FILE AND READ IN DATA
C
WRITE(*,*)'ENTER THE NAME OF THE INPUT FILE'
READ(*,*) FILE1

OPEN (6, FILE= FILE1, STATUS = 'OLD', IOSTAT = IERROR)

C CREATE AND OPEN OUTPUT FILE

WRITE(*,*)'ENTER THE NAME OF THE OUTPUT FILE'
READ(*,*) FILE2

OPEN (12, FILE = FILE2, STATUS ='UNKNOWN')

C
WRITE(*,1)
1 FORMAT('debug 1')
C
C BRIDGE DATA, SOIL DATA

READ (6,*)
READ (6,*)
READ (6,*)
READ (6,*)
READ (6,*) b, D50M, YTM500, VM500, QM500
READ (6,*)
C

```

```

C ANNUAL MAXIMUM DISCHARGE VELOCITY AND DEPTH
C
      WRITE(*,2)
2  FORMAT('debug 2')
      READ (6,*)
      READ (6,*)
      READ (6,*) (YTMAX(I),I=1,100)
      READ (6,*)

      WRITE(*,3)
3  FORMAT('debug 3')
      READ (6,*) (QMAX(I),I=1,100)
      READ (6,*)

      WRITE(*,4)
4  FORMAT('debug 4')
      READ (6,*) (VMAX(I),I=1,100)

C
C      COMPUTATION INPUT DATA DATA for 100 yr events
C      avg is used for the upstream conditions

      CONVER = 3.28
C      CONVER is the conversion factor from meters to feet
C      PARAMETERS

      g = 32.2
      PI = 3.142
      gm = 9.81
      bm = 0.3048*b
      D50MET= D50M/1000

C      KS and KTHETA is 1 for cylindrical piers

      K = 1
      KS = 1
      KTHET = 1
      KI = 1
      K1 = 1
      K2 = 1
      K3 = 1
      K4 = 1
      K5 = 1

C      COMPUTED VARIABLES AND CHANGE COMPUTED VARIABLES TO S I UNITS

      Do 10 I=1,100

      QMMAX(I) = 0.028*QMAX(I)

      VMMA(I) = 0.3048*VMAX(I)

      YMMAX(I) = 0.3048*YTMAX(I)

      FRMAX(I) = VMAX(I)/(g*YTMAX(I))**0.5

```



```

VCRITM(I)= 1.75*(D50M)**0.33*(YTMAX(I))**0.17

FRCMAX(I)= VCRITM(I)/(g*YTMAX(I))**0.5
10 CONTINUE
C   COMPUTE 500yr VARIABLES

QMM500 = 0.028*QM500

VMM500 = 0.3048*VM500

YMM500 = 0.3048*YTM500

FRM500 = VM500/(g*YTM500)**0.5

VCR500= 1.75*(D50M)**0.33*(YTM500)**0.17

FRC500= VCR500/(g*YTM500)**0.5

WRITE(*,13)
13 FORMAT('debug 13')

*****
C                               SCOUR EQUATIONS
*****

C      5      Laursen &Toch      dse/b=1.5(y/b)**0.30

C      13      Jain & Fischer      dse/b=2.0(y/b)**0.5[Fr -Frc]**0.25
C                                     ; Frc is the Froud number at the critical
velocity

C      14      HEC18      ds=2yK1 K2 K3 K4[b/y]**0.65 Fr**0.34
C                                     Terms are defined in the HEC 18 manual.
C                                     These terms are equivalent to Ks, KI , KG ,
Ktheta

C      Hancu dse/b=2.42(y/b)**0.33*Fr**0.67  Dimensionless ratio
eqn

C      28      Froelich
ds=b*0.32K1(b'/b)**.62*(y/b)**0.46*F**0.2*(b/d50)**0.08 +1

C      SCOUR EQUATIONS COMPUTATION

*****
C                                     MODELS
*****

      Do 100 I=1,100

C      DSE5 Laursen &Toch      dse/b=1.5(y/b)**0.30 independent of Q, V
C      Dimensionless ratio-equation

```

```

DSLTM(I) = b*1.5*(YTMAX(I)/b)**0.30

C      Hancu dse/b=2.42(y/b)**0.33*Fr**0.67 Dimensionless ratio eqn
      DSHA1M(I) = b*2.42*(YTMAX(I)/b)**0.33*FRMAX(I)**0.67

C      Froelich's eqn 1988 with adjustments for circular piers
C      Ref Peggy Johnson's Dissertation
C      ds=b*0.32K1(b'/b)**.62*(y/b)**0.46*F**0.2*(b/d50)**0.08 +1

      DSFROM(I) = CONVER*bm*0.32*(YMMAX(I)/bm)*0.46*
      (VMMAX(I)/(gm*bm)**0.5)**0.2*(bm/D50MET)**0.08 + CONVER

C      Jain & Fischer dse/b=2.0(y/b)**0.5[Fr - Frc]**0.25
Dimensionless

      DSJFM(I) = 0
      IF(FRMAX(I).GT.FRCMAX(I)) DSJFM(I) = b*2.0*(YTMAX(I)/b)**0.5*
      (FRMAX(I) - FRCMAX(I))**0.25

C      Colorado state University HEC18 ds=2yK1 K2[b/y]**0.65 Fr**0.43
dimensionless

      DSCSUM(I) = 2*YTMAX(I)*K1*K2*(b/YTMAX(I))**0.65*FRMAX(I)**0.43

100 CONTINUE

C                                     COMPUTE 500YR SCOUR VALUES

C      DSE5 Laursen & Toch dse/b=1.5(y/b)**0.30 independent of Q, V
C      Dimensionless ratio-equation

      DSL500 = b*1.5*(YTM500/b)**0.30

C      Hancu dse/b=2.42(y/b)**0.33*Fr**0.67 Dimensionless ratio eqn

      DSH500 = b*2.42*(YTM500/b)**0.33*FRM500**0.67

C      Froelich's eqn 1988 with adjustments for circular piers
C      Ref Peggy Johnson's Dissertation
C      ds=b*0.32K1(b'/b)**.62*(y/b)**0.46*F**0.2*(b/d50)**0.08 +1

      DSF500 = CONVER*bm*0.32*(YMM500/bm)*0.46*
      (VMM500/(gm*bm)**0.5)**0.2*(bm/D50MET)**0.08 + CONVER

C      Jain & Fischer dse/b=2.0(y/b)**0.5[Fr - Frc]**0.25
Dimensionless

      DSJ500 = 0
      IF(FRM500.GT.FRC500) DSJ500 = b*2.0*(YTM500/b)**0.5*
      (FRM500 - FRC500)**0.25

```

```
C      Colorado state University HEC18 ds=2yK1 K2[b/y]**0.65 Fr**0.43
dimensionless
```

$$DSC500 = 2*YTM500*K1*K2*(b/YTM500)**0.65*FRM500**0.43$$

```
*****
```

```
C      DISPLAY RESULTS
```

```
C
*****
```

```
WRITE(12,*)
WRITE(12,*)
WRITE(12,*)'Laursen &Toch = ', DSLTM
```

```
WRITE(12,*)'Hancu eq1 = ',DSHA1M
```

```
WRITE(12,*)'Froelichs eqn 1988 for circular piers = ',DSFROM
```

```
WRITE(12,*)'Jain & Fischer,Dimensionless= ',DSJFM
```

```
WRITE(12,*)'Colorado state University HEC18= ',DSCSUM
```

```
WRITE(12,*)
WRITE(12,*)
WRITE(12,*)'Laursen &Toch 500 yr scour= ', DSL500
```

```
WRITE(12,*)'Hancu eq1 500 yr scour= ',DSH500
```

```
WRITE(12,*)'Froelichs eqn 1988 500 yr scour = ',DSF500
```

```
WRITE(12,*)'Jain & Fischer,500 yr scour= ',DSJ500
```

```
WRITE(12,*)'CSU HEC18 500 yr scour= ',DSC500
```

```
CLOSE (12, STATUS = 'REPLACE')
END
```

## APPENDIX E-5

TITLE: DETAILED MODEL COMPARISON

PROJECT NAME: MONIE BAY

UPSTREAM PIER FACE

DATE: 4/06/05

pier diam (ft), Soil mean diameter(mm)

b	D50M	YTM500	VM500	QM500
5.0	0.135	10.25	1.17	61228

ARRAY OF ANNUAL MAXIMUM FLOW DEPTH (ft) YTMAX

8.657200	8.657200		
9.245000	8.745000	8.657200	8.685199
8.657200	8.657200	8.995000	8.995000
8.657200	8.495000	8.405587	9.098116
9.098116	9.098116	9.098116	9.098116
9.098116	9.098116	9.098116	9.098116
9.098116	9.098116	9.098116	9.098116
9.098116	9.098116	9.098116	9.098116
9.098116	9.098116	9.098116	9.098116
9.245000	9.098116	9.098116	9.098116
9.098116	9.098116	9.098116	9.098116
9.098116	8.459832	8.473576	8.995000
8.745000	8.712579	8.712579	8.712579
8.712579	8.712579	8.712579	8.712579
8.745000	8.712579	8.712579	9.245000
8.712579	8.712579	8.803782	8.803782
8.803782	8.803782	8.807333	8.807333
8.495000	8.245000	8.419100	8.433814
8.403076	8.495000	8.606614	8.403076
8.403076	8.745000	8.745000	8.403076
8.438987	8.415760	8.415760	8.495000
8.415760	8.624671	8.624671	8.768705
8.729970	8.729970	8.729970	8.729970
8.729970	8.729970	8.729970	8.729970
8.745000	8.729970	8.729970	8.729970
8.219649	8.495000		

ARRAY OF ANNUAL MAXIMUM FLOW DISCHARGE (cfs) QMAX

42260.360000	46294.350000		
39052.300000	38336.210000	37122.910000	46120.300000
40900.280000	39417.710000	39495.010000	41446.280000
44743.130000	40732.450000	38975.200000	41123.180000
40065.100000	39780.430000	43761.570000	38918.530000
38466.910000	37476.450000	46476.340000	39971.160000
40856.950000	42989.710000	38730.840000	39490.440000
39941.790000	40277.840000	48205.020000	39240.370000
38818.900000	50310.730000	45380.140000	43482.230000
41444.170000	38137.000000	39815.410000	42885.430000
39249.690000	36437.070000	41748.240000	45222.660000
43947.140000	38526.940000	40144.940000	46450.780000
45254.520000	42240.390000	42708.150000	44584.510000
39084.580000	48614.580000	45936.610000	42806.260000
40580.690000	40832.010000	45412.540000	44164.660000
37221.000000	39774.620000	46403.720000	45263.160000
44099.450000	50550.990000	43612.590000	46703.000000
41031.530000	42483.130000	42433.430000	45847.930000

40207.440000	41969.850000	47465.260000	36405.490000
39522.370000	43367.290000	42157.160000	38177.070000
35529.040000	38673.780000	38242.650000	45145.970000
43383.730000	38605.820000	41419.160000	40127.180000
39367.160000	43866.840000	38574.390000	38117.390000
42014.850000	39717.740000	39910.520000	45257.870000
41601.530000	48060.140000	36925.500000	45117.640000
40001.260000	42598.130000		
ARRAY OF ANNUAL MAXIMUM FLOW VELOCITY (ft/sec) VMAX			
5.905355E-01	6.177908E-01		
5.878229E-01	5.512557E-01	6.251256E-01	6.171355E-01
6.009783E-01	6.035676E-01	6.137961E-01	5.659245E-01
6.159304E-01	5.853845E-01	5.426438E-01	5.862695E-01
5.879153E-01	5.700608E-01	5.698293E-01	5.610082E-01
5.965563E-01	5.649116E-01	6.160181E-01	5.974163E-01
6.024175E-01	5.794241E-01	5.754811E-01	5.595501E-01
5.791355E-01	5.496882E-01	6.065647E-01	5.898461E-01
5.686995E-01	5.637906E-01	5.711054E-01	5.795109E-01
6.018610E-01	5.774754E-01	6.266273E-01	5.618666E-01
5.779951E-01	5.952319E-01	5.417353E-01	5.950171E-01
5.772915E-01	5.721473E-01	5.989382E-01	6.137170E-01
5.726511E-01	5.509964E-01	5.699242E-01	5.649636E-01
5.932547E-01	5.748895E-01	5.913566E-01	5.867468E-01
5.690062E-01	5.437918E-01	6.615236E-01	5.710542E-01
5.768998E-01	6.101898E-01	6.399040E-01	6.011847E-01
5.809631E-01	5.615147E-01	5.636551E-01	5.957874E-01
5.409352E-01	5.842665E-01	5.652792E-01	5.724488E-01
5.625614E-01	6.121222E-01	5.815270E-01	5.580202E-01
6.007769E-01	6.170388E-01	5.756883E-01	6.030960E-01
5.530685E-01	5.614761E-01	5.576924E-01	5.507864E-01
6.327173E-01	5.812076E-01	5.953085E-01	6.442097E-01
5.842042E-01	5.863311E-01	5.789304E-01	5.561932E-01
5.531400E-01	5.757112E-01	5.661561E-01	5.763102E-01
5.998825E-01	5.616366E-01	5.675319E-01	5.661818E-01
6.021416E-01	5.773752E-01		

TITLE: DETAILED MODEL COMPARISON

PROJECT NAME: MONIE BAY

DOWNSTREAM PIER FACE

DATE: 4/06/05

pier diam (ft), Soil mean diameter(mm)

b	D50M	YTM500	VM500	QM500
5.0	0.135	10.00	1.41	61861

ARRAY OF ANNUAL MAXIMUM FLOW DEPTH (ft) YTMAX

9.245000	8.995000		
9.245000	8.773869	8.995000	9.173283
9.245000	9.745000	9.495000	9.495000
9.495000	8.995000	8.995000	9.152212
8.995000	9.245000	9.245000	8.745000
8.995000	9.245000	9.245000	9.745000
8.995000	9.245000	9.745000	8.646978
8.995000	8.895731	8.745000	9.245000
9.495000	9.245000	8.995000	9.245000
9.495000	9.245000	8.995000	9.245000
8.745000	8.995000	8.995000	8.995000

9.245000	9.495000	8.995000	8.995000
9.245000	8.758671	8.995000	9.245000
9.495000	9.745000	8.995000	9.245000
9.245000	8.995000	9.072608	9.245000
8.995000	9.495000	8.995000	9.245000
8.745000	9.245000	9.745000	9.495000
9.245000	8.995000	8.995000	9.245000
9.495000	8.745000	9.745000	8.745000
8.745000	9.245000	8.995000	9.745000
9.245000	8.995000	8.745000	8.995000
8.745000	8.745000	9.245000	8.772450
8.995000	9.245000	9.995000	9.245000
9.245000	8.745000	8.995000	8.995000
8.995000	8.995000	9.245000	8.995000
9.245000	8.995000		
ARRAY OF ANNUAL MAXIMUM FLOW DISCHARGE (cfs) QMAX			
38153.320000	36247.680000		
44181.130000	40013.980000	39989.510000	40196.160000
40965.180000	44915.560000	43982.100000	44293.310000
46072.500000	39927.250000	36176.960000	46328.020000
37001.330000	37755.020000	35393.060000	39121.630000
38855.370000	36704.820000	40191.920000	41416.060000
37415.640000	38648.340000	38008.010000	33793.230000
38251.300000	38345.520000	45582.750000	36600.710000
41931.360000	38334.090000	36028.250000	43558.490000
42573.480000	41332.240000	39670.800000	35744.990000
38465.000000	37740.670000	43849.810000	39288.420000
32514.440000	39698.610000	36239.620000	38273.780000
41099.040000	37072.810000	40021.040000	43272.600000
42051.950000	39704.330000	40343.160000	39672.310000
41289.760000	35781.860000	46155.250000	46361.590000
44155.710000	44775.870000	40017.540000	42456.630000
37820.870000	44841.440000	44377.740000	38177.930000
40710.420000	37266.040000	43547.880000	42838.450000
37080.180000	41145.910000	44556.070000	38273.710000
42574.390000	35274.710000	40929.000000	40959.880000
38340.290000	42965.260000	39102.070000	36493.270000
43469.790000	35043.200000	39061.770000	38802.070000
39780.000000	40713.550000	50527.050000	41476.210000
43315.590000	40930.940000	39278.940000	36563.270000
45651.320000	40742.810000	39773.370000	34777.730000
41766.860000	41450.060000		
ARRAY OF ANNUAL MAXIMUM FLOW VELOCITY (ft/sec) VMAX			
1.065757	1.242033		
1.096860	1.016291	9.927958E-01	9.111453E-01
1.017369	1.115101	1.091918	1.107990
1.143996	9.912748E-01	9.297574E-01	1.150177
1.005615	1.014722	1.091742	9.716369E-01
9.646621E-01	9.471502E-01	1.085657	1.084739
9.294004E-01	9.491114E-01	1.052660	1.013822
1.084523	9.794714E-01	1.050517	1.105743
1.041013	1.108922	8.889236E-01	1.081407
1.134108	1.026132	1.084295	1.118204
9.550909E-01	9.373394E-01	1.015939	1.042482
8.510341E-01	1.066193	9.571586E-01	1.180248
1.103804	1.150056	1.007385	1.248806
1.044277	1.071354	1.011807	9.877745E-01

1.008518	9.609995E-01	1.146057	1.151071
1.101770	1.111636	9.940314E-01	1.112264
9.393173E-01	1.408754	1.032768	9.111736E-01
1.093367	1.220187	1.026058	1.063695
9.850203E-01	1.105063	1.058946	9.502029E-01
1.056969	1.015734	1.030061	1.251362
1.102096	1.206404	1.066230	1.022726
1.079199	9.270074E-01	9.697666E-01	9.636766E-01
9.878467E-01	1.059033	1.254408	9.738631E-01
1.075373	9.417990E-01	9.368961E-01	9.740301E-01
1.133360	1.045197	1.082743	8.815030E-01
1.046169	1.029162		

-----  
 -----  
 -----

TITLE: DETAILED MODEL COMPARISON

PROJECT NAME: BLACK RIVER U/STREAM PIER FACE

DATE: 4/09/05

pier diam (ft), Soil mean diameter(mm)

b	D50M	YTM500	VM500	QM500
5.0	0.15	16.25	1.66	263352

ARRAY OF ANNUAL MAXIMUM FLOW DEPTH (ft) YTMAX

14.750000	14.750000		
14.500000	14.750000	14.250000	14.250000
14.750000	14.250000	14.750000	14.500000
14.750000	14.750000	14.750000	14.750000
15.250000	15.250000	15.500000	14.250000
14.750000	14.750000	15.000000	14.500000
15.250000	14.750000	15.000000	14.500000
14.500000	14.500000	14.500000	15.000000
14.750000	15.000000	14.750000	14.500000
14.500000	14.500000	14.750000	14.500000
14.750000	15.000000	14.500000	14.500000
14.250000	14.750000	14.500000	14.500000
14.500000	14.250000	14.750000	14.750000
15.000000	15.000000	15.500000	14.250000
14.750000	14.750000	15.000000	14.750000
14.500000	15.250000	14.750000	14.500000
14.500000	15.000000	14.750000	14.750000
14.500000	15.000000	14.750000	15.000000
14.500000	14.750000	14.250000	15.000000
14.250000	15.000000	14.750000	14.750000
14.750000	14.000000	14.750000	15.000000
15.000000	15.250000	14.750000	14.250000
14.500000	15.000000	15.000000	14.000000
14.500000	14.500000	14.750000	14.500000
14.250000	14.500000	15.000000	15.000000
15.000000	15.250000		

ARRAY OF ANNUAL MAXIMUM FLOW DISCHARGE (cfs) QMAX

165773.000000	167696.200000		
177459.100000	166158.500000	200283.900000	170374.500000
168939.700000	178733.500000	177786.600000	176563.200000
169417.500000	200280.000000	179151.000000	179332.900000

177346.300000	181356.700000	180127.100000	186925.200000
168306.400000	175002.500000	177814.500000	174446.500000
179683.300000	176718.900000	156416.000000	186593.300000
172212.300000	166493.400000	168926.000000	164891.800000
180778.300000	178967.200000	187892.600000	171078.800000
185138.100000	167545.400000	172365.700000	157013.700000
151401.400000	176306.800000	180839.300000	181036.200000
178908.000000	176872.400000	159074.100000	172348.800000
169600.600000	173774.700000	163148.300000	174265.100000
166705.600000	154806.500000	158873.400000	157185.500000
176675.500000	164076.700000	168220.100000	206526.800000
167154.600000	169632.800000	178822.900000	174422.200000
206457.500000	157730.800000	172431.600000	182212.400000
160759.000000	211024.000000	170237.200000	177922.900000
157548.100000	168808.500000	161342.800000	179240.000000
196824.700000	198290.400000	177784.000000	189105.900000
153694.700000	159845.700000	171449.200000	155912.900000
183224.800000	181967.700000	176804.000000	157184.600000
173345.800000	171945.400000	154879.500000	168332.600000
166539.800000	182220.700000	188590.700000	176143.200000
188165.900000	169542.500000	164638.600000	178708.000000
171794.400000	172166.200000		

ARRAY OF ANNUAL MAXIMUM FLOW VELOCITY (ft/sec) VMAX

1.076251	1.100536		
1.083966	1.067267	1.060633	1.044742
1.172818	1.055049	1.118029	1.114566
1.058959	1.082243	1.069519	1.054579
1.066565	1.020598	1.085199	1.047609
1.030108	1.125532	1.170992	1.029543
1.096134	1.139649	9.671694E-01	1.045652
1.039393	1.037774	1.079204	1.060638
1.084756	1.085083	1.162544	1.070577
1.084399	1.008123	1.053244	1.098652
1.121133	1.139383	1.067886	1.036920
1.030201	1.136870	1.067541	1.031031
1.072946	1.091731	1.206410	1.017204
1.038495	1.084033	1.061325	1.129092
1.122931	1.111003	9.928966E-01	1.125171
1.155915	1.140743	1.026227	1.124109
1.093720	9.939406E-01	1.065292	1.028262
1.038539	1.152570	1.144485	1.085982
1.068316	1.052236	1.088445	1.052743
1.078273	1.049927	1.014927	1.132474
1.091274	1.117049	1.121627	1.096303
1.109313	1.112770	1.118885	1.055501
1.019678	1.027945	1.076688	1.145859
1.209202	9.937201E-01	1.117168	1.099066
1.067919	1.193063	9.653108E-01	1.175126

TITLE: DETAILED MODEL COMPARISON

PROJECT NAME: BLACK RIVER DOWN/STREAM PIER FACE

DATE: 4/09/05

pier diam (ft), Soil mean diameter(mm)

b	D50M	YTM500	VM500	QM500
5.0	0.15	16.75	2.33	271238



ARRAY OF ANNUAL MAXIMUM FLOW DEPTH (ft) YTMAX

13.500000	13.750000		
13.591020	13.750000	13.390770	13.500000
13.750000	13.500000	14.500000	13.500000
13.250000	13.750000	14.000000	13.750000
13.500000	13.750000	13.750000	13.250000
13.750000	13.750000	14.000000	14.250000
15.000000	14.000000	13.500000	13.500000
14.000000	14.000000	13.500000	14.250000
13.750000	13.750000	13.500000	13.750000
13.750000	13.750000	14.000000	13.750000
13.750000	13.750000	13.750000	14.000000
13.750000	14.000000	13.500000	13.750000
13.781830	13.250000	14.250000	14.000000
13.500000	14.750000	14.000000	14.000000
14.000000	13.750000	14.000000	14.250000
14.000000	14.500000	13.750000	13.750000
14.000000	13.500000	14.000000	14.000000
13.750000	14.000000	13.750000	14.000000
14.000000	14.000000	13.628000	13.628000
13.750000	14.002110	14.250000	13.750000
14.000000	13.750000	14.000000	13.750000
14.000000	13.273480	13.250000	13.750000
13.001940	14.250000	13.750000	13.250000
14.250000	13.250000	13.189790	13.500000
13.423270	13.747820	13.750000	15.000000
13.750000	13.750000		

ARRAY OF ANNUAL MAXIMUM FLOW DISCHARGE (cfs) QMAX

168718.900000	168469.100000		
172411.800000	181716.900000	162947.700000	160218.300000
156320.100000	156990.500000	155620.100000	180691.500000
167471.300000	163707.000000	150757.300000	196746.000000
183788.700000	166130.700000	162270.300000	192664.700000
153764.100000	201669.900000	153404.000000	167332.500000
176479.700000	160804.600000	157356.800000	176649.400000
148858.600000	173534.000000	151301.700000	191122.500000
167041.100000	168920.500000	175107.800000	183932.300000
180960.100000	153710.800000	153378.900000	151216.800000
171802.800000	180439.000000	168844.900000	180831.400000
149138.700000	147156.000000	158702.200000	180633.600000
175237.600000	168159.200000	178409.300000	165845.100000
159199.300000	187783.500000	158894.200000	180260.900000
169255.800000	170983.000000	179399.400000	164515.000000
171253.000000	164247.700000	174139.600000	169100.300000
156644.400000	182169.000000	162621.400000	153408.300000
154365.700000	157306.100000	166521.300000	186364.900000
182343.500000	167571.700000	148450.700000	156995.300000
149865.300000	171486.700000	170438.100000	186855.600000
164504.800000	158882.700000	155233.700000	183728.100000
155151.800000	155001.500000	178533.900000	165892.200000
181763.300000	161988.400000	178935.700000	163215.500000
153674.000000	161069.300000	163229.100000	184221.700000
166750.800000	156234.900000	183499.800000	187543.200000
170409.400000	153057.100000		

ARRAY OF ANNUAL MAXIMUM FLOW VELOCITY (ft/sec) VMAX

1.359432	1.508331		
1.424561	1.531120	1.337672	1.315226

1.341980	1.243831	1.371419	1.533581
1.374736	1.436547	1.300901	1.615046
1.537985	1.345207	1.558331	1.581566
1.371512	1.597703	1.384094	1.511501
1.587445	1.341504	1.320199	1.450077
1.391628	1.449286	1.368573	1.626851
1.371205	1.386672	1.501420	1.565648
1.485469	1.270007	1.471844	1.307586
1.410293	1.562620	1.386015	1.432727
1.288257	1.525587	1.302753	1.435589
1.417276	1.380431	1.464552	1.390948
1.324835	1.541474	1.747105	1.479736
1.518512	1.403571	1.503291	1.512363
1.478217	1.458973	1.379576	1.411471
1.358255	1.495390	1.345740	1.381623
1.283140	1.417771	1.450821	1.586354
1.496821	1.458416	1.242488	1.334101
1.436632	1.407714	1.583390	1.533863
1.346003	1.281022	1.390143	1.508234
1.347024	1.398928	1.968874	1.361775
1.440047	1.501706	1.664297	1.302159
1.355824	1.322184	1.534005	1.459441
1.386060	1.350760	1.453740	1.629114
1.500762	1.452992		

-----

-----

-----

TITLE: DETAILED MODEL COMPARISON

PROJECT NAME: PATUXENT RIVER U/STREAM PIER FACE

DATE: 4/09/05

pier diam (ft), Soil mean diameter(mm)

b	D50M	YTM500	VM500	QM500
5.0	0.25	19.80	2.98	154789

ARRAY OF ANNUAL MAXIMUM FLOW DEPTH (ft) YTMAX

17.800000	17.800000		
17.872540	17.951540	17.721280	17.800000
17.800000	17.800000	17.800000	17.732740
17.550000	17.800000	17.557800	18.050000
17.800000	17.550000	17.550000	17.550000
17.800000	18.050000	17.550000	18.050000
17.800000	17.550000	18.050000	17.800000
17.800000	17.550000	18.050000	17.550000
18.050000	17.847600	17.550000	18.050000
18.050000	18.300000	17.800000	17.800000
18.050000	17.800000	17.800000	17.846730
17.800000	18.050000	17.800000	17.858470
18.050000	17.800000	17.800000	17.594640
17.550000	17.550000	17.550000	18.300000
18.050000	18.050000	17.800000	17.800000
18.050000	17.467900	18.050000	17.800000
17.800000	17.800000	17.800000	17.800000
18.050000	17.550000	17.550000	17.800000
18.050000	18.050000	18.300000	17.800000
17.754200	18.144820	17.630890	17.800000

17.499710	18.050000	17.750140	17.800000
17.565610	17.800000	17.800000	17.800000
17.800000	17.800000	18.300000	17.800000
18.050000	18.050000	17.800000	17.800000
17.800000	17.629910	17.800000	18.050000
17.568650	17.550000		
ARRAY OF ANNUAL MAXIMUM FLOW DISCHARGE (cfs) QMAX			
79161.950000	88153.960000		
106844.400000	92259.420000	93468.190000	88192.940000
90017.660000	76578.520000	79571.480000	101360.400000
91641.430000	88352.810000	83317.870000	94273.980000
93274.920000	78764.690000	94026.500000	88145.920000
105925.400000	101187.600000	98754.040000	100933.900000
100770.400000	86391.080000	92192.330000	100297.600000
82737.700000	85998.210000	81889.880000	83491.770000
125435.500000	109593.400000	86992.830000	78994.300000
94823.330000	114850.500000	93556.890000	97543.170000
79705.310000	89045.950000	85721.580000	80730.420000
98219.420000	98747.830000	81804.410000	103093.100000
83246.900000	87923.680000	87191.780000	93343.550000
77715.410000	92859.380000	88731.390000	102512.200000
88970.480000	97059.090000	93883.950000	99081.650000
88267.850000	82854.630000	98887.410000	89644.800000
95116.190000	109906.500000	95088.250000	102234.700000
89547.730000	98817.210000	90044.630000	87576.540000
86876.380000	96361.300000	83110.530000	84806.490000
91436.480000	83718.430000	87106.410000	92753.540000
80499.910000	95264.410000	92159.450000	100096.500000
85120.060000	91211.360000	90805.070000	83943.880000
88511.660000	90779.170000	87210.950000	113414.200000
96593.080000	89590.530000	90497.060000	90408.090000
90107.480000	97568.230000	115020.500000	109018.400000
93293.640000	89909.560000		
ARRAY OF ANNUAL MAXIMUM FLOW VELOCITY (ft/sec) VMAX			
1.464173	1.476181		
1.999984	1.946745	2.688903	2.490155
1.564070	1.563139	1.459940	1.498440
1.904922	1.505974	1.608830	2.410543
1.435449	1.430291	1.661848	1.956090
2.078062	1.834023	2.036304	1.618747
1.874203	1.585056	1.880477	1.780695
1.459238	1.380437	1.856357	1.387382
1.818105	2.146832	1.562753	1.809073
2.096366	2.531136	1.588615	1.415374
1.449562	1.414503	1.553368	1.372086
1.954260	2.059736	1.701590	1.661102
1.404088	1.942392	1.483912	1.683647
1.451882	1.550318	1.583688	2.711949
1.902168	1.500196	2.289214	1.735584
2.194894	1.614069	1.549613	1.566894
1.685224	1.765664	1.634830	1.631412
2.364820	1.663724	1.881617	1.577147
1.687603	1.679485	2.188611	1.680995
1.403233	1.514496	1.722323	1.520904
1.362301	1.552143	2.156016	1.899855
1.441149	1.432899	1.691357	1.923167
1.576486	2.327169	1.490382	2.571936

1.690863	1.730314	2.072342	1.593996
1.613682	1.558330	1.602563	2.640761
1.675236	1.370121		

TITLE: DETAILED MODEL COMPARISON

PROJECT NAME: PATUXENT RIVER DOWNSTREAM PIER FACE

DATE: 4/09/05

pier diam (ft), Soil mean diameter(mm)

b	D50M	YTM500	VM500	QM500
5.0	0.25	20.05	5.70	234269

ARRAY OF ANNUAL MAXIMUM FLOW DEPTH (ft) YTMAX

17.527210	17.332160		
17.714210	17.950450	17.550000	17.471910
17.604190	17.406810	17.300000	17.509870
17.419050	17.550000	17.552330	17.550000
17.399100	17.397650	17.452770	17.345190
17.266800	17.692980	17.374260	17.721910
17.446550	17.368180	17.339370	17.344870
17.550000	17.482780	17.550000	17.372360
17.550000	17.592870	17.369020	17.415830
17.550000	18.050000	17.550000	17.550000
17.444080	17.688170	17.590290	17.585780
17.550000	17.550000	17.433400	17.607270
17.525250	17.432220	17.407400	17.544880
17.295400	17.501800	17.397220	17.386160
17.439330	17.391480	17.800000	17.550000
17.800000	17.408920	17.800000	17.403270
17.515290	17.522340	17.550000	17.474210
17.295790	17.375390	17.300000	17.358520
17.427340	17.735000	17.308380	17.419150
17.645870	17.804540	17.544580	17.387470
17.497510	17.421670	17.387580	17.521650
17.556740	17.233510	17.579030	17.476660
17.208370	17.800000	17.587650	17.800000
17.727440	17.445990	17.335350	17.550000
17.401180	17.456740	17.662330	17.550000
17.550000	17.484650		

ARRAY OF ANNUAL MAXIMUM FLOW DISCHARGE (cfs) QMAX

87157.880000	106094.900000		
79727.400000	87983.480000	76674.880000	70394.590000
94157.970000	85754.730000	88232.610000	94702.070000
87525.600000	84704.440000	81984.840000	84718.550000
77276.140000	74656.300000	72663.800000	86520.680000
84547.850000	87233.450000	78493.700000	68199.840000
84456.230000	79789.270000	85797.700000	90727.910000
81027.310000	81027.310000	85633.980000	90318.090000
81066.870000	91508.050000	98677.390000	102497.800000
99356.750000	81576.300000	98823.590000	82662.690000
89502.740000	90991.430000	77001.690000	83560.720000
92510.520000	77380.280000	105632.300000	98436.450000
84078.200000	79292.660000	78006.930000	81871.930000
69115.980000	81234.890000	84544.770000	81818.480000
73273.670000	91795.820000	84250.810000	95808.200000
80896.530000	81559.680000	97137.500000	87999.310000
106351.200000	83278.960000	93217.340000	78567.650000
87194.670000	105937.200000	105937.200000	79124.250000

87999.640000	87763.880000	79040.630000	82412.900000
94499.020000	83668.720000	89804.160000	78609.400000
74976.790000	85580.280000	84820.300000	75050.670000
75653.340000	69394.630000	83879.350000	76865.410000
89899.700000	89945.930000	94122.010000	74733.850000
84687.740000	69446.700000	83958.590000	88987.660000
89107.840000	84805.380000	76299.470000	82495.500000
83249.240000	79349.280000		

ARRAY OF ANNUAL MAXIMUM FLOW VELOCITY (ft/sec) VMAX

1.567170	1.884795		
1.741027	1.563060	1.488132	1.732842
1.781514	1.769986	1.733798	1.630951
1.554986	1.644161	1.583825	1.584878
1.511380	1.612089	1.588335	1.586137
1.801724	1.833766	1.438960	1.735371
1.605883	1.689497	1.477512	1.838591
1.692273	1.499201	1.752849	1.655729
1.650799	1.727695	1.809078	1.879026
1.821498	1.647550	1.811663	1.644336
1.777379	1.585487	1.471010	1.751842
1.750343	1.334382	1.936495	1.804598
1.900772	1.621735	1.806643	1.500918
1.586794	1.489300	1.653678	1.524542
1.866763	1.740348	1.671500	1.809932
1.688887	1.516733	1.780856	1.515332
1.949662	1.610359	1.716997	1.641194
1.769831	1.942062	1.594874	1.451216
1.766730	1.692337	1.538771	1.514773
1.743561	1.766951	1.646306	1.837900
1.568531	1.769240	1.624406	1.754077
1.430896	1.493503	1.604264	1.770634
1.902038	1.672451	1.843853	1.503074
1.980304	1.575525	1.583574	1.808084
1.633552	1.566845	1.498644	1.616985
1.587658	1.792825		

TITLE: DETAILED MODEL COMPARISON

PROJECT NAME: WICOMICO U/STREAM PIER FACE

DATE: 4/07/05

pier diam (ft),d50

b	D50M	YTM500	VM500	QTM500
5.0	0.325	21.06	2.74	93489

ARRAY OF ANNUAL MAXIMUM FLOW DEPTH (ft) YTMAX

20.486830	20.346900		
20.839950	20.755460	20.573200	20.306630
20.473560	20.314040	20.145000	20.696520
20.162380	20.414500	20.275210	20.536290
20.290500	20.252690	20.520040	20.363770
20.395940	20.530700	20.253780	20.632050
20.225840	20.465400	20.404150	20.192320
20.064920	20.456220	20.405500	20.365410

20.314670	20.795080	20.409210	20.471390
20.417240	20.612220	20.478430	20.569610
20.569610	20.688110	20.506020	20.730080
20.585560	20.229530	20.328770	20.530270
20.602810	20.335460	20.689490	20.381230
20.183600	20.274610	20.305950	20.423090
20.409470	20.279480	20.394530	20.303630
20.456850	20.440370	20.479070	20.351370
20.396400	20.252140	20.402320	20.343310
20.233570	20.169360	20.076940	20.376320
20.360290	20.248750	20.313690	20.349400
20.586030	20.766530	20.604860	20.455870
20.288320	20.438450	20.669140	20.356510
20.392380	20.423620	20.489960	20.254130
20.254730	20.428440	20.699280	20.332670
20.677570	20.303160	20.287120	20.355340
20.142970	20.525550	20.490360	20.556580
20.506690	20.360810		

ARRAY OF ANNUAL MAXIMUM FLOW DISCHARGE (cfs) QMAX

75404	71152.15		
67198.41	72515.7	64939.28	67117.96
80195.63	71642.74	73545.8	68491.52
73038.41	81578.51	77736.66	74027.74
71285.83	76870.33	67759.8	68295.04
73683.68	71842.34	71137.81	69789.34
63338.7	69344.34	67412.24	76155.9
71528.25	70723.13	71955.03	70085.66
83066.78	69741.25	74797.87	72512.16
75105.72	65197.18	81657.34	68959.35
70695.84	72345.52	71020.24	68569.3
67158	68579.02	69902.98	74145.4
71802.28	63697.57	68141.67	67792.91
69447	69470.93	74570.88	62660.29
66453.07	71021.32	70064.91	71807.47
72305.44	80219.85	80873.13	77533.99
67276.46	72339.95	72845.03	72763.3
71595.96	74607.15	69254.94	68653.74
70008.99	86716.8	73134.05	71175.43
77669.48	76620.71	70989.85	70097.71
72950.94	77613.09	67404.59	70318.5
71313.94	74493.33	75085.89	74469.3
62397.55	82732.33	66392.21	66888.5
78352.2	70234.17	73190.25	82189.74
68382.95	80541.04	68555.5	68258.92
67394.86	69608.8		

ARRAY OF ANNUAL MAXIMUM FLOW VELOCITY (ft/sec) VMAX

1.821532	1.816269		
1.851572	1.994957	2.169101	1.83086
1.713217	1.781865	1.789728	1.97743
1.791858	1.81524	1.904375	1.862026
1.703549	1.75186	1.710914	1.722576
2.156173	1.763084	1.737903	1.775806
1.860806	1.868693	1.725446	2.067293
1.76893	1.712817	1.740279	1.773467
1.776126	1.913507	1.752242	1.826217
2.000971	2.031474	1.886993	1.803148

1.952907	1.940556	1.782908	1.778918
1.751305	1.875536	1.708586	1.857862
1.869472	1.965102	1.856906	1.845039
1.69777	1.894582	1.889264	1.747865
1.926507	1.863116	1.977738	1.86072
1.823056	1.823082	1.917357	1.917076
1.579566	1.754919	1.790583	1.771878
1.664985	1.682107	1.718342	1.761162
1.921671	1.794858	1.968936	1.803161
1.821153	1.830766	1.897418	1.754951
1.696062	1.822237	1.702986	1.739395
1.775386	1.786921	1.885039	1.768051
1.838659	1.970756	1.876183	1.873237
1.840946	1.733713	1.82737	1.85294
1.762858	1.901042	1.840441	2.10781
1.885355	1.81234		

TITLE: DETAILED MODEL COMPARISON

PROJECT NAME: WICOMICO D/STREAM PIER FACE

DATE: 4/07/05

pier diam (ft),d50

b	D50M	YTM500	VM500	QTM500
5.0	0.325	21.8	3.55	92540

ARRAY OF ANNUAL MAXIMUM FLOW DEPTH (ft) YTMAX

20.493580	20.537200		
20.920080	20.784440	20.562890	20.701020
20.587550	20.409530	20.593820	20.729630
20.903150	20.789530	20.999290	20.664220
20.620850	20.620330	20.685360	20.711070
20.837940	20.689450	20.463340	20.698000
20.594460	20.556350	20.556820	20.639030
20.464930	20.507210	20.487610	20.392380
20.544240	20.796930	20.692760	20.500520
20.732520	20.784030	20.566070	20.856640
20.380820	20.808230	20.539900	20.826490
20.706870	20.462740	20.742400	20.758190
20.902800	20.479220	20.730380	20.472640
20.368260	20.498170	20.468250	20.521700
20.596840	20.425190	20.426270	20.741470
20.833040	20.624640	20.479880	20.636960
20.458120	20.619460	20.781830	20.642930
20.506300	20.482030	20.567930	20.572010
20.445600	20.539170	20.422910	20.631080
20.668990	20.855750	20.794540	20.583310
20.574660	20.622640	20.781080	20.521410
20.412460	20.875220	20.529480	20.456050
20.499200	20.918500	20.785180	20.376270
20.706360	20.502290	20.513850	20.567130
20.647720	20.553000	20.499280	20.640130
20.522770	20.649360		

ARRAY OF ANNUAL MAXIMUM FLOW DISCHARGE (cfs) QMAX

67747.32	62789.14		
73646.02	63035.07	77233.63	62687.9
71781.36	73616.83	66825.71	71043.34
65361.34	61498.26	69200.21	75406.18

70957.57	67570.54	67093.52	67093.52
66520.63	62152.64	64878.47	63609.03
64869.11	70419.3	64094.68	58432.16
64711.26	70378.79	67842.27	62656.34
60547.45	64382.08	67121.48	65403.91
63032.9	63551.89	67006.26	71188.97
74254.33	65643.77	63229.61	71987.12
64731.14	69504.48	62605.57	62003.6
64653.38	61337.28	67998.47	62319.73
67673.62	61061.71	66864.8	64691.14
66974	67566.38	67899.98	70492.45
61050.64	63379.48	62710.21	65084.98
61823.16	64232.04	63276.52	65885.59
67044.11	59234.16	66041.72	64418.84
66856.24	62292.71	67829.55	72151.36
70446.87	63977.29	62992.02	69949.37
64907.92	70523.29	62205.99	64925.91
58179.64	67298.57	64334.3	64651.23
69827.28	80450.06	63176.53	63754.75
67577.34	63064.58	67289.95	64550.05
69276.47	69512.09	59231.03	67429.31
62996.96	78261.61		
ARRAY OF ANNUAL MAXIMUM FLOW VELOCITY (ft/sec) VMAX			
2.257031	2.157247		
2.452946	2.305281	2.572725	2.136336
2.390796	2.452071	2.20661	2.366519
2.177101	2.154559	2.469816	2.511524
2.146433	2.306036	2.210821	2.166484
2.451684	2.296778	2.205621	2.17107
2.133322	2.345441	2.134962	2.643292
2.156808	2.390297	2.315309	2.117939
2.112857	2.387876	2.176033	2.227109
2.107565	2.190026	2.314231	2.371798
2.473184	2.38132	2.235625	2.456764
2.165903	2.321932	2.126019	2.080171
2.12382	2.069941	2.265144	2.126837
2.309554	2.322697	2.228547	2.207768
2.375772	2.250506	2.299999	2.405754
2.11641	2.297915	2.109399	2.167768
2.392966	2.1921	2.054062	2.13987
2.189528	2.024424	2.141492	2.147034
2.226782	2.189152	2.259224	2.403189
2.346864	2.116083	2.325758	2.20594
2.209811	2.287028	2.490083	2.162787
2.131427	2.242718	2.276067	2.20416
2.265275	2.679556	2.369963	2.601057
2.250819	2.046666	2.241501	2.377903
2.268325	2.3153	2.30872	2.247273
2.21294	2.606858		

-----

-----

-----

TITLE: DETAILED MODEL COMPARISON



PROJECT NAME: BALTIMORE US PIER FACE  
 pier diam (ft), Soil mean diameter(mm)  
 b D50M YTM500 VM500 QTM500  
 5.0 0.15 41.00 4.51 250761

DATE: 4/07/05

ARRAY OF ANNUAL MAXIMUM FLOW DEPTH (ft) YTMAX

37.000000	36.750000		
37.750000	37.072270	38.500000	37.000000
36.750000	36.521670	37.000000	36.848270
37.250000	36.577110	36.750000	38.750000
36.442030	36.750000	36.750000	37.750000
37.750000	37.005220	37.250000	36.886850
36.531910	36.750000	37.000000	36.750000
36.478960	37.000000	37.000000	37.000000
36.750000	37.136490	37.250000	36.579070
36.750000	37.500000	36.750000	36.648090
36.248020	36.770110	37.250000	37.007350
36.581620	37.250000	36.750000	37.000000
36.500000	36.750000	36.678760	36.608150
36.417620	36.420900	36.500000	38.250000
37.750000	36.750000	37.250000	37.250000
37.000000	36.509580	36.767600	36.750000
36.696990	37.000000	36.742070	36.500000
37.500000	36.295560	38.000000	36.750000
36.718870	37.025590	37.750000	37.250000
36.929230	37.176140	36.978160	36.507170
37.000000	36.770600	36.750000	37.500000
36.596460	36.552930	37.000000	37.500000
36.500000	37.000000	36.860860	37.250000
36.873590	36.750000	37.750000	37.750000
36.990760	36.737800	36.527760	38.500000
36.397140	36.429580		

ARRAY OF ANNUAL MAXIMUM FLOW DISCHARGE (cfs) QMAX

69359.780000	70384.750000		
85428.480000	72355.230000	128380.300000	81406.340000
67928.010000	62545.160000	72016.200000	74108.050000
81994.550000	65098.840000	92550.460000	128609.000000
67476.610000	66371.840000	74996.100000	90670.270000
76761.450000	89339.340000	78906.750000	73337.240000
73155.010000	62889.940000	68943.090000	86301.360000
63984.850000	64959.950000	80379.270000	61317.500000
60824.140000	92691.780000	77742.890000	82489.300000
88007.500000	98426.950000	80751.460000	71797.900000
66950.420000	62003.840000	80053.030000	62381.270000
67999.840000	100210.500000	73925.590000	73703.030000
66898.870000	88358.390000	66186.140000	74933.470000
71600.720000	79067.510000	63090.090000	109376.500000
89750.790000	74718.730000	114865.600000	81788.640000
80371.810000	62889.770000	63858.810000	64572.220000
68698.480000	70631.630000	89248.010000	69728.960000
102987.100000	68370.690000	106630.100000	74198.620000
67487.520000	70064.450000	90776.750000	67853.300000
66336.020000	70505.390000	60361.820000	69530.800000
65925.120000	75637.910000	79168.710000	72955.430000
66246.590000	73700.840000	85769.910000	92997.700000
73752.400000	76660.290000	62931.380000	129931.500000

75174.190000	69996.440000	87583.160000	74075.980000
74564.890000	75550.390000	67803.700000	119192.300000
63080.890000	67732.130000		
ARRAY OF ANNUAL MAXIMUM FLOW VELOCITY (ft/sec) VMAX			
1.238974	1.371984		
1.965574	1.777336	2.580252	1.783640
1.114192	1.212872	1.108562	1.181335
1.820592	1.289675	1.292715	2.502550
1.007562	1.247173	1.022056	2.100950
1.742546	2.004594	1.820264	1.402171
1.428923	7.909279E-01	1.485274	1.551212
8.543501E-01	1.065620	1.529689	1.113761
8.070495E-01	1.869717	1.359676	1.651781
1.728025	2.054943	1.292238	9.769673E-01
9.021355E-01	1.238472	1.542575	9.711797E-01
1.386620	1.782023	1.622180	1.253182
1.112272	1.906992	8.172714E-01	1.726371
1.322417	9.102172E-01	1.363127	2.219834
1.906485	1.259358	2.070082	1.675835
1.903465	1.203892	1.124138	1.184530
1.135547	1.321566	1.716703	1.326909
2.263973	1.349324	2.073964	1.303249
1.092813	9.069383E-01	1.881641	1.657262
1.156878	1.526664	1.341791	1.098983
1.188592	1.195654	1.773570	1.419667
9.900039E-01	9.459242E-01	1.565590	1.976120
1.026446	1.456572	1.041493	2.415179
1.619750	1.170977	1.778872	1.691023
8.795996E-01	1.313238	1.112654	2.555676
1.306080	1.171398		

TITLE: DETAILED MODEL COMPARISON

PROJECT NAME: BALTIMORE DS PIER FACE

DATE: 4/07/05

pier diam (ft), Soil mean diameter(mm)

b	D50M	YTM500	VM500	QTM500
5.0	0.15	41.25	2.51	100678

ARRAY OF ANNUAL MAXIMUM FLOW DEPTH (ft) YTMAX

37.750000	37.750000		
38.500000	38.750000	39.250000	38.500000
37.000000	37.000000	37.000000	37.000000
38.250000	37.250000	37.250000	39.250000
37.000000	36.750000	37.000000	39.000000
37.750000	39.250000	37.750000	37.000000
37.750000	37.000000	38.000000	37.250000
36.750000	37.000000	37.750000	37.500000
37.000000	38.000000	38.000000	37.750000
38.000000	38.250000	38.250000	37.250000
36.750000	37.000000	37.500000	37.250000
37.000000	37.500000	38.250000	37.500000
36.750000	38.500000	37.250000	38.250000
37.000000	37.000000	37.000000	38.750000
38.250000	37.250000	38.750000	37.750000
37.500000	36.750000	37.750000	37.750000
37.035150	37.500000	38.250000	37.000000
38.500000	37.000000	39.250000	38.250000

37.000000	37.116000	37.750000	37.500000
36.966450	37.250000	37.250000	37.250000
37.000000	37.000000	37.250000	38.250000
37.000000	37.137940	37.250000	39.000000
36.820180	37.514030	37.500000	38.750000
37.250000	37.000000	37.750000	38.250000
37.250000	37.500000	36.750000	39.000000
37.250000	36.805500		
ARRAY OF ANNUAL MAXIMUM FLOW DISCHARGE (cfs) QMAX			
72080.800000	62550.910000		
63603.070000	65408.390000	55927.660000	60000.680000
62844.090000	73845.560000	66035.050000	53809.260000
65556.720000	70223.560000	70555.800000	58270.650000
69768.910000	63019.640000	67290.240000	69609.480000
65633.950000	74646.430000	66281.270000	57018.670000
67918.110000	71915.050000	66097.610000	60897.140000
61560.700000	60805.460000	67194.590000	65143.040000
62704.110000	65860.160000	54381.200000	65625.590000
70834.200000	55900.210000	61086.660000	60288.740000
61555.870000	60131.480000	59086.070000	64734.820000
61391.410000	62776.910000	78784.160000	65173.640000
70351.110000	59197.120000	54254.070000	65722.730000
58924.350000	58924.350000	64981.250000	57250.790000
62601.050000	65396.360000	64577.840000	82579.710000
66211.520000	60692.830000	62296.490000	61728.300000
72582.650000	59910.890000	63646.740000	56931.600000
61361.100000	58255.770000	54943.960000	58543.830000
65874.910000	62545.860000	58853.770000	59407.390000
70390.640000	60335.770000	59600.630000	67407.470000
65207.320000	76828.780000	67909.360000	67910.220000
61471.250000	69531.660000	60211.140000	68608.550000
75625.810000	63136.890000	65012.360000	62587.760000
58705.700000	63496.390000	61574.880000	65889.610000
59811.620000	56819.950000	58471.730000	71702.450000
60449.980000	60244.410000		
ARRAY OF ANNUAL MAXIMUM FLOW VELOCITY (ft/sec) VMAX			
1.042961	1.015477		
9.462508E-01	9.464179E-01	8.246149E-01	8.852946E-01
9.748330E-01	1.068496	9.554860E-01	8.905261E-01
9.229528E-01	1.015435	1.040308	9.520143E-01
1.009560	1.025659	9.633124E-01	1.007240
1.009279	1.050810	9.462192E-01	8.287537E-01
9.827309E-01	1.026613	9.436362E-01	9.876090E-01
8.879385E-01	8.798143E-01	9.592052E-01	9.489326E-01
9.581022E-01	9.529543E-01	9.379629E-01	9.495699E-01
1.011150	9.510589E-01	8.877410E-01	9.160058E-01
9.031009E-01	9.251480E-01	9.028993E-01	1.059280
8.883025E-01	8.906776E-01	1.139979	9.430666E-01
1.017978	8.565441E-01	1.111339	9.509873E-01
9.395388E-01	9.953431E-01	9.576279E-01	8.312370E-01
1.001465	1.016914	9.104413E-01	1.194882
9.322065E-01	8.782240E-01	1.059895	9.037853E-01
1.021940	1.007887	9.544667E-01	9.044439E-01
9.441676E-01	1.174592	9.803725E-01	9.750562E-01
9.532123E-01	9.598794E-01	8.738623E-01	9.369457E-01
1.018518	9.508025E-01	8.865155E-01	9.753418E-01
9.559017E-01	1.111661	9.826078E-01	1.020182

8.949619E-01	1.006080	9.069943E-01	9.927385E-01
1.079597	9.135489E-01	1.016304	9.497236E-01
8.771642E-01	9.281113E-01	9.031460E-01	9.534972E-01
9.713302E-01	8.803160E-01	8.991486E-01	1.009521
8.872234E-01	1.153860		

# APPENDIX E-6

Raw scour results from annual series data. These data were  
Later sorted in ascending order to simulate annual  
scour.

## Monie Bay Upstream Pier Face

Laursen &Tosh =	8.914099	8.944799	8.944799
9.091148	8.944799	8.944799	8.869481
9.091148	9.006008	9.091148	8.869481
8.944799	9.018666	9.018666	9.018666
9.018666	9.018666	9.162307	9.018666
9.018666	9.162307	8.944799	9.043643
9.018666	8.869481	8.869481	8.944799
8.944799	8.900755	8.869481	8.944799
8.869481	9.091148	8.869481	9.091148
8.944799	8.869481	8.944799	9.018666
9.018666	8.944799	8.944799	8.964895
9.091148	8.944799	8.944799	8.944799
8.944799	8.944799	9.018666	8.944799
9.091148	8.999912	8.944990	8.944799
9.091148	8.869481	9.018666	8.944799
8.963928	9.018666	8.869481	9.018666
8.944799	9.091148	8.944799	8.944799
8.944799	8.835526	8.944799	8.897306
8.869481	9.162307	9.091148	9.018666
8.944799	8.944799	8.869481	9.018666
9.018666	9.018666	8.944799	8.944799
8.944799	8.869481	8.869481	9.018666
9.018666	8.944799	8.944799	8.944799
8.944799	8.869481	9.091148	9.018666
8.944799	8.869481	9.091148	8.944799
9.018666			
Hancu eq1 =	1.531956	1.519521	1.544167
1.543750			
1.528345	1.533628	1.462635	1.568198
1.531694	1.524406	1.539119	1.538902
1.473014	1.570146	1.543956	1.563183
1.571885	1.508293	1.469423	1.549211
1.517145	1.651085	1.529827	1.592672
1.459030	1.539119	1.494675	1.507123
1.496580	1.539119	1.503572	1.475218
1.527932	1.480595	1.590732	1.573838
1.507336	1.594617	1.577094	1.557951
1.640889	1.601513	1.507067	1.503165
1.466029	1.475011	1.478595	1.519521
1.524819	1.533418	1.568622	1.499611
1.473066	1.466029	1.487539	1.510262
1.544385	1.559696	1.542413	1.491056
1.531659	1.484174	1.487335	1.531868
1.497832	1.512443	1.538902	1.503572
1.530421	1.523054	1.570501	1.528561
1.529495	1.555997	1.531659	1.480386
1.582512	1.537362	1.557951	1.499811
1.590945	1.498237	1.526583	1.531868



0.000000E+00			
Colorado state University HEC18=		2.874268	2.863804
2.893530	2.914739	2.874467	2.880840
2.783663	2.944280	2.887566	2.891246
2.876229	2.887194	2.817895	2.935781
2.904258	2.927419	2.937867	2.881928
2.813485	2.910599	2.892772	3.020564
2.890855	2.962743	2.779257	2.876229
2.833663	2.848787	2.829538	2.876229
2.844476	2.799009	2.895536	2.805552
2.971364	2.929090	2.837967	2.953851
2.944112	2.921127	3.008580	2.962044
2.851665	2.865326	2.798688	2.809680
2.814060	2.863804	2.870208	2.891522
2.922857	2.860976	2.815257	2.798715
2.824973	2.874000	2.882540	2.923226
2.891420	2.832044	2.889392	2.809902
2.835448	2.878718	2.858797	2.855236
2.887194	2.844476	2.860727	2.868076
2.917938	2.863550	2.907863	2.929559
2.889392	2.816248	2.939441	2.874121
2.921127	2.850688	2.960680	2.837995
2.872339	2.878718	2.913828	2.850796
2.833261	2.800197	2.850938	2.831494
2.853088	2.868076	2.848664	3.008334
2.876567	2.916605	2.878335	2.823637
2.878718	2.867975		

### Monie Bay Downstream Pier Face

Laursen &Tosh =	8.955679	8.955679	8.944799
8.869481	8.703862	8.869481	8.747146
8.860285	8.998845	8.955732	8.955732
8.955732	8.955732	8.760336	8.778270
8.820265	8.760336	8.792640	8.797494
8.785483	8.785483	8.785483	8.785483
8.792640	8.792640	8.689665	8.841716
8.689665	8.897180	8.887177	8.910285
8.859996	8.859996	8.859996	8.859996
8.869481	8.859996	8.859996	8.869481
8.859996	8.869481	8.859996	8.869481
8.859996	8.859996	8.859996	8.823463
8.819262	8.819262	8.869481	8.792640
8.869481	8.887123	8.887123	8.887123
8.887123	8.887123	8.759210	8.714199
8.848153	8.848153	8.848153	8.848153
8.848153	8.848153	8.848153	8.848153
8.848153	8.848153	8.848153	8.892816
8.864029	8.864029	8.714933	8.792640
8.716727	8.842306	8.833043	8.833043
8.833043	8.833043	8.944799	8.821267
8.809767	8.809767	8.809767	8.809767
8.809767	8.809767	8.809767	8.809767
8.714199	8.712676	8.777403	8.754848
8.792640	8.731025	8.732303	8.731025

8.779115			
Hancu eq1 =	2.203421	2.313548	2.271467
2.309974			
2.223029	2.126502	2.309077	2.288448
2.301778	2.198947	2.307073	2.209921
2.209589	2.223438	2.255189	2.276492
2.333076	2.174496	2.276581	2.220104
2.288111	2.313438	2.210279	2.229522
2.243819	2.233377	2.347427	2.254727
2.238976	2.325376	2.271007	2.251728
2.213270	2.296280	2.289787	2.288340
2.227876	2.296576	2.233492	2.165319
2.220291	2.245349	2.122005	2.210451
2.177182	2.214964	2.314170	2.282029
2.183270	2.352980	2.269742	2.275330
2.145863	2.207297	2.216918	2.169661
2.264543	2.323391	2.223378	2.283804
2.258741	2.252137	2.146020	2.326861
2.234089	2.252541	2.237093	2.270311
2.169820	2.256871	2.287126	2.204433
2.200047	2.222872	2.268081	2.264101
2.246401	2.268733	2.267185	2.312970
2.210437	2.274510	2.280259	2.200622
2.193650	2.248206	2.291103	2.214579
2.348353	2.203626	2.296866	2.293685
2.268026	2.173076	2.271563	2.283034
2.255374	2.164357	2.290654	2.173069
Froelichs eqn 1988 for circular piers =			4.967993
4.992748			
4.976490	4.937567	4.818754	4.897120
4.862284	4.927227	5.097815	4.967002
4.991349	4.969512	4.969436	4.852423
4.869911	4.899984	4.875179	4.861322
4.886084	4.866832	4.881188	4.886459
4.864732	4.873163	4.876205	4.812514
4.928202	4.816873	4.939374	4.951946
4.954635	4.919113	4.910706	4.928728
4.927335	4.932918	4.913911	4.928791
4.920990	4.900079	4.918089	4.917726
4.896098	4.910086	4.902723	4.911078
4.909914	4.900544	4.879283	4.946719
4.881688	4.930107	4.912293	4.926105
4.928244	4.917676	4.938735	4.872516
4.824935	4.918715	4.913326	4.911899
4.888556	4.927877	4.907985	4.911986
4.908638	4.915819	4.893861	4.912922
4.947215	4.911236	4.910266	4.825265
4.881338	4.834834	4.907063	4.906174
4.905843	4.915575	4.893587	4.977168
4.901399	4.877313	4.875801	4.887546
4.896641	4.880330	4.908596	4.877964
4.897854	4.839360	4.833225	4.851887
4.859200	4.884482	4.841563	4.823232
4.848814	4.852908		
Jain & Fischer, Dimensionless=		0.000000E+00	0.000000E+00
0.000000E+00			
0.000000E+00	0.000000E+00	0.000000E+00	0.000000E+00





# Black River Upstream Pier Face

Laursen	&Tosh	10.15924	10.15924
10.2143	10.15924	10.15924	10.01195
10.156	10.3224	10.2143	10.15924
10.10347	10.10347	10.06446	10.2143
10.15924	10.2143	10.10347	10.10347
10.15924	10.2143	10.15924	10.2143
10.15924	10.10347	10.04697	10.20767
10.10347	10.15924	10.15924	10.2143
10.15924	10.2143	10.15924	10.05269
10.2143	10.2143	10.10347	10.15924
10.37547	10.10347	10.09871	10.15924
10.09871	10.15924	10.26868	10.15924
10.2143	10.2143	10.15924	10.10347
10.26868	10.2143	10.17099	10.37547
10.17099	10.04697	10.15924	10.10347
10.15924	10.15924	10.26868	10.10347
10.04697	10.3224	10.10347	10.10347
10.15924	10.2143	10.26868	10.16322
10.10347	10.3224	10.10347	10.15924
10.26868	10.12699	10.10414	10.26868
10.2143	10.10624	10.22856	10.10347
10.04697	10.2143	10.15924	10.10347
10.15924	10.2143	10.15924	10.06919
10.15924	10.15924	10.15924	10.2143
10.04697	10.2143	10.10347	10.15924
10.2143	10.13596		
Hancu	eq1	2.292994	2.291391
2.313755	2.270306	2.314096	2.320533
2.299111	2.301486	2.219855	2.320159
2.235506	2.337419	2.326823	2.232313
2.363889	2.351433	2.291785	2.302574
2.367364	2.31262	2.248995	2.302999
2.539489	2.316375	2.325545	2.320864
2.259399	2.434538	2.252129	2.339501
2.397962	2.223859	2.537109	2.285168
2.252178	2.300436	2.32724	2.391145
2.225875	2.462538	2.41545	2.290005
2.290931	2.200048	2.405413	2.377116
2.391952	2.214721	2.358566	2.279078
2.157228	2.332365	2.208271	2.267773
2.314991	2.277297	2.244895	2.329067
2.445789	2.296075	2.221411	2.383817
2.176075	2.330938	2.296549	2.47937
2.228045	2.284488	2.293414	2.246736
2.461447	2.38485	2.267386	2.398255
2.312295	2.181277	2.350529	2.246352
2.287093	2.300024	2.256201	2.315315
2.249719	2.268004	2.313737	2.278922

FrøelichsEqn		1988	for	circular	piers
5.853121	5.907406	5.867371	5.85277		
5.744363	5.866875	6.00355	5.910307		
5.835569	5.822355	5.794303	5.795293		
5.918917	5.839842	5.931396	5.832536		
5.813034	5.863632	5.932559	5.866992		
5.892254	5.863774	5.891838	5.773989		
5.912772	5.822585	5.849075	5.906971		
5.89334	5.875931	5.942748	5.836945		
5.847558	5.904726	5.893357	5.815884		
5.871863	6.08323	5.791065	5.863891		
5.900806	5.808467	5.859725	5.921564		
5.897551	5.935816	5.940753	5.833804		
5.834845	5.949539	5.85997	5.8836		
6.017437	5.861864	5.773544	5.855133		
5.797451	5.87247	5.91059	5.955467		
5.789561	5.795447	5.9592	5.825875		
5.814604	5.92132	5.884966	5.951429		
5.863941	5.798067	6.059587	5.843311		
5.851782	5.990467	5.839574	5.776497		
5.974252	5.891337	5.813804	5.922085		
5.801229	5.773648	5.892505	5.851991		
5.820252	5.855681	5.967777	5.85653		
5.800416	5.890647	5.913127	5.858249		
5.976097	5.802972	5.920216	5.817719		
5.876743	5.901891	5.85988	5.840724		

857

0.00E+00	0.00E+00	0.00E+00	0.00E+00
0.00E+00	0.00E+00	0.00E+00	0.00E+00
0.00E+00	0.00E+00	0.00E+00	0.00E+00
0.00E+00	0.00E+00	0.00E+00	0.00E+00
0.00E+00	0.00E+00	0.00E+00	0.00E+00
0.00E+00	0.00E+00	0.00E+00	
Colorado	State	University	HEC18
3.930581	3.964447	3.97753	3.92943
3.951232	3.984418	3.990539	3.973865
3.873163	3.974499	3.880813	3.986339
4.001886	3.8871	4.042684	4.0088
3.943236	3.965183	4.046497	3.976277
3.915456	3.965652	4.211715	3.960094
3.999279	3.975274	3.917304	4.10957
3.918957	4.005878	4.079987	3.877645
4.199422	3.955758	3.919012	3.952782
3.992391	4.102017	3.870074	4.128461
4.088862	3.940415	3.952304	3.870005
4.07795	4.057188	4.07342	3.867412
4.0166	3.958661	3.812157	4.000163
3.897817	3.928709	3.958576	3.937191
3.891266	3.994403	4.121749	3.977584
3.865091	4.033711	3.852136	3.98634
3.948495	4.157981	3.892009	3.96469
3.955767	3.893313	4.169156	4.04527
3.926186	4.0903	3.970099	3.820246
4.037871	3.912503	3.93855	3.974798
3.903831	3.958931	3.916265	3.926872
3.967435	3.938994	4.162888	3.941784
3.9912	4.054862	4.130303	3.947442
4.19064	4.0597	4.006121	3.958936
4.008571	3.946577	3.952812	3.950383

### Black River Downstream Pier Face

L&T	Hancu	Froelichs	Jain	HEC18
10.27	2.66	6.08	0	4.38
10.27	2.66	6.09	0	4.38
10.27	2.67	6.1	0	4.39
10.27	2.7	6.1	0	4.41
10.27	2.7	6.11	0	4.42
10.27	2.7	6.12	0	4.44
10.27	2.7	6.12	0	4.44
10.27	2.72	6.12	0	4.45
10.27	2.72	6.12	0	4.45
10.27	2.72	6.13	0	4.46
10.27	2.73	6.14	0	4.46

10.32	2.74	6.14	0	4.46
10.32	2.74	6.14	0	4.46
10.32	2.74	6.15	0	4.47
10.32	2.74	6.15	0	4.47
10.32	2.74	6.15	0	4.48
10.32	2.75	6.15	0	4.48
10.32	2.75	6.15	0	4.49
10.32	2.76	6.15	0	4.49
10.32	2.76	6.16	0	4.49
10.32	2.76	6.16	0	4.49
10.32	2.76	6.16	0	4.5
10.32	2.76	6.16	0	4.5
10.32	2.76	6.16	0	4.5
10.32	2.76	6.16	0	4.5
10.32	2.77	6.16	0	4.5
10.32	2.77	6.17	0	4.5
10.32	2.77	6.17	0	4.51
10.32	2.77	6.17	0	4.51
10.32	2.77	6.17	0	4.51
10.32	2.78	6.17	0	4.51
10.32	2.78	6.18	0	4.51
10.32	2.78	6.18	0	4.51
10.32	2.78	6.18	0	4.51
10.32	2.78	6.18	0	4.51
10.32	2.78	6.19	0	4.51
10.32	2.78	6.19	0	4.52
10.32	2.78	6.19	0	4.52
10.32	2.79	6.2	0	4.52
10.38	2.79	6.2	0	4.52
10.38	2.79	6.21	0	4.52
10.38	2.79	6.21	0	4.52
10.38	2.79	6.21	0	4.53
10.38	2.79	6.21	0	4.53
10.38	2.79	6.21	0	4.53
10.38	2.8	6.21	0	4.54
10.38	2.8	6.21	0	4.54
10.38	2.8	6.21	0	4.54
10.38	2.8	6.21	0	4.54
10.38	2.8	6.22	0	4.54
10.38	2.8	6.22	0	4.54
10.38	2.8	6.23	0	4.55
10.38	2.81	6.23	0	4.55
10.38	2.81	6.23	0	4.55
10.38	2.81	6.23	0	4.55
10.38	2.81	6.23	0	4.56
10.38	2.82	6.24	0	4.56
10.38	2.82	6.24	0	4.56
10.38	2.82	6.24	0	4.56
10.38	2.82	6.25	0	4.57

10.38	2.82	6.25	0	4.57
10.38	2.82	6.25	0	4.57
10.43	2.83	6.25	0	4.57
10.43	2.83	6.26	0	4.57
10.43	2.83	6.26	0	4.57
10.43	2.83	6.26	0	4.57
10.43	2.83	6.26	0	4.58
10.43	2.83	6.26	0	4.58
10.43	2.83	6.27	0	4.58
10.43	2.83	6.27	0	4.58
10.43	2.84	6.27	0	4.58
10.43	2.84	6.27	0	4.59
10.43	2.84	6.27	0	4.59
10.43	2.85	6.27	1.29	4.59
10.43	2.87	6.27	1.99	4.6
10.43	2.87	6.28	2.41	4.6
10.43	2.87	6.28	2.6	4.6
10.43	2.87	6.28	2.7	4.61
10.43	2.87	6.28	2.76	4.61
10.43	2.87	6.28	2.82	4.62
10.43	2.88	6.28	2.85	4.62
10.43	2.88	6.29	3	4.62
10.43	2.88	6.29	3.3	4.63
10.43	2.89	6.29	3.32	4.63
10.43	2.89	6.3	3.33	4.63
10.48	2.89	6.3	3.44	4.64
10.48	2.9	6.3	3.45	4.64
10.48	2.9	6.31	3.55	4.64
10.48	2.9	6.31	3.57	4.65
10.48	2.9	6.32	3.57	4.65
10.48	2.91	6.33	3.6	4.66
10.48	2.91	6.34	3.69	4.67
10.48	2.92	6.35	3.76	4.67
10.48	2.93	6.36	3.77	4.68
10.53	2.93	6.37	3.87	4.69
10.53	2.93	6.39	3.91	4.7
10.53	2.94	6.41	4.22	4.72
10.53	2.97	6.42	4.68	4.74
10.58	3.21	6.55	5.90	5.01

#### Patuxent River Upstream Pier Face

Laursen	&Tosh	10.93084	11.02335
10.94027	10.97732	11.02335	10.97732
11.06893	11.05596	10.97732	10.97732
11.02335	10.94023	10.97732	10.97732
10.97732	10.97732	11.02335	10.97732
10.97732	10.97732	10.93084	11.02335

10.93084	10.93084	10.97732	10.93084	
11.02335	11.00729	10.97732	11.01994	
10.97299	10.97732	11.02335	11.06408	
10.93084	11.02335	10.97732	10.97732	
11.0688	10.93084	11.02335	10.93084	
10.96721	10.9898	10.98205	10.97732	
10.97732	11.1588	11.02335	10.97732	
10.97732	10.97732	10.97732	10.93305	
11.06893	10.97732	10.97732	10.93084	
11.06893	11.02335	10.93084	10.97732	
10.97732	10.93084	10.93084	10.97732	
10.97732	10.93084	10.97732	11.02335	
11.02335	10.97732	10.93331	10.97732	
10.97732	10.99105	11.06893	10.97732	
11.06893	11.02335	11.06893	10.97732	
11.02335	10.97732	11.02335	10.97732	
10.93084	10.97732	10.94536	11.02335	
10.93084	10.9355	11.02335	10.94362	
11.06893	10.97732	10.95217	10.97732	
10.96839	10.97732			
Hancu	eq1	3.54431	3.752291	3.246265
2.896186	4.22854	3.523396	4.239205	2.918951
2.941134	3.383576	3.096216	3.569129	
2.943677	2.884648	2.726073	3.366836	
3.318461	2.757977	2.913245	3.231745	
2.859548	2.909662	3.220976	2.746351	
2.794893	3.383073	2.76675	3.524884	
3.15122	3.057341	3.495235	2.819801	
3.014681	2.756642	3.639394	3.003754	
3.625691	2.98066	2.858543	4.268195	
3.2402	2.80621	3.40607	2.868816	
3.21529	3.526649	3.064949	2.807688	
4.271465	2.925429	2.945946	3.080941	
3.509171	2.998073	2.699004	2.91596	
3.309211	3.429843	3.709756	2.85828	
3.202134	2.90355	3.605061	3.63323	
2.9146	2.986299	3.563072	3.03259	
3.068408	3.389489	3.889623	3.009288	
3.797316	3.061707	3.012607	3.228007	
3.941898	3.981743	2.965034	3.976844	
3.288263	3.775657	2.936877	2.970119	
2.973217	3.141263	3.055378	2.924108	
2.918363	3.025176	2.885539	2.765907	
2.986331	2.774255	2.740323	3.915539	
3.254044	2.97048	2.974866	3.356238	
Froelichs	Eqn	1988	for	circular piers
6.881896	6.688916	6.719557	7.185105	
6.926834	7.201954	6.818736	6.883019	
6.788817	6.992394	6.69747	6.715461	
6.657965	6.877689	6.86218	6.717397	

6.725593	6.833978	6.706511	6.67588	
6.880379	6.617827	6.63533	6.88286	
6.625208	6.978597	6.839563	6.775608	
6.965476	6.687736	6.760976	6.716901	
7.117655	6.708295	7.00986	6.749203	
6.706151	7.257498	6.786722	6.735233	
6.839373	6.699292	6.842053	6.933095	
6.778202	6.687841	7.181914	6.778414	
6.737092	6.783641	6.922433	6.75524	
6.602789	6.82351	6.859197	6.897656	
6.931285	6.80244	6.874079	6.673749	
6.951863	6.960404	6.677599	6.702336	
6.939044	6.767136	6.730158	6.884898	
7.088921	6.808053	7.009255	6.730515	
6.760261	6.83275	7.066855	7.168833	
6.743764	7.167404	6.902668	7.107626	
6.733912	6.794282	6.746615	6.853547	
6.774938	6.680904	6.727398	6.730835	
6.764106	6.624904	6.70722	6.723441	
6.628677	7.149418	6.84128	6.719229	
6.747189	6.864552	7.048269	6.838737	
		Fischer,Dim		
Jain		& ensionless=	6.904938	0.00E+00 5.979359
0.00E+00	0.00E+00	8.248211	5.871424	
8.383392	0.00E+00	4.859764	0.00E+00	
6.122305	0.00E+00	0.00E+00	0.00E+00	
4.688281	4.047586	0.00E+00	0.00E+00	
0.00E+00	0.00E+00	0.00E+00	0.00E+00	
0.00E+00	0.00E+00	4.854867	0.00E+00	
5.883749	0.00E+00	0.00E+00	5.706948	
0.00E+00	0.00E+00	0.00E+00	6.479881	
0.00E+00	6.393375	0.00E+00	0.00E+00	
9.61757	0.00E+00	0.00E+00	5.080049	
0.00E+00	0.00E+00	5.8901	0.00E+00	
0.00E+00	8.323394	0.00E+00	0.00E+00	
0.00E+00	5.789785	0.00E+00	0.00E+00	
0.00E+00	3.883769	5.259268	6.709537	
0.00E+00	0.00E+00	0.00E+00	6.287221	
6.414123	0.00E+00	0.00E+00	6.083508	
0.00E+00	0.00E+00	4.916309	7.362359	
0.00E+00	7.042472	0.00E+00	0.00E+00	
0.00E+00	7.499282	7.658054	0.00E+00	
7.644265	3.280688	7.008811	0.00E+00	
0.00E+00	0.00E+00	0.00E+00	0.00E+00	
0.00E+00	0.00E+00	0.00E+00	0.00E+00	
0.00E+00	0.00E+00	0.00E+00	0.00E+00	
7.465798	0.00E+00	0.00E+00	0.00E+00	
4.575726				
Colorado	State	University	HEC18=	5.6326 5.122654
5.409148	4.777442	4.760904	6.081545	
5.399186	6.044129	4.824032	5.260683	



4.969406	5.454564	4.803367	4.748723
4.579493	5.243964	5.195483	4.62272
4.778883	5.107938	4.722163	4.765784
5.106842	4.59234	4.644271	5.260181
4.614203	5.411071	5.032203	4.929271
5.381049	4.679082	4.885018	4.621284
5.544138	4.864129	5.509885	4.849566
4.721098	6.132178	5.106517	4.674444
5.272783	4.729971	5.093896	5.403459
4.93714	4.66702	6.058257	4.800946
4.813241	4.953658	5.385187	4.86773
4.541794	4.800083	5.186183	5.306737
5.569871	4.738928	5.087648	4.759357
5.479171	5.50661	4.770973	4.845969
5.438129	4.903623	4.931066	5.266582
5.764052	4.888823	5.664954	4.924665
4.882861	5.104145	5.805798	5.862432
4.833233	5.857801	5.175056	5.665847
4.803726	4.847888	4.841791	5.025365
4.92724	4.780956	4.784269	4.889353
4.758829	4.613301	4.846955	4.640213
4.588338	5.799686	5.130529	4.833819
4.843513	5.231402		

#### Patuxent River Downstream Pier Face

Laursen	&Tosh		10.92658	10.88995	10.96142
11.06507	10.93084	10.91622	10.94095		
10.90401	10.88389	10.92333	10.9063		
10.93084	10.93127	10.93084	10.90256		
10.90228	10.91263	10.89241	10.87762		
10.95748	10.89788	10.96285	10.91147		
10.89674	10.89131	10.89235	10.93084		
10.91826	10.93084	10.89753	10.93084		
10.93884	10.8969	10.9057	10.93084		
11.02335	10.93084	10.93084	10.911		
10.95658	10.93836	10.93752	10.93084		
10.93084	10.909	10.94153	10.92621		
10.90878	10.90412	10.92988	10.88302		
10.92182	10.9022	10.90012	10.91011		
10.90112	10.97732	10.93084	10.97732		
10.9044	10.97732	10.90334	10.92435		
10.92567	10.93084	10.91665	10.88309		
10.8981	10.88389	10.89492	10.90786		
10.96528	10.88547	10.90632	10.94872		
10.97816	10.92982	10.90037	10.92102		

10.9068	10.90039	10.92554	10.9321		
10.87132	10.93626	10.91711	10.86656		
10.97732	10.93787	10.97732	10.96387		
10.91136	10.89056	10.93084	10.90295		
10.91338	10.95178	10.93084	10.93084		
10.91861					
Hancu	eq1	=	2.961439	3.3514	3.177545
2.8605	3.167746	3.226965	3.213141		
3.169074	3.041673	2.946084	3.058122		
2.982467	2.983798	2.890489	3.018157		
2.98824	2.985561	3.251761	3.289993		
2.796962	3.170618	3.010324	3.114528		
2.846978	3.296118	3.117794	2.874793		
3.192133	3.072678	3.066389	3.16133		
3.260551	3.344443	3.275363	3.061914		
3.263503	3.058341	3.222092	2.984449		
2.838374	3.190872	3.189075	2.658948		
3.412617	3.254918	3.370221	3.030214		
3.257574	2.876948	2.986432	2.862043		
3.070105	2.907341	3.329781	3.177006		
3.091881	3.261414	3.113392	2.897336		
3.225988	2.895547	3.428066	3.015878		
3.148239	3.05449	3.213055	3.419245		
2.996608	2.812914	3.20916	3.117709		
2.925559	2.894818	3.180704	3.209086		
3.0608	3.295248	2.963187	3.21222		
3.033596	3.193657	2.786306	2.867674		
3.008177	3.213865	3.372032	3.093059		
3.302206	2.879508	3.463863	2.972077		
2.982336	3.259182	3.045017	2.961087		
2.873931	3.024163	2.987303	3.240788		
Froelichs	Eqn	1988	for	circular	piers
6.799012	6.769862	6.65865	6.747608		
6.793272	6.749373	6.713868	6.713277		
6.663043	6.726702	6.70148	6.70148		
6.64	6.683347	6.684008	6.662089		
6.733722	6.831465	6.602415	6.798251		
6.690281	6.709601	6.613323	6.76342		
6.746642	6.650702	6.771112	6.696603		
6.729481	6.769538	6.756999	6.792922		
6.798039	6.826359	6.794232	6.726776		
6.759701	6.728683	6.658578	6.777828		
6.770113	6.585757	6.817718	6.802946		
6.823138	6.69418	6.763743	6.663449		
6.65266	6.6499	6.700644	6.643329		
6.793059	6.73463	6.78735	6.79356		
6.794616	6.644275	6.832087	6.642561		
6.839156	6.707003	6.756713	6.710578		
6.727185	6.807971	6.656985	6.605041		
6.752185	6.783212	6.63451	6.645381		

6.786455	6.827427	6.726537	6.771713		
6.684182	6.752042	6.686559	6.765961		
6.633539	6.600112	6.715483	6.76355		
6.759536	6.787749	6.814198	6.713633		
7.013518	6.677179	6.659077	6.792842		
6.693054	6.675519	6.685066	6.715232		
6.70268	6.773835				
		Fischer,Dim			
Jain		& ensionless=	0.00E+00	4.574289	0.00E+00
0.00E+00	0.00E+00	0.00E+00	0.00E+00		
0.00E+00	0.00E+00	0.00E+00	0.00E+00		
0.00E+00	0.00E+00	0.00E+00	0.00E+00		
0.00E+00	0.00E+00	0.00E+00	2.141748		
3.50401	0.00E+00	0.00E+00	0.00E+00		
0.00E+00	0.00E+00	3.769455	0.00E+00		
0.00E+00	0.00E+00	0.00E+00	0.00E+00		
0.00E+00	2.653077	4.48297	3.148295		
0.00E+00	2.622109	0.00E+00	0.00E+00		
0.00E+00	0.00E+00	0.00E+00	0.00E+00		
0.00E+00	5.139629	1.531928	4.752752		
0.00E+00	2.410933	0.00E+00	0.00E+00		
0.00E+00	0.00E+00	0.00E+00	4.292924		
0.00E+00	0.00E+00	2.487712	0.00E+00		
0.00E+00	0.00E+00	0.00E+00	5.256289		
0.00E+00	0.00E+00	0.00E+00	0.00E+00		
5.194267	0.00E+00	0.00E+00	0.00E+00		
0.00E+00	0.00E+00	0.00E+00	0.00E+00		
0.00E+00	0.00E+00	3.738161	0.00E+00		
0.00E+00	0.00E+00	0.00E+00	0.00E+00		
0.00E+00	0.00E+00	0.00E+00	4.800192		
0.00E+00	3.81296	0.00E+00	5.485975		
0.00E+00	0.00E+00	2.315026	0.00E+00		
0.00E+00	0.00E+00	0.00E+00	0.00E+00		
0.00E+00					
Colorado	State	University	HEC18=	4.819174	5.20931
5.049418	4.829267	4.713947	5.029836		
5.095292	5.073359	5.024317	4.901898		
4.799016	4.920452	4.842067	4.843364		
4.739945	4.873209	4.844269	4.837346		
5.106708	5.162529	4.640019	5.042654		
4.866977	4.971346	4.691798	5.15452		
4.981856	4.726543	5.05777	4.928535		
4.928984	5.028087	5.119739	5.205831		
5.142014	4.943522	5.130057	4.920677		
5.083928	4.849295	4.692	5.05791		
5.054659	4.497999	5.274425	5.123698		
5.236077	4.887035	5.118299	4.731134		
4.83633	4.713788	4.926859	4.757173		
5.19214	5.036055	4.964939	5.127949		
4.987082	4.747518	5.102095	4.745424		
5.293164	4.875658	5.013024	4.91376		

5.068788	5.278564	4.847079	4.656402
5.07015	4.988995	4.773324	4.745255
5.049941	5.085102	4.923006	5.155394
4.81987	5.073024	4.888802	5.058189
4.635354	4.709671	4.869837	5.076902
5.224691	4.966154	5.170551	4.743291
5.357445	4.827178	4.833613	5.125697
4.901136	4.816124	4.732311	4.885314
4.847015	5.104479		

# **Wicomico River Upstream Pier Face**

	Laursen	&Tosh		11.45132	11.45863	11.5023
11.49984	11.46293	11.48597	11.46705			
11.43721	11.4681	11.49073	11.5195			
11.50068	11.50537	11.47984	11.47261			
11.47252	11.48337	11.48765	11.50871			
11.48405	11.44625	11.48547	11.4682			
11.46183	11.46191	11.47564	11.44652			
11.45361	11.45032	11.43433	11.45981			
11.50191	11.4846	11.45249	11.49121			
11.49977	11.46346	11.51181	11.43238			
11.50379	11.45908	11.50681	11.48695			
11.44615	11.49286	11.49548	11.51945			
11.44891	11.49086	11.44781	11.43027			
11.45209	11.44707	11.45603	11.4686			
11.43984	11.44003	11.4927	11.5079			
11.47324	11.44902	11.4753	11.44537			
11.47238	11.49941	11.47629	11.45345			
11.44939	11.46377	11.46445	11.44327			
11.45896	11.43946	11.47432	11.48064			
11.51166	11.50152	11.46634	11.46489			
11.47291	11.49928	11.45599	11.43771			
11.51488	11.45734	11.44503	11.45226			
11.52204	11.49996	11.43162	11.48686			
11.45278	11.45472	11.46364	11.47709			
11.46127	11.45228	11.47583	11.45621			
11.47737						
	Hancu	eq1	3.478246	3.272865	3.266492	3.30859
3.679049	3.28392	3.141086	3.225006			
3.234388	3.457788	3.236726	3.265052			
3.37145	3.321298	3.129173	3.188355			
3.138182	3.152478	3.6641	3.201973			
3.171435	3.217428	3.319896	3.329348			
3.156114	3.562374	3.209258	3.140656			
3.17432	3.214828	3.217937	3.382437			

3.188765	3.278497	3.485312	3.520777	
3.35115	3.250412	3.429289	3.414388	
3.226168	3.221106	3.187611	3.337588	
3.135277	3.316245	3.33	3.443539	
3.315124	3.301121	3.12225	3.36023	
3.353932	3.183558	3.39798	3.322794	
3.458404	3.319676	3.274431	3.274626	
3.387255	3.386793	2.974812	3.192085	
3.235277	3.212701	3.08162	3.102834	
3.147393	3.199725	3.392388	3.24064	
3.448086	3.250604	3.272269	3.283684	
3.363358	3.192152	3.119987	3.273611	
3.128359	3.173214	3.217142	3.23077	
3.348855	3.208196	3.293447	3.449808	
3.338099	3.334917	3.296025	3.16628	
3.279873	3.310509	3.201731	3.367857	
3.295585	3.609002	3.349236	3.261667	
Froelichs eqn	1988	for	circular	piers
7.399968	7.434773	7.459867	7.347664	7.302792
7.27199	7.268691	7.308252	7.416511	
7.369731	7.358062	7.43889	7.354164	
7.273924	7.296223	7.289877	7.300319	
7.520715	7.314836	7.259275	7.322312	
7.339878	7.335794	7.271706	7.435201	
7.273693	7.256226	7.265083	7.261575	
7.292428	7.402756	7.310506	7.306222	
7.426891	7.449792	7.345629	7.365761	
7.336769	7.416592	7.294639	7.348831	
7.312823	7.320278	7.299839	7.370859	
7.404493	7.361434	7.364958	7.309	
7.222322	7.33546	7.327264	7.275188	
7.368623	7.307508	7.356103	7.368821	
7.37011	7.329207	7.341536	7.372568	
7.182974	7.297455	7.345416	7.309772	
7.233591	7.237	7.270569	7.291058	
7.336561	7.299863	7.351799	7.32158	
7.337055	7.378026	7.395326	7.290426	
7.261469	7.328439	7.304692	7.271252	
7.266357	7.362013	7.337554	7.271564	
7.311434	7.451377	7.384225	7.302217	
7.353187	7.264925	7.309348	7.331056	
7.306594	7.349077	7.312231	7.451584	
7.336364	7.329271			
	Fischer,Di			
	mensionles			
Jain	&	s=	0.00E+00	0.00E+00 0.00E+00
0.00E+00	5.602417	0.00E+00	0.00E+00	
0.00E+00	0.00E+00	0.00E+00	0.00E+00	
0.00E+00	0.00E+00	0.00E+00	0.00E+00	
0.00E+00	0.00E+00	0.00E+00	5.458381	
0.00E+00	0.00E+00	0.00E+00	0.00E+00	

0.00E+00	0.00E+00	4.193817	0.00E+00		
0.00E+00	0.00E+00	0.00E+00	0.00E+00		
0.00E+00	0.00E+00	0.00E+00	0.00E+00		
2.751216	0.00E+00	0.00E+00	0.00E+00		
0.00E+00	0.00E+00	0.00E+00	0.00E+00		
0.00E+00	0.00E+00	0.00E+00	0.00E+00		
0.00E+00	0.00E+00	0.00E+00	0.00E+00		
0.00E+00	0.00E+00	0.00E+00	0.00E+00		
0.00E+00	0.00E+00	0.00E+00	0.00E+00		
0.00E+00	0.00E+00	0.00E+00	0.00E+00		
0.00E+00	0.00E+00	0.00E+00	0.00E+00		
0.00E+00	0.00E+00	0.00E+00	0.00E+00		
0.00E+00	0.00E+00	0.00E+00	0.00E+00		
0.00E+00	0.00E+00	0.00E+00	0.00E+00		
0.00E+00	0.00E+00	0.00E+00	0.00E+00		
0.00E+00	0.00E+00	0.00E+00	0.00E+00		
0.00E+00	0.00E+00	0.00E+00	0.00E+00		
0.00E+00	0.00E+00	0.00E+00	0.00E+00		
0.00E+00	0.00E+00	0.00E+00	0.00E+00		
0.00E+00	0.00E+00	0.00E+00	0.00E+00		
0.00E+00	0.00E+00	0.00E+00	0.00E+00		
0.00E+00	0.00E+00	0.00E+00	0.00E+00		
0.00E+00	0.00E+00	0.00E+00	0.00E+00		
0.00E+00	0.00E+00	4.901238	0.00E+00		
0.00E+00					
Colorado	state	University	HEC18=	5.250827	5.245804
5.302614	5.470633	5.66289	5.269533		
5.117377	5.198465	5.214641	5.447971		
5.22782	5.253179	5.369856	5.306643		
5.106054	5.167805	5.117692	5.133523		
5.658494	5.184358	5.14475	5.200701		
5.302727	5.311052	5.132018	5.549801		
5.184101	5.114163	5.148597	5.187326		
5.195871	5.373884	5.170737	5.25687		
5.475869	5.513455	5.333694	5.240382		
5.406416	5.406815	5.204245	5.208968		
5.170023	5.316129	5.116598	5.304786		
5.324002	5.424433	5.302652	5.27913		
5.090122	5.340523	5.33302	5.159394		
5.382524	5.299648	5.437504	5.307716		
5.264379	5.25727	5.367388	5.372589		
4.937529	5.171654	5.222115	5.193883		
5.052225	5.073689	5.123295	5.177947		
5.371362	5.21919	5.426964	5.232712		
5.256402	5.274716	5.354325	5.17047		
5.094849	5.256154	5.110665	5.148618		
5.190429	5.220679	5.330037	5.18269		
5.272195	5.446723	5.328152	5.310289		
5.282179	5.140732	5.258759	5.292128		
5.18266	5.350275	5.274395	5.596354		
5.330186	5.244776				

# Wicomico River Downstream Pier Face

Laursen	&Tosh	11.45019	11.42667	11.50904
11.49503	11.46465	11.41988	11.44796	
11.42113	11.39254	11.48522	11.39548	
11.43805	11.41458	11.45848	11.41716	
11.41077	11.45576	11.42951	11.43493	
11.45754	11.41096	11.47448	11.40623	
11.4466	11.43631	11.40056	11.37893	
11.44506	11.43653	11.42979	11.42124	
11.50161	11.43716	11.4476	11.43851	
11.47117	11.44878	11.46405	11.46405	
11.48382	11.45341	11.49081	11.46672	
11.40686	11.42362	11.45747	11.4696	
11.42474	11.48405	11.43245	11.39908	
11.41448	11.41977	11.43949	11.4372	
11.4153	11.43469	11.41938	11.44516	
11.44239	11.44889	11.42742	11.435	
11.41068	11.436	11.42607	11.40754	
11.39667	11.38098	11.43163	11.42893	
11.41011	11.42107	11.42709	11.46679	
11.49687	11.46994	11.445	11.41679	
11.44207	11.48066	11.42829	11.43433	
11.43958	11.45072	11.41102	11.41112	
11.44039	11.48568	11.42427	11.48207	
11.4193	11.41659	11.42809	11.39219	
11.45668	11.45078	11.46187	11.45352	
11.42901				
Hancu	eq1	3.832065	3.778386	3.66576 3.994754
4.124683	3.64195	3.927001	3.994309	
3.721936	3.900028	3.688498	3.662638	
4.013691	4.058719	3.653488	3.833376	
3.726349	3.676254	3.993807	3.822797	
3.720718	3.681225	3.638579	3.876938	
3.640293	4.200537	3.665515	3.926469	
3.843553	3.620855	3.615077	3.923482	
3.687061	3.744765	3.608916	3.702746	
3.842285	3.905975	4.017069	3.916362	
3.754321	3.999024	3.675394	3.851082	
3.630137	3.577321	3.627378	3.565695	
3.787294	3.631026	3.837359	3.851889	
3.746537	3.722989	3.910512	3.771255	
3.826516	3.943611	3.619022	3.82415	
3.610966	3.677724	3.929463	3.705422	
3.547286	3.645952	3.702525	3.513113	
3.648044	3.654096	3.744499	3.702085	
3.781006	3.940748	3.8784	3.618375	
3.854978	3.720893	3.72542	3.812003	
4.035341	3.672056	3.636264	3.762374	
3.799705	3.719066	3.787843	4.238815	

3.903827	4.155306	3.771241	3.53881		
3.761132	3.912913	3.791364	3.84343		
3.836141	3.767369	3.728754	4.161484		
Froelichs	Eqn	1988	for	circular	piers
7.621668	7.550704	7.607159	7.39523		
7.5235	7.511801	7.388987	7.560965		
7.381473	7.424124	7.509808	7.578647		
7.395841	7.447526	7.46708	7.418392		
7.528728	7.501336	7.410804	7.474686		
7.3777	7.505591	7.414461	7.550096		
7.35401	7.519729	7.482342	7.400009		
7.38777	7.589087	7.431276	7.46329		
7.40644	7.477947	7.496968	7.536611		
7.572395	7.564565	7.473567	7.600121		
7.463241	7.448483	7.39573	7.418441		
7.450348	7.375133	7.522202	7.406668		
7.434575	7.458047	7.430018	7.446146		
7.504886	7.432745	7.474513	7.493532		
7.41791	7.483179	7.419657	7.416362		
7.508275	7.405393	7.382274	7.404026		
7.400643	7.323661	7.350644	7.41348		
7.440465	7.403593	7.442967	7.502129		
7.531014	7.480421	7.527222	7.452141		
7.41942	7.478794	7.599043	7.415504		
7.410707	7.459362	7.485333	7.410328		
7.433105	7.731817	7.562781	7.565947		
7.514381	7.359391	7.430979	7.494437		
7.411301	7.507062	7.497414	7.488277		
7.465158	7.573791				
		Fischer,Di			
		mensionle			
Jain	&	ss=	6.287422	5.502018	7.324286
6.589457	7.767257	5.29012	7.025509		
7.287577	5.933126	6.91787	5.693212		
5.471296	7.357823	7.540234	5.398012		
6.581418	5.958042	5.588709	7.291198		
6.534805	5.923352	5.617098	5.264191		
6.801186	5.266416	7.968294	5.514725		
7.022295	6.637517	5.070463	5.012419		
7.027178	5.673225	6.080887	4.929265		
5.786697	6.633565	6.938598	7.391305		
6.990499	6.141588	7.333666	5.570998		
6.668466	5.171731	4.481168	5.116157		
4.333067	6.341681	5.175971	6.59921		
6.674049	6.09272	5.936396	6.950721		
6.243486	6.550531	7.085739	5.040409		
6.539492	4.94566	5.601225	7.031801		
5.81601	3.951463	5.325198	5.795495		
2.947784	5.363115	5.397872	6.079607		
5.791903	6.300618	7.076541	6.813102		
4.99712	6.701069	5.921381	5.954835		



6.475116	7.466094	5.554502	5.227773	
6.191237	6.409044	5.912019	6.338675	
8.133669	6.935184	7.843758	6.246402	
3.784324	6.183065	6.958457	6.356429	
6.640855	6.602825	6.22226	5.974644	
7.865612				
Colorado	State	University	HEC18=	5.757603 5.641514
5.981201	5.820437	6.094476	5.616432	
5.901411	5.959683	5.689002	5.884166	
5.656821	5.641016	5.976647	6.030246	
5.627228	5.802018	5.707863	5.652522	
5.962517	5.802661	5.692042	5.667669	
5.610003	5.852694	5.618511	6.150268	
5.630403	5.900207	5.81794	5.597767	
5.590105	5.910731	5.664925	5.724074	
5.587878	5.688156	5.819577	5.884918	
5.9918	5.899639	5.734784	5.980933	
5.660141	5.818284	5.605577	5.560673	
5.613222	5.54176	5.774161	5.608456	
5.803145	5.820857	5.719394	5.700827	
5.882946	5.742548	5.800945	5.910605	
5.599415	5.800442	5.592251	5.653497	
5.900705	5.67695	5.525887	5.621795	
5.673382	5.482954	5.613629	5.631113	
5.719509	5.673537	5.753412	5.909691	
5.858866	5.610411	5.836872	5.700031	
5.697999	5.788536	6.013288	5.6481	
5.614072	5.73948	5.778553	5.690434	
5.757773	6.206126	5.887953	6.113532	
5.757983	5.513695	5.732948	5.883104	
5.756804	5.822539	5.814071	5.749524	
5.709714	6.120533			

# **Patapsco River Upstream Pier Face**

Laursen	&Tosh		13.67196	13.63971	13.58822
13.83593	13.61627	13.62484	13.64418		
13.61897	13.67196	13.69961	13.72713		
13.72713	13.61627	13.69048	13.65887		
13.67196	13.61959	13.67196	13.67196		
13.64418	13.78178	13.61627	13.62963		
13.64401	13.69961	13.65944	13.5852		
13.75452	13.61627	13.6382	13.61627		
13.65629	13.62191	13.69961	13.61632		
13.64418	13.61627	13.57112	13.78178		
13.67196	13.64363	13.66195	13.6352		
13.72713	13.69961	13.67196	13.61627		

13.62279	13.61627	13.61627	13.83593
13.58923	13.78178	13.72713	13.64418
13.67196	13.67196	13.80892	13.69961
13.65738	13.62496	13.75452	13.64418
13.62936	13.63723	13.61627	13.61825
13.64418	13.67196	13.66115	13.61627
13.72713	13.64077	13.60155	13.64418
13.62254	13.69961	13.64418	13.69961
13.61627	13.75452	13.64764	13.64418
13.64418	13.64418	13.78178	13.80892
13.58822	13.83593	13.64597	13.637
13.58822	13.72713	13.72713	13.63281
13.72713	13.61915	13.72713	13.72713
13.64918			
Hancu	eq1	3.859215	2.918043 2.861397 2.063566
3.059437	2.209999	2.859164	2.383198
2.718227	3.04779	3.487449	3.259804
2.510194	2.128984	2.075405	2.489174
2.015065	2.892918	3.476558	2.314653
3.642084	2.526827	2.389987	3.285958
2.74069	2.493208	2.013628	3.130536
2.534641	2.667338	2.520112	2.694602
2.168976	3.621696	2.476122	3.025163
2.353137	3.034545	3.566999	2.761587
2.255079	2.29566	2.154237	2.667852
3.535602	2.439722	2.881696	2.670591
2.886517	2.684538	3.96769	2.157303
4.047843	3.17771	3.164675	3.022732
2.839315	4.099521	3.067377	2.523208
2.152791	3.231638	2.859977	2.290993
2.633987	2.986578	2.100933	2.700914
3.015985	1.964423	2.565544	2.8089
2.480351	2.329901	2.983255	2.615462
2.873281	2.416843	3.178265	2.344023
3.453618	3.082802	2.584195	2.585432
3.397448	3.497561	3.693428	1.92432
3.531711	2.19592	3.001445	2.314597
2.951628	3.131425	2.105367	3.446073
2.339592	3.427169	3.282358	2.692387
Froelichs	eqn	1988	for circular piers
9.881716	11.73292	10.75649	10.07901 10.75276 10.65082
10.65717	10.22389	10.5962	10.90167
11.26783	11.10848	10.32767	10.11239
10.00848	10.40645	9.885667	10.7335
11.15381	10.20629	11.48001	10.34158
10.24796	10.96967	10.66382	10.38812
9.828753	11.06614	10.34809	10.49525
10.33597	10.54927	10.03624	11.30447
10.29907	10.7825	10.19305	10.65605
11.42917	10.63084	10.15166	10.21937

10.04449	10.65392	11.24704	10.36389
10.6241	10.47068	10.62777	10.47037
11.89316	9.971498	11.74268	11.0491
10.88416	10.8318	10.692	11.83076
10.91625	10.40997	10.02619	11.14036
10.6578	10.16007	10.46649	10.70289
9.966264	10.53284	10.82677	9.902687
10.37371	10.7682	10.34482	10.14777
10.75133	10.42561	10.76869	10.29619
10.99764	10.18505	11.2978	10.83129
10.43783	10.43885	11.04698	11.38149
11.5686	9.745465	11.51209	10.10126
10.75176	10.11187	10.87982	11.01515
9.994389	11.23942	10.18603	11.22636
11.12461	10.53487		
	Fischer,Di		
	mensionle		
Jain	&	ss=	0.00E+00 0.00E+00 0.00E+00
10.02561	0.00E+00	0.00E+00	0.00E+00
0.00E+00	0.00E+00	0.00E+00	8.197328
6.110696	0.00E+00	0.00E+00	0.00E+00
0.00E+00	0.00E+00	0.00E+00	8.114769
0.00E+00	9.06986	0.00E+00	0.00E+00
6.499434	0.00E+00	0.00E+00	0.00E+00
0.00E+00	0.00E+00	0.00E+00	0.00E+00
0.00E+00	0.00E+00	8.933707	0.00E+00
0.00E+00	0.00E+00	0.00E+00	8.682132
0.00E+00	0.00E+00	0.00E+00	0.00E+00
0.00E+00	8.478235	0.00E+00	0.00E+00
0.00E+00	0.00E+00	0.00E+00	10.41532
0.00E+00	10.64062	4.142681	3.791827
0.00E+00	0.00E+00	10.84216	0.00E+00
0.00E+00	0.00E+00	5.61643	0.00E+00
0.00E+00	0.00E+00	0.00E+00	0.00E+00
0.00E+00	0.00E+00	0.00E+00	0.00E+00
0.00E+00	0.00E+00	0.00E+00	0.00E+00
0.00E+00	0.00E+00	0.00E+00	4.259106
0.00E+00	7.979939	0.00E+00	0.00E+00
0.00E+00	7.556315	8.27486	9.32436
0.00E+00	8.498667	0.00E+00	0.00E+00
0.00E+00	0.00E+00	0.00E+00	0.00E+00
7.922907	0.00E+00	7.788024	6.420089
0.00E+00			
Colorado	state University	HEC18=	5.293042 5.221183
4.225749	6.368084	5.445997	4.421306
5.219356	4.639751	5.057482	5.447975
5.945605	5.693522	4.796512	4.32616
4.251438	4.779675	4.16616	5.263748
5.922684	4.55754	6.124685	4.816886
4.649904	5.706808	5.089001	4.782626
4.159404	5.55267	4.82644	4.990822

4.808667	5.02657	4.368024	6.085869
4.754635	5.411866	4.601685	5.409235
6.043346	5.109111	4.481822	4.536224
4.350906	5.006407	5.99262	4.718514
5.24077	4.992127	5.246395	5.007739
6.48239	4.34811	6.624282	5.601081
5.570747	5.414144	5.200943	6.613854
5.47042	4.819147	4.347527	5.667104
5.220307	4.52532	4.950521	5.362401
4.27905	5.032068	5.406385	4.104413
4.864125	5.174708	4.763779	4.570193
5.363629	4.9257	5.245668	4.685675
5.596532	4.590238	5.913952	5.478459
4.891402	4.892905	5.830366	5.967578
6.185563	4.040463	6.015767	4.406354
5.383291	4.548849	5.341961	5.548584
4.286954	5.900236	4.585115	5.879443
5.718773	5.022714		

#### Patapsco River Downstream Pier Face

Laursen	&Tosh	=	13.69961	13.72713	13.67196
13.83593	13.72713	13.68216	13.78178		
13.72713	13.78178	13.72713	13.91625		
13.75452	13.67196	13.69725	13.66323		
13.67196	13.67196	13.72713	13.78178		
13.67196	13.83593	13.67196	13.66961		
13.80892	13.69961	13.67196	13.68618		
13.78178	13.66157	13.75452	13.67196		
13.67864	13.67196	13.8896	13.69961		
13.67196	13.75452	13.69961	13.80892		
13.69961	13.75452	13.69961	13.69961		
13.72713	13.86283	13.72713	13.72713		
13.78178	13.69961	13.78178	13.8896		
13.69961	13.86283	13.78178	13.78178		
13.78178	13.75452	14.02168	13.78178		
13.67196	13.67196	13.80892	13.72713		
13.71444	13.67313	13.72713	13.64792		
13.69961	13.8896	13.69341	13.67196		
13.78178	13.67196	13.64418	13.72713		
13.67196	13.80892	13.67196	13.78178		
13.67196	13.78178	13.69961	13.67196		
13.67196	13.78178	13.83593	13.80892		
13.64418	13.91625	13.65229	13.80892		
13.69961	13.78178	13.75452	13.67259		
13.78178	13.67196	13.78178	13.78178		

13.69961					
Hancu	eq1	2.369952	2.343824	2.185366	2.306437
2.167229	2.085833	2.196645	2.010233		
2.139103	2.100655	2.245229	2.12289		
2.123103	2.245886	1.962877	2.112707		
2.194744	2.108103	2.107963	2.048285		
2.15224	2.010368	1.987454	2.21483		
2.177568	2.105266	2.070834	2.146484		
2.165934	2.221023	2.211251	2.267233		
2.294666	2.077824	2.094757	2.145295		
2.253624	2.115609	2.006986	2.03006		
2.31012	2.121548	2.04066	2.312497		
2.026626	2.001081	2.216808	2.057059		
2.043684	2.147959	2.116608	2.111149		
2.352646	2.002475	2.216024	2.116883		
2.183278	2.053455	2.043481	2.292923		
2.168843	2.285964	2.096179	2.066256		
2.158553	2.201285	1.970615	2.204983		
2.260409	2.031591	2.19565	2.348115		
2.143819	2.039286	2.103635	2.17031		
2.194037	2.179106	2.227339	2.03316		
1.98105	2.157012	2.06185	2.124586		
2.0101	2.324	2.206324	2.093405		
2.123959	2.02866	2.197088	2.207189		
2.204221	2.121406	2.483677	2.102006		
2.05884	1.970294	2.362636	2.241985		
Froelichs	Eqn	1988	for	circular	piers
10.24608	10.58794	10.21037	10.05698	10.32697	10.22763
10.33123	10.05653	10.27558	10.14612		
10.61125	10.21372	10.07596	10.23376		
9.904492	10.06602	10.14362	10.15338		
10.24502	10.00357	10.38073	9.966177		
9.939511	10.39518	10.17388	10.05887		
10.04904	10.28278	10.09927	10.30789		
10.15899	10.22184	10.23545	10.39793		
10.09456	10.09709	10.33852	10.11473		
10.18893	10.03104	10.39089	10.12046		
10.04154	10.34589	10.29976	10.04731		
10.25732	10.19438	10.04453	10.28421		
10.43733	10.11043	10.61939	10.1391		
10.34974	10.25381	10.27202	11.29058		
10.18073	10.23387	10.11934	10.46264		
10.14175	10.09131	10.11159	10.2427		
9.8875	10.19968	10.57915	10.02236		
10.14447	10.47299	10.09569	9.949306		
10.14903	10.12073	10.37517	10.12899		
10.3605	9.988715	10.11711	10.15439		
10.01684	10.07738	10.14688	10.54535		
10.38701	10.00165	10.49074	9.952137		
10.37812	10.20174	10.33848	10.21227		

[illegible]

4.235465	4.317729	4.182315	4.598816
4.443978	4.272946	4.352276	4.188802
4.432029	4.42885	4.437235	4.325561
4.773	4.304057	4.231494	4.128971
4.63935	4.473535		

## **APPENDIX F**

### **THE PHYSICS OF THE HORSESHOE VORTEX AND DOWNFLOW FORMATION**

#### **INTRODUCTION**

The mechanism of local scour around bridge piers involves a complex three-dimensional separation of the flow just upstream of the pier. This separation leads to the formation of a system of horseshoe vortices and the periodic vortex shedding in the downstream region. While the scientific community accepts the existence of the horseshoe vortex system, researchers differ on the mechanism by which it is formed. In recent years, research engineers have identified another phenomena described as the downflow, which some believe play a part in the formation of the horseshoe vortex and in the actual scour process. Presented below are the various view points gathered from engineers and scientists who have studied this process. These descriptions were used to develop a conceptual mechanism that combines the two processes and explains the formation of the horseshoe vortex.

#### **FLUID MECHANICS THEORIES**

Experts in the field of fluid mechanics, such as Vennard and Street (1982) and Ahmed (1987), have studied the flow around cylindrical objects. All have noted the formation of a secondary flow that travels downwards along the front face of an object placed in the flow field. Vennard and Street (1982) recognized this secondary flow as the consequence of wall friction and determined that the secondary flow was related to the horizontal velocity profile in a flow field. They explained that the stagnation pressure at the obstruction was greater at higher vertical levels in the flow field than at lower levels



(as may be deduced from the velocity profile shown in Fig. F-1). Accordingly, this pressure difference maintained a downward secondary flow, thus inducing a vortex type motion with the core of the vortex being swept downstream around both sides of the projection. Hung (1968) also studied the velocity and pressure distributions near a circular cylinder in an open channel. He found that the secondary flows along the front and rear of the cylinder were due to the resulting pressure gradient created by the horizontal flow.

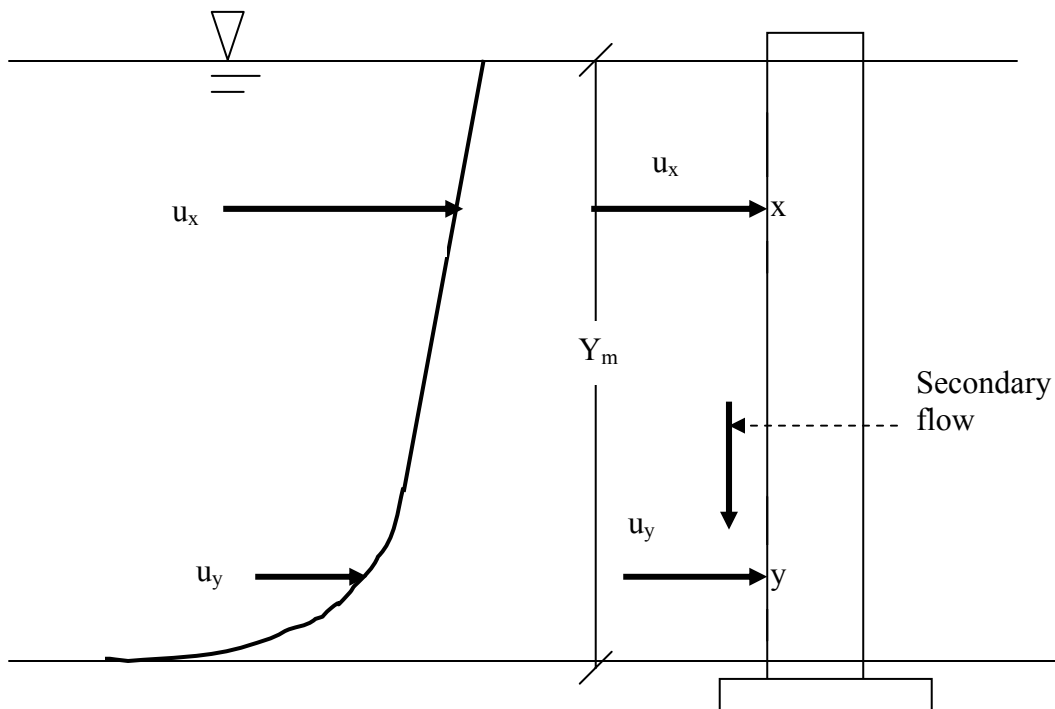


**Fig. F-1. The development of the secondary flow along a bridge pier as explained by Vennard and Street (1982).  $Y_m$  is the flow depth,  $u_x$  is the horizontal velocity vector close to the surface, and  $u_y$  is the horizontal velocity vector close to the invert. The curve represents the turbulent stream velocity profile developed by Grover and Harrington (1966).**

## RESEARCH OF THE HORSESHOE VORTEX SYSTEM

Early researchers such as Keutner (1932), Tison (1940), Laursen and Tosh (1956), and Roper et al. (1967) concluded that the dominant feature of the flow near a pier was the large eddy structure or the system of vortices that developed around the pier. These researchers recognized the vortex system as the basic mechanism of local scour. Roper et al. (1967) concluded that, depending on the type of pier and free-stream conditions, the eddy structure could be composed of any, all, or none of the three basic vortex systems: the horseshoe vortex system, the wake vortex system, and the trailing vortex system. They believed that the vortex systems were an integral part of the flow structure and strongly affected the vertical component of the flow velocity in the neighborhood of the pier.

Baker (1979) conducted experiments using flow visualization in a smoke tunnel. The flow pattern in the plane of symmetry upstream of the cylinder was determined using flow visualization techniques. In addition, measurements of the pressure and velocity distribution upstream of the cylinder were made. Figure F-2 shows the flow pattern seen in the smoke tunnel. At lower flow speeds, three vortices (1, 2, and 3) rotated in a clockwise direction and three smaller vortices (1a, 2a, and  $S_0$ ) rotated in a counter-clockwise direction. The exact number of vortices depended on the diameter of the obstruction and flow speed, with more vortices appearing as either the flow speed or diameter of the obstruction increased. Baker (1979) showed that the number of vortices was a function of the Reynolds number  $UD/\nu$  and a dimensionless parameter  $D/\delta$ , where  $\delta$  is the boundary layer thickness,  $D$  is the pier diameter, and  $\nu$  is the kinematic viscosity. The quantity  $UD/\nu$  is defined as the pier Reynolds number, as it uses the pier diameter as

the length dimension in the Reynolds equation in lieu of the flow depth or hydraulic radius. Above a certain flow speed ( $0.65 \text{ ms}^{-1}$ ), Baker found that the entire vortex system oscillated with Strouhal number ( $fU/D$ ) of the range from 0.26 to 0.6 with  $f$  from 0.8 to 1.4 hertz, where  $f$  is the oscillation frequency (hertz).

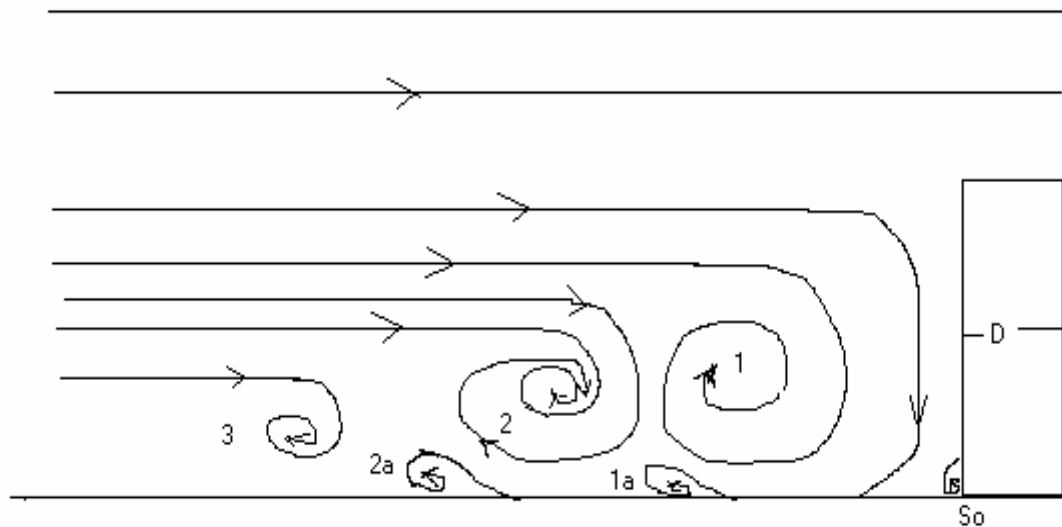


**Fig. F-2. Streamline patterns and vortex systems (Baker 1979) showing a weak counter clockwise vortex  $S_o$  at the base of the cylinder along with small counter clockwise vortices 1a, and 2a at the invert of the flume.**

Using hydrogen bubble flow visualization, Dargahi (1989) also experimentally investigated the flow field around a circular cylinder mounted vertically. Dargahi (1989) determined that the main characteristic of the flow upstream of the cylinder was a system of horseshoe vortices, similar to those identified by Baker (1978), which were shed quasi periodically with a frequency of 0.1 to 2 hertz. Dargahi (1989) also identified a relatively large secondary flow region that had a skewed horizontal velocity distribution in the vertical direction. The implication being that the vortices produced affected the vertical velocity distribution in the flume used for the experiments. He determined that for pier

Reynolds number from 20,000 to 39,000 the vortex system was similar to that obtained by Baker with vortices 1, 2,  $S_o$ , 1a, and 2a being clearly identified.

## **DOWNFLOW RESEARCH**

Baker (1979, 1980) studied the formation of a turbulent horseshoe vortex around the base of a cylinder placed in a wind tunnel and determined that the pressure coefficient at the base of the cylinder was  $(u/U)^2$  where  $u$  is the velocity of the streamline that passed down the face of the cylinder and  $U$  is the free-stream velocity. Baker's finding was an indication that  $u$  was equivalent to the downflow velocity along the face of the cylinder. Baker (1980) further postulated that the weak anti-clockwise vortex ( $S_o$ ) was formed when the streamline with velocity  $u$  directed down the face of the pier (the downflow) was forced to rotate in an anti-clockwise direction because of the no-slip condition that exists in the boundary layer along the pier face. Baker (1980) believed that, depending on the flow conditions, the weak counter clockwise vortex ( $S_o$ ) induced the formation of the large clockwise vortex just upstream (vortex 1). Vortex 1 in turn induced the formation of the counter clockwise vortex 1a, which induced the large clockwise vortex 2, and so on.

Using wind tunnel experiments, Ettema (1980) measured the downflow induced by a cylindrical obstruction placed in the flow in the vertical plane of symmetry. He found that the downflow velocity varied with the vertical displacement from the channel bottom. He also found that at any given elevation the value of the downflow varied horizontally, with the downflow velocity being zero in contact with the pier and again some distance upstream of it. The velocity profiles shown in Fig. F-3 are based on

experimental data by Ettema (1980) and represent the maximum downflow distribution at any elevation, where  $d$  is the pier diameter and  $y$  is the distance from the channel invert. Studies conducted by Ettema showed that the magnitude of the downflow varied with the vertical distance from the bed, as shown in Fig. F-3. Ettema also found that the vertical location of the maximum downflow was dependent on scour depth ( $d_s$ ), while the horizontal location of the maximum downflow was 0.05 to 0.02 pier diameters upstream of the pier, being closer to the pier at lower elevations. Figure F-3 shows that the maximum value of  $V_{dmax}/U$  increases from 0.4 (at  $d_s/d = 0$ ) to 0.8 (at  $d_s/d = 2.3$ ), where  $V_{dmax}$  is the maximum downflow at a given elevation in the flow field and  $d$  is the diameter of the obstruction.

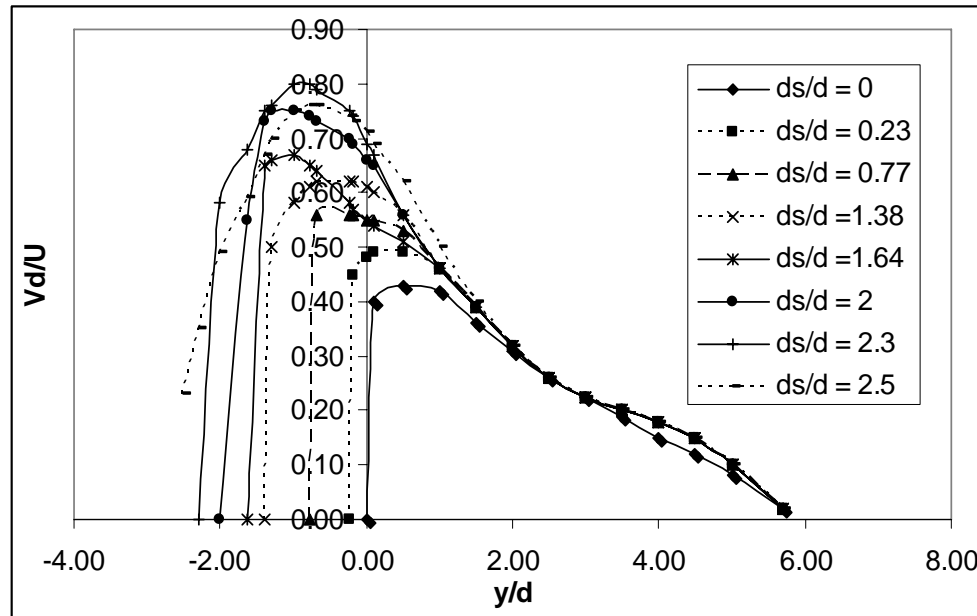


**Fig. F-3. Downflow in front of a pier according to Ettema (1980) for values of  $d_s/d = 0, 0.23, 0.77, 1.38, 1.64, 2.0, 2.3, 2.5$  where  $d_s$  represents scour depth,  $d$  the pier diameter, and  $y$  the vertical distance from the channel invert.**

Raudkivi (1986) conducted laboratory research into the flow field developed around circular piers. He also postulated that the downflow around bridge piers was primarily due to an adverse pressure gradient set up by the stagnation pressure produced by the pier obstruction. He reasoned that, because the horizontal velocity in turbulent flow decreased with depth, then the stagnation pressure also decreases with depth, which establishes the adverse pressure gradient. Raudkivi (1986) was also able to develop relationships between the magnitude of the downflow and the scour depth. He found that the downflow close to the base of a pier was approximately 40% of the mean free stream velocity when the scour depth was zero. He also determined that the downflow increased to a maximum value of 80% of the mean free stream velocity when the scour depth was 2.3 times the pier diameter.

Ahmed and Rajaratnam (1998) conducted laboratory flume experiments on the flow past cylindrical piers. The experiments were conducted using a flume 20-m long and 1.22-m wide. The flume was fitted with a sediment recess 0.2-m deep, 0.78-m wide and 0.78-m long. They observed frontal downflow velocities as large as 95% of the approach velocity during the development of the scour hole.

Melville and Coleman (2000) attributed the downflow velocity to an adverse pressure gradient induced by the bridge pier. According to Melville and Coleman (2000) the stagnation pressures on the face of a pier were highest near the surface, where the deceleration is greatest, and decreases with depth. The resulting downward pressure gradient at the pier face generated the downflow.

## **THE ROLE OF THE DOWNFLOW AND THE VORTEX SYSTEM IN LOCAL SCOUR**

Melville (1975) measured the velocities of the flow at different stages in the development of the scour hole. He also found that a strong vertically downward flow also developed as the scour hole enlarged. Melville (1975) concluded that the downflow played a role in the development of the horseshow vortex system that was directly responsible for the development of the scour hole.

Chiew (1984) determined that the rate of erosion of the scour hole formed around bridge piers was directly related to the magnitude of the downflow that was in turn due to the adverse pressure gradient induced by the bridge pier. Under Chiew's concept the vortices responsible for local scour could be separated into the following components as shown in Fig. F-4: the downflow in front of the pier, the horseshoe vortex system, the wake vortex system, and the trailing vortex. Chiew indicated that the jet of water in the downflow played an important role in the formation and strength of the vortex. However, it was the vortex that caused the erosion of the bed material around the pier, thus forming the scour hole.

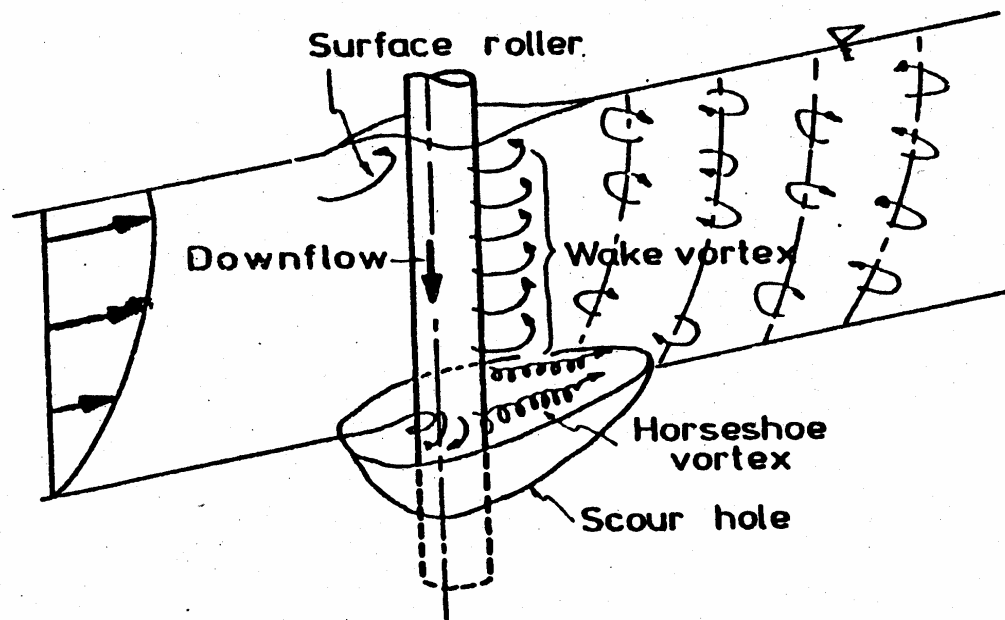


**Fig. F-4. Downflow-Vortex System around a Bridge Pier - Chiew (1984)**

Raudkivi (1986) believed that local scour around piers was caused only by the downflow jet, which represented the primary cause of scour and developed in direct relationship with the scour hole. He further stated that the horseshoe vortex system that developed in and around the scour hole was a consequence of the local scour hole and not the cause of it.

Dargahi (1989) believed that the secondary flow or downflow did not play a direct role in the scour process but was responsible for the flow separation that occurred just upstream of the pier obstruction, which eventually led to the development of a vortex system. He observed that the downflow in the stagnation plane of the cylinder separated



from the pier surface and rotated, thus forming a small anti-clockwise vortex (Baker's  $S_0$ ) at the base of the pier.

Melville and Coleman (2000) identified the principal features of the flow around a bridge pier as the downflow at the upstream face of the pier, horseshoe vortex system, the surface roller, and the wake vortex system. According to Melville and Coleman (2000) the downflow impinged on the bed as a vertical jet and immediately eroded a groove at the base of the front face of the pier. This groove further developed into a small scour hole that helped to create a lee eddy known as the horseshoe vortex. Melville and Coleman (2000) postulated that the downflow and horseshoe vortex system together were responsible for the early development of the local scour hole. Figure F-5 depicts Melville and Coleman's (2000) concept of the roles played by the downflow and horseshoe vortex in the local scour process.

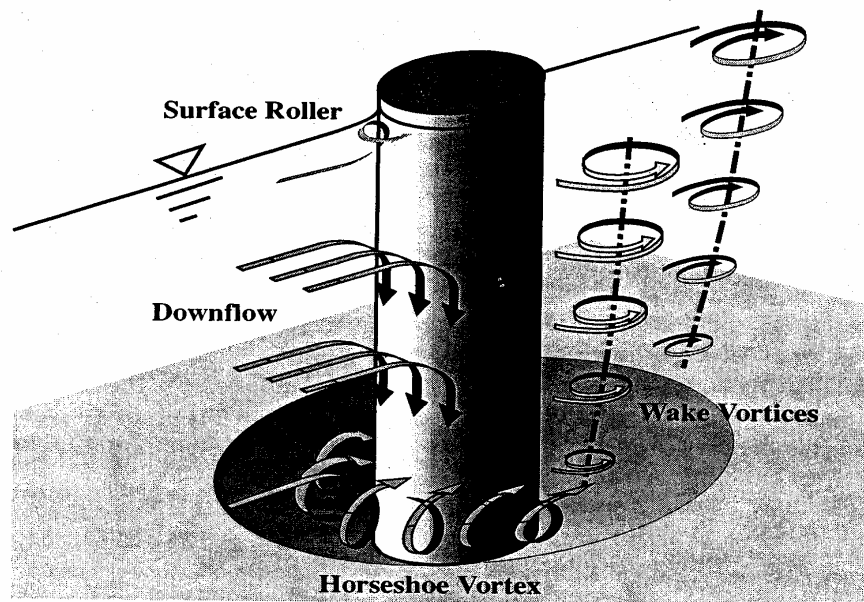


**Fig. F-5. The Downflow-Horseshoe Vortex System of Melville and Coleman (2000)**

## **THE ROLE OF THE DOWNFLOW AND VORTEX AFTER THE DEVELOPMENT OF THE SCOUR HOLE**

Most researchers attribute the latter stages of the development of the scour hole to the erosive activities of the horseshoe vortex system. Dargahi (1989) determined that the scour hole grew with time under the action of the vortex system. Dey et al. (1995) also observed the activities of the horseshoe vortex system during the latter stages of the development of the scour hole. Richardson and Panchang (1998) plotted the flow field in a developed scour hole and deduced that the erosion was caused by a rotating elliptical vortex.

## **CONCLUSIONS**

From the preceding discussions the following may be deduced. First, a downward velocity component (the downflow) is developed along the face of a pier or obstruction placed a flow field. Second, the downflow contributes to the formation of the horseshoe vortex system at the base of the pier. Third, the downflow and vortex systems both contribute to the local scour mechanism during the early development of the scour hole; however, it appears that the horseshoe vortex system plays the major role after the development of the scour hole.

## REFERENCES

- ADC (Alexandria Drafting Company). (1998). *Chesapeake Bay chartbook (Maryland and Virginia)*, Alexandria Drafting Company, Alexandria, Virginia.
- Ahmad, M. (1962). Discussions paper: "Scour at bridge crossings." (E. M. Laursen). *Trans. ASCE*, 127: 1848-1853.
- Ahmed, F. and Rajaratnam, N. (1998). "Flow around bridge piers." *Journal of Hydraulic Engineering*, ASCE, 124(3): 288-300.
- Ahmed, N. (1987). *Fluid mechanics*, Engineering Press, Inc., San Jose, CA.
- Ansari, S. A. and Qadar, A. (1994). "Ultimate depth of scour around bridge piers." *Proc., National Hydraulic Conference*, ASCE, Buffalo, New York, 51-55.
- Apmann, R. P. (1970). "Validity of two-point method of velocity sampling." *Journal of the Hydraulic Division, Proceedings*, ASCE, 96(HY10): 2171-2176.
- Arunachalan, K. (1965). "Scour around bridge piers." *Journal of Indian Roads Congress*, 29: 189-200.
- Baker, C. J. (1979). "The laminar horseshoe vortex." *Journal of Fluid Mechanics*, 95(2): 347-367.
- Baker, C. J. (1980). "The turbulent horseshoe vortex." *Journal of Wind and Industrial Aerodynamics*, 6: 9-23.
- Barkau, L. (1996). *UNET one-dimensional unsteady flow through a network of open channels*, U.S. Army Corps of Engineers, Hydrologic Engineering Center, Davis, CA.
- Basak, V. (1975). "Scour at square piles." *Report No. 583*, Delvet Su isteri genel mudurlugu, Ankara, Turkey.
- Blench, T. (1969). *Mobile-bed fluviology*, University of Alberta Press, Edmonton, Canada.
- Breusers, H. N. C. (1965). "Scour around drilling platforms." *Bulletin, Hydraulic Research, 1964 and 1965*, I.A.H.R., 19: 276-288.
- Breusers, H. N. C., Nicollet, G., and Shen, H. W. (1977). "Local scour around cylindrical piers." *Journal of Hydraulic Research*, I.A.H.R., 15(3): 211-252.
- Briaud, J., Ting, F. C. K., Chen, H. C., Gudavilli, R., Perugu, S., and Wei, G. (1999). "SRICOS: Predictions of scour rates in cohesive soils at bridge piers." *Journal of Geotechnical and Geoenvironmental Engineering*, 125(4): 237-246.

- Chang, F. (1998). "Modification of Neill's equation for tidal flow analysis." *ASCE Compendium of Papers on Bridge Scour*, Maryland State Highway Administration, Office of Bridge Development, Baltimore, Maryland, 723-727.
- Chapra, S. C. (1997). *Surface water quality modeling*, The McGraw Hill Book Company, Inc., New York.
- Chiew, Y. M. (1984). "Local scour at bridge piers." *Report No. 355*, University of Auckland, School of Engineering, Auckland, New Zealand.
- Chitale, W. S. (1962). Discussion paper: "Scour at bridge crossings." (E. M. Laursen). *Trans.*, ASCE, 217(1): 191-196.
- Chitale, W. S. (1988). "Estimation of scour at bridge piers." *Journal of Irrigation and Power*, India, 1: 57-68.
- Chow, V. T. (1959). *Open-channel hydraulics*, McGraw-Hill Book Company, Inc., New York.
- Coleman, N. L. (1971). "Analyzing laboratory measurements of scour at cylindrical piers in sand beds." *Proc.*, 14<sup>th</sup> Congress I.A.H.R., 3: 238-250.
- Daily, J. W. and Harleman, D. F. R. (1966). *Fluid dynamics*, Addison-Wesley Publ. Co., Reading, CA.
- Dargahi, B. (1989). "The turbulent flow field around a circular cylinder." *Experiments in Fluids*, 8: 1-12.
- Demetrius, D. R., Brubaker K., and Davis S. R. (2002). "Modification of Neill's equation for storm-tide design flow analysis." *Journal of the American Water Resources Association*, 38(1): 275-288.
- Demetrius, D. R. and McCuen R. H. (2003). "A conceptual downflow model for circular bridge piers." *Journal of Floodplain Management*, 3(2): 19-38.
- Dey, S., Bose, S. K., and Sastry, G. L. N. (1995). "Clear water scour at circular piers, a model." *Journal of Hydraulic Engineering*, 121(12): 869-876.
- Dongguang, G., Pasada, L., and Nordin, F. C. (1993). "Pier scour equations used in the People's Republic of China." *Rep. No. FHWA-SA-93-076*, Federal Highway Administration, U.S. Department of Transportation, Washington, D.C.
- Edge, B. L., Scheffner, N. W., Fisher, J. S., and Vignet, S. N. (1998). "Determination of velocity in estuary for bridge scour computations." *Journal of Hydraulic Engineering*, ASCE, 124(6): 619-628.

- Einstein, H. A. (1942). "Formulas for the transportation of bed load." *Trans.*, ASCE, 107: 561-570.
- Engel, J. J., Hotchkiss, R. H., and Hall, B. R. (1995). "Three-dimensional sediment transport modeling using CH3D computer model." *Proc., First National Conference on Water Resource Engineering*, ASCE, San Antonio, Texas, 628-632.
- Ettema, R. (1980). "Scour at bridge piers." *Report No 216*, University of Auckland, School of Engineering, Auckland, New Zealand.
- E2RC, Inc. (2001). *Final geotechnical report for the preliminary feasibility study of Parson Island, Chesapeake Bay, Maryland*, E2CR, Inc., Baltimore, Maryland.
- Froelich, D. C. (1988). "Analysis of on-site measurements of scour at piers." *Proceedings, National Hydraulic Engineering Conference*, ASCE, New York.
- Gao, D., Posada, G. L., and Nordin, C. F. (1993). "Pier scour equations used in the Peoples Republic of China – review and summary." *Proc., National Hydraulics Conference*, ASCE, California, 1031-1036.
- Garde, R. J. (1961). "Local bed variations at bridge piers in alluvial channels." *University of Roorkee Research Journal*, IV(1): 101-116.
- Grover, C. and Harrington, A. (1966). *Stream flow measurements records and their uses*, Dover Publication Inc., New York.
- Hancu, S. (1971). "Sur de calcul des affouillements locaux la zone des piles des ponts." *Proc., 14<sup>th</sup> I.A.H.R. Congress*, Paris, 3: 299-313.
- Henderson, F. M. (1966). *Open channel flow*, Macmillan Publishing Co., Inc., New York.
- Hu G., Johnson, M. L., and Krone, R. E. (1995). "Hydraulic and sediment models for design of restoration of former tidal marshland." *Estuarine and Coastal Modeling, Proceedings of the 4<sup>th</sup> International Conference*, ASCE, 215-228.
- Hung, C. S. (1968). *A preliminary study on the resistance of cylinders in open channel flow*, Colorado State University, Fort Collins, Colorado.
- Inglis, C. C. (1949). "The behavior and control of rivers and canals part II." *Research Publication #13*, Central Water Power Irrigation and Navigation Research Station, Poona, India.
- Jain, S. C. (1981). "Maximum clear-water scour around cylindrical piers." *Journal of Hydraulic Engineering*, ASCE, 107(5): 611-625.
- Jain, S. C. and Fischer, E. E., (1979). "Scour around bridge piers at high Froude numbers." *Federal Highway Administration, Research Report No. FHWA-RD-79-*

104. Federal Highway Administration, U.S. Department of Transportation, Washington, D.C.
- Jain, S. C. and Modi, P. N. (1986). "Comparative study of various formulae on scour around bridge piers." *Journal of the Institute of Engineers (India)*, 67(CI3): 149-159.
- Johnson, P. A. (1995). "Comparison of pier-scour equations using field data." *Journal of Hydraulic Engineering*, ASCE, 121(8): 626-629.
- Johnson, P. A. (1996). "Uncertainty of hydraulic parameters." *Journal of Hydraulic Engineering*, ASCE, Vol. 122(2): 112-114.
- Johnson, P. A. and McCuen, R. H. (1991). "A temporal spatial pier scour model." *Transp. Res. Rec. 1319*, Transportation Research Board, Washington D.C., 143-149.
- Keutner, C. (1932). "The flow around bridge piers of different shapes and its effects on the river bed." *Die Bautechnik*, 10(2): 161-172
- Kreeb, B. L. and McCuen, R. H. (2003). *Hydrologic efficiency and design sensitivity of bioretention facilities*, Department of Civil and Environmental Engineering, University of Maryland, College Park, MD.
- Krone, R. B. (1962). *Flume study in the transport of sediment in estuarial shoaling process*, Final report to San Francisco District, U.S. Army Corps of Engineers, Hydraulic Engineering Lab., and Sanitary Engineering Res. Lab., University of California, Berkeley, CA.
- Lacey, G. (1930). "Stable channels in alluvium." *Paper 4736, Minutes of the Proc.*, Institution of Civil Engineers, William Clowes and Sons Ltd., London, 229: 259-292.
- Landers, M. N. and Mueller, D. S. (1996). "Scour processes observed in field data." *North American Water and Environmental Congress*, ASCE, Anaheim, CA.
- Larras, J. (1963). "Profondeurs maximales d'érosion des fonds mobiles autour des piles en rivière." *Ann. Ponts et Chaussées*, 133(4): 411-424.
- Laursen, E. M. (1962). "Scour at bridge crossings." *Trans.*, ASCE, 127(1): 116-179.
- Laursen, E. M. and Tosh, A. (1956). "Scour around bridge piers and abutments." *Bulletin No. 4*, Iowa Highway Research Board, Ames, Iowa.
- Leopold, L. B. (1994). *A view of the river*, Harvard University Press, Cambridge, Massachusetts.

- Leopold, L. B. and Maddock, B. (1953). "The hydraulic geometry of channels and some physiographic implications." *Geological Survey Professional Paper 252*, Washington, D.C.
- Liu, H. K., Chang, F. M., and Skinner, M. M. (1961). "Effects of bridge constriction on scour and backwater." *CER 60 KHL 22*, Engineering Research Center, Colorado State University, Fort Collins, Colorado.
- Maryland Geological Survey (2003). *Surficial sediment distribution of Maryland's Chesapeake Bay*, [www.mgs.md.gov/coastal/vmap/baysed.html](http://www.mgs.md.gov/coastal/vmap/baysed.html).
- McCuen, R. H. (1973). "The role of sensitivity analysis in hydrologic modeling." *Journal of Hydrology*, 18: 37-53.
- McCuen, R. H. (2003). *Modeling hydrologic change-statistical methods*, Lewis Publishers, Boca Raton, Florida.
- Melville, B. W. (1975). "Local scour at bridge piers." *Report #117*, University of Auckland, Auckland, New Zealand.
- Melville, B. W. (1997). "Pier and abutment scour – an integrated approach." *Journal of Hydraulic Engineering*, ASCE, 123(2): 125-136.
- Melville, B. W. and Coleman, S. E. (2000). *Bridge scour*, Water Resources Publications, LLC, Littleton, Colorado.
- Melville, B. W. and Sutherland, A. J. (1988). "Design methods for local scour at bridge piers." *Journal of Hydraulic Engineering*, ASCE, 114(10): 1210-1226.
- Metha, A. J. and Prakash B. J. (1988). "Tidal inlet hydraulics." *Journal of Hydraulic Engineering*, 114(11): 1321-1335.
- Modarres, M. (1993). *What every engineer should know about reliability and risk analysis*, Marcel Dekker, Inc., New York.
- Moglen E., Thomas W., and Cuneo, G. (2006). *Evaluation of alternative statistical methods for estimating frequency of peak flows in Maryland*. Maryland State Highway Administration, Baltimore, Maryland.
- Muir, L. R. (1978). "A one-dimensional tidal model for estuarine networks." *Proceedings of the 9<sup>th</sup> International Liege Colloquium on Ocean Hydrodynamics*, Elsevier Oceanography Series, 23: 243-260.
- National Oceanographic and Atmospheric Agency. (1977). *National hurricane operations plan*. Department of Commerce, Washington, D.C.

- National Weather Service. (1961). "Rainfall frequency atlas of the United States, 30-minutes to 24-hour durations, 1-year to 100-year return periods." *TP 40*. National Weather Service, Silver Spring, Maryland
- Neill, C. R. (1968). "Note on initial movement of coarse uniformed bed material." *Journal of Hydraulic Research*, 17(2): 247-249.
- Neill, C. R. (1973). *Guide to bridge hydraulics*, Road and Transportation Association of Canada (RTAC).
- Odgaard, A. J. (1986). "Free-surface air core vortex." *Journal of Hydraulic Engineering*, 112(7): 610-620.
- Parola, A. C., Hagerty, D. J., Mueller, D. S., Melville, B. W., Parker, G., and Usher, J. S. (1995). "Scour at bridge foundations, research needs." *NCHRP Project 24-8 Interim Report*, National Co-operative Highway Research Program, Washington D.C.
- Parola, A. C., Hagerty, D. J., Mueller, D. S., Melville, B. W., Parker, G., and Usher, J. S. (1996). "Scour at bridge foundations, research needs." *NCHRP Project 24-8 Interim Report, Preliminary Draft Strategic Plan*, National Co-operative Highway Research Program, Washington D.C.
- Pillsbury, G. B. (1956). *Tidal hydraulics*, Corps of Engineers, U.S. Army, Waterways Experiment Station, Vicksburg, Mississippi.
- Prandle, D. (1982). "Generalized theory of estuarine dynamics." Institute of Oceanographic Sciences, U.K. *Proceedings of Coastal Engineering Conference*, ASCE, Houston, Texas, 42-57.
- Pritchard, D. W. and Cameron, W. M. (1963). "Estuaries." *The sea*, (M.N. Hill, ed.), Wiley, New York, 2: 306-324.
- Raudjkivi, A. J. (1986). "Functional trends of scour at bridge piers." *Journal of Hydraulic Engineering*, 112(1): 1-13.
- R.D.S.O. (1968). "Scour around bridge piers of Ganga Pul at Mokameh." *Bridges and Floods Report No. BRF-5*, Progress Report No. 2, New Delhi, India.
- Richardson, E. V., Davis, S. R., and Lawrence J. H. (1991). "Evaluating scour at bridges." *Report No. FHWA-IP-90-017*, Hydraulic Engineering Circular No.18 (HEC 18), Office of Research and Development, Federal Highway Administration, U.S. Department of Transportation, Washington, D.C.
- Richardson, E.V. and Davis, S.R., (1995). "Evaluating scour at bridges." *Report No. FHWA-IP-90-017*, Hydraulic Engineering Circular No.18 (HEC 18), Third Edition,



- Office of Technology Applications. HTA-22, Federal Highway Administration, U.S. Department of Transportation, Washington, D.C.
- Richardson, E. V. and Davis, S. R., (2001). "Evaluating scour at bridges." *Report No. FHWA NHI-01-001*, Hydraulic Engineering Circular No.18 (HEC 18), Fourth Edition, Office of Bridge Technology, Federal Highway Administration, U.S. Department of Transportation, Washington, D.C.
- Richardson, E. V. and Edge, B. L. (1997). *Tidal hydraulic modeling for bridges, users manual*, Ayers and Associates, Columbia, SC.
- Richardson, J. E. and Panchang, V. G. (1998). "Three-dimensional simulation of scour inducing flow at bridge piers." *Journal of Hydraulic Engineering*, 124(5): 530-540.
- Rosgen, D. (1996). *Applied river morphology*, Wildland Hydrology, Pagosa Springs, Colorado.
- Roper, A. T., Schneider, V. R., and Shen, H. W. (1967). "Analytical approach to local scour." *Proc., 12<sup>th</sup> Congress*, I.A.H.R, Ft Collins, Colorado, 3:151-161.
- Savenije, H. H. G. (1998). "Analytical expression for tidal damping in alluvial estuaries." *Journal of Hydraulic Engineering*, 124(6): 615-618.
- Shelden, J. G. and Martin, J. D. (1998). "Hydrodynamic modeling Croatan / Pamlico Sound system, NC." *Estuarine and Coastal Modeling, Proceedings of the 7<sup>th</sup> International Conference*, ASCE, St. Petersburg, Florida, 308-317.
- Shen, H. W., Schneider, V. R., and Karak, S. (1966). "Mechanics of local scour and supplement methods of reducing scour." *Report No. CER66HW536*, Civ. Engr. Dept., Colorado State Univ., Fort Collins, Colorado.
- Shen, H. W., Schneider, V. R., and Karaki, S. (1966). "Mechanics of local scour and supplement methods of reducing scour." *Colorado State University CER 66 HWS-VRS-SK-22 prepared for US Department of Commerce*, Bureau of Public Roads, Office of Research and Development, Structures and Applied Mechanics Division, Fort Collins, Colorado.
- Shen, H. W., Schneider, V. R., and Karaki, S. (1969). "Local scour around bridge piers." *Journal of the Hydraulics Division, Proceedings*, ASCE, 95(HY6): 1919-1940.
- Simmons, H.B. (1955). "Some effects of upland discharges on estuarine hydraulics." *Proceedings*, ASCE, 81: 2002-2022.
- Soil Conservation Service. (1984). *TR-20 computer program for project formulation hydrology*, Third Edition, Soil Conservation Service, USDA, Washington, D.C.

- Soil Conservation Service. (1986). "Urban hydrology for small watersheds." *Technical Release 55*, Soil Conservation Service, USDA, Washington, D.C.
- Stelling, G. S. (1980). "Improved stability of Dronkers' tidal schemes." *Journal of the Hydraulics Division*, 106(HY8): 1365-1379.
- Thurman, H.V. (1993). *Essentials of oceanography*, (4<sup>th</sup> ed.), Macmillan Publishing Co., Inc., New York.
- Tison, L. J. (1962). Discussions paper: "Scour at bridge crossings." (E. M. Laursen). *Trans. ASCE*, 127: 188-191.
- U.S. Army Corps of Engineers. (1977). "Scour and deposition in rivers and reservoirs, HEC 6." *Rep 723-G2-L2470*, Hydraulic Engineering Center, Davis, California.
- U.S. Army Corps of Engineers. (1986). "Storm surge analysis and design water level determinations." *EM 1110-2-1412*, U.S. Army Corps of Engineers, Washington, D.C.
- U.S. Army Corps of Engineers. (1989). "Sedimentation investigations of rivers and reservoirs." *CECW-EH-Y, Engineer Manual 1110-2-4000*, Department of the Army, U.S. Army Corps of Engineers, Washington, DC.
- U.S. Army Corps of Engineers. (1991). "Tidal hydraulics." *EM 1110-2-1607*, U.S. Army Corps of Engineers, Washington, D.C.
- Vennard, J. K. and Street, R. L. (1982). *Elementary fluid mechanics*, (6<sup>th</sup> ed.), John Wiley and Sons, New York.
- Wang, D. P. (1980). "Observation and modeling of the circulation in the Chesapeake Bay." *Workshop on Estuarine and Wetland Process*, Plenum Press, New York, 35-47.
- Yeh, K. C. and Tung, Y. K. (1993). "Uncertainty and sensitivity analyses of pit migration model." *Journal of Hydraulic Engineering*, ASCE, 119(2): 262-283.
- Zai-Jin, Y. (1998). "Initial motion of sediment in oscillatory flow." *Journal of Waterway, Ports, Coastal, and Ocean Engineering*, 124(2): 68-72.
- Zhuravlyov, M. M. (1978). "New methods for the estimation of local scour due to bridge piers and its substantiation." *Trans., Ministry of Transport Constr.*, State All Union Scientific Res. Inst. on Roads, Moscow, Russia, 4-51.